



PHD

Development of Axially Chiral Biazulenes for Catalysis

Gee, Anthony

Award date:
2016

Awarding institution:
University of Bath

[Link to publication](#)

Alternative formats

If you require this document in an alternative format, please contact:
openaccess@bath.ac.uk

Copyright of this thesis rests with the author. Access is subject to the above licence, if given. If no licence is specified above, original content in this thesis is licensed under the terms of the Creative Commons Attribution-NonCommercial 4.0 International (CC BY-NC-ND 4.0) Licence (<https://creativecommons.org/licenses/by-nc-nd/4.0/>). Any third-party copyright material present remains the property of its respective owner(s) and is licensed under its existing terms.

Take down policy

If you consider content within Bath's Research Portal to be in breach of UK law, please contact: openaccess@bath.ac.uk with the details. Your claim will be investigated and, where appropriate, the item will be removed from public view as soon as possible.



Development of Axially Chiral Biazulenes for Catalysis

Anthony Philip Gee

A thesis submitted for the degree of Doctor of Philosophy

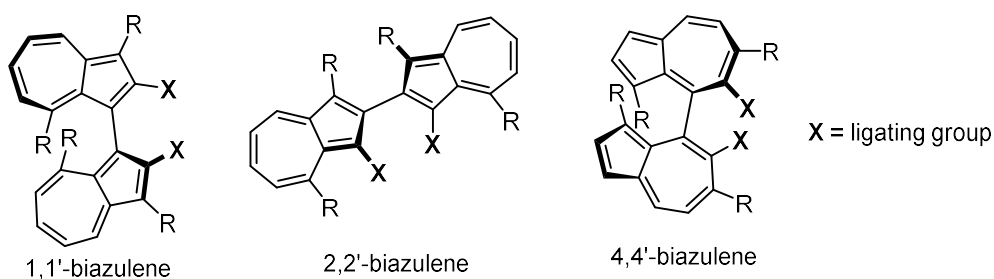
University of Bath

Department of Chemistry

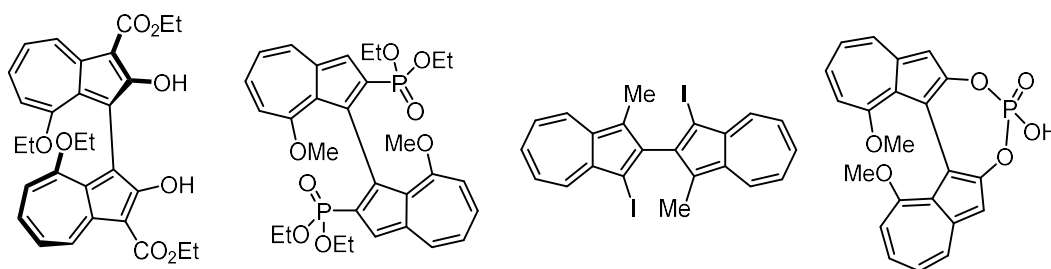
September 2016

i. ABSTRACT

Axially chiral biaryl ligands are ubiquitous in asymmetric transition metal-catalysed homogeneous catalysis. However, biazulene motifs have not previously been incorporated in the design of chiral ligands in asymmetric catalysis, despite the unique geometric and electronic properties of azulene derivatives. The aims of this project were to develop novel axially chiral biazulene-diphosphine, -diol and related species, encompassing the synthesis and resolution of their enantiomers, and to screen these compounds in the application towards common asymmetric reactions.



The most significant achievement reached in this project was the synthesis and resolution of practicable quantities of an atropisomeric 1,1'-biazulene-2,2'-diol species ("1,1'-BazOL"), which has been employed in an asymmetric Ti-catalysed Diels–Alder reaction. Much progress has also been made towards the synthesis of other targets, like 1,1'-biazulene-2,2'-diphosphine ("1,1'-BazPhos"), 2,2'-biazulene-1,1'-diphosphine ("2,2'-BazPhos") and 1,1'-biazulene-2,2'-phosphoric acid ("1,1'-BazPA").



ii. ACKNOWLEDGMENTS

Undertaking this project would not have been possible without key contributions and assistance from colleagues and friends around the department. Firstly, I would like to offer many heartfelt thanks to my primary supervisor, Dr. Simon E. Lewis, for all his help, ideas, support and great enthusiasm towards this research. Similarly, I would also thank all postgraduate students and post-doctoral researchers who have worked in the Lewis group throughout my PhD studentship – Paul Cowper, Dr. Catherine Lyall, Dr. Julia Griffen, Dr. Kathryn Wills, Dr. Matthew Palframan, Georgina Gregory, Toby Nash, Ben Alexander, Dr. Monica Ali Khan, Carlos López Alled, Dominic Ferdani, Yu Jin – as well as all of the undergraduate students, for their help, support and companionship.

Also, there have been several other people from around the department whose contributions to the project have been greatly appreciated. I would like to thank Dr. Gabriele Kociok-Köhn and Dr. Mary Mahon for their X-ray crystallography expertise; my secondary supervisor, Dr. Andrew L. Johnson, as well as Dr. Sam Cosham, for their help with air-sensitive phosphine synthesis; for their help with CD spectrometry, Dr. G. Dan Pantoş and Tibi Gianga; for their tuition of chiral HPLC, Robert Chapman and Dr. G. Dan Pantoş, once again and for his help with chiral GC, Dr. Matthew Jones. Special thanks also go to the EPSRC for funding this research.

Finally, I would like to thank my girlfriend, Hope, as well as my mother, Kaisu and father, Phil, for all of their love and support, and for looking after me while I have been writing this thesis.

iii. ABBREVIATIONS

R	residual group
°C	degrees Celsius
2D	2-dimensional
Å	Ångstroms
Ac	acetyl
AMC	active methylene compound
app	apparent
aq	aqueous
Ar	aryl
ASAP	atmospheric solids analysis probe
atm	atmosphere(s)
B ₂ pin ₂	bis(pinacolato)diboron
BAr _F	[B[3,5-(CF ₃) ₂ C ₆ H ₃] ₄] anion
BHT	butylated hydroxytoluene
Bn	benzyl
Boc	<i>tert</i> -butyloxycarbonyl
bpy	bipyridine
Bu	butyl
calc	calculated
cat.	catalyst or catalysed
Cbz	carboxybenzyl
CCD	charge-coupled device
CD	circular dichroism
cm	centimetres
COD	cyclooctadiene
Cp	cyclopentadienyl
Cy	cyclohexyl
d	days
d	doublet
<i>d.e.</i>	diastereomeric excess
DABCO	1,4-diazabicyclo[2.2.2]octane
dba	dibenzylideneacetone
DCE	dichloroethane
DCM	dichloromethane
DDQ	2,3-dichloro-5,6-dicyano-1,4-benzoquinone
dec.	decomposed
DIBAL-H	<i>di</i> isobutylaluminium hydride
DIPEA	<i>N,N</i> -Diisopropylethylamine (Hünig's base)
dm	decimetre
DMAP	4-dimethylaminopyridine
DME	1,2-dimethoxyethane

DMF	dimethylformamide
DMSO	dimethyl sulfoxide
DNA	deoxyribonucleic acid
dppb	bis-(diphenylphosphino)butane
dppe	bis-(diphenylphosphino)ethane
dppf	1,1'-bis-(diphenylphosphino)ferrocene
e.e.	enantiomeric excess
EDG	electron donating group
EI	electron impact
eq.	equivalents
ESI	electrospray ionisation
Et	ethyl
<i>et al.</i>	and others
EWG	electron withdrawing group
FT	Fourier transformed
G	Gibbs free energy
g	grams
GC	gas chromatography
<i>gem</i>	geminal
h	hour(s)
H	enthalpy
<i>het</i>	hetero
HMBC	heteronuclear multiple bond correlation
HOMO	highest occupied molecular orbital
HPLC	high performance liquid chromatography
HRMS	high-resolution mass spectrometry
HSQC	heteronuclear single quantum correlation
Hz	Hertz
<i>i</i>	<i>iso</i>
ID	internal diameter
IPA	isopropyl alcohol
IR	infra red
<i>J</i>	NMR coupling constant
k	rate constant
K	degrees Kelvin
kcal	kilocalories
L	ligand
L	litre
LDA	lithium diisopropylamide
L-DOPA	L-3,4-dihydroxyphenylalanine
LG	leaving group
LTMP	lithium 2,2,6,6-tetramethylpiperidide
LUMO	lowest unoccupied molecular orbital
M	metal

<i>m</i>	<i>meta</i>
m	metres
M	moles per dm ³
m	multiplet
m.p.	melting point
<i>m/z</i>	mass per unit charge
maj	major
Me	methyl
mg	milligrams
MHz	mega Hertz
min	minute(s)
min	minor
mL	millilitre
mM	millimoles per dm ³
MM2	Molecular Mechanics 2
mmol	millimolar
mol	moles or molecular
<i>n</i>	linear (alkyl chain)
nbd	norbornadiene
NBS	<i>N</i> -bromosuccinimide
NCS	<i>N</i> -chlorosuccinimide
NIS	<i>N</i> -iodosuccinimide
nm	nanometre
ν_{\max}	wavenumber of maximum absorption
NMP	<i>N</i> -methyl-2-pyrrolidone
NMR	nuclear magnetic resonance
<i>o</i>	<i>ortho</i>
Oct	octyl
ORTEP	Oak Ridge Thermal Ellipsoid Plot
<i>p</i>	<i>para</i>
Ph	phenyl
pH	potential of hydrogen
pK_a	logarithmic acid dissociation constant
PMP	1,2,2,6,6-pentamethylpiperidine
Pr	propyl
py	pyridine
q	quartet
quint	quintet
r.t.	room temperature
<i>rac</i>	racemic
R_f	retention factor
s	seconds
S	entropy

t	triplet
TBAB	tetra- <i>n</i> -butylammonium bromide
TBAI	tetra- <i>n</i> -butylammonium iodide
TEMPO	2,2,6,6-tetramethyl-1-piperidinyloxy
<i>tert</i>	tertiary
<i>tert</i>	tertiary
Tf	trifluoromethanesulfonyl
TFA	trifluoroacetic acid
TFAA	trifluoroacetic anhydride
tfc	3-(trifluoromethylhydroxymethylene)-(+)-camphorate
TFE	2,2,2-trifluoroethanol
THF	tetrahydrofuran
TLC	thin layer chromatography
TMEDA	<i>N,N,N',N'</i> -tetramethylethylenediamine
TMS	trimethylsilyl
TOF	time of flight
tol	tolyl
TRIP	3,3'-bis(2,4,6-triisopropylphenyl)-1,1'-binaphthyl-2,2'-diyl hydrogenphosphate
Ts	<i>p</i> -toluenesulfonyl
UV	ultraviolet
v	volume
V	volts
wt.	weight
X	halide or pseudohalide
xyl	xylyl
Δ	heat at reflux
μL	microlitre
μw	microwave radiation
v	wavenumber

iv. CONTENTS

1. INTRODUCTION	1
1.1. Chirality and chiral induction	1
1.2. Chiral phosphine ligands in homogeneous catalysis	8
1.2.1. Wilkinson's catalyst	8
1.2.2. First chiral phosphine ligands for asymmetric hydrogenation	10
1.2.3. DIOP, CAMP and DIPAMP	12
1.2.4. BINAP by Noyori	16
1.3. Dihedral angles of axially chiral diphosphine ligands	21
1.3.1. BIPHEMP and MeO-BIPHEP	23
1.3.2. H ₈ -BINAP	26
1.3.3. SEGPPOS	31
1.3.4. TunePhos	34
1.3.5. Supramolecular tuning of the ligand bite angle	38
1.4. Electron-rich and electron-poor diphosphine ligands	40
1.4.1. Increased Lewis basicity in diphosphine ligands	40
1.4.2. Assessment of biaryl diphosphine Lewis basicity by IR	41
1.4.3. Electron-rich axially chiral diphosphine ligands	42
1.4.4. Decreased Lewis basicity in diphosphine ligands	48
1.4.5. Electron-poor axially chiral diphosphine ligands	49
1.4.6. DIFLUORPHOS	52
1.5. Biheteroaryl diphosphine ligands with 5-membered rings	56
1.5.1. Sulfur as the heteroatom	56
1.5.2. Nitrogen as the heteroatom	58
1.5.3. Oxygen as the heteroatom	59
1.6. Dihedral angles of axially chiral biaryl diol ligands	60
1.6.1. BINOL by Noyori	60
1.6.2. Modification of biaryl diol dihedral angle	63
1.6.3. H ₈ -BINOL	66
1.7. Conclusion	69
2. RESULTS AND DISCUSSION	71
2.1. Project aims and rationale	71
2.1.1. Properties of azulenes	73
2.1.2. Azulene as a motif in chiral ligand design	77
2.1.3. Nozoe's method for the synthesis of azulenes	84
2.2. Development of 1,1'-biazulene-2,2'-diphosphine ("1,1'-BazPhos")	90
2.2.1. Foundations of synthesis based around Nozoe's method	90
2.2.2. Improvements to synthetic steps	96
2.2.3. Chemical transformations of monoazulenes	103
2.2.4. Synthesis of 3-aryl-2 <i>H</i> -cyclohepta[<i>b</i>]furan-2-one precursors	109

2.2.5. 1,1'-biazulene formation through Cu-catalysed oxidative homocoupling	113
2.2.6. Chemical transformations of ester-containing 1,1'-biazulene-2,2'-diol	116
2.2.7. Removal of ester groups	121
2.2.8. Installation of phosphorus-containing functional groups	126
2.3. Development of 1,1'-biazulene-2,2'-diol ("1,1'-BazOL")	136
2.3.1. Asymmetric synthesis of 1,1'-BazOL	139
2.3.2. Resolution of 1,1'-BazOL	145
2.3.4. CD spectrometry and configurational stability	155
2.4. Development of 2,2'-biazulene-1,1'-diphosphine ("2,2'-BazPhos")	163
2.4.1. Formation of 2,2'-biazulene through Pd-catalysed homocoupling	163
2.4.2. Installation of phosphine groups at 1-position	165
2.4.3. Reduction of ester groups	171
2.4.4. Synthesis towards 2,2'-BazPhos	174
2.5. Development of "1,1'-BazPhos" through the Hafner method	183
2.5.1. C-H activation of azulene 2-position	183
2.5.2. Hafner's method for the synthesis of azulenes	187
2.5.3. Synthesis of azulene-2-yl phosphines	189
2.5.4. Limitations and future synthetic developments	199
2.6. Development of 1,1-biazulene-2,2'-phosphoric acid ("1,1'-BazPA")	201
2.6.1. Ideal chiral biazulene-acid targets	201
2.6.2. Synthesis of 1,1'-BazPa	203
2.6.3. Limitations	205
2.7. Asymmetric Diels–Alder reaction	206
2.7.1. Ti-catalysed Diels–Alder reaction with 1,1'-BazOL	207
2.8. Conclusions and future work	210
 3. EXPERIMENTAL	 216
 4. REFERENCES	 332
 5. APPENDICES	 352
5.1. NMR appendix	352
5.2. X-ray crystallography appendix	463

1. INTRODUCTION

1.1. Chirality and chiral induction

If an object possesses a mirror image, onto which it cannot be superimposed, it is described as having chirality. This concept is ubiquitous in organic chemistry, as a tetrahedral carbon atom that has four different substituents is known as a stereocentre and, in most cases, leads to chirality in a molecule. The mirrored depictions of the chiral molecule are the enantiomers of each other (Figure 1). Other tetrahedral atoms, such as phosphorus and sulfur, can exhibit chirality in the same way, often with a lone pair acting as a fourth 'substituent'.

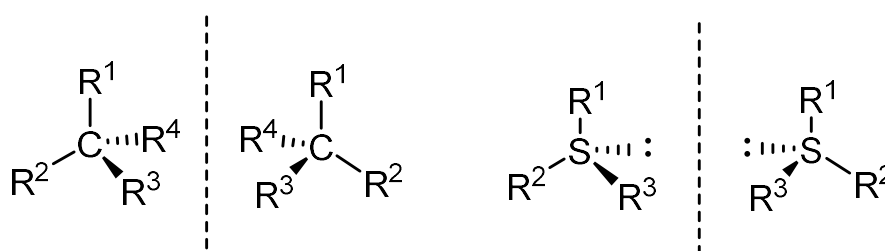


Figure 1: Tetrahedral atoms, carbon and sulfur, with four different substituents, reflected with a plane of symmetry to depict their enantiomers.

While it is the most common form of chirality in organic chemistry, having a stereocentre is not compulsory for a molecule to be chiral (Figure 2). If a biaryl molecule has restricted rotation around the biaryl bond, often caused by steric hindrance of substituents positioned *ortho*- to that bond, it can have two enantiomeric forms (**1**). If that molecule is comprised of identical arene species, it possesses a C₂ axis of rotational symmetry, despite the planar asymmetry, called axial chirality, associated with its structure. Axial chirality also occurs in other molecules that do not have stereocentres, but have restricted rotation around an axis; allene derivatives **2** with inequivalent substituents R₁ and R₂ at each terminus

do not have a mirror plane of symmetry, and are therefore chiral. Spiro compounds **3** can also exhibit axial chirality, when the quaternary centre has fewer than four different substituents, due to the fixed configuration at that carbon atom. Helicenes **4** are aromatic hydrocarbons, made up of benzene rings that are fused in a spiral formation, and thus exhibit helical chirality, similar to the symmetrical properties of a screw.

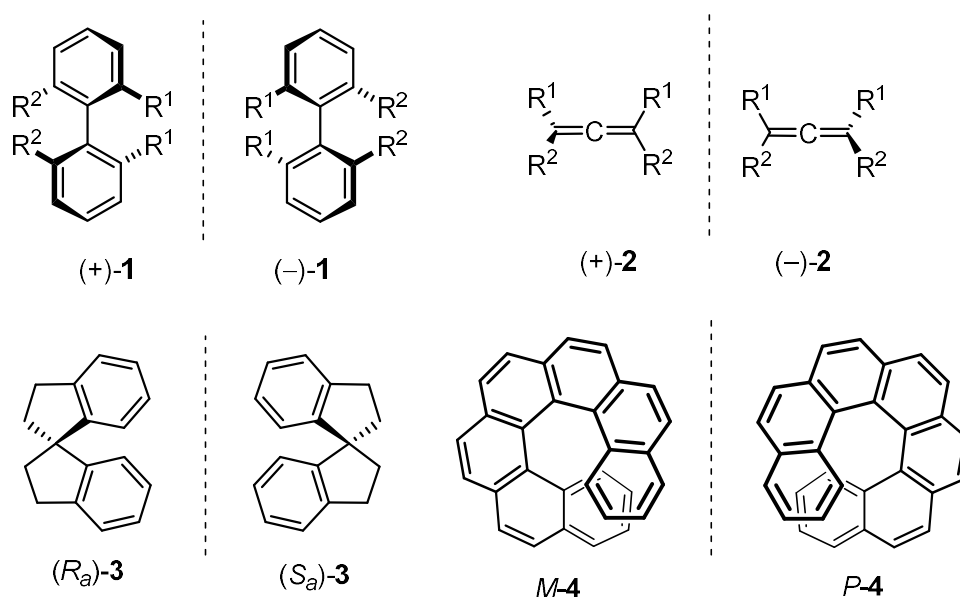


Figure 2: Chiral molecules without a stereogenic centre: axially chiral biaryl derivatives **1**, allenes **2**, spiro compounds **3** and helicenes **4**.

Enantiomers of a chiral molecule have identical physical and chemical properties, apart from the opposite rotation of plane-polarised light that passes through an enantioenriched medium. Despite this similarity, enantiomers of a chiral molecule behave differently when in proximity to a chiral environment, analogous to a hand fitting a glove, such as the active site of an enzyme, a chiral stationary phase for chromatography, and human DNA. Crucially for the pharmaceutical industry, enantiomers have different biological activity, so any chiral drug must be synthesised to be enantiomerically pure if there are undesirable side effects from the mirror

image of that drug. The most famous case of a racemic drug misguidedly released on the market was Thalidomide **5** (Figure 3) in the late 1950s, which is a good illustration to a non-chemist of the importance of chirality in medicine. Ostensibly prescribed as a treatment for morning sickness in pregnant women, the (*S*)-isomer of the drug led to teratogenic deformities in around 10,000 children worldwide, which led to greater awareness in the pharmaceutical industry of the importance of treating enantiomers as separate entities with regards to their bioactivity. However, even if the compound was administered in the body enantioenriched with the (*R*)-isomer, the acidity of the proton at the stereocentre would mean the molecule racemises when the pH of the body is acidic or alkaline. Despite the difference in the physiological effects of enantiomers, many drugs are sold as a racemate for convenience, if the side effects associated with the enantiomer of the active drug are non-harmful, or deemed not to outweigh the benefits of that desired enantiomer.¹ While the (*S*)-enantiomer of anti-depressant drug citalopram **6** (Figure 3) (known as escitalopram) has been shown to be more potent at treating major depression, with fewer side effects,² the drug is still available as a racemate because of the additional costs associated with a stereoselective synthesis.

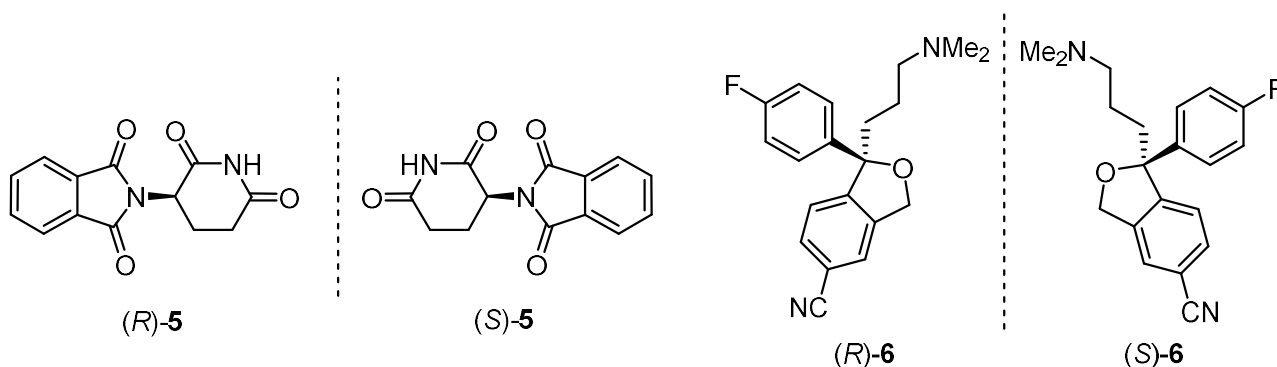


Figure 3: Examples of drugs where only one enantiomer has the desired treatment effect, thalidomide **5** and citalopram **6**.

The configuration of the stereocentres of a molecule can also affect its smell and taste, making chirality a key consideration in the flavouring and fragrance industries.^{3,4} With chiral odour molecules, it is often the case that one enantiomer simply has a stronger smell than the other, but there are many exceptions where they are completely different from one another. The (*R*)-enantiomer of limonene **7**, a cyclic terpene, smells of citrus fruits, while the (*S*)-enantiomer has a lemon/turpentine-like odour. With carvone **8**, a terpenoid molecule, the (*R*)-enantiomer smells of spearmint and the (*S*)-enantiomer smells of caraway seeds. Detailed analysis has been carried out on widely produced fragrance Tropional[®] **9**, which in its racemic form, has fresh, sea-like notes. Its (*R*)-enantiomer was described as “green floral”, having a “fruity, cumin-like” scent with “marine, ozone-like” notes while its (*S*)-enantiomer, which was around 5 times less potent, was more like “citrus” and “lily of the valley”.⁵

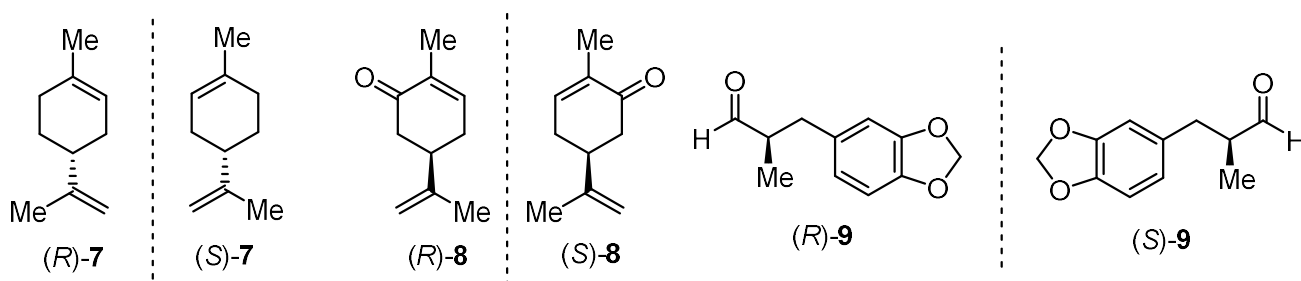
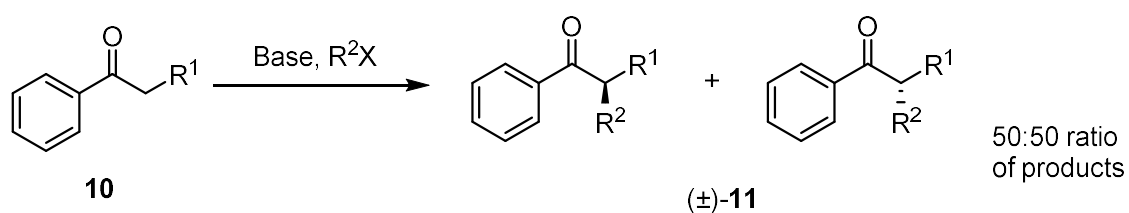


Figure 4: Enantiomers with different scents: limonene **7**, carvone **8** and Tropional[®] **9**.

To synthesise chiral compounds as single enantiomers in a laboratory, one needs a means of biasing the reaction to favour the formation of one configuration of that molecule over the other. Without a form of stereocontrol, for example, for the reaction of prochiral ketone **10** with an alkyl halide, an equimolar mixture of alkylated stereoisomers is produced, i.e. a racemic mixture of **11** (Scheme 1). One would have

to likely purify the two enantiomers by using preparative chiral HPLC, which is very expensive and not practical on a large scale; or by forming and crystallising a diastereomeric derivative of the product with a chiral auxiliary, which adds steps to the synthesis to install and remove. After purification, it is possible that only one pure enantiomer is useful to the purpose at hand, resulting in a maximum of 50% yield in that step to produce the desirable compound.



Scheme 1: The alkylation of a prochiral ketone 10 without controlling the stereochemistry, giving racemic product (±)-11.

To minimise waste produced by such a synthetic method, there are several approaches to control the stereochemistry and increase the efficiency (Figure 5). One way is to use a ‘chiral pool’ approach, making use of cheap, enantiopure compounds that widely occur in nature as building blocks, such as amino acids, tartrates, terpenes and sugars. Because this approach generally involves introducing the stereochemistry at the start of a synthetic route, care must be taken not induce racemisation/epimerisation in subsequent chemical steps. A more flexible approach is to use a chiral additive to induce the stereoselectivity for the transformation of a prochiral substrate. These modifications can involve covalently attaching an enantiopure chiral auxiliary to that prochiral substrate. The auxiliary can sterically or electronically restrict the approach of a reactant or reagent to one side of the substrate. This approach generally leads to very high enantioselectivity, but involves adding steps to the synthesis to install and remove a stoichiometric quantity of a

homochiral fragment to and from the molecule. The auxiliary may be used multiple times if said steps can be efficiently performed. Another method of inducing the stereoselectivity is to incorporate the chiral environment in a catalyst, known as asymmetric catalysis. This technique is advantageous as only a relatively small amount of the compound that brings about the stereoselectivity is needed, with no extra chemical steps, and as it is not consumed by the reaction taking place, can potentially be recovered. The most common way of doing this is through homogeneous catalysis, where either a transition metal complex or an organic species brings about stereoselectivity within the same phase as the substrates. Its ubiquity as an approach in asymmetric synthesis is due to the flexibility allowed by modifications of the catalyst, the relative ease with which the mechanisms can be studied and elucidated, the tolerance of a range of conditions and the ability to increase the scale of the reaction. These advantages have meant that the range of asymmetric transformations that can be performed through homogeneous catalysis has developed much further than those achieved with heterogeneous catalysis and biocatalysis.

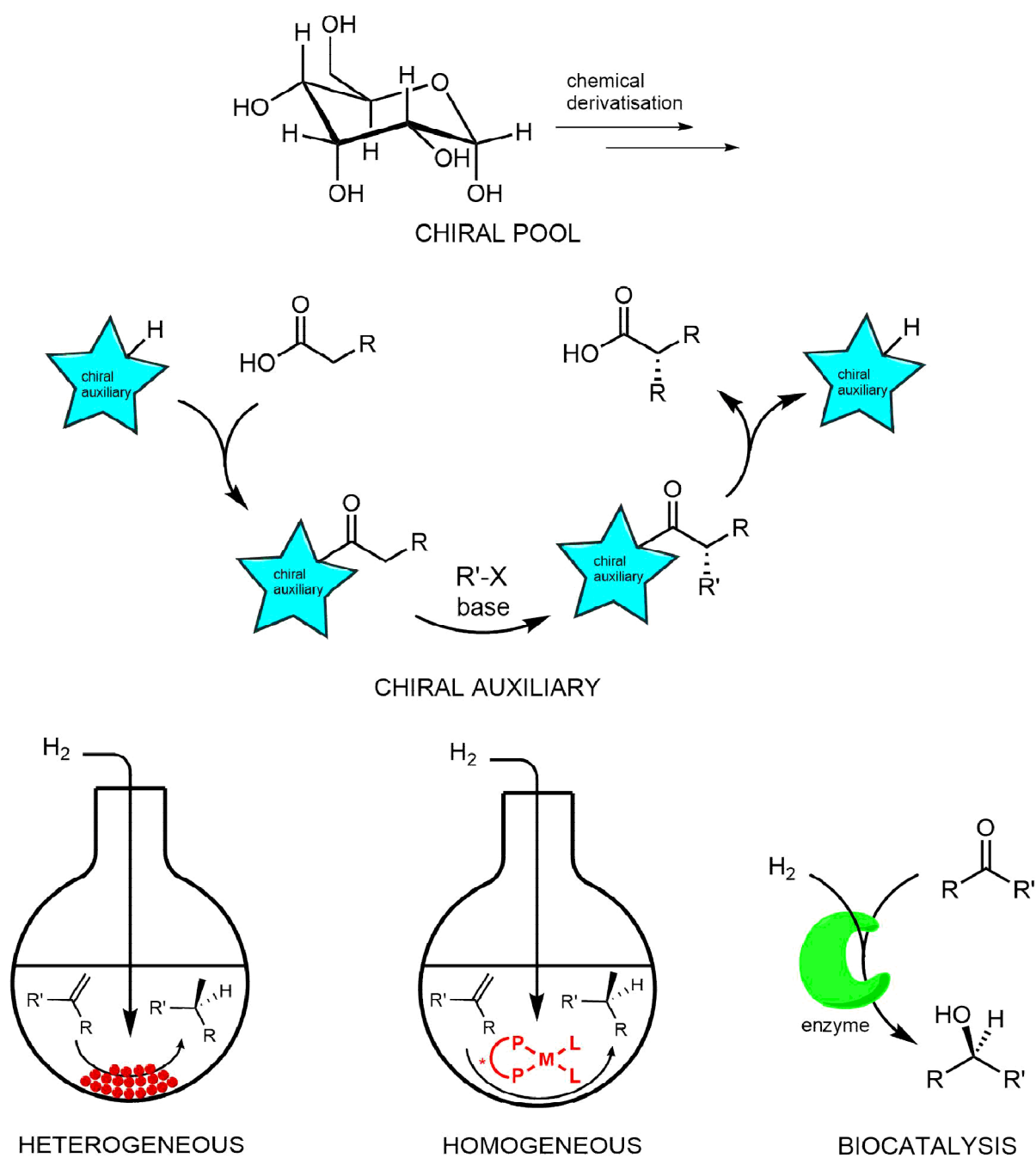
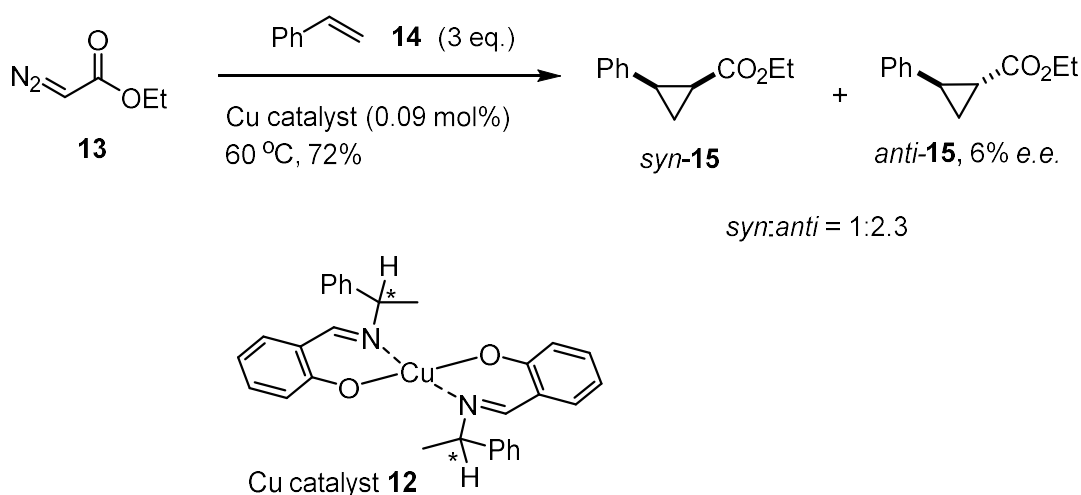


Figure 5: Various methods to introduce homochirality in molecules.

The first instance of an enantioselective form of homogeneous catalysis was reported by a pioneer of asymmetric catalysis, Ryoji Noyori *et al.*, in 1966.⁶ With the use of a chiral iminomethylphenol-Cu(II) complex **12**, the authors were able to perform the reaction of ethyl diazoacetate **13** with styrene **14** to form the

diastereomeric cyclopropane products **15** in 72% yield. With a *syn/anti* ratio of 1:2.3, the *anti* product was determined to have been formed in 6% e.e. (the same result for both (*R*)- and (*S*)-ligand isomers), representing a groundbreaking result that was to lead to a paradigm shift in asymmetric synthesis (Scheme 2). The chiral iminomethylphenol ligand induced the stereoselectivity by rendering one side of the substrate more sterically hindered than the other for the incoming nucleophile, which was a simple rationalisation, but one that was an underlying principle for the design of chiral transition metal complexes thereon.



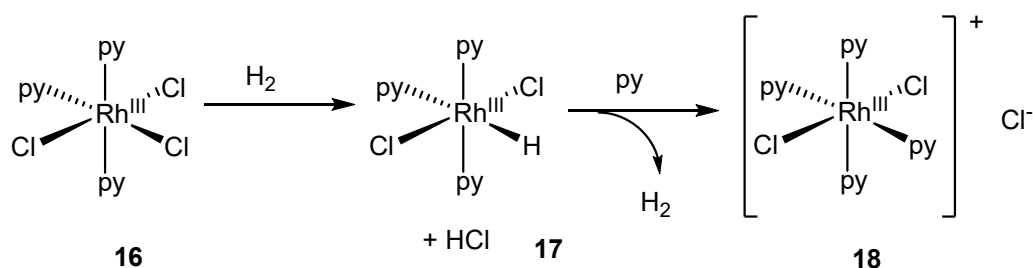
Scheme 2: The Cu-catalysed enantioselective formation of cyclopropane **15**, the first example asymmetric homogeneous catalysis.

1.2. Chiral phosphine ligands in homogeneous catalysis

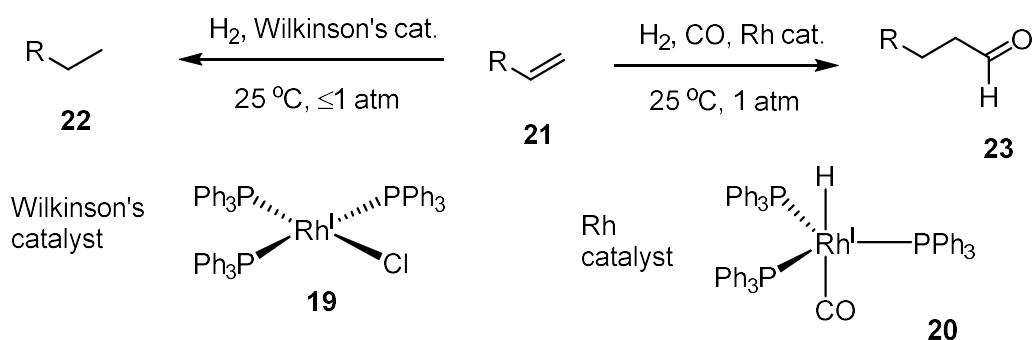
1.2.1. Wilkinson's catalyst

In the 1960s, Sir Geoffrey Wilkinson made the observation that under mild conditions, the nucleophilic displacement of a chloride ligand on trichlorotris(pyridine)rhodium **16** with a molecule of pyridine was catalysed by molecular hydrogen (Scheme 3).⁷ Because the molecule of hydrogen underwent heterolytic cleavage easily, forming a hydride as a catalytic intermediate, the group

saw potential in the use of rhodium complexes as hydrogenation catalysts. They designed a different rhodium complex with triphenylphosphine ligands, chosen due to their superior π -acceptor ability compared to pyridine, forming the air-stable metal complex tris(triphenylphosphine)rhodium(I) chloride **19**. This complex, later known as Wilkinson's catalyst, could be used for the catalytic hydrogenation of a variety of double and triple bonds at ambient pressure and temperature, with high turnover, and represented a very important breakthrough in the field of homogeneous catalysis (Scheme 4).^{8,9} This method of hydrogenation was shown also to be tolerant of other double bonds, such as ketones, esters, acids, nitriles and nitro groups; only ever reducing the alkene. The versatility of rhodium catalysts was shown by the ability of a similar complex **20** to catalyse the hydroformylation of alkenes with hydrogen and carbon monoxide.^{10,11} Since its advent, Wilkinson's catalyst has had a number of important applications, such as the selective hydrogenation of the natural anti-parasitic drug Avermectin to its more effective analogue Ivermectin, used for the treatment of scabies, river blindness and other parasitic infections.¹² It is also used for the widespread industrial production of nitrile rubber.¹³ The catalyst has endured very well in synthetic chemistry research, as it is still used frequently today, most recently for processes such as a disilane formation via oxidative homocoupling of tertiary silanes,¹⁴ and a regioselective reduction of an enone alkene in the synthesis of 1-tuberculosinyl adenosine, a virulence factor of *Mycobacterium tuberculosis*.¹⁵



Scheme 3: The nucleophilic displacement of trichlorotris(pyridine)rhodium(III) **16**, catalysed by hydrogen.

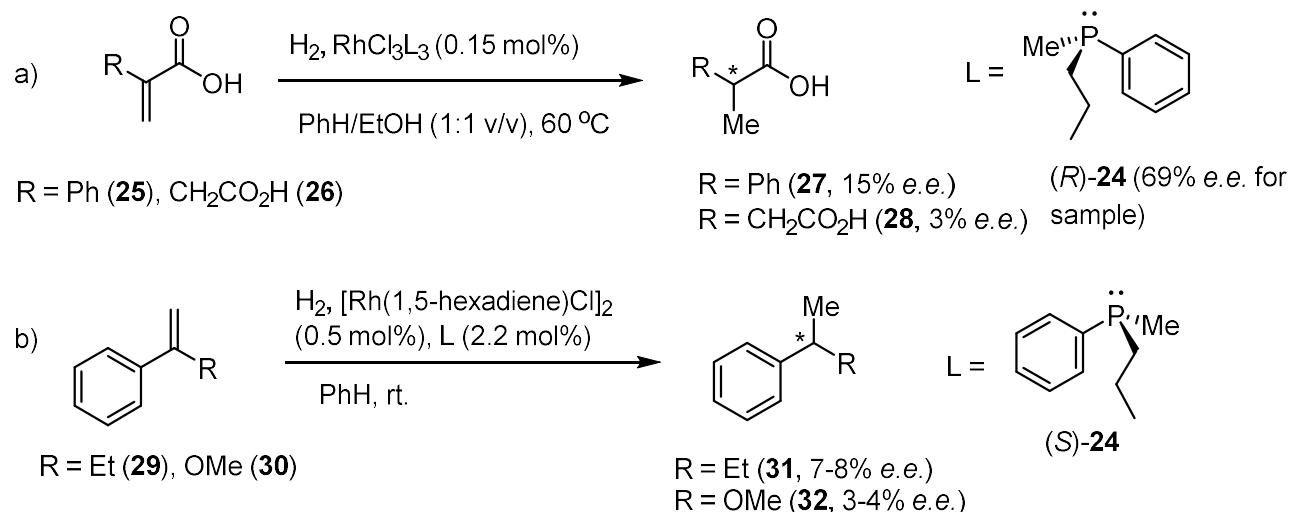


Scheme 4: The efficient Rh-catalysed hydrogenation and hydroformylation processes by Wilkinson.

1.2.2. First chiral phosphine ligands for asymmetric hydrogenation

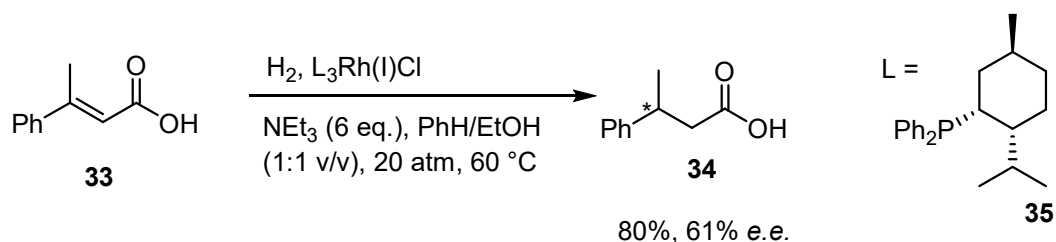
By combining the efficiency and practicality of Wilkinson's rhodium complexes, and the use of the chiral Cu-catalyst **12** by Noyori, the first examples of asymmetric hydrogenation by homogeneous catalysis were reported independently by Knowles *et al.* and Büthe *et al.* in 1968 (Scheme 5).^{16,17} Both groups replaced the achiral triphenylphosphine ligands on the rhodium complexes with *n*-propylmethylphenylphosphine ligands **24**, which are *P*-chiral because of a lone pair as a fourth 'substituent' and an energetic barrier to inversion. The former group used the complex tris(*n*-propylmethylphenylphosphine)rhodium(III) chloride (in which the ligands were prepared in 69% e.e.) to catalyse the hydrogenation of α -phenylacrylic acid **25** and itaconic acid **26**, resulting in 15% e.e. and 3% e.e. respectively for the formation of the saturated acids **27** and **28**. The latter group used a similar Rh

complex, analogous to Wilkinson's catalyst, formed *in situ* from the same chiral phosphine ligand **24** and $[\text{Rh}(1,5\text{-hexadiene})\text{Cl}]_2$, achieving hydrogenation of α -ethylstyrene **29** and α -methoxystyrene **30** to form saturated species **31** and **32** in 7-8% e.e. and 3-4% e.e. respectively.



Scheme 5: The first asymmetric hydrogenation processes through homogeneous catalysis, by Knowles (a) and Büthe (b).

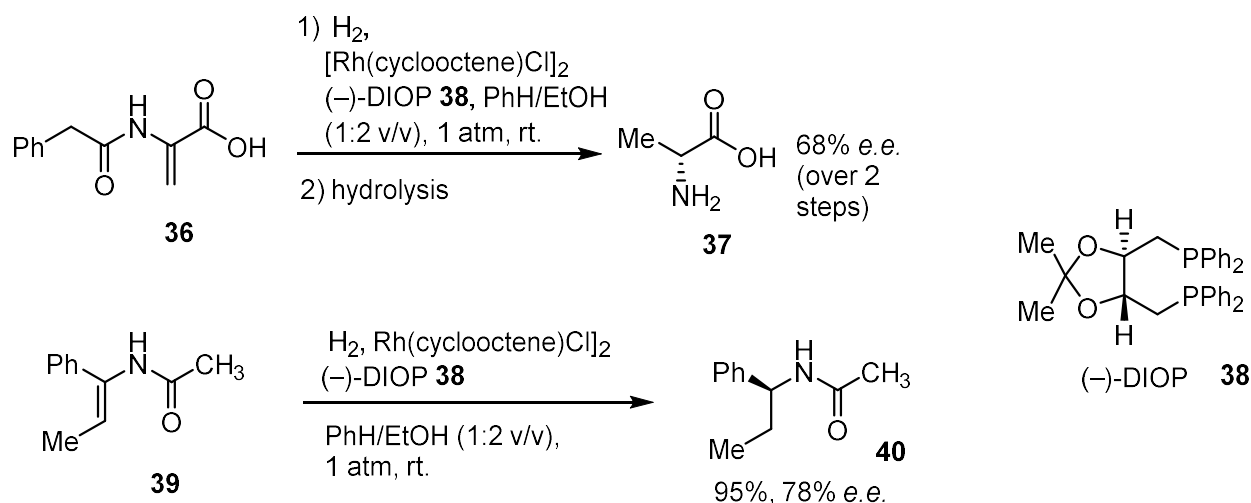
Following these successful developments, other groups began to use similar Rh complexes with modifications of the phosphine ligand. Instead of using *P*-chiral ligands, in 1971 Morrison *et al.* reported the use of tris(neomenthyl)diphenylphosphine)rhodium(I) chloride for the hydrogenation of *E*- β -methylcinnamic acid **33** to produce 3-phenylbutanoic acid **34** in a much improved 61% e.e., which started to hint towards practical application of asymmetric homogeneous catalysis (Scheme 6).¹⁸ The choice of neomenthylphosphine **35** avoided the requirement of a resolution, as it was synthesised from naturally occurring (–)-menthol. This process also demonstrated that the chirality could instead be located on the *P*-substituents rather than on the phosphorus atom itself.



Scheme 6: The asymmetric hydrogenation of *E*-β-methylcinnamic acid **33** with a rhodium(I)-neomenthylphosphine catalyst.

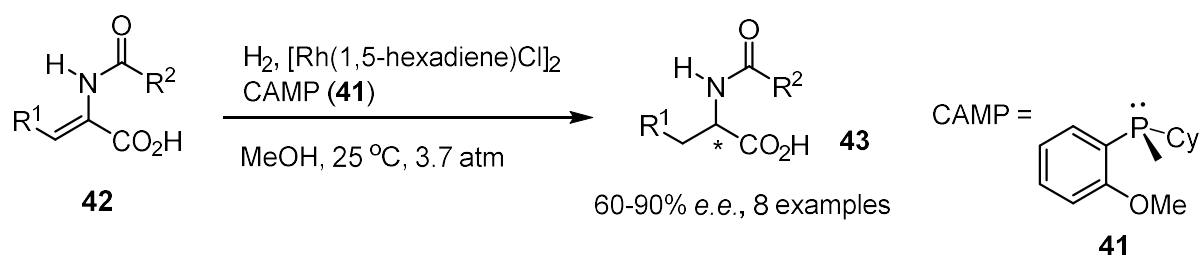
1.2.3. DIOP, CAMP and DIPAMP

In the same year, Kagan *et al.* reported the use of a Rh(I)((-)-DIOP) complex for the hydrogenation of α-phenylacrylic acid **25** in 63% e.e., and a range of other α-acetamidoacrylate derivatives in 60-80% e.e., including α-phenylacetamidoacrylic acid **36** to form (*R*)-alanine **37** in 68% e.e. following a hydrolysis (Scheme 7).^{19,20} Again, the DIOP ligand **38** (an abbreviation of 2,3-O-isopropylidene-2,3-dihydroxyl-1,4-bis(diphenylphosphino)butane) has its stereocentre away from the phosphorus atom, and was synthesised from (+)-diethyl tartrate, an ester form of the naturally occurring (+)-tartaric acid. The innovation in this design was the C₂-symmetric, chelating properties of this ligand, which increased the rigidity of the chiral catalyst, so the bulky diphenylphosphine groups could have a greater influence on the orientation of the olefin substrate, thus stabilising more greatly a single diastereomeric transition state of substrate and catalyst. These properties allowed the hydrogenation of enamide **39** in 78% e.e., despite lacking the fixed orientation that would be provided from a coordinating carboxylate group.

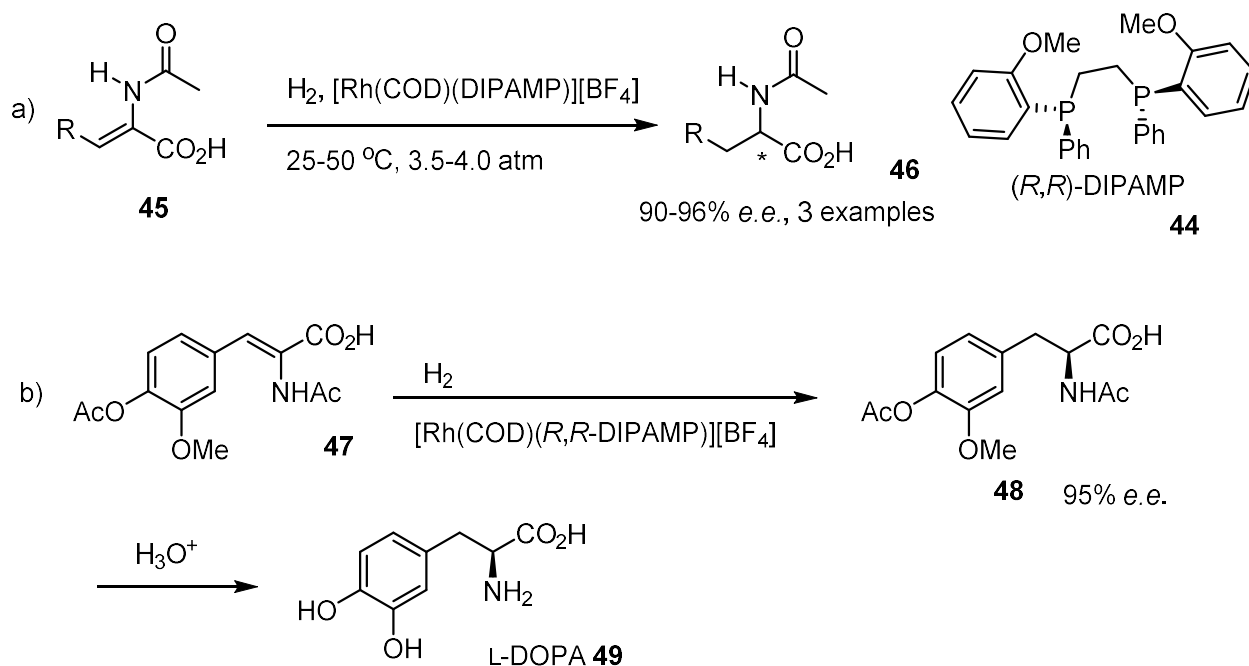


Scheme 7: Asymmetric hydrogenation of olefins with an $\text{Rh(I)}((-)\text{-DIOP})$ complex.

Meanwhile, Knowles *et al.* showed that high enantioselectivities for asymmetric hydrogenation could be achieved also with *P*-chiral monodentate ligands, as demonstrated with cyclohexyl-*o*-anisylmethylphosphine **41** (CAMP). Because of the bulkiness of CAMP **41**, as well as the methoxy group on the *o*-anisyl moiety acting as an H-bond acceptor, the *in situ* formed $\text{Rh(I)}\text{-(CAMP)}$ complex could be used for the hydrogenation of several α -acetamidoacrylic acid derivatives **42** in 60-90% e.e. (Scheme 8).²¹ To combine the high selectivity obtained with these ligands with the rigidity of a bidentate diphosphine ligand, Knowles *et al.* designed the DIPAMP ligand **44**, replacing the methyl groups of CAMP **41** with an ethylene linker between two cyclohexyl-*o*-anisylphosphine groups. By using the cationic $[\text{Rh}(\text{COD})(\text{DIPAMP})]^+[\text{BF}_4]^-$ complex as a catalyst, several α -acetamidoacrylic acid derivatives **45**, now the standard test for this process, could be hydrogenated in 90-96% e.e. (Scheme 9).^{22,23} Since this selectivity now rivalled that associated with enzyme catalysts, this complex could be applied towards the industrial manufacture of L-DOPA **49**, a treatment for Parkinson's disease.²⁴



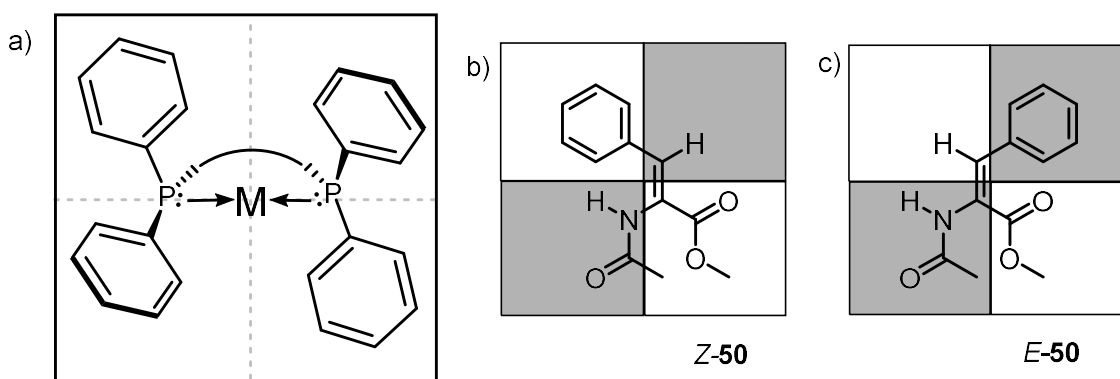
Scheme 8: The asymmetric hydrogenation of α -acetamidoacrylic acid derivatives **42** with a rhodium-CAMP catalyst.



Scheme 9: The asymmetric hydrogenation of α -acetamidoacrylic acid derivatives **45** (a) and the industrial synthesis of L-DOPA **49** (b) with a cationic Rh(I)-DIPAMP complex **X** as catalyst.

There are, however, limitations with the DIPAMP ligand **44**. While ‘tridentate’ substrates, involving coordination of olefin, carboxylate and amide, could be hydrogenated smoothly and in high selectivity, selectivity decreased dramatically for ‘bidentate’ substrates like *Z*-enamide **50**, which only possessed an olefin and amide. Virtually no selectivity was observed for *E*- and *Z*-2-methyl-3-phenylacrylic acid, indicating the influence of H-bonds interactions between the amide and methoxy group. Rates and selectivity for *Z*-alkenes were much greater than their respective *E*-isomers, which were later rationalised with quadrant diagrams.²⁵ As shown by crystal

structures such as that of a rhodium(I)-DIPAMP complex, the phenyl groups on the phosphines adopt edge-face interactions between each other. Thus, a projection from the perspective of the oncoming substrate show two hindered ‘quadrants’ where the edge of the pseudo-equatorial phenyl groups point out of the page, and the perpendicular pseudo-axial phenyl groups occupy the two unhindered ‘quadrants’ (Scheme 10, a). The approaching alkene would be biased to align with the unhindered quadrants, leading to induction of stereoselectivity. For the α -acetamidoacrylic acid substrates tested in the report on DIPAMP **44**, *Z*-alkenes have the bulkiest groups (carboxylate and phenyl) *trans* to each other, so therefore those groups can both align with the unhindered quadrants (Scheme 10, b). This contrasts with the *E*-alkenes, which have bulky groups *cis* to each other, so at least one of these groups clashes with a hindered quadrant (Scheme 10, c). The quadrant diagram is a simple rationalisation of selectivity, but one that is still oft-cited in the theory of asymmetric catalysis.²⁶



Scheme 10: Quadrant diagram of a metal-bis(diarylphosphine) complex to rationalise stereoselectivity (a), and the alignment *Z*- and *E*-isomers of α -acetamidoacrylate **50** (b and c respectively) towards hindered (shaded) and unhindered (white) quadrants.

1.2.4. BINAP by Noyori

Another chiral ligand that fits into the quadrant diagram model, which is possibly the most successful, versatile and influential chiral phosphine of all time, is 2,2'-bis(diphenylphosphino)-1,1'-binaphthyl, or BINAP **51**, first introduced by Ryōji Noyori in 1980.²⁷ There are no stereocentres in the structure of BINAP **51**, so the source of its chirality is through atropisomerism; that is, the large kinetic barrier preventing the two naphthyl moieties from freely rotating around the biaryl bond. While axial chirality had previously been explored in diphosphine ligands, for instance, with NAPHOS **52** (2,2'-bis(diphenylphosphinomethyl)-1,1'-binaphthyl) by Kumada *et al.*²⁸ and BINAPO **53** (2,2'-bis(diphenylphosphinooxy)-1,1'-binaphthyl) by Grubbs *et al.*,²⁹ BINAP **51** has no additional atom between the phosphine groups and biaryl backbone (Figure 6). This meant that only sp²-hybridised carbon atoms made up the ligand-metal cycle in a transition metal complex, leading to a highly rigid chiral environment. Thus, a range of α -acetamidoacrylic acids and esters **54** (consisting of both *E*- and *Z*-isomers) could be hydrogenated with [Rh(BINAP)(nbd)][ClO₄] as a pre-catalyst in ethanol, giving optical purities of 67-100% e.e., several of which were over 90% e.e. (Scheme 11), which were equal to or greater than selectivities induced with DIPAMP **44**.³⁰ These results were remarkable as the selectivity was driven purely by sterics, as BINAP **51** has no capability to make hydrogen bonds between the ligand and substrate. This property meant that use of BINAP **51** potentially had a previously unprecedented generality for the asymmetric hydrogenation of olefins.

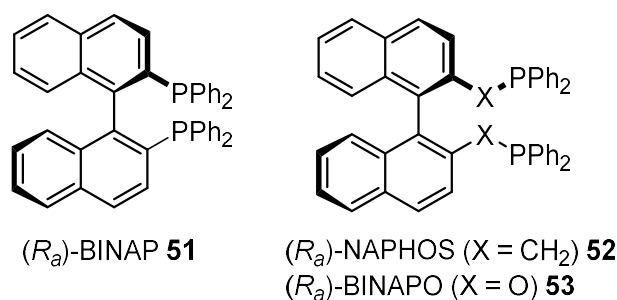
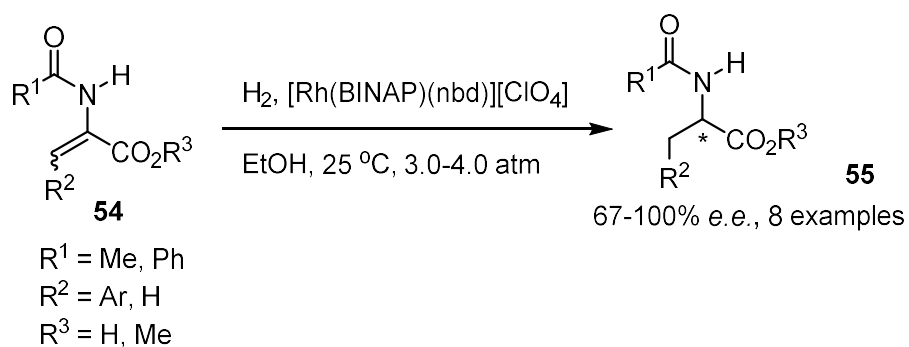
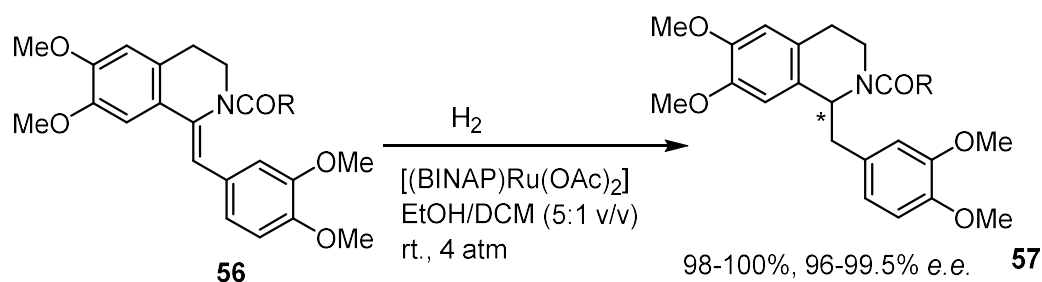


Figure 6: Axially chiral ligands NAPHOS **52** and BINAPO **53**, which have an atom between the naphthyl and phosphine group, and BINAP **51**, which has phosphine groups bonded to the binaphthyl.



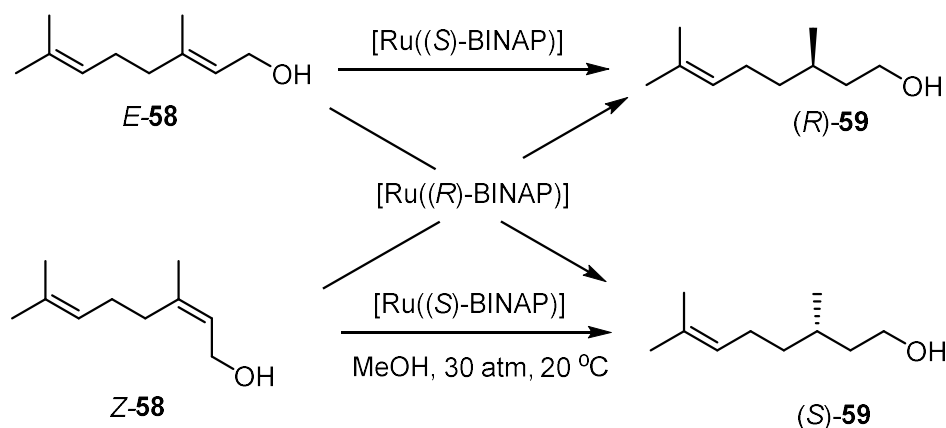
Scheme 11: The Rh(BINAP)-catalysed asymmetric hydrogenation of α -acetamidoacrylate derivatives **54**.

While the enantioselectivities induced by Rh-BINAP complexes for asymmetric hydrogenation were high, results like this were restricted to α -acetamidoacrylate derivatives, due to the multiple coordinating groups on these substrates. However, the substrate scope was widened with the use of BINAP-Ru(II) diacetate complexes, which permitted the highly enantioselective catalytic hydrogenation of precursors **56** to biologically relevant isoquinoline-derived alkaloids **57** in 96-99.5% e.e. (Scheme 12).³¹ The saturated products included (*R*)-laudanosine, a metabolite of the muscle relaxant drug atracurium;³² and (*R*)-norreticuline, a precursor in the biosynthesis of morphine.³³ When Rh(I)-BINAP complexes were used for the same purpose, for the *Z*-alkene where R = Me, only ~70% e.e. was achieved.

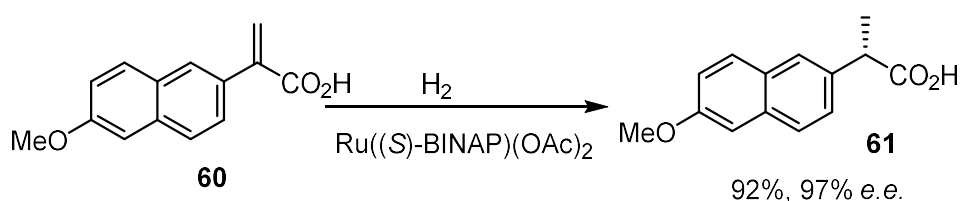


Scheme 12: The Ru-BINAP catalysed asymmetric synthesis of isoquinoline-derived alkaloids **57**.

Other alkene substrates, such as allylic and homoallylic alcohols, could be hydrogenated in high enantioselectivity.³⁴ The naturally occurring geraniol *E*-**58**, and its geometrical isomer nerol *Z*-**58**, notable for not possessing a carbonyl group to coordinate to the metal, could be hydrogenated to give citronellol **59** in 96-99% e.e., with only a minimal trace of overreaction to form dihydrocitronellol, the hydrogenation product of the terminal alkene. Interestingly, the configuration of the product **59** could be controlled with the choice of alkene stereoisomer and BINAP **51** enantiomer (Scheme 13). Starting with geraniol *E*-**58**, use of Ru((*S*)-BINAP)(OAc)₂ gave (*R*)-citronellol **59**, and Ru((*R*)-BINAP)(OAc)₂ gave the (*S*)-enantiomer of **59**, but the opposite occurred with nerol *Z*-**58** - Ru((*R*)-BINAP)(OAc)₂ gave (*R*)-citronellol **59** and vice versa. The same Ru(BINAP)(OAc)₂ complex could also catalyse, with high enantioselectivity, the hydrogenation of a range of acrylic acid derivatives, a class of compounds for which successful results were difficult to achieve with previous catalysts.³⁵ Among the substrates was included a precursor **60** to (*S*)-Naproxen **61**, an anti-inflammatory agent (Scheme 14). This process has since been adapted to synthesise this drug on an industrial scale, as, the (*S*)-enantiomer is 28 times more biologically potent than the (*R*)-enantiomer.³⁶



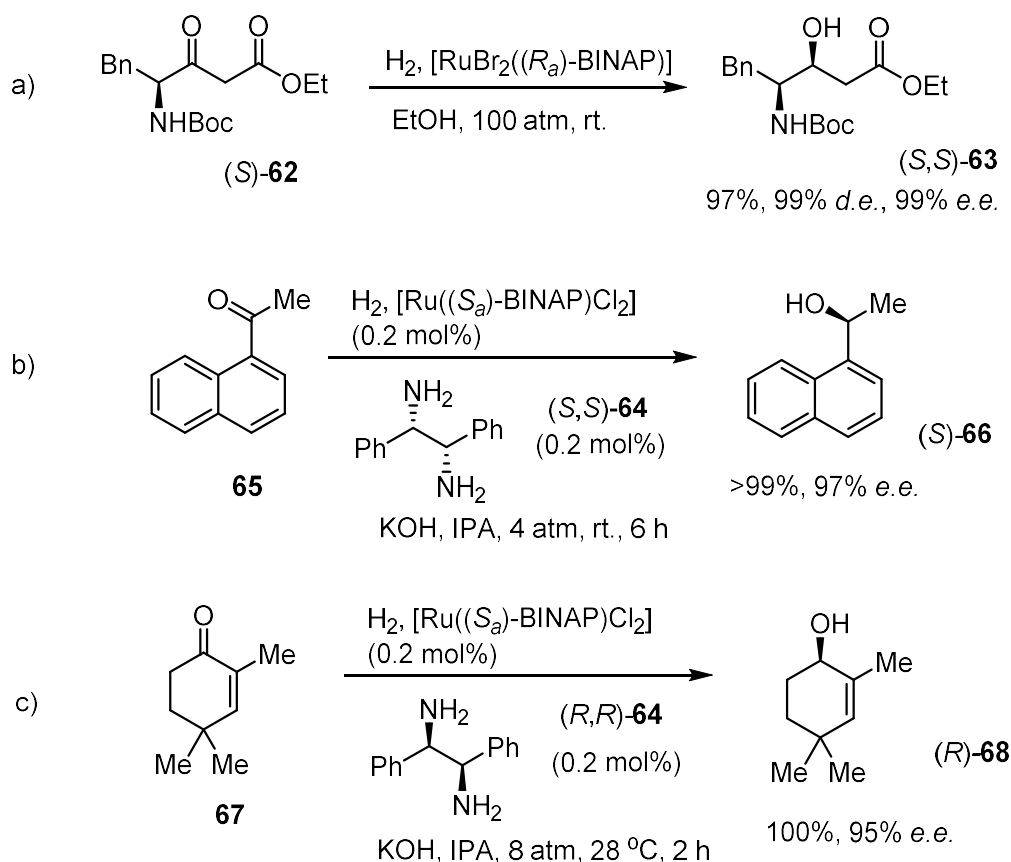
Scheme 13: The Ru-BINAP catalysed asymmetric hydrogenation of geraniol *E*-58 or nerol *Z*-58 to yield either enantiomer of citronellol **59**.



Scheme 14: The Ru-BINAP catalysed asymmetric synthesis of (*S*)-naproxen **61**.

Since the 1980s, BINAP **51** has become a prime example of what is termed a 'privileged ligand', as it has been applied to induce stereoselectivity in many, mechanistically different catalytic processes. As well as being highly effective for the asymmetric hydrogenation of alkenes possessing a variety of proximal functional groups, it has also been applied towards the stereoselective reduction of prochiral ketones, such as β -keto ester precursors (**62**) of analogues (**63**) of statine, a diastereomeric β -hydroxy- γ -amino acid (Scheme 15, a).³⁷ With the addition of enantiopure chiral diamines, such as (*S,S*)-1,2-diphenylethylenediamine **64**, even ketones lacking an additional Lewis basic functional group, such as 1-acetonaphthone **65**, could be hydrogenated with consistently high enantioselectivity (Scheme 15, b).^{38,39} With this amine additive, even α,β -unsaturated ketones (**67**)

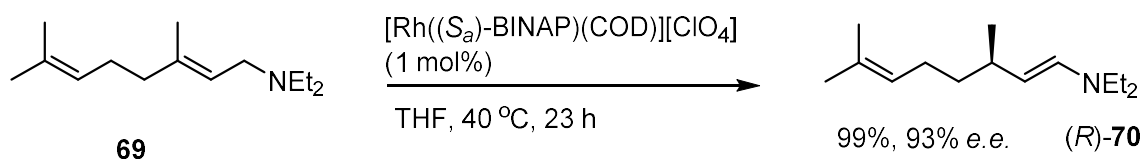
could be selectively reduced at the carbonyl group, rather than at the alkene, to synthesise chiral allylic alcohols (**68**) (Scheme 15, c).^{40,41}



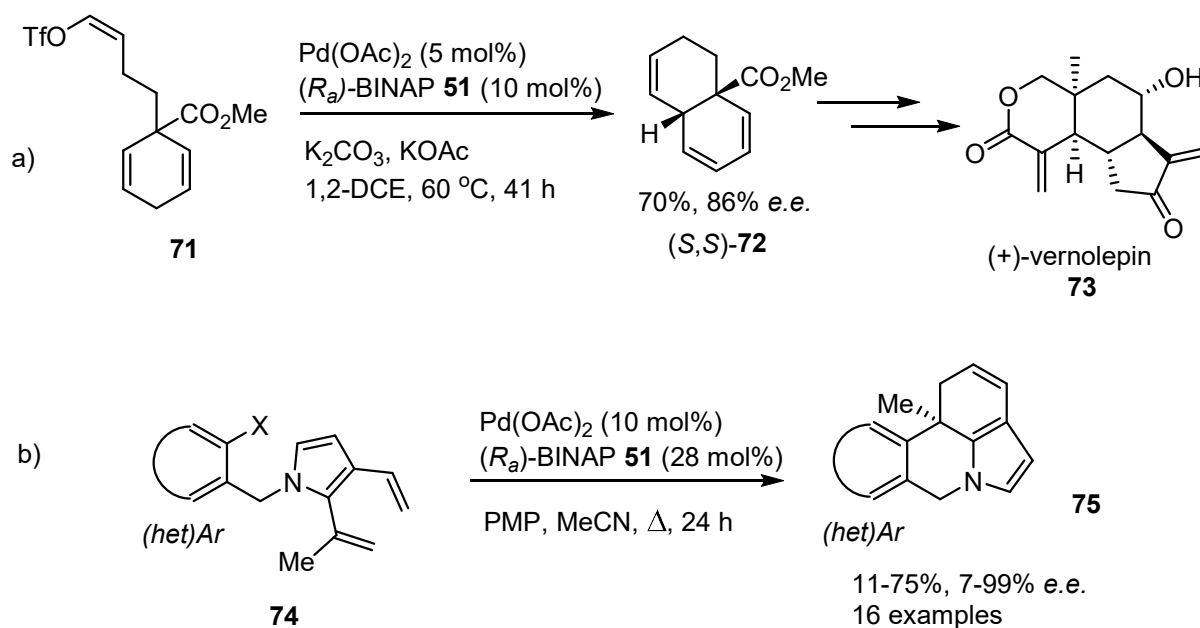
Scheme 15: Ru-BINAP catalysed asymmetric hydrogenation of ketones.

Additionally, the enantioselective 1,3-hydride shift of prochiral allylamines (**69**) to enamines (**70**) may be achieved with a cationic Rh-BINAP catalyst (Scheme 16), which is exploited for the industrial synthesis of (–)-menthol.^{42,43} As it is able to rotate around the biaryl bond to a degree without too much strain, the BINAP ligand is able to coordinate to a variety of metals such as palladium, to induce enantioselectivity for cross coupling reactions. The asymmetric synthesis of (+)-vernolepin **73**, a sesquiterpene with anti-tumour activity, was achieved this way, through a Pd-BINAP catalysed intramolecular Heck reaction (Scheme 17, a).⁴⁴ More recently, a Pd-BINAP

system was used for an asymmetric Heck cascade reaction to synthesise the tetracyclic core **75** of lycorane alkaloids (Scheme 17, b).⁴⁵



Scheme 16: The Rh-BINAP catalysed asymmetric isomerisation of allylamine **69** to enamine **70**.



Scheme 17: Asymmetric Heck reactions with enantioselectivity induced by BINAP **51**.

1.3. Dihedral angles of axially chiral diphosphine ligands

The list of applications for BINAP **51** goes on,^{46,47,48} but it is clear that the versatility of this ligand has led to it, or more generally the axially chiral biaryl unit, becoming a template in chiral ligand design. The inventor of the first chiral ligand (DIPAMP **44**) to induce enantioselectivity to rival that of biocatalysts, W. S. Knowles, who shared the 2001 Nobel Prize in Chemistry along with Ryōji Noyori and K. Barry Sharpless for pioneering work in asymmetric homogeneous catalysis, stated that:⁴⁹

"Since achieving 95% e.e. only involves energy differences of about 2 kcal, which is no more than the barrier encountered in a simple rotation of ethane, it is unlikely that before the fact one can predict what kind of ligand structures would be effective."

This key statement emphasises how sensitive the enantiomeric excess is to a change in electronic and steric properties, whether in the substrate or catalyst, and that the optimisation of the stereoselectivity of a reaction will often involve trial and improvement with regards to choosing and designing ligands. It follows that one single ligand like BINAP **51** will never produce universally optimal results for the stereoselectivity of an asymmetric chemical transformation of every prochiral substrate. Modifications, no matter how small or large, have to be made to change the steric, geometric and electronic properties of the ligand, and by extension, the catalyst, in order to improve stereoselectivity in reactions in which >95% e.e. is not induced by BINAP **51**.

One key geometric property of a diphosphine ligand, concerning the stereoselectivity of a reaction, is the dihedral angle (θ), which generally relates directly to its bite angle (β) on coordination to a metal centre (Figure 7). Because the stereoselectivity induced by a diphosphine ligand-metal complex is largely a result of the bulky ancillary aryl groups bonded to the phosphorus atoms, the orientation of the substrate is very sensitive to the positions these groups occupy in space, which is a direct result of the bite angle. The biphenyl unit is a very useful backbone for a chiral ligand, as the variation of substituents located at the back of the ligand, often at the 6,6'-positions, is a source of tuning of the dihedral angle.

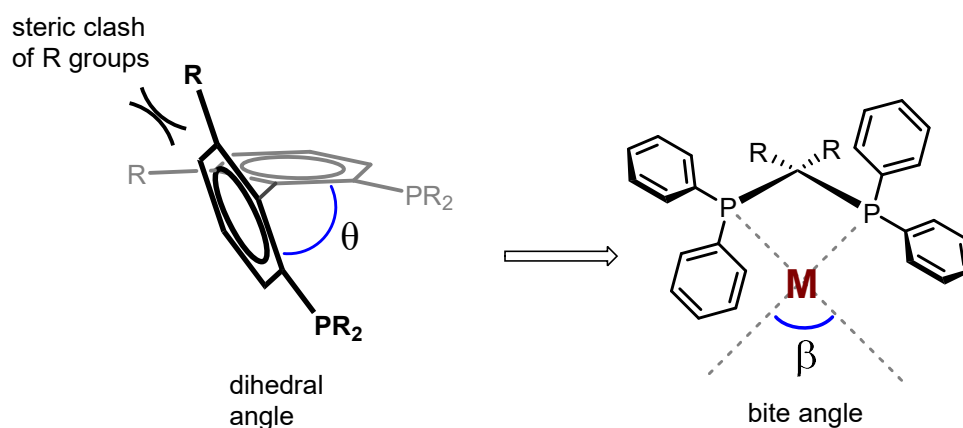
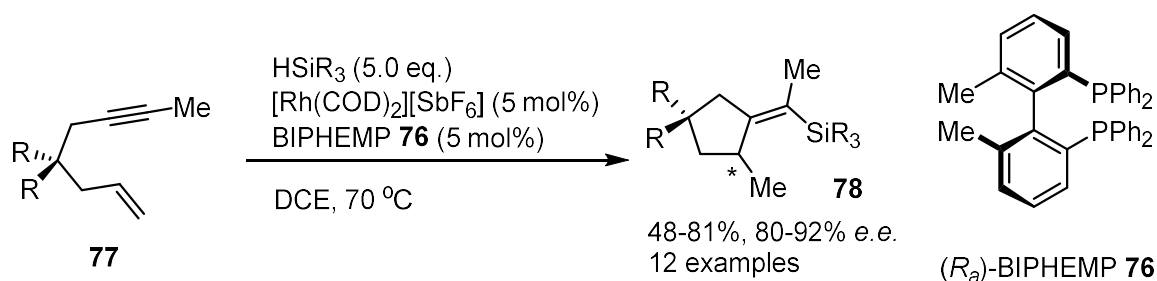


Figure 7: The dihedral angle (θ) of a biaryl diphosphine ligand, and bite angle (β) in a metal complex.

1.3.1. BIPHEMP and MeO-BIPHEP

One of the earliest examples of examining the variation of 6,6'-substituents of the 1,1'-biphenyl structure was BIPHEMP **76**, which consisted of methyl groups at these positions. The crystal structure of the cationic $[\text{Rh}((R_a)\text{-BIPHEMP})(\text{nbd})][\text{BF}_4]$ complex was first reported by Frejd *et al.*, which revealed key differences compared the analogous Rh-BINAP complex.⁵⁰ The dihedral angle of the Rh-BIPHEMP structure was $71.8(3)^\circ$, which was smaller than that of Rh-BINAP at $74.4(2)^\circ$, because the methyl groups of BIPHEMP **76** are less bulky compared to the fused benzene rings of BINAP **51**. Furthermore, the 7-membered ring chelate of the Rh-BIPHEMP complex was revealed be distorted from the twist-boat conformation of Rh-BINAP, and in constrast to ligands like BINAP **51** and DIPAMP **44**, the phenyl groups on the phosphorus atoms of Rh-BIPHEMP were aligned in an edge-face face-face manner (as opposed to edge-face edge-face). The ligand was also independently reported by Schmid *et al.*, who made similar observations regarding the X-ray crystal analysis of the same Rh-BIPHEMP complex.⁵¹ While the use of BIPHEMP **76** was shown to improve the enantioselectivity for the asymmetric Pd-catalysed Kumada coupling of 1-bromo-2-methylnaphthalene,⁵² the

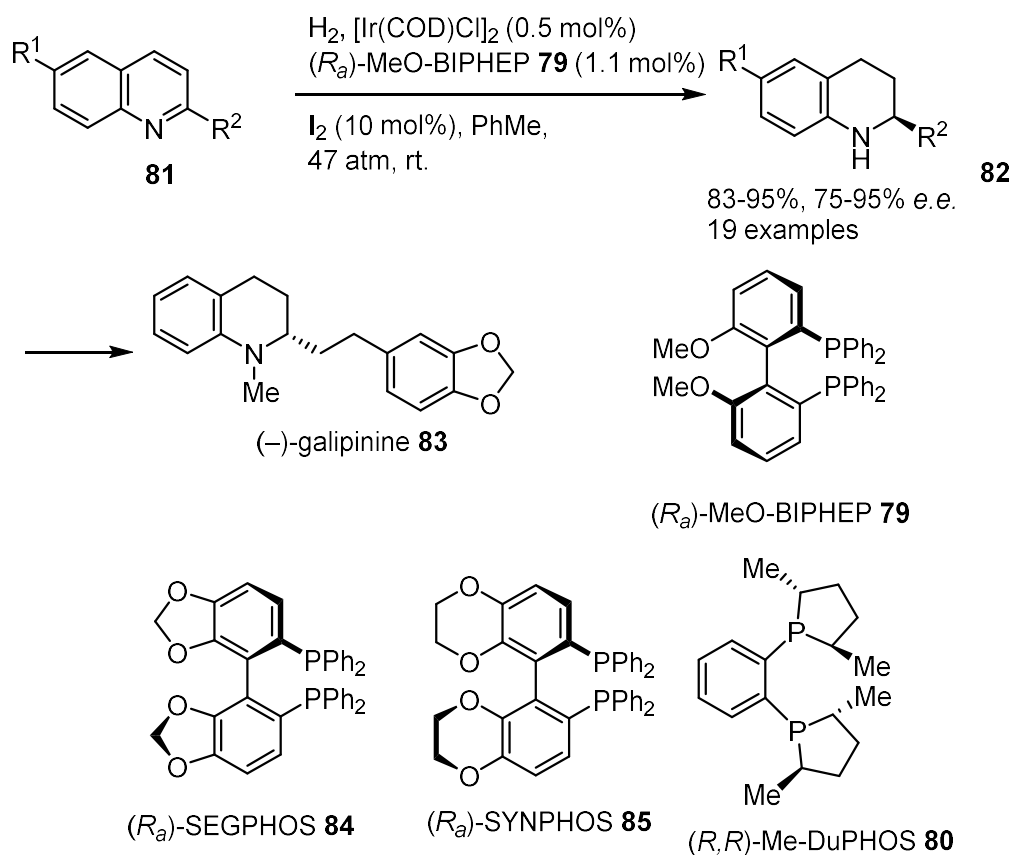
enantioselectivities achieved for the isomerisation of *N,N*-diethylnerylamine **69**⁵¹ (a step in the synthesis of (–)-menthol) and the Rh- and Ru-catalysed^{53,54} hydrogenation of various prochiral substrates were comparable to those obtained by using BINAP **51**. However, a cationic Rh-BIPHEMP complex was shown by Widenhoefer *et al.* to be an effective catalyst for the asymmetric tandem hydrosilylation and cyclisation of 1,6-enynes **77** to produce a wide variety of chiral 1-silylmethylenecyclopentanes **78** (Scheme 18); a reaction that could not be effectively carried out with analogous BINAP **51** complexes.⁵⁵



Scheme 18: The Rh-BIPHEMP-catalysed tandem hydrosilylation/cyclisation of 1,6-enynes **77**.

A similar ligand, MeO-BIPHEP **79**, was also first reported by Schmid *et al.*, in which the 6,6'-substituents are methoxy groups.⁵⁶ The X-ray crystal structure of a cationic (MeO-BIPHEP)-Pd complex revealed that the 7-membered chelating ring adopted a distorted twist-boat conformation, and that the dihedral angle of the ligand in the complex was 70.8°, both of which characteristics showed a similarity to the cationic BIPHEMP-Rh complex. Since the advent of this ligand, despite these geometric similarities to BIPHEMP **76**, it has been subjected to more widespread usage in asymmetric catalysis, possibly as a consequence of the different electronic properties, and that the methoxy group has more flexibility as a handle for further derivatisation of the structure. For the Ru-catalysed asymmetric hydrogenation of β -keto esters at atmospheric pressure, conducted by Genêt *et al.*, the

enantioselectivities obtained using MeO-BIPHEP **79** were comparable to those of BINAP **51**.⁵⁷ However, Zhou *et al.* found the optimised conditions for the iodine-promoted Ir-catalysed asymmetric hydrogenation of 2-methylquinoline achieved 94% e.e. with the use of MeO-BIPHEP **79**, while enantioselectivity decreased by using BINAP **51** (87% e.e.), DIOP **38** (53% e.e.) or Me-DuPhos **80** (51% e.e.).⁵⁸ The Ir-MeO-BIPHEP catalytic system could be applied for the hydrogenation of a range of 2- and 6-substituted quinolines **81**, including the precursors (**82**) to some tetrahydroquinoline alkaloid natural products, such as (–)-galipinine **83** (Scheme 19). In a later report, for the optimisation of the Ir-catalysed hydrogenation of 2-benzylquinoline, the enantioselectivity achieved with MeO-BIPHEP **79** (94% e.e.) was considerably greater than that of BINAP **51** and Me-DuPhos **80** (72% e.e. and 3% e.e. respectively) and slightly greater than that of other narrow-dihedral angled ligands SEGPHOS **84** and SYNPHOS **85** (93% e.e. and 91% e.e. respectively).⁵⁹ By lowering the hydrogen pressure, from 47-54 atm to 3 atm, and raising the temperature from room temperature to 70 °C, this changed the rates of the enantiodetermining steps to favour high e.e. values for the formation of the already favoured *syn*-isomers of 2,3-disubstituted tetrahydroquinolines.

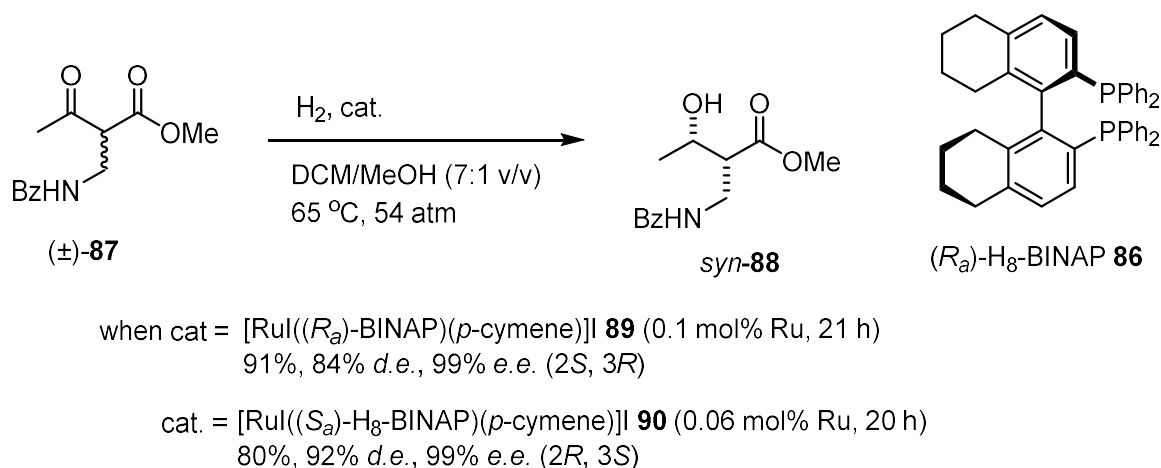


Scheme 19: The Ir-MeO-BIPHEP-catalysed asymmetric hydrogenation of quinolines **81**, and other ligands used for comparison.

1.3.2. $H_8\text{-BINAP}$

Another common alternative ligand to BINAP **51** is the partially hydrogenated variant $H_8\text{-BINAP } \mathbf{86}$, which is saturated at the 5,5',6,6',7,7',8,8'-carbon atoms. First synthesised in 1991 by Takaya *et al.* through the regioselective Ru/C-catalysed hydrogenation of 2,2'-dibromo-1,1'-binaphthalene to the bitetralin product,⁶⁰ X-ray studies revealed the dihedral angle of $[\text{Rh}(H_8\text{-BINAP})(\text{COD})][\text{ClO}_4]$ complex to be $80.3(4)^\circ$,⁶¹ which is larger than that of an analogous BINAP **51** complex $[\text{Rh}(\text{BINAP})(\text{nbd})][\text{ClO}_4]$, at $74.4(2)^\circ$.⁶² This increase in the angle size is due to the non-planarity of the saturated domain of the ligand **86**, which increases steric repulsion between the two tetralin rings. In the same report,⁶¹ for the asymmetric

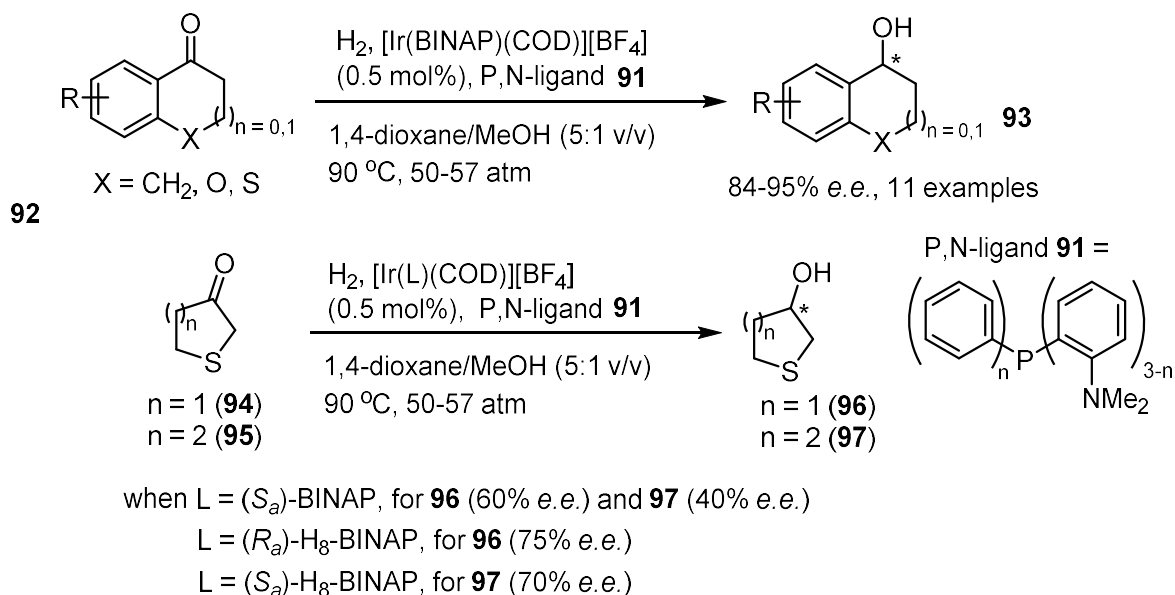
hydrogenation of racemic methyl 2-(benzamidomethyl)-3-oxobutanoate **87** at 54 atm and 65°C in the optimal solvent system of DCM/MeOH (7:1 v/v), after 20 hours the results achieved with the Ru-H₈-BINAP complex **90** (80% conversion, 92% *d.e.*, 99% *e.e.* for the (2*R*-3*S*)-product **88**) were comparable to that obtained with a similar Ru-BINAP-cymene complex **89** (91% conversion, 84% *d.e.*, 99% *e.e.*) (Scheme 20).



Scheme 20: The asymmetric hydrogenation of methyl 2-(benzamidomethyl)-3-oxobutanoate **87**, catalysed by Ru-BINAP and Ru-H₈-BINAP complexes **89** and **90**.

Due to the different geometric properties of H₈-BINAP **86**, the use of this ligand has improved results with certain reactions compared to analogous BINAP **51** complexes. For the asymmetric hydrogenation of cycloalkanones, in which a catalytic system of [Ir(ligand)(COD)][BF₄] and 2-(diphenylphosphino)-*N,N*-dimethylaniline (or similar) **91** was used, the use of BINAP **51** led to high enantioselectivity (80-95% *e.e.*) for various benzocyclohexanones **92** with electron-withdrawing and donating substituents on the benzene ring.⁶³ Also, when the C4-atom of the benzocyclohexanones **92** was replaced with oxygen or sulfur, or when benzocyclopentanones were used as substrates, similar results were achieved. However, β-thiacycloalkanones **94** and **95**, without a fused benzene ring, could only be hydrogenated in 60% *e.e.* 40% *e.e.* respectively. By using H₈-BINAP **86**, because

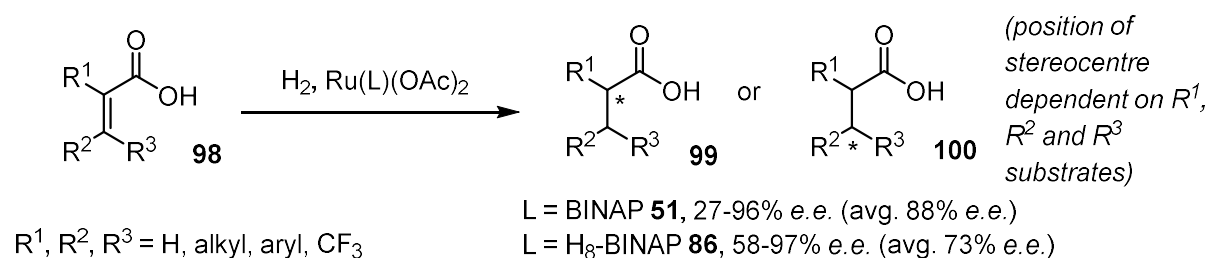
of its altered steric environment around the metal centre, these enantioselectivities were raised to 75% e.e. and 70% e.e. respectively (Scheme 21). However, it appeared that the sulfur atom was imperative for good enantioselectivity, as the analogous tetrahydrofuran-3-one could only be hydrogenated in 12% e.e. using the Ir-(H₈-BINAP) complex.



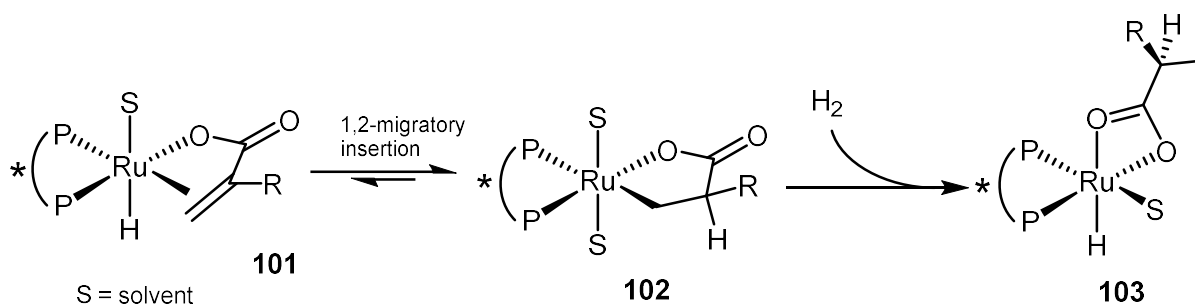
Scheme 21: The Ir-catalysed asymmetric hydrogenation of benzocyclohexanones **92** and β -thiacycloalkanones **94** and **95**, using BINAP **51** and H₈-BINAP **86** as ligands.

A key study by Takaya *et al.* demonstrated a speciality of the H₈-BINAP **86**, which was on the Ru-catalysed asymmetric hydrogenation of acrylic acid derivatives **98**, substituted with alkyl and aryl groups at the α - and/or β -positions.⁶⁴ For the 11 reported examples comparing H₈-BINAP **86** with BINAP **51** within the Ru(ligand)(OAc)₂ catalyst system, the stereoselectivity for H₈-BINAP **86** was greater than that of BINAP **51** for 10 examples, and equal for the other, with an increase in 15% e.e. on average (Scheme 22). By taking into account the difference of the dihedral angles of the two ligands **51** and **86** in previously reported rhodium complexes, and constructing a simple model of the ruthenium diphosphine diacetate

complexes, the authors found that differences in conformation of the phenyl groups on the phosphorus atoms led to a more sterically crowded equatorial site of coordination for the olefin. The substrate is thus coordinated more rigidly to the metal centre, leading to greater enantioselectivity (Scheme 23). Additionally, with H₈-BINAP **86** as the ligand, the axial sites around the metal complex are rendered wider than with BINAP **51**. This change in geometry increases the rate of hydrogenolysis of the Ru-C bond of the intermediate **102** that follows 1,2-migratory insertion of the hydride to the olefin. Finally, the authors pointed out that it was the steric, rather than electronic, effects of H₈-BINAP **86** that contributed to the enhanced the enantioselectivity, as Ru-complexes with other ligands with electron donating groups such as MeO-BINAP and *p*-tol-BINAP gave similar e.e. values to BINAP **51**.



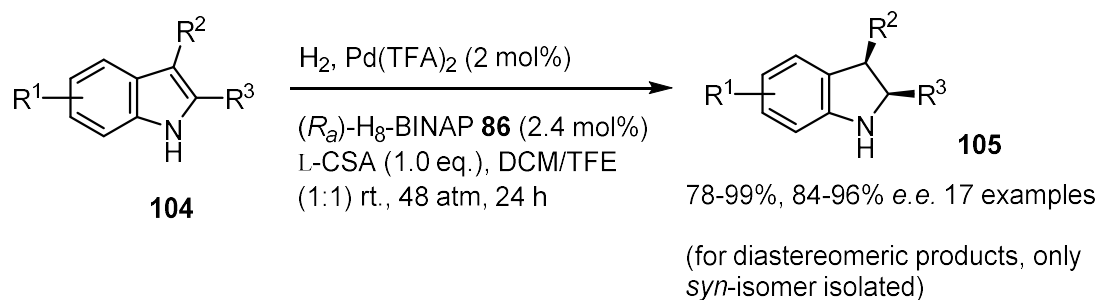
Scheme 22: The Ru-catalysed asymmetric hydrogenation of acrylic acid derivatives **98**, comparing enantioselectivities achieved between BINAP **51** and H₈-BINAP **86**.



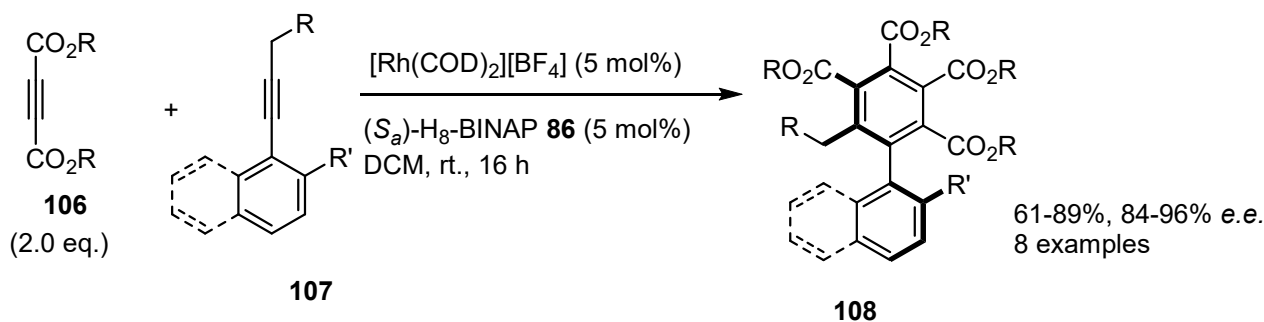
Scheme 23: Coordination of the prochiral olefin to the Ru-centre (the enantiodefining step), followed by hydrogenolysis of the Ru-carbon bond (part of mechanism by Takaya *et al.*).

Another example in which the use of H₈-BINAP **86** has resulted in optimal stereoselectivity, by Zhou *et al.*, is the Pd-catalysed asymmetric hydrogenation of *N*-unprotected indoles.⁶⁵ The group had previously found that after Brønsted acid activation of quinolines, they could undergo asymmetric hydrogenation in high enantioselectivity.⁶⁶ Logically, they then found that iminium intermediate of indoles without an *N*-carbamate group could also be formed by using L-camphorsulfonic acid, and for the optimisation of the asymmetric hydrogenation on 2-methylindole, it was found that H₈-BINAP **86** gave the better enantioselectivity than a variety of chiral diphosphine ligands at 91% e.e., compared to 85% e.e. obtained with BINAP. With H₈-BINAP **86**, 16 more examples of 2-, 3-, 5- and 7-substituted *N*-unprotected indoles **104** could be hydrogenated in 84-96% e.e., with consistently high isolated yield (Scheme 24).

A final example that displays the versatility of H₈-BINAP **86**, by Tanaka *et al.*, is the Rh-catalysed cyclotrimerisation of alkynes to form phenyl rings.⁶⁷ In a previous report, the authors had described the use of a cationic Rh(I)/chiral diphosphine ligand system for the synthesis of achiral arenes, with good regioselectivity, from one molecule of a functionalised terminal alkyne and two molecules of a dialkyl acetylenedicarboxylate **106**.⁶⁸ By changing the substituent on the former alkyne to an *ortho*-functionalised phenyl ring (**107**), axial chirality could be incorporated into the product. For the optimisation, the use of H₈-BINAP **86** the reaction of diethyl acetylenedicarboxylate and 3-(*o*-tolyl)propargyl acetate gave the product in 81% yield and 89% e.e., compared to 16% yield and 77% e.e. with BINAP **51**, and minimal product formation with SEGPHOS **84**. A further 7 similar examples of atropisomeric biaryls **108** could be made in 84-96% e.e. with the Rh(I)/H₈-BINAP catalytic system (Scheme 25).



Scheme 24: The Pd/ $\text{H}_8\text{-BINAP}$ **86** catalysed asymmetric hydrogenation of unprotected indoles **104**.

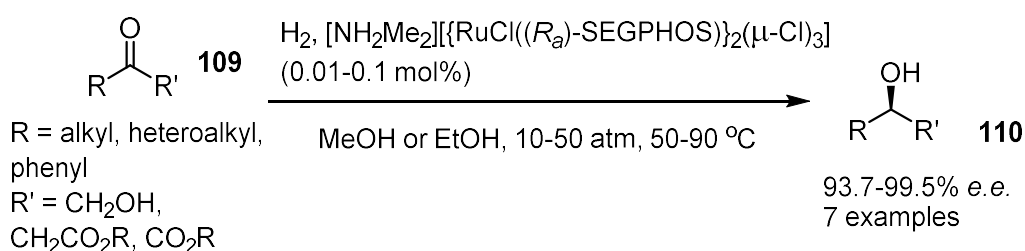


Scheme 25: The Rh(I)/ $\text{H}_8\text{-BINAP}$ **86** catalysed cyclotrimerisation of alkynes to produce chiral biaryls **108**.

1.3.3. SEGPHOS

The development of SEGPHOS **84** (Scheme 29) by Saito *et al.* showed that metal-ligand complexes with small bite angles prevail in asymmetric catalysis as much as those with large ones.⁶⁹ The group noticed that for the Ru-catalysed asymmetric hydrogenation of 2-oxo-1-propanol, the enantioselectivity increased along with the decrease in the MM2-calculated dihedral angles for the Ru-complexes for BINAP **51** (89.0% e.e., 73.49°), BIPHEMP **76** (92.5% e.e., 72.07°) and MeO-BIPHEP **79** (96.0% e.e., 68.56°). Building upon the design of MeO-BIPHEP **79**, the SEGPHOS **84** ligand is made up of two benzodioxole rings, so without a freely rotating alkoxy group, the steric repulsion between the rings in the biaryl system is reduced. This reduces the dihedral angle of the ligand to the calculated value of 64.0° for a Ru-

SEGPPOS-complex. Consequently, the Ru-catalysed asymmetric hydrogenation of 2-oxo-1-propanol proceeded in 98.5% e.e. with just 0.01 mol% of catalyst. The catalyst system also provided superior enantioselectivity to BINAP- and MeO-BIPHEP-complexes for various β -ketoester and α -ketoester substrates **109** (Scheme 26). The small dihedral angle was especially beneficial for the hydrogenation ethyl 4-chloro-3-oxobutanoate, as it prevented the chlorine atom from competing with the ester for coordination to the metal.

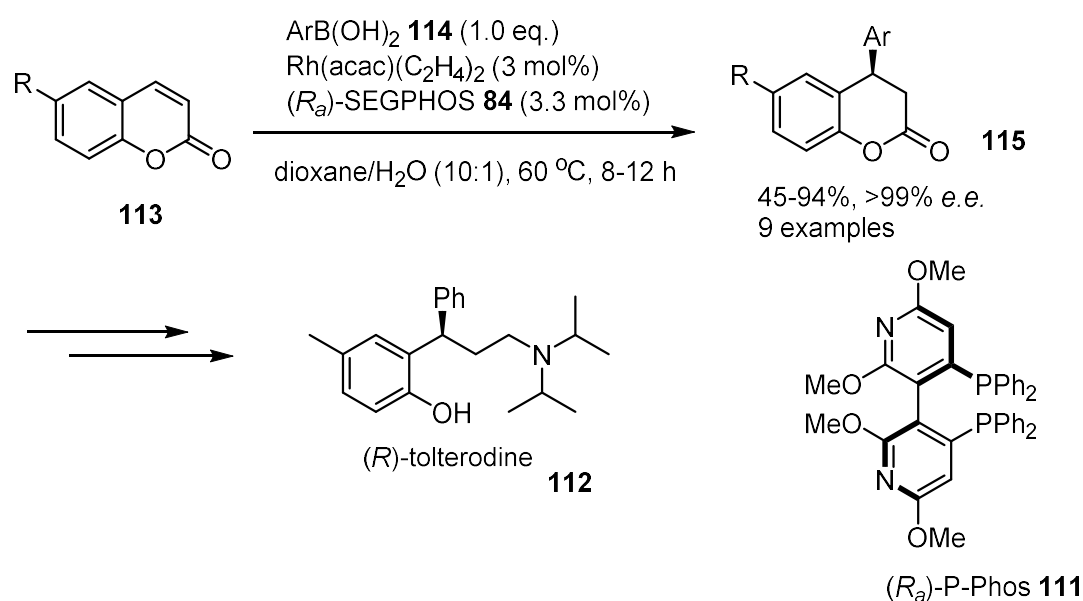


Scheme 26: The Ru-SEGPPOS-catalysed asymmetric hydrogenation of ketones **109**.

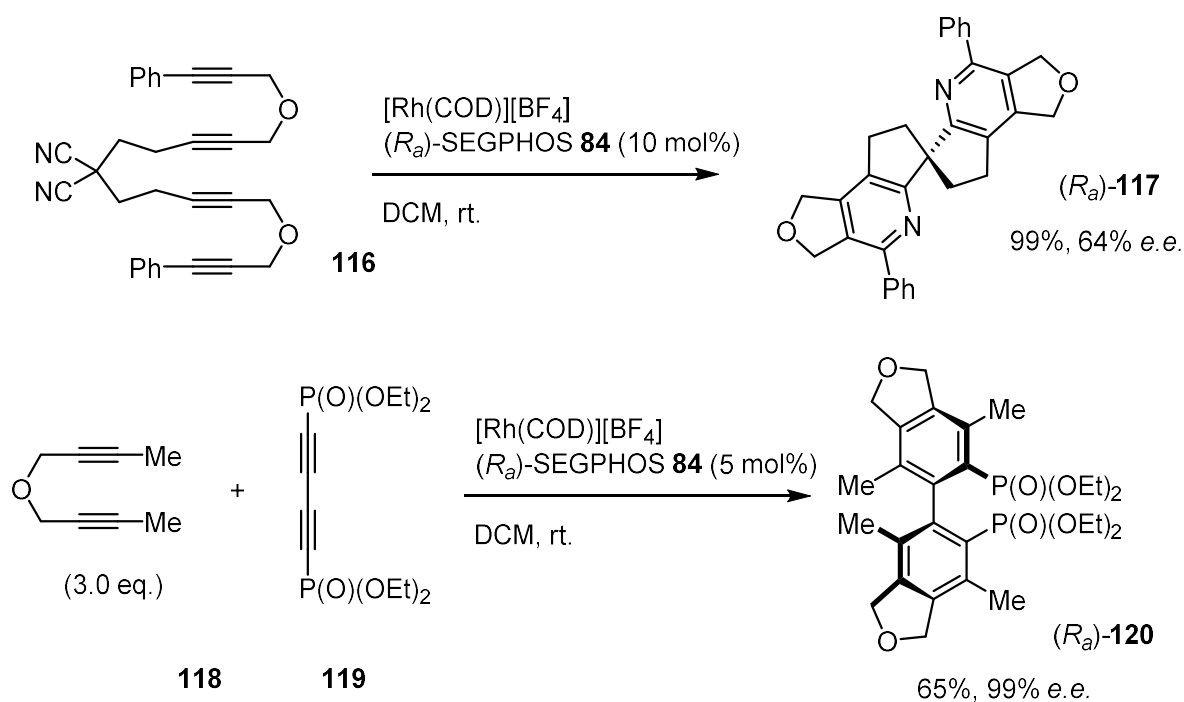
The versatility of SEGPPOS **84** has been demonstrated by Hayashi *et al.*, with their work on the Rh-catalysed asymmetric 1,4-addition of arylboronic acids to coumarin derivatives.⁷⁰ For the reaction of 6-methylcoumarin with phenylboronic acid, which was chosen for optimisation purposes, while BINAP **51** and P-Phos **111** induced excellent enantioselectivities of 94-96% e.e., the results were improved to >99% e.e. by using a Rh-SEGPPOS catalyst. The conjugate addition product could also be converted to (*R*)-tolterodine **112**, a widely used urological drug. Impressively, the high enantioselectivity of >99% e.e. with the Rh-SEGPPOS catalyst could be reproduced for a range of electron-rich and -poor 6-substituted coumarins **113** and arylboronic acids **114** (Scheme 27).

Furthermore, for Tanaka *et al.*, the use of SEGPPOS **84** has been instrumental for high enantioselectivity towards the asymmetric Rh-catalysed double [2+2+2]

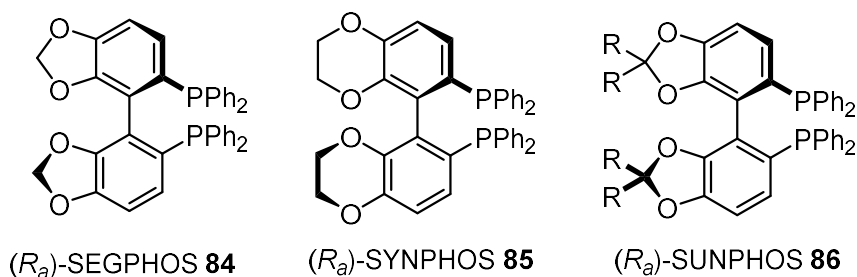
cycloaddition of alkynes and nitriles to produce chiral *spiro*-bipyridines (**117**)⁷¹ and axially chiral biaryl diphosphonates (**120**) and dicarboxylates (Scheme 28).⁷² The design of SEGPHOS **84** has also led to other successful variants such as SYNPHOS **85**^{73,74} and SUNPHOS **121**^{75,76} (Scheme 29), made up of benzodioxane and *gem*-dimethylbenzodioxole units respectively, to vary the dihedral angle in their metal-ligand complexes.



Scheme 27: The Rh-SEGPHOS-catalysed asymmetric 1,4-addition of arylboronic acids **114** to coumarins **113**, and P-Phos **111**, which was used for comparison.



Scheme 28: Asymmetric Rh-SEGPHOS-catalysed [2 + 2 + 2]-cycloadditions of alkynes and nitriles.



Scheme 29: Chiral biphenyl ligands functionalised with cyclic ethers.

1.3.4. TunePhos

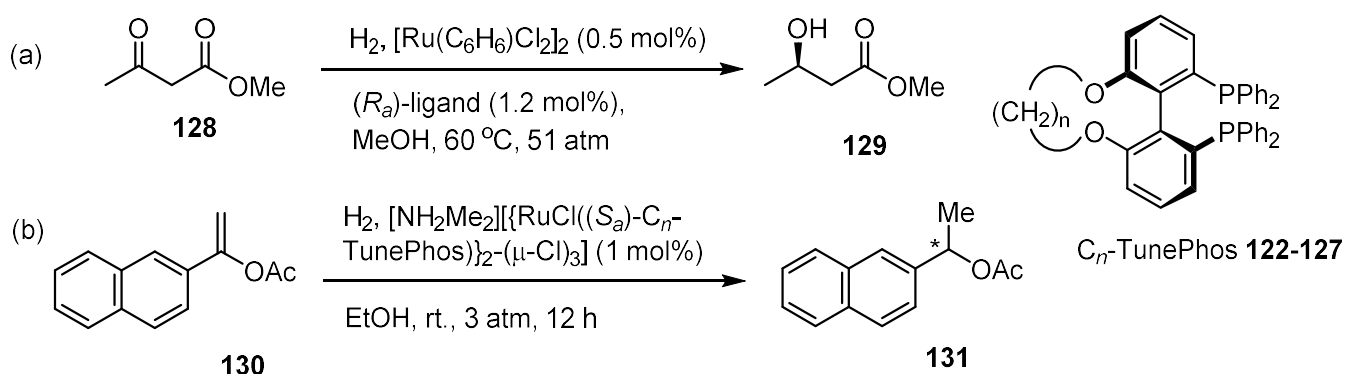
The TunePhos series of ligands **122-127** by Zhang *et al.* represented a highly important study into the relationship between the dihedral angle of the biaryl diphosphine and stereoselectivity. Starting from MeO-BIPHEP **79**, the ether groups were dealkylated, and treatment of the resultant biphenol with a dihaloalkane of the formula $\text{X}(\text{CH}_2)_n\text{X}$ gave a series of biaryl diphosphine ligands with systematically varying length of the ether linkage.⁷⁷ As the n value increases for the ether linkage,

the dihedral angle of the TunePhos ligand increases, as shown by the MM2-calculated values. These ligands were first tested in the application to a Ru-catalysed asymmetric hydrogenation of β -ketoesters (**128**). For all 7 substrates that were tested, the highest enantioselectivity was obtained by using C₄-TunePhos **125**, with a general decrease in e.e. as the *n* value for the ligand increased or decreased (Table 1, a). This observation was rationalised by C₄-TunePhos **125** having the most similar dihedral angle (88°) to BINAP **51** (87°) and MeO-BIPHEP **79** (87°), though an inferior enantioselectivity was achieved for each β -ketoester substrate with the latter two ligands, due to the added rigidity resulting from the atropisomerism-inducing groups in TunePhos being covalently linked to each other.

The series of ligands **122-127** were then tested for the Ru-catalysed asymmetric hydrogenation of enol acetate derivatives.⁷⁸ These substrates are a good alternative to their unfunctionalised keto-forms, due to the ability of the substrate to chelate to the metal centre, aiding enantioselectivity in the hydrogenation process. Furthermore, low hydrogen pressures are typically required for the hydrogenation of alkenes compared to ketones. In this report, an unusual trend was observed for the hydrogenation of 1-(naphth-2-yl)-1-acetoxyethene **130**, catalysed by the anionic dimeric [NH₂Me₂][{RuCl((S_a)-C_{*n*}-TunePhos)}₂-(μ -Cl)₃] complexes. While optimal results were achieved using C₁-TunePhos **122** and C₂-TunePhos **123**, each with 95.9% e.e., the selectivity decreased for C₃-TunePhos **124** and C₄-TunePhos **125**, with 92.1% e.e. and 88.9% e.e. respectively, but a further increase in dihedral angle led to an increase in selectivity, with 91.9% e.e. for C₅-TunePhos **126** and 92.3% e.e. for C₆-TunePhos **127** (Table 1, b). This non-linear relationship demonstrates the complicated consequences of small changes in geometric properties of the catalyst, due to the low energy differences between achieving high and low e.e. values.

Further optimisation was applied to the reaction, and 97.7% e.e. was achieved by using EtOH/DCM (4:1 v/v) as the solvent and C₂-TunePhos **123** as the ligand, and 5 other aryl enol acetate derivatives could be hydrogenated in 94-99% e.e. under these conditions.

Table 1: The Ru-catalysed asymmetric hydrogenation of methyl acetoacetate **128** (a) and 1-(naphth-2-yl)-1-acetoxyethene **130** (b), showing the variation of the ligand dihedral angle with enantioselectivity.

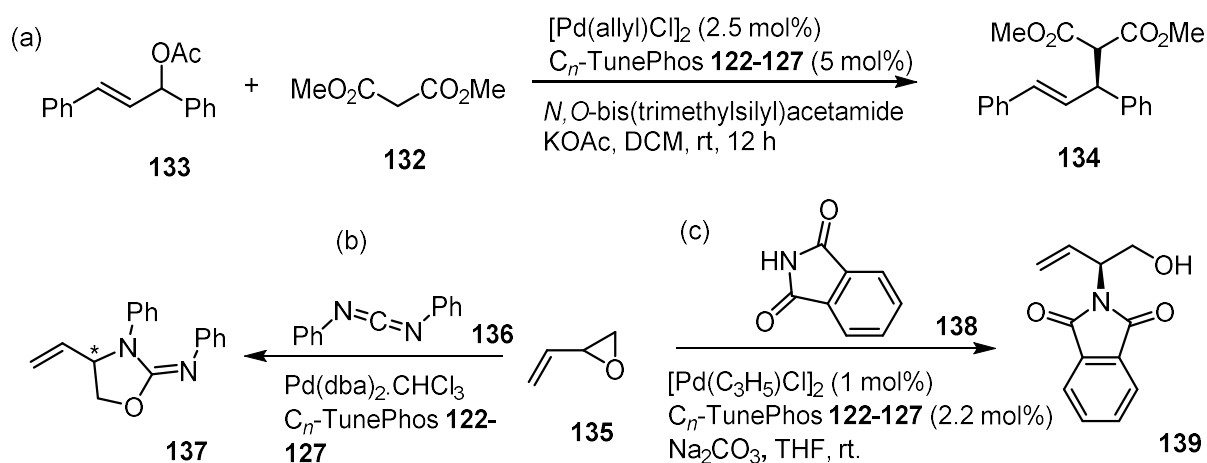


Ligand	Calculated dihedral angle (°)	% e.e. for (a)	% e.e. for (b)
BINAP 51	88	98.4	N/A
MeO-BIPHEP 79	88	97.9	N/A
C ₁ -TunePhos 122	60	90.9	95.9
C ₂ -TunePhos 123	74	90.8	95.9
C ₃ -TunePhos 124	77	97.7	92.1
C ₄ -TunePhos 125	88	99.1	88.9
C ₅ -TunePhos 126	94	97.1	91.9
C ₆ -TunePhos 127	106	96.5	92.3

The TunePhos ligand series **122-127** was also tested on asymmetric Pd-catalysed C-C and C-N bond formations (Table 2).⁷⁹ For the asymmetric allylic addition of dimethyl malonate **132** to 1,3-diphenylallyl acetate **133**, it was found that the enantioselectivity increased along with an increase in the ligand dihedral angle, with 95% e.e. obtained with a Pd-C₆-TunePhos **127** catalyst (Table 2, a). This observation is consistent with the high selectivity achieved for this type of reaction

when Trost ligands are used; the metal complexes of which are characterised by a large bite angle.^{80,81,82} The metal centre is thus more greatly enveloped within the chiral environment, and so the bulky diphenylphosphine groups are able to exert a greater influence on the orientation of the incoming nucleophilic reaction partner towards the Pd-allyl cation. This trend in enantioselectivity, however, was not reflected in other examples in the report. For the Pd-catalysed cycloaddition of butadiene monoxide **135** with diphenyl carbodiimide **136**, which mechanistically resembles an intramolecular variant of asymmetric allylic alkylation,⁸³ the trend opposite to that in the aforementioned Tsuji–Trost reaction was observed (Table 2, b). The best e.e. value of 83% was achieved with C₁-TunePhos **122**, and an increase in dihedral angle led to a loss of enantioselectivity. For the reaction of butadiene monoxide **135** with phthalimide **138**, optimal results were obtained with C₄-TunePhos **125**, with a decrease in enantioselectivity as the dihedral angle was increased or decreased (Table 2, c). While C₆-TunePhos **127** has the largest dihedral angle, which would be ideal for influencing the alignment of the phthalimide **138** molecule, the enantioselectivity was diminished by a loss of rigidity in the structure that came from the long, flexible ether group, according to the authors.

Table 2: The Pd-C_n-TunePhos-catalysed asymmetric C-C and C-N bond formations, showing variation of enantioselectivity with the ligand dihedral angle.



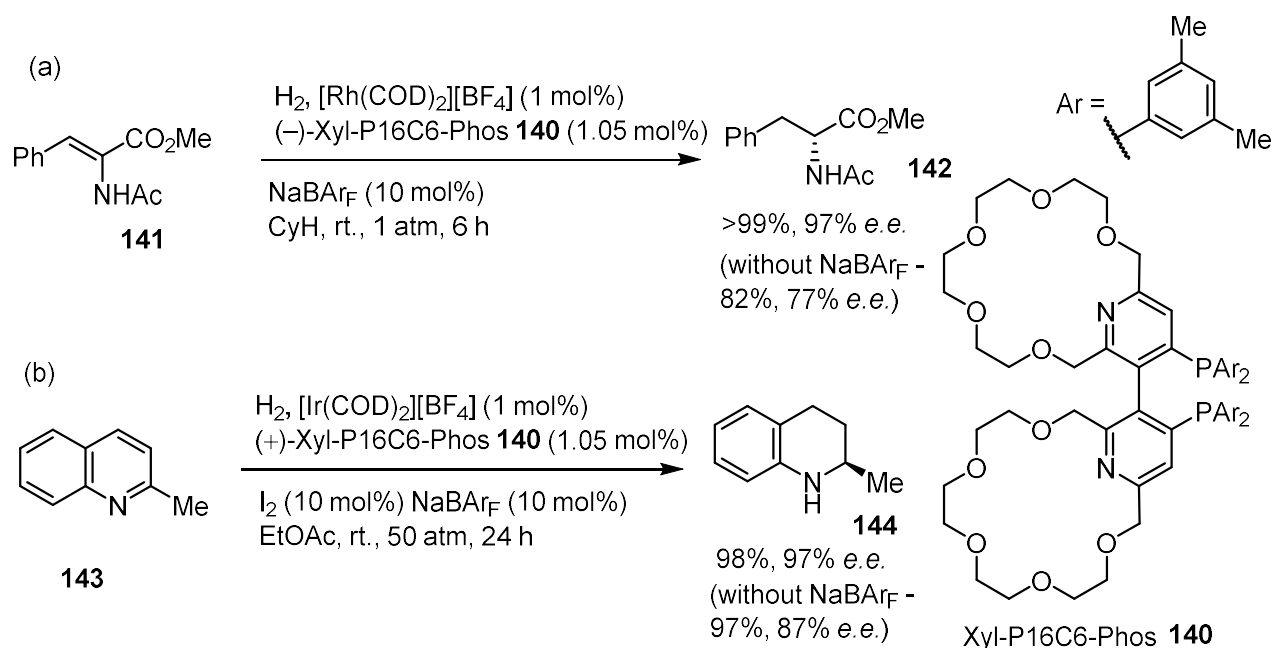
Ligand	Calculated dihedral angle (°)	% e.e. for (a)	% e.e. for (b)	% e.e. for (c)
C ₁ -TunePhos 122	60	77	83	65
C ₂ -TunePhos 123	74	82	79	75
C ₃ -TunePhos 124	77	84	70	76
C ₄ -TunePhos 125	88	87	60	82
C ₅ -TunePhos 126	94	92	58	70
C ₆ -TunePhos 127	106	95	57	68

The TunePhos series of ligands enjoy continued usage in synthetic research today, showing that they induce excellent enantioselectivity in their own right, rather than simply being a useful tool to systematically examine the influence of a catalyst bite angle towards selectivity. For example, C₄-TunePhos **125** was found to induce greater enantioselectivity than a variety of chiral mono- and diphosphine ligands for the Pd-catalysed salicylic acid-promoted hydrogenation of acetophenone, and showed good generality for the asymmetric hydrogenation of other aryl and alkyl-substituted unfunctionalised ketones.⁸⁴ For the Ru-catalysed hydrogenation of cyclic β -amido enones, the enantioselectivity obtained by using C₃-TunePhos **124** was superior to that of BINAP **51** and a few chiral bis(phospholane) ligands.⁸⁵

1.3.5. Supramolecular tuning of the ligand bite angle

Furthermore, these ligands have been greatly influential in the design of new chiral ligands. An exceptional example of building upon the tunability of a biaryl diphosphine was reported by Li, Wu and co-workers with the design of Xyl-P16C6-Phos **140**, a bipyridyl diphosphine ligand functionalised with crown ethers (Scheme 30).⁸⁶ While the idea of controlling the geometry of a chiral ligand in a supramolecular fashion was not novel,⁸⁷ this was the first instance of the incorporation of crown ethers to alter the dihedral angle of a biaryl unit. With this design, one can theoretically change the geometric properties of the final product,

that is, by the addition of different size metal cations to the system, without a change in the preceding chemical steps to synthesise the ligand. For the asymmetric hydrogenation of methyl (Z)-2-acetamidocinnamate **141** catalysed by the Rh-Xyl-P16C6-Phos complex, the enantioselectivity was improved by a gradually increased quantity of NaBAr_F (from 0 to 10 mol%). Furthermore, when the same loading of LiBAr_F and KBAr_F, the enantioselectivity was diminished, showing that the ligand had been 'tuned' most suitably for this reaction. The effect of the cation was confirmed when only a small increase in e.e. was observed when using tetra-*n*-butylammonium BAr_F as a control. On optimising the solvent, the effect was particularly enhanced by using the non-polar cyclohexane as a solvent (from 77% e.e. to 97% e.e.) (Scheme 30, a), encouraging the complexation of sodium ions into the crown ether of **140**. A similar enhancement of enantioselectivity was also observed for the Ir-catalysed asymmetric hydrogenation of 2-methylquinoline **143** – a significant rise from 87% e.e. to 97% e.e. was engendered with the addition of 10 mol% of NaBAr_F to the system (Scheme 30, b). Currently, the group are working on analysing the properties of the catalysts and thus elucidating the mechanistic basis of these fascinating phenomena.



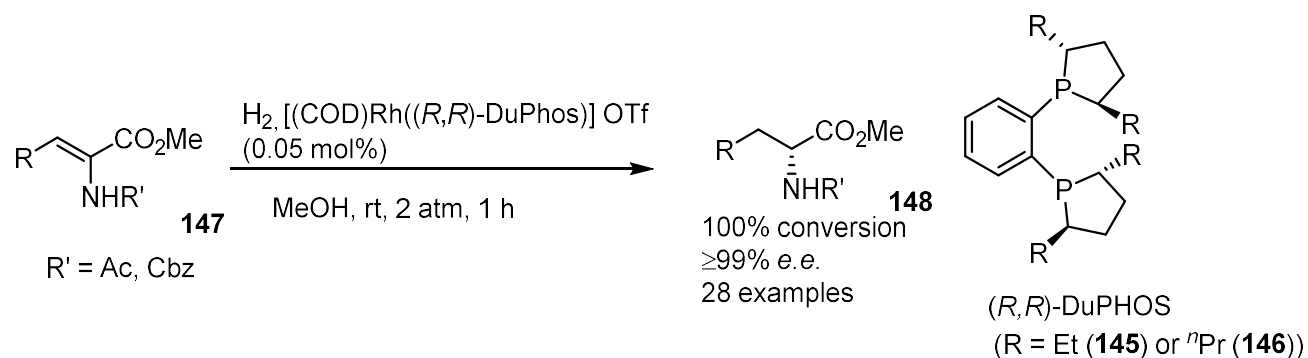
Scheme 30: The asymmetric hydrogenation of methyl (Z)-2-acetamidocinnamate **141** (a) and 2-methylquinoline **143** (b) with a Xyl-P16C6-Phos **140** ligand.

Electron-rich and electron-poor diphosphine ligands

1.4.1. Increased Lewis basicity in diphosphine ligands

In the early 1990s, Burk *et al.* introduced DuPhos, a ligand made up of two *P*-chiral phospholane groups linked with a 1,2-phenylene bridge, which was a landmark in asymmetric catalysis.⁸⁸ With a rhodium catalyst consisting of either Et-DuPhos **145** or ⁿPr-DuPhos **146**, the asymmetric hydrogenation of 25 different examples of methyl α-amidoacrylates **147** could be achieved in >99% e.e. under mild conditions (Scheme 31).⁸⁹ These results were previously unprecedented and the success of the ligands, along with their highly rigid structure, was rationalised by the electron-rich nature of the alkyl-phosphine groups. As the ligands have high Lewis basicity, this forces backbonding from the metal d-orbitals to the π*-orbital of the olefin, strengthening the bond between substrate and catalyst and allowing greater transfer

of stereochemical information from the chiral ligand to the olefin, leading to near 100% enantioselectivity.



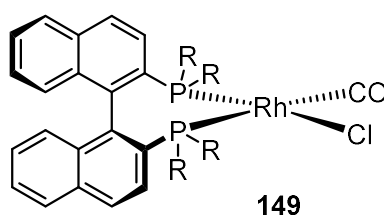
Scheme 31: The Rh-DuPhos-catalysed asymmetric hydrogenation of methyl α -amidoacrylates **147**.

1.4.2. Assessment of biaryl diphosphine Lewis basicity by IR

Because of the flexibility allowed in the design of axially chiral biaryl diphosphine ligands, there has been a tendency to modify ligands of this type to increase the Lewis basicity of the phosphorus atoms. On this subject, an important study of this property was conducted by Takaya *et al.*, in which the Lewis basicities of BINAP derivatives with various electron-rich and -poor *P*-aryl groups (as well as cyclohexyl groups) were assessed by forming the corresponding $\text{Rh}(\text{phosphine})(\text{CO})\text{Cl}$ complexes **149**.⁹⁰ As the degree of donation from the phosphine to the Rh centre is increased, the wavenumber of the ν_{CO} stretch by IR spectrometry decreases due to the increased backbonding to the π^* -orbital of the carbonyl. As the data in Table 3 shows, the ν_{CO} value with cyclohexyl groups (1990 cm^{-1}) on the phosphorus atom indicates that they are significantly more electron-donating than the electron-rich aryl groups, as the ν_{CO} values for *p*-anisyl, 3,5-di(*tert*-butyl)phenyl, *p*-tolyl, and 3,5-xylyl are much closer to that of phenyl (BINAP **51**). It follows that the cyclohexyl group would have a much greater electronic effect on the selectivity, than electron-rich

arenes, for asymmetric hydrogenation. For the reported substrates tested in the paper for Ru-catalysed asymmetric hydrogenation, BINAP **51** generally resulted in the best enantioselectivities, except for methyl 2-(benzamidomethyl)-3-oxobutanoate when 3,5-di(*tert*-butyl)-BINAP gave the optimal result. However, Cy-BINAP **150** was not tested in any experiments in this account.

Table 3: The effect of the ligand phosphorus atom substituents on the ν_{CO} wavenumber for the Rh(phosphine)(CO)Cl complexes **149**.



R	ν_{CO} wavenumber /cm ⁻¹
Cy	1990
<i>p</i> -anisyl	2004
3,5-di(<i>tert</i> -butyl)phenyl	2006
<i>p</i> -tolyl	2010
3,5-xylyl	2011
Ph	2013
4-fluorophenyl	2018
4-chlorophenyl	2020

1.4.3. Electron-rich axially chiral diphosphine ligands

Prior to their work in the application of ruthenium complexes towards asymmetric hydrogenation, Noyori *et al.* found that for the asymmetric hydrogenation of the naturally occurring allylic alcohol nerol **Z-58**, the use of a Rh-Cy-BINAP **150** catalyst led to formation of the product in 66% e.e., compared to the 52% e.e. achieved with the analogous BINAP **51** complex.⁹¹ The application by Takaya *et al.* of BICHEP **151** (Figure 8), the cyclohexyl-substituted variant of BIPHEMP **76**, towards the rhodium-catalysed asymmetric hydrogenation of ethyl (*Z*)- α -benzamidocinnamate **152** resulted in 98% e.e., whereas only 14% e.e. was obtained using the analogous

BIPHEMP **76** catalyst.⁹² A similar improvement to the enantioselectivity was observed by Miyashita *et al.* for the Ru-catalysed hydrogenation of methyl phenylglyoxylate **153** – using BINAP **51** as a ligand resulted in 45% e.e., whereas an impressive >99% e.e. was achieved using BICHEP **151**.⁹³

The structure of BIPHEMP **76** was modified by Achiwa *et al.* to include electron donating methyl and methoxy groups on the biphenyl backbone to make BIMOP **154** (Figure 8).⁹⁴ This ligand was applied to the Ru-catalysed hydrogenation of methyl acetoacetate **128** to give the alcohol product in 99% e.e., which was slightly better than the 98% produced by BINAP **51**. For the Ru-catalysed hydrogenation of 2,3-dimethylacrylic acid **155**, the olefin was reduced in 91% e.e., compared to 87% e.e. with BINAP **51**. Curiously, the enantioselectivity for these two reactions diminished (95% e.e. and 86% e.e. respectively) with the ligand *p*-MeO-BIMOP **X** (Figure 8), which consists of *p*-anisyl groups on the phosphine and would therefore be expected to have a higher Lewis basicity.

In a later report, the same authors reported that for the Rh-catalysed hydrogenation of itaconic acid **26**, they observed that the best enantioselectivity of 80% e.e. was obtained by using Cy-BIMOP **157** (Figure 8), the cyclohexyl substituted analogue of BIMOP **154**.⁹⁵ This value exceeded that of MOC-BIMOP **158** (Figure 8) (71% e.e.), which consists of a PPh₂ group and a PCy₃ group, and that of BIMOP **154** (51% e.e.), while BINAP **51** resulted in a racemate. However, for the Rh-catalysed hydrogenation of 2-aminoacetophenone **159**, the best selectivity was obtained with MOC-BIMOP **158** (93% e.e., with a cationic precatalyst), exceeding those of Cy-BIMOP **157** (55% e.e., with a neutral precatalyst) and BIMOP **154** (8% e.e., neutral precatalyst). These results indicate that with some substrates, an optimal amount of

steric bulk around the metal centre outweighs the influence of electronic properties of the ligand.

Another intriguing quality of the geometric properties for a cyclohexyl group, compared to a phenyl group, is that its presence within the ligand led to a reversal of the configuration of the major product for the hydrogenation of 2-aminoacetophenone **159**. Normally with a Rh-diphosphine-catalysed asymmetric hydrogenation, somewhat counterintuitively, the minor, higher in energy diastereomeric intermediate **160** leads to the major enantiomer for the product, because this intermediate is more reactive towards the oxidative addition of H₂ to the metal than the major diastereomer **161** (Figure 10).^{96,89,97} However, by changing the phenyl group to cyclohexyl, Achiwa *et al.* suggested the upper axial site of the Rh centre for the minor diastereomeric intermediate **164**, where the oxidative addition takes place, is more sterically hindered (Figure 11). Thus, the higher energy caused by a 'mis-matched' substrate orientation no longer induces reactivity of the metal with hydrogen. Furthermore, the electron donation from the cyclohexyl group perhaps facilitates the oxidative addition by stabilising the higher oxidation state of the metal. Therefore, the intermediate diastereomer **165** with the longer lifetime, i.e. the major one, now leads to the major product enantiomer.

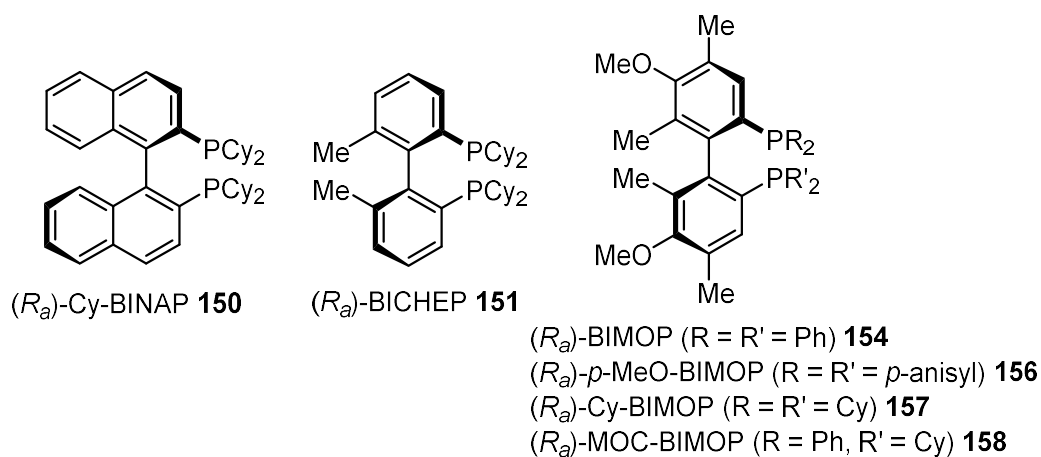


Figure 8: Electron-rich variants of biaryl diphosphine ligands.

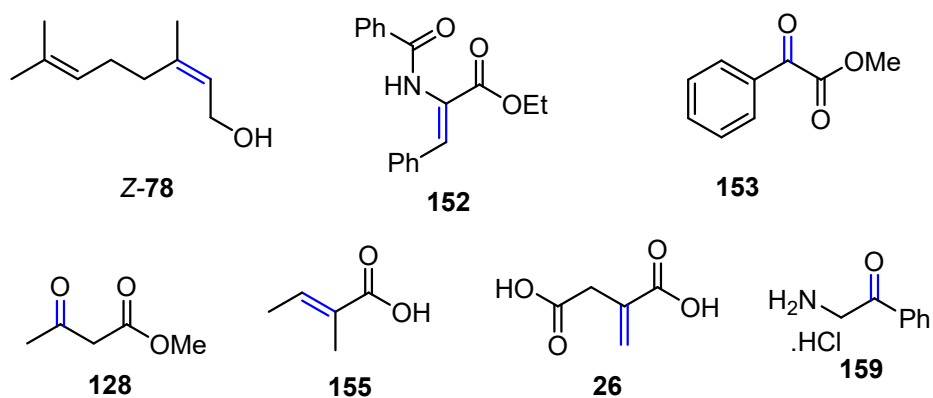


Figure 9: Substrates for which the enantioselectivity was improved in asymmetric hydrogenation, with the use of a more electron-rich biaryl diphosphine ligand. Reactive double bonds are highlighted in blue.

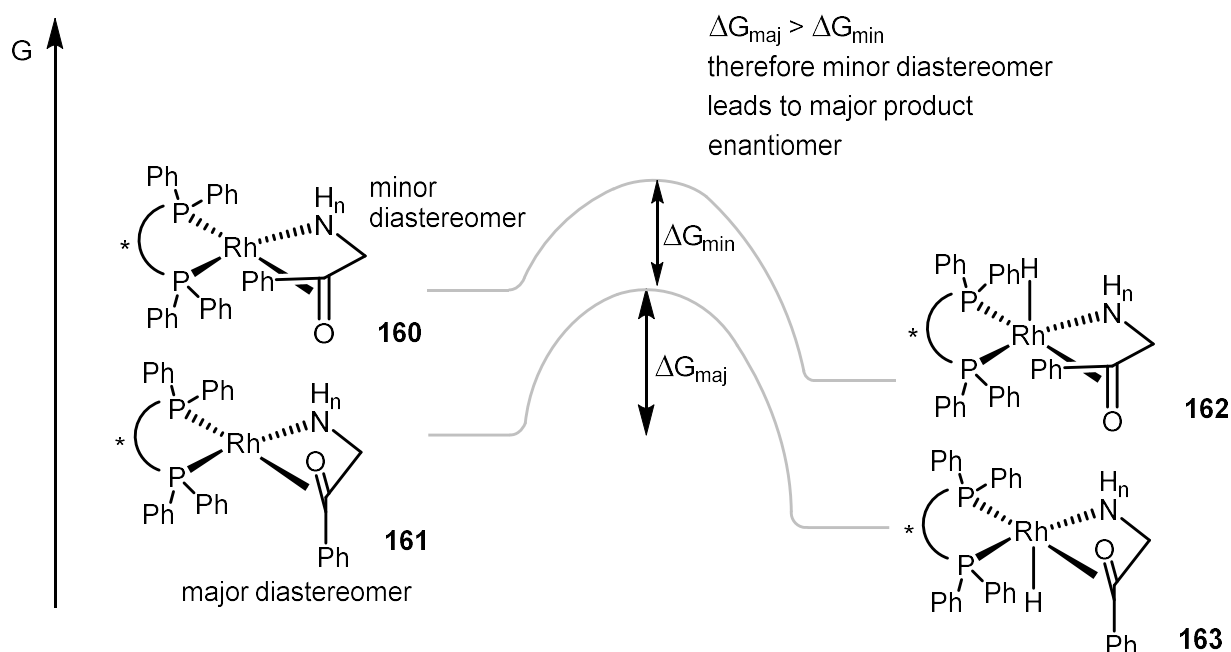


Figure 10: Reaction profile diagram for the oxidative addition of H_2 to Rh-centre with $RPPH_2$ groups, for the asymmetric hydrogenation of 2-aminoacetophenone **159**.

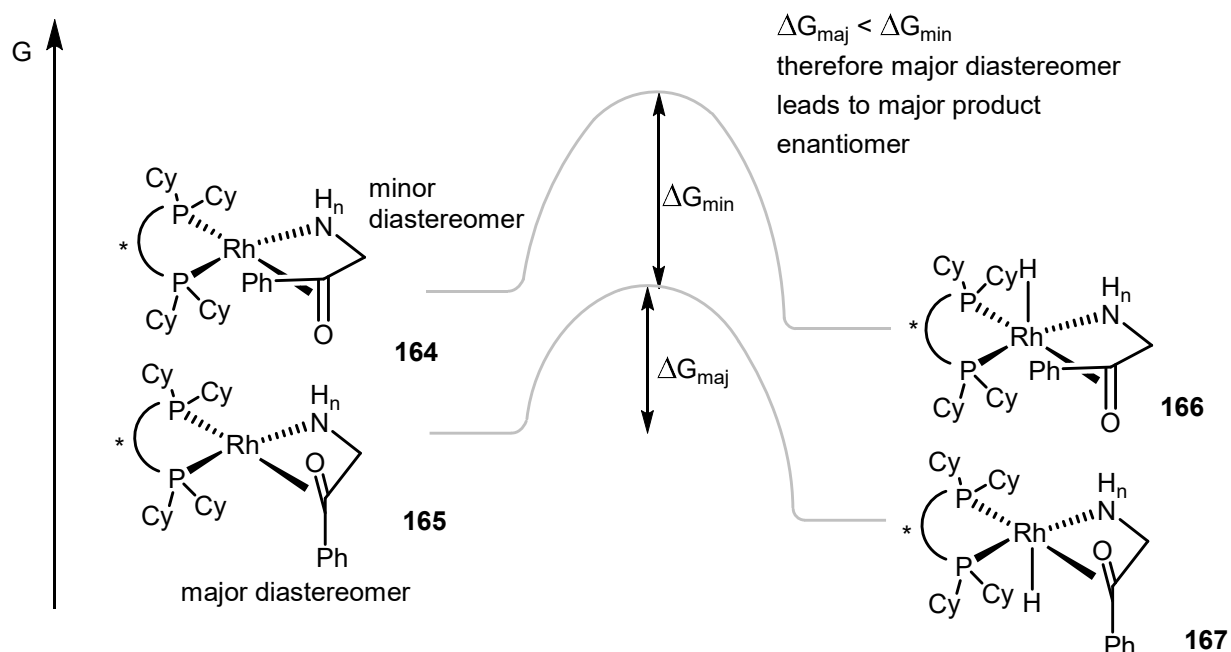


Figure 11: Reaction profile diagram for the oxidative addition of H_2 to Rh-centre with $RPCy_2$ groups, for the asymmetric hydrogenation of 2-aminoacetophenone **159**.

A lot of developments towards asymmetric hydrogenation, conducted by Imamoto *et al.*, involve the use of *P*-chiral diphosphine ligands such as MiniPhos **168**,⁹⁸ BisP* **169**^{99,100} and BenzP* **170**¹⁰¹ (Figure 12). These ligands deliver high enantioselectivity for the hydrogenation of olefins due to having electron-rich alkyl groups, and the difference in bulk between the two non-bridging *P*-alkyl groups (usually *tert*-butyl and methyl) creates a well-defined chiral pocket for the substrate. However, Imamoto *et al.* also demonstrated the beneficial effect of electron-donating substrates in axially chiral biaryl ligands for Rh-catalysed asymmetric hydrogenation, using various octamethyl-1,1'-biphenyl diphosphine (Me₈-BIPHEP) species (Table 4).¹⁰² For the hydrogenation of methyl (Z)- α -acetamidocinnamate **141**, the use of Me₈-BIPHEP **171** with Ph groups achieved 88% e.e. requiring 15 hours at 50 °C and 50 atm to go to completion (Table 4, entry 1). For *rac*-Me₈-BIPHEP **172** with Cy groups, which could not be resolved, the reaction was complete in 15 hours, requiring only room temperature and 3 atm (Table 4, entry 2). With Et groups on the phosphorus atom (**173**), the reaction was complete in 10 minutes under the same mild conditions because of the lack of steric hindrance in the catalyst (Table 4, entry 3). Despite the lack of steric bulk in the ligand **173**, 74% e.e. was still achieved because of the high Lewis basicity of the phosphine groups. By reducing the temperature and increasing the reaction time to 60 hours, the product **142** was obtained in 84% e.e. at -20 °C (Table 4, entry 4), and in 89% e.e. at -40 °C (Table 4, entry 5). The completion of the reaction at this low temperature demonstrates the high catalytic activity due to the electron-rich ligands, the explanation being that a higher oxidation state is stabilised, facilitating the oxidative addition of H₂ to the metal.

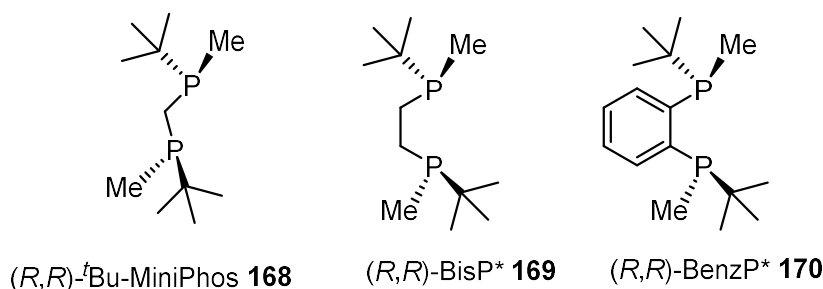
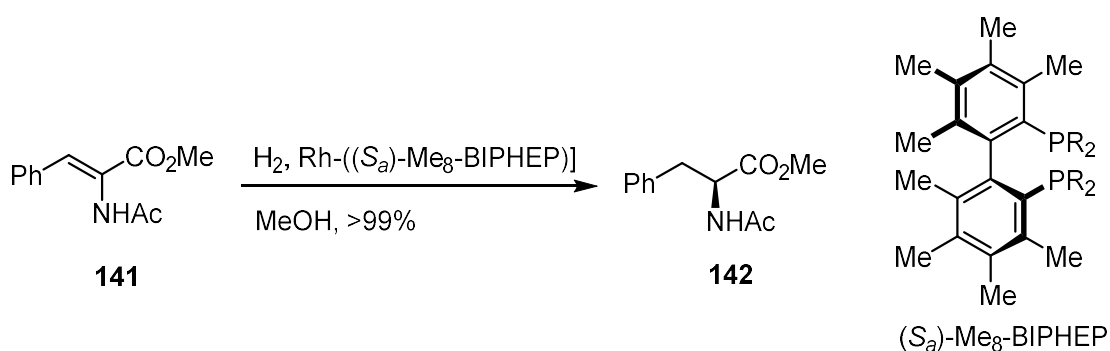


Figure 12: Electron-rich *P*-chiral diphosphine ligands for asymmetric hydrogenation, by Imamoto.

Table 4: The Rh-catalysed asymmetric hydrogenation of methyl (Z)- α -acetamidocinnamate **141**, with Me₈-BIPHEP derivatives as ligands.



Entry	R	Temperature /°C	Pressure /atm	Running time	% e.e.
1	Ph (171)	50	50	15 h	88
2	Cy (<i>racemic</i>) ((\pm)- 172)	r.t.	3	15 h	N/A
3	Et (173)	r.t.	3	<10 min	74
4	Et (173)	-20	3	36 h	84
5	Et (173)	-40	3	60 h	89

1.4.4. Decreased Lewis basicity in diphosphine ligands

Increasing the diphosphine ligand donation ability is not a universal way of enhancing the enantioselectivity in asymmetric catalysis; examples in which the results are improved by using an electron-poor diphosphine ligand are just as frequent. For instance, by reducing the Lewis basicity of the ligand, the Lewis acidity of the metal centre is increased; a characteristic which has been exploited by Kundig *et al.* for asymmetric Diels–Alder reactions. One of the most common methods to create electron-poor character in a ligand is to incorporate fluorinated substituents in the structure. This way, one can modify the electronic properties of the structure

without greatly changing the steric properties, which makes it easier to infer cause and effect for the outcome of the experiment. With a cationic Fe-complex consisting of a CYCLOP-F ligand **174**, made up of two di(pentafluorophenyl)phosphine groups linked together with a *trans*-1,2-cyclopentandiol unit (Figure 13), the authors could induce high enantioselectivities for the Diels–Alder reaction between several α,β -unsaturated aldehydes and dienes.¹⁰³ To put this catalyst design into perspective, it was found by Hossain *et al.* that an analogous Fe-complex with triphenylphosphine ligands was completely inactive for similar reactions.¹⁰⁴ The authors have since expanded the substrate scope and improved catalytic activity by changing the diol linker to a *trans*-1,2-diarylethane-1,2-diol unit (BIPHOP-F **175** or Me₄-BIPHOP-F **176**) and with the use of cationic Ru-complexes.^{105,106,107}

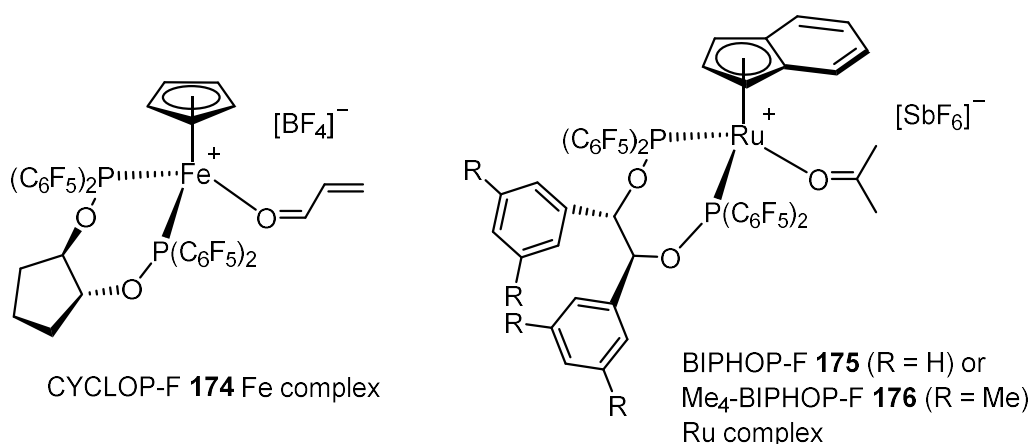


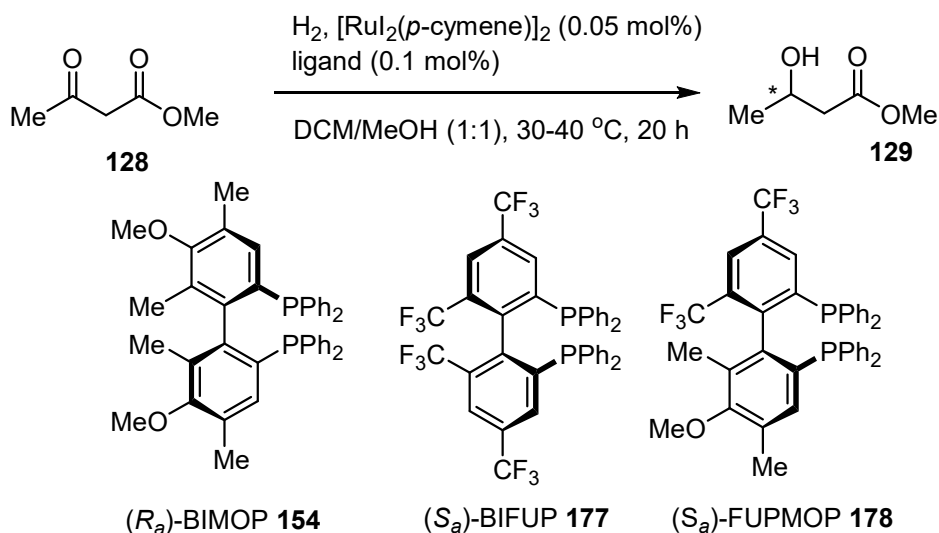
Figure 13: Chiral Lewis acids with electron-poor diphosphinite ligands for asymmetric Diels–Alder reactions.

1.4.5. Electron-poor axially chiral diphosphine ligands

The modification of ligands to reduce electron donor ability has also been carried out many times within the context of axially chiral biaryl diphosphines. Along with the electron-rich ligand BIMOP **154**, Achiwa *et al.* also reported the analogous electron-poor tetra-(trifluoromethyl)biphenyldiphosphine ligand BIFUP **177**, along with the

mixed non-C₂-symmetric ligand FUPMOP **178**.¹⁰⁸ However, for the Ru-catalysed asymmetric hydrogenation of methyl acetoacetate **128**, while >99% e.e. and quantitative conversion was achieved after 20 hours by using either BIMOP **154**, FUPMOP **178** or BINAP **51** as ligands, the activity was diminished greatly with the use of BIFUP **177**, giving only 95% e.e. and 13% conversion at a higher pressure (Table 5). These findings are consistent with the improvements brought about with a more electron-rich ligand for asymmetric hydrogenation, as previously discussed in this report.

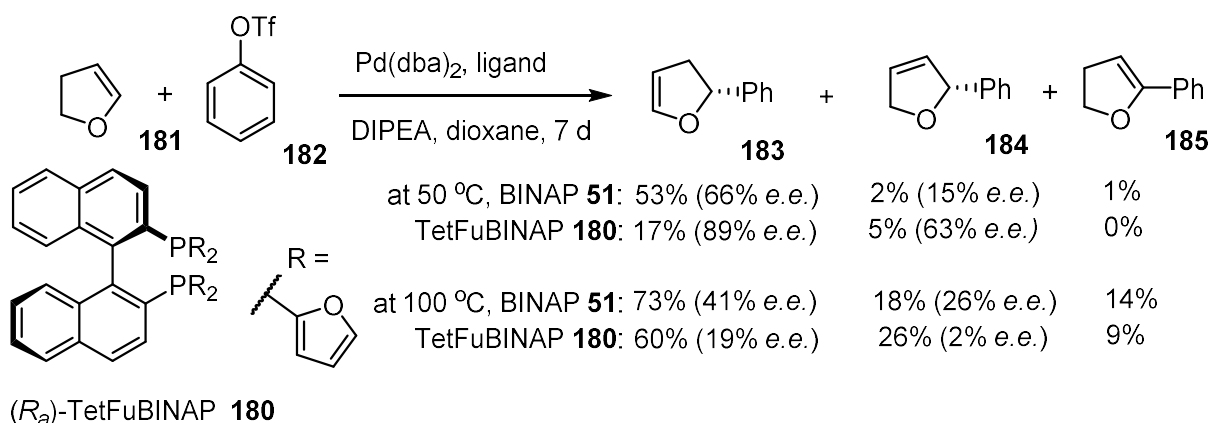
Table 5: The Ru-catalysed asymmetric hydrogenation with ligands of varying Lewis basicity.



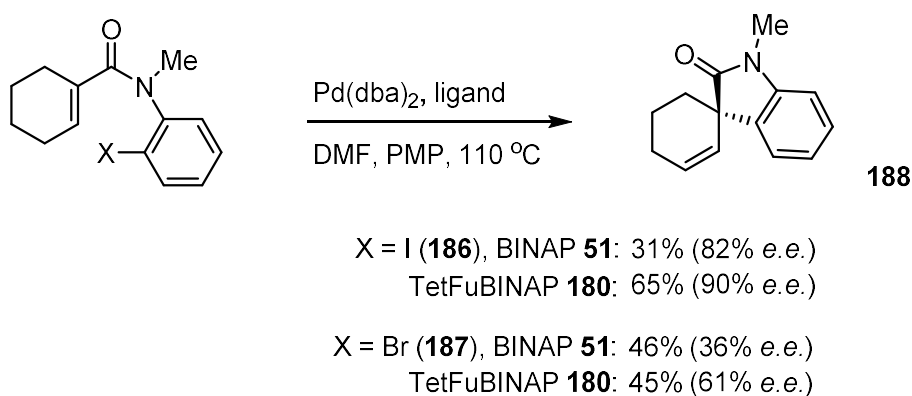
Ligand	H ₂ pressure /atm	Conversion /%	% e.e.
(R _a)-BINAP 51	10	>99	>99
(R _a)-BIMOP 154	10	>99	>99
(S _a)-FUPMOP 178	10	>99	>99
(S _a)-BIFUP 177	90	13	95

Building upon their work on the development of BINAPFu **179**¹⁰⁹ (Scheme 37, vide infra), Keay *et al.* designed TetFuBINAP **180**,¹¹⁰ a modified form of BINAP **51** with electron-withdrawing 2-furyl units in place of the phenyl groups on the phosphorus atoms. A standard method to measure the Lewis basicity of a phosphine ligand is to use the ¹J_{PSe} value of ³¹P-NMR spectrum for the corresponding phosphine

selenide.¹¹¹ An increase in the $^1J_{\text{PSe}}$ value indicates an increase in the s-character on the phosphorus lone pair orbital, meaning it is less basic. From the phosphine selenide derivative of TetFuBINAP **180**, it was observed from measuring the $^1J_{\text{PSe}}$ value (767 Hz) that the phosphorus atom was less basic than that of BINAP **51** (738 Hz) and BINAPFu **179** (762 Hz). Furthermore, the X-ray crystal structure for the (TetFuBINAP)PdCl₂ complex displayed a similar bite angle (91.7°) to that of BINAP **51** (92.7°), so any differences in performance with asymmetric catalysis would be down to either the difference in electronic properties, or ring size, between the furyl and phenyl rings. For the asymmetric Heck reaction between 2,3-dihydrofuran **181** and phenyl triflate **182** at 50 °C, the desired coupled product **183** was synthesised with better enantioselectivity with TetFuBINAP **180** (89% e.e.) than BINAP **51** (66% e.e.), but conversion and regioisomeric selectivity were considerably worse (Scheme 32). By raising the temperature to 100 °C, the conversion was increased to 100% for both ligands, but the enantioselectivity of the desired product **183** suffered a lot more for TetFuBINAP **180** (19% e.e.) than for BINAP **51** (41% e.e.). For the intramolecular asymmetric Heck reaction of (*E*)- α,β -unsaturated 2-haloanilides **186** and **187**, mechanistic studies by Overman *et al.* had determined that the diphosphine ligand remains chelated to the Pd centre while the reactive olefin occupies a 5th coordination site.¹¹² It was postulated by Keay *et al.* that an electron-poor diphosphine would facilitate this mechanistic step by increasing the electrophilicity of the metal centre. Indeed, for the reaction of both the iodo- **186** and bromo-derivative **187**, the use of TetFuBINAP **180** generally achieved superior enantioselectivity compared to BINAP **51**, particularly when DMF was used as solvent (90% e.e. vs. 82% e.e. for iodoanilide **186**, 61% e.e. vs. 36% e.e. for bromoanilide **187**) (Scheme 33).



Scheme 32: The asymmetric Heck reaction between 2,3-dihydrofuran **181** and phenyl triflate **182**, with TetFuBINAP **180** and BINAP **51** as ligands.



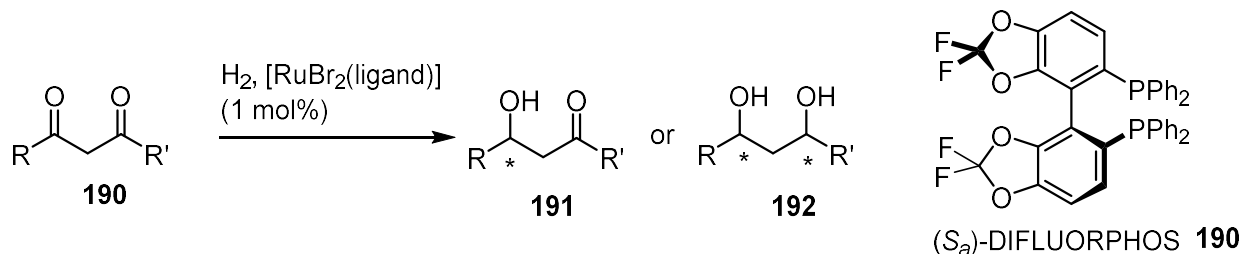
Scheme 33: The asymmetric intramolecular Heck reaction of (*E*)-α,β-unsaturated 2-haloanilides **186** and **187**, with TetFuBINAP **180** and BINAP **51** as ligands.

1.4.6. DIFLUORPHOS

One of the most widely employed electron-poor diphosphine ligands, DIFLUORPHOS **189**, developed by Genêt *et al.*, is a modified form of SEGPHOS **84**, wherein the methylene is replaced with a difluoromethylene group.^{113,114} Indeed, DIFLUOROPHOS **189** was demonstrated to be a more electron-poor ligand than the analogous SEGPHOS **84**, as the $^1J_{\text{PSe}}$ value for the phosphine selenide derivative was greater (749 Hz and 738 Hz respectively) and the ν_{CO} value in the IR spectrum for the corresponding $[\text{RhCl}(\text{diphosphine})(\text{CO})]$ complex was, as expected, also

greater (2023 cm^{-1} and 2016 cm^{-1}). The Lewis basicity of DIFLUORPHOS **189** was also demonstrated, in a similar way, to be lower than BINAP **51**, MeO-BIPHEP **79** and SYNPHOS **85**. Furthermore, the calculated dihedral angle of DIFLUORPHOS **189** (67.6°) was very close to that of SEGPHOS **84** (67.2°), so it follows that any difference in performance between these ligands is a consequence of electronic properties. For the Ru-catalysed asymmetric hydrogenation of β -keto-carbonyls **190**, the use of DIFLUORPHOS **189** achieved a consistently higher enantioselectivity than SEGPHOS **84** with fluorinated substrates, despite the similarity in geometric properties with these ligands (Table 6). The e.e. values obtained with DIFLUORPHOS **189** also consistently exceeded those obtained with BINAP **51**, MeO-BIPHEP **79** and SYNPHOS **85**.

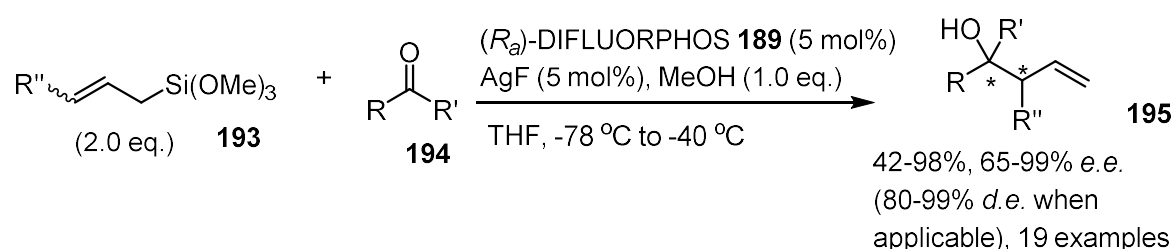
Table 6: The Ru-catalysed asymmetric hydrogenation of fluorinated β -keto-carbonyls **190**, with SEGPHOS **84** and DIFLUORPHOS **189** as ligands.



R	R'	Conditions	Product	(S _a)-SEGPHOS 84 % e.e.	(S _a)-DIFLUORPHOS 189 % e.e.
CF ₃	OEt	10 atm, 110 °C, 1 h, EtOH	191	59	70
C ₂ F ₅	OEt		191	76	81
CF ₃	CF ₃	50 atm, 50 °C, 24 h, MeOH	192	88 (71% d.e.)	98 (86% d.e.)

The applications of DIFLUORPHOS **189** have been rich in diversity. One example was the Ag-catalysed asymmetric addition of allyl siloxanes to ketones (Sakurai–Hosomi allylation) by Yamamoto *et al.*,¹¹⁵ in which DIFLUORPHOS **189** was demonstrated to induce the highest enantioselectivity for the reaction between acetophenone and allyltrimethoxysilane, which was chosen for the optimisation. The

high selectivity was rationalised by DIFLUORPHOS **189** forming the highest proportion, compared to BINAP **51**, SEGPHOS **84** and MeO-BIPHEP **79**, of the monochelated diphosphine-silver complex relative to the chelated bis(diphosphine)-silver and bridging diphosphine-disilver complexes; presumably a result of the low Lewis basicity of the ligand. The DIFLUORPHOS-silver catalyst system was then shown to induce high enantioselectivity for the reaction of a variety of allylsiloxanes **193** with ketones **194** (and high diastereoselectivity with γ -substituted allylsiloxanes), with exclusive 1,2-addition when enone substrates were used (Scheme 34).

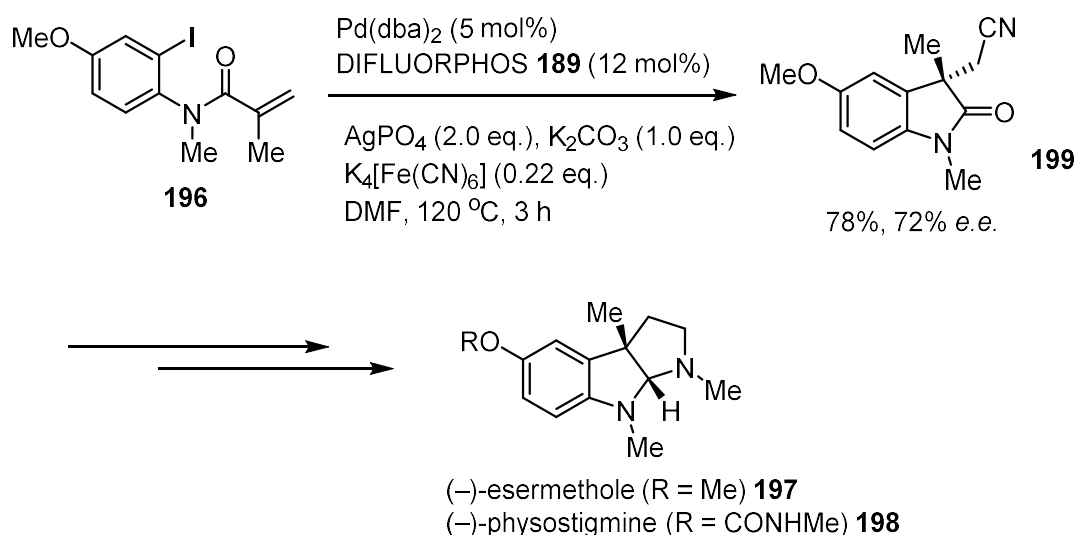


Scheme 34: The asymmetric Ag-catalysed Sakurai-Hosomi allylation of ketones **194**, with DIFLUORPHOS **189** as a ligand.

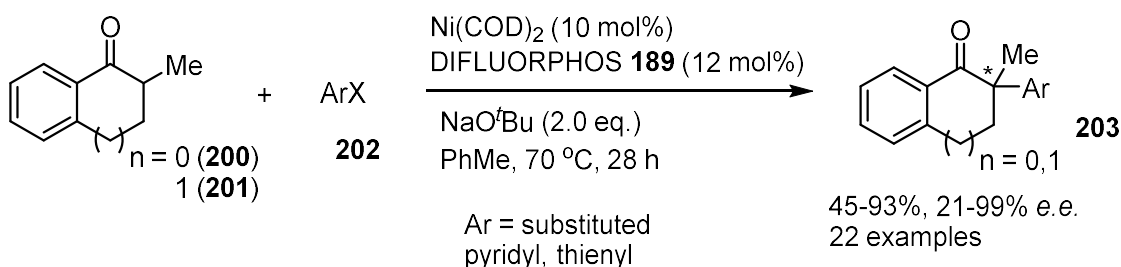
Other notable examples include the work by Zhu *et al.* on the asymmetric tandem Heck-cyanation of a 2-iodoanilide precursor **196** in the formal synthesis of natural products (–)-esermethole **197** and (–)-physostigmine **198**,¹¹⁶ which are inhibitors of acetyl- and butyrylcholineesterase. The cyano-oxindole product **199** was synthesised in a maximum of 72% e.e. by using DIFLUORPHOS **189** as a ligand (Scheme 35) – its superior enantioselectivity perhaps rationalised by an increase in electrophilicity of the Pd-centre, similar to that described by Keay *et al.* earlier in this report. For the Ni-catalysed asymmetric α -arylation of ketones, Hartwig *et al.* found that the substrate scope could be expanded from aryl chlorides to heteroaryl chlorides by using DIFLUORPHOS **189** as the ligand, rather than BINAP **51**.¹¹⁷ With the DIFLUORPHOS-Ni catalytic system, indanone **200** and tetralone **201** could be

arylated consistently with >90% e.e. with a range of pyridyl and thienyl halides **202** with electron-donating and electron-withdrawing substituents (Scheme 36).

Similar to DIFLUORPHOS **189**, other fluorinated electron-poor biaryl diposphine ligands include MeO-F₁₂-BIPHEP **204**^{118,119} reported by Sakai *et al.* and F₁₂-C₃-TunePhos **205**¹²⁰ by Zhou *et al.* (Figure 14); the latter being an fluorinated analogue of C₃-TunePhos **124** with a (*R,R*)-pentane-2,4-diol linker at the back of the structure. Both of these ligands were used to induce high enantioselectivity for the Rh-catalysed conjugate addition of arylboronic acids to α,β -unsaturated ketones, due to the enhanced Lewis acidity of the metal centre.



Scheme 35: The asymmetric synthesis of (-)-esermethole **197** and (-)-physostigmine **198**, via a Pd-DIFLUORPHOS-catalysed Heck-cyanation process.



Scheme 36: The asymmetric α -heteroarylation of ketones **200** and **201**, catalysed with a Ni-DIFLUORPHOS **189** system.

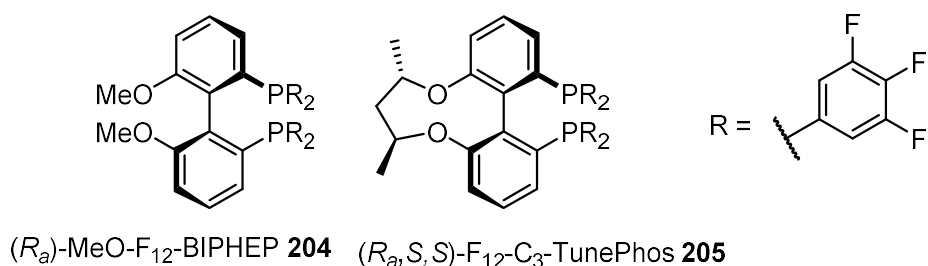


Figure 14: Other examples of fluorinated electron-poor biaryl diphosphine ligands.

1.5. Biheteroaryl diphosphine ligands with 5-membered rings

A method to simultaneously adjust the geometric and electronic properties of a biaryl diphosphine ligand, relative to a typical biphenyl based design, is to employ 5-membered heteroaromatic rings in the structure. The heteroatom in moieties such as furan and thiophene has mesomeric effects on the aromatic ring, so the electronic properties of the phosphine group can be tuned, depending on where it is bonded to the ring. Furthermore, if the biaryl bond links together two 5-membered rings, rather than 6-membered rings, the groups located *ortho*- to that bond, often the ligating phosphines, are positioned further away from each other in space, which potentially changes the bite angle in a metal-ligand complex.

1.5.1. Sulfur as the heteroatom

The first ligands of this kind, reported by Sannicolò *et al.*, were 2,2'-bis(diphenylphosphino)-4,4',6,6'-tetramethyl-3,3'-bibenzo[*b*]thiophene (TetraMe-BITIANP **206**) and the analogous compound without methyl groups, 2,2'-bis(diphenylphosphino)-3,3'-bibenzo[*b*]thiophene (BITIANP **207**) (Figure 15).^{121,122} The configurational stability of these ligands was confirmed by the ³¹P-NMR spectra of corresponding diastereomeric Pd-complexes, showing that the configuration was

retained in refluxing xylenes during the reduction of the corresponding phosphine oxide. However, the analogous 2,2'-bis(diphenylphosphino)-3,3'-bibenzo[*b*]furan ligand did not retain its configuration under the same conditions, perhaps due to the shorter C-O bond lengths (1.39 Å compared to 1.74 Å for C-S bonds) preventing atropisomerism. For the X-ray crystal analysis of (tetraMe-BITIANP)- and (BITIANP)-PdCl₂ complexes, despite the differences in structure between these ligands and BINAP **51**, similarities in geometry with the 7-membered metal-ligand chelating ring with analogous BINAP complexes were observed. The bibenzothiophene ligands **206** and **207** were also tested in the Ru-catalysed asymmetric hydrogenation of α - and β -ketoesters, as well as prochiral olefinic substrates; while high e.e. values were achieved, there was no overall improvement on those obtained with similar BINAP **51** complexes.

A similar ligand, 4,4'-bis(diphenylphosphino)-2,2',5,5'-tetramethyl-3,3'-bithiophene (BITIOP **208**) was later developed, in which the phosphine groups are positioned on the electron-rich 3-carbons.¹²³ The enhanced availability of the electron density to the phosphorus atom was shown by its electrochemical oxidation potential (0.57 V), which was lower than that of (non-atropisomeric) 2,2'-bis(diphenylphosphino)-5,5'-tetramethyl-3,3'-bithiophene (0.70 V). While the enantioselectivity obtained in asymmetric hydrogenation reactions was similar to that of BINAP **51** (oxidation potential of 0.63 V), the rate was increased by the greater Lewis basicity of BITIOP **208**.

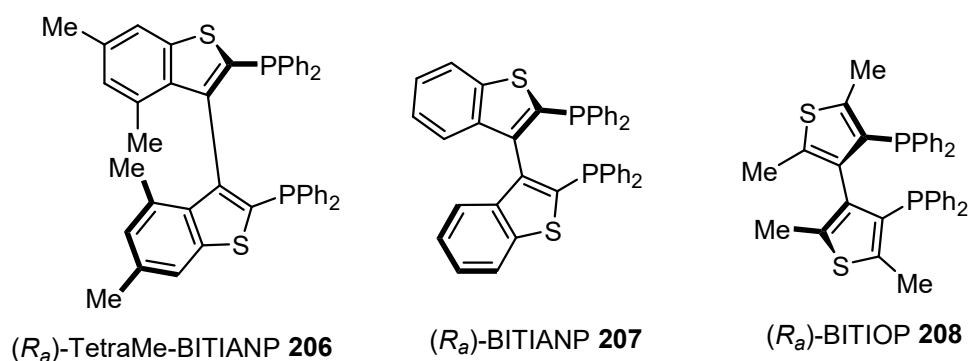


Figure 15: Axially chiral bibenzo[*b*]thiophene and bithiophene diphosphine ligands.

1.5.2. Nitrogen as the heteroatom

While the first biindolyl diphosphine ligand was synthesised by Berens *et al.*, no application towards an enantioselective reaction was reported.¹²⁴ Shortly afterwards, configurationally stable 3,3-dimethyl-1,1'-bis(diphenylphosphino)-2,2'-biindole (BISCAP **209**) and 2,2'-bis(diphenylphosphino)-1,1'-bibenzimidazole (BIMIP **210**) were reported by Sannicolò *et al.*, continuing their work on heterobiaryl diphosphine ligands (Figure 16).¹²⁵ The X-ray crystal data for (BIMIP)-PdCl₂ indicated a P-Pd-P bite angle of 95.02(5)°, ~3-5° wider than that of similar BINAP **51** complexes,^{62,126,127} which perhaps reflects the change in geometry due to the 5-membered rings in the ligand structure. In a later paper, the same authors, aiming to vary the electronic properties with the position of the phosphine groups, also reported the synthesis of 3,3'-bis(diphenylphosphino)-1,1'-dimethyl-2,2'-biindole (N-Me-2-BINP **211**) as well as the 1,1'-bis(methoxymethyl) derivative (N-MOM-2-BINP **212**).¹²⁸ Interestingly, a very close negative correlation was found between the electrochemical oxidation potential and log(*k_{obs}*) values for the Ru-catalysed hydrogenation of ethyl acetoacetate. This relationship demonstrates that an electron-rich ligand accelerates the rate of hydrogenation, but no correlation was found for the enantioselectivity.

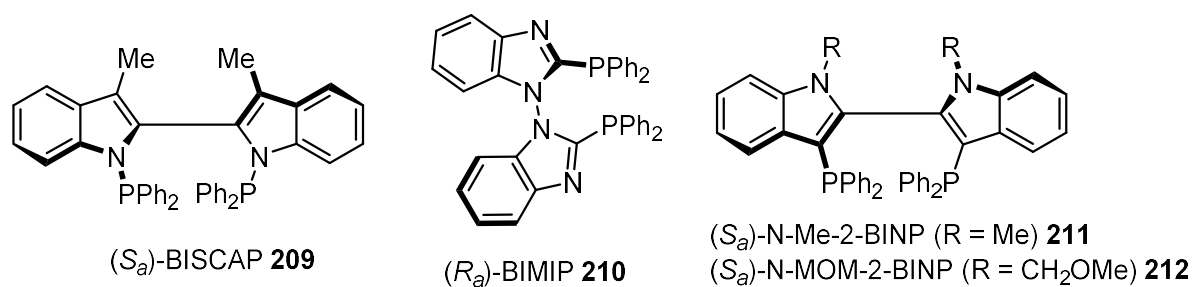
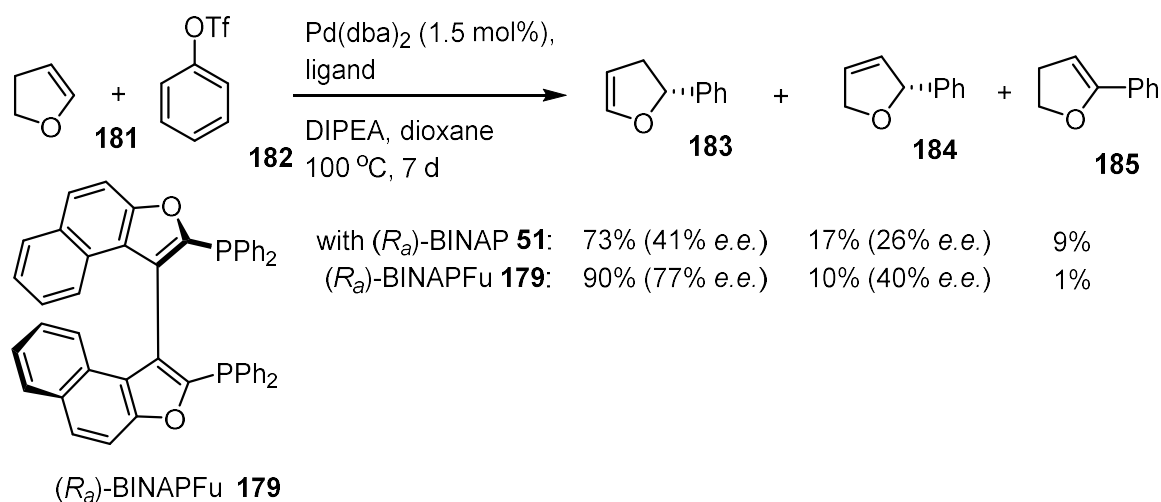


Figure 16: Axially chiral biindole and biimidazole disphosphine ligands.

1.5.3. Oxygen as the heteroatom

The design of the non-atropisomeric bibenzo[*b*]furan diphosphine ligand was modified by Keay *et al.* with the development of the axially chiral 2,2'-bis(diphenylphosphino)-3,3'-binaphtho[2,1-*b*]furan (BINAPFu **179**).¹⁰⁹ The authors assessed the Lewis basicity of the phosphorus atoms in the ligand by measuring the $^1J_{\text{PSe}}$ coupling constant of the corresponding phosphine selenide, and the value of 762 Hz indicated a more electron-poor ligand than BINAP **51** (738 Hz). For the asymmetric Heck reaction of 2,3-dihydrofuran **181** and phenyl triflate **182**, a variety of temperatures, solvents, bases and pre-catalysts were tested, but the enantioselectivity of BINAPFu **179** exceeded that of BINAP **51** every time. The optimised conditions of using Pd₂(dba)₃, Hünig's base and dioxane for 7 days at 100 °C formed the desired 2-phenyl-2,3-dihydrofuran product in 90% yield and 77% e.e., compared to the 73% and 41% e.e. obtained with BINAP **51** as the ligand (Scheme 37). Since the performance of BINAPFu **179**, for this reaction, was superior to that of the more electron-poor TetFuBINAP **180** (Scheme 37; *c.f.* Scheme 33), this suggests either that the small size of the furyl rings of TetFuBINAP **180** diminished the enantioselectivity, the moderate electron-poor character of BINAPFu **179** was key for optimal results, or that the change in geometry from the biaryl bond linking two 5-

membered rings in BINAPFu **179** was favourable for this intermolecular Heck process.

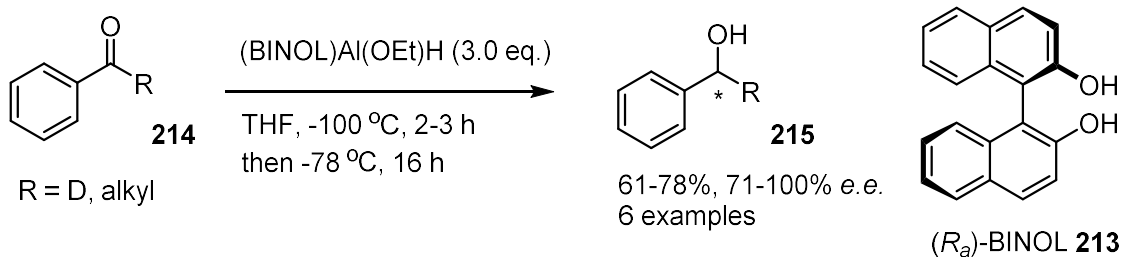


Scheme 37: The asymmetric Heck reaction of 2,3-dihydrofuran **181** and phenyl triflate **182**, with BINAPFu **179** and BINAP **51** as ligands.

1.6. Dihedral angles of axially chiral biaryl diol ligands

1.6.1. BINOL by Noyori

The axially chiral 1,1'-biaryl unit is also effective for transmitting chiral information from catalyst to substrate when present in diol ligands. As well as developing BINAP **51**, Noyori *et al.* first reported the use of the analogous diol ligand, BINOL **213**, in asymmetric synthesis.¹²⁹ The authors were able to use a BINOL-Al-hydride complex to reduce a series of alkyl phenyl ketones **214** in 71-100% e.e., thereby demonstrating the ability of an axially chiral biaryl unit to bias the orientation of the substrate towards the aluminium centre (Scheme 38). However, a super-stoichiometric quantity of the Al-BINOL reagent was required for this transformation, though the ligand was recoverable from the reaction mixture.

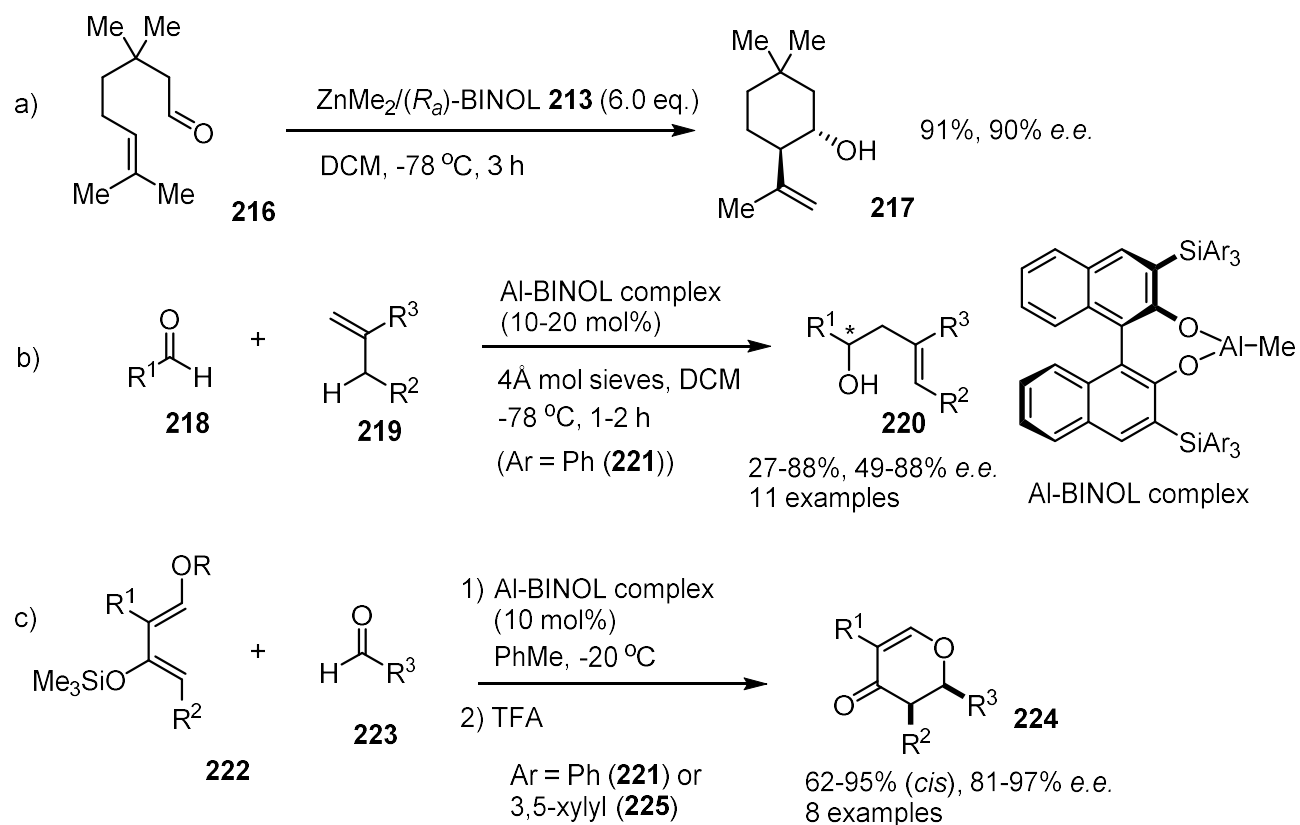


Scheme 38: The first application of BINOL **213** in asymmetric synthesis: the aluminium hydride mediated reduction of prochiral carbonyls **214**.

The Zn-BINOL-mediated asymmetric cyclisation of unsaturated aldehydes was reported by Yamamoto *et al.*, in which, for example, 3-methylcitronellal **216** was converted in 91% yield and 90% e.e. to the chiral cyclic alcohol **217** (Scheme 39, a).¹³⁰ While the *in situ* generated Zn-BINOL reagent acts as a Lewis acid in this transformation, and presumably is not consumed by the reaction, a superstoichiometric quantity of the reagent was required to induce the enantioselectivity.¹³¹

Nonetheless, the first instance of a BINOL derivative applied in catalytic amounts was also reported by the Yamamoto *et al.*, towards an asymmetric ene reaction.¹³² After the addition of 4Å molecular sieves to the system, for the reaction between several electron-poor aldehydes **218** and electron-rich olefins **219**, most of the enantioselectivity was retained when the molar quantity of a 3,3'-bis(triphenylsilyl)BINOL-Al complex **221** was reduced from 110 mol% to 10-20 mol% (Scheme 39, a). The enantioselectivity of the catalysed reactions were in the range of 49-88% e.e., and in some cases, these values were even improved compared to stoichiometric loadings. This chiral catalyst was also applied to the asymmetric hetero-Diels–Alder reaction between siloxydienes **222** and aldehydes **223**, followed by treatment of trifluoroacetic acid, to synthesise dihydro-γ-pyrone products **224** with excellent diastereo- and enantioselectivity (Scheme 39, b).¹³³ For some substrates,

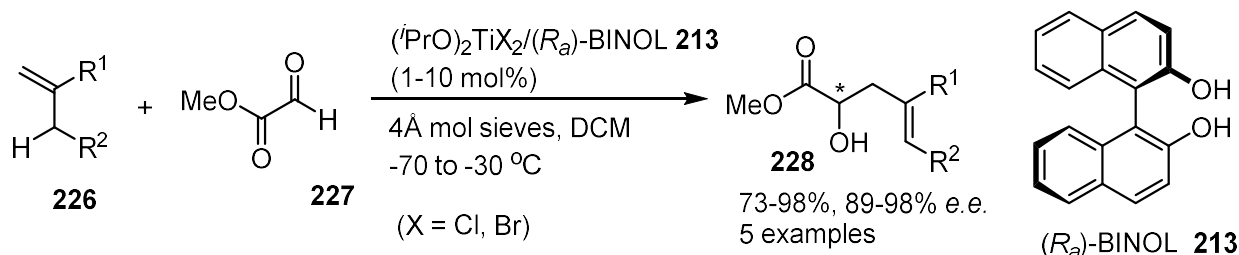
the selectivity could be improved by using the bulkier tri(3,5-xylyl)silyl derivative **225**, rather than triphenyl **221**, biasing further the orientation of the diene towards the aldehyde-Lewis acid complex.



Scheme 39: The Zn-BINOL-mediated asymmetric cyclisation of 3-methylcitronellal **216** (a), and the first examples of a BINOL **213** and derivatives in a chiral catalyst: the ene reaction with aldehydes **218** and olefins **219** (b), and the hetero-Diels–Alder with siloxydienes **222** and aldehydes **223** (c).

The first example of BINOL **213** itself, rather than a derivative, as a ligand in a chiral catalyst was reported by Nakai *et al.*, with an asymmetric ene reaction.¹³⁴ An *in situ* prepared Ti-BINOL complex was used to catalyse the reactions between several olefins **226** and methyl glyoxylate **227**. The chiral alcohols **228** were produced in 89-98% e.e. with as little as 1 mol% catalyst loading, and again, the presence of 4 Å molecular sieves was essential for the high selectivity (Scheme 40). Nonetheless,

with the absence of the bulky silyl groups, the great stereochemical influence of the axially chiral backbone of the catalyst was demonstrated with these reactions.



Scheme 40: The first example of BINOL **213** as a chiral ligand, for the ene reaction between methyl glyoxylate **227** and olefins **226**.

1.6.2. Modification of biaryl diol dihedral angle

Since these first examples, BINOL **213** has been applied as a ligand in asymmetric Lewis acid catalysis towards a seemingly endless range of reactions and substrates, due to the flexibility of the binaphthyl backbone permitting coordination to many metals and metalloids, and the rigidity of those BINOL complexes.¹³⁵ However, like with BINAP **51** optimal results are not universally obtained by using BINOL **213**, so it is essential to tailor the structure of the chiral diol to maximise the stereoselectivity for certain reactions or substrates. Similar to chiral diphosphine ligands, the axially chiral biphenyl unit offers great flexibility to alter the bite angle (β) of a metal-diol complex, as sterically different substituents, particularly at the 6,6'-positions, lead to a different dihedral angle (θ) of the ligand (Figure 17, *c.f.* Figure 7).

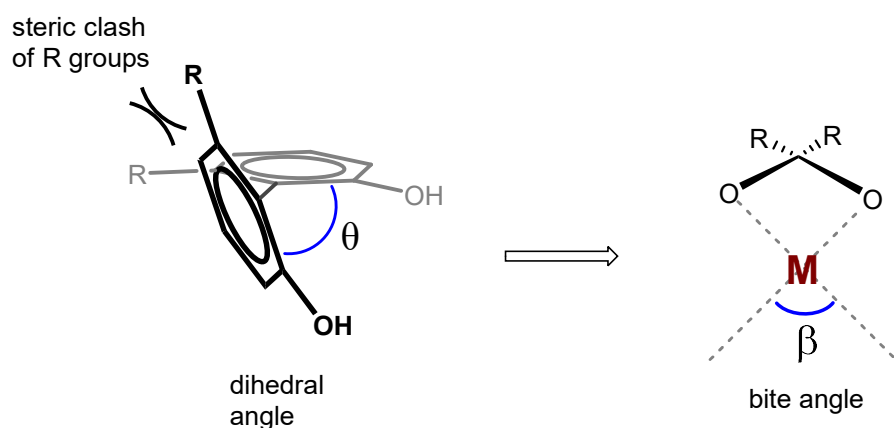
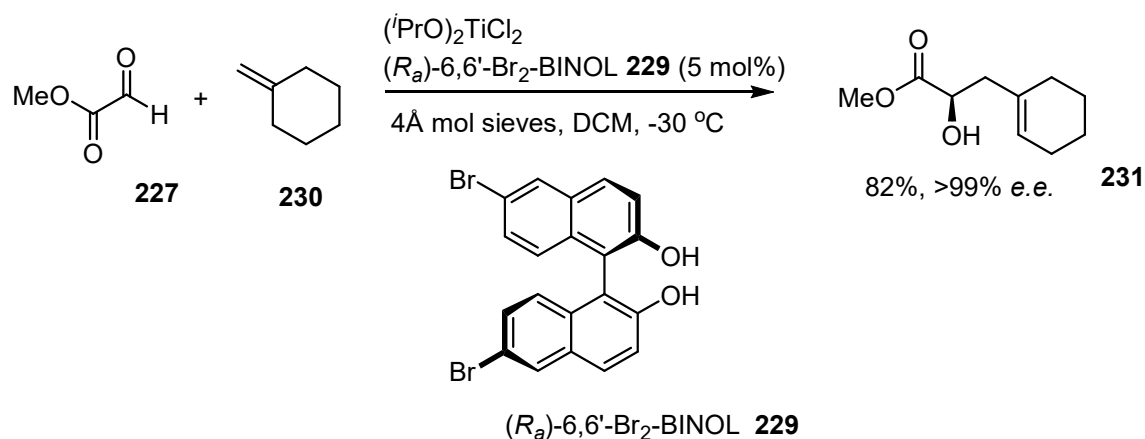


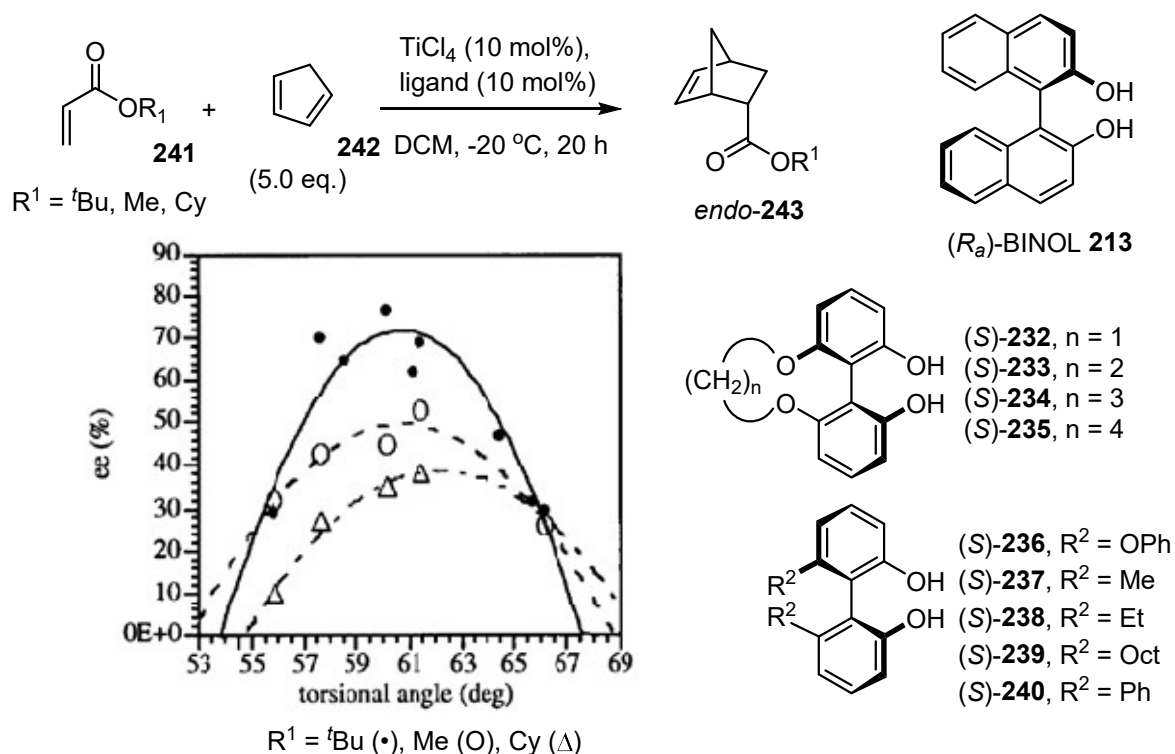
Figure 17: The dihedral angle (θ) of an axially chiral biphenyl-diol ligand, and its relationship with the bite angle (β) of the metal-diol complex.

With this rationale in mind, Mikami *et al.* applied a 6,6'-dibromo-BINOL derivative **229** as a ligand for the Ti-catalysed ene reaction between olefins and methyl glyoxylate.¹³⁶ The authors hypothesised that the orientation of the halide ligands X in the (BINOL)TiX₂ complexes in Scheme 40 helped to direct the trajectory of the olefin towards the coordinated glyoxylate. By increasing the metal-diol ligand bite angle (O-Ti-O), from the increased repulsion of the brominated naphthyl rings of **X**, the metal-dihalide internal angle (X-Ti-X) is compressed, increasing the degree of shielding of one of the glyoxylate enantiofaces. Consequently, the reaction between methyl glyoxylate **227** and methylenecyclohexane **230** was improved to >99% e.e. (Scheme 41). Intriguingly, the reaction with α -methylstyrene achieved 85% e.e. even when the catalyst had an enantiopurity of only 70%, which demonstrated an asymmetric amplification effect.



Scheme 41: The Ti-catalysed ene reaction with methyl glyoxylate **227** and methylenecyclohexane **230**, with 6,6'-Br₂-BINOL **229** as a ligand.

A variety of axially chiral 6,6'-dialkoxy-1,1'-biphenyl-2,2'-diol derivatives **232-240** were synthesised in high enantiopurity, by Harada *et al.*, from the achiral 1,1'-biphenyl-2,2',6,6'-tetrol by using (–)-menthone as a chiral template.^{137,138} This library of ligands included a series of biphenyl diols in which the two phenyl groups were linked by an ether bridge of a systematically varied length (**232-235**), similar to TunePhos (*c.f.* Table 1). Using this ligand library, the authors studied the relationship between the calculated dihedral angle and the enantioselectivity of a Ti-catalysed Diels–Alder reaction with acrylate esters **241** and cyclopentadiene **242** (Scheme 42).¹³⁹ Despite the small difference (~10°) between the smallest and largest dihedral angle, an angle of 61-63° was clearly shown to be optimal for the enantioselectivity for these reactions. Any deviation from the optimal angle resulted in a sharp decrease in e.e. values, thereby demonstrating the high sensitivity of the selectivity towards the ligand geometry.



Scheme 42: The Ti-catalysed asymmetric Diels–Alder reaction of acrylate esters **241** and cyclopentadiene **242**, using biphenyldiol ligands **232-240** varying in dihedral angle.

1.6.3. *H₈*-BINOL

After their work on the Ti-BINOL-catalysed asymmetric addition of diethylzinc to benzaldehyde derivatives,¹⁴⁰ Chan *et al.* investigated the use of the partially hydrogenated variant *H₈*-BINOL **244** in similar reactions.¹⁴¹ Similar to *H₈*-BINAP **86**, the saturated domain of the *H₈*-BINOL **244** ligand (Figure 18) is non-planar, resulting in increased steric repulsion between the aryl groups and thus, an increased dihedral angle. The change in geometry meant that, for a collection of *ortho*-, *meta*- and *para*-substituted benzaldehydes **245**, using *H₈*-BINOL **244** as a ligand led to an improvement in enantioselectivity every time compared to using BINOL **213** (Scheme 43). Furthermore, by using triethylaluminium instead of diethylzinc, the formation of undesired aldehyde reduction products was reduced to a minimum.¹⁴² Also under these conditions, similar improvements to the enantioselectivity could be

made by using H₈-BINOL **244** rather than BINOL **213** as the ligand. However, the catalyst system was not general for the choice of alkyl group on the alkylating agent, as the use of trimethylaluminium reduced the selectivity dramatically from 90-99% e.e. to 40-50% e.e., and using triisobutylaluminium led to exclusive reduction of the aldehydes. The influence of a dihedral angle towards the enantioselectivity of this reaction was corroborated by Ding *et al.*, as they found the e.e. values obtained with the non-C₂-symmetric H₄-BINOL **247** ligand (Figure 18) fell in between those obtained with the less saturated BINOL **213** and the more saturated H₈-BINOL **244**.¹⁴³

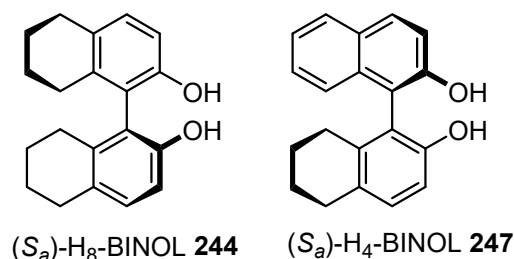
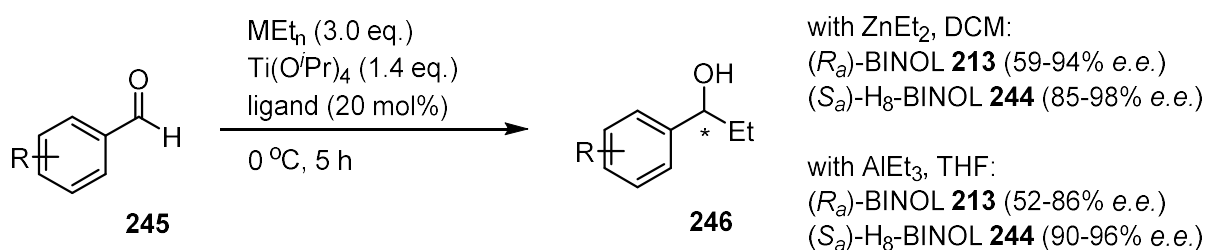


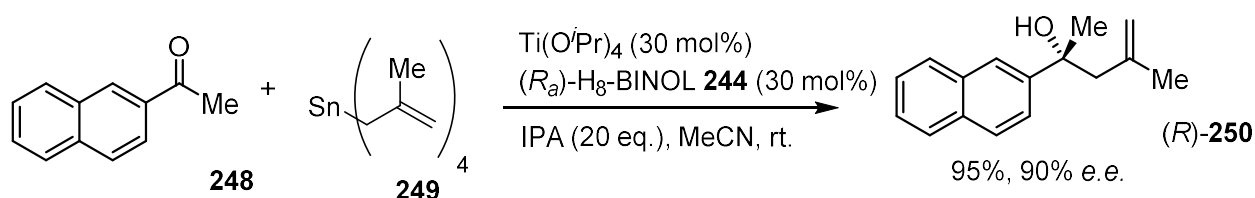
Figure 18: Partially hydrogenated derivatives of BINOL **213**.



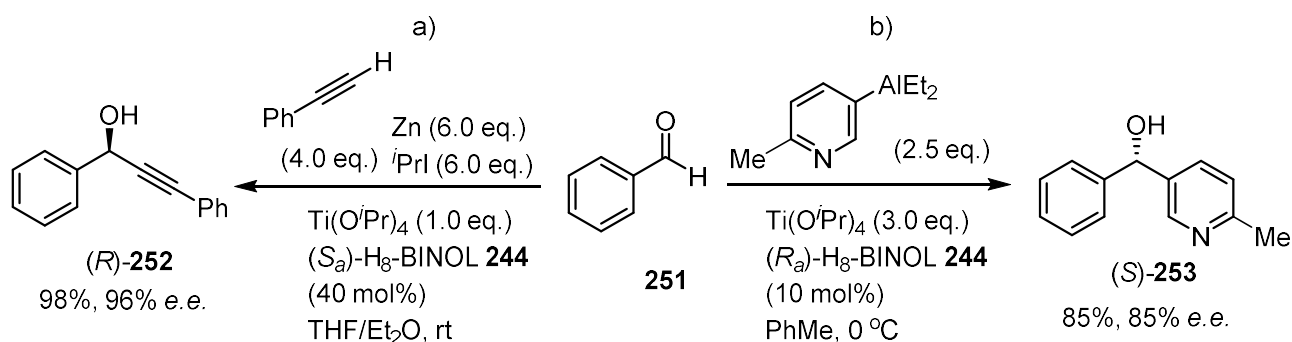
Scheme 43: The Ti-catalysed asymmetric addition of diethylzinc and triethylaluminium to benzaldehyde derivatives **245**, with BINOL **213** and H₈-BINOL **244** as ligands.

The wide dihedral angle of H₈-BINOL **244** has led to a privileged status for this ligand. It has been shown to be specialised for the asymmetric Ti-catalysed nucleophilic addition of organometallic reagents to carbonyls, providing superior enantioselectivities compared to other chiral diol ligands for the addition of

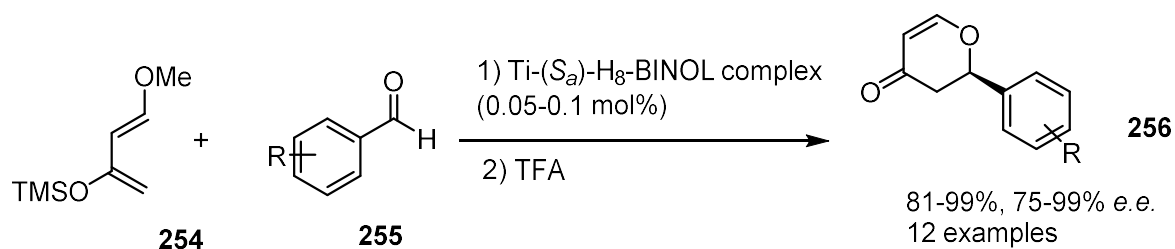
methallylstannanes **249** to ketones (**248**) (Scheme 44),¹⁴⁴ reactions of *in situ* generated alkynylzinc reagents with aldehydes (e.g. **251**) (Scheme 45, a),¹⁴⁵ and addition of pyridylaluminium reagents to benzaldehyde **251** and derivatives thereof (Scheme 45, b).¹⁴⁶ Furthermore, the versatility of H₈-BINOL **244** has also been shown by Ding *et al.* to induce the highest enantioselectivities in a solvent free Ti-catalysed hetero-Diels–Alder reaction to synthesise dihydro-γ-pyrones **256** (Scheme 46), in a unique, high-throughput combinatorial optimisation process involving 13 different chiral diol ligands.¹⁴⁷ Finally, the enantioselectivities for asymmetric Sm-catalysed epoxidation of α,β-unsaturated *N*-acylpyrroles by Shibasaki *et al.* were improved upon by switching the ligand from BINOL **213** to H₈-BINOL **244**.¹⁴⁸ This transformation was exploited for the synthesis of intermediates **257** and **258** towards natural antifungal products such as strictifolione **259**, as well as the marine natural product (+)-phorboxazole A **260** (Figure 19).¹⁴⁹



Scheme 44: An example of the asymmetric Ti-H₈-BINOL-catalysed methallylation of ketones.



Scheme 45: Examples of the Ti-catalysed asymmetric addition of alkynes (a) and substituted pyridines (b) to aldehydes, with H₈-BINOL **244** as a ligand.



Scheme 46: The solvent-free asymmetric Ti-catalysed hetero-Diels–Alder reaction, with H₈-BINOL **244** as a ligand.

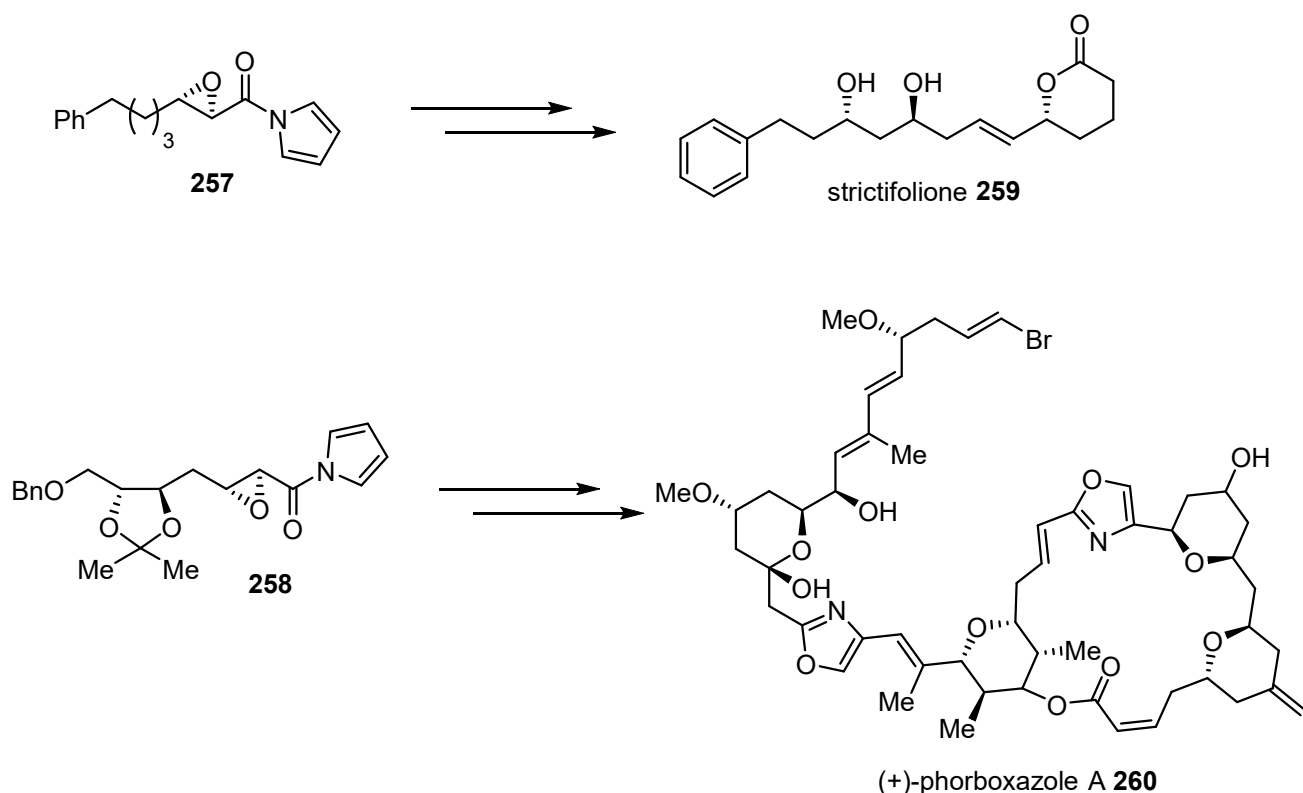


Figure 19: Chiral epoxide intermediates **257** and **258** towards natural products, synthesised through the Sm-H₈-BINOL-catalysed epoxidation of α,β -unsaturated *N*-acylpyrroles.

1.7. Conclusion

To conclude, the examples of chiral phosphine and diol ligands detailed in this introduction represent just a small fraction of those that have ever been employed towards asymmetric homogeneous catalysis, since research on the subject was first reported half a century ago. However, they demonstrate the endurance of the axially

chiral biaryl motif when it comes to chiral ligand design. The biaryl unit is structurally rigid when coordinated to a metal centre and it has plentiful flexibility towards the incorporation of functional groups to systematically alter the bite angle of its metal-ligand complex and/or vary the electronic properties of the ligating atom. It is for these reasons that axially chiral ligands have been, and will for a long time continue to be hugely prevalent for an extraordinary variety of enantioselective catalytic reactions, from the milligram scale of the research laboratory to the tonne scale of industrial processes.

2. RESULTS AND DISCUSSION

2.1. Project aims and rationale

Axially chiral molecules are used ubiquitously as chiral homogeneous catalysts for asymmetric synthesis. The first examples of axially chiral diol and diphosphine ligands, BINOL **213** and BINAP **51** respectively (Figure 20), are incredibly versatile in their application and influential in their design. Both of these groundbreaking chiral ligands were introduced by Nobel-prize winning chemist Ryoji Noyori.^{27,129} Due to the simple synthetic methods to produce and resolve their individual enantiomers,^{150,151,152} they both are widely available on a large scale and constitute a common starting point as ligands in the optimisation of stereoselective synthetic transformations. Because these ligands can be used for many, mechanistically quite different, asymmetric reactions, they are often described as ‘privileged structures’.¹⁵³

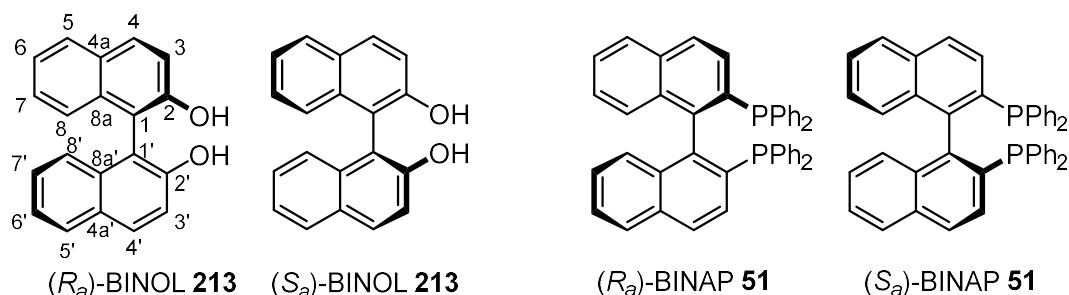


Figure 20: The two enantiomers of BINOL **213** and BINAP **51**. The numbering system for the aromatic structure is included for (R_a) -BINOL **213**.

As widely applicable as BINOL **213** and BINAP **51** are, it is near impossible for a chiral catalyst to be ‘universally applicable’, which is why derivatives of these compounds are continually synthesised and screened in new asymmetric reactions. These processes may be chemical reactions which have not yet had an element of chirality applied successfully towards them, so a chiral catalyst is applied for the first

time in order to induce stereoselectivity in that chemical context. Sometimes, good enantiomeric excesses have already been achieved for particular substrates, and the successful ligand is required to be derivatised to broaden the scope of prochiral substrates that can be transformed with high stereoselectivity. Other times, high enantiomeric excesses may have only been achieved for a reaction via an approach other than homogeneous catalysis, such as heterogeneous catalysis, biocatalysis or the use of a chiral auxiliary. One may then wish to exploit the advantages that homogeneous catalysis could have over these alternatives, such as a tolerance of more forcing conditions, flexibility in the scale at which the reaction is being operated, or an ability to perform mechanistic studies in more detail, on the reaction in question.

If the vast quantity of different axially chiral catalysts that have been applied in asymmetric catalysis in the literature is considered, it is apparent that, for a particular transformation on a particular prochiral substrate, a 'tailor-made' catalyst tends to be needed in order to bring about the maximum stereoselectivity. Since the advent of BINOL **213** and BINAP **51**, the property of axial chirality has endured well in the design of chiral diol and phosphine ligands, because binaphthyl, and other atropisomeric biphenyl motifs, can reliably transfer their stereochemical information to the orientation the substrates adopt towards the catalyst. In order to design derivatives of this core of the ligand (**261** and **262**), substituents on the aromatic rings can be put in place of hydrogen atoms, by changing the starting materials used to make the ligand, or by installing the groups at some stage midway through the synthesis (Figure 21). For example, electronic properties of the coordinating groups can be manipulated by installing electron-donating or -withdrawing groups on the biphenyl backbone. With diphosphine ligands, the ancillary groups directly bonded to

the phosphorus atom are another source of diversity within this template. When the donating ability of the oxygen or phosphorus atom is changed, this can promote certain steps of the catalytic cycle by stabilising or destabilising certain oxidation states, for example. Steric properties of the ligand can also be affected by substituents in multiple ways. The use of bulky substituents at the 3,3'-positions of the backbone, adjacent to the donor atom, can restrict the freedom of the substituent in the chiral pocket, and therefore possibly enhance the selectivity of the reaction. Alternatively, changing the substituents at the 6,6'-positions of the structure can change the dihedral angle of the molecule, and therefore the bite angle on coordination to a metal centre, which can either change the freedom of the substituent or favour certain geometries of the metal complex.

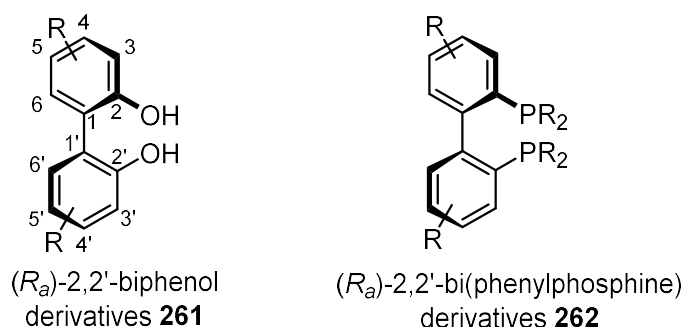
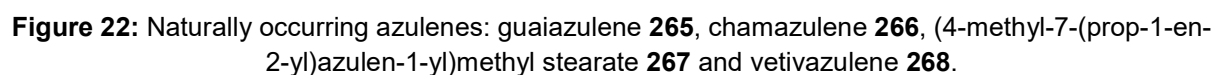


Figure 21: Typical templates for axially chiral biaryl diol **261** and diphosphine ligands **262**. The numbering system for the aromatic structure of 2,2'-biphenol derivatives **261** is included.

2.1.1. Properties of azulenes

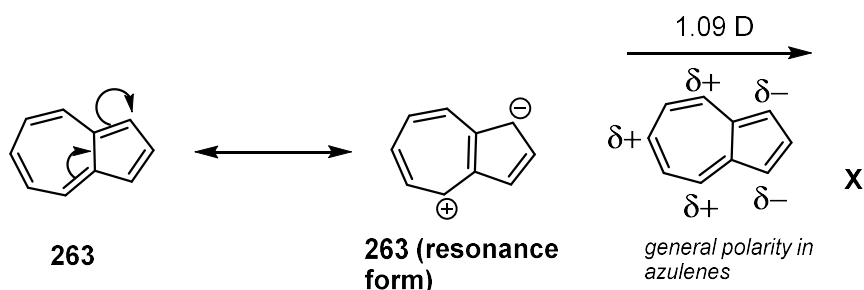
These variations of the ligand templates above allow for great flexibility in catalytic design. However, the variation of the aromatic motif has received relatively little consideration; the persistence in the use of benzenoid molecules is evidence of a degree of conservatism when manipulating the factors that influence enantioselectivity. Azulene **263**, a non-benzenoid aromatic isomer of naphthalene **264**, has not yet been incorporated in the design of chiral molecules for asymmetric

Derived from the Spanish word for its colour ('*azul*', meaning 'blue'), the azulene motif is made up of a 5-membered ring fused to a 7-membered ring, instead of two fused phenyl rings. This class of molecule is ordinarily not sourced from crude oil, but is found as the chromophores of certain pigments within organisms (Figure 22). Guaiazulene **265**, the most widely occurring azulene derivative in nature, is a terpene-derived substance found in oil of guaiac, from the wood of the Pala Santo tree in South America. A similarly structured compound, chamazulene **266**, is found in chamomile blue, a deep blue essential oil of the chamomile plant. The indigo milk cap mushroom, or *Lactarius indigo*, contains (4-methyl-7-(prop-1-en-2-yl)azulen-1-yl)methyl stearate **267** as a pigment, which gives it a vivid blue colour. Another terpenoid, vetivazulene **268**, is isomeric with guaiazulene **265** and is extracted from vetiver oil.



74

structures both individually satisfy Hückel's rule of $4n+2$ π -electrons and thus, are aromatic. As a result, azulene has a dipole value of 1.09 D, and is therefore remarkably polarised for a hydrocarbon.¹⁵⁴



Scheme 47: Resonance forms and polarity of azulene **263**.

The chromophoric properties of azulene **263** contrast with the isomeric naphthalene **264**, since the latter is a colourless solid. This characteristic is explained by viewing the molecular orbital coefficients for the frontier molecular orbitals (Figure 23).¹⁵⁵ Azulene **263** is a non-alternant molecule, so the HOMO and LUMO are spatially different from each other. Thus, in the S_1 electronic state (one electron in each orbital), there is little overlap and therefore only a small amount of repulsive pairing energy. This S_0 – S_1 gap corresponds to the absorption of visible light. With naphthalene, an alternant hydrocarbon, the HOMO and LUMO are spatially similar, so there is a greater repulsive energy between the two electrons when in an S_1 state. Therefore, with the greater energy gap, naphthalene **264** does not absorb electronically in the visible region, but only in the UV region.

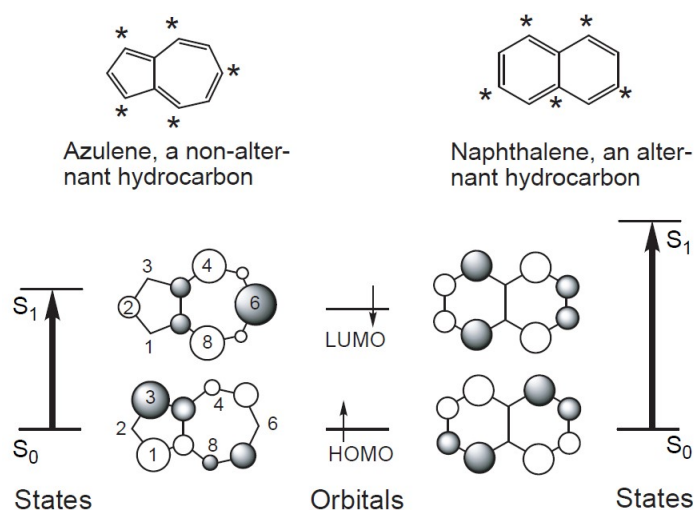


Figure 23: The frontier molecular orbitals for azulene **263** and naphthalene **264**, showing differences in molecular orbital coefficients (asterisks denote carbons alternating between S_0 and S_1), taken from Liu.

Because of their unique properties, azulene derivatives have featured in a wide range of applications: in medicine, they have shown activity as anti-inflammatory agents,¹⁵⁶ as anti-arrhythmic agents,¹⁵⁷ as anti-diabetic agents,¹⁵⁸ as anti-cancer agents,¹⁵⁹ in treatment for erectile dysfunction¹⁶⁰ and in anti-retroviral drugs for HIV treatment.¹⁶¹ Their vivid, tuneable¹⁶² colours have been exploited in their application towards solar cells,^{163,164} electrochromic materials,¹⁶⁵ halochromic materials,^{166,167} visible light triggered photoswitches,¹⁶⁸ near-infrared absorbing pigments¹⁶⁹ and as probes for soft metal cations¹⁷⁰ and fluoride anions.¹⁷¹ Their dipole moment has meant they have shown promising results as semiconductors.^{172,173} The tunability of the absorption properties of the aromatic system has allowed application in fluorescent bioimaging.¹⁷⁴ The chemistry of azulene-containing porphyrin analogues and their transition metal complexes have also been extensively studied by Lash *et al.*¹⁷⁵

2.1.2. Azulene as a motif in chiral ligand design

Referring back to the template for axially chiral diol and diphosphine ligands (Figure 21), the incorporation of a biazulene group in place of the biphenyl (or binaphthyl) group would change the ligand properties in a different, more creative way compared to a simple change of substituents on the aromatic system, or on the phosphorus atom. Since azulene **263** has very different electronic and steric properties to naphthalene **264**, it follows that any chiral ligands made from a binaphthalene moiety will behave differently if replaced with biazulene. The azulene monomers are unsymmetrical, so they may also be coupled together at different sites to make, for instance, either 1,1'-biazulene **269**, 2,2'-biazulene **270** or 4,4'-biazulene **271** moieties (Figure 24), each possessing significantly different properties.

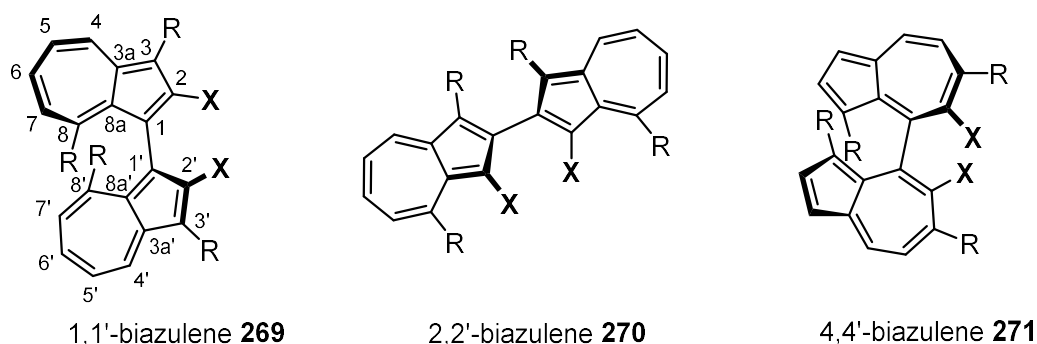


Figure 24: Designs for different biazulene-based ligands, where donor group X = OH, PR₂ and R groups to induce atropisomerism or point towards the reactive site in the catalyst. The numbering system for the aromatic structure of 1,1'-biazulene **269** is included.

If the 1,1'-biazulene-based ligands **269** are compared side by side with 1,1'-binaphthalene based ligands **272**, it is clear to see that there would be a larger bite angle on coordination to a metal for the 1,1'-biazulene (Figure 25). In the 1,1'-biazulene skeleton, the biaryl bond connects two aromatic 5-membered rings rather than 6-membered rings. Thus, any ligating atoms in the 2,2'-positions are now

further away in space from each other because of the smaller internal angle of the aromatic ring. The geometry of the R-groups in the 3,3'-positions is also affected as they are also further away from each other in space, which can also have an effect on the orientation of the substrate.

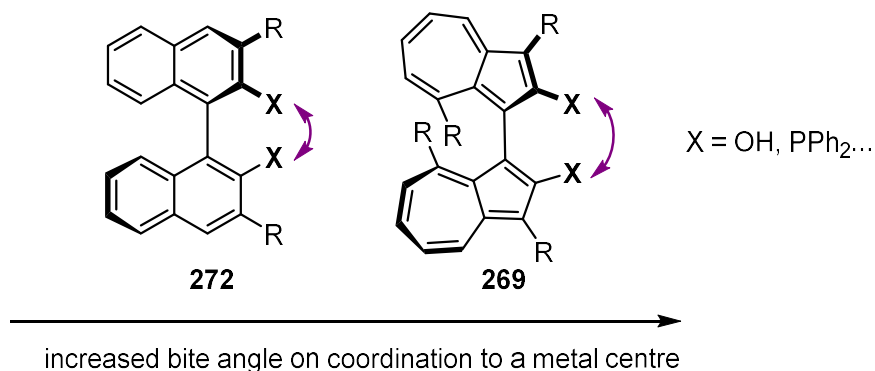


Figure 25: The proposed increase in bite angle for a chelating ligand coordinating to a metal centre, if the biaryl bond connects two 5-membered rings rather than 6-membered rings.

As a consequence of the biaryl bond connecting 5-membered rather than 6-membered rings, the hydrogen atoms on the 8,8'-positions may have insufficient steric interaction to ensure atropisomerism in the 1,1'-biazulene-based ligands **269**, unlike in analogous 1,1'-binaphthyl species **272**. Biazulene species such as 2,2'-dimethyl-1,1'-biazulene **273**,¹⁷⁶ diethyl 2,2'-diamino-8,8'-diphenyl-[1,1'-biazulene]-3,3'-dicarboxylate **274**¹⁷⁷ and 10,10'-bibenzo[a]azulene **275**¹⁷⁸ have all been resolved into configurationally stable enantiomers, whereas the enantiomers of 2,2'-dimethoxy-1,1'-biazulene **276**,¹⁷⁶ once resolved, racemised rapidly at room temperature (Figure 26). The configurational instability of the latter biazulene **276** may be explained by additional degrees of freedom of the 2,2'-methoxy groups compared to 2,2'-methyl groups, allowing rotation around the axial bond. Several derivatives of dimethyl 4,4',8,8'-dimethyl-[1,1'-biazulene]-2,2'-dicarboxylate **277** have

also been synthesised, which would probably be expected to be chiral, but no analysis into their axial chirality had been carried out by the authors.¹⁷⁹

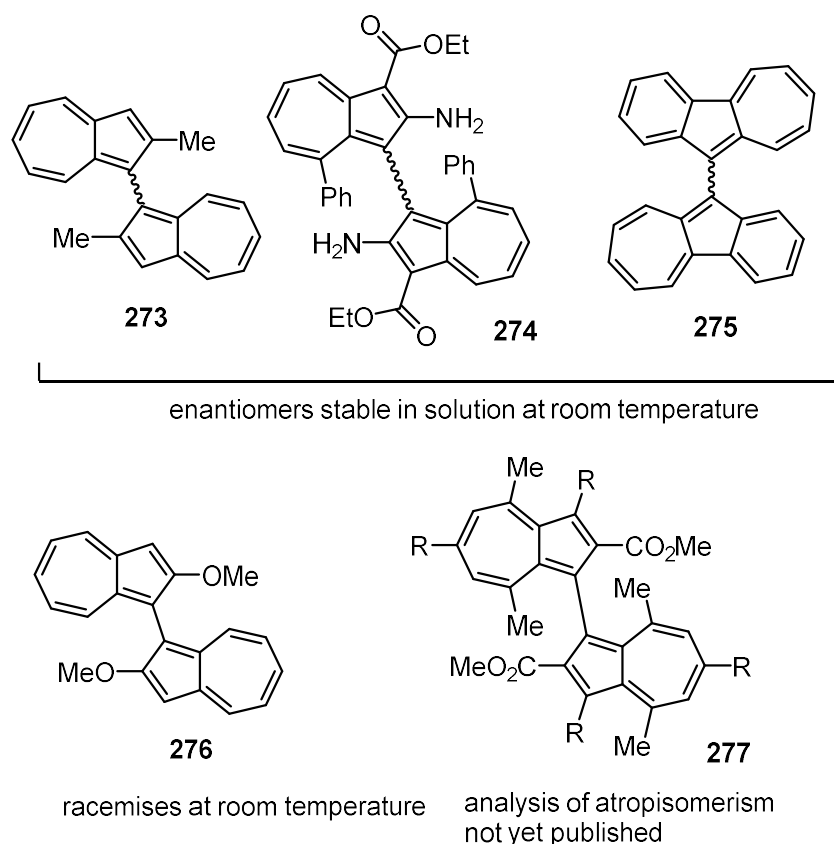


Figure 26: Derivatives of 1,1'-biazulene, of which the axial chirality and configurational stability has been studied, or would be expected to exhibit atropisomerism.

The usual ways to vary the bite angle of axially chiral metal-chelating ligands are either to change the substituents around the biphenyl unit, e.g. the methylene acetal group of SEGPHOS **84** in place of the fused phenyl ring on BINAP **51** gives the former ligand a smaller dihedral angle (67.2° and 86.2° respectively¹¹⁴ for free diphosphine); or to increase the number of atoms in the metal-ligand cycle, like with NAPHOS **52** or BINAPO **53**, which possess methylene groups and oxygen atoms, respectively, between the binaphthyl unit and phosphine groups (Figure 27). Aside from the bithiophene, biindole and biimidazole diphosphine ligands reported by Sannicolò *et al.* (Figure 15, Figure 16) or BINAPFu **179** by Keay *et al.* (Figure 17),

changing the number of atoms in the rings either side of the biaryl bond is underexplored as a means of changing the bite angle for a chelating biaryl ligand. It is noteworthy that this change in bite angle is brought about without necessarily an alteration with the dihedral angle, which adds to the uniqueness of the design of the biazulene ligands. Furthermore, if the bite angle of a chelating ligand-metal complex can be increased without an accompanying increase in the number of atoms in the metal ligand cycle, in the style of NAPHOS **52**, then the rigidity of the complex does not need to be compromised.

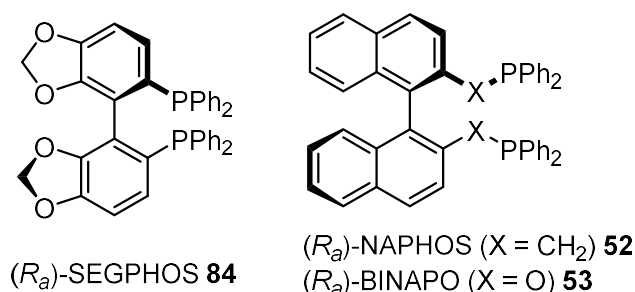


Figure 27: Examples of ligands with different bite angles to BINAP **51**: SEGPBOS **84**, which has a smaller dihedral angle, NAPHOS **52**, which has methylene groups between the chiral backbone and phosphorus atoms, and BINAPO **53**, which has oxygen atoms between the chiral backbone and phosphorus atoms.

If the use of a 1,1'-biazulene unit (**269**) increases the bite angle of the ligand compared to 1,1'-binaphthyl units (**272**), it follows that using a 4,4'-biazulene unit (**271**) as a core of the ligand would result in a decrease in bite angle (Figure 28). This time, since the axial bond links together two 7-membered rings rather than 5-membered or 6-membered rings, it follows that the ligating atoms 'ortho' to that bond will be oriented closer to each other in space. The unsymmetrical nature of azulenes therefore lends itself well to flexible ligand design, with regards to their geometric properties.

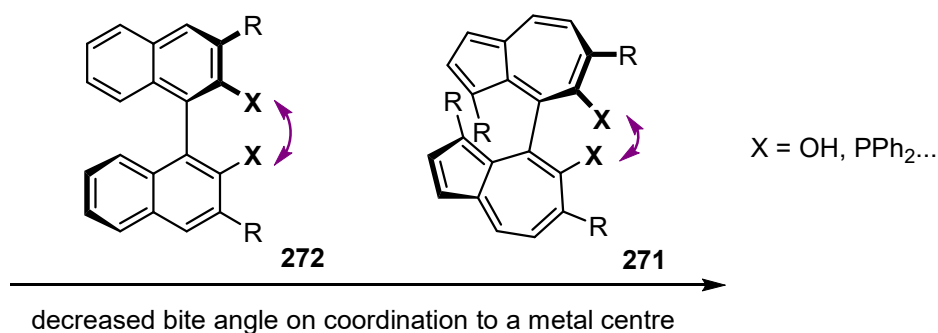


Figure 28: The proposed decrease in bite angle for a chelating ligand coordinating to a metal centre, if the biaryl bond connects two 7-membered rings rather than 6-membered rings.

The unusual electronic, as well as geometric, properties of azulene may also be exploited to change the characteristics of the ligand. With a 2,2'-biazulene moiety as a backbone (**270**), installing the ligating atoms at the adjacent electron-rich 1,1'-positions of the azulene would lead to an increased donation ability for that ligand compared to any position on the less polarised benzene or naphthalene moiety (Figure 29).

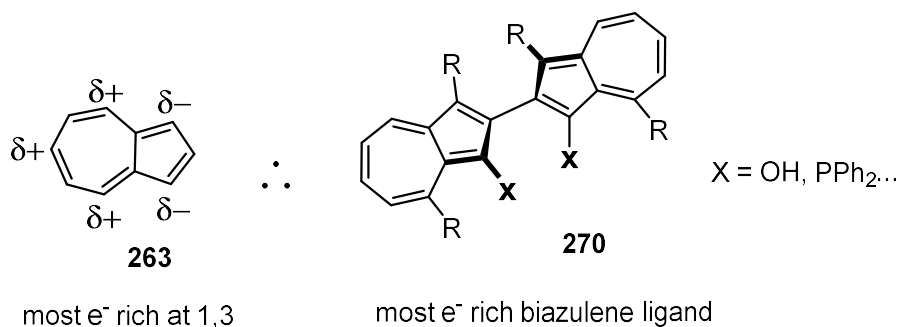
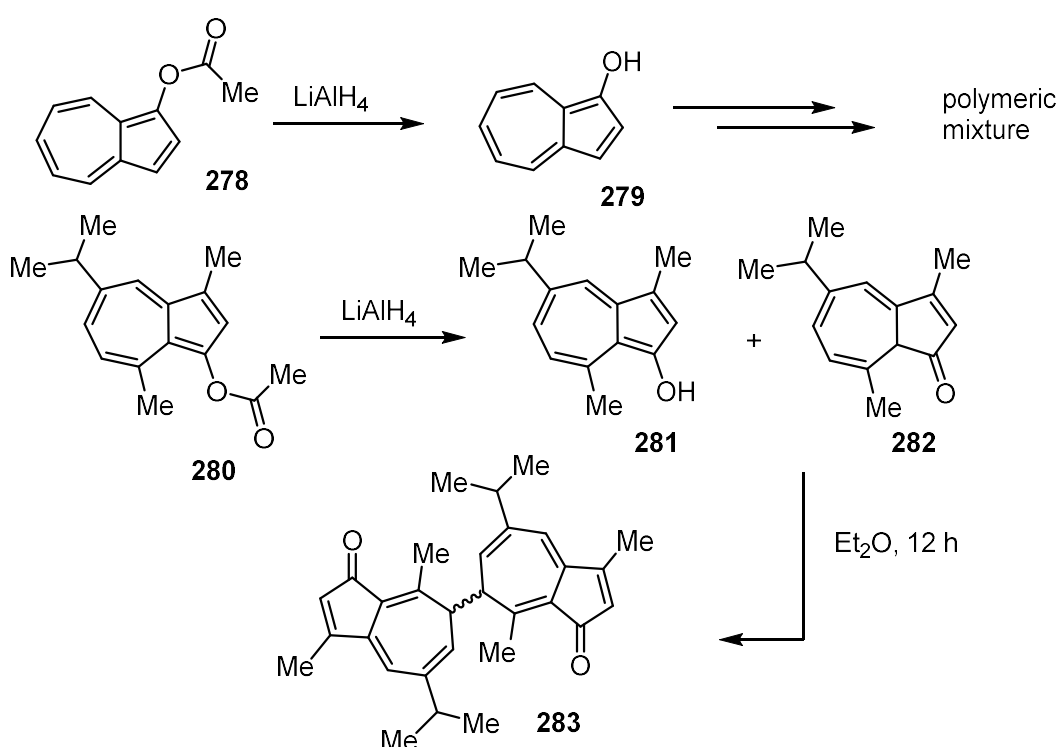


Figure 29: Since the 1- (and 3-) positions on azulene are the most electron-rich, a 2,2'-biazulene with ligating atoms at 1,1'-positions will have maximised electron donation to the metal centre.

The potential drawback with this ligand design is that azulenes hydroxylated at the 1-position have been shown to be unstable at room temperature. The simplest form, 1-hydroxyazulene **279**²⁷⁸ itself, was formed by Asao *et al.* through LiAlH₄ reduction of its O-acetyl protected form **278**, but on warming to room temperature from -30 °C,

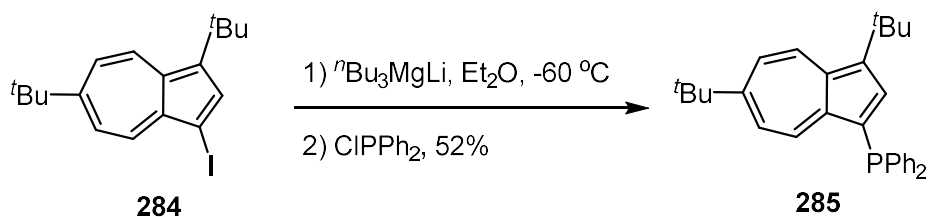
decomposed to a polymeric mixture.¹⁸⁰ The derivative 3-hydroxyguaiazulene **281**, formed through the same methodology, reacted with its tautomeric form **282** to make a dimeric diketone species **283** (Scheme 48). It may be possible prevent these mechanisms from taking place if electron-withdrawing substituents are present in the azulene structure at the 3,3'-positions. However, since the primary motivation to design these ligands is to maximise the donating ability, the electron-withdrawing group may negate the desired electronic properties.



Scheme 48: The formation and fate of 1-hydroxyazulene **278** and 3-hydroxyguaiazulene **281**.

Fortunately, an azulene with a phosphine group at the 1-position has previously been isolated under ambient conditions. The azulen-1-yl phosphine **285** was formed in a satisfactory yield by Ito *et al.* through a halogen-magnesium exchange of 1,6-di-*tert*-butyl-3-iodoazulene **284** with lithium tri-*n*-butylmagnesate, followed by quenching with chlorodiphenylphosphine (Scheme 49).¹⁸¹ Thus, a 2,2'-biazulene-1,1'-

diphosphine may be more feasible to synthesise and apply in asymmetric catalysis than the corresponding diol ligand.



Scheme 49: The formation of (3,6-di-*tert*-butylazulen-1-yl)diphenylphosphine **285**, an electron-rich phosphine species.

By the same principle, if the ligating atom is bonded to the electron-poor positions of azulene, this will cause the lone pair of that atom to become more extensively conjugated with the aromatic system and reduce donation to the metal centre. As a result, there is a choice as to where the ligating atom should be for an electron-poor ligand, that is, either the 6-position or 4-position, which therefore allows some flexibility in this design (Figure 30). Assuming a 5,5'-biazulene as the core of the structure, having the ligating atoms at the 4,4'-positions (**286**) would perhaps result in a chiral 'pocket' formed by the surrounding fused 5-membered rings, resembling the 'vaulted' biaryl diol ligands VANOL **288** and VAPOL **289** (Figure 31).¹⁸² Conversely, installing the donor atoms at the 6,6'-positions (**287**) would produce a more sterically 'open' reactive site, perhaps more suitable for more sterically encumbered substrates.

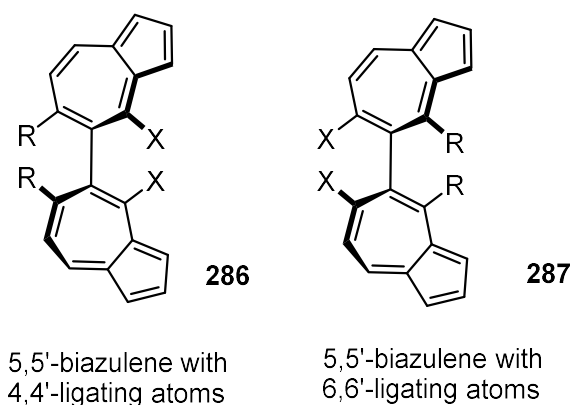


Figure 30: Electron-poor ligands designed around 5,5'-biazulene backbone, with R groups to ensure atropisomerism X = OH, PR₃.

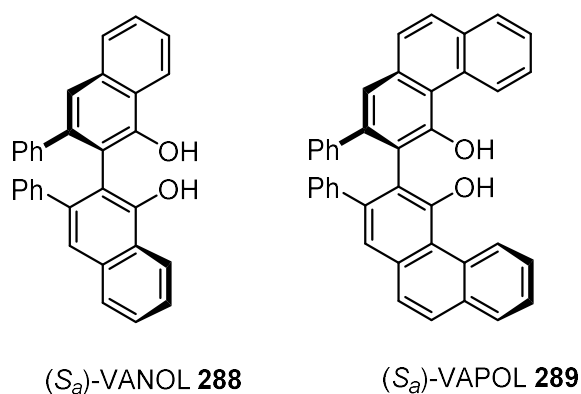
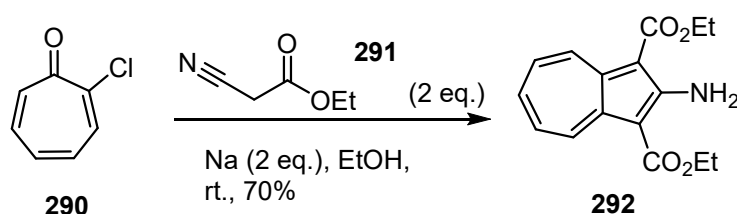


Figure 31: The 'vaulted' biaryl diol ligands, (S_a)-VANOL **288** and (S_a)-VAPOL **289**.

2.1.3. Nozoe's method for the synthesis of azulenes

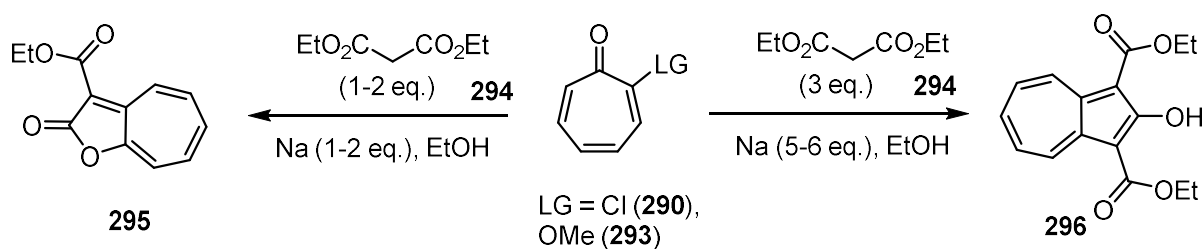
With an extensive range of molecular designs, of varying steric and electronic character, there was an opportunity to build a library of interesting, uniquely constructed ligands for asymmetric catalysis. It was decided for the focus to be placed, at first, on the synthesis of the ligands based around the 1,1'-biazulene unit, due to the relative abundance of dependable chemistry in the literature for the functionalisation of the 5-membered ring of the azulene. One of the most common ways to construct an azulene skeleton is through the method of renowned Japanese chemist Tetsuo Nozoe, who had an extensive career primarily studying azulenes and

other troponoids over a timescale of seven decades. The reaction is characterised by the condensation of an active methylene compound (AMC) (i.e. a species with a methylene group directly between two electron-withdrawing groups, which gives the protons a low pK_a value) and a tropone derivative with a leaving group adjacent to the carbonyl group. The process was first described in 1956, where 2-chlorotropone **290** was introduced to an ethanolic solution of ethyl cyanoacetate **291** and sodium ethoxide to give diethyl 2-aminoazulene-1,3-dicarboxylate **292** in 70% yield (Scheme 50).¹⁸³



Scheme 50: One of the earliest examples of an azulene produced by the reaction of a troponoid with an active methylene, with diethyl 2-aminoazulene-1,3-dicarboxylate **292** produced from 2-chlorotropone **290** and ethyl cyanoacetate **291**.

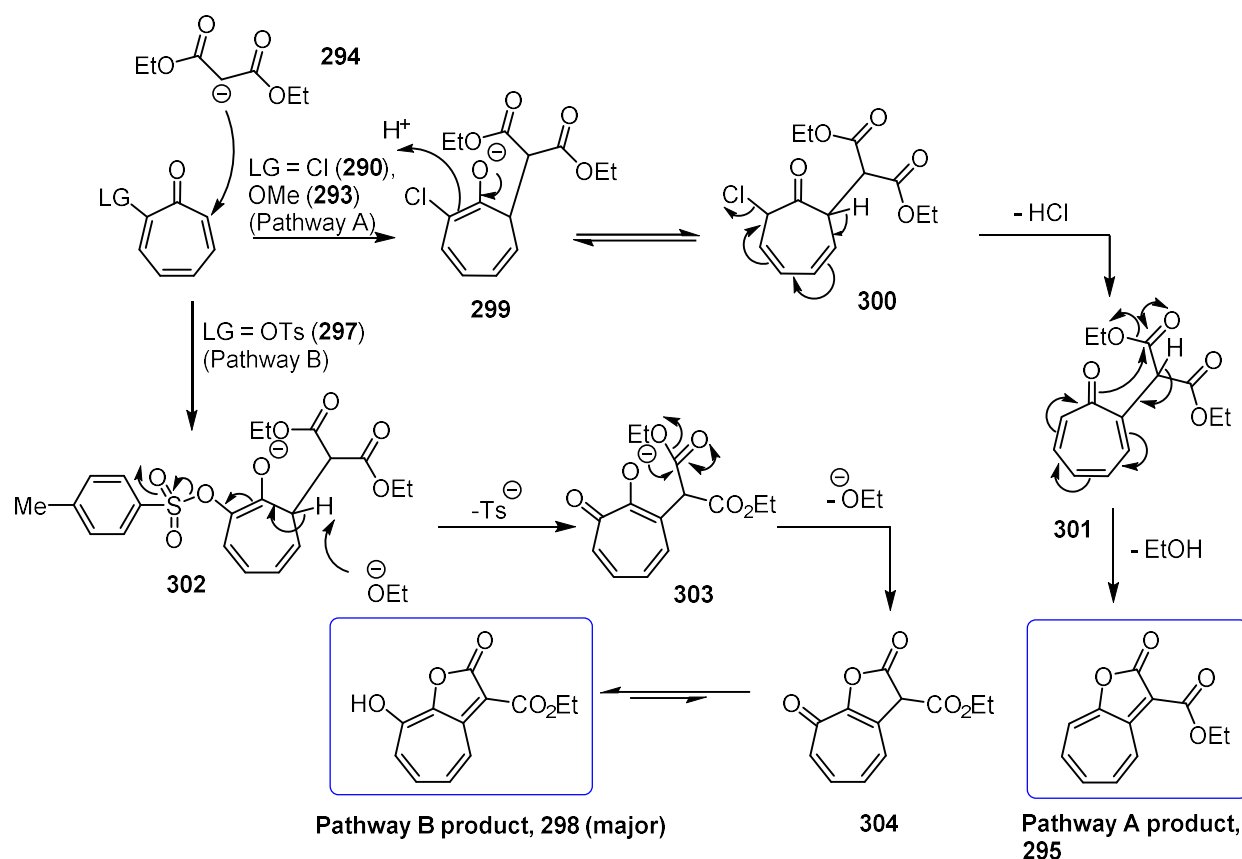
In some cases, the conditions can be changed to favour formation of different products. In the case of the reaction of either 2-chlorotropone **290** or 2-methoxytropone **293** with diethyl malonate **294** and sodium ethoxide, using one or two equivalents each of the active methylene compound and base favoured ethyl 2-oxo-2*H*-cyclohepta[*b*]furan-3-carboxylate **295** as the product; whereas a larger excess of active methylene (3 equivalents) and base (5-6 equivalents) produced diethyl 2-hydroxyazulene-1,3-dicarboxylate **296** (Scheme 51).¹⁸⁴ This observation is logical, since a molecule of troponoid, which possesses multiple electrophilic sites, is more likely to be attacked by two molecules of the sodium salt of diethyl malonate when the equivalents of diethyl malonate and sodium ethoxide are both increased.



Scheme 51: Changing the equivalents of active methylene and base relative to the troponoid can favour either the azulene (**296**) or *2H*-cyclohepta[*b*]furan-2-one (**295**) derivatives.

If a tosylate (**297**) (or benzenesulfonate) is the leaving group on the troponoid, the reaction of these species with various active methylenes in the presence of sodium ethoxide results in a *2H*-cyclohepta[*b*]furan-2-one product, but with a hydroxy group at the 8-position (**298**). When there is a small excess of sodium ethoxide (1-2 equivalents), referring to previous mechanistic postulations and studies,^{185,186} the sodium salt of diethyl malonate **294** will begin by attacking the 7-position of the tropone derivative (Scheme 52). For leaving groups like chloride or methoxide (Pathway A), the intermediate adduct **299** then tautomerises back to the keto form **300**, followed by elimination of hydrogen chloride (or methanol), and the basic conditions drive the cyclisation of **301** to produce ethyl 2-oxo-*2H*-cyclohepta[*b*]furan-3-carboxylate **295**. A more unusual process takes place when the leaving group is a tosylate (Pathway B). As with pathway A, the sodium salt of diethyl malonate attacks the 7-position, but this is followed by an ethoxide promoted elimination of a *p*-toluenesulfinate anion from **302**. The cyclisation of **303** occurs to form the lactone **304**, and then the ketone at the 8-position tautomerises to form ethyl 8-hydroxy-2-oxo-*2H*-cyclohepta[*b*]furan-3-carboxylate **298**. When tosyloxypone **297** is used, the product **295** from pathway A is also formed in a low yield, but the two compounds can be separated during the work-up procedure. Due to the low pK_a of the hydroxy group on product **298**, the anionic form is aqueous-soluble at a basic pH, so the

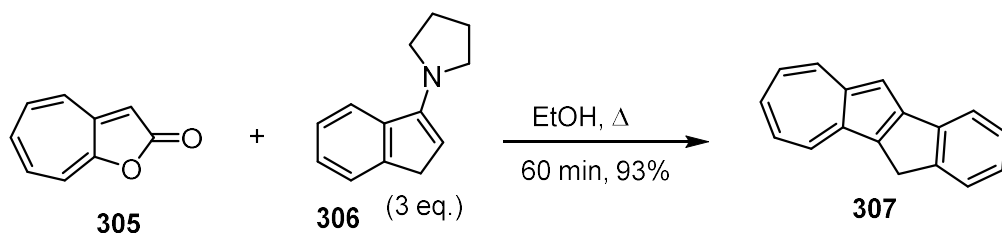
minor component **295** can be washed out with organic solvent. The presence of a base as strong as sodium ethoxide may be key towards pathway B taking place, as similar treatment of 2-tosyloxypone **297** with dimethyl malonate and sodium methoxide in methanol favours formation of methyl 2-oxo-2*H*-cyclohepta[*b*]furan-3-carboxylate i.e. the product obtained via pathway a, without a hydroxy group.¹⁸⁷



Scheme 52: The mechanisms to show the formation of ethyl 2-oxo-2*H*-cyclohepta[*b*]furan-3-carboxylate **295** and 2-chlorotropone **290**, and the formation of ethyl 8-hydroxy-2-oxo-2*H*-cyclohepta[*b*]furan-3-carboxylate **298** from 2-tosyloxypone **297**.

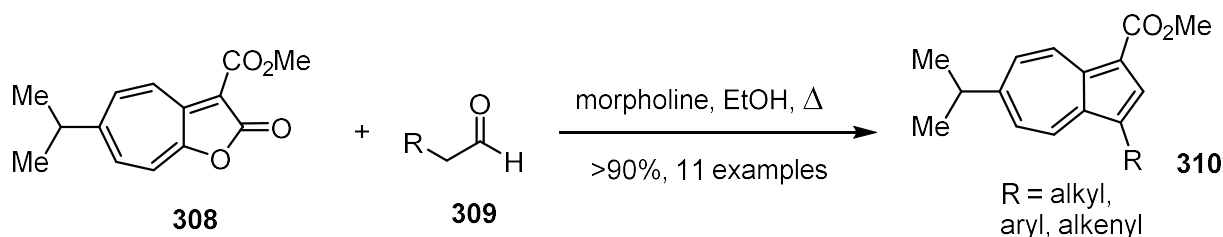
The 2*H*-cyclohepta[*b*]furan-2-one derivatives can be converted to an azulene through an [8+2]-addition-elimination process with an electron-rich olefin, expelling carbon dioxide as the leaving group. This transformation was achieved at first in 1971 by Takase *et al.*, with enamines as the olefinic component,¹⁸⁸ and an impressive later example came from the formation of the fused product 11*H*-

indeno[2,1-*a*]azulene **307** from 2*H*-cyclohepta[*b*]furan-2-one **305** and 1-(1*H*-inden-3-yl)pyrrolidine **306** in 93% yield (Scheme 53).¹⁸⁹



Scheme 53: The formation of 11*H*-indeno[2,1-*a*]azulene **307** from 1-(1*H*-inden-3-yl)pyrrolidine **306** and 2*H*-cyclohepta[*b*]furan-2-one **305**.

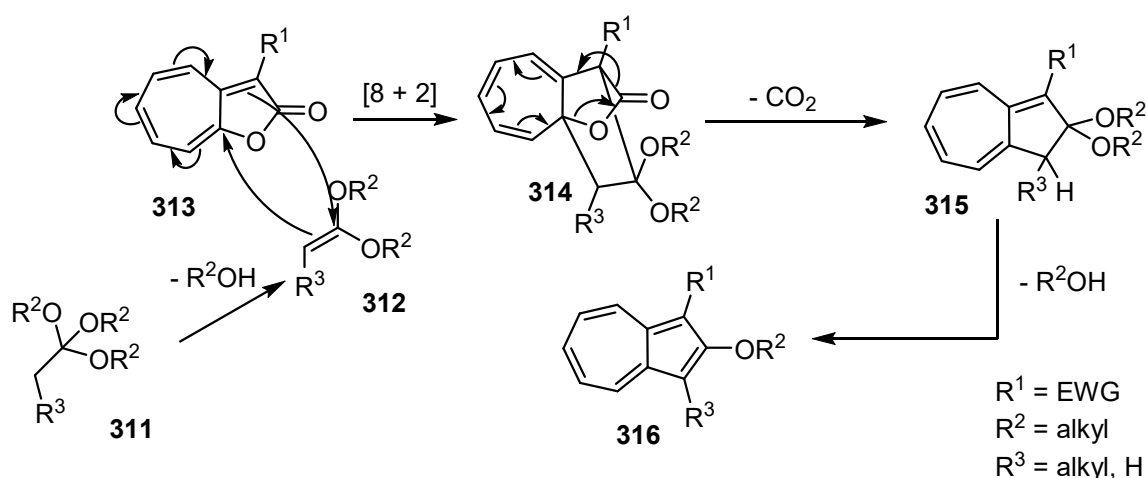
The scope was then expanded to include aldehyde-derived enamines,¹⁹⁰ and a further development came in the synthesis of methyl 6-isopropylazulene-1-carboxylate derivatives **310** substituted at the 3-position with various alkyl, alkenyl and aryl groups.¹⁹¹ These azulenes **310** were formed in over 90% yield each time from methyl 6-isopropyl-2-oxo-2*H*-cyclohepta[*b*]furan-3-carboxylate **308** and *in situ* generated morpholino-enamines from the corresponding aldehydes **309** (Scheme 54). These azulenes were then converted to various azulen-1-ylsulfonates, which were shown to have anti-ulcer activity.



Scheme 54: The formation of 3-substituted azulenes **310** from methyl 6-isopropyl-2-oxo-2*H*-cyclohepta[*b*]furan-3-carboxylate **308** and *in situ* generated enamines.

A similar transformation was then achieved by Nozoe *et al.*, using vinyl ethers as the olefinic component, albeit at a higher temperature due to their reduced

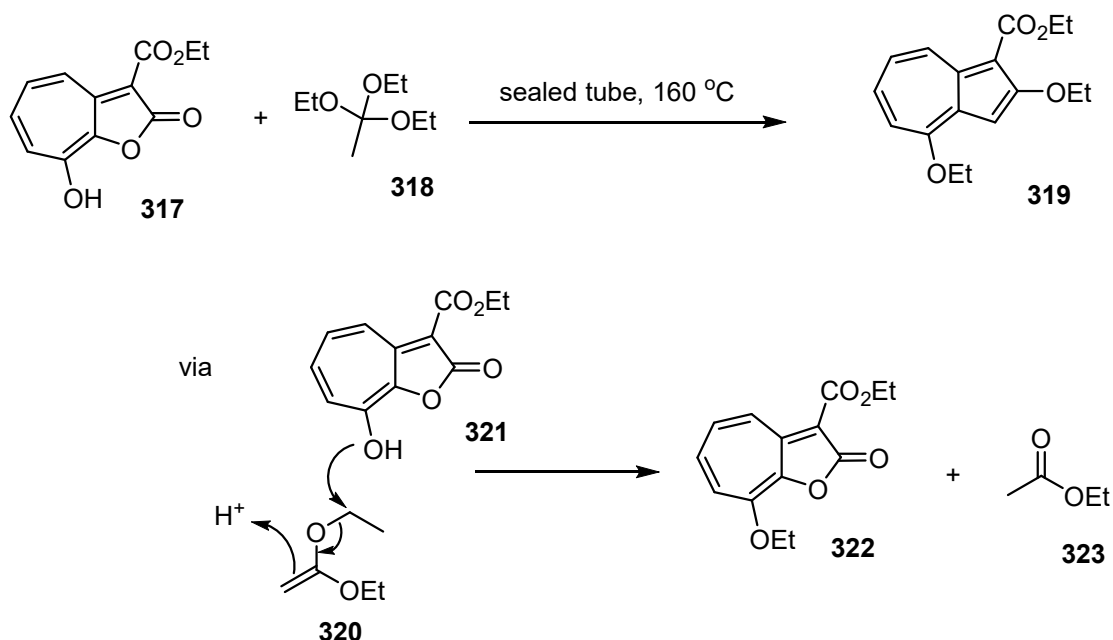
nucleophilicity compared to enamines.¹⁹² The key advantage of this reaction is that a ketene acetal can be made thermally, *in situ*, through the elimination of an alcohol from an orthoester (**311**).¹⁹² The use of a ketene acetal provides a convenient method to synthesise an azulene with an ether functionality at the 2-position. As shown by the mechanism (Scheme 55), the *in situ* generated ketene acetal **312** undergoes a cycloaddition to the 2*H*-cyclohepta[*b*]furan-2-one **313**, leading to the elimination of carbon dioxide from the adduct **314**. The alcohol is then eliminated from the final intermediate **315** to yield the azulene **316**, gaining aromaticity. When the azulene has already been made with just a hydrogen atom or alkyl group at the 2-position, it is challenging to subsequently introduce different functionalities at this position, so an alkoxy group provides a useful handle for further functional group interconversion.



Scheme 55: The plausible mechanism for the synthesis of 2-alkoxyazulenes **316** from the 2*H*-cyclohepta[*b*]furan-2-one **313** and orthoester **311**.

In addition to this, the reaction of ethyl 2-oxo-2*H*-cyclohepta[*b*]furan-3-carboxylate **317** with triethyl orthoacetate **318** produced the corresponding azulene product **319**, accompanied with the alkylation of the 8-hydroxy group (Scheme 56). It appears

energetically favourable for the ketene acetal **320** to act as the alkylating agent, as it would result in the production of a stable ester **322**, though the mechanism was not discussed in the paper.



Scheme 56: The synthesis of ethyl 2,4-diethoxyazulene-1-carboxylate **319** from ethyl 2-oxo-2H-cyclohepta[b]furan-3-carboxylate **317** and triethylorthoacetate **318**, with mechanism suggested by us for the ethylation step.

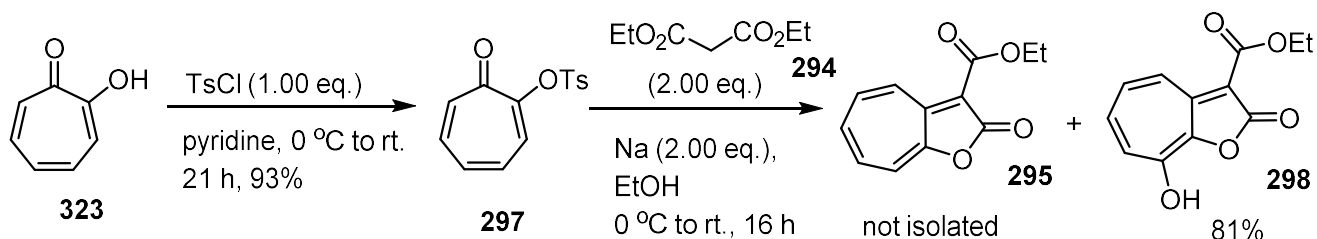
2.2. Development of 1,1'-biazulene-2,2'-diphosphine ("1,1'-BazPhos")

2.2.1. Foundations of synthesis based around Nozoe's method

Originally, the focus of the project was the synthesis and application of 1,1'-biazulene-2,2'-diphosphine ligands, rather than of 1,1'-biazulene-2,2'-diol ligands. An azulene species like **319**, created by Nozoe's process outlined in Scheme 56, seemed like an ideal precursor towards the 1,1'-biazulene-2,2'-diphosphine ligand for a number of reasons. Firstly, it was envisaged that the aforementioned alkoxy group at the 2-position could be converted to a triflate in two steps, which could be then converted to diphenylphosphine in a nickel-catalysed cross coupling reaction

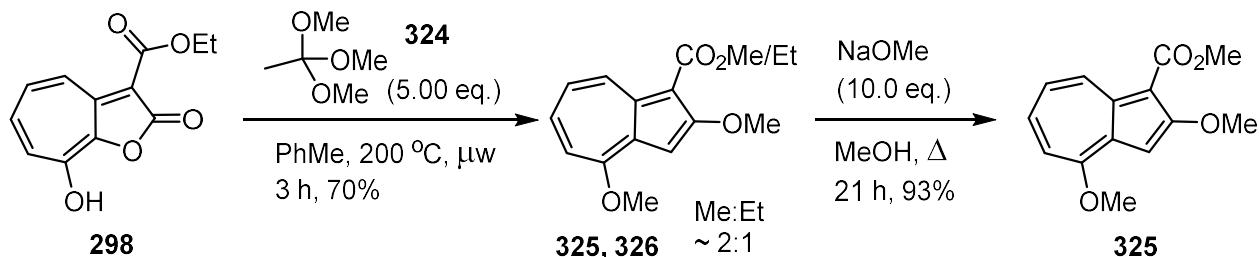
analogous to that used in the synthesis of BINAP **51**.¹⁵² Also, one of the electron-rich 1- and 3-positions is already occupied, or “protected”, by an ester group, reducing the risk of oligomerisation with whichever process is chosen to couple the two azulene units together. If required, the ester group should also be removed by the treatment with hot *orthophosphoric acid*,¹⁹⁴ or with the treatment with DIBAL-H, reduced to a methyl group.¹⁹⁵ Finally, the 4-position of the azulene is also substituted with an alkoxy group, which has more steric hindrance than a hydrogen atom, and would therefore hopefully ensure atropisomerism in the 1,1'-biazulene species.

The first step of the synthesis was to produce 2-tosyloxypone **297**, which was achieved through the reaction of commercially available tropolone **323** with 4-toluenesulfonyl chloride, with pyridine as the solvent (Scheme 57).¹⁹⁶ This reaction could be operated at a scale of 100 mmol in a near-quantitative yield every time. The product, 2-tosyloxypone **297** was then reacted with diethyl malonate **294** in the presence of freshly made sodium ethoxide to form ethyl 8-hydroxy-2-oxo-2*H*-cyclohepta[*b*]furan-3-carboxylate **298** in a good yield.¹⁹⁷ This procedure produced a small amount of a similar compound, ethyl 2-oxo-2*H*-cyclohepta[*b*]furan-3-carboxylate **295** (the product of pathway A, Scheme 52), which lacked the hydroxy group at the 8-position. This side product could be separated with an acid-base extraction technique, due to the low pK_a of the desired product.



Scheme 57: The synthesis of 2-tosyloxytropone **297** from commercially available tropolone **323**, followed by the condensation reaction to form ethyl 8-hydroxy-2-oxo-2H-cyclohepta[b]furan-3-carboxylate **298**, the precursor to the azulene structure.

To synthesise the azulene, ethyl 8-hydroxy-2-oxo-2H-cyclohepta[b]furan-3-carboxylate **298** was heated at 200 °C under microwave irradiation with trimethyl orthoacetate **324** and toluene (Scheme 58).¹⁹⁸ While the reaction was successful in forming an azulene through the [8+2] addition-elimination mechanism, and methylating the hydroxy group, some transesterification took place, giving a mixture of methyl (**325**) and ethyl (**326**) esters. Thus, an additional step, which was to heat the mixture at reflux with excess sodium methoxide, was undertaken to give pure methyl ester **325**. Initially, it was anticipated that a methoxy group at the 2-position would be easier to convert to a hydroxy group in subsequent steps than larger alkyl groups, which is why trimethyl orthoacetate **324** was chosen in preference to triethyl orthoacetate **318** in these initial studies.



Scheme 58: The [8+2] addition-elimination reaction of ethyl 8-hydroxy-2-oxo-2H-cyclohepta[b]furan-3-carboxylate **298** with trimethyl orthoacetate **324**, followed by a transesterification reaction, to form methyl 2,4-dimethoxyazulene-1-carboxylate **325**.

Looking ahead to make the 1,1'-biazulene, a method by Iyoda was found, in which azulene was treated with *N*-bromosuccinimide to produce an inseparable mixture of 1-bromoazulene and 1,3-dibromoazulene.¹⁹⁹ This mixture was then heated in THF at 50 °C with Ni(PPh₃)₂Br₂ as a catalyst, zinc powder as a reductant, and tetraethylammonium iodide as an organic-soluble source of iodide to give 1,1'-biazulene in 55% yield. Because of the presence of 1,3-dibromoazulene, higher oligoazulenes were also made and isolated in the process. Applying the method to this project, methyl 2,4-dimethoxyazulene-1-carboxylate **325** was treated with *N*-bromosuccinimide in benzene to form methyl 3-bromo-2,4-dimethoxyazulene-1-carboxylate **327** through electrophilic aromatic substitution exclusively at the 3-position, in high yield (Scheme 59). The brominated azulene **327** underwent a reductive homocoupling reaction using Ni(PPh₃)₂Br₂, zinc powder and tetra-*n*-butylammonium iodide to produce dimethyl 2,2',8,8'-tetramethoxy-[1,1'-biazulene]-3,3'-dicarboxylate (±)-**328** in 49% yield (Scheme 59 and Table 7, entry 1, page 102), which was similar to that of the reported method. However, the yield diminished to 29% when the homocoupling reaction was approximately quadrupled in scale (Table 7, entry 2). Evidence to support the atropisomerism of the biazulene **328** was obtained through chiral HPLC, displaying resolution of two peaks which were of approximately equal size (Figure 32). A crystal structure of the (±)-1,1'-biazulene **328** also was obtained by Dr. Mary Mahon, which confirmed the structure and to an extent, gave a visual impression of the steric interaction of the 8,8'-methoxy groups (Figure 33). The non-planarity of the structure was evidenced by a dihedral angle of 102.0(2)° (C2-C1-C1'-C2').

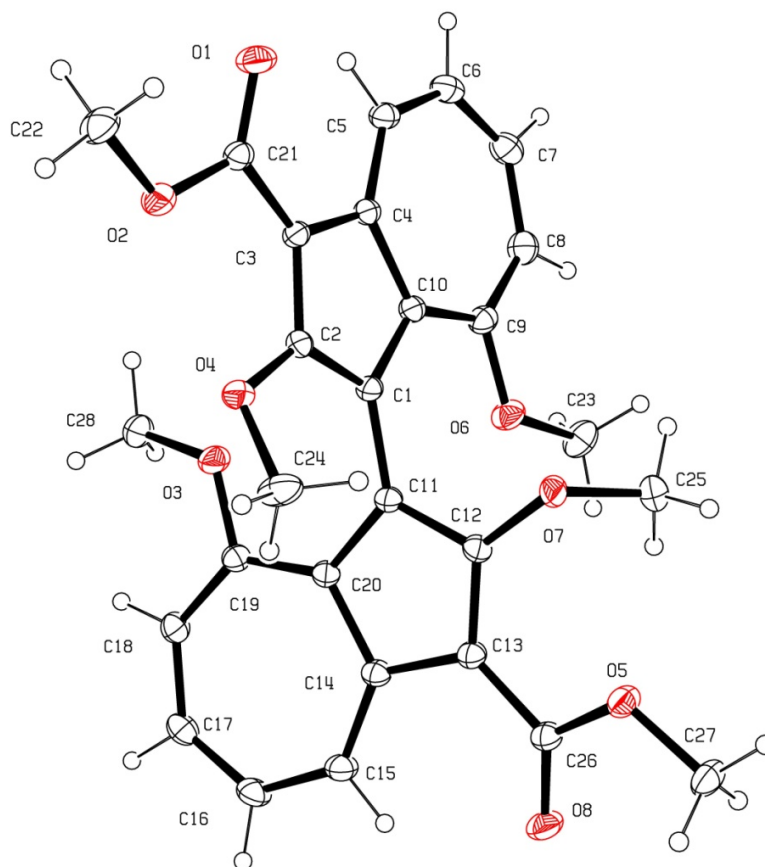
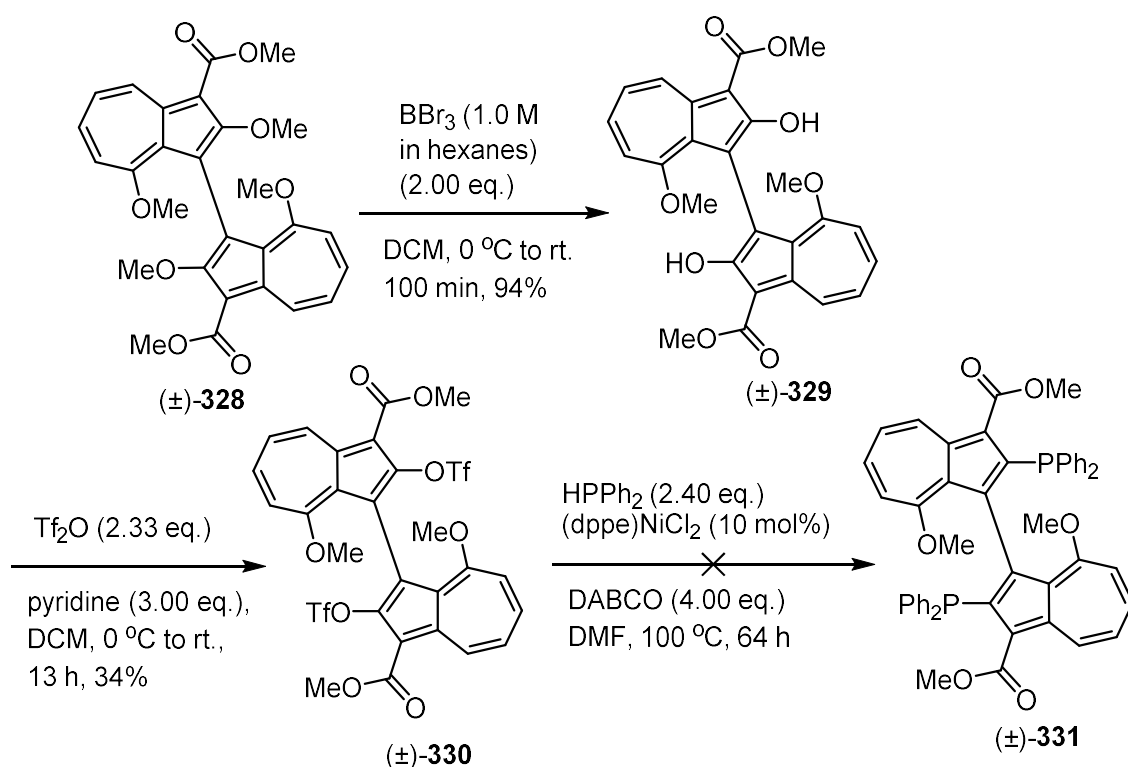


Figure 33: ORTEP diagram of (±)-dimethyl 2,2',8,8'-tetramethoxy-[1,1'-biazulene]-3,3'-dicarboxylate (±)-**328** showing ellipsoids of 30% probability. H atoms are shown as spheres of arbitrary radius.

With the 1,1'-biazulene (±)-**328** in hand, the next step towards the diphosphine was the demethylation of the 2,2'-methoxy groups. This transformation was achieved very efficiently by using two equivalents of boron tribromide,²⁰⁰ as dimethyl 2,2'-dihydroxy-8,8'-dimethoxy-[1,1'-biazulene]-3,3'-dicarboxylate (±)-**329** was produced in near quantitative yield (Scheme 60). There was no evidence of demethylation of the 8,8'-methoxy groups, as these azulene positions are electron-poor and the oxygen lone pairs are more extensively conjugated with the aromatic system, so the product could be used for the next step without further purification. Adapting the procedure for the preparation of BINAP as outlined in *Organic Syntheses*,¹⁵² the 1,1'-biazulene-2,2'-diol product (±)-**329** was then converted to the ditriflate (±)-**330** in 34% yield,

using trifluoromethanesulfonic anhydride and pyridine as a base. Unfortunately, the cross coupling reaction of the 1,1'-biazulene-2,2'-ditriflate (\pm)-**330** with diphenylphosphine, mediated by [1,2-bis-(diphenylphosphino)ethane]nickel(II) chloride as the catalyst and DABCO as base, resulted only in degradation of the starting material. It was postulated that the reaction required more rigorous exclusion of oxygen to work, and for the reaction to be operated on a larger scale to allow, more conveniently, the portionwise addition of diphenylphosphine, as directed in the original procedure.

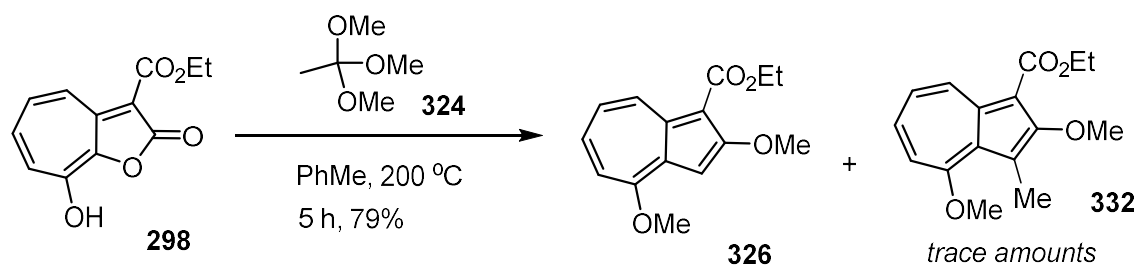


Scheme 60: The demethylation of the 2,2'-methoxy groups with boron tribromide of 2,2',8,8'-dimethoxy-[1,1'-biazulene]-3,3'-dicarboxylate (\pm)-**328**, followed by triflation of the 1,1'-biazulene-2,2'-diol (\pm)-**329**, and attempted formation of 1,1'-biazulene-2,2'-diphosphine (\pm)-**331**.

2.2.2. Improvements to synthetic steps

At this stage, the synthetic pathway was limited by the scale at which the [8+2]-addition-elimination reaction to initially form the azulene could be carried out, since

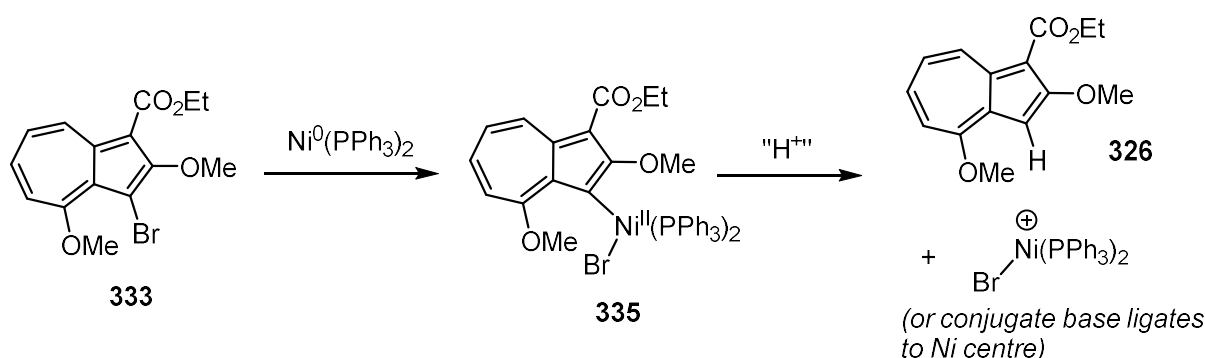
the reaction took place under microwave irradiation, and was therefore being carried out in a microwave tube with a capacity of about 10 mL, limiting each run to convert only 1.70 mmol of ethyl 8-hydroxy-2-oxo-2*H*-cyclohepta[*b*]furan-3-carboxylate **298**. To put this quantity into perspective, both preceding steps (Scheme 57) could be operating at a scale of tens of millimoles at a time. By operating the azulene synthesis outside the microwave reactor, with the use of an Asynt aluminium heating block, up to seven of these sealed tubes containing this reaction could be used on a single hotplate stirrer. This change in protocol allowed an increase in scale of up to 12.0 mmol of ethyl 8-hydroxy-2-oxo-2*H*-cyclohepta[*b*]furan-3-carboxylate **298** starting material. To add to this, when the reaction was carried out in a series of sealed microwave tubes (each containing 400 mg of **298**, 1.10 mL of trimethyl orthoacetate **324** and 1.0 mL of toluene) the absence of microwave irradiation minimised the undesirable process of transesterification. This process would produce ethyl 2,4-dimethoxyazulene-1-carboxylate **326** with just a trace of the methyl ester **325**, in an improved yield compared to that of Scheme 58 when the reaction time is increased by a few hours. That time is saved by the azulene product **326** not needing further transesterification for the conversion to a single ester. Interestingly, these [8+2]-addition-elimination reactions yielded a trace of the side product ethyl 2,4-dimethoxy-3-methylazulene-1-carboxylate **332**, having been alkylated at the 3-position through electrophilic aromatic substitution, as well as at the hydroxy group.



Scheme 61: The [8+2]-addition-elimination reaction of trimethyl orthoacetate **324** with 8-hydroxy-2-oxo-2H-cyclohepta[b]furan-3-carboxylate **298** in the absence of microwave irradiation to give ethyl 2,4-dimethoxyazulene-1-carboxylate **326**.

Using the azulene product **326** with the ethyl ester instead, the Ni-catalysed homocoupling reaction proved difficult to replicate (Table 7, entry 3), although the bromination with *N*-bromosuccinimide appeared to proceed as well as that with the methyl ester **325**. This problem seemed strange, as the change of alkyl group on the azulene-1-yl carboxylate would not be expected to cause a significant change in the steric or electronic properties, especially with regards to the reactivity at the 3-position of this azulene. It was shown that at this stage that even using inseparable mixtures of the methyl and ethyl ester of the azulene was not yielding any 1,1'-biazulene product (Table 7, entry 4), so it was unlikely that the choice of alkyl group was influencing the outcome of the reaction. Several changes were made to the conditions in order to reproduce formation of the desired 1,1'-biazulene product **334**, with the ethyl ester groups: the molar quantity of zinc metal was increased from 1.50 to 2.00 (Table 7, entry 5), and in addition to that, in a separate run, the Ni(PPh₃)₂Br₂ complex, the zinc and the tetra-*n*-butylammonium iodide were stirred for 30 min in THF at room temperature (Table 7, entry 6); neither of these modifications were successful in yielding the 1,1'-biazulene **334**. The only products isolated were the 3-bromoazulene **333** and ethyl 2,4-dimethoxyazulene-1-carboxylate **326**, the latter of which was perhaps produced by nickel(0) insertion between the azulene-bromine

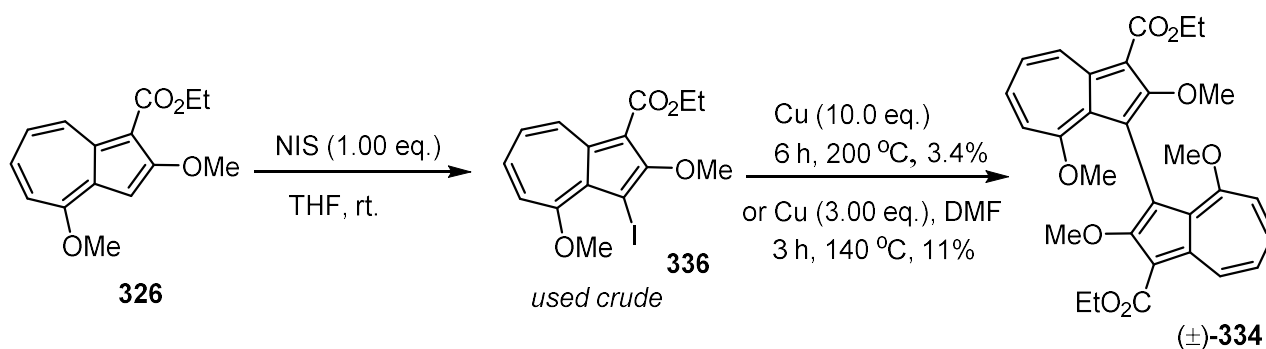
bond, followed by a reaction of azulenylnickel species **335** with a proton source, which seems feasible, based on proposed mechanisms in previous literature²⁰¹ (Scheme 62). Other methodologies were tested, such as the Fe-catalysed Kumada-like homocoupling^{202,203} of the *in situ* generated azulene-3-yl magnesium bromide (Table 7, entries 7 and 8), and a homocoupling reaction mediated by glucose-generated Pd(0)-nanoparticles²⁰⁴ (Table 7, entry 9); both of which yielded none of 1,1'-biazulene **334**.



Scheme 62: Proposed mechanism of the oxidative addition of the azulene-3-yl bromide **333** to the Ni(0) centre, followed by protonolysis to make ethyl 2,4-dimethoxyazulene-1-carboxylate **326**.

Given the struggle to reproduce the Ni-catalysed homocoupling method by Iyoda, alternative literature methods, in which 1,1'-biazulenenes had been synthesised, were explored. In 1982, Morita reported the synthesis of diethyl 1,1'-biazulene-3,3'-dicarboxylate by heating ethyl 3-iodoazulene-1-carboxylate with a superstoichiometric quantity of copper metal, without any solvent, in 83% yield.²⁰⁵ Although both of these methods were precented to form 1,1'-biazulenenes, the Ni-catalysed method had been seen as the more attractive because of the milder conditions. However, despite the energy intensive nature, the high yield of the Cu-mediated process appeared to demonstrate good functional group tolerance. To apply this methodology to this project, ethyl 2,4-dimethoxyazulene-1-carboxylate **326**

was treated with *N*-iodosuccinimide to give the crude 3-iodinated azulene **336**, which was heated with 10 equivalents of copper powder at 200 °C for 6 hours. This process gave the desired product of (±)-diethyl 2,2',8,8'-tetramethoxy-[1,1'-biazulene]-3,3'-dicarboxylate (±)-**334**, but only in 3.4% yield (Scheme 63; Table 7, entry 10). To improve the mixing of the azulenyl iodide **336** and copper, DMF was used as a solvent, and by using 3 equivalents of copper powder at a reduced temperature and reaction time of 140 °C and 3 hours respectively, the 1,1'-biazulene (±)-**334** was produced in an improved 11% yield (Scheme 63, Table 7, entry 11).



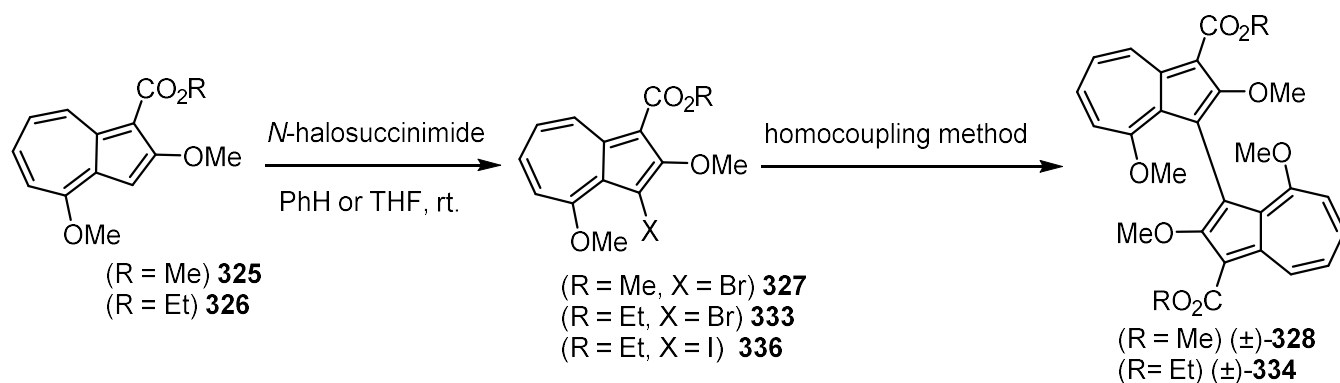
Scheme 63: The iodination of ethyl 2,4-dimethoxyazulene-1-carboxylate **326** with *N*-iodosuccinimide, followed by copper-mediated homocoupling of the resultant 3-iodoazulene **336** to form (±)-diethyl 2,2',8,8'-tetramethoxy-[1,1'-biazulene]-3,3'-dicarboxylate (±)-**334** (Table 7, entries 10 and 11).

The iodinated azulene **336** was also applied in the Ni-catalysed homocoupling methodology. Since the 3-iodoazulene **336** was visibly less stable than the 3-bromoazulene **333** during the work-up procedure, two experiments were carried out in which the azulene **326** was treated with *N*-iodosuccinimide in THF, and on completion of the reaction, the mixture was immediately treated with the homocoupling conditions (Table 7, entries 12 and 13). Unfortunately, this did not produce any of the 1,1'-biazulene **334** either, but because of the presumed presence of the acidic byproduct succinimide, it was decided to apply a basic aqueous wash of the crude 3-haloazulene during the work-up process. Thus, after bromination of the

azulene **326** with *N*-bromosuccinimide in THF, the crude mixture was washed with aqueous sodium carbonate during the work-up process, and when the crude 3-bromoazulene **333** was then treated with the homocoupling conditions as in Scheme 59, the desired product (\pm)-diethyl 2,2',8,8'-tetramethoxy-[1,1'-biazulene]-3,3'-dicarboxylate (\pm)-**334** was produced in 24% yield (Table 7, entry 14). The yield was increased to 29% if the reaction was allowed to run for 17 hours (Table 7, entry 15). Unfortunately, when the scale of this reaction was increased to 2.15 millimoles, the 1,1'-biazulene product (\pm)-**334** was not detected (Table 7, entry 17).

By applying the basic aqueous wash to the Cu-mediated Ullmann homocoupling procedure, as in Scheme 63, the yield was slightly increased from 11% to 13% (Table 7, entry 16); though in this case, the procedure was carried out with 0.384 millimoles of azulene **326** (i.e. half of the 0.768 millimoles used before).

Table 7: Summary of the attempts towards a 1,1'-biazulene **334** through a homocoupling reaction of 3-haloazulenes.

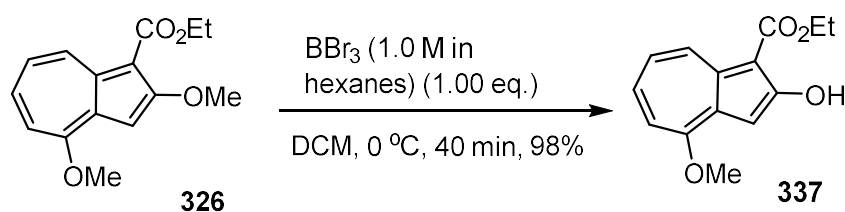


Entry	R ^a	X	Basic aqueous wash ^c	Homocoupling method ^d	Running time /h	Scale of AzX /mmol	Yield ^f /%	Notes
1	Me	Br	No	1	3	0.489	49	
2	Me	Br	No	1	2	1.90	29	
3	Et	Br	No	1	2	1.37	0	
4	Me/Et	Br	No	1	24	2.5	0	Heated at reflux for final 3 h
5	Me/Et	Br	No	1	3	2.4	0	2.0 eq. of Zn used
6	Me/Et (2:1)	Br	No	1	18	0.73	0	2.0 eq. of Zn used; Ni(PPh ₃) ₂ Br ₂ , Zn and TBAI stirred in THF for 30 min at r.t. before addition of Az-X
7	Me/Et (2:1)	Br	No	2	19	0.47	0	
8	Me/Et (1:1)	Br	No	2	1	0.68	0	Molecular iodine used to assist formation of Az-MgBr
9	Me/Et (2:1)	Br	No	3	21	0.15	0	
10	Et	I ^b	No	4	6	0.768 ^e	3.4	10.0 eq. of Cu, no solvent, T = 200 °C
11	Et	I ^b	No	4	3	0.768 ^e	11	
12	Et	I ^b	No	1	20	0.384 ^e	0	No aqueous work-up applied to halogenation step
13	Et	I ^b	No	1	20	0.384 ^e	0	No aqueous work-up applied to halogenation step; Ni(PPh ₃) ₂ Br ₂ , Zn and TBAI stirred in THF for 1 h at r.t. before addition of Az-X
14	Et	Br ^b	Yes	1	3	0.384 ^e	24	
15	Et	Br ^b	Yes	1	17	0.423 ^e	29	
16	Et	I ^b	Yes	4	16	0.384 ^e	13	
17	Et	Br ^b	Yes	1	16	2.15 ^e	0	

a) Mixtures of esters resulted from formation of azulene, from a procedure that deviated from 400 mg of **298**, 1.10 mL of trimethyl orthoacetate **324** and 1.0 mL of PhMe in 10 mL capacity microwave tubes **b)** Halogenation of azulene was carried out in THF, rather than benzene **c)** After the halogenation reaction, the crude mixture was washed with either Na₂CO_{3(aq)} or K₂CO_{3(aq)} (1.0 M or 2.0 M) **d)** Procedure for homocoupling the 3-haloazulene, unless other stated in "Notes": **1** = Ni(PPh₃)₂Br₂ (10 mol%), Zn (1.50 eq.), ^tBu₄NI (1.00 eq.), THF, 50 °C; **2** = Mg (1.10 eq.), THF, Δ, followed by FeCl₃ (5 mol%), 1,2-dibromoethane (1.00 eq.), THF, r.t.; **3** = Pd(OAc)₂ (3 mol%), glucose (0.50 eq.), ^tBu₄NOH_(aq) (40 wt. %, 3.00 eq.), H₂O/dioxane (3:7), 90 °C; **4** = Cu (3.00 eq.), DMF, 140 °C **e)** Yield of halogenation of azulene was not recorded, and so assumed to be quantitative with respect to azulene **f)** Yield of 1,1'-biazulene with respect to molar quantity in "Scale of AzX" column.

2.2.3. Chemical transformations of monoazulenes

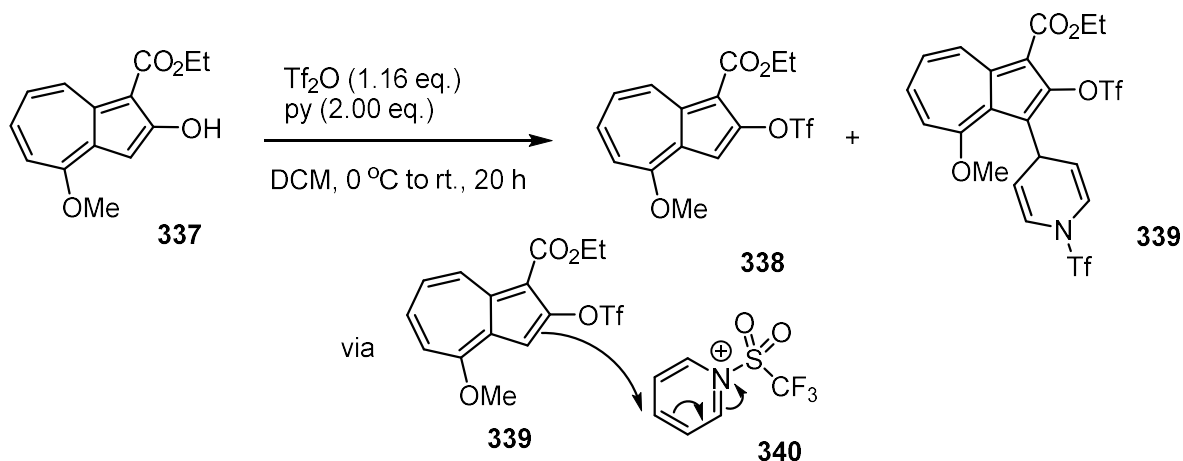
The formation of a 1,1'-biazulene was shown to be a difficult synthetic step to develop, so during this stage of the project, focus was also brought to the improvement of other chemical steps useful towards the synthesis of the target 1,1'-biazulene-2,2'-diphosphine ligand. Since it was difficult at this time to produce large, useful quantities of either (\pm)-diethyl 2,2',8,8'-tetramethoxy-[1,1'-biazulene]-3,3'-dicarboxylate (\pm)-**334** or the dimethyl ester (\pm)-**328**, experiments were instead carried out on monoazulene derivatives. Since the procedure had worked so well on the 1,1'-biazulene species (\pm)-**328** (Scheme 60), the demethylation of the monomeric azulene **326**, mediated by boron tribromide, was attempted and proceeded smoothly to produce ethyl 2-hydroxy-4-methoxyazulene-1-carboxylate **337** in high yield (Scheme 110). Again, the reaction was entirely selective towards the 2-methoxy group, rather than that at the 4-position.



Scheme 64: The selective demethylation of ethyl 2,4-dimethoxyazulene-1-carboxylate **326**, with boron tribromide, to give ethyl 2-hydroxy-4-methoxyazulene-1-carboxylate **337**.

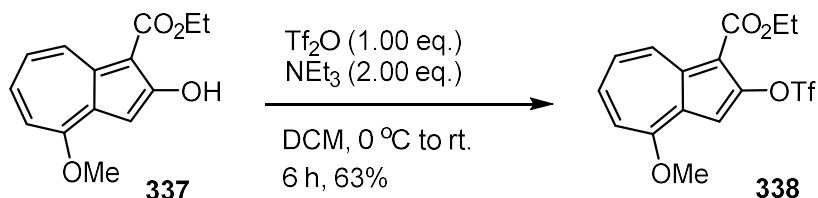
The next step was to convert the 2-hydroxy group into a triflate, which would act as a leaving group for the installation of the phosphine group. However, when the triflation procedure applied to the 2,2'-dihydroxy-1,1'-biazulene **329** (Scheme 60) was adapted to the monomeric 2-hydroxyazulene **337**, the desired product was inseparable from a side product on the silica column (Scheme 65). It emerged that because the pyridine in the system was acting as a nucleophilic catalyst to promote

the triflation, as well as a base, it meant the desired product **338** reacted further with the pyridinium triflate intermediate **340** at the nucleophilic 3-position of the azulene in a precedence manner,²⁰⁶ giving side product **339**, the identity of which was confirmed by NMR and mass spectrometry.



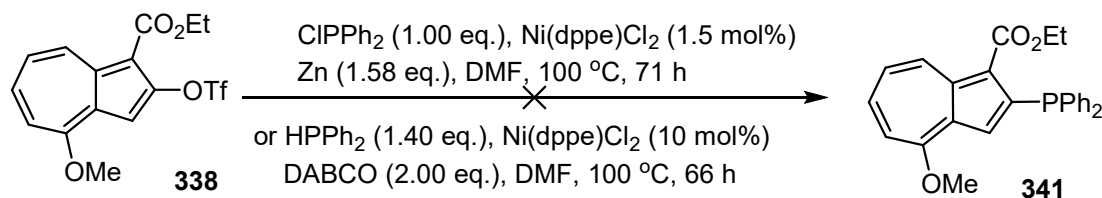
Scheme 65: The triflation of ethyl 2-hydroxy-4-methoxyazulene-1-carboxylate **337** with triflic anhydride and pyridine to form the desired product **338** and *N*-trifluoromethanesulfonate-1,4-dihydropyridin-4-yl adduct **339**.

By switching pyridine with a less nucleophilic base, it was predicted that triflation would only occur at the hydroxyl group, and not at the 3-position. As expected, the treatment of ethyl 2-hydroxy-4-methoxyazulene-1-carboxylate **337** with triflic anhydride and triethylamine solely produced the desired azulene-2-yl trifluoromethanesulfonate **338** in 63% yield in 6 hours (Scheme 66).



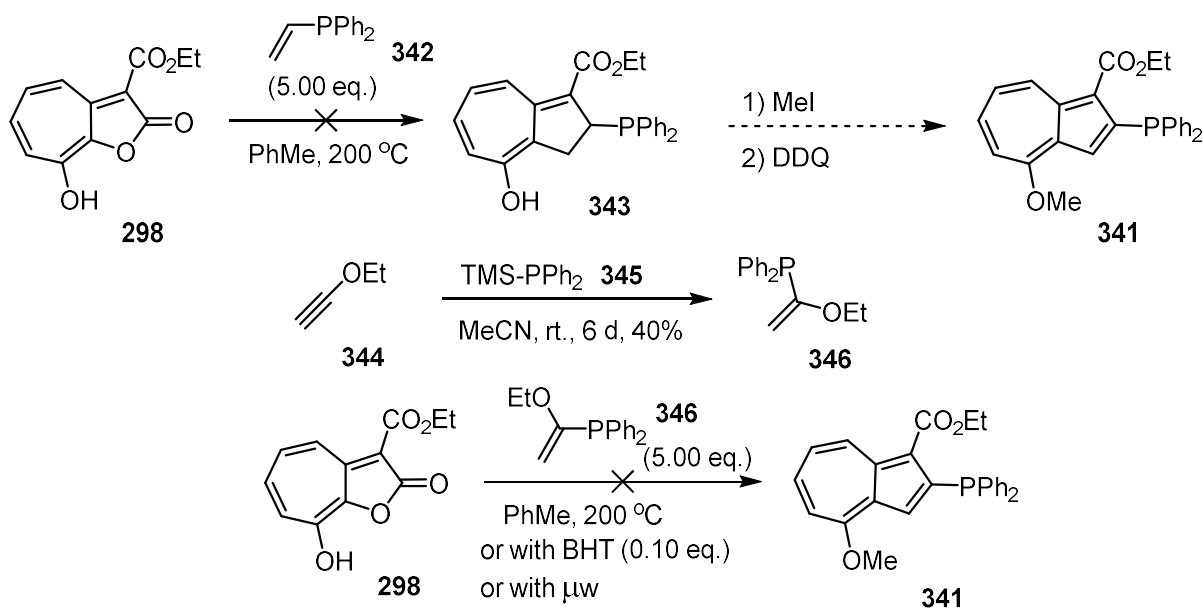
Scheme 66: The triflation of ethyl 2-hydroxy-4-methoxyazulene-1-carboxylate **337** with triflic anhydride and triethylamine to exclusively form azulene-2-yl triflate **338**, the desired product.

Since the azulene-2-yl triflate **338** was now accessible on a scale of 2 millimoles, it was now more convenient to test methodologies for installing the phosphine group at the 2-position, that might be later applicable to an analogous biazulene (Scheme 67). An account by Laneman *et al.* described the cross coupling reaction of chlorodiphenylphosphine with several aryl, alkenyl and alkyl halides and triflates, in the presence of [1,2-bis-(diphenylphosphino)ethane]nickel(II) chloride and zinc in DMF in moderate to high yield.²⁰⁷ Unfortunately, when this methodology was applied to the azulene-2-yl trifluoromethanesulfonate **338**, the only product isolated, other than starting material, was ethyl 2-hydroxy-4-methoxyazulene-1-carboxylate **337**. The presence of the latter product was unusual, as the cleavage of the azulene-triflate C-O bond would be expected, during the oxidative addition to either the zinc or nickel centres. The next experiment carried out was the application of the cross coupling method outlined in the *Organic Syntheses* paper for the synthesis of BINAP **51**, similar to that in Scheme 60. On this occasion, the scale of the reaction was large enough to allow accurate portionwise addition of diphenylphosphine, but the desired product of azulene-2-yl diphenylphosphine **341** was not detected. However, instead of degradation of starting material, the products isolated, other than starting material, were ethyl 2-hydroxy-4-methoxyazulene-1-carboxylate **337** and an azulene derivative that could not be identified, but appeared to possess no methyl groups.



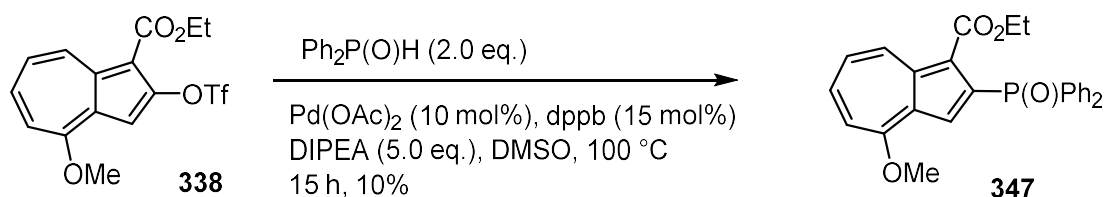
Scheme 67: The attempts to carry out a cross coupling reaction on azulene-2-yl trifluoromethanesulfonate **338** to synthesise azulene-2-yl diphenylphosphine **341**.

A less typical method to install the phosphine group came through attempts to carry out the [8+2]-addition-elimination on ethyl 8-hydroxy-2-oxo-2*H*-cyclohepta[*b*]furan-3-carboxylate **298** with a diphenylphosphine-containing olefinic species. This unprecedented transformation appeared attractive, as it would represent a very direct way of synthesizing an azulene-2-yl phosphine without resorting to functional group interconversions and transition metal catalysed cross coupling reactions. To test this reaction, the 2*H*-cyclohepta[*b*]furan-2-one **298** was heated at 200 °C with 5.0 equivalents of diphenylvinylphosphine **342**, which would produce 2,3-dihydroazulene **343** if successful. Alkylation of the acidic 4-hydroxy group, followed by aromatisation with the oxidant 2,3-dichloro-5,6-dicyano-1,4-benzoquinone (DDQ) would yield the desired azulene-2-yl phosphine **341**. Unfortunately, the reaction resulted only in degradation of the starting material (Scheme 68). After this experiment, the olefin partner was changed from diphenylvinylphosphine **342** to (1-ethoxyvinyl)diphenylphosphine **346**, which could be synthesised through the reaction of ethoxyacetylene **344** with diphenyl(trimethylsilyl)phosphine **345**.²⁰⁸ This way, the 2,3-dihydroazulene product from an [8+2]-addition-elimination reaction could subsequently eliminate a molecule of ethanol *in situ* to form the azulene **341**. However, after carrying out this process with similar conditions to the attempt to make 2,3-dihydroazulene **343**, repeating with butylated hydroxytoluene (BHT) added to suppress radical pathways, and with microwave irradiation, none of the desired azulene-2-yl phosphine product **341** was detected.



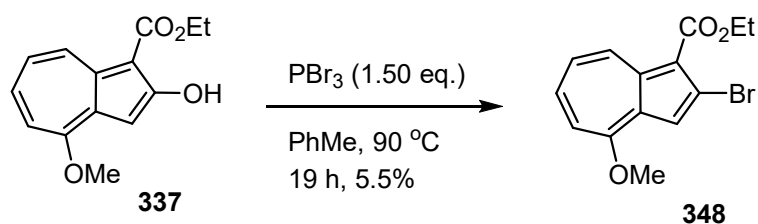
Scheme 68: Attempts at synthesizing azulene-2-yl phosphine derivative **341** from ethyl 8-hydroxy-2-oxo-2H-cyclohepta[b]furan-3-carboxylate **298** and phosphine-containing olefins.

Because of the difficulty involved in forming an azulene species with a phosphine group at the 2-position, cross coupling reactions to form azulene-2-yl phosphine oxide derivatives were explored instead. The oxygen atom therefore would serve as a protecting group, and could be reduced at the end of the synthesis, which is why this approach is often employed to make phosphine ligands. A promising result was obtained from the palladium-catalysed cross coupling reaction of diphenylphosphine oxide and the monomeric azulene-2-yl triflate **338** in DMSO, with Hünig's base and 1,4-bis-(diphenylphosphino)butane (dppb) as a ligand.²⁰⁹ After purification by column chromatography and recrystallisation, the desired azulene-2-yl phosphine oxide **347** was obtained in 10% yield (Scheme 69). This experiment represented the first azulene carbon-phosphorus bond formation of the project. The reaction was repeated, with the scale doubled from 0.132 mmol to 0.264 mmol, but the product could not be isolated with the same purity as before.



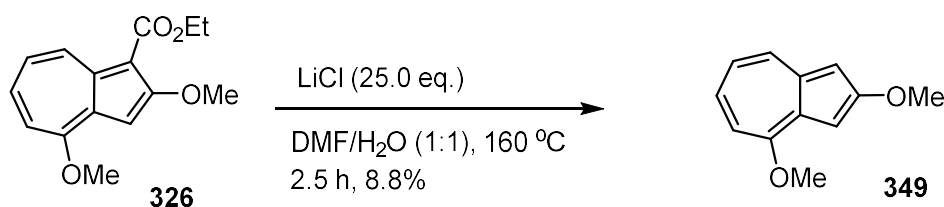
Scheme 69: The Pd-catalysed cross coupling reaction of azulene-2-yl triflate **338** with diphenylphosphine oxide to form ethyl 2-(diphenylphosphoryl)-4-methoxyazulene-1-carboxylate **341**.

To extend the variety of the leaving group at the 2-position of the azulene, the reaction of ethyl 2-hydroxy-4-methoxyazulene-1-carboxylate **337** with phosphorus tribromide in toluene at $90\text{ }^\circ\text{C}$ gave a small amount of the desired product ethyl 2-bromo-4-methoxyazulene-1-carboxylate **348**, in 5.5% yield (Scheme 70).²¹⁰ If the reaction was optimised, the product would be suitable as an alternative to an azulene-2-yl triflate species in carbon-phosphorus cross coupling reactions. If the ester was converted to a different group, such as through decarboxylation to give the unsubstituted 1-position, or through reduction to form the 1-methyl group, it may be possible to carry out a halogen-lithium exchange process. The azulene-2-yllithium intermediate could then be quenched with an electrophilic source of phosphorus, such as chlorodiphenylphosphine, to form an azulene-2-yl phosphine species.



Scheme 70: The substitution of the hydroxy group of ethyl 2-hydroxy-4-methoxyazulene-1-carboxylate **337** with phosphorus tribromide to give ethyl 2-bromo-4-methoxyazulene-1-carboxylate **348**.

One method of removing the ester group by decarboxylation is to heat the alkyl azulene-1-carboxylate with lithium chloride, giving the unsubstituted 1-position, which proceeds by dealkylation of the ester by the chloride ion, followed by decarboxylation.²¹¹ When this reaction was tested on ethyl 2,4-dimethoxyazulene-1-carboxylate **326** by heating it with 25 equivalents of lithium chloride in a 1:1 mixture by volume of DMF and water, this gave the desired decarboxylated product **349** in 8.8% yield (Scheme 71). About 8% of the starting material was recovered, which suggests conversion could be improved, particularly if degassed solvents were to be used.



Scheme 71: The lithium chloride-mediated decarboxylation of ethyl 2,4-dimethoxyazulene-1-carboxylate **326** to give 2,4-dimethoxyazulene **349**.

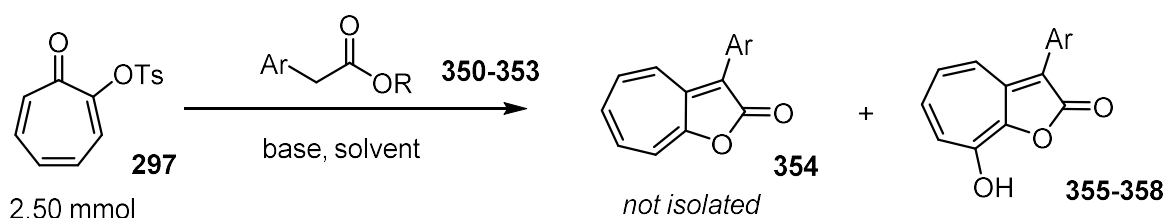
2.2.4. Synthesis of 3-aryl-2H-cyclohepta[b]furan-2-one precursors

At this stage, it appeared that the only purpose that the ester was serving, once the azulene had been formed, was to protect one of the electron-rich 1- and 3-positions of the azulene to prevent oligomerisation during a homocoupling reaction. It was also likely that these groups would have to be removed at some stage after a 1,1'-biazulene had been formed, and to have bulky aryl groups in place of those esters, which could be required for the chiral ligand to induce good stereoselectivity. In order to reduce the number of steps, it was postulated that instead of synthesising the 2H-cyclohepta[b]furan-2-one precursor with diethyl malonate **294** as the active methylene compound, that an arene-containing active methylene group could be

used instead, which had never been carried out previously. This way, the aryl group in the 3-aryl-2*H*-cyclohepta[*b*]furan-2-one product could be retained throughout the synthesis of the ligand, as it would likely be less reactive than the ester group. Encouragingly, a few derivatives of 3-aryl-2*H*-cyclohepta[*b*]furan-2-one were synthesised in a facile manner, on a scale of 2.50 mmol (Table 8). The first reaction that was attempted was the synthesis of 8-hydroxy-3-(4-nitrophenyl)-2*H*-cyclohepta[*b*]furan-2-one **355** from 2-tosyloxypone **297** and ethyl 4-nitrophenylacetate **350** in 52% yield (Table 8, entry 1); the 4-nitrophenyl group was chosen because of its electron withdrawing ability, keeping the pK_a of the methylene group low. When ethyl phenylacetate **351** was used as the active methylene compound, using otherwise the same method as with ethyl 4-nitrophenylacetate **350**, the product of 8-hydroxy-3-phenyl-2*H*-cyclohepta[*b*]furan-2-one **356** was produced in only approximately 5% yield (Table 8, entry 2). Carrying out this reaction at 60 °C rather than ambient temperature doubled the product yield to 10%, with a higher purity as the NMR spectrum showed no trace of ethyl phenylacetate (Table 8, entry 3). For the active methylene compound, the 4-nitrophenyl group has a greater ability to stabilise an adjacent negative charge than a phenyl group, so it was predicted that a stronger base would improve the yield of the 2*H*-cyclohepta[*b*]furan-2-one derivative. As expected, the reaction of 2-tosyloxypone **297** and ethyl phenylacetate **351** at ambient temperature, using potassium *tert*-butoxide as the base, gave 8-hydroxy-3-phenyl-2*H*-cyclohepta[*b*]furan-2-one **356** in 34% yield (Table 8, entry 4). When this process was undertaken at an elevated temperature of 60 °C, exactly the same yield was achieved (Table 8, entry 5). Other 2*H*-cyclohepta[*b*]furan-2-one derivatives synthesised in a similar way, using potassium *tert*-butoxide as the base, were 8-hydroxy-3-(naphthalen-1-yl)-2*H*-cyclohepta[*b*]furan-2-one **357**, from

methyl-1-naphthaleneacetate **352**, in approximately 55% yield (Table 8, entry 6), with a small amount of impurity in the product; and methyl 4-(8-hydroxy-2-oxo-2*H*-cyclohepta[*b*]furan-3-yl)benzoate **358**, from methyl 4-(2-methoxy-2-oxoethyl)benzoate **353**, in a pleasing 71% yield (Table 8, entry 7). For each of these examples in Table 8, it is assumed that a small amount of side product **354** was produced, without the 8-hydroxy group (via the mechanism of Pathway A, Scheme 52). The yields of these side products **354** were not recorded, as they were removed during the work-up process each time by washing the aqueous layer, under basic conditions, with toluene. The organic solvent extracted the side product and excess activated methylene compound, while the desired product remained in the aqueous layer in its anionic form, due to the acidic 8-hydroxy group. Instead of isolating the side products from the excess active methylene compound, which would have required column chromatography or a distillation, they were simply discarded.

Table 8: The synthesis of various 3-aryl-2*H*-cyclohepta[*b*]furan-2-one derivatives, from 2-tosyloxypone **297** and the corresponding aryl active methylene compounds.



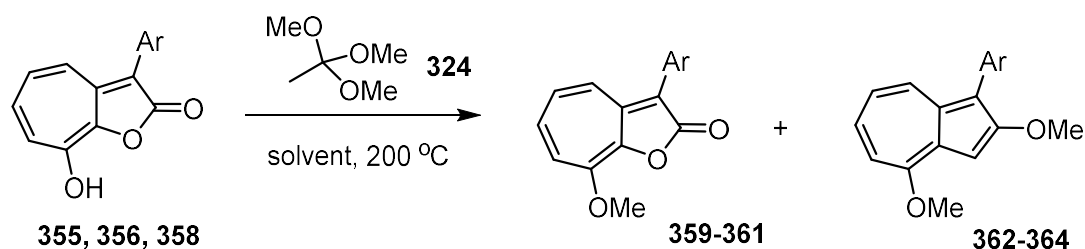
Entry	AMC ^a	Ar	R	Base	Solvent	Temperature /°C	Running time /h	Product	Yield /%
1	350	-C ₆ H ₄ (<i>p</i> -NO ₂)	Et	NaOEt ^b	EtOH	0→r.t.	20	355	52
2	351	Ph	Et	NaOEt ^b	EtOH	0→r.t.	26	356	5 ^c
3	351	Ph	Et	NaOEt ^b	EtOH	60	21	356	10
4	351	Ph	Et	<i>t</i> -BuOK ^c	<i>t</i> -BuOH	r.t.	20	356	34
5	351	Ph	Et	<i>t</i> -BuOK ^c	<i>t</i> -BuOH	60	17	356	34
6	352	1-naphthyl	Me	<i>t</i> -BuOK ^c	<i>t</i> -BuOH	r.t.	24	357	55 ^d
7	353	-C ₆ H ₄ (<i>p</i> -CO ₂ Me)	Me	<i>t</i> -BuOK ^c	<i>t</i> -BuOH	r.t.	17	358	71

a) AMC = active methylene compound **b)** Prepared freshly by dissolving sodium metal in ethanol **c)** Sourced from ready-made bottle from Sigma-Aldrich, at a concentration of 1.0 M in *tert*-butanol **d)** Contained a small amount of impurity.

After being able to synthesise a few derivatives of 3-aryl-2*H*-cyclohepta[*b*]furan-2-one, the conversion of some of these compounds to azulenes was attempted (Table 9). At first, the *p*-nitrophenyl derivative **355** was heated with trimethyl orthoacetate **324** in toluene at 200 °C for 3 hours (Table 9, entry 1). This experiment produced a mostly clean sample of the desired azulene product **362** in approximately 5% yield, which co-eluted with traces of unidentified side products. However, the majority product from this reaction was 8-methoxy-3-(4-nitrophenyl)-2*H*-cyclohepta[*b*]furan-2-one **359**, i.e. the methylated derivative of the starting material, in 66% yield. This solid had crystallised out of the reaction mixture after allowing it to cool to room temperature, so it was simply collected by filtration before the remaining filtrate was purified by column chromatography. Because of the polarity induced by the nitro group, this reduced the solubility of the starting material, presumably due to increased π -stacking interactions between molecules. To improve the solubility for the reaction mixture, *N*-methylpyrrolidone (NMP)²¹² was used as a solvent in place of toluene. With this change applied, the yield of azulene **362** improved to around 13% (Table 9, entry 2), though this product was not isolated cleanly as the presence of NMP caused streaking of the crude mixture through the silica. This experiment was repeated with an aqueous work-up applied before column chromatography, which permitted some pure azulene **362** to be separated, but only in 6% yield (Table 9, entry 3). The methylated derivative **359** could not be isolated when NMP was used as the solvent. When the conversion of the phenyl derivative **356** of 3-aryl-2*H*-cyclohepta[*b*]furan-2-one to the azulene was attempted, with toluene as the solvent, a lower yield of 2.8% was obtained for 1-phenylazulene **363** (Table 9, entry 4). This result was expected, due to the reduced electrophilicity of phenyl derivative **356** compared to *p*-nitrophenyl derivative **355**. Similar to the *p*-nitrophenyl derivative **359**,

the methylated byproduct **360** was obtained in 41% yield, which was collected by filtration after the reaction had cooled to room temperature. Finally, the same [8+2]-addition-elimination reaction was attempted with the methyl *p*-benzoate derivative **358**, in which only the methylated byproduct **361** could be detected, and was isolated in 38% yield (Table 9, entry 5). Overall, while the synthesis of these novel azulene products had formed the basis of an interesting tangent from the main work, the yields were too low to be of immediate use to this project, so any further developments were postponed for the future.

Table 9: The attempts at transforming the 3-aryl-2*H*-cyclohepta[*b*]furan-2-one derivatives into corresponding azulenes, through the [8+2]-addition-elimination reaction with trimethyl orthoacetate **324**.



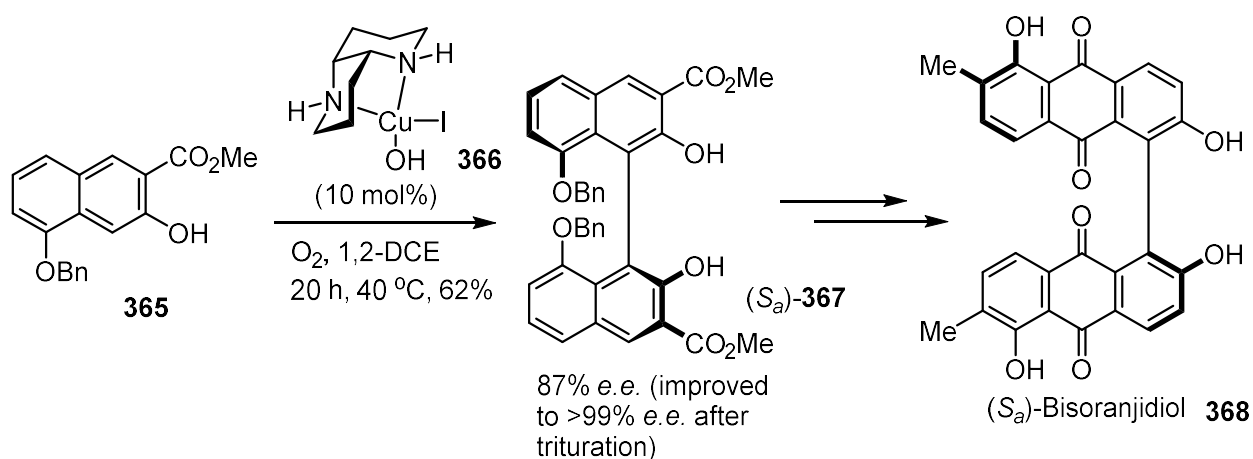
Entry ^a	Ar	Solvent	Running time /h	Yield of 359-361 /%	Yield of 362-364 /%
1	–C ₆ H ₄ (<i>p</i> -NO ₂)	Toluene	3	66 (359)	5.2 (impure) (362)
2	–C ₆ H ₄ (<i>p</i> -NO ₂)	NMP	6	not isolated (359)	13 (impure) (362)
3 ^b	–C ₆ H ₄ (<i>p</i> -NO ₂)	NMP	6	not isolated (359)	5.8 (362)
4 ^c	Ph	Toluene	6	41 (360)	2.8 (363)
5 ^d	–C ₆ H ₄ (<i>p</i> -CO ₂ Me)	Toluene	5	38 (361)	0 (364)

a) Unless otherwise stated, experiments were carried out with 0.706 mmol of **355**, **356** or **358**, 1.5 mL of trimethyl orthoacetate and 1.5 mL of solvent, under an atmosphere of air at 200 °C in a sealed microwave tube (capacity 10 mL), and reaction mixture was loaded directly onto silica column after completion of reaction **b)** After completion of reaction, diluted with ethyl acetate and washed with water, dried and concentrated under reduced pressure before column chromatography **c)** 0.210 mmol of **356**, 1.0 mL of trimethyl orthoacetate and 1.0 mL of solvent used **d)** 0.337 mmol of **358**, 1.0 mL of trimethyl orthoacetate and 1.0 mL of solvent used.

2.2.5. 1,1'-biazulene formation through Cu-catalysed oxidative homocoupling

While there had been some fruitful results for the experiments on monoazulenes, the synthetic route towards a ligand was still limited, as a satisfactory method to couple the azulene units together had not been achieved. Previous methods from the

literature to form the 1,1'-biazulene could only achieve low yields, on a small scale, from the azulene monomers involved in this project. It was therefore decided to search for homocoupling methods that had worked for benzenoid aromatic molecules, rather than azulene, that possessed similar substituents to the monomeric azulene compounds that had been already reliably synthesised in this project. It was at this time that a promising precedent was found from the extensive work of Kozlowski *et al.*, towards the asymmetric oxidative homocoupling reactions of 2-hydroxynaphthalene derivatives²¹³ for the synthesis of axially chiral natural products. For the total synthesis of (*S_a*)-bisoranjidiol **368**, the group were able to employ a 1,5-diaza-*cis*-decalin copper(II) catalyst **366** to induce stereoselectivity for the asymmetric oxidative homocoupling reaction of methyl 5-(benzyloxy)-3-hydroxy-2-naphthoate **365**, giving the axially chiral 1,1'-binaphthyl product **367** in 87% e.e. and 62% yield (Scheme 72).²¹⁴ After purifying the product to a single enantiomer with a trituration, it was eventually transformed into the target natural product **368**.

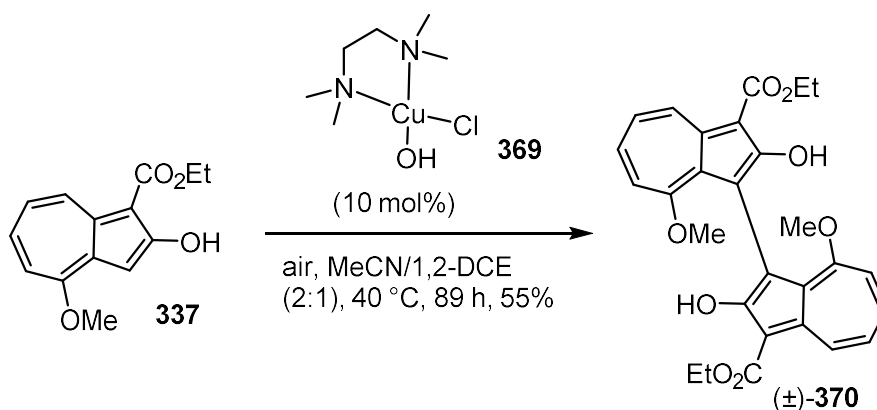


Scheme 72: The asymmetric synthesis of 1,1'-binaphthyl product **367**, the precursor for the axially chiral natural product (*S_a*)-bisoranjidiol **368**, by Kozlowski.

Due to the similarity between the hydroxynaphthalene **365** and ethyl 2-hydroxy-4-methoxyazulene-1-carboxylate **337**, which was readily available from synthetic

methods employed in this project, Kozlowski's method appeared to be suitable not only to produce a 1,1'-biazulene, but also potentially to induce stereoselectivity and produce enantioenriched 1,1'-biazulene products. However, the enantioselectivity of the homocoupling reaction on an azulene monomer, at a point when it was unknown whether the process would even yield any 1,1'-biazulene product, was a consideration for a later time. Conveniently, the paper also described the synthesis of the racemic form of 1,1'-binaphthol **367** in 91% yield using a TMEDA-copper(II) catalyst **369**, which is inexpensive compared to the chiral 1,5-diaza-*cis*-decalin copper(II) complex **366**. Adapting Kozlowski's reported procedure, ethyl 2-hydroxy-4-methoxyazulene-1-carboxylate **337** was stirred with the TMEDA-copper(II) complex **369** in acetonitrile and 1,2-dichloroethane (2:1) under an oxygen atmosphere for 16 hours at room temperature, and then for 47 hours at 40 °C. A similar additional experiment was also set up, carried out on this occasion under atmosphere of air at 40 °C, stirred for 21 hours, to see if the oxygen atmosphere was necessary for this substrate. Both experiments appeared to produce the desired 1,1'-biazulene-2,2'-diol product (\pm)-**370**. However, after aqueous washes of both reaction mixtures, followed by column chromatography, the high polarity of the compound resulted in too great an affinity to the silica gel to purify it this way. Encouragingly, it had been noticed that on completion of the reaction, a red precipitate had been produced. Another experiment was then carried out, under an atmosphere of air at 40 °C for 47 hours. The red precipitate was simply collected by filtration after cooling the mixture at -18 °C for an hour, which transpired to be the desired pure 1,1'-biazulene-2,2'-diol (\pm)-**370** in 28% yield. On increasing the scale of the procedure from 0.411 mmol, eventually to 8.94 mmol, the desired product could be produced in 55% yield (Scheme 73). Given that this result was reproducible, this procedure represented a

great improvement in yield, scalability and reliability compared to the Ullmann-like methods to produce a 1,1'-biazulene species.



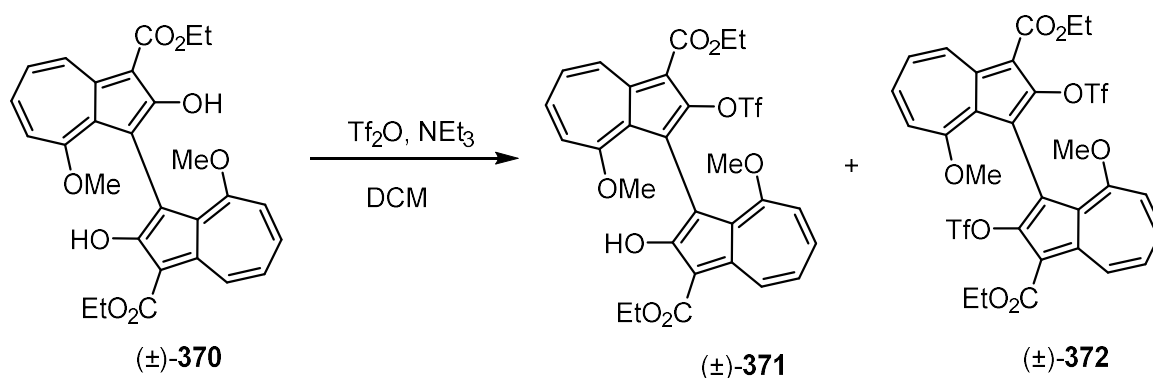
Scheme 73: The copper-catalysed oxidative homocoupling reaction to produce (±)-diethyl 2,2'-dihydroxy-8,8'-dimethoxy-[1,1'-biazulene]-3,3'-dicarboxylate (±)-**370**.

2.2.6. Chemical transformations of ester-containing 1,1'-biazulene-2,2'-diol

Now that a 1,1'-biazulene species could be easily synthesised, the next step was to convert the two hydroxy groups to triflates. Disappointingly, when the procedure described in Scheme 66 was adapted for the biazulene diol **370**, the result was a mere 9.1% yield of the desired biazulene ditriflate (±)-**372** (Table 10, entry 1), compared to the 63% yield achieved for the triflation of the monomeric ethyl 2-hydroxy-4-methoxyazulene-1-carboxylate **337**. Although the 1,1'-biazulene-2,2'-diol (±)-**370** was more sparingly soluble than its corresponding monomer, the expected implication of this would be a slower reaction. Instead, the monotriflated product (±)-**371** was only produced in 7.1% yield, and there was no recovered starting material. As the reaction proceeded, the mixture changed colour from deep red to black, which is more indicative of a degradation process of the azulene structure. A similar reaction was carried out with the addition of triflic anhydride taking place at – 78 °C, resulting in a purple solution at this temperature. However, on allowing the

mixture to warm to room temperature, the colour changed to black, and the desired product (\pm)-**372** could not be isolated purely (Table 10, entry 2). The logical next step was to maintain the mixture at $-78\text{ }^{\circ}\text{C}$ for the duration of the reaction. When this was done, using 6.0 equivalents of triethylamine and 3.0 equivalents of triflic anhydride (plus another 2.0 equivalents added after 90 minutes to ensure complete conversion of starting material), running for 2 hours, the desired biazulene ditriflate (\pm)-**372** was produced in an improved 30% yield (Table 10, entry 3). When the scale of the experiment was increased from 0.12 mmol to 1.0 mmol, but without the additional 2.0 equivalents of triflic anhydride, the yield of the ditriflate (\pm)-**372** was 22% (Table 10, entry 4). Because of the larger scale, the remaining starting material (\pm)-**370** could be recovered in 10% yield, collected by filtration immediately after the reaction had finished.

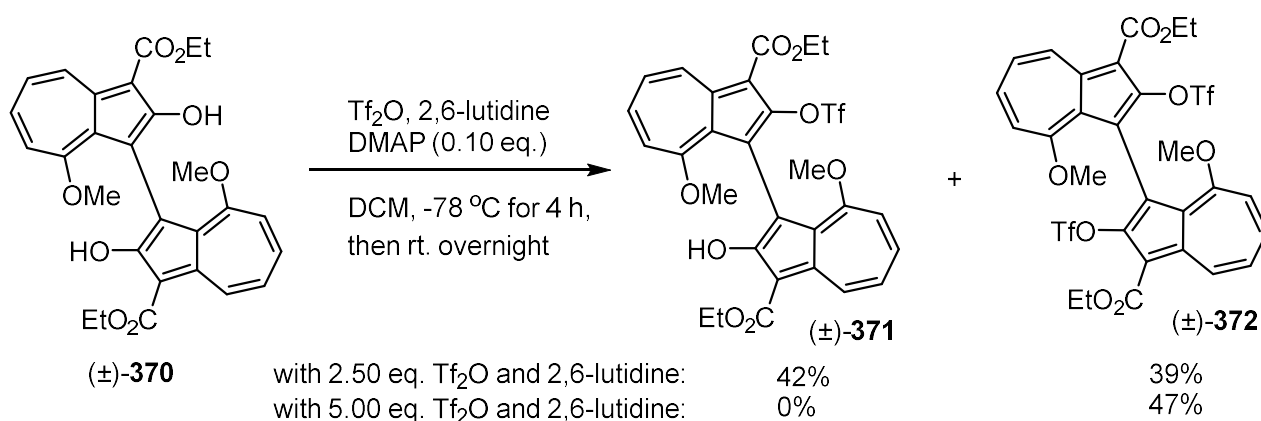
Table 10: The attempts to convert 1,1'-biazulene-2,2'-diol (\pm)-**370** to 1,1'-biazulene-2,2'-ditriflate (\pm)-**372** using triflic anhydride and triethylamine as base.



Entry	Scale /mmol	Equivalents of Tf ₂ O	Equivalents of NEt ₃	Temperature ^b	Running time /h	Yield of (\pm)- 371	Yield of (\pm)- 372
1	0.612	4.35 ^a	6.22 ^a	0 \rightarrow rt.	18	7.6	9.1
2	0.204	3.00	5.28	$-78\rightarrow$ rt.	22	4.9	impure
3	0.120	5.00 ^a	12.0 ^a	-78	2	impure	30
4	1.02	3.00	5.00	-78	7	0 ^c	22

a) Reagent added in two portions **b)** Changes in temperature were effected immediately after the first addition of triflic anhydride, and for second addition of reagents, the reaction was cooled to starting temperature **c)** The starting material (\pm)-**370** was recovered in 10% yield.

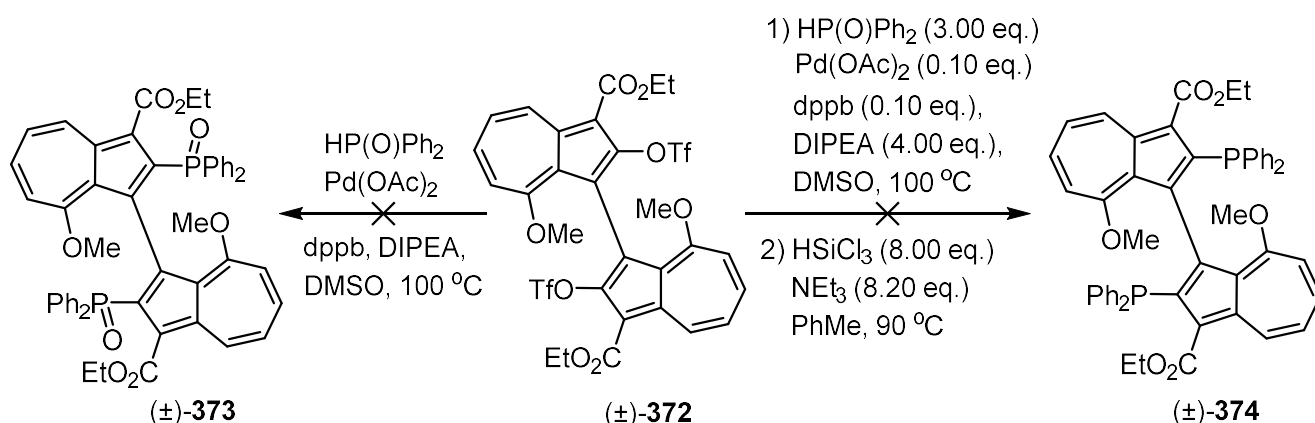
Since none of the protocols, in which triethylamine was used as the base, were affording the desired ditriflate (\pm)-**372** in a satisfactory yield, other methods in the literature were explored. It appeared that the triflation reaction had to be treated more carefully for the 1,1'-biazulene-2,2'-diol (\pm)-**370** than for the 2-hydroxyazulene **337**. After searching for a procedure that worked specifically for a biaryl diol, a report by Mikami *et al.* was found, describing the ditriflation of 4,4'-di-*tert*-butyl-[1,1'-biphenyl]-2,2'-diol with 2.5 equivalents each of triflic anhydride and 2,6-lutidine, and 0.1 equivalents of *N,N*-dimethylaminopyridine (DMAP), which gave the corresponding ditriflate product in 97% yield.²¹⁵ This procedure was applied to the 1,1'-biazulene-2,2'-diol (\pm)-**370**, on a scale of 0.41 mmol, at $-78\text{ }^{\circ}\text{C}$ for 4 hours, followed by stirring overnight at room temperature (Scheme 74). It proved to be a much cleaner reaction, producing the biazulene ditriflate (\pm)-**372** in 39% yield, though also along with the monotriflated product (\pm)-**371** in 42% yield. By increasing the quantities of triflic anhydride and 2,6-lutidine to 5.0 equivalents each, and adding the triflic anhydride to the mixture in two portions, the yield of biazulene ditriflate (\pm)-**372** improved to 47%, without a trace of the monotriflated biazulene (\pm)-**371**. When the scale of the reaction was doubled to 0.82 mmol, the yield of biazulene ditriflate (\pm)-**372** was mostly retained, at 44%.



Scheme 74: The ditriflation of diethyl 2,2'-dihydroxy-8,8'-dimethoxy-[1,1'-biazulene]-3,3'-dicarboxylate (±)-**370** with triflic anhydride, with 2,6-lutidine as the base, and in the presence of DMAP, to make biazulene monotriflate (±)-**371** and biazulene ditriflate (±)-**372**.

Now that practicable quantities of 1,1'-biazulene-2,2'-ditriflate (±)-**372** could be isolated, the most challenging step of the synthesis followed, which was to carry out a double cross coupling reaction to install phosphine groups at the 2,2'-positions. Due to the previous success in forming the monomeric azulene-2-yl phosphine oxide **347**, as in Scheme 69, this method was adapted for the biazulene ditriflate (±)-**372** by increasing the molar quantities of all of the reagents by a factor of two. This reaction was run twice: once with degassed, anhydrous DMSO as the solvent, and the other in DMSO that was merely anhydrous. Neither of these experiments yielded neither the desired biazulene diphosphine oxide (±)-**373**, nor the semi-complete biazulene monophosphine oxide monotriflate; the only identified product was 1,4-bis-(diphenylphosphino)butane dioxide from the experiment with non-degassed solvent (Scheme 75). In a similar manner to improving the double triflation reaction, other literature methods were explored, specifically to convert a biaryl ditriflate rather than a monomer. The same paper, by Mikami *et al.*, that described the double triflation using 2,6-lutidine and DMAP, reported a subsequent process to convert 4,4'-*tert*-butyl-[1,1'-biphenyl]-2,2'-diyl bis-(triflate) to the corresponding biaryl bis-

(diphenylphosphine oxide) in 72% yield.²¹⁵ The conditions were similar to what had already been tried in this project, but specified a reaction time of 48 hours, rather than overnight. Following this protocol, the conditions used for the next attempt at converting the biazulene ditriflate (\pm)-**372** to the biazulene diphosphine oxide (\pm)-**373** were 3.0 equivalents of diphenylphosphine oxide, 0.1 equivalents of palladium diacetate, 4.0 equivalents of Hünig's base and 0.1 equivalents of dppb. Unfortunately, after heating this mixture in degassed DMSO at 100 °C for 63 hours, the only identified product, again after column chromatography, was dppb dioxide. The possibility was then considered that the desired biazulene diphenylphosphine oxide product could be too polarised to elute through the silica column, and was hidden amongst a stationary fraction at the baseline. To test this hypothesis, the experiment was repeated, in which an attempted reduction of the two phosphine oxide groups with trichlorosilane was carried out on the crude mixture to try forming diphosphine (\pm)-**374**. Once this process had taken place, the proton NMR spectrum of the subsequent crude mixture revealed a trace of an azulene-like product, which could not be identified. It was after this experiment that it was accepted that perhaps the pseudohalides on the biazulene ditriflate (\pm)-**372** were too sterically hindered to react, leading to competing processes that led to degradation of the starting material.

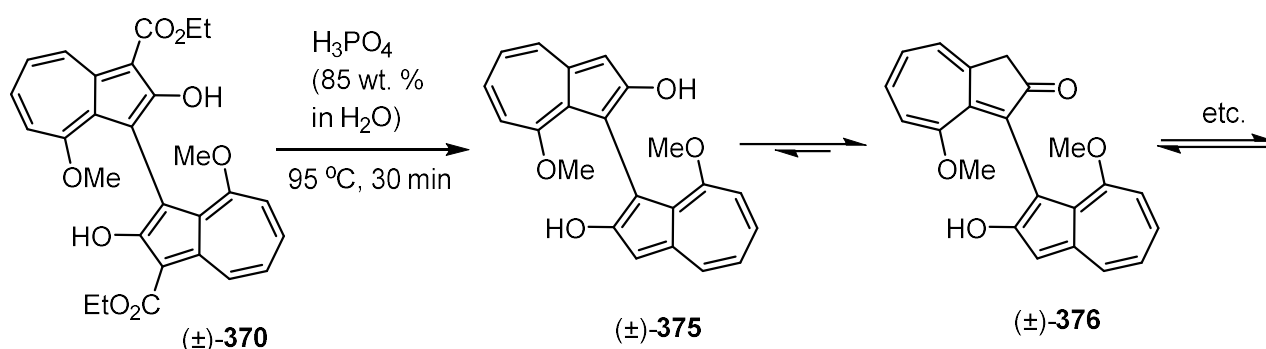


Scheme 75: The attempts at the Pd-catalysed cross coupling reaction of diphenylphosphine oxide and 1,1'-biazulene-2,2'-ditriflate (±)-**372** (left), and the trichlorosilane-mediated reduction of the assumed crude bis-(diphenylphosphine) oxide product (±)-**373** (right).

2.2.7. Removal of ester groups

In order to decrease steric bulk around the triflate groups, one option was to remove the ester groups in a decarboxylation reaction, as they had already served their purposes in the synthesis; that is, to activate the 2*H*-cyclohepta[*b*]furan-2-one derivative **298** for the [8+2]-addition-elimination reaction to form the azulene **326**, and to coordinate to the copper(II) catalyst to facilitate the oxidative homocoupling reaction, forming the 1,1'-biazulene (±)-**370**. The lithium chloride-mediated method described in Scheme 71 was low yielding, so it was decided that an alternative method, which was to heat the azulenyl carboxylate in *orthophosphoric acid*, was to be tested instead, as it had been previously shown to work for alkyl 2-hydroxyazulene-1-carboxylate derivatives.¹⁹⁴ At first, the process was tested by heating 1,1'-biazulene-2,2'-diol (±)-**370** with the standard commercially available form of *orthophosphoric acid*, which is 85 wt. % in water, at 95 °C for 30 minutes. The desired product of 2,2'-dihydroxy-8,8'-dimethoxy-1,1'-biazulene (±)-**375** appeared to be the majority product of the crude mixture by mass spectrometry.

However, the proton NMR spectrum was not well-defined, and appeared to show alkene-like signals, which may indicate that the compound prefers to form the keto tautomer (\pm)-**376** in CDCl_3 ,²¹⁶ rather than the enol tautomer (\pm)-**375** (Scheme 76). In addition, the product lacked stability on silica, possibly due to the acidic environment causing aldol-like degradation processes and oligomerisation, and could not be purified.

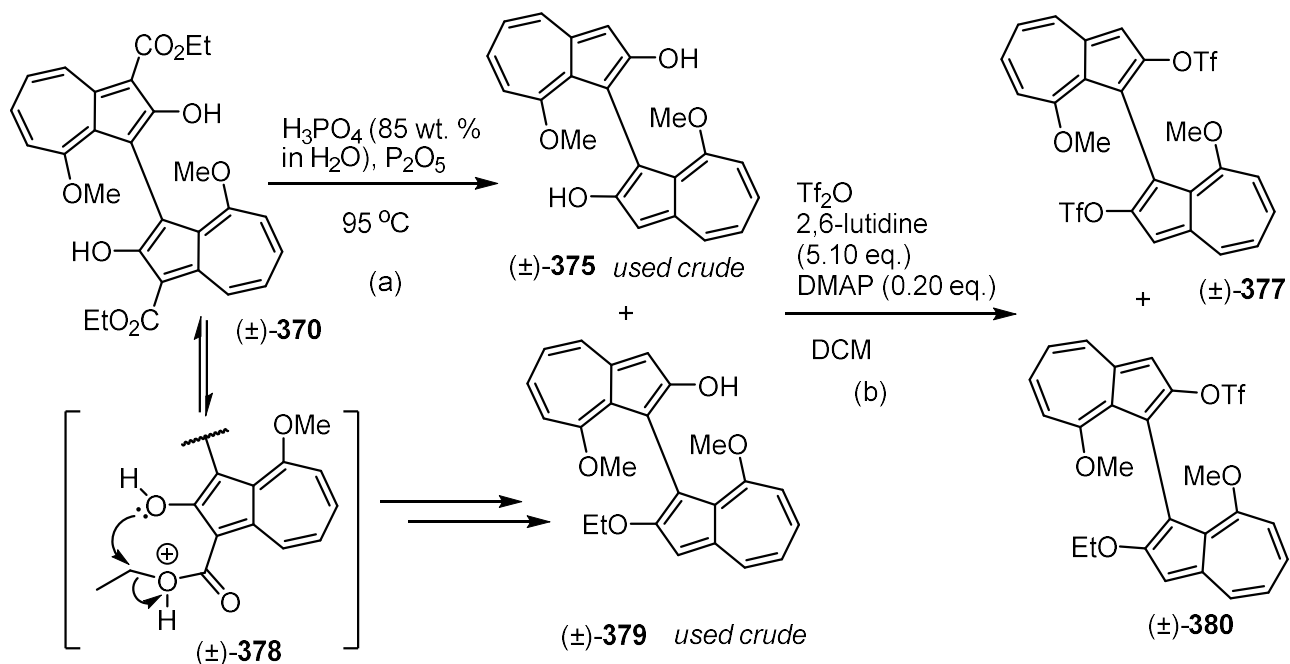


Scheme 76: The attempted removal of the ester groups from diethyl 2,2'-dihydroxy-8,8'-dimethoxy-[1,1'-biazulene]-3,3'-dicarboxylate (\pm)-**370** with aqueous *orthophosphoric acid*, giving the unstable 2,2'-diol (\pm)-**375**.

To combat this lack of stability, it was hypothesised that the 1,1'-biazulene-2,2'-diol product (\pm)-**375** could be trapped in the desired bis-(enol) tautomer through rapid *O*-substitution. With this idea in mind, the reaction was repeated with anhydrous *orthophosphoric acid* (dried by using phosphorus pentoxide) this time, and instead of purification with column chromatography, the crude 1,1'-biazulene-2,2'-diol (\pm)-**375** was treated with a similar procedure to that previously used in this project for a double triflation, as described in Scheme 74. After stirring with triflic anhydride, 2,6-lutidine and DMAP at $-78\text{ }^\circ\text{C}$ for 8 hours, the desired 1,1'-biazulene-2,2'-ditriflate (\pm)-**377** was isolated in 45% yield with respect to the ester-containing biazulene diol (\pm)-**370** (Table 11, entry 1). An unusual side product of 2'-ethoxy-[1,1'-biazulene]-2-yl

triflate (\pm)-**380** was also obtained in 8% yield, which was probably formed from the 2-hydroxy-2'-ethoxy-1,1'-biazulene intermediate (\pm)-**379**, which itself could have formed by an acid-mediated migration of the ethyl group from the ester to the hydroxyl group. When the scale of this reaction was doubled to 0.41 mmol, the yield of (\pm)-**377** was essentially retained, giving 44% of the desired 1,1'-biazulene-2,2'-ditriflate (\pm)-**377** after a much shorter length of time to carry out the triflation process (Table 11, entry 2). Again, the side product (\pm)-**380** was formed (in 4.8% yield), and it was from this experiment that the structure of (\pm)-**380** could be elucidated, due to the higher purity of this sample than that of entry 1. The scale of the experiment was increased again to 0.88 mmol, and the triflation was allowed to warm up to room temperature after the addition of triflic anhydride at $-78\text{ }^{\circ}\text{C}$, which resulted in a slight decrease of the yield of (\pm)-**377** to 39% (Table 11, entry 3). No trace of side product (\pm)-**380** was detected this time, although it is unclear why this was the case. The best yield, at 52%, of biazulene triflate (\pm)-**377** was achieved because of a running time for the decarboxylation being increased to nearly 2 hours, or due to using 2.5 equivalents of triflic anhydride in the second step, which was half of what was previously used, or due to both of these changes (Table 11, entry 4). This experiment produced some of side product (\pm)-**380**, but the yield of this could not be determined as it could not be isolated in pure form. Overall, despite consisting of two chemical steps, it was felt that this procedure was more convenient than that of Scheme 74, as the triflation step could be run at room temperature without degradation of the starting material. This process also added flexibility in the construction of the ligand, as the removal of the ester groups would allow derivatisation of the 3,3'-positions at a later stage, if this was required in order to improve the stereoselectivity of a particular reaction.

Table 11: The phosphoric acid-mediated decarboxylation of diethyl 2,2'-dihydroxy-8,8'-dimethoxy-[1,1'-biazulene]-3,3'-dicarboxylate (\pm)-**370**, followed by the double triflation of the hydroxyl groups.

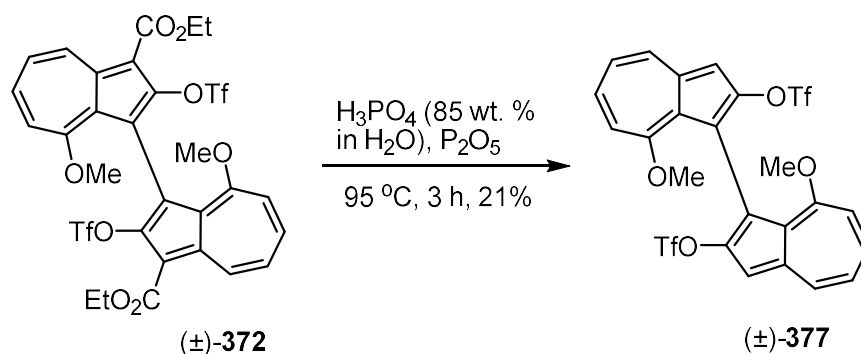


Entry	Scale /mmol	Running time (a) /min	Equivalents of Tf_2O^a	Temperature /°C	Running time (b) /h	Yield of (\pm)- 377 /%	Yield of (\pm)- 380 /%
1	0.204	30	5.00	-78	8	45	~8 (slight impurity) ^c
2	0.408	40	5.00	-78	2	44	4.8
3	0.877	55	5.00	-78→rt. ^b	15	39	0
4	0.532	110	2.50	-78→rt.	18	52	(impure) ^c

a) When 5.00 equivalents were used, triflic anhydride was added in two portions **b)** Temperature was lowered to -78 °C again for second addition of triflic anhydride **c)** Identity of impurity unknown.

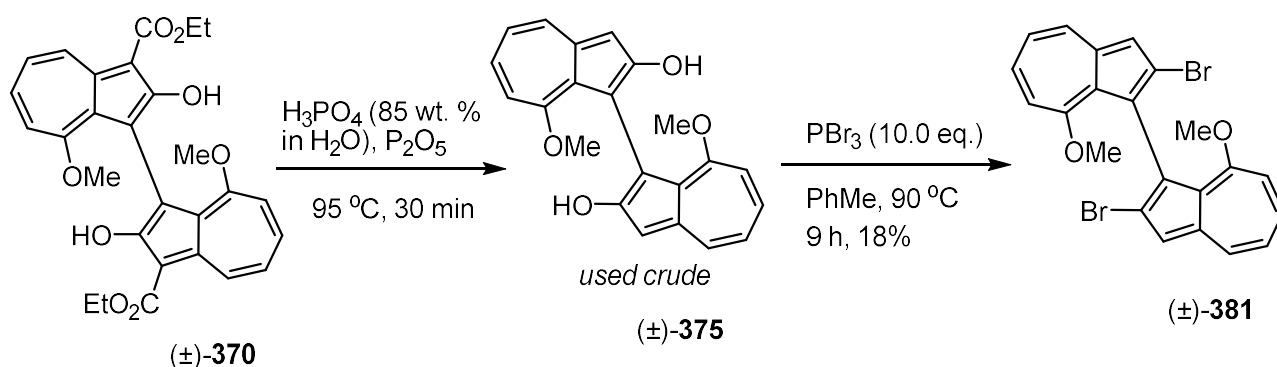
The reversal of the order of the above two steps was tested as well, i.e. double triflation of the ester-containing biazulene diol (\pm)-**370**, followed by *orthophosphoric* acid-mediated decarboxylation. The decarboxylation process required 3 hours of heating the ester-containing 1,1'-biazulene-2,2'-ditriflate (\pm)-**372** with anhydrous *orthophosphoric* acid at 95 °C to completely consume the starting material, and this only resulted in 21% yield of the decarboxylated biazulene ditriflate (\pm)-**377** (Scheme 77). The decarboxylation of the ester-containing biazulene diol (\pm)-**375** probably works more efficiently than for the ditriflate (\pm)-**372**, as the hydroxy group can act as

a hydrogen bond donor towards the carbonyl, polarising the ester moiety and increasing the reaction rate.



Scheme 77: The decarboxylation reaction of the ester-containing 1,1'-biazulene-2,2'-ditriflate (±)-372.

It was decided that the decarboxylation-triflation procedure should be undertaken in that order, as described in Table 11. This protocol was shown to have some versatility in the choice of the electrophile, as phosphorus tribromide could be used in place of triflic anhydride, to install bromines at the 2,2'-positions of the biazulene. The treatment of 1,1'-biazulene-2,2'-diol (±)-370 with anhydrous *orthophosphoric* acid at 95 °C for 30 minutes, followed by the reaction of the crude mixture with phosphorus tribromide in toluene at 90 °C for 9 hours, produced 2,2'-dibromo-8,8'-dimethoxy-1,1'-biazulene (±)-381 in 18% yield (Scheme 78).

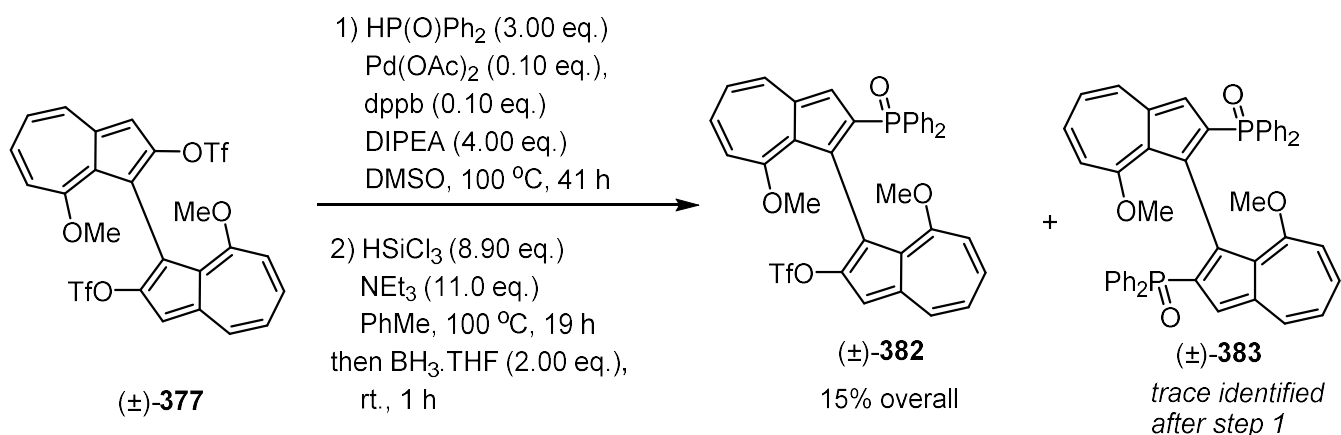


Scheme 78: The decarboxylation of 1,1'-biazulene-2,2'-diol (±)-370, followed by treatment with phosphorus tribromide, to give the dibromo biazulene (±)-381.

2.2.8. Installation of phosphorus-containing functional groups

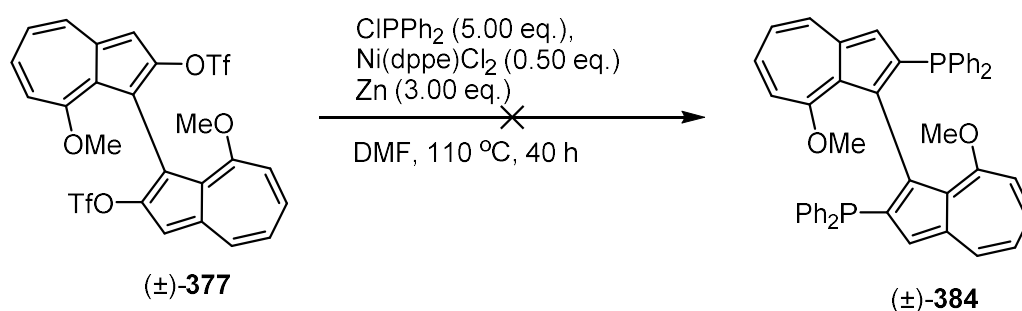
Now that a method had been developed to produce a 1,1'-biazulene-2,2'-ditriflate compound with the ester groups removed, this species would now be less sterically hindered, and would perhaps be better suited for the carbon-phosphorus bond formation to synthesise a 1,1-biazulene-2,2'-diphosphine ligand. As the only successful carbon-phosphorus cross coupling reaction had taken place with the palladium-catalysed formation of the azulene-2-yl phosphine oxide **347**, as described in Scheme 69, this methodology was applied towards the decarboxylated biazulene ditriflate (\pm)-**372**. This species was heated at 100 °C with diphenylphosphine oxide, palladium diacetate, bis-1,4(diphenylphosphino)butane and Hünig's base in DMSO for 41 hours (Scheme 79). Inspection of the proton NMR spectrum of the crude mixture showed that virtually all of the starting material had been consumed, and had been replaced by several azulene-like species. The mass spectrum of the mixture showed matching m/z values for both the desired product (\pm)-**383** and mono-phosphine oxide species (\pm)-**382**. The application of column chromatography gave a fraction of several inseparable azulene-like species. In order to aid separation, this fraction was treated with trichlorosilane and triethylamine in toluene at 100 °C to reduce the phosphine oxide, and to this resultant mixture was added borane to form the phosphine borane adduct, to prevent spontaneous re-oxidation. Unfortunately, after column chromatography, the only product isolated was the mono-phosphine oxide species (\pm)-**382** in 15% overall yield, implying that the cross coupling reaction had only worked on one triflate group, and that the reduction step had not worked. Despite not being able to isolate the desired biazulene diphenylphosphine oxide, this

experiment still represented progress towards the target ligand, as the presence of esters had previously prevented any reaction of the triflate groups from taking place.



Scheme 79: The Pd-catalysed cross coupling reaction of diphenylphosphine oxide with 1,1'-biazulene-2,2'-ditriflate (**(±)-377**), followed by attempted trichlorosilane reduction and borane protection of the phosphine groups.

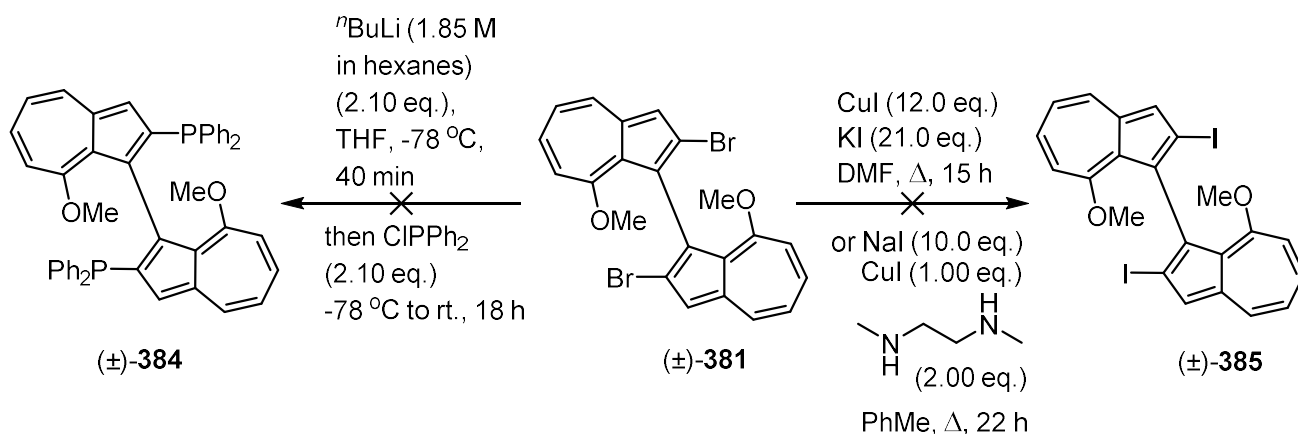
The nickel-catalysed cross coupling reaction of chlorodiphenylphosphine with 1,1'-biazulene-2,2'-ditriflate (**(±)-377**) was also attempted, to access directly the diphosphine without requiring a reduction step for any phosphine oxide groups. This procedure was similar to that described in Scheme 68, except the equivalents of reagent and conditions were adjusted according to the procedure by Wu *et al.*²¹⁷ Rather than resulting in degradation of starting material, however, this experiment appeared to have no effect on the biazulene ditriflate (**(±)-377**), as this was the only product shown in the crude analysis (Scheme 80). This result supports the idea that ester groups at the 1- or 3-positions of the azulene lead to instability of the structure under the conditions of this sort of nickel-catalysed carbon-phosphorus bond formation.



Scheme 80: The attempted Ni-catalysed cross coupling reaction between chlorodiphenylphosphine and 1,1'-biazulene-2,2'-dinitrile (\pm)-**377**.

The 2,2'-dibromobiazulene derivative (\pm)-**381** was also readily accessible, so a strategy to access the 1,1'-biazulene-2,2'-diphosphine ligand through a halogen-lithium exchange, followed by quenching the azulene-2-yl lithium with an electrophile, was also explored. The drawback to this approach was that bromine-lithium exchange chemistry at the 2-position of an azulene structure had not previously been carried out in the literature, so it was likely that carrying out two lithiations on the biazulene would be challenging. The 2,2'-dibromo derivative (\pm)-**381** was thus treated with *n*-butyllithium in THF at $-78\text{ }^\circ\text{C}$, and at the same temperature, the presumed biazulen-2,2'-diyl dilithium intermediate was treated with chlorodiphenylphosphine, and allowed to warm to room temperature (Scheme 81). The reaction did not yield the desired product but unexpectedly, the starting material was largely recovered from the experiment. To try facilitating the halogen-lithium exchange process, the 2,2'-dibromobiazulene (\pm)-**381** was subjected to two literature methods for a Finkelstein-like reaction to access the 2,2'-diiodo-1,1'-biazulene (\pm)-**385**. The first method was to heat at reflux the dibromo derivative (\pm)-**381** with an excess of both copper(I) iodide and potassium iodide in DMF,¹⁹⁴ which only resulted in the degradation of starting material. The second attempt was similar to the first, but with sodium iodide in place of potassium iodide, *N,N'*-dimethylethylenediamine

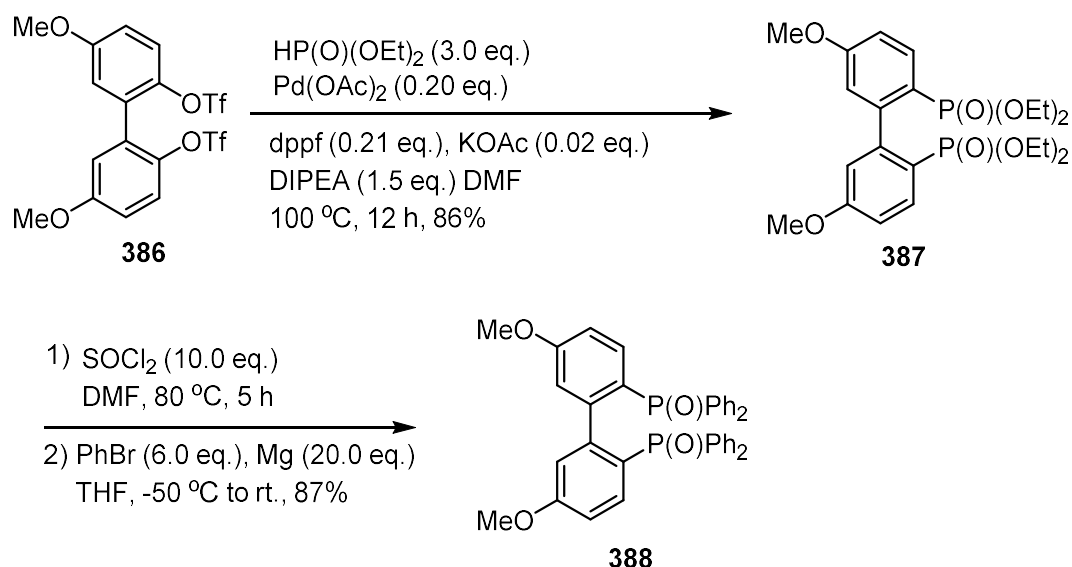
as a ligand, and with heating at reflux in toluene.²¹⁸ No conversion of the starting material was observed after 22 hours of reaction time. As the 2,2'-bromo-1,1'-azulene (\pm)-**381** could not be synthesised as efficiently as the analogous ditriflate species (\pm)-**377**, the focus was shifted away from the halogen-lithium exchange strategy and back to a transition metal cross-coupling method.



Scheme 81: The attempted installation of diphenylphosphine groups by halogen-lithium exchange of 2,2'-dibromo-8,8'-dimethoxy-1,1'-biazulene (\pm)-**381**, and attempted substitution of bromide groups with iodides.

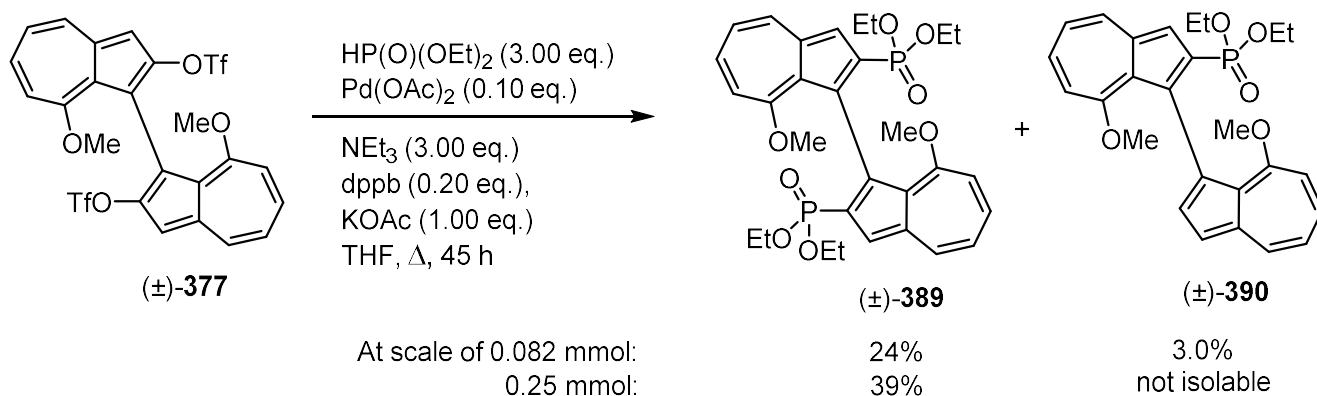
Although the removal of the 3,3'-ester groups had enabled some reactivity of the 1,1'-biazulene-2,2'-ditriflate (\pm)-**377** to take place in the palladium-catalysed cross coupling reaction with diphenylphosphine oxide, the reaction had only taken place at one rather than two sites, and in low yield. Also, it was difficult to know which reagents or conditions to change in this process to improve the yield. An alternative method was to carry out the carbon-phosphorus bond formation by using a dialkylphosphite species, giving the aryl dialkylphosphonate product. This species could be converted to the phosphine ligand through nucleophilic substitution of the alkoxy groups with the desired Grignard reagent, followed by reduction of the resultant phosphine oxide to the phosphine. A detailed study by Stawinski *et al.* demonstrated the generality of this carbon-phosphorus bond formation, showing that

both electron-rich and electron-poor aryl halides and triflates could be converted to aryl phosphonate esters.²¹⁹ The reaction also showed good functional group tolerance, as more elaborate biologically-relevant dinucleoside H-phosphonates could be coupled with bromobenzene in good yield. What made this reaction more appealing was that the aryl triflates showed a much greater degree of reactivity than the aryl halides, as the non-coordinating nature of the leaving group means it does not deactivate the catalyst. Additionally, the reaction had previously been shown take place twice in one pot to convert a 1,1'-biphenyl-2,2'-ditriflate derivative **386** to the corresponding biphenyl bis-(diethylphosphonate) **387** by Zhang *et al.*, in the synthesis of the BridgePhos series of ligands (Scheme 82).²²⁰ The phosphonate esters were then converted to the phosphine oxides through the reaction with thionyl chloride to form the bis-(phosphonic dichloride), which then could be reacted with various Grignard reagents to get the desired product **388**.



Scheme 82: The palladium-catalysed cross coupling reaction of biphenyl ditriflate **386** with diethyl phosphite to give the bis-(phosphonate ester) **387**, which was then treated with thionyl chloride and phenyl magnesium bromide to yield the bis-(diphenylphosphine oxide) **388**, by Zhang.

Adhering to a combination of the methods described by Stawinski and Zhang, 8,8'-dimethoxy-[1,1'-biazulene]-2,2'-diyl ditriflate (\pm)-**377** was heated at reflux with diethyl phosphite, palladium diacetate as the pre-catalyst, dppb as a ligand, triethylamine as a base, and potassium acetate as an additive in THF for 45 hours (Scheme 83). The TLC analysis showed complete conversion from the starting material to two different blue spots, and mass spectrometry showed a peak that corresponded to the desired product (\pm)-**389**. After column chromatography, the proton NMR spectrum of one of the fractions showed what appeared to be the desired product, but with large ethyl-like signals. It was deduced that the product had co-eluted with triethylammonium triflate, which required a simple aqueous wash to remove, giving the pure 1,1'-biazulene-2,2'-bis-(diethylphosphonate) (\pm)-**389** in 24% yield. The other product isolated was mono(diethylphosphonate) species (\pm)-**390** in 3.0% yield, which was possibly a reduction product of the palladium(II)-azulene intermediate species formed after oxidative addition of the biazulene triflate (\pm)-**377**. On increasing the scale of the reaction from 0.082 mmol to 0.25 mmol, the yield of biazulene bis-(diethylphosphonate) (\pm)-**389** increased to 39%, which meant practicable quantities of a biazulene with two phosphorus-containing functional groups at the 2,2'-positions could now be synthesised. On this occasion, the biazulene mono(diethylphosphonate) side product (\pm)-**390** was detected, but the yield could not be calculated as it had co-eluted with an additional, unidentified, unsymmetrically substituted biazulene species.



Scheme 83: The palladium-catalysed double cross coupling reaction of 8,8'-dimethoxy-[1,1'-biazulene]-2,2'-diyl ditriflate (±)-**377** with diethylphosphite.

The proton NMR spectrum for the 1,1'-biazulene bis-(diethylphosphonate) (±)-**389** showed important evidence of its axial chirality, particularly from the inequivalent nature of the ethyl groups in the phosphonate esters (Figure 34). The methylene signals (11,11',13,13'-CH₂) were comprised of four different complex multiplets, split in this manner because of their diastereotopicity, coupling with the geminal methylene proton, the methyl group and the phosphorus atom. While not a result of the axial chirality from the biazulene skeleton, an interesting observation comes from the methyl groups (12,12',14,14'-CH₃) being divided into two triplets, showing significantly different chemical shifts to each other. The change is brought about probably because one methyl group, for each phosphonate ester group, is closely aligned with the centre of the aromatic system. The induced magnetic field of the azulene (anisotropic effect) has a shielding effect on the protons of that methyl group, lowering the chemical shift value.

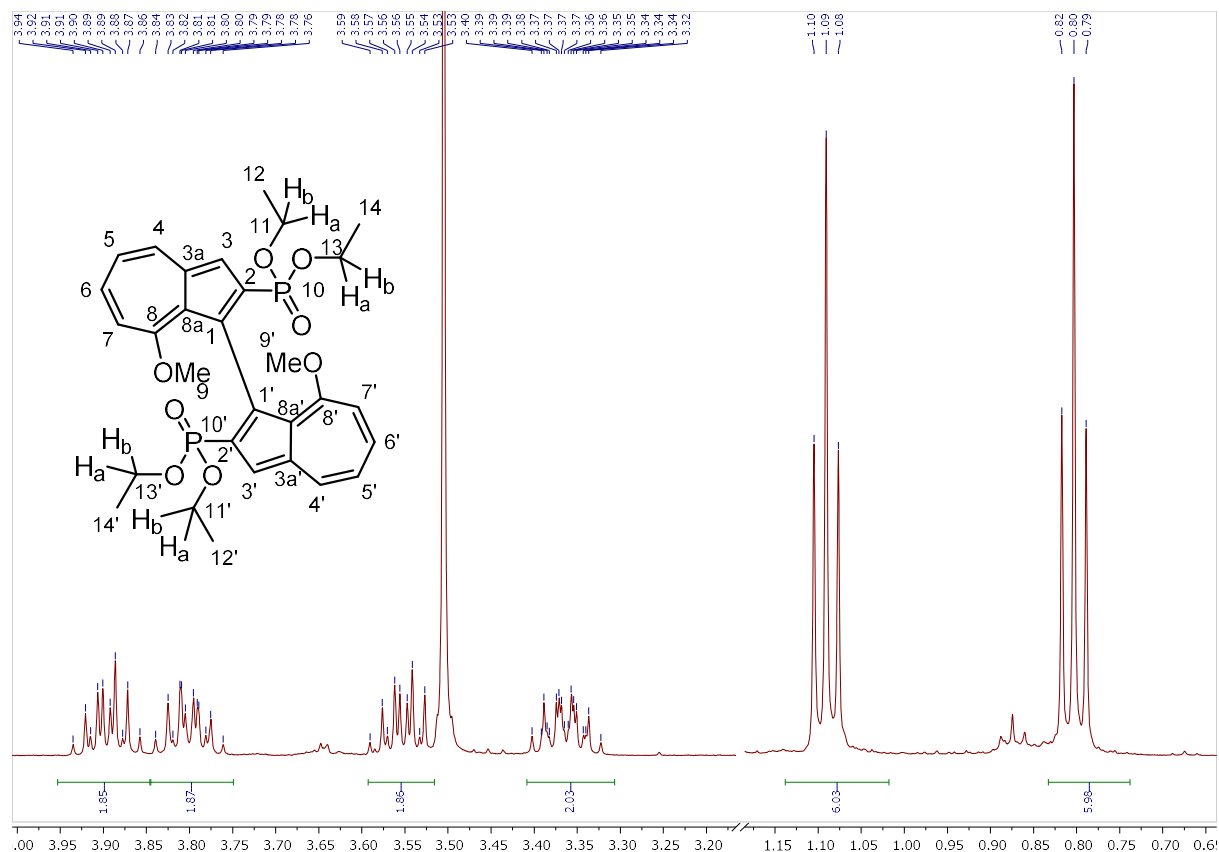
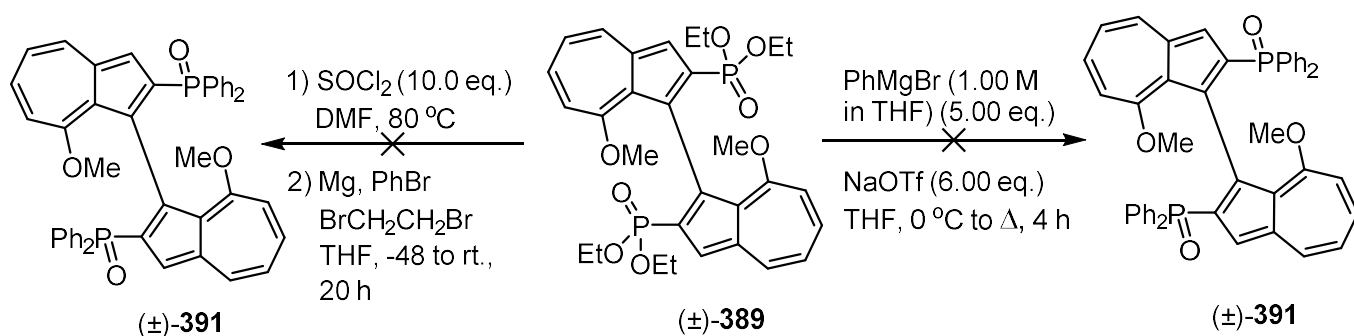


Figure 34: Proton NMR spectrum of 1,1'-biazulene bis-(diethylphosphonate) (±)-**389** in CDCl_3 , highlighting peaks for the ethyl groups on the phosphonate esters (11,11',12,12',13,13',14,14'- CH_n). The region between 3.20-1.20 ppm is omitted for clarity.

The next step towards the synthesis of the 1,1'-biazulene-2,2'-diphosphine ligand was the nucleophilic displacement of the ethoxy groups with a nucleophilic arene species, to make the 1,1'-biazulene-2,2'-bis-(diarylphosphine oxide) (±)-**391**. Following the procedure of Zhang, the 1,1'-biazulene bis-(diethylphosphonate) (±)-**389** was treated with 10.0 equivalents of thionyl chloride, with DMF acting as the solvent and catalyst, and heated at 80 °C for 2 hours in order to make the bis-(phosphonic dichloride) intermediate (Scheme 84). The second step was the treatment with freshly prepared phenyl magnesium bromide at –48 °C at first, then allowing it to stir at room temperature overnight. Disappointingly, the proton NMR spectrum of the brown crude mixture indicated the degradation of the starting material. A similar result was achieved when instead, the thionyl chloride was

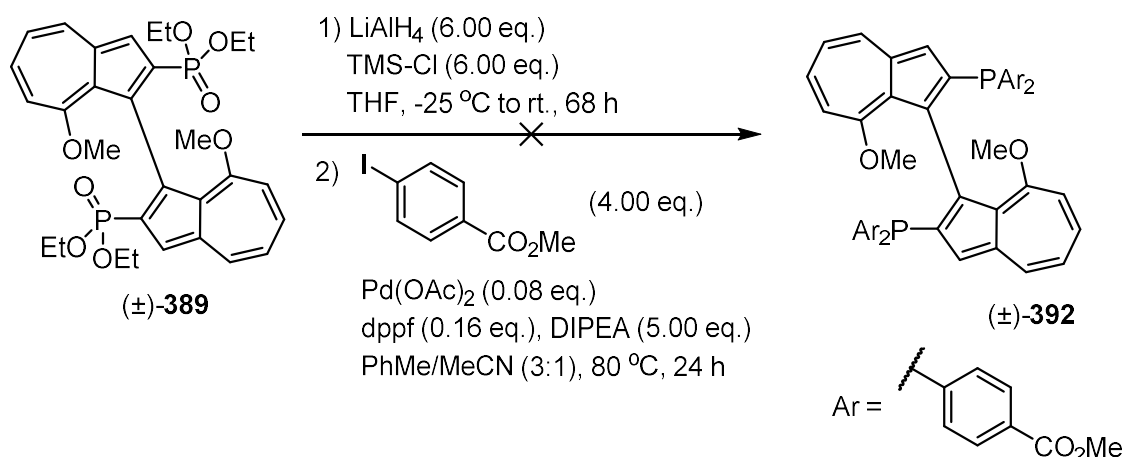
applied in a very large excess, effectively acting as the solvent, while 15.0 equivalents of DMF were used, and phenyl magnesium bromide was sourced from a commercially made solution. As it was possible that the attempts to form the bis-(phosphonic dichloride) intermediate were resulting in the decomposition of the azulene, the method developed by Tyler *et al.*, in which the aryl phosphonate ester could be converted directly to the aryl phosphine oxide, was appealing.²²¹ The group could treat the aryl dialkylphosphonate with a Grignard reagent in the presence of sodium triflate to form the product. The additive was crucial, as it precipitated the sodium halide out of the reaction mixture, preventing halide-mediated formation of coordination oligomers from the Grignard addition intermediates. Following this method, 1,1'-biazulene bis-(diethylphosphonate) (\pm)-**389** was treated with 5.0 equivalents of phenyl magnesium bromide and 6.0 equivalents of sodium triflate, and was heated at reflux in THF for 4 hours. The brown crude product was then treated with *p*-chloranil to rearomatise the azulene structure, if the Grignard addition had taken place at the electron-poor positions of the azulene. There was no change in colour, however, and NMR spectrum of this crude product showed only indeterminate aromatic peaks.



Scheme 84: Attempts to convert the 1,1'-biazulene bis-(diethylphosphonate) (\pm)-**389** to 1,1'-biazulene bis-(diphenylphosphine oxide) (\pm)-**391** through Grignard addition.

An alternative, established way to convert phosphonate esters to tertiary phosphines is through a reduction to the primary phosphine,²²² followed by a transition metal cross-coupling reaction to attach the desired aryl or alkyl groups to the phosphorus atom.²²³ This method was attractive as it avoided the use of highly reactive organometallic reagents, to which the azulene backbone was potentially sensitive. The process was applied to the 1,1'-biazulene bis-(diethylphosphonate) (\pm)-**389** by adding to it a mixture of lithium aluminium hydride and trimethylsilyl chloride at -25°C , and stirring at room temperature for 68 hours (Scheme 85). The work-up procedure was carried out with degassed solvents and aqueous solutions, and while the NMR spectra was difficult to characterise, the formation of the 1,1'-biazulene bis-(primary phosphine) was not ruled out, due to the persistence of aromatic proton peaks. The ^{31}P -NMR spectrum showed signals at -15 and -153 ppm; the latter of which was more likely to correspond to a primary phosphine.

The second half of the method was carried out according to the procedure by Michelet *et al.* in which the presumed 1,1'-biazulene bis-(primary phosphine) was treated with methyl 4-iodobenzoate as the cross-coupling partner (as it showed good reactivity in the literature report), palladium diacetate as the pre-catalyst, 1,1'-bis-(diphenylphosphino)ferrocene (dppf) as a ligand, and Hünig's base. This mixture was heated at 80°C in toluene/acetonitrile (3:1) for 24 hours, but after an aqueous work-up, only methyl 4-iodobenzoate could be seen on the NMR spectrum.



Scheme 85: The attempted reduction of 1,1'-biazulene-2,2'-diyl bis-(diethylphosphonate) (\pm)-**389** to the bis-(primary phosphine), followed by palladium-catalysed cross coupling of aryl groups to the phosphorus atom.

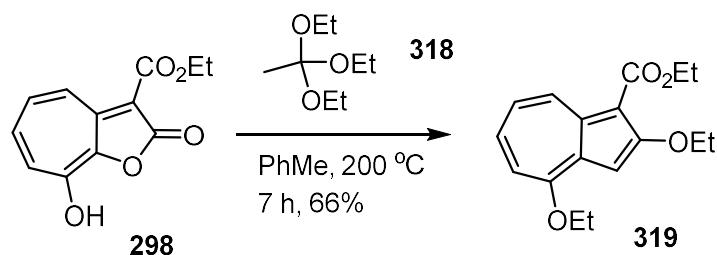
2.3. Development of 1,1'-biazulene-2,2'-diol (“1,1'-BazOL”)

After this series of unsuccessful reactions, it was decided that the studies towards the synthesis of a 1,1'-biazulene-2,2'-diphosphine ligand had been taken as far as possible at this point, and any further developments towards this target would be postponed for another time. However, the incomplete route encompassed a method to make a racemic form of the 1,1'-biazulene-2,2'-diol derivative (\pm)-**370** as a synthetic intermediate, which could itself be employed instead as a ligand for asymmetric catalysis, analogous to BINOL **213** and derivatives. The biazulene diol (\pm)-**370** in question possesses ester groups at the 3,3'-positions to retain the enol form of the structure, which lead to a minor issue if this structure was indeed to be considered the target molecule. At this time, the [8+2]-addition-elimination to synthesise the azulene from any 2*H*-cyclohepta[*b*]furan-2-one derivative (Scheme 61) was carried out in a sealed microwave tube, heated by a stirrer hotplate, and the method to increase the scale of this process was simply to run several of these reactions at once. However, as quantity of reaction vessels increases, the more they

have to be positioned away from the centre of the stirrer hotplate, which compromises the efficiency of the stirring, reducing the yield of azulene product. Sometimes, once an experiment had been carried out and starting material was still visibly present in the reaction tube, a small amount of trimethyl orthoacetate **324** would be added to the vessel, and then the vessel heated again to 200 °C, to help with conversion. However, this increased ratio of trimethyl orthoacetate **324** to toluene appeared to be the reason why unwanted transesterification from the ethyl (**326**) to the methyl ester (**325**) would take place, giving an inseparable mixture of esters. Another way to perform this reaction on a multi-gram scale was by using a round bottom pressure flask (Ace Glass Inc.), which was, advantageously, a lot more physically robust than the microwave tube. On a scale of 9.20 mmol, the azulene derivative could be made in 60% yield; however, the product was a mixture of methyl and ethyl esters, in a ratio of ~2:1.

In the synthetic route towards the diphosphine ligand, working with a mixture of esters did not matter, as the esters were removed at a later stage. However, as the esters were important for favouring the enol form in the 1,1'-biazulene-2,2'-diol target, using a methyl/ethyl mixture would not be acceptable. To get around this problem, triethyl orthoacetate **318** was used instead of trimethyl orthoacetate **324**, as the transesterification process would result in no change to the structure. To our delight, it transpired that ethyl 2,4-diethoxyazulene-1-carboxylate **319** could be synthesised in 66% yield by heating ethyl 8-hydroxy-2-oxo-2*H*-cyclohepta[*b*]furan-3-carboxylate **298** in triethyl orthoacetate **324** and toluene at 200 °C for 7 hours, on a scale of 12.8 mmol, in a single round bottom pressure flask (Scheme 86). In hindsight, the change in orthoester reagent used should have been made earlier in the project, but the reluctance to do so was due to the variety of chemical

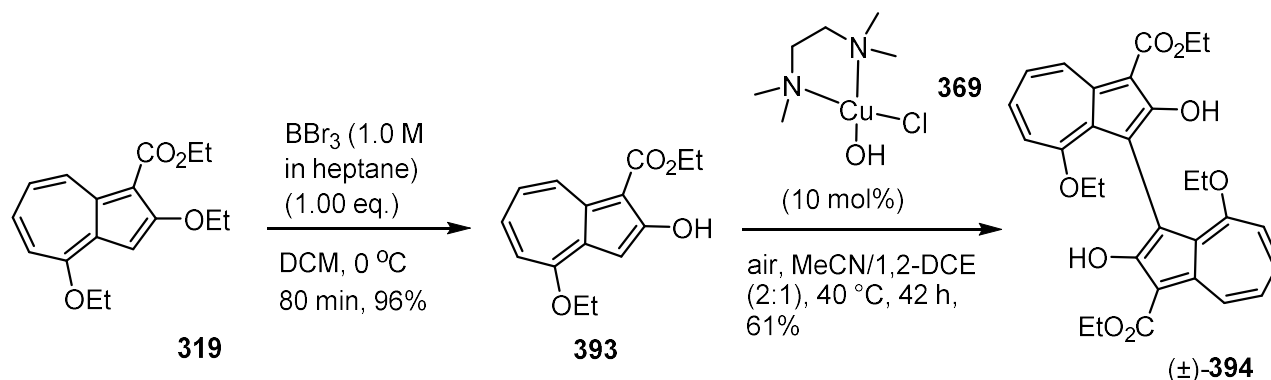
transformations that had been accomplished by starting from ethyl 2,4-dimethoxyazulene-1-carboxylate **326**, and due also to the general unwillingness to change the structure of a compound that was present at an early stage of the synthesis.



Scheme 86: The [8+2]-addition-elimination reaction of triethyl orthoacetate **318** with ethyl 8-hydroxy-2-oxo-2H-cyclohepta[b]furan-3-carboxylate **298** to make ethyl 2,4-diethoxyazulene-1-carboxylate **319**.

Following the procedure for the dealkylation of the 2-methoxy group of ethyl 2,4-dimethoxyazulene-1-carboxylate **326**, as described in Scheme 64, the treatment of ethyl 2,4-diethoxyazulene-1-carboxylate **319** with one equivalent of boron tribromide gave the deethylated product ethyl 4-ethoxy-2-hydroxyazulene-1-carboxylate **393** in near-quantitative yield (Scheme 87). Again, there was no evidence of dealkylation of the 4-ethoxy group, which meant, like all the previous examples of this reaction, the product could be taken forward to the next step without column chromatography. Similar to the reaction in Scheme 73, in which ethyl 4-methoxy-2-hydroxyazulene-1-carboxylate **337** was converted to the biazulene (±)-**370**, the copper-catalysed oxidative homocoupling was applied to ethyl 4-ethoxy-2-hydroxyazulene-1-carboxylate **393**. After stirring the 2-hydroxyazulene **393**, on a scale of 8.0 mmol, with the TMEDA-copper(II) complex **369** in acetonitrile and 1,2-dichloroethane (2:1) under air at 40 °C for 42 hours, the racemic biazulene product (±)-**394**, or “(±)-1,1'-BazOL”, could be isolated in 61% yield (Scheme 87), which was a slight improvement on the homocoupling of 4-methoxy-2-hydroxyazulene **337**. Because

biazulene product (\pm)-**394** had ethoxy, rather than methoxy, groups at the 8,8'-positions, it meant that it could not be isolated by precipitation and filtration from the reaction mixture as before. Instead, this structural change meant the product was mobile on silica, and was therefore purified by column chromatography.

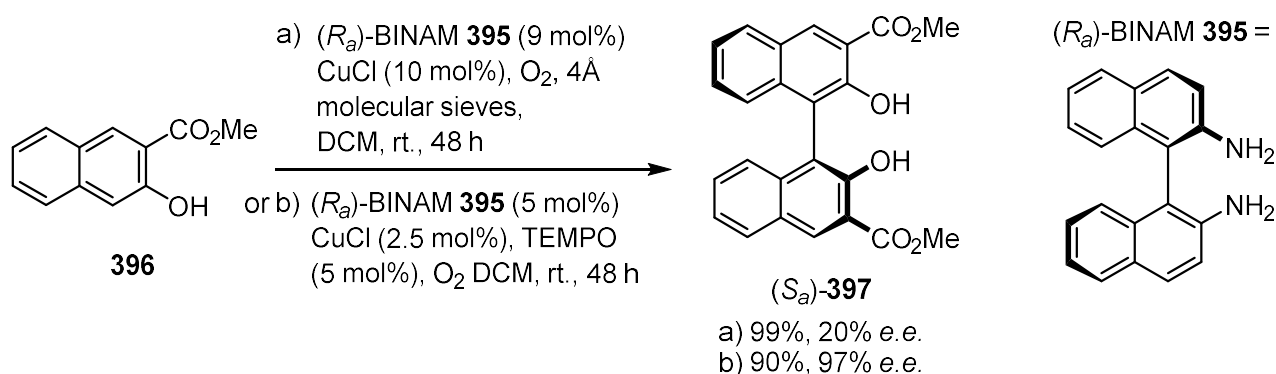


Scheme 87: The selective boron tribromide-mediated dealkylation of ethyl 2,4-diethoxyazulene-1-carboxylate **319**, and the copper-catalysed oxidative homocoupling of the 2-hydroxyazulene **393** product to make racemic 1,1'-biazulene-2,2'-diol (\pm)-**394** ("(\pm)-1,1'-BazOL").

2.3.1. Asymmetric synthesis of 1,1'-BazOL

A robust, scalable synthesis for (\pm)-BazOL **394**, consisting solely of ethyl esters, had now been fully developed. In order to screen the ligand for enantioselectivity imparted in a catalytic reaction, access to its single enantiomers was required, and the first approach considered to achieve this was through an enantioselective form of the copper-catalysed oxidative homocoupling reaction. As shown in Scheme 72, much development of this type of asymmetric reaction had been accomplished by Kozlowski, particularly with the application of 1,5-diaza-*cis*-decalin copper(II) complex **366** for the 1,1'-homocoupling of alkyl 2-hydroxy-3-naphthoate derivatives.²¹⁴ However, before this complex could be applied in an attempted homocoupling of ethyl 4-ethoxy-2-hydroxyazulene-1-carboxylate **393**, an alternative, more widely commercially available ligand, 1,1'-binaphthyl-2,2'-diamine (BINAM)

395, was found in the literature to give similar results with similar substrates (Scheme 88). This ligand was first employed for this reaction by Ha *et al.*, with the oxidative homocoupling of methyl 2-hydroxy-3-naphthoate **396**, using copper(I) chloride under an oxygen atmosphere in DCM at room temperature, to produce (*S_a*)-1,1'-binaphthol **397** in 20% e.e. and 99% yield.²²⁴ While the enantioselectivity was modest, near complete conversion of starting material had occurred by 24 hours, representing a faster rate compared with aliphatic amine ligands. This observation was ascribed to the aromatic amine being less basic than aliphatic amines, making the copper(II) complex more electrophilic and therefore more easily reduced to the copper(I) species by the substrate. By adding catalytic 2,2,6,6-tetramethyl-1-piperidinyloxy (TEMPO) to the reaction, with otherwise similar conditions, Sekar *et al.* could achieve 97% e.e. and 90% yield for the homocoupling of the same substrate **396**, as well as good enantioselectivity and yields for several other 2-hydroxy-3-naphthoate derivatives.²²⁵



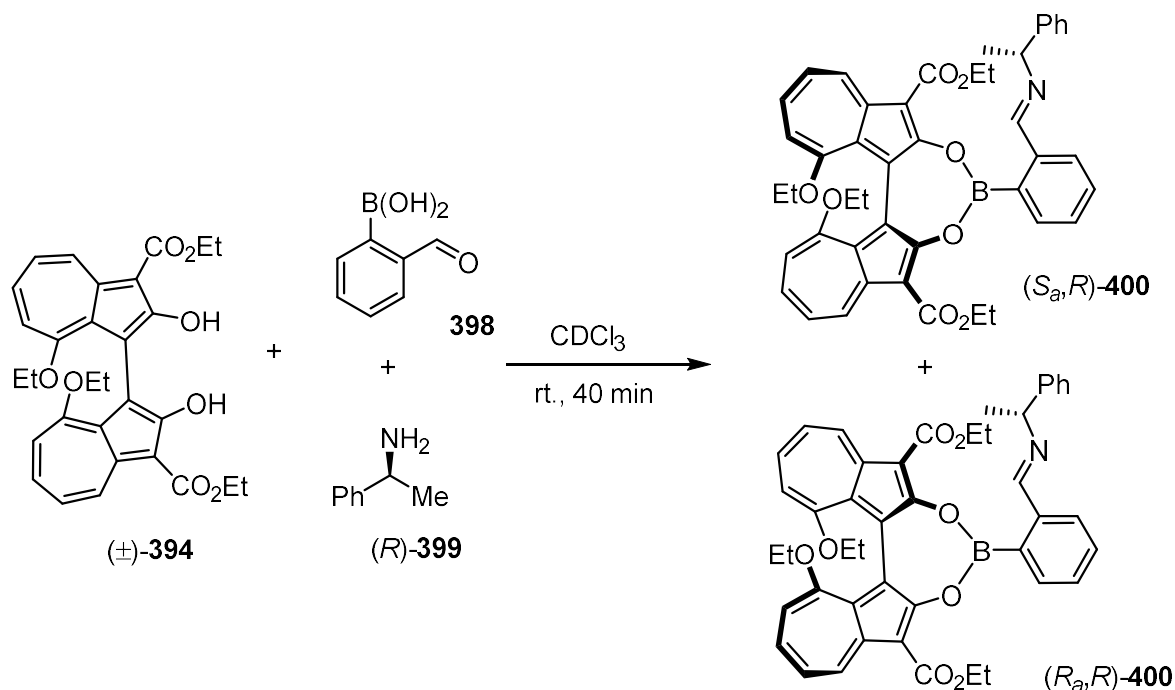
Scheme 88: Literature examples of the asymmetric oxidative homocoupling of methyl 2-hydroxy-3-naphthoate **396**, achieved with a copper(I) chloride/(*R_a*)-BINAM **395** system (a = Ha (2004); b = Sekar (2013)).

The method of Sekar was applied to this project. Accordingly, ethyl 4-ethoxy-2-hydroxyazulene-1-carboxylate **393** was added to a mixture of (*R_a*)-BINAM **395**, one

of three copper salts (CuCl, CuCl₂ or CuBr•SMe₂) and TEMPO in DCM, and was stirred at room temperature in DCM for 18 days (Table 12). Since this 2-hydroxyazulene derivative **393** could conveniently undergo a homocoupling reaction under an atmosphere of air, this condition was applied to these experiments rather than the oxygen atmosphere as described in the literature. Unfortunately, each copper salt used in this asymmetric protocol gave lower yields than for the method with the Cu(II)-TMEDA complex **369**, as in Scheme 87: using CuBr•SMe₂ led to the best yield, at 30% (Table 12, entry 3), followed by CuCl at 26% (Table 12, entry 1), while CuCl₂ gave the worst yield, at 5.5% (Table 12, entry 2). The reaction with CuBr•SMe₂ also proceeded more cleanly than that with CuCl, as more starting material could be recovered.

Methods were then explored for the calculation of the enantiomeric excess for each reaction. A report by James *et al.* described a protocol to determine the enantiopurity of chiral diols with proton NMR analysis.²²⁶ By treating the diol with an equimolar amount of 2-formylbenzene boronic acid and a slight excess of (S)- α -methylbenzylamine in chloroform-*d*, calculation of the enantiopurity of that diol may be carried out by integration of the resolved diastereotopic protons in the ¹H-NMR spectrum of the diastereomeric iminoboronate ester products. Unlike previous chiral derivatisation agents for diols, this method was quite general, as it could be applied to 1,2- and 1,3-diols, as well as BINOL. Applying the method to this project, a sample of the (±)-1,1'-BazOL **394** was mixed with 2-formylbenzene boronic acid **398** and (R)- α -methylbenzylamine **399** in chloroform-*d*, and after stirring at room temperature for 40 minutes, by TLC the reaction appeared to go to completion (Scheme 89). On examining the proton NMR spectrum, the formation of the iminoboronate ester product (*S_a*,*R*)/(*R_a*,*R*)-**400** was confirmed, showing the excess amine left in the

sample. However, the key signals to differentiate between the two enantiomers of BazOL ($\underline{\text{HC}}=\text{N}$, $\text{Ph}-\underline{\text{CH}}-\text{N}$, $\underline{\text{H}}_3\text{C}-\text{CH}$) were not sufficiently resolved, despite the use of a 500 MHz NMR spectrometer, and therefore would not be useful to calculate the enantiopurity of the sample.

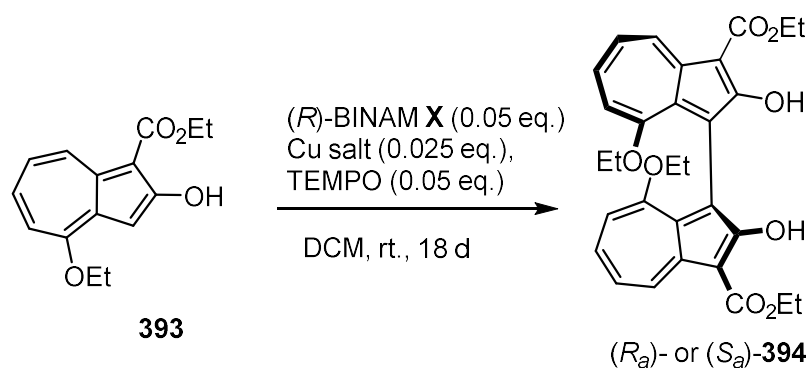


Scheme 89: The attempted calculation of the enantiopurity of (±)-1,1'-BazOL **394** by formation of diastereomeric iminoboronate esters (S_a, R)/(R_a, R)-**400**.

As the iminoboronate diastereomer derivatives did not allow the calculation of the enantioselectivity, chiral HPLC was adopted for this purpose instead. Initial optimisation for the chromatographic separation of the diol ligands was difficult, so the weakly acidic hydroxy groups were converted to acetoxy groups. To achieve this, the 1,1'-BazOL ligand **394** was treated with acetyl chloride and triethylamine,¹⁶⁴ and after stirring in DCM for 17 hours, the bis-acetoxy-1,1'-biazulene **401** could be isolated in 77% yield (Scheme 90). The product could be resolved using a Chiralcel OD column (25 x 4.6 mm) with hexane/isopropanol (9:1) with a flow rate 0.75 mL min⁻¹ at 20 °C, with UV detection (238 nm). The enantiomeric excess of the product

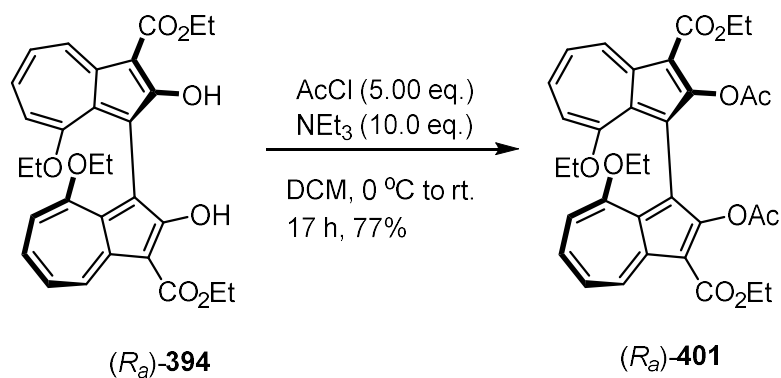
from the asymmetric homocoupling reaction could now be calculated. When using (*R_a*)-BINAM **395** as the chiral ligand, both CuBr•SMe₂ (Table 12, entry 3) and CuCl (Table 12, entry 1) favoured the (*S_a*)-enantiomer of **394**, with 16% e.e. and 13% e.e. respectively. This enantiomeric sense was consistent with the results obtained by Sekar. Interestingly, the best selectivity, at 21% e.e., was produced by using CuCl₂, this time in favour of the (*R_a*)-enantiomer of **394** (Table 12, entry 2). However, these results need to be interpreted with caution, as the chromatograms for each experiment showed 'trailing' for the peak corresponding to the (*R_a*)-enantiomer of **401** (Figure 35). Each proton NMR spectrum for each derivative **401** displayed some unidentified impurity between 2-3 ppm, which may account for this 'trail', rather than purely the (*R_a*)-enantiomer.

Table 12: The Cu-catalysed asymmetric oxidative homocoupling of 2-hydroxyazulene **393**.



Entry	Cu salt	Recovered 393 /%	Yield of 1,1'-biazulene 394 ^a /%	% e.e. ^b
1	CuCl	33	26	13 (S)
2	CuCl ₂	67	5.5	21 (R)
3	CuBr.SMe ₂	49	30	16 (S)

a) During purification by column chromatography, partial co-elution of 1,1'-biazulene **394** and (R_a) -BINAM **395** occurred, so part of the yield was calculated by integration of the ¹H-NMR **b)** Calculated by chiral HPLC of the bis-acetoxy derivative of the BazOL product.



Scheme 90: The diacetylation of (R_a) -BazOL **394** (for resolution procedure, vide infra) with acetyl chloride and triethylamine.

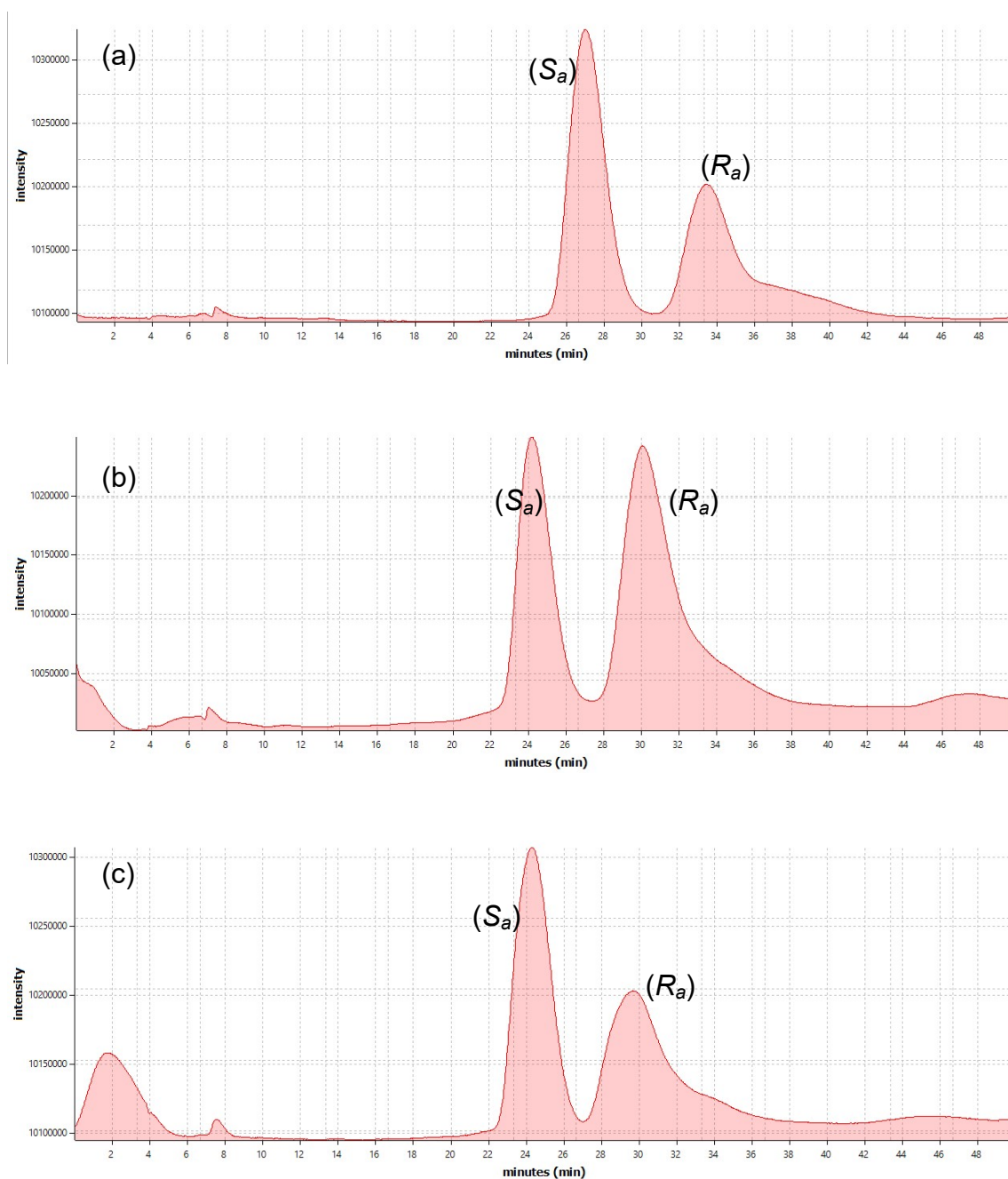
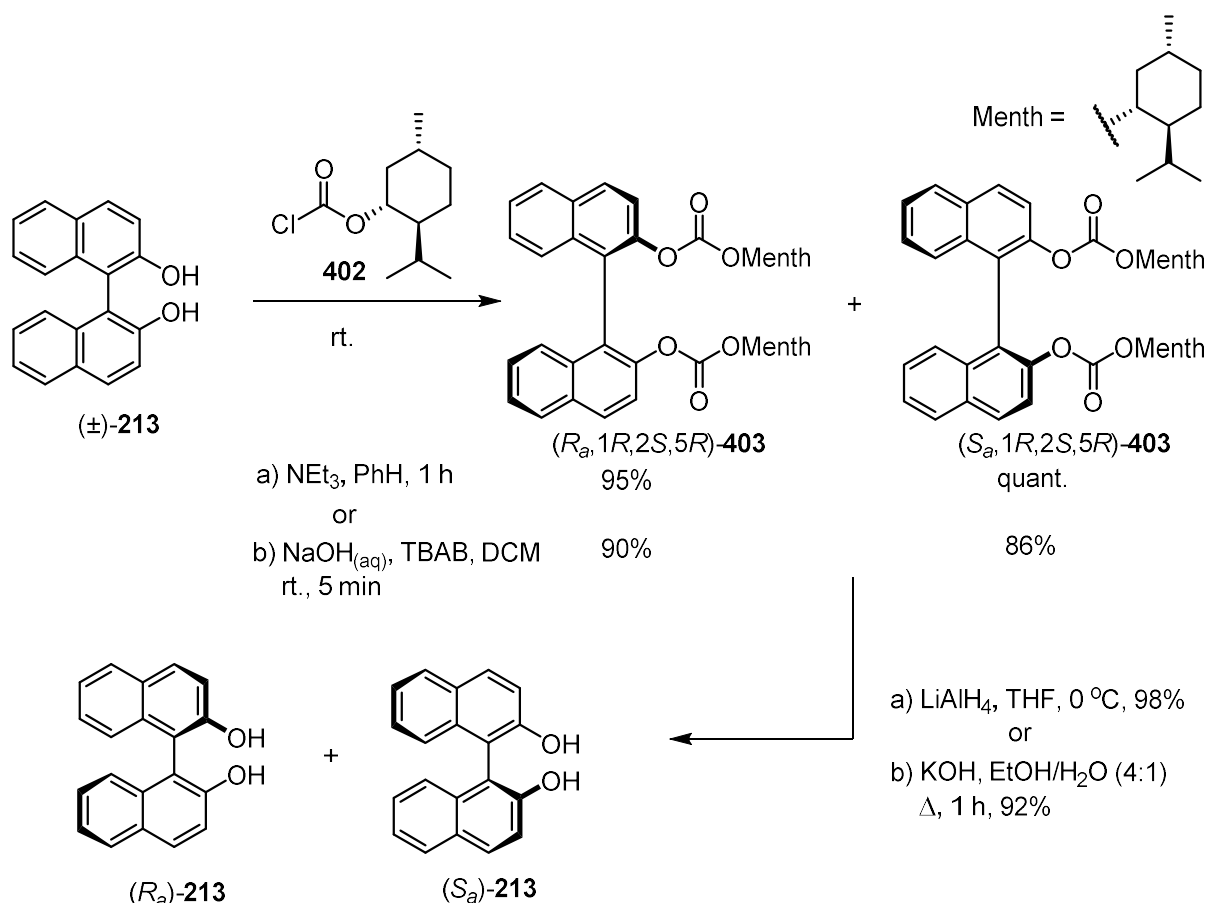


Figure 35: The chiral HPLC chromatograms for the bis-acetoxy derivatives **401** of the diol products obtained from the asymmetric homocoupling, using CuCl (a), CuCl_2 (b) and $\text{CuBr} \cdot \text{SMe}_2$ (c) (Chiralcel OD 250 x 4.6 mm ID, 9:1 hexane/2-propanol, UV detection 238 nm, flow rate 0.75 mL min^{-1} , 20°C).

2.3.2. Resolution of 1,1'-BazOL

While the development of an asymmetric oxidative homocoupling reaction for ethyl 4-ethoxy-2-hydroxyazulene-1-carboxylate **393** was taking place, methods for the

enantiomeric resolution of (±)-BazOL **394** were also explored. It was demonstrated by De Lucchi *et al.* that various axially chiral binaphthol and mercapto-binaphthol species could be resolved by forming the bis-(–)-menthyl carbonate derivatives of these compounds, followed by selective crystallisation by using hexane (Scheme 91).²²⁷ Once the diastereomers (eg. **403**) had been separated and purified, conversion back to the diol, or thiol, could be achieved through a reduction with lithium aluminium hydride. The method was appealing because (–)-menthyl chloroformate **402**, the reactive partner for the racemic ligand, is commercially available, and the reactions were complete within one hour at room temperature. Whilst optimising a method to resolve 4,4'-dibromo-SPINOL, Wan *et al.* discovered the reaction of (±)-BINOL **213** with (–)-menthyl chloroformate **402** could be carried out in 5 minutes by using a biphasic aqueous NaOH/DCM system, with tetra-*n*-butylammonium bromide (TBAB) as a phase transfer catalyst, rather than simply using triethylamine in benzene.²²⁸ Subsequently, rather than converting the (–)-menthyl carbonate group back to the hydroxy group with LiAlH₄, Wan *et al.* employed basic hydrolysis with potassium hydroxide in ethanol and water.



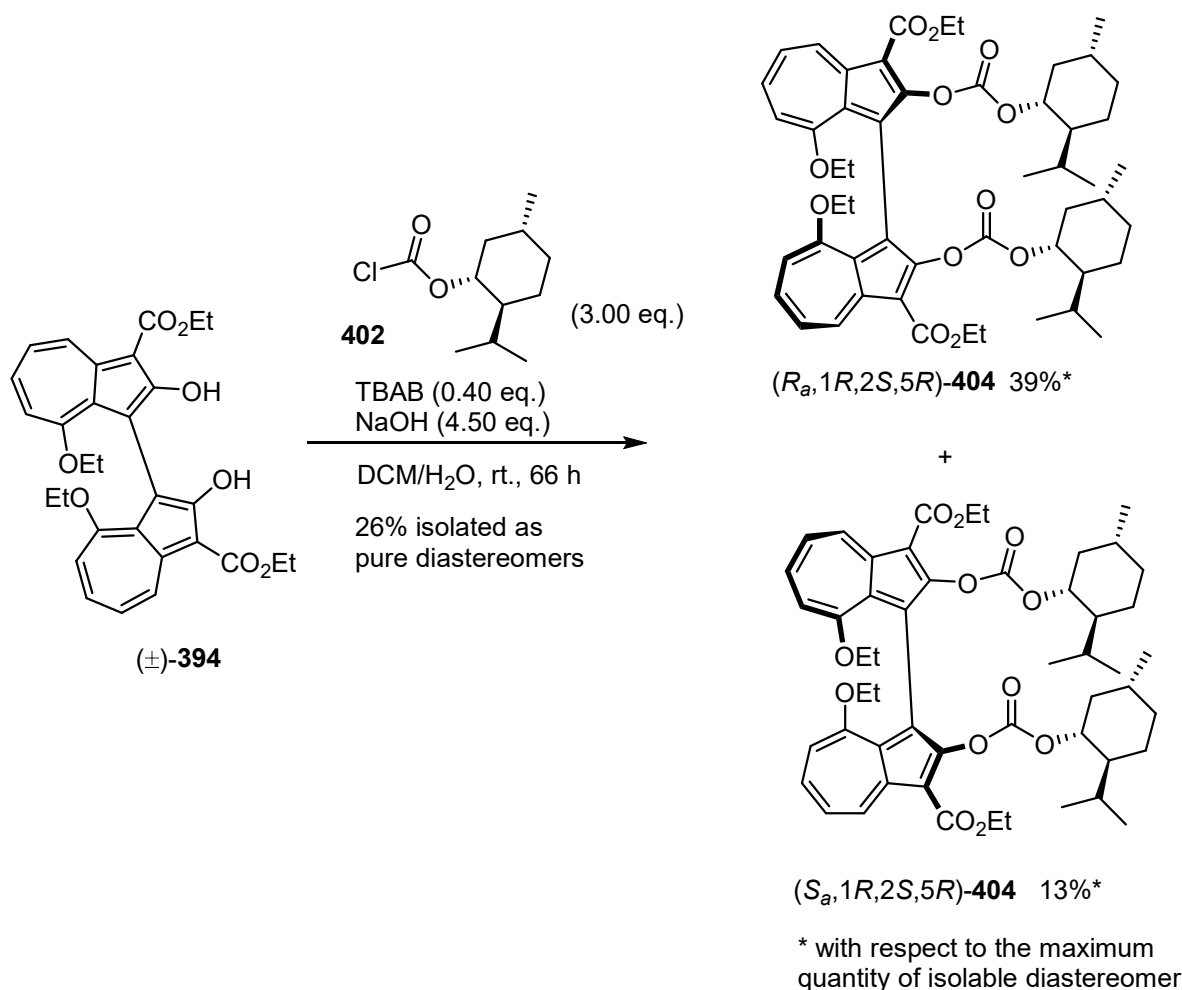
Scheme 91: Literature examples of the resolution of (\pm) -BINOL **213** through selective crystallisation of its bis-((-)-menthyl carbonate) derivatives **403** (a = de Lucchi (1995); b = Wan (2004)).

The method of Wan was applied to (\pm) -BazOL **394**, on a scale of 0.19 mmol, and the diol was almost completely consumed after 21 hours. This slow reaction time could be rationalised by the delocalisation of the oxygen lone pairs towards the ester carbonyls. When column chromatography was applied to the crude product, minimal separation of the diastereomers of **404** was achieved. The fraction of inseparable diastereomers was recrystallised in ethanol, but rather than precipitating a pure diastereomer, each individual crystal in the sample was made up of conglomerates of either the (R_a) -BazOL or (S_a) -BazOL **394** derivative. The reaction was carried out again, on a larger scale of 0.78 mmol to facilitate the selective recrystallisation of **404**. This time, through column chromatography, small amounts of almost

diastereomerically pure product could be isolated, for both (*R_a*)-BazOL-bis-((-)-menthyl carbonate) **404** (8.4% yield with respect to the maximum quantity of isolable diastereomer, 96:4 *d.r.*) and (*S_a*)-BazOL-bis-((-)-menthyl carbonate) **404** (8.0% yield with respect to the maximum quantity of isolable diastereomer, 94:6 *d.r.*) derivatives. The remaining fractions of mixed diastereomers, which were eluted from the column, were recrystallised in hexane, but the crystalline precipitate consisted of equal amounts of each diastereomer. This precipitate was recrystallised again, this time in hexane/THF (7:1 v/v), and after storage at 2 °C, yielded (*R_a*)-BazOL-bis-((-)-menthyl carbonate) **404**, corresponding to 15% yield. Further attempts at crystallising the solid from the filtrate did not yield any more pure diastereomer.

The scale of the experiment was increased further, to 2.07 mmol of (±)-BazOL **394** (Scheme 92). After filtering the crude mixture through a pad of silica, recrystallisation with hexane/THF (7:1 v/v) once again gave pure (*R_a*)-BazOL-bis-((-)-menthyl carbonate) **404** in 32% yield. The mother liquor was evaporated to give a solid that was recrystallised with the same solvent composition, which gave a precipitate comprising an equimolar quantity of (*R_a*)-BazOL derivative of **404** and (*S_a*)-BazOL derivative of **404**. However, the mother liquor of this second recrystallisation was evaporated to give a solid that was enriched with the (*S_a*)-BazOL derivative of **404**. Thus, this solid was recrystallised in a different ratio of hexane/THF (9:1 v/v), from which precipitated on cooling pure (*S_a*)-BazOL-bis-((-)-menthyl carbonate) **404** in 13% yield. The mother liquor from this third recrystallisation was then combined with the precipitate from the second recrystallisation, and was purified by column chromatography to separate out unreacted starting material. The product fraction underwent a fourth recrystallisation using at first hexane/THF (19:1 v/v), with THF continually added until complete solvation occurred. This final recrystallisation

precipitated additional pure (*R_a*)-BazOL-bis-((-)-menthyl carbonate) **404** in a further 7% yield. While this resolution was far from perfect in its efficiency, it still represented great progress in the project, as only one step remained in order to obtain synthetically useful quantities of each enantiomer of 1,1'-BazOL **394**.



Scheme 92: The resolution of (**±**)-BazOL **394** (scale of 2.0 mmol) through the formation of its bis-((-)-menthyl carbonate) derivatives **404** and fractional recrystallisation of the diastereomeric products.

One interesting feature of the two BazOL-bis-((-)-menthyl carbonate) derivatives (*R_a*,1*R*,2*S*,5*R*)-**404** and (*S_a*,1*R*,2*S*,5*R*)-**404** is the differences discernable in their proton NMR spectra in CDCl₃, particularly in the upfield alkyl region where peaks for the (-)-menthyl group are situated. For (*S_a*)-BazOL-bis-((-)-menthyl carbonate) **404**,

the methyl groups of the isopropyl unit are inequivalent and have upfield chemical shifts, with chemical shifts of 0.57 ppm and 0.69 ppm (Figure 36). These values are lower than that of the equivalent signal for (–)-menthol, at 0.81 ppm.²²⁹ Whereas for (*R_a*)-BazOL-bis-(–)-menthyl carbonate **404**, these signals are significantly more upfield, with shifts of 0.06 ppm and 0.46 ppm (Figure 37). These values suggest that the protons of the isopropyl methyl groups on (*R_a*)-BazOL-bis-(–)-menthyl carbonate **404** experience shielding by the ring current induced on the aromatic azulene ring system, to a much greater extent than for (*S_a*)-BazOL-bis-(–)-menthyl carbonate **404**.

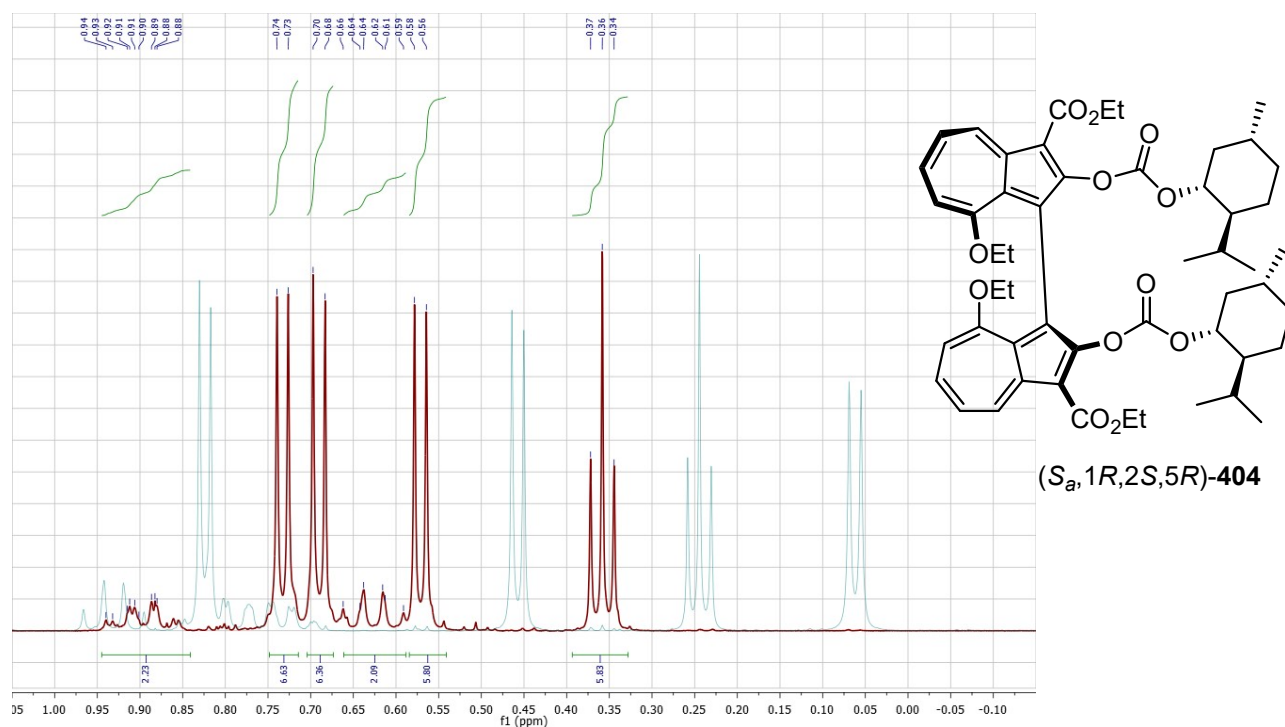


Figure 36: The ¹H-NMR spectrum (region of δ 0-1 ppm) in CDCl₃ of (*S_a*)-BazOL-bis-(–)-menthyl carbonate **404** (highlighted, maroon), superimposed over the ¹H-NMR spectrum in CDCl₃ (*R_a*)-BazOL-bis-(–)-menthyl carbonate **404** (pale blue).

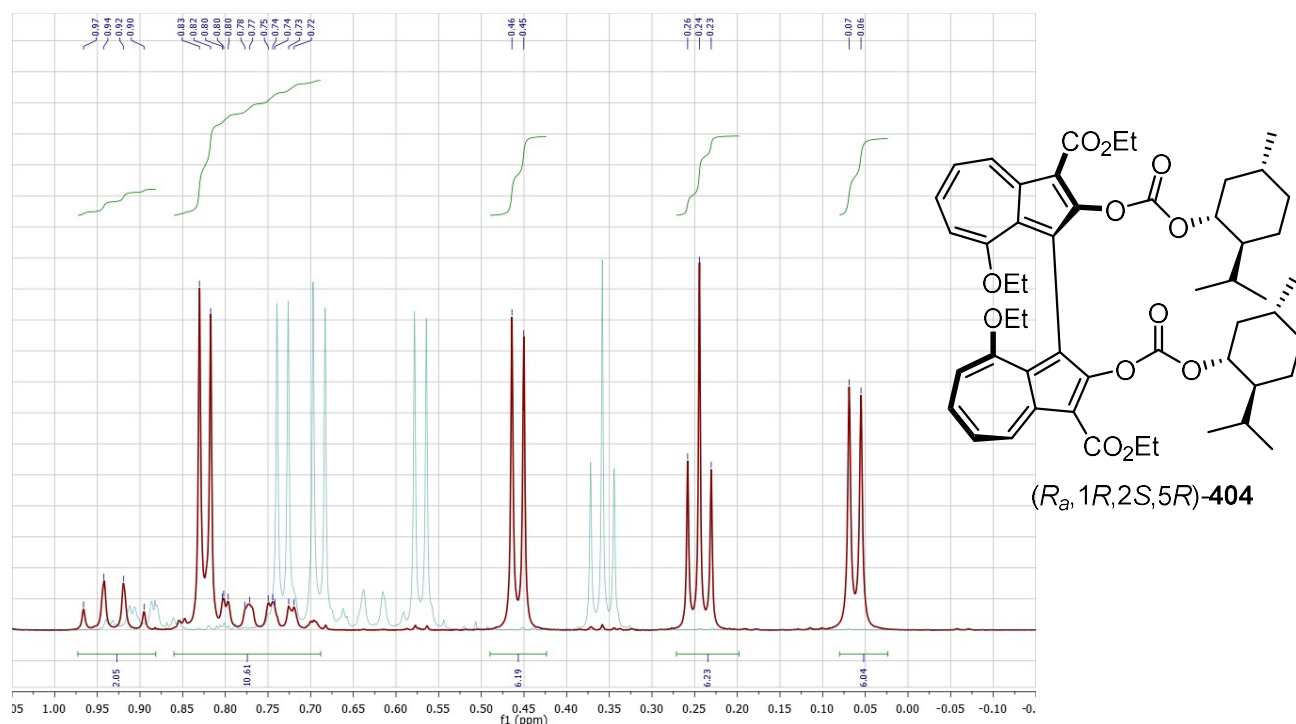


Figure 37: The ^1H -NMR spectrum (region of δ 0-1 ppm) in CDCl_3 of (R_a) -BazOL-bis((-)-menthyl carbonate **404** (highlighted, maroon), superimposed over the ^1H -NMR spectrum in CDCl_3 (S_a) -BazOL-bis((-)-menthyl carbonate **404** (pale blue).

This hypothesis on the alignment of the methyl groups is corroborated by the X-ray crystal structures (obtained by Dr. Gabriele Kociok-Köhn) of both diastereomers, when observing the distances between the centroid of the 7-membered ring and the hydrogen atoms on the isopropyl group. For the structure of (S_a) -BazOL-bis((-)-menthyl carbonate **404**, the non-perpendicular distance of 4.600 Å shows that this methyl group is not aligned with the midpoint of the aromatic structure (Figure 38). This position in space means that the hydrogen atoms experience a limited shielding effect from the magnetic field induced by the NMR spectrometers. For the structure of (R_a) -BazOL-bis((-)-menthyl carbonate **404**, the near-perpendicular distance of 2.866 Å is much shorter, which indicates that the methyl hydrogen atoms are aligned with the centre of the 7-membered ring (Figure 39). As a consequence, the

hydrogens experience a great degree of shielding, resulting in a low chemical shift of 0.05 ppm.

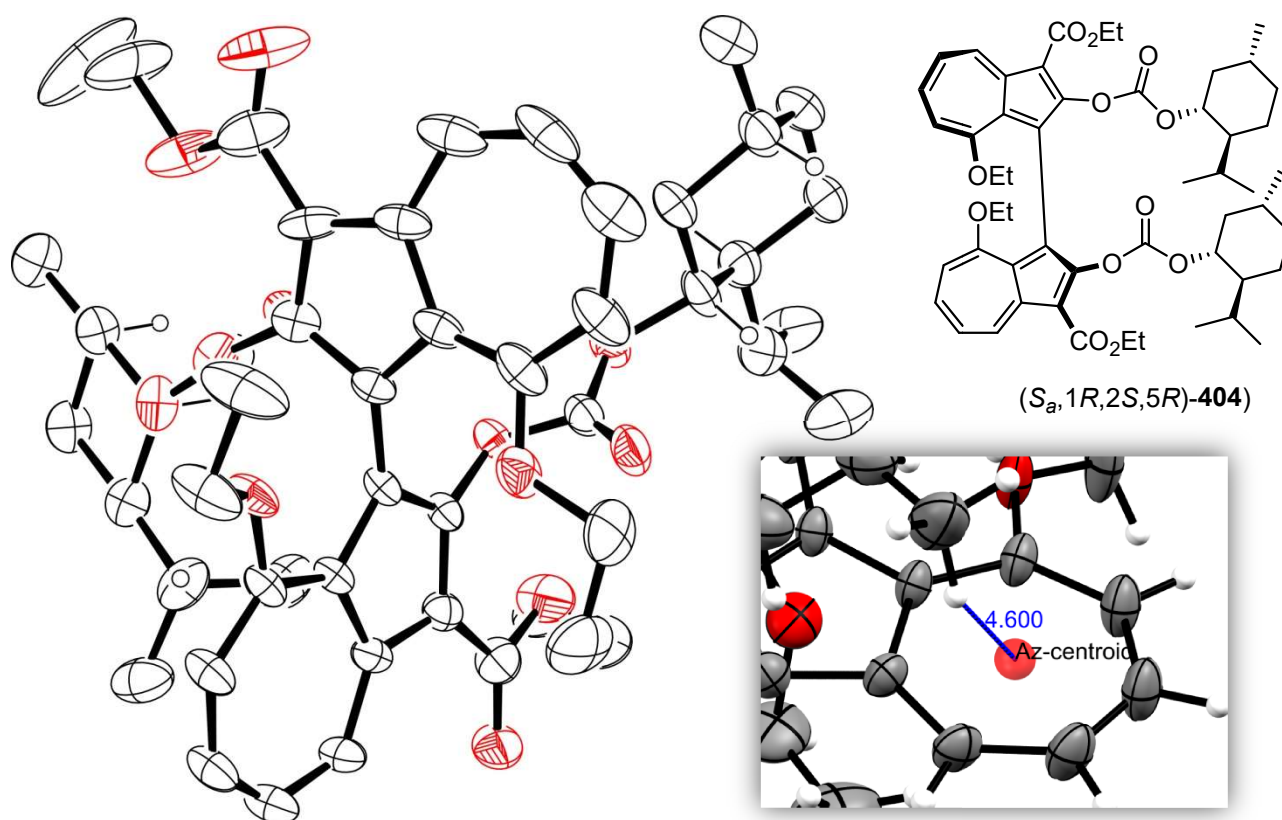


Figure 38: ORTEP diagram of *(S_a)-BazOL-bis-((-)-menthyl carbonate 404* showing ellipsoids at 30% probability. H atoms are shown as spheres of arbitrary radius.

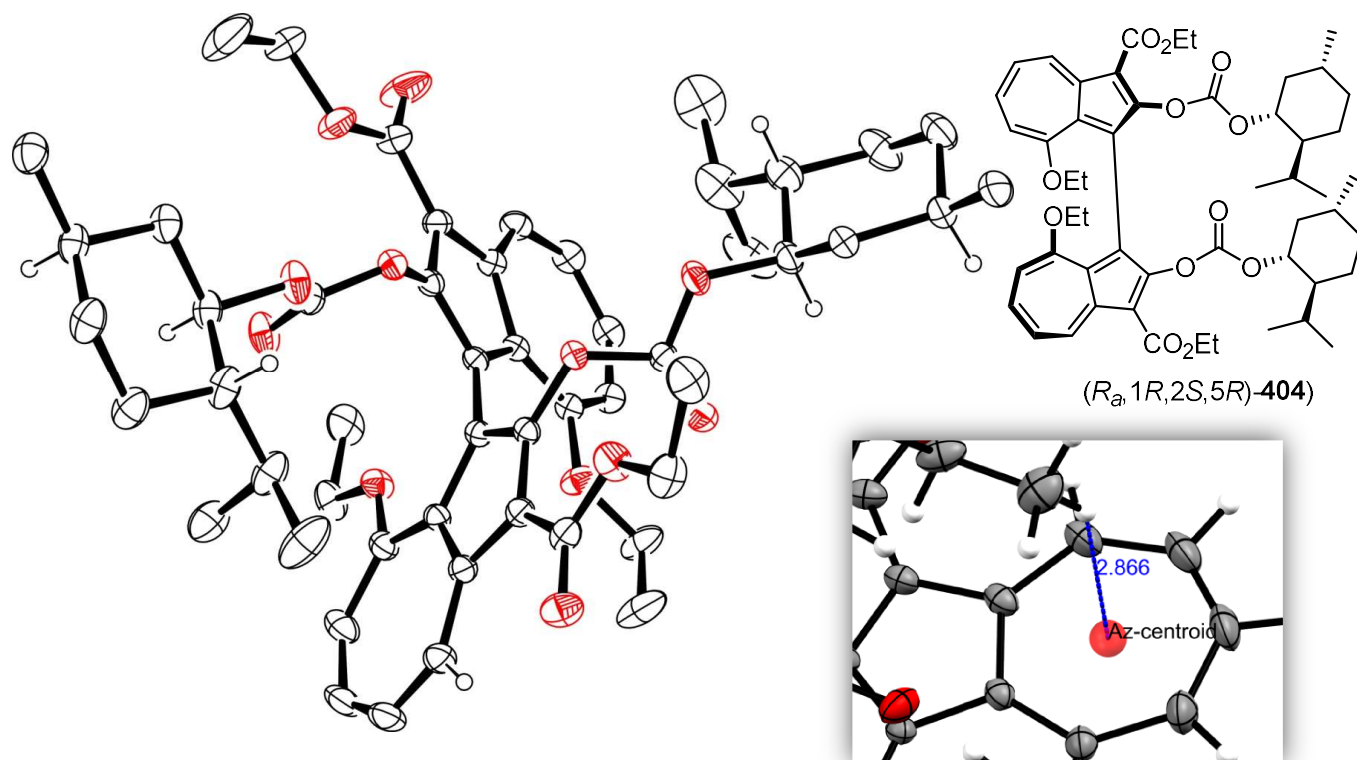
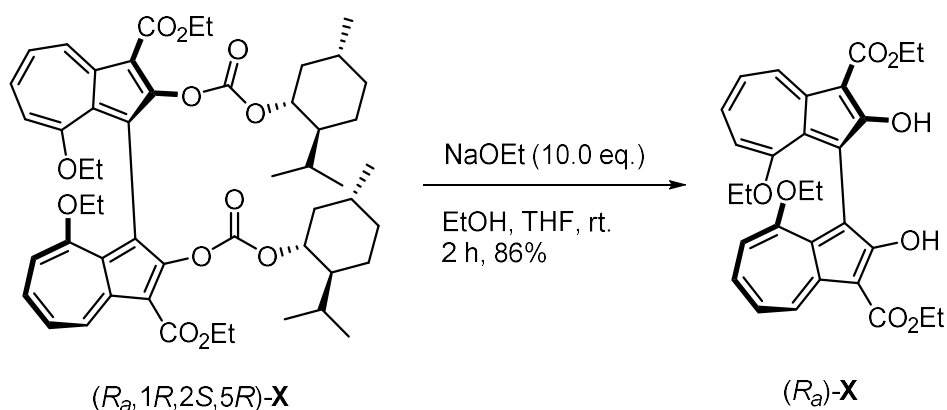


Figure 39: ORTEP diagram of (*R_a*)-BazOL-bis-((-)-menthyl carbonate **404** showing ellipsoids at 30% probability. H atoms are shown as spheres of arbitrary radius.

While the data from the NMR spectra and X-ray crystallography are consistent with each other, it is important to consider that the NMR is a study of the compound in solution, while the X-ray crystallography is a study of the solid state. Therefore, the lowest energy conformation of the diastereomers as shown by the X-ray crystal structure may not be entirely accurate geometric depictions of the structures from the NMR spectra. Another reason to treat this data tentatively is that the solid crystals of the (*S_a*)-BazOL derivative of **404** did not diffract to high angles, which compromised some of the quality of the structural data, particularly for the ester groups. The crystallographic data for this structure may need to be recorded again to ensure an accurate depiction of the conformation.

The final step of the synthesis involved the conversion of the separate bis-((-)-menthyl carbonate diastereomers **404** back to diols. Neither of the methods

described in Scheme 92 to achieve this transformation, that is, through reduction with lithium aluminium hydride or hydrolysis with potassium hydroxide would be suited to the BazOL derivatives **404**, as the ester groups may also react under these conditions. Instead, the treatment of both BazOL-bis-((-)-menthyl carbonate diastereomers (*R_a*,1*R*,2*S*,5*R*)-**404** and (*S_a*,1*R*,2*S*,5*R*)-**404** with sodium ethoxide in THF/ethanol at room temperature, similar to a method by Katsuki *et al.*,²³⁰ gave pure (*R_a*)-BazOL (-)-**394** or (*S_a*)-BazOL (+)-**394** in 86% yield (Scheme 93). In the absence of water, hydrolysis of the ester groups could not occur, and any transesterification that may have taken place would not have changed the structure of the product. The X-ray crystal structure for (*R_a*)-BazOL (-)-**394** was obtained, showing a dihedral angle of 111.8(6)° (C2-C1-C1'-C2') (Figure 40). This angle is significantly larger than the corresponding angle for 1,1'-biazulene **328** in Figure 33, which was 102.0(2)°, and may be a result of the increased steric repulsion of ethoxy groups, compared to methoxy groups, at the 8,8'-positions of the biazulene.



Scheme 93: The sodium ethoxide-mediated conversion of (*R_a*)-BazOL-bis-((-)-menthyl carbonate **404** to (*R_a*)-BazOL (-)-**394**.

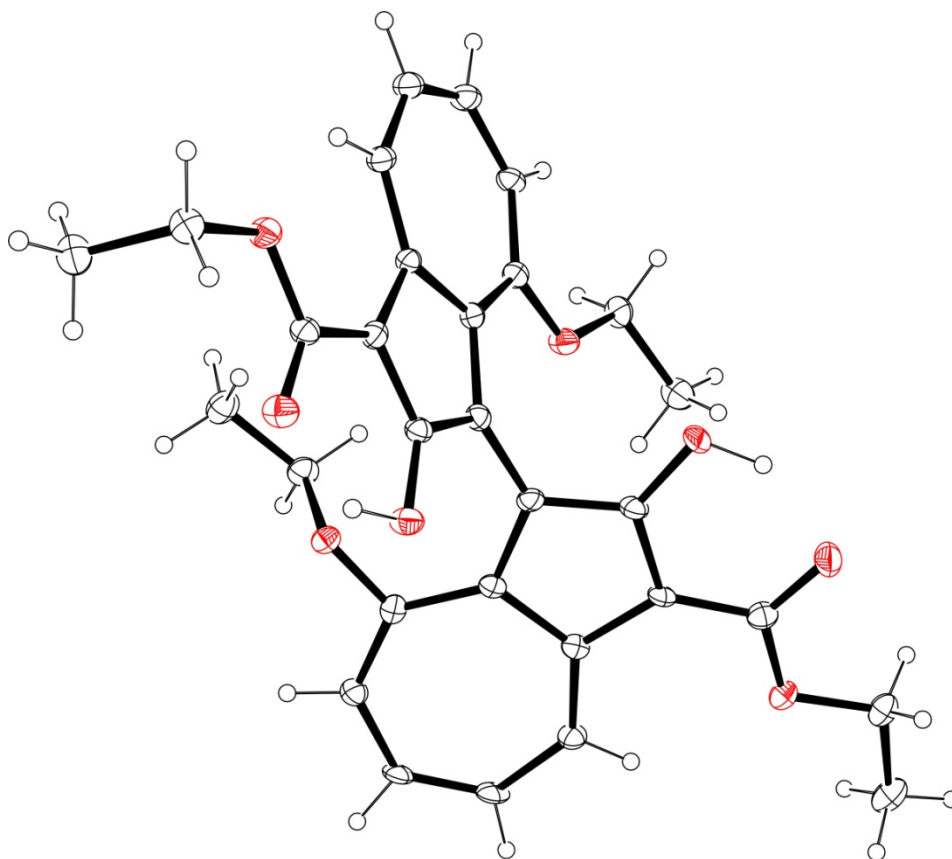


Figure 40: ORTEP diagram of (R_a)-BazOL (–)-**394** showing ellipsoids at 30% probability. H atoms are shown as spheres of arbitrary radius.

2.3.4. CD spectrometry and configurational stability

Further analysis relating to the axial chirality of (R_a)-BazOL (–)-**394** and (S_a)-BazOL (+)-**394** was subsequently carried out by Dr. G. Dan Pantoş and Mr. Tiberiu Gianga; their results and analysis are reproduced and discussed below. The circular dichroism (CD) plots of each enantiomer were shown to be mirror images of one another, which confirms their configurational stability in solution at room temperature, as well as their enantiopurity (Figure 41). Variable temperature CD experiments were also carried out on both (R_a)-BazOL (Figure 42) (–)-**394** and (S_a)-BazOL (+)-**394** (Figure 43). At 5 °C, each enantiomer showed the greatest selective absorption of circular polarised light. As this temperature was increased, incrementally in intervals

of 10 °C, from 5 °C to 95 °C, the selective absorption decreased, indicating a gradual loss of configurational stability. A repeat experiment at 25 °C showed that permanent partial racemisation of each sample had taken place. However, these data only showed a qualitative relationship between the temperature of the solution and the configurational stability, so further experiments on the kinetics of the molecules were required to calculate the energy barrier to racemisation, and therefore the half-life.

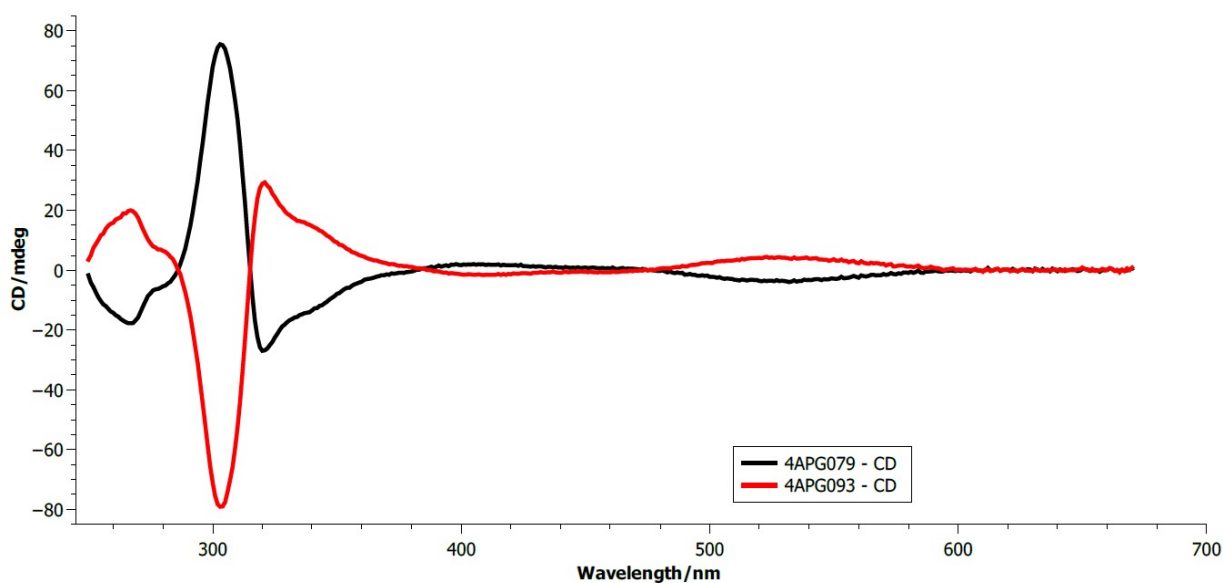


Figure 41: The circular dichroism plots of (*R*_a)-BazOL (–)-**394** (black) and (*S*_a)-BazOL (+)-**394** (red), recorded as a 0.01 mM solution of each enantiomer in CHCl₃.

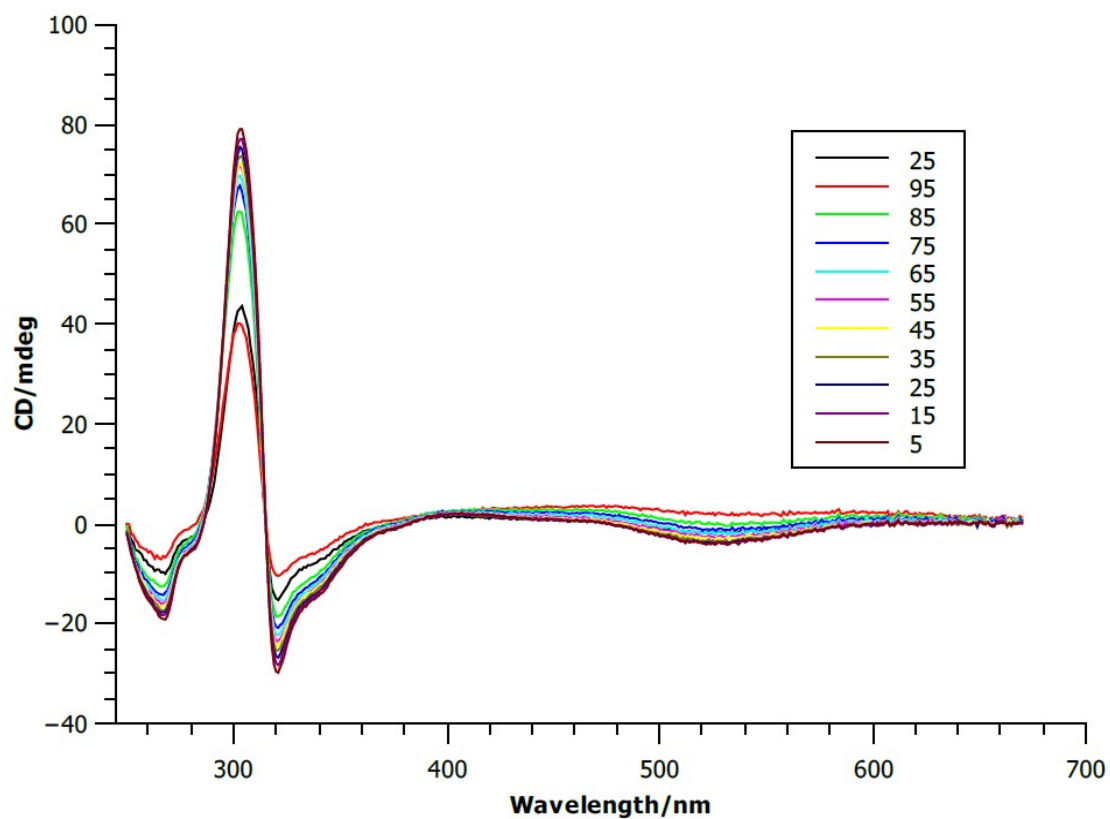


Figure 42: The variable temperature CD spectra of a 0.01 mM solution of (*R_a*)-BazOL (–)-**394** in 1,1,2,2-tetrachloroethane.

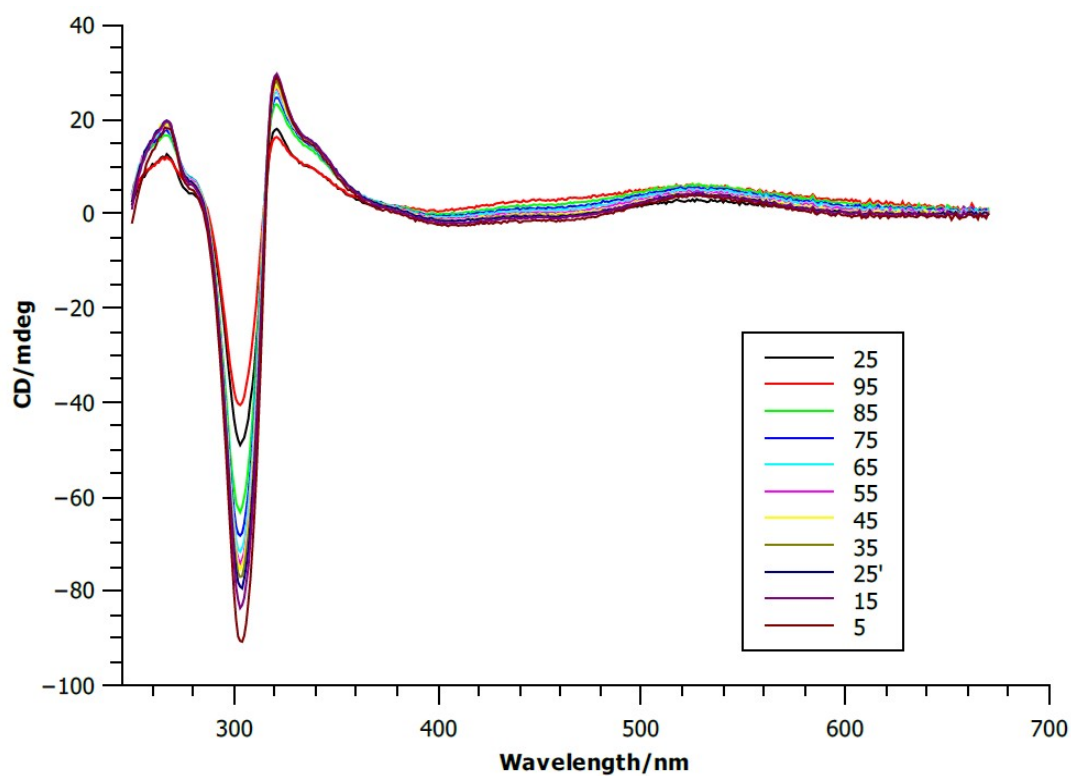


Figure 43: The variable temperature CD spectra of a 0.01 mM solution of (*S_a*)-BazOL (+)-**394** in 1,1,2,2-tetrachloroethane.

To calculate the relevant kinetic parameters, a CD spectrum of a 0.01 mM solution of (*S_a*)-BazOL (+)-**394** in 1,1,2,2-tetrachloroethane was recorded every 5 minutes for 845 minutes at three temperatures: 333.15 K, 343.15 K, 353.15 K (60 °C, 70 °C, 80 °C) (Figure 44). As expected, the rate of racemisation increased with a higher temperature.

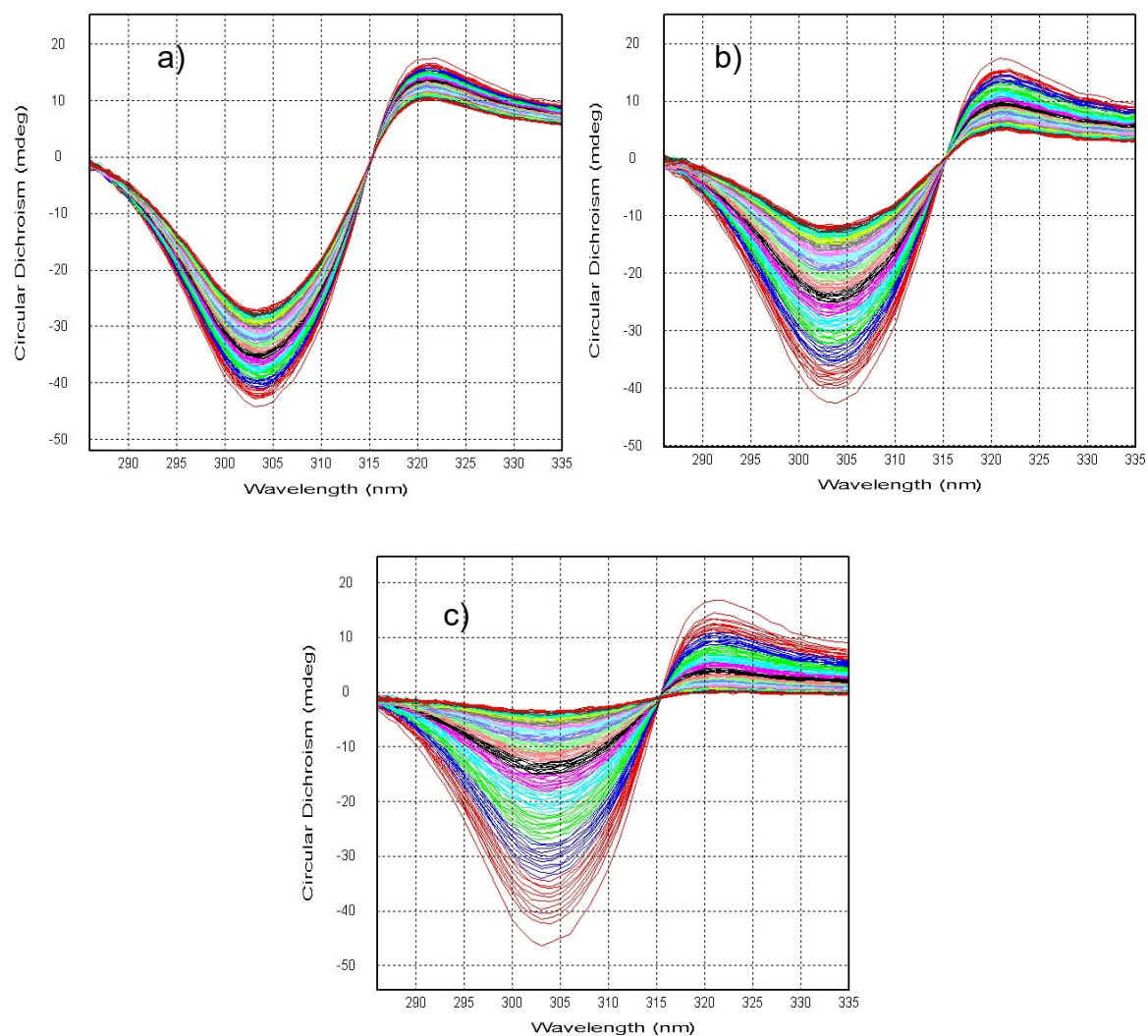


Figure 44: CD spectra of (*S_a*)-BazOL (+)-**394** in 1,1,2,2-tetrachloroethane at 0.01 mM concentration at 333.15 K (a), 343.15 K (b), 353.15 K (c).

To calculate the barrier to racemisation from this data, the rate constant (k) of the racemisation had to be calculated for each temperature. Since the absorption of the circular polarised light was strong at 304 nm, a first order rate equation was adopted for the data at this wavelength (Figure 45).

$$\ln \frac{C}{C_0} = -kt$$

$$\ln C = -kt - \ln C_0$$

where: $\ln C = \ln(-CD)_t$; t = time; $\ln A_0 = \ln(-CD)_0$

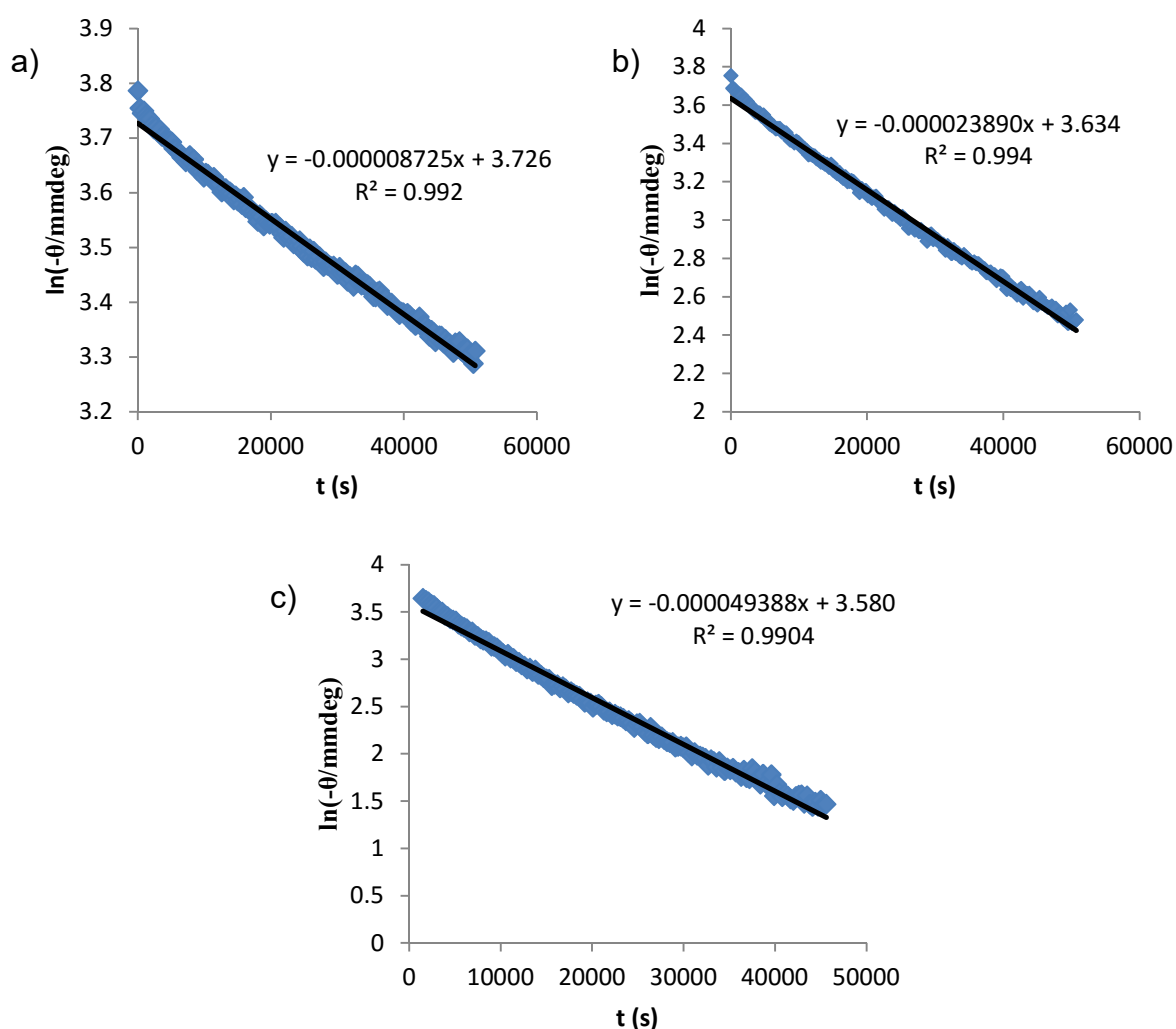


Figure 45: Linear regression analysis of the kinetic measurements at 333.15 K (a); 343.15 K (b); 353.15 K (c); using data points at $\lambda = 304$ nm.

Table 13: The rate constants calculated from the linear regression analysis of the kinetic measurements at different temperatures.

T (K)	k (s ⁻¹)	1/T (K ⁻¹)
333.15	8.725 × 10 ⁻⁶	0.003002
343.15	23.890 × 10 ⁻⁶	0.002914
353.15	49.388 × 10 ⁻⁶	0.002832

From the three values for the rate constant k , the activation energy (E_a) could now be calculated using the linear form of the Arrhenius equation (Figure 46).

$$\ln k = -\frac{E_a}{R} \frac{1}{T} + \ln A$$

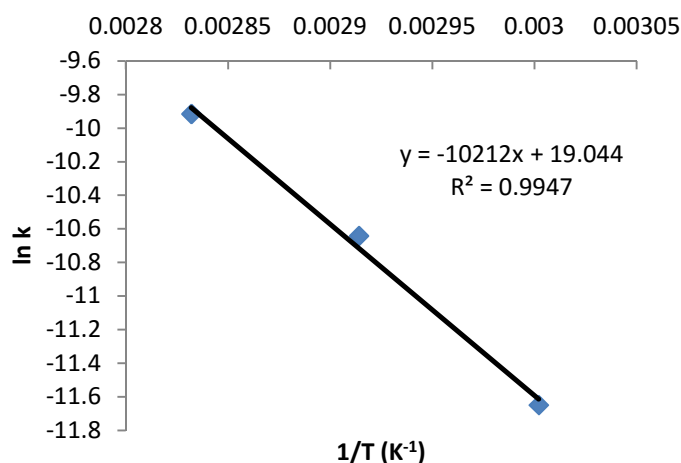


Figure 46: Linear regression analysis of the rate constants k , related to the different temperatures.

The activation energy E_a is therefore 84.902 kJ mol⁻¹, with the pre-exponential factor equating to e^{19.044} s⁻¹. These values can be used to calculate the half-life of racemisation in solution of (*S_a*)-BazOL (+)-**394** at 293.15 K (20 °C) through application to the Arrhenius equation. The rate constant at this temperature is 1.38 × 10⁻⁷ s⁻¹, so therefore the half-life is 1389 h, or 57.9 days. To quantify the barrier to racemisation, or the Gibbs free energy of activation ΔG^\ddagger , the linear form of the Eyring equation can be employed, plotting the $\ln(k/T)$ against $1/T$ (Figure 47).

$$\ln \frac{k}{T} = -\left(\frac{\Delta H^\ddagger}{R}\right) \frac{1}{T} + \frac{\Delta S^\ddagger}{R} + \ln \frac{k_B}{h}$$

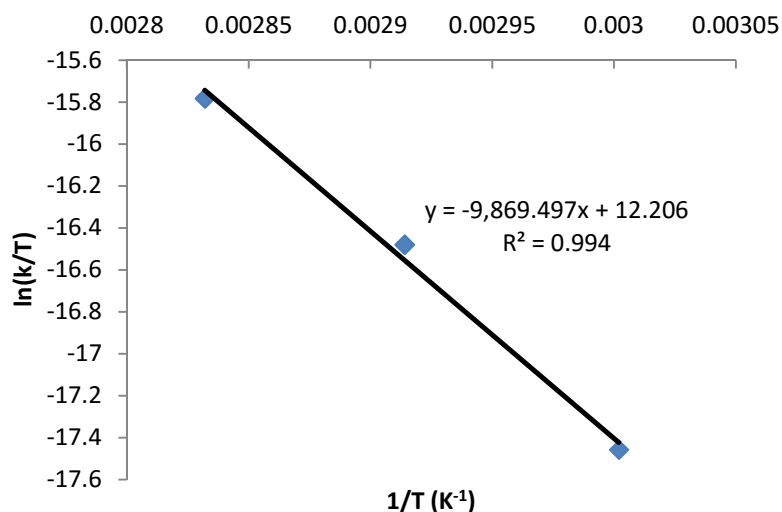


Figure 47: Linear regression analysis of the Eyring equation for the calculation of thermodynamic quantities of activation.

From the linear Eyring plot, the enthalpy and entropy of activation can be calculated as $\Delta H^\ddagger = 82.055 \text{ kJ mol}^{-1}$ and $\Delta S^\ddagger = -96.060 \text{ J mol}^{-1} \text{ K}^{-1}$, respectively. The equation for ΔG^\ddagger is expressed as:

$$\Delta G^\ddagger = \Delta H^\ddagger - T\Delta S^\ddagger$$

Therefore, the Gibbs free energy of activation, or barrier to racemisation, at 293.15 K (20 °C) is:

$$\Delta G_{293.15 \text{ K}}^\ddagger = 110.25 \text{ kJ mol}^{-1}$$

The thermodynamic and kinetic values are summarised in Table 14.

Table 14: Summary of the thermodynamic and kinetic quantities for (S_a)-BazOL (+)-**394**.

$k_{333.15\text{ K}}/\text{s}^{-1}$	$k_{343.15\text{ K}}/\text{s}^{-1}$	$k_{353.15\text{ K}}/\text{s}^{-1}$	$E_a/\text{kJ mol}^{-1}$	A/s^{-1}	$\Delta H^\ddagger/\text{kJ mol}^{-1}$	$\Delta S^\ddagger/\text{J mol}^{-1}\text{ K}^{-1}$	$\Delta G^\ddagger_{293.15\text{ K}}/\text{kJ mol}^{-1}$
8.725×10^{-6}	23.890×10^{-6}	49.388×10^{-6}	84.902	1.865×10^8	82.055	-96.060	110.215

By using the equation for the Gibbs free energy of activation, the relationship between ΔG^\ddagger and temperature can be plotted (Figure 48). For comparison, while the ΔG^\ddagger value at 493.15 K for BINOL **213** has previously been calculated to be 158 kJ mol^{-1} ,²³¹ the corresponding value for (S_a)-BazOL (+)-**394** at 493.15 K is 129.4 kJ mol^{-1} , according to the experimental data in this project. The increased stability to racemisation of BINOL **213** suggests that the distance in space (d_{nap}), parallel to the biaryl bond, between the fused 6-membered rings (through C4a-C5-C6-C7-C8-C8a) has to be much shorter than that (d_{az}) of the fused 7-membered rings (through C3a-C4-C5-C6-C7-C8-C8a) of (S_a)-BazOL (+)-**394** (Figure 49). The distance d_{nap} is shorter than d_{az} , as the biaryl bond of BINOL **213** links two 6-membered rings together, rather than the two 5-membered rings of (S_a)-BazOL (+)-**394**. The difference in these distances is evidently more influential, compared to the steric repulsion of the blocking groups, towards the stability to racemisation, since the 8,8'-ethoxy groups of (S_a)-BazOL (+)-**394** are larger than the 8,8'-hydrogens of BINOL **213**.

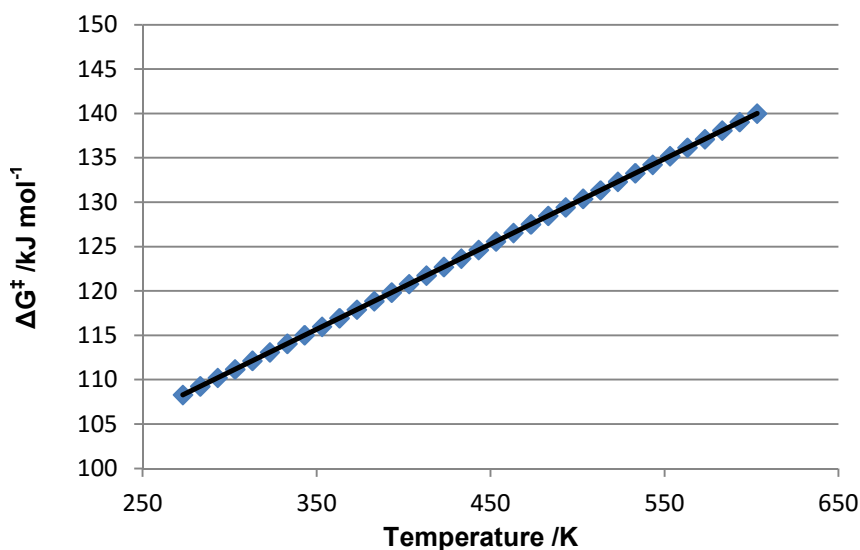


Figure 48: The Gibbs free energy of activation of (*S_a*)-BazOL (+)-**394** as a function of temperature.

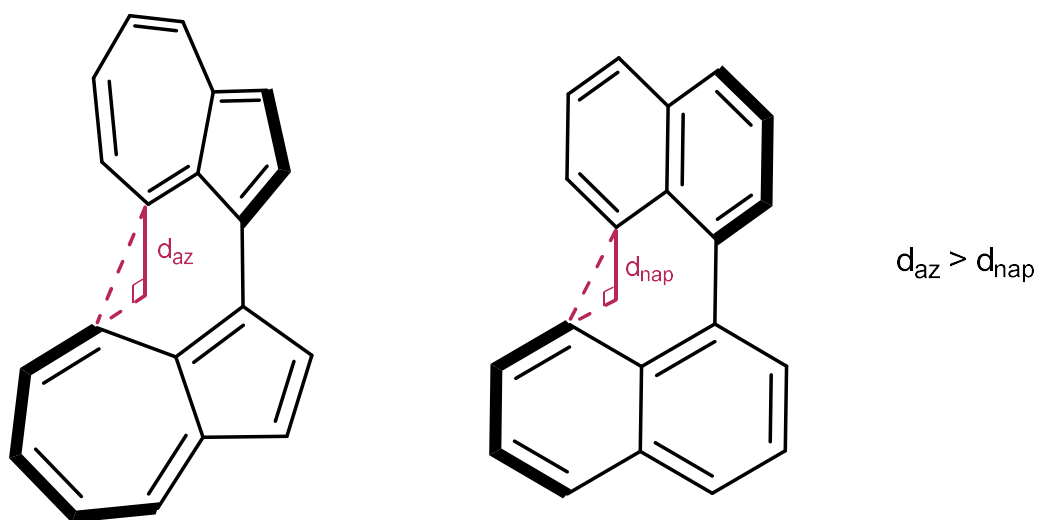


Figure 49: The distances, parallel to the biaryl bond, between the 7-membered rings (C3a-C4-C5-C6-C7-C8-C8a) of a 1,1'-biazulene (d_{az}) and between the 6-membered rings (C4a-C5-C6-C7-C8-C8a) of 1,1'-binaphthalene (d_{nap}).

2.4. Development of 2,2'-biazulene-1,1'-diphosphine (“2,2’-BazPhos”)

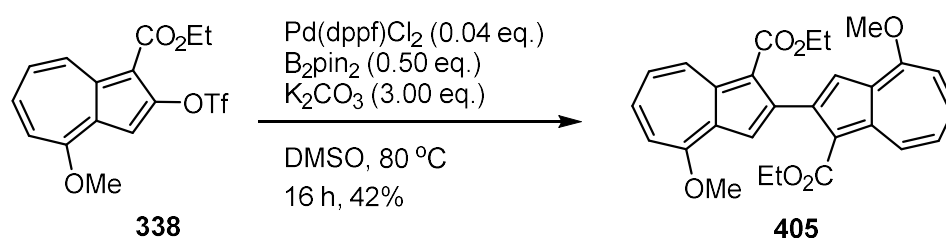
2.4.1. 2,2'-biazulene formation through Pd-catalysed homocoupling

During the stage of the project in which the development of the nickel-catalysed homocoupling reaction of ethyl 3-bromo-2,4-dimethoxyazulene-1-carboxylate **333**

was taking place (Table 7), other reactions useful towards the synthesis of the 1,1'-biazulene-2,2'-diphosphine target were being carried out concurrently, but on monoazulene derivatives. One example of these experiments not mentioned earlier in this report, was the palladium-catalysed homocoupling reaction of azulene-2-yl triflate **338**, mediated by bis(pinacolato)diboron (B_2pin_2), to form diethyl 4,4'-dimethoxy-2,2'-biazulene-1,1'-dicarboxylate **405**. This type of biaryl formation, introduced by Miyaura *et al.*, originated from a side process for the palladium-catalysed cross coupling of dialkoxydiboron species with aryl halides to form aryl boronic esters.²³² The same group later expanded the substrate scope for the borylation of aryl triflates, and also tailored the reaction to favour the previously unwanted biaryl formation in a two step, one-pot procedure.²³³ The biaryl formation from the homocoupling of aryl halides or aryl triflates was optimised and streamlined to a one-step process by Bräse *et al.*, applying the reaction to a variety of electron-rich and electron-poor substrates.²³⁴

This methodology was thus applied to azulene-2-yl triflate **338** by heating 0.13 mmol of this substrate with 0.5 equivalents of B_2pin_2 , 4 mol% of $Pd(dppf)Cl_2$, and 3.0 equivalents of potassium carbonate in anhydrous DMSO for 14 hours. Unfortunately, the only product identified from this reaction was ethyl 2-hydroxy-4-methoxyazulene-1-carboxylate **337**, formed as a result of losing the triflyl group. This experiment was repeated with dioxane as the solvent, but only a trace of desired 2,2'-biazulene **405** was detected by mass spectrometry. To combat the possibility of the reaction failing as a result of the presence of oxygen, another reaction was carried out with DMSO that was degassed by sparging with nitrogen. To our delight, this resulted in the formation of the desired 2,2'-biazulene **405** in 34% yield. On increasing the scale of the reaction to 0.42 mmol, the 2,2'-biazulene **405** was isolated in an improved 42%

yield (Scheme 94). Very recently, and subsequent to the research described here, in the synthesis of biazulene diimides by Gao *et al.*, the formation of tetraethyl [2,2'-biazulene]-1,1',3,3'-tetracarboxylate could be achieved in 71% yield.²³⁵ This was achieved through the homocoupling of diethyl 2-chloroazulene-1,3-dicarboxylate, by heating with Ni(COD)₂ in DMF at 50 °C. A more impressive 97% yield was achieved for the homocoupling of the 6-(azulen-2-yl) derivative of this starting material, so this may represent an alternative protocol to improve the formation of 2,2'-biazulenenes in this project.

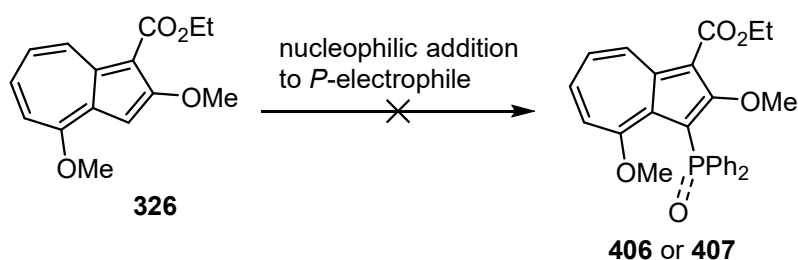


Scheme 94: The Pd-catalysed homocoupling reaction of azulene-2-yl triflate **338**, via Miyaura borylation, to form diethyl 4,4'-dimethoxy-[2,2'-biazulene]-1,1'-dicarboxylate **405**.

2.4.2. Installation of phosphine groups at 1-position

After the success of the 2,2'-homocoupling reaction, strategies for the installation of a phosphine group at the 1-position were explored to potentially complete the synthesis of a *rac*-2,2'-biazulene-1,1'-diphosphine ligand, using ethyl 2,4-dimethoxyazulene-1-carboxylate **326** as a (monomeric) model substrate due to its availability. At first, attempts were made to exploit the nucleophilic nature of the 3-position of this azulene derivative, by treating it with phosphorus-containing electrophiles to make the desired 3-(diphenylphosphino)-azulene via an S_EAr process (Scheme 95). However, no reactivity was observed between this azulene and chlorodiphenylphosphine at room temperature. The treatment of azulene **326** with chlorodiphenylphosphine in the presence of DMAP, heated to reflux in THF,

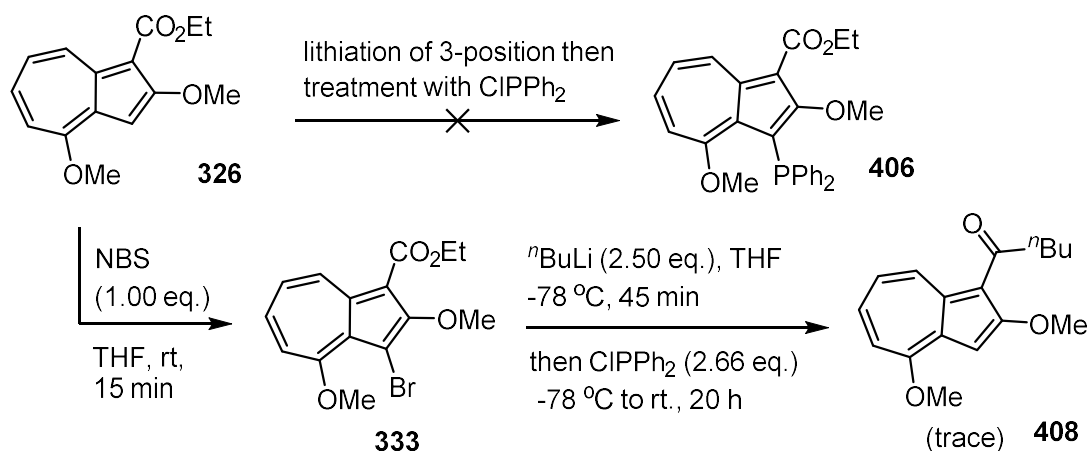
also induced no reaction. No reaction was produced when azulene **326** was treated with diphenylphosphinic chloride and catalytic DMAP at room temperature, either. Interestingly, the same reaction but with 1.1 equivalents of DMAP produced a small amount of 2,4-dimethoxyazulene **349**. However, it was clear from the lack of reactivity in this process that the 3-position of the azulene needed some prior activation in order to form the desired carbon-phosphorus bond.



Scheme 95: No reaction was observed between ethyl 2,4-dimethoxyazulene-1-carboxylate **326** and phosphorus-containing electrophiles chlorodiphenylphosphine, nor diphenylphosphinic chloride.

Efforts were made to install the phosphine group using organolithium reagents, in the hope that the two methoxy groups at 2,4-positions could direct the lithiation to the 3-position (Scheme 96). The first experiment through this approach involved the treatment of the same model azulene **326** with *n*-butyllithium at $-78\text{ }^{\circ}\text{C}$ and allowing to warm up to room temperature. The presumed azulene-3-yl lithium intermediate was cooled again to $-78\text{ }^{\circ}\text{C}$ and quenched with chlorodiphenylphosphine. Unfortunately, only olefinic degradation products were detected, which were perhaps produced through nucleophilic addition of *n*-butyllithium to the 7-membered ring of the azulene. For increased control over the lithiation, *n*-butyllithium was instead added to the 3-bromoazulene **333**, with the temperature maintained at $-78\text{ }^{\circ}\text{C}$ until quenching with chlorodiphenylphosphine. A different azulene-like product was detected by NMR, but instead of the desired product **406**, mass spectrometry showed formation of 1-(2,4-

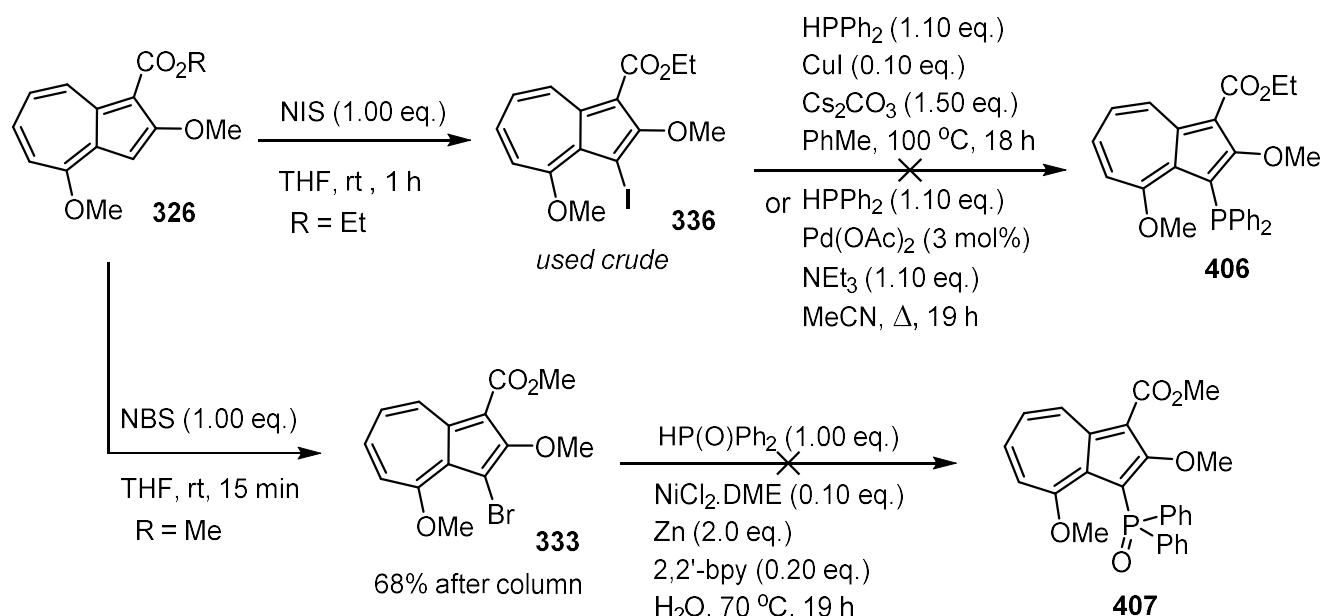
dimethoxyazulen-1-yl)pentan-1-one **408**, which is the result of nucleophilic addition of the organolithium to the ester group.



Scheme 96: The attempts at 3-lithiation of ethyl 2,4-dimethoxyazulene-1-carboxylate **326**, followed by quenching with chlorodiphenylphosphine.

As there was too much functionality that was sensitive to side reactions on the treatment with organolithium reagents, transition metal cross coupling reactions were also explored (Scheme 97). The treatment of ethyl 2,4-dimethoxyazulene-1-carboxylate **326** with *N*-iodosuccinimide gave the crude 3-iodoazulene **336**, which was then heated with diphenylphosphine, copper(I) iodide and caesium carbonate in toluene at 100 °C for 18 hours, according to a process reported by Venkataraman *et al.*²³⁶ Unfortunately, this process only converted the 3-iodoazulene **336** back to the dehalogenated azulene **326**. The same result was achieved, following a process originally developed by Stelzer *et al.*, when the same 3-iodoazulene **336** was heated with diphenylphosphine, palladium diacetate and triethylamine at reflux in acetonitrile.²³⁷ Another attempt at a carbon-phosphorus cross coupling came from following the procedure reported by Tang *et al.*, in which diphenylphosphine oxide could be coupled with aryl halides by using nickel(II) chloride, zinc, and 2,2'-bipyridine in water.²³⁸ After forming the 3-bromoazulene **333** through treatment of

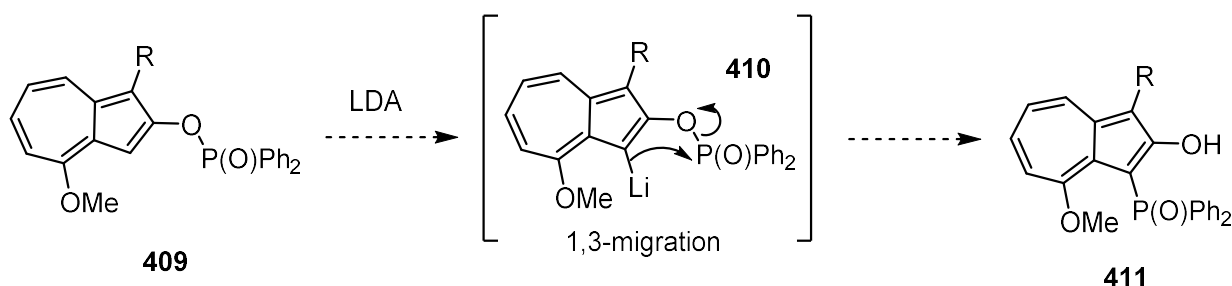
azulene **326** with *N*-bromosuccinimide, the application of this method only resulted in conversion back to dehalogenated azulene **326**.



Scheme 97: The attempts at the formation of azulene-1-yl phosphine **406** or phosphine oxide **407** through transition metal cross coupling.

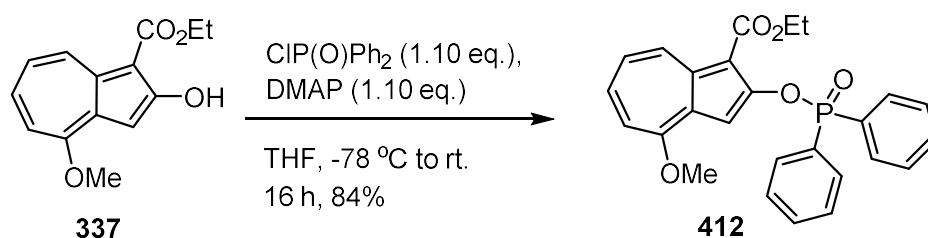
The next idea explored was to form a 2-((diphenylphosphoryl)oxy)azulene **409** that could be lithiated at the 3-position, leading to a 1,3-migration of the diphenylphosphoryl group from the oxygen atom to the azulene, producing an azulene-3-yl phosphine oxide **411**. First developed by Heinicke *et al.*, the reaction works well with arenes generally, due to the excellent *ortho*-directing ability for lithiation of the oxy-phosphoryl group.^{239,240} The method was appealing for this project, as it looked like an easier way of installing a phosphine group on the compound, through the nucleophilicity of the oxygen rather than the azulene. Once the 2-((diphenylphosphoryl)oxy)azulene **409** is formed, an intramolecular, rather than intermolecular, process is then required for the installation of a phosphine group at the 3-position (Scheme 98). The base used for the lithiation is lithium

diisopropylamide (LDA), rather than *n*-butyllithium, so the ester at the 1-position of the azulene is less likely to react in this process.



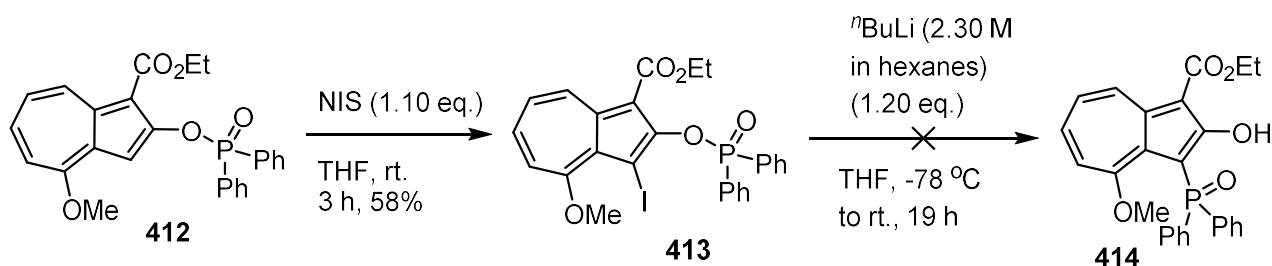
Scheme 98: The plan to lithiate the 3-position of the azulene, leading to migration of the phosphoryl group to there from the oxygen atom.

Following the method of Díez-González *et al.*,²⁴¹ ethyl 2-hydroxy-4-methoxyazulene-3-carboxylate **337** was treated with chlorodiphenylphosphine, triethylamine and catalytic DMAP in THF at room temperature for 3 days, followed by heating at 40 °C for 15 hours. The crude mixture was then treated with hydrogen peroxide to oxidise the phosphanyl to a phosphoryl group. The process yielded the desired 2-((diphenylphosphoryl)oxy)azulene **412**, but it could not be separated from diphenylphosphine oxide and another aromatic, phosphorus-containing impurity. Instead of carrying out the reaction as a two-step process, the 2-hydroxyazulene **337** was treated with diphenylphosphinic chloride at –78 °C to access the desired 2-((diphenylphosphoryl)oxy)azulene **412** directly (Scheme 99). Using a stoichiometric quantity of DMAP, according to Parquette *et al.*,²⁴² the reaction was run for 16 hours, and it proceeded a lot more smoothly, giving the product **412** in 84% yield, with no difficulties in the purification.



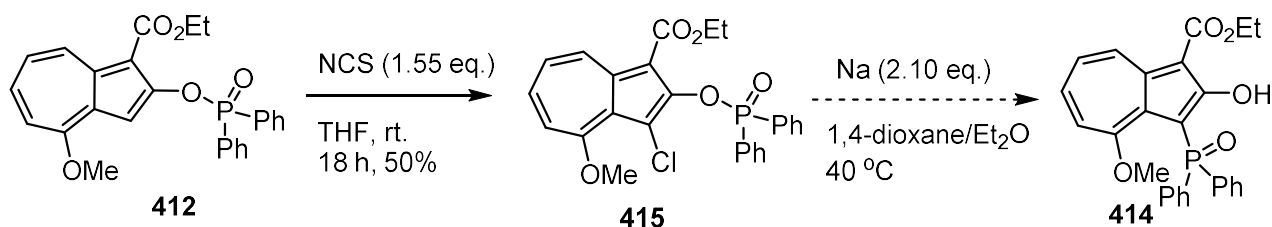
Scheme 99: The treatment of ethyl 2-hydroxy-4-methoxyazulene-3-carboxylate **337** with diphenylphosphinic chloride and DMAP to give ethyl 2-((diphenylphosphoryl)oxy)-4-methoxyazulene-1-carboxylate **412**.

The 2-((diphenylphosphoryl)oxy)azulene **412** was treated with 1.0 equivalent of freshly made lithium diisopropylamide at $-78\text{ }^\circ\text{C}$ in THF, stirring at this temperature for 2.5 hours, and then allowing to warm to room temperature to induce the migration step of the reaction. Oddly, the crude product consisted mostly of 2-hydroxyazulene **337**, which is what one might expect if the solvent is moist, and the quenching of the LDA results in nucleophilic hydroxide ions that react with the phosphoryl group. The THF was sourced by distillation over sodium and benzophenone, so the near complete conversion of the starting material to 2-hydroxyazulene **337** through this route seems implausible. To facilitate the lithiation step, 2-((diphenylphosphoryl)oxy)azulene **412** was treated with *N*-iodosuccinimide, which produced a near-clean crude sample of the 3-iodoazulene product **413** in 58% yield (Scheme 100). Unfortunately, when the 3-iodoazulene **413** was treated with *n*-butyllithium for the halogen-lithium exchange, degradation of the azulene occurred. This result may be a consequence of the instability of iodo groups at the 1- or 3-positions of azulenes.^{243,244}



Scheme 100: The iodination of 2-((diphenylphosphoryl)oxy)azulene **412** with *N*-iodosuccinimide, followed by attempted lithiation of the 3-iodoazulene **413** to induce the migration of the phosphoryl group.

The 2-((diphenylphosphoryl)oxy)azulene **412** could also react with *N*-chlorosuccinimide to produce the 3-chloroazulene **415**, which was stable to column chromatography, in 49% yield (Scheme 101). This product was made with a view to react with sodium in a halogen-sodium exchange to produce the arylsodium intermediate, which then would undergo the migration.²⁴⁰ This process, however, was not carried out in this project.

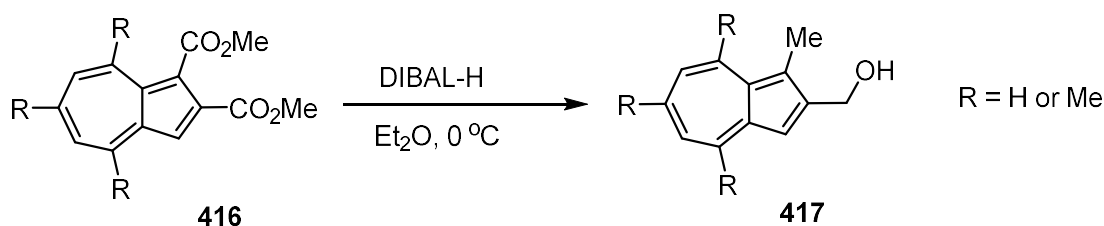


Scheme 101: The chlorination of 2-((diphenylphosphoryl)oxy)azulene **412** with *N*-chlorosuccinimide, and planned halogen-sodium exchange of the 3-chloroazulene **415** to induce the migration step.

2.4.3. Reduction of ester groups

To allow more flexibility in the reactions that could be performed in this synthetic route, methods were explored to convert the ester group of **326** into something less influential in the outcome of reactions in which it ostensibly is not participating. The ester could not simply be converted to a hydrogen atom, by decarboxylation with

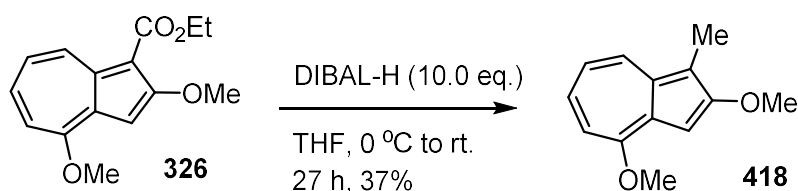
orthophosphoric acid, as a larger group would probably be needed to ensure atropisomerism in the final ligand. Fortunately, it was revealed in two papers by Hansen *et al.* that an ester group at the 1- or 3-position of the azulene could be reduced to a methyl group by reacting it with diisobutylaluminium hydride (DIBAL-H), a relatively mild reducing agent.^{195,245} The authors used this reagent to convert several examples of dimethyl azulene-1,2-dicarboxylates **416** to (1-methylazulen-2-yl)methanol derivatives **417** (Scheme 102). The 1-ester is reduced further than the 2-ester because, on formation of the (azulen-1-ylmethoxy)diisobutylaluminum intermediate, the carbon-oxygen bond is cleaved and the electron density shifts from the 7-membered ring to the 1-position, stabilising the carbocation, and eventually forming a methyl group. A 2-methyl carbocation cannot be stabilised by resonance in the same fashion, so the hydroxymethyl group is retained here.



Scheme 102: The reaction of DIBAL-H with dimethyl azulene-1,2-dicarboxylates **416** to give (1-methylazulen-2-yl)methanol derivatives **417**, by Hansen.

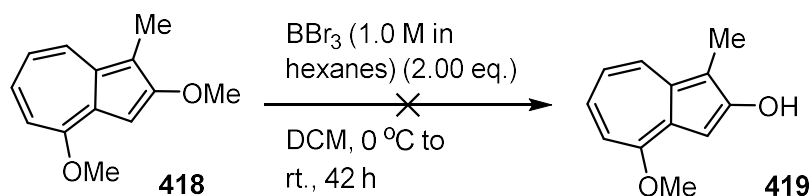
Following this method, to ethyl 2,4-dimethoxyazulene-1-carboxylate **326** was added 10.0 equivalents of DIBAL-H in two portions at 0 °C and allowed to warm up to room temperature, stirring for 27 hours. Happily, the desired 2,4-dimethoxy-1-methylazulene product **418** was isolated in 37% yield, which was oddly low considering the crude NMR spectrum showed that the product was almost clean at this stage (Scheme 103). When the reaction was repeated, increasing the scale from 0.20 mmol to 1.6 mmol, the mass of the crude product **418** corresponded to a yield

that was over 100%, despite appearing mostly clean by NMR. Therefore, while the product may be unstable on silica, the column is perhaps required to more rigorously remove inorganic aluminium salts are not visible by proton NMR.



Scheme 103: The reduction by DIBAL-H of ethyl 2,4-dimethoxyazulene-1-carboxylate **326** to 2,4-dimethoxy-1-methylazulene **418**.

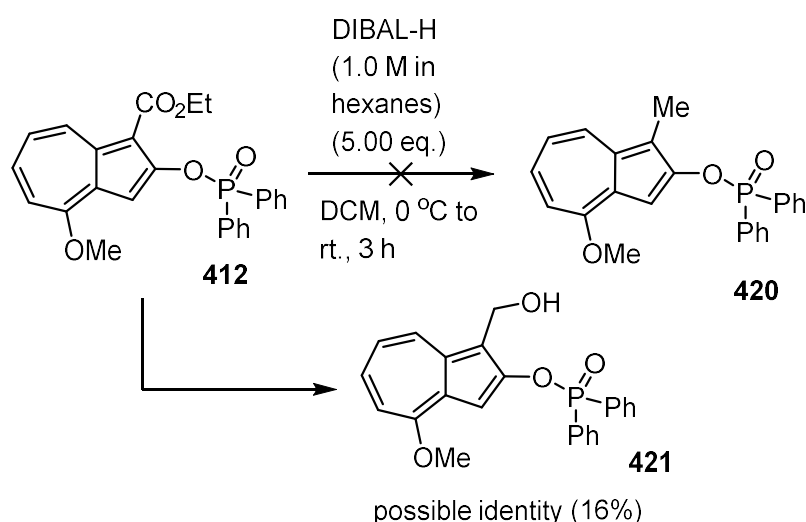
The next consideration was choosing at which point this step could be performed within the synthetic route towards a 2,2'-biazulene-1,1'-diphosphine ligand. The azulene product **418** obtained from this reduction was treated with boron tribromide in order to form the corresponding 2-hydroxyazulene **419** (Scheme 104). After the addition of one equivalent of boron tribromide and stirring overnight in DCM, not much conversion had taken place according to the TLC. The addition of another equivalent resulted in degradation of the product. Thus, an ester at the 1-position is perhaps essential for a clean dealkylation, with degradation pathways a result of keto-enol tautomerisation.²¹⁶



Scheme 104: The attempted dealkylation of 2,4-dimethoxy-1-methylazulene **418** with boron tribromide.

Another option was to reduce the ester to the methyl group once the 2-((diphenylphosphoryl)oxy)azulene **412** had been made. Accordingly, this azulene

was treated with 5.0 equivalents of DIBAL-H and stirred in DCM for 3 hours (Scheme 105). This reaction produced a small amount of what was tentatively identified as perhaps the azulene-1-yl methanol **421**. If this was the correct identity, it was produced in ~16% yield. This compound **421** is probably unstable, as the hydroxy group could be eliminated by the movement of electron density from the 7-membered ring, stabilising the resultant carbocation. If this reaction were to be repeated, an increased quantity of DIBAL-H may be required to completely reduce the ester to the methyl group.



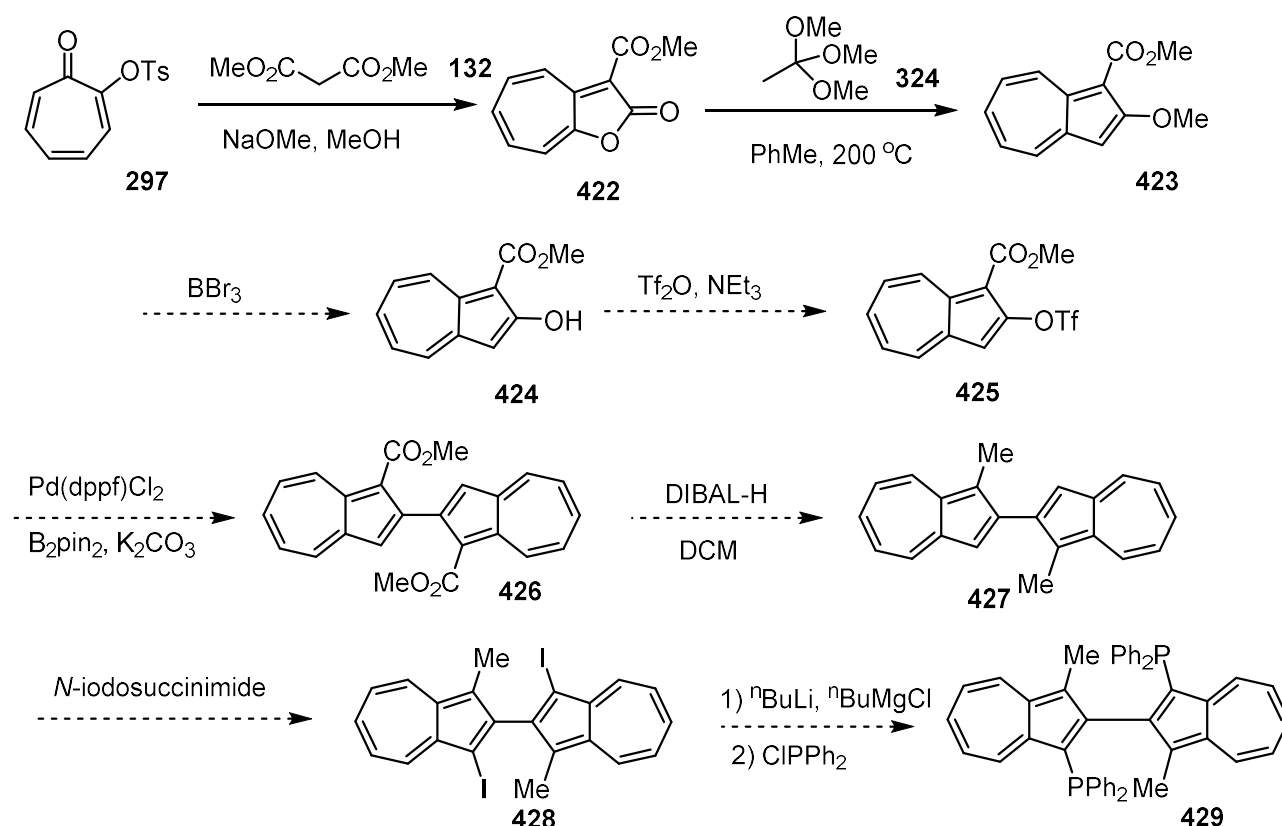
Scheme 105: The reduction with DIBAL-H on 2-((diphenylphosphoryl)oxy)azulene **412**, which yielded possibly azulene-1-yl methanol **421**.

2.4.4. Synthesis towards 2,2'-BazPhos

The desired precursor for the lithiation and migration of the diphenylphosphoryl group, which was 4-methoxy-1-methylazulene-2-yl diphenylphosphinate **420**, could not be synthesised cleanly from the methods that were tested. Therefore, it was decided to abandon this strategy for the installation of a phosphine group at the 1-position of the ligand, and different synthetic methods were considered. As mentioned previously in this account, Ito and co-workers had been able to form (3,6-

di-*tert*-butylazulen-1-yl)diphenylphosphine **285** by halogen-lithium exchange of the corresponding 1-iodoazulene **284**, achieved by using lithium tri-*n*-butylmagnesate (Scheme 49).¹⁸¹ Crucially, this reaction had literature precedent, and it was possible to reduce esters in the electron-rich positions of the azulene, so a new plan was devised around these methods (Scheme 106). The tosyl derivative of tropolone **297** can undergo a condensation reaction with the sodium salt of dimethyl malonate **132** to produce methyl 2-oxo-2*H*-cyclohepta[*b*]furan-3-carboxylate **422**.¹⁸⁷ Due possibly to the lower pK_{aH} of methoxide compared to ethoxide, the major pathway of the reaction is different to that of the synthesis of the ethyl ester derivative **298**, and leads to the absence of the 8-hydroxy group (see mechanism in Scheme 52). A hydrogen atom in this position is desirable, as there is no requirement for a bulky group here for atropisomerism, and reduced steric hindrance at this position may allow greater flexibility and efficiency in the synthetic route. The 2*H*-cyclohepta[*b*]furan-2-one **422** reacts with the thermally *in situ* generated ketene acetal from trimethyl orthoacetate **324** to make methyl 2-methoxyazulene-1-carboxylate **423**.¹⁸⁷ After this point, each proposed chemical step had not yet been performed on the corresponding substrate, but was preceded for other substrates, either in this project or in the literature. The azulene product **423** of the [8+2]-addition-elimination reaction could probably be dealkylated to form the 2-hydroxyazulene **424**, and then converted to the triflate **425**. In a process similar to that in Scheme 94, the azulen-2-yl triflate could hopefully be converted to the 2,2'-biazulene **426**, via the palladium-catalysed Miyaura borylation and Suzuki cross-coupling. The ester groups on this 2,2'-biazulene **426** could probably be reduced by using DIBAL-H to produce 1,1'-dimethyl-2,2'-biazulene **427**, which would potentially permit halogen-lithium exchange chemistry to take place cleanly to synthesise the

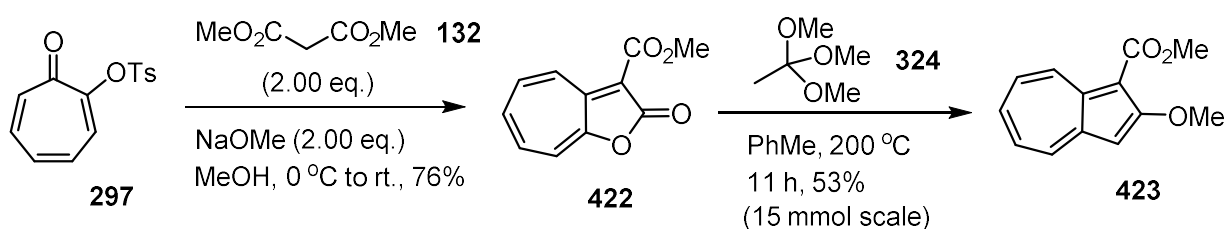
diphosphine. Because of the methyl groups at 1,1'-positions, this substrate should only react with *N*-iodosuccinimide at the other two remaining electron-rich positions, giving 1,1'-diiodo-3,3'-dimethyl-2,2'-biazulene **428**. This biazulene **428** would hopefully then be converted to the (2,2'-biazulene-1,1-diyl)-bis-(diphenylphosphine) **429** via the literature method depicted in Scheme 49.



Scheme 106: Synthetic plan for a 2,2'-biazulene-1,1'-diphosphine ligand. Solid reaction arrows signify that the reaction has been previously performed in the literature, specifically on that compound; each dashed arrow represents a chemical step previously unreported for that compound.

The first two steps of this planned synthesis were adopted from a paper by Pham (Scheme 107). On a scale of 20 mmol, a freshly made solution of sodium methoxide was added to 2-tosyloxycyclohepta-2,4,6-trien-1-one **297** and dimethyl malonate **132** in methanol at 0 °C, and was allowed to warm to room temperature, stirring for 6 hours. The desired 2H-cyclohepta[b]furan-2-one **422** was then smoothly isolated in 55% yield. When the

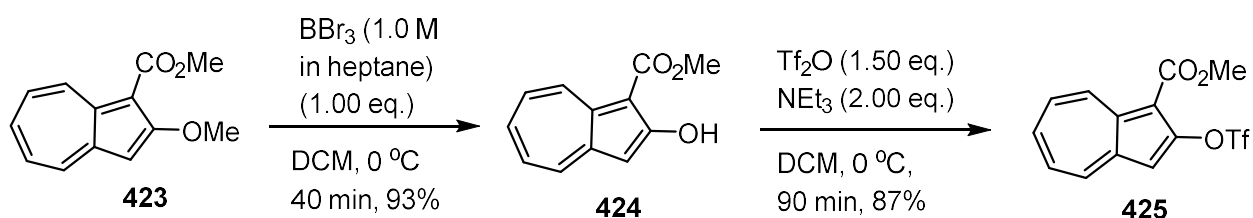
scale of the process was increased to 60 mmol, this resulted in an increased 76% yield of **422**, though this experiment was only carried out once. Nevertheless, this step made for a solid basis of the synthetic route. To test the next step, the [8+2]-addition-elimination to synthesise the azulene moiety, *2H*-cyclohepta[*b*]furan-2-one **422** was heated with trimethyl orthoacetate and toluene at 200 °C for 6 hours, on a relatively small scale of 2 mmol in a microwave tube. This process gave the desired compound of methyl 2-methoxyazulene-1-carboxylate **423** in 48% yield. When the scale of the reaction was increased to 10 mmol, carried out in an round bottom pressure flask (Ace Glass Inc.) and heated for 7 hours, the yield was increased to 68%. When the limit to the capacity of the pressure flask was approached, at a scale of 15 mmol, the product **423** could still be made in 53% yield, after heating for 11 hours in total.



Scheme 107: The condensation reaction of 2-tosyloxypyrone **297** with dimethyl malonate **132** to form *2H*-cyclohepta[*b*]furan-2-one **422**, followed by the [8+2] reaction with trimethyl orthoacetate **324** to form methyl 2-methoxyazulene-1-carboxylate **423**.

The demethylation reaction was first carried out on a scale of 0.46 mmol, whereby methyl 2-methoxyazulene-1-carboxylate **423** was treated with an equivalent of boron tribromide for 45 minutes. As expected, the reaction smoothly produced methyl 2-hydroxyazulene-1-carboxylate **424** in 88% yield, without the requirement of chromatographic separation (Scheme 108). This experiment could be performed on a larger scale; for instance, using 7.0 mmol of starting material, a yield of 93% for the

2-hydroxyazulene **424** was obtained. The conversion of the hydroxy group to a triflate was also uncomplicated. Testing this reaction on a small scale of 0.40 mmol, the 2-hydroxyazulene **424** was stirred with 1.5 equivalents of triflic anhydride and 2.0 equivalents of triethylamine in DCM at 0 °C for 40 minutes. After column chromatography, the azulene-2-yl triflate **425** was isolated in 72% yield. By increasing the scale to 6.5 mmol, and by adding the triflic anhydride as a solution in DCM rather than neat, the yield of this reaction increased to 87%. Since the both the demethylation and triflation reactions worked so reliably, these two steps could be combined into a single, two-pot process. This meant that the crude mixture for demethylation reaction could be given a simple aqueous wash, dried, and without recording the yield or crude NMR analysis, the triflation reaction could be immediately carried out. This modification meant the two steps could be completed within 6 hours, and on a scale of 10.6 mmol, resulted in 78% overall yield of **425**.

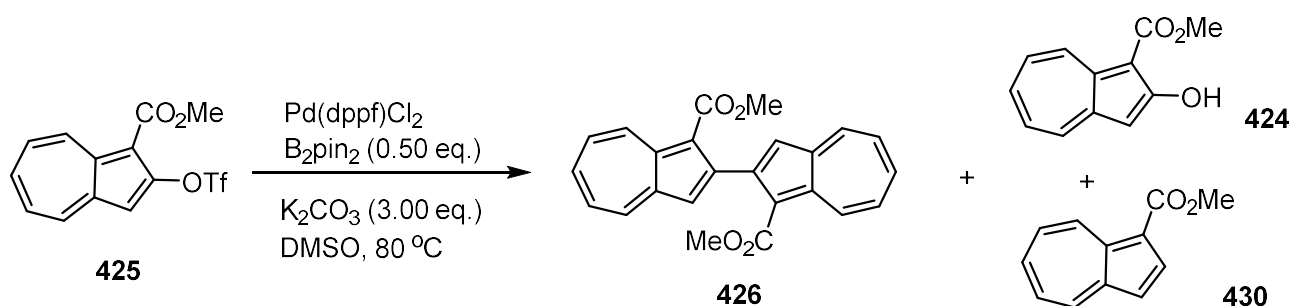


Scheme 108: The boron tribromide-mediated demethylation of methyl 2-methoxyazulene-1-carboxylate **423**, followed by conversion of the hydroxy group to a triflate.

The palladium-catalysed homocoupling reaction was also successful (Table 15). On the first attempt, 0.30 mmol of azulene-2-yl triflate **425** was stirred with 4 mol% of $\text{Pd}(\text{dppf})\text{Cl}_2$, 0.5 equivalents of B_2pin_2 and 3.0 equivalents of potassium carbonate in 2 mL of degassed DMSO at 80 °C for 15 hours. This reaction yielded the desired 2,2'-biazulene **426** in 23% yield (Table 15, entry 1). By increasing the reaction scale almost ten-fold, at 5.6 mmol, and at roughly double the concentration (0.28 M with

respect to the azulene-2-yl triflate **425**), a much improved 44% yield of **426** was produced (Table 15, entry 2). Another experiment, on a scale of 3.2 mmol, employed a loading of the palladium complex at 3.1 mol%, gave a further increase in yield at 48% (Table 15, entry 3). However, it is difficult to say which of the two parameter changes, if any of them, led to this improved result. When the palladium loading was reduced to 2 mol%, at scales of 4.8 mmol and 8.3 mmol, this gave yields of 29% (Table 15, entry 4) and 20% (Table 15, entry 5) respectively. Though the latter was carried out at a significantly higher concentration than the others of 0.42 M, the reduced yields were probably either a result of the lower palladium loading, or increased quantity of moisture in the bottle of solvent. The latter factor may have had some influence in the significant formation of both 2-hydroxyazulene **424** and methyl azulene-1-carboxylate **430**, which were inseparable from each other by column chromatography.

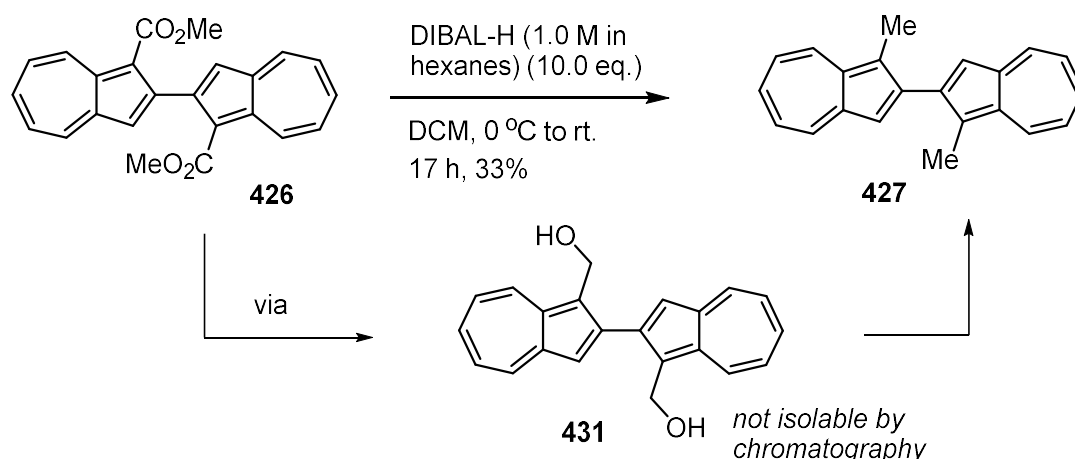
Table 15: Summary of the Pd-catalysed homocoupling reaction of azulene-2-yl triflate **425** to form dimethyl [2,2'-biazulene]-1,1'-dicarboxylate **426**.



Entry	Scale ^a /mmol	Pd mol%	Concentration ^b /M	Running time ^c /h	Yield of 426 /%	Yield of 424 ^d /%	Yield of 430 ^d /%
1	0.29	4.0	0.15	15	23	0	0
2	5.6	4.0	0.28	15	44	0	trace ^e
3	3.2	3.1	0.21	21	48	0	3.4
4	4.8	2.0	0.27	6	29	12	3.4
5	8.3	2.0	0.42	12	20	7.0	3.8

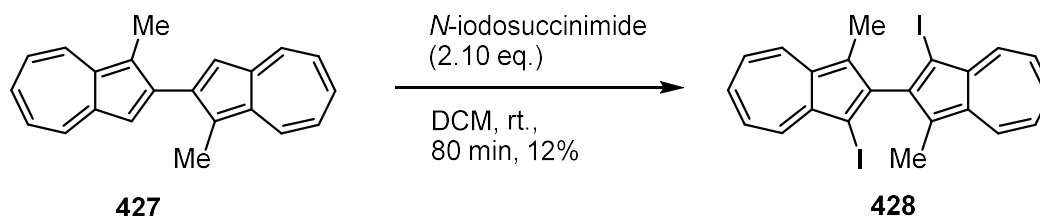
a) Scale of the reaction with respect to the molar quantity of azulene-2-yl triflate **425** **b)** Concentration with respect to the molar quantity of azulene-2-yl triflate **425** in the volume of DMSO **c)** Reaction was allowed to operate overnight, or until the starting material had been completely consumed by TLC **d)** Compounds **424** and **430** were inseparable by column chromatography; thus for entries 4 and 5, yields were estimated by integration of peaks in proton NMR spectrum **e)** Yield was not recorded.

Now with practicable amounts of a 2,2'-biazulene species **426**, the structure had to be modified to be compatible with strongly nucleophilic organometallic reagents. In order to reduce the two ester groups, the biazulene **426** was mixed with 10 equivalents of DIBAL-H in DCM at 0 °C. The TLC analysis of the reaction mixture after 80 minutes showed the complete consumption of the starting material, so a work-up procedure was applied at this point. However, instead of the expected 1,1'-dimethyl-2,2'-biazulene **427**, the NMR and mass spectrometry analysis of the crude mixture revealed an impure sample of [2,2'-biazulene]-1,1'-diyl dimethanol **431**, which was not stable to column chromatography, and so could not be isolated. The reaction was repeated, this time allowing to stir at room temperature overnight, which gave 1,1'-dimethyl-2,2'-biazulene **427** in 33% yield (Scheme 109). Unfortunately, with an increase in the scale of the reaction to 0.74 mmol, the reaction took place less smoothly. At first, 10 equivalents of DIBAL-H were added, but after allowing the mixture to stir for 18 hours, the reaction was still incomplete, so another 10 equivalents of DIBAL-H were added. After running for another 4 hours, the 1,1'-dimethyl-2,2'-biazulene **427** was inseparable from small amounts of unidentified side products by column chromatography, but still corresponded to approximately the same yield.



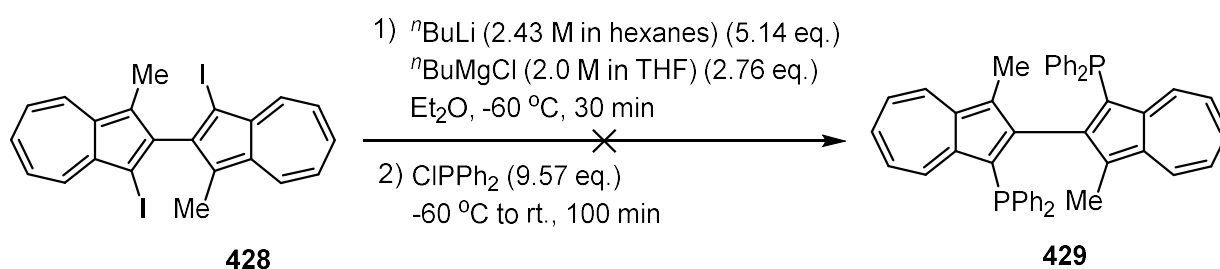
Scheme 109: The reduction of dimethyl [2,2'-biazulene]-1,1'-dicarboxylate **426** with DIBAL-H to yield 1,1'-dimethyl-2,2'-biazulene **427**.

The less pure, but more plentiful sample of 1,1'-dimethyl-2,2'-biazulene **427** was then treated with *N*-iodosuccinimide. Because of concerns over how stable the desired 1,1'-diiodoazulene product **428** would be, the reaction mixture was shielded from light with aluminium foil. After near completion of the reaction by TLC analysis after 100 minutes, neutral alumina was added to the solution, and the mixture was concentrated under reduced pressure to prepare a dry-loaded sample for column chromatography. This purification method gave the desired diiodo product **428** in 12% yield, and the product was stable enough for full characterisation (Scheme 110).



Scheme 110: The reaction of 1,1'-dimethyl-2,2'-biazulene **427** with *N*-iodosuccinimide to produce 1,1'-diiodo-3,3'-dimethyl-2,2'-biazulene **428**.

At this stage, the synthesis was potentially one step away from accessing racemic (3,3'-dimethyl-[2,2'-biazulene]-1,1'-diyl)bis-(diphenylphosphine) **429**, or “(±)-2,2'-BazPhos”, assuming the methyl groups are oriented in such a way as to induce atropisomerism. Following the methods of Ito¹⁸¹ and Oshima *et al.*,²⁴⁶ the organometallic species lithium tri-*n*-butylmagnesate was made *in situ* through the addition of *n*-butyllithium to a solution of *n*-butylmagnesium chloride in ether at –60 °C (Scheme 111). After 10 minutes, a solution of the 1,1'-diiodo-2,2'-biazulene **428** in ether was added at the same temperature, and the mixture was allowed to stir for 30 minutes, before the addition of chlorodiphenylphosphine. After allowing it to warm up to room temperature, the reaction was allowed to run for 100 minutes. However, after column chromatography, the only products isolated were *n*-butyldiphenylphosphine oxide and the starting material. Oddly, this indicates that not only did the 1,1'-diiodo-2,2'-biazulene **428** not undergo halogen-lithium exchange, but was stable to the reaction conditions, work-up and column chromatography on silica. This left a nucleophilic source of an *n*-butyl fragment to react with chlorodiphenylphosphine, which was then oxidised on exposure to air.



Scheme 111: The attempted magnesium-iodide exchange of 1,1'-diiodo-2,2'-biazulene **428** with tri-*n*-butylmagnesate, followed by the reaction with chlorodiphenylphosphine.

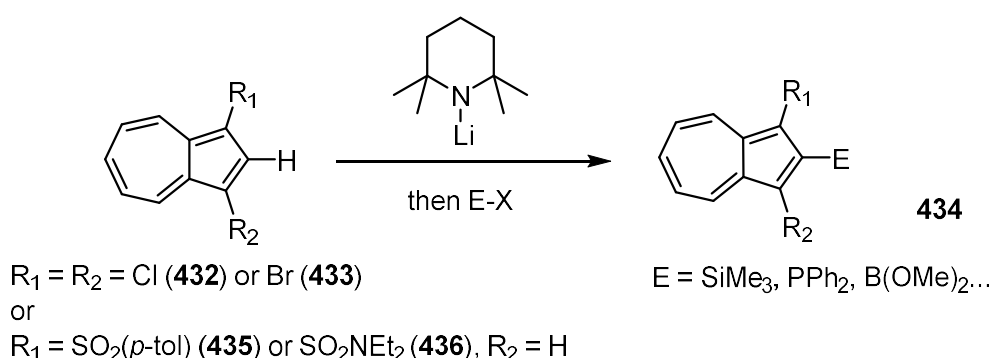
2.5. Development of “1,1’-BazPhos” through the Hafner method

2.5.1. C-H activation of azulene 2-position

So far, the routes towards a chiral ligand described in this account have been based around Nozoe’s method for the construction of the azulene skeleton, that is, the condensation reaction of a tropone derivative with an active methylene compound. One key reason why this reaction had led to success was that it allowed the 2-position of the azulene to be functionalised with an alkyl ether group, which could be converted to a hydroxy group in one step for the 1,1’-BazOL ligand **394**. However, several synthetic steps were required to convert the ether to a phosphonate ester (**389**), which would then most likely need a further two steps to access the phosphine group. With this disadvantage in mind, it would be desirable to access the phosphine more directly. The inherent problem with the 2-position is that it is not as reactive as the most electron-rich (1 and 3) and most electron-poor (4, 6 and 8) positions,^{247,248} towards electrophiles and nucleophiles respectively. Thus, special protocols have to be adopted for C-H activation at this position.

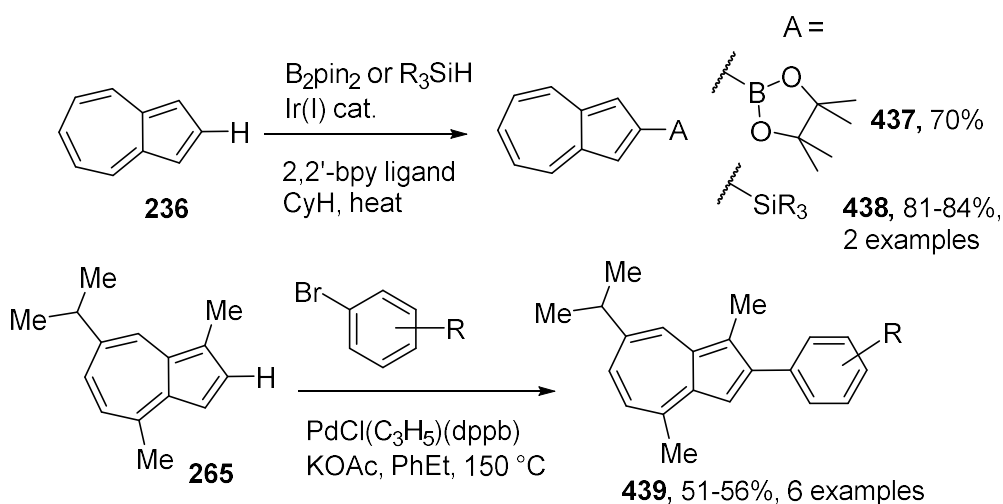
Some success has been achieved in functionalising the 2-position via deprotonation, followed by quenching the conjugate base with an electrophile (Scheme 112). The challenged faced with this strategy is that the electrophilic positions of azulene are potentially incompatible with strong organometallic bases, if they can also behave as nucleophilic species. Moreover, for unsubstituted azulene, Sugihara *et al.* had calculated that there was only a small energy difference between the azulen-2-yl anion (without a counteraction) and the diradical species formed by single electron donation from the 7-membered ring to the 5-membered ring, with the latter canonical form leading to decomposition.²⁴⁹ Nevertheless, the authors were able to use lithium

tetramethylpiperidide (LTMP), a non-nucleophilic base, for the lithiation of 1,3-dihaloazulenes (**432** and **433**) at the 2-position. The intermediates, stabilised by the electron withdrawing ability of the halide groups, could be subsequently quenched with various electrophiles, such as chlorotrimethylsilane, chlorodiphenylphosphine, trimethylborate, dimethylformamide and carbon dioxide to obtain a versatile library of 2-functionalised azulene derivatives **434** in moderate to good yields. With later developments, the group were able to carry out a lithiation at the 2-position of 1-tosylazulene **435** at $-100\text{ }^{\circ}\text{C}$, followed by the addition of similar electrophiles.²⁵⁰ The strong directing ability of the sulfone was demonstrated in a competition reaction with 1,3-dichloroazulene **432**, showing that 1-tosylazulene **435** was more readily lithiated. However, if the reaction was performed at $-70\text{ }^{\circ}\text{C}$, the lithiation suffered issues with selectivity, as the *ortho*-position of the *p*-tolyl group could be deprotonated instead of the azulene. This side intermediate would undergo cyclisation via nucleophilic aromatic substitution at the 8-position of the azulene. This side process could be prevented either by performing the reaction at $-100\text{ }^{\circ}\text{C}$, or by using *N,N*-diethylsulfonamide (**436**), rather than *p*-toluenesulfonate, as the directing group.



Scheme 112: The directed deprotonation of azulenes with LTMP, followed by quenching with electrophiles to produce azulen-2-yl derivatives **434**, by Sugihara.

The same group was also able to employ late transition metal catalyzed C-H activation to carry out similar transformations (Scheme 113). By treating azulene **263** with bis-(pinacolato)diboron, in the presence of an iridium(I) complex and with bipyridine as a ligand, the azulen-2-yl boronate ester **437** was made selectively in 70% yield.²¹⁶ The regioselectivity arises from the coordination of the 5-membered ring of the azulene to the iridium centre, forming an η^5 -complex. The insertion of the metal then takes place at the proximal 2-position, as it is more electron-poor and therefore more acidic than the 1- and 3- positions. The reaction was, however, sensitive to sterics, as derivatives 4,6,8-trimethylazulene and guaiazulene gave respective yields of 32% and 5% for the azulen-2-yl boronate ester products. The versatility of this iridium chemistry was built upon by Takai *et al.*, who were able to carry out similar chemistry with tertiary silanes, to produce 2-silylazulenes **438** with no regioisomeric side products.²⁵¹ Studies have been reported by Doucet *et al.* on the palladium-catalyzed direct arylation of guaiazulene **265**, an inexpensive, naturally occurring azulene derivative.²⁵² Given the various sites on this molecule that are reactive under these conditions (2-CH, 3-CH and 4-C-Me), achieving a good level of regioselectivity presented a challenge. By employing conditions that favoured Heck-like pathways, various 2-arylguiaiazulene species **439** were selectively synthesized in 51-56% yield.

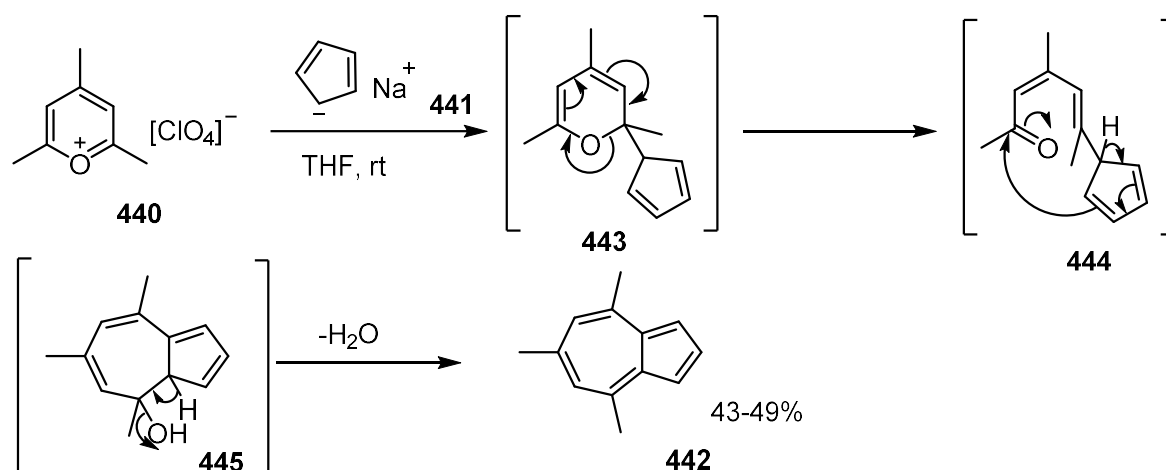


Scheme 113: The late transition metal catalysed C-H activation reactions of azulene **263** and guaiazulene **265**.

While both of these types of C-H functionalisation show versatility in the derivatisation of the 2-position, they may not be immediately suitable for the aims of this project. It has been shown that chlorodiphenylphosphine is a suitable electrophile to combine with the azulene-2-yl lithium intermediate, but the formation of this intermediate in the first place is a delicate process, with its success heavily dependent on the choice of substituents on the starting material. A method with a transition metal catalyst may show greater functional group tolerance, but has not yet been adapted for the creation of azulene-phosphorus bonds, and a lot of time would therefore be demanded for the development of such a process.

2.5.2. Hafner's method for the synthesis of azulenes

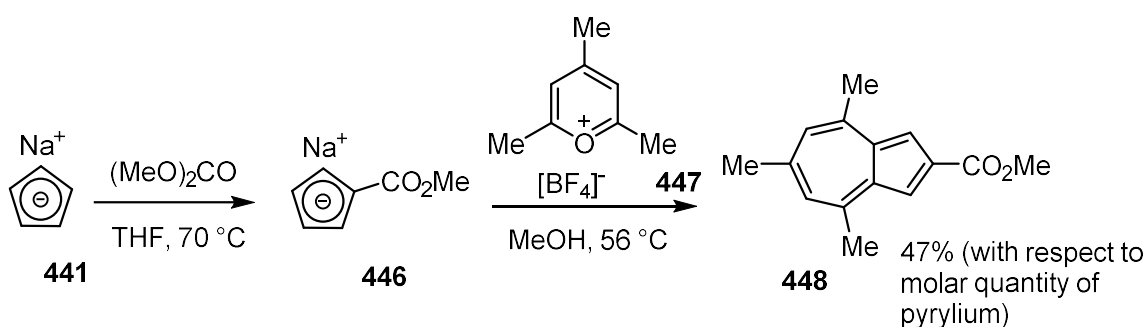
Another ubiquitous method to make azulenes, around which a synthetic method towards a chiral ligand could be based, was originally developed by German chemist Klaus Hafner. Originally published in 1958,²⁵³ the reaction of 2,4,6-trimethylpyrylium perchlorate **440** with an excess of sodium cyclopentadienide **441** yielded 43-49% of 4,6,8-trimethylazulene **442** according to a later account from *Organic Syntheses* (Scheme 114).²⁵⁴ The reaction works by nucleophilic addition of the cyclopentadienide anion to the pyrylium species, followed by an electrocyclic ring opening of **443** to extend the conjugated π -system. Cyclisation of **444** and elimination of a molecule of water from **445**, yields the azulene product **442**. A similar process can also be carried out with less reactive pyridinium salts – for example, Lash *et al.* were able to synthesise 6-*tert*-butylazulene and 6-phenylazulene from the reaction of sodium cyclopentadienide **441** with the corresponding *N*-butylpyridinium bromide salts in 66% and 81% yields, respectively.²⁵⁵



Scheme 114: The synthesis of 4,6,8-trimethylazulene **442** by Hafner, with mechanism.

There has been some variation of the substituents on the pyrylium or pyridinium reaction partner, for example, with the synthesis of 6-methoxy-4,8-dimethylazulene

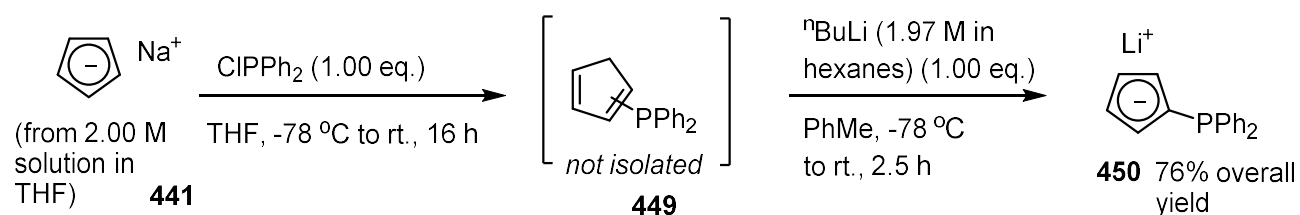
from 4-methoxy-2,6-dimethylpyrylium tetrafluoroborate by Hansen *et al.*,²⁵⁶ or, by Razus *et al.*,²⁵⁷ of various 1,6-biazulene derivatives from the corresponding 4-(azulen-1-yl)pyrylium perchlorate salts. The use of substituted derivatives of cyclopentadienide, particularly to yield an azulene derivative with a substituent at the 2-position, is comparatively rare. The only examples of this type of reaction found in the literature, to the best of our knowledge, were of the synthesis of alkyl azulene-2-carboxylate derivatives. When *N*-butyl 4-methylpyridinium bromide was treated with sodium (ethoxycarbonyl)cyclopentadienide by Koenig *et al.*, an equimolar mixture of ethyl 6-methylazulene-1-carboxylate and ethyl 6-methylazulene-2-carboxylate was obtained; the product of selective hydrolysis of this mixture, 6-methylazulene-2-carboxylic acid, was isolated in 9.3% overall yield.²⁵⁸ A more efficient result was obtained by Hansen, for the reaction of sodium (methoxycarbonyl)cyclopentadienide **446** with 2,4,6-trimethylpyrylium tetrafluoroborate **447** (Scheme 115). When methanol was used as the solvent, methyl 4,6,8-trimethylazulene-2-carboxylate **448** was formed in 47% yield, and was the only regioisomer detected, perhaps because of the steric hindrance of the 4,8-methyl groups.²⁵⁹



Scheme 115: The selective synthesis of methyl 4,6,8-trimethylazulene-2-carboxylate **448** from sodium (methoxycarbonyl)cyclopentadienide **446** with 2,4,6-trimethylpyrylium tetrafluoroborate **447**, by Hansen.

2.5.3. Synthesis of azulene-2-yl phosphines

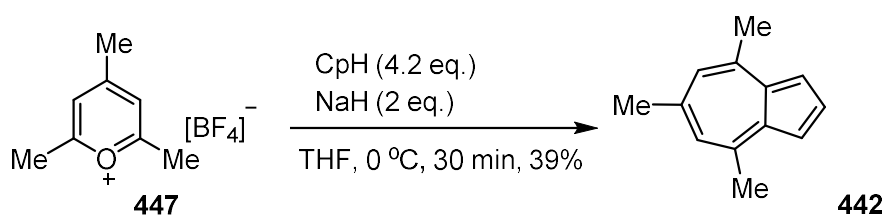
Given the remarkable selectivity, and without the use of harsh organometallic reagents on the azulene structure, or expensive transition metal complexes, this method in Scheme 115 could potentially be adapted towards the synthesis of a 1,1'-BazPhos ligand. While several literature methods^{260,261,262} exist for the synthesis of the (diphenylphosphino)cyclopentadienide salt **450**, this species has never been treated with a pyrylium or pyridinium cation to make an azulene-2-yl phosphine species, and would make a very direct way of doing so. Following the method of Erker *et al.*, on a scale of 30 mmol, sodium cyclopentadienide **441** was treated with chlorodiphenylphosphine in THF at $-78\text{ }^{\circ}\text{C}$, and the solution was allowed to stir overnight at room temperature (Scheme 116). After concentrating the mixture in vacuo, the residue was then dissolved in toluene and filtered through Celite, before treating with $n\text{BuLi}$ to deprotonate the 5-membered ring. This procedure gave the desired product of lithium (diphenylphosphino)cyclopentadienide **450** in 76% yield, which was stored under an atmosphere of argon to prevent any reaction with oxygen or water.



Scheme 116: The synthesis of lithium (diphenylphosphino)cyclopentadienide **450** from chlorodiphenylphosphine and sodium cyclopentadienide **441**.

Before the idea for the synthesis of azulene-2-yl phosphine in this manner had been considered, the synthesis of 4,6,8-trimethylazulene **442** had been carried out earlier in this laboratory, following the method of Hansen *et al.*, which was an adaptation of

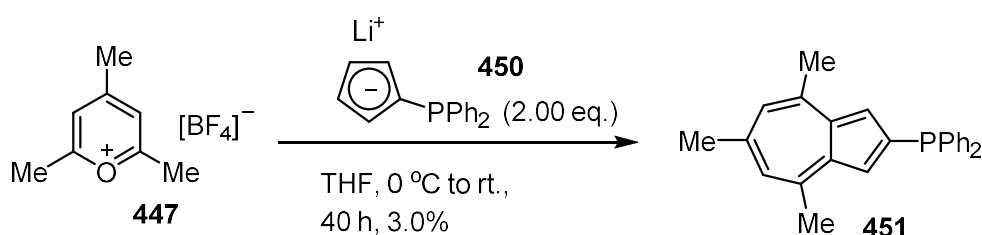
the original by Hafner.²⁵⁶ At 0 °C, to 2,4,6-trimethylpyrylium tetrafluoroborate **447** was added sodium cyclopentadienide **441** (freshly made from cyclopentadiene and sodium hydride), and the mixture was stirred for 30 min to give 4,6,8-trimethylazulene **442** in 39% yield (Scheme 117). The extra equivalent of sodium cyclopentadienide **441** is required as it reacts with the water that is eliminated in the formation of the azulene.



Scheme 117: The synthesis of 4,6,8-trimethylazulene **442** from 2,4,6-trimethylpyrylium tetrafluoroborate **447**.

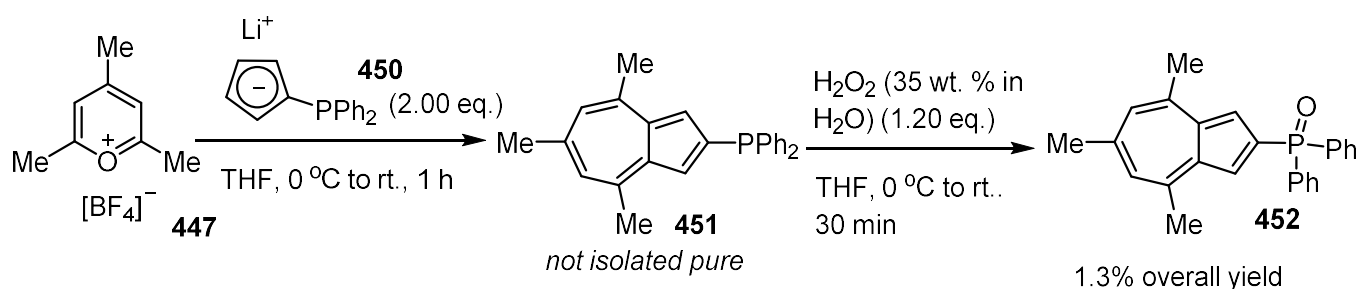
A similar method could thus be applied to the phosphine-functionalised cyclopentadienide species **450**. The first time this reaction was carried out, the addition of a solution of lithium (diphenylphosphino)cyclopentadienide **450** in THF to 2,4,6-trimethylpyrylium tetrafluoroborate **447**, at 0 °C, resulted in a brilliant blue mixture. However, the colour changed to a dull brown during the aqueous work-up, but despite this, the desired product **451** was stable to column chromatography, co-eluting with excess (diphenylphosphino)cyclopentadiene **449** (CpPPh₂). Another fraction from the column contained the analogous oxides of these products: the azulene-2-yl phosphine oxide **452** and (diphenylphosphinyl)cyclopentadiene **453** (CpP(O)Ph₂), showing that these phosphine species were sensitive to air oxidation. The reaction was repeated, allowing the azulene formation to complete overnight. Instead of an aqueous work-up, a silica plug was applied under the argon atmosphere to the crude reaction mixture to either neutralise or remove any ionic

species from the system that could be leading to any decomposition of the azulene. After column chromatography, the fraction of azulene-2-yl phosphine **451** with excess CpPPh₂ **449** could be purified by crystallisation with hot ethanol to give the desired product **451** in 3.0% yield (Scheme 118). A second recrystallisation with hot ethanol was applied to the solid that was dissolved in the filtrate, but this second crop yielded the corresponding azulene-2-yl phosphine oxide **452** instead, in 2.0% yield.



Scheme 118: The synthesis of diphenyl(4,6,8-trimethylazulen-2-yl)phosphine **451** from 2,4,6-trimethylpyrylium tetrafluoroborate **447** and lithium (diphenylphosphino)cyclopentadienide **450**.

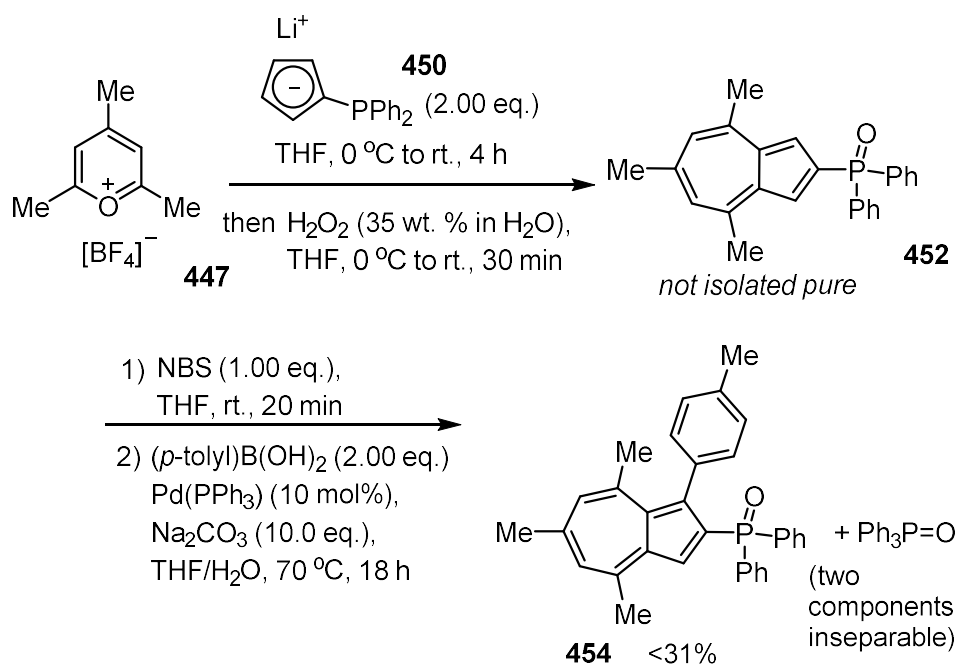
The reaction was increased in scale, from 1.42 mmol to 11.2 mmol of pyrylium salt **447**, but this time, the recrystallisation did not yield pure azulene-2-yl phosphine **451**. Instead, as it was evident that the phosphine group was sensitive to air oxidation, this fraction was treated with hydrogen peroxide to convert it to the phosphine oxide **452**, with a view to reducing the diphenylphosphinyl group at the end of the ligand synthesis. After column chromatography, and recrystallisation (THF/hexane 4:1), azulene-2-yl phosphine oxide **452** was produced in 1.3% overall yield (Scheme 119).



Scheme 119: The synthesis of diphenyl(4,6,8-trimethylazulen-2-yl)phosphine oxide **452**, through the oxidation of azulene-2-yl phosphine **451**.

In order to increase the yield and efficiency of this process, the hydrogen peroxide oxidation step was applied immediately after the formation of the azulene. Unfortunately, after column chromatography, the recrystallisation could not be repeated successfully to isolate the azulene-2-yl phosphine oxide **452** (Scheme 120). The purity could, however, be improved through the selective solvation of the desired product in *tert*-methyl butyl ether, but not to the extent that an accurate yield of the compound could be determined. Nevertheless, this impure sample of azulene-2-yl phosphine oxide **452** was treated with *N*-bromosuccinimide, completely converting the starting material to a mixture of the corresponding 1-bromoazulene and a smaller amount of the corresponding 1,3-dibromoazulene. A Suzuki reaction on this substrate was performed by adding to the reaction mixture *p*-tolylboronic acid, catalytic Pd(PPh₃)₄, sodium carbonate as the base and water, and the mixture was heated at 70 °C for 18 hours.²⁶³ The procedure yielded a sample of the 1-*p*-tolylazulene-2-yl phosphine **454**, which co-eluted with triphenylphosphine oxide sourced from the palladium complex, in <31% yield (derived from total mass of the fraction). The ferric chloride catalysed oxidative homocoupling reaction was attempted on this substrate **454**, once in methanol¹⁷⁷ and once in benzene.²⁶⁴ However, the only substance identified from these reactions was recovered starting

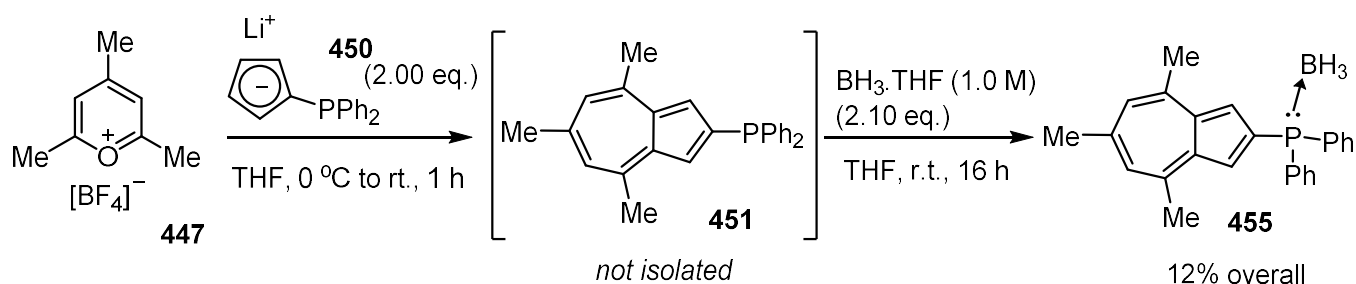
material, with the formation of the 1,1'-biazulene product perhaps prevented by steric hindrance of the phosphine and 4-methyl groups.



Scheme 120: The synthesis of azulene-2-yl phosphine oxide **452** through azulene formation and then H₂O₂ oxidation in one pot, followed by bromination and Suzuki coupling for form 1-(*p*-tolyl)azulene-2-yl phosphine **454**.

To try improving the yield of azulene-2-yl phosphine oxide **452**, the reaction was repeated with a filtration through neutral alumina, rather than through silica, between the azulene formation and oxidation steps. Since this change in protocol did not facilitate the purification of this azulene, the impure sample from this reaction was treated with trichlorosilane and triethylamine, heating at reflux in toluene for 15 hours. This process completely reduced the phosphine oxide to the phosphine, so to the mixture was added borane, to protect the free phosphine from oxidation. Fortunately, after purification by column chromatography, the azulene-2-yl phosphine borane adduct **455** was isolated, without recrystallisation, in 1.6% overall yield. With this positive result in mind, the procedure for the formation of the azulene-2-yl phosphine was changed to include treatment with borane, in place of an oxidation

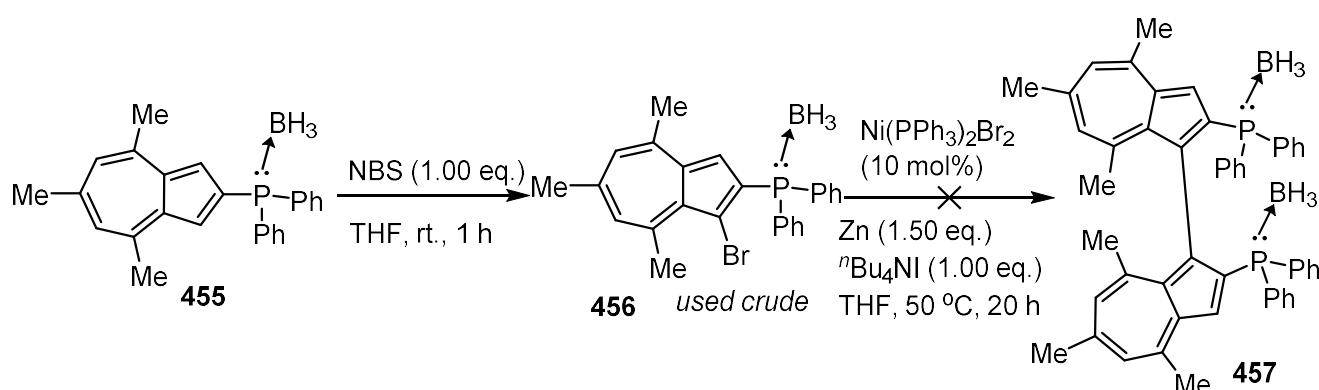
step. By doing this, the azulen-2-yl phosphine borane **455** could be isolated in a much improved 12% yield, again without requiring crystallisation (Scheme 121). This therefore represented a much more efficient protocol than what was achieved previously for the synthesis of a pure azulen-2-yl phosphine species. A few changes were made to try improving this yield, none of which succeeded in doing so: the quantity of phosphino-cyclopentadienide was doubled to 4 equivalents, giving 11% yield of **455** and making purification by column chromatography more difficult; the order of addition was changed, by adding the pyrylium salt **447** to the solution of phosphino-cyclopentadienide **450**, which gave 3.0% yield of **455**; also, carrying out the azulene formation at 60 °C resulted in 6.8% yield of **455**.



Scheme 121: The formation of azulen-2-yl phosphine **451**, followed by the addition of borane in the same pot to form the azulen-2-yl phosphine borane adduct **452**.

While the yield of 12% was still modest, the reaction gave practicable quantities of the phosphine borane adduct **455**. To make the corresponding 1,1'-biazulene **457** the phosphine borane adduct **455** was treated with *N*-bromosuccinimide in THF, and stirred until the reaction was virtually complete by TLC, giving a mixture of the corresponding 1-bromoazulene **456** and corresponding 1,3-dibromoazulene (Scheme 122). The crude mixture was added to $\text{Ni}(\text{PPh}_3)_2\text{Br}_2$, zinc powder and tetra-*n*-butylammonium iodide for a homocoupling reaction similar to that in Table 7. After heating at 50 °C for 20 hours, purification by column chromatography gave the free

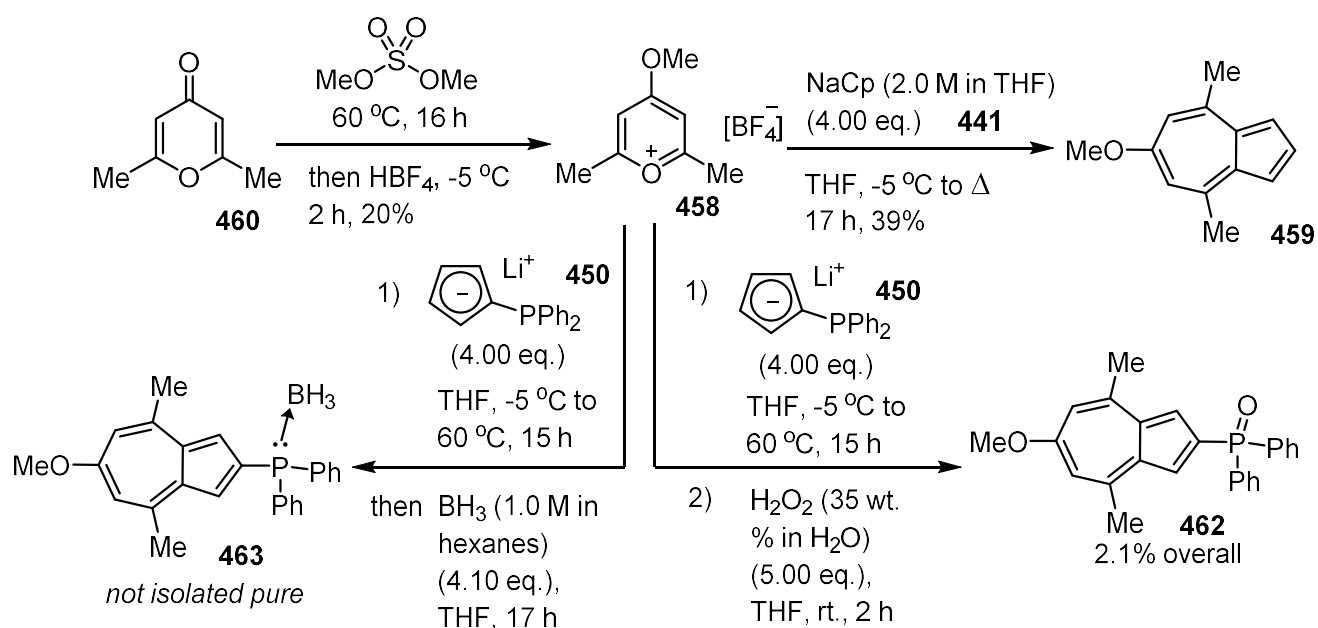
azulen-2-yl phosphine **451** in 19% yield, recovered azulene-2-yl phosphine borane **455** in 17% yield, some azulene-2-yl phosphine oxide **452** that co-eluted with triphenylphosphine oxide, and another fraction that could not be identified. The mass spectrum of the latter fraction gave an m/z value of 721.3408, which corresponds to a species that perhaps consists of a 1,1'-biazulene skeleton, but the integrations of the peaks on the proton NMR spectrum indicated a symmetrically substituted monomeric azulene. This unidentified substance was heated with morpholine to displace the phosphine group from the borane, but this process gave an inseparable mixture of azulene-2-yl phosphine oxide **452** and morpholine-borane adduct. The homocoupling reaction was later repeated to include a basic aqueous wash in the work-up procedure for the brominated azulene mixture, but neither the unidentified species, nor any 1,1'-biazulene species were produced.



Scheme 122: Bromination of azulene-2-yl phosphine borane **455**, followed by attempted homocoupling to form the 1,1'-biazulene **457**.

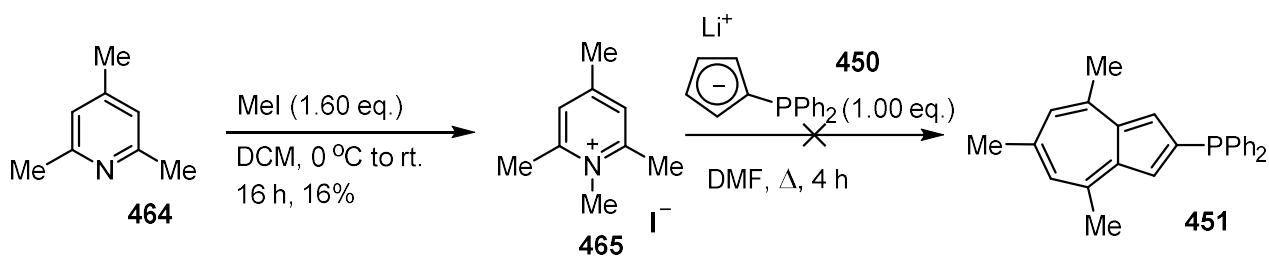
Another idea that was explored was to use a less electrophilic pyrylium derivative, in order to eliminate possible side reactions and gain more control over the synthesis of the azulene. The account by Hansen *et al.*, which had a procedure that was followed for this mode of synthesising azulenes, described the synthesis of 6-methoxy-4,8-

dimethylazulene **459** from sodium cyclopentadienide **441** and 4-methoxy-2,6-dimethylpyrylium tetrafluoroborate **447**, in 48% yield.²⁵⁶ In contrast to the 2,4,6-trimethylpyrylium salts, this reaction required heating at reflux in THF, which demonstrates the effect of the electron donating 4-methoxy group on the electrophilic reaction partner. Following the method in this paper, the 4-methoxypyrylium salt **458** was synthesised in 20% yield by alkylation of 2,6-dimethyl- γ -pyrone **460** with dimethyl sulfate, followed by the anion exchange with tetrafluoroboric acid (Scheme 123). For a preliminary test, the 4-methoxypyrylium salt **458** was added to 4 equivalents unfunctionalised sodium cyclopentadienide **441** and after heating at reflux for 17 hours, the desired product of 6-methoxy-4,8-dimethylazulene **459** was isolated in 39% yield. After this, the 4-methoxypyrylium salt **458** was added to 4 equivalents of lithium (diphenylphosphino)cyclopentadienide **450**, and was heated in THF at 60 °C for 15 hours. The reaction was simply quenched by pouring over ice, and purification by column chromatography gave an impure sample of the desired 6-methoxyazulen-2-yl phosphine **461**. This sample was later oxidised with hydrogen peroxide, which produced a pure sample of the phosphine oxide **462** in 2.1% yield overall, after column chromatography. The synthesis of the 6-methoxyazulen-2-yl phosphine **461** was repeated, but the crude product was treated with borane in THF to protect the phosphine from oxidation. Unfortunately, the desired phosphine borane **463** could not be purified adequately through column chromatography and recrystallisation with ethanol. Thus, the use of 4-methoxy-2,6-dimethylpyrylium tetrafluoroborate **458** did not improve the yield or efficiency of the formation of an azulene-2-yl phosphine species.



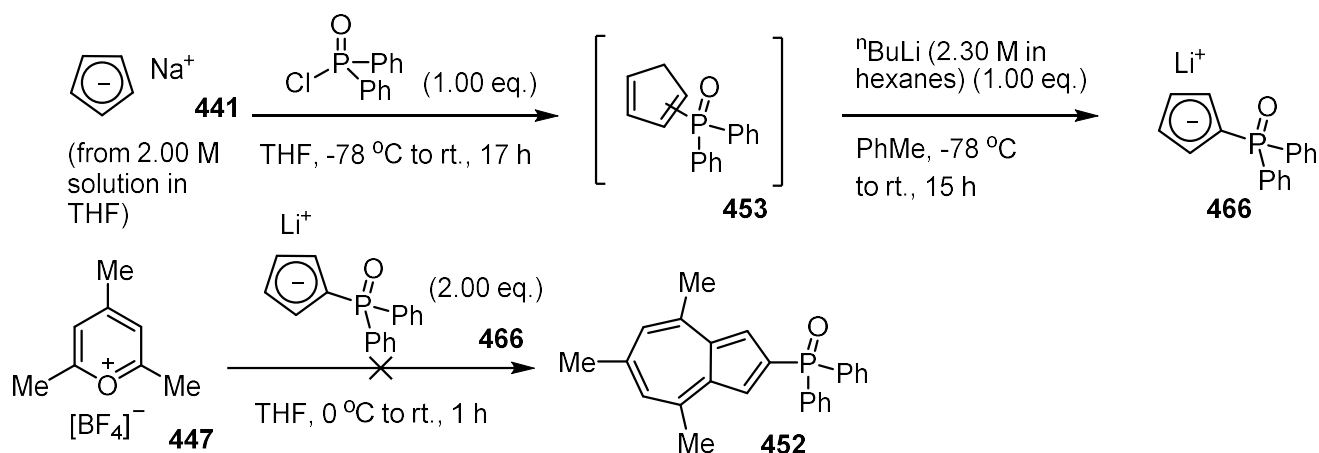
Scheme 123: The synthesis of 4-methoxy-2,6-dimethylpyrylium tetrafluoroborate **458**, and from this, the synthesis of 6-methoxy-2,4-dimethylazulene **459**, 6-methoxyazulene phosphine oxide **462**, and 6-methoxyazulene phosphine borane **463**.

Another attractive option was to try using an analogous pyridinium salt for the formation of the same trimethylazulen-2-yl phosphine **451**, due to the impressive yields obtained by Lash *et al.* for the formation of 6-*tert*-butylazulene and 6-phenylazulene in this way, mentioned earlier in this report.²⁵⁵ Another advantage was the requirement of only one equivalent of cyclopentadienide for the reaction to work. Following the method of Tang *et al.*,²⁶⁵ the pyridinium salt **465** was formed by the alkylation of 2,4,6-collidine **464** with methyl iodide, and allowing the mixture to stir overnight gave the desired alkylated product **465** in an unusually low 16% yield, which was attributed to the age of the sample of alkylating agent (Scheme 124). The pyridinium salt **465** was then mixed with 1.0 equivalent of phosphino-cyclopentadienide **450**, and heated at reflux in DMF for 4 hours. Unfortunately, the reaction only produced a sample with indeterminate aromatic peaks by NMR, containing a small amount of azulene-2-yl phosphine oxide **452**.



Scheme 124: The attempted synthesis of azulene-2-yl phosphine **451** from *N*-methyl-2,4,6-collidinium iodide **465**.

The final idea explored towards this mode of synthesising azulene-2-yl phosphine derivatives, was to form the lithium cyclopentadienide derivative through the reaction of sodium cyclopentadienide **441** with diphenylphosphinyl chloride, followed by deprotonation with *n*-butyllithium. This way, the neutral CpP(O)Ph₂ intermediate **453** could be handled under air, making the work-up procedure more convenient. Once this procedure had been carried out, the lithium (phosphinyl)cyclopentadienide salt **466** was not characterised by NMR, but the formation of the desired product was suggested by the addition of a small amount of the sample to a suspension of trimethylpyrylium salt **447**, which resulted in a purple solution (Scheme 125). However, when the remainder of the sample was treated with trimethylpyrylium salt **447**, no azulene product could be isolated, perhaps due to the now reduced nucleophilicity of the cyclopentadienide derivative **466**.



Scheme 125: The attempted synthesis of azulene-2-yl phosphine oxide **452** from lithium (diphenylphosphinyl)cyclopentadienide **466**.

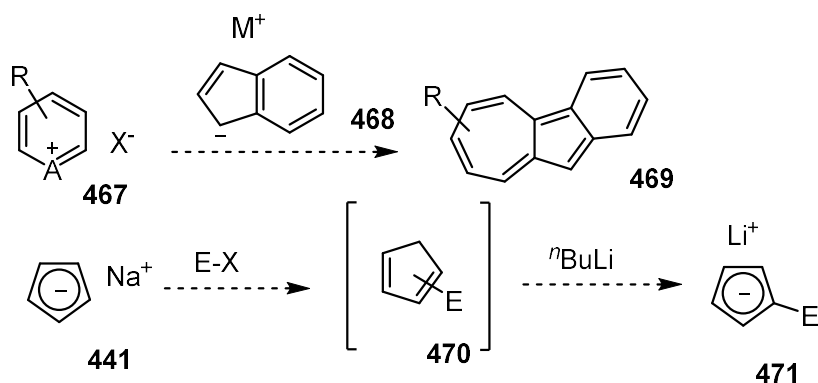
2.5.4. Limitations and future synthetic developments

Overall, the application of this alternative method towards the synthesis of a 1,1'-BazPhos ligand, based around the azulene chemistry pioneered by Hafner, yielded a very direct method of accessing azulene-2-yl phosphine species. However, the poor yields and often difficult purification for this azulene formation are obvious disadvantages, and represent a great hindrance in the synthesis of a chiral ligand. The chemistry based around the Nozoe-type azulenenes has been more facile to develop, despite requiring a greater number of functional group interconversions to reach the target ligands.

The best yield achieved for a pure azulene-2-yl phosphine was 12% (as its borane adduct **455**), which was low probably due mostly to the steric hindrance of the bulky phosphine groups on the cyclopentadienide nucleophile. Nonetheless, the chemistry of this Hafner type of azulene synthesis seems to be inherently inefficient, as the best literature examples only reach a maximum of around 50% yield with pyrylium derivatives as the electrophilic partner. This poor performance is probably due to the

elimination of water into the system leading to side reactions and necessitating the use of an excess of cyclopentadienide. The performance may perhaps be improved by including a means of quickly scavenging water out of the system, e.g. the use of 4Å molecular sieves. To add to this, the azulene motif itself probably makes a competing nucleophile, as it has been shown that it can undergo conjugate addition to α,β -unsaturated carbonyls.²⁶⁶ The side products that are made are also not often easy to identify, which makes it difficult to obtain a clear understanding of the reaction.

On the bright side, as the azulene-2-yl phosphine species **451** is accessible, it would be interesting to investigate how the geometric and electronic properties of this species translate into its performance as a non-chiral ligand in homogeneous catalysis. Monophosphine ligands are ubiquitous for this purpose, particularly for transition metal catalysed hydrogenation and carbon-carbon bond formation. The success of this result can also inspire further investigation into the use of other cyclopentadienide derivatives for the synthesis of azulenes (Scheme 126). The inexpensive hydrocarbon indene has relatively acidic carbon-hydrogen bonds, and through the reaction of indenide salts **468** with pyrylium or pyridinium salts **467**, could make a convenient method of making benzoazulene derivatives **469**. Other cyclopentadienide derivatives **471** may be accessed by addition of sodium cyclopentadienide **441** to electrophiles, followed by deprotonation, in a similar way to reactions described in Scheme 115 and Scheme 116.



Scheme 126: The proposed formation of benzo[a]azulene derivatives **469** from an indenide anion **468**, and derivatisation of cyclopentadienide **441** through addition to electrophiles.

2.6. Development of 1,1-biazulene-2,2'-phosphoric acid ("1,1'-BazPA")

2.6.1. Ideal chiral biazulene-acid targets

The application of axially chiral biaryl diol-derived phosphoric acids in organocatalysis is a relatively new field in asymmetric synthesis.^{267,268,269} One of the original targets of this project was to synthesise a biazulene-based phosphoric acid, to examine how the unique geometric and electronic properties of azulene translates into the performance at 'specific' acid catalysis. Based on previous literature showing that the high enantioselectivity generally results from a narrow chiral pocket, for example with chiral spinol-derived phosphoric acids **472**,^{270,271,272} the ideal biazulene-phosphoric acid would probably possess a biaryl bond between the two 7-membered rings, so that any bulky groups positioned '*ortho*' to the hydrogen phosphate group are closer together in space. To decrease the pK_a value by induction, the hydrogen phosphate can be positioned on either the 4-carbon or the 6-carbon on the azulene. Combining these two design criteria together leads to two ideal options: the 5,5'-biazulene-4,4'-phosphoric acid **473** or the 5,5'-biazulene-6,6'-phosphoric acid **474** (Figure 50). From the synthetic point of view, the former structure **473** has an advantage, as the 5-membered rings positioned above and

below the hydrogen phosphate may have sufficient steric bulk to influence the orientation of the substrate. If not, a substituent (R_2), such as mesityl, can be introduced to the 3,3'-positions of the structure of **473** by halogenation and a Suzuki reaction.

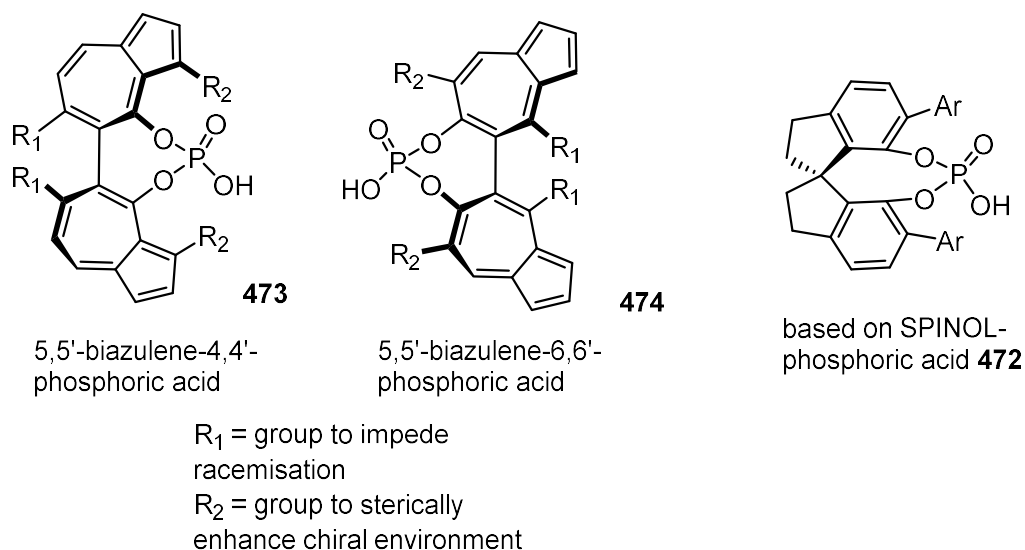
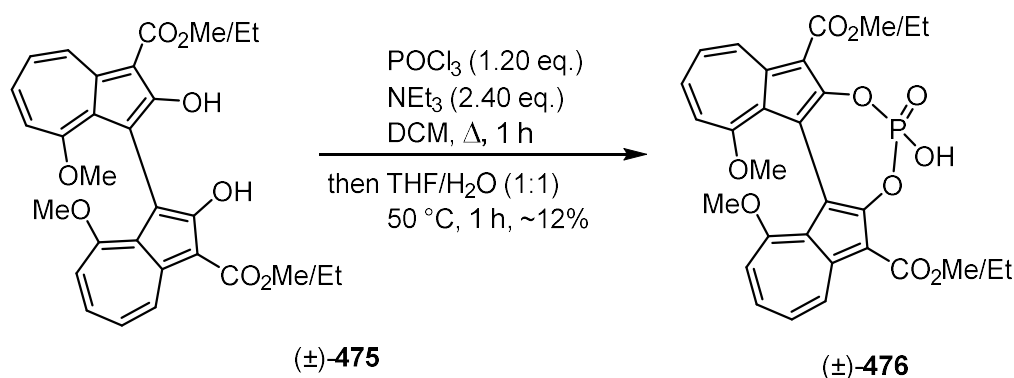


Figure 50: Ideal designs for a biazulene-based chiral phosphoric acid.

The structures in Figure 50 are greatly different from the 1,1'-biazulene or 2,2'-biazulene derivatives that were synthesised or targeted in this project, so their development was not explored. However, a 1,1'-biazulene-2,2'-phosphoric acid could potentially be accessed in one step from the 1,1'-biazulene-2,2'-diol structures that were synthesised for different purposes, and would therefore not represent a great investment of time. These more immediately accessible chiral acids would most likely not be the final design, because in order to have an effective chiral acid catalyst, the esters at the 3,3'-positions would probably have to be replaced with more rigid, bulky aryl groups (*c.f.* "TRIP" catalyst).²⁷³ This type of structure may be accessed in the same number of steps by synthesising the 2*H*-cyclohepta[*b*]furan-2-one precursors derived from aryl active methylene compounds, as in Table 8.

2.6.2. Synthesis of 1,1'-BazPa

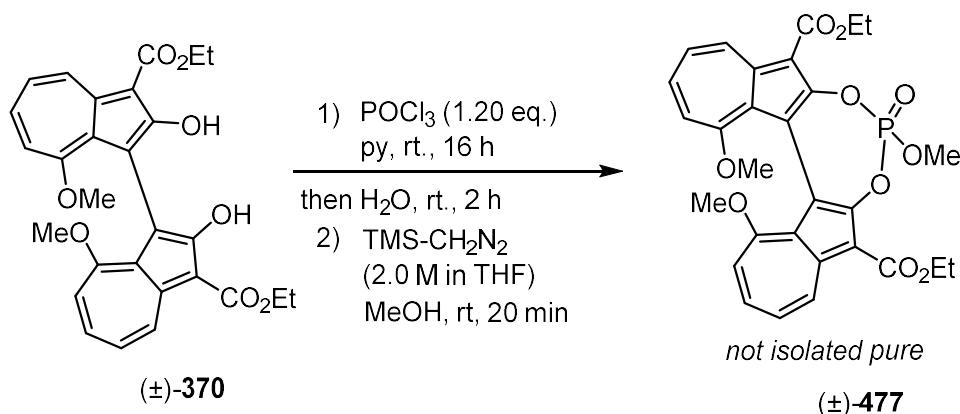
For the first attempt to synthesise the phosphoric acid, the 1,1'-biazulene-2,2'-diol (as an inseparable mixture of methyl and ethyl esters (\pm)-**475**) was treated with 1.2 equivalents of phosphorus oxychloride and 2.4 equivalents of triethylamine, and heated at reflux in DCM for an hour (Scheme 127).²⁷⁴ After hydrolysis of the phosphorochloridate intermediate and treating the organic solution with dilute HCl, the work-up procedure was not straight-forward. The proton NMR spectrum of the solute from the organic layer was messy and indeterminate. It was dissolved in DCM again, and after washing with dilute aqueous NaOH solution, most of the distinct azulene colour remained in the organic layer, so the organic layer was filtered through silica. The NMR spectrum showed mostly clean product (\pm)-**476**, as a mixture of methyl and ethyl esters carried over from the starting material. After applying column chromatography, the NMR spectrum looking no different, the product (\pm)-**476** was isolated in ~12% yield (based on the molecular weight of the diethyl ester).



Scheme 127: The conversion of 1,1'-biazulene-2,2'-diol (\pm)-**475** (mixed esters) into its corresponding phosphoric acid (\pm)-**476**.

The product (\pm)-**476**, due to the hydrogen phosphate group, streaked on the silica column, so to improve the isolable yield for a repeat experiment, the phosphate was

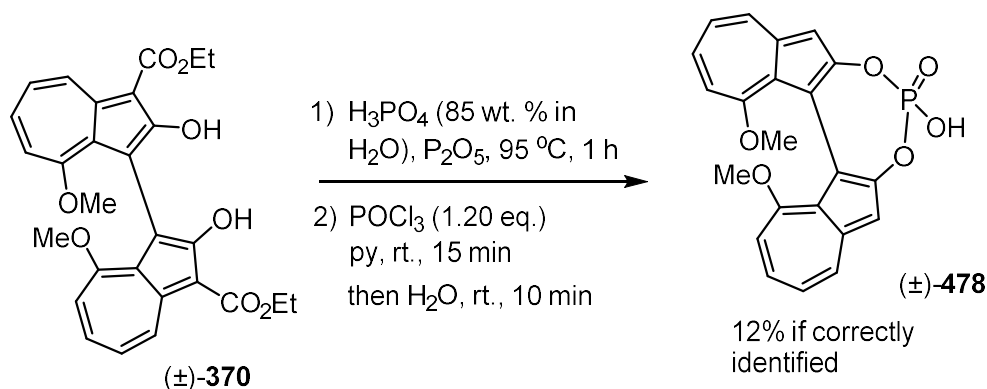
to be alkylated before column chromatography (Scheme 128). A different procedure was adopted, following a paper by MacMillan,²⁷⁵ by which the biazulene diol (\pm)-**370**, this time comprising pure ethyl ester, was treated with 2.0 equivalents of POCl₃ and using pyridine as the solvent. The crude acid product was treated with a solution of TMS-diazomethane in THF, and while the identity of the methylated product (\pm)-**477** was confirmed by mass spectrometry, it could not be isolated cleanly after column chromatography. Interestingly, the NMR spectrum of (\pm)-**477** showed that the two azulene moieties were no longer equivalent, due to the symmetry lost from the conversion of a hydrogen phosphate to a methyl phosphate.



Scheme 128: The conversion of 1,1'-biazulene-2,2'-diol (\pm)-**370** into its corresponding phosphoric acid, with subsequent alkylation to the methyl phosphate ester (\pm)-**477**.

The final attempt at synthesising a 1,1'-biazulene-2,2'-phosphoric acid was carried out by heating biazulene diol (\pm)-**370** in anhydrous *orthophosphoric acid* to remove the ester groups, and the crude diol was treated with POCl₃ in pyridine (Scheme 129). After hydrolysis with water and treatment with dilute aqueous HCl, the work-up procedure was problematic, as the crude product appeared to be partly aqueous and partly organic-soluble. The NMR spectra of the organic extracts, using DCM, and then ethyl acetate, showed no evidence of the formation of the desired product (\pm)-**478**. The aqueous layer, however, was allowed to evaporate to dryness, and a

solution of the residue in chloroform was filtered through silica. The NMR spectrum of this residue showed a clean sample of what appeared to be the desired product, although the structure could not be confirmed by mass spectrometry. If this sample was of the desired compound (\pm)-**478**, the mass corresponded to 12% yield.



Scheme 129: The H_3PO_4 -mediated deethoxycarbonylation of 1,1'-biazulene-2,2'-diol (\pm)-**370**, followed by conversion of the crude diol to the phosphoric acid (\pm)-**478**.

2.6.3. Limitations

Overall, there were a number of factors that constituted problems with the synthesis of these biazulene-phosphoric acid targets. While the isolated yields of the products were low, the starting material was either mostly or completely consumed each time, as evidenced by the NMR spectra of the crude material. Observing the experiment taking place, the reactions did not appear to proceed cleanly, as they tended to produce intractable material in the flask. This observation was common with the reaction of the same biazulene diol species (\pm)-**370** with triflic anhydride to make the biazulene ditriflate (\pm)-**372**, so perhaps the treatment with strong electrophiles lead to decomposition of the starting material. The solubility of the starting material may be a factor in how cleanly the reaction proceeds, as the 1,1'-biazulene-2,2'-diol (\pm)-**370** with 8,8'-methoxy groups generally had poor solubility in most organic solvents. However, the analogous compound with 8,8'-ethoxy groups (\pm)-**394** had much

improved general solubility, so the conversion of this species to the phosphoric acid, which was not attempted in this project, may result in a cleaner reaction.

Another factor that added complication to the procedure was the amphiphilic properties of the phosphoric acid targets, due to the polar hydrogen phosphate group at one end of the molecule, and the large, relatively apolar aromatic hydrocarbon structure at the other end. This property perhaps was the reason why purification by a simple acid-base extraction could not be performed on the biazulene phosphoric acid product with 3,3'-ester groups (\pm)-**476**. Despite this, the biazulene phosphoric acid without the 3,3'-ester groups (\pm)-**478** was retained in the aqueous layer, and could be isolated after evaporation of the water. The low yield in this case may be due to the multiple steps incorporated in the procedure to make that product, as well as the questionable stability of the intermediate diol.

2.7. Asymmetric Diels–Alder reaction

The chiral 1,1'-BazOL ligand, diethyl 2,2'-dihydroxy-8,8'-diethoxy-[1,1'-biazulene]-3,3'-dicarboxylate **394**, had been synthesised and resolved to yield workable quantities of its individual enantiomers. Thus, the next step in the project was to apply the ligands to an asymmetric reaction. The Diels–Alder cycloaddition was seen as an appropriate choice due to its ubiquity in synthetic chemistry. As covered in the introduction of this report, the paper by Harada *et al.* described the Ti-catalysed reaction between cyclopentadiene and several α,β -unsaturated esters, using 1,1'-biphenyl diols that varied in bite angle as the chiral ligands (Scheme 42).¹³⁹ The results showed that the reaction was highly sensitive towards the bite angle of the diol ligand. The best results obtained were at a moderate 70-80% e.e., which was

ideal for the purposes of this project because, while the process was clearly suited for this Diels–Alder reaction, it meant there was room to improve the selectivity by screening new ligands.

2.7.1. *Ti-catalysed Diels–Alder reaction with 1,1'-BazOL*

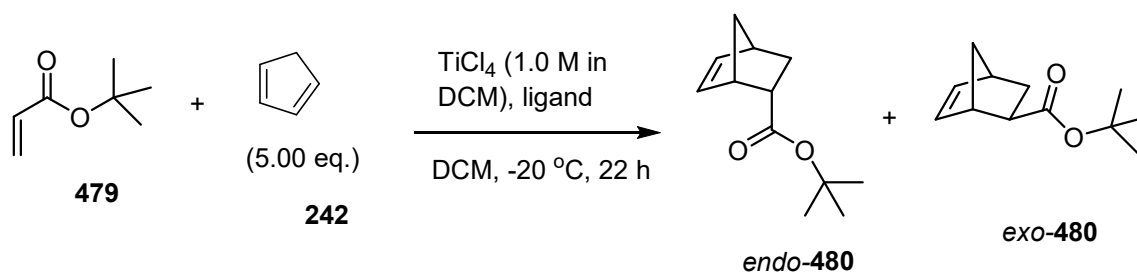
Unfortunately, as the paper by Harada was a letter, no detailed method was included in the content. In lieu of this, the experimental method described by Wulff *et al.* for the Al-catalysed Diels–Alder reaction of cyclopentadiene with various α,β -unsaturated carbonyl compounds, using VANOL **288** and VAPOL **289** as ligands, was adapted for a Ti-catalysed process in this project (Table 16).²⁷⁶ For each experiment, the chosen ligand was stirred with titanium(IV) chloride in DCM for 30 minutes at room temperature. After cooling to $-20\text{ }^{\circ}\text{C}$, *tert*-butyl acrylate **479** was added and the mixture was stirred for 15 minutes, which was followed by the addition of cyclopentadiene **242**, and allowing the reaction to take place for 22 hours. The mixture was then given an aqueous wash, and purified by column chromatography. The ligands chosen for comparison with (*R_a*)-1,1'-BazOL (–)-**394** and (*S_a*)-1,1'-BazOL (+)-**394** were (*R_a*)-BINOL **213** and (*S_a*)-VAPOL **289**. The reactions were run with a catalytic loading, which encompasses both the loading of the ligand and TiCl₄, at 10 mol%, aside from a comparison between (*R_a*)-BINOL **213** and (*R_a*)-1,1'-BazOL (–)-**394** at 5 mol% (Table 16, entries 2 and 5). Initially, the determination of the total yield of norbornene adducts *endo*-**480** and *exo*-**480** was attempted by integration of the product peaks on the proton NMR spectrum, using the ligand as an internal standard. Unfortunately, this method tended to calculate yields of over 100%, so the isolated yields of **480** are instead listed. These values may not be truly representative of the quantity of products synthesised, as small quantities were probably lost due to their volatility. The ratio of *endo*- to *exo*-adducts was

consistently good for each experiment, achieving above 90:10 each time; changing the ligand did not show a clear influence on these results. Disappointingly, none of the experiments showed any enantioselectivity. Initially to calculate the e.e. values, attempts were made to optimise the resolution of the products by chiral HPLC, as the equipment was readily accessible, but the peaks could not be completely separated. The use of a chiral NMR shift reagent was also investigated towards determining the enantiomeric excess. A sample of the norbornene adduct (*endo*- and *exo*-adducts **480** mixed) was mixed with a gradually increased quantity of $\text{Eu}(\text{tfc})_3$ **481**,²⁷⁷ recording the proton NMR spectrum at 0, 0.2, 0.5 and 1.0 equivalents (Figure 51). Gradual shifts of the peaks were observed with each addition, particularly with the olefinic peaks, but the resolution of the enantiomers observed was insufficient.

Several Diels–Alder experiments were carried out, varying the ligand and catalytic loading, before the enantioselectivities were able to be determined. Eventually, the e.e. values were calculated through chiral GC, but by the time the apparatus could be used, there was no time left to further change the conditions of the procedure. It is evident that the chiral element of the reaction i.e. the ligand, was not able to induce enantioselectivity in the synthesis of the adducts because of a fundamental fault with the set-up of the experiments. It is unlikely that more time was required to form the Ti-ligand complex, as the addition of the ligand to the solution of TiCl_4 brought about an instant colour change. It is more likely that the diene and dienophile were able to react without the assistance of the Lewis acid. Thus, to suppress this uncatalysed process, the experiment could be carried out at a lower temperature, so that the carbonyl group will be required to coordinate to the Lewis acid to activate the cycloaddition. More rigorous measures could also be made to exclude water and

oxygen from the system, as it is possible that multicentre Ti-complexes, comprising bridging oxo ligands, may have formed, shutting down the catalysed reaction.

Table 16: The attempts at the Ti-catalysed asymmetric Diels-Alder reaction between *tert*-butyl acrylate **479** and cyclopentadiene **242**.



Entry	Ligand	Catalyst loading /mol%	Isolated yield /%	endo/exo	% e.e.
1	(<i>R</i> _a)-BINOL 213	10	40	96:4	0
2	(<i>R</i> _a)-BINOL 213	5	37	95:5	0
3	(<i>S</i> _a)-VAPOL 289	10	30*	93:7	0
4	(<i>R</i> _a)-BazOL 394	10	20	95:5	0
5	(<i>R</i> _a)-BazOL 394	5	33	96:4	0
6	(<i>S</i> _a)-BazOL 394	10	29	95:5	0

*sample also contained indeterminate dicyclopentadienide-like species.

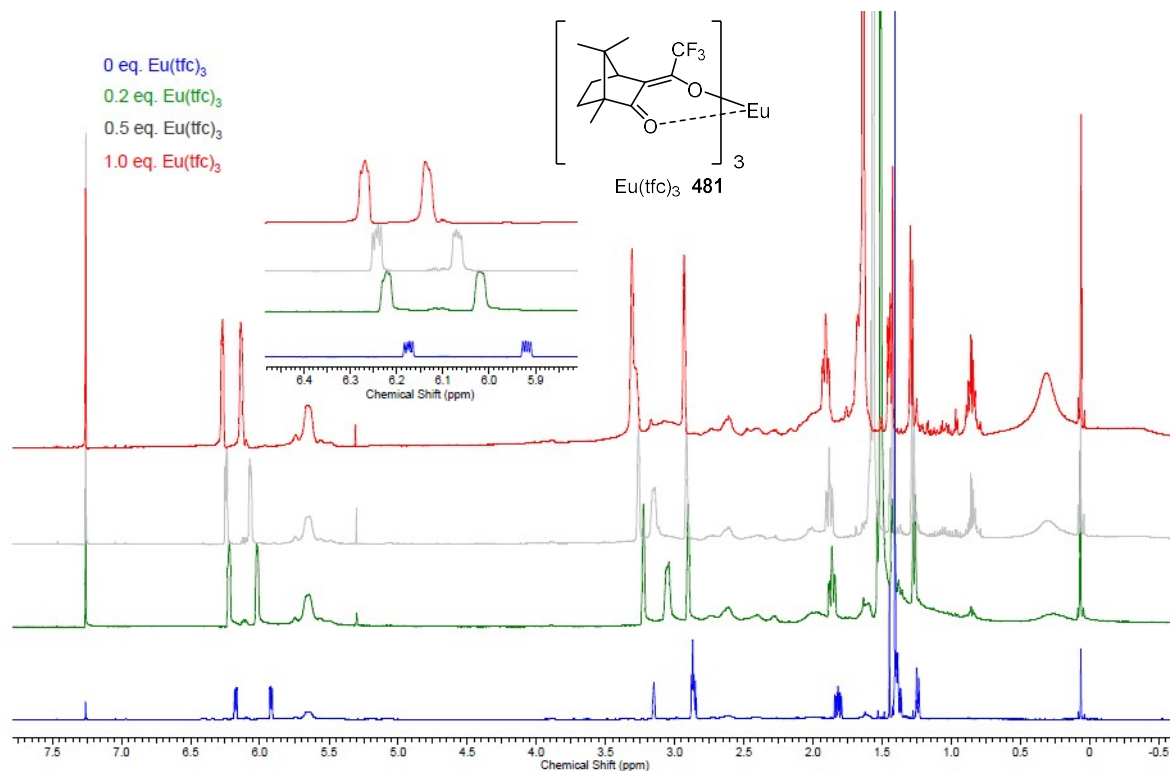


Figure 51: The proton NMR spectra in CDCl_3 of a sample of norbornene adduct **480**, with gradual addition of $\text{Eu}(\text{tfc})_3$ **481**.

2.8. Conclusions and future work

While it would be desirable at this stage to have employed a chiral biazulene ligand or acid to induce enantioselectivity in asymmetric catalysis, several notable objectives have been achieved. That desired stage was nearly reached, with the synthesis, resolution and detailed characterisation of an atropisomeric 1,1'-biazulene-2,2'-diol ("1,1'-BazOL", **394**), plus the attempted application of this ligand to an asymmetric Ti-catalysed Diels–Alder reaction. Before deciding to investigate the effects of the biazulene moiety within the context of diol ligands, the original aim of the project was to develop a chiral 1,1'-biazulene-based diphosphine ligand. This objective was almost achieved with the synthesis of the atropisomeric 1,1'-biazulene-2,2'-diphosphonate ester species (\pm)-**389**, which is likely to be two synthetic steps away from a racemic 1,1'-biazulene-2,2'-diphosphine. The incorporation of the resolution procedure, using the 1,1'-BazOL-((bis)menthyl carbonate) derivative **404**, could allow access to single enantiomers of the diphosphine ligand, assuming the configuration is retained throughout the subsequent synthetic steps. Another synthetic target that was pursued was a 2,2'-biazulene-1,1'-diphosphine, and access to a racemic form of this ligand is potentially one step away, using 1,1'-iodo-3,3'-dimethyl-2,2'-biazulene **428**. However, it has not yet been confirmed that the 3,3'-methyl groups are sufficiently large to induce atropisomerism in a 2,2'-biazulene species.

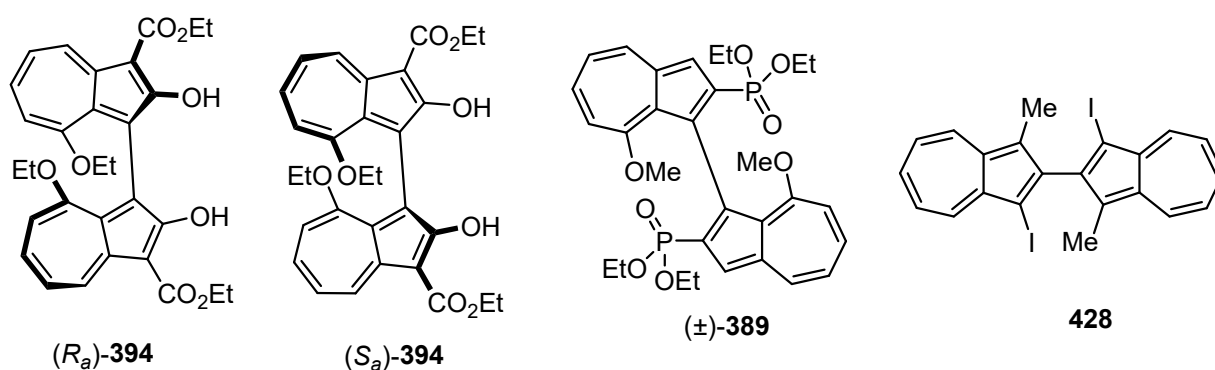
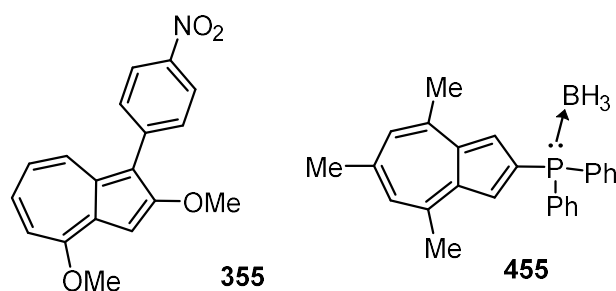


Figure 52: Key compounds synthesised in the routes towards biazulene ligands: (*R_a*)- and (*S_a*)-1,1'-BazOL **394**, (±)-1,1'-biazulene-2,2'-diphosphonate **389** and 1,1'-diiodo-2,2'-biazulene **428**.

During a project that is characterised by the aim to synthesise unusual, novel compounds, it is necessary to develop novel chemical processes along the way to make those compounds. This project has been no exception, as a variety of new reactions and compounds based around azulene have been developed in order to access these new, unique chiral ligands. These chemical transformations can be categorised by those that have not previously been reported on azulene substrates, such as a transition metal catalysed coupling of a biazulene triflate with a dialkyl phosphite, or the boron tribromide-mediated selective 2-dealkylation of a 2,4-dialkoxyazulene. Other new developments can be categorised by the expansion of the substrate scope of precursors towards azulenes (Scheme 130), such as the novel 3-aryl-2*H*-cyclohepta[*b*]furan-2-ones synthesised from arene-containing active methylene compounds; some of which could then be directly converted to the corresponding 1-arylazulene. In addition, the selective synthesis of a monomeric azulen-2-yl phosphine species has been achieved from a pyrylium salt and a phosphine-functionalised cyclopentadienide has been accomplished. This reaction paves the way to expand further the substrate scope of functionalised Cp rings to be converted to azulenes in a Hafner-like process.

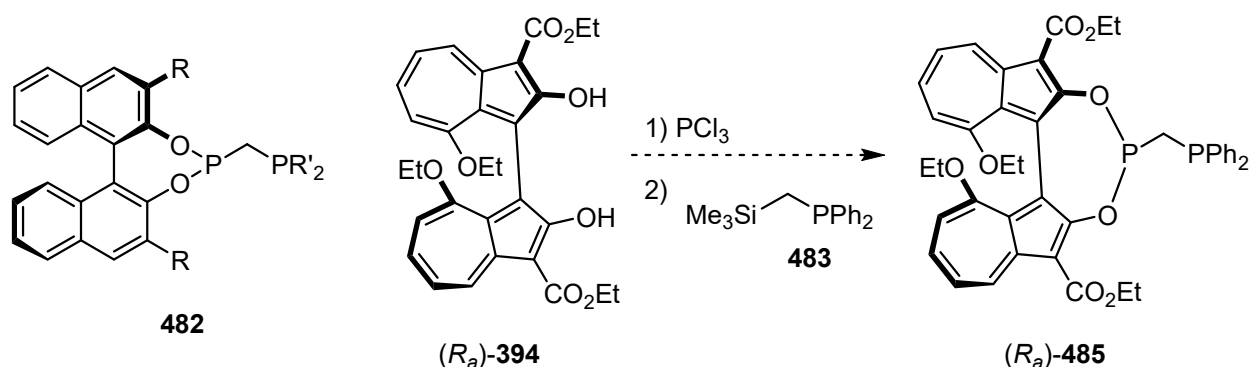


Scheme 130: Examples of novel azulene compounds synthesised from components that had not previously been used to prepare azulene derivatives.

This project now has plenty of exciting developments to be carried out in the future, with the most immediate aim of continuing the application of the resolved 1,1'-BazOL ligand **394** towards asymmetric catalysis. While the biazulene motif was designed to be a privileged ligand, that is, to be employed for wide-ranging asymmetric reactions, further efforts are most urgently required to be expended towards inducing enantioselectivity in the same asymmetric Ti-catalysed Diels–Alder reactions. The experiments thus far were carried out under atmosphere of N₂ with standard Schlenk techniques, using alumina-filtered DCM as solvent. Instead, storage of reagents in a glovebox and purifying the solvent by distillation over calcium hydride will ensure a more rigorous exclusion of oxygen from the system, thereby helping to prevent deactivation of the titanium-1,1'-BazOL catalyst.

An X-ray crystal structure has been obtained for 1,1'-BazOL **394**, which revealed some important geometric and steric properties of the free ligand, but it would also be desirable to obtain quantitative information of geometric properties, such as the bite angle, of a 1,1'-BazOL-metal complex. This can be achieved either through X-ray crystal analysis of that complex, or by computer modelling studies, and this data will give a more accurate idea of suitable asymmetric reactions to which the ligand can be applied.

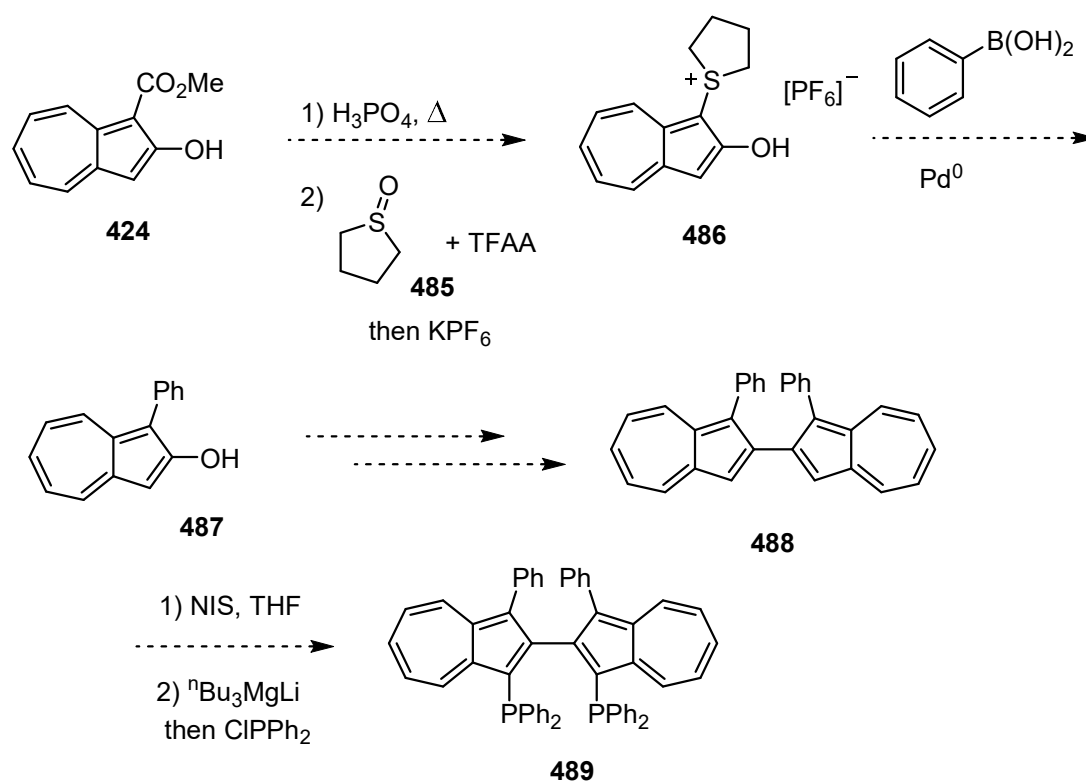
Because of the success in resolving the 1,1-BazOL species **394**, it could be used as a new moiety in the library of BINOL-phosphonite-phosphine ligands **482** reported by Pringle *et al.* (Scheme 131), which were applied successfully towards rhodium-catalysed asymmetric hydrogenation of olefins.²⁷⁸ These ligands **482** are suited towards asymmetric catalysis because of the combined rigidity of the axially chiral BINOL unit and the 4-membered chelating ligand-metal ring, similar to the MiniPhos series of ligands **168** (Figure 12). The reaction of 1,1'-BazOL **394** with phosphorus trichloride, followed by diphenyl((trimethylsilyl)methyl)phosphine **483** may allow easier access to a chelating diphosphine-like chiral ligand like **484**, than the transition-metal cross coupling methods that have been explored so far in the project.



Scheme 131: The BINOL-phosphonite-phosphine ligand series **482**, and the proposed application of 1,1'-BazOL **394** to this series.

The step to potentially complete the synthesis of (3,3'-dimethyl-[2,2'-biazulene]-1,1'-diyl)bis(diphenylphosphine) **429**, that is, the double halogen-lithium exchange process of 1,1'-diiodo-3,3'-dimethyl-2,2'-biazulene **428** followed by quenching with chlorodiphenylphosphine (Scheme 111), was only attempted once, only yielding recovered starting material. The repetition of this experiment, with variation of reagents, like the organolithium species, or conditions, such as temperature, may be

sufficient to bring about the desired chemical transformation. However, if these modifications do not work, it may be necessary to alter the synthetic route to access a wider range of 2,2'-biazulene precursors (Scheme 132). One idea could be to start from the easily accessible methyl 2-hydroxyazulene-1-carboxylate **424** and undergo *orthophosphoric* acid-mediated deethoxycarbonylation to remove the ester group. Following this, the corresponding azulene-1-yl sulfonium hexafluorophosphate salt **486** would hopefully be formed through a reaction, recently reported by Lewis *et al.*, with tetrahydrothiophene 1-oxide **485**, trifluoroacetic anhydride (TFAA) and potassium hexafluorophosphate.²⁷⁹ The azulene-1-yl sulfonium salts like **486** tetrahydrothiophene oxide have been shown to be stable and make excellent cross coupling partners for Suzuki reactions; a strategy which could be exploited to synthesise 1-phenyl-2-hydroxyazulene **487**. The steps outlined in Scheme 106 may be then applied to create the potentially atropisomeric 1,1'-diphenyl-2,2'-biazulene **488**, avoiding the difficult DIBAL-H reduction process to convert esters to methyl groups (Scheme 109). Finally, this precursor may be treated with *N*-iodosuccinimide to install iodines at the electron rich positions, which then may be converted to the diphosphine **489** through halogen-lithium exchange.



Scheme 132: A synthetic plan to access the potentially atropisomeric (3,3'-diphenyl-[2,2'-biazulene]-1,1'-diyl)bis(diphenylphosphine) **489**.

3. EXPERIMENTAL

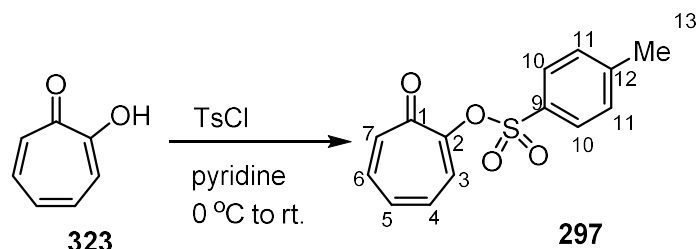
General directions

All reactions were carried out under an atmosphere of N₂ or argon, through the use of a Schlenk line, unless otherwise stated. Anhydrous solvents were either purchased from Fisher Scientific or Sigma-Aldrich, or purified through anhydrous alumina columns using an Innovative Technology Inc. PS-400-7 solvent purification system, or purified by distillation (over sodium/benzophenone ketyl or calcium hydride). Solvents were deoxygenated either by channelling a stream of N₂ through the liquid (sparging), or by the freeze-thaw-pump method. Thin layer chromatography (TLC) was carried out on aluminium plates coated with silica gel (Alugram[®]SIL G/UV₂₅₄ nm), and visualisation was achieved with UV light or KMnO₄, ceric ammonium molybdate and iodine dips, followed by gentle heating. Solvents were removed using Büchi rotary evaporators and with high vacuum on a Schlenk line. Flash column chromatography was carried out using Davisil LC 60 Å silica gel (35-70 micron) purchased from Sigma-Aldrich.

NMR spectra were run in CDCl₃ unless otherwise stated, on Bruker Avance 250, Bruker Avance 300, Bruker Avance 400, Bruker Avance 500 II+ or Agilent A500a instruments. IR spectra were recorded on a Perkin-Elmer 1600 FT-IR instrument. Capillary melting points were recorded on a Büchi 535 melting point apparatus, and are uncorrected. High resolution mass spectrometry (HRMS) was carried out using a micrOTOF ESI-TOF spectrometer coupled to an Agilent 1200 LC system for auto-sampling. X-ray crystallography was carried out on a Nonius Kappa CCD diffractometer with Mo-K α radiation (λ = 0.71073 Å). Chiral HPLC was carried out with a Chiralcel OD (200 × 4.6 mm, particle size 20 μ m) or Chiralcel OC stationary

phases (200 × 4.6 mm, particle size 20 µm), using UV detection. Chiral GC analysis was carried out on an Agilent 5977A GC-MS apparatus, with a Beta-Dex 120 column (60 m × 0.25 mm × 0.25 µm) with helium as carrier gas. The GC runs were conducted at 90 °C for 15 min, then increased by 10 °C per min until 200 °C was reached, and maintained at 200 °C for 10 min.

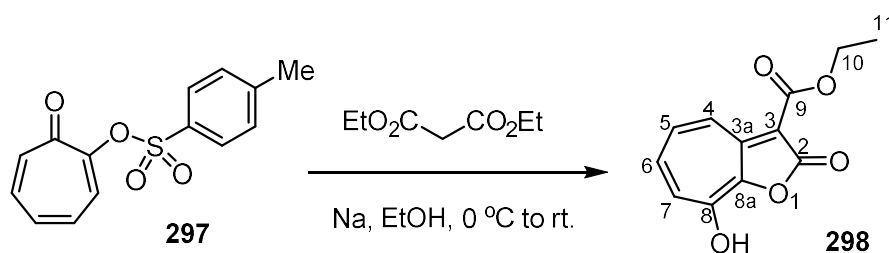
7-Oxocyclohepta-1,3,5-trien-1-yl 4-methylbenzene-1-sulfonate **297**



The preparation of this compound was based on a method by von Eggers Doering.¹⁹⁶ At 0 °C, to a stirred mixture of tropolone **323** (12.2 g, 100 mmol, 1.00 eq.) and *p*-toluenesulfonyl chloride (19.1 g, 100 mmol, 1.00 eq.) was slowly added pyridine (30 mL), and then was allowed to warm to r.t. The mixture was stirred for 3 h, forming a viscous consistency after 1 h. To the mixture was added water (120 mL), stirred for 15 min and the precipitate was collected by filtration to give 7-oxocyclohepta-1,3,5-trien-1-yl 4-methylbenzene-1-sulfonate **297** (25.7 g, 93.1 mmol, 93%) as an off-white solid, used without further purification; R_f 0.60 (EtOAc); δ_H (250 MHz, $CDCl_3$) 7.92 (2H, d, J 8.5 Hz, 10-CH), 7.46 (1H, dd, J 9.0 Hz, 1.0 Hz, 7-CH), 7.37-7.33 (2H, dd, J 8.5 Hz, 1.0 Hz, 11-CH), 7.24-6.95 (4H, m, 3,4,5,6-CH), 2.45 (3H, s, 15-CH₃).

Data in agreement with those previously reported.²⁸⁰

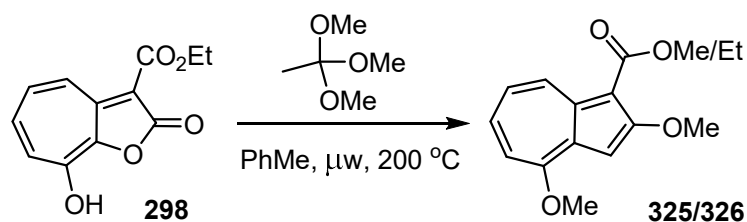
Ethyl 8-hydroxy-2-oxo-2H-cyclohepta[b]furan-3-carboxylate **298**



The preparation of this compound was based on method by Nozoe.¹⁹⁷ At 0 °C, to a stirred suspension of 7-oxocyclohepta-1,3,5-trien-1-yl 4-methylbenzene-1-sulfonate **297** (13.8 g, 50.0 mmol, 1.00 eq.) and diethyl malonate **294** (14.0 mL, 100.0 mmol, 2.00 eq.) in ethanol (100 mL) was added by cannula NaOEt solution (freshly prepared from Na metal (2.30 g, 100.0 mmol, 2.00 eq.) and ethanol (100 mL)). The mixture was allowed to warm to r.t. in the ice bath, while the ice melted, forming a gel-like consistency after 10 min. After 16 h, to the mixture was added water (250 mL), and the solution was extracted with DCM (3 × 100 mL). The organic extracts were discarded, and to the aqueous layer was added HCl_(aq) (5 M, 150 mL), which changed from an orange/brown solution to a bright yellow suspension. After chilling at 2 °C for 2 h, the mixture was filtered to give *ethyl 8-hydroxy-2-oxo-2H-cyclohepta[b]furan-3-carboxylate* **298** (9.48 g, 40.5 mmol, 81%) as a bright yellow fluffy solid; R_f 0.00 (EtOAc); δ_H (250 MHz, DMSO-*d*₆) 8.76 (1H, d, *J* 10.5 Hz, 4-CH), 7.70-7.47 (3H, m, 5,6,7-CH), 4.23 (2H, q, *J* 7.0 Hz, 10-CH₂), 1.28 (3H, t, *J* 7.0 Hz, 11-CH₃).

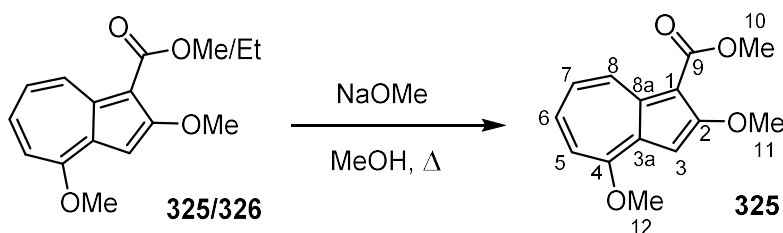
Data in agreement with those previously reported.¹⁹⁷

Methyl (325) and ethyl 2,4-methoxyazulene-1-carboxylate 326



The preparation of this compound was based on a method by Pham.¹⁹⁸ Under atmosphere of air, at r.t., to a suspension of ethyl 8-hydroxy-2-oxo-2H-cyclohepta[b]furan-3-carboxylate **298** (400 mg, 1.71 mmol, 1.00 eq.) in trimethyl orthoacetate **324** (1.08 mL, 8.54 mmol, 5.00 eq.) was added toluene (1.00 mL), and then heated in at 200 °C for 3 h, under microwave radiation. The resultant deep red solution, loaded directly onto a column, was purified by column chromatography (20→100% EtOAc in petroleum ether) to give an inseparable mixture of *methyl* **325** and *ethyl 2,4-methoxyazulene-1-carboxylate* **326** (299 mg, 1.17 mmol, 70%, Me/Et ~2:1) as a red solid.

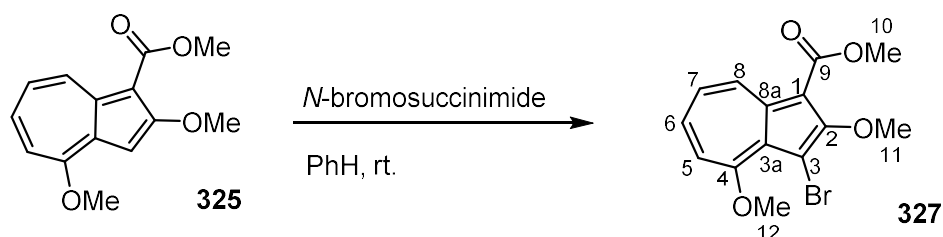
Methyl 2,4-methoxyazulene-1-carboxylate **325**



At r.t., to a stirred suspension of sodium methoxide (659 mg, 12.2 mmol, 10.5 eq.) in methanol (4.00 mL) was added a solution of methyl **325** and ethyl 2,4-methoxyazulene-1-carboxylate **326** (296 mg, ~1.16 mmol, 1.00 eq.) in methanol (11.0 mL). The mixture was heated at reflux and stirred for 21 h, then allowed to cool. To the mixture was then added HCl_(aq) (1 M, 30 mL) and extracted with DCM (3 × 20 mL). The combined organic extracts were washed with water (20 mL), dried over anhydrous MgSO₄ and filtered. The filtrate was concentrated under reduced pressure to give *methyl 2,4-methoxyazulene-1-carboxylate* **325** (266 mg, 1.08 mmol, 93%) as a red solid; *R_f* 0.62 (EtOAc); δ_{H} (250 MHz, CDCl₃) 9.44 (1H, dd, *J* 10.0 Hz, 1.0 Hz, 8-CH), 7.57 (1H, ddd, *J* 11.0 Hz, 10.0 Hz, 1.0 Hz, 6-CH), 7.34 (1H, td, *J* 10.0 Hz, 1.0 Hz, 7-CH), 7.17 (1H, d, *J* 11.0 Hz, 5-CH), 7.03 (1H, s, 3-CH), 4.16 (3H, s, 12-CH₃), 4.14 (3H, s, 11-CH₃), 3.96 (3H, s, 10-CH₃).

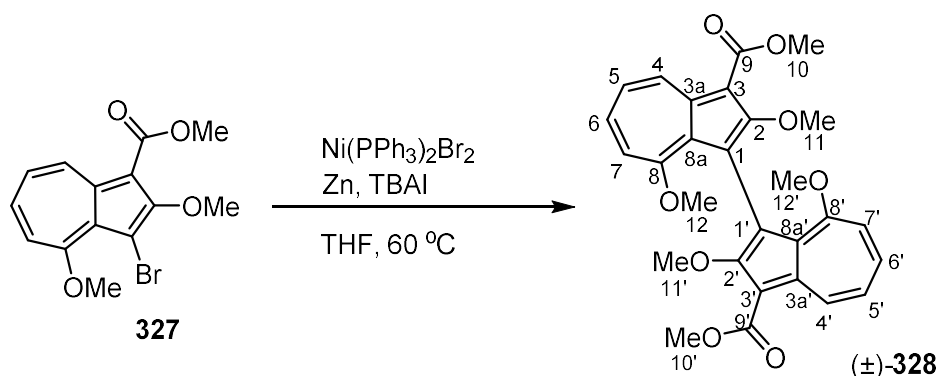
Data in agreement with those previously reported.¹⁹³

Methyl 2,4-dimethoxy-3-bromoazulene-1-carboxylate **327**



The preparation of this compound was based on a method by Nozoe.¹⁹⁴ Under atmosphere of air, at r.t., to an aluminium foil-covered stirred suspension of *N*-bromosuccinimide (410 mg, 2.30 mmol, 1.10 eq.) in benzene (50 mL) was gradually added methyl 2,4-dimethoxyazulene-1-carboxylate **325** (515 mg, 2.09 mmol, 1.00 eq.). After stirring for 1 h, to the reaction mixture was added *N*-bromosuccinimide (83 mg, 0.466 mmol, 0.40 eq.) and was further stirred for 20 min. The mixture was washed with water (50 mL), and the organic phase was separated, dried over anhydrous MgSO_4 and filtered. The filtrate was concentrated under reduced pressure to give methyl 2,4-dimethoxy-3-bromoazulene-1-carboxylate **327** (610 mg, 1.88 mmol, 89%) as a purple solid (m.p. 69-73 °C), and was used without further purification; R_f 0.41 (2:1 petroleum ether/EtOAc); δ_H (300 MHz, CDCl_3) 9.33 (1H, dd, J 10.0 Hz, 1.0 Hz, 8-CH), 7.55 (1H, ddd, J 11.0 Hz, 10.0 Hz, 1.0 Hz, 6-CH), 7.20 (1H, td, J 10.0 Hz, 1.0 Hz, 7-CH), 7.04 (1H, d, J 11.0 Hz, 5-CH), 4.10 (3H, s, 12-CH₃), 4.09 (3H, s, 11-CH₃), 3.98 (3H, s, 10-CH₃); δ_C (75 MHz, CDCl_3) 164.7 (9-C), 163.8 (4-C), 163.6 (2-C), 137.6 (8a-C), 136.9 (8-C), 136.4 (6-C), 126.0 (3a-C), 123.3 (7-C), 112.1 (5-C), 105.6 (1-C), 95.4 (3-C), 62.2 (12-C), 56.2 (11-C), 51.3 (10-C); ν_{max} (film) 2982, 2931, 2846, 1677, 1594, 1569, 1527, 1481, 1454, 1403, 1377, 1336, 1298, 1264, 1212, 1191, 1098, 1000, 969, 941, 902, 871, 788, 762, 715 cm^{-1} ; HRMS (ESI+) m/z calc for $[\text{C}_{14}\text{H}_{13}\text{O}_4\text{Br} + \text{H}]^+$, 325.0075; found, 325.0073.

(±)-Dimethyl 2,2',8,8'-tetramethoxy-1,1'-biazulene-3,3'-dicarboxylate **328**

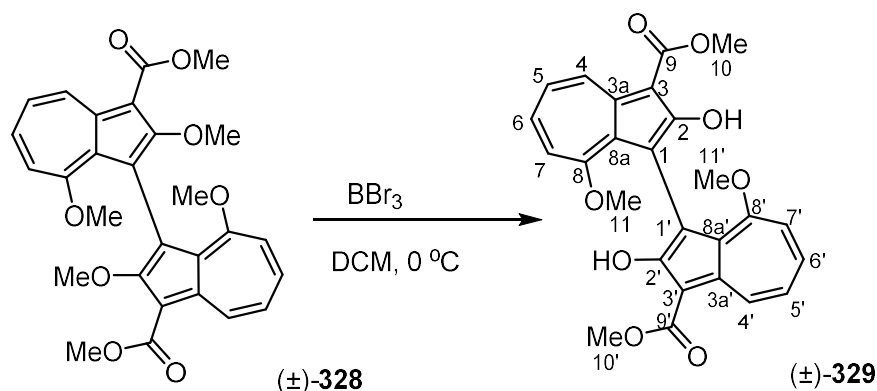


The preparation of this compound was based on a method by Iyoda.¹⁹⁹ At r.t., to a mixture of zinc powder (48 mg, 0.734 mmol, 1.50 eq.), tetrabutylammonium iodide (180 mg, 0.489 mmol, 1.00 eq.) and, dispensed within a glovebox, bis(diphenylphosphine)nickel(II) bromide (36 mg, 0.049 mmol, 0.10 eq.) was added a solution of methyl 2,4-methoxy-3-bromoazulene-1-carboxylate **327** (158 mg, 0.489 mmol, 1.00 eq.) in THF (1.20 mL). The stirred mixture was heated at 50 °C for 3 h and then allowed to cool. The reaction mixture was loaded directly onto a silica column. Purification by column chromatography (2:1 petroleum ether/EtOAc) yielded (*±*)-dimethyl 2,2',8,8'-tetramethoxy-1,1'-biazulene-3,3'-dicarboxylate **328** (59 mg, 0.120 mmol, 49%) as a pink/purple crystalline solid (m.p. 208-211 °C, crystals suitable for X-ray crystallography were grown by slow vapour diffusion of hexane into a solution of **328** in DCM); *R*_f 0.40 (1:1 petroleum ether/EtOAc); δ_H (300 MHz, CDCl₃) 9.41 (2H, dd, *J* 10.0, 1.0 Hz, 4,4'-CH), 7.46 (2H, *J* 11.0 Hz, 10.0 Hz, 1.0 Hz, 6,6'-CH), 7.22 (2H, td, *J* 10.0 Hz, 1.0 Hz, 5,5'-CH), 6.88 (2H, d, *J* 10.5 Hz, 7,7'-CH), 3.99 (6H, s, 10,10'-CH₃), 3.72 (6H, s, 11,11'-CH₃), 3.43 (6H, s, 12,12'-CH₃); δ_C (75 MHz, CDCl₃) 166.0 (9,9'-C), 165.9 (2,2'-C), 163.5 (8,8'-C), 138.5 (3a,3a'-C), 135.0 (4,4'-C), 133.8 (6,6'-C), 129.1 (8a,8a'-C), 123.0 (5,5'-C), 115.8 (1,1'-C), 111.8 (7,7'-C), 104.2 (3,3'-C), 61.0 (11,11'-C), 56.5 (12,12'-C), 51.1 (10,10'-C); ν_{max} (film) 2986, 2942,

2843, 1673, 1591, 1570, 1526, 1473, 1448, 1387, 1334, 1300, 1261, 1209, 1186, 1164, 1093, 1074, 990, 938, 872, 790, 644 cm^{-1} ; HRMS (ESI+) m/z calc for $[\text{C}_{28}\text{H}_{26}\text{O}_8 + \text{H}]^+$, 491.1705; found, 491.1704.

(±)-Dimethyl 2,2'-dihydroxy-8,8'-dimethoxy-1,1'-biazulene-3,3'-dicarboxylate

329

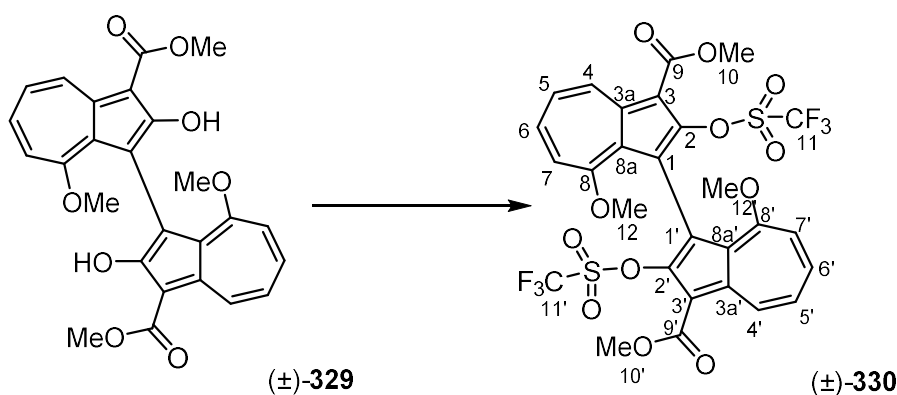


The preparation of this compound was based on a method by Talaz.²⁰⁰ At 0 °C, to a stirred solution of (±)-dimethyl 2,2',8,8'-tetramethoxy-1,1'-biazulene-3,3'-dicarboxylate **328** (132 mg, 0.268 mmol, 1.00 eq.) in DCM (2 mL) was added dropwise BBr₃ (1.0 M in hexanes, 0.540 mL, 0.540 mmol, 2.00 eq.). The mixture was allowed to warm to r.t., and stirred for 105 min. To the mixture was added methanol (5 mL), and then was poured into DCM (20 mL). The solution was washed with water (2 × 10 mL), dried over anhydrous MgSO₄ and filtered. The filtrate was concentrated under reduced pressure to give (±)-dimethyl 2,2'-dihydroxy-8,8'-dimethoxy-1,1'-biazulene-3,3'-dicarboxylate **329** (117 mg, 0.253 mmol, 94%) as a deep red solid; R_f 0.44 (1:1 petroleum ether/EtOAc); δ_H (250 MHz, CDCl₃)* 10.78 (2H, s, 11,11'-OH), 8.98 (2H, dd, *J* 9.6 Hz, 0.9 Hz, 4,4'-CH), 7.39 (2H, td, *J* 10.0 Hz, 1.0 Hz, 6,6'-CH), 7.19 (2H, t, *J* 10.0 Hz, 5,5'-CH), 6.91 (2H, d, *J* 10.5 Hz, 7,7'-CH), 4.05 (6H, s, 10,10'-CH₃), 3.56 (6H, s, 11,11'-CH₃); δ_C (63 MHz, CDCl₃)* 169.3 (9,9'-C or 2,2'-C), 169.0 (9,9'-C or 2,2'-C), 163.0 (8,8'-C), 137.6 (3a,3a'-C), 132.4 (4,4'-C or 6,6'-C), 132.1 (4,4'-C or 6,6'-C), 130.5 (8a,8a'-C), 123.5 (5,5'-C), 111.9 (1,1'-C), 111.8 (7,7'-C), 97.8 (3,3'-C), 56.4 (11,11'-C), 51.2 (10,10'-C); ν_{max} (film) 3376, 2953, 2922, 2852, 1738, 1702, 1630, 1596, 1574, 1452, 1438, 1398, 1315, 1265, 1245,

1218, 1202, 1182, 1166, 1099, 1083, 1005, 989, 961, 871, 789, 723, 684 cm^{-1} ;
HRMS (ESI+) m/z calc for $[\text{C}_{26}\text{H}_{22}\text{O}_8 + \text{Na}]^+$, 485.1212; found, 485.1214.

* due to the lack of 2D NMR spectra recorded, carbon and hydrogen atoms are assigned tentatively, based on those of biazulene diol **370**.

(±)-Dimethyl 2,2'-di(trifluoromethanesulfonyloxy)-8,8'-dimethoxy-1,1'-biazulene-3,3-dicarboxylate **330**

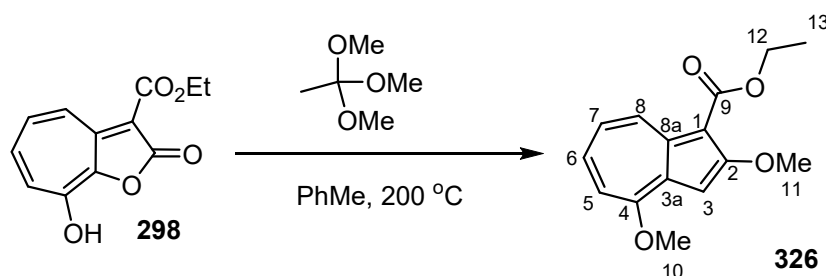


This compound was prepared based on a method by Cai.¹⁵² At 0 °C, to a stirred solution of (±)-dimethyl 2,2'-dihydroxy-8,8'-dimethoxy-1,1'-biazulene-3,3'-dicarboxylate **329** (117 mg, 0.253 mmol, 1.00 eq.) and pyridine (0.060 mL, 0.760 mmol, 3.00 eq.) in DCM (2.5 mL) was added dropwise trifluoromethanesulfonic anhydride (0.10 mL, 0.591 mmol, 2.33 eq.), immediately changing colour from deep red to red/purple. The mixture was allowed to warm to r.t., and stirred for 14 h. To the mixture was added pentane (3 mL), loaded onto pad of silica and filtered through with DCM/pentane (1:1, 80 mL). The filtrate was concentrated under reduced pressure to give the crude product, which was purified by column chromatography (20→50% EtOAc in petroleum ether) to give (±)-dimethyl 2,2'-di(trifluoromethanesulfonyloxy)-8,8'-dimethoxy-1,1'-biazulene-3,3-dicarboxylate **330** (62 mg, 0.0853 mmol, 34%) as a deep purple crystalline solid (m.p. 242-245 °C, dec.); R_f 0.32 (1:1 petroleum ether/EtOAc); δ_H (300 MHz, $CDCl_3$)* 9.80 (2H, dd, J 10.0 Hz, 1.0 Hz, 4,4'-CH), 7.81 (2H, ddd, J 11.0 Hz, 9.5 Hz, 1.0 Hz, 6,6'-CH), 7.44 (2H, t, J 9.8 Hz, 5,5'-CH), 7.13 (2H, d, J 11.0 Hz, 7,7'-CH), 3.99 (6H, s, 10,10'-CH₃), 3.60 (6H, s, 12,12'-CH₃); δ_C (75 MHz, $CDCl_3$)* 167.2 (8,8'-C), 164.1 (9,9'-C), 149.4 (2,2'-C), 140.1 (4,4'-C), 138.9 (6,6'-C), 136.6 (3a,3a'-C), 126.6 (8a,8a'-C), 124.4

(5,5'-C), 117.9 (q, $^1J_{CF}$ 321.0 Hz, 11,11'-C), 113.2 (7,7'-C), 112.7 (1,1'-C), 106.1 (3,3'-C), 56.6 (12,12'-C), 51.1 (10,10'-C); ν_{\max} (film) 3000, 2955, 2849, 1707, 1688, 1598, 1569, 1532, 1515, 1459, 1441, 1416, 1387, 1317, 1299, 1270, 1218, 1190, 1132, 1090, 1048, 1002, 982, 947, 918, 901, 856, 814, 797, 753, 724, 709, 686, 669, 653 cm^{-1} ; HRMS (ESI+) m/z calc for $[\text{C}_{28}\text{H}_{20}\text{F}_6\text{O}_{12}\text{S}_2 + \text{H}]^+$, 727.0379; found, 727.0375.

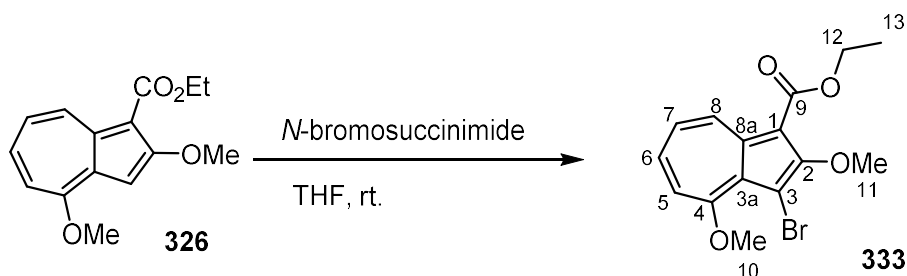
* due to the lack of 2D NMR spectra recorded, carbon and hydrogen atoms are assigned tentatively, based on those of biazulene ditriflate **372**.

Ethyl 2,4-dimethoxyazulene-1-carboxylate **326**



The preparation of this compound was based on a method by Pham.¹⁹⁸ Under atmosphere of air at r.t., to microwave tubes (7 × 10 mL capacity) was added ethyl 8-hydroxy-2-oxo-2*H*-cyclohepta[*b*]furan-3-carboxylate **298** (2.80 g, 12.0 mmol, 1.00 eq.), trimethyl orthoacetate **324** (7.70 mL, 60.5 mmol, 5.05 eq.) and toluene (7.0 mL). The tubes were sealed, and the suspension was stirred, heating under air at 200 °C, for 5 h (CAUTION: the reaction was run behind a blast shield). The resultant deep red solution was loaded onto a silica column, and purified by column chromatography (5→25% EtOAc in petroleum ether) to give *ethyl 2,4-dimethoxyazulene-1-carboxylate* **326** (2.45 g, 9.40 mmol, 79%) as a red, crystalline solid (m.p. 103-105 °C); R_f 0.51 (1:1 petroleum ether/EtOAc); δ_H (500 MHz, $CDCl_3$) 9.39 (1H, d, J 10.3 Hz, 8-CH), 7.51 (1H, ddd, J 10.9 Hz, 9.9 Hz, 1.0 Hz, 6-CH), 7.29 (1H, t, J 10.0 Hz, 7-CH), 7.11 (1H, d, J 10.8 Hz, 5-CH), 7.01 (1H, s, 3-CH), 4.45 (2H, q, J 6.8 Hz, 12-CH₂), 4.12 (3H, s, 11-CH₃), 4.11 (3H, s, 10-CH₃), 1.45 (3H, t, J 7.1 Hz, 13-CH₃); δ_C (126 MHz, $CDCl_3$) 167.6 (2-C), 165.2 (9-C), 160.3 (4-C), 138.9 (8a-C), 135.0 (8-C), 132.8 (6-C), 131.8 (3a-C), 124.0 (7-C), 111.3 (5-C), 96.9 (3-C), 96.8 (1-C), 59.4 (12-C), 58.1 (11-C), 56.4 (10-C), 14.6 (13-C); ν_{max} (film) 2977, 2938, 2837, 1659, 1589, 1575, 1540, 1501, 1455, 1420, 1394, 1344, 1309, 1265, 1198, 1171, 1130, 1088, 1029, 980, 786, 745, 700, 658 cm^{-1} ; HRMS (ESI+) m/z calc for $[C_{15}H_{16}O_4 + Na]^+$, 283.0941; found, 283.0953.

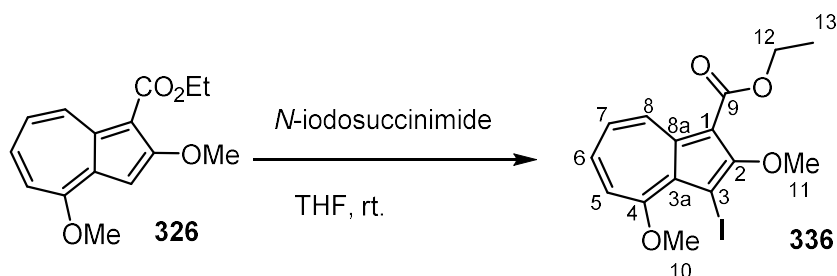
Ethyl 3-bromo-2,4-dimethoxyazulene-1-carboxylate **333**



The preparation of this compound was based on a method by Nozoe.¹⁹³ Under atmosphere of air, at r.t., to a stirred solution of ethyl 2,4-dimethoxyazulene-1-carboxylate **326** (150 mg, 0.576 mmol, 1.00 eq.) in THF (10.0 mL) was added *N*-bromosuccinimide (103 mg, 0.576 mmol, 1.00 eq.). After 5 min, the reaction mixture was concentrated under reduced pressure, and dissolved in ethyl acetate (30 mL). The solution was washed with K₂CO_{3(aq)} (1.0 M, 15 mL), water (2 × 10 mL) and saturated brine. The organic layer was then dried over anhydrous MgSO₄ and filtered. The filtrate was concentrated under reduced pressure to give the crude product, which was purified by column chromatography (10% EtOAc in petroleum ether) to give *ethyl 3-bromo-2,4-dimethoxyazulene-1-carboxylate* **333** (172 mg, 0.506 mmol, 88%) as a maroon/purple oily solid; *R*_f 0.63 (1:1 petroleum ether/EtOAc); δ_{H} (500 MHz, CDCl₃) 9.34 (1H, dd, *J* 9.9 Hz, 1.1 Hz, 8-CH), 7.56 (1H, ddd, *J* 10.9 Hz, 9.8 Hz, 1.2 Hz, 6-CH), 7.20 (1H, td, *J* 9.9 Hz, 0.7 Hz, 7-CH), 7.05 (1H, d, *J* 11.0 Hz, 5-CH), 4.43 (2H, q, *J* 7.0 Hz, 12-CH₂), 4.10 (3H, s, 10-CH₃) 4.09 (3H, s, 11-CH₃), 1.45 (3H, t, *J* 7.1 Hz, 13-CH₃); δ_{C} (126 MHz, CDCl₃) 164.4 (9-C), 163.8 (4-C), 163.5 (2-C), 137.7 (8a-C), 136.9 (8-C), 136.3 (6-C), 125.9 (3a-C), 123.3 (7-C), 112.0 (5-C), 106.0 (1-C), 95.5 (3-C), 62.2 (11-C), 60.1 (12-C), 56.2 (10-C), 14.4 (13-C); ν_{max} (film) 2927, 2853, 1675, 1592, 1572, 1535, 1500, 1480, 1456, 1406, 1381, 1310, 1265, 1211, 1195, 1167, 1117, 1093, 1082, 1030, 999, 956, 856, 789,

748, 721, 696 cm^{-1} ; HRMS (ESI+) m/z calc for $[\text{C}_{15}\text{H}_{15}\text{BrO}_4 + \text{Na}]^+$, 361.0046; found, 361.0061.

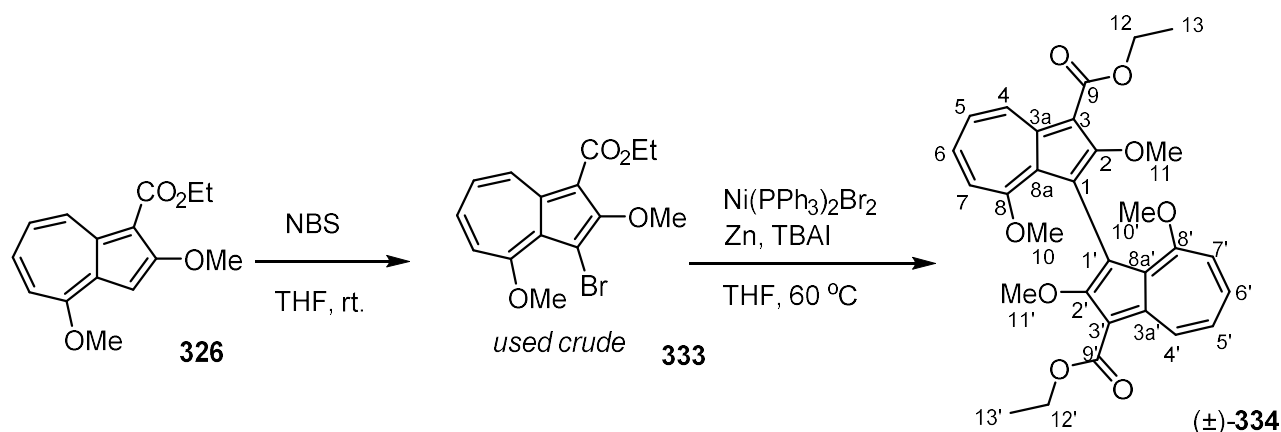
Ethyl 3-iodo-2,4-dimethoxyazulene-1-carboxylate **336**



Under atmosphere of air, to a stirred solution of ethyl 2,4-dimethoxyazulene-1-carboxylate **326** (44 mg, 0.169 mmol, 1.00 eq.) in THF (5.0 mL) was added *N*-iodosuccinimide (38 mg, 0.169 mmol, 1.00 eq.), and the mixture was allowed to stir for 2 h. The mixture was then concentrated under reduced pressure, dissolved in diethyl ether (15 mL), washed with Na₂CO_{3(aq)} (1.0 M, 10 mL), with water (2 × 10 mL) and with saturated brine. The organic layer was dried over anhydrous MgSO₄, and filtered. The filtrate was concentrated under reduced pressure to give *ethyl 3-iodo-2,4-dimethoxyazulene-1-carboxylate* **336** (59 mg, 0.153 mmol, 90%) as a thick burgundy oil; *R_f* 0.62 (1:1 petroleum ether/EtOAc); δ_{H} (300 MHz, CDCl₃) 9.36 (1H, dd, *J* 10.0 Hz, 1.0 Hz, 8-CH), 7.56 (1H, ddd, *J* 11.0 Hz, 10.0 Hz, 1.0 Hz, 6-CH), 7.19 (1H, td, *J* 10.0 Hz, 0.5 Hz, 7-CH), 7.02 (1H, d, *J* 11.0 Hz, 5-CH), 4.44 (2H, q, *J* 7.0 Hz, 12-CH₂), 4.12 (3H, s, 10-CH₃), 4.11 (3H, s, 11-CH₃), 1.45 (3H, t, *J* 7.0 Hz, 13-CH₃); δ_{C} (75 MHz, CDCl₃) 164.5 (9-C), 164.1 (4-C), 162.2 (2-C), 137.0 (8-C), 136.1 (6-C), 135.9 (8a-C), 124.3 (3a-C), 123.1 (7-C), 111.6 (5-C), 108.5 (3-C), 105.4 (1-C), 62.1 (11-C), 60.1 (12-C), 56.4 (10-C), 14.5 (13-C); ν_{max} (film) 2976, 2933, 1679, 1593, 1535, 1485, 1456, 1409, 1382, 1347, 1301, 1267, 1211, 1193, 1094, 1078, 1028, 990, 953, 855, 821, 789, 763, 723, 702, 680 cm⁻¹.

No corresponding *m/z* value could be obtained by mass spectrometry.

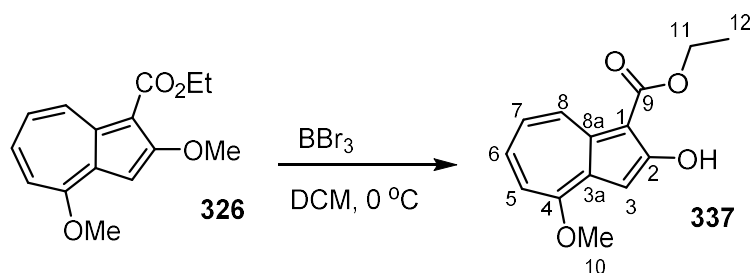
(±)-3,3'-Diethyl 2,2',8,8'-tetramethoxy-[1,1'-biazulene]-3,3'-dicarboxylate **334**



The preparation of this compound was based on a method by Iyoda.¹⁹⁹ Under atmosphere of air, at r.t., to a stirred solution of ethyl 2,4-dimethoxyazulene-1-carboxylate **326** (110 mg, 0.423 mmol, 1.00 eq.) in THF (10 mL) was added *N*-bromosuccinimide (75 mg, 1.00 eq.). After 15 min, the reaction mixture was concentrated under reduced pressure, and dissolved in ethyl acetate (25 mL). The solution was washed with $\text{Na}_2\text{CO}_{3(\text{aq})}$ (2.0 M, 2 × 15 mL), water (15 mL) and the organic layer was dried over anhydrous MgSO_4 and filtered. The filtrate was concentrated to give crude *ethyl 3-bromo-2,4-dimethoxyazulene-1-carboxylate* **333**. Under atmosphere of N_2 , to a microwave tube charged with $\text{Ni(PPh}_3)_2\text{Br}_2$ (31 mg, 0.0423 mmol, 0.10 eq.), Zn powder (41 mg, 0.625 mmol, 1.50 eq.) and tetra-*n*-butylammonium iodide (156 mg, 0.423 mmol, 1.00 eq.) was added a solution of the crude bromoazulene in THF (1.50 mL), and the mixture was stirred and heated at 50 °C for 17 h. After cooling, the mixture was loaded directly onto a silica column and purified by column chromatography (5→33% EtOAc in petroleum ether) to give (±)-3,3'-diethyl 2,2',8,8'-tetramethoxy-[1,1'-biazulene]-3,3'-dicarboxylate **334** (32 mg, 0.0607 mmol, 29%) as a pink/red solid (m.p. 199-201 °C); R_f 0.43 (1:1 petroleum ether/EtOAc); δ_{H} (500 MHz, CDCl_3) 9.39 (2H, dd, J 9.9 Hz, 1.1 Hz, 4,4'-CH), 7.45

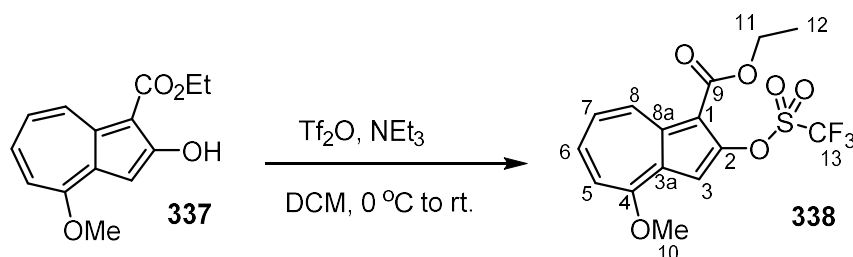
(2H, ddd, J 10.8 Hz, 9.8 Hz, 1.1 Hz, 6,6'-CH), 7.21 (2H, td, J 9.9 Hz, 0.8 Hz, 5,5'-CH), 6.87 (2H, d, J 10.7 Hz, 7,7'-CH), 4.47 (4H, q, J 7.1 Hz, 12,12'-CH₂), 3.72 (6H, s, 11,11'-CH₃), 3.43 (6H, s, 10,10'-CH₃), 1.45 (6H, t, J 7.1 Hz, 13,13'-CH₃); δ_c (75 MHz, CDCl₃) 166.1 (9,9'-C), 165.7 (2,2'-C), 163.5 (8,8'-C), 138.5 (3a,3a'-C), 135.0 (4,4'-C), 133.8 (6,6'-C), 128.7 (8a,8a'-C), 122.8 (5,5'-C), 116.2 (1,1'-C), 111.5 (7,7'-C), 104.8 (3,3'-C), 61.1 (11,11'-C), 59.8 (12,12'-C), 56.5 (10,10'-C), 14.6 (13,13'-C); $\nu_{\max}(\text{film})$ 2978, 2926, 2842, 1665, 1591, 1571, 1526, 1472, 1453, 1437, 1396, 1379, 1361, 1332, 1312, 1300, 1262, 1207, 1188, 1165, 1132, 1089, 1072, 984, 947, 894, 874, 825, 790, 751, 707, 687 cm⁻¹; HRMS (ESI+) m/z calc for [C₃₀H₃₀O₈ + Na]⁺, 541.1838; found, 541.1813.

Ethyl 2-hydroxy-4-methoxyazulene-1-carboxylate **337**



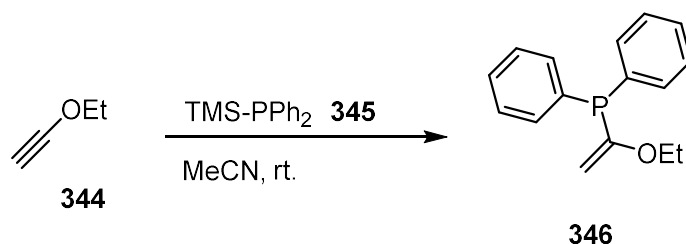
The preparation of this compound was based on a method by Talaz.²⁰⁰ At 0 °C, to a stirred solution of ethyl 2,4-dimethoxyazulene-1-carboxylate **326** (2.45 g, 9.41 mmol, 1.00 eq.) in DCM (50 mL) was added slowly BBr₃ (1.0 M in hexanes, 9.50 mL, 1.01 eq.). After stirring for 40 min, to the reaction mixture was added methanol (5.0 mL) to quench. The solution was diluted with DCM (100 mL) and washed with water (3 × 50 mL). The organic layer was dried over anhydrous MgSO₄, filtered and the filtrate was concentrated under reduced pressure to give *2-hydroxy-4-methoxyazulene-1-carboxylate* **337** (2.28 g, 9.23 mmol, 98%) as an orange/brown crystalline solid (m.p. 98-100 °C); *R_f* 0.37 (4:1 petroleum ether/EtOAc); δ_{H} (300 MHz, CDCl₃) 10.82 (1H, s, 2-OH), 8.84 (1H, d, *J* 9.5 Hz, 8-CH), 7.38 (1H, td, *J* 10.2 Hz, 0.9 Hz, 6-CH), 7.17 (1H, t, *J* 10.0 Hz, 7-CH), 6.94 (1H, s, 3-CH), 6.93 (1H, d, *J* 10.6 Hz, 5-CH), 4.50 (2H, q, *J* 7.2 Hz, 10-CH₂), 4.01 (3H, s, 12-CH₃), 1.51 (3H, t, *J* 7.2 Hz, 11-CH₃); δ_{C} (75 MHz, CDCl₃) 169.4 (2-C), 168.6 (9-C), 160.4 (4-C), 136.6 (8a-C), 133.6 (3a-C), 132.7 (8-C), 132.0 (6-C), 123.5 (7-C), 110.5 (5-C), 101.3 (3-C), 98.5 (1-C), 60.0 (11-C), 55.9 (10-C), 14.3 (12-C); ν_{max} (film) 2981, 2936, 2908, 2837, 1628, 1596, 1535, 1478, 1450, 1436, 1396, 1381, 1351, 1316, 1266, 1171, 1128, 1091, 1069, 1021, 958, 924, 871, 821, 806, 785, 763, 739, 714, 670 cm⁻¹; HRMS (ESI+) *m/z* calc for [C₁₄H₁₄O₄ + Na]⁺, 269.0790; found, 269.0785.

Ethyl 4-methoxy-2-(trifluoromethanesulfonyloxy)azulene-1-carboxylate **338**



The preparation of this compound was based on a method by Morita.²⁰⁶ At 0 °C, to a stirred solution of ethyl 2-hydroxy-4-methoxyazulene-1-carboxylate **337** (502 mg, 2.04 mmol, 1.00 eq.) and triethylamine (570 μL , 4.08 mmol, 2.00 eq.) in DCM (5.0 mL) was added dropwise trifluoromethanesulfonic anhydride (520 μL , 3.06 mmol, 1.50 eq.). The mixture was allowed to warm to r.t., and after 6 h, was poured into DCM (25 mL) and washed with water (2 \times 15 mL). The organic layer was dried over anhydrous MgSO_4 , and filtered. The filtrate was concentrated under reduced pressure to give the crude product, which was purified by column chromatography (20% EtOAc in petroleum ether) to give *ethyl 4-methoxy-2-(trifluoromethanesulfonyloxy)azulene-1-carboxylate* **338** (484 mg, 1.28 mmol, 63%) as a vivid red solid (m.p. 101-103 °C); R_f 0.44 (1:1 petroleum ether/EtOAc); δ_{H} (250 MHz, CDCl_3) 9.64 (1H, d, J 10.0 Hz, 8-CH), 7.77 (1H, t, J 10.5 Hz, 6-CH), 7.37 (1H, t, J 10.0 Hz, 7-CH), 7.24 (1H, s, 3-CH), 7.19 (1H, d, J 11.0 Hz, 5-CH), 4.48 (2H, q, J 7.0 Hz, 11- CH_2), 4.16 (3H, s, 10- CH_3), 1.47 (3H, t, J 7.0 Hz, 12- CH_3); δ_{C} (75 MHz, CDCl_3) 165.2 (4-C), 163.5 (9-C), 150.4 (2-C), 140.5 (8-C), 138.8 (6-C), 136.5 (8a-C), 128.5 (3a-C), 124.6 (7-C), 118.9 (q, $^1J_{\text{CF}}$ 320 Hz, 13-C), 112.4 (5-C), 106.5 (1-C), 104.4 (3-C), 60.3 (11-C), 56.8 (10-C), 14.3 (12-C); ν_{max} (film) 2994, 2955, 1683, 1597, 1570, 1538, 1516, 1463, 1440, 1416, 1395, 1382, 1335, 1299, 1273, 1237, 1201, 1134, 1119, 1046, 1017, 987, 958, 922, 888, 857, 839, 788, 752, 736, 704, 669, 655 cm^{-1} ; HRMS (ESI+) m/z calc for $[\text{C}_{15}\text{H}_{13}\text{F}_3\text{O}_6\text{S} + \text{Na}]^+$, 401.0283; found, 401.0276.

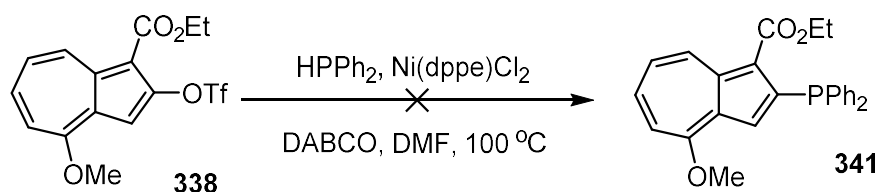
(1-ethoxyvinyl)diphenylphosphine 346



The preparation of this compound was based on a method by Kochetkov.²⁰⁸ At r.t., to a solution of ethoxyacetylene **344** (40% wt. in hexanes, 0.926 mL, 3.87 mmol, 1.00 eq.) in acetonitrile (degassed by sparging with N₂, 2.00 mL) was added diphenyl(trimethylsilyl)phosphine **345** (1.00 g, 3.87 mmol, 1.00 eq.), and the mixture was allowed to stir for 68 h. The mixture was then concentrated *in vacuo*, and the residue was purified by distillation (0.51 Torr) to give (1-ethoxyvinyl)diphenylphosphine **346** (790 mg, 3.08 mmol, 40%) as a pale yellow oil; δ_{H} (300 MHz, CDCl₃) 7.51-7.45 (4H, m), 7.34-7.31 (6H, m), 4.75 (1H, dd, *J* 24.5 Hz, 2.2 Hz), 4.45 (1H, dd, *J* 8.4 Hz, 2.2 Hz), 3.81 (2H, q, *J* 6.9 Hz), 1.23 (3H, t, *J* 7.1 Hz); δ_{P} (122 MHz, CDCl₃) -3.38.

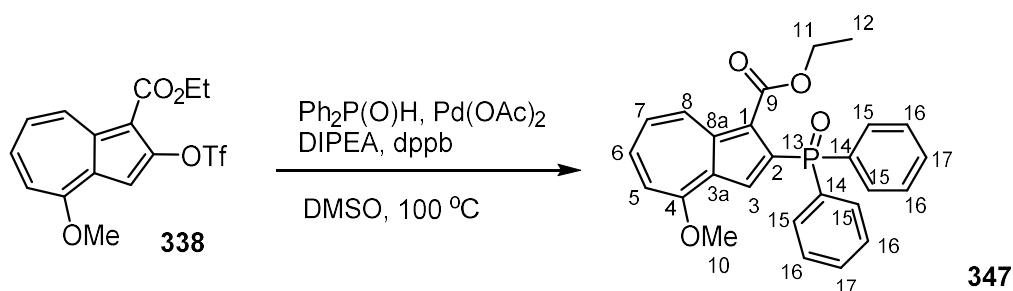
Data in agreement with those previously reported.²⁰⁸

Ethyl 2-(diphenylphosphino)-4-methoxyazulene-1-carboxylate **341**



The preparation of this compound was based on a method by Cai.¹⁵² At r.t., to a solution of [1,3-bis(diphenylphosphino)propane]dichloronickel(II) (28 mg, 0.0528 mmol, 0.10 eq.) in DMF (degassed by sparging with N_2 , 0.75 mL) was added diphenylphosphine (60 μL , 0.345 mmol, 0.65 eq.), and the mixture was stirred at $100\text{ }^\circ\text{C}$ for 45 min. To the mixture was then added a solution of ethyl 4-methoxy-2-(trifluoromethanesulfonyloxy)azulene-1-carboxylate **338** (200 mg, 0.528 mmol, 1.00 eq.) and 1,4-diazabicyclo[2.2.2]octane (118 mg, 1.06 mmol, 2.00 eq.) in DMF (degassed by sparging with N_2 , 1.25 mL). After stirring at $100\text{ }^\circ\text{C}$ for another 55 min, to the mixture was added diphenylphosphine (70 μL , 0.403 mmol, 0.76 eq.). The mixture was stirred at $100\text{ }^\circ\text{C}$ for another 18 h, then allowed to cool and diluted with EtOAc (25 mL). The mixture was washed with water ($4 \times 20\text{ mL}$), dried over anhydrous MgSO_4 and filtered. The filtrate was concentrated under reduced pressure to give the crude product, which was purified by column chromatography (10 \rightarrow 100% EtOAc in petroleum ether, then to 10% MeOH in EtOAc), but the only identified compounds were starting material **338** and 2-hydroxyazulene **337**.

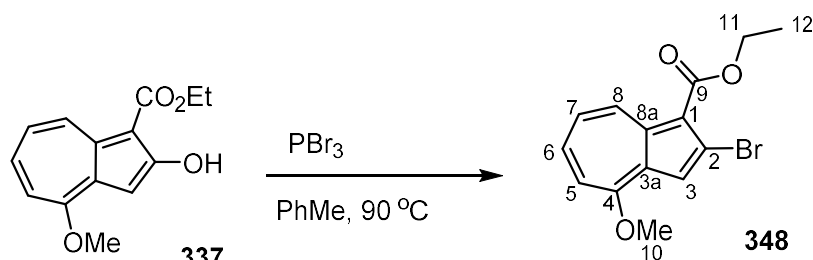
Ethyl 1-(diphenylphosphoryl)-4-methoxyazulene-1-carboxylate **347**



The preparation of this compound was based on a method by Zhang.²⁰⁹ At r.t., to a mixture of ethyl 4-methoxy-2-(trifluoromethanesulfonyloxy)azulene-1-carboxylate **338** (50 mg, 0.132 mmol, 1.00 eq.), diphenylphosphine oxide (53 mg, 0.264 mmol, 2.00 eq.), palladium diacetate (3 mg, 0.0132 mmol, 0.10 eq.) and 1,4-bis(diphenylphosphino)butane (9 mg, 0.0199 mmol, 0.15 eq.) in DMSO (degassed by freeze-pump-thaw, 0.50 mL) was added diisopropylethylamine (120 μL , 0.690 mmol, 5.22 eq.). The mixture was then stirred and heated at 100 °C for 15 h, then allowed to cool. After diluting with ethyl acetate (50 mL), the organic phase was washed with water (3 \times 15 mL), dried over anhydrous MgSO_4 , and filtered. The filtrate was concentrated under reduced pressure to give the crude product, which was purified by column chromatography (50 \rightarrow 100% EtOAc in petroleum ether, then 5% MeOH in EtOAc) and recrystallisation (1:1 THF/hexane) to give *ethyl 1-(diphenylphosphoryl)-4-methoxyazulene-1-carboxylate* **347** (5.5 mg, 0.0128 mmol, 10%) as a magenta solid (m.p. 220-223 °C (dec.)); R_f 0.07 (EtOAc); δ_{H} (500 MHz, CDCl_3) 9.73 (1H, d, J 10.2 Hz, 8-CH), 7.85 (1H, t, J 10.4 Hz, 6-CH), 7.75-7.70 (4H, m, 15-CH), 7.53-7.48 (2H, m, 17-CH), 7.46-7.41 (4H, m, 16-CH), 7.36 (1H, t, J 10.0 Hz, 7-CH), 7.31 (1H, d, $^3J_{\text{PH}}$ 6.9 Hz, 3-CH), 7.19 (1H, d, J 11.3 Hz, 5-CH), 4.11 (3H, s, 10-CH₃), 3.96 (2H, q, J 7.2 Hz, 11-CH₂), 0.95 (3H, t, J 7.3 Hz, 12-CH₃); δ_{C} (126 MHz, CDCl_3) 166.2 (4-C), 164.8 (9-C), 141.6 (8-C), 140.7 (6-C), 140.3 (d, $^3J_{\text{CP}}$ 10.9

Hz, 8a-C), 136.6 (d, $^1J_{\text{CP}}$ 106.8 Hz, 2-C), 135.0 (d, $^1J_{\text{CP}}$ 108.8 Hz, 14-C), 131.6 (d, $^2J_{\text{CP}}$ 9.7 Hz, 15-C), 131.1 (d, $^4J_{\text{CP}}$ 2.7 Hz, 17-C), 129.8 (d, $^3J_{\text{CP}}$ 15.3 Hz, 3a-C), 128.1 (d, $^3J_{\text{CP}}$ 12.4 Hz, 16-C), 123.7 (7-C), 122.3 (d, $^2J_{\text{CP}}$ 13.8 Hz, 3-C), 119.8 (d, $^2J_{\text{CP}}$ 8.1 Hz, 1-C), 112.2 (5-C), 60.0 (11-C), 56.9 (10-C), 13.7 (12-C); δ_{P} (202 MHz, CDCl_3) 26.3 (13-P); $\nu_{\text{max}}(\text{film})$ 3057, 2919, 2855, 1683, 1596, 1566, 1534, 1461, 1437, 1408, 1385, 1323, 1271, 1221, 1177, 1115, 1104, 1039, 954, 893, 790, 720 cm^{-1} ; HRMS (ESI+) m/z *calc* for $[\text{C}_{26}\text{H}_{23}\text{O}_4\text{P} + \text{H}]^+$, 431.1412; found, 431.1420.

Ethyl 2-bromo-4-methoxyazulene-1-carboxylate **348**

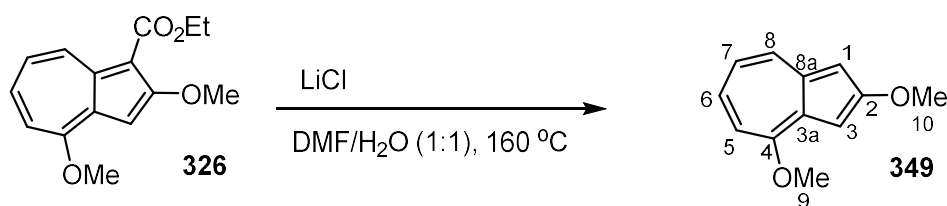


The preparation of this compound was based on a method by Ito.²¹⁰ At r.t., to a stirred solution of ethyl 2-hydroxy-4-methoxyazulene-1-carboxylate **337** (174 mg, 0.707 mmol, 1.00 eq.) in toluene (degassed by sparging with N₂, 45 mL) was added PBr₃ (100 μ L, 1.06 mmol, 1.50 eq.), and the mixture was stirred at 90 °C for 26 h. After allowing to cool to r.t., to the mixture was added PBr₃ (100 μ L, 1.06 mmol, 1.50 eq.), and the mixture was stirred at 100 °C for 19 h, and then allowed to cool to r.t. The mixture was then washed with water (3 \times 40 mL) and with saturated brine, and the organic layer was dried over anhydrous MgSO₄, and filtered. The filtrate was concentrated under reduced pressure to give the crude product, which was purified by column chromatography (0 \rightarrow 20% EtOAc in petroleum ether) to give *ethyl 2-bromo-4-methoxyazulene-1-carboxylate* **348** (12 mg, 0.0388 mmol, 5.5%) as a maroon solid (m.p. 104-106 °C); *R*_f 0.17 (4:1 petroleum ether/EtOAc); δ_{H} (300 MHz, CDCl₃) 9.47 (1H, d, *J* 10.0 Hz, 8-CH), 7.75 (1H, ddd, *J* 11.0 Hz, 10.0 Hz, 1.1 Hz, 6-CH), 7.55 (1H, s, 3-CH), 7.31 (1H, t, *J* 10.0 Hz, 7-CH), 7.17 (1H, d, *J* 11.0 Hz, 5-CH), 4.47 (2H, q, *J* 7.0 Hz, 11-CH₂), 4.16 (3H, s, 10-CH₃), 1.48 (3H, t, *J* 7.0 Hz, 12-CH₃); δ_{C} (75 MHz, CDCl₃) 164.8 (9-C), 162.7 (4-C), 138.8 (8a-C), 137.9 (8-C), 137.4 (6-C), 130.8 (3a-C), 126.2 (2-C), 123.5 (7-C), 117.8 (3-C), 115.3 (1-C), 111.5 (5-C), 60.2 (11-C), 56.7 (10-C), 14.5 (12-C); ν_{max} (film) 2971, 2921, 2846, 1674, 1639, 1592, 1567, 1534, 1475, 1456, 1403, 1381, 1354, 1320, 1283, 1260, 1215, 1174, 1109,

1078, 1033, 995, 982, 951, 879, 845, 820, 808, 782, 752, 730, 706, 678, 653 cm^{-1} ;

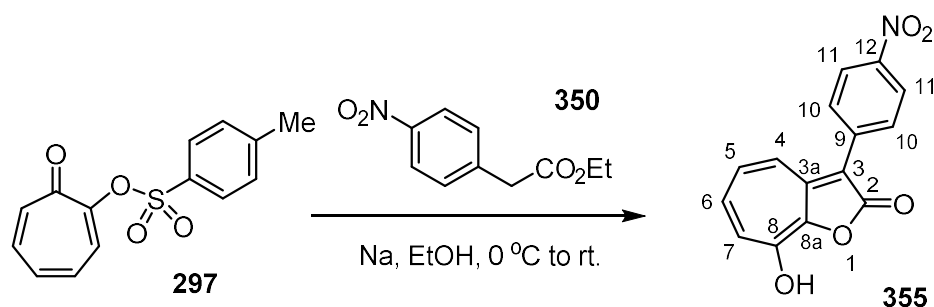
HRMS (ESI+) m/z calc for $[\text{C}_{14}\text{H}_{13}\text{BrO}_3 + \text{Na}]^+$, 330.9946; found, 330.9945.

2,4-dimethoxyazulene **349**



The preparation of this compound was based on a method by Koch.²¹¹ Under atmosphere of air, a sealed tube charged with a suspension of ethyl 2,4-dimethoxyazulene-1-carboxylate **326** (100 mg, 0.384 mmol, 1.00 eq.) and LiCl (407 mg, 9.60 mmol, 25.0 eq.) in DMF/H₂O (1:1, 2.0 mL) was heated at 160 °C, stirring for 2.5 h. After allowing it to cool to r.t., the resultant brown oil was dissolved in ethyl acetate (40 mL), washed with water (2 × 20 mL) and saturated brine (2 × 10 mL), and the organic layer was dried over anhydrous MgSO₄, and filtered. The filtrate was concentrated under reduced pressure to give the crude product, which was purified by column chromatography (10→33% EtOAc in petroleum ether) to give 2,4-dimethoxyazulene **349** (6 mg, 0.0319 mmol, 8.3%) as a red solid (m.p. 62-65 °C); *R*_f 0.57 (3:1 petroleum ether/EtOAc); δ_{H} (500 MHz, CDCl₃) 8.05 (1H, d, *J* 9.4 Hz, 8-CH), 7.39 (1H, ddd, *J* 10.9 Hz, 10.0 Hz, 1.0 Hz, 6-CH), 7.07 (1H, d, *J* 2.4 Hz, 3-CH), 7.02 (1H, t, *J* 9.7 Hz, 7-CH), 6.98 (1H, d, *J* 10.9 Hz, 5-CH), 6.69 (1H, d, *J* 2.3 Hz, 1-CH), 4.13 (3H, s, 9-CH₃), 4.03 (3H, s, 10-CH₃); δ_{C} (126 MHz, CDCl₃) 166.4 (2-C), 159.4 (4-C), 138.7 (8a-C), 133.1 (8-C), 131.0 (6-C), 127.8 (3a-C), 120.1 (7-C), 108.5 (5-C), 100.2 (3-C), 99.5 (1-C), 57.5 (10-C), 56.3 (9-C); ν_{max} (film) 3113, 3013, 2928, 2833, 1594, 1568, 1539, 1512, 1451, 1436, 1395, 1356, 1333, 1289, 1257, 1220, 1221, 1194, 1170, 1127, 1068, 1024, 988, 936, 860, 820, 814, 772, 728, 704, 666 cm⁻¹; HRMS (ESI+) *m/z* calc for [C₁₂H₁₂O₂ + H]⁺, 189.0910; found, 189.0909.

8-Hydroxy-3-(4-nitrophenyl)-2H-cyclohepta[b]furan-2-one **355**

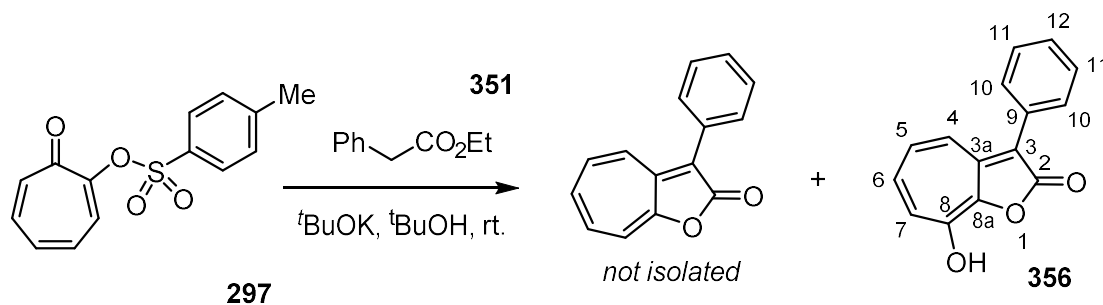


The preparation of this compound was based on a method by Nozoe.¹⁹⁷ At 0 °C, to a stirred suspension of 7-oxocyclohepta-1,3,5-trien-1-yl 4-methylbenzene-1-sulfonate **297** (690 mg, 2.50 mmol, 1.00 eq.) and ethyl 4-nitrophenylacetate **350** (1.04 g, 5.00 mmol, 2.00 eq.) in ethanol (7.5 mL) was slowly added NaOEt solution (freshly prepared from Na metal (118 mg, 5.13 mmol, 2.05 eq.) and ethanol (5.0 mL)), instantly forming a deep purple mixture. The mixture was stirred at 0 °C for 1 h, then allowed to warm to r.t., before it was stirred for another 3 h, becoming brown/orange in colour. After allowing it to stand for 16 h, to the mixture was added water (25 mL), forming a solid precipitate that was then collected by filtration, washing with water. The solid was dissolved in DMF (20 mL), forming a purple solution, and to this was added HCl_(aq) (5 M, 10 mL), forming an orange suspension that was stored at 2 °C for 2 h. The mixture was then filtered, washing the collected precipitate with water to give the crude product, which was purified by recrystallisation (hot DMF, 60 mL) to produce 8-hydroxy-3-(4-nitrophenyl)-2H-cyclohepta[b]furan-2-one **355** (370 mg, 1.31 mmol, 52%) as an orange solid (m.p. >300 °C (dec.)); δ_{H} (500 MHz, DMSO-*d*₆) 11.93 (1H, br s, 8-OH), 8.30 (2H, d, *J* 8.9 Hz, 11-CH), 7.92 (2H, d, *J* 9.0 Hz, 10-CH), 7.91-7.88 (1H, m), 7.33-7.21 (3H, m); δ_{C} (126 MHz, DMSO-*d*₆) 166.1 (2-C), 145.0 (13-C), 141.8, 139.4 (9-C), 134.2, 132.7, 131.2, 128.3 (10-C), 127.8, 123.8 (11-C), 100.0 (3-C); ν_{max} (film) 3110, 1728, 1634, 1590, 1565, 1518, 1465, 1420, 1340, 1320, 1281,

1239, 1149, 1109, 1085, 1034, 1009, 934, 858, 811, 785, 758, 734, 713, 687, 674, 653 cm^{-1} ; HRMS (ESI-) m/z calc for $[\text{C}_{15}\text{H}_8\text{NO}_5]^-$, 282.0402; found, 282.0420.

Due to the limited solubility of **355**, some peaks in the ^{13}C -NMR data could not be observed, and HMBC spectrum was of limited quality. The signal at $\delta_{\text{C}} = 100.0$ ppm was apparent by HMBC, but not by ^{13}C -NMR.

8-Hydroxy-3-phenyl-2H-cyclohepta[b]furan-2-one **356**

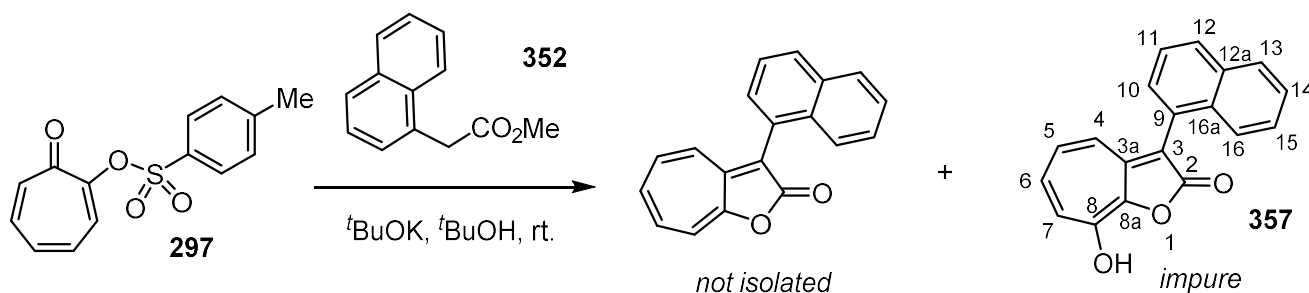


The preparation of this compound was based on a method by Nozoe.¹⁹⁷ At r.t., to a stirred suspension of 7-oxocyclohepta-1,3,5-trien-1-yl 4-methylbenzene-1-sulfonate **297** (690 mg, 2.50 mmol, 1.00 eq.) and ethyl phenylacetate **351** (800 μL , 4.88 mmol, 1.95 eq.) in *tert*-butanol (12.5 mL) was added a solution of potassium *tert*-butoxide (1.0 M in *tert*-butanol, 5.00 mL, 2.00 eq.), forming an orange/brown mixture, which was allowed to stir for 20 h. To the mixture was then added water (60 mL) and extracted with toluene (3 \times 40 mL). The combined organic extracts were washed with saturated brine, dried over anhydrous MgSO_4 and filtered. The filtrate was concentrated under reduced pressure to give 3-phenyl-2H-cyclohepta[b]furan-2-one as an inseparable mixture with ethyl phenylacetate **351**.

The aqueous layer was then concentrated under reduced pressure to remove toluene and *tert*-butanol. To this solution was added $\text{HCl}_{(\text{aq})}$ (5 M, 18 mL), forming a precipitate, which was stored at 2 $^{\circ}\text{C}$ for 1 h. The precipitate collected by filtration to give crude 8-hydroxy-3-phenyl-2H-cyclohepta[b]furan-2-one **356** (201 mg, 0.845 mmol, 34%) as a copper coloured solid, used without further purification; δ_{H} (500 MHz, $\text{DMSO}-d_6$) 11.47 (1H, br s, 8-OH), 7.66 (1H, d, J 11.3 Hz, 4-CH), 7.56 (2H, dd, J 8.2 Hz, 1.2 Hz, 10-CH), 7.46 (2H, t, J 7.5 Hz, 11-CH), 7.33 (1H, tt, J 7.5 Hz, 1.4 Hz, 12-CH), 7.11-7.15 (2H, m, 5,7-CH), 7.07-7.02 (1H, m, 6-CH); δ_{C} (126 MHz, $\text{DMSO}-d_6$) 166.7 (2-C), 145.2 (8-C), 144.7 (3a-C), 140.7 (8a-C), 133.2 (5-C or 7-C), 131.4

(6-C and 9-C), 130.2 (5-C or 7-C), 128.5 (11-C), 128.1 (10-C), 127.5 (4-C), 127.0 (12-C), 103.4 (3-C); $\nu_{\text{max}}(\text{film})$ 3049, 1765, 1702, 1633, 1593, 1576, 1536, 1497, 1466, 1444, 1398, 1318, 1302, 1276, 1226, 1166, 1101, 1078, 1061, 1027, 967, 930, 910, 866, 845, 816, 750, 736, 696, 677 cm^{-1} ; HRMS (ESI-) m/z calc for $[\text{C}_{15}\text{H}_9\text{O}_3]^-$, 237.0551; found, 237.0544.

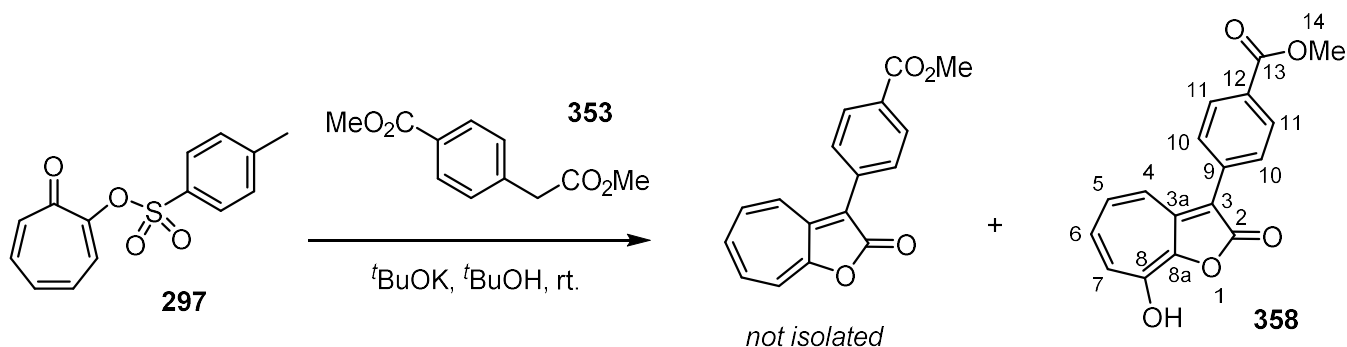
8-Hydroxy-3-(naphthalen-1-yl)-2H-cyclohepta[b]furan-2-one **357**



The preparation of this compound was based on a method by Nozoe.¹⁹⁷ At r.t., to a stirred suspension of 7-oxocyclohepta-1,3,5-trien-1-yl 4-methylbenzene-1-sulfonate **297** (690 mg, 2.50 mmol, 1.00 eq.) and methyl-1-naphthaleneacetate **352** (880 μL , 5.00 mmol, 2.00 eq.) in *tert*-butanol (7.5 mL) was added a solution of potassium *tert*-butoxide (1.0 M in *tert*-butanol, 5.00 mL, 2.00 eq.), forming an orange/brown mixture after 5 min. The mixture was allowed to stir for 24 h, and to it was added water (30 mL) and allowed to stir for 2 min, before concentrating under reduced pressure to remove any *tert*-butanol. The aqueous solution was extracted with toluene (2 \times 50 mL), and the combined organic extracts were discarded. To the aqueous layer was added $\text{HCl}_{(\text{aq})}$ (5 M, 20 mL), forming an orange/yellow precipitate. After storing at 2 $^{\circ}\text{C}$ for 2 h, the precipitate was collected by filtration, washing with water, giving crude 8-hydroxy-3-(naphthalen-1-yl)-2H-cyclohepta[b]furan-2-one **357** (398 mg, 1.38 mmol, 55%) as an orange solid, and was used without further purification (m.p. 225-230 $^{\circ}\text{C}$ (dec.)); δ_{H} (500 MHz, $\text{DMSO}-d_6$) 11.55 (1H, br s, 8-OH), 8.00 (2H, app tt, J 8.5 Hz, 1.0 Hz), 7.64-7.44 (6H, m), 7.21-7.16 (1H, m), 7.06-7.01 (2H, m); $\nu_{\text{max}}(\text{film})$ 3046, 1697, 1630, 1595, 1530, 1457, 1430, 1398, 1334, 1304, 1274, 1255, 1226, 1210, 1165, 1141, 1129, 1083, 1061, 1032, 1013, 981, 966, 865, 805, 792, 778, 762, 732, 681, 670 cm^{-1} ; HRMS (ESI+) m/z calc for $[\text{C}_{19}\text{H}_{12}\text{O}_3 + \text{H}]^+$, 289.0865; found, 289.0883.

Sample of compound **357** contained some impurity, making it difficult to correlate signals between ^1H -NMR and ^{13}C -NMR spectra, and therefore know which peaks in the ^{13}C -NMR spectrum correspond to the product.

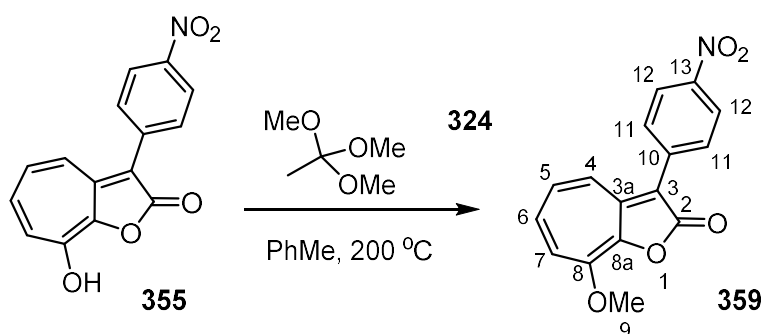
Methyl 4-(8-hydroxy-2-oxo-2H-cyclohepta[b]furan-3-yl)benzoate **358**



The preparation of this compound was based on a method by Nozoe.¹⁹⁷ At r.t., to a stirred suspension of 7-oxocyclohepta-1,3,5-trien-1-yl 4-methylbenzene-1-sulfonate **297** (690 mg, 2.50 mmol, 1.00 eq.) and methyl 4-(2-methoxy-2-oxoethyl)benzoate **353** (1.04 g, 5.00 mmol, 2.00 eq.) in *tert*-butanol (7.5 mL) was added a solution of potassium *tert*-butoxide (1.0 M in *tert*-butanol, 5.00 mL, 2.00 eq.), forming an viscous orange/brown mixture after 5 min. After allowing it to stir for 17 h, water (50 mL) was added to the mixture. The aqueous mixture was extracted with toluene (3 × 40 mL), and the combined organic extracts were discarded. The aqueous layer was concentrated under reduced pressure to remove residual toluene, and then to it was added HCl_(aq) (5 M, 18 mL), forming an orange suspension. The mixture was stored at 2 °C for 24 h, and then the precipitate was collected by filtration, washing with water, to give crude *methyl 4-(8-hydroxy-2-oxo-2H-cyclohepta[b]furan-3-yl)benzoate* **358** (526 mg, 1.77 mmol, 71%) as an orange solid, which was used without further purification (m.p. 280-284 °C (dec.)); δ_{H} (300 MHz, DMSO-*d*₆) 11.77 (1H, br s, 8-OH), 8.02 (2H, d, *J* 8.5 Hz, 11-CH), 7.81-7.74 (1H, m, 4-CH), 7.76 (2H, d, *J* 8.5 Hz, 10-CH), 7.27-7.12 (3H, m, 5,6,7-CH), 3.87 (3H, s, 14-CH₃); δ_{C} (75 MHz, DMSO-*d*₆) 166.3 (13-C), 166.0 (2-C), 146.6 (8-C), 145.2 (3a-C), 141.2 (8a-C), 136.8 (9-C), 134.0 (5-C or 6-C or 7-C), 132.2 (5-C or 6-C or 7-C), 130.6 (5-C or 6-C or 7-C),

129.4 (11-C), 128.0 (10-C), 127.8 (4-C), 127.4 (12-C), 101.6 (3-C), 52.2 (14-C);
 $\nu_{\text{max}}(\text{film})$ 3074, 1720, 1666, 1633, 1602, 1567, 1530, 1509, 1467, 1417, 1348, 1314,
1282, 1235, 1182, 1113, 1096, 1070, 1019, 970, 902, 873, 856, 821, 767, 756, 739,
711, 697, 688 cm^{-1} ; HRMS (ESI+) m/z calc for $[\text{C}_{17}\text{H}_{12}\text{O}_5 + \text{Na}]^+$, 319.0577; found,
319.0539.

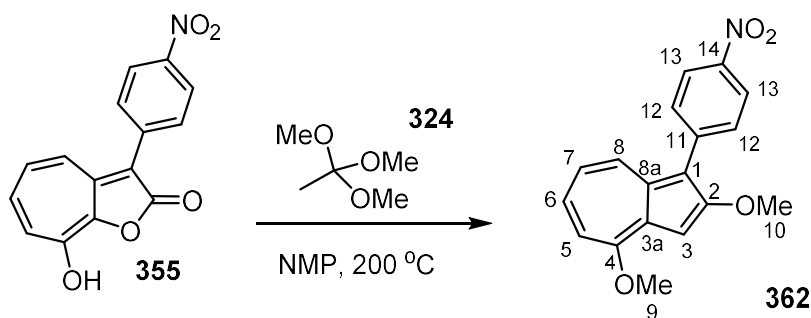
8-Methoxy-3-(4-nitrophenyl)-2H-cyclohepta[b]furan-2-one **359**



The preparation of this compound was based on a method by Pham.¹⁹⁸ Under atmosphere of air, a sealed tube charged with 8-hydroxy-3-(4-nitrophenyl)-2H-cyclohepta[b]furan-2-one **355** (200 mg, 0.706 mmol, 1.00 eq.), trimethyl orthoacetate **324** (1.50 mL) and toluene (1.50 mL) was heated under air at 200 °C, stirring for 3 h (CAUTION: the reaction was run behind a blast shield).. The mixture was allowed to cool to r.t., producing a maroon precipitate. The solid was collected by filtration, washing with DCM to produce 8-methoxy-3-(4-nitrophenyl)-2H-cyclohepta[b]furan-2-one **359** (139 mg, 0.467 mmol, 66%) as a fluffy maroon solid, which required no further purification (m.p. >300 °C (dec.)); δ_{H} (500 MHz, DMSO- d_6 , 70 °C) 8.30 (2H, d, J 8.9 Hz, 12-CH), 7.92 (2H, d, J 9.0 Hz, 11-CH), 7.93-7.90 (1H, m, 4-CH), 7.58 (1H, d, J 11.9 Hz, 7-CH), 7.39-7.35 (1H, m, 5-CH), 7.32-7.28 (1H, m, 6-CH), 4.11 (3H, s, 9-CH₃); δ_{C} (126 MHz, DMSO- d_6 , 70 °C) 147.4 (8-C), 145.6, 145.4, 144.4, 138.4 (10-C), 134.5 (5-C), 132.1 (6-C), 128.2 (11-C), 127.8 (4-C), 126.9 (7-C), 123.3 (12-C), 101.1 (3-C), 58.1 (9-C); ν_{max} (film) 3080, 2996, 1726, 1708, 1621, 1593, 1581, 1538, 1497, 1459, 1447, 1416, 1381, 1362, 1318, 1268, 1237, 1189, 1142, 1117, 1106, 1079, 1036, 968, 912, 872, 850, 821, 805, 780, 765, 744, 732, 710, 687 cm^{-1} ; HRMS (ESI+) m/z calc for [C₁₆H₁₁NO₅ + Na]⁺, 320.0535; found, 320.0513.

The solubility of **359** in DMSO- d_6 in the NMR tube, even at raised temperature, was limited, so therefore the carbonyl peak was absent from ^{13}C -NMR spectrum and assignments for quaternary carbons are tentative due to limited quality of the 2D NMR data.

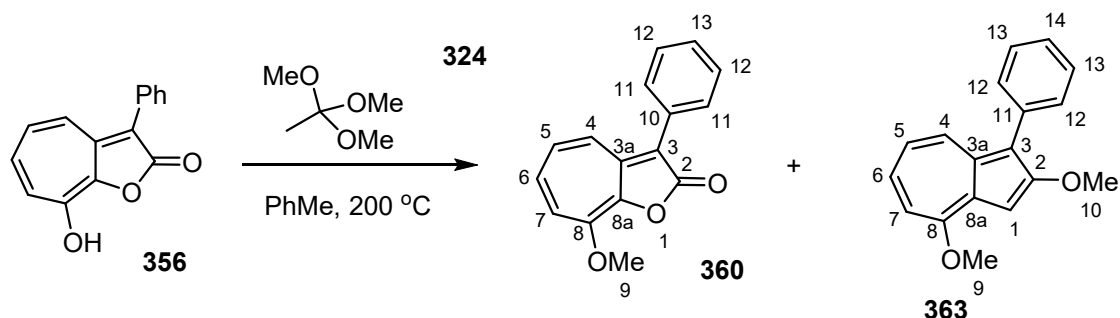
2,4-Dimethoxy-1-(4-nitrophenyl)azulene **362**



The preparation of this compound was based on methods by Pham and Hansen.²¹² Under atmosphere of air, a sealed tube charged with 8-hydroxy-3-(4-nitrophenyl)-2H-cyclohepta[b]furan-2-one **355** (200 mg, 0.706 mmol, 1.00 eq.), trimethyl orthoacetate **324** (1.50 mL) and *N*-methylpyrrolidone (1.50 mL) was stirred at 200 °C for 6 h, then allowed to cool to r.t. The mixture was diluted with ethyl acetate (20 mL), and then washed with water (4 × 10 mL) and with saturated brine. The organic layer was dried over anhydrous MgSO₄, and filtered. The filtrate was concentrated under reduced pressure. The crude product was dissolved in DCM (2 mL) and filtered through a pad of silica, washing through with petroleum ether/ethyl acetate (19:1), and concentrated under reduced pressure to give the crude product, which was purified by column chromatography (5→10% EtOAc in petroleum ether) to give 2,4-dimethoxy-1-(4-nitrophenyl)azulene **362** (13 mg, 0.420 mmol, 6.0%) as a red/brown solid (m.p. 196-199 °C); *R*_f 0.26 (4:1 petroleum ether/EtOAc); δ_{H} (300 MHz, CDCl₃) 8.31 (2H, d, *J* 9.0 Hz, 13-CH), 8.30 (1H, d, *J* 10.0 Hz, 8-CH), 7.78 (2H, d, *J* 9.0 Hz, 12-CH), 7.50 (1H, ddd, *J* 11.0 Hz, 10.0 Hz, 1.0 Hz, 6-CH), 7.20 (1H, s, 3-CH), 7.12 (1H, d, *J* 11.0 Hz, 5-CH), 7.11 (1H, t, *J* 9.5 Hz, 7-CH), 4.19 (3H, s, 9-CH₃), 4.11 (3H, s, 10-CH₃); δ_{C} (75 MHz, CDCl₃) 163.3 (2-C), 159.9 (4-C), 145.3 (14-C), 142.2 (11-C), 134.7 (8a-C), 132.7 (6-C), 132.3 (8-C), 130.7 (12-C), 128.6 (3a-C), 123.6 (13-C), 121.7 (7-C), 113.0 (1-C), 110.5 (5-C), 96.2 (3-C), 57.8 (10-C), 56.6 (9-C); ν_{max} (film)

2923, 2852, 1586, 1572, 1540, 1496, 1456, 1420, 1407, 1327, 1307, 1258, 1217, 1191, 1167, 1119, 1106, 1079, 1053, 996, 953, 882, 843, 822, 759, 745, 704, 682, 667 cm⁻¹; HRMS (ESI+) *m/z* calc for [C₁₈H₁₅NO₄ + Na]⁺, 332.0893; found, 332.0928.

8-methoxy-3-phenyl-2H-cyclohepta[b]furan-2-one 360 and 2,4-dimethoxy-1-phenylazulene 363

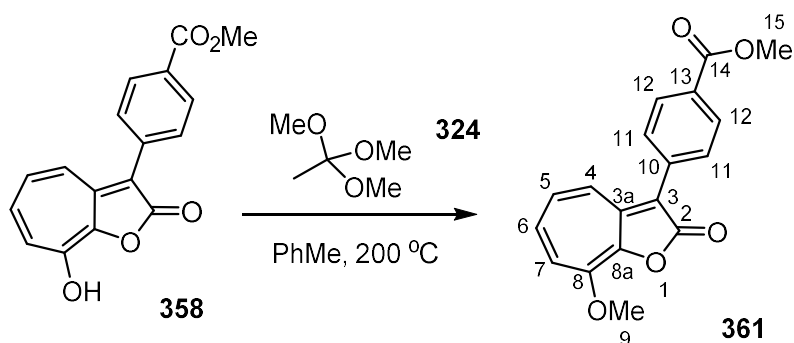


The preparation of this compound was based on a method by Pham.¹⁹⁸ Under atmosphere of air, a sealed tube charged with 8-hydroxy-3-phenyl-2H-cyclohepta[b]furan-2-one **356** (50 mg, 0.210 mmol, 1.00 eq.), trimethyl orthoacetate **324** (1.0 mL) and toluene (1.0 mL) was heated under air at 200 °C, stirring for 6.5 h (CAUTION: the reaction was run behind a blast shield). After cooling to r.t., a copper coloured fluffy precipitate of 8-methoxy-3-phenyl-2H-cyclohepta[b]furan-2-one **360** (21.5 mg, 0.0852 mmol, 41%) was collected by filtration, washing with toluene, and no further purification was required (m.p. 208-210 °C); R_f 0.37 (1:1 petroleum ether/EtOAc); δ_H (500 MHz, $CDCl_3$) 7.62-7.58 (3H, m, 4,11-CH), 7.44 (2H, t, J 7.8 Hz, 12-CH), 7.33 (1H, t, J 7.3 Hz, 13-CH), 7.00 (1H, d, J 12.2 Hz, 7-CH), 6.89 (1H, dd, J 11.2 Hz, 8.4 Hz, 5-CH), 6.80 (1H, dd, J 12.0 Hz, 8.4 Hz, 6-CH), 4.11 (3H, s, 9-CH₃); δ_C (126 MHz, $CDCl_3$) 167.4 (2-C), 145.4 (3a-C), 145.3 (8-C), 144.9 (8a-C), 132.4 (5-C), 130.9 (10-C), 129.8 (6-C), 128.7 (12-C), 128.4 (11-C), 128.2 (4-C), 128.1 (7-C), 127.6 (13-C), 107.4 (3-C), 59.4 (9-C); $\nu_{max}(\text{film})$ 3069, 2989, 2941, 2852, 1702, 1623, 1584, 1535, 1511, 1473, 1463, 1443, 1427, 1385, 1324, 1304, 1292, 1269, 1238, 1184, 1156, 1092, 1066, 1028, 999, 923, 904, 896, 861, 763, 745, 727, 703, 678 cm^{-1} ; HRMS (ESI+) m/z calc for $[C_{16}H_{13}O_3 + H]^+$, 253.0865; found, 253.0859.

The filtrate was concentrated under reduced pressure and purified by column chromatography (5→25% EtOAc in petroleum ether) and *2,4-dimethoxy-1-phenylazulene* **363** (1.6 mg, 0.00605 mmol, 2.8%) as a pale pink residue; R_f 0.68 (1:1 petroleum ether/EtOAc); δ_H (250 MHz, $CDCl_3$) 8.28 (1H, d, J 10.0 Hz), 7.61-7.28 (6H, m), 7.20 (1H, s), 7.05 (1H, d, J 11.0 Hz), 7.02 (1H, t, J 10.0 Hz), 4.17 (3H, s), 4.08 (3H, s); HRMS (ESI+) m/z *calc* for $[C_{18}H_{16}O_2 + H]^+$, 265.1229; found, 265.1218.

Insufficient quantity isolated to carry out further characterisation.

Methyl 4-(8-methoxy-2-oxo-2H-cyclohepta[b]furan-3-yl)benzoate **361**

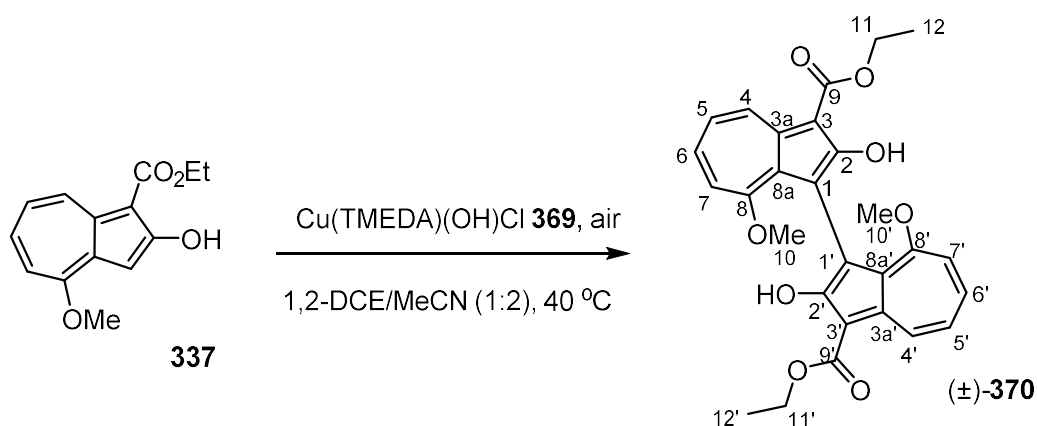


The preparation of this compound was based on a method by Pham.¹⁹⁸ Under atmosphere of air, a sealed tube charged with methyl 4-(8-hydroxy-2-oxo-2H-cyclohepta[b]furan-3-yl)benzoate **358** (100 mg, 0.337 mmol, 1.00 eq.), trimethyl orthoacetate **324** (1.0 mL) and toluene (1.0 mL) was heated at 200 °C, stirring for 5 h. The mixture was allowed to cool to r.t., producing a crimson coloured precipitate. The solid was collected by filtration, washing with toluene, giving *methyl 4-(8-methoxy-2-oxo-2H-cyclohepta[b]furan-3-yl)benzoate* **361** (40 mg, 0.129 mmol, 38%) as a fluffy crimson solid, used without further purification (m.p. 248-251 °C); δ_{H} (500 MHz, $\text{CDCl}_3/\text{CD}_3\text{OD}$ 1:1)* 7.95-7.93 (2H, m, 12-CH), 7.59 (1H, d, J 11.0 Hz, 4-CH), 7.54-7.52 (2H, m, 11-CH), 7.06 (1H, d, J 11.9 Hz, 7-CH), 6.98-6.87 (2H, m, 5,6-CH), 3.98 (3H, s, 9-CH₃), 3.77 (3H, s, 15-CH₃); δ_{C} (126 MHz, $\text{CDCl}_3/\text{CD}_3\text{OD}$ 1:1)* 167.5 (2-C), 167.0 (14-C), 146.9 (8-C), 146.0 (3a-C), 144.6 (8a-C), 135.8 (10-C), 133.2 (6-C), 131.1 (5-C), 129.6 (12-C), 128.4 (13-C), 128.2 (4-C), 127.9 (11-C), 127.0 (7-C), 105.9 (3-C), 58.5 (9-C), 51.9 (15-C); ν_{max} (film) 2958, 2849, 1789, 1740, 1717, 1625, 1608, 1591, 1567, 1543, 1520, 1504, 1453, 1425, 1413, 1375, 1316, 1280, 1259, 1233, 1184, 1171, 1149, 1102, 1078, 1019, 970, 955, 896, 870, 857, 822, 780, 757, 748, 733, 707, 686 cm^{-1} ; HRMS (ESI+) m/z calc for $[\text{C}_{18}\text{H}_{14}\text{O}_5 + \text{Na}]^+$, 333.0739; found, 333.0716.

* Residual CHCl_3 solvent peak calibrated at δ_{H} 7.26 ppm, δ_{C} 77.00 ppm.

(±)-3,3'-Diethyl 2,2'-dihydroxy-8,8'-dimethoxy-[1,1'-biazulene]-3,3'-dicarboxylate

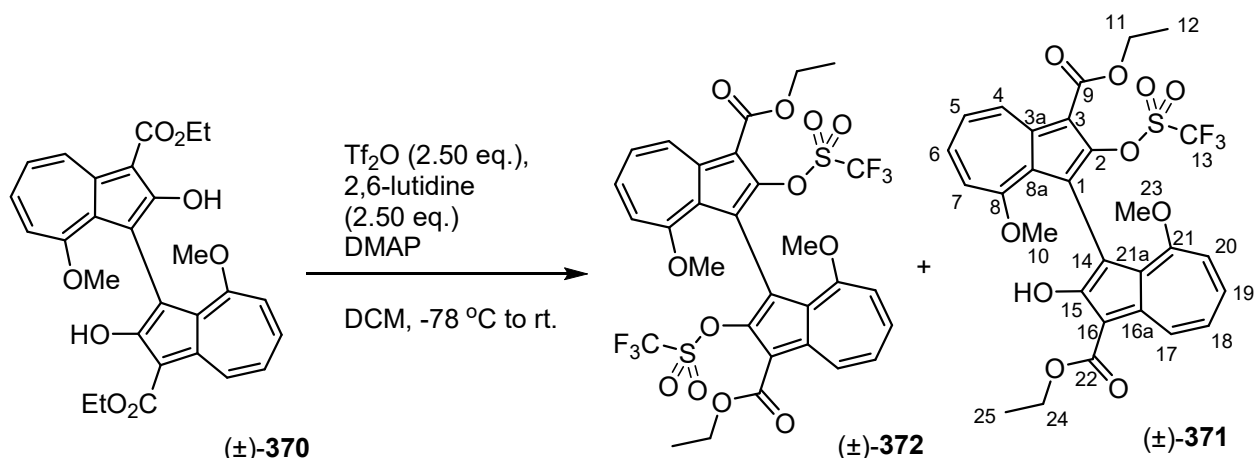
370



The preparation of this compound was based on a method by Kozłowski.²¹⁴ Under atmosphere of air, at r.t., to a stirred solution of ethyl 2-hydroxy-4-methoxyazulene-1-carboxylate **337** (2.20 g, 8.94 mmol, 1.00 eq.) in 1,2-dichloroethane (10 mL) and acetonitrile (20 mL) was added di-μ-hydroxo-bis[*N,N,N',N'*-tetramethylethylenediamine]copper(II) chloride **369** (208 mg, 0.894 mmol (by mol. weight of monomer), 0.10 eq.). The mixture was stirred at 40 °C for 89 h in a sealed vessel. After allowing to cool to r.t., the suspension was stored at −18 °C for 2 h, and the mixture was filtered, washing with cold CHCl_3 , to give (±)-3,3'-diethyl 2,2'-dihydroxy-8,8'-dimethoxy-[1,1'-biazulene]-3,3'-dicarboxylate **370** (1.08 g, 2.20 mmol, 49%) as a red solid. After storing the filtrate for an additional 3 days at −18 °C, a 2nd crop of product (124 mg, 0.252 mmol, 5.6%) was collected by filtration as a red solid (m.p. >300 °C (dec. ca. 233 °C)); δ_{H} (250 MHz, CDCl_3) 10.84 (2H, br s, 2,2'-OH), 9.03 (2H, d, J 9.5 Hz, 4,4'-CH), 7.41 (2H, t, J 10.2 Hz, 6,6'-CH), 7.21 (2H, t, J 10.0 Hz, 5,5'-CH), 6.93 (2H, d, J 10.5 Hz, 7,7'-CH), 4.60-4.50 (4H, m, 11,11'-CH₂), 3.58 (6H, s, 10,10'-CH₃), 1.52 (6H, t, J 7.0 Hz, 12,12'-CH₃); δ_{C} (75 MHz, CDCl_3) 169.1 (9,9'-C or 2,2'-C), 169.0 (9,9'-C or 2,2'-C), 163.0 (8,8'-C), 137.7 (3a,3a'-C), 132.3

(4,4'-C or 6,6'-C), 132.0 (4,4'-C or 6,6'-C), 130.4 (8a,8a'-C), 123.5 (5,5'-C), 111.9 (1,1'-C), 111.7 (7,7'-C), 98.0 (3,3'-C), 60.3 (11,11'-C), 56.5 (10,10'-C), 14.7 (12,12'-C); $\nu_{\text{max}}(\text{film})$ 2924, 2852, 1740, 1686, 1628, 1595, 1572, 1449, 1422, 1396, 1380, 1357, 1313, 1259, 1215, 1205, 1183, 1170, 1130, 1098, 1082, 1022, 957, 870, 838, 810, 789, 746, 725, 698 cm^{-1} ; HRMS (ESI+) m/z calc for $[\text{C}_{28}\text{H}_{26}\text{O}_8 + \text{Na}]^+$, 513.1525; found, 513.1551.

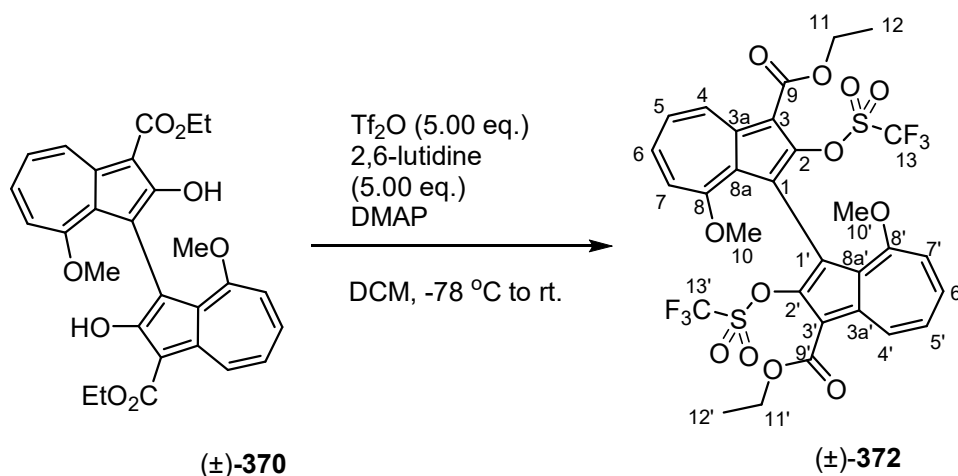
(±)-Diethyl 2-hydroxy-8,8'-dimethoxy-2'-(((trifluoromethyl)sulfonyl)oxy)-[1,1'-biazulene]-3,3'-dicarboxylate **371**



The preparation of this compound was based on a method by Mikami.²¹⁵ At $-78\text{ }^\circ\text{C}$, to a stirred suspension of **(±)-3,3'-diethyl 2,2'-dihydroxy-8,8'-dimethoxy-[1,1'-biazulene]-3,3'-dicarboxylate 370** (200 mg, 0.408 mmol, 1.00 eq.), 4-(dimethylamino)pyridine (10 mg, 0.0816 mmol, 0.20 eq.) and 2,6-lutidine (120 μL , 1.02 mmol, 2.50 eq.) in DCM (10.0 mL) was added dropwise trifluoromethanesulfonic anhydride (170 μL , 1.01 mmol, 2.48 eq.), and the mixture was stirred at $-78\text{ }^\circ\text{C}$ for 4 h. The reaction was allowed to warm to r.t., stirred for another 17 h, and to it was added water (5.0 mL) to quench, stirring for 10 min. The mixture was diluted with DCM (30 mL), and the phases were separated. The organic layer was washed further with water ($2 \times 20\text{ mL}$), dried over anhydrous MgSO_4 , and filtered. The filtrate was concentrated under reduced pressure to give the crude product, which was purified by column chromatography to give **(±)-3,3'-diethyl 8,8'-dimethoxy-2,2'-bis(trifluoromethanesulfonyloxy)-[1,1'-biazulene]-3,3'-dicarboxylate 372** (121 mg, 0.160 mmol, 39%) and **(±)-diethyl 2-hydroxy-8,8'-dimethoxy-2'-(((trifluoromethyl)sulfonyl)oxy)-[1,1'-biazulene]-3,3'-dicarboxylate 371** (106 mg, 0.170

mmol, 42%) as a red/brown solid (m.p. 128-131 °C); R_f 0.40 (1:1 petroleum ether/EtOAc); δ_H (300 MHz, $CDCl_3$) 10.87 (1H, s, 15-OH), 9.72 (1H, d, J 10.0 Hz, 4-CH), 9.06 (1H, d, J 9.5 Hz, 17-CH), 7.72 (1H, t, J 10.5 Hz, 6-CH), 7.44 (1H, t, J 10.5 Hz, 19-CH), 7.34 (1H, t, J 10.0 Hz, 5-CH), 7.26 (1H, t, J 10.0 Hz, 18-CH), 7.08 (1H, d, J 11.0 Hz, 7-CH), 6.98 (1H, d, J 10.5 Hz, 20-CH), 4.54 (2H, q, J 7.0 Hz, 24-CH₂), 4.57-4.42 (2H, m, 11-CH₂), 3.66 (3H, s, 10-CH₃), 3.60 (3H, s, 23-CH₃), 1.54 (3H, t, J 7.0 Hz, 12-CH₃ or 25-CH₃), 1.45 (3H, t, J 7.0 Hz, 12-CH₃ or 25-CH₃); δ_C (75 MHz, $CDCl_3$) 169.4 (15-C), 169.0 (22-C), 167.4 (8-C), 164.0 (9-C), 162.6 (21-C), 149.5 (2-C), 139.7 (4-C), 138.4 (6-C), 137.7 (16a-C), 136.4 (3a-C), 132.6 (17-C), 132.3 (19-C), 130.3 (21a-C), 125.8 (8a-C), 123.8 (5-C or 18-C), 123.7 (5-C or 18-C), 118.0 (d, $^1J_{CF}$ 321.0 Hz, 13-C), 114.8 (1-C), 112.9 (7-C), 111.9 (20-C), 109.8 (14-C), 106.5 (3-C), 97.8 (16-C), 60.4 (11-C or 24-C), 60.3 (11-C or 24-C), 56.6 (10-C), 56.2 (23-C), 14.6 (12-C or 25-C), 14.3 (12-C or 25-C); $\nu_{max}(\text{film})$ 2989, 2940, 2849, 1698, 1633, 1596, 1570, 1518, 1476, 1456, 1420, 1402, 1385, 1321, 1309, 1266, 1237, 1210, 1195, 1133, 1082, 1058, 1018, 953, 928, 865, 835, 788, 765, 731, 697, 682 cm^{-1} ; HRMS (ESI+) m/z calc for $[C_{29}H_{25}F_3O_{10}S + Na]^+$, 645.1018; found, 645.1032.

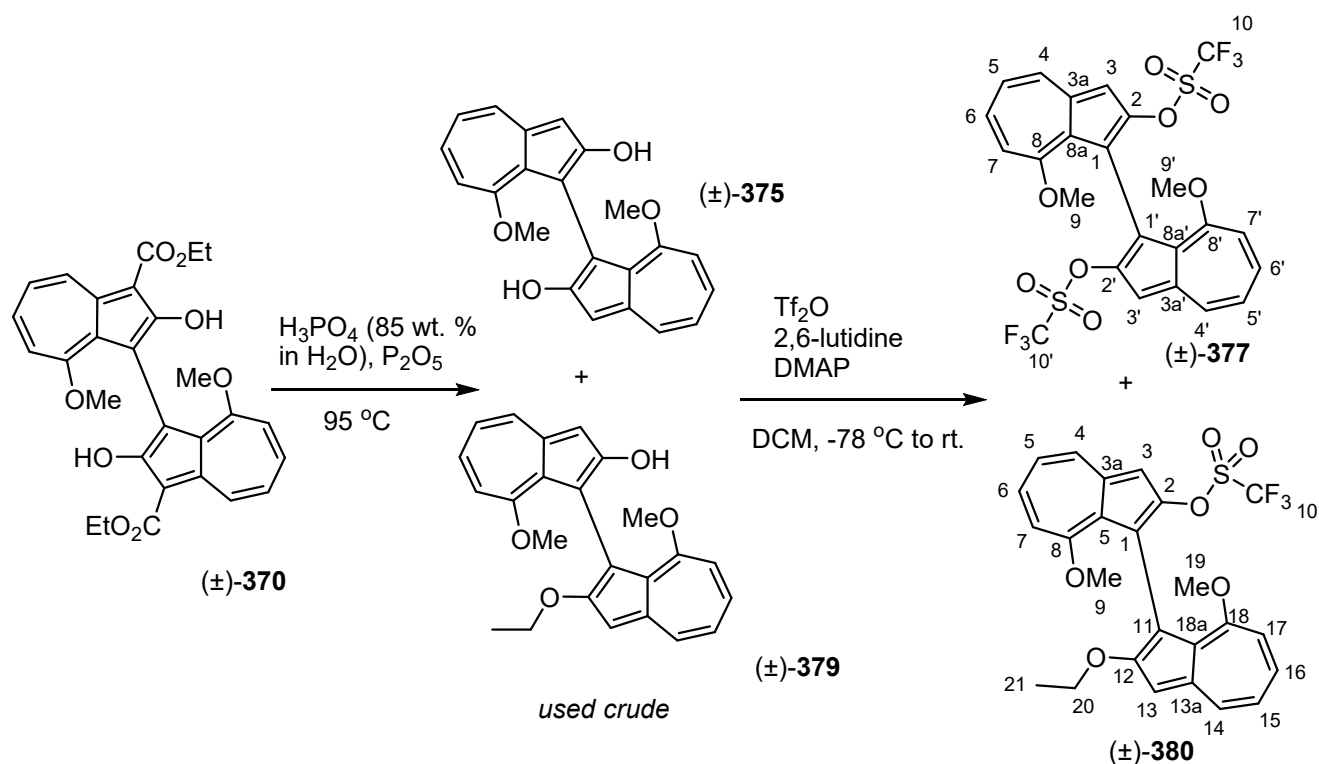
(±)-3,3'-Diethyl 8,8'-dimethoxy-2,2'-bis(trifluoromethanesulfonyloxy)-[1,1'-biazulene]-3,3'-dicarboxylate **372**



The preparation of this compound was based on a method by Mikami.²¹⁵ At $-78\text{ }^\circ\text{C}$, to a stirred suspension of 3,3'-diethyl 2,2'-dihydroxy-8,8'-dimethoxy-[1,1'-biazulene]-3,3'-dicarboxylate **370** (200 mg, 0.408 mmol, 1.00 eq.), 4-(dimethylamino)pyridine (10 mg, 0.0816 mmol, 0.20 eq.) and 2,6-lutidine (240 μL , 2.07 mmol, 5.06 eq.) in DCM (10.0 mL) was added trifluoromethanesulfonic anhydride (170 μL , 1.01 mmol, 2.46 eq.). The mixture temperature was maintained at $-78\text{ }^\circ\text{C}$ for 5 h. To it was then added trifluoromethanesulfonic anhydride (170 μL , 1.01 mmol, 2.46 eq.), the mixture was allowed to warm to r.t. in dry ice/acetone bath. After stirring for an additional 17 h, water (5.0 mL) was added slowly, and allowed to stir for 5 min. The mixture was diluted with DCM (30 mL), and the two phases were separated. The organic phase was washed further with water ($3 \times 15\text{ mL}$), dried over anhydrous MgSO_4 , and filtered. The filtrate was concentrated under reduced pressure to give the crude product, which was purified by column chromatography (10 \rightarrow 50% EtOAc in petroleum ether) to give (±)-3,3'-diethyl 8,8'-dimethoxy-2,2'-bis(trifluoromethanesulfonyloxy)-[1,1'-biazulene]-3,3'-dicarboxylate **372** (145 mg, 0.193 mmol, 47%) as a magenta solid (m.p. $183\text{--}185\text{ }^\circ\text{C}$); R_f 0.23 (1:1 petroleum

ether/EtOAc); δ_{H} (500 MHz, CDCl_3) 9.81 (2H, dd, J 10.2 Hz, 1.1 Hz, 4,4'-CH), 7.81 (2H, ddd, J 10.9 Hz, 9.7 Hz, 1.1 Hz, 6,6'-CH), 7.43 (2H, t, J 9.8 Hz, 5,5'-CH), 7.14 (2H, d, J 11.1 Hz, 7,7'-CH), 4.51 (4H, q, J 7.0 Hz, 11,11'-CH₂), 3.61 (6H, s, 10,10'-CH₃), 1.47 (6H, t, J 7.1 Hz, 12,12'-CH₃); δ_{C} (126 MHz, CDCl_3) 167.2 (8,8'-C), 163.8 (9,9'-C), 149.4 (2,2'-C), 140.1 (4,4'-C), 138.7 (6,6'-C), 136.6 (3a,3a'-C), 126.4 (8a,8a'-C), 124.2 (5,5'-C), 117.9 (q, $^1J_{\text{CF}}$ 321.0 Hz, 13,13'-C) 113.0 (7,7'-C), 112.6 (1,1'-C), 106.8 (3,3'-C), 60.5 (11,11'-C), 56.6 (10,10'-C), 14.3 (12,12'-C); ν_{max} (film) 2924, 2851, 1690, 1598, 1570, 1516, 1458, 1412, 1391, 1316, 1268, 1191, 1135, 1086, 1048, 1021, 954, 923, 875, 846, 832, 805, 790, 759, 726, 690 cm^{-1} ; HRMS (ESI+) m/z calc for $[\text{C}_{30}\text{H}_{24}\text{F}_6\text{O}_{12}\text{S}_2 + \text{Na}]^+$, 777.0511; found, 777.0513.

(±)-8,8'-Dimethoxy-2'-(trifluoromethanesulfonyloxy)-[1,1'-biazulene]-2-yl trifluoromethanesulfonate **377 and (±)-2'-ethoxy-8,8'-dimethoxy-[1,1'-biazulen]-2-yl trifluoromethanesulfonate **380****



The preparation of this compound was based on methods by Ito¹⁹⁴ and Mikami.²¹⁵ Under atmosphere of air, at $0\text{ }^\circ\text{C}$, to phosphorus pentoxide (800 mg) was added $\text{H}_3\text{PO}_{4(\text{aq})}$ (85 wt. %, 1.20 mL). The mixture was then stirred at $95\text{ }^\circ\text{C}$, and to it was added **(±)-3,3'-diethyl 2,2'-dihydroxy-8,8'-dimethoxy-[1,1'-biazulene]-3,3'-dicarboxylate **370**** (200 mg, 0.408 mmol, 1.00 eq.), stirred for 2 h, and then allowed to cool to r.t. To the resultant slurry was slowly added water (20 mL), and extracted with DCM ($2 \times 25\text{ mL}$). The organic extracts were combined and washed with saturated aqueous NaHCO_3 (20 mL) and water ($2 \times 20\text{ mL}$). The organic layer was then dried over anhydrous MgSO_4 , and filtered. The filtrate was concentrated under reduced pressure to give the crude intermediate mixture as a maroon oil. Under

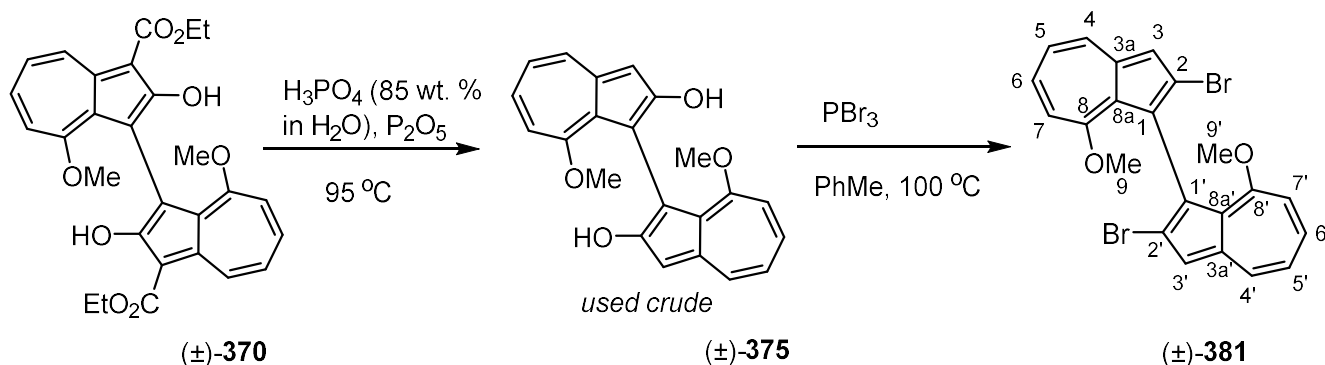
atmosphere of N₂, at –78 °C, to a stirred solution of the crude diol, 4-(dimethylamino)pyridine (10 mg, 0.0816 mmol, 0.20 eq.) and 2,6-lutidine (250 µL, 2.15 mmol, 5.27 eq.) in DCM (20 mL) was added dropwise trifluoromethanesulfonic anhydride (170 µL, 1.01 mmol, 2.47 eq.), and the mixture was allowed to stir at –78 °C for 45 min. To this was then added trifluoromethanesulfonic anhydride (170 µL, 1.01 mmol, 2.47 eq.), and stirred at –78 °C for another 45 min. The mixture was allowed to warm to r.t., and to it was added water (20 mL), allowing to stir for 10 min, and then the phases were separated. The aqueous layer was extracted with DCM (60 mL), and the combined organic extracts were washed with water (2 × 20 mL), dried over anhydrous MgSO₄, and filtered. The filtrate was concentrated under reduced pressure to give the crude product, which was purified by column chromatography (10→50% EtOAc in petroleum ether) to give (±)-8,8'-dimethoxy-2'-(trifluoromethanesulfonyloxy)-[1,1'-biazulene]-2-yl trifluoromethanesulfonate **377** (110 mg, 0.181 mmol, 44%) as a purple crystalline solid (m.p. 174-176 °C); R_f 0.19 (4:1 petroleum ether/EtOAc); δ_H (500 MHz, CDCl₃) 8.28 (2H, d, *J* 9.2 Hz, 4,4'-CH), 7.59 (2H, td, *J* 11.0 Hz, 9.8 Hz, 1.2 Hz, 6,6'-CH), 7.21 (2H, s, 3,3'-CH), 7.08 (2H, t, *J* 9.5 Hz, 5,5'-CH), 6.91 (2H, d, *J* 11.0 Hz, 7,7'-CH), 3.69 (6H, s, 9-CH₃); δ_C (126 MHz, CDCl₃) 165.6 (8,8'-C), 150.0 (2,2'-C), 139.1 (4,4'-C), 136.6 (6,6'-C), 136.3 (3a,3a'-C), 122.1 (8a,8a'-C), 120.3 (5,5'-C), 118.4 (d, ¹*J*_{CF} 320.4 Hz, 10,10'-C), 112.4 (1,1'-C), 109.6 (7,7'-C), 105.2 (3,3'-C), 56.3 (9,9'-C); ν_{max}(film) 3015, 2939, 2844, 1597, 1568, 1523, 1482, 1457, 1441, 1411, 1382, 1265 1241, 1230, 1196, 1181, 1162, 1078, 1004, 958, 916, 875, 822, 788, 781, 764, 745, 725, 690, 679 cm⁻¹; HRMS (ESI+) *m/z* calc for [C₂₄H₁₆F₆O₄S₂ + H]⁺, 611.0264; found, 611.0277.

From the column was also isolated (±)-2'-ethoxy-8,8'-dimethoxy-[1,1'-biazulen]-2-yl trifluoromethanesulfonate **380** (10 mg, 0.0197 mmol, 4.8%) as a pale purple solid

(m.p. 127-130 °C); R_f 0.23 (4:1 petroleum ether/EtOAc); δ_H (500 MHz, $CDCl_3$) 8.23 (1H, d, J 9.6 Hz, 4-CH), 8.01 (1H, d, J 9.1 Hz, 14-CH), 7.51 (1H, ddd, J 11.0 Hz, 9.8 Hz, 1.2 Hz, 6-CH), 7.28 (1H, ddd, J 10.8 Hz, 10.0 Hz, 1.0 Hz, 16-CH), 7.19 (1H, s, 3-CH), 7.00 (1H, t, J 9.6 Hz, 5-CH), 6.96 (1H, t, J 9.6 Hz, 15-CH), 6.82 (1H, d, J 11.0 Hz, 7-CH), 6.77 (1H, d, J 10.7 Hz, 17-CH), 6.70 (1H, s, 13-CH), 4.23 (2H, q, J 7.0 Hz, 20-CH₂), 3.60 (3H, s, 9-CH₃), 3.53 (3H, s, 19-CH₃), 1.32 (3H, t, J 7.0 Hz, 21-CH₃); δ_C (126 MHz, $CDCl_3$) 166.2 (8-C), 164.7 (12-C), 161.3 (18-C), 150.2 (2-C), 139.9 (13a-C), 138.7 (4-C), 136.2 (6-C), 136.1 (3a-C), 131.8 (14-C), 130.4 (16-C), 124.3 (18a-C), 122.4 (8a-C), 119.7 (15-C), 119.5 (5-C), 118.4 (q, $^1J_{CF}$ 321 Hz, 10-C), 115.9 (1-C), 111.6 (11-C), 109.3 (7-C), 108.6 (17-C), 105.5 (3-C), 97.3 (13-C), 65.6 (20-C), 56.23 (9-C or 19-C), 56.19 (9-C or 19-C), 14.8 (21-C); $\nu_{max}(\text{film})$ 2985, 2935, 2849, 1594, 1567, 1518, 1494, 1456, 1408, 1387, 1359, 1261, 1243, 1202, 1187, 1163, 1137, 1116, 1100, 1041, 1006, 974, 942, 887, 843, 827, 784, 767, 728, 707, 684, 662 cm^{-1} ; HRMS (ESI+) m/z calc for $[C_{25}H_{21}F_3O_6S + Na]^+$, 529.0903; found, 529.0912.

In a separate experiment under similar conditions, the desired product (\pm)-8,8'-dimethoxy-2'-(trifluoromethanesulfonyloxy)-[1,1'-biazulene]-2-yl trifluoromethanesulfonate **377** was isolated in an increased yield (168 mg, 0.274 mmol, 52%), with only a trace of side product (\pm)-2'-ethoxy-8,8'-dimethoxy-[1,1'-biazulen]-2-yl trifluoromethanesulfonate **380**.

(±)-2,2'-Dibromo-8,8'-dimethoxy-1,1'-biazulene 381



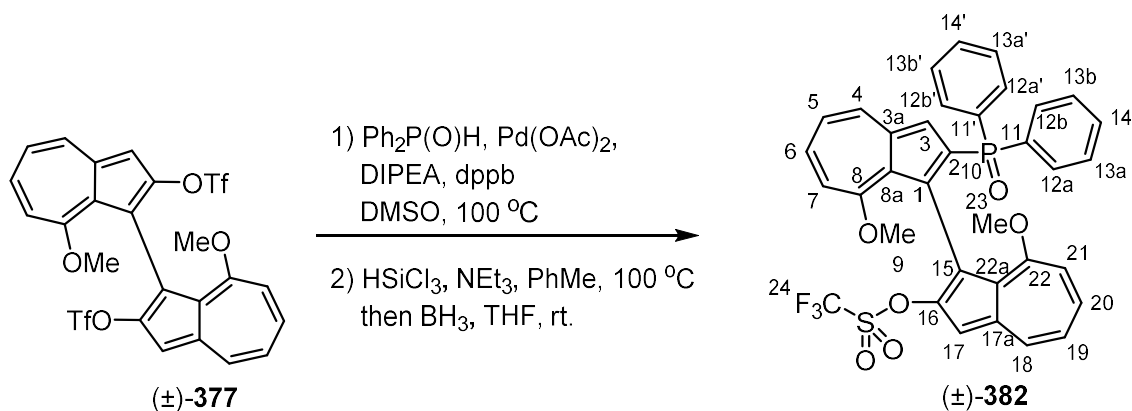
The preparation of this compound was based on methods by Ito.^{194,210} Under atmosphere of air, at 95 °C, to a stirred mixture of phosphorus pentoxide (800 mg) in H₃PO_{4(aq)} (85 wt. %, 1.20 mL) was added (±)-3,3'-diethyl 2,2'-dihydroxy-8,8'-dimethoxy-[1,1'-biazulene]-3,3'-dicarboxylate **370** (200 mg, 0.408 mmol, 1.00 eq.). The mixture was stirred at 95 °C for 30 min, and then allowed to cool to r.t. To the resultant slurry was slowly added water (20 mL), and the aqueous mixture was extracted with DCM (2 × 20 mL). The organic extracts were combined and washed with saturated aqueous NaHCO₃ (20 mL) and water (3 × 20 mL). The organic phase was then dried over anhydrous MgSO₄, and filtered. The filtrate was concentrated under reduced pressure to give the crude (±)-8,8'-dimethoxy-[1,1'-biazulene]-2,2'-diol **375** as a maroon oil. Under atmosphere of N₂, at r.t., to a stirred solution of the crude diol in toluene (12.5 mL) was added phosphorus tribromide (400 µL, 4.22 mmol, 10.3 eq.). The mixture was then heated at 110 °C for 9 h, and allowed to cool to r.t. The excess reagent was quenched by the addition of water (20 mL) and the mixture was extracted with ethyl acetate (40 mL). The organic extract was washed with water (3 × 15 mL), dried over anhydrous MgSO₄, and filtered. The filtrate was concentrated under reduced pressure to give the crude product, which was purified by column chromatography (10→25% EtOAc in petroleum ether) to yield (±)-2,2'-dibromo-8,8'-

dimethoxy-1,1'-biazulene **381** (34 mg, 0.0709 mmol, 17%) as a purple solid (m.p. 187-189 °C); R_f 0.23 (4:1 petroleum ether/EtOAc); δ_H (500 MHz, $CDCl_3$) 8.18 (2H, d, J 9.5 Hz, 4,4'-CH), 7.49 (2H, ddd, J 11.0 Hz, 9.9 Hz, 1.2 Hz, 6,6'-CH), 7.41 (2H, s, 3,3'-CH), 6.96 (2H, t, J 9.6 Hz, 5,5'-CH), 6.79 (2H, d, J 11.1 Hz, 7,7'-CH), 3.56 (6H, s, 9,9'-CH₃); δ_C (126 MHz, $CDCl_3$)* 163.2 (8,8'-C), 138.7 (2,2'-C), 136.2 (4,4'-C), 135.5 (6,6'-C), 127.7 (3a,3a'-C), 126.4 (8a,8a'-C), 123.9 (1,1'-C), 119.2 (5,5'-C), 118.9 (7,7'-C), 109.5 (3,3'-C), 56.6 (9,9'-C); $\nu_{max}(\text{film})$ 2929, 2852, 1592, 1562, 1523, 1487, 1450, 1397, 1376, 1358, 1256, 1211, 1190, 1173, 1154, 1012, 940, 877, 793, 752, 720, 668, 632 cm^{-1} ; HRMS (ESI+) m/z calc for $[C_{22}H_{16}Br_2O_2 + Na]^+$, 492.9409; found, 492.9466.

* carbon atoms are assigned tentatively, due to lack of 2D spectra obtained for compound **381**.

(±)-2'-(Diphenylphosphoryl)-8,8'-dimethoxy-[1,1'-biazulen]-2-yl

trifluoromethanesulfonate 382

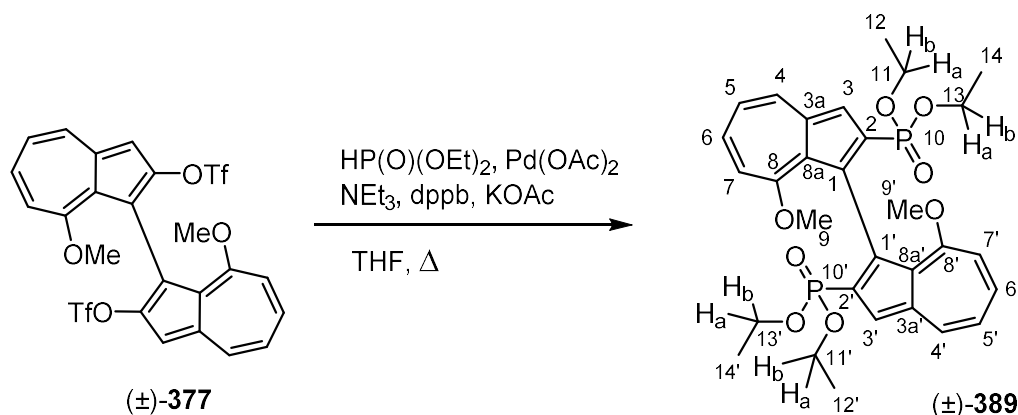


The preparation of this compound was based on a method by Zhang.²⁰⁹ At r.t., to a mixture of diphenylphosphine oxide (50 mg, 0.245 mmol, 3.00 eq.), palladium diacetate (2.0 mg, 0.0082 mmol, 0.10 eq.) and 1,4-bis(diphenylphosphino)butane (3.5 mg, 0.0082 mmol, 0.10 eq.) was added a solution of (±)-8,8'-dimethoxy-2'-(trifluoromethanesulfonyloxy)-[1,1'-biazulene]-2-yl trifluoromethanesulfonate **377** (50 mg, 0.0819 mmol, 1.00 eq.) in DMSO (degassed by freeze-thaw-pump, 1.0 mL), and allowed to stir for 10 min. To the mixture was then added *N,N*-diisopropylethylamine (60 μL , 0.345 mmol, 4.21 eq.), stirred at 100 °C for 41 h, and then allowed to cool to r.t. The mixture was diluted with ethyl acetate (20 mL), washed with water (4 \times 10 mL) and with saturated brine. The organic layer was then dried over anhydrous MgSO_4 , and filtered. The filtrate was concentrated under reduced pressure to give the crude product, which could not be completely purified by column chromatography (0 \rightarrow 5% MeOH in DCM). At 0 °C, to a stirred solution of the impure product (23 mg, <0.0328 mmol, 1.00 eq.) and triethylamine (50 μL , 0.358 mmol, 11.0 eq.) in toluene (degassed by freeze-thaw-pump, 1.0 mL) was added dropwise trichlorosilane (30 μL , 0.291 mmol, 8.90 eq.). The mixture was then stirred at 100 °C for 19 h, allowed to

cool to r.t., and then to this was added borane-THF complex (1.0 M in THF, 70 μ L, 0.070 mmol, 2.10 eq.), and stirred for 1 h. The mixture was then quenched by the addition of MeOH (1.0 mL), diluted with DCM (10 mL) and washed with water (3 \times 10 mL). The organic layer was dried over anhydrous MgSO₄, and filtered. The filtrate was concentrated under reduced pressure to give the crude product, which was purified by column chromatography (0 \rightarrow 2% MeOH in DCM) to give (\pm)-2'-(diphenylphosphoryl)-8,8'-dimethoxy-[1,1'-biazulen]-2-yl trifluoromethanesulfonate **382** (8.1 mg, 0.0122 mmol, 15% overall) as a deep blue solid (m.p. 125-130 $^{\circ}$ C); R_f 0.22 (19:1 DCM/MeOH); δ_H (500 MHz, CDCl₃) 8.26 (1H, d, J 9.3 Hz, 4-CH), 7.96 (1H, d, J 9.5 Hz, 18-CH), 7.70 (1H, dd, J 11.8 Hz, 1.3 Hz, 12a-CH or 12a'-CH), 7.68 (1H, dd, J 11.8 Hz, 1.4 Hz, 12a-CH or 12a'-CH), 7.56 (1H, d, $^3J_{PH}$ 6.2 Hz, 3-CH), 7.56 (1H, ddd, J 11.0 Hz, 9.6 Hz, 1.1 Hz, 6-CH) 7.45 (1H, ddd, J 10.9 Hz, 9.8 Hz, 1.2 Hz, 20-CH), 7.44-7.42 (1H, m, 14-CH), 7.38-7.34 (2H, m, 13a,13a'-CH), 7.03 (1H, dd, J 12.2 Hz, 1.3 Hz, 12b-CH or 12b'-CH) 7.02 (1H, dd, J 12.2 Hz, 1.4 Hz, 12b-CH or 12b'-CH), 7.01-6.97 (1H, m, 14'-CH), 6.93 (1H, t, J 9.5 Hz, 5-CH) 6.91 (1H, t, J 9.5 Hz, 19-CH), 6.87-6.83 (2H, m, 13a',13b'-CH), 6.73 (1H, d, J 11.3 Hz, 7-CH) 6.71 (1H, d, J 11.2 Hz, 21-CH), 6.64 (1H, s, 17-CH), 3.57 (3H, s, 23-CH₃), 3.53 (3H, s, 9-CH₃); δ_C (126 MHz, CDCl₃) 167.0 (8-C), 166.0 (22-C), 148.8 (16-C), 140.8 (4-C), 138.9 (6-C), 138.6 (d, $^3J_{CP}$ 15.9 Hz, 3a-C), 138.3 (18-C), 136.9 (d, $^1J_{CP}$ 110.0 Hz, 2-C), 136.2 (20-C), 135.7 (17a-C), 135.0 (d, $^1J_{CP}$ 105.1 Hz, 11-C), 133.0 (d, $^1J_{CP}$ 105.7 Hz, 11'-C), 131.9 (d, $^2J_{CP}$ 9.5 Hz, 12a,12a'-C), 131.0 (d, $^4J_{CP}$ 2.8 Hz, 14-C), 130.4 (d, $^2J_{CP}$ 9.9 Hz, 12b,12b'-C), 129.7 (d, $^4J_{CP}$ 2.9 Hz, 14'-C), 127.9 (d, $^3J_{CP}$ 11.7 Hz, 13a,13a'-C), 127.0 (d, $^3J_{CP}$ 12.3 Hz, 13b,13b'-C), 126.0 (d, $^2J_{CP}$ 11.9 Hz, 3-C), 125.7 (d, $^2J_{CP}$ 11.8 Hz, 1-C), 125.0 (d, $^3J_{CP}$ 12.0 Hz, 8a-C), 122.9 (22a-C), 119.3 (19-C), 118.8 (5-C), 118.4 (q, $^1J_{CF}$ 322 Hz, 24-C), 116.5 (15-C), 109.9 (21-C), 108.6 (7-C),

103.6 (17-C), 56.3 (9-C or 23-C), 56.2 (9-C or 23-C); δ_P (202 MHz, $CDCl_3$) 23.0 (10-P); $\nu_{max}(\text{film})$ 2924, 2859, 1667, 1597, 1561, 1525, 1455, 1264, 1209, 1163, 1143, 950, 887, 807, 721, 698 cm^{-1} ; HRMS (ESI+) m/z calc for $[C_{35}H_{26}F_3O_6PS + H]^+$, 663.1213; found 663.1197.

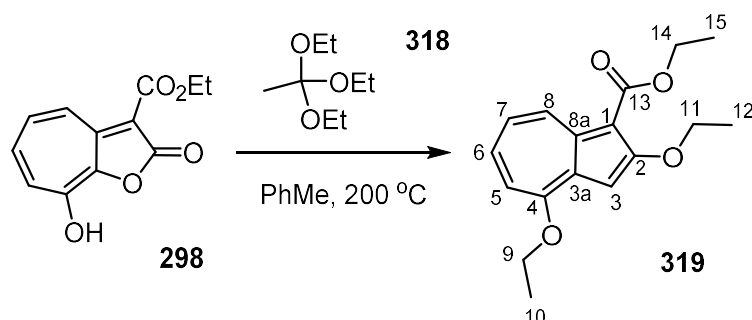
(±)-Diethyl (2'-(diethoxyphosphoryl)-8,8'-dimethoxy-[1,1'-biazulene]-2-yl)phosphonate **389**



The preparation of this compound was based on a method by Stawinski.²¹⁹ A mixture of palladium diacetate (5.5 mg, 0.0246 mmol, 0.10 eq.), 1,4-bis(diphenylphosphino)butane (21 mg, 0.0492 mmol, 0.20 eq.), potassium acetate (24 mg, 0.246 mmol, 1.00 eq.) was dissolved in THF (0.5 mL) and stirred at 60 °C for 30 min. To the mixture was then added triethylamine (100 μL , 0.738 mmol, 3.00 eq.), diethyl phosphite (100 μL , 0.738 mmol, 3.00 eq.) and a solution of (±)-8,8'-dimethoxy-2'-(trifluoromethanesulfonyloxy)-[1,1'-biazulene]-2-yl trifluoromethanesulfonate **377** (150 mg, 0.246 mmol, 1.00 eq.) in THF (1.5 mL), and heated at 68 °C for 45 h. After allowing to cool to r.t., the mixture was concentrated under reduced pressure and purified by column chromatography (0→10% MeOH in DCM) to give the crude product. After dissolving in ethyl acetate (20 mL), washing with water (5 × 10 mL) and with saturated brine, the solution was concentrated under reduced pressure to give (±)-diethyl [2'-(diethoxyphosphoryl)-8,8'-dimethoxy-[1,1'-biazulene]-2-yl]phosphonate **389** (56 mg, 0.0958 mmol, 39%) as a deep blue solid (m.p. 156-158 °C); R_f 0.21 (19:1 DCM/MeOH); δ_{H} (500 MHz, CDCl_3) 8.25 (2H, d, J 9.3 Hz, 4,4'-CH), 7.69 (2H, d, $^3J_{\text{PH}}$ 6.9 Hz, 3,3'-CH), 7.48 (2H, t, J 10.2 Hz, 6,6'-CH),

6.84 (2H, t, J 9.6 Hz, 5,5'-CH), 6.66 (2H, d, J 10.8 Hz, 7,7'-CH), 3.94-3.87 (2H, m, 11a,11a'-CH₂), 3.85-3.77 (2H, m, 11b,11b'-CH₂), 3.60-3.54 (2H, m, 13a,13a'-CH₂), 3.52 (6H, s, 9,9'-CH₃), 3.42-3.34 (2H, m, 13b,13b'-CH₂), 1.10 (6H, t, J 7.1 Hz, 12,12'-CH₃), 0.81 (6H, t, J 7.1 Hz, 14,14'-CH₃); δ_C 167.5 (8,8'-C), 140.2 (4,4'-C), 138.5 (6,6'-C), 138.3 (d, $^3J_{CP}$ 20.0 Hz, 3a,3a'-C), 132.3 (d, $^1J_{CP}$ 199.9 Hz, 2,2'-C), 130.3 (d, $^2J_{CP}$ 14.2 Hz, 1,1'-C) 124.6 (d, $^3J_{CP}$ 17.4 Hz, 8a,8a'-C), 123.9 (d, $^2J_{CP}$ 13.4 Hz, 3,3'-C), 117.9 (d, $^5J_{CP}$ 1.9 Hz, 5,5'-C), 108.5 (d, $^5J_{CP}$ 1.2 Hz, 7,7'-C), 61.1 (d, $^2J_{CP}$ 5.9 Hz, 11,11'-C), 60.9 (d, $^2J_{CP}$ 6.3 Hz, 13,13'-C), 56.3 (9,9'-C), 16.2 (d, $^3J_{CP}$ 6.7 Hz, 12,12'-C), 16.1 (d, $^3J_{CP}$ 6.3 Hz, 14,14'-C); δ_P (202 MHz, CDCl₃) 17.6 (10,10'-P); $\nu_{max}(\text{film})$ 2975, 2925, 2850, 1597, 1561, 1528, 1496, 1477, 1450, 1436, 1408, 1386, 1364, 1341, 1292, 1264, 1242, 1229, 1217, 1193, 1178, 1159, 1122, 1095, 1047, 1025, 941, 909, 841, 824, 789, 726, 695, 666 cm⁻¹; HRMS (ESI+) m/z calc for [C₃₀H₃₆O₈P₂ + H]⁺, 587.1964; found 587.1929.

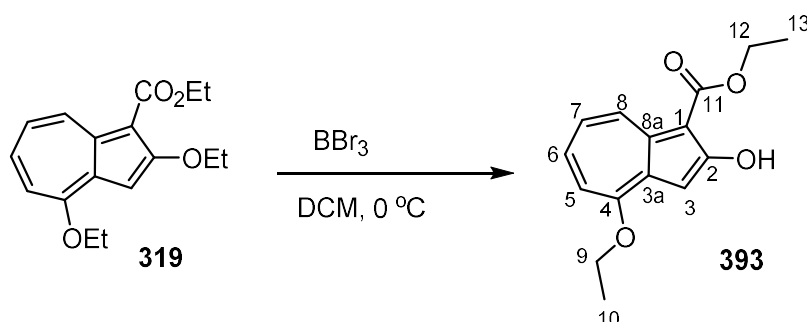
Ethyl 2,4-diethoxyazulene-1-carboxylate **319**



The preparation of this compound was based on a method by Pham.¹⁹⁸ Under atmosphere of air, an ACE pressure RBF (capacity 50 mL) was charged with 8-hydroxy-2-oxo-2H-cyclohepta[b]furan-3-carboxylate **298** (3.00 g, 12.8 mmol), triethyl orthoacetate **318** (9.0 mL) and toluene (6.0 mL) and heated under air at 200 °C, stirring for 6 h (CAUTION: the reaction was run behind a blast shield). After cooling to r.t., the resultant deep red solution was loaded onto a silica column, and purified by column chromatography (5→25% EtOAc in petroleum ether) to give *ethyl 2,4-diethoxyazulene-1-carboxylate* **319** (2.43 g, 8.42 mmol, 66%) as a red crystalline solid; R_f 0.45 (1:1 petroleum ether/EtOAc); δ_H (250 MHz, $CDCl_3$) 9.38 (1H, d, J 10.0 Hz, 8-CH), 7.40 (1H, ddd, J 11.0 Hz, 10.0 Hz, 1.0 Hz, 6-CH), 7.22 (1H, td, J 10.0 Hz, 1.0 Hz, 7-CH), 6.98 (1H, d, J 10.5 Hz, 5-CH), 6.93 (1H, s, 3-CH), 4.42 (2H, q, J 7.0 Hz, CH_2), 4.33 (2H, q, J 7.0 Hz, CH_2), 4.21 (2H, q, J 7.0 Hz, CH_2), 1.54 (3H, t, J 7.0 Hz, CH_3), 1.51 (3H, t, J 7.0 Hz, CH_3), 1.44 (3H, t, J 7.0 Hz, CH_3).

No NMR data has been previously reported for **319**; the only data previously reported is a description (“reddish orange needles”) and a melting point (119-120 °C).¹⁹³

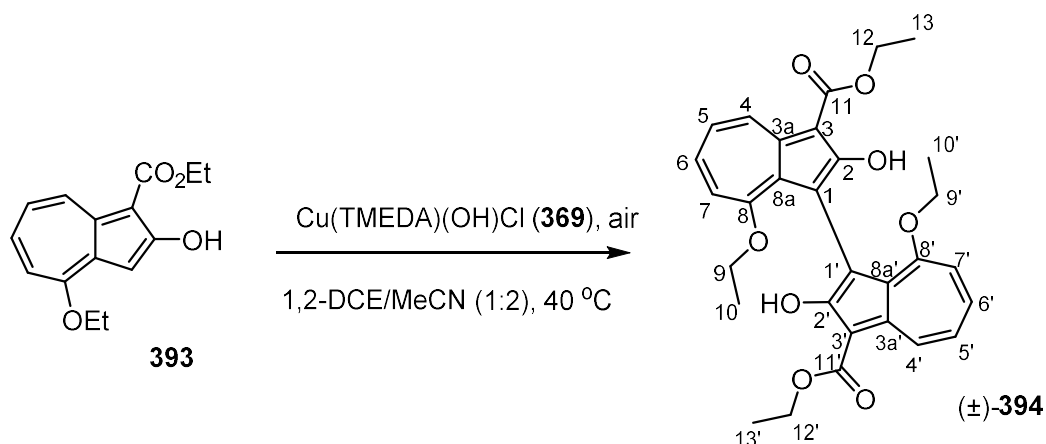
Ethyl 4-ethoxy-2-hydroxyazulene-1-carboxylate **393**



The preparation of this compound was based on a method by Talaz.²⁰⁰ To a stirred solution of ethyl 2,4-diethoxyazulene-1-carboxylate **319** (2.43 g, 8.43 mmol, 1.00 eq.) in DCM (80 mL), at $0\text{ }^\circ\text{C}$, was slowly added BBr_3 (1.0 M in heptane, 8.50 mL, 1.01 eq.), instantly forming a yellow/brown solution. The mixture was allowed to stir for 80 min, then to it was added MeOH (10 mL), forming an orange solution. The solution was diluted with DCM (80 mL) and washed with water ($2 \times 60\text{ mL}$). After drying with anhydrous MgSO_4 , the organic phase was filtered. The filtrate was concentrated under reduced pressure to give pure *ethyl 4-ethoxy-2-hydroxyazulene-1-carboxylate* **393** (2.10 g, 8.08 mmol, 96%) as an orange/brown solid, which was used without further purification (m.p. $107\text{--}110\text{ }^\circ\text{C}$); R_f 0.45 (3:1 petroleum ether/EtOAc); δ_{H} (300 MHz, CDCl_3) 10.70 (1H, br s, 2-OH), 8.90 (1H, d, J 9.5 Hz, 8-CH), 7.53 (1H, td, J 10.5 Hz, 1.0 Hz, 6-CH), 7.22 (1H, t, J 10.0 Hz, 7-CH), 7.02 (1H, d, J 10.6 Hz, 5-CH), 6.98 (1H, s, 3-CH), 4.51 (2H, q, J 7.0 Hz, 12- CH_2), 4.29 (2H, q, J 7.0 Hz, 9- CH_2), 1.56 (3H, t, J 7.0 Hz, 10- CH_3), 1.50 (3H, t, J 7.0 Hz, 13- CH_3); δ_{C} (75 MHz, CDCl_3) 169.6 (2-C), 168.8 (11-C), 160.4 (4-C), 137.0 (8a-C), 134.1 (3a-C, 133.0 (8-C), 132.3 (6-C), 123.7 (7-C), 111.7 (5-C), 101.6 (3-C), 98.8 (1-C), 64.8 (9-C), 60.2 (12-C), 14.8 (10-C), 14.6 (13-C); ν_{max} (film) 2986, 2933, 2894, 1628, 1596, 1532, 1478, 1454, 1441, 1421, 1385, 1356, 1316, 1264, 1221, 1200, 1135, 1082, 1067, 1004, 993, 959,

925, 894, 836, 827, 785, 741, 729, 667 cm^{-1} ; HRMS (ESI+) m/z calc for $[\text{C}_{15}\text{H}_{16}\text{O}_4 + \text{Na}]^+$, 283.0946; found, 283.0946.

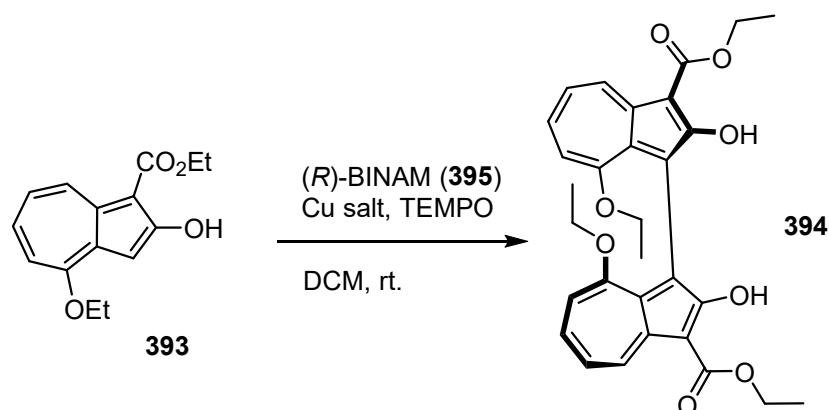
(±)-3,3'-Diethyl 2,2'-dihydroxy-8,8'-diethoxy-[1,1'-biazulene]-3,3'-dicarboxylate
394



The preparation of this compound was based on a method by Kozłowski.²¹⁴ Under atmosphere of air, to a stirred solution of ethyl 4-ethoxy-2-hydroxyazulene-1-carboxylate **393** (2.01 g, 8.06 mmol, 1.00 eq.) in acetonitrile (40 mL) and 1,2-dichloroethane (20 mL) was added di-μ-hydroxo-bis[(*N,N,N',N'*-tetramethylethylenediamine)copper(II)] chloride **369** (187 mg, 0.806 mmol (by mol. weight of monomer), 0.10 eq.). The mixture was stirred at 40 °C for 42 h, allowed to cool to r.t., and then diluted with DCM (100 mL). The solution was washed with HCl_(aq) (0.5 M, 70 mL) and with water (2 × 60 mL). The organic layer was then dried over anhydrous MgSO₄, and filtered. The filtrate was concentrated under reduced pressure to give the crude product, which was then purified by column chromatography (20→100% EtOAc in petroleum ether, then 5% MeOH in EtOAc) to give (±)-3,3'-diethyl 2,2'-dihydroxy-8,8'-diethoxy-[1,1'-biazulene]-3,3'-dicarboxylate **394** (1.27 g, 2.44 mmol, 61%) as a red solid (m.p. 210-212 °C); *R*_f 0.54 (1:1 petroleum ether/EtOAc); δ_H (500 MHz, CDCl₃) 10.74 (2H, br s, 2,2'-OH), 9.02 (2H, dd, *J* 9.7 Hz, 1.0 Hz, 4,4'-CH), 7.32 (2H, td, *J* 10.2 Hz, 1.1 Hz, 6,6'-CH), 7.14 (2H, t, *J* 9.8 Hz, 5,5'-CH), 6.82 (2H, d, *J* 10.3 Hz, 7,7'-CH), 4.52 (4H, m, 12,12'-CH₂), 3.85-

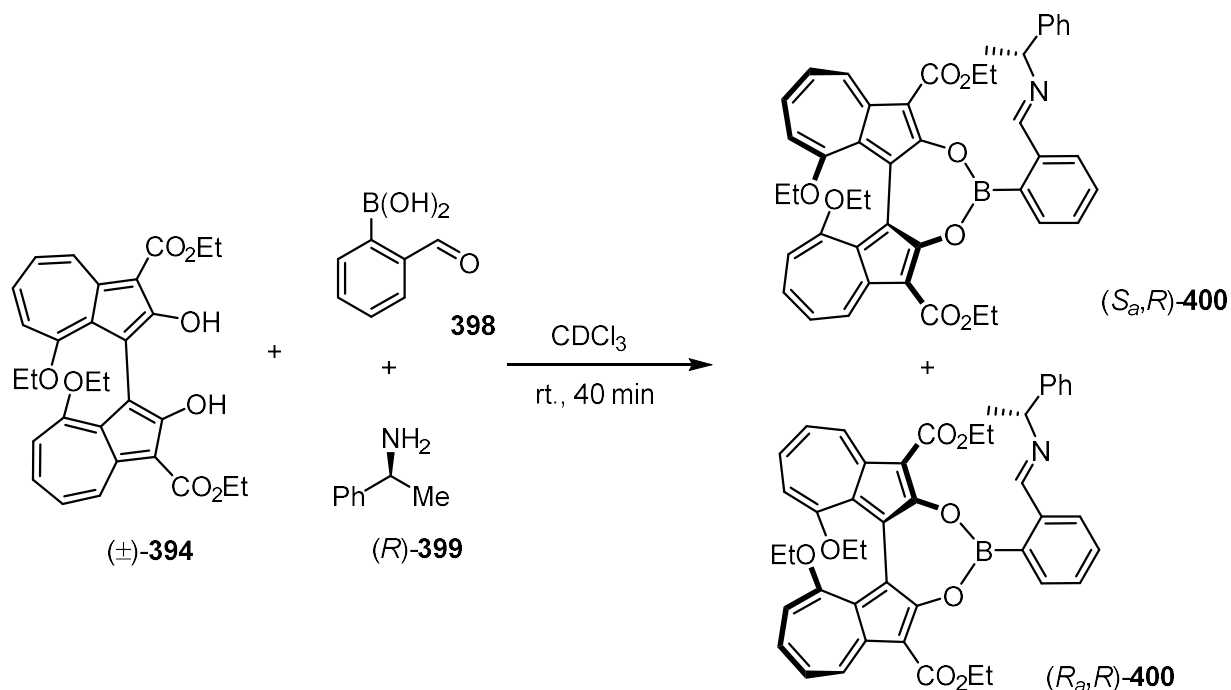
3.70 (4H, m, 9,9'-CH₂), 1.50 (6H, t, *J* 7.1 Hz, 13,13'-CH₃), 0.41 (6H, t, *J* 6.9 Hz, 10,10'-CH₃); δ_{C} (126 MHz, CDCl₃) 168.7 (11,11'-C), 168.5 (2,2'-C), 162.4 (8,8'-C), 137.6 (3a,3a'-C), 132.4 (4,4'-C), 132.0 (6,6'-C), 131.1 (8a,8a'-C), 123.0 (5,5'-C), 112.1 (1,1'-C), 111.8 (7,7'-C), 97.8 (3,3'-C), 64.2 (9,9'-C), 60.1 (12,12'-C), 14.6 (13,13'-C), 13.2 (10,10'-C); ν_{max} (film) 2978, 2925, 1625, 1596, 1572, 1527, 1470, 1438, 1418, 1380, 1356, 1312, 1261, 1214, 1178, 1118, 1095, 1007, 956, 927, 889, 869, 813, 788, 731, 701, 683 cm⁻¹; HRMS (ESI+) *m/z* calc for [C₃₀H₃₀O₈ + Na]⁺, 541.1838; found, 541.1883.

General method: (*R_a*)-3,3'-Diethyl 2,2'-dihydroxy-8,8'-diethoxy-[1,1'-biazulene]-3,3'-dicarboxylate **X**



The preparation of this compound was based on a method by Sekar.²²⁵ At r.t., to a vial charged with Cu salt (0.125 mmol, 0.025 eq.) and (*R_a*)-1,1'-bi(2-naphthylamine) (7 mg, 0.025 mmol, 0.050 eq.) was added DCM (2.0 mL), and the mixture was allowed to stir for 3 h. To this was then added 2,2,6,6-tetramethyl-1-piperidinyloxy (4 mg, 0.025 mmol, 0.050 eq.), and the mixture was stirred for 30 min before adding ethyl 4-ethoxy-2-hydroxyazulene-1-carboxylate **393** (130 mg, 0.500 mmol, 1.00 eq.), and fitting onto the vial a pierced cap to allow intake of air. The mixture was stirred for 18 days, loaded directly onto a silica column and purified by column chromatography (5→50% EtOAc in petroleum ether) to give scalemic 3,3'-diethyl 2,2'-dihydroxy-8,8'-diethoxy-[1,1'-biazulene]-3,3'-dicarboxylate) **394** as a red solid.

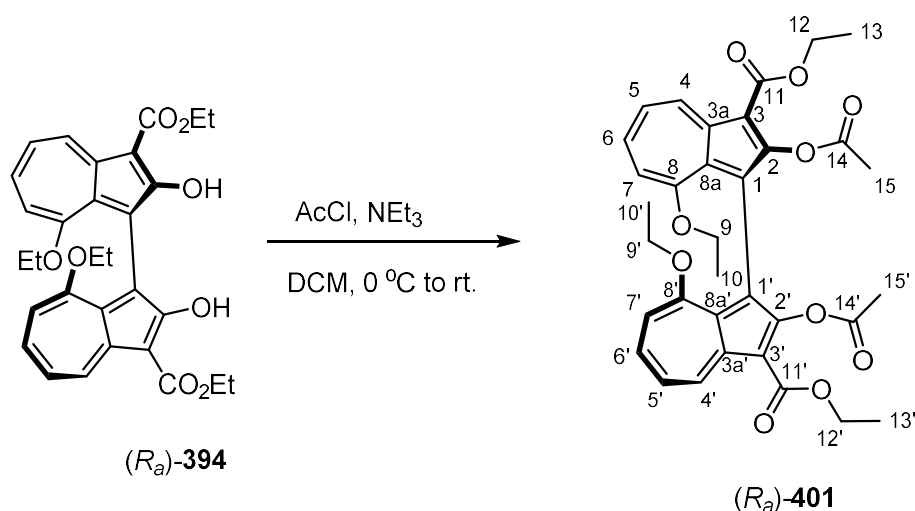
(*R_a*)/(*S_a*)- diethyl 1,15-diethoxy-8-(2-((*E*)-(((*R*)-1-phenylethyl)imino)methyl)phenyl)diazuleno[2,1-*d*:1',2'-*f*][1,3,2]dioxaborepine-6,10-dicarboxylate **400**



The preparation of this compound was based on a method by James.²²⁶ Under atmosphere of air, at r.t., to a solution of **(±)-3,3'-diethyl 2,2'-dihydroxy-8,8'-diethoxy-[1,1'-biazulene]-3,3'-dicarboxylate** **394** (52 mg, 0.100 mmol, 1.00 eq.) and 2-formylphenylboronic acid (15 mg, 0.100 mmol, 1.00 eq.) in CDCl_3 (2.0 mL) was added **(*R*)-α-methylbenzylamine** (0.55 M in CDCl_3 , 200 μL , 1.10 eq.), and the mixture was allowed to stir for 40 min. After this, an aliquot of the mixture was analysed by $^1\text{H-NMR}$ spectroscopy; δ_{H} (500 MHz, CDCl_3) 9.04 (2H, dd, J 9.7 Hz, 1.0 Hz), 8.34 (1H, s), 7.51-7.21 (m), 7.16 (2H, t, J 9.8 Hz), 6.85 (2H, d, J 10.6 Hz), 4.63 (1H, q, J 6.7 Hz), 4.58-4.47 (4H, m), 4.12 (4H, q, J 6.6 Hz), 3.88-3.74 (4H, m), 1.70 (3H, d, J 6.7 Hz), 1.50 (6H, t, J 7.1 Hz), 0.44 (6H, t, J 6.9 Hz).

(*R_a*)-3,3'-diethyl 2,2'-diacetoxy-8,8'-diethoxy-[1,1'-biazulene]-3,3'-dicarboxylate

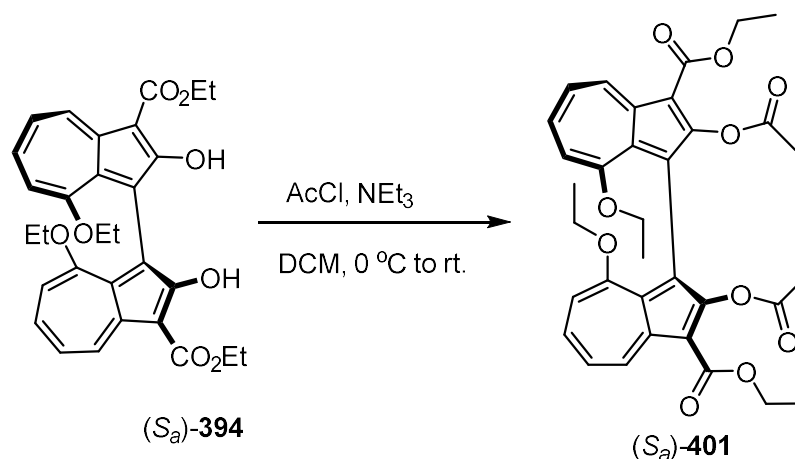
401



The preparation of this compound was based on a method by Emrick.¹⁶⁴ At 0 °C, to a stirred solution of (*R_a*)-3,3'-diethyl 2,2'-dihydroxy-8,8'-diethoxy-[1,1'-biazulene]-3,3'-dicarboxylate **394** (30 mg, 0.0578 mmol, 1.00 eq.) and triethylamine (80 μL, 0.578 mmol, 10.0 eq) in DCM (1.0 mL) was slowly added acetyl chloride (30 μL, 0.413 mmol, 7.14 eq.), changing from red to magenta in colour, forming a precipitate. The mixture was allowed to warm to r.t., and stirred for 17 h. The reaction was quenched by the addition of water (10 mL). After adding ethyl acetate (15 mL), the phases were separated, and the organic layer was washed with water (2 × 10 mL). The organic layer was then dried over anhydrous MgSO₄, and filtered. The filtrate was concentrated under reduced pressure to give the crude product, which was purified by column chromatography (10→50% EtOAc in petroleum ether) to give (*R_a*)-3,3'-diethyl 2,2'-diacetoxy-8,8'-diethoxy-[1,1'-biazulene]-3,3'-dicarboxylate **401** (27 mg, 0.0446 mmol, 77%) as a magenta solid (m.p. 86-90 °C); *R_f* 0.32 (1:1 petroleum ether/EtOAc); [*α*]_D¹⁹ -1400 (c 0.005, CHCl₃); HPLC retention time, 30.7 min (Chiralcel OD 250 x 4.6 mm ID, 9:1 hexane/2-propanol, UV detection 238 nm, flow

rate 0.75 mL min⁻¹, 20 °C); δ_{H} (500 MHz, CDCl₃) 9.68 (2H, dd, *J* 10.1 Hz, 1.0 Hz, 4,4'-CH), 7.59 (2H, ddd, *J* 10.3 Hz, 9.7 Hz, 1.2 Hz, 6,6'-CH), 7.26 (2H, t, *J* 10.2 Hz, 5,5'-CH), 6.92 (2H, d, 10.9 Hz, 7,7'-CH), 4.42-4.34 (4H, m, 12,12'-CH₂), 3.80-3.72 (4H, m, 9,9'-CH₂), 2.09 (6H, s, 15,15'-CH₃), 1.39 (6H, t, *J* 7.0 Hz, 13,13'-CH₃), 0.24 (6H, t, *J* 6.9 Hz, 10,10'-CH₃); δ_{C} (75 MHz, CDCl₃) 169.0 (14,14'-C), 165.0 (8,8'-C), 164.7 (11,11'-C), 154.2 (2,2'-C), 138.0 (4,4'-C), 137.9 (3a,3a'-C), 136.4 (6,6'-C), 128.6 (8a,8a'-C), 122.8 (5,5'-C), 115.8 (1,1'-C), 112.5 (7,7'-C), 105.7 (3,3'-C), 64.4 (9,9'-C), 59.6 (12,12'-C), 21.1 (15,15'-C), 14.5 (13,13'-C), 13.1 (10,10'-C); Chiral HPLC ν_{max} (film) 2962, 2924, 2852, 1767, 1680, 1595, 1570, 1531, 1509, 1451, 1429, 1410, 1383, 1364, 1314, 1266, 1234, 1200, 1171, 1074, 1026, 997, 934, 890, 789, 753, 724, 665 cm⁻¹; HRMS (ESI+) *m/z* calc for [C₃₄H₃₄O₁₀ + Na]⁺, 625.2050; found, 625.2053.

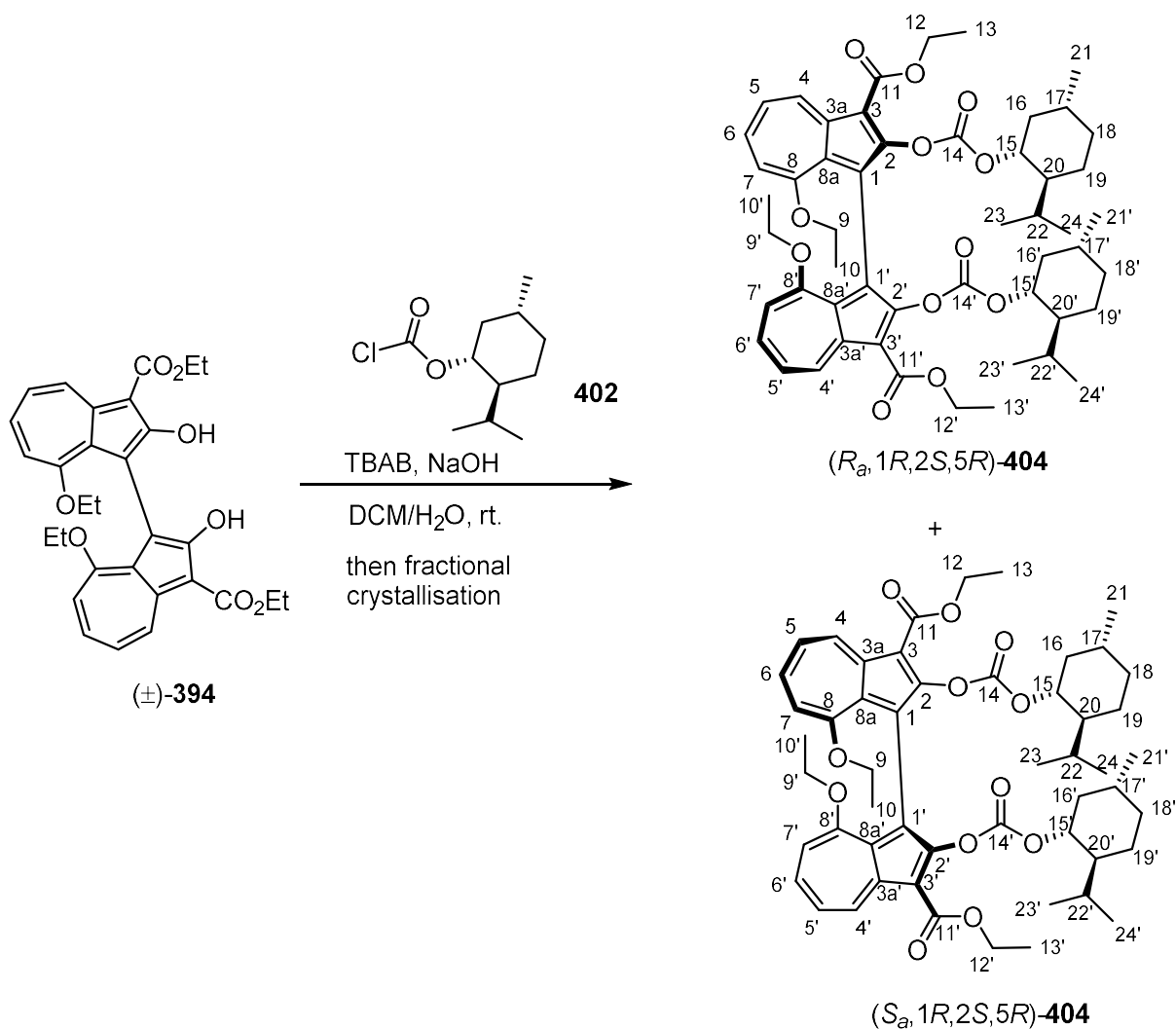
(S_a)-3,3'-diethyl 2,2'-diacetoxy-8,8'-diethoxy-[1,1'-biazulene]-3,3'-dicarboxylate
401



The preparation of this compound was based on a method by Emrick.¹⁶⁴ At 0 °C, to a stirred solution of (S_a)-3,3'-diethyl 2,2'-dihydroxy-8,8'-diethoxy-[1,1'-biazulene]-3,3'-dicarboxylate **394** (14.5 mg, 0.0280 mmol, 1.00 eq.) and triethylamine (50 μL, 0.363 mmol, 13.0 eq.) in DCM (1.0 mL) was added acetyl chloride (20 μL, 0.280 mmol, 10.0 eq.), and the mixture was allowed to warm to r.t., and stirred for 80 min. To the reaction mixture was added water (3.0 mL) to quench. The mixture was diluted with ethyl acetate (15 mL) and the phases were separated. The organic layer was washed with water (3 × 10 mL), dried over anhydrous MgSO₄ and filtered. The filtrate was concentrated under reduced pressure to give the crude product, which was purified by column chromatography (20→40% EtOAc in petroleum ether) to give (S_a)-3,3'-diethyl 2,2'-diacetoxy-8,8'-diethoxy-[1,1'-biazulene]-3,3'-dicarboxylate **401** (8.6 mg, 0.0143 mmol, 51%) as a magenta solid; [α]_D¹⁹ +1400 (c 0.005, CHCl₃); HPLC retention time, 25.0 min (Chiralcel OD 250 x 4.6 mm ID, 9:1 hexane/2-propanol, UV detection 238 nm, flow rate 0.75 mL min⁻¹, 20 °C).

(*R_a*)-Diethyl (8,8'-diethoxy-2,2'-bis((((1*R*,2*S*,5*R*)-2-isopropyl-5-methylcyclohexyl)oxy)carbonyl)oxy)-[1,1'-biazulene]-3,3'-dicarboxylate **404**

and (*S_a*)-Diethyl (8,8'-diethoxy-2,2'-bis((((1*R*,2*S*,5*R*)-2-isopropyl-5-methylcyclohexyl)oxy)carbonyl)oxy)-[1,1'-biazulene]-3,3'-dicarboxylate **404**



The preparation of these compounds was based on a method by Wan.²²⁸ At r.t., to a mixture of (±)-3,3'-diethyl 2,2'-dihydroxy-8,8'-diethoxy-[1,1'-biazulene]-3,3'-dicarboxylate **394** (1.08 g, 2.07 mmol, 1.00 eq.) and tetra-*n*-butylammonium bromide (267 mg, 0.829 mmol, 0.40 eq.) in DCM (10 mL) was added a solution of NaOH (375

mg, 9.33 mmol, 4.50 eq.) in H₂O (10 mL) and the biphasic mixture was allowed to stir. To this was then slowly added (–)-menthyl chloroformate **402** (1.30 mL, 6.22 mmol, 3.00 eq.), and the mixture was stirred vigorously for 66 h. The mixture was then diluted with DCM (30 mL) and the two phases were separated. The aqueous layer was further extracted with DCM (30 mL), and the combined organic extracts were dried over anhydrous MgSO₄, filtered, and concentrated under reduced pressure to a small volume of DCM. The solution was filtered through a plug of silica gel (25→50% EtOAc/1% NEt₃ in petroleum ether) and concentrated under reduced pressure to give the crude product. Separation of the diastereomers was achieved by recrystallisation (7:1 hexane/THF) to give pure (*R_a*)-diethyl (8,8'-diethoxy-2,2'-bis((((1*R*,2*S*,5*R*)-2-isopropyl-5-methylcyclohexyl)oxy)carbonyl)oxy)-[1,1'-biazulene]-3,3'-dicarboxylate **404** (295 mg, 0.333 mmol, 32%) as a fluffy magenta solid, isolated by filtration. The filtrate was then concentrated under reduced pressure, and purified by further recrystallisation (9:1 hexane/THF) to give pure (*S_a*)-diethyl (8,8'-diethoxy-2,2'-bis((((1*R*,2*S*,5*R*)-2-isopropyl-5-methylcyclohexyl)oxy)carbonyl)oxy)-[1,1'-biazulene]-3,3'-dicarboxylate **404** (116 mg, 0.131 mmol, 13%) as a fluffy magenta solid, isolated by filtration. The filtrate was then purified by column chromatography (10→17% EtOAc in petroleum ether) and recrystallisation (19:1 hexane/THF) to give a 2nd crop of pure (*R_a*)-diethyl (8,8'-diethoxy-2,2'-bis((((1*R*,2*S*,5*R*)-2-isopropyl-5-methylcyclohexyl)oxy)carbonyl)oxy)-[1,1'-biazulene]-3,3'-dicarboxylate **404** (59 mg, 0.0666 mmol, 6.4%) as a fluffy magenta solid.

(*R_a*,1*R*,2*S*,5*R*)-**404**: (m.p. 219-221 °C, crystals suitable for X-ray crystallography were grown by storage of a solution of **404** in EtOH at –18 °C); *R_f* 0.29 (3:1 petroleum ether/EtOAc); [α]_D¹⁹ -1900 (c 0.005, CHCl₃) δ_H (500 MHz, CDCl₃) 9.71 (2H, dd, *J* 10.0 Hz, 1.1 Hz, 4,4'-CH), 7.58 (2H, ddd, *J* 10.9 Hz, 9.8 Hz, 1.1 Hz, 6,6'-CH),

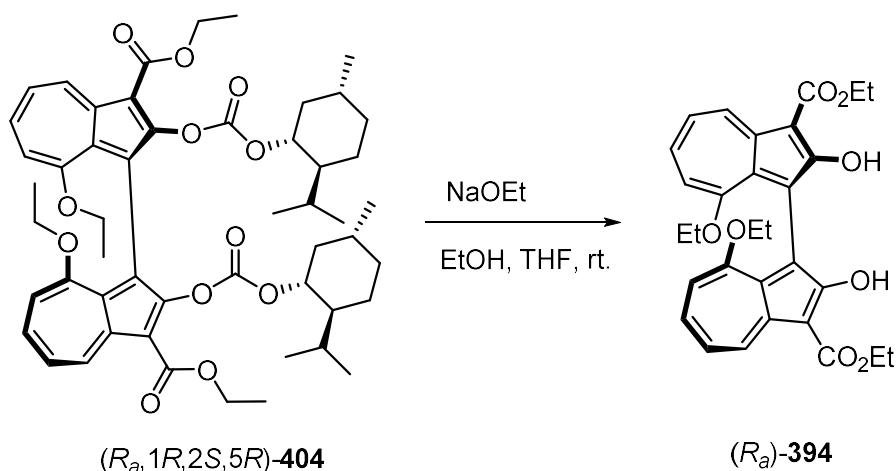
7.25 (2H, td, J 9.9 Hz, 0.6 Hz, 5,5'-CH), 6.92 (2H, d, J 10.9 Hz, 7,7'-CH), 4.37 (2H, q, J 7.3 Hz, 12-CH₂ or 12'-CH₂), 4.37 (2H, q, J 7.3 Hz, 12-CH₂ or 12'-CH₂), 4.28 (2H, td, J 11.0 Hz, 4.4 Hz, 15,15'-CH), 3.82 (app dq, J 8.6 Hz, 6.8 Hz, 9,9'-CH_H), 3.75 (2H, app dq, J 8.4 Hz, 6.9 Hz, 9,9'-CH_H), 1.91-1.86 (2H, m, 16,16'-CH_{eq}), 1.57-1.52 (2H, m, 18,18'-CH_H), 1.46 (2H, dq, J 13.0 Hz, 3.4 Hz, 19,19'-CH_{eq}), 1.38 (6H, t, J 7.1 Hz, 13,13'-CH₂), 1.32-1.25 (2H, m, 17,17'-CH), 1.16 (2H, tt, J 11.9 Hz, 3.1 Hz, 20,20'-CH), 1.12-1.07 (2H, m, 22,22'-CH), 0.93 (2H, q, J 11.5 Hz, 16,16'-CH_{ax}), 0.83 (6H, d, J 6.7 Hz, 21,21'-CH₃), 0.85-0.72 (4H, m, 18,18'-CH_H, 19,19'-CH_{ax}), 0.46 (6H, d, J 6.9 Hz, 24,24'-CH₃), 0.24 (6H, t, J 7.1 Hz, 10,10'-CH₃), 0.06 (6H, d, J 6.9 Hz, 23,23'-CH₃); δ_c (126 MHz, CDCl₃) 165.4 (8,8'-C), 164.8 (11,11'-C), 153.8 (2,2'-C), 152.0 (14,14'-C), 138.2 (4,4'-C), 137.8 (3a,3a'-C), 136.4 (6,6'-C), 128.3 (8a,8a'-C), 122.7 (5,5'-C), 116.0 (1,1'-C), 112.4 (7,7'-C), 105.7 (3,3'-C), 78.3 (15,15'-C), 64.6 (9,9'-C), 59.6 (12,12'-C), 46.9 (20,20'-C), 40.6 (16,16'-C), 34.0 (18,18'-C), 31.3 (17,17'-C), 25.8 (22,22'-C), 23.3 (19,19'-C), 22.0 (21,21'-C), 20.1 (24,24'-C), 15.7 (23,23'-C), 14.5 (13,13'-C), 13.1 (10,10'-C); ν_{\max} (film) 2953, 2930, 2869, 1757, 1685, 1595, 1571, 1512, 1450, 1434, 1410, 1384, 1330, 1270, 1227, 1207, 1178, 1094, 1074, 1033, 1000, 980, 958, 925, 891, 827, 781, 720 cm⁻¹; HRMS (ESI+) m/z calc for [C₅₂H₆₆O₁₂ + H]⁺, 883.4633; found, 883.4631.

(*S_a*,1*R*,2*S*,5*R*)-**404**: (m.p. 213-215 °C, crystals suitable for X-ray crystallography were grown by storage of a solution of **404** in hexane/THF (9:1 v/v) at -18 °C); [α]_D¹⁹ -1500 (c 0.005, CHCl₃); R_f 0.26 (3:1 petroleum ether/EtOAc); δ_H (500 MHz, CDCl₃) 9.68 (2H, dd, J 10.0 Hz, 1.0 Hz, 4,4'-CH), 7.58 (2H, ddd, J 10.9 Hz, 9.8 Hz, 1.1 Hz, 6,6'-CH), 7.25 (2H, td, J 9.8 Hz, 0.6 Hz, 5,5'-CH), 6.93 (2H, d, J 11.0 Hz, 7,7'-CH), 4.41-4.31 (4H, m, 12,12'-CH₂), 4.25 (2H, td, J 10.8 Hz, 4.4 Hz, 15,15'-CH), 3.91-3.79 (4H, m, 9,9'-CH₂), 1.70 (2H, app quint d, J 7.0 Hz, 2.4 Hz, 22,22'-CH), 1.56-1.50 (6H,

m, 16,16'-CH_{eq}, 18,18'-CH_H, 19,19'-CH_{eq}), 1.36 (6H, t, *J* 7.1 Hz, 13,13'-CH₃), 1.27-1.23 (2H, m, 17,17'-CH), 1.22 (2H, tt, *J* 11.6 Hz, 3.0 Hz, 20,20'-CH), 0.90 (2H, qd, *J* 12.8 Hz, 3.4 Hz, 19,19'-CH_{ax}), 0.73 (6H, d, *J* 6.6 Hz, 21,21'-CH₃), 0.71 (2H, m, 18,18'-CH_H), 0.69 (6H, d, *J* 7.0, 24,24'-CH₃), 0.63 (2H, app q, *J* 12.1 Hz, 16,16'-CH_{ax}), 0.57 (6H, d, *J* 7.0 Hz, 23,23'-CH₃), 0.36 (6H, t, *J* 6.9 Hz, 10,10'-CH₃); δ_c (126 MHz, CDCl₃) 165.1 (8,8'-C), 164.7 (11,11'-C), 154.0 (2,2'-C), 151.4 (14,14'-C), 138.0 (4,4'-C), 137.5 (3a,3a'-C), 136.4 (6,6'-C), 127.3 (8a,8a'-C), 122.6 (5,5'-C), 116.1 (1,1'-C), 112.2 (7,7'-C), 105.8 (3,3'-C), 78.8 (15,15'-C), 64.5 (9,9'-C), 59.6 (12,12'-C), 46.3 (20,20'-C), 39.6 (16,16'-C), 34.0 (18,18'-C), 31.0 (17,17'-C), 25.7 (22,22'-C), 23.2 (19,19'-C), 21.9 (21,21'-C), 20.5 (24,24'-C), 16.0 (23,23'-C), 14.5 (13,13'-C), 13.2 (10,10'-C); ν_{\max} (film) 2952, 2952, 2870, 1755, 1678, 1594, 1568, 1511, 1451, 1437, 1409, 1382, 1330, 1233, 1208, 1189, 1179, 1107, 1094, 1074, 1033, 1001, 978, 957, 926, 912, 890, 862, 827, 792, 781, 767, 721, 669 cm⁻¹; HRMS (ESI+) *m/z* calc for [C₅₂H₆₆O₁₂ + H]⁺, 883.4633; found, 883.4643.

(*R_a*)-3,3'-Diethyl 2,2'-dihydroxy-8,8'-diethoxy-[1,1'-biazulene]-3,3'-dicarboxylate

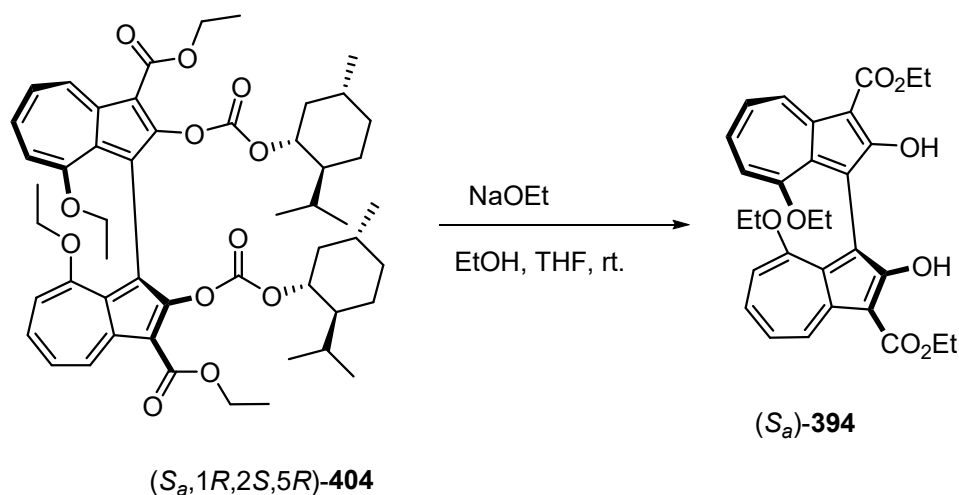
394



The preparation of this compound was based on a method by Katsuki.²³⁰ At r.t., to a stirred solution of (*R_a*)-diethyl (8,8'-diethoxy-2,2'-bis((((1*R*,2*S*,5*R*)-2-isopropyl-5-methylcyclohexyl)oxy)carbonyl)oxy)-[1,1'-biazulene]-3,3'-dicarboxylate **404** (280 mg, 0.317 mmol, 1.00 eq.) in THF (10 mL) was slowly added NaOEt (2.0 M in EtOH, 1.60 mL, 3.20 mmol, 10.0 eq.). After stirring for 2 h, the solution was concentrated under reduced pressure, dissolved in KOH_(aq) (1.0 M, 150 mL), and washed with hexane (2 × 40 mL). To the aqueous layer was added HCl_(aq) (5.0 M, 60 mL), forming a deep red precipitate, and stored at 2 °C for 1.5 h. The mixture was then filtered, washing with water, to give (*R_a*)-3,3'-diethyl 2,2'-dihydroxy-8,8'-diethoxy-[1,1'-biazulene]-3,3'-dicarboxylate **394** (142 mg, 0.274 mmol, 86%) as a deep red solid (crystals suitable for X-ray crystallography were grown by storage of a solution of **394** in EtOH at −18 °C); $[\alpha]_D^{19}$ -2400 (c 0.005, CHCl₃).

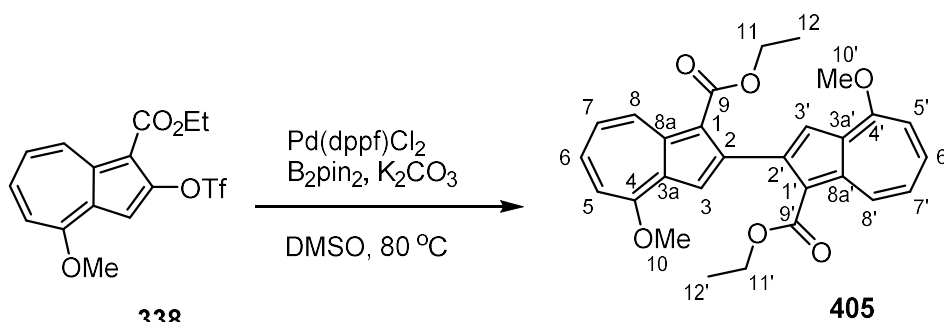
(S_a)-3,3'-diethyl 2,2'-dihydroxy-8,8'-diethoxy-[1,1'-biazulene]-3,3'-dicarboxylate

394



The preparation of this compound was based on a method by Katsuki.²³⁰ At 0 °C, to a stirred solution of (S_a)-diethyl (8,8'-diethoxy-2,2'-bis((((1R,2S,5R)-2-isopropyl-5-methylcyclohexyl)oxy)carbonyl)oxy)-[1,1'-biazulene]-3,3'-dicarboxylate **404** (131 mg, 0.148 mmol, 1.00 eq.) was slowly added NaOEt (2.0 M in EtOH, 740 μL, 1.48 mmol, 10.0 eq.). On completion of addition, the solution was raised out of ice bath and allowed to warm to r.t., and stirred for 1.5 h. After concentrating under reduced pressure, the solid was dissolved in KOH_(aq) (1 M, 30 mL) and water (70 mL), and washed with hexane (2 × 25 mL). On addition of HCl_(aq) (5.0 M, 20 mL) to the aqueous layer, a red precipitate formed instantly. After storing at 2 °C for 2.5 h, the mixture was filtered, washing with water, to give (S_a)-3,3'-diethyl 2,2'-dihydroxy-8,8'-diethoxy-[1,1'-biazulene]-3,3'-dicarboxylate **394** (66 mg, 0.128 mmol, 86%) as a deep red solid; $[\alpha]_D^{19} +2400$ (c 0.005, CHCl₃).

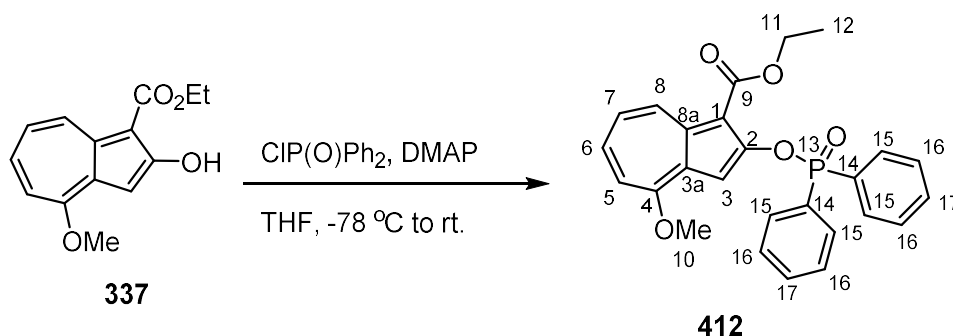
Diethyl 4,4'-dimethoxy-[2,2'-biazulene]-1,1'-dicarboxylate **405**



The preparation of this compound was based on a method by Bräse.²³⁴ At r.t., to a mixture of bis(diphenylphosphino)ferrocene]palladium dichloride (14 mg, 0.0169 mmol, 0.04 eq.), bis(pinacolato)diboron (54 mg, 0.212 mmol, 0.50 eq.) and potassium carbonate (175 mg, 1.27 mmol, 0.50 eq.) was added a solution of ethyl 4-methoxy-2-(trifluoromethanesulfonyloxy)azulene-1-carboxylate **338** (160 mg, 0.423 mmol, 1.00 eq.) in DMSO (degassed by sparging with N₂, 5.0 mL). The resulting suspension was stirred at 80 °C for 16 h, and then allowed to cool to r.t. The mixture was diluted with DCM (30 mL) and washed with water (3 × 20 mL). The organic phase was dried over anhydrous MgSO₄, and filtered. The filtrate was concentrated under reduced pressure to give the crude product, which was purified by column chromatography (20→50% EtOAc in petroleum ether) to give *diethyl 4,4'-dimethoxy-[2,2'-biazulene]-1,1'-dicarboxylate* **405** (41 mg, 0.0883 mmol, 42%) as a maroon solid (m.p. 97-100 °C); *R*_f 0.45 (1:1 petroleum ether/EtOAc); δ_H (500 MHz, CDCl₃) 9.59 (2H, d, *J* 9.8 Hz, 8,8'-CH), 7.68 (2H, t, *J* 10.5 Hz, 6,6'-CH), 7.64 (2H, s, 3,3'-CH), 7.30 (2H, t, *J* 10.3 Hz, 7,7'-CH), 7.14 (2H, d, *J* 10.8 Hz, 5,5'-CH), 4.17 (6H, s, 10,10'-CH₃), 4.10 (4H, q, *J* 6.9 Hz, 11,11'-CH₂), 0.91 (6H, t, *J* 6.9 Hz, 12,12'-CH₃); δ_C (126 MHz, CDCl₃) 166.2 (9,9'-C), 163.3 (4,4'-C), 147.9 (2,2'-C), 139.8 (8a,8a'-C), 138.2 (8,8'-C), 136.4 (6,6'-C), 130.8 (3a,3a'-C), 122.8 (7,7'-C), 116.7 (3,3'-C), 116.1 (1,1'-C), 110.6 (5,5'-C), 59.5 (11,11'-C), 56.5 (10,10'-C), 13.7 (12,12'-C); ν_{max}(film)

2986, 1687, 1600, 1568, 1515, 1461, 1419, 1381, 1329, 1305, 1274, 1200, 1169, 1134, 1106, 1088, 1062, 1021, 955, 926, 881, 865, 831, 785, 753, 721, 710, 672 cm^{-1} ; HRMS (ESI+) m/z calc for $[\text{C}_{28}\text{H}_{26}\text{O}_6 + \text{Na}]^+$, 481.1622; found, 481.1689.

Ethyl 2-((diphenylphosphoryl)oxy)-4-methoxyazulene-1-carboxylate **412**

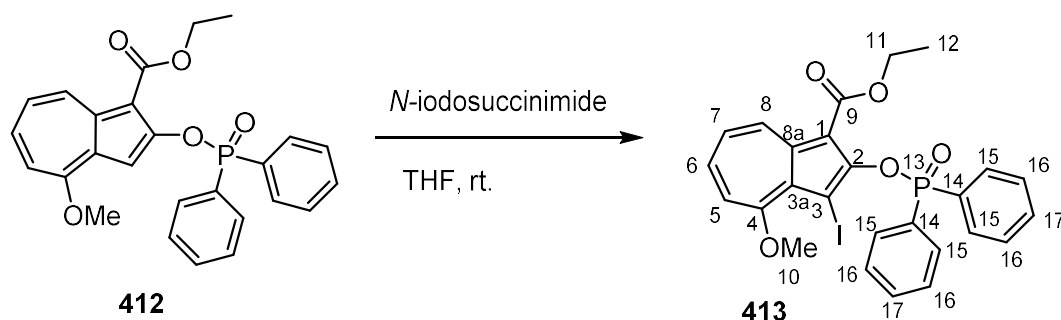


The preparation of this compound was based on a method by Parquette.²⁴² At -78 $^\circ\text{C}$, to a stirred solution of ethyl 2-hydroxy-4-methoxyazulene-1-carboxylate **337** (160 mg, 0.650 mmol, 1.00 eq.) and DMAP (87 mg, 0.715 mmol, 1.10 eq.) in THF (6.0 mL) was added dropwise diphenylphosphinic chloride (140 μL , 0.730 mmol, 1.12 eq.). The resultant mixture was stirred for 16 h, allowing it to warm up to r.t. inside the acetone/dry ice bath. The solution was quenched with water (20 mL) and extracted with ethyl acetate (50 mL). The organic extract was then washed with water (2×20 mL) and saturated brine, dried over MgSO_4 , and filtered. The filtrate was concentrated under reduced pressure to give the crude product, which was purified by column chromatography (10 \rightarrow 66% EtOAc in petroleum ether) to give *ethyl 2-((diphenylphosphoryl)oxy)-4-methoxyazulene-1-carboxylate* **412** (243 mg, 0.544 mmol, 84%) as a bright red solid (m.p. $183\text{--}185$ $^\circ\text{C}$); R_f 0.15 (1:1 petroleum ether/EtOAc); δ_{H} (500 MHz, CDCl_3) 9.47 (1H, d, J 9.8 Hz, 8-CH), 8.10–8.05 (4H, m, 15-CH), 7.57 (1H, ddd, J 10.3 Hz, 10.0 Hz, 0.9 Hz, 6-CH), 7.51–7.48 (2H, m, 17-CH), 7.50 (1H, s, 3-CH), 7.46–7.42 (4H, m, 16-CH), 7.27 (1H, t, J 9.8 Hz, 7-CH), 7.05 (1H, d, J 10.8 Hz, 5-CH), 4.50 (2H, q, J 7.2 Hz, 11- CH_2), 4.04 (3H, s, 10- CH_3), 1.43 (3H, t, J 7.2 Hz, 12- CH_3); δ_{C} (126 MHz, CDCl_3) 164.7 (9-C), 162.8 (4-C), 155.7 (d, $^2J_{\text{CP}}$ 7.6 Hz, 2-C), 137.4 (8a-C), 137.3 (8-C), 135.5 (6-C), 132.3 (d, $^4J_{\text{CP}}$ 2.9 Hz, 17-

C), 131.9 (d, $^2J_{\text{CP}}$ 10.5 Hz, 15-C), 131.3 (d, $^1J_{\text{CP}}$ 138.8 Hz, 14-C), 130.6 (3a-C), 128.5 (d, $^3J_{\text{CP}}$ 13.4 Hz, 16-C), 123.7 (7-C), 111.5 (5-C), 104.8 (1-C)*, 104.6 (d, $^3J_{\text{CP}}$ 4.2 Hz, 3-C), 59.7 (11-C), 56.3 (10-C), 14.7 (12-C); δ_{P} (202 MHz, CDCl_3) 30.5 (13-P); ν_{max} (film) 3079, 2977, 2921, 2842, 1673, 1591, 1573, 1539, 1505, 1468, 1452, 1452, 1407, 1396, 1385, 1355, 1342, 1303, 1269, 1236, 1206, 1178, 1130, 1111, 1069, 1035, 998, 958, 934, 895, 862, 831, 810, 787, 749, 730, 690, 669 cm^{-1} ; HRMS (ESI+) m/z calc for $[\text{C}_{26}\text{H}_{23}\text{O}_5\text{P} + \text{H}]^+$, 447.1361; found, 447.1344.

*possibly a doublet, hidden by adjacent doublet.

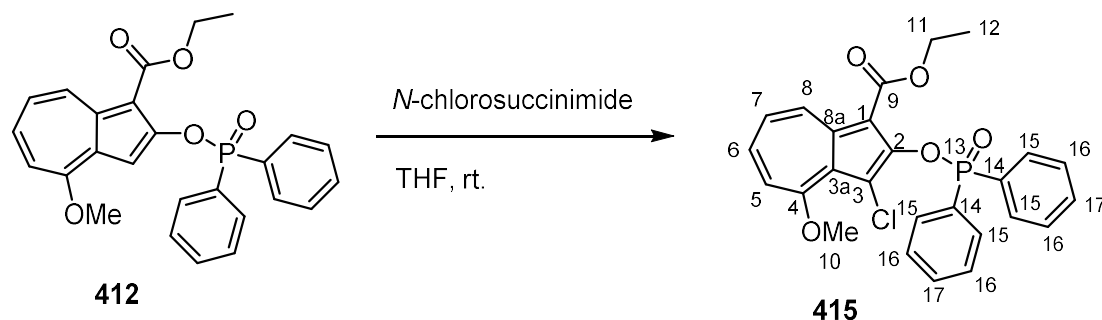
Ethyl 2-((diphenylphosphoryl)oxy)-3-iodo-4-methoxyazulene-1-carboxylate
413



Under atmosphere of air at r.t., to a round-bottom flask wrapped in aluminium foil, charged with a stirred solution of ethyl 2-((diphenylphosphoryl)oxy)-4-methoxyazulene-1-carboxylate **412** (50 mg, 0.112 mmol, 1.00 eq.) in THF (5.0 mL) was added portionwise *N*-iodosuccinimide (28 mg, 0.123 mmol, 1.10 eq.), and the mixture was allowed to stir for 1 h. To the mixture was added more *N*-iodosuccinimide (10 mg, 0.0444 mmol, 0.40 eq.), allowing then to stir for 30 min to make a pink/red suspension. The mixture was diluted with ethyl acetate (20 mL), washed with $\text{Na}_2\text{CO}_{3(\text{aq})}$ (1 M, 5.0 mL), with water (2×10 mL) and with saturated brine. The organic layer was dried over anhydrous MgSO_4 , and filtered. The filtrate was concentrated under reduced pressure to give crude *ethyl 2-((diphenylphosphoryl)oxy)-3-iodo-4-methoxyazulene-1-carboxylate* **413** (37 mg, 0.0647 mmol, 58%) as a pink/red solid (m.p. 133-139 °C); δ_{H} (300 MHz, CDCl_3) 9.47 (1H, d, J 10.0 Hz, 8-CH), 8.11-8.03 (4H, m, 15-CH), 7.59 (1H, ddd, J 11.0 Hz, 10.0 Hz, 1.1 Hz, 6-CH), 7.50-7.43 (6H, m, 16,17-CH), 7.28 (1H, t, J 9.9 Hz, 7-CH), 7.06 (1H, d, J 10.8 Hz, 5-CH), 4.49 (2H, q, J 7.1 Hz, 11- CH_2), 4.04 (3H, s, 10- CH_3), 1.42 (3H, t, J 7.1 Hz, 12- CH_3); δ_{C} (75 MHz, CDCl_3) 164.7 (9-C), 162.8 (4-C), 155.6 (d, $^2J_{\text{CP}}$ 7.8 Hz, 2-C), 137.3 (8-C), 135.6 (6-C), 132.3 (d, $^4J_{\text{CP}}$ 2.9 Hz, 17-C), 131.9 (d, $^2J_{\text{CP}}$ 10.7 Hz, 15-C), 130.6 (3a-C), 129.3 (d, $^1J_{\text{CP}}$ 141.2 Hz, 14-C), 128.5 (d, $^3J_{\text{CP}}$ 13.6 Hz,

16-C), 124.3 (8a-C), 123.7 (7-C), 112.9 (3-C), 111.5 (5-C), 104.6 (1-C), 59.7 (11-C), 56.3 (10-C), 14.7 (12-C); δ_P (121 MHz, $CDCl_3$) 31.3 (13-P); $\nu_{max}(\text{film})$ 2952, 2923, 2850, 1673, 1633, 1592, 1573, 1539, 1468, 1452, 1437, 1408, 1396, 1355, 1342, 1303, 1268, 1236, 1206, 1177, 1130, 1111, 1069, 1034, 958, 934, 895, 862, 832, 787, 750, 710, 690, 669 cm^{-1} ; HRMS (ESI+) m/z calc for $[C_{26}H_{22}IO_5P + H]^+$, 573.0328; found, 573.0323.

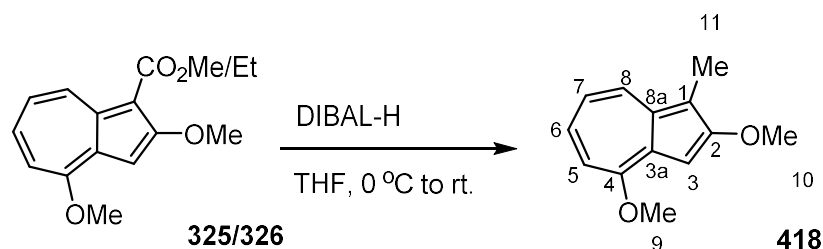
Ethyl 3-chloro-((diphenylphosphoryl)oxy)-4-methoxyazulene-1-carboxylate **415**



Under atmosphere of air, at r.t., to a stirred solution of ethyl 2-((diphenylphosphoryl)oxy)-4-methoxyazulene-1-carboxylate **412** (30 mg, 0.067 mmol, 1.00 eq.) in DCM (4.0 mL) was added *N*-chlorosuccinimide (10 mg, 0.074 mmol, 1.10 eq.), and the mixture was allowed to stir for 1 h. To the mixture was then added more *N*-chlorosuccinimide (4 mg, 0.030 mmol, 0.45 eq.), allowing then to stir for 17 h. The mixture was diluted with DCM (15 mL), washed with Na₂CO_{3(aq)} (1 M, 10 mL) and with water (2 × 10 mL), and the organic layer was dried over anhydrous MgSO₄, and filtered. The filtrate was concentrated under reduced pressure to give the crude product, which was purified by column chromatography (25→50% EtOAc in petroleum ether) to give ethyl 3-chloro-((diphenylphosphoryl)oxy)-4-methoxyazulene-1-carboxylate **415** (16 mg, 0.0333 mmol, 50%) as a pink/red solid (m.p. 212-215 °C (dec.)); *R*_f 0.43 (1:3 petroleum ether/EtOAc); δ_H (300 MHz, CDCl₃) 9.36 (1H, d, *J* 10.0 Hz, 8-CH), 8.03-7.95 (4H, m, 15-CH), 7.58 (1H, t, *J* 10.3 Hz, 6-CH), 7.55-7.43 (6H, m, 16,17-CH), 7.16 (1H, t, *J* 9.9 Hz, 7-CH), 6.98 (1H, d, *J* 11.0 Hz, 5-CH), 4.04 (3H, s, 10-CH₃), 3.99 (2H, q, *J* 7.2 Hz, 11-CH₂), 1.00 (3H, t, *J* 7.1 Hz, 12-CH₃); δ_C (75 MHz, CDCl₃) 165.0 (4-C), 164.0 (9-C), 149.8 (d, ²*J*_{CP} 9.8 Hz, 2-C), 138.4 (8-C), 137.4 (6-C), 135.0 (d, ⁴*J*_{CP} 1.1 Hz, 8a-C), 132.2 (d, ⁴*J*_{CP} 2.9 Hz, 17-C), 131.9 (d, ²*J*_{CP} 10.6 Hz, 15-C), 131.8 (d, ¹*J*_{CP} 138 Hz, 14-C), 128.2 (d, ³*J*_{CP} 13.7 Hz, 16-C), 123.3 (d, ⁴*J*_{CP} 1.4 Hz, 3a-C), 123.1 (7-C), 111.8 (5-C), 107.9 (1-C or 3-C),

107.7 (1-C or 3-C), 60.0 (11-C), 56.4 (10-C), 14.1 (12-C); δ_P (121 MHz, $CDCl_3$) 32.9 (13-P); $\nu_{max}(\text{film})$ 3061, 2924, 2852, 1772, 1687, 1596, 1572, 1530, 1508, 1462, 1453, 1439, 1409, 1382, 1342, 1307, 1272, 1232, 1212, 1198, 1168, 1128, 1109, 1076, 1025, 997, 954, 928, 882, 836, 800, 785, 770, 754, 728, 715, 699, 674 cm^{-1} ; HRMS (ESI+) m/z calc for $[C_{26}H_{22}ClO_5P + Na]^+$, 503.0791; found, 503.0799.

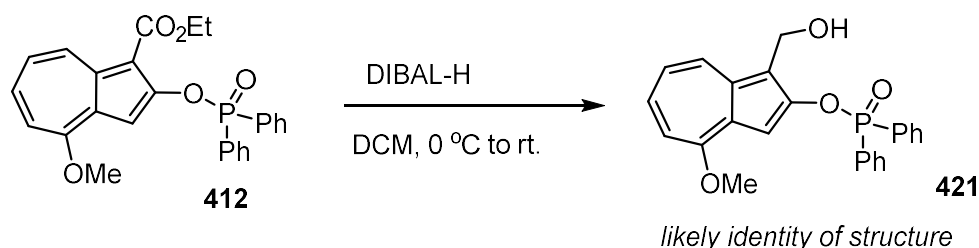
2,4-Dimethoxy-1-methylazulene **418**



The preparation of this compound was based on a method by Hansen.¹⁹⁵ At 0 °C, to a stirred solution of mixed methyl 2,4-dimethoxyazulene-1-carboxylate **325** and ethyl 2,4-dimethoxyazulene-1-carboxylate **326** (~1:3 Me/Et, 50 mg, 0.195 mmol, 1.00 eq.) in THF (3.0 mL) was slowly added DIBAL-H (1.0 M in DCM, 980 µL, 0.980 mmol, 5.00 eq.), changing in colour from orange/red to pink/red within 5 min. The solution was allowed to warm up to r.t., and stirred for 3 h. The mixture was cooled again to 0 °C, and to it was added DIBAL-H (1.0 M in DCM, 980 µL, 0.980 mmol, 5.00 eq.), before allowing to warm to r.t. The mixture was allowed to stir for 24 h, then to it was added ethyl acetate (25 mL) and water (5.0 mL), before filtering through Celite. The crude product was washed through with ethyl acetate (20 mL), and the phases were separated. The organic solution was washed with water (3 × 10 mL) and saturated brine, dried over anhydrous MgSO₄, and filtered. The filtrate was concentrated under reduced pressure to give the crude product, which was purified by column chromatography (10% EtOAc in petroleum ether) to give *2,4-dimethoxy-1-methylazulene* **418** (15 mg, 0.0741 mmol, 38%) as a violet solid (m.p. 101-104 °C); *R*_f 0.51 (4:1 petroleum ether/EtOAc); δ_H (300 MHz, CDCl₃) 8.08 (1H, d, *J* 10.0 Hz, 8-CH), 7.38 (1H, t, *J* 10.5 Hz, 6-CH), 7.10 (1H, s, 3-CH), 7.01 (1H, t, *J* 10.0 Hz, 7-CH), 6.99 (1H, d, *J* 10.5 Hz 7-CH), 4.13 (3H, s, 9-CH₃), 4.07 (3H, s, 10-CH₃), 2.44 (3H, s, 11-CH₃); δ_C (75 MHz, CDCl₃) 164.2 (2-C), 158.3 (4-C), 134.4 (8a-C), 130.9 (6-C), 130.7 (8-C), 126.3 (3a-C), 118.7 (7-C), 110.2 (1-C), 109.4 (5-C), 94.9 (3-C), 57.5

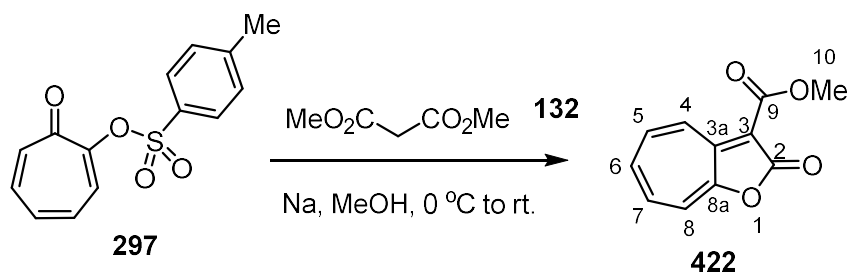
(10-C), 56.6 (9-C), 8.3 (11-C); $\nu_{\text{max}}(\text{film})$ 2998, 2966, 2919, 2844, 1591, 1563, 1538, 1524, 1496, 1455, 1418, 1385, 1370, 1342, 1302, 1256, 1229, 1211, 1196, 1168, 1142, 1099, 1021, 1008, 973, 939, 854, 777, 748, 699, 659 cm^{-1} ; HRMS (ESI+) m/z calc for $[\text{C}_{13}\text{H}_{14}\text{O}_2 + \text{H}]^+$, 203.1072; found, 203.1072.

1-(Hydroxymethyl)-4-methoxyazulen-2-yl diphenylphosphinate **421**



The preparation of this compound was based on a method by Hansen.¹⁹⁵ At 0 °C, to a solution of ethyl 2-((diphenylphosphoryl)oxy)-4-methoxyazulene-1-carboxylate **412** (68 mg, 0.152 mmol, 1.00 eq.) in THF (3.0 mL) was slowly added DIBAL-H (1.0 M in hexanes, 760 μ L, 5.00 eq.). The mixture was allowed to warm to r.t., stirred for 3 h. The mixture was diluted with EtOAc (10 mL) and at 0 °C, to it was added water (5.0 mL) and allowed to stir for 5 min. The mixture was diluted further with EtOAc (10 mL), and filtered through Celite. The filtrate was then washed with saturated aqueous Rochelle salt (2 \times 10 mL), with water (2 \times 15 mL) and with saturated brine. The organic layer was dried over anhydrous MgSO_4 and filtered. The filtrate was concentrated under reduced pressure to give the crude product, which was purified by column chromatography (0 \rightarrow 5% MeOH in DCM) to give impure 1-(hydroxymethyl)-4-methoxyazulen-2-yl diphenylphosphinate **418** (10 mg, <0.025 mmol, <16%) as a red/brown solid; R_f 0.33 (5% MeOH in DCM); δ_H (500 MHz, CDCl_3) 8.45 (1H, d, J 9.6 Hz), 7.99-7.94 (4H, m), 7.60-7.55 (m), 7.53-7.48 (m), 7.10 (1H, t, J 9.7 Hz), 6.94-6.92 (2H, m), 5.01 (2H, br s), 4.04 (3H, s); δ_P (202 MHz, CDCl_3) 32.07.

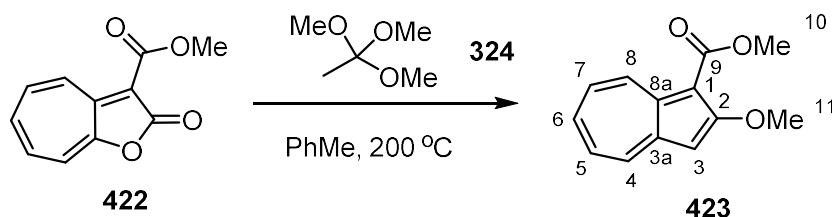
Methyl 2-oxo-2H-cyclohepta[b]furan-3-carboxylate **422**



The preparation of this compound was based on a method by Pham.¹⁸⁷ At 0 °C, to a stirred suspension of 7-oxocyclohepta-1,3,5-trien-1-yl 4-methylbenzene-1-sulfonate **297** (16.6 g, 60.0 mmol, 1.00 eq.) and dimethyl malonate **132** (14.0 mL, 123 mmol, 2.04 eq.) in MeOH (100 mL) was added by cannula NaOMe solution (freshly prepared from Na metal (2.77 g, 120 mmol, 2.00 eq.) and MeOH (100 mL)). After 5 min, the suspension had changed from cream to yellow/brown in colour, and was allowed to warm to r.t. After stirring for 6 h, water was added (200 mL), and the mixture was stored at -18 °C for 16 h. The precipitate collected by filtration, washing with water to give pure *methyl 2-oxo-2H-cyclohepta[b]furan-3-carboxylate* **422** (9.31 g, 45.6 mmol, 76%) as a yellow solid; δ_{H} (500 MHz, CDCl_3) 8.87 (1H, d, J 11.4 Hz, CH), 7.65-7.61 (1H, m, CH), 7.51-7.47 (2H, m, CH), 7.36-7.34 (1H, m, CH), 3.94 (3H, s, 10-CH₃).

Data in agreement with those previously reported.¹⁸⁷

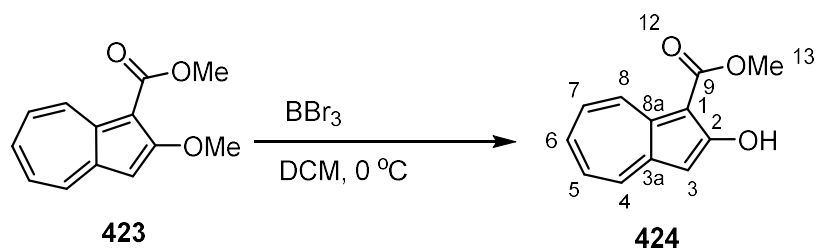
Methyl 2-methoxyazulene-1-carboxylate **423**



The preparation of this compound was based on a method by Pham.¹⁸⁷ To an ACE pressure round-bottom flask (capacity 50 mL) was added methyl 2-oxo-2H-cyclohepta[b]furan-3-carboxylate **422** (3.00 g, 14.7 mmol, 1.00 eq.), trimethyl orthoacetate **324** (8.00 mL) and toluene (7.00 mL). The mixture was stirred under air at 200 °C for 8 h, allowed to cool to r.t. overnight, and then stirred at 200 °C again for a further 3 h (CAUTION: the reaction was run behind a blast shield). After allowing to cool, the mixture was loaded onto a silica column and purified by column chromatography (5→14% EtOAc in petroleum ether) to give *methyl 2-methoxyazulene-1-carboxylate* **423** (1.68 g, 7.78 mmol, 53%) as a red, crystalline solid; R_f 0.22 (3:1 petroleum ether/EtOAc); δ_H (500 MHz, $CDCl_3$) 9.35 (1H, dd, J 9.7 Hz, 1.5 Hz, 8-CH), 8.05 (1H, d, J 9.8 Hz, 4-CH), 7.50-7.42 (2H, m, 6-CH and either 7-CH or 5-CH), 7.32-7.27 (1H, m, 5-CH or 7-CH), 6.65 (1H, s, 3-CH), 4.03 (3H, s, 10,11-CH₃), 3.93 (3H, s, 10,11-CH₃).

Data in agreement with those previously reported.¹⁹²

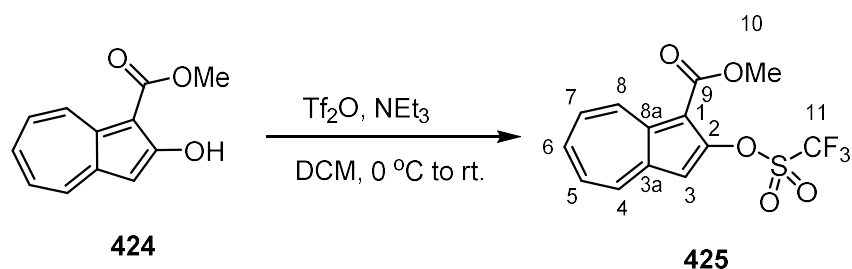
Methyl 2-hydroxyazulene-1-carboxylate **424**



The preparation of this compound was based on a method by Talaz.²⁰⁰ At $0\text{ }^\circ\text{C}$, to a stirred solution of methyl 2-methoxyazulene-1-carboxylate **423** (1.52 g, 7.04 mmol, 1.00 eq.) in DCM (100 mL) was added boron tribromide (1.0 M in heptanes, 7.10 mL, 7.10 mmol, 1.01 eq.), which instantly formed a brown/yellow cloudy mixture. After stirring for 40 min, MeOH (10 mL) was added, forming an orange/red solution, which was washed with water ($2 \times 50\text{ mL}$). The organic layer was dried over anhydrous MgSO_4 , and filtered. The filtrate was concentrated under reduced pressure to give *methyl 2-hydroxyazulene-1-carboxylate* **424** (1.33 g, 6.55 mmol, 93%) as an orange solid; R_f 0.49 (3:1 petroleum ether/EtOAc); δ_{H} (500 MHz, CDCl_3) 10.73 (1H, br s, 2-OH), 8.83 (1H, dd, J 9.5 Hz, 1.4 Hz, 8-CH), 8.07 (1H, d, J 10.0 Hz, 4-CH), 7.46 (1H, tt, J 9.1 Hz, 1.2 Hz, 6-CH), 7.44 (1H, td, J 9.9 Hz, 1.3 Hz, 5-CH or 7-CH), 7.32 (1H, ddd, J 10.3 Hz, 8.9 Hz, 1.3 Hz, 5-CH or 7-CH), 6.72 (1H, s, 3-CH), 4.02 (3H, s, 10- CH_3).

Compound **424** has previously been reported in the literature, but without accompanying NMR data.^{281,282}

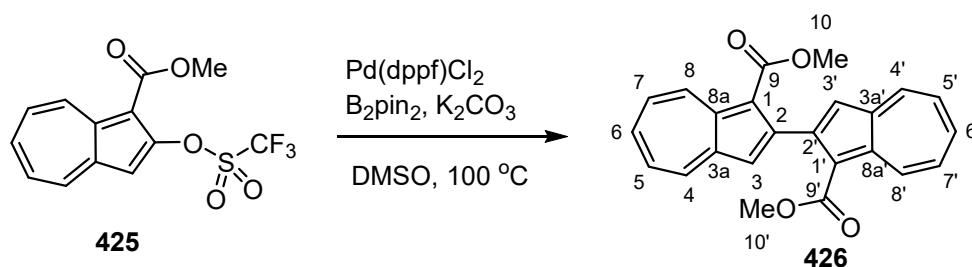
Methyl 2-(((trifluoromethyl)sulfonyl)oxy)azulene-1-carboxylate **425**



The preparation of this compound was based on a method by Morita.²⁰⁶ At 0 °C, to a stirred solution of methyl 2-hydroxyazulene-1-carboxylate **424** (1.33 g, 6.55 mmol, 1.00 eq.) and triethylamine (1.82 mL, 13.1 mmol, 2.00 eq.) in DCM (70 mL) was added by cannula a solution of trifluoromethanesulfonic anhydride (1.66 mL, 9.82 mmol, 1.50 eq.) in DCM (50 mL), which instantly changed colour from orange to magenta. The mixture was allowed to warm to r.t., and stirred for 90 min before the addition of H₂O (20 mL) to quench. The mixture was diluted with DCM (50 mL), and the phases were separated. The organic layer was washed with HCl_(aq) (0.5 M, 50 mL) and with water (2 × 50 mL), dried over anhydrous MgSO₄, and filtered. The filtrate was concentrated under reduced pressure to give the crude product, which was purified by column chromatography (20% EtOAc in petroleum ether) to give *methyl 2-(((trifluoromethyl)sulfonyl)oxy)azulene-1-carboxylate* **425** (1.91 g, 5.71 mmol, 87%) as a purple, crystalline solid (m.p. 68-70 °C); *R_f* 0.32 (3:1 petroleum ether/EtOAc); δ_{H} (500 MHz, CDCl₃) 9.73 (1H, dd, *J* 10.1 Hz, 0.6 Hz, 8-CH), 8.47 (1H, dd, *J* 9.7 Hz, 1.0 Hz, 4-CH), 7.91 (1H, tt, *J* 9.9 Hz, 1.1 Hz, 6-CH), 7.69 (1H, t, *J* 10.0 Hz, 7-CH), 7.58 (1H, t, *J* 9.8 Hz, 5-CH), 7.13 (1H, s, 3-CH), 4.00 (3H, s, 10-CH₃); δ_{C} (75 MHz, CDCl₃) 163.6 (9-C), 153.2 (2-C), 140.4 (3a-C), 140.3 (6-C), 139.89 (4-C or 8-C), 139.88 (4-C or 8-C), 139.2 (8a-C), 129.9 (7-C), 128.8 (5-C), 118.8 (q, ¹*J*_{CF} 320 Hz, 11-C), 107.9 (3-C), 106.5 (1-C), 51.3 (10-C); ν_{max} (film) 2961, 1691, 1612, 1595,

1581, 1535, 1514, 1462, 1424, 1407, 1306, 1292, 1228, 1197, 1137, 1055, 1042, 987, 968, 940, 898, 860, 817, 790, 764, 730, 706, 673 cm⁻¹; HRMS (ESI+) *m/z* calc for [C₁₃H₉F₃O₅S + Na]⁺, 357.0020; found 357.0039.

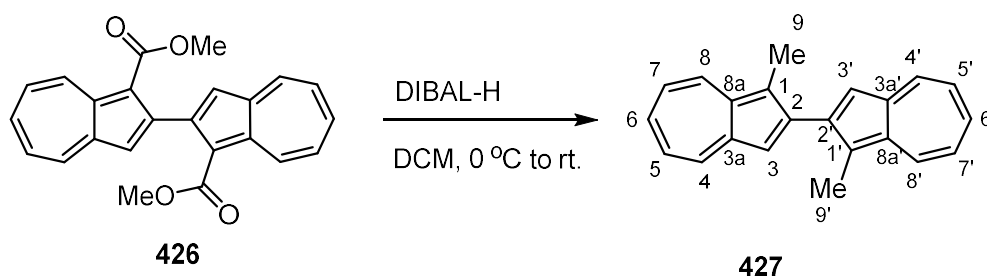
Dimethyl [2,2'-biazulene]-1,1'-dicarboxylate **426**



The preparation of this compound was based on a method by Bräse.²³⁴ At r.t., to a mixture of Pd(dppf)Cl₂ (163 mg, 0.225 mmol, 0.04 eq.), B₂pin₂ (714 mg, 2.82 mmol, 0.50 eq.) and K₂CO₃ (2.35 g, 16.9 mmol, 3.00 eq.) was added a solution of methyl 2-(((trifluoromethyl)sulfonyl)oxy)azulene-1-carboxylate **425** (1.88 g, 5.63 mmol, 1.00 eq.) in DMSO (degassed by freeze-pump-thaw, 20 mL). The mixture was stirred at 80 °C for 15 h, allowed to cool, and then diluted with DCM (120 mL). The solution was washed with NaOH_(aq) (2.5 M, 50 mL) and water (2 × 50 mL), and the organic layer was dried over anhydrous MgSO₄, and filtered. The filtrate was concentrated under reduced pressure to give the crude product, which was purified by column chromatography (10→50% EtOAc in petroleum ether) to give *dimethyl [2,2'-biazulene]-1,1'-dicarboxylate* **426** (459 mg, 1.24 mmol, 44%) as a blue/violet solid; R_f 0.18 (3:1 petroleum ether/EtOAc); δ_H (500 MHz, CDCl₃) 9.59 (2H, d, *J* 10.0 Hz, 8,8'-CH), 8.39 (2H, d, *J* 9.6 Hz, 4,4'-CH), 7.73 (2H, tt, *J* 9.8 Hz, 1.1 Hz, 6,6'-CH) 7.53 (2H, t, *J* 10.0 Hz, 7,7'-CH), 7.42 (2H, s, 3,3'-CH), 7.39 (2H, t, *J* 9.7 Hz, 5,5'-CH), 3.67 (6H, s, 10,10'-CH₃).

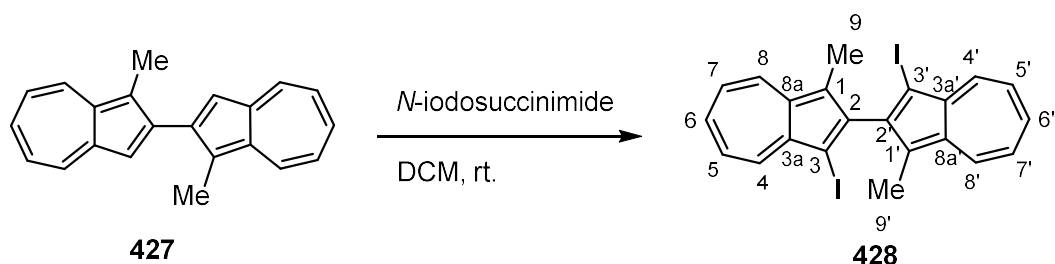
Data in agreement with those previously reported.²⁰⁵

1,1'-dimethyl-2,2'-biazulene **427**



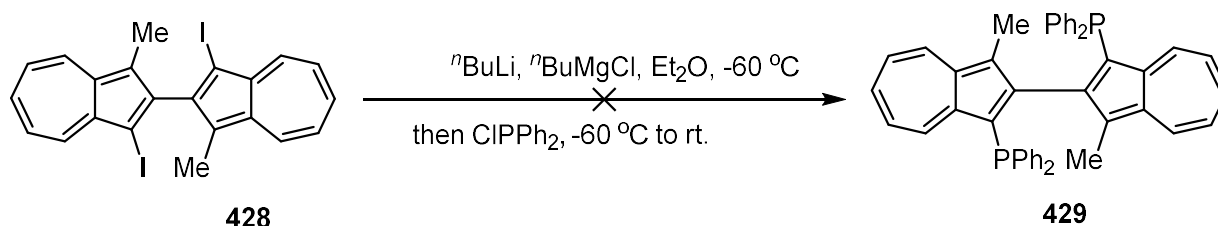
The preparation of this compound was based on a method by Hansen.¹⁹⁵ At 0 °C, to a stirred solution of dimethyl [2,2'-biazulene]-1,1'-dicarboxylate **426** (50 mg, 0.135 mmol, 1.00 eq.) in DCM (4.0 mL) was slowly added DIBAL-H (1.0 M in hexanes, 1.35 mL, 10.0 eq.), instantly changing colour from deep violet to blue/green. The solution was allowed warm to r.t., stirred for 17 h, and quenched with water (1.0 mL). The mixture was diluted with DCM (10 mL) and filtered through a bed of Celite, washing through with DCM (4 × 10 mL). The filtrate was dried over anhydrous MgSO₄, and filtered. The filtrate was concentrated under reduced pressure to give the crude product, which was purified by column chromatography (5→10% EtOAc in petroleum ether) to give 1,1'-dimethyl-2,2'-biazulene **427** (12 mg, 0.0439 mmol, 33%) as a dark green solid (m.p. 199-201 °C); *R*_f 0.47 (9:1 petroleum ether/EtOAc); δ_{H} (500 MHz, CDCl₃) 8.33 (2H, d, *J* 9.7 Hz, 8,8'-CH) 8.28 (2H, d, *J* 9.4 Hz, 4,4'-CH), 7.56 (2H, s, 3,3'-CH), 7.53 (2H, tt, *J* 9.9 Hz, 1.1 Hz, 6,6'-CH), 7.15 (2H, t, *J* 9.8 Hz, 7,7'-CH), 7.11 (2H, t, *J* 9.6 Hz, 5,5'-CH), 2.75 (6H, s, 9,9'-CH₃); δ_{C} (126 MHz, CDCl₃) 146.8 (2,2'-C), 139.7 (3a,3a'-C), 137.5 (8a,8a'-C), 136.8 (6,6'-C), 135.7 (4,4'-C), 133.6 (8,8'-C), 124.7 (1,1'-C), 122.6 (5,5'-C), 121.9 (7,7'-C), 118.4 (3,3'-C), 11.9 (9,9'-C); ν_{max} (film) 2963, 2915, 2849, 1566, 1532, 1460, 1410, 1381, 1293, 1259, 1215, 1181, 1086, 1015, 967, 951, 930, 879, 856, 809, 795, 731, 720, 695, 677 cm⁻¹; HRMS (ESI+) *m/z* calc for [C₂₂H₁₈ + H]⁺, 283.1487; found, 283.1500.

1,1'-Diiodo-3,3'-dimethyl-2,2'-biazulene **428**



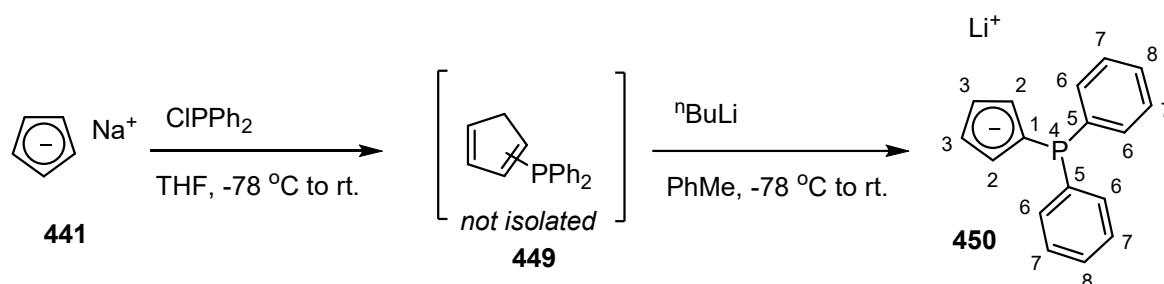
Under atmosphere of air at r.t., to a round-bottom flask wrapped in aluminium foil, charged with a stirred solution of 1,1'-dimethyl-2,2'-biazulene **427** (68 mg, 0.241 mmol, 1.00 eq.) in DCM (17 mL) was added *N*-iodosuccinimide (114 mg, 0.506 mmol, 2.10 eq.), and allowed to stir for 80 min. To the mixture was then added neutral alumina (~0.5 g), the solvent was removed in vacuo, and the crude product was purified by column chromatography (1→5% EtOAc in petroleum ether, neutral alumina) to give 1,1'-diiodo-3,3'-dimethyl-2,2'-biazulene **428** (15 mg, 0.0285 mmol, 12%) as a dark blue solid (m.p. >300 °C (dec.)); R_f 0.54 (9:1 petroleum ether/EtOAc, neutral alumina); δ_H (500 MHz, C_6D_6) 8.35 (2H, dd, J 9.7 Hz, 1.0 Hz, 4,4'-CH), 7.87 (2H, dd, J 9.5 Hz, 1.0 Hz, 8,8'-CH), 7.14 (2H, tt, J 9.9 Hz, 1.0 Hz, 6,6'-CH), 6.77 (2H, t, J 10.1 Hz, 5,5'-CH), 6.75 (2H, t, J 10.1 Hz, 7,7'-CH), 2.35 (6H, s, 9,9'-CH₃); δ_C (126 MHz, C_6D_6) 151.9 (2,2'-C), 140.1 (3a,3a'-C), 138.8 (4,4'-C), 138.7 (8a,8a'-C), 138.0 (6,6'-C), 134.0 (8,8'-C), 126.6 (1,1'-C), 123.7 (5,5'-C), 123.0 (7,7'-C), 79.4 (3,3'-C), 12.2 (9,9'-C); $\nu_{max}(\text{film})$ 2982, 2905, 2852, 1573, 1447, 1373, 1318, 1293, 1259, 1218, 1157, 1047, 1016, 959, 944, 879, 830, 785, 734, 721, 681 cm^{-1} ; HRMS (ASAP+) m/z calc for $[C_{22}H_{16}I_2 + H]^+$, 534.9420; found, 534.9426.

(3,3'-dimethyl-[2,2'-biazulene]-1,1'-diyl)bis(diphenylphosphine) 429



The preparation of this compound was based on a method by Ito.¹⁸¹ At $-60\text{ }^\circ\text{C}$, to a solution of *n*.butylmagnesium chloride (2.0 M in THF, 40 μL , 2.76 eq.) in Et_2O (degassed by sparging with N_2 , 0.50 mL) was added dropwise a solution of *n*-butyllithium (2.43 M in hexanes, 60 μL , 5.14 eq.), and the mixture was allowed to stir for 10 min. To the mixture was added dropwise a solution of 1,1'-diiodo-3,3'-dimethyl-2,2'-biazulene **428** (15 mg, 0.0285 mmol, 1.00 eq.) in Et_2O (degassed by sparging with N_2 , 1.50 mL), forming a dark green solution. After allowing to stir for 35 min, to the mixture was added dropwise chlorodiphenylphosphine (50 μL , 0.273 mmol, 9.57 eq.), and the reaction was allowed to warm to r.t. while in the dry ice/chloroform bath. After allowing to stir for 100 min, water (2.0 mL) was added and the mixture was extracted with Et_2O (10 mL). The organic extract was washed with saturated $\text{NH}_4\text{Cl}_{(\text{aq})}$ (10 mL), dried over anhydrous MgSO_4 and filtered. The filtrate was concentrated under reduced pressure to give the crude product, and purified by column chromatography (1 \rightarrow 25% EtOAc in petroleum ether) to give impure starting material.

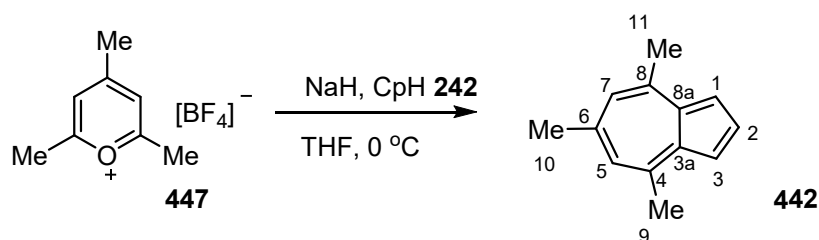
Lithium (diphenylphosphino)cyclopentadienide **450**



The preparation of this compound was based on a method by Erker.²⁶² To a Schlenk flask charged with THF (30 mL) was added a solution of sodium cyclopentadienide **441** (2.0 M in THF, 15.0 mL, 1.00 eq.). At $-78\text{ }^\circ\text{C}$, to this stirred solution was added dropwise chlorodiphenylphosphine (5.50 mL, 30.0 mmol, 1.00 eq.), and stirred for 16 h, allowing to warm up to r.t. The solvent was then removed *in vacuo* to give a brown/red solid, which was dissolved in toluene (60 mL) and filtered through a pad of Celite. The Celite was then washed with toluene (30 mL). At $-78\text{ }^\circ\text{C}$, to the combined filtrate, with stirring, was added dropwise a solution of *n*-butyllithium (1.97 M in hexanes, 15.5 mL, 1.00 eq.), then allowed to warm to r.t. After stirring for 2.5 h, the solvent was removed *in vacuo*, and the resultant solid was triturated with hexane ($2 \times 30\text{ mL}$) and dried *in vacuo* to give *lithium (diphenylphosphinyl)cyclopentadienide* **450** (5.88 g, 22.9 mmol, 76%) as a golden yellow solid; δ_{H} (300 MHz, $\text{THF-}d_8$) 7.30-7.24 (4H, m, 6-CH), 7.14-7.06 (6H, m, 7,8-CH), 5.95-5.89 (4H, m, 2,3-CH); δ_{P} (122 MHz, $\text{THF-}d_8$) -20.47 (4-P).

Data in agreement with those previously reported.²⁶²

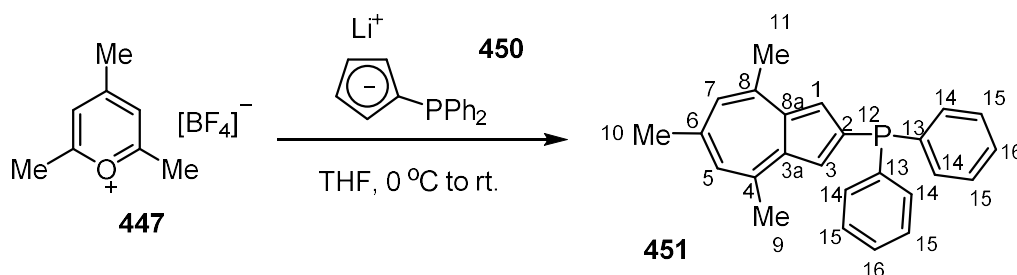
4,6,8-trimethylazulene **442**



This compound was prepared according to the method by Hansen.²⁵⁶ At 0 °C, to a stirred suspension of sodium hydride (60% suspension in oil, 938 mg, 23.4 mmol, 1.80 eq.) in THF (50 mL) was added dropwise freshly cracked cyclopentadiene **242** (4.50 mL, 53.5 mmol, 4.20 eq.). The reaction mixture was stirred for 30 min at 0 °C. After 5 min, the suspension had changed colour from white to deep red. At room temperature, to a stirred suspension of 2,4,6-trimethylpyrylium tetrafluoroborate **447** (2.69 g, 12.8 mmol, 1.0 eq.) in THF (50 mL) was added by cannula the solution of sodium cyclopentadienide, immediately forming a deep purple colour, and was stirred for 2 h. The solvent was removed under reduced pressure, then crude mixture was dissolved in Et₂O (150 mL), washed with water (4 × 75 mL) and again with saturated brine. The organic phase was dried over anhydrous MgSO₄, filtered, and the filtrate was concentrated under reduced pressure. The crude product was purified by column chromatography (pentane), followed by recrystallisation (EtOH) to yield 4,6,8-trimethylazulene **442** (854 mg, 5.01 mmol, 39%) as deep purple plates; *R*_f 0.22 (pentane); δ_H (250 MHz, CDCl₃) 7.67 (1H, s, 2-CH), 7.37 (2H, br s, 5,7-CH), 7.08 (2H, s, 1,3-CH), 2.90 (6H, s, 9,11-CH₃), 2.67 (3H, s, 10-CH₃).

Data in agreement with those previously reported.²⁴⁵

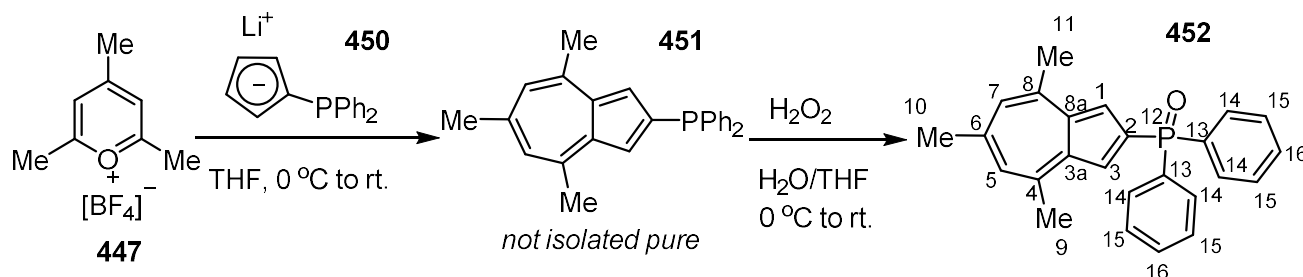
Diphenyl(4,6,8-trimethylazulen-2-yl)phosphine **451**



The preparation of this compound was based on a method by Hansen.²⁵⁶ At 0 °C, to a stirred suspension of 2,4,6-trimethylpyrylium tetrafluoroborate **447** (300 mg, 1.42 mmol, 1.00 eq.) in THF (10 mL) was added by cannula lithium (diphenylphosphinyl)cyclopentadienide **450** (732 mg, 2.84 mmol, 2.00 eq.) in THF (10 mL), forming a deep blue/violet mixture, which was allowed to stir for 40 h before filtering through a silica plug, under atmosphere of argon. The filtrate was concentrated under reduced pressure to give the crude product, which was purified by column chromatography (0→4% EtOAc in petroleum ether) and recrystallisation (EtOH) to give *diphenyl(4,6,8-trimethylazulen-2-yl)phosphine* **451** (15 mg, 0.0423 mmol, 3.0%) as purple plates (m.p. 135-137 °C); R_f 0.45 (9:1 petroleum ether/EtOAc); δ_H (300 MHz, $CDCl_3$) 7.47-7.41 (4H, m, 14-CH), 7.35-7.32 (6H, m, 15,16-CH), 7.20 (2H, d, $^3J_{PH}$ 3.1 Hz, 1,3-CH), 7.03 (2H, s, J 5,7-CH), 2.75 (6H, s, 9,11-CH₃), 2.60 (3H, s, 10-CH₃); δ_P (122 MHz, $CDCl_3$) -14.92 (12-P); ν_{max} (film) 3051, 2980, 2967, 2926, 1578, 1537, 1466, 1433, 1372, 1333, 1291, 1217, 1185, 1141, 1109, 1084, 1023, 997, 909, 847, 806, 745, 721, 694, 627 cm^{-1} ; HRMS (ESI+) m/z calc for $[C_{25}H_{23}P + H]^+$, 355.1616; found, 355.1631.

^{13}C -NMR spectrum not obtained due to insufficient quantity and stability of compound.

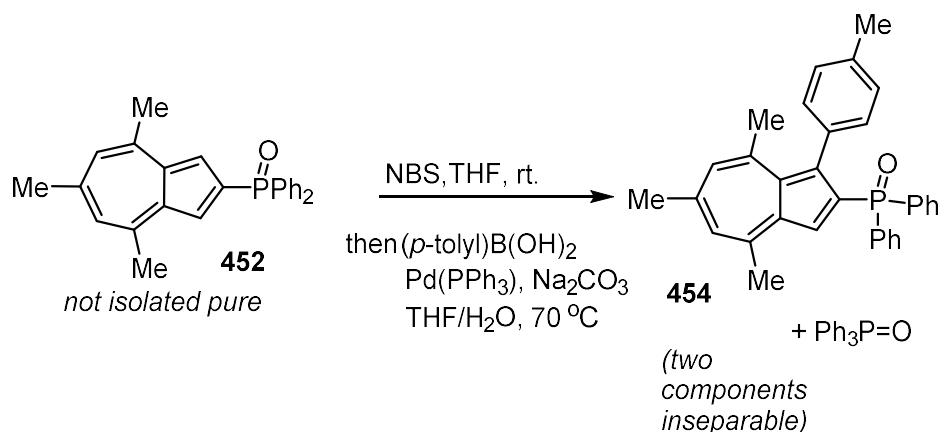
Diphenyl(4,6,8-trimethylazulen-2-yl)phosphine oxide **452**



The preparation of this compound was based on a method by Hansen.²⁵⁶ At 0 °C, to a stirred solution of 2,4,6-trimethylpyrylium tetrafluoroborate **447** (2.36 g, 11.2 mmol, 1.00 eq.) in THF (40 mL) was added by cannula a solution of lithium (diphenylphosphinyl)cyclopentadienide **450** (5.76 g, 22.5 mmol, 2.00 eq.) in THF (40 mL). After stirring for 1 h, under an atmosphere of argon, the solution was filtered through a pad of silica, washing through with ethyl acetate (40 mL), and was concentrated under reduced pressure to give the crude *diphenyl(4,6,8-trimethylazulen-2-yl)phosphine* **451**, which could not be completely purified by column chromatography (0→2% EtOAc in petroleum ether) or recrystallisation (EtOH). Thus, at 0 °C, to a stirred solution of the impure *diphenyl(4,6,8-trimethylazulen-2-yl)phosphine* **451** (1.06 g, <2.98 mmol, 1.00 eq.) in THF (10 mL) was added hydrogen peroxide solution (35% wt. in H₂O, 0.350 mL, 3.57 mmol, 1.20 eq.), and allowed to stir for 25 min, before the addition of Na₂S₂O_{3(aq)} (10 wt. %, 10 mL) to quench excess hydrogen peroxide. The aqueous solution was extracted with CHCl₃ (2 × 10 mL), and the combined organic extracts were dried over anhydrous MgSO₄, and filtered. The filtrate was concentrated under reduced pressure to give the crude product, which was purified by column chromatography (50→100% EtOAc in petroleum ether) and recrystallisation (4:1 THF/hexane) to give *diphenyl(4,6,8-trimethylazulen-2-yl)phosphine oxide* **452** (54 mg, 0.145 mmol, 1.3%) as purple

plates (m.p. 181-183 °C); R_f 0.20 (EtOAc); δ_H (300 MHz, $CDCl_3$) 7.81-7.73 (4H, m, 14-CH), 7.56-7.41 (6H, m, 15,16-CH), 7.54 (2H, d, $^3J_{PH}$ 5.5 Hz, 1,3-CH), 7.11 (2H, s, 5,7-CH), 2.82 (6H, s, 9,11-CH₃), 2.63 (3H, s, 10-CH₃); δ_C (75 MHz, $CDCl_3$) 150.1 (6-C), 149.2 (4,8-C), 136.3 (d, $^3J_{CP}$ 14.0 Hz, 3a,8a-C), 134.3 (d, $^1J_{CP}$ 110.2 Hz, 2-C), 133.7 (d, $^1J_{CP}$ 105.0 Hz, 13-C), 131.9 (d, $^2J_{CP}$ 10.2 Hz, 14-C), 131.6 (d, $^4J_{CP}$ 2.8 Hz, 16-C), 128.3 (5,7-C), 128.3 (d, $^3J_{CP}$ 12.3 Hz, 15-C), 120.2 (d, $^2J_{CP}$ 12.1 Hz, 1,3-C), 29.0 (10-C), 25.2 (9,11-C); δ_P (122 MHz, $CDCl_3$) 26.3 (12-P); $\nu_{max}(\text{film})$ 3054, 2918, 2855, 1578, 1537, 1481, 1467, 1435, 1368, 1335, 1292, 1219, 1182, 1159, 1141, 1098, 1084, 1072, 1024, 940, 911, 845, 805, 745, 720, 694 cm^{-1} ; HRMS (ESI+) m/z calc for $[C_{25}H_{23}OP + H]^+$, 371.1564; found, 371.1575.

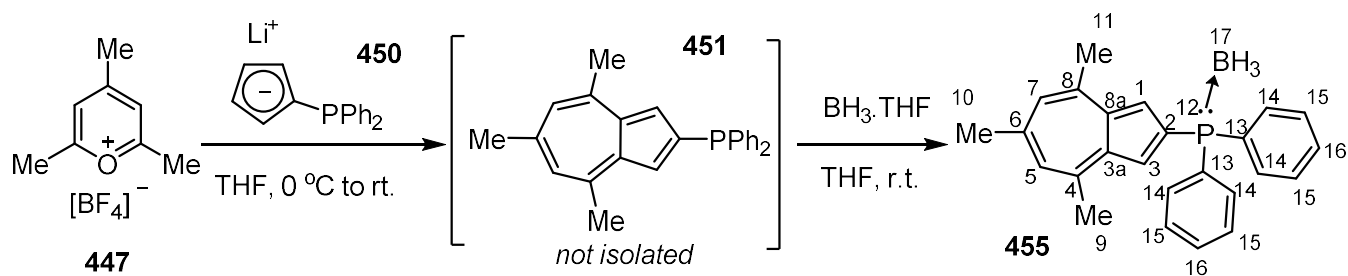
Diphenyl(4,6,8-trimethyl-1-(*p*-tolyl)azulen-2-yl)phosphine oxide **454**



The preparation of this compound was based on a method by Zhang.²⁶³ Under atmosphere of air, at r.t., to an aluminium foil-covered solution of crude diphenyl(4,6,8-trimethylazulen-2-yl)phosphine oxide **452** (100 mg, ~0.270 mmol, 1.00 eq.) in THF (degassed by sparging with N_2 , 10 mL) was added portionwise *N*-bromosuccinimide (48 mg, 0.270 mmol, 1.00 eq.). After allowing to stir for 20 min, to the mixture was added sodium carbonate (286 mg, 2.70 mmol, 10.0 eq.), *p*-tolylboronic acid (74 mg, 0.540 mmol, 2.00 eq.), tetrakis(triphenylphosphine)palladium (31 mg, 0.027 mmol, 0.10 eq.) and water (3.0 mL), and the mixture was stirred at 70 °C for 18 h. After allowing it to cool, the mixture was diluted with water (25 mL) and extracted with EtOAc (3 × 20 mL). The combined organic extracts were dried over anhydrous MgSO_4 and filtered. The filtrate was concentrated under reduced pressure to give the crude product, which was purified by column chromatography (50→100% EtOAc in petroleum ether) to give *diphenyl(4,6,8-trimethyl-1-(p-tolyl)azulen-2-yl)phosphine oxide* **454**, which co-eluted with triphenylphosphine oxide (39 mg, <0.0846 mmol, <31%) as a dark blue solid; R_f 0.35 (EtOAc); δ_{H} (300 MHz, CDCl_3) 7.70-7.63 (m), 7.57-7.42 (m), 7.41-7.38 (2H, m), 7.31-7.25 (4H, m), 7.04 (1H, s), 6.91 (1H, s), 6.87 (2H, d, J 8.0 Hz), 6.73

(2H, d, *J* 7.8 Hz), 2.78 (3H, s), 2.58 (3H, s), 2.24 (3H, s), 2.23 (3H, s); δ_P (122 MHz, $CDCl_3$) 24.7; HRMS (ESI+) *m/z* calc for $[C_{32}H_{29}OP + H]^+$, 461.2034; found, 461.2020.

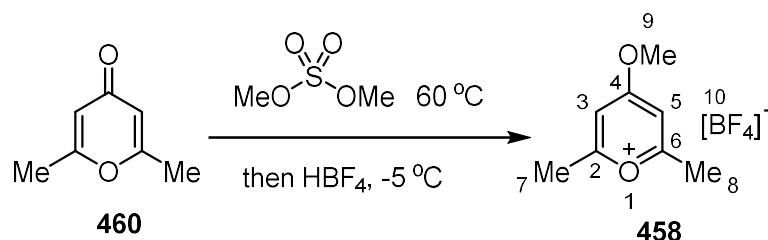
Boranyldiphenyl(4,6,8-trimethylazulen-2-yl)phosphine **455**



The preparation of this compound was based on a method by Hansen.²⁵⁶ At 0 °C, to a suspension of 2,4,6-trimethylpyrylium tetrafluoroborate **447** (1.10 g, 5.23 mmol, 1.00 eq.) in THF (30 mL) was added a solution of lithium (diphenylphosphinyl)cyclopentadienide **450** (2.68 g, 10.5 mmol, 2.00 eq.) in THF (30 mL). After stirring at 0 °C for 1 h, the mixture was filtered through a pad of neutral alumina under atmosphere of argon. To the stirred filtrate, at r.t., was slowly added a solution of borane-THF complex (11.0 mL, 1.0 M in THF, 2.10 eq.). After stirring for 16 h, the reaction was quenched by the addition of methanol (10 mL). The solution was then concentrated under reduced pressure to a small volume, and added to ethyl acetate (60 mL). The solution was washed with water (3 × 50 mL) and with saturated brine, and the organic layer was dried over anhydrous MgSO_4 , and filtered. The filtrate was concentrated under reduced pressure to give the crude product, which was purified by column chromatography (0→10% EtOAc in petroleum ether) to give *boranyldiphenyl(4,6,8-trimethylazulen-2-yl)phosphine* **455** (228 mg, 0.621 mmol, 12%) as a purple solid (m.p. 148-150 °C); R_f 0.53 (3:1 petroleum ether/EtOAc); δ_{H} (300 MHz, CDCl_3) 7.73-7.66 (4H, m, 14-CH), 7.51-7.41 (6H, m, 15,16-CH), 7.46 (2H, d, $^3J_{\text{PH}}$ 5.1 Hz, 1,3-CH), 7.12 (2H, s, 5,7-CH), 2.83 (6H, s, 9,11-CH₃), 2.65 (3H, s, 10-CH₃), 1.44 (3H, br d, 17-BH₃); δ_{C} (75 MHz, CDCl_3) 149.7 (6-C), 148.7 (4,8-C), 136.5 (d, $^3J_{\text{CP}}$ 11.5 Hz, 3a,8a-C), 133.0 (d, $^2J_{\text{CP}}$ 9.9 Hz, 14-C), 131.1

(d, $^1J_{CP}$ 62.7 Hz, 2-C), 130.8 (d, $^4J_{CP}$ 2.5 Hz, 16-C), 130.6 (d, $^1J_{CP}$ 58.9 Hz, 13-C), 128.5 (d, $^3J_{CP}$ 10.2 Hz, 15-C), 128.3 (d, $^5J_{CP}$ 1.2 Hz, 5,7-C), 120.8 (d, $^2J_{CP}$ 10.5 Hz, 1,3-C), 29.0 (10-C), 25.2 (9,11-C); δ_P (122 MHz, $CDCl_3$) 12.38-11.65 (m, 12-P); δ_B (96 MHz, $CDCl_3$) -34.5 (17-B); ν_{max} (film) 3675, 2987, 2971, 2901, 2380 (ν_{BH}), 1578, 1537, 1483, 1468, 1435, 1408, 1394, 1377, 1333, 1290, 1218, 1187, 1140, 1102, 1027, 1066, 907, 882, 847, 809, 797, 766, 740, 690 cm^{-1} ; HRMS (ESI+) m/z calc for $[C_{25}H_{26}BP + Na]^+$, 391.1763; found, 391.1796.

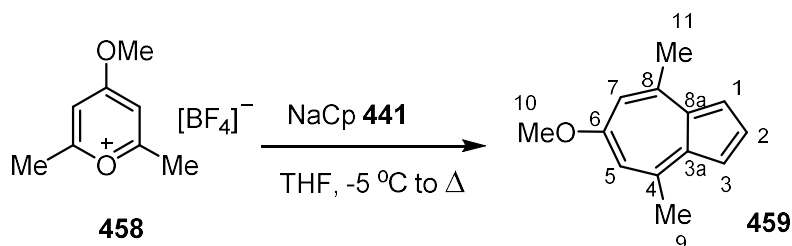
4-Methoxy-2,6-dimethylpyrylium tetrafluoroborate **458**



The preparation of this compound was based on a method by Hansen.²⁵⁶ At r.t., to 2,6-dimethyl-γ-pyrone **460** (1.00 g, 8.06 mmol, 1.00 eq.) was added dimethyl sulfate (1.20 mL, 12.7 mmol, 1.57 eq.), and the mixture was stirred at 60 °C for 16 h. The mixture was then cooled to -5 °C, and to it was slowly added HBF_{4(aq)} (50 wt. %, 1.45 mL, 8.20 mmol, 1.01 eq.) and stirred for 2 h. The mixture was allowed to warm to r.t., and to it was added *tert*-butyl methyl ether (1.00 mL), stirring for another 1 h. The solid product was collected by filtration, washing with DCM, to give *4-methoxy-2,6-dimethylpyrylium tetrafluoroborate* **458** (361 mg, 1.60 mmol, 20%) as an off-white solid; δ_{H} (300 MHz, DMSO-*d*₆) 6.08 (2H, s, 3,5-CH), 3.16 (3H, s, 9-CH₃), 2.23 (6H, s, 7,8-CH₃); δ_{B} (96 MHz, DMSO-*d*₆) 1.94 (10-B).

Compound **458** has previously been reported in the literature, but without accompanying NMR data.

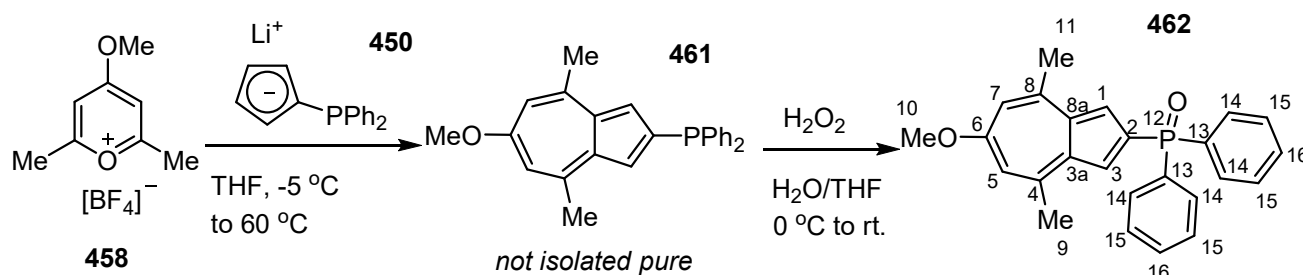
6-Methoxy-4,8-dimethylazulene **459**



The preparation of this compound was based on a method by Hansen.²⁵⁶ At r.t., to a 2-neck round bottom flask charged with THF (2.0 mL) was added sodium cyclopentadienide **441** (2.0 M in THF, 2.65 mL, 5.31 mmol, 4.00 eq.). At -5 °C, to this stirred solution was added portionwise 4-methoxy-2,6-dimethylpyrylium tetrafluoroborate **458** (300 mg, 1.33 mmol, 1.00 eq.), instantly forming a magenta solution, which was then allowed to warm to r.t. and then stirred at 68 °C for 17 h. After allowing it to cool to r.t., the reaction mixture was poured over crushed ice. The aqueous mixture was extracted with ethyl acetate (2 × 50 mL), and the combined organic extracts were washed with saturated brine, dried over anhydrous MgSO₄, and filtered. The filtrate was concentrated under reduced pressure to give the crude product, which was purified by column chromatography (0→1% EtOAc in petroleum ether) to give *6-methoxy-4,8-dimethylazulene* **459** (97 mg, 0.521 mmol, 39%) as a magenta solid; *R*_f 0.48 (9:1 petroleum ether/EtOAc); δ_{H} (250 MHz, CDCl₃) 7.54 (1H, t, *J* 3.9 Hz, 2-CH), 7.37 (2H, d, *J* 3.9 Hz, 1,3-CH), 6.81 (2H, s, 5,7-CH), 3.96 (3H, s, 10-CH₃), 2.91 (6H, s, 9,11-CH₃).

Data in agreement with those previously reported.²⁵⁶

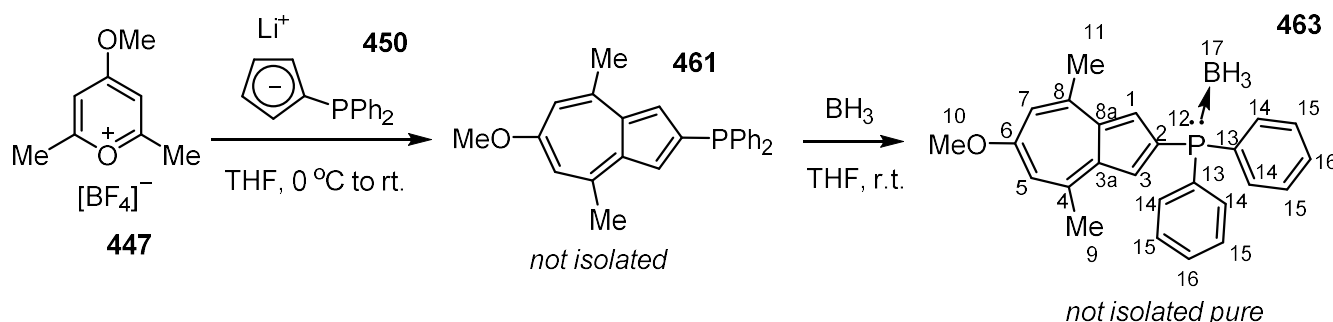
(6-Methoxy-4,8-dimethylazulen-2-yl)diphenylphosphine oxide 462



The preparation of this compound was based on a method by Hansen.²⁵⁶ At $-5\text{ }^\circ\text{C}$, to a stirred solution of lithium (diphenylphosphinyl)cyclopentadienide **450** (1.36 g, 5.31 mmol, 4.00 eq.) in THF (5.0 mL) was added portionwise 4-methoxy-2,6-dimethylpyrylium tetrafluoroborate **458** (300 mg, 1.33 mmol, 1.00 eq.), and the mixture was stirred at $-5\text{ }^\circ\text{C}$ for 20 min, changing in colour to deep purple. The mixture was then stirred at $60\text{ }^\circ\text{C}$ for 15 h, and then allowed to cool to r.t., and poured onto crushed ice. The aqueous mixture was extracted with ethyl acetate ($2 \times 50\text{ mL}$), and the combined organic extracts were dried over anhydrous MgSO_4 , and filtered. The filtrate was concentrated under reduced pressure to give crude (6-methoxy-4,8-dimethylazulen-2-yl)diphenylphosphine **461**, which could not be completely purified by column chromatography (0 \rightarrow 1% EtOAc in petroleum ether). Thus, at r.t., to a stirred solution of the impure (6-methoxy-4,8-dimethylazulen-2-yl)diphenylphosphine **461** (93 mg, $<0.251\text{ mmol}$, 1.00 eq.) in THF (2.0 mL) was added hydrogen peroxide (35 wt. % in H_2O , $120\text{ }\mu\text{L}$, 1.26 mmol , 5.00 eq.), and the mixture was allowed to stir for 2 h. The reaction was quenched by the addition of $\text{Na}_2\text{S}_2\text{O}_3(\text{aq})$ (10 wt. % in H_2O , 2.0 mL), and to this was added ethyl acetate (20 mL), and the phases were separated. The organic layer was washed with water ($3 \times 10\text{ mL}$), dried over anhydrous MgSO_4 , and filtered. The filtrate was concentrated under reduced pressure to give the crude product, which was purified by column

chromatography (0→2% MeOH in DCM) to give (6-methoxy-4,8-dimethylazulen-2-yl)diphenylphosphine oxide **462** (11 mg, 0.0285 mmol, 2.1% overall) as a red/purple solid (m.p. 180-183 °C); R_f 0.26 (19:1 DCM/MeOH); δ_H (500 MHz, $CDCl_3$) 7.79-7.74 (4H, m, 14-CH), 7.53-7.49 (2H, m, 16-CH), 7.50 (2H, d, $^3J_{PH}$ 5.4 Hz, 1,3-CH), 7.46-7.43 (4H, m, 15-CH), 6.79 (2H, s, 5,7-CH), 3.96 (3H, s, 10-CH₃), 2.81 (6H, s, 9,11-CH₃); δ_C (126 MHz, $CDCl_3$) 166.9 (6-C), 149.9 (4,8-C), 134.3 (d, $^1J_{CP}$ 104.8 Hz, 13-C), 133.8 (d, $^3J_{CP}$ 14.3 Hz, 3a,8a-C), 131.9 (d, $^2J_{CP}$ 10.4 Hz, 14-C), 131.6 (d, $^1J_{CP}$ 112.2 Hz, 2-C), 131.4 (d, $^4J_{CP}$ 2.8 Hz, 16-C) 128.2 (d, $^3J_{CP}$ 12.0 Hz, 15-C), 121.1 (d, $^2J_{CP}$ 12.3 Hz, 1,3-C), 113.9 (5,7-C), 55.9 (10-C), 25.6 (9,11-C); δ_P (202 MHz, $CDCl_3$) 25.1 (12-P); ν_{max} (film) 3071, 2999, 2918, 2850, 1581, 1556, 1526, 1483, 1461, 1454, 1436, 1357, 1337, 1294, 1262, 1217, 1173, 1132, 1113, 1097, 1083, 1062, 1026, 997, 965, 928, 908, 885, 836, 812, 741, 720, 693 cm^{-1} ; HRMS (ESI+) m/z calc for $[C_{25}H_{23}O_2P + Na]^+$, 409.1328; found, 409.1347.

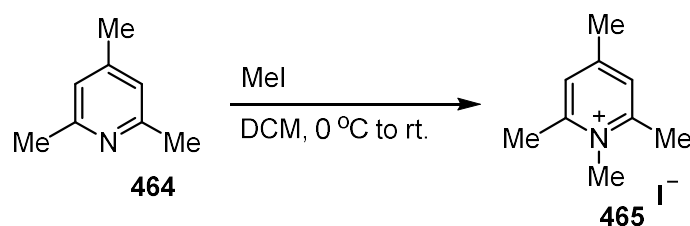
Boranyldiphenyl(6-methoxy-4,8-dimethylazulen-2-yl)phosphine **463**



The preparation of this compound was based on a method by Hansen.²⁵⁶ At -5 °C, to a stirred solution of lithium (diphenylphosphinyl)cyclopentadienide **450** (1.36 g, 5.31 mmol, 4.00 eq.) in THF (5.0 mL) was added portionwise 4-methoxy-2,6-dimethylpyrylium tetrafluoroborate **458** (300 mg, 1.33 mmol, 1.00 eq.), immediately changing in colour to deep purple. The mixture was then stirred at 60 °C for 17 h, allowed to cool to r.t., and then was poured onto crushed ice. The aqueous mixture was extracted with ethyl acetate (2 × 50 mL), and the combined organic extracts were washed with saturated brine, dried over anhydrous MgSO_4 , and filtered. The filtrate was concentrated under reduced pressure to give the crude *diphenyl*(6-methoxy-4,8-dimethylazulen-2-yl)phosphine **461** as a thick brown oil. Under atmosphere of N_2 , at 0 °C, to a solution of the crude *diphenyl*(6-methoxy-4,8-dimethylazulen-2-yl)phosphine **461** in THF (20 mL) was added borane (1.0 M in hexanes, 5.50 mL, 5.50 mmol, 4.13 eq.), and the mixture was allowed to warm to r.t. and stirred for 1 h. To the mixture was then added more borane (1.0 M in hexanes, 1.40 mL, 1.40 mmol, 1.05 eq.), and stirred for 17 h. The reaction was quenched by the addition of MeOH (10 mL), and the solution was concentrated under reduced pressure. The residue was dissolved in ethyl acetate (100 mL), washed with water (100 mL) and with saturated brine, and the organic layer was dried over anhydrous

MgSO₄, and filtered. The filtrate was concentrated under reduced pressure to give the crude product, on which purification was attempted by column chromatography (0→20% EtOAc in petroleum ether) and recrystallisation (EtOH) to give impure *boranyldiphenyl(6-methoxy-4,8-dimethylazulen-2-yl)phosphine* **463** (69 mg, <0.180 mmol, <14%) as a red/maroon solid (m.p. 99-103 °C (dec.)); R_f 0.24 (4:1 petroleum ether/EtOAc); δ_H (500 MHz, CDCl₃) 7.78-7.57 (m), 7.50-7.40 (m), 7.42 (2H, d, ³J_{PH} 5.1 Hz, 1,3-CH), 6.79 (2H, s, 5,7-CH), 3.95 (3H, s, 10-CH₃), 2.80 (6H, s, 9,11-CH₃); δ_P (122 MHz, CDCl₃) 13.6-10.5 (m, 12-P); δ_B (96 MHz, CDCl₃) 35.1 (17-B); HRMS (ESI+) *m/z* calc for [C₂₅H₂₆BOP + Na]⁺, 407.1707; found, 407.1715.

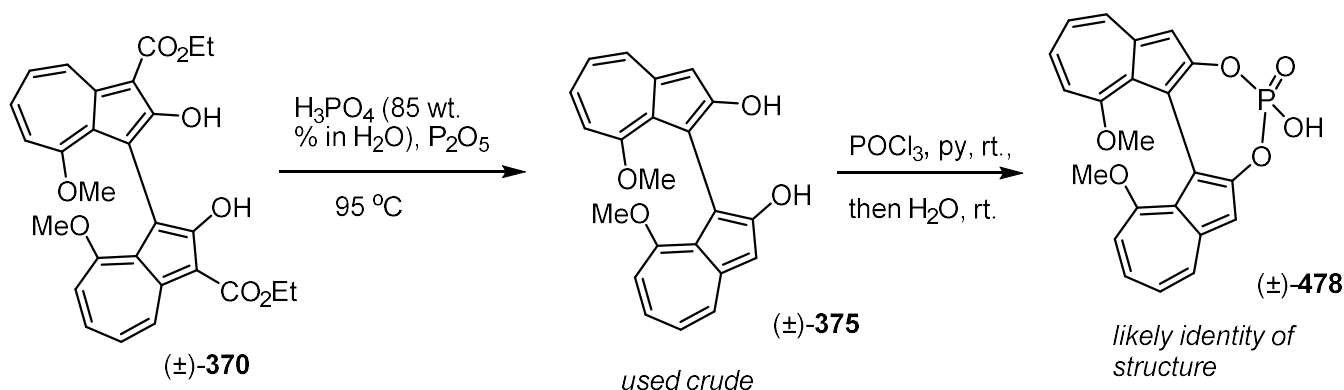
1-methyl-2,4,6-collidinium iodide **465**



The preparation of this compound was based on a method by Tang.²⁶⁵ At 0 °C, to a solution of 2,4,6-collidine **464** (1.32 mL, 10.0 mmol, 1.00 eq.) in DCM (10 mL) was added dropwise methyl iodide (1.00 mL, 16.0 mmol, 1.60 eq.). The mixture was allowed to warm to r.t. and stirred for 16 h, forming an off white precipitate. The precipitate was collected by filtration, and purified by recrystallisation (MeOH) to give *1-methyl-2,4,6-collidinium iodide* **465** (159 mg, 0.604 mmol, 6.0%) as a white needle-like solid. The two mother liquors were combined, concentrated under reduced pressure, and purified by recrystallisation to give a 2nd crop of *1-methyl-2,4,6-collidinium iodide* **465** (101 mg, 0.383 mmol, 3.8%) as an off-white, needle-like solid. The mother liquor from the 2nd recrystallation was allowed to concentrate at atmospheric pressure to give a 3rd crop of *1-methyl-2,4,6-collidinium iodide* **465** (157 mg, 0.600 mmol, 6.0%) as a pink-tinted crystalline solid; δ_{H} (500 MHz, CDCl₃) 7.55 (2H, s), 4.00 (3H, s), 2.73 (6H, s), 2.50 (3H, s).

Data in agreement with those previously reported.²⁶⁵

(±)-8,8'-dimethoxy-1,1'-biazulene-2,2'-diyl hydrogenphosphate 478



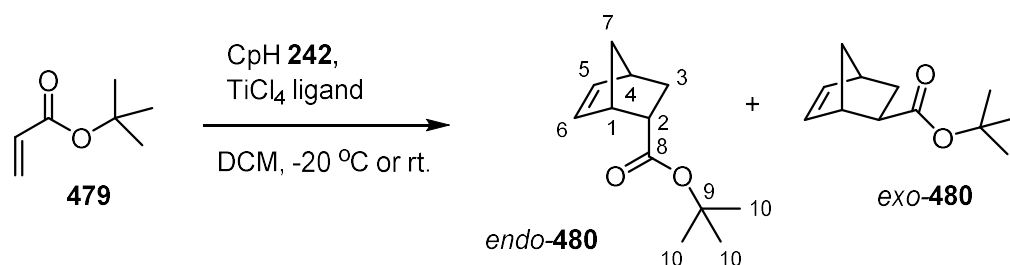
The preparation of this compound was based on methods by Ito¹⁹⁴ and MacMillan.²⁷⁵

Under atmosphere of air, at $0\text{ }^\circ\text{C}$, to phosphorus pentoxide (800 mg) was added $\text{H}_3\text{PO}_{4(\text{aq})}$ (85 wt. %, 1.20 mL). The mixture was then stirred at $95\text{ }^\circ\text{C}$, and to it was added (\pm) -3,3'-diethyl 2,2'-dihydroxy-8,8'-dimethoxy-[1,1'-biazulene]-3,3'-dicarboxylate **370** (200 mg, 0.408 mmol, 1.00 eq.), stirred for 1 h, and then allowed to cool to r.t. To the resultant slurry was slowly added water (20 mL), and extracted with DCM ($2 \times 20\text{ mL}$). The organic extracts were combined and washed with water ($3 \times 20\text{ mL}$), dried over anhydrous MgSO_4 , and filtered. The filtrate was concentrated under reduced pressure to give the crude intermediate mixture as a maroon oil.

Under atmosphere of N_2 , at r.t., to a stirred solution of the crude diol in pyridine (1.50 mL) was added dropwise phosphoryl chloride (80 μL , 0.816 mmol, 2.00 eq.), forming a dark brown precipitate. The mixture was stirred for 15 min, and to it was added water (5.0 mL), and allowed to stir for another 10 min. The mixture was diluted with $\text{HCl}_{(\text{aq})}$ (1 M, 30 mL), extracted with DCM (30 mL), and extracted with EtOAc (25 mL). The aqueous layer was allowed to concentrate at atmospheric pressure. To the resultant burgundy residue was added CHCl_3 (30 mL), and the solution was filtered through a pad of silica. The filtrate was concentrated under reduced pressure to give

(±)-8,8'-dimethoxy-1,1'-biazulene-2,2'-diyl hydrogenphosphate **478** (20 mg, 0.0480 mmol, 12%) as a burgundy solid; δ_{H} (500 MHz, CDCl_3) 8.18 (2H, d, J 9.3 Hz), 7.49 (2H, ddd, J 11.0 Hz, 9.8 Hz, 1.2 Hz), 7.41 (2H, s), 6.96 (2H, t, J 9.6 Hz), 6.78 (2H, d, J 11.0 Hz), 3.55 (6H, s).

General method: *tert*-Butyl (1*S,2*S**,4*S**)-bicyclo[2.2.1]hept-5-ene-2-carboxylate *endo*-480 and *tert*-Butyl (1*S**,2*R**,4*S**)-bicyclo[2.2.1]hept-5-ene-2-carboxylate *exo*-480**



The preparation of this compound was based on methods by Harada¹³⁹ and Wulff.²⁷⁶ At r.t., to a stirred solution of the chosen ligand in DCM (1.0 mL) was slowly added titanium tetrachloride (1.0 M in DCM), and the mixture was allowed to stir for 30 min. The mixture was then either cooled to -20 °C or left at r.t. To the mixture was added *tert*-butyl acrylate **479** (1.00 eq.), and the mixture was stirred for 15 min, before cyclopentadiene **242** (5.00 eq.) was added, and the mixture was stirred for 22 h. The reaction was quenched by adding saturated brine (1.0 mL), then the mixture was allowed to warm to r.t. and diluted with DCM (20 mL). The organic layer was washed with water (10 mL), dried over anhydrous MgSO₄ and filtered. The filtrate was concentrated under reduced pressure to give the crude product, which was purified by column chromatography (0→5% Et₂O in pentane) to give a mixture of *tert*-butyl (1*S**,2*S**,4*S**)-bicyclo[2.2.1]hept-5-ene-2-carboxylate (**endo-480**) and *tert*-butyl (1*S**,2*R**,4*S**)-bicyclo[2.2.1]hept-5-ene-2-carboxylate (**exo-480**) as a pale yellow oil; R_f 0.56 (9:1 pentane/Et₂O).

tert-Butyl (1*S**,2*S**,4*S**)-bicyclo[2.2.1]hept-5-ene-2-carboxylate (**endo-480**): Chiral GC retention times, 27.50 min and 27.70 min; δ_H (500 MHz, CDCl₃) 6.18 (1H, dd, *J* 5.7 Hz, 3.1 Hz), 5.93 (1H, dd, *J* 5.7 Hz, 2.8 Hz), 3.17-3.15 (1H, m), 2.88-2.85 (2H,

m), 1.83 (1H, ddd, *J* 11.7 Hz, 9.3 Hz, 3.7 Hz), 1.41 (9H, s), 1.40-1.36 (2H, m), 1.25 (1H, d, *J* 8.1 Hz).

Data in agreement with those previously reported.²⁸³

4. REFERENCES

1. McConathy, J.; Owens, M. J., *Primary Care Companion J. Clin. Psychiatry* **2003**, 5, 70-73.
2. Owens, M. J.; Rosenbaum, J. F., *CNS Spectr.* **2002**, 7, 34-39.
3. Brenna, E.; Fuganti, C.; Serra, S., *Tetrahedron: Asymmetry* **2003**, 14, 1-42.
4. Bentley, R., *Chem. Rev.* **2006**, 106, 4099-4112.
5. Enders, D.; Backes, M., *Tetrahedron: Asymmetry* **2004**, 15, 1813-1817.
6. Nozaki, H.; Moriuti, S.; Takaya, H.; Noyori, R., *Tetrahedron Lett.* **1966**, 7(43), 5239.
7. Gillard, R. D.; Wilkinson, G.; Osborn, J. A.; Stockwell, P. B., *Proc. Chem. Soc. (London)* **1964**, 284-285.
8. Young, J. F.; Osborn, J. A.; Jardine, F. H.; Wilkinson, G., *Chem. Commun.* **1965**, (7), 131-132.
9. Osborn, J. A.; Jardine, F. H.; Young, J. F.; Wilkinson, G., *J. Chem. Soc. A* **1966**, (12), 1711-1732.
10. Osborn, J. A.; Wilkinson, G.; Young, J. F., *Chem. Commun.* **1965**, (2), 17.
11. Evans, D.; Osborn, J.; Wilkinson, G., *J. Chem. Soc. A* **1968**, (12), 3133-3142.
12. Chabala, J. C.; Mrozik, H.; Tolman, R. L.; Eskola, P.; Lusi, A.; Peterson, L. H.; Woods, M. F.; Fisher, M. H., *J. Med. Chem.* **1980**, 23, 1134-1136.
13. Mohammadi, N. A.; Rempel, G. L., *Macromolecules* **1987**, 20, 2363-2368.
14. Azpeitia, S.; Fernández, B.; Garralda, M. A.; Huertos, M. A., *Eur. J. Inorg. Chem.* **2016**, 2891-2895.
15. Buter, J.; Heijnen, D.; Wan, I. C.; Bickelhaupt, F. M.; Young, D. C.; Otten, E.; Moody, D. B.; Minnaard, A. J., *J. Org. Chem.* **2016**, 81, 6686-6696.
16. Knowles, W. S.; Sabacky, M. J., *Chem. Commun.* **1968**, (22), 1445-1446.

17. Horner, L.; Buthe, H.; Siegel, H., *Tetrahedron Lett.* **1968**, 9(37), 4023-4026.
18. Morrison, J.; Burnett, R. E.; Aguiar, A. M.; Morrow, C. J.; Phillips, C., *J. Am. Chem. Soc.* **1971**, 93(5), 1301-1303.
19. Dang, T. P.; Kagan, H. B., *J. Chem. Soc. D* **1971**, (10), 481.
20. Kagan, H. B.; Dang, T. P., *J. Am. Chem. Soc.* **1972**, 94 (18), 6429-6433.
21. Knowles, W. S.; Vineyard, B. D.; Sabacky, M. J., *Chem. Commun.* **1972**, (1), 10-11.
22. Knowles, W. S.; Sabacky, M. J.; Vineyard, B. D.; Weinkauff, D. J., *J. Am. Chem. Soc.* **1975**, 97(9), 2567-2568.
23. Vineyard, B. D.; Knowles, W. S.; Sabacky, M. J.; Bachman, G. L.; Weinkauff, D. J., *J. Am. Chem. Soc.* **1977**, 99(18), 5946-5952.
24. Knowles, W. S., *Adv. Synth. Catal.* **2003**, 345(1-2), 3-13.
25. Koenig, K. E.; Sabacky, M. J.; Bachman, G. L.; Christopfel, W. C.; Barnstorff, H. D.; Friedman, R. B.; Knowles, W. S.; Stults, B. R.; Vineyard, B. D.; Weinkauff, D. J., *Ann. N. Y. Acad. Sci.* **1980**, 333(1), 16-22.
26. Zhang, W.; Chi, Y.; Zhang, X., *Acc. Chem. Res.* **2007**, 40, 1278-1290.
27. Miyashita, A.; Yasuda, A.; Takaya, H.; Toriumu, K.; Ito, T.; Souchi, T.; Noyori, R., *J. Am. Chem. Soc.* **1980**, 102(27), 7932-7934.
28. Tamao, K.; Yamamoto, H.; Matsumoto, H.; Miyake, N.; Hayashi, T.; Kumada, M., *Tetrahedron Lett.* **1977**, 18(16), 1389-1392.
29. Grubbs, R. H.; DeVries, R. A., *Tetrahedron Lett.* **1977**, 18(22), 1879-1880.
30. Miyashita, A.; Takaya, H.; Souchi, T.; Noyori, R., *Tetrahedron* **1984**, 40(8), 1245-1253.
31. Noyori, R.; Ohta, M.; Hsiao, Y.; Kitamura, M.; Ohta, T.; Takaya, H., *J. Am. Chem. Soc.* **1986**, 108 (22), 7117-7119.

32. Fodale, V.; Santamaria, L. B., *Eur. J. Anaesthesiol.* **2002**, *19*(7), 466–473.
33. Gesell, A.; Rolf, M.; Ziegler, J.; Díaz Chavez, M. L.; Huang, F-C.; Kutchan, T. M., *J. Biol. Chem.* **2009**, *284*(36), 24432-24442.
34. Takaya, H.; Ohta, T.; Sayo, N.; Kumobayashi, H.; Akutagawa, S.; Inoue, S.; Kasahara, I.; Noyori, R., *J. Am. Chem. Soc.* **1987**, *109*(5), 1596-1597.
35. Ohta, T.; Takaya, H.; Kitamura, M.; Nagai, K.; Noyori, R., *J. Org. Chem.* **1987**, *52*(14), 3174-3176.
36. Harrison, I. T.; Lewis, B.; Nelson, P.; Rooks, W.; Roszowski, A.; Tomolonis, A.; Fried, J. H., *J. Med. Chem.* **1970**, *13*, 203-205.
37. Nishi, T.; Kitamura, M.; Ohkuma, T.; Noyori, R., *Tetrahedron Lett.* **1988**, *29*(48), 6327-6330.
38. Ohkuma, T.; Ooka, H.; Hashiguchi, S.; Ikariya, T.; Noyori, R., *J. Am. Chem. Soc.* **1995**, *117*, 2675-2676.
39. Ohkuma, T.; Ooka, H.; Yamakawa, M.; Ikariya, T.; Noyori, R., *J. Org. Chem.* **1996**, *61*, 4872-4873.
40. Ohkuma, T.; Ikehira, H.; Ikariya, T.; Noyori, R., *Synlett* **1997**, 467-468.
41. Ohkuma, T.; Koizumi, M.; Doucet, H.; Pham, T.; Kozawa, M.; Murata, K.; Katayama, E.; Yokozawa, T.; Ikariya, T.; Noyori, R., *J. Am. Chem. Soc.* **1998**, *120*, 13529-13530.
42. Tani, K.; Yamagata, T.; Akutagawa, S.; Kumobayashi, H.; Taketomi, T.; Takaya, H.; Miyashita, A.; Noyori, R.; Otsuka, S., *J. Am. Chem. Soc.* **1984**, *106*, 5208-5217.
43. Noyori, R., *Angew. Chem. Int. Ed.* **2002**, *41*, 2008-2022.
44. Ohrai, K.; Kondo, K.; Sodeoka, M.; Shibasaki, M., *J. Am. Chem. Soc.* **1994**, *116*, 11737-11748.

45. Coya, E.; Sotomayor, N.; Lete, E., *Adv. Synth. Catal.* **2015**, 357, 3206-3214.
46. Noyori, R.; Takaya, H., *Acc. Chem. Res.* **1990**, 23, 345-350.
47. Akutagawa, S., *App. Catal., A* **1995**, 128, 171-207.
48. Christoffers, J.; Koripelly, G.; Rosiak, A.; Rössle, M., *Synthesis*, **2007**, (9), 1279-1300.
49. Knowles, W. S., *Acc. Chem. Res.* **1983**, 16 (3), 106-112.
50. Svensson, G.; Albertsson, J.; Frejd, T.; Klingstedt, T., *Acta Cryst. C* **1986**, 42, 1324-1327.
51. Schmid, R.; Cereghetti, M.; Heiser, B.; Schönholzer, P.; Hansen, H.-J., *Helv. Chim. Acta* **1988**, 71, 897-929.
52. Frejd, T.; Klingstedt, T., *Acta Chem. Scand.* **1989**, 43, 670-675.
53. Heiser, B.; Broger, E. A.; Cramer, Y., *Tetrahedron: Asymmetry* **1991**, 2(1), 51-62.
54. Mezzetti, A.; Tschumper, A.; Consiglio, G., *J. Chem. Soc. Dalton Trans.* **1995**, 49-56.
55. Chakrapani, H.; Liu, C.; Widenhoefer, R. A., *Org. Lett.* **2003**, 5(2), 157-159.
56. Schmid, R.; Foricher, J.; Cereghetti, M.; Schönholzer, P., *Helv. Chim. Acta* **1991**, 74, 370-389.
57. Genêt, J.-P.; Ratovelomanana-Vidal, V.; Caño de Andrade, M. C.; Pfister, X.; Guerreiro, P.; Lenoir, J. Y., *Tetrahedron Lett.* **1995**, 36(27), 4801-4804.
58. Wang, W.-B.; Lu, S.-M.; Yang, P.-Y.; Han, X.-W.; Zhou, Y.-G., *J. Am. Chem. Soc.* **2003**, 125, 10536-10537.
59. Wang, D.-W.; Wang, X.-B.; Wang, D.-S.; Lu, S.-M.; Zhou, Y.-G.; Li, Y.-X., *J. Org. Chem.* **2009**, 74, 2780-2787.

60. Zhang, X.; Mashima, K.; Koyano, K.; Sayo, N.; Kumobayashi, H.; Akutagawa, S.; Takaya, H., *Tetrahedron Lett.* **1991**, 32(49), 7283-7286.
61. Zhang, X.; Mashima, K.; Koyano, K.; Sayo, N.; Kumobayashi, H.; Akutagawa, S.; Takaya, H., *J. Chem. Soc. Perkin Trans. 1.* **1994**, 2309-2322.
62. Toriumi, K.; Ito, T.; Takaya, H.; Souchi, T.; Noyori, R., *Acta Cryst. B.* **1982**, 38, 807-812.
63. Zhang, X.; Taketomi, T.; Yoshizumi, T.; Kumobayashi, H.; Akutagawa, S.; Mashima, K.; Takaya, H., *J. Am. Chem. Soc.* **1993**, 115, 3318-3319.
64. Uemura, T.; Zhang, X.; Matsumura, K.; Sayo, N.; Kumobayashi, H.; Ohta, T.; Nozaki, K.; Takaya, H., *J. Org. Chem.* **1996**, 61, 5510-5516.
65. Wang, D.-S.; Chen, Q.-A.; Li, W.; Yu, C.-B.; Zhou, Y.-G.; Zhang, X., *J. Am. Chem. Soc.* **2010**, 132, 8909-8911.
66. Wang, D.-S.; Zhou, Y.-G., *Tetrahedron Lett.* **2010**, 51, 3014.
67. Tanaka, K.; Nishida, G.; Ogino, M.; Hirano, M.; Noguchi, K., *Org. Lett.* **2005**, 7(14), 3119-3121.
68. Tanaka, K.; Shirasaka, K., *Org. Lett.* **2003**, 5(24), 4697-4699.
69. Saito, T.; Yokozawa, T.; Ishizaki, T.; Moroi, T.; Sayo, N.; Miura, T.; Kumobayashi, H., *Adv. Synth. Catal.* **2001**, 343, 264-267.
70. Chen, G.; Tokunaga, N.; Hayashi, T., *Org. Lett.* **2005**, 7(11), 2285-2288.
71. Wada, A.; Noguchi, K.; Hirano, M.; Tanaka, K., *Org. Lett.* **2007**, 9(7), 1295-1298.
72. Nishida, G.; Ogaki, S.; Yusa, Y.; Yokozawa, T.; Noguchi, K.; Tanaka, K., *Org. Lett.* **2008**, 10(13), 2849-2852.
73. Pai, C.-C.; Li, Y.-M.; Zhou, Z.-Y.; Chan, A. S. C., *Tetrahedron Lett.* **2002**, 2789-2792.

74. de Paule, S. D.; Jeulin, S.; Ratovelomanana-Vidal, V.; Genêt, J.-P.; Champion, N.; Dellis, P., *Tetrahedron Lett.* **2003**, *44*, 823-826.
75. Sun, Y.; Wan, X.; Guo, M.; Wang, D.; Dong, X.; Pan, Y.; Zhang, Z., *Tetrahedron: Asymmetry* **2004**, *15*, 2185-2188.
76. Yang, M.; Zhang, X.; Lu, X., *Org. Lett.* **2007**, *9*(24), 5131-5133.
77. Zhang, Z.; Qian, H.; Longmire, J.; Zhang, X., *J. Org. Chem.* **2000**, *65*, 6223-6226.
78. Wu, S.; Wang, W.; Tang, W.; Lin, M.; Zhang, X., *Org. Lett.* **2002**, *4*(25), 4495-4497.
79. Raghunath, M.; Zhang, X., *Tetrahedron Lett.* **2005**, *46*, 8213-8216.
80. Trost, B. M.; Van Vranken, D. L.; Bingel, C., *J. Am. Chem. Soc.* **1992**, *114*, 9327-9343.
81. Trost, B. M., *Acc. Chem. Res.* **1996**, *29*(8), 355-364.
82. Trost, B. M.; Zambrano, J. L.; Richter, W., *Synlett* **2001**, 907-909.
83. Larksarp, C.; Alper, H., *J. Am. Chem. Soc.* **1997**, *119*, 3709-3715.
84. Zhou, X.-Y.; Wang, D.-S.; Bao, M.; Zhou, Y.-G., *Tetrahedron Lett.* **2011**, *52*, 2826-2829.
85. Huang, K.; Guan, Z.-H.; Zhang, X., *Tetrahedron Lett.* **2014**, *55*, 1686-1688.
86. Zhang, C.-X.; Hu, Y.-H.; Chen, C.-F.; Fang, Q.; Yang, L.-Y.; Lu, Y.-B.; Xie, L.-J.; Wu, J.; Li, S.; Fang, W., *Chem. Sci.* **2016**, *7*, 4594.
87. Vidal-Ferran, A.; Mon, I.; Bauzá, A.; Frontera, A.; Rovira, L., *Chem. Eur. J.* **2015**, *21*, 11417-11426.
88. Burk, M. J.; Feaster, J. E.; Harlow, R. L., *Organometallics* **1990**, 2653-2655.
89. Burk, M. J.; Feaster, J. E.; Nugent, W. A.; Harlow, R. L., *J. Am. Chem. Soc.* **1993**, *115*, 10125-10138.

90. Mashima, K.; Kusano, K.-H.; Sato, N.; Matsumura, Y.; Nozaki, K.; Kumobayashi, H.; Sayo, N.; Hori, Y.; Ishizaki, T.; Akutagawa, S.; Takaya, H., *J. Org. Chem.* **1994**, *59*, 3064-3076.
91. Inoue, S.; Osada, M.; Koyano, K.; Takaya, H.; Noyori, R., *Chem. Lett.* **1985**, 1007-1008.
92. Miyashita, A.; Karino, H.; Shimamura, J.; Chiba, T.; Nagano, K.; Nohira, H.; Takaya, H., *Chem Lett.* **1989**, 1849-1852.
93. Chiba, T.; Miyashita, A.; Nohira, H., *Tetrahedron Lett.* **1993**, *34*(14), 2351-2354.
94. Yamamoto, N.; Murata, M.; Morimoto, M.; Achiwa, K., *Chem. Pharm. Bull.* **1991**, *39*(4), 1085-1087.
95. Yoshikawa, K.; Yamamoto, N.; Murata, M.; Awano, K.; Morimoto, T.; Achiwa, K., *Tetrahedron: Asymmetry* **1992**, *3*(1), 13-16.
96. Landis, C. R.; Halpern, J., *J. Am. Chem. Soc.* **1987**, *109*, 1746-1754.
97. Sakuraba, S.; Morimoto, T.; Achiwa, K., *Tetrahedron: Asymmetry* **1991**, *2*(7), 597-600.
98. Yamanoi, Y.; Imamoto, T., *J. Org. Chem.* **1998**, *64*, 2988-2989.
99. Imamoto, T.; Wanatabe, J.; Wada, Y.; Masuda, H.; Yamada, H.; Tsuruta, H.; Matsukawa, S.; Yamaguchi, K., *J. Am. Chem. Soc.* **1998**, *120*, 1635.
100. Gridnev, I. D.; Yasutake, M.; Imamoto, T.; Beletskaya, I. P., *Proc. Natl. Acad. Sci.* **2004**, *101*(15), 5385-5390.
101. Tamura, K.; Sugiya, M.; Yoshida, K.; Yanagisawa, A.; Imamoto, T., *Org. Lett.* **2010**, *12*(19), 4400-4403.
102. Shibata, T.; Tsuruta, H.; Danjo, H.; Imamoto, T., *J. Mol. Catal. A: Chem.* **2003**, *196*, 117-124.

103. Kündig, E. P.; Bourdin, B.; Bernardinelli G., *Angew. Chem. Int. Ed. Engl.* **1994**, 33(18), 1856-1858.
104. Olson, A. S.; Seitz, W. J.; Hossain, M. M., *Tetrahedron Lett.* **1991**, 32(39), 5299-5302.
105. Bruin, M. E.; Kündig, E. P., *Chem. Commun.* **1998**, 2635–2636.
106. Kündig, E. P.; Saudan, C. M.; Bernardinelli, G., *Angew. Chem. Int. Ed.* **2001**, 38(9), 1219-1223.
107. Thamapipol, S.; Bernardinelli, G.; Besnard, C.; Kündig, E. P., *Org. Lett.* **2010**, 5604-5607.
108. Murata, M.; Morimoto, T.; Achiwa, K., *Synlett* **1991**, 827-829.
109. Andersen, N. G.; Parvez, M.; Keay, B. M., *Org. Lett.* **2000**, 2(18), 2817-2820.
110. Andersen, N. G.; McDonald, R.; Keay, B. M., *Tetrahedron: Asymmetry* **2001**, 12, 263-269.
111. Allen, D. W.; Taylor, B. F., *J. Chem. Soc., Dalton Trans.* **1982**, 51-53.
112. Poon, D. J.; Overman, L. E., *Angew. Chem. Int. Ed. Engl.* **1997**, 36(5), 518-521.
113. Jeulin, S.; de Paule, S. D.; Ratovelomanana-Vidal, V.; Genêt, J.-P.; Champion, N.; Dellis, P., *Angew. Chem. Int. Ed.* **2004**, 43, 320-325.
114. Jeulin, S.; de Paule, S. D.; Ratovelomanana-Vidal, V.; Genêt, J.-P.; Champion, N.; Dellis, P., *Proc. Natl. Acad. Sci.* **2004**, 101(16), 5799-5804.
115. Wadamoto, M.; Yamamoto, H., *J. Am. Chem. Soc.* **2005**, 127, 14556-14557.
116. Pinto, A.; Jia, Y.; Neuville, L.; Zhu, J., *Chem. Eur. J.* **2007**, 13, 961-967.
117. Ge, S.; Hartwig, J. F., *J. Am. Chem. Soc.* **2011**, 133, 16330-16333.

118. Korenaga, T.; Osaki, K.; Maenishi, R.; Sakai, T., *Org. Lett.* **2009**, *11*(11), 2325-2328.
119. Korenaga, T.; Maenishi, R.; Hayashi, K.; Sakai, T., *Adv. Synth. Catal.* **2010**, *352*, 3247-3254.
120. Hu, S.-B.; Chen, Z.-P.; Zhou, J.; Zhou, Y.-G., *Tetrahedron Lett.* **2016**, *57*, 1925-1929.
121. Benincori, T.; Brenna, E.; Sannicolò, F.; Trimarco, L.; Antognazza, P.; Cesarotti, E., *J. Chem. Soc., Chem. Commun.* **1995**, 685-686.
122. Benincori, T.; Brenna, E.; Sannicolò, F.; Trimarco, L.; Antognazza, P.; Cesarotti, E.; Demartin, F.; Pilati, T., *J. Org. Chem.* **1996**, *61*, 6244-6251.
123. Benincori, T.; Cesarotti, E.; Piccolo, O.; Sannicolò, F., *J. Org. Chem.* **2000**, *65*, 2043-2047.
124. Berens, U.; Brown, J. M.; Long, J.; Selke, R., *Tetrahedron: Asymmetry* **1996**, *7*(1), 285-292.
125. Benincori, T.; Brenna, E.; Sannicolò, F.; Trimarco, L.; Antognazza, P.; Cesarotti, E.; Demartin, F.; Pilati, T.; Zotti, G., *J. Organomet. Chem.* **1997**, *529*, 445-453.
126. Ohta, T.; Takaya, H.; Noyori, R., *Inorg. Chem.* **1988**, *27*, 566-569.
127. Ozawa, F.; Kubo, A.; Matsumoto, Y.; Hayashi, T., *Organometallics* **1993**, *12*, 4188-4196.
128. Benincori, T.; Piccolo, O.; Rizzo, S.; Sannicolò, F., *J. Org. Chem.* **2000**, *65*, 8340-8347.
129. Noyori, R.; Tomino, I.; Tanimoto, Y., *J. Am. Chem. Soc.* **1979**, 3129-3131.
130. Sakane, S.; Maruoka, K.; Yamamoto, H., *Tetrahedron Lett.* **1985**, *26*(45), 5535-5538.

131. Sakane, S.; Maruoka, K.; Yamamoto, H., *Tetrahedron* **1986**, 42(8), 2203-2209.
132. Maruoka, K.; Hoshino, Y.; Shirasaka, T.; Yamamoto, H., *Tetrahedron Lett.* **1988**, 29(32), 3967-3970.
133. Maruoka, K.; Itoh, T.; Shirasaka, T.; Yamamoto, T., *J. Am. Chem. Soc.* **1988**, 110, 310-312.
134. Mikami, K.; Terada, M.; Nakai, T., *J. Am. Chem. Soc.* **1989**, 111, 1940-1941.
135. Brunel, J. M., *Chem. Rev.* **2005**, 105, 857-897.
136. Mikami, K.; Motoyama, Y.; Terada, M., *Inorg. Chim. Acta* **1994**, 222, 71-75.
137. Harada, T.; Ueda, S.; Yoshida, T.; Inoue, A.; Takeuchi, M.; Ogawa, N.; Oku, A., *J. Org. Chem.* **1994**, 59, 7575-7576.
138. Harada, T.; Yoshida, T.; Inoue, A.; Takeuchi, M.; Oku, A., *Synlett* **1995**, 283-284.
139. Harada, T.; Takeuchi, M.; Hatsuda, M.; Ueda, S.; Oku, A., *Tetrahedron: Asymmetry* **1996**, 7(9), 2479-2482.
140. Zhang, F.-Y.; Yip, C.-W.; Cao, R.; Chan, A. S. C., *Tetrahedron: Asymmetry* **1997**, 8(4), 585-589.
141. Zhang, F.-Y.; Chan, A. S. C., *Tetrahedron: Asymmetry* **1997**, 8(21), 3651-3655.
142. Zhang, F.-Y.; Yip, C.-W.; Chan, A. S. C., *J. Am. Chem. Soc.* **1997**, 119, 4080-4081.
143. Shen, X.; Guo, H.; Ding, K., *Tetrahedron: Asymmetry* **2000**, 11, 4321-4327.
144. Kim, J. G.; Camp, E. H.; Walsh, P. J., *Org. Lett.* **2006**, 8(20), 4413-4416.

145. Huang, W.-C.; Liu, W.; Wu, X.-D.; Ying, J.; Pu, L., *J. Org. Chem.* **2015**, *80*, 11480-11484.
146. Zhang, L.; Tu, B.; Ge, M.; Li, Y.; Chen, L.; Wang, W.; Zhou, S., *J. Org. Chem.* **2015**, *80*, 8307-8313.
147. Long, J.; Hu, J.; Shen, X.; Ji, B.; Ding, K., *J. Am. Chem. Soc.* **2002**, *124*, 10-11.
148. Kinoshita, T.; Okada, S.; Park, S.-R.; Matsunaga, S.; Shibasaki, M., *Angew. Chem. Int. Ed.* **2003**, *42*, 4680-4684.
149. Matsunaga, S.; Kinoshita, T.; Okada, S.; Harada, S.; Shibasaki, M., *J. Am. Chem. Soc.* **2004**, *126*, 7559-7570.
150. Brussee, J.; Jansen, A. C. A., *Tetrahedron Lett.* **1983**, *24*(31), 3261-3262.
151. Dongwai, C.; Hughes, D. L.; Verhoeven, T. R.; Reider, P. J.; van Rijn, R.; Smith, A. B., *Org. Synth.* **1999**, *76*, 1-3.
152. Dongwai, C.; Payack, J. F.; Bender, D. R.; Hughes, D. L.; Verhoeven, L. L.; Reider, P. J.; van Rijn, R.; Smith, A. B., *Org. Synth.* **1999**, *76*, 6-9.
153. Yoon, T. P.; Jacobsen, E. N., *Science* **2003**, *299*, 1691-1693.
154. Anderson, A. G.; Steckler, B. M., *J. Am. Chem. Soc.* **1959**, *81*(18), 4941-4946.
155. Liu, R. S. H., *J. Chem. Educ.* **2002**, *79*(2), 183-185.
156. Guarrera, M.; Turbino, L.; Rebora, A., *J. Eur. Acad. Dermatol. Veneareol.* **2001**, *15*, 486-496.
157. Tanaka, Y.; Shigenobu, K., *Cardiovasc. Drug Rev.* **2001**, *19*, 297-312.
158. Ikegai, K.; Imamura, M.; Suzuki, T.; Nakanishi, K.; Murakami, T.; Kurosaki, E.; Noda, A.; Kobayashi, Y.; Yokota, M.; Koide, T.; Kosakai, K.; Okhura, Y.;

- Takeuchi, M.; Tomiyama, H.; Ohta, M., *Bioorg. Med. Chem.* **2013**, *21*, 3934–3948.
159. Asato, A. E.; Peng, A.; Hossain, M. Z.; Mirzadegan, T.; Bertram, J. S., *J. Med. Chem.* **1993**, *36*, 3137-3147.
160. Löber, S.; Hübner, H.; Buschauer, A.; Sanna, F.; Argiolas, A.; Melis, M. R.; Gmeiner, P., *Bioorg. Med. Chem. Lett.* **2012**, *22*, 7151-7154.
161. Peet, J.; Selyutina, A.; Bredihhin, A., *Bioorg. Med. Chem.* **2016**, *24*, 1653-1657.
162. Liu, R. S. H.; Asato, A. E., *J. Photochem. Photobiol. C* **2003**, *4*(3), 179-194.
163. Zhang, X.-H.; Li, C.; Wang, W.-B.; Cheng, X.-X.; Wang, X.-S.; Zhang, B.-W., *J. Mater. Chem.* **2007**, *17*, 642-649.
164. Puodziukynaite, E.; Wang, H.-W.; Lawrence, J.; Wise, A. J.; Russell, T. P.; Barnes, M. D.; Emrick, T., *J. Am. Chem. Soc.* **2014**, *136*, 11043-11049.
165. Ito, S.; Morita, N., *Eur. J. Org. Chem.* **2009**, 4567-4579.
166. Ghazvini Zadeh, E. H.; Tang, S.; Woodward, A. W.; Liu, T.; Bondar, M. V.; Belfield, K. D., *J. Mater. Chem. C.* **2015**, *3*, 8495-8503.
167. Murai, M.; Ku, S.-Y.; Treat, N. D.; Robb, M. J.; Chabinyk, M. L.; Hawker, C. J., *Chem. Sci.* **2014**, *5*, 3753-3760.
168. Dragu, E. A.; Ion, A. E.; Shova, S.; Bala, D.; Mihailciuc, C.; Voicescu, M.; Ionescu, S.; Nica, S., *RSC Adv.* **2015**, *5*, 63282-63286.
169. Wang, F.; Lin, T. T. He, C.; Chi, H.; Tang, T.; Lai, Y.-H., *J. Mater. Chem.*, **2012**, *22*, 10448-10451.
170. Wabayashi, S.; Kato, Y.; Mochizuki, K.; Suzuki, R.; Matsumoto, M.; Sugihara, Y.; Shimizu, M., *J. Org. Chem.* **2007**, *72*, 744-749.

171. Son, Y.-A.; Gwon, S.-Y.; Kim, S.-H., *Mol. Cryst. Liq. Cryst.* **2014**, *600*, 189-195.
172. Yamaguchi, Y.; Ogawa, K.; Nakayama, K.; Ohba, Y.; Katagiri, H., *J. Am. Chem. Soc.* **2013**, *135*, 19095-19098.
173. Yao, J.; Cai, Z.; Liu, Z.; Yu, C.; Luo, H.; Yang, Y.; Yang, S.; Zhang, G.; Zhang, D., *Macromolecules* **2015**, *48*, 2039-2047.
174. Gosavi, P. M.; Moroz, Y. S.; Korendovych, I. V., *Chem. Commun.* **2015**, *51*, 5347-5350.
175. Lash, T. D., *Acc. Chem. Res.* **2016**, *49*, 471-482.
176. Tajiri, A.; Fukuda, M.; Hatano, M.; Morita, T.; Takase, K., *Angew. Chem. Int. Ed.* **1983**, *22*(11), 870-871.
177. Chen, A. H.; Yen, H. H.; Kuo, Y. C.; Chen, W. Z., *Synth. Commun.* **2007**, *37*(17), 2975-2987.
178. Sigrist, R.; Hansen, H.-J., *Helv. Chim. Acta.* **2014**, *97*, 1165-1175.
179. Ostaszewski, R.; Hansen, H.-J., *Heterocycles*, **2015**, *90*(2), 1135-1141.
180. Asao, T.; Ito, S.; Morita, N., *Tetrahedron Lett.* **1989**, *30*(48), 6693-6696.
181. Ito, S.; Kubo, T.; Morita, N.; Matsui, Y.; Wanatabe, T.; Ohta, A.; Fujimori, K.; Murafuji, T.; Sugihara, Y.; Tajiri, A., *Tetrahedron Lett.* **2004**, *45*, 2891-2894.
182. Bao, J.; Wulff, W. D.; Rheingold, A. L., *J. Am. Chem. Soc.* **1993**, *115*, 3814-3815.
183. Nozoe, T.; Seto, S.; Matsumura, S.; Takashi, A., *Proc. Japan. Acad.* **1956**, *5*, 339-343.
184. Nozoe, T.; Takase, K.; Shimazaki, N., *Bull. Chem. Soc. Jpn.* **1964**, *37*(11), 1644-1648.

185. Nozoe, T.; Takase, K.; Kato, M.; Nogi, T., *Tetrahedron* **1971**, 27 (24), 6023-6035.
186. Cavazza, M.; Guella, G.; Pietra, F., *Tetrahedron* **2000**, 56 (13), 1917-1922.
187. Nolting, D. D.; Nickels, M.; Price, R.; Gore, J. C.; Pham, W., *Nat. Protoc.* **2009**, 4(8), 1113-1117.
188. Yang, P.-W.; Yasunami, M.; Takase, K., *Tetrahedron Lett.* **1971**, (45), 4275-4278.
189. Chen, A.; Yasunami, M.; Takase, K., *Tetrahedron Lett.* **1974**, (30), 2581-2584.
190. Yasunami, M.; Chen, A.; Yang, P. W.; Takase, K., *Chem. Lett.* **1980**, 579-582.
191. Yanagisawa, T.; Kosakai, K.; Tomiyama, T.; Yasunami, M.; Takase, K., *Chem. Pharm. Bull.* **1990**, 38(12), 3355-3358.
192. Nozoe, T.; Yang, P. W.; Wu, C. P.; Huang, T. S.; Lee, T. H.; Okai, H.; Wakabayashi, H.; Ishikawa, S., *Heterocycles* **1989**, 29 (7), 1225-1232.
193. Nozoe, T.; Wakabayashi, H.; Shindo, K.; Ishikawa, S.; Wu, C. P.; Yang, P. W., *Heterocycles* **1991**, 32 (2), 213-220.
194. Ito, S.; Ando, M.; Nomura, A.; Morita, N.; Kabuto, C.; Mukai, H.; Ohta, K.; Kawakami, J.; Yoshizawa, A.; Tajiri, A., *J. Org. Chem.* **2005**, 70, 3939-3949.
195. Fallahpour, R. A.; Hansen, H.-J., *Helv. Chim. Acta.* **1992**, 75(7), 2210-2214.
196. Doering, W. V. E.; Hiskey, C. F., *J. Am. Chem. Soc.* **1952**, 74 (22), 5688-5693.
197. Nozoe, T.; Asao, T.; Yasunami, M.; Wakui, H.; Suzuki, T.; Masayoshi, A., *J. Org. Chem.* **1995**, 60, 5919-5924.
198. Pham, W.; Weissleder, R.; Tung, C., *Tetrahedron Lett.* **2002**, 43 (1), 19-20.

199. Iyoda, M.; Sato, K.; Oda, M., *Tetrahedron Lett.* **1985**, 26 (32), 3829-3832.
200. Talaz, O.; Gulcin, I.; Goksu, S.; Saracoglu, N., *Bioorg. Med. Chem.* **2009**, 17(18), 6583-6589.
201. Iyoda, M.; Otsuka, H.; Sato, K.; Nisato, N., Oda, M., *Bull. Chem. Soc. Jpn.* **1990**, 63, 80-87.
202. Cahiez, G.; Chaboche, C.; Mahuteau-Betzer, F.; Ahr, M., *Org. Lett.* **2005**, 7(10), 1943-1946.
203. Nagano, T.; Hayashi, T., *Org. Lett.* **2005**, 7(3), 491-493.
204. Monopoli, A.; Calò, V.; Ciminale, F.; Cotugno, P.; Angelici, C.; Cioffi, N.; Nacci, A., *J. Org. Chem.* **2010**, 75, 3908-3911.
205. Morita, N.; Takase, K., *Bull. Chem. Soc. Jpn.* **1982**, 55, 1144-1152.
206. Ito, S.; Yokoyama, R.; Okujima, T.; Terazono, T.; Kubo, T.; Tajiri, A.; Wanatabe, M.; Morita, N., *Org. Biomol. Chem.* **2003**, 1, 1947-1952.
207. Ager, D. J.; East, M. B.; Eisenstadt, A.; Laneman, S. A., *Chem. Commun.* **1997**, 2359-2360.
208. Kochetkov, A. N.; Efimova, I. V.; Trotsyanskaya, I. G.; Kazankova, M. A.; Beletskaya, I. P., *Russ. Chem. Bull.* **1998**, 47(9), 1744-1748.
209. Zhang, T.-Z.; Dai, L.-X.; Hou, X.-L., *Tetrahedron: Asymmetry* **2007**, 18, 251-259.
210. Ito, S.; Nomura, A.; Morita, N.; Kabuto, C.; Kobayashi, H.; Maejima, S.; Fujimori, K.; Yasunami, M., *J. Org. Chem.* **2002**, 67, 7295-7302.
211. Koch, M.; Blacque, O.; Venkatesan, K., *Org. Lett.* **2012**, 14(6), 1580-1583.
212. Nagel, M.; Hansen, H.-J., *Synlett* **2002**, 692-696.
213. Li, X.; Hewgley, B. J.; Mulrooney, C. A.; Yang, J.; Kozlowski, M. C., *J. Org. Chem.* **2003**, 68, 5500-5511.

214. Podlesny, E. E.; Kozlowski, M. C., *J. Org. Chem.* **2013**, 78, 466-476.
215. Aikawa, K.; Miyazaki, Y.; Mikami, K., *Bull. Chem. Soc. Jpn.* **2012**, 85(2), 201-208.
216. Kurotobi, K.; Miyachi, M.; Takakura, K.; Murafuji, T.; Sugihara, Y., *Eur. J. Org. Chem.* **2003**, 3663-3665.
217. Liu, L.; Wu, H.-C.; Yu, J.-Q., *Chem. Eur. J.* **2011**, 17, 10828-10831.
218. Antilla, J. C.; Baskin, J. M.; Barder, T. E.; Buchwald, S. L., *J. Org. Chem.* **2004**, 67, 5578-5587.
219. Kalek, M.; Jezowska, M.; Stawinski, J., *Adv. Synth. Catal.* **2009**, 351, 3207-3216.
220. Chen, J.; Liu, D.; Fan, D.; Liu, Y.; Zhang, W., *Tetrahedron* **2013**, 69, 8161-8168.
221. Kendall, A. J.; Salazar, C. S.; Martino, P. F.; Tyler, D. R., *Organometallics* **2014**, 33, 6171-6178.
222. Koh, J.-H.; Larsen, A. O.; White, P. S.; Gagné, M. R., *Organometallics* **2002**, 21(1), 7-9.
223. Leseurre, L.; Le Boucher d'Herouville, F.; Püntener, K.; Scalone, M.; Genêt, J.-P.; Michelet, V., *Org. Lett.* **2011**, 13(12), 3250-3253.
224. Kim, K. H.; Lee, D.-W.; Lee, Y.-S.; Ko, D.-H.; Ha, D.-C., *Tetrahedron* **2004**, 60, 9037-9042.
225. Alamsetti, S. K.; Poonguzhali, E.; Ganapathy, D.; Sekar, G., *Adv. Synth. Catal.* **2013**, 355, 2803-2808.
226. Kelly, A. M.; Pérez-Fuertes, Y.; Fossey, J. S.; Yeste, S. L.; Bull, S. D.; James, T. D., *Nat. Protoc.* **2008**, 3(2), 215-219.
227. Fabbri, D.; Delogu, G.; De Lucchi, O., *J. Org. Chem.* **1995**, 60, 6599-6601.

228. Li, Z.; Liang, X.; Wu, F.; Wan, B., *Tetrahedron: Asymmetry* **2004**, *15*, 665-669.
229. Kennedy, N.; Cohen, T., *J. Org. Chem.* **2015**, *80*, 8134-8141.
230. Irie, R.; Noda, K.; Ito, Y.; Matsumoto, N.; Katsuki, T., *Tetrahedron: Asymmetry* **1991**, *2*(7), 481-494.
231. Meca, L.; Řeha, D.; Havlas, Z., *J. Org. Chem.* **2003**, *68*, 5677-5680.
232. Ishiyama, T.; Murata, M.; Miyaura, N., *J. Org. Chem.* **1995**, *60*, 7508-7510.
233. Ishiyama, T.; Itoh, Y.; Kitano, T.; Miyaura, N., *Tetrahedron Lett.* **1997**, *38*(19), 3447-3450.
234. Nising, C. F.; Schmid, U. K.; Nieger, M.; Bräse, S., *J. Org. Chem.* **2004**, *69*, 6830-6833.
235. Xin, H.; Ge, C.; Yang, X.; Gao, H.; Yang, X.; Gao, X., *Chem. Sci.* **2016**, DOI:10.1039/c6sc02504h.
236. Van Allen, D.; Venkataraman D., *J. Org. Chem.* **2003**, *68*, 4590-4593.
237. Brauer, D. J.; Hingst, M.; Kottsieper, K. W.; Liek, C.; Nickel, T.; Tepper, M.; Stelzer, O.; Sheldrick, W. S., *J. Organomet. Chem.* **2002**, *645*, 14-26.
238. Zhang, X.; Liu, H.; Hu, X.; Tang, G.; Zhu, J.; Zhao, Y., *Org. Lett.* **2011**, *13*(13), 3478-3481.
239. Heinicke, J.; Böhle, I.; Tzschach, A., *J. Organomet. Chem.* **1986**, *317*, 11-21
240. Heinicke, J.; Kadyrov, R., *J. Organomet. Chem.* **1996**, *520*, 131-137.
241. Lal, S.; McNally, J.; White, A. J. P.; Díez-González, S., *Organometallics* **2011**, *30*(22), 6225-6232.
242. Yu, J.; RajanBabu, T. V.; Parquette, J. R., *J. Am. Chem. Soc.* **2008**, *130*, 7845-7847.

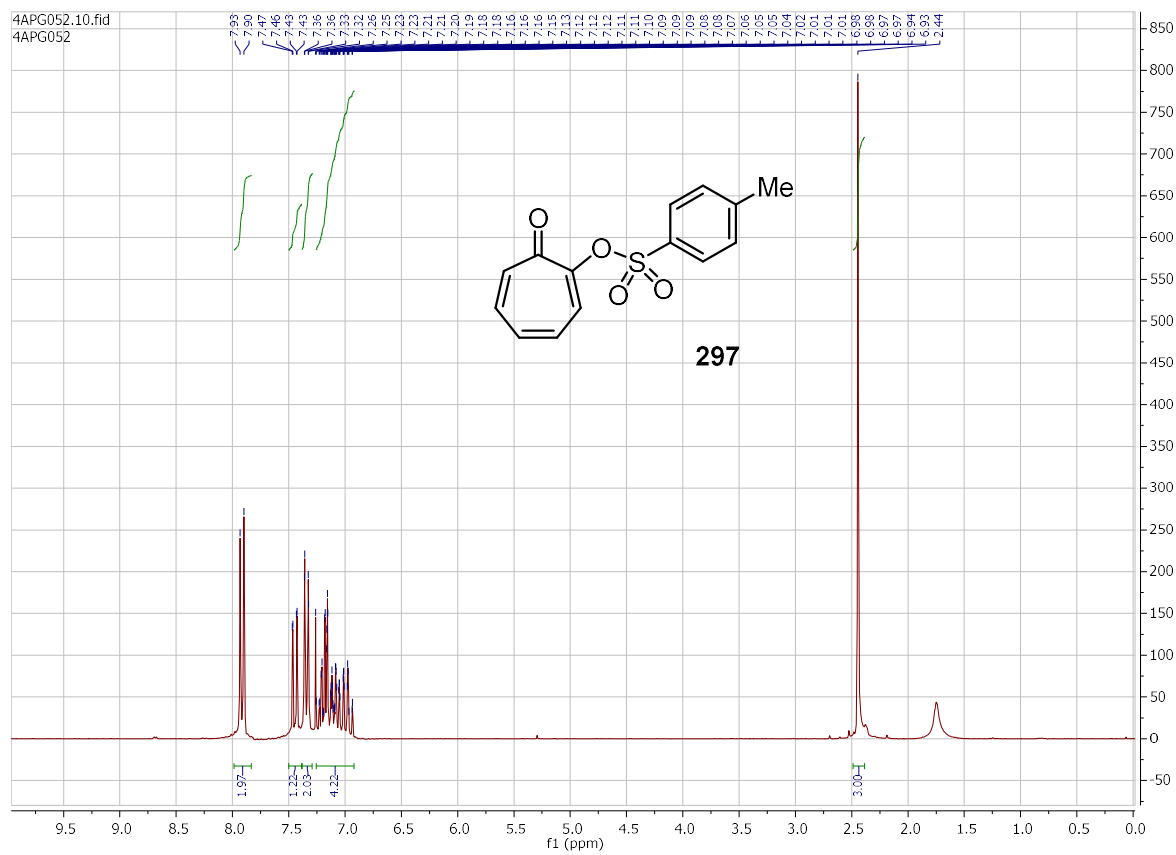
243. Leino, T. O.; Baumann, M.; Yli-Kauhaluoma, J.; Baxendale, I. R.; Wallén, E. A. A., *J. Org. Chem.* **2015**, *80*, 11513-11520.
244. Dubovik, J.; Bredihhin, A., *Synthesis* **2015**, *47*, 2663-2669.
245. Fallahpour, R.-A.; Sigrist, R.; Hansen, H.-J., *Helv. Chim. Acta* **1995**, *78*(6), 1408-1418
246. Inoue, A.; Kitagawa, K.; Shinokubo, H.; Oshima, K., *J. Org. Chem.* **2001**, *66*, 4333-4339.
247. McDonald, R. N.; Petty, H. E.; Wolfe, N. L.; Paukstelis, J. V., *J. Org. Chem.* **1974**, *39*, 1877-1887.
248. Chen, S.-L.; Klein, R.; Hafner, K., *Eur. J. Org. Chem.* **1998**, 423-433.
249. Kurotobi, K.; Tabata, H.; Miyauchi, M.; Mustafizur, R. A. F. M.; Migita, K.; Murafuji, T.; Sugihara, Y.; Shimoyama, H.; Fujimori, K., *Synthesis* **2003**, (1), 30-34.
250. Shibasaki, T.; Oishi, T.; Yamanouchi, N.; Murafuji, T.; Kurotobi, K.; Sugihara, Y., *J. Org. Chem.* **2008**, *73*, 7971-7977.
251. Murai, M.; Takami, K.; Takeshima, H.; Takai, K., *Org. Lett.* **2015**, *17*, 1798-1801.
252. Zhao, L.; Bruneau, C.; Doucet, H., *Chem. Commun.* **2013**, *49*, 5598.
253. Hafner, K.; Kaiser, H., *Liebigs Ann. Chem.* **1958**, *618* (1-3), 140-152.
254. Hafner, K.; Kaiser, H.; Bangert, K.; Boekelheide, V., *Org. Synth.* **1964**, *44*, 94.
255. Lash, T. D.; El-Beck, J. A.; Ferrence, G. M., *J. Org. Chem.* **2007**, *72*, 8402-8415.
256. Rogano, F.; Stojnic, D.; Linden, A.; Abou-Hadeed, K.; Hansen, H., *Helv. Chim. Acta* **2011**, *94* (7), 1194-1215.

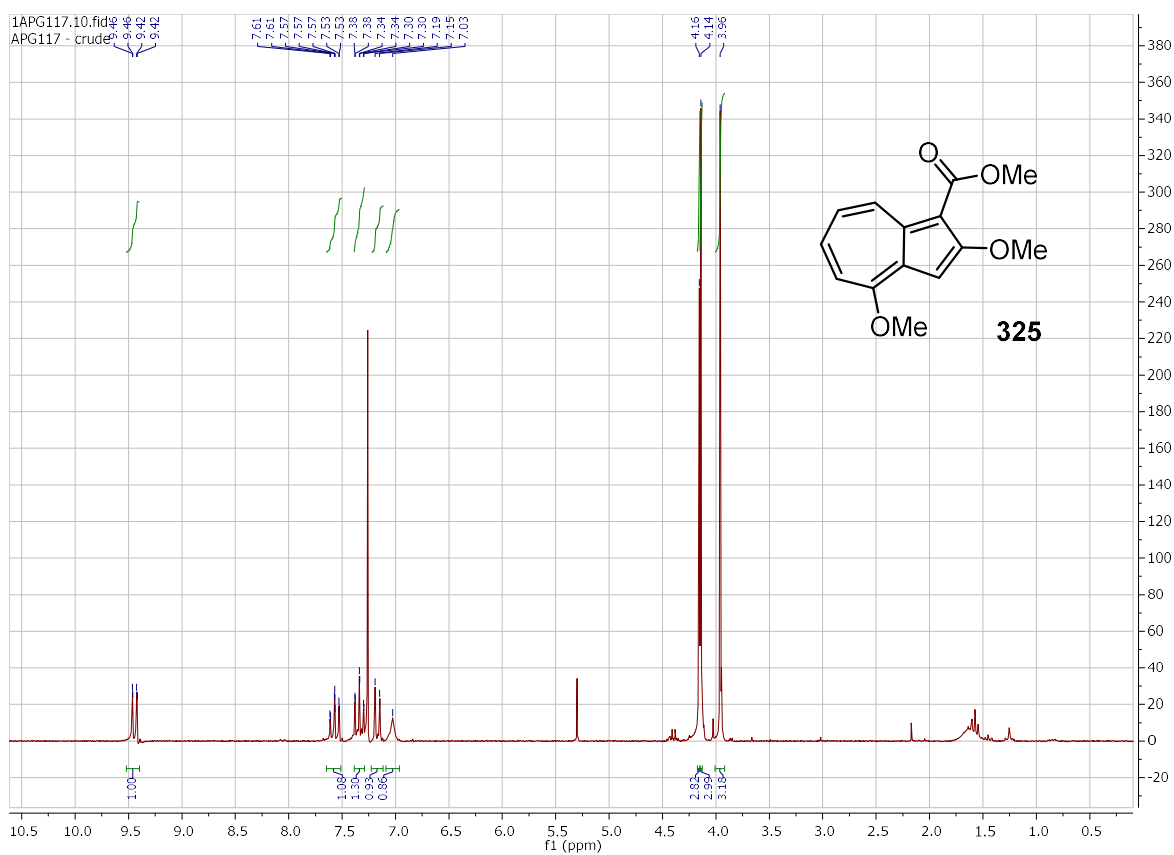
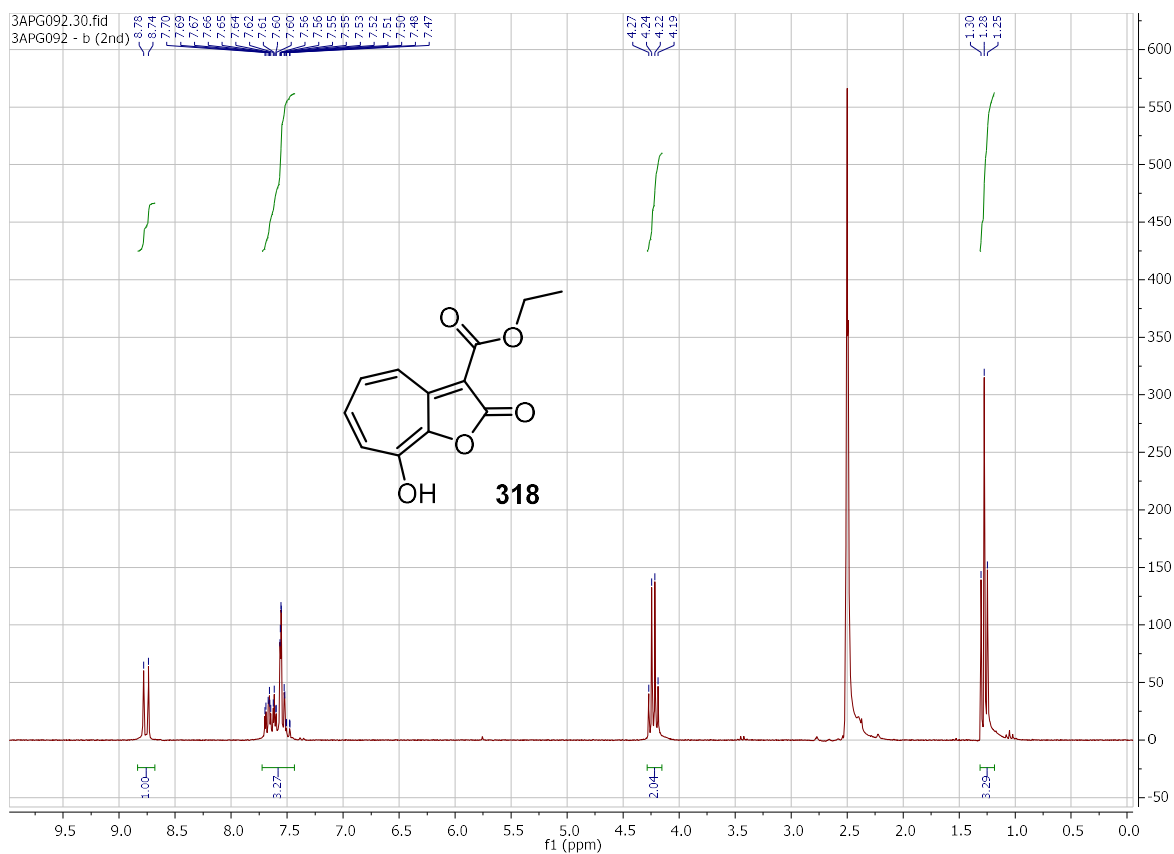
257. Razus, A. C.; Pavel, C.; Lehadus, O.; Nica, S.; Birzan, L., *Tetrahedron* **2008**, *64*, 1792-1797.
258. Koenig, T.; Rudolf, K.; Chadwick, R.; Geiselman, H.; Patapoff, T.; Klopfenstein, C. E., *J. Am. Chem. Soc.* **1986**, *108*, 5024-5025.
259. Rippert, A. J.; Hansen, H.-J., *Helv. Chim. Acta* **1995**, *78*, 238-241.
260. Casey, C. P.; Bullock, R. M.; Fultz, W. C.; Rheingold, A. L., *Organometallics* **1982**, *1*, 1591-1596.
261. Brasse, C. C.; Englert, U.; Salzer, A.; Waffenschmidt, H.; Wasserscheid, P., *Organometallics* **2000**, *19*, 3818-3823.
262. Cornelissen, C.; Erker, G.; Kehr, G.; Fröhlich, R., *Organometallics* **2005**, *24*, 214-225.
263. Li, F.; Song, Q.; Yang, L.; Wu, G.; Zhang, X., *Chem. Commun.* **2013**, *49*, 1808-1810.
264. Razus, A. C.; Nitu, C.; Carvac, S.; Birzan, L.; Razus, S. A.; Pop, M.; Tarko, L., *J. Chem. Soc. Perkin Trans. 1* **2001**, 1227-1233.
265. Yang, F.; Xu, X.-L.; Gong, Y.-H.; Qiu, W.-W.; Sun, Z.-R.; Zhou, J.-W.; Audebert, P.; Tang, J., *Tetrahedron* **2007**, *63*, 9188-9194.
266. Wu, C.; Devendar, B.; Su, H.; Chang, Y.; Ku, C., *Tetrahedron Lett.* **2012**, *53*(37), 5019-5022.
267. Terada, M., *Synthesis* **2010**, (12), 1929-1982.
268. Parmar, D.; Sugiono, E.; Raja, S.; Rueping, M., *Chem. Rev.* **2015**, *114*(18), 9047-9153.
269. Correia, J. T. M., *Synlett* **2015**, *26*, 416-417.
270. Xu, F.; Huang, D.; Han, C.; Shen, W.; Lin, X.; Wang, Y., *J. Org. Chem.* **2010**, *75*, 8677-8680.

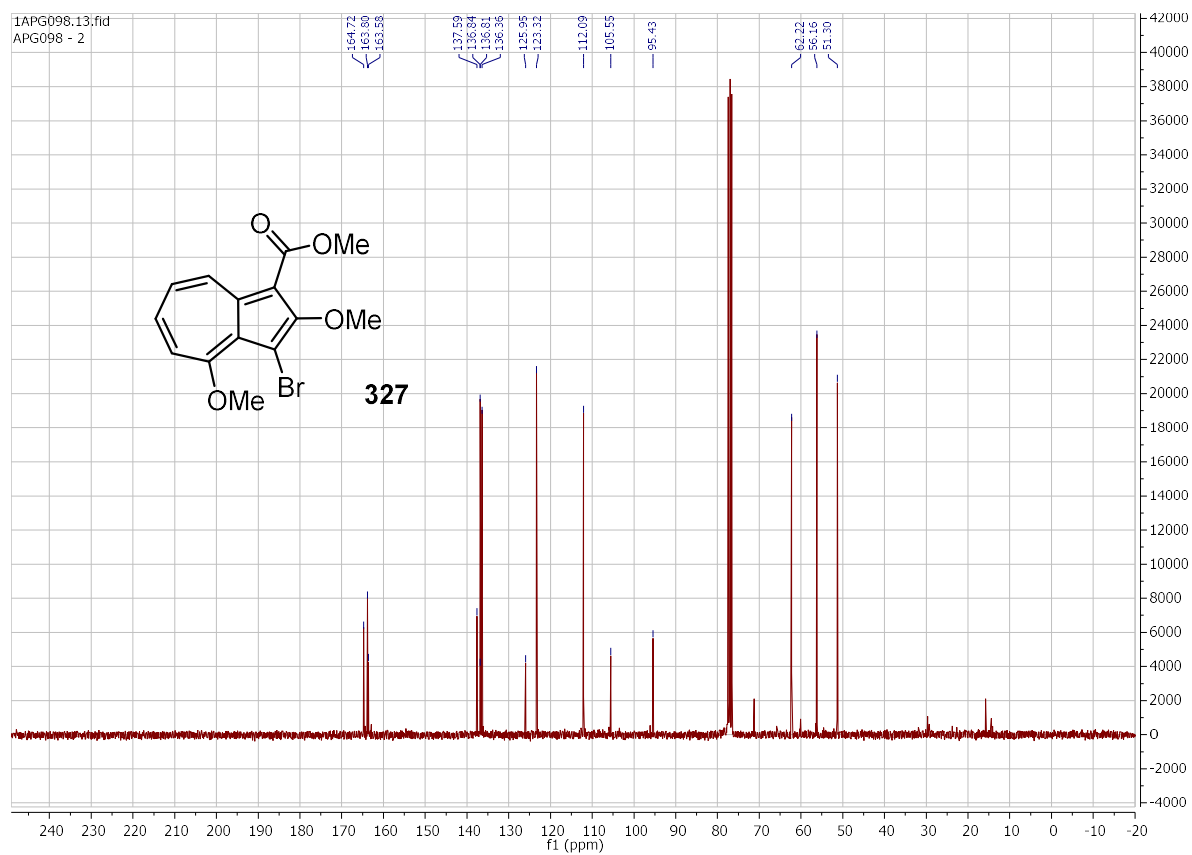
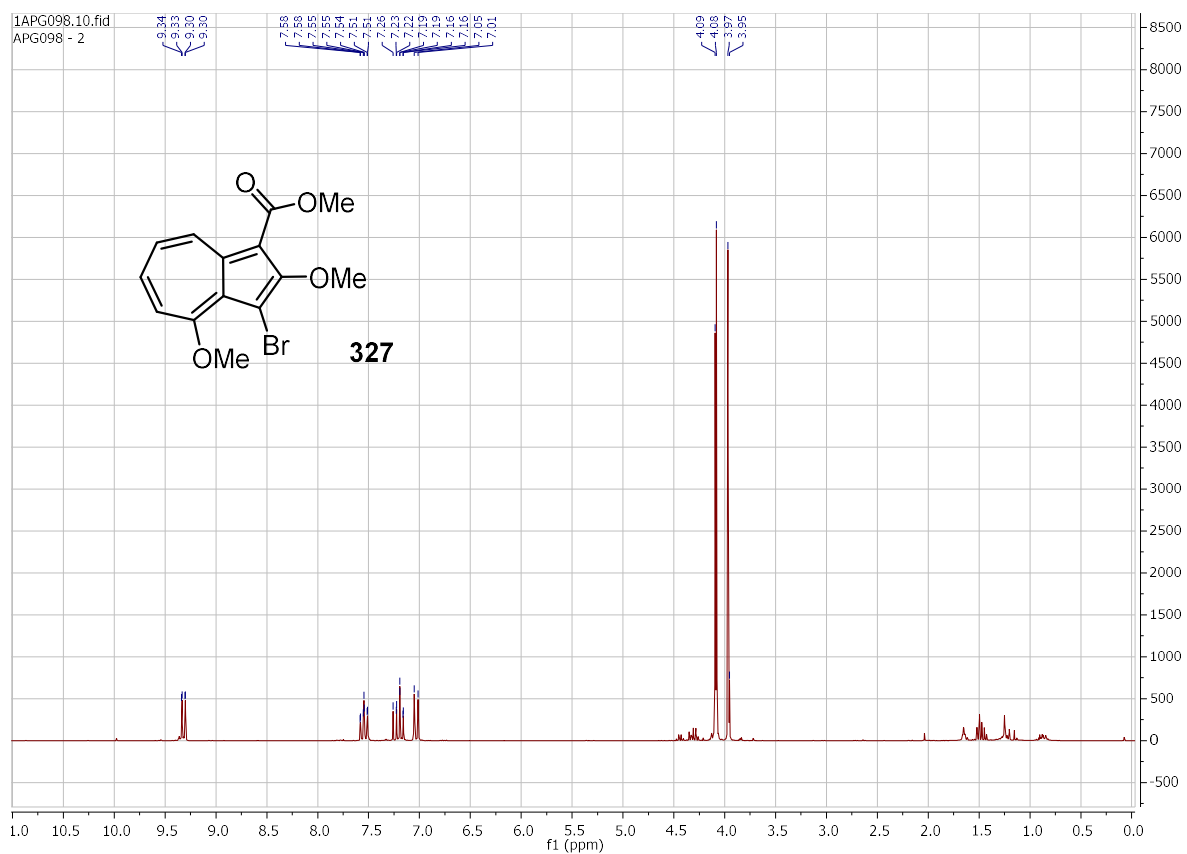
271. Xu, B.; Zhu, S.-F.; Xie, X.-L.; Shen, J.-J.; Zhou, Q.-L., *Angew. Chem. Int. Ed.* **2011**, *50*, 11483-11486.
272. Zhang, Y.; Zhao, R.; Bao, R. L.-Y.; Shi, L., *Eur. J. Org. Chem.* **2015**, 3344-3351.
273. Adair, G.; Mukherjee, S.; List, B., *Aldrichim. Acta* **2008**, *41*(2), 29-51.
274. Holzwarth, R.; Bartsch, R.; Cherkaoui, Z.; Solladié, *Eur. J. Org. Chem* **2005**, 3536-3541.
275. Storer, R. I.; Carrera, D. E.; Ni, Y.; MacMillan, D. W. C., *J. Am. Chem. Soc.* **2006**, *128*, 84-86.
276. Heller, D. P.; Goldberg, D. R.; Wu, H.; Wulff, W. D., *Can. J. Chem.* **2006**, *84*, 1487-1503.
277. Byrne, B.; Rothchild, R., *Chirality* **1999**, *11*, 529-535.
278. Hazeland, E. L.; Chapman, A. M.; Pringle, P. G.; Sparkes, H. A., *Chem. Commun.* **2015**, *51*, 10206-10209.
279. Cowper, P.; Jin, Y.; Turton, M. D.; Kociok-Köhn, G.; Lewis, S. E., *Angew. Chem. Int. Ed.* **2016**, *55*, 2564-2568.
280. Claramunt, R. M.; Sanz, D.; Pérez-Torrallba, M.; Pinilla, E.; Torres, M. R., *Eur. J. Org. Chem.* **2004**, 4452-4466.
281. Matsubara, Y.; Morita, M.; Takekuma, S.; Zhao, Z.; Yamamoto, H.; Nozoe, T., *Bull. Chem. Soc. Jpn.* **1991**, *64*, 2865-2867.
282. Lee, D.-S.; Yang, P.-W.; Morita, T.; Nozoe, T., *Heterocycles* **1995**, *41*(2), 249-253.
283. Kim, T.-S.; Seo, S.-Y.; Shin, D., *Synlett* **2015**, 1243-1247.

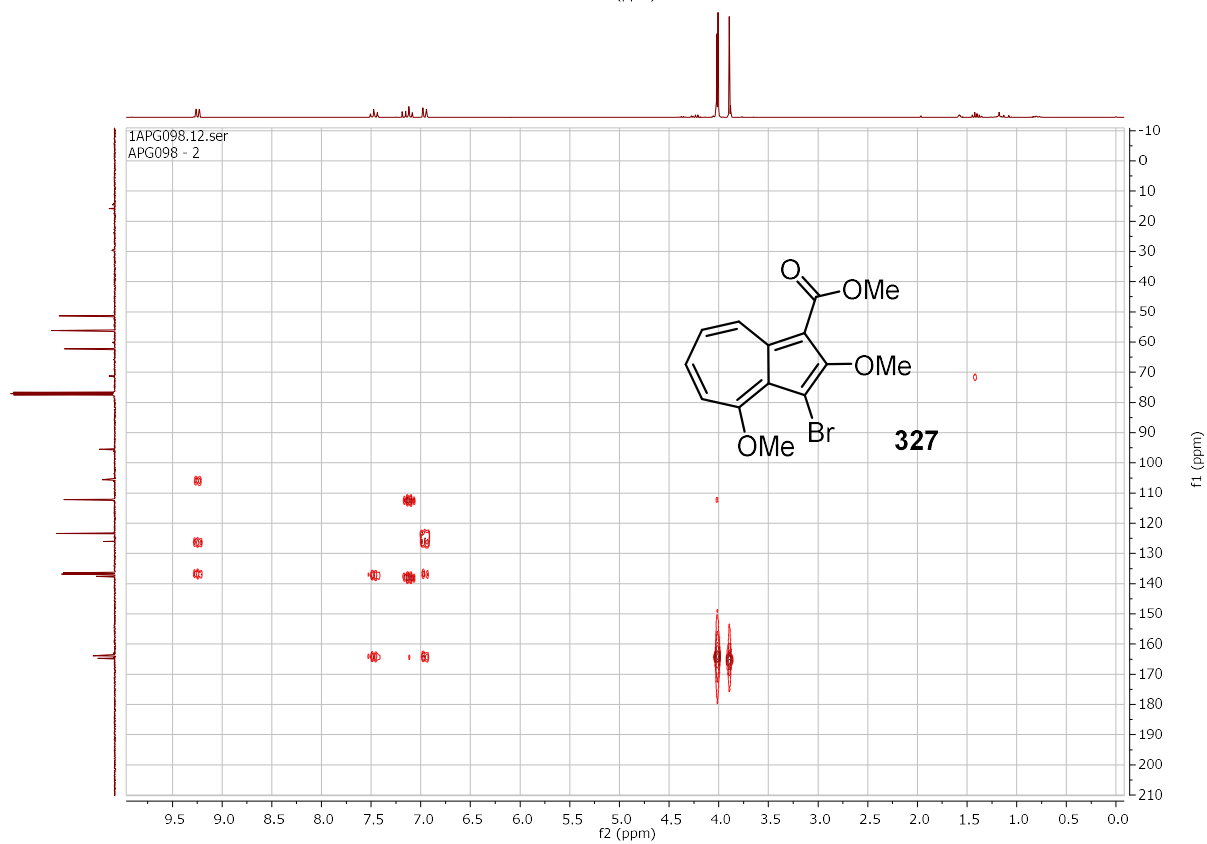
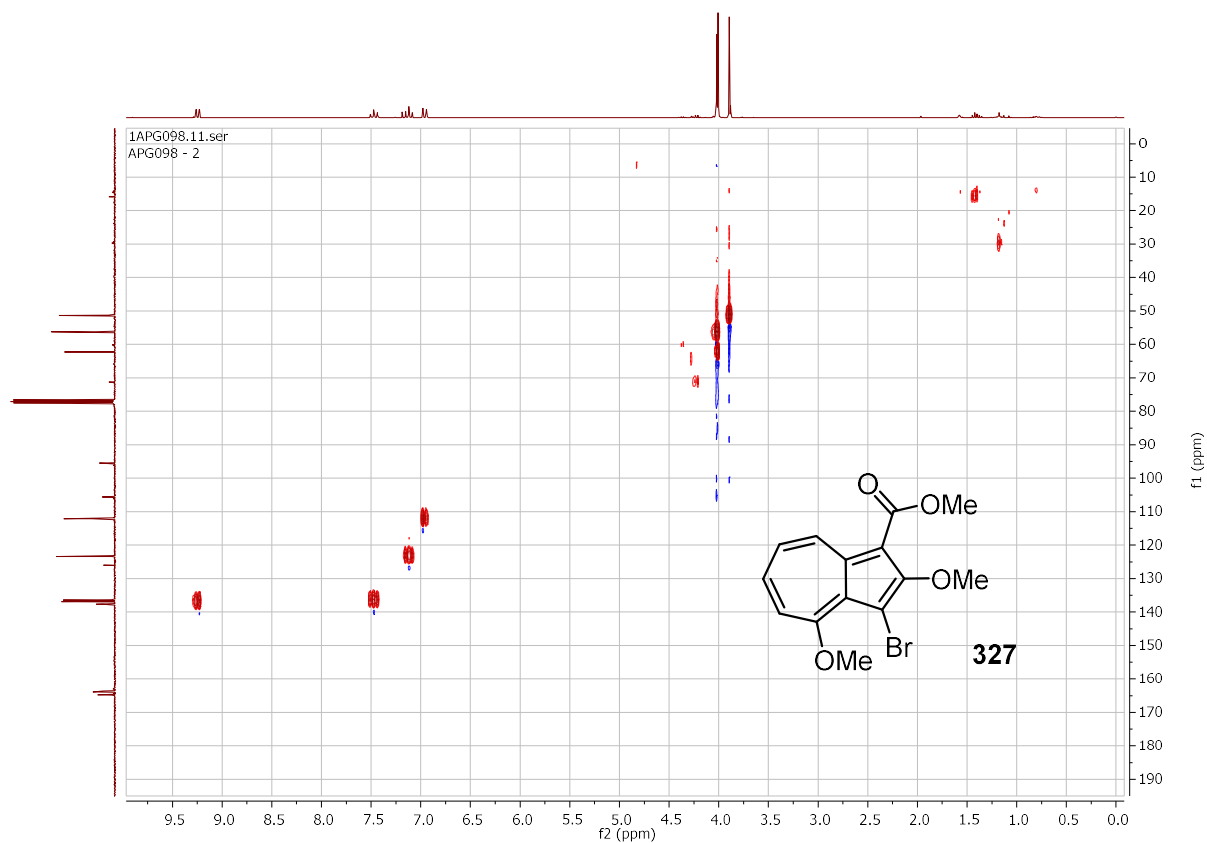
5. APPENDICES

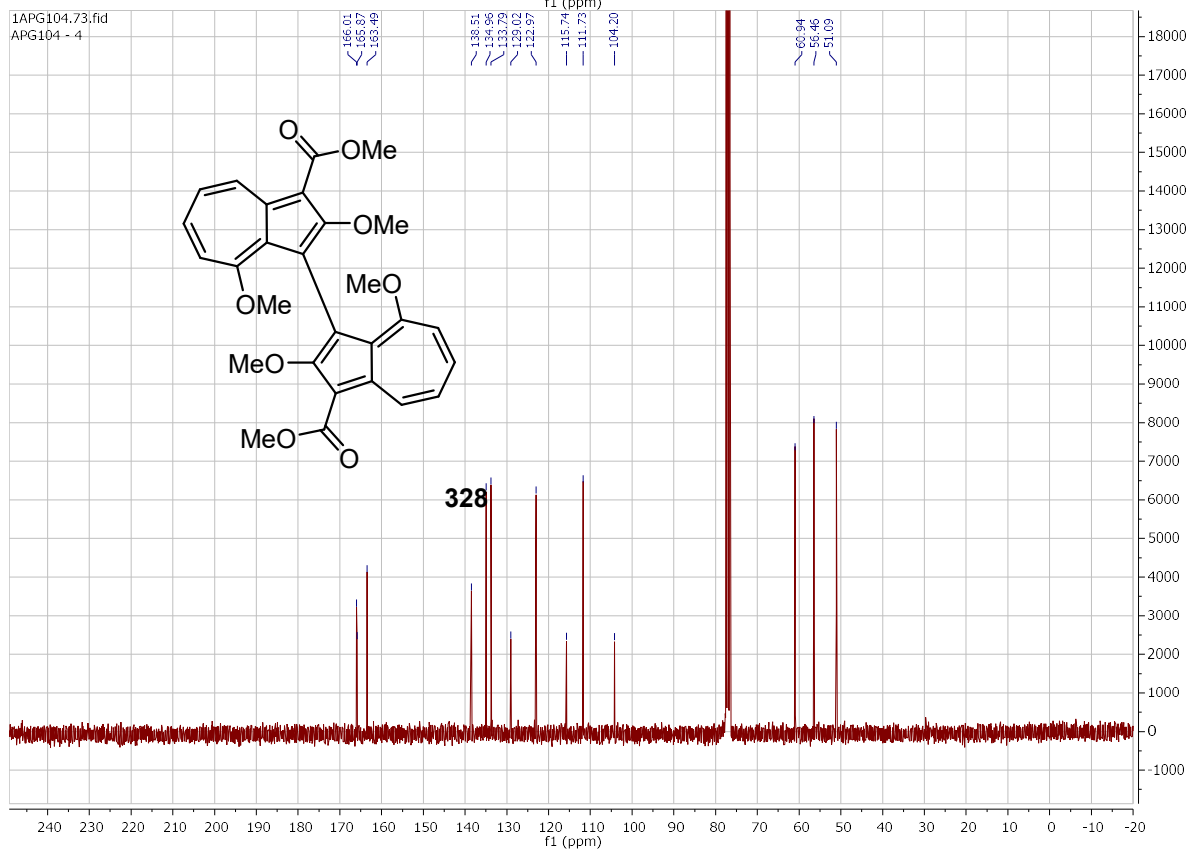
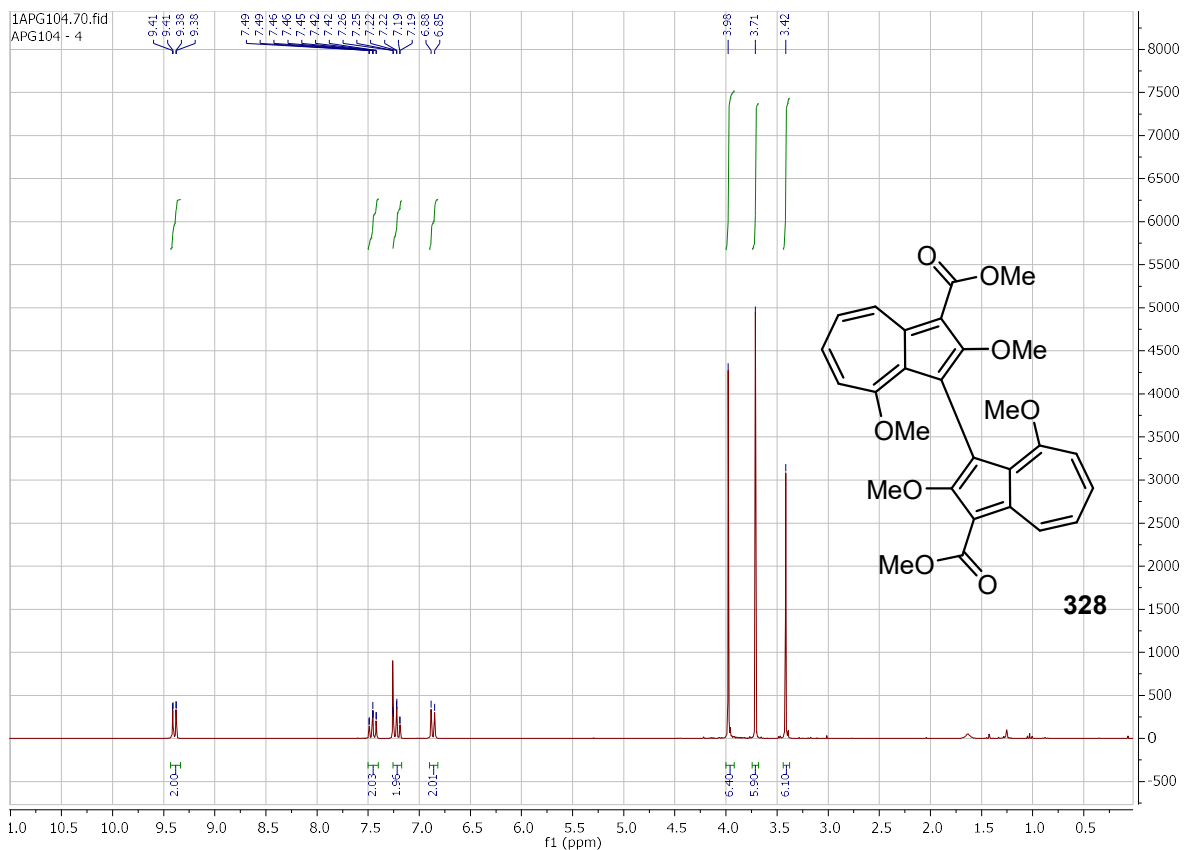
5.1 NMR appendix

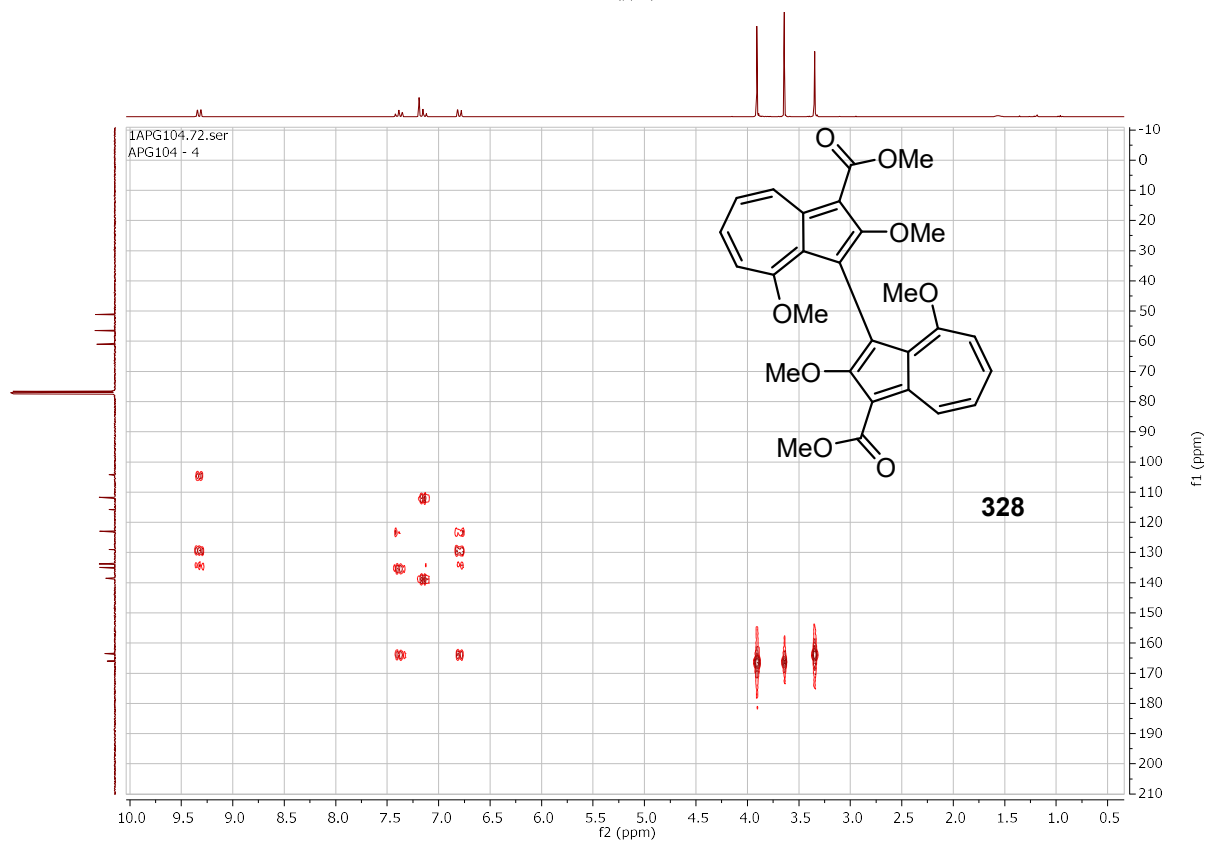
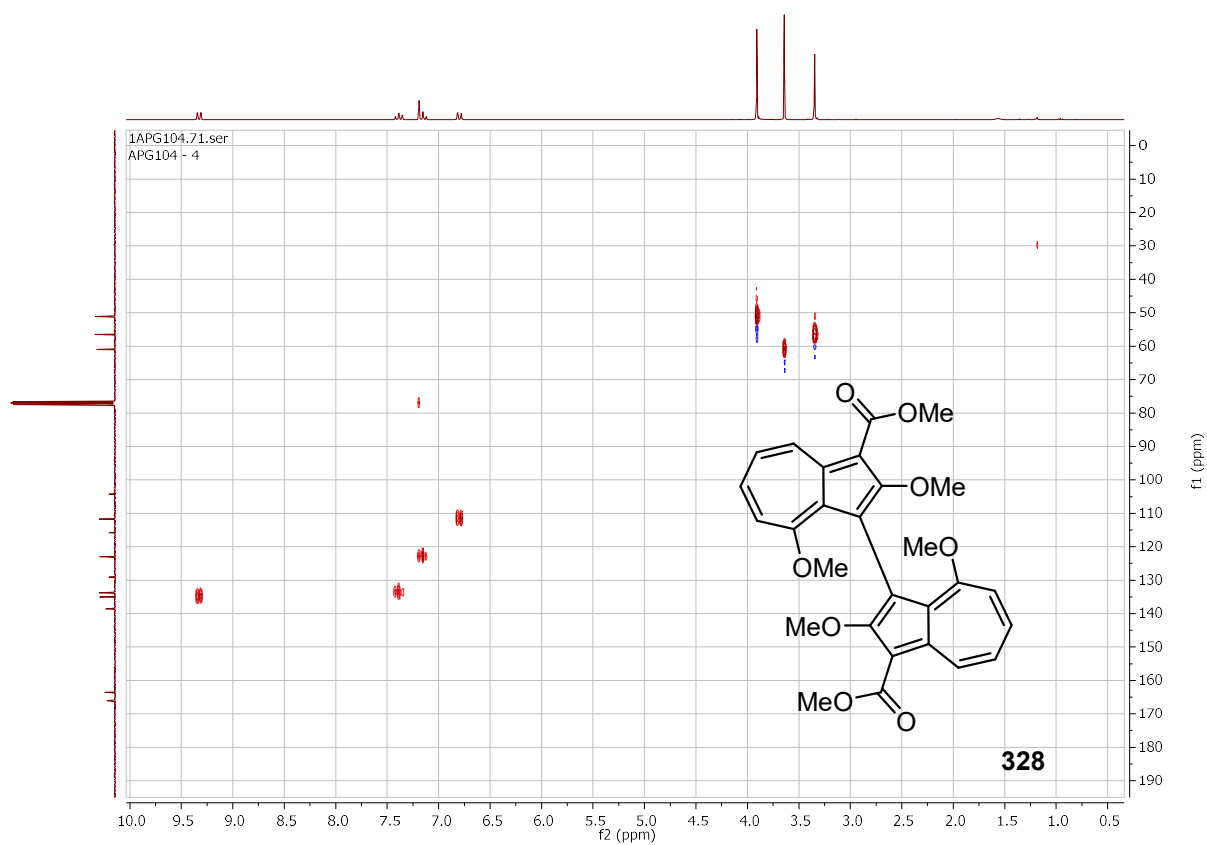


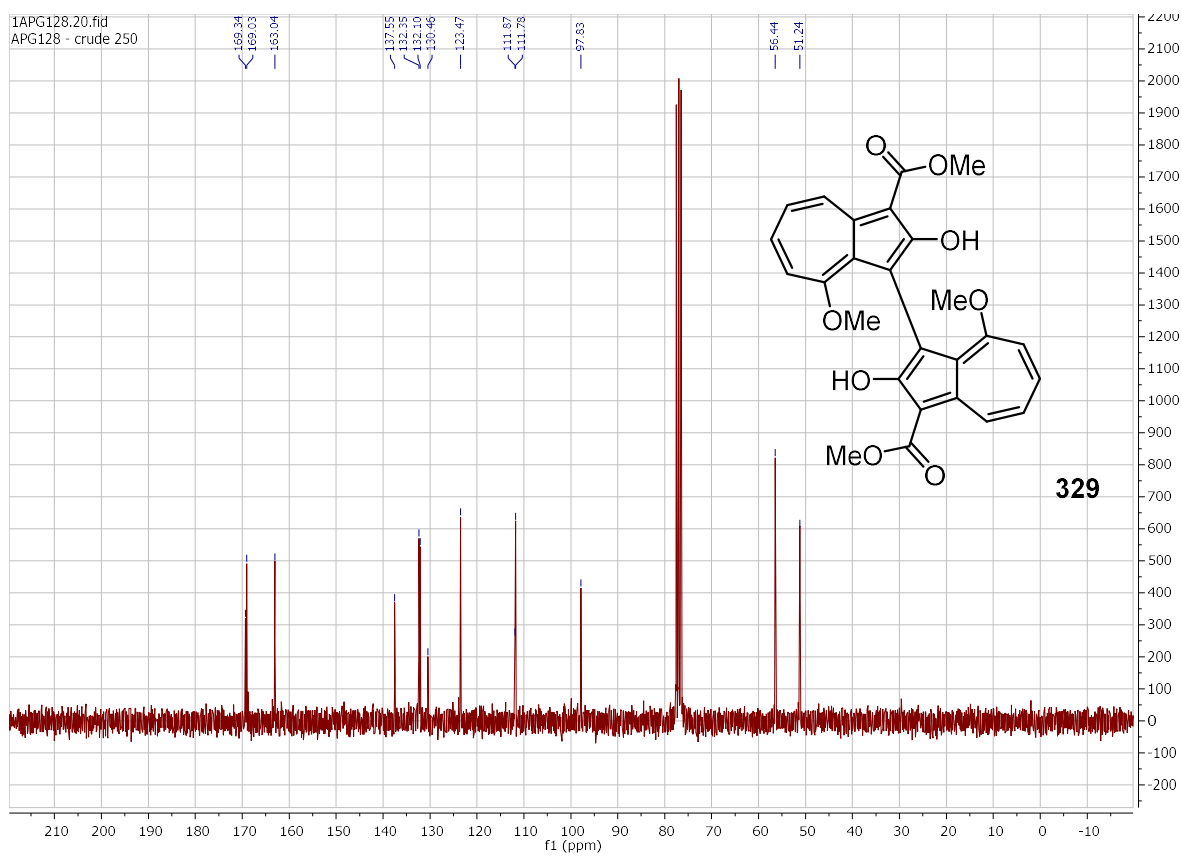
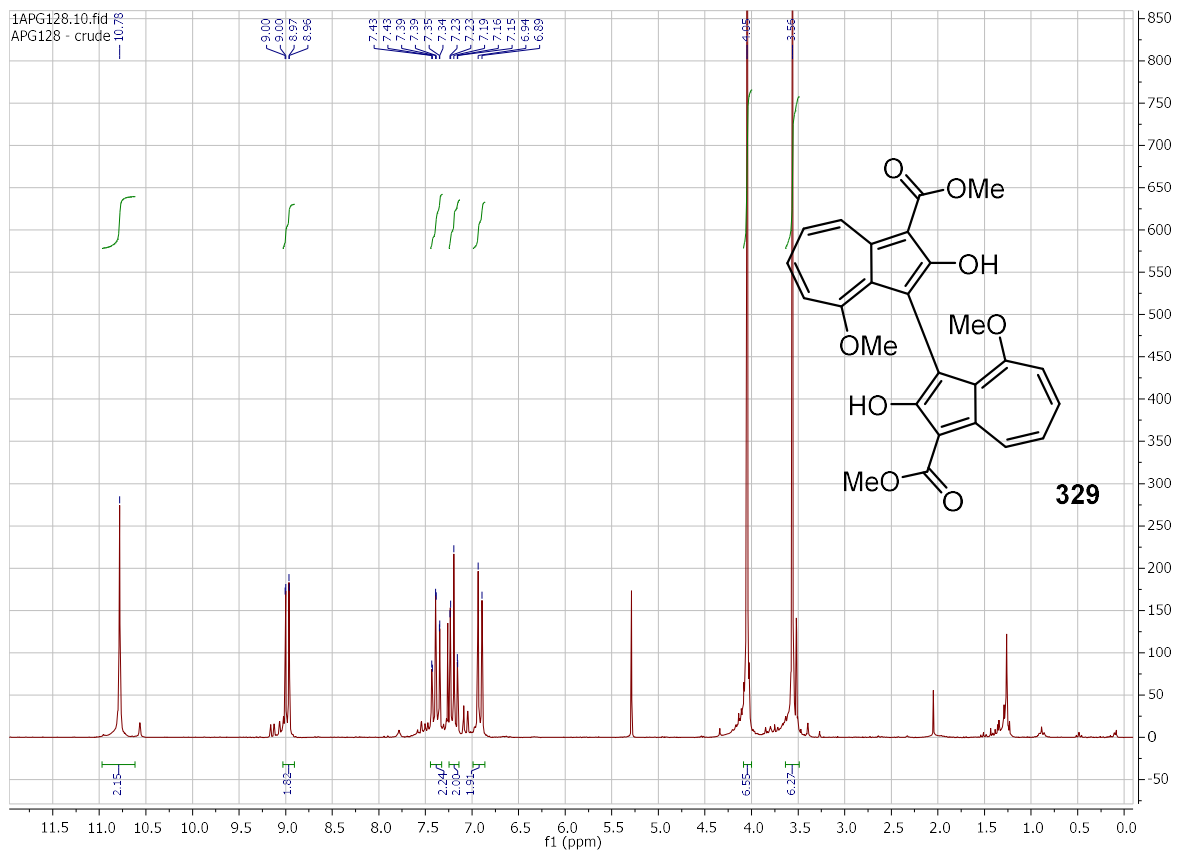


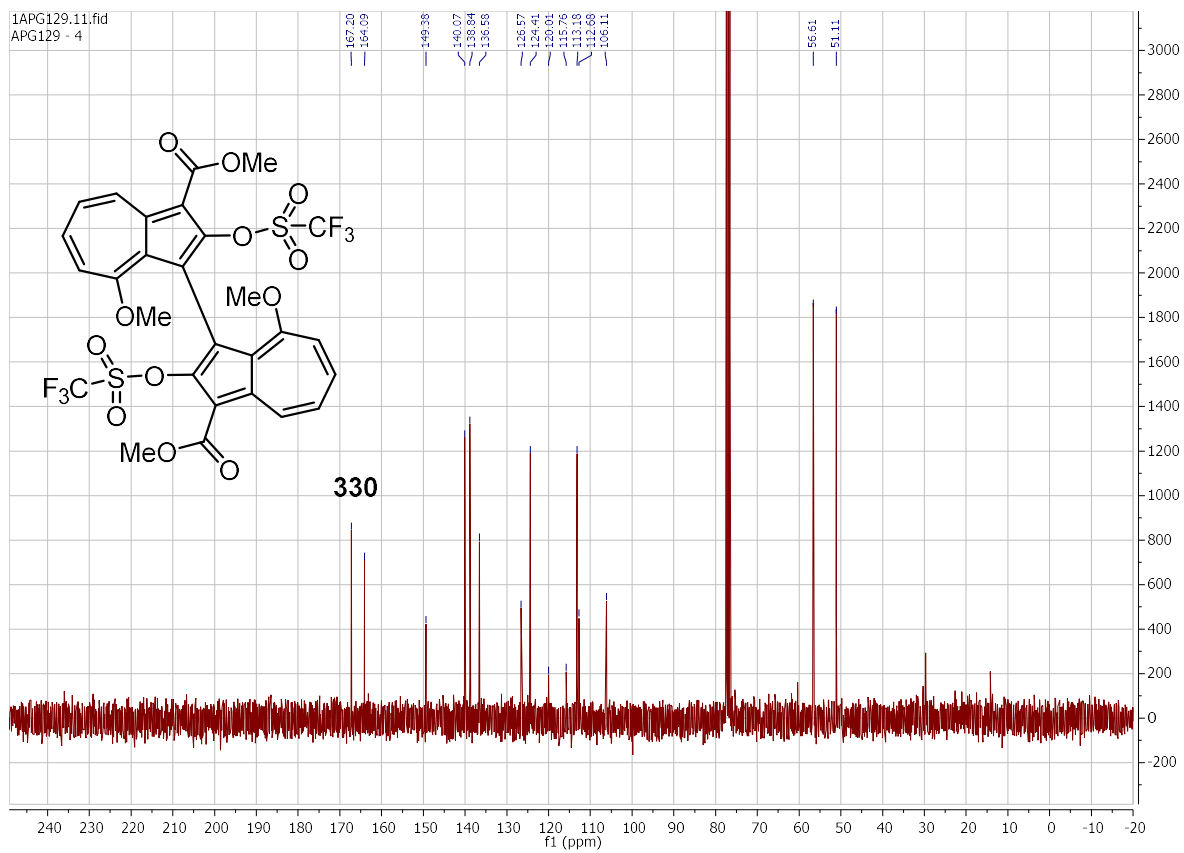
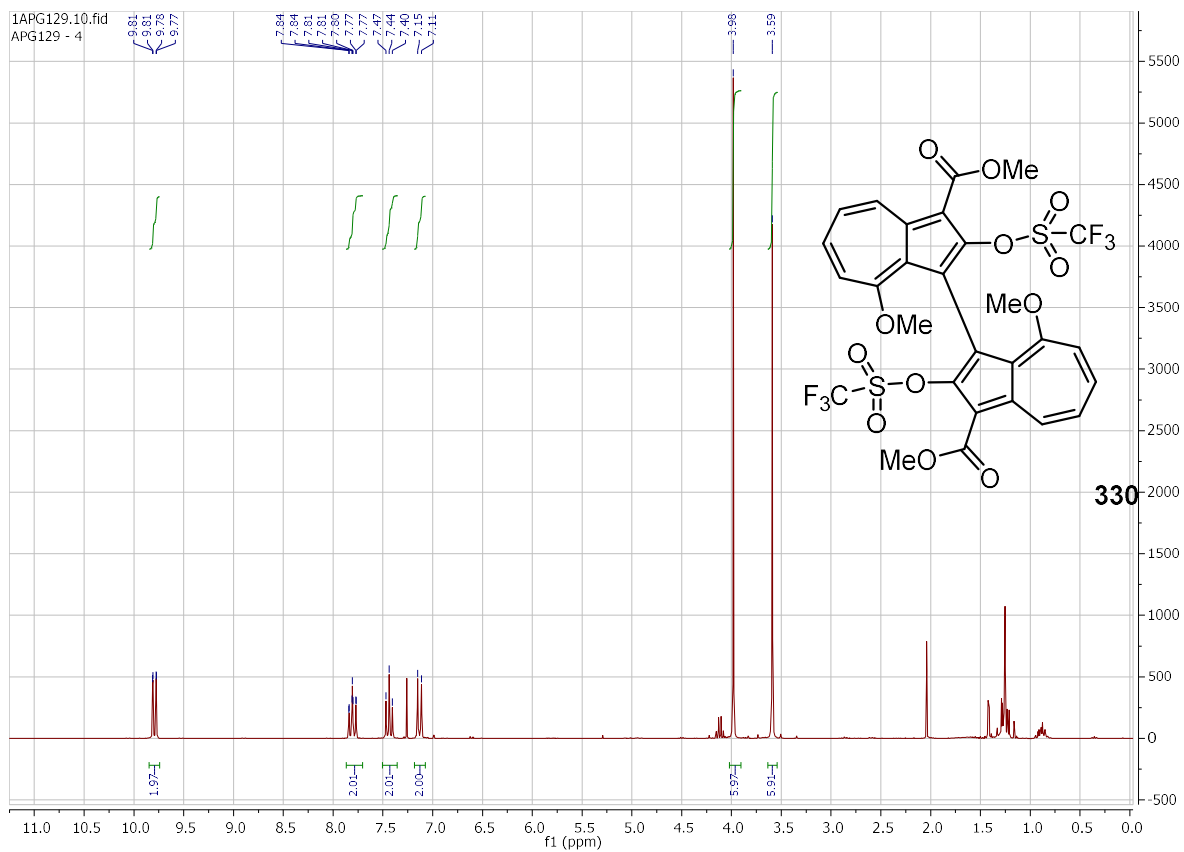


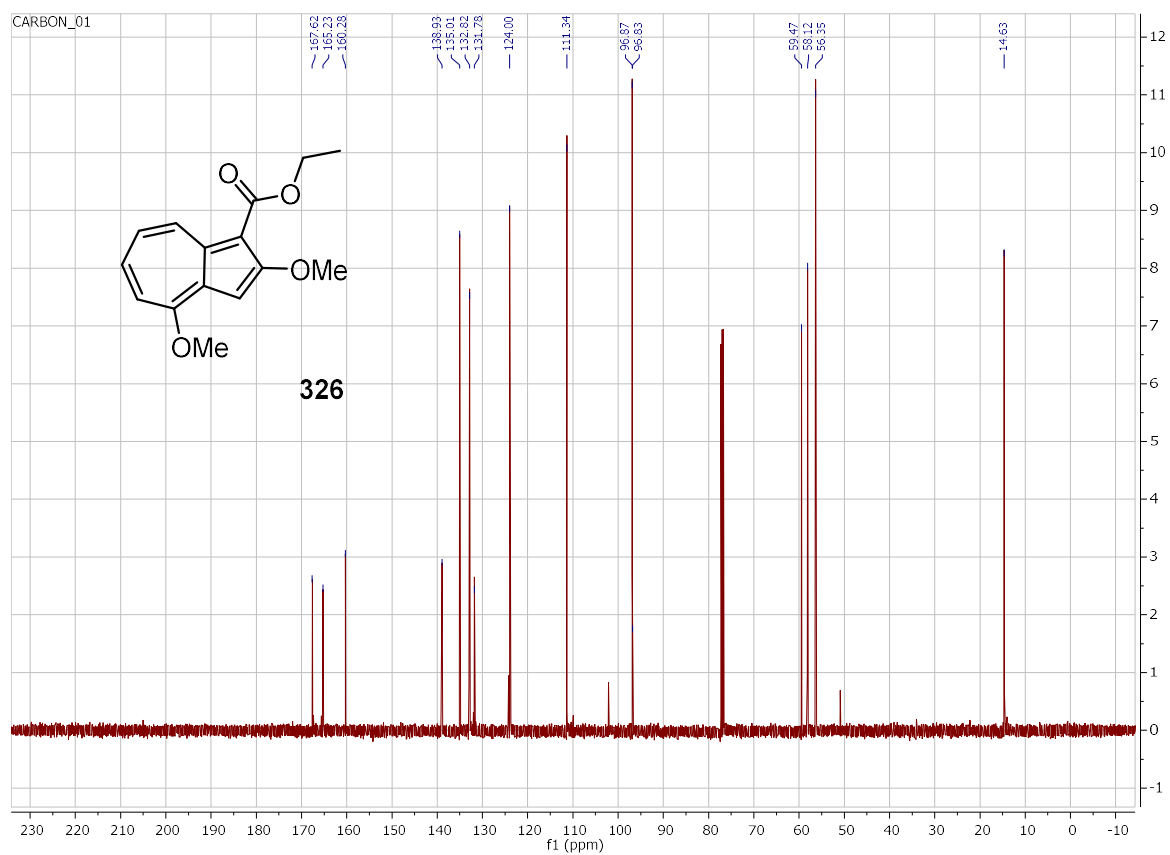
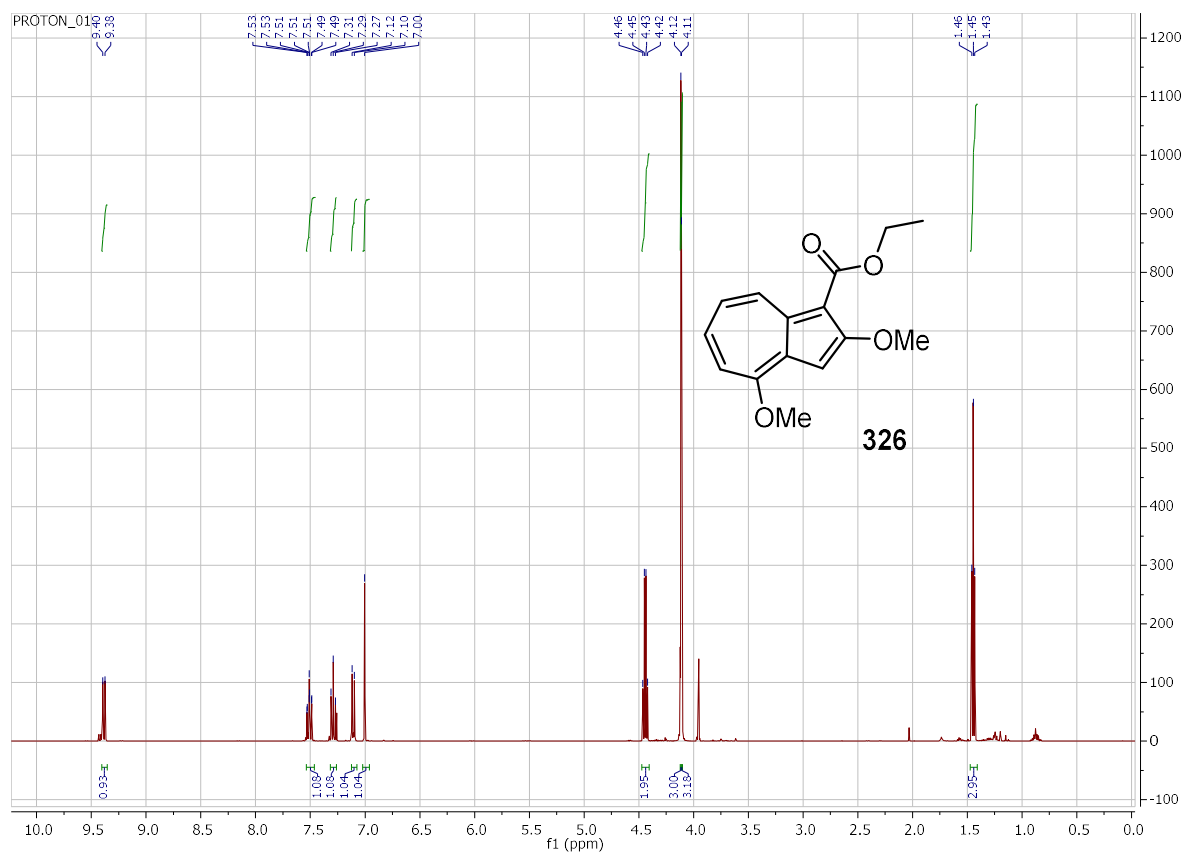


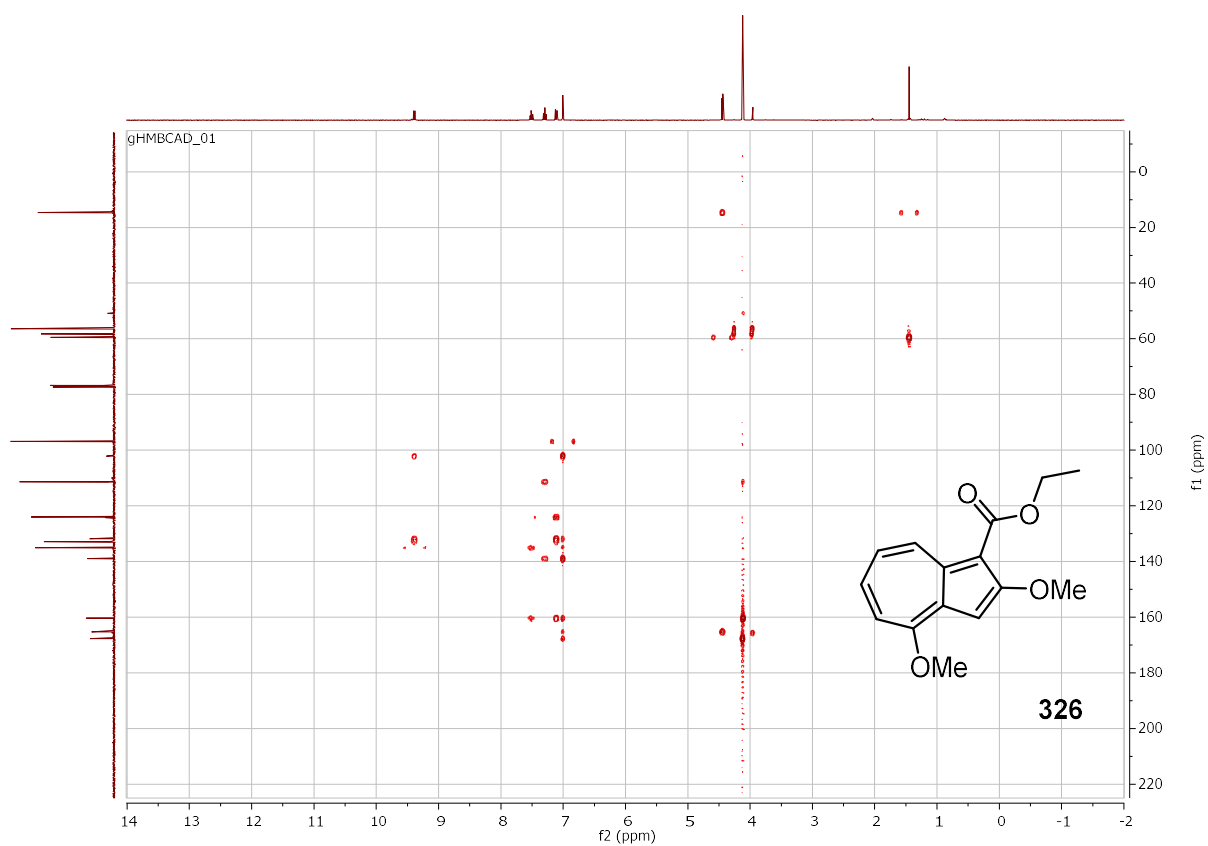
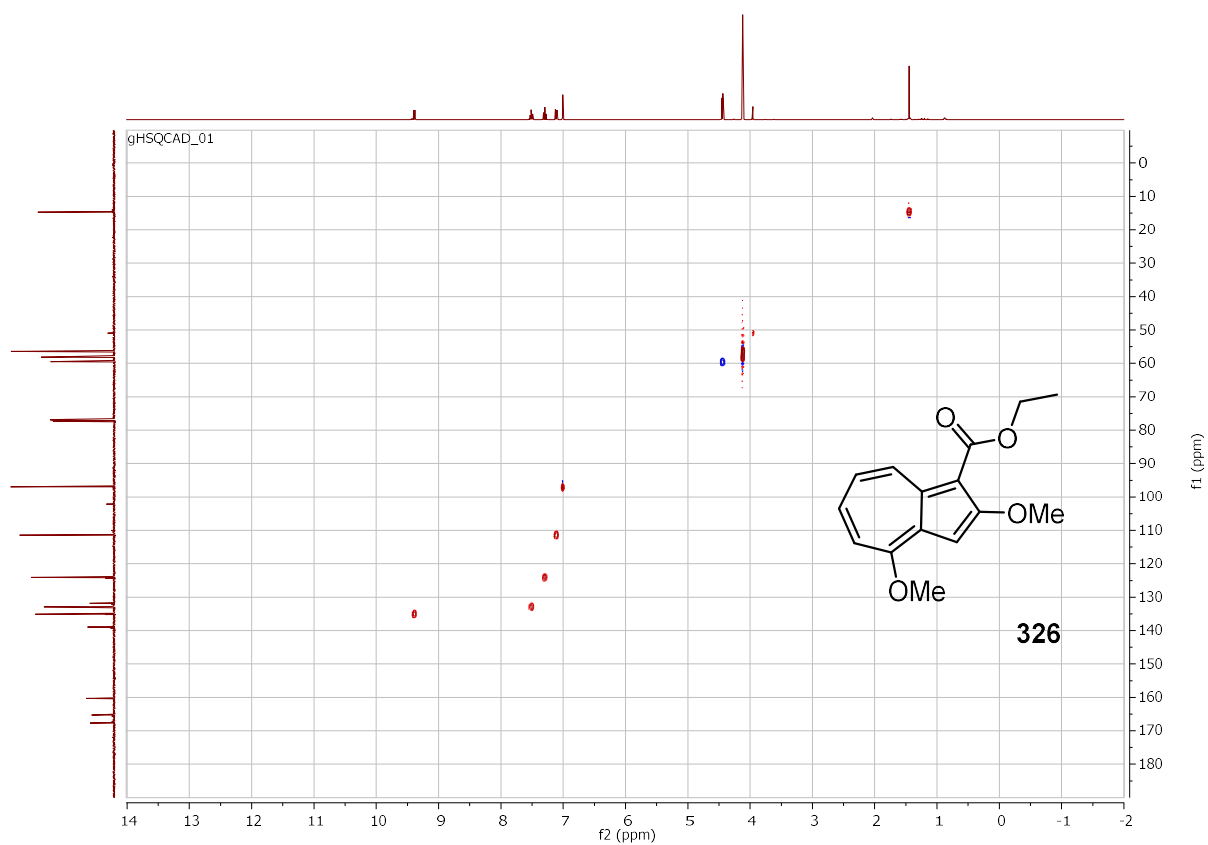


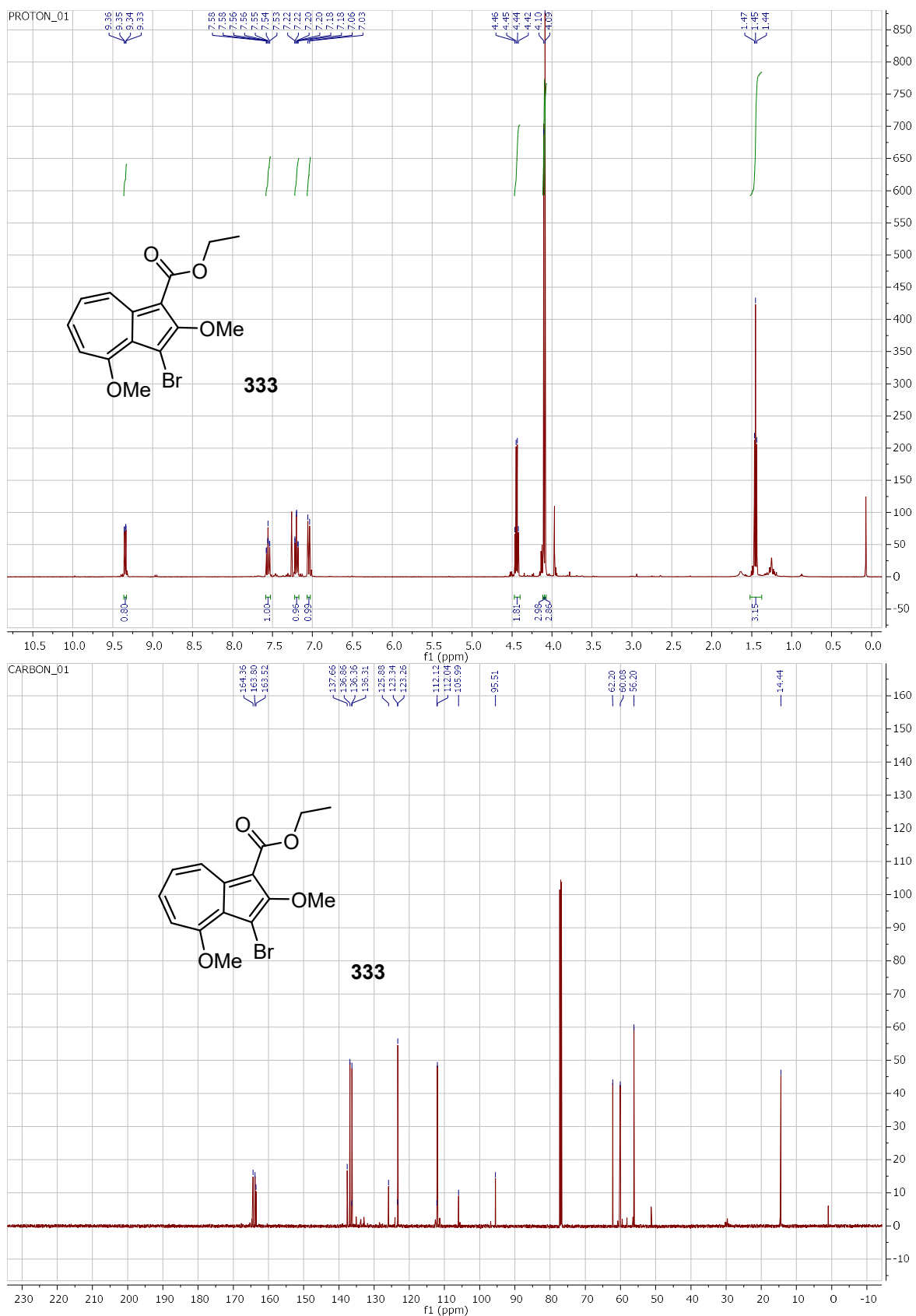


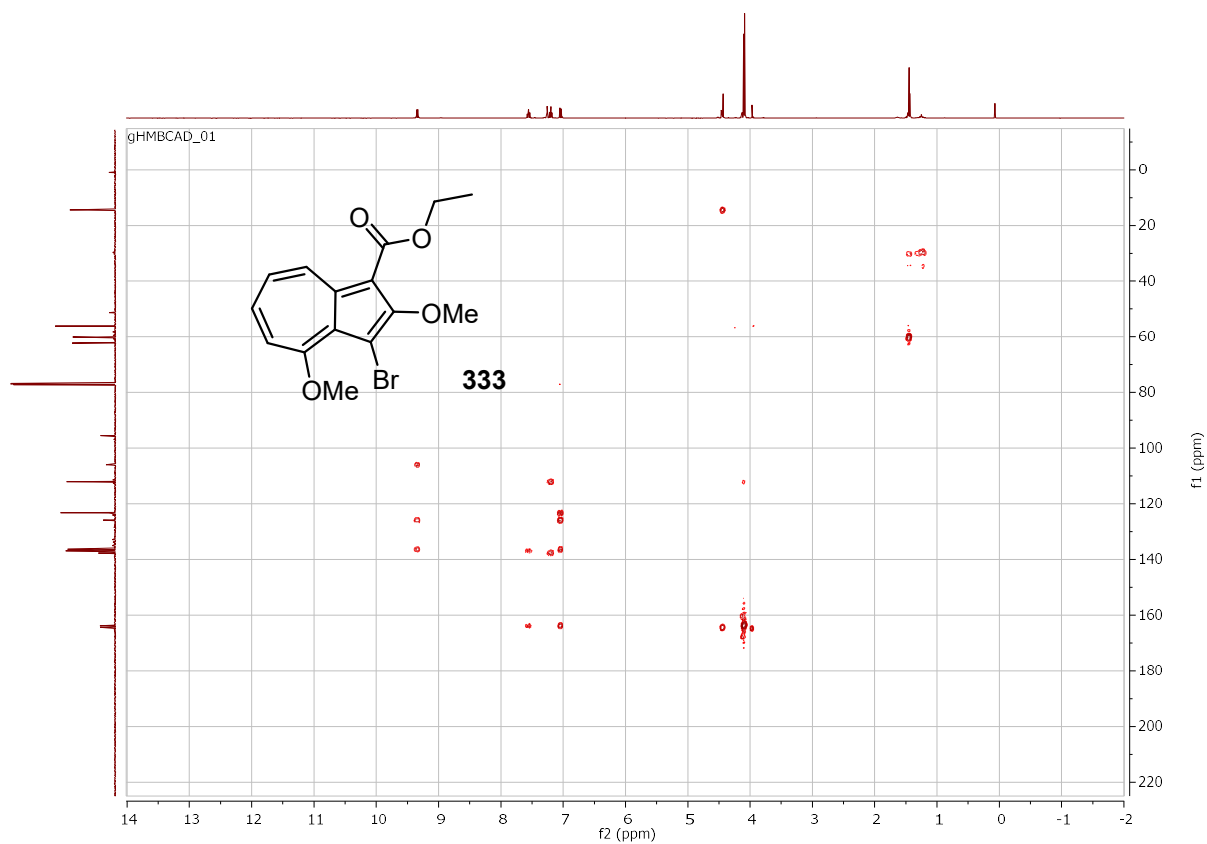
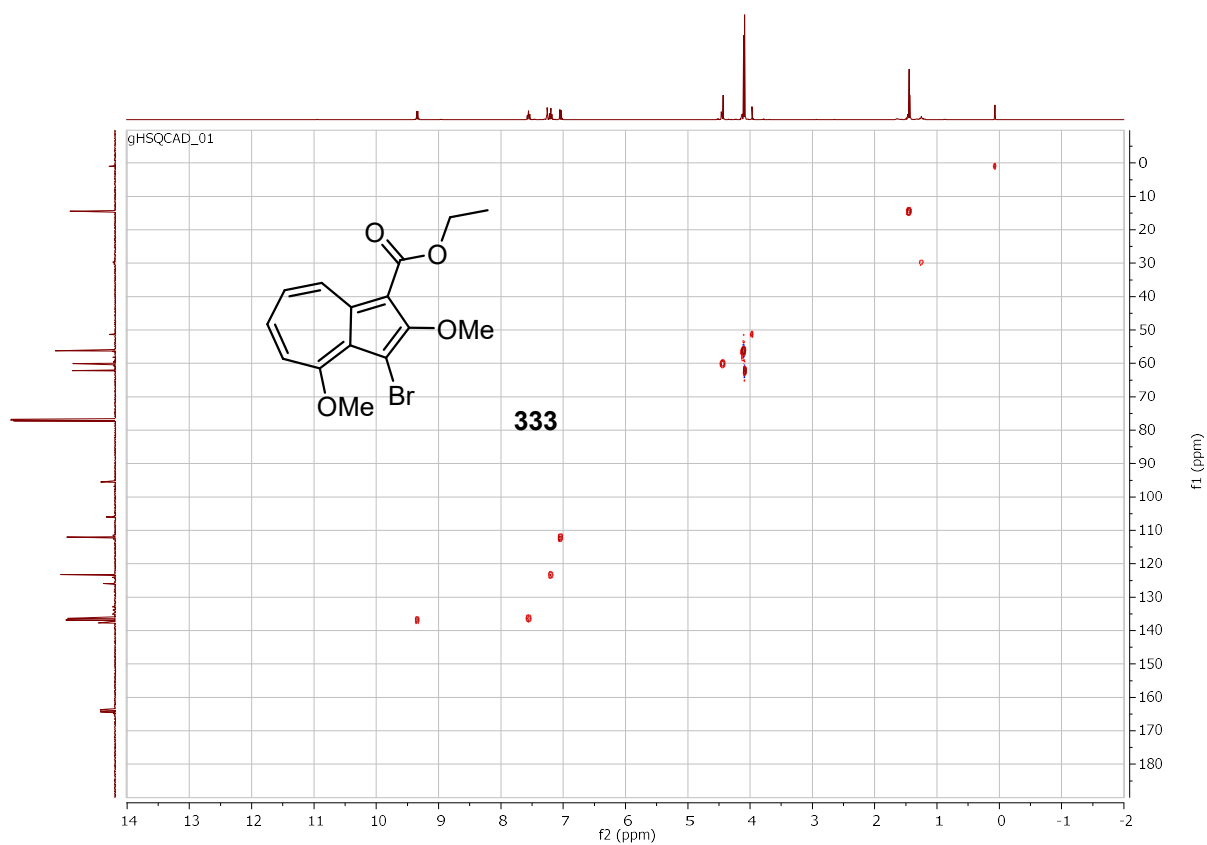


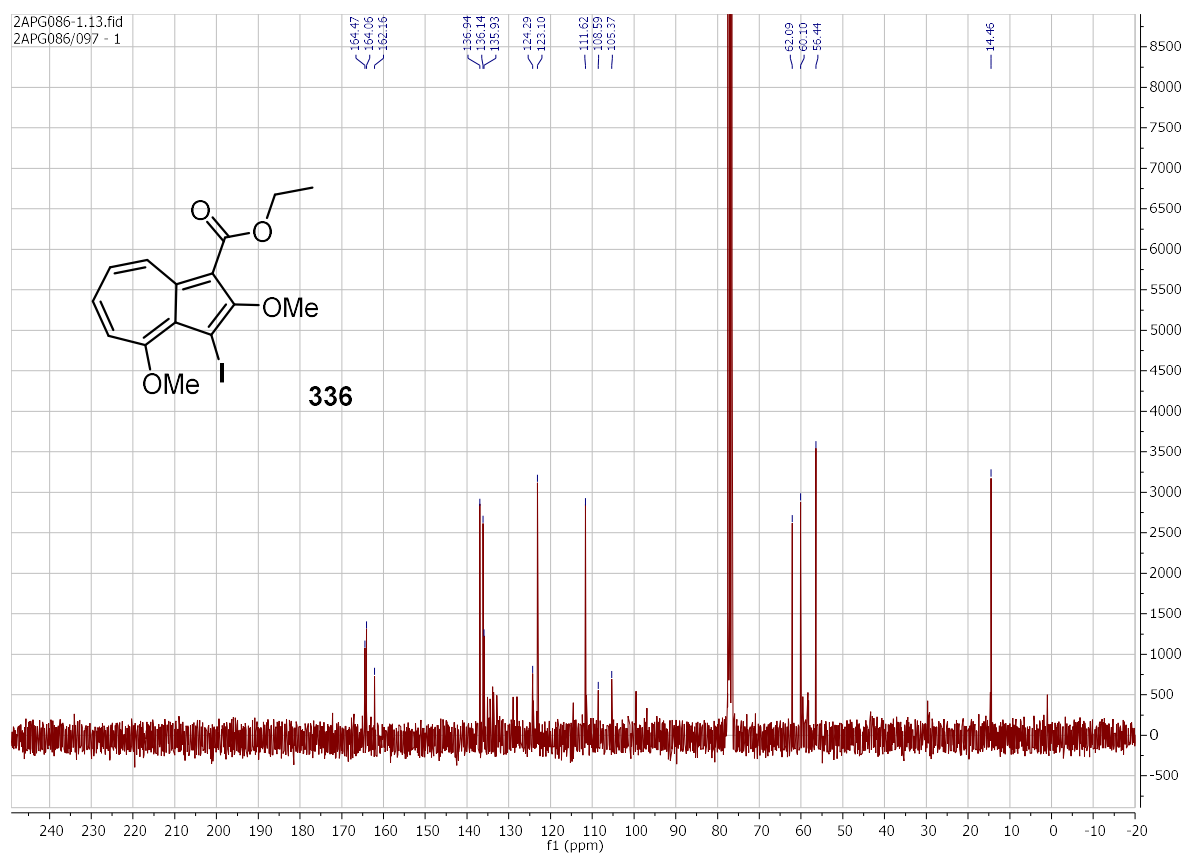
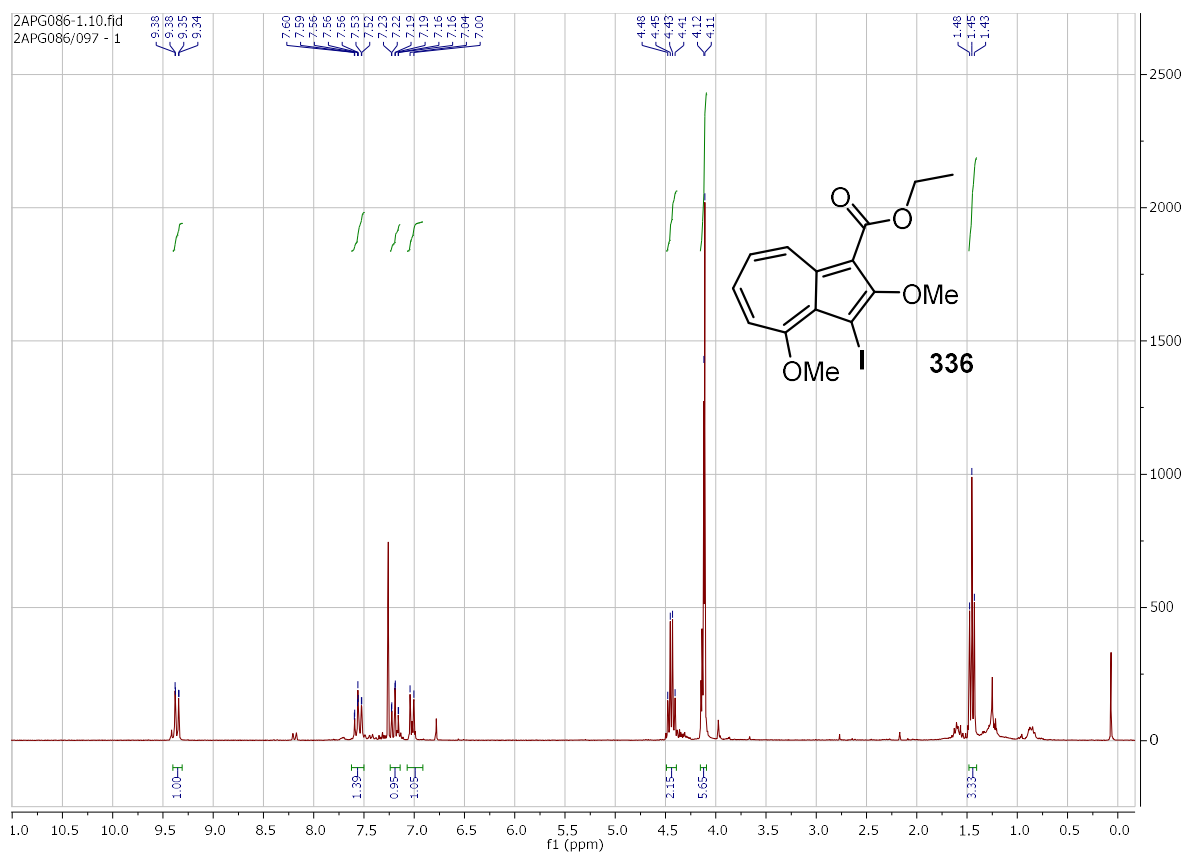


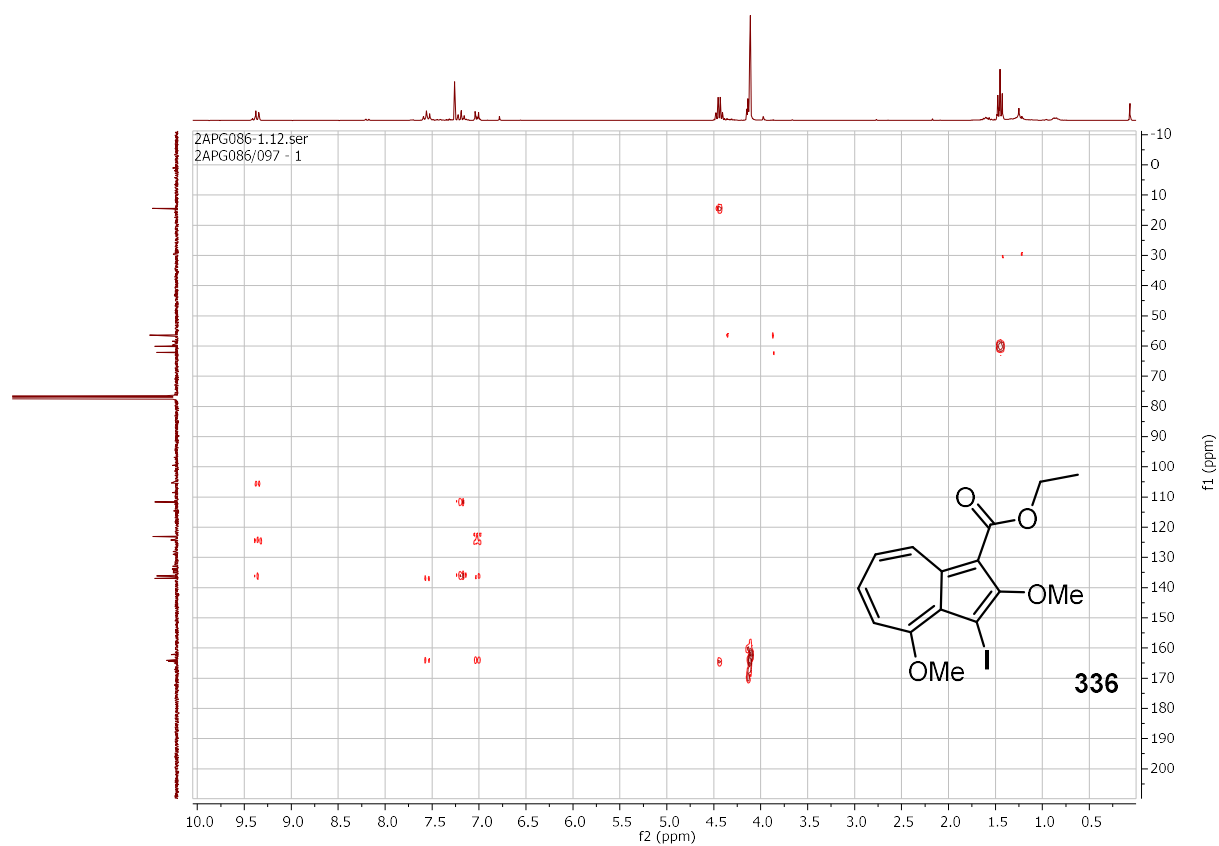
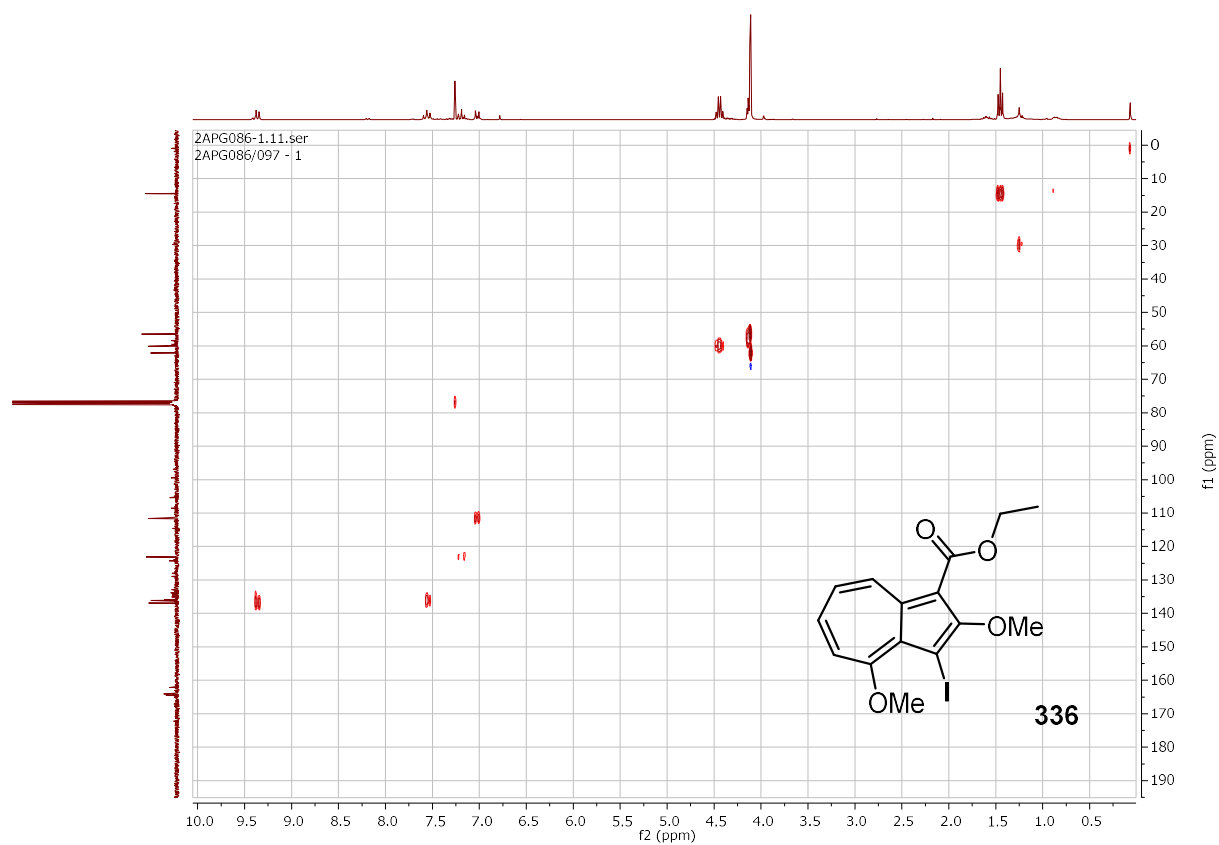


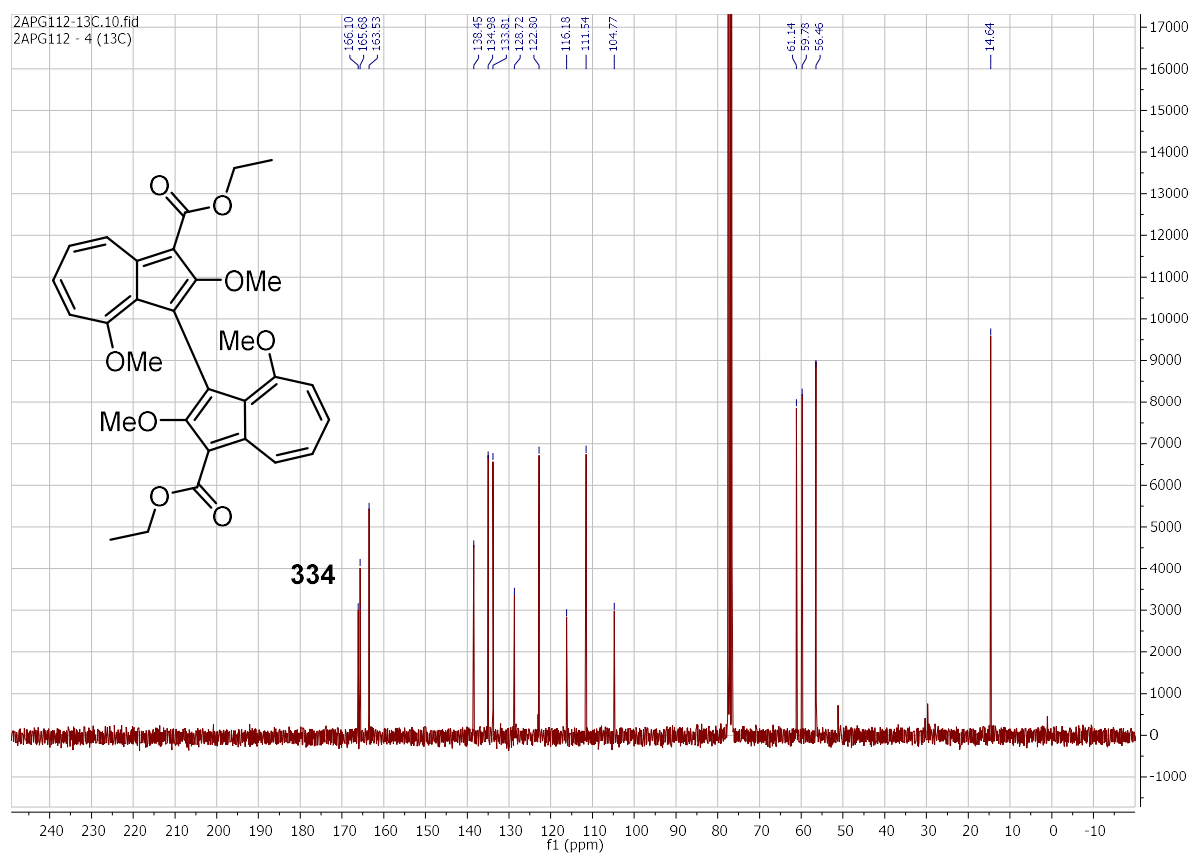
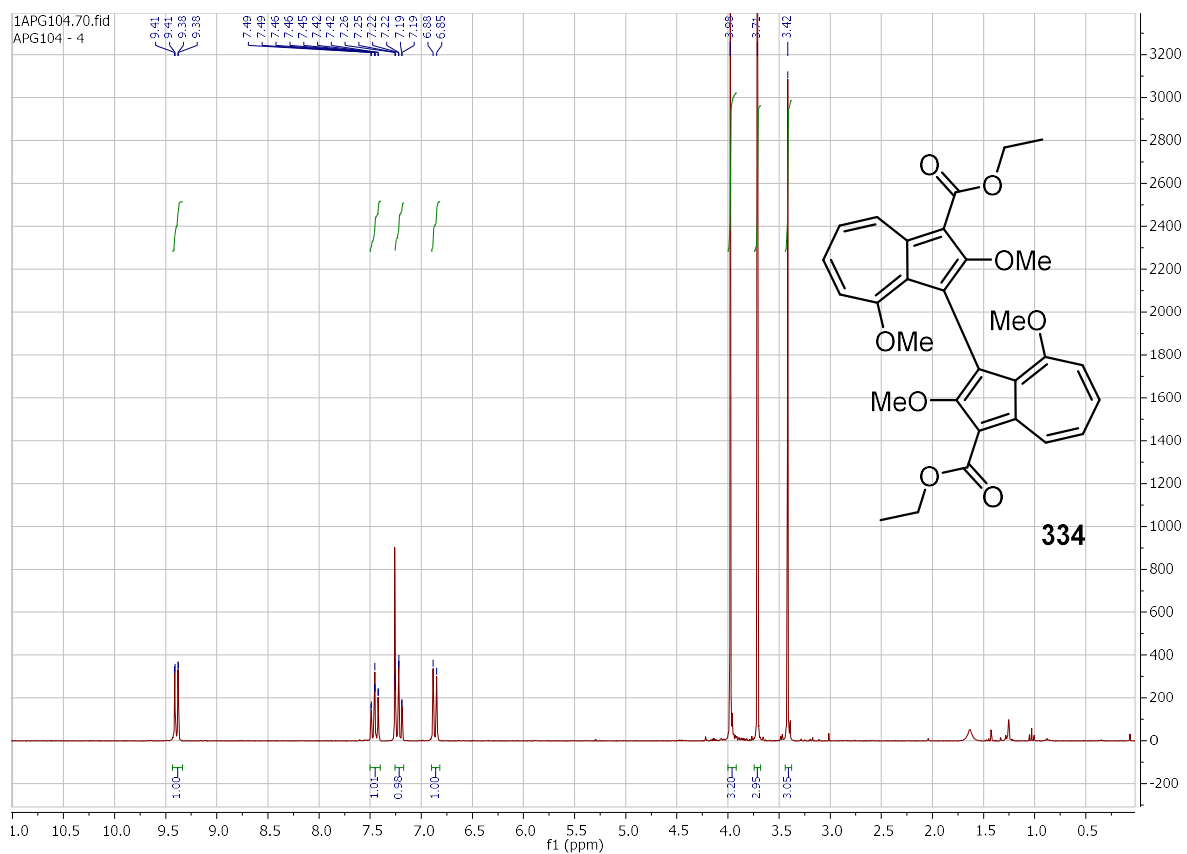


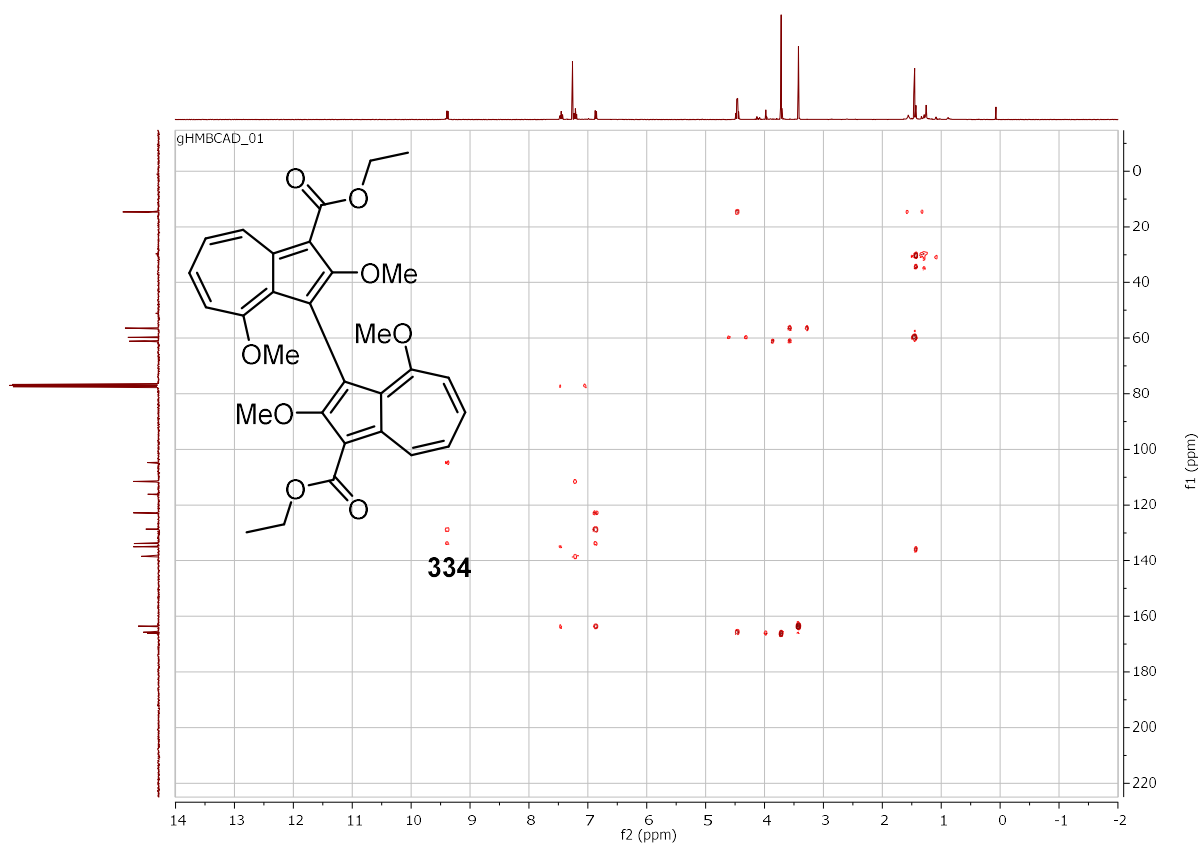
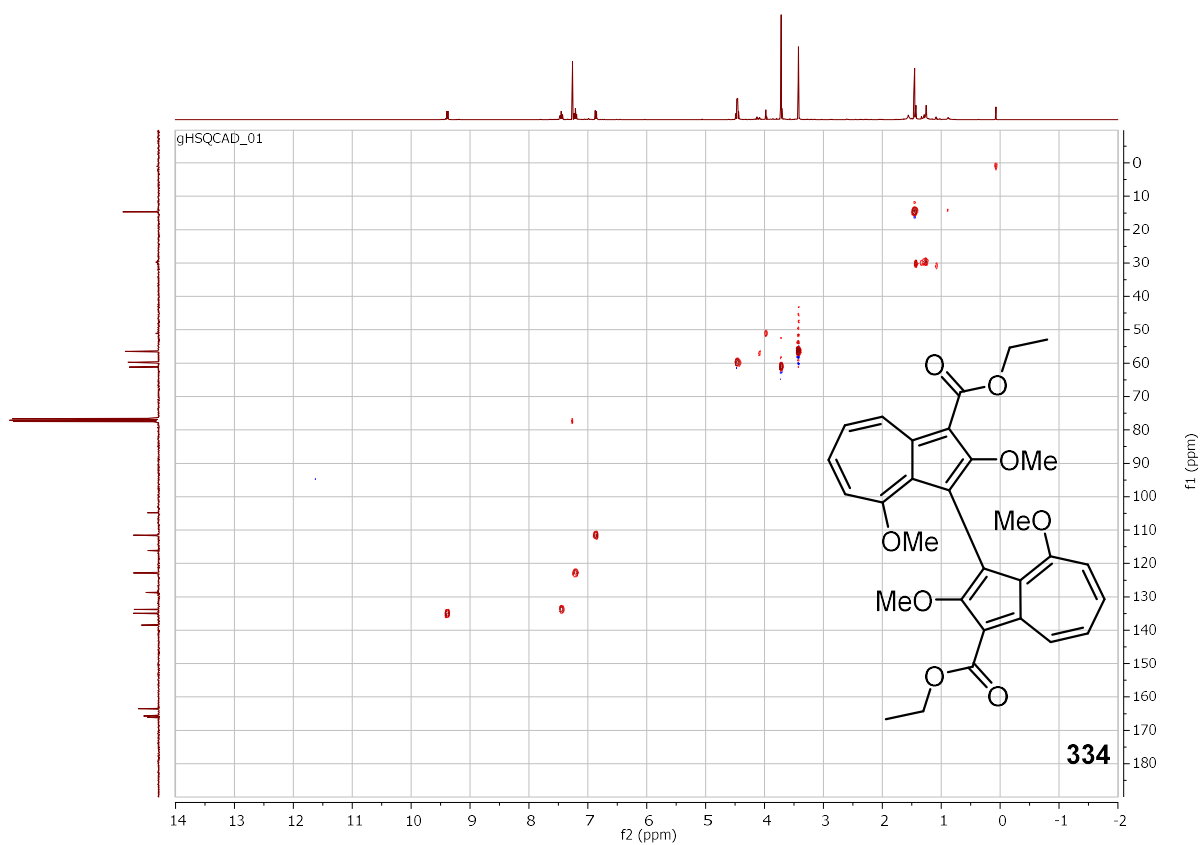


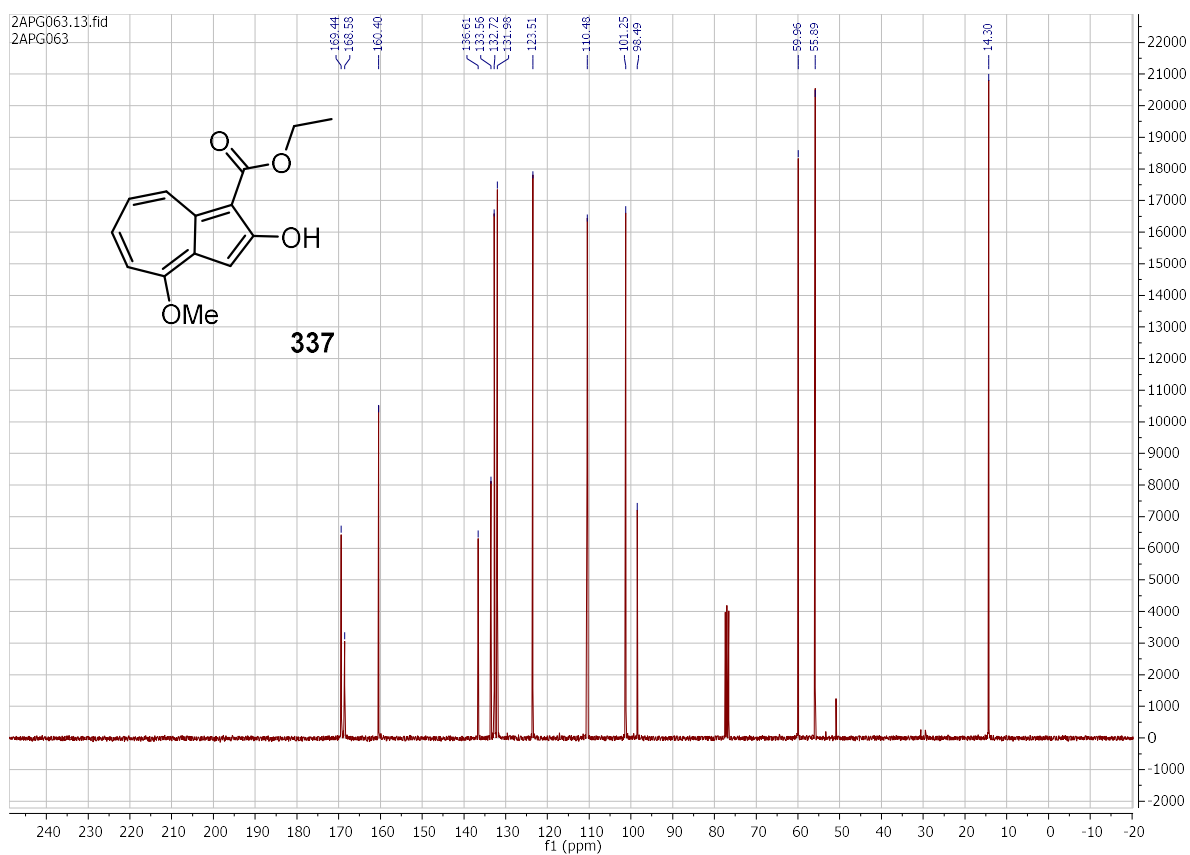
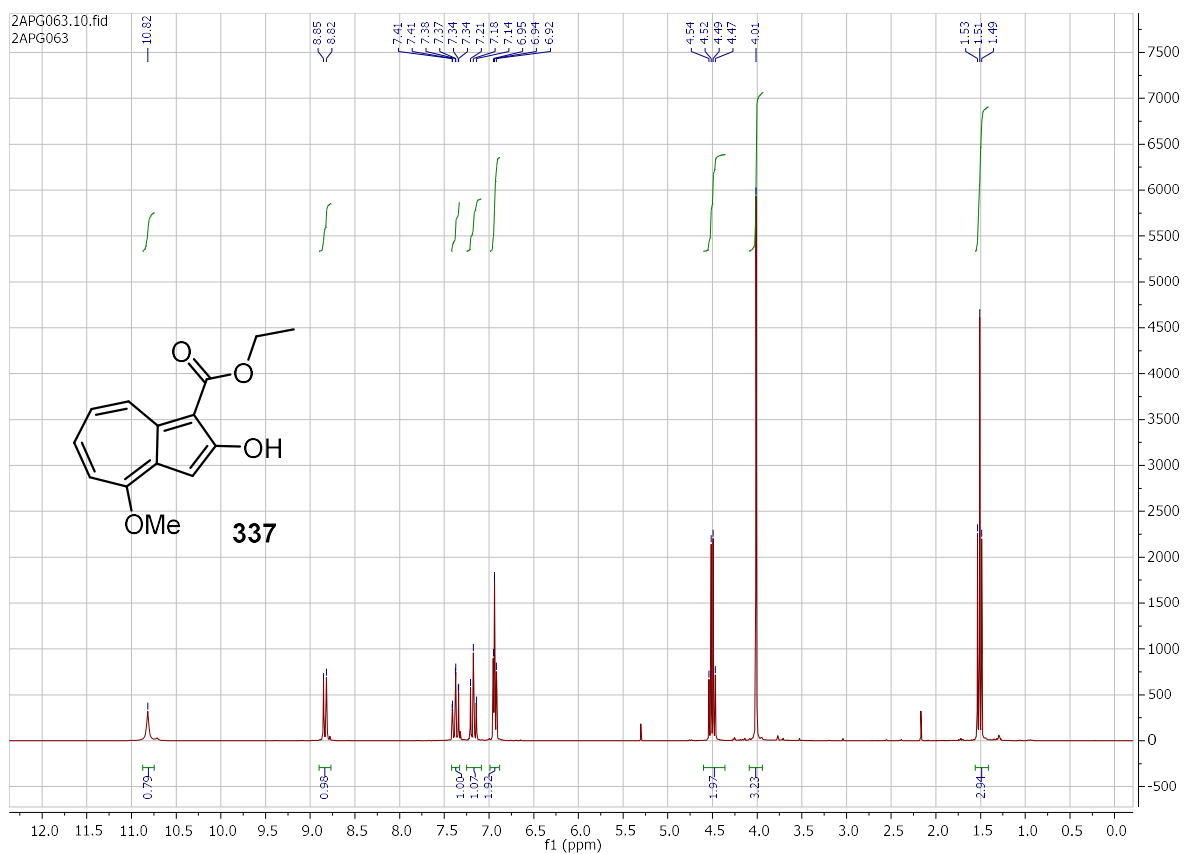


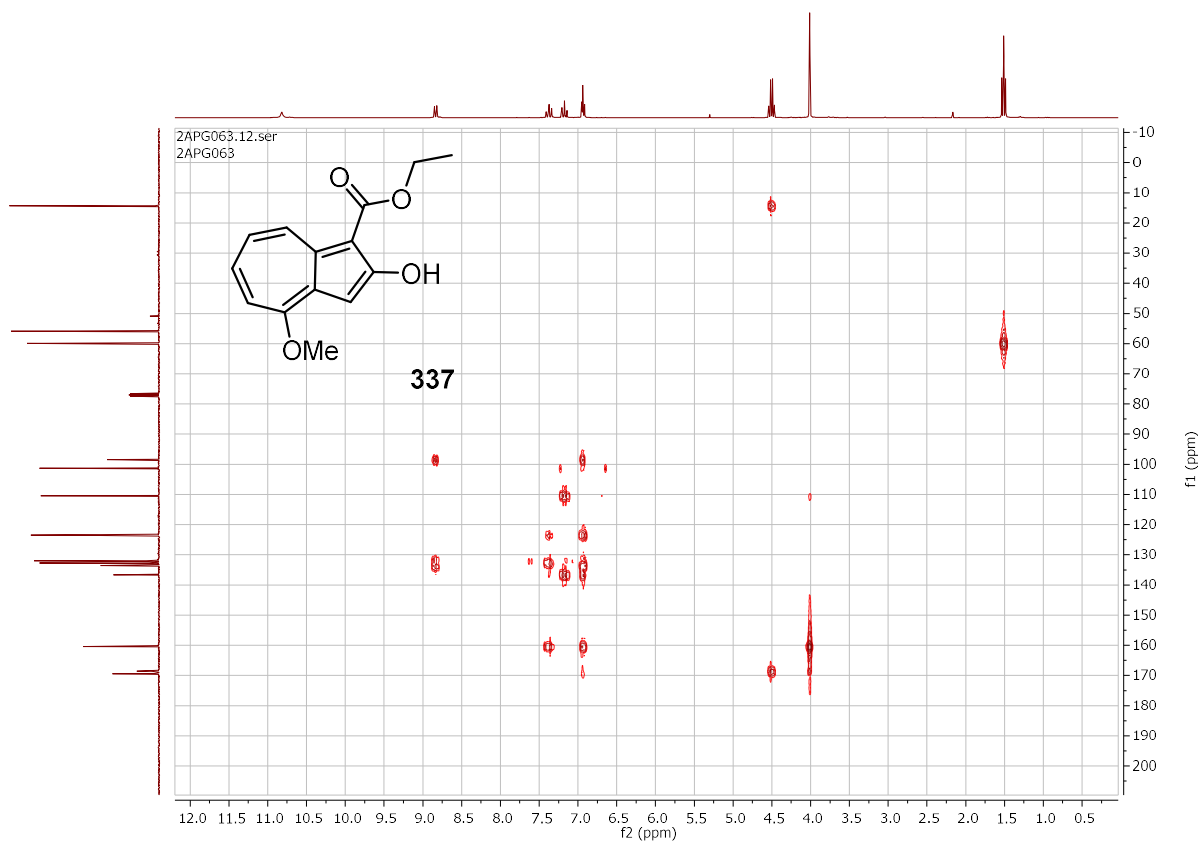
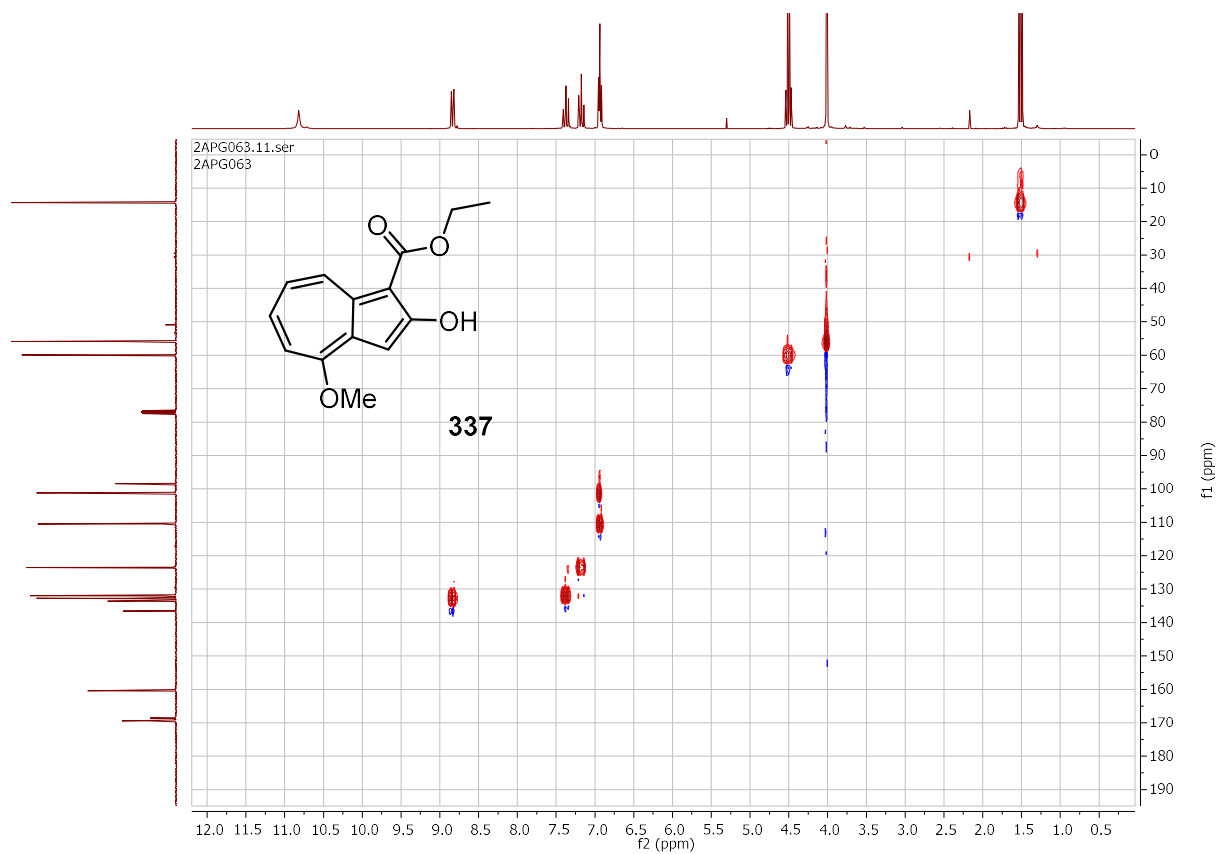


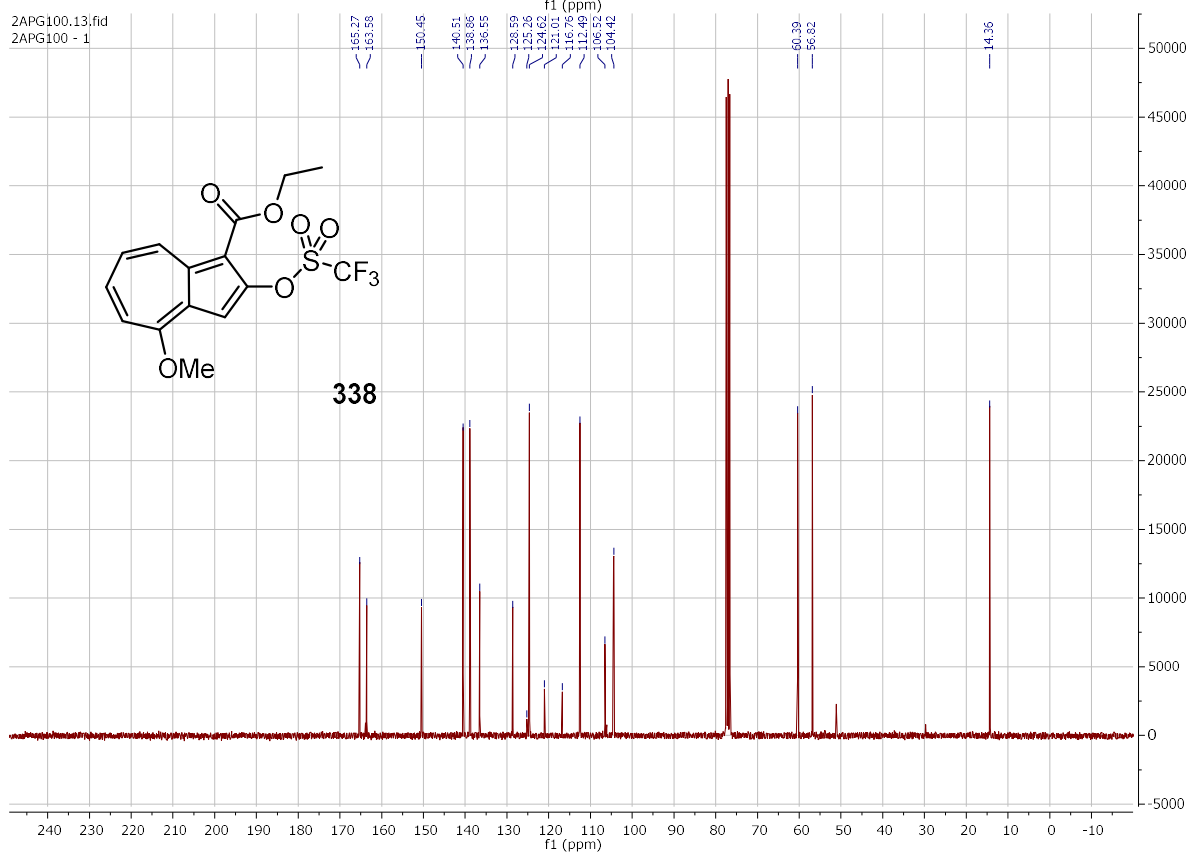
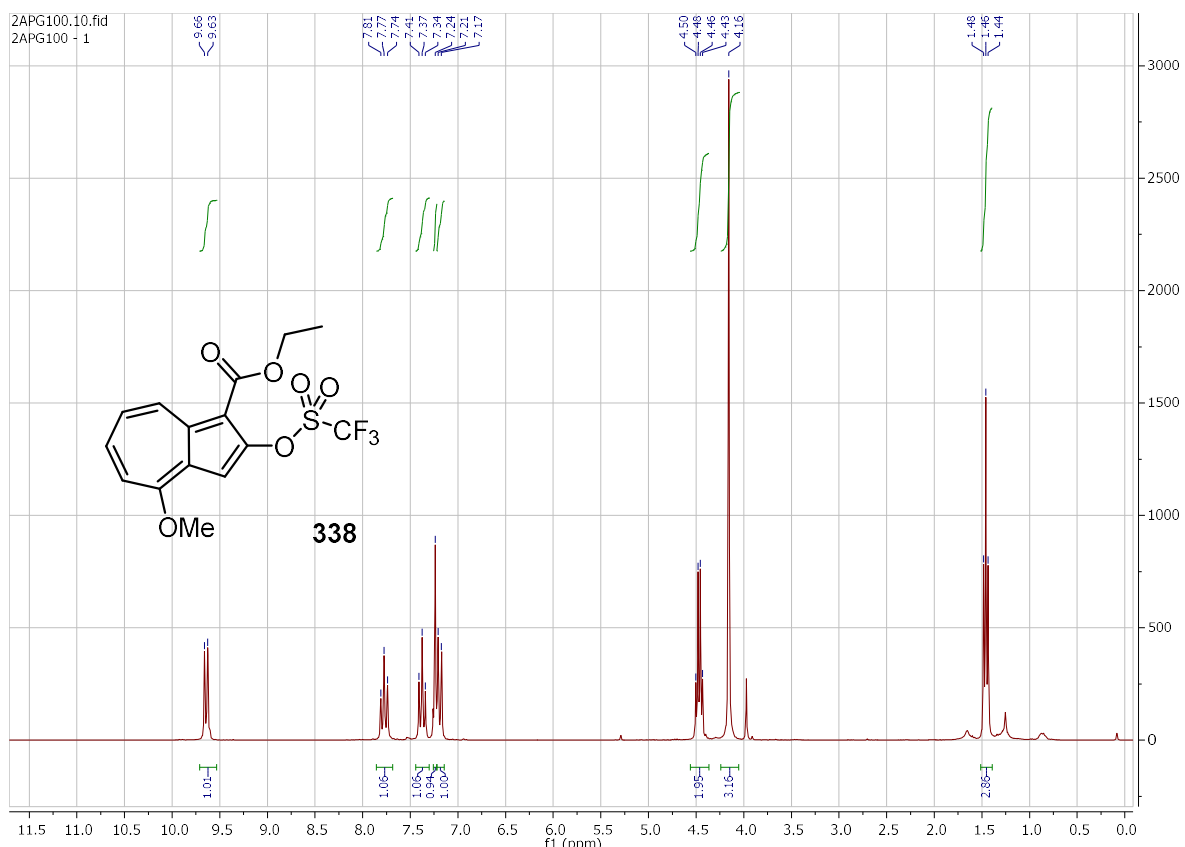


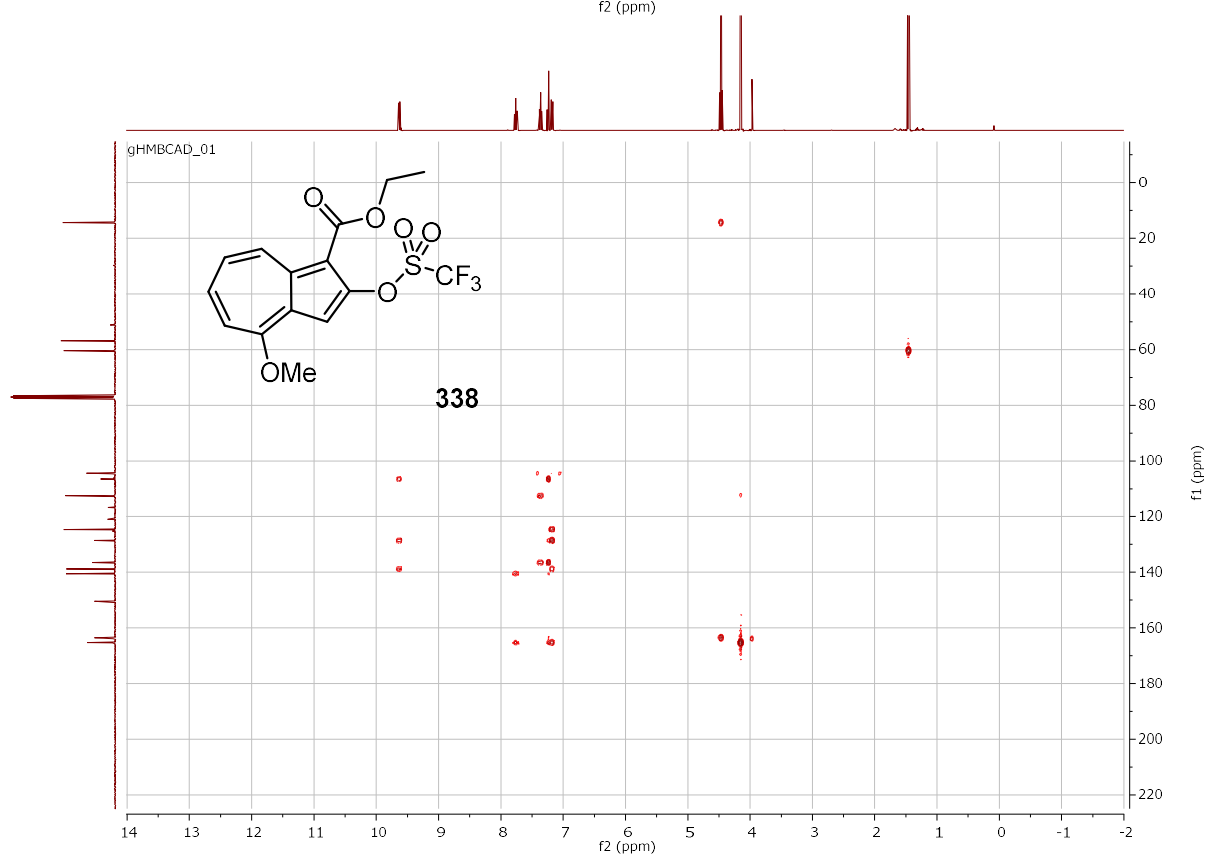
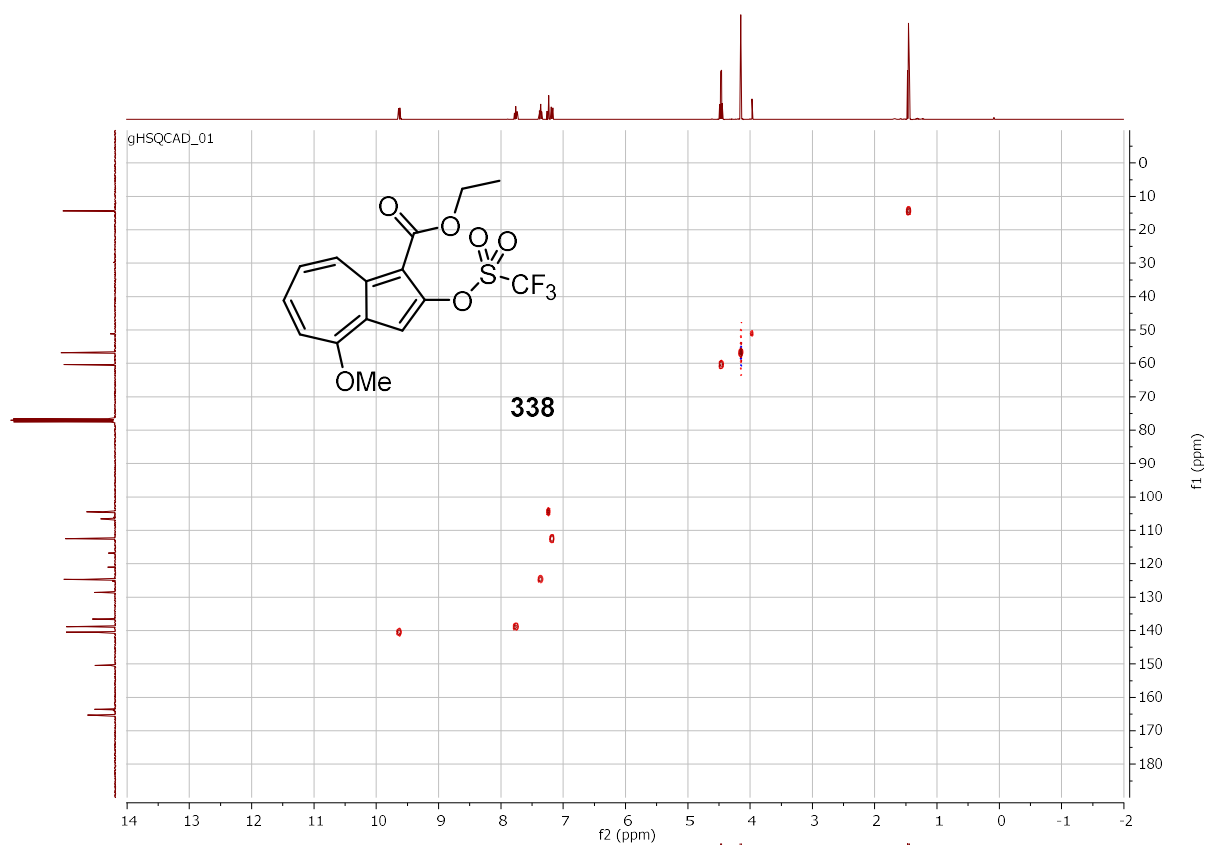


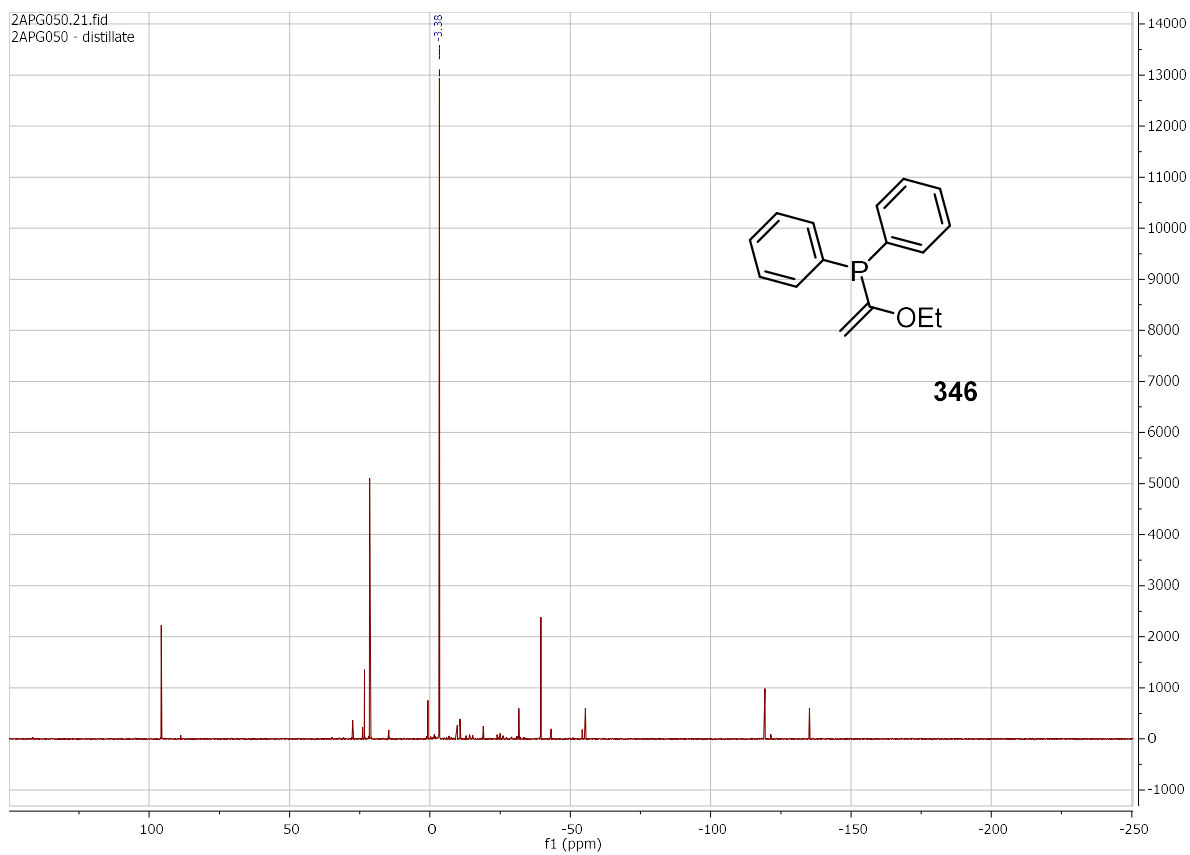
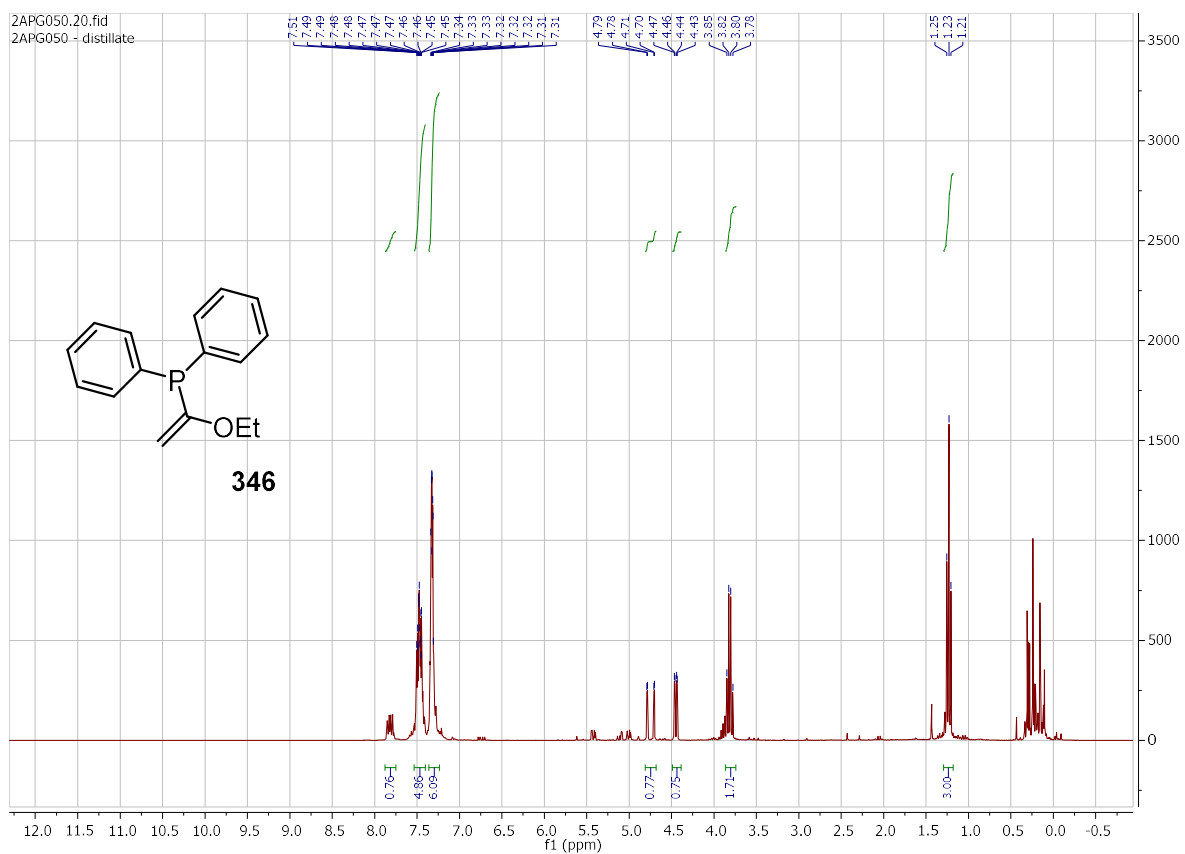


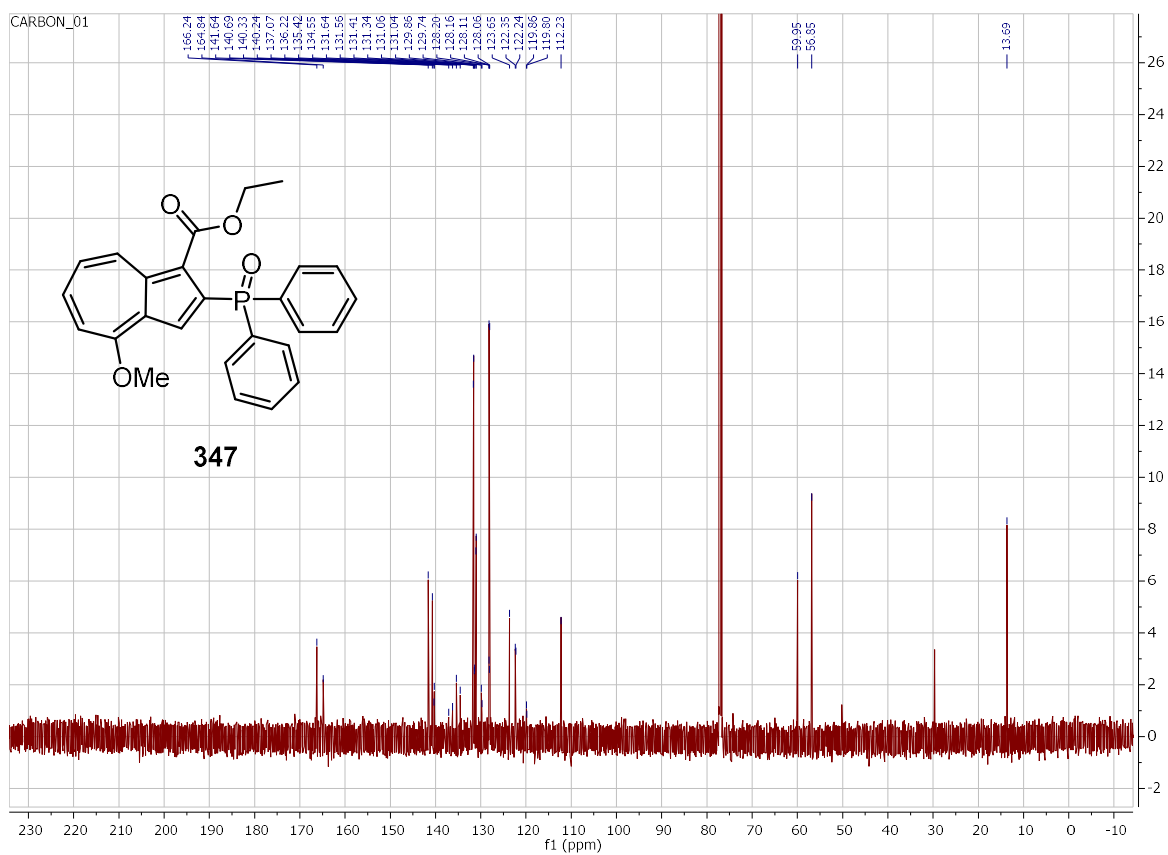
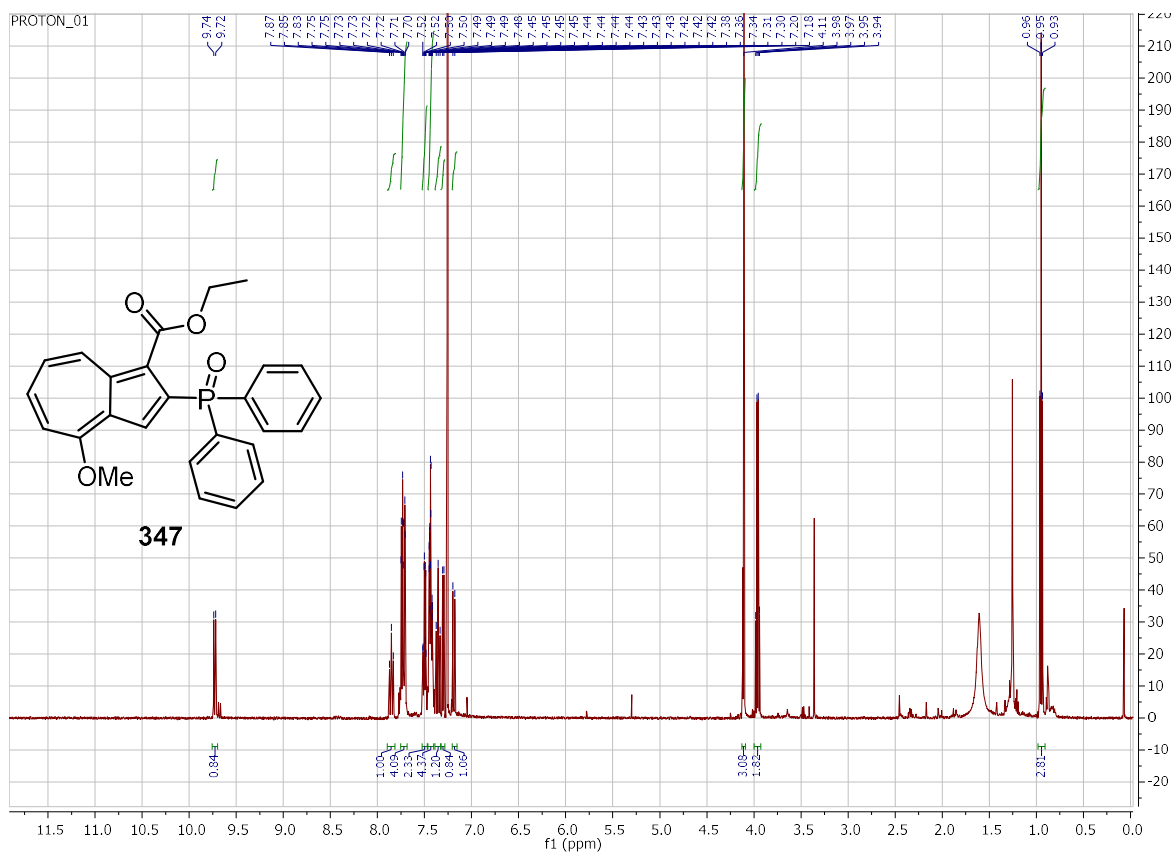


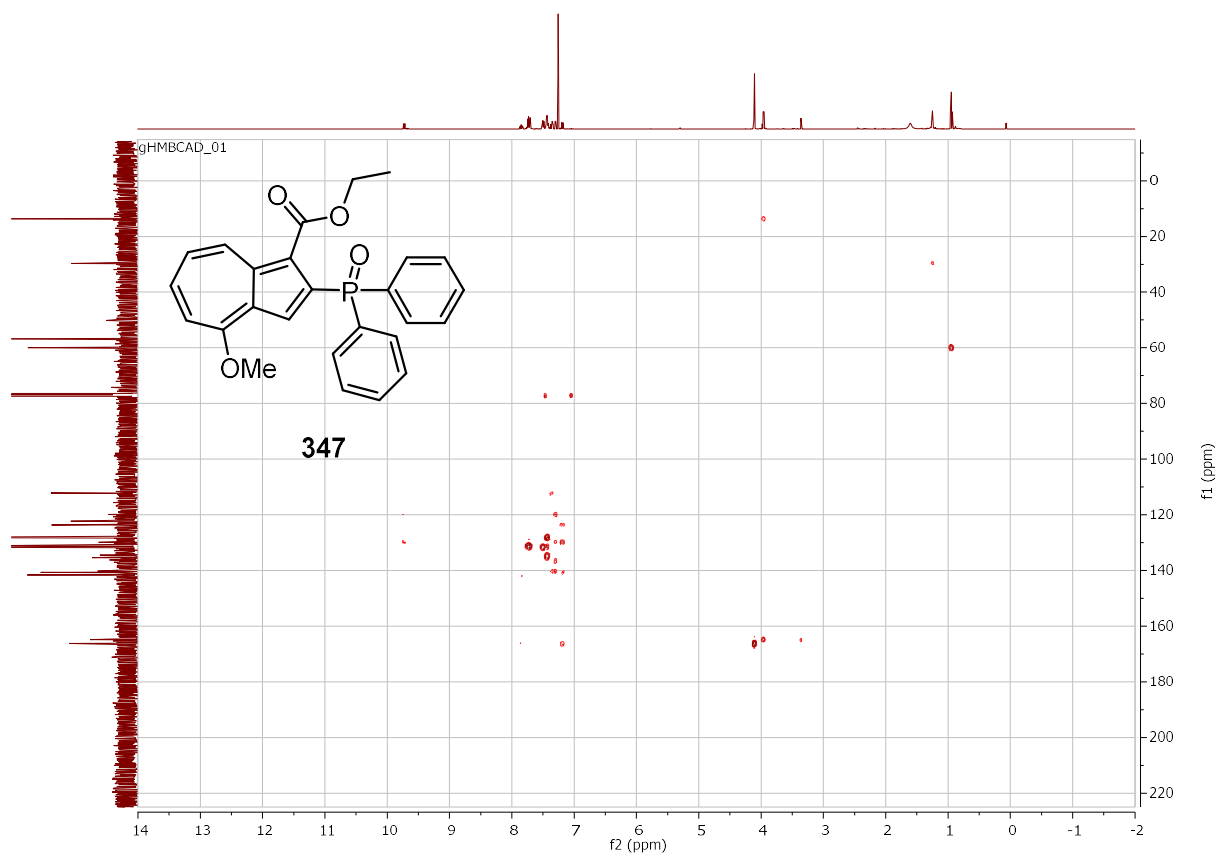
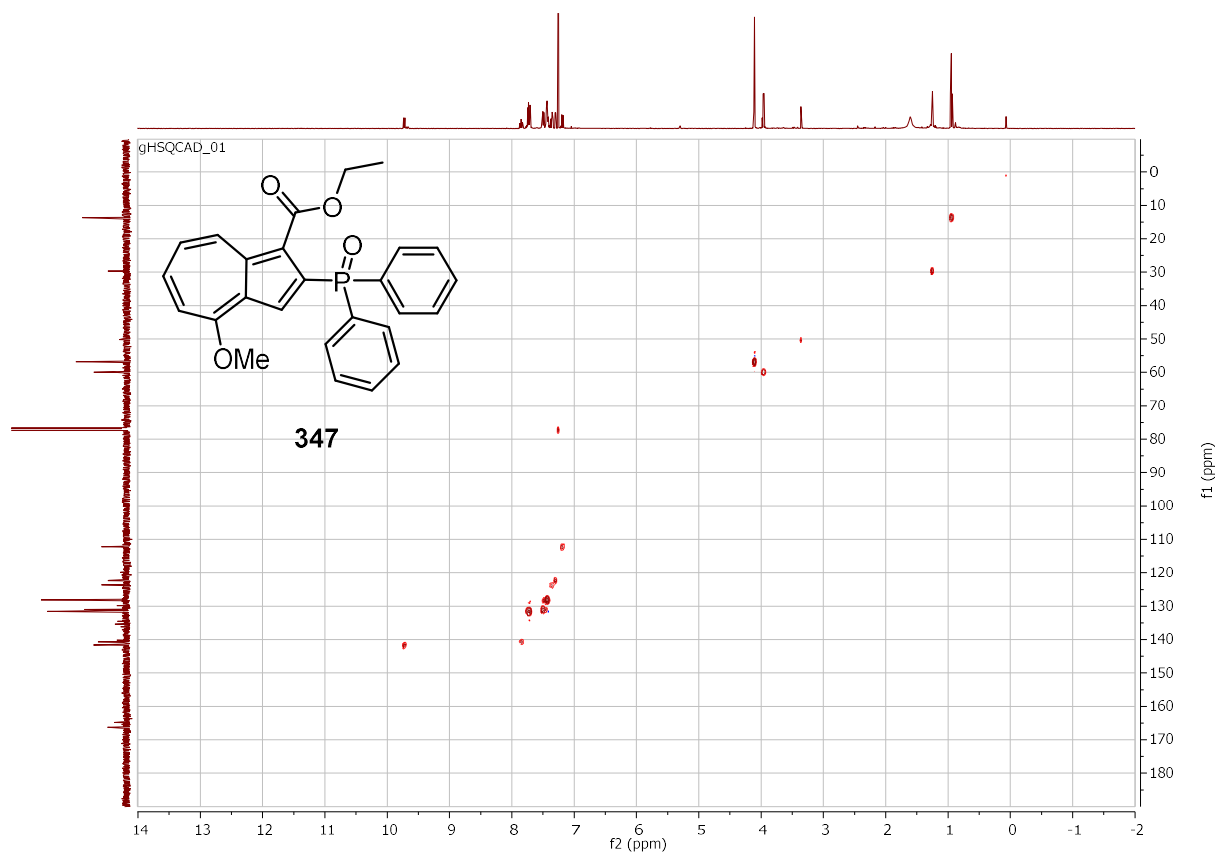


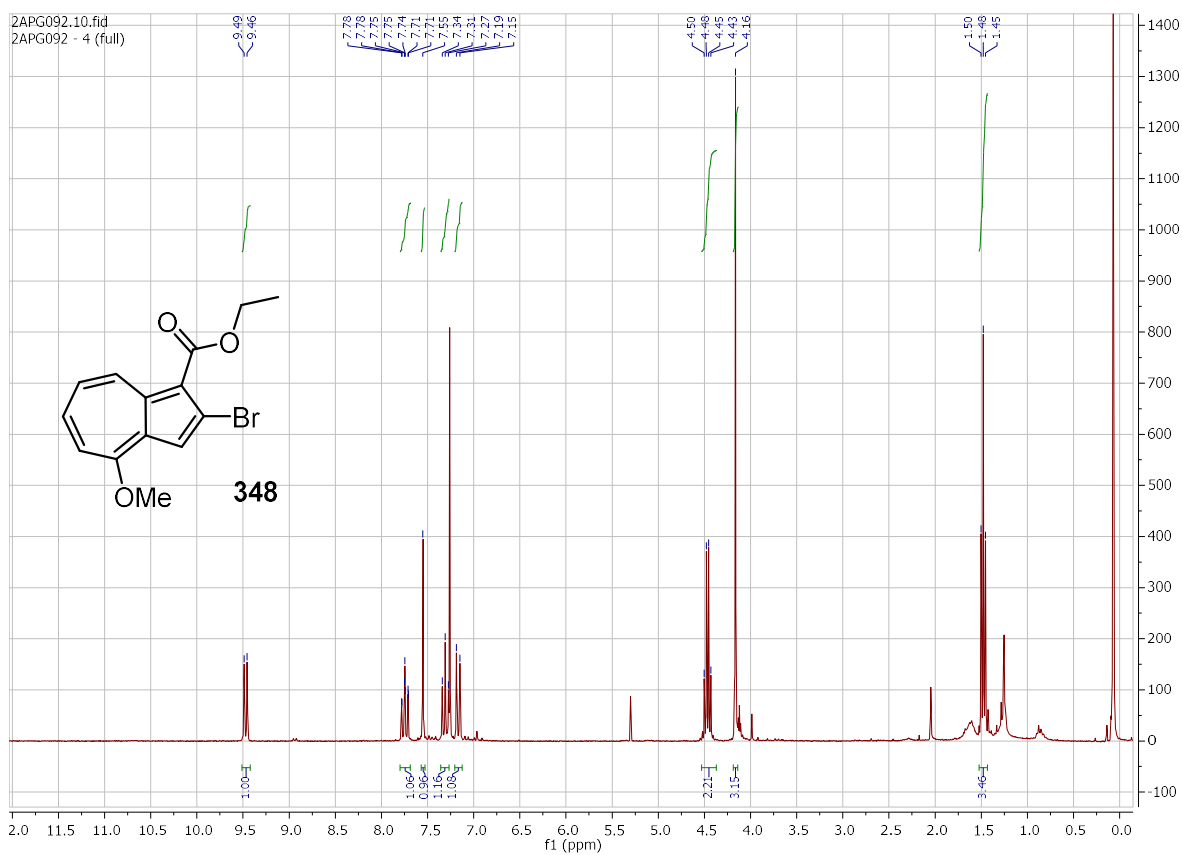
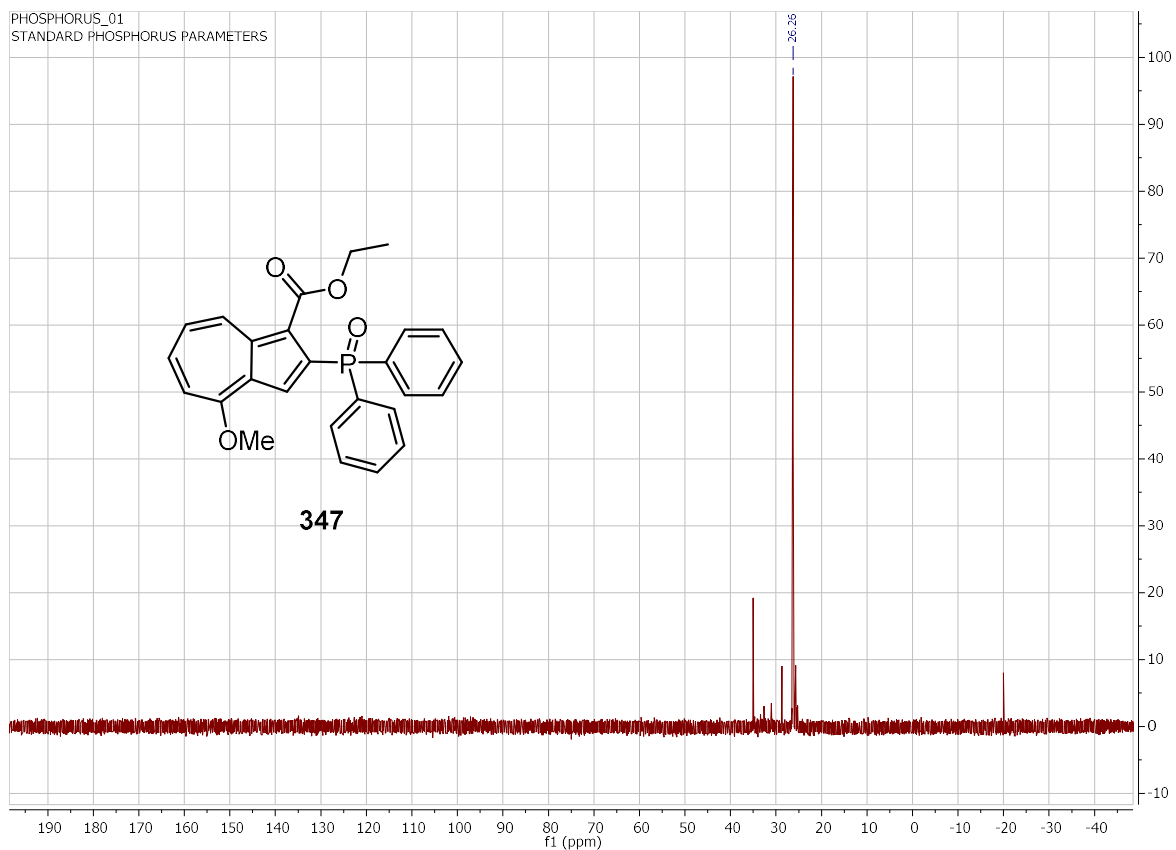


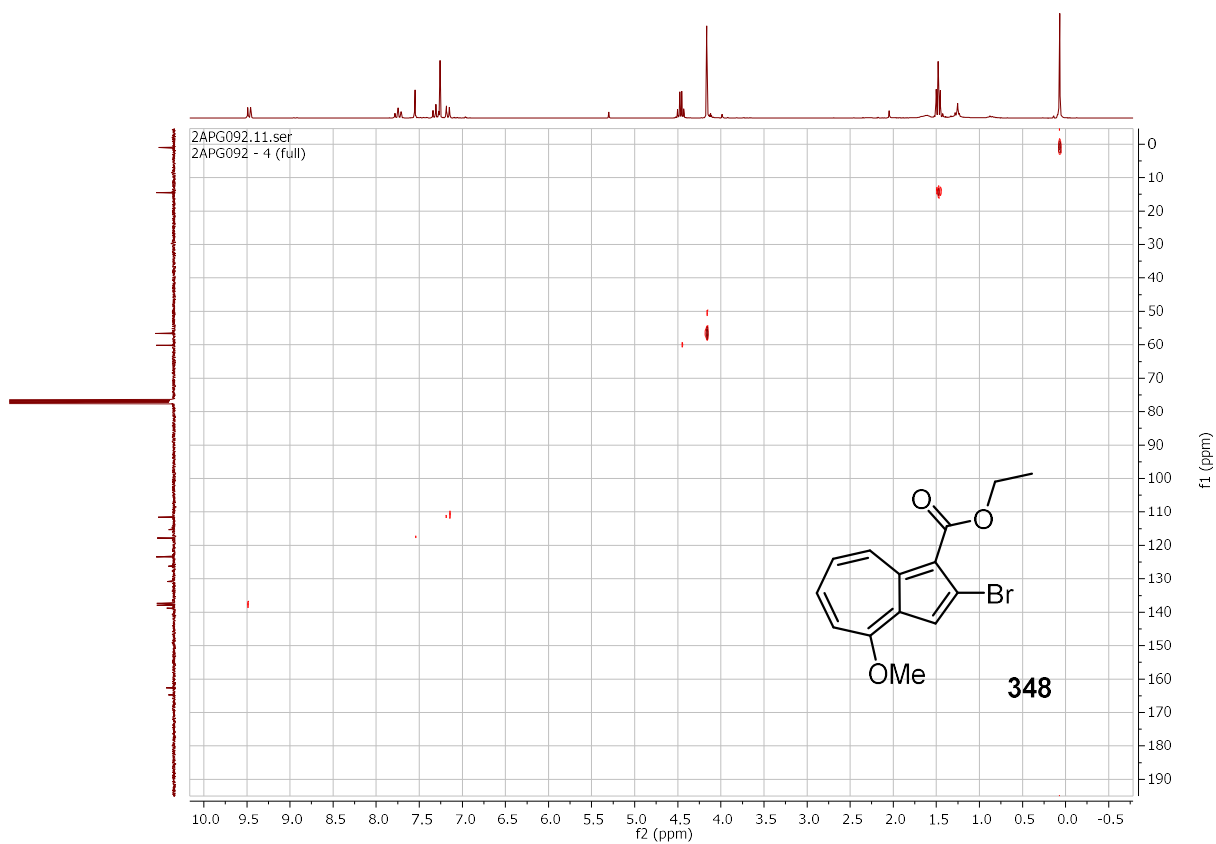
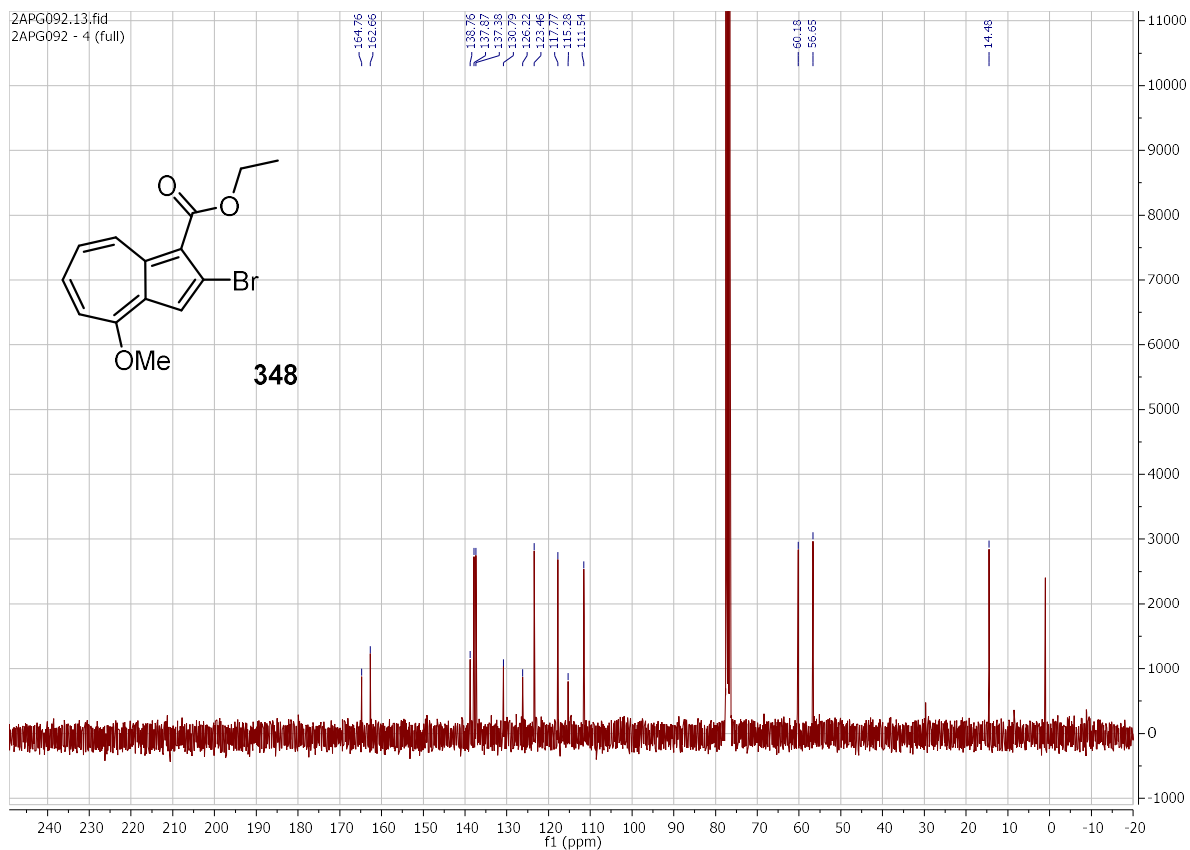


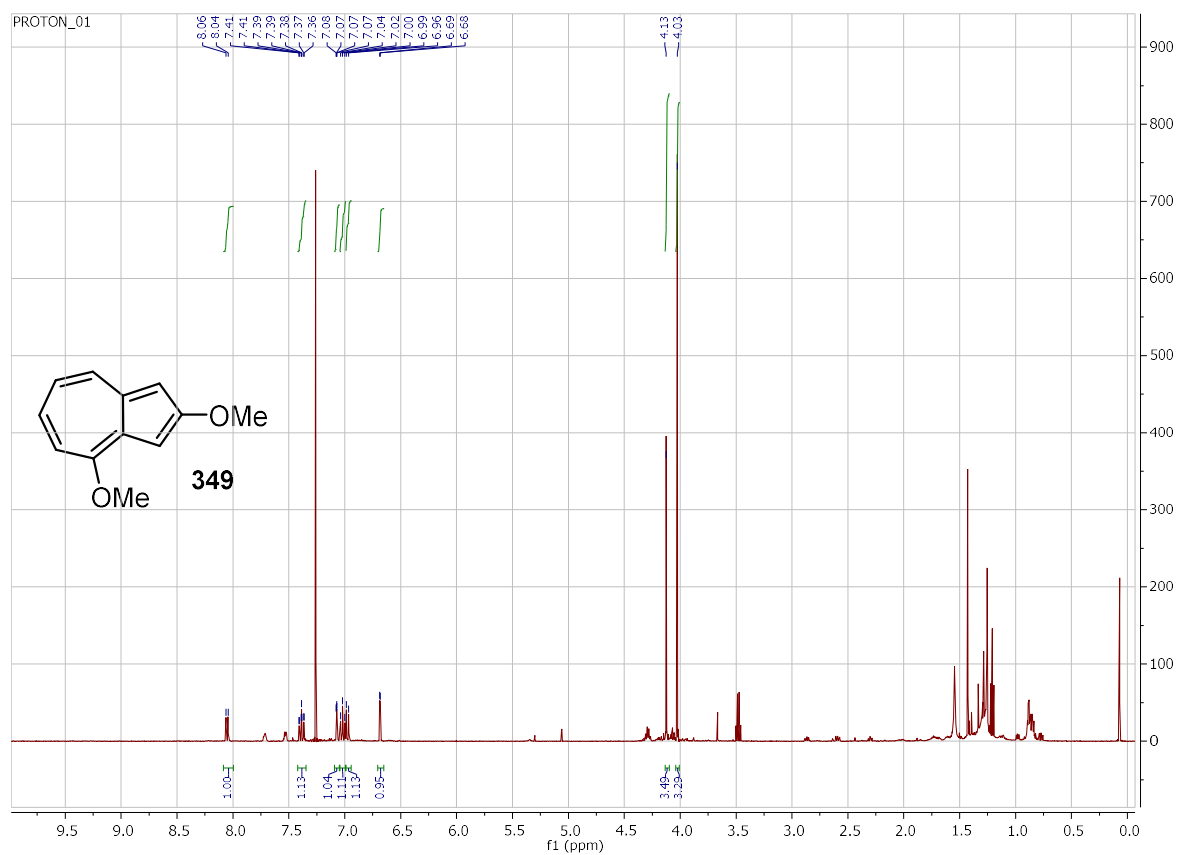
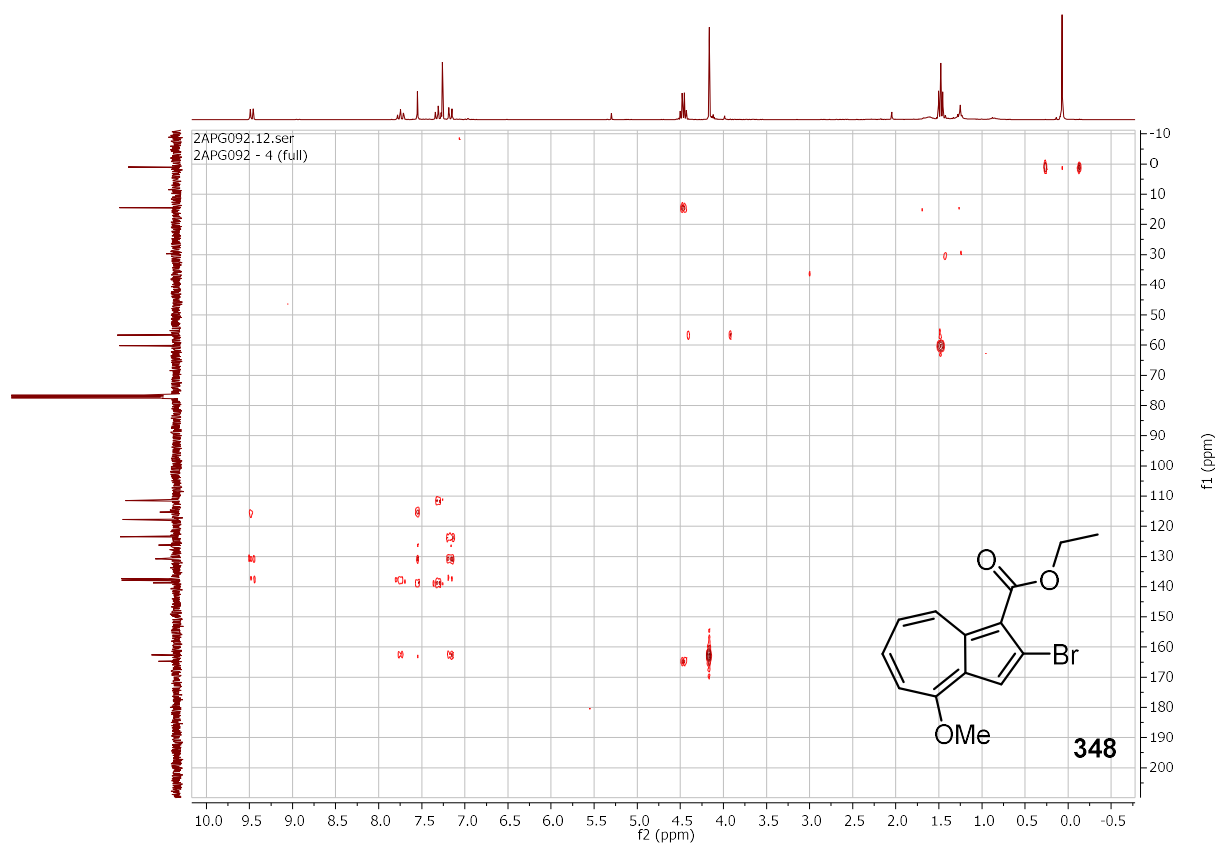


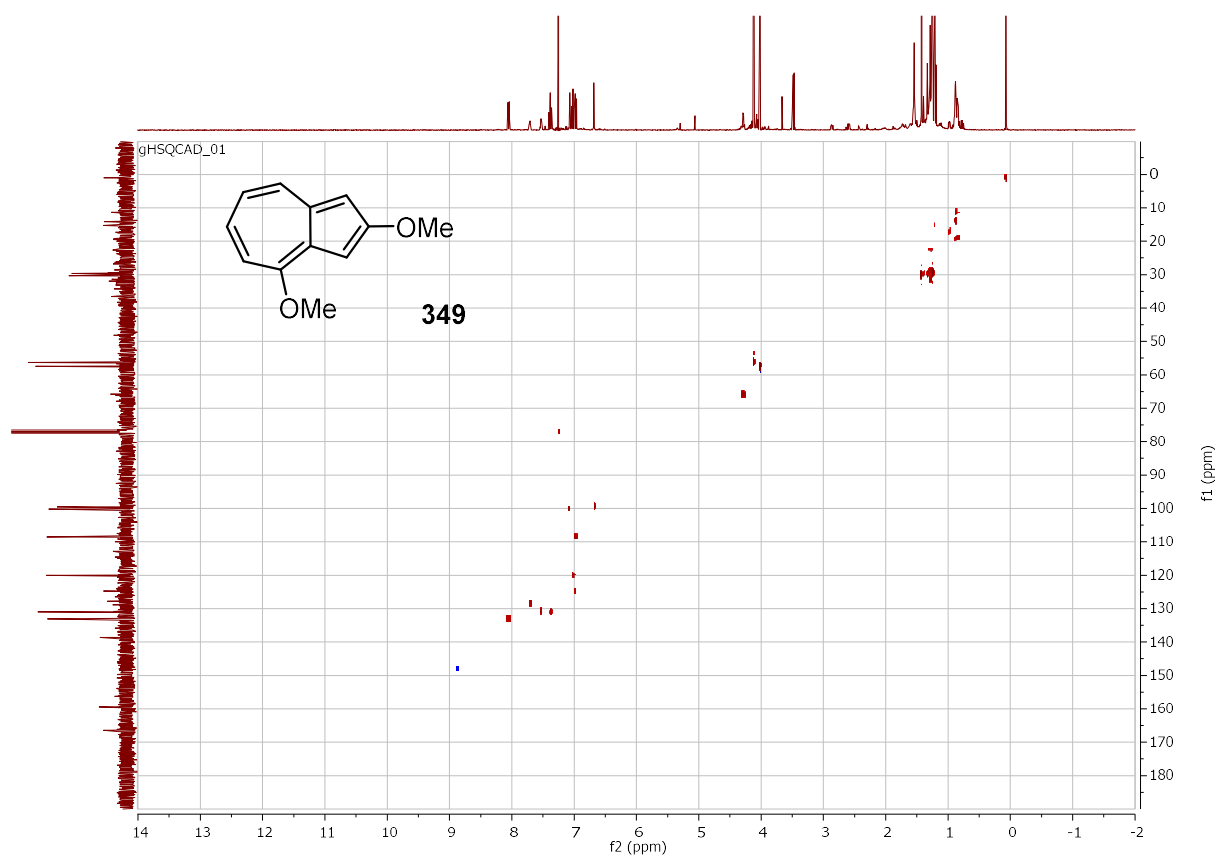
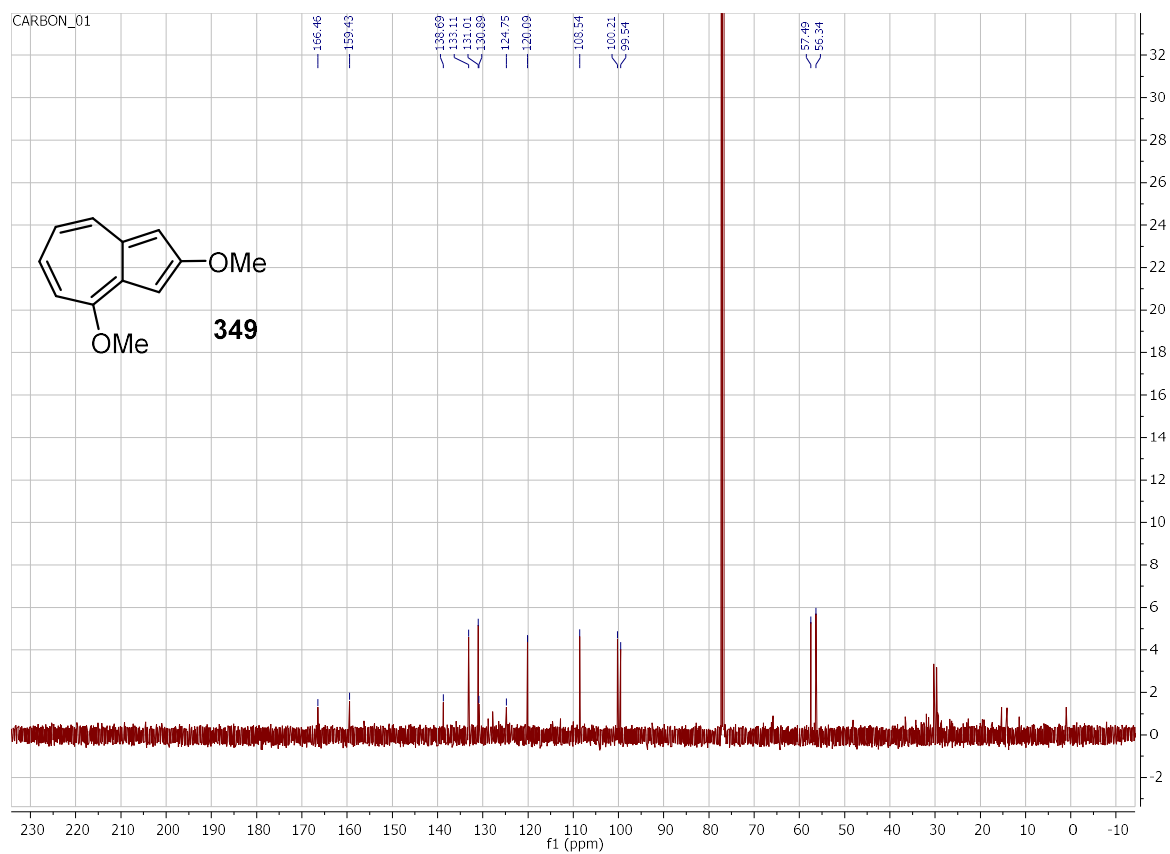


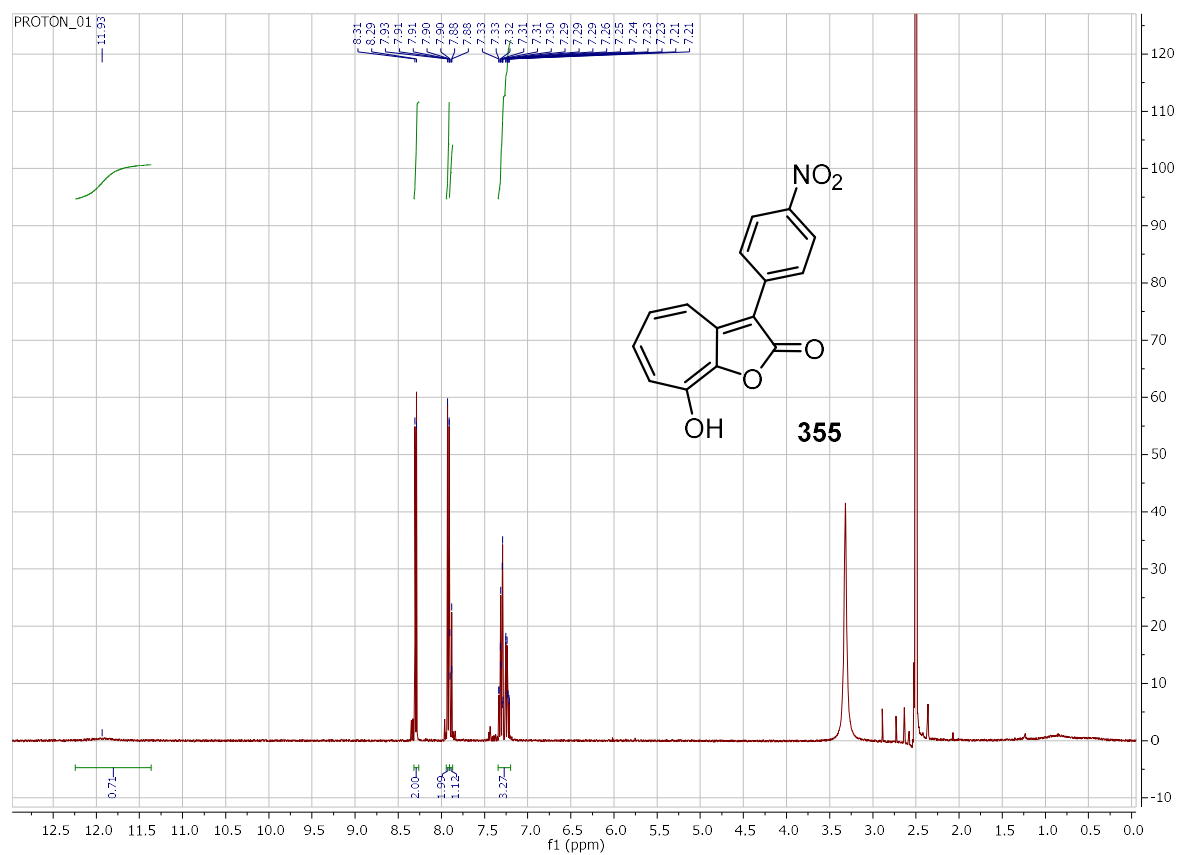
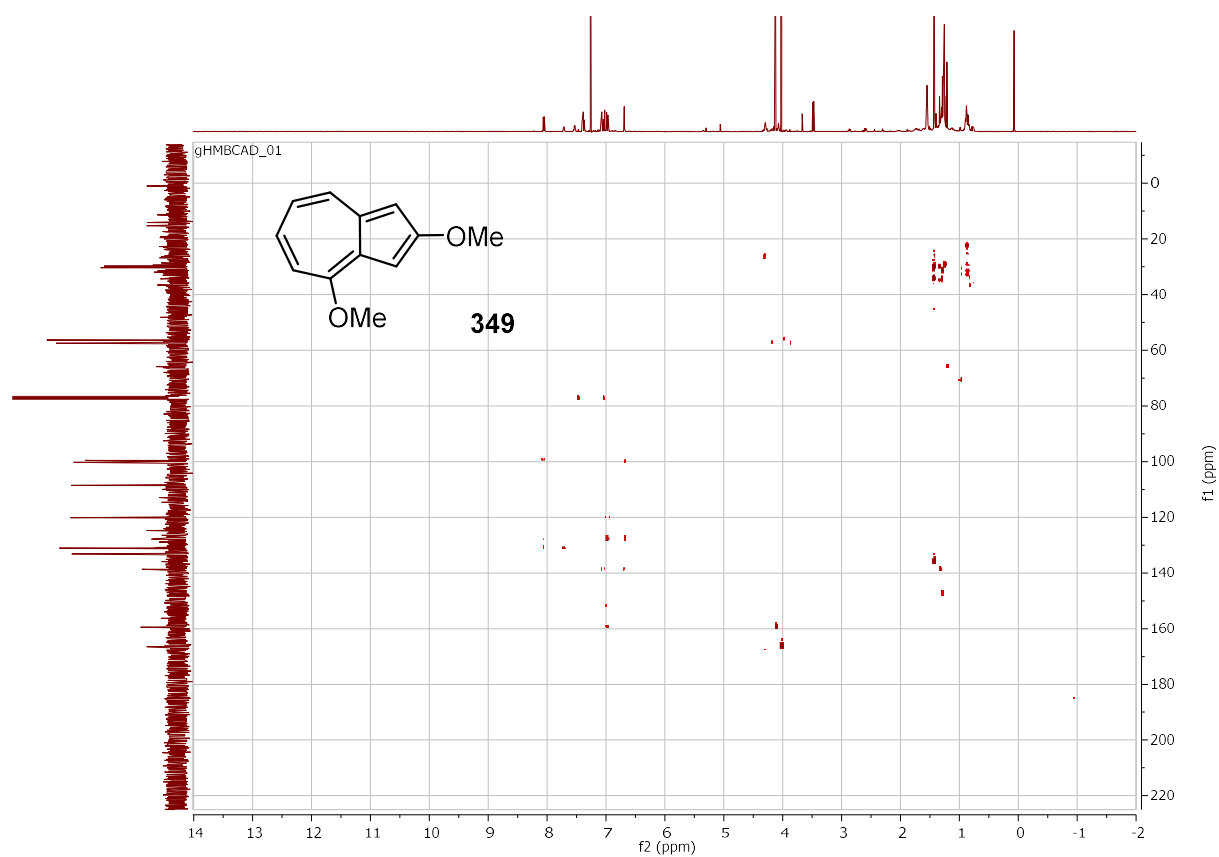


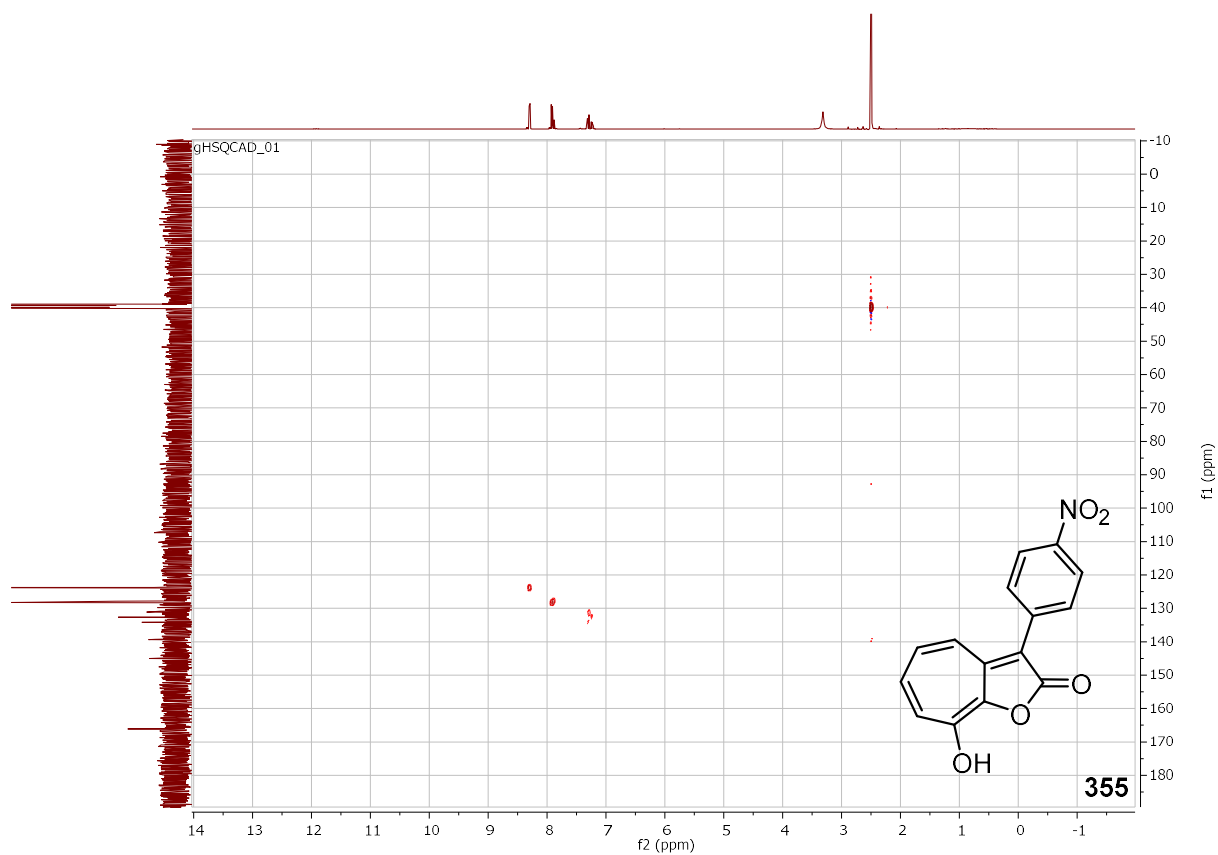
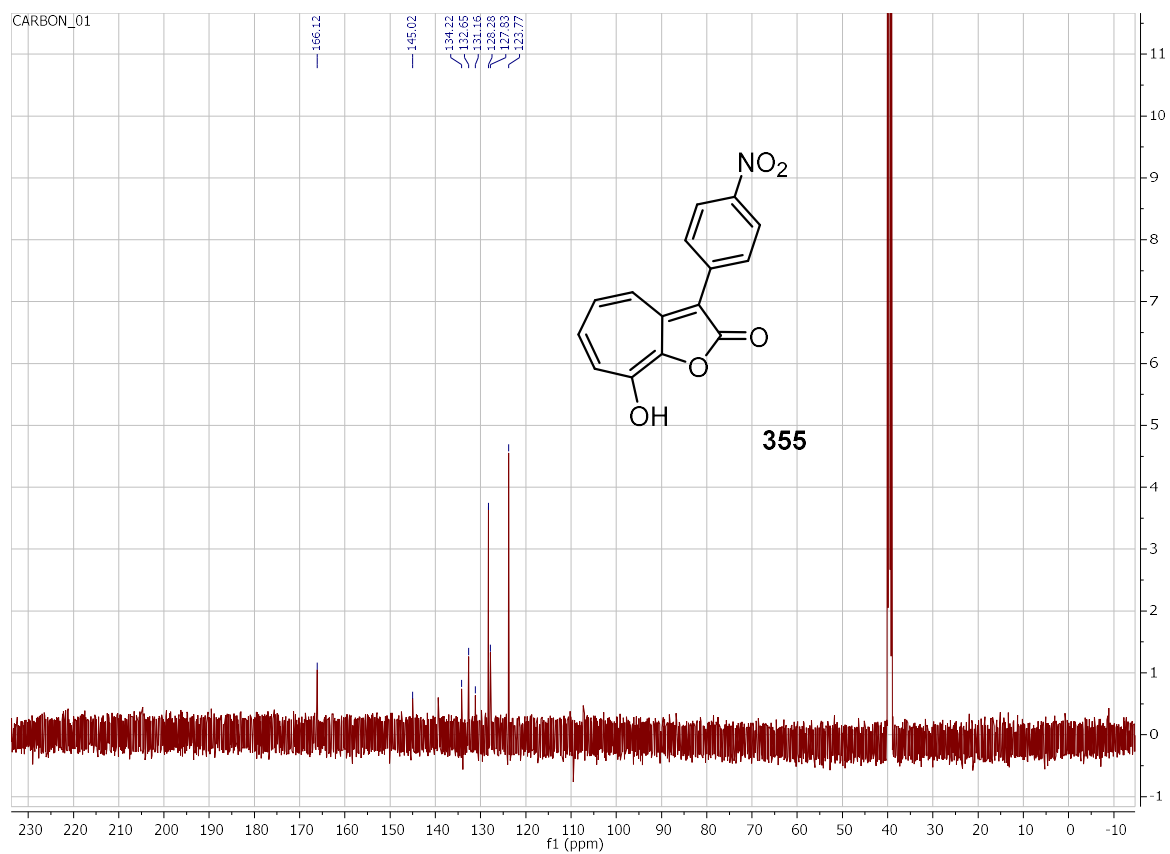


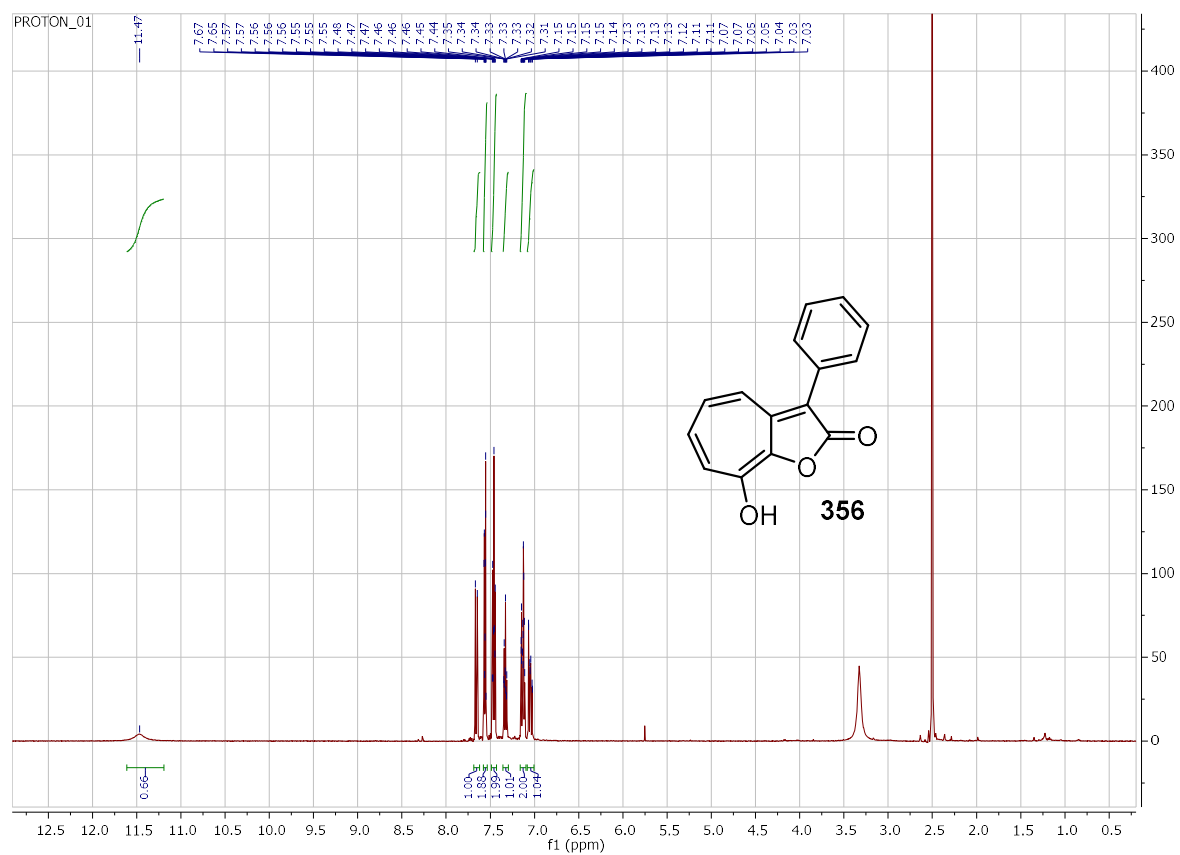
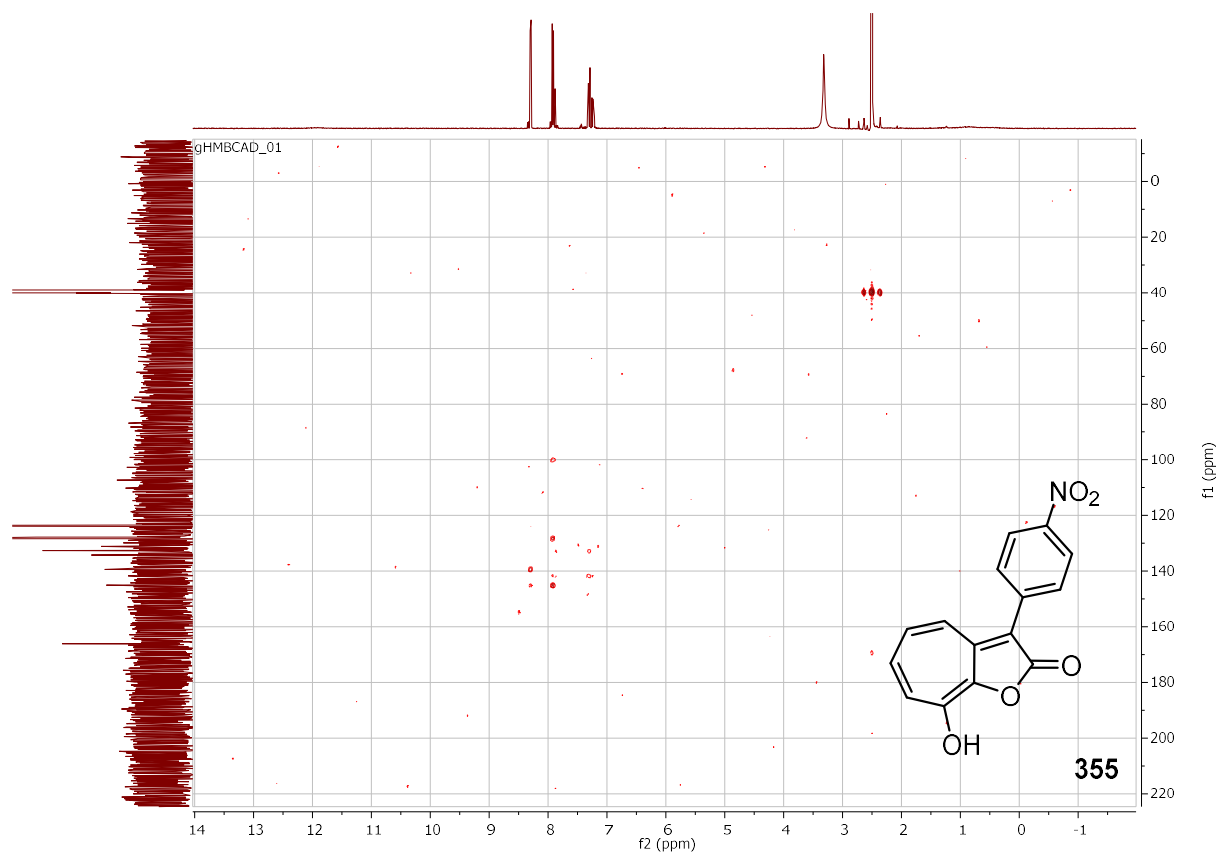


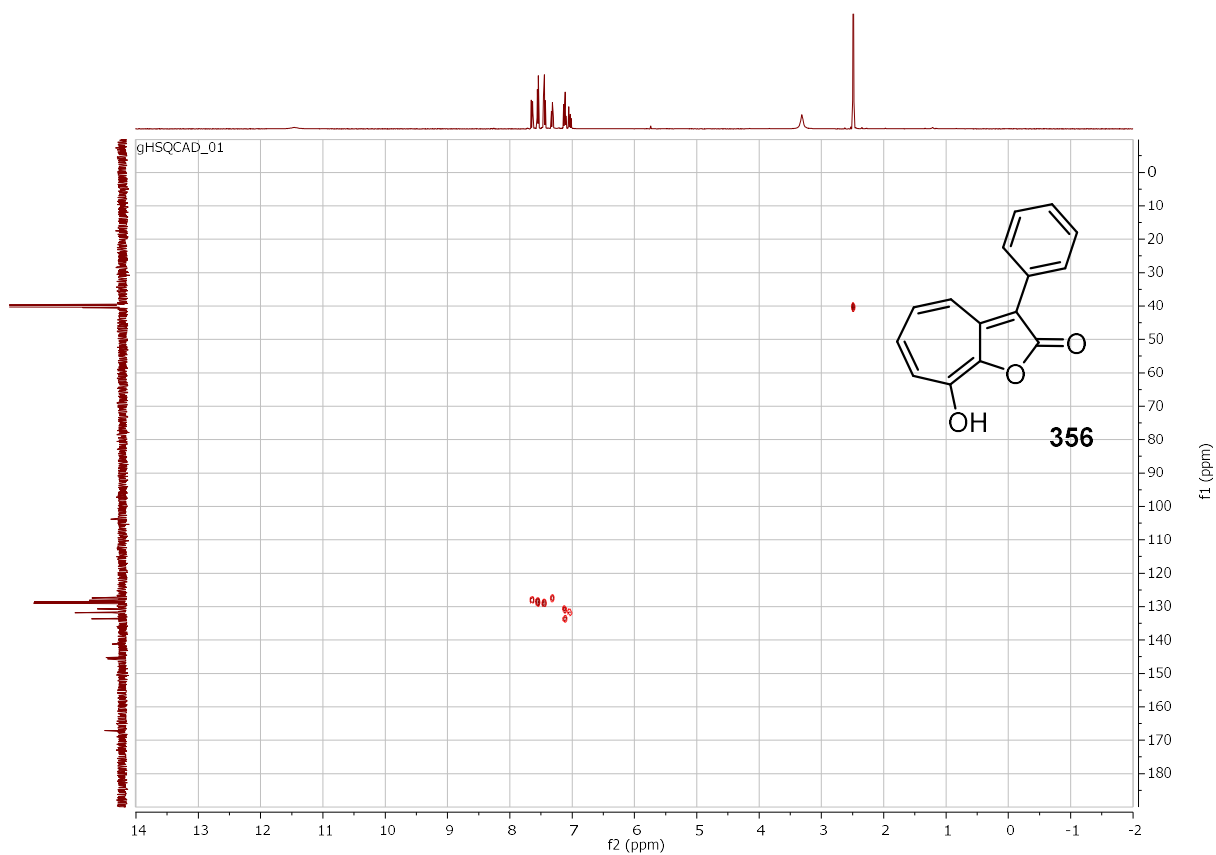
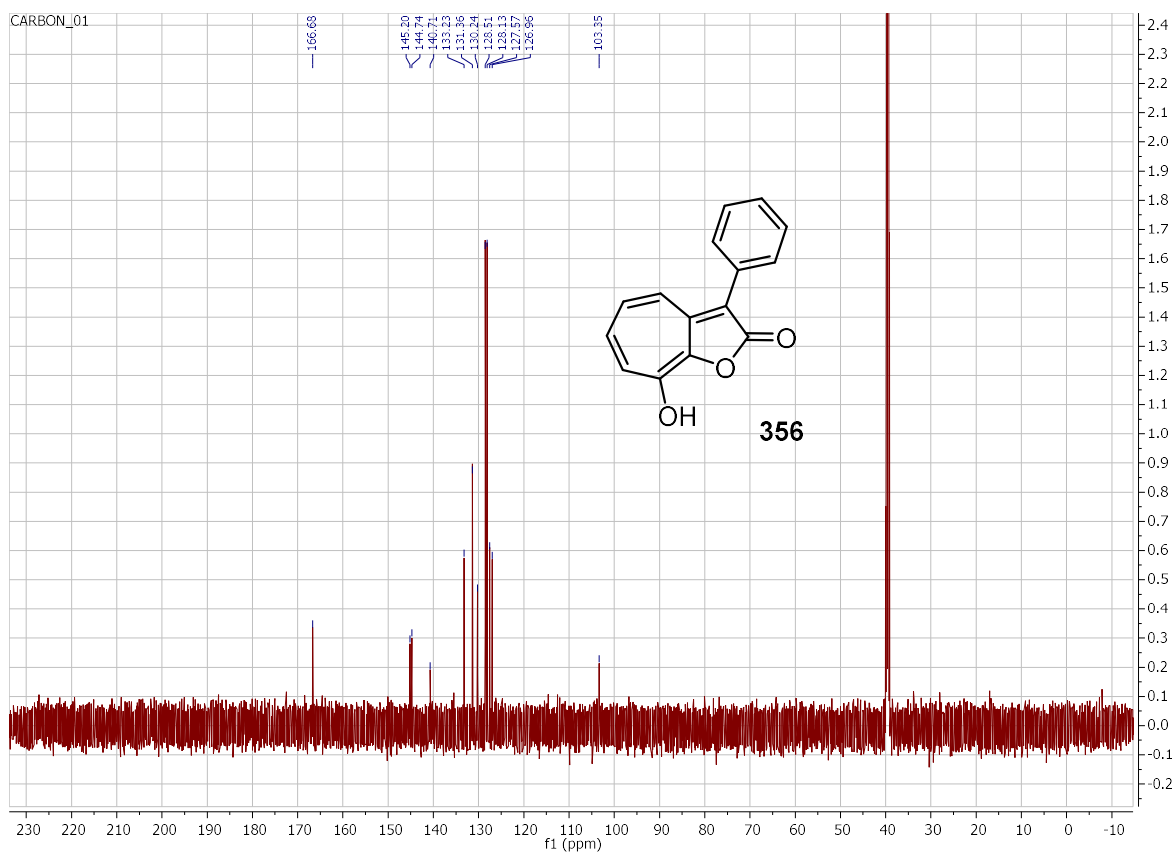


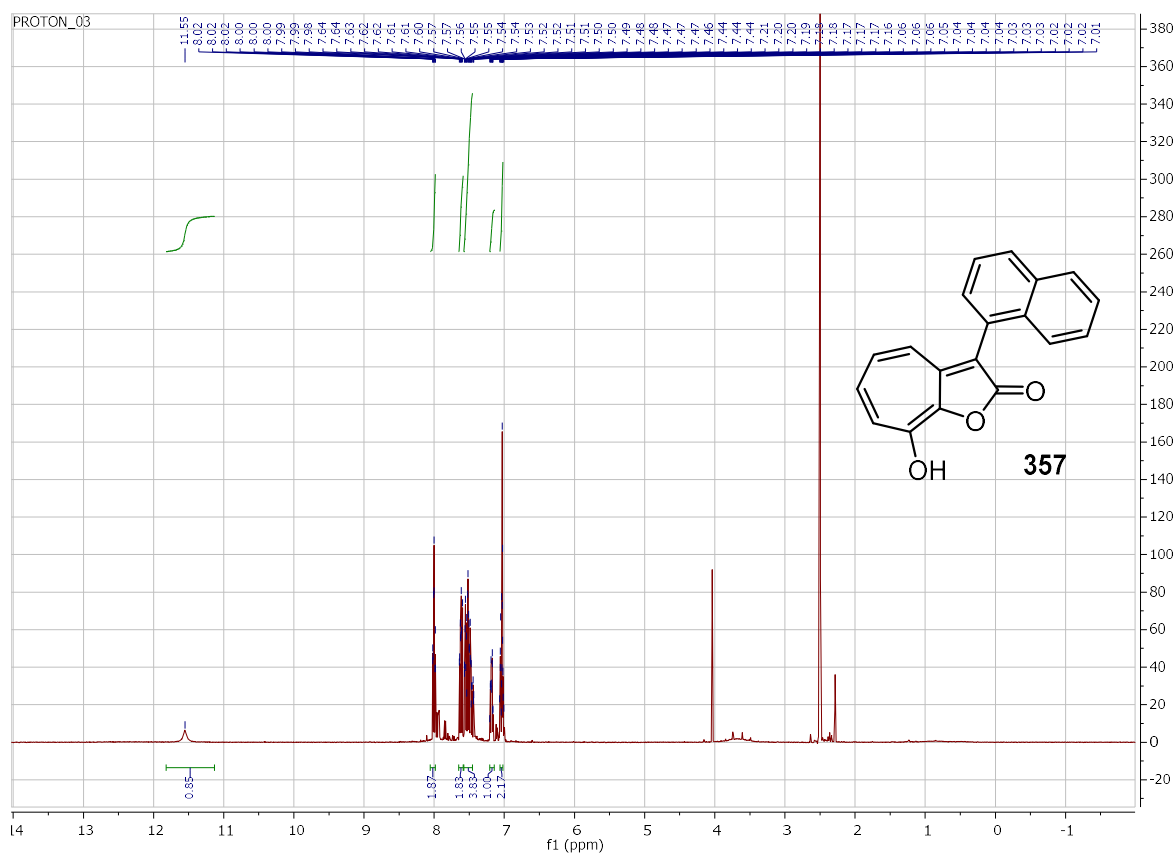
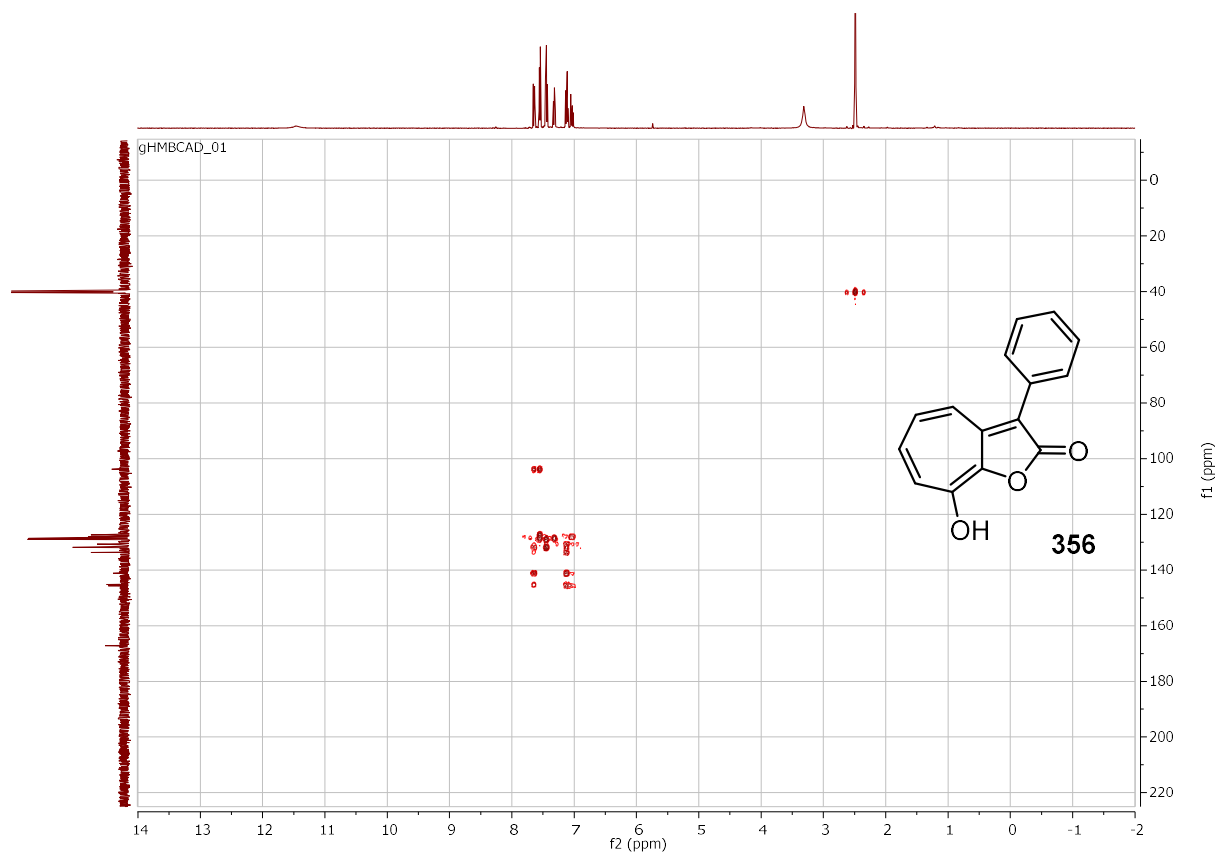


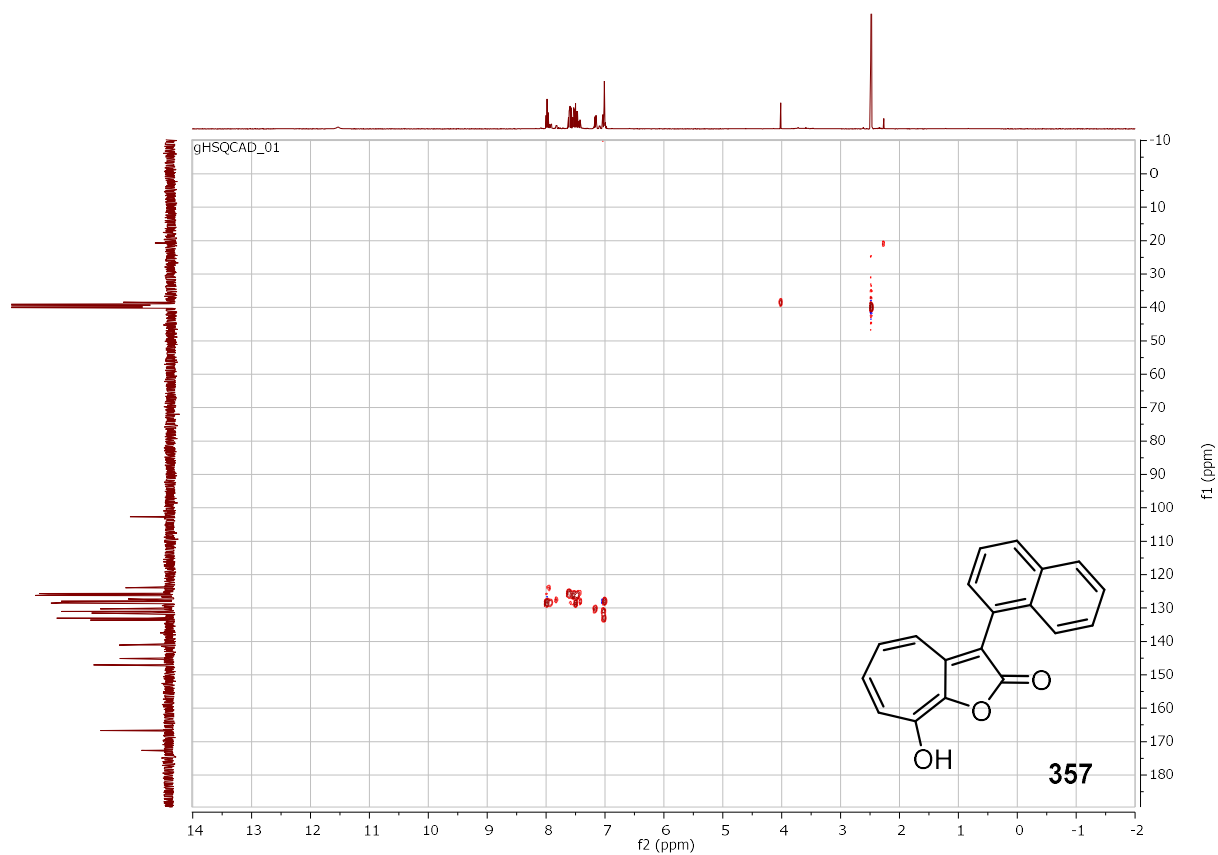
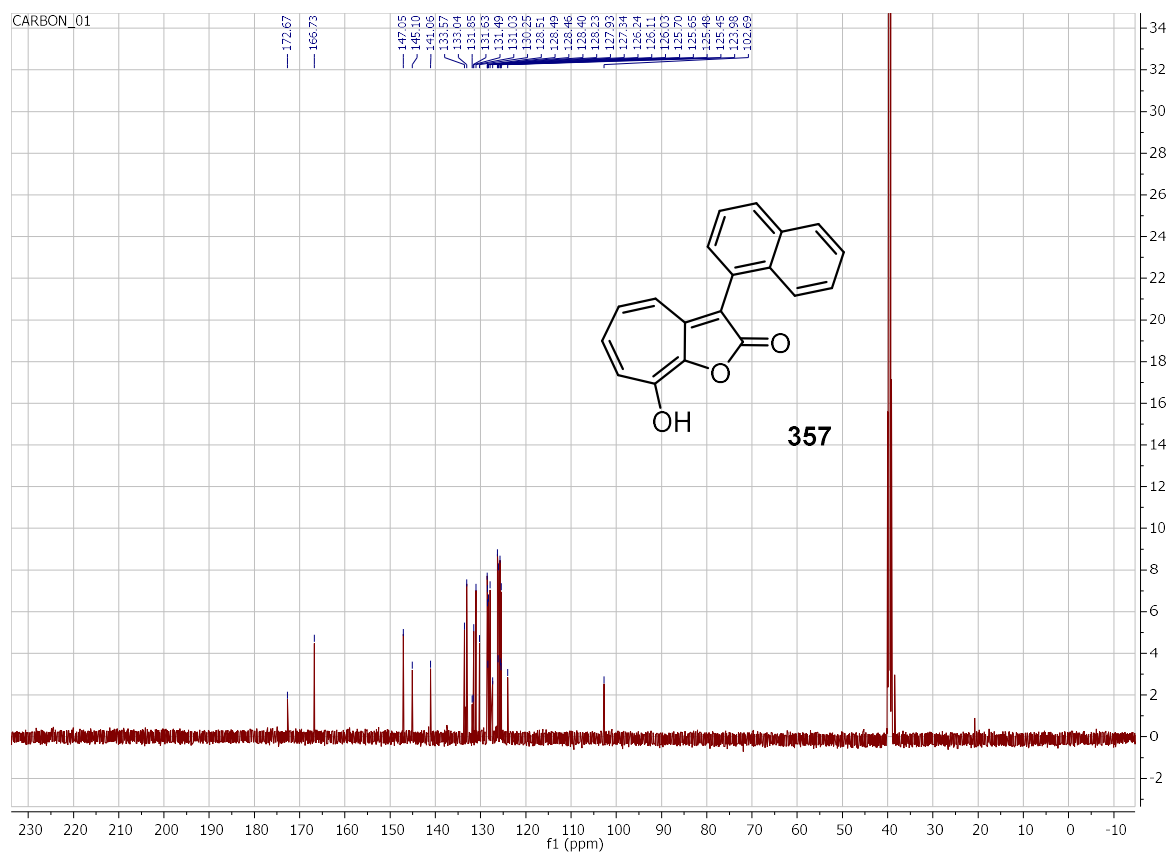


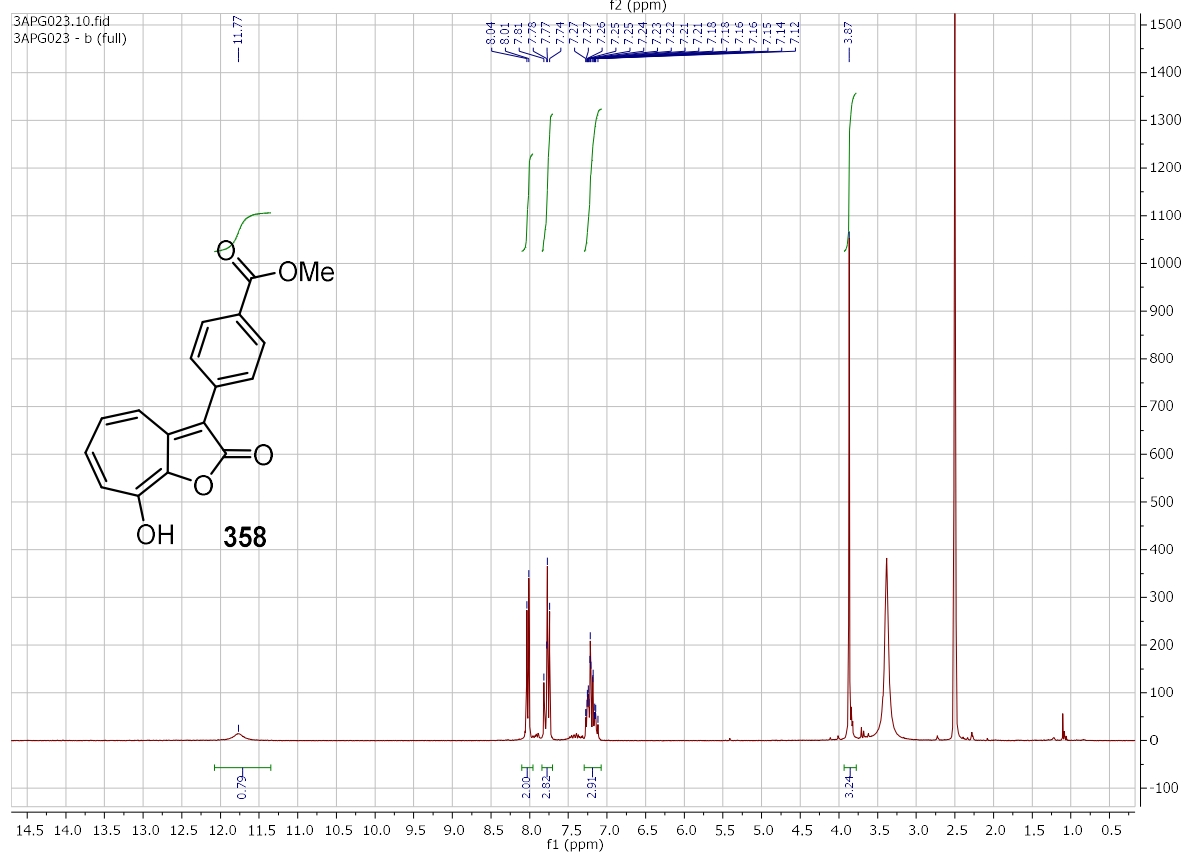
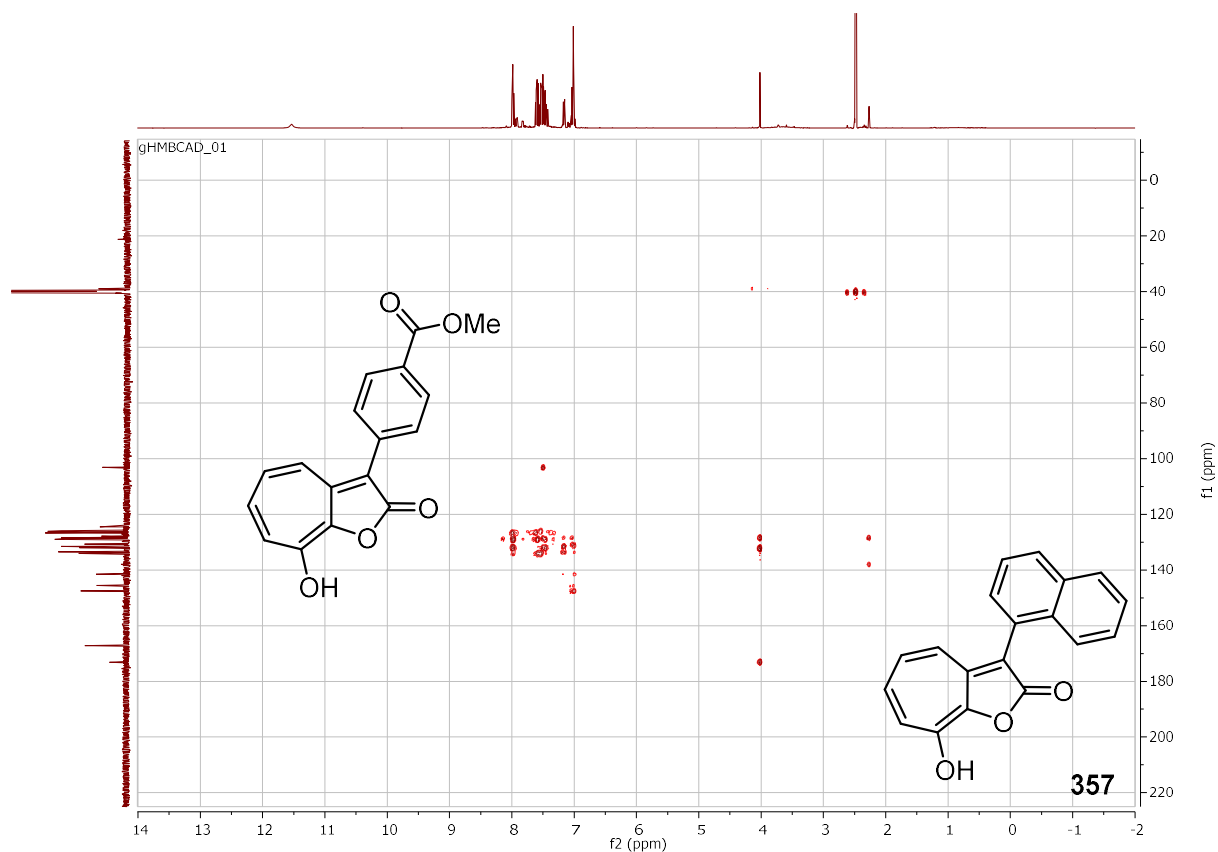


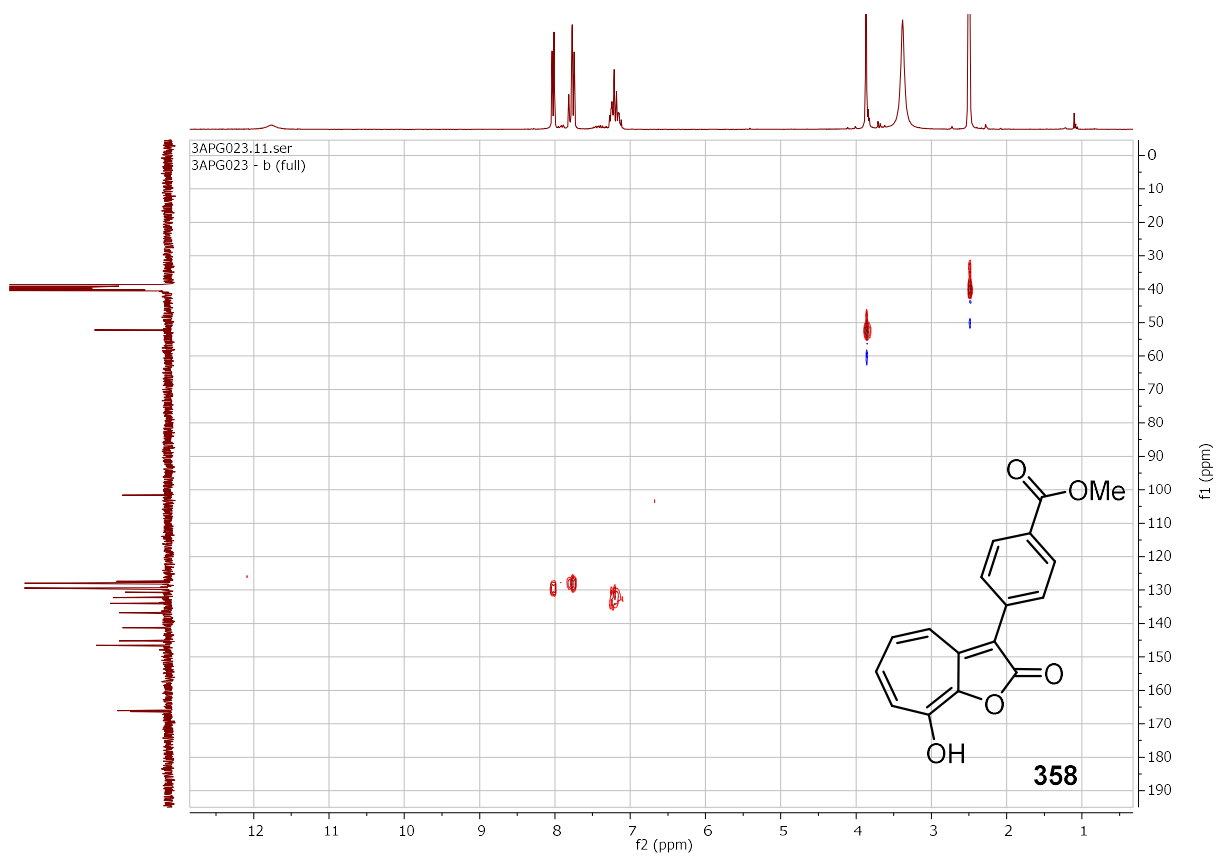
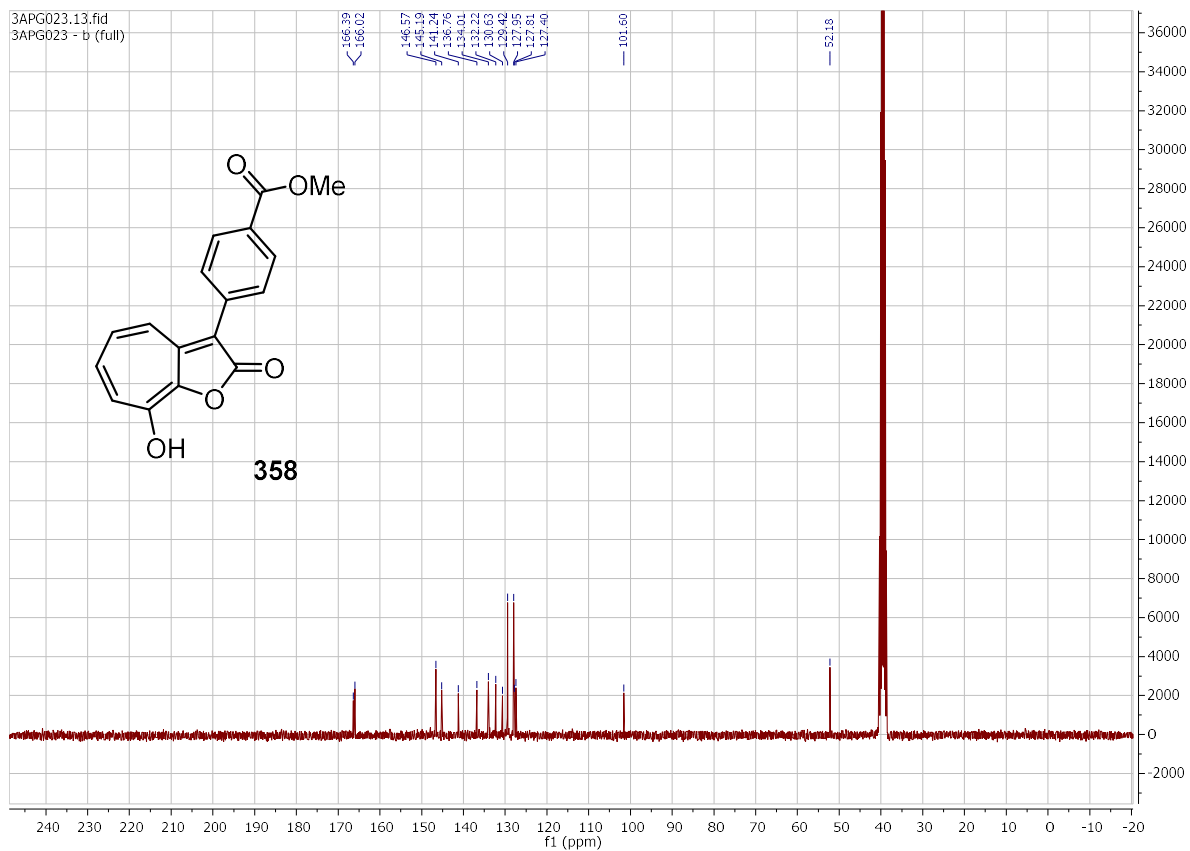


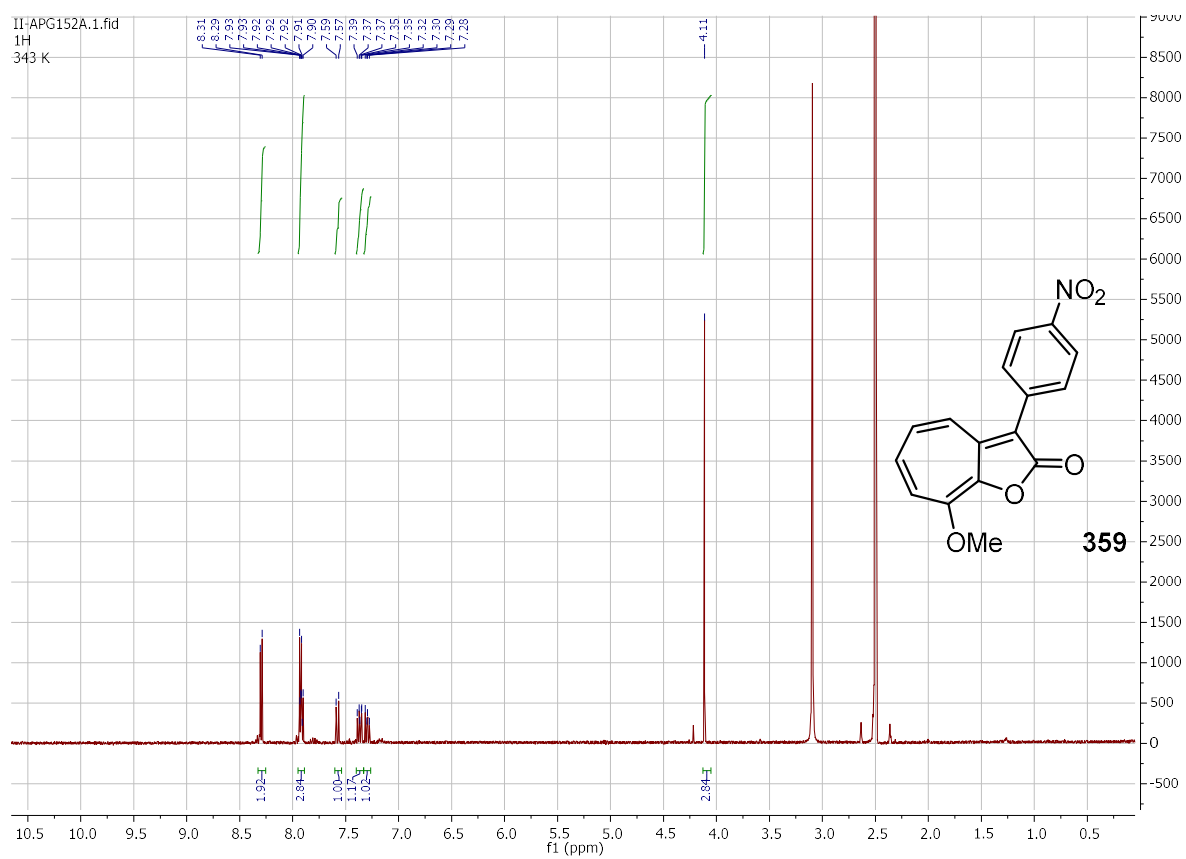
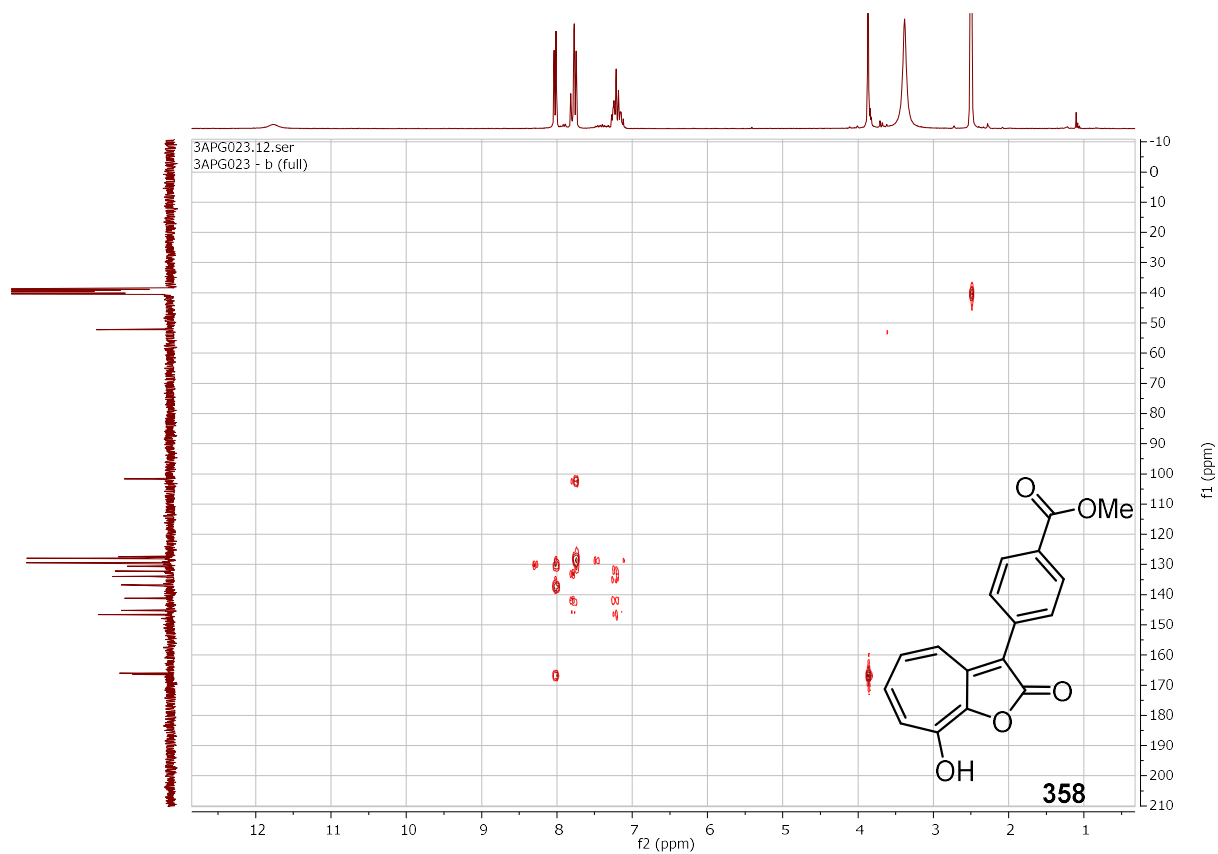


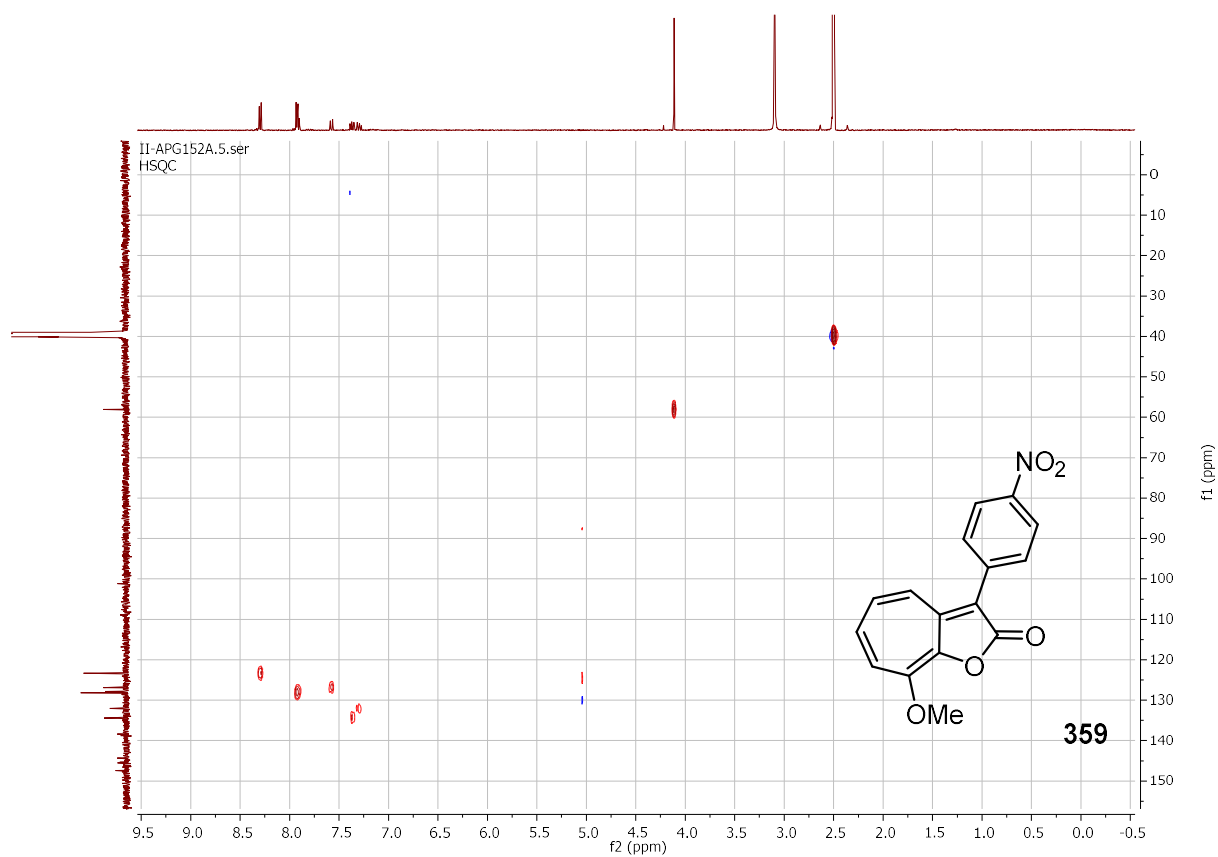
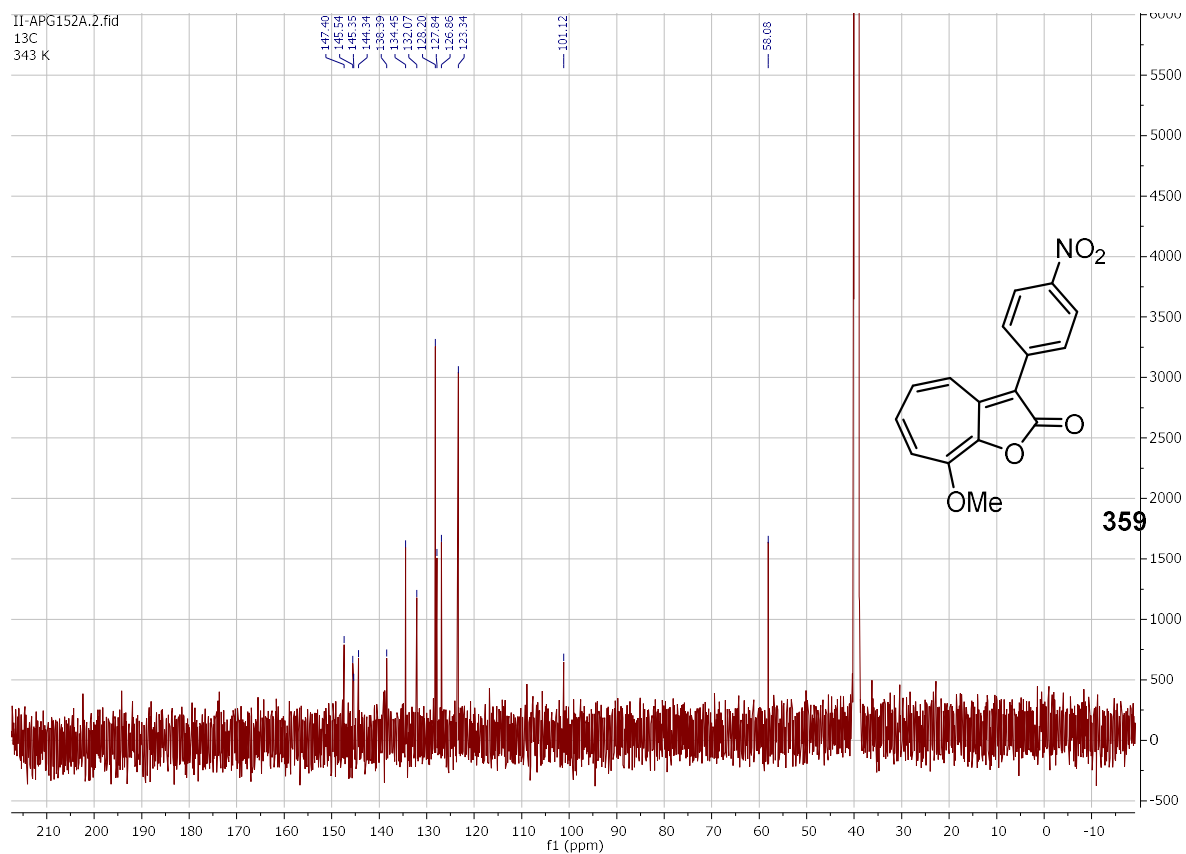


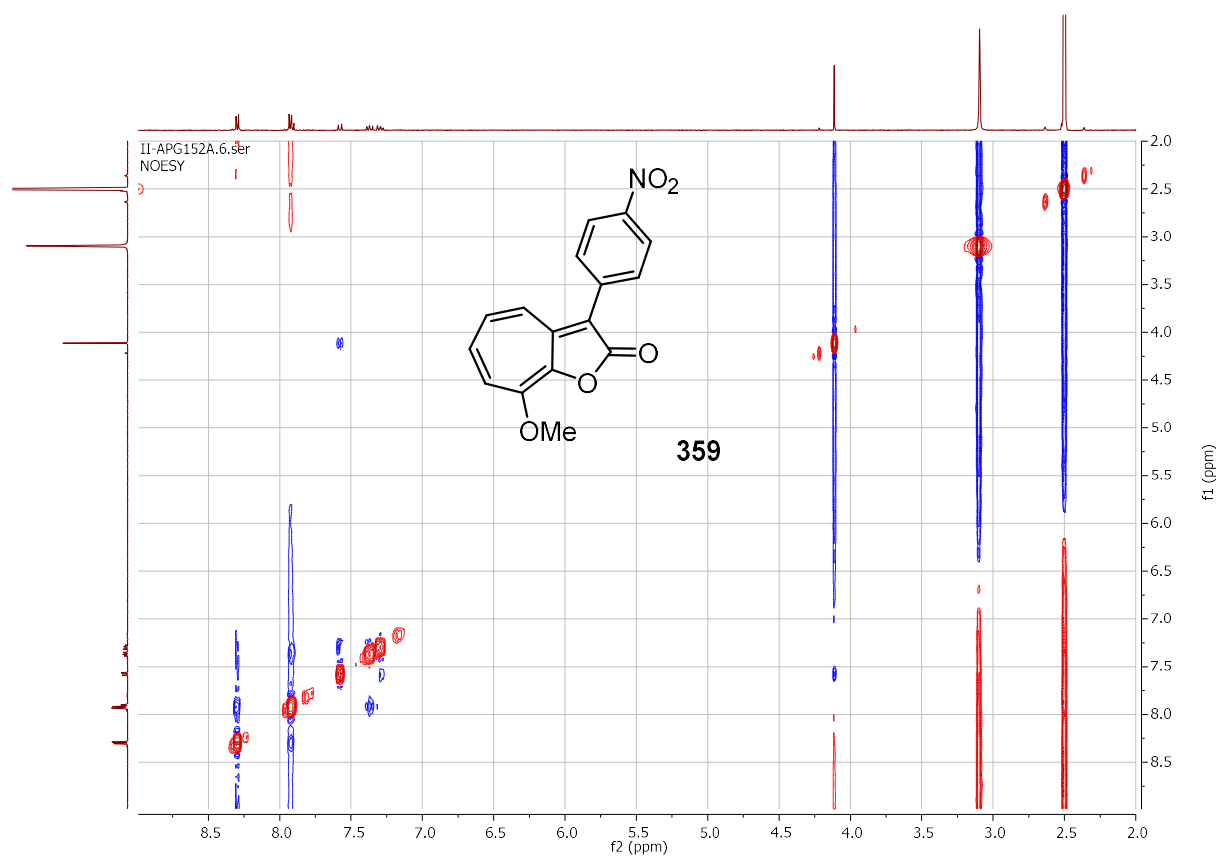
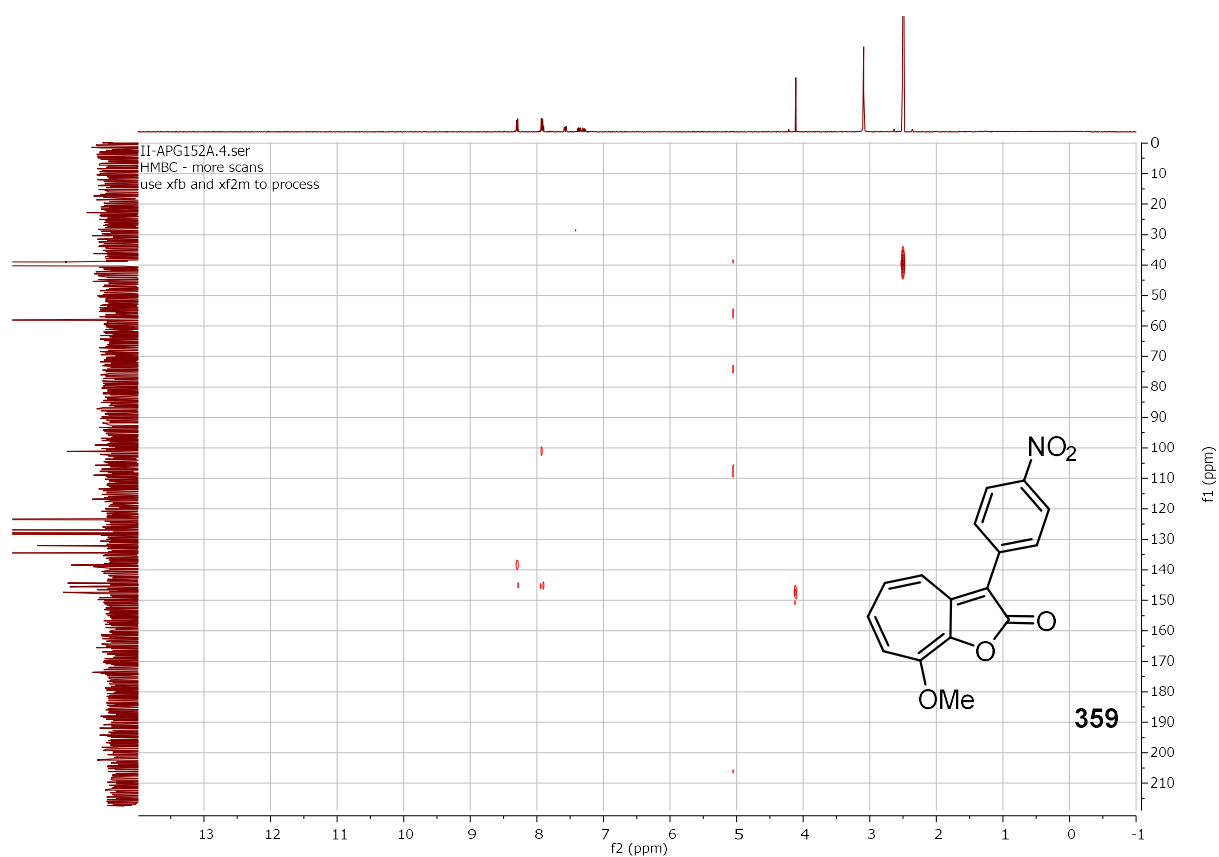


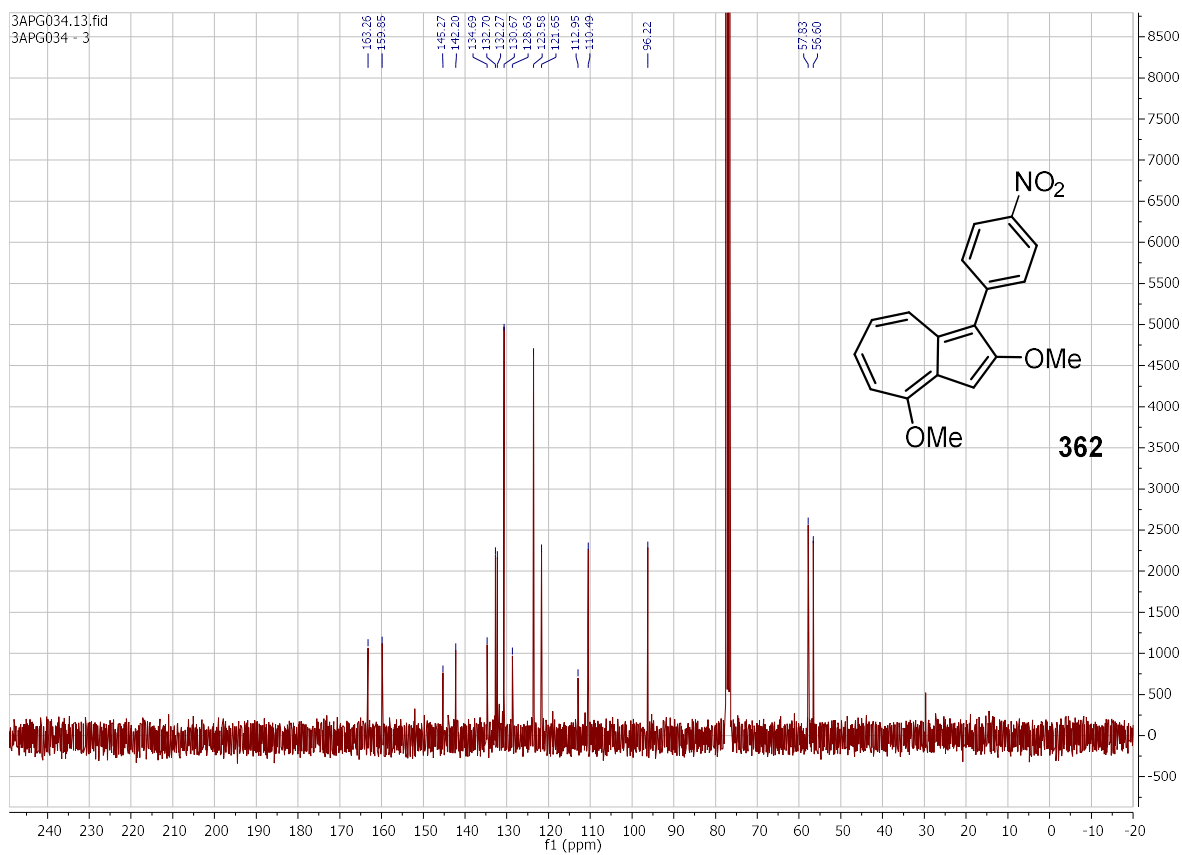
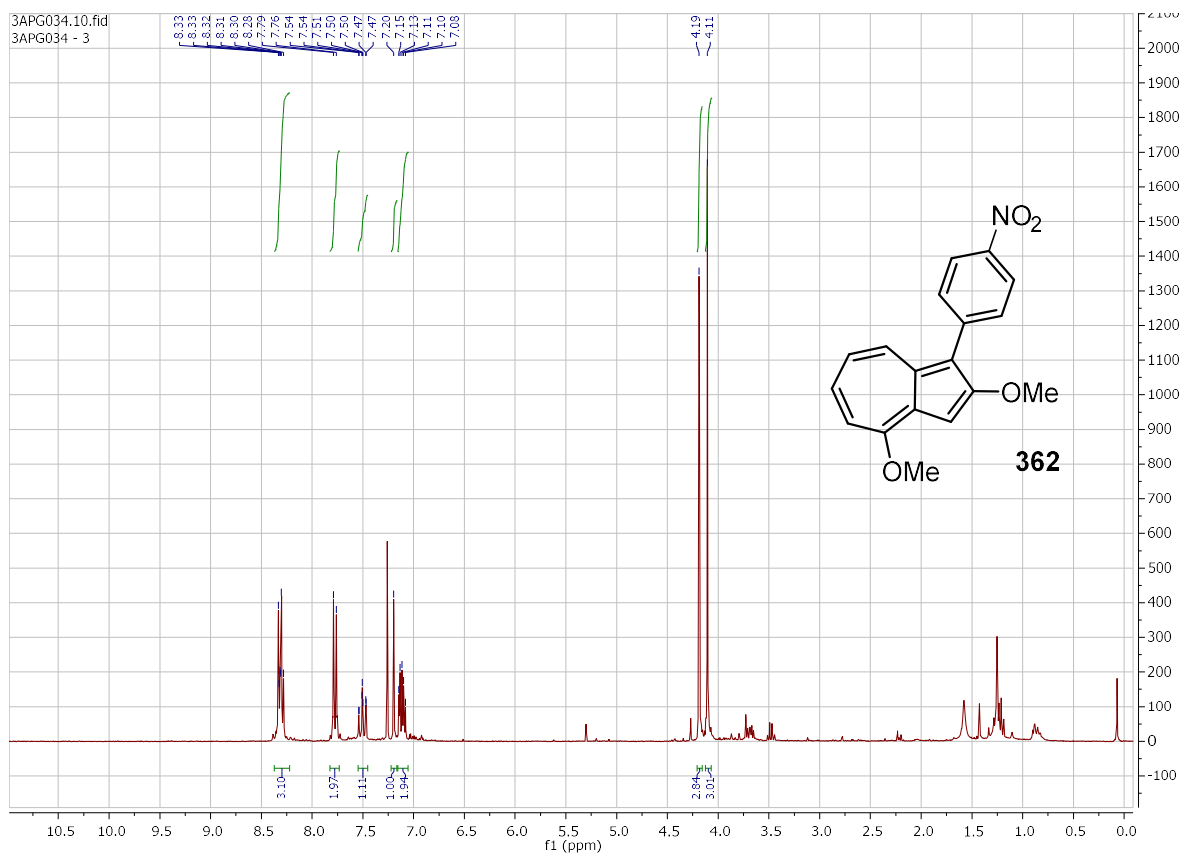


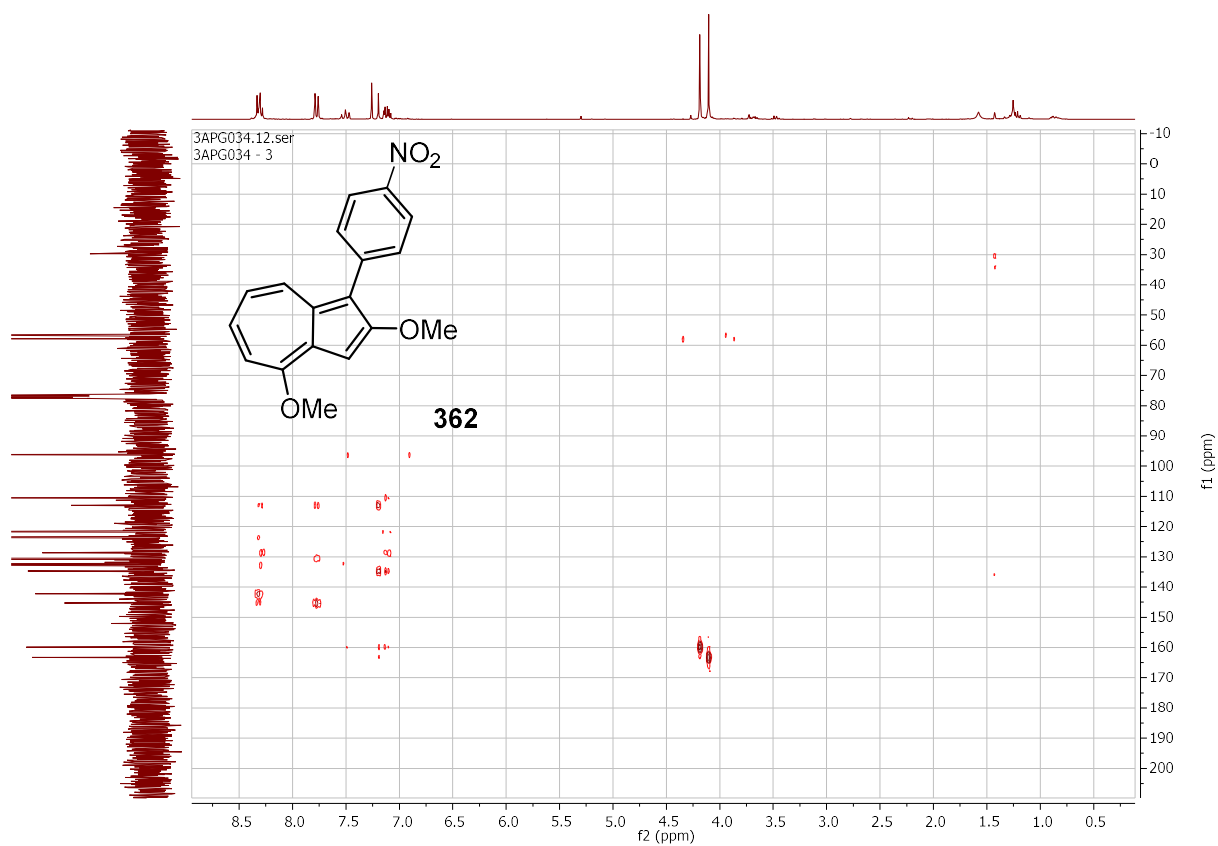
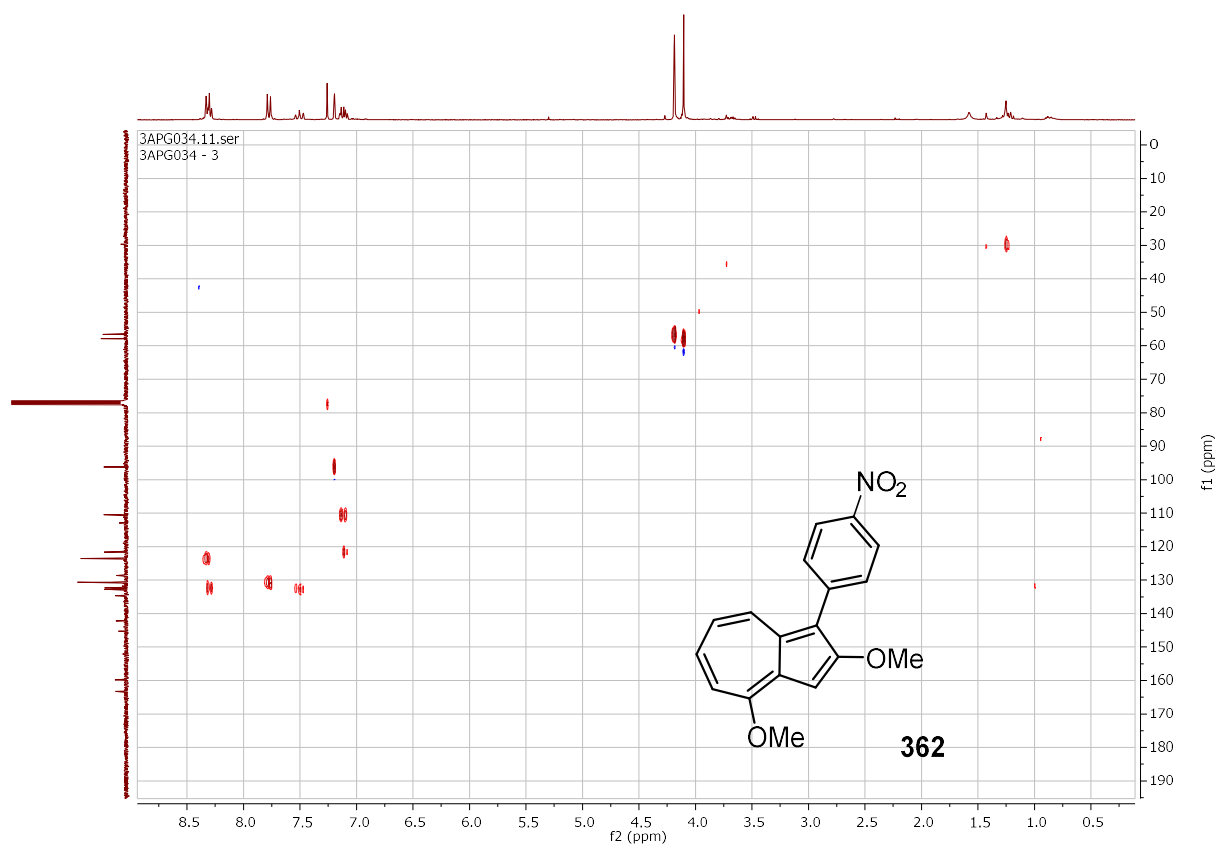


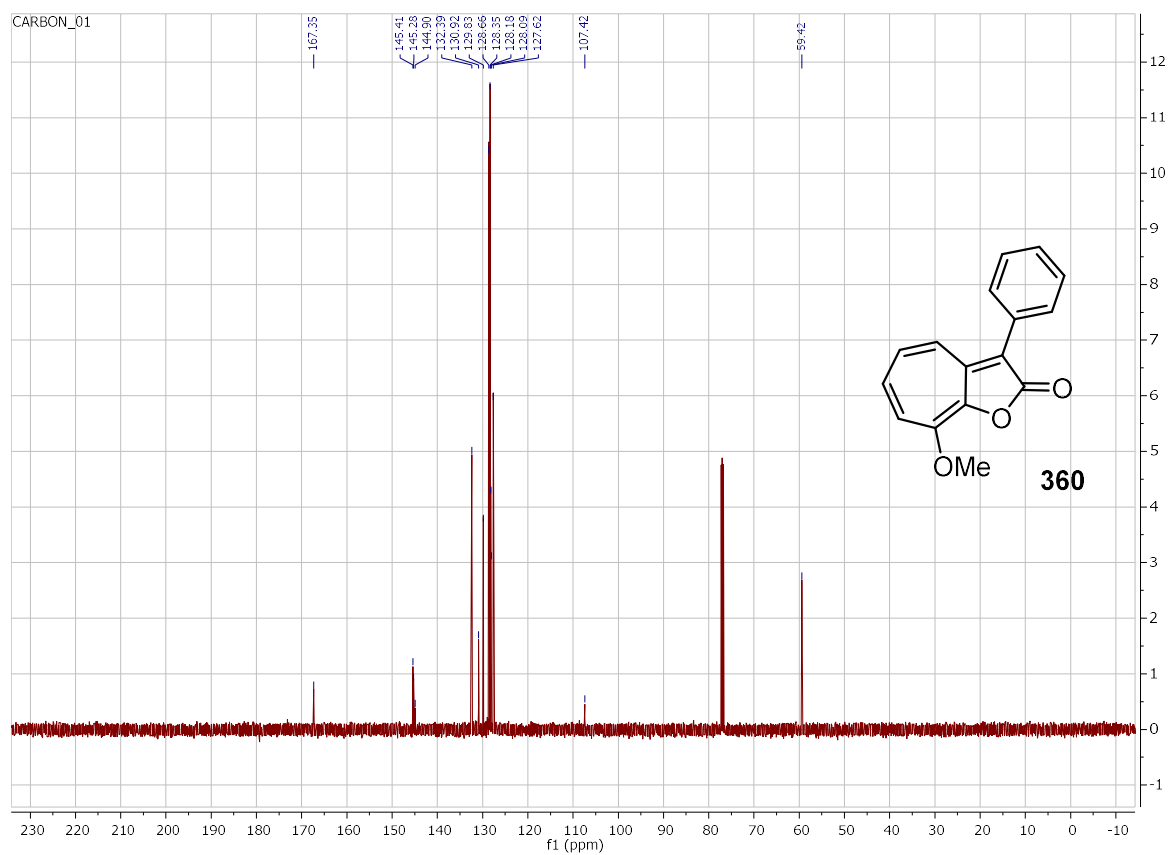
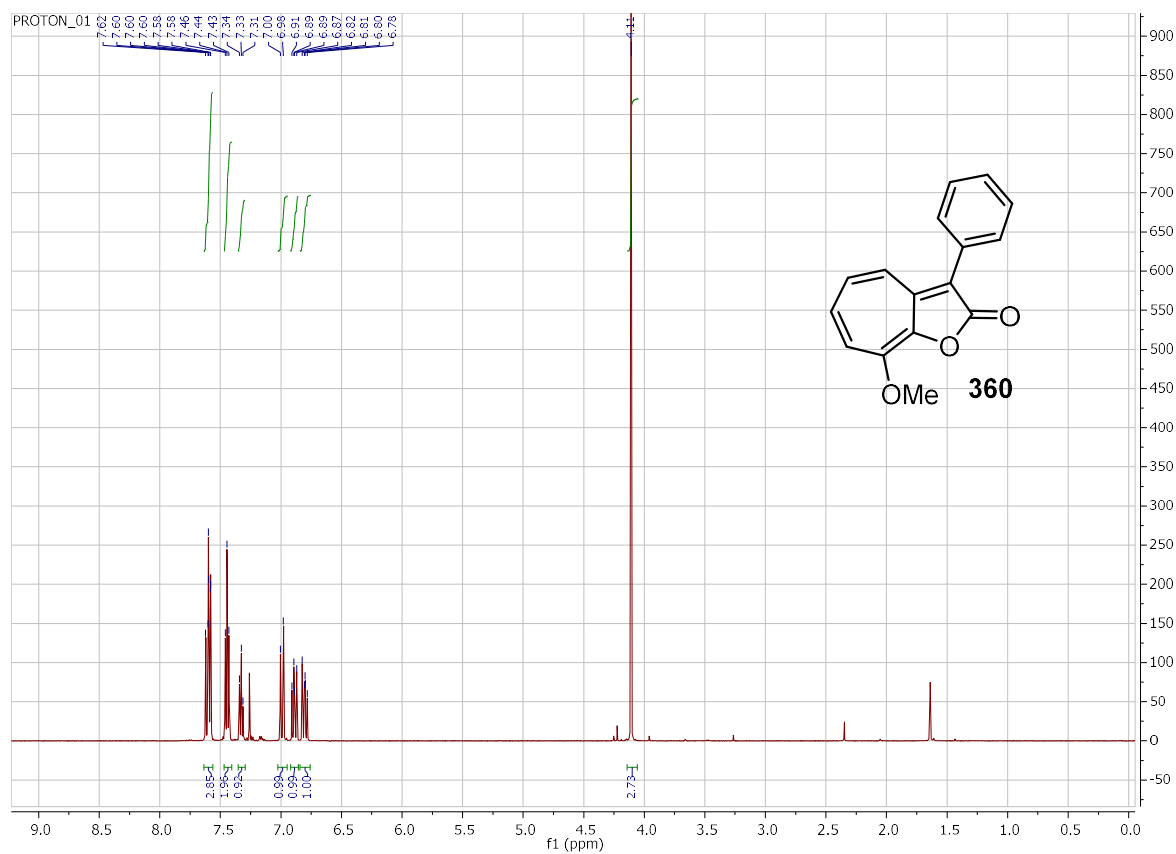


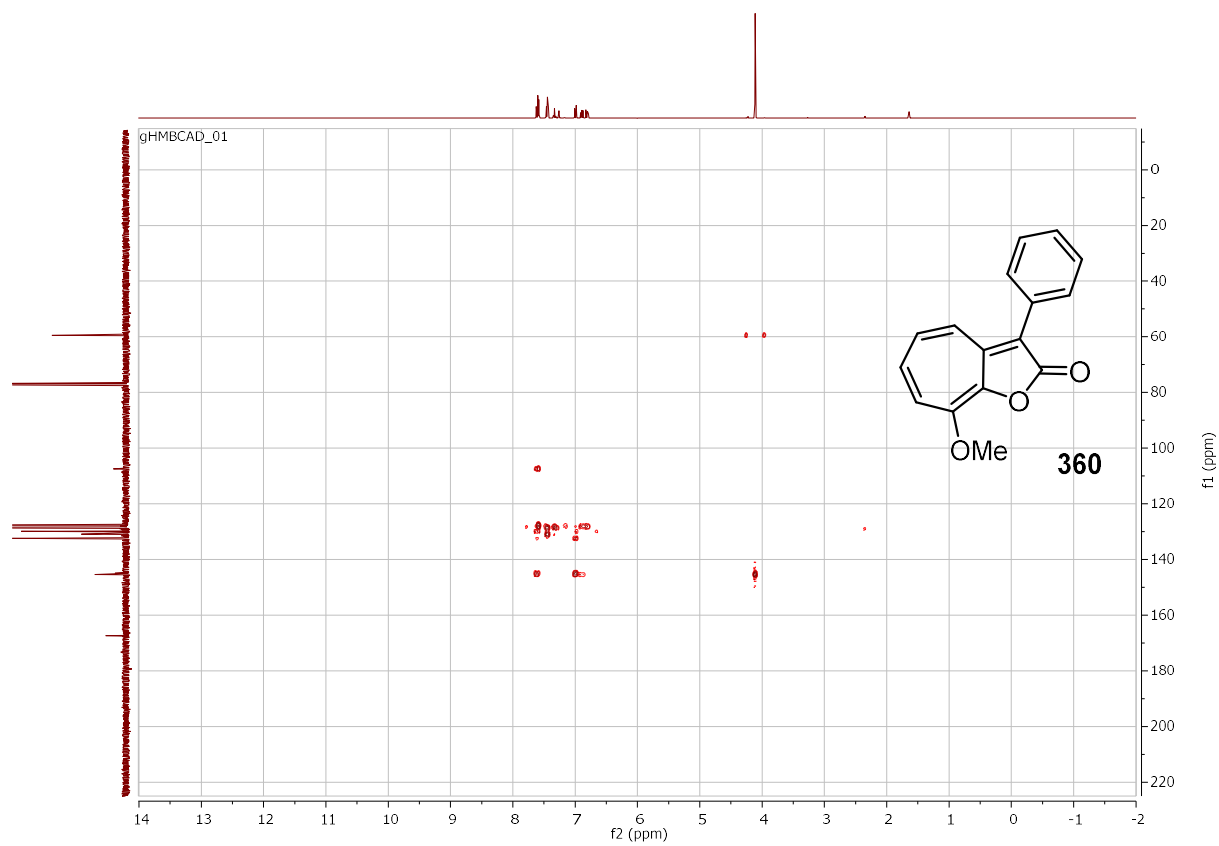
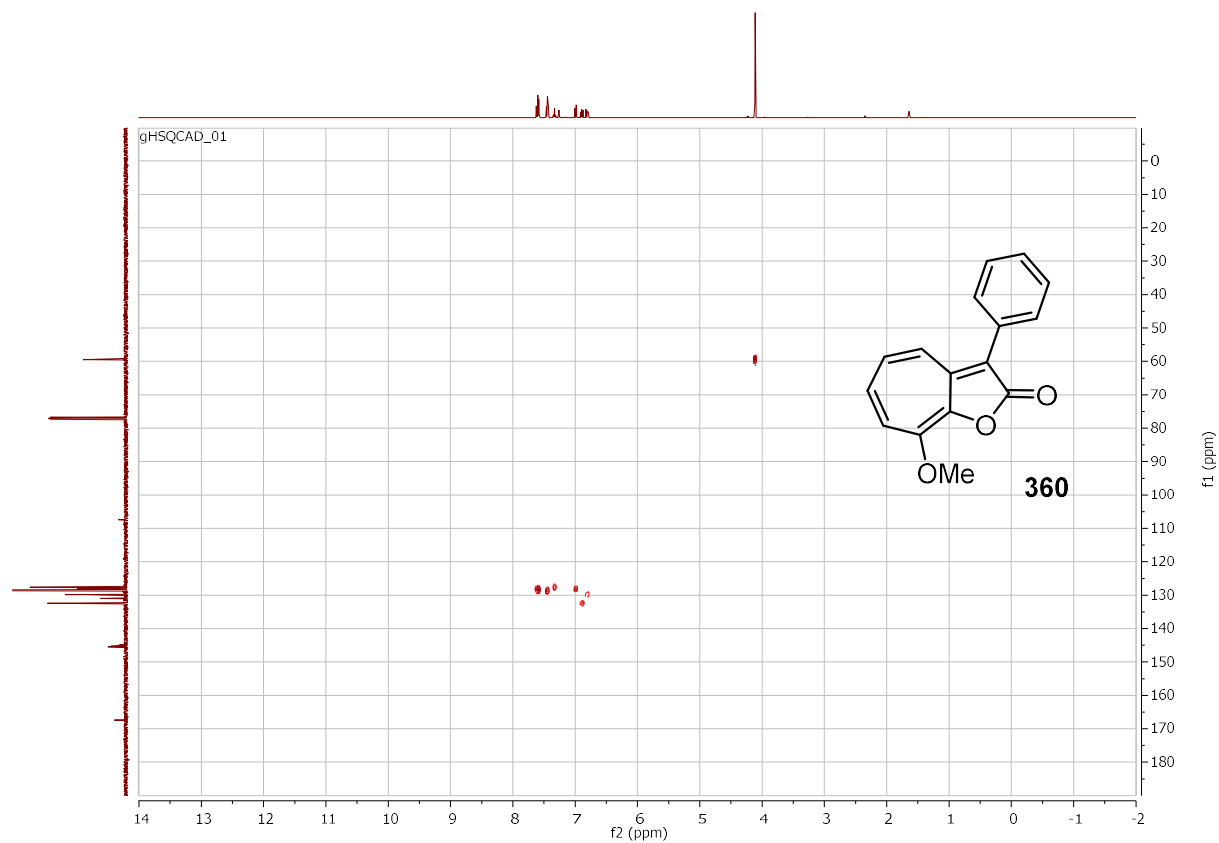


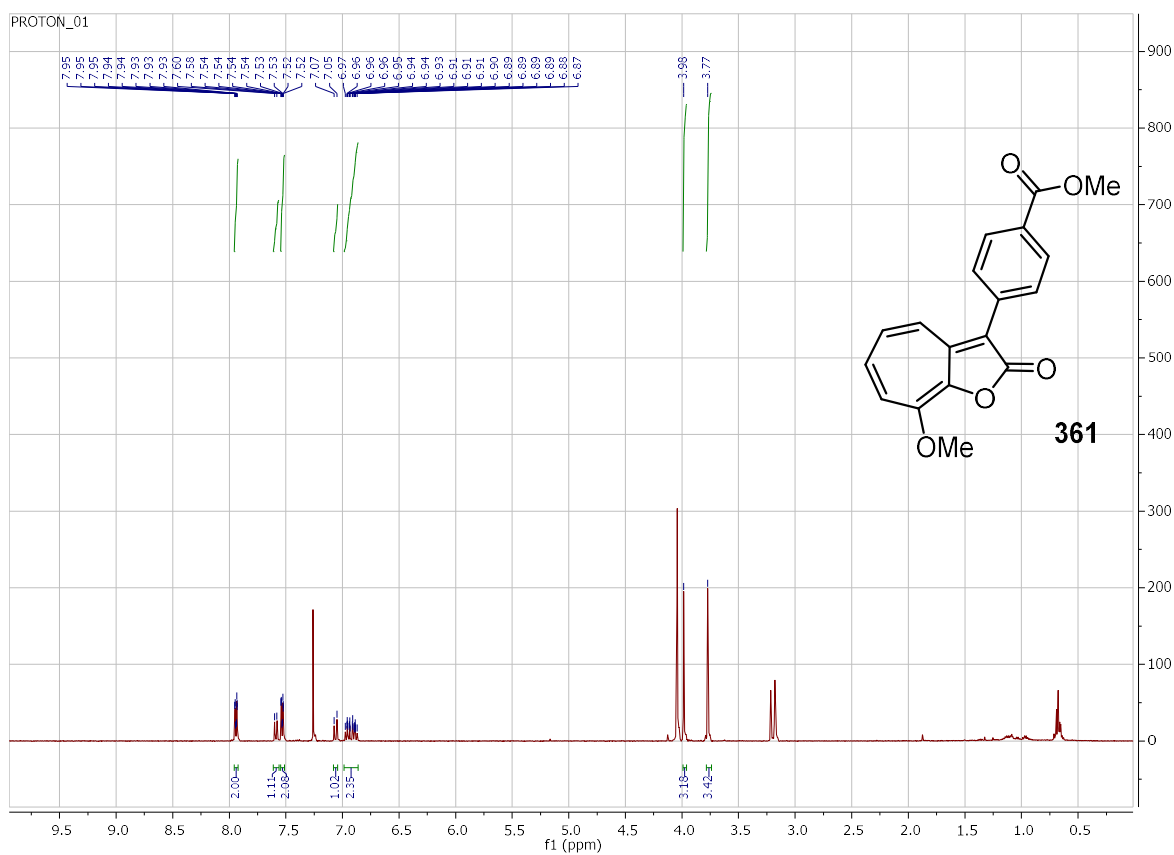
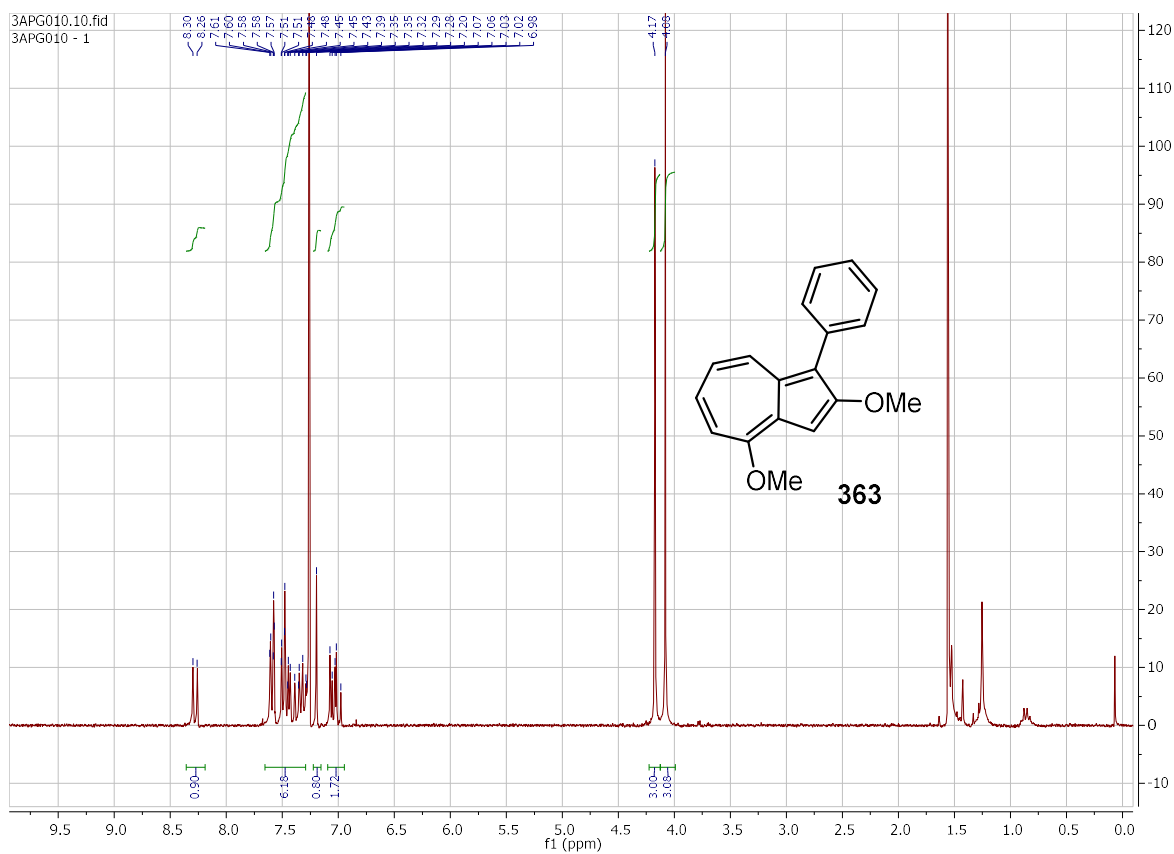


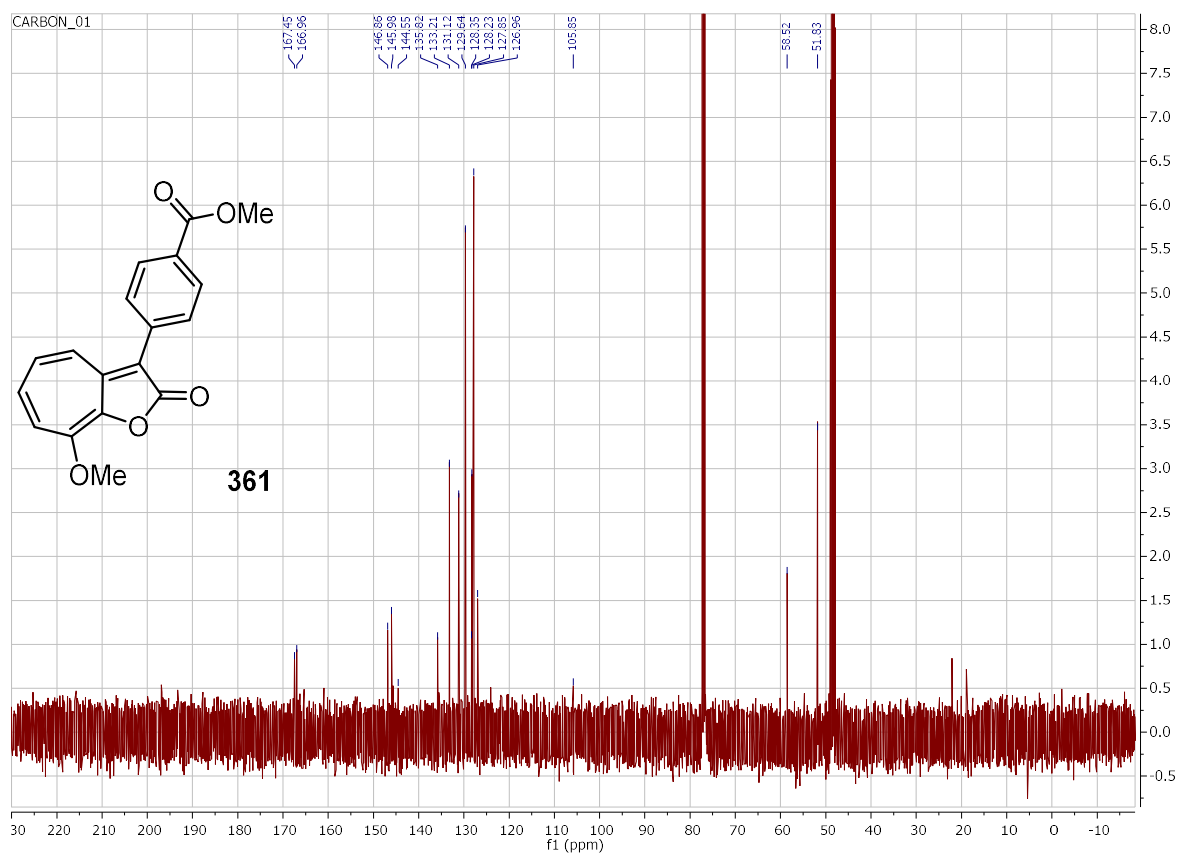
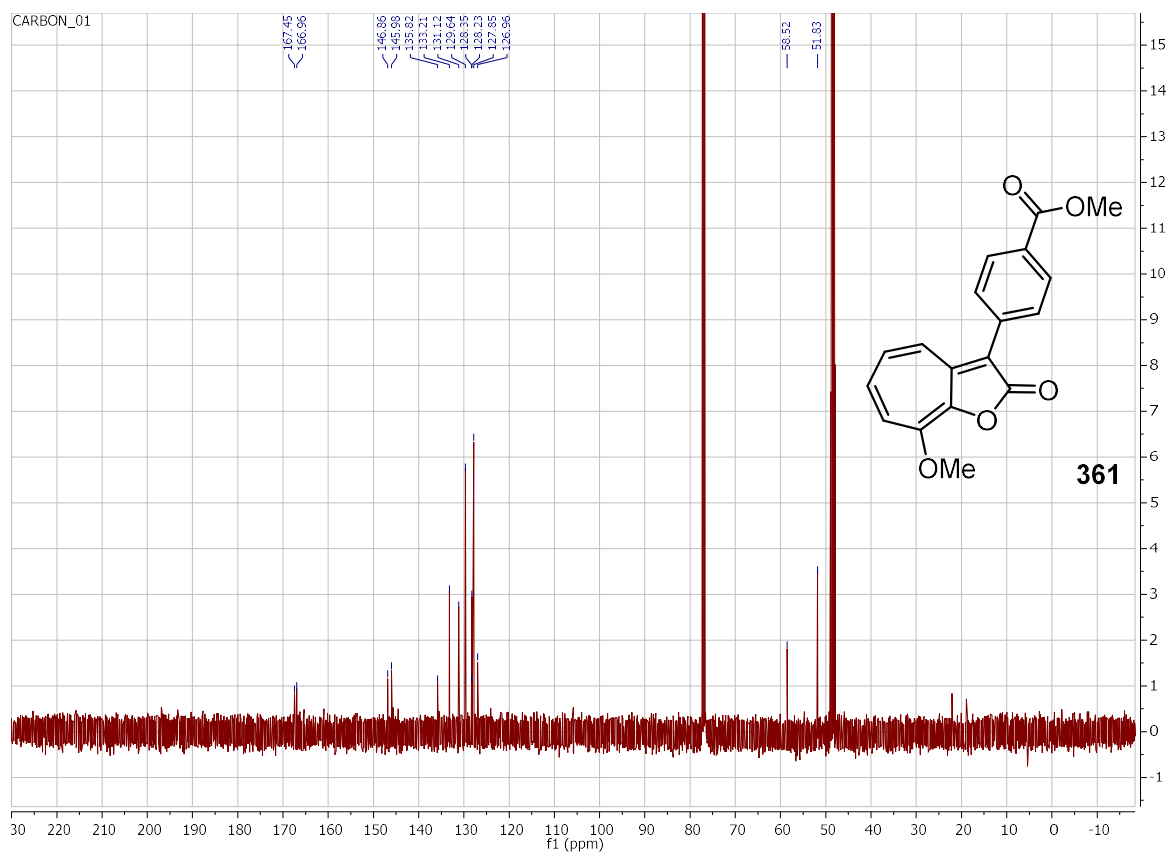


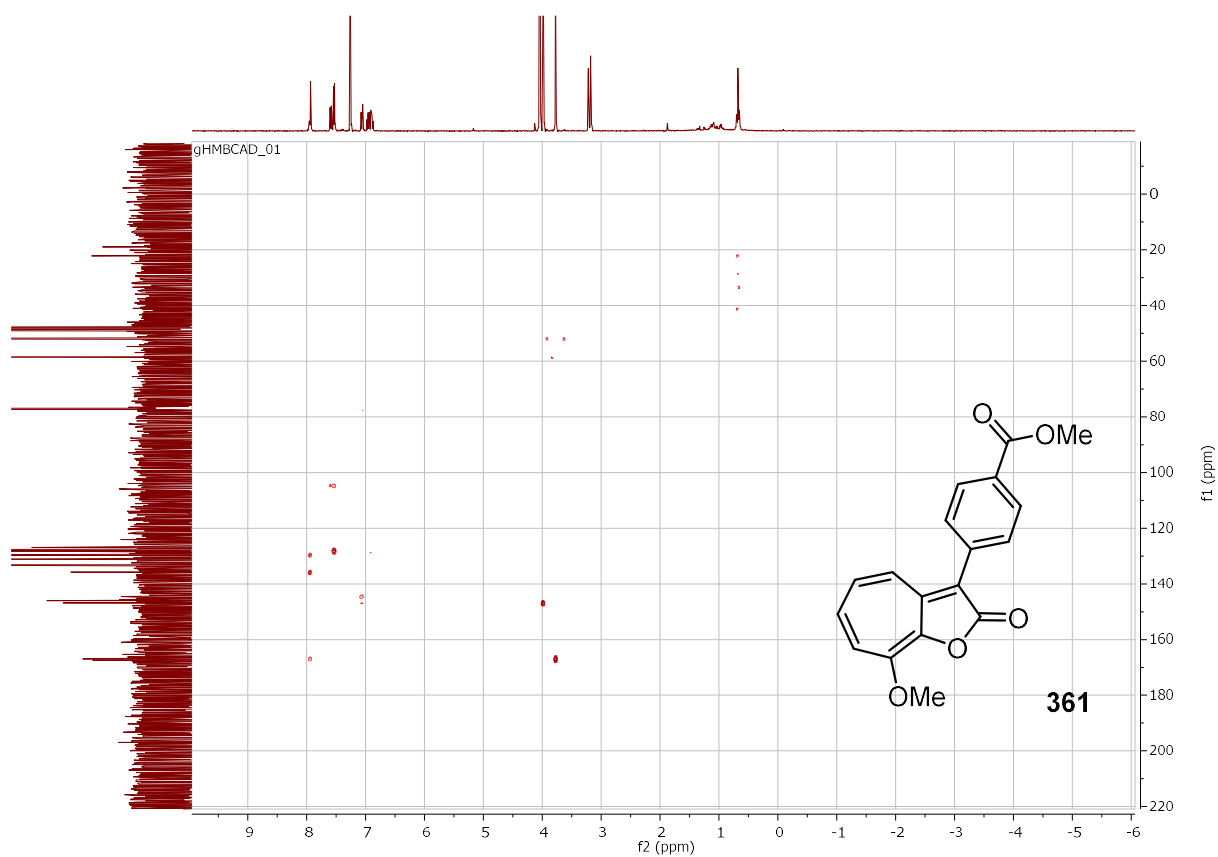
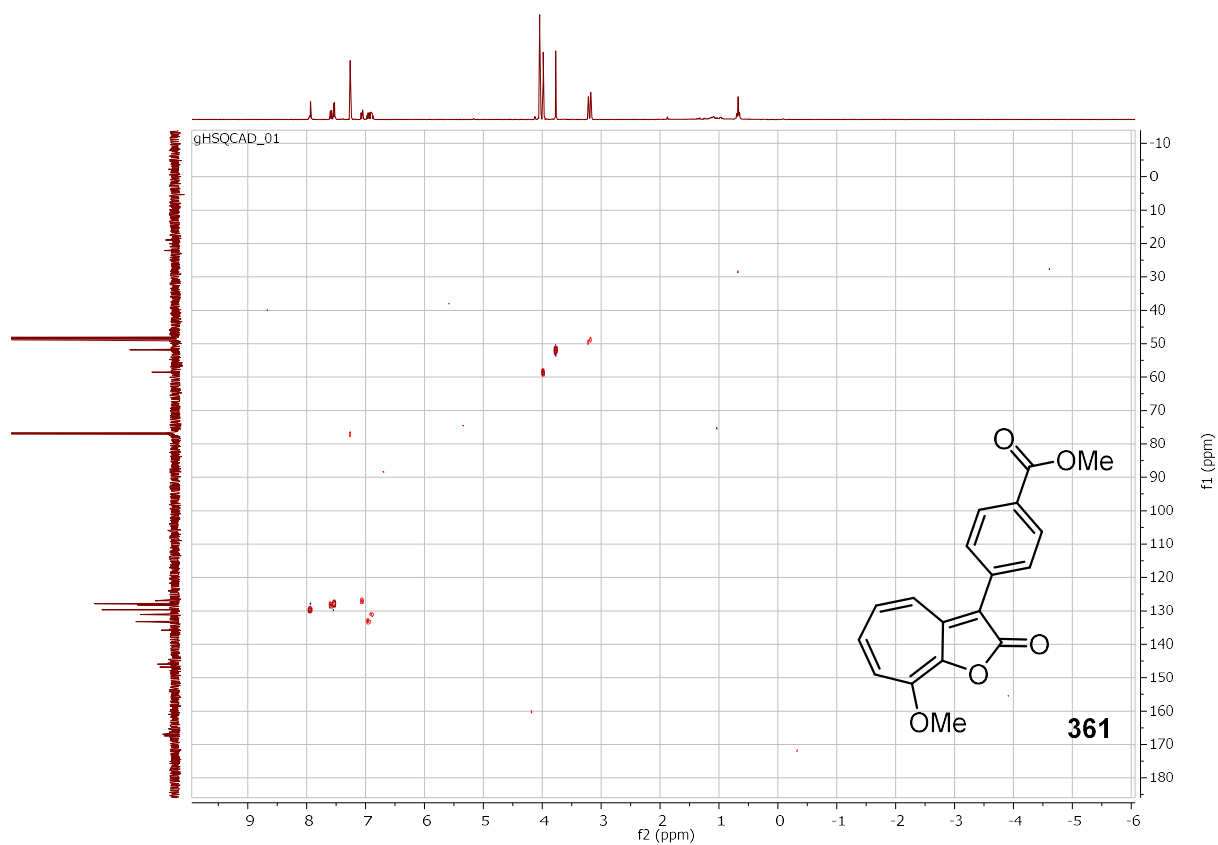


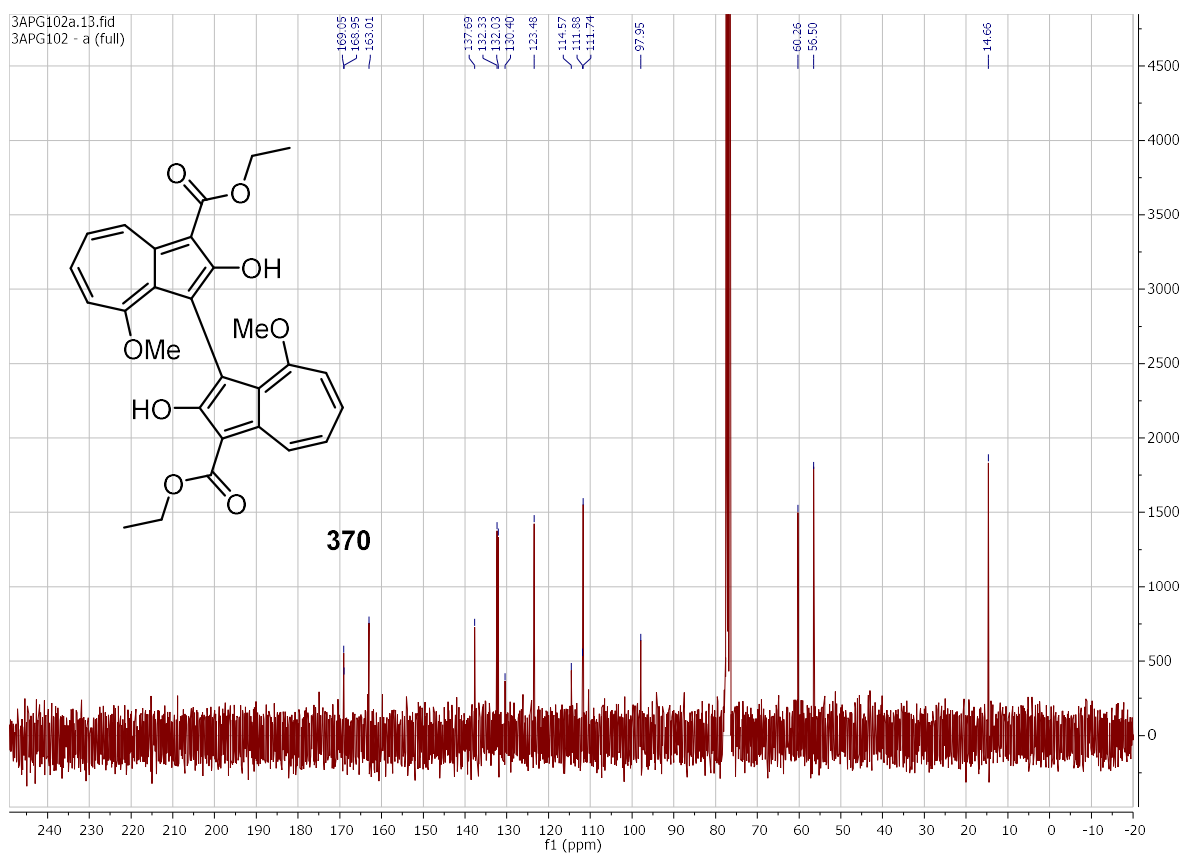
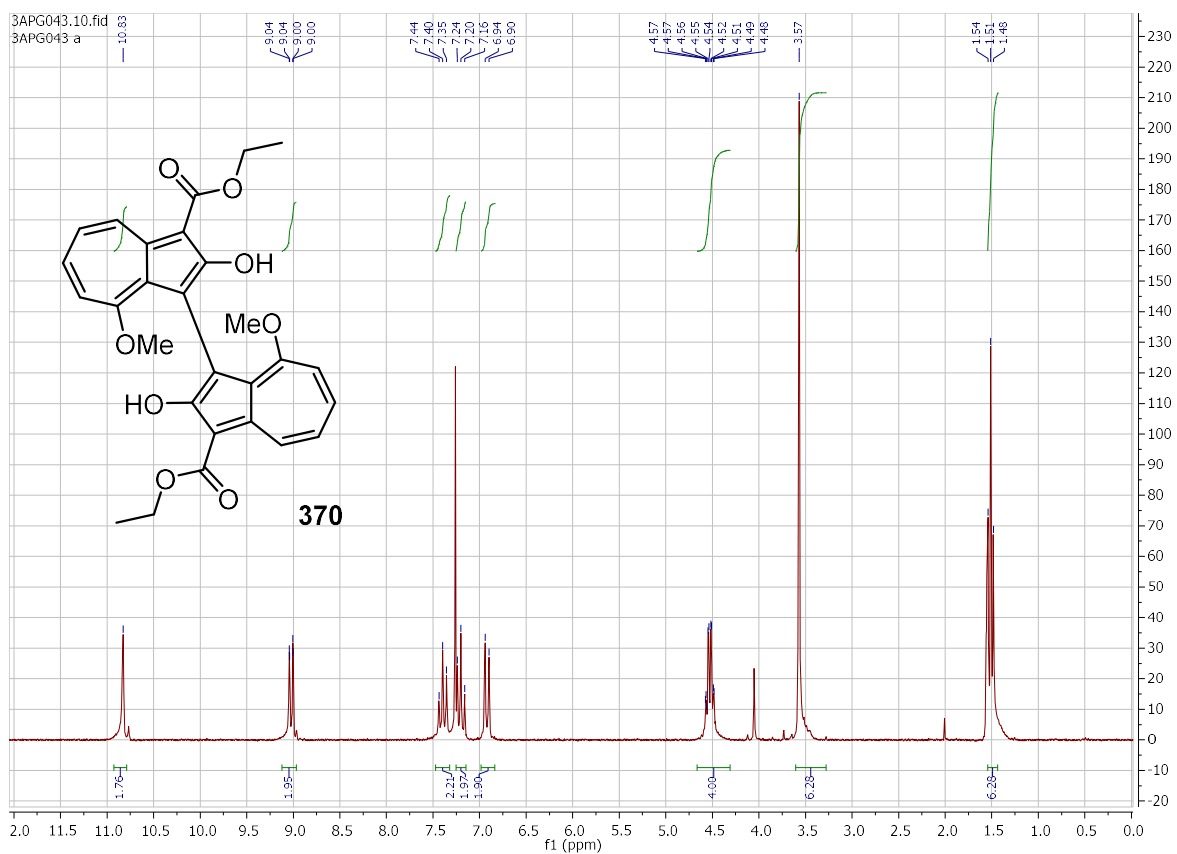


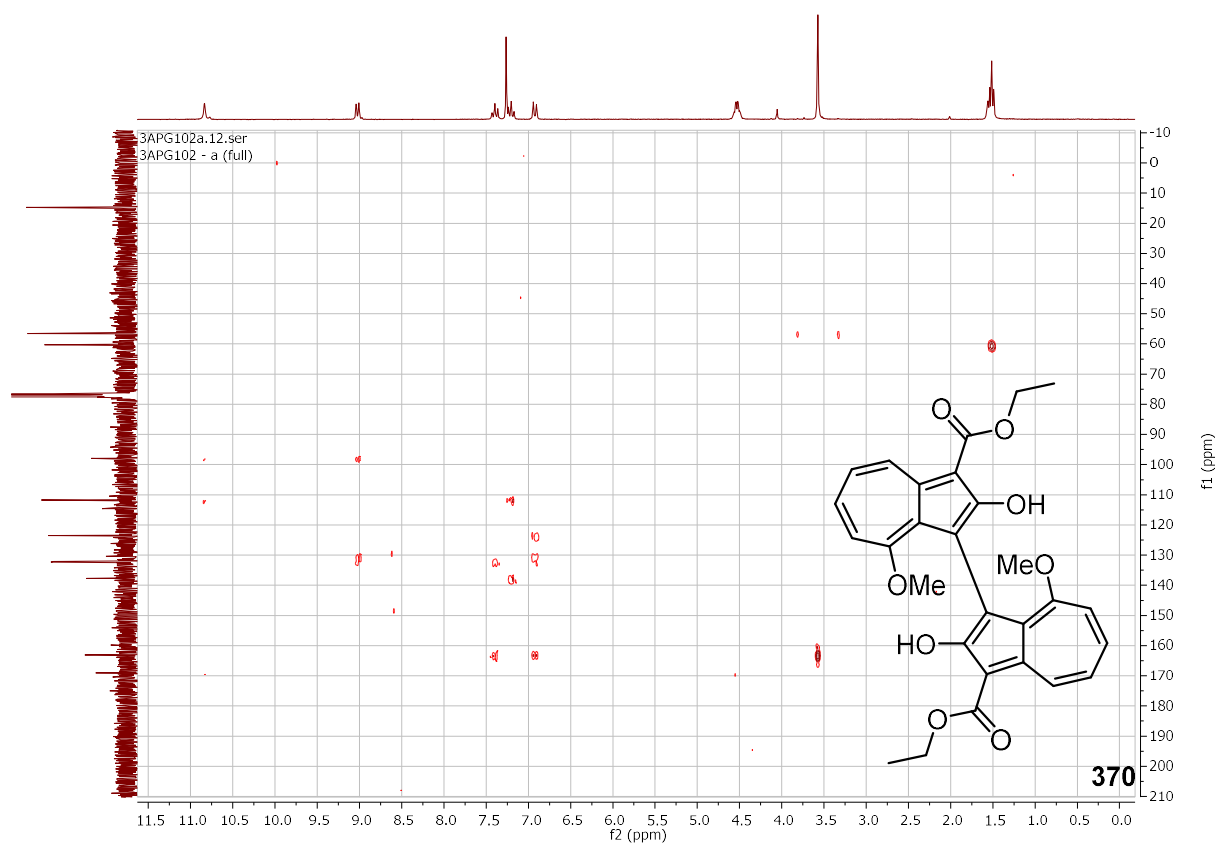
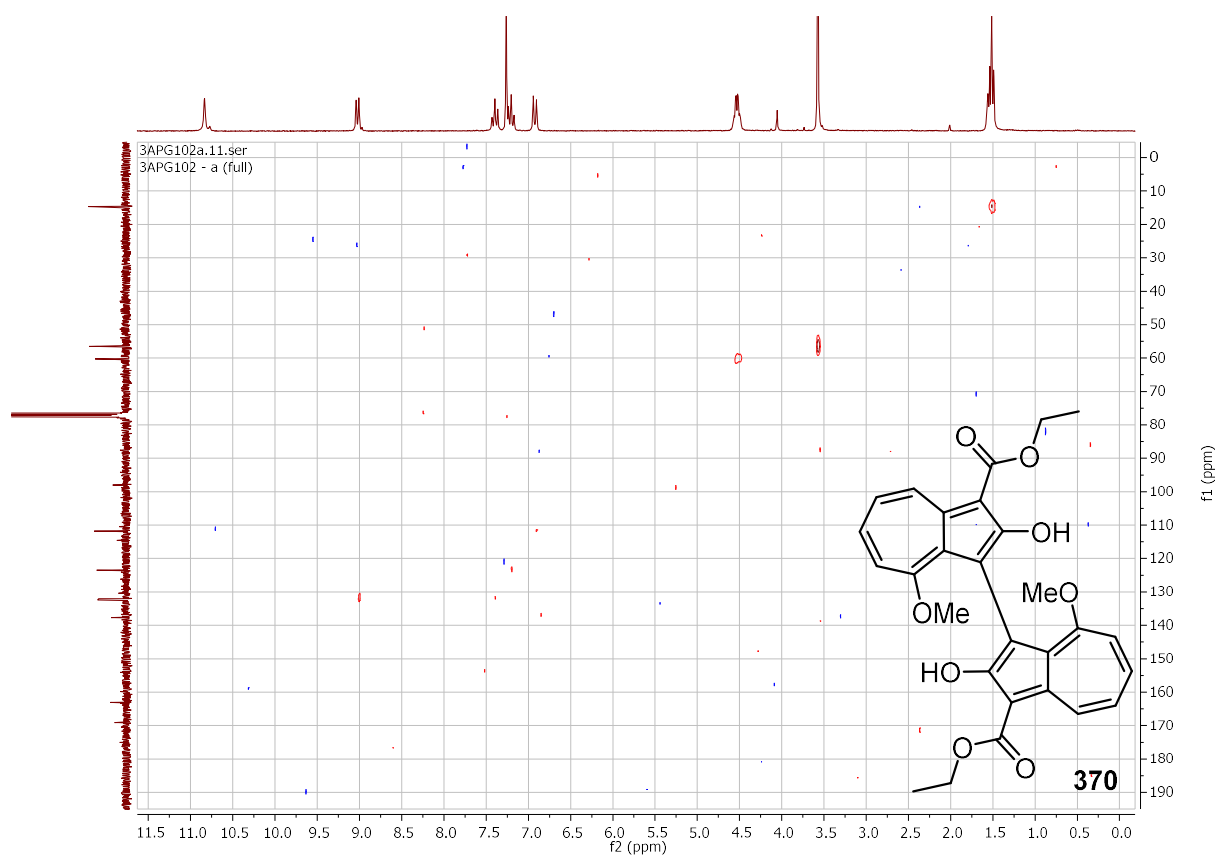


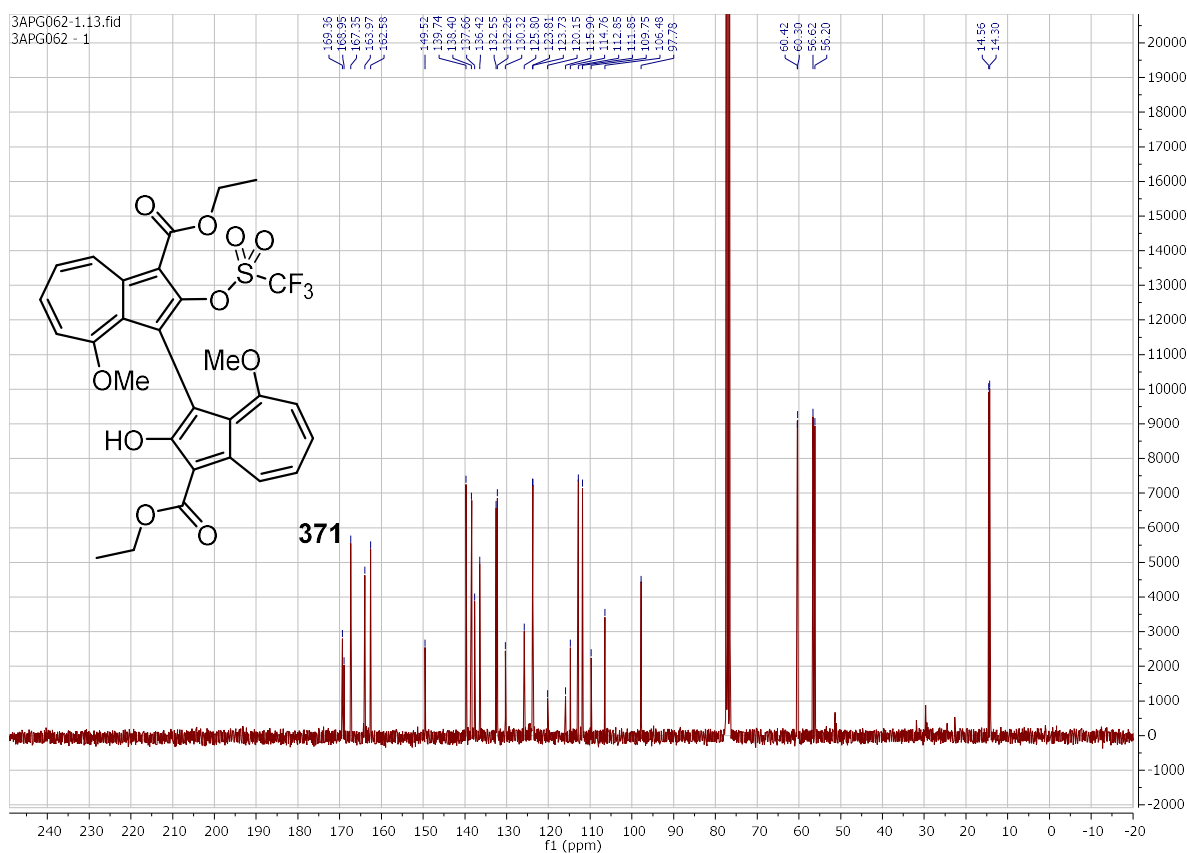
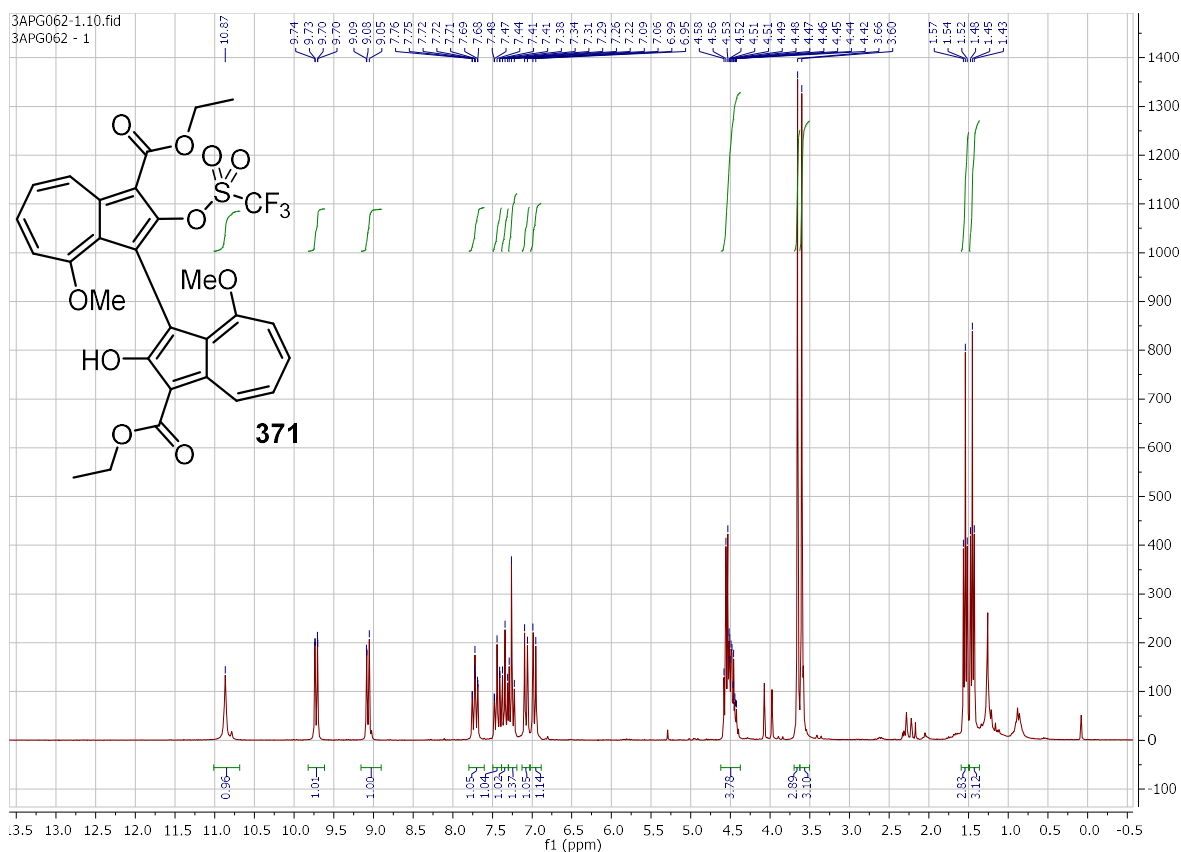


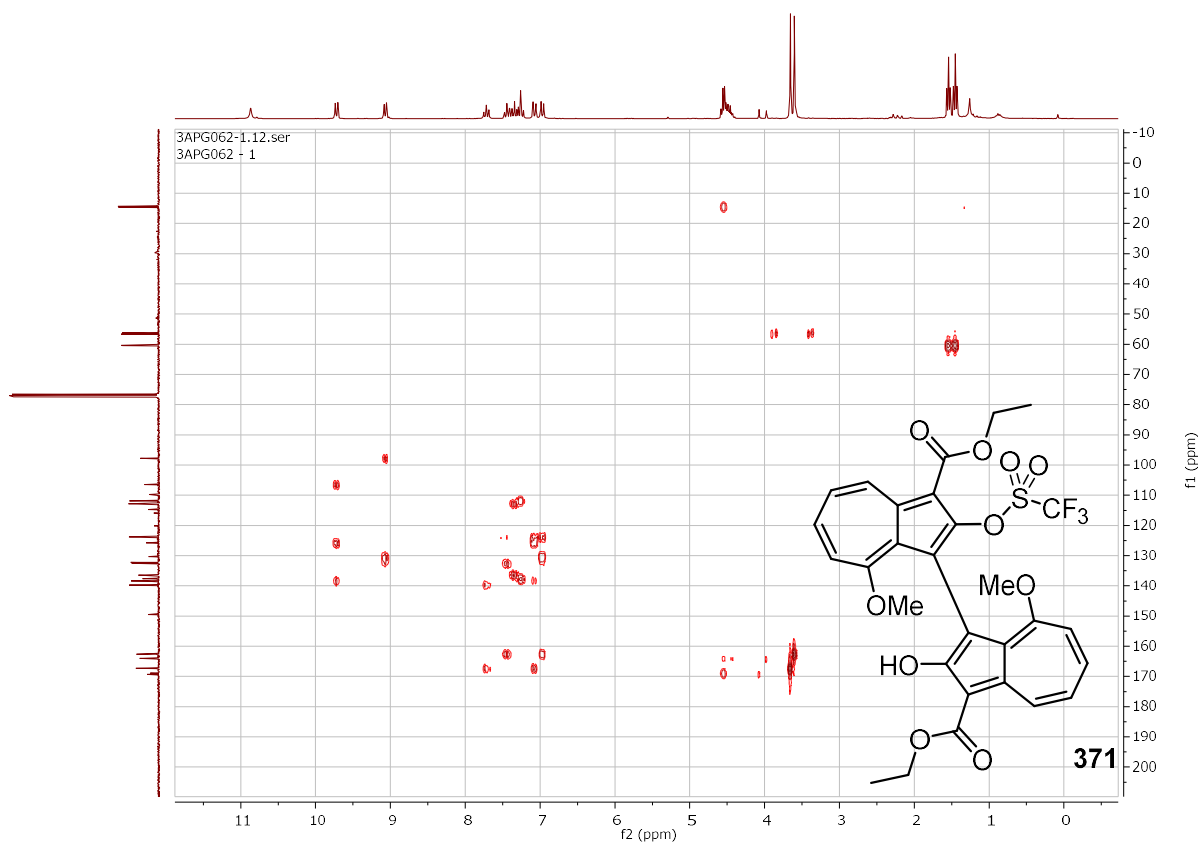
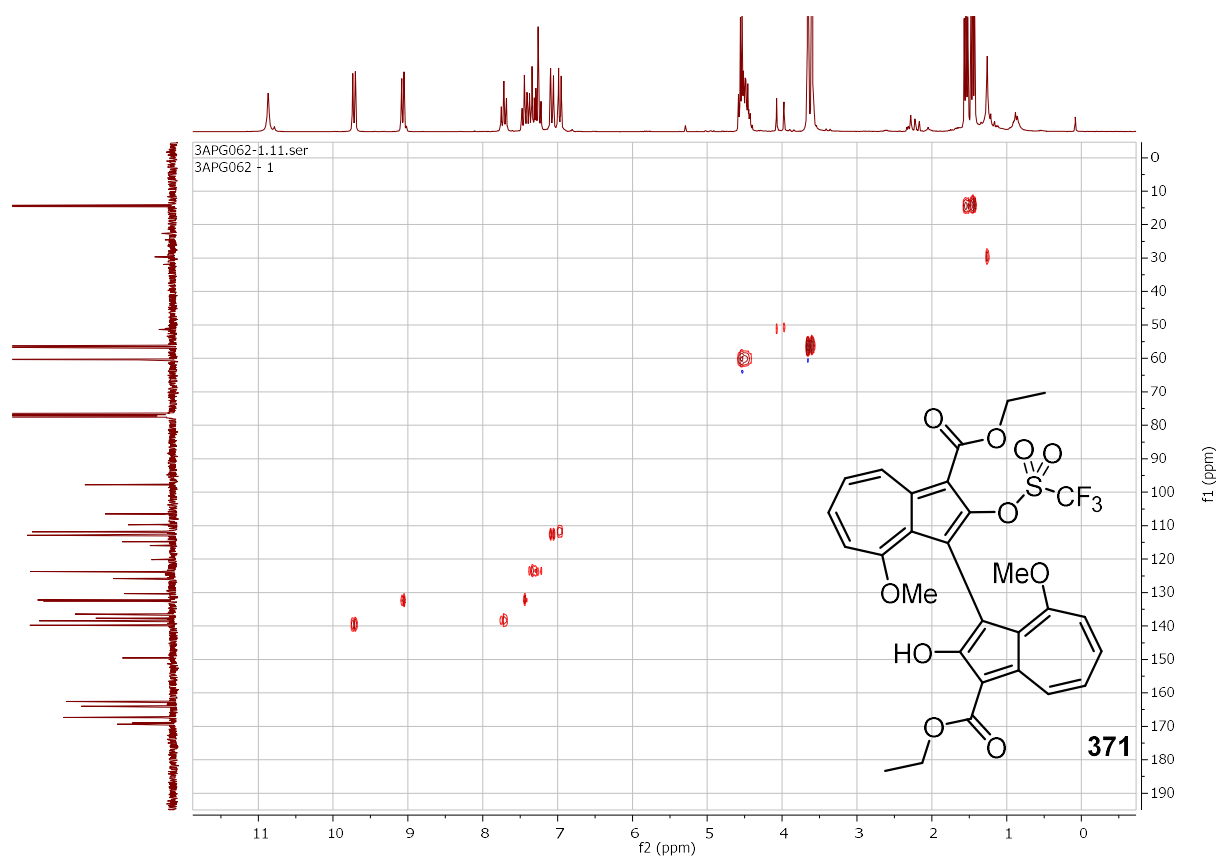


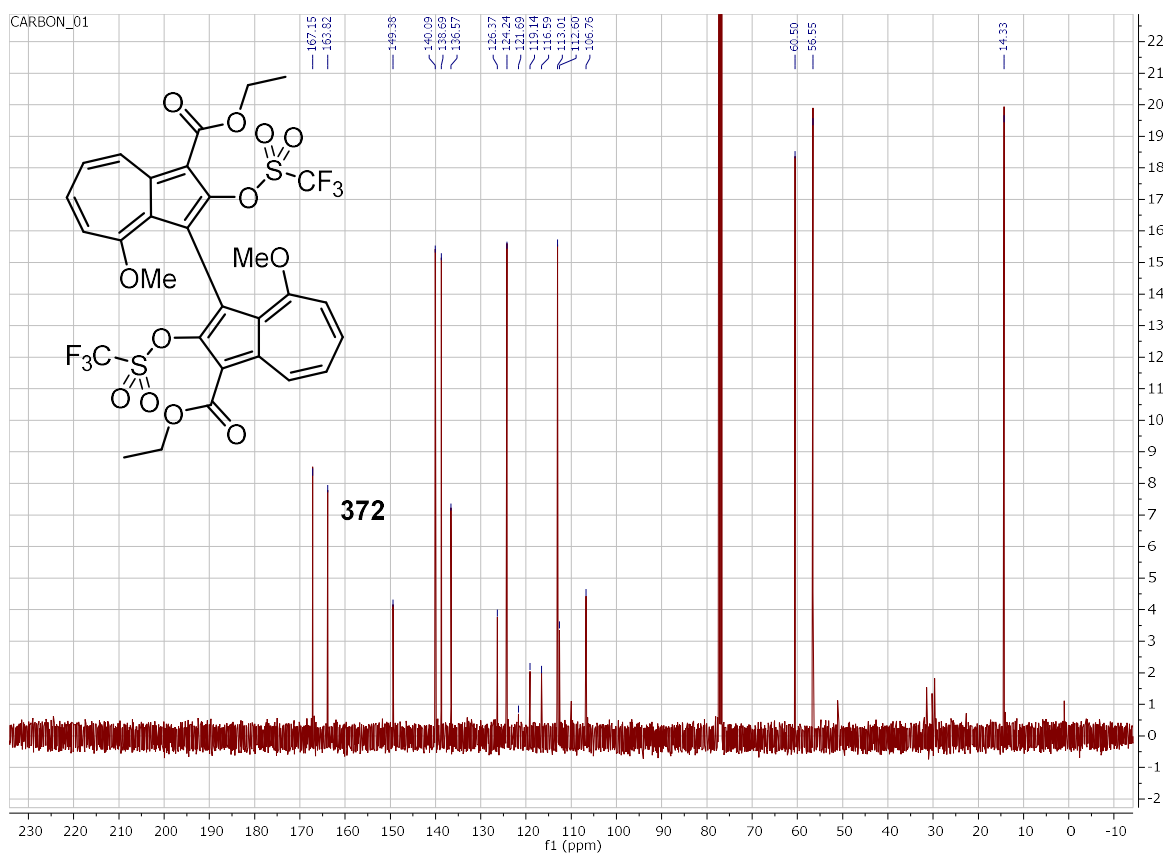
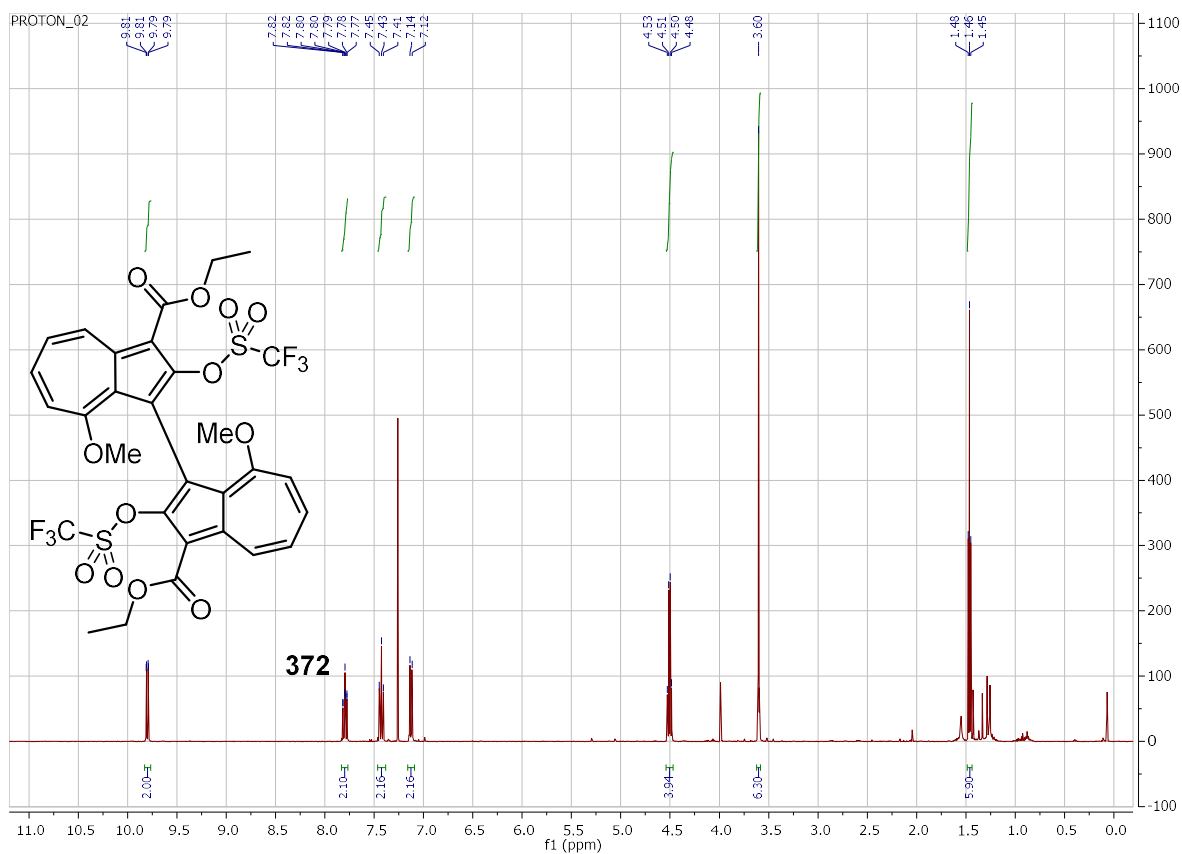


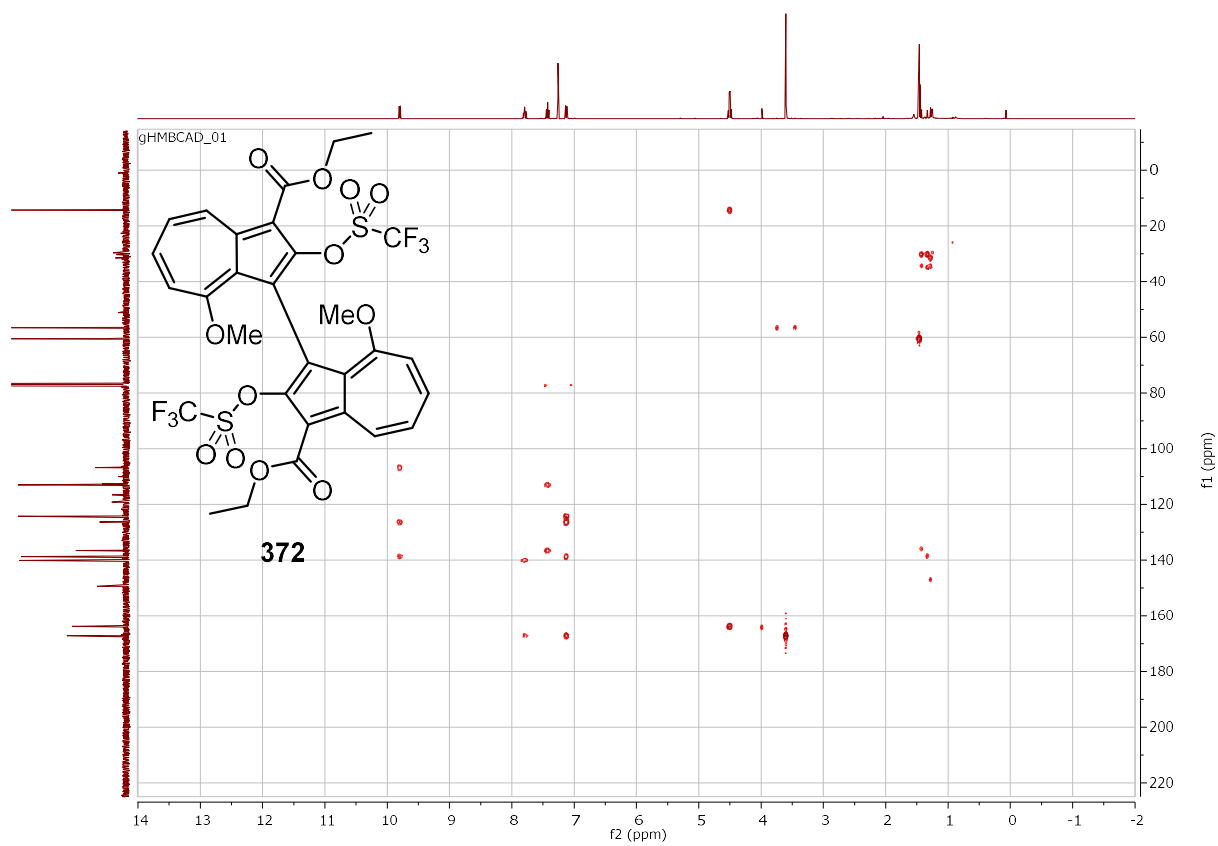
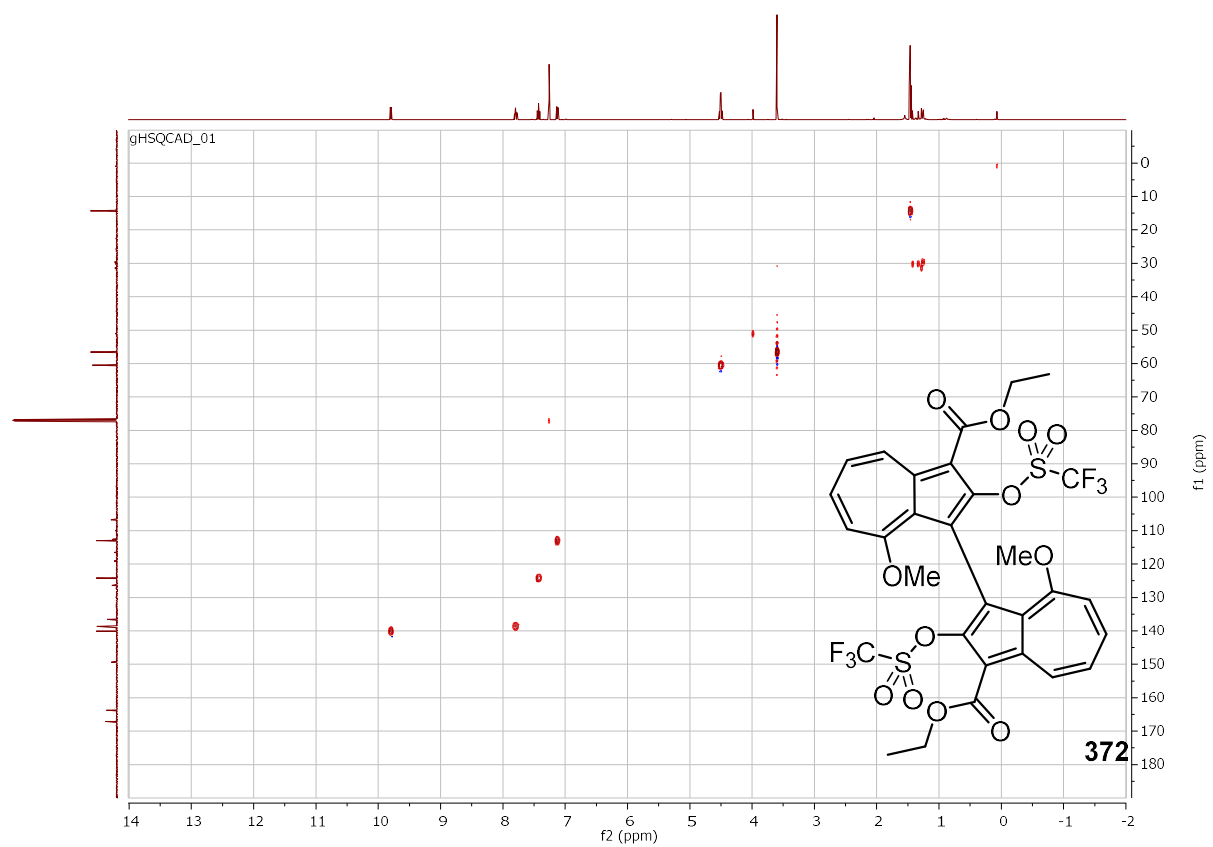


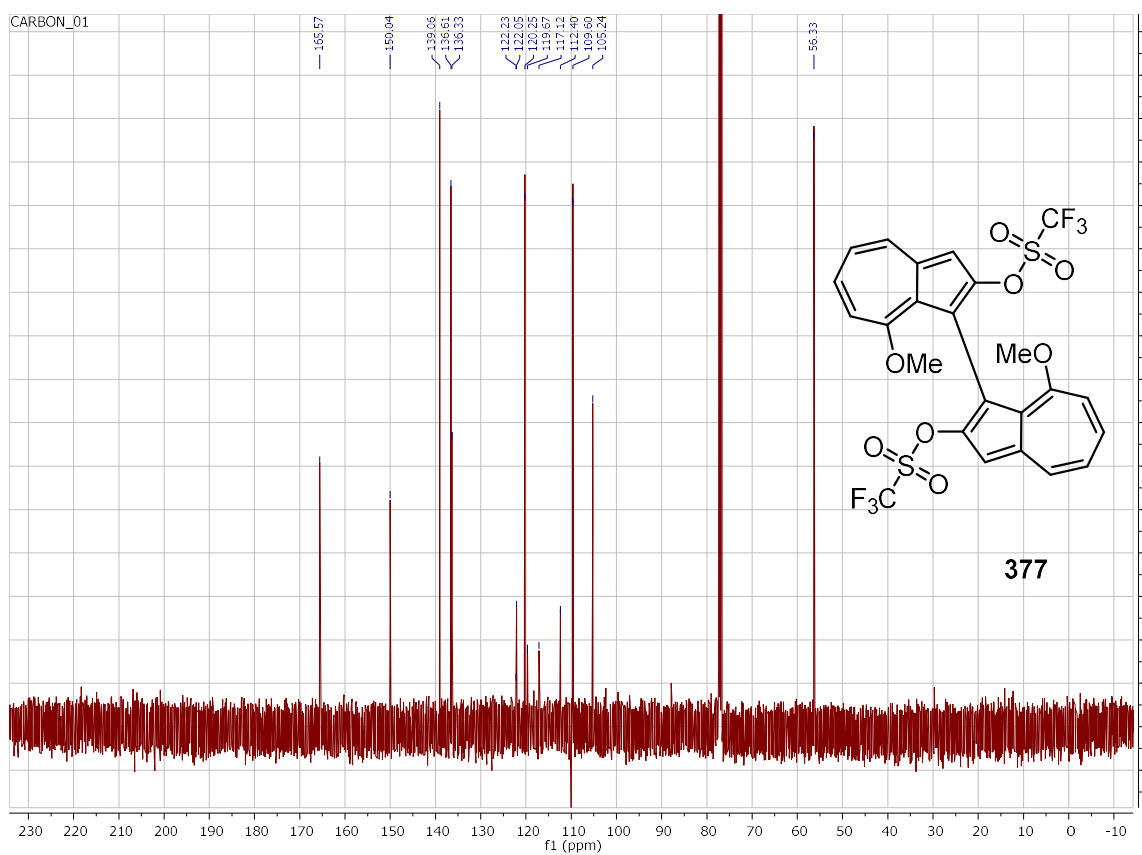
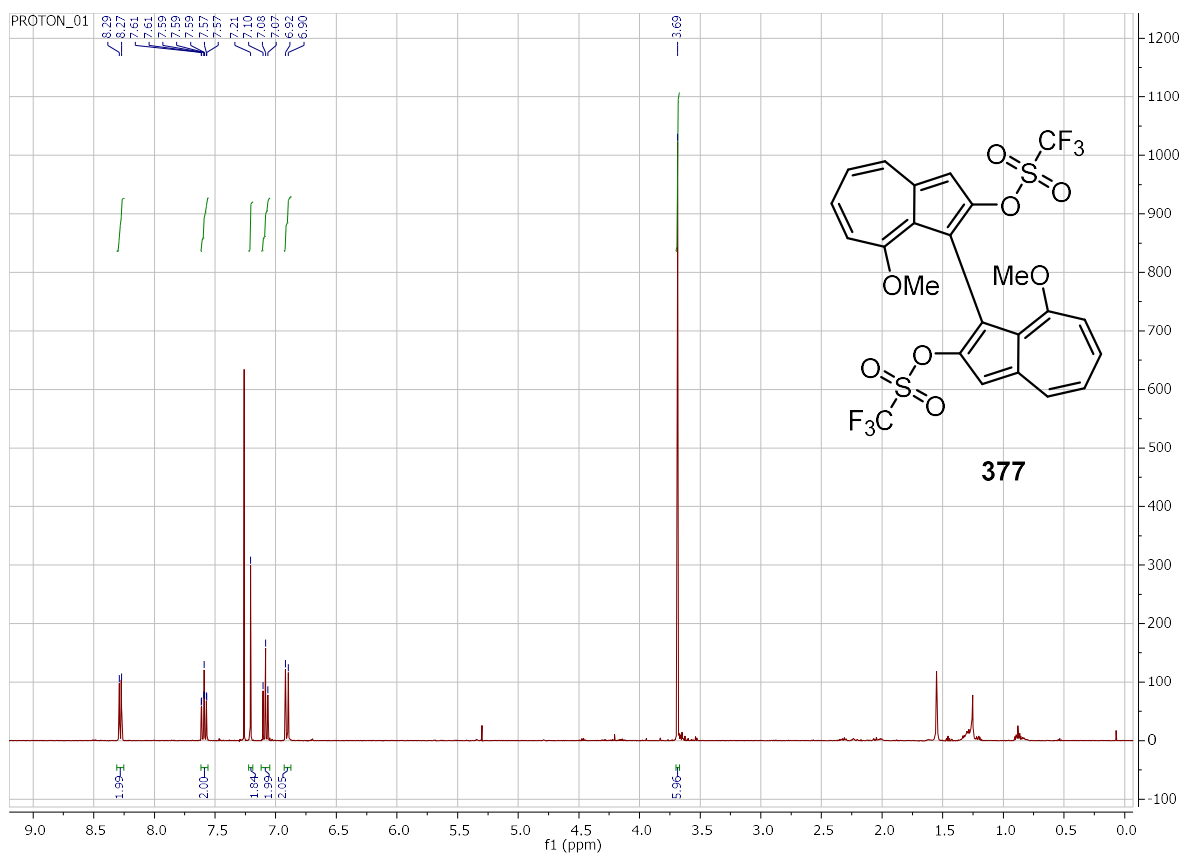


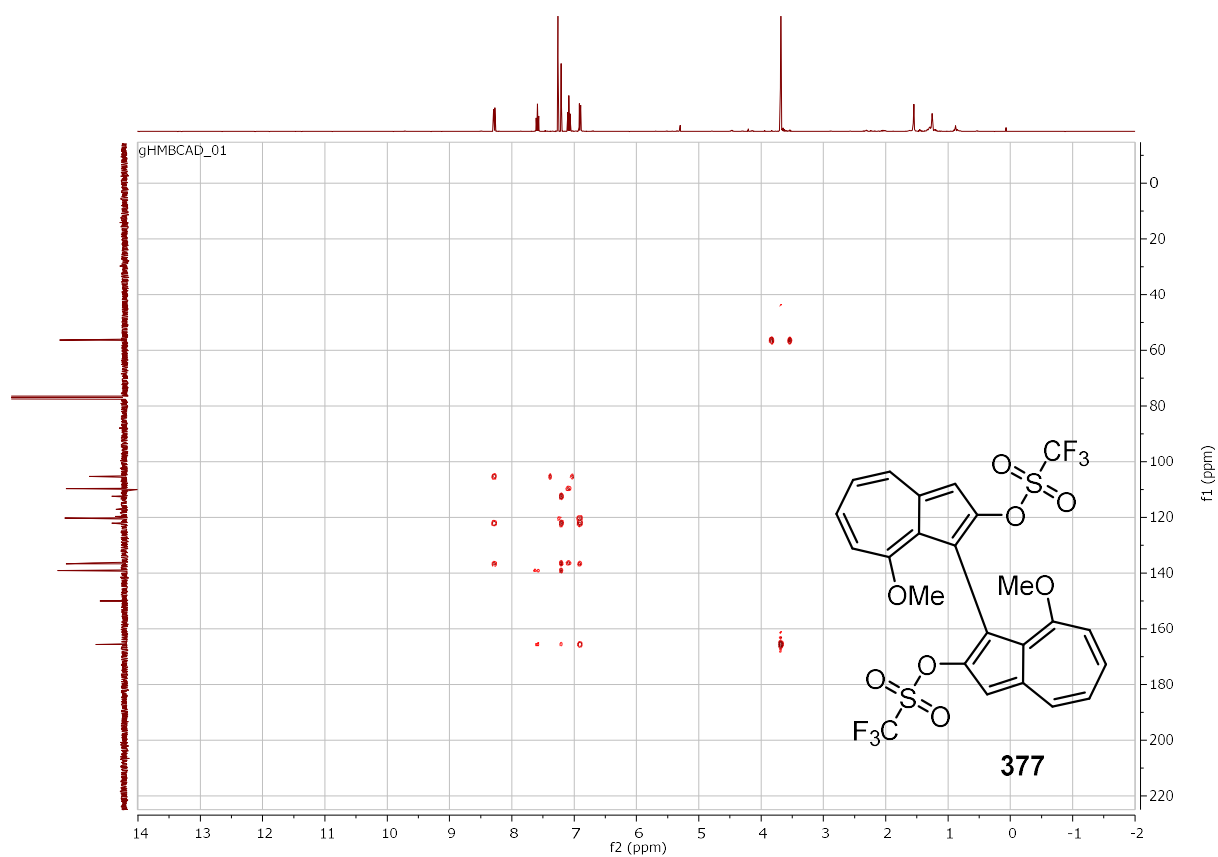
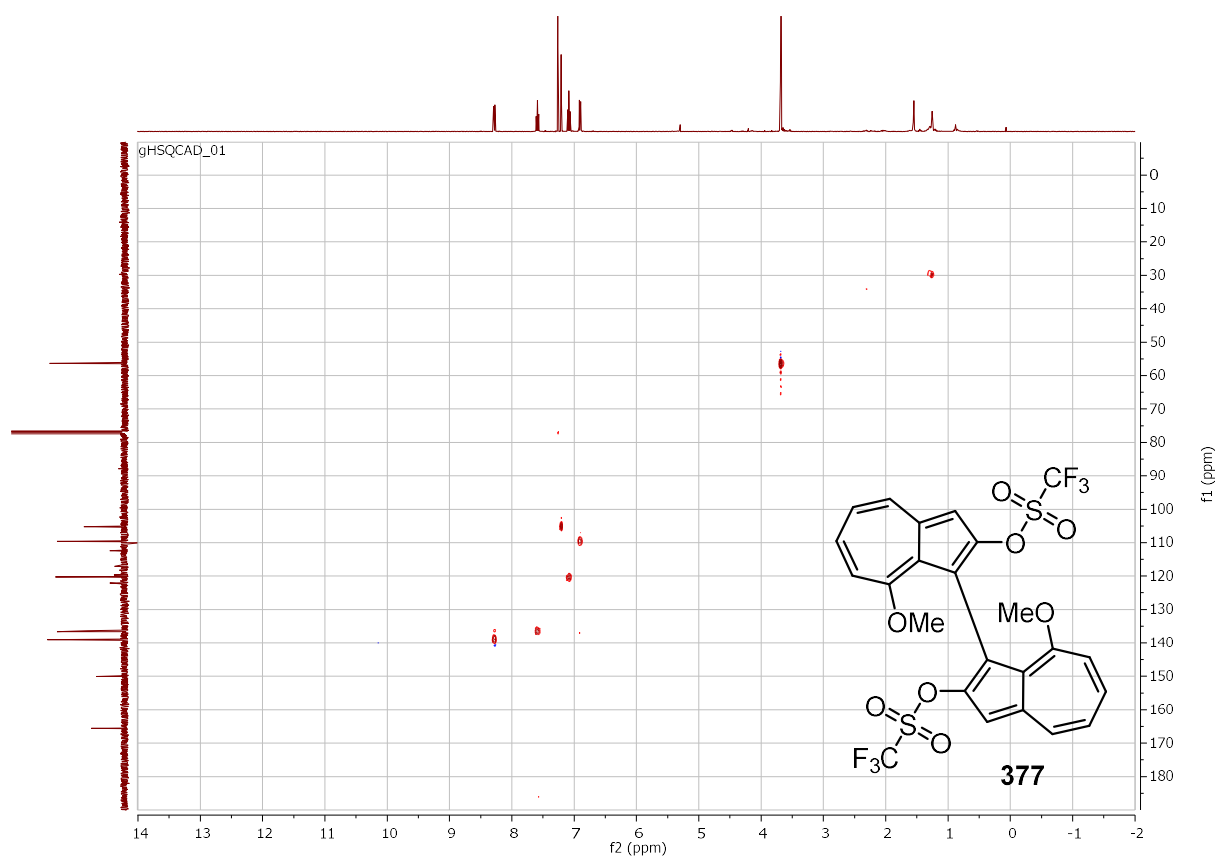


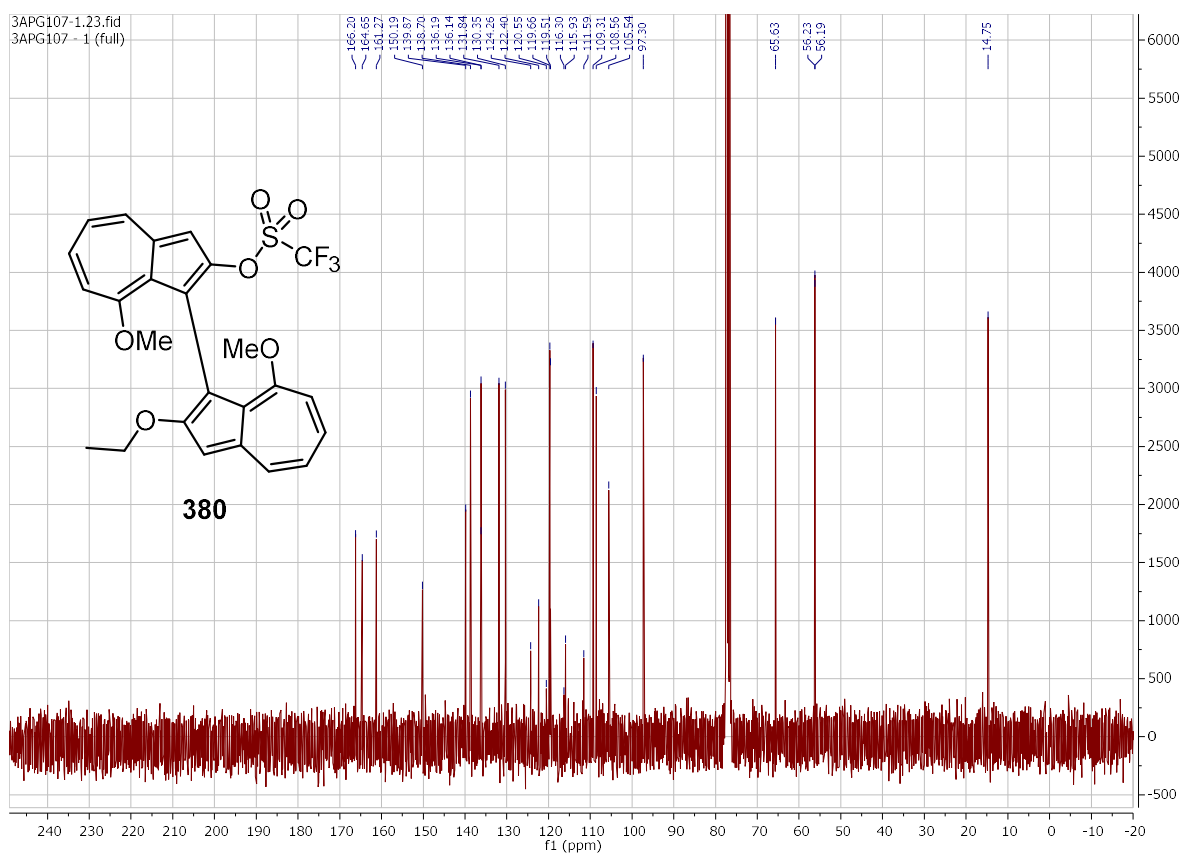
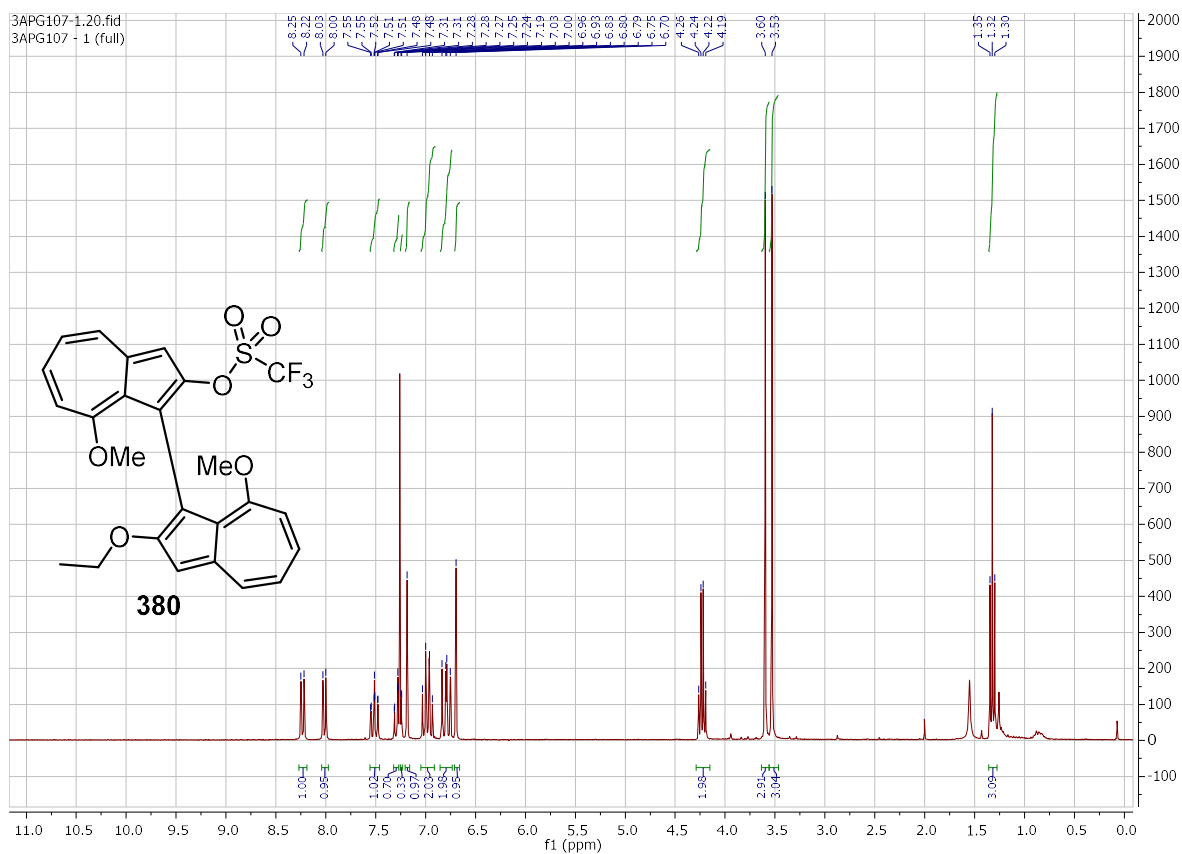


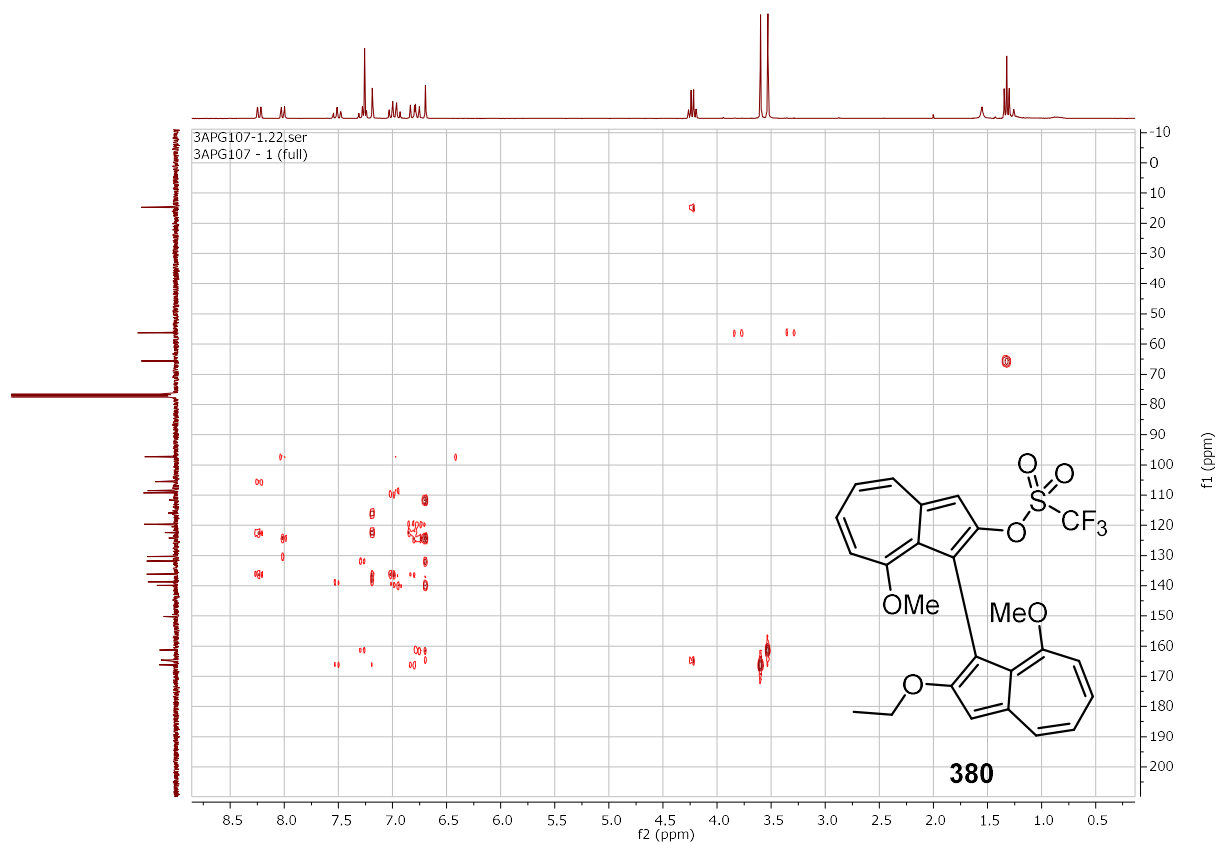
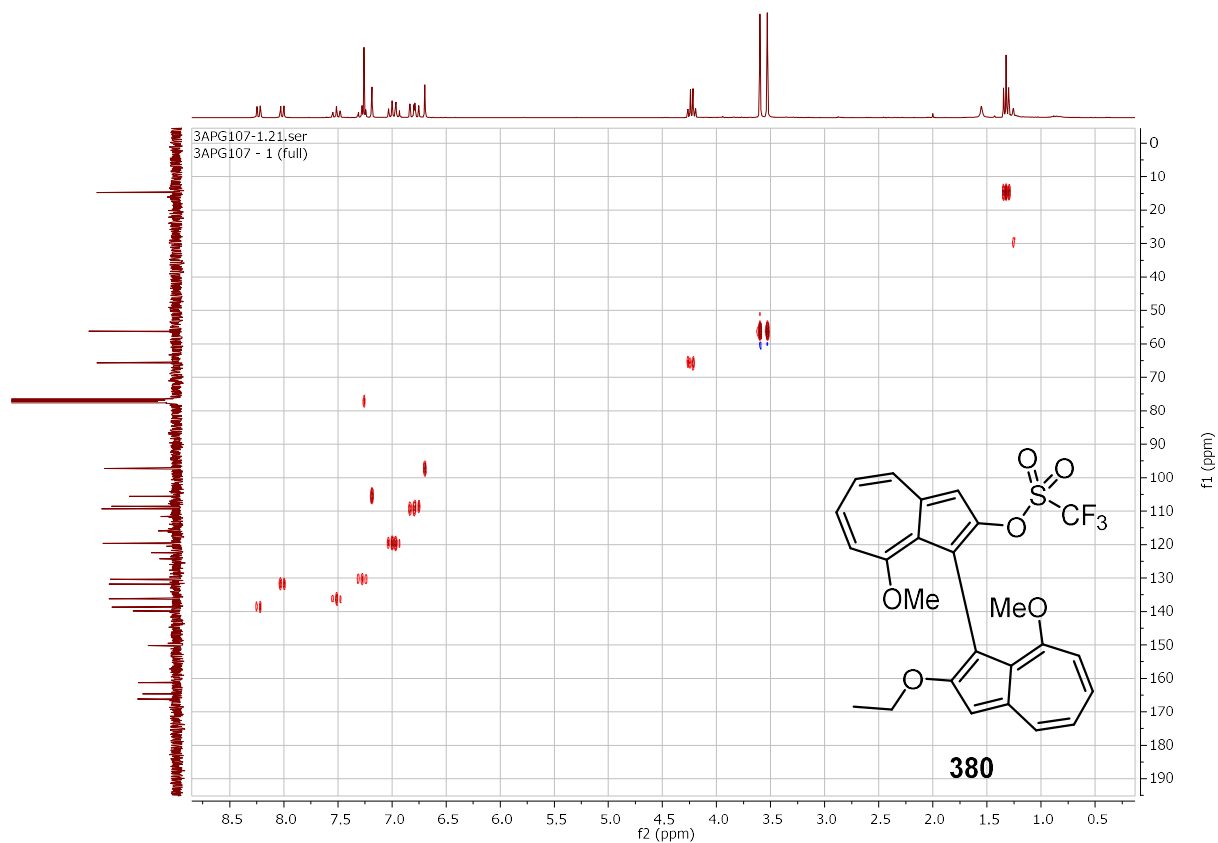


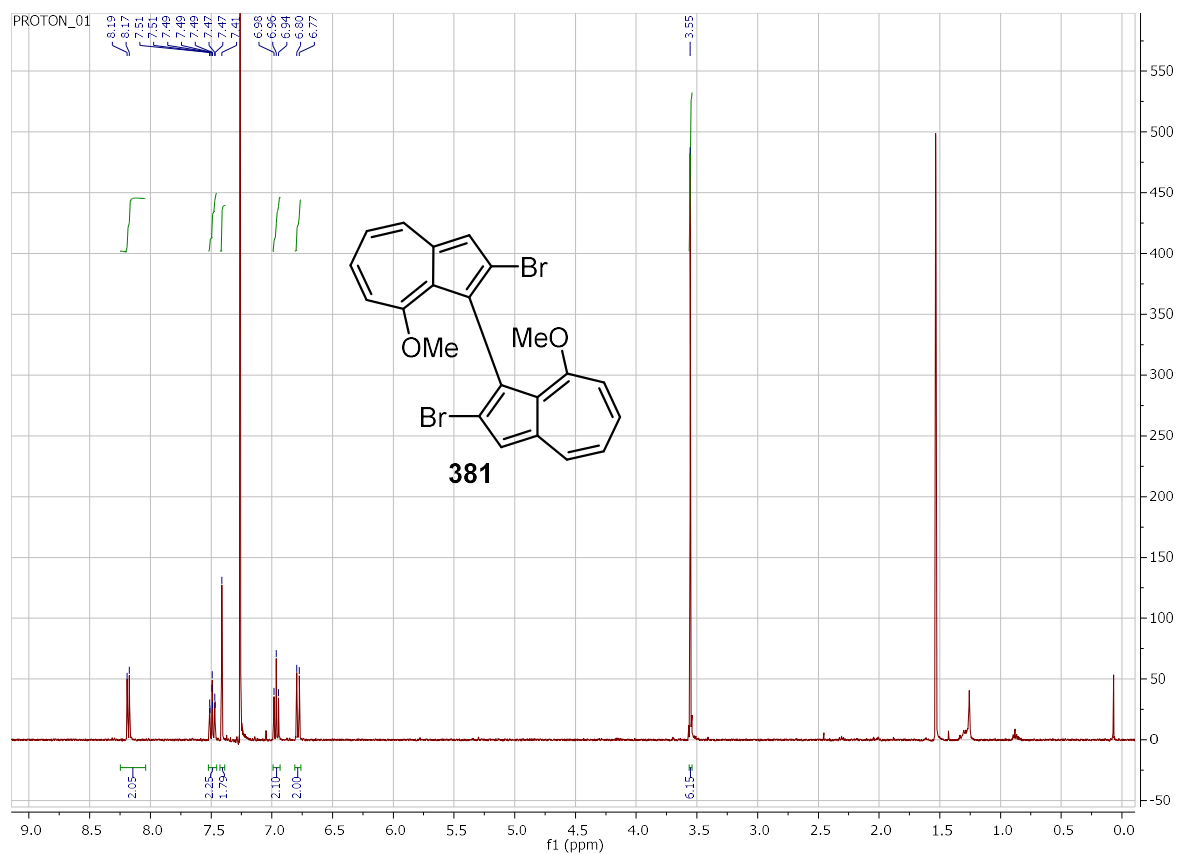




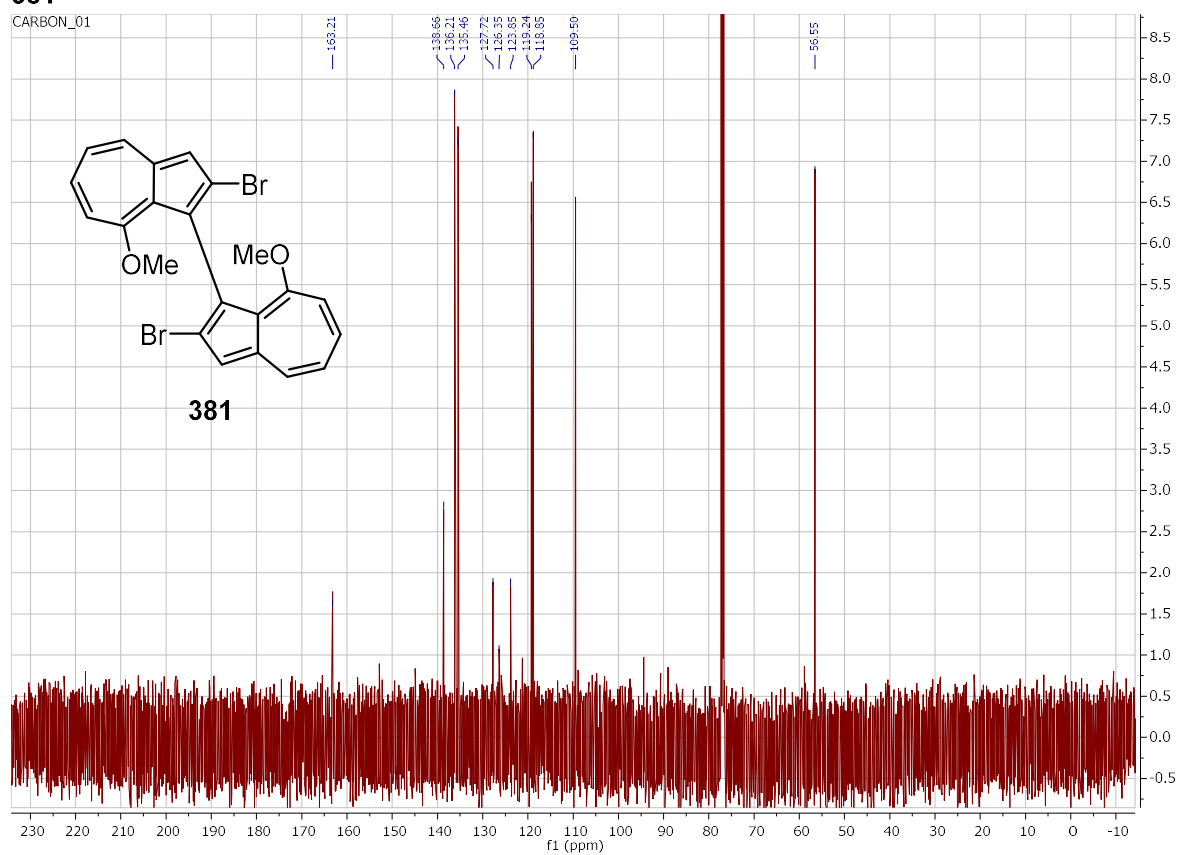


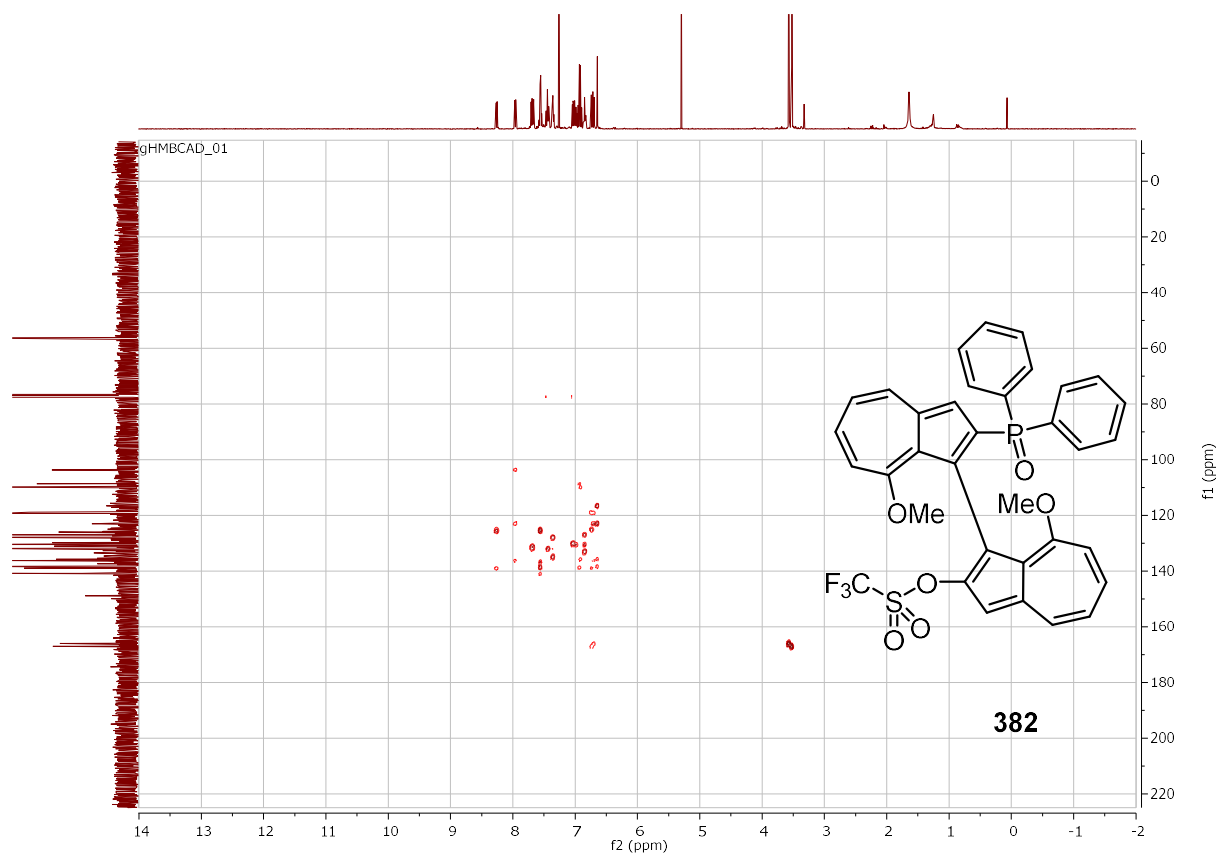
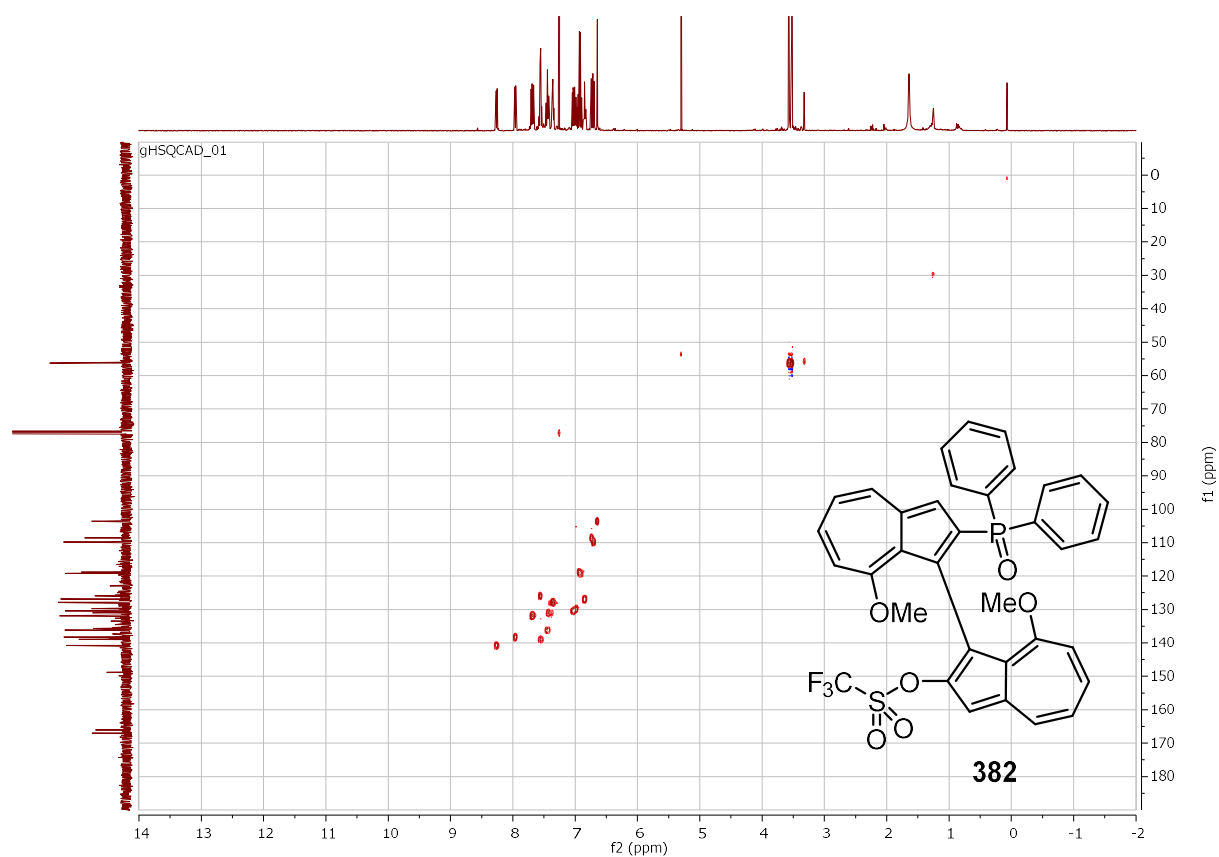






381





PHOSPHORUS_01
STANDARD PHOSPHORUS PARAMETERS

Chemical structure of compound 382 is displayed above the spectrum. The structure features a central benzene ring substituted with a trifluoromethanesulfonyl group (OTf), a methoxy group (OMe), and a phosphonate group (P(=O)(Ph)₂). The phosphonate group is attached to a phenyl ring, which is further substituted with a methoxy group (OMe) and a trifluoromethanesulfonyl group (OTf).

382

155.0

154.8

154.6

154.4

154.2

154.0

153.8

153.6

153.4

153.2

153.0

152.8

152.6

152.4

152.2

152.0

151.8

151.6

151.4

151.2

151.0

150.8

150.6

150.4

150.2

150.0

149.8

149.6

149.4

149.2

149.0

148.8

148.6

148.4

148.2

148.0

147.8

147.6

147.4

147.2

147.0

146.8

146.6

146.4

146.2

146.0

145.8

145.6

145.4

145.2

145.0

144.8

144.6

144.4

144.2

144.0

143.8

143.6

143.4

143.2

143.0

142.8

142.6

142.4

142.2

142.0

141.8

141.6

141.4

141.2

141.0

140.8

140.6

140.4

140.2

140.0

139.8

139.6

139.4

139.2

139.0

138.8

138.6

138.4

138.2

138.0

137.8

137.6

137.4

137.2

137.0

136.8

136.6

136.4

136.2

136.0

135.8

135.6

135.4

135.2

135.0

134.8

134.6

134.4

134.2

134.0

133.8

133.6

133.4

133.2

133.0

132.8

132.6

132.4

132.2

132.0

131.8

131.6

131.4

131.2

131.0

130.8

130.6

130.4

130.2

130.0

129.8

129.6

129.4

129.2

129.0

128.8

128.6

128.4

128.2

128.0

127.8

127.6

127.4

127.2

127.0

126.8

126.6

126.4

126.2

126.0

125.8

125.6

125.4

125.2

125.0

124.8

124.6

124.4

124.2

124.0

123.8

123.6

123.4

123.2

123.0

122.8

122.6

122.4

122.2

122.0

121.8

121.6

121.4

121.2

121.0

120.8

120.6

120.4

120.2

120.0

119.8

119.6

119.4

119.2

119.0

118.8

118.6

118.4

118.2

118.0

117.8

117.6

117.4

117.2

117.0

116.8

116.6

116.4

116.2

116.0

115.8

115.6

115.4

115.2

115.0

114.8

114.6

114.4

114.2

114.0

113.8

113.6

113.4

113.2

113.0

112.8

112.6

112.4

112.2

112.0

111.8

111.6

111.4

111.2

111.0

110.8

110.6

110.4

110.2

110.0

109.8

109.6

109.4

109.2

109.0

108.8

108.6

108.4

108.2

108.0

107.8

107.6

107.4

107.2

107.0

106.8

106.6

106.4

106.2

106.0

105.8

105.6

105.4

105.2

105.0

104.8

104.6

104.4

104.2

104.0

103.8

103.6

103.4

103.2

103.0

102.8

102.6

102.4

102.2

102.0

101.8

101.6

101.4

101.2

101.0

100.8

100.6

100.4

100.2

100.0

99.8

99.6

99.4

99.2

99.0

98.8

98.6

98.4

98.2

98.0

97.8

97.6

97.4

97.2

97.0

96.8

96.6

96.4

96.2

96.0

95.8

95.6

95.4

95.2

95.0

94.8

94.6

94.4

94.2

94.0

93.8

93.6

93.4

93.2

93.0

92.8

92.6

92.4

92.2

92.0

91.8

91.6

91.4

91.2

91.0

90.8

90.6

90.4

90.2

90.0

89.8

89.6

89.4

89.2

89.0

88.8

88.6

88.4

88.2

88.0

87.8

87.6

87.4

87.2

87.0

86.8

86.6

86.4

86.2

86.0

85.8

85.6

85.4

85.2

85.0

84.8

84.6

84.4

84.2

84.0

83.8

83.6

83.4

83.2

83.0

82.8

82.6

82.4

82.2

82.0

81.8

81.6

81.4

81.2

81.0

80.8

80.6

80.4

80.2

80.0

79.8

79.6

79.4

79.2

79.0

78.8

78.6

78.4

78.2

78.0

77.8

77.6

77.4

77.2

77.0

76.8

76.6

76.4

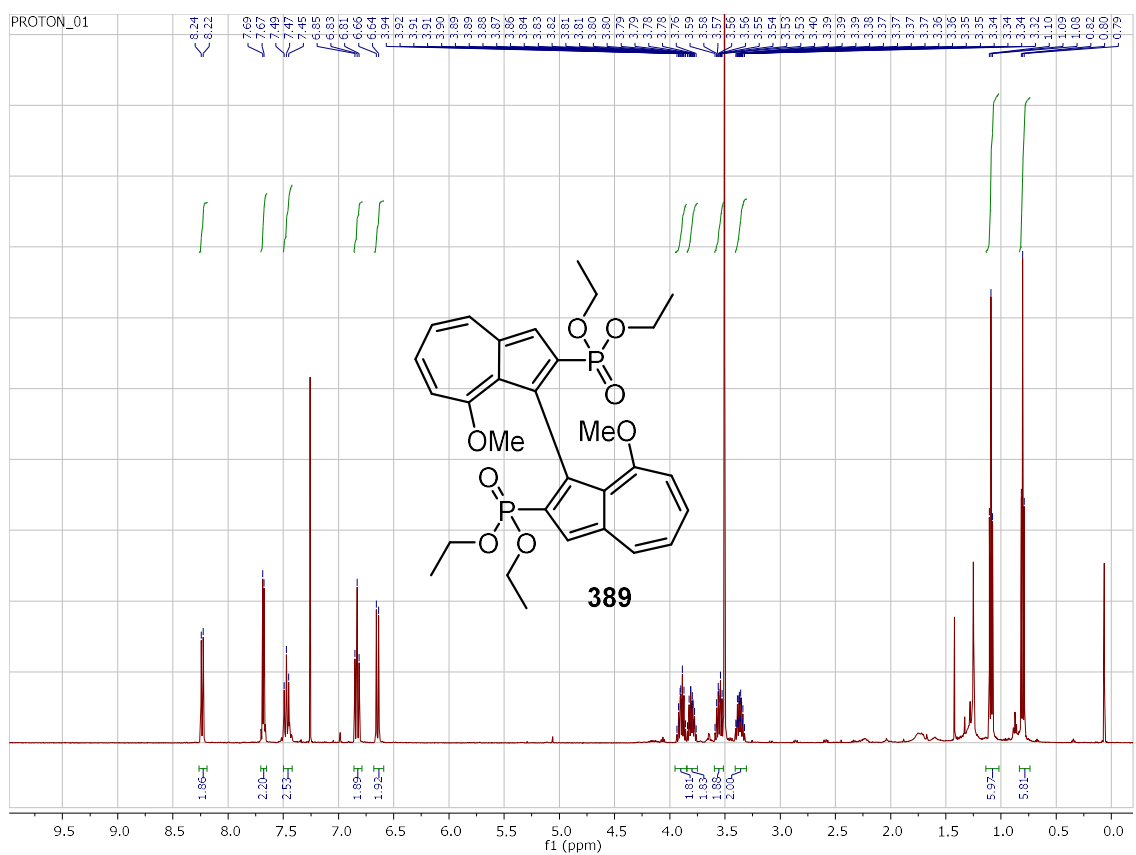
76.2

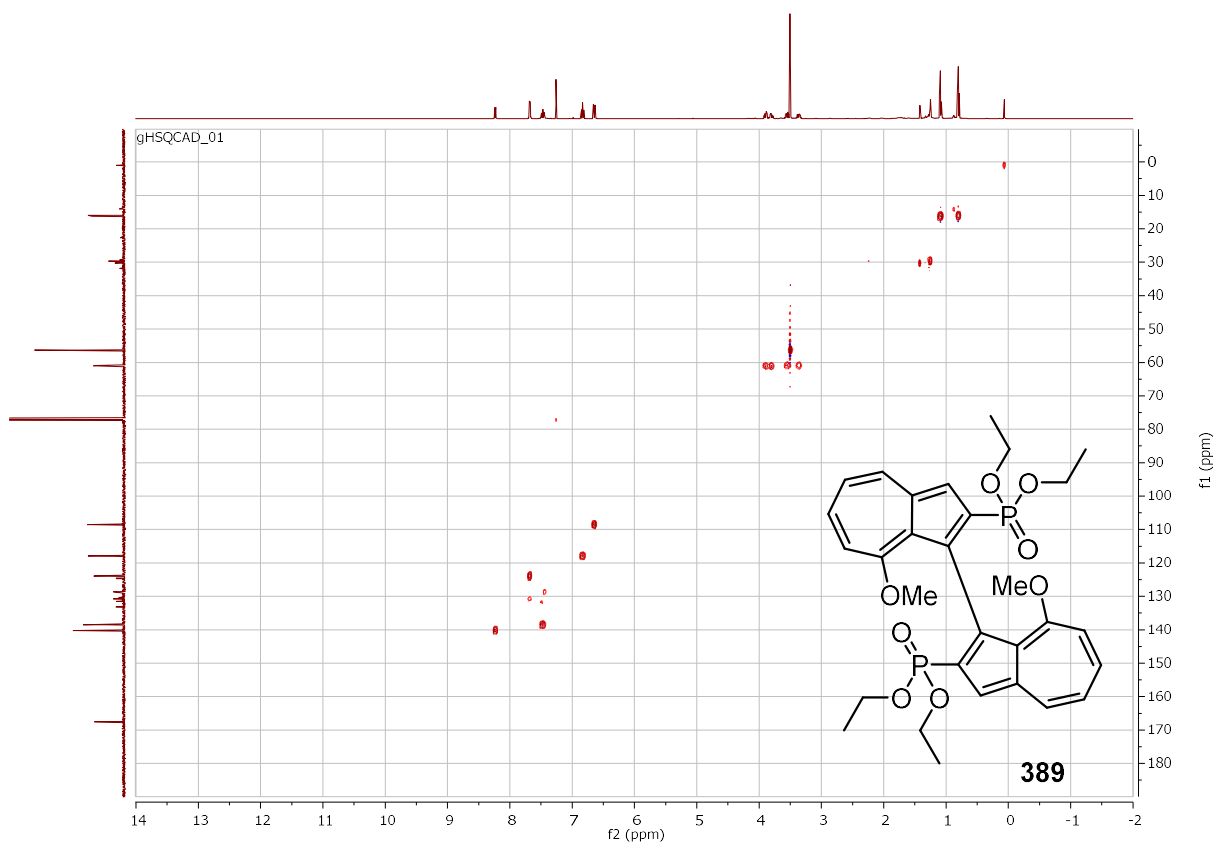
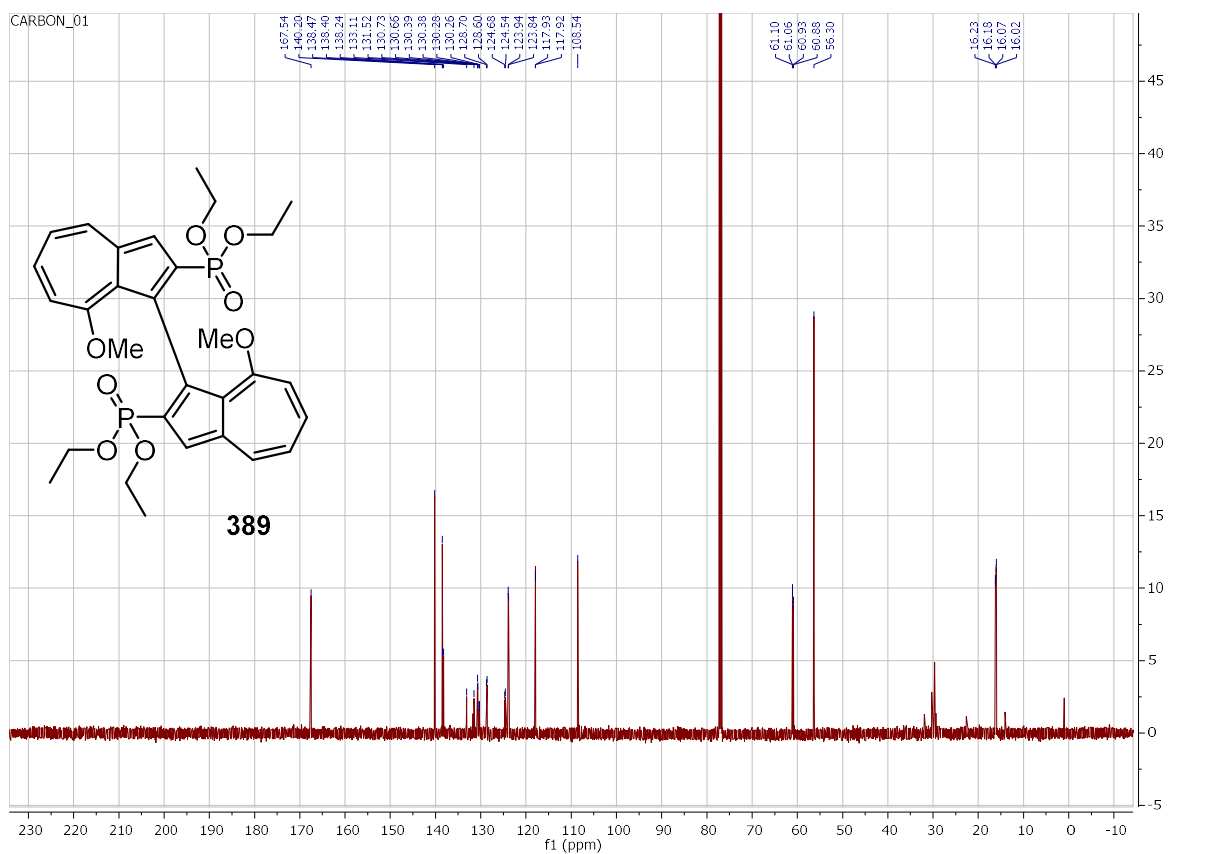
76.0

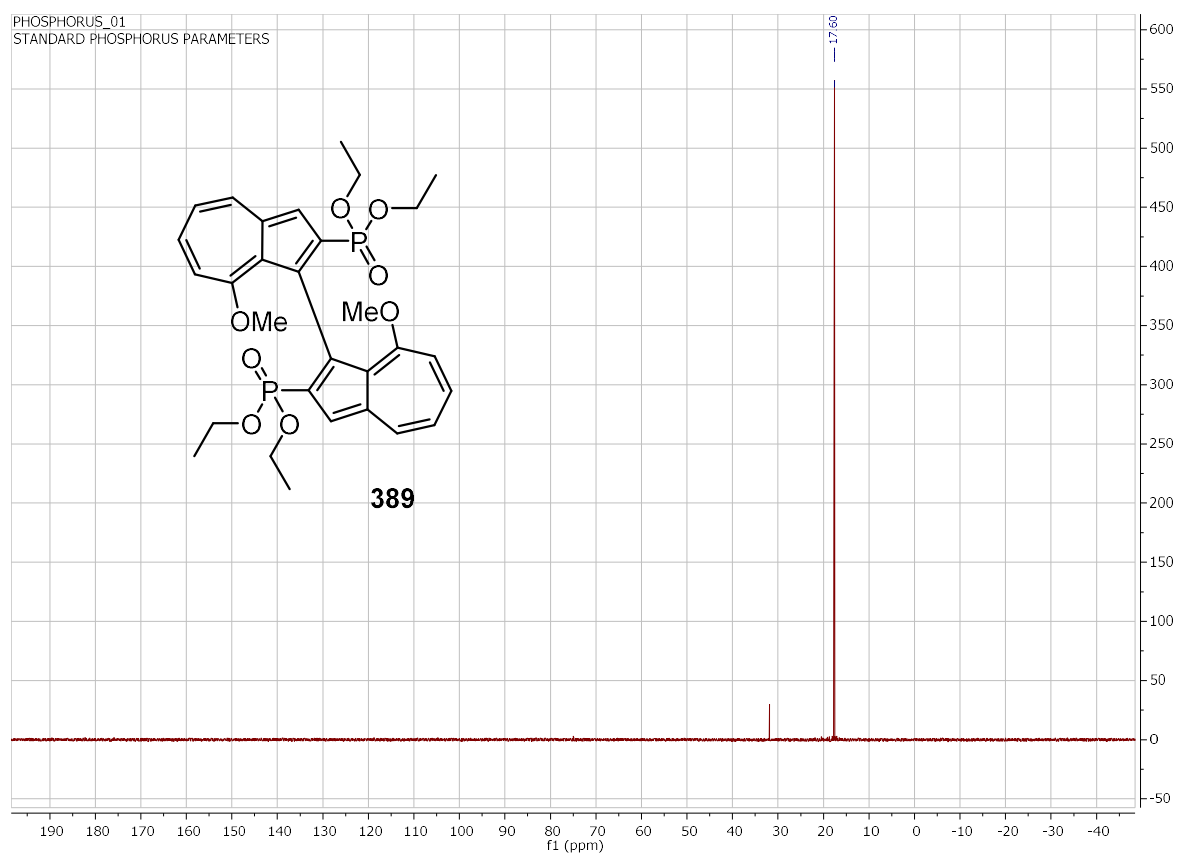
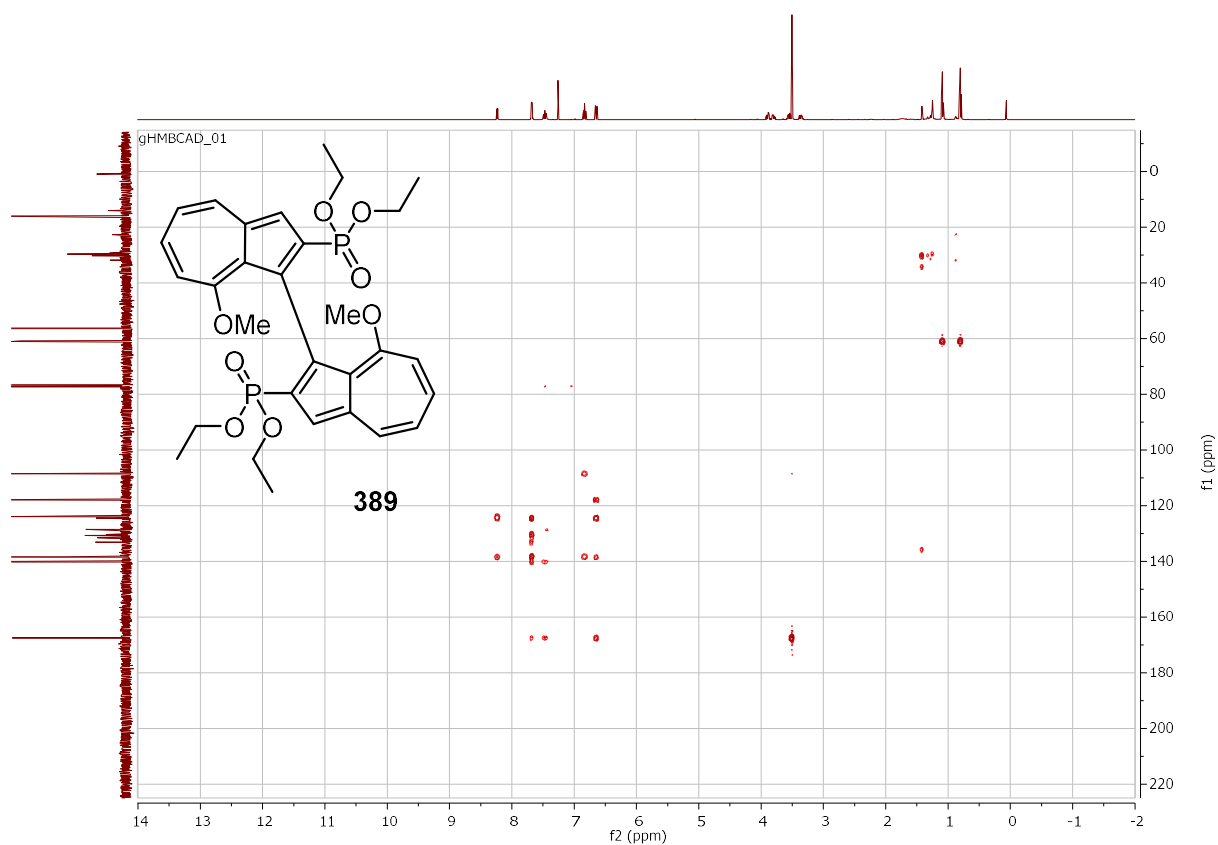
75.8

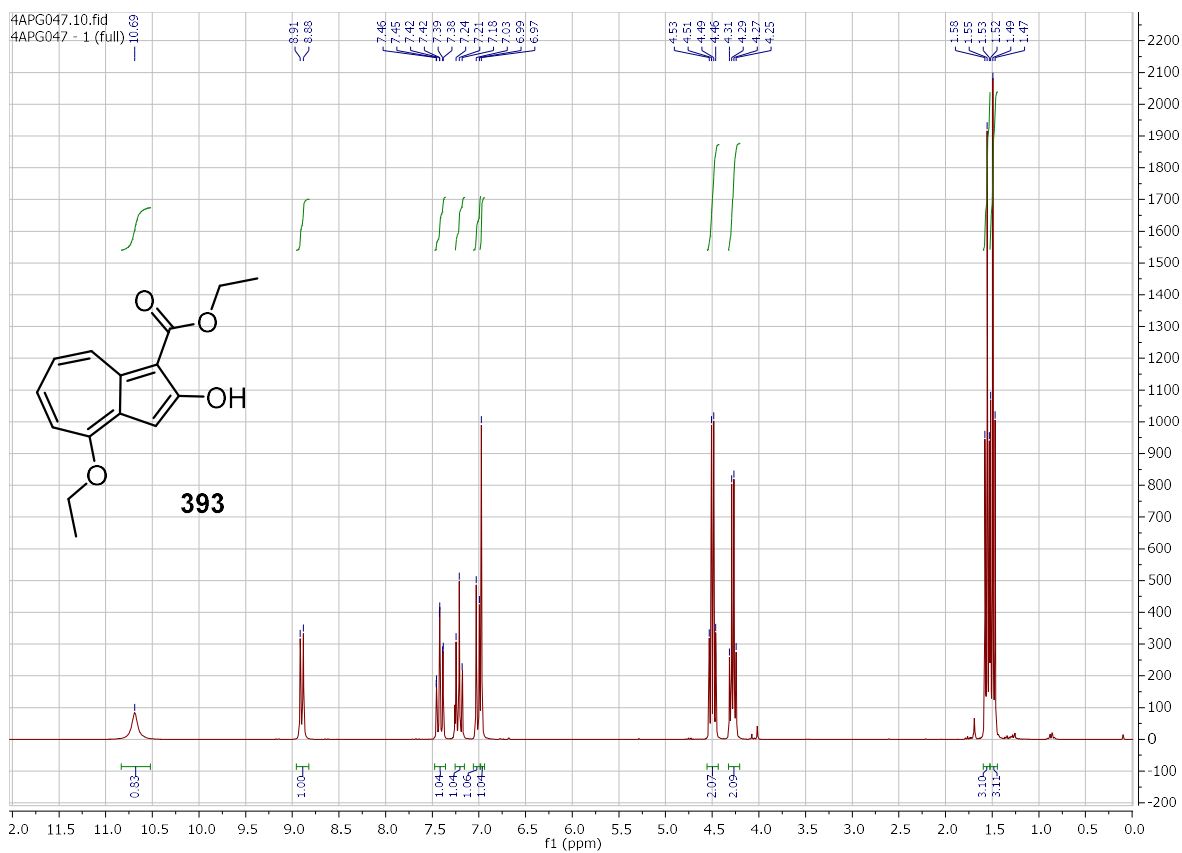
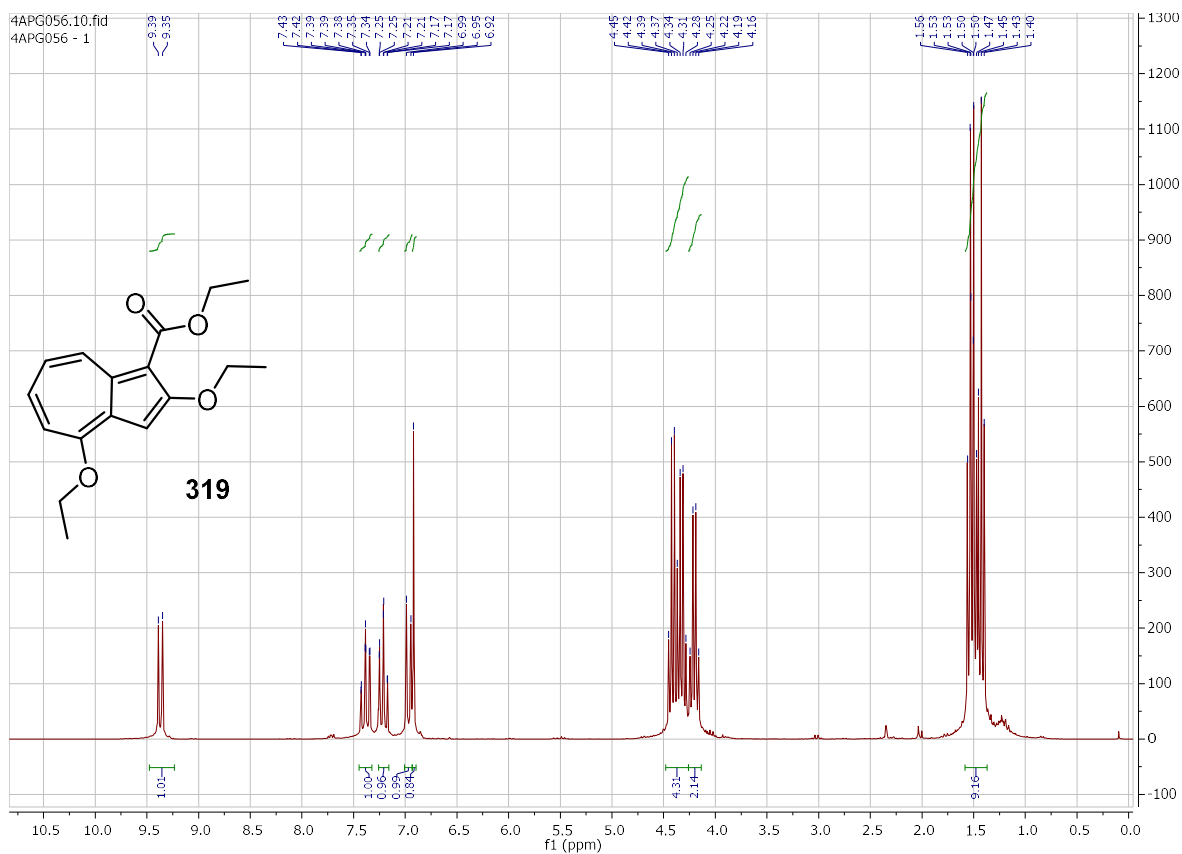
75.6

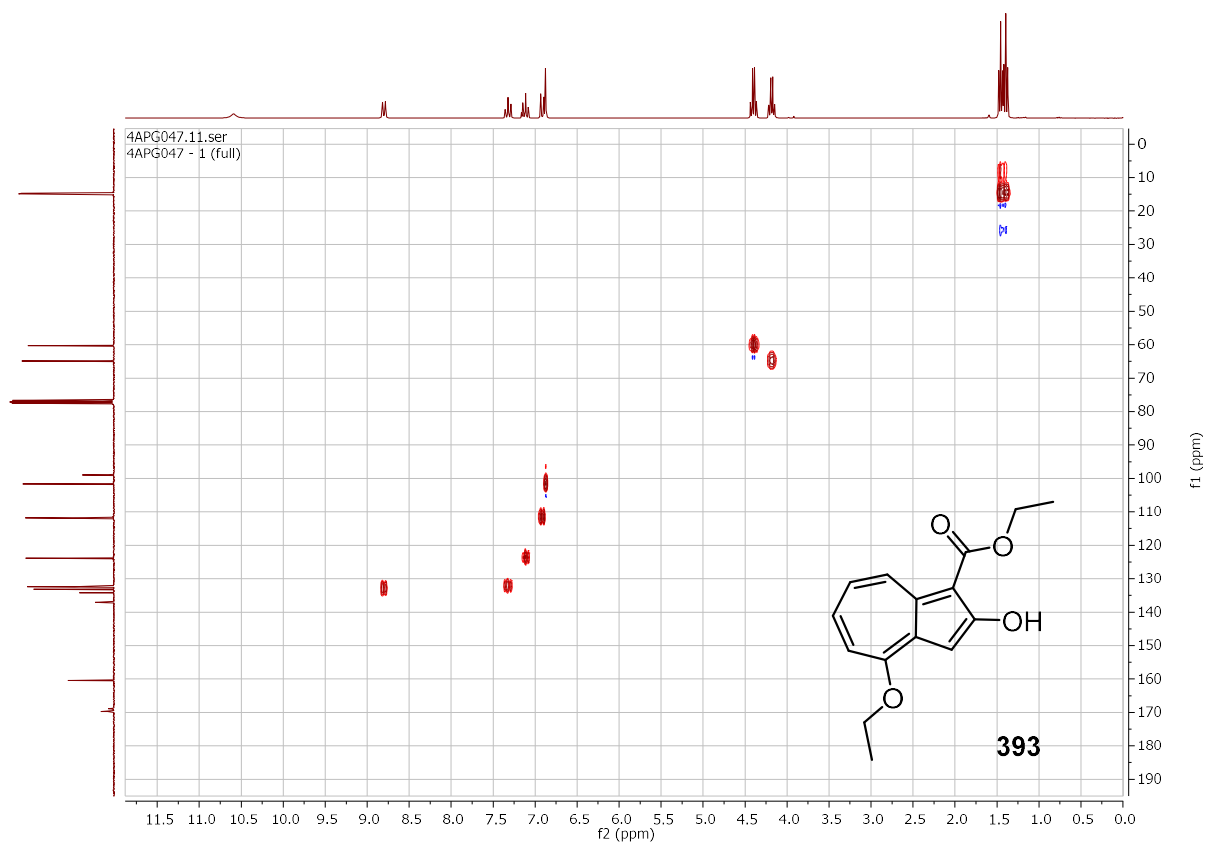
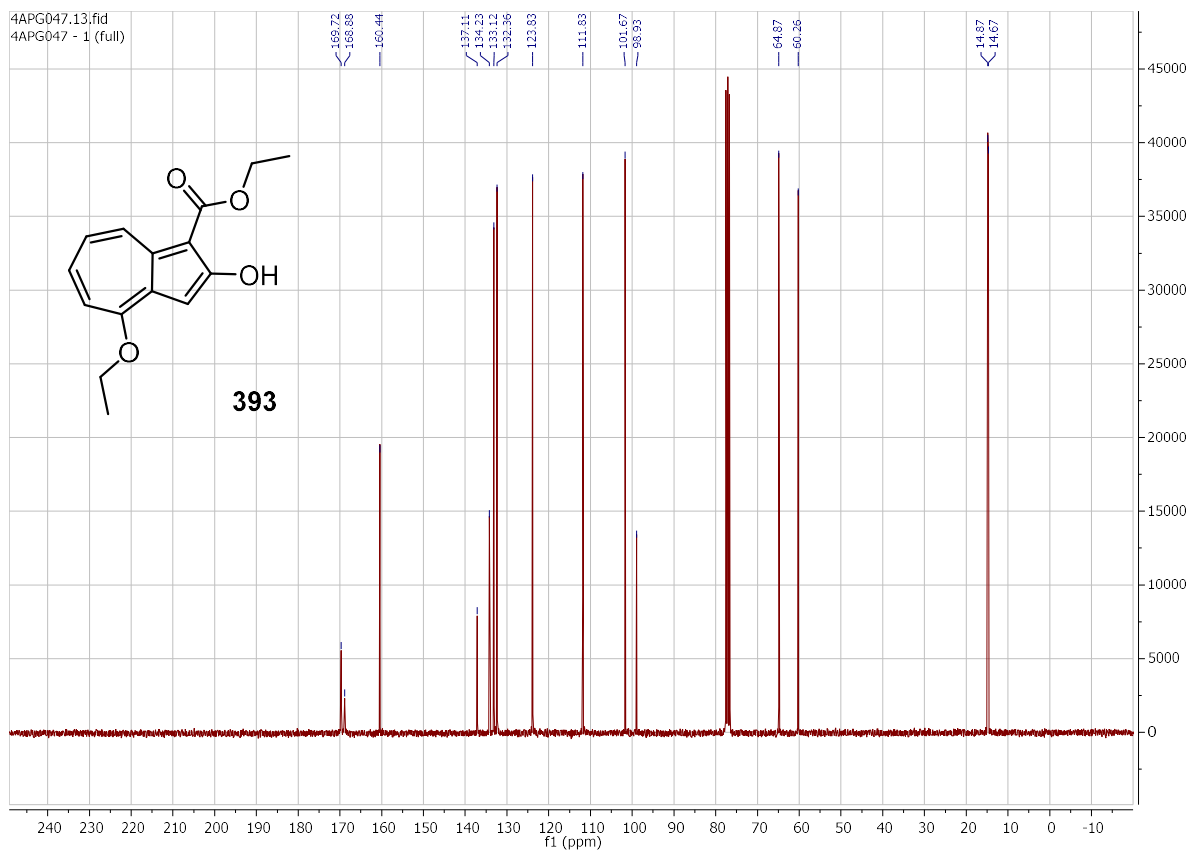
75.4

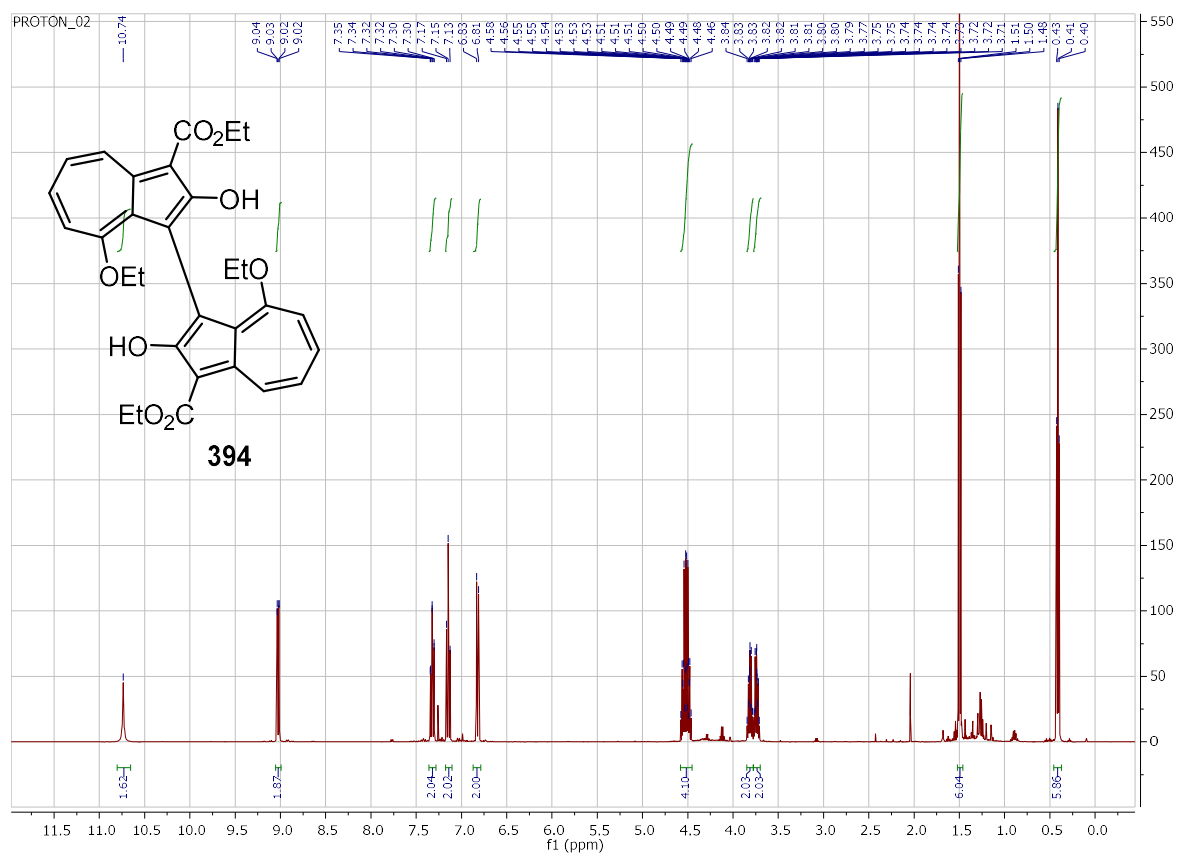
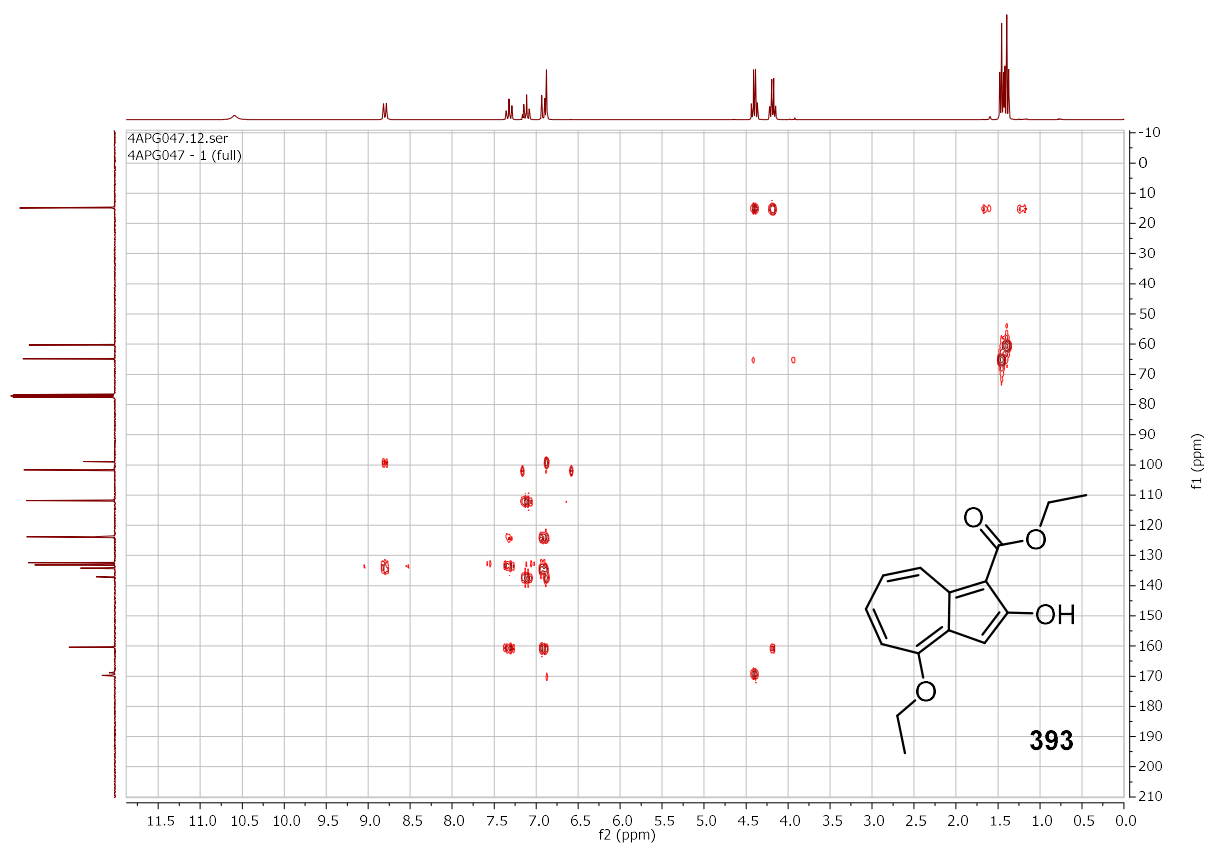


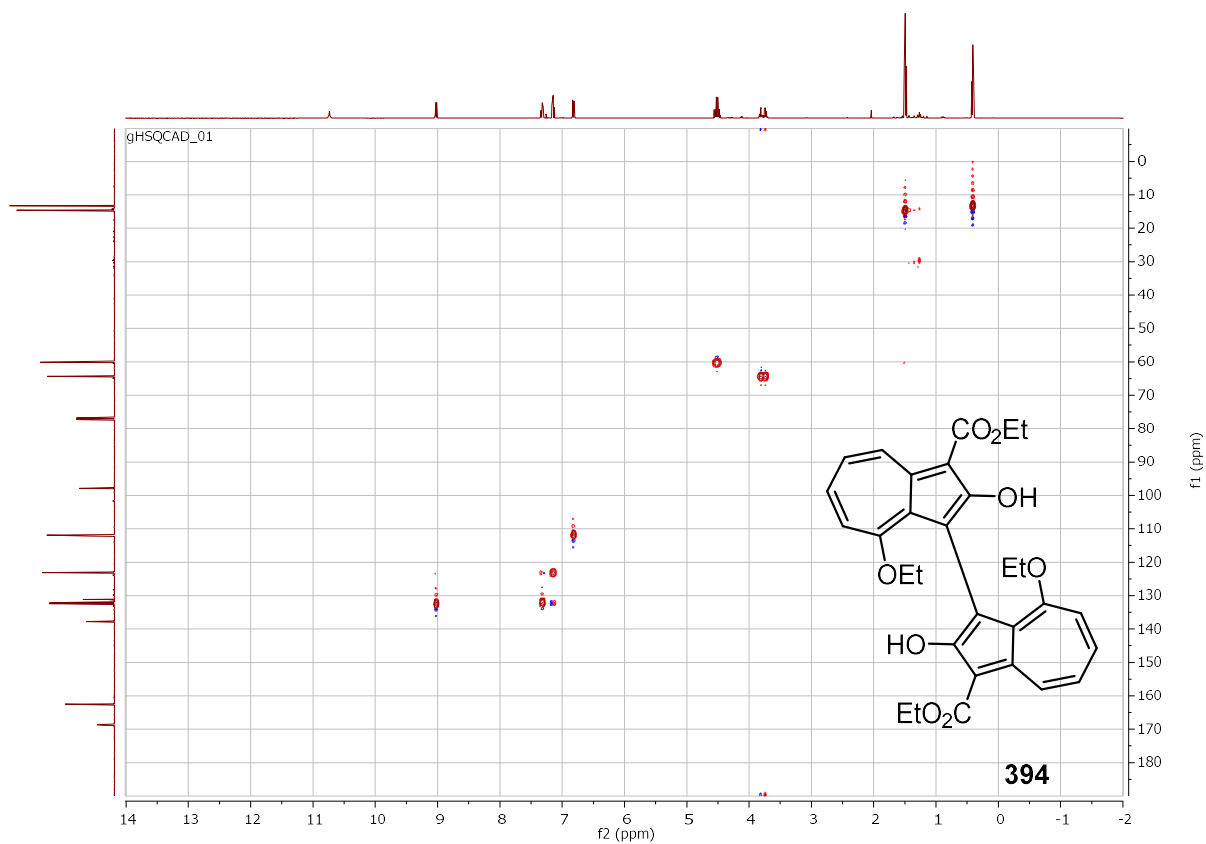
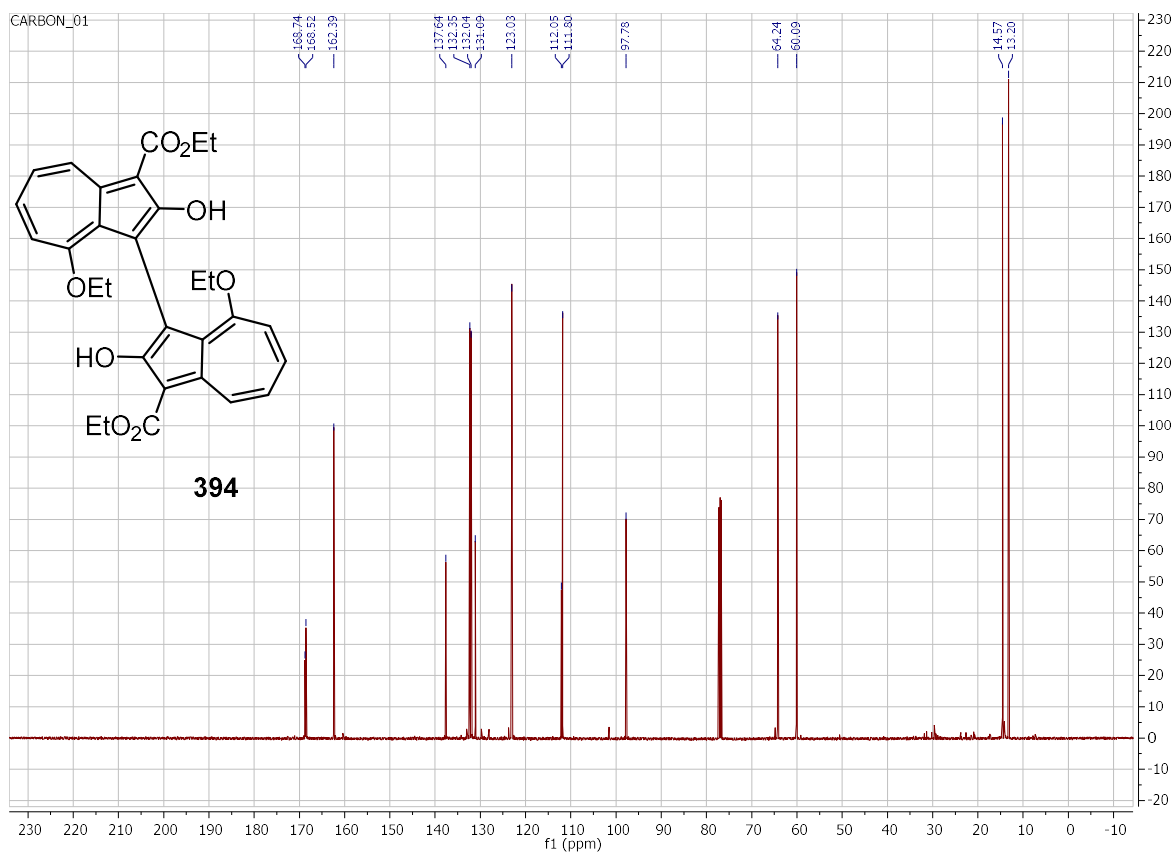


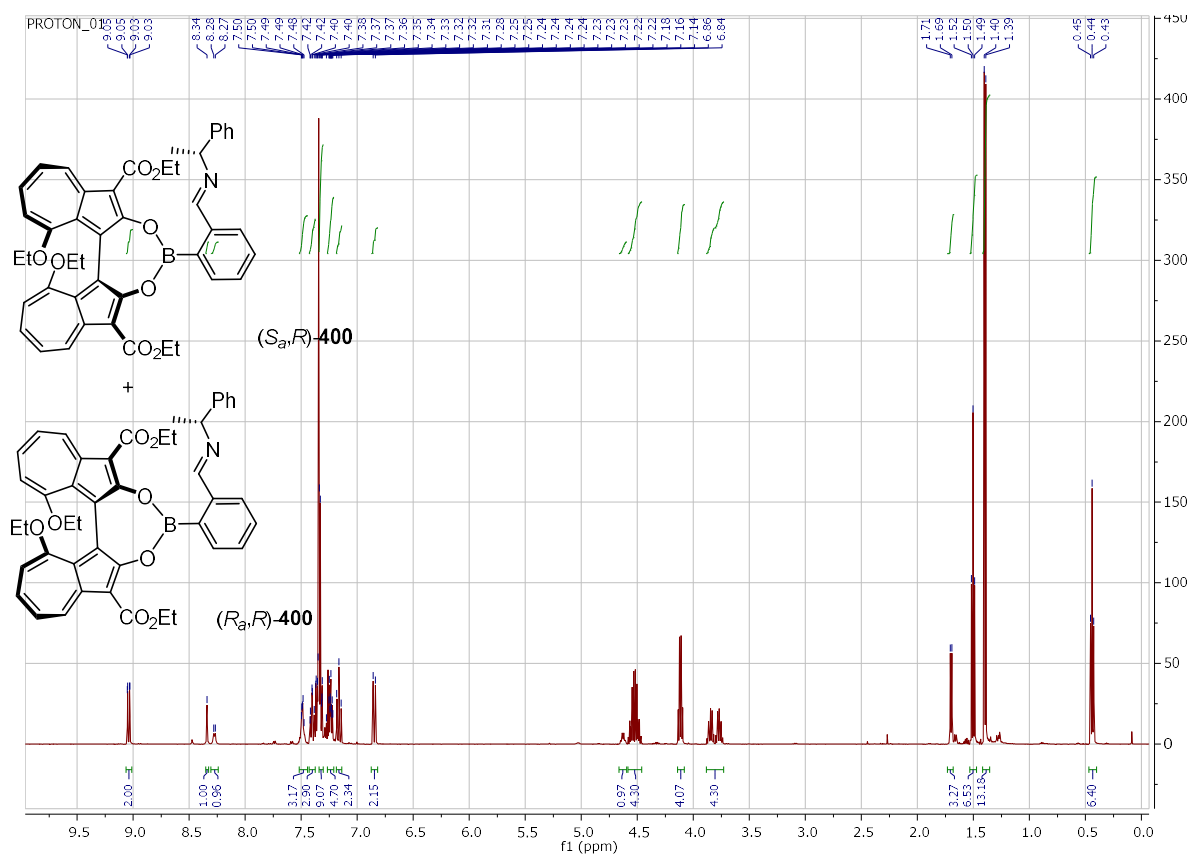
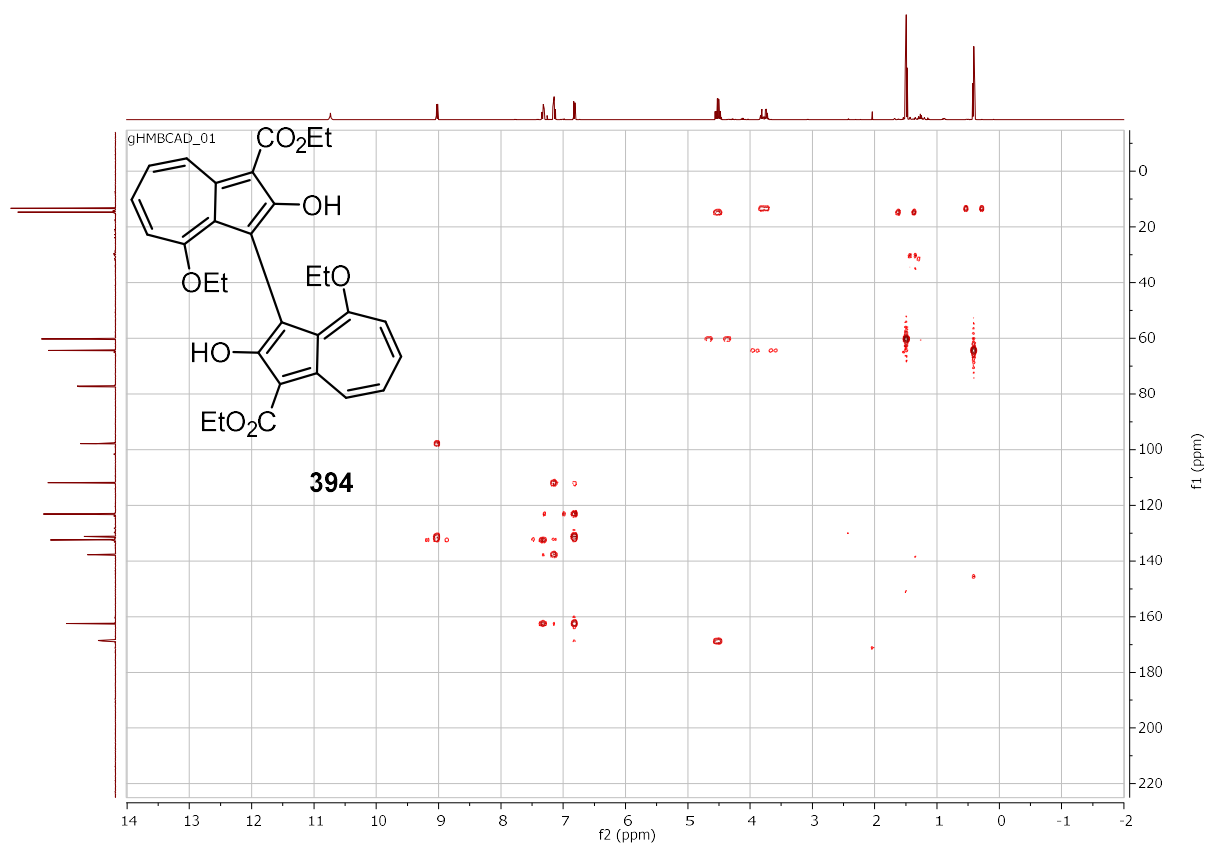


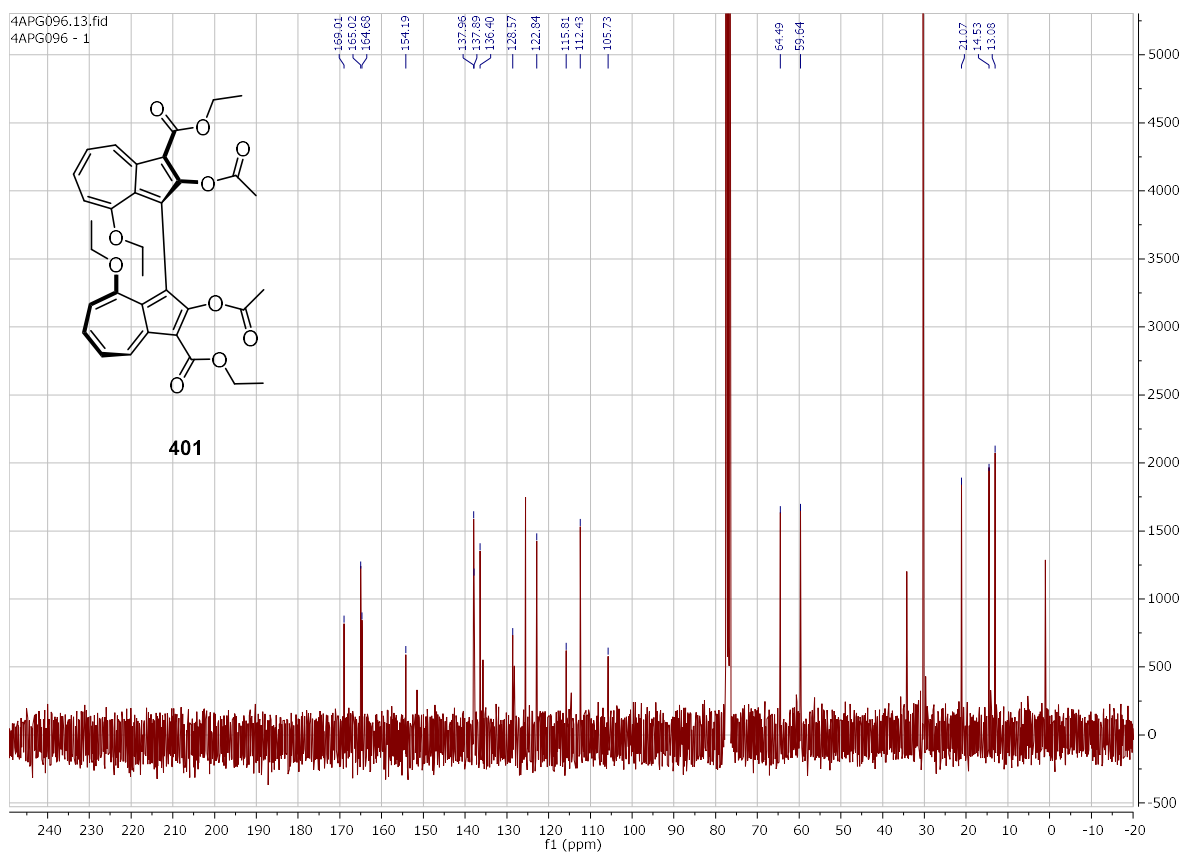
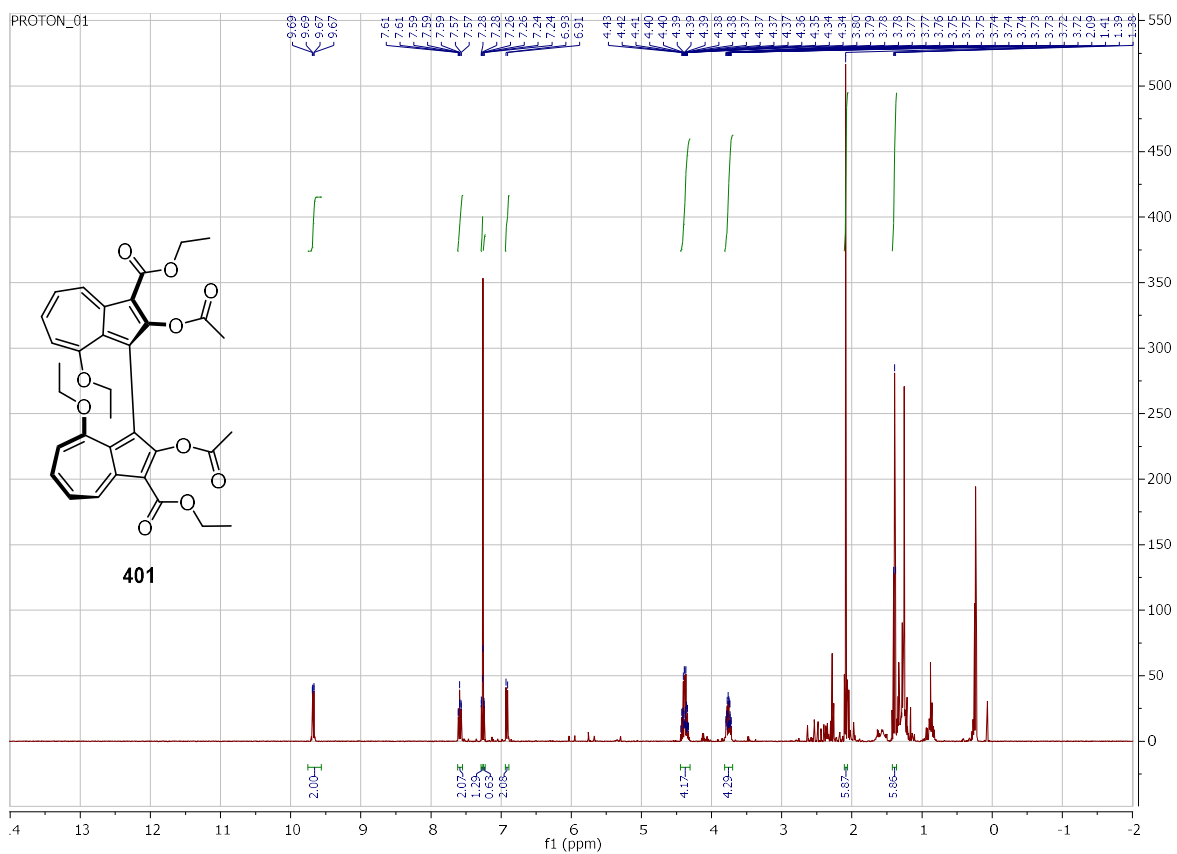


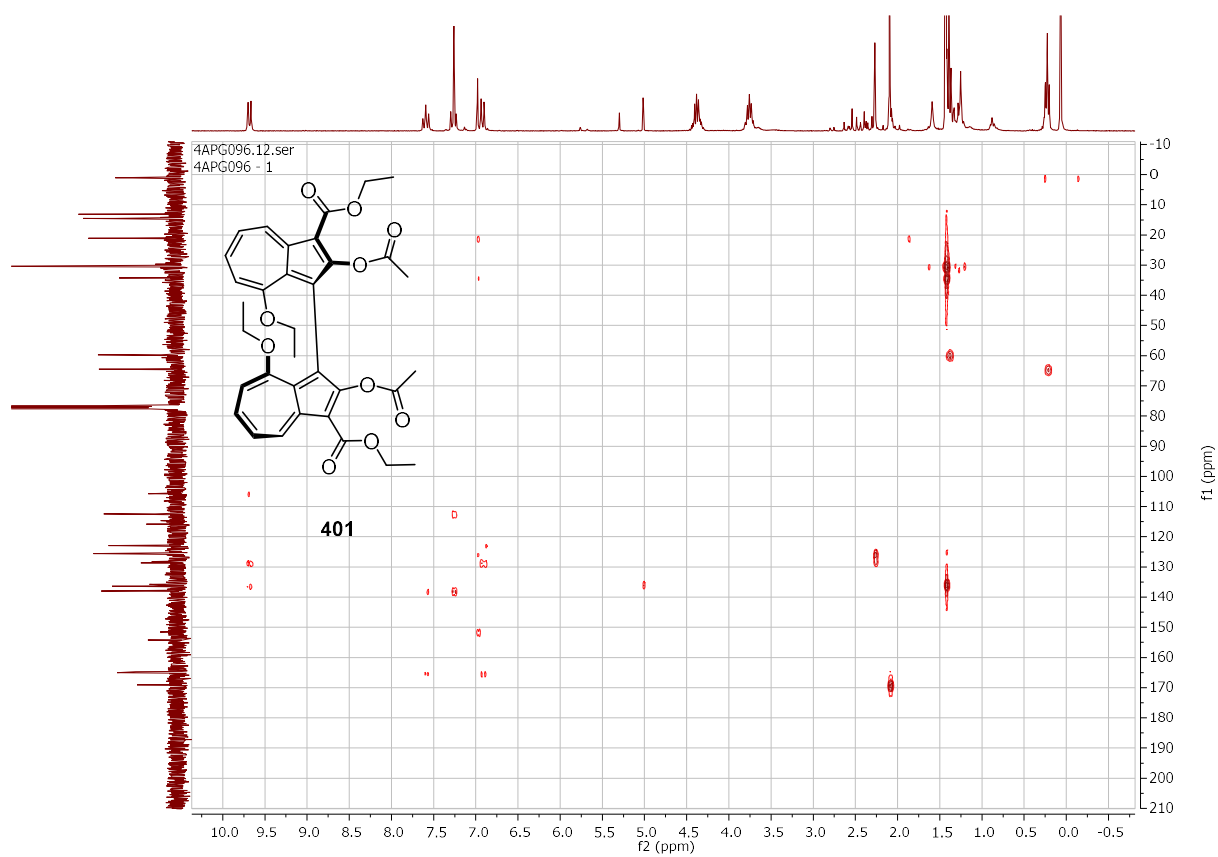
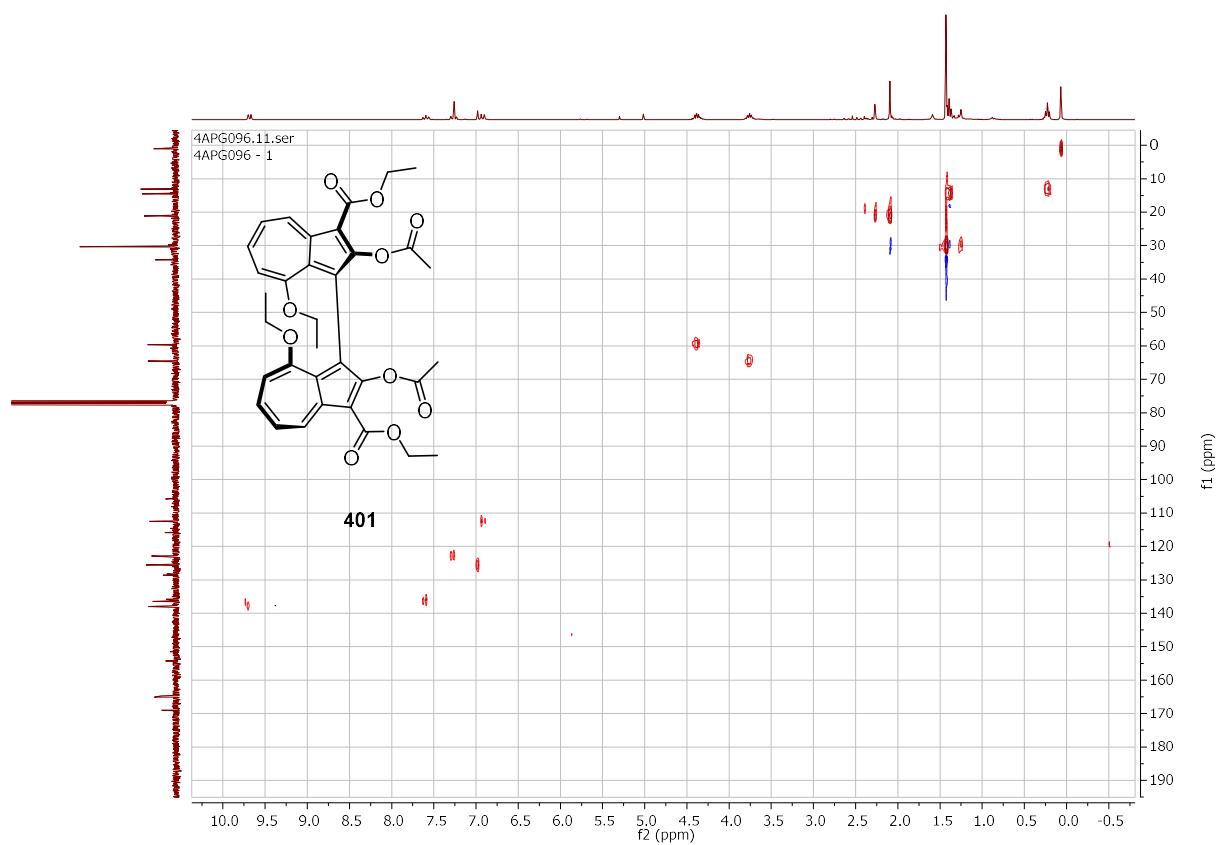


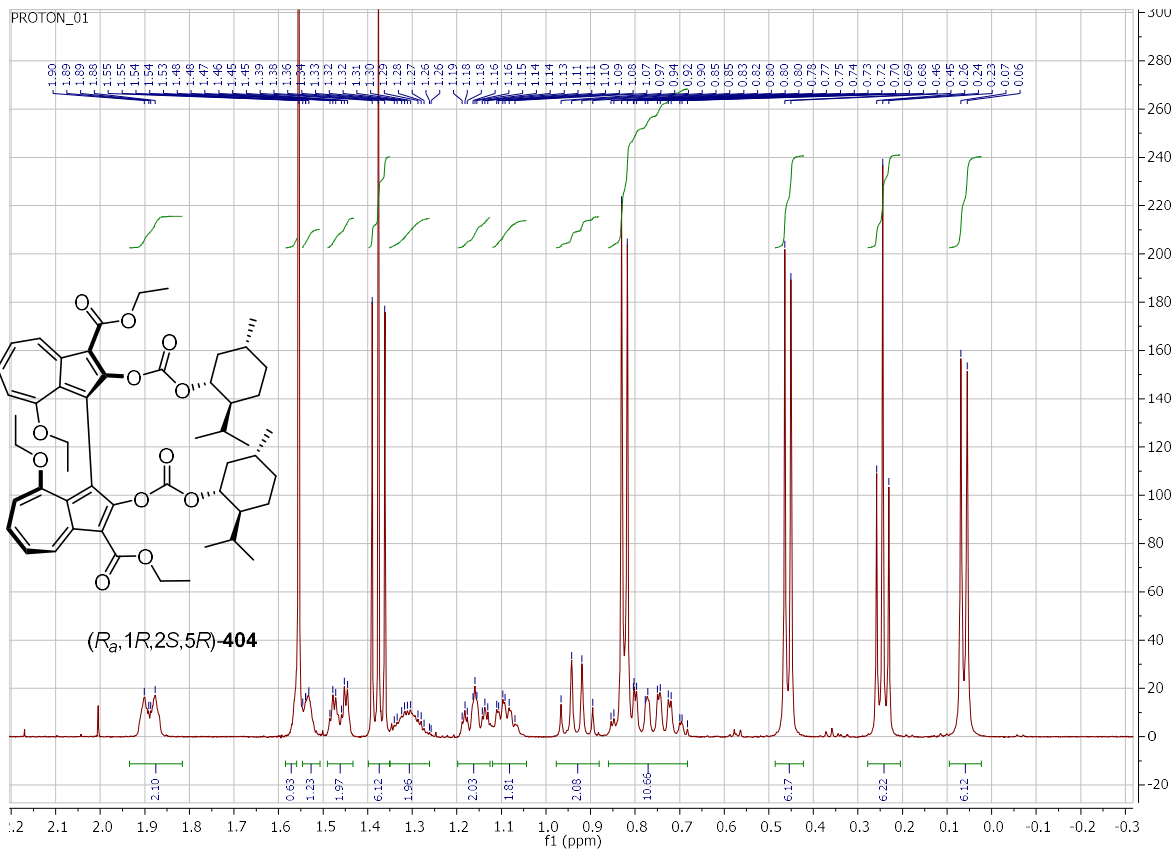


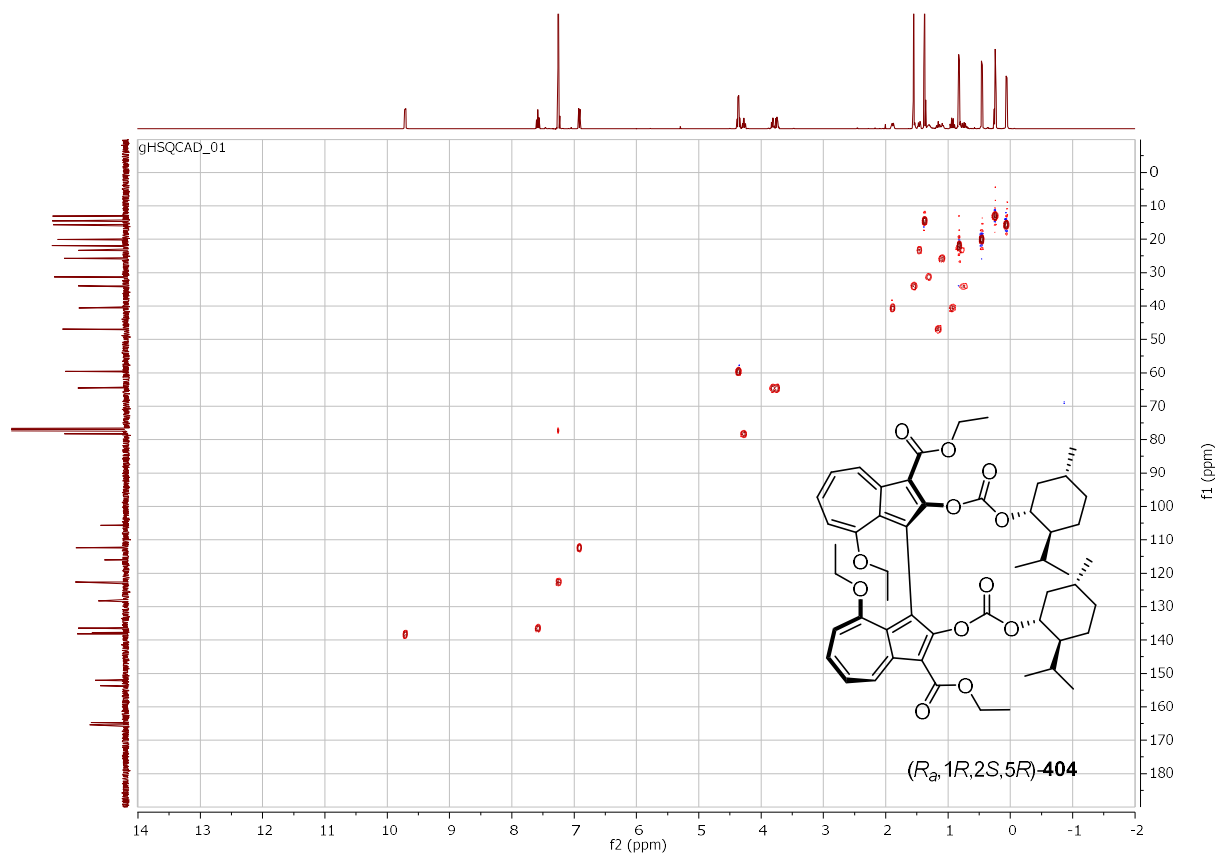
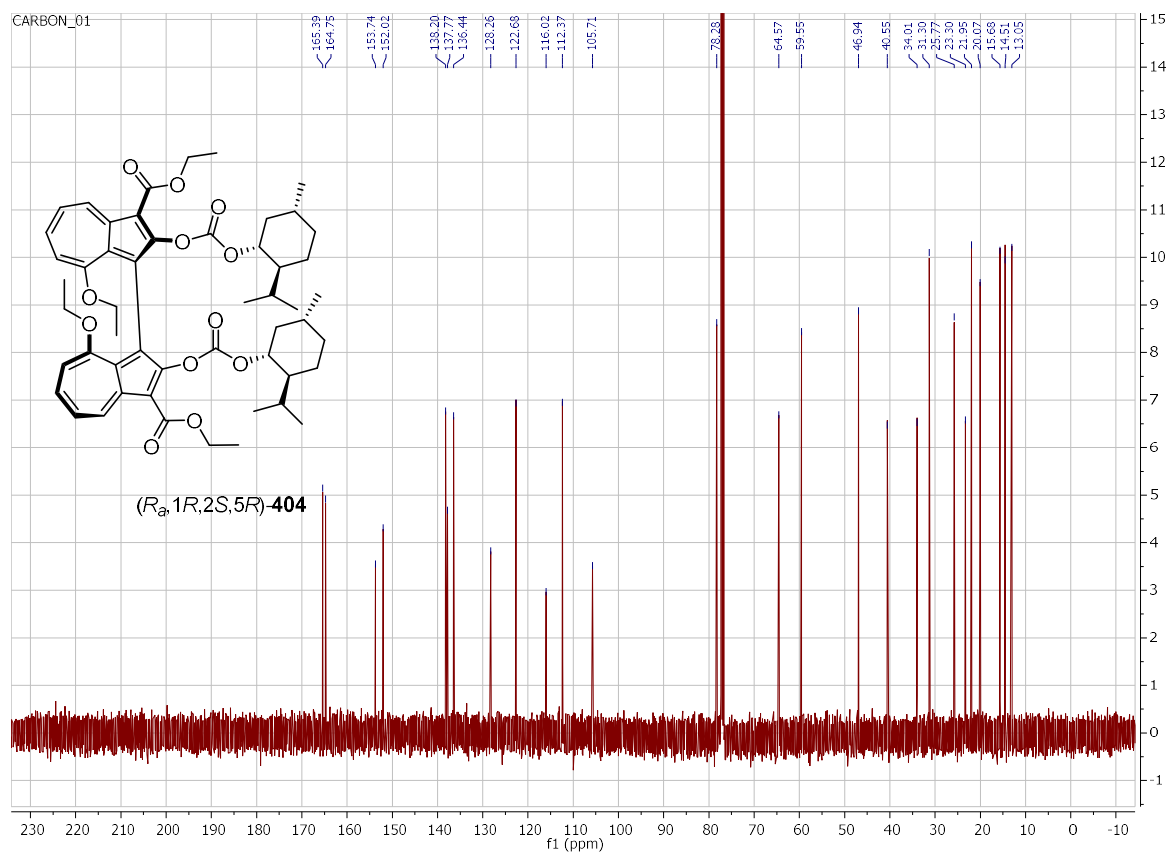


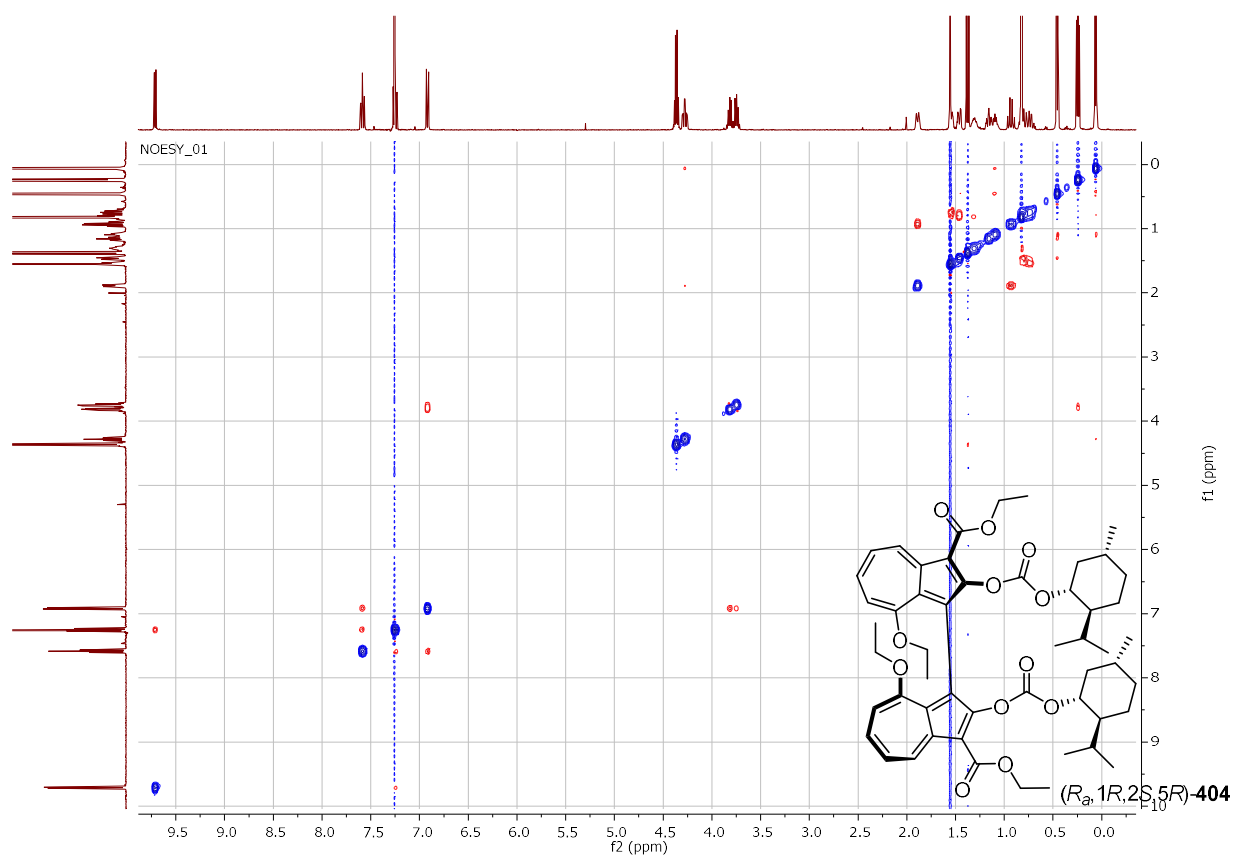
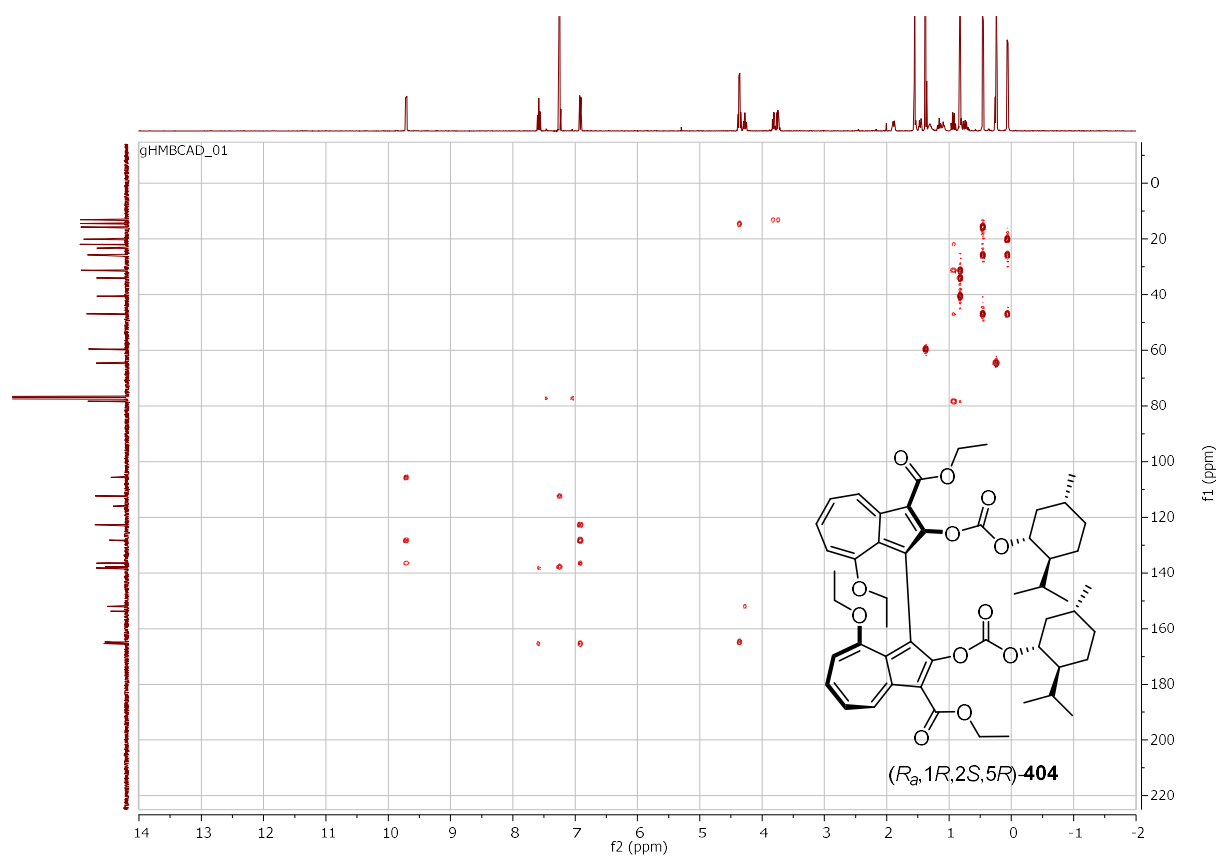


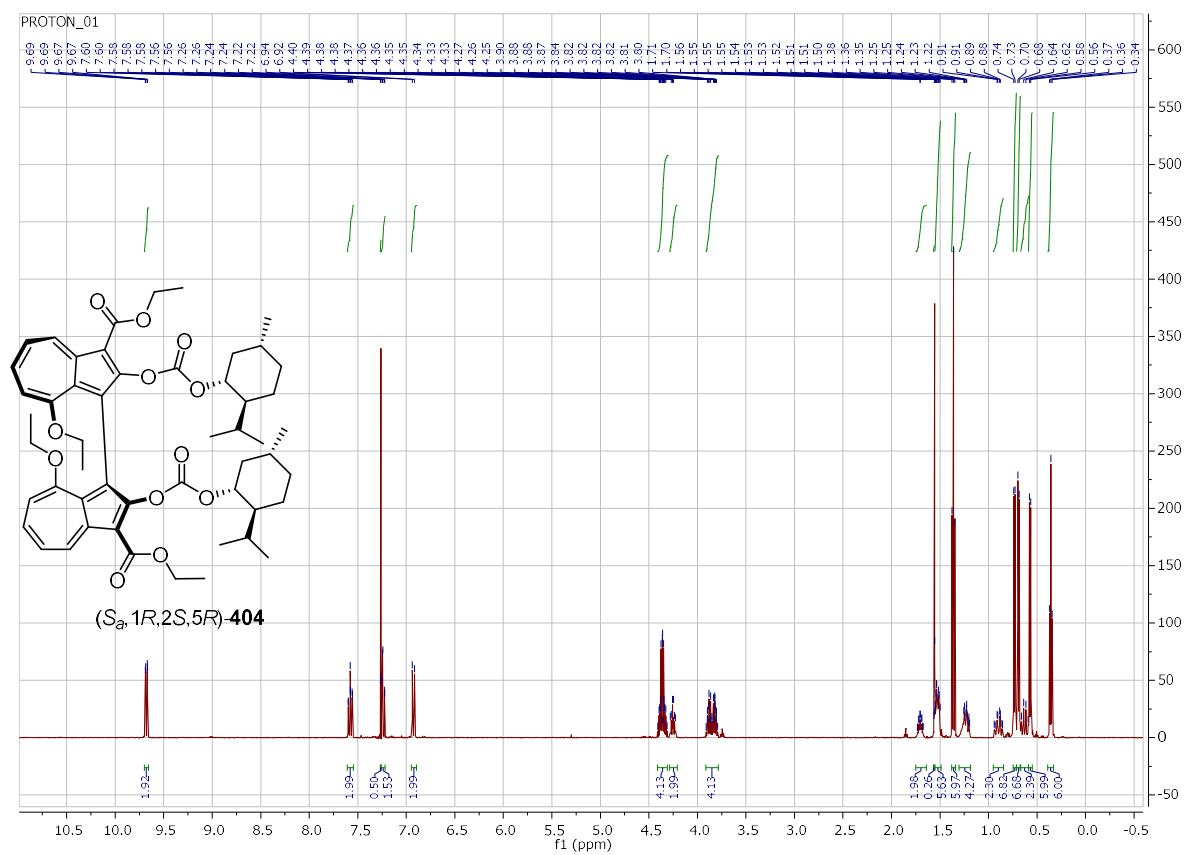
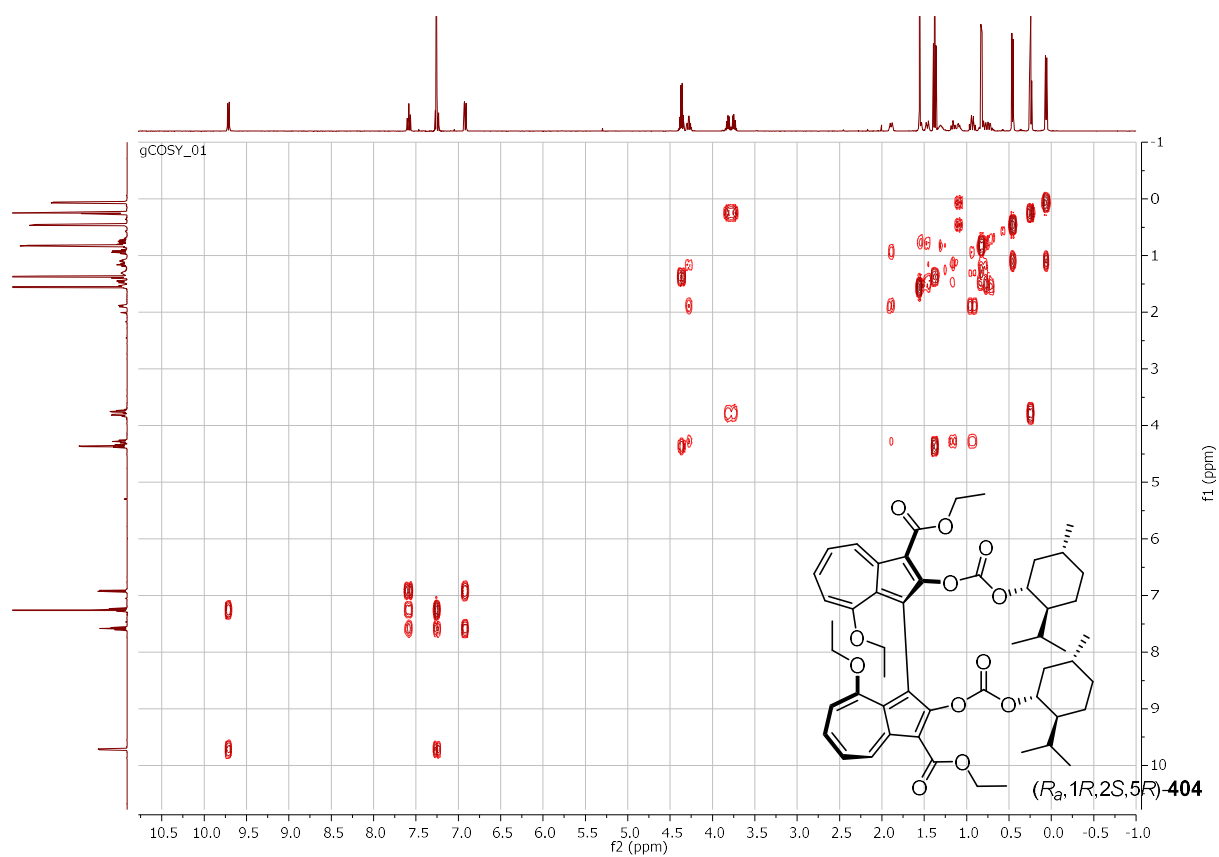


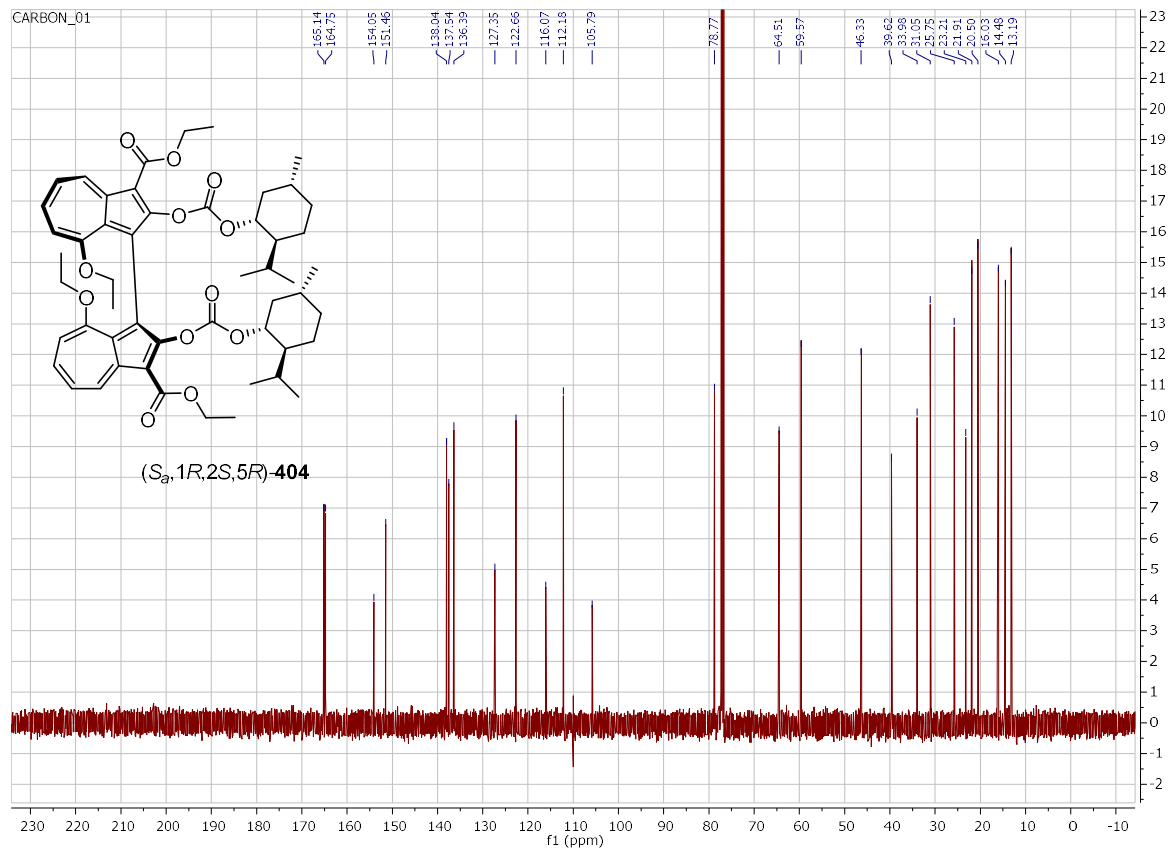
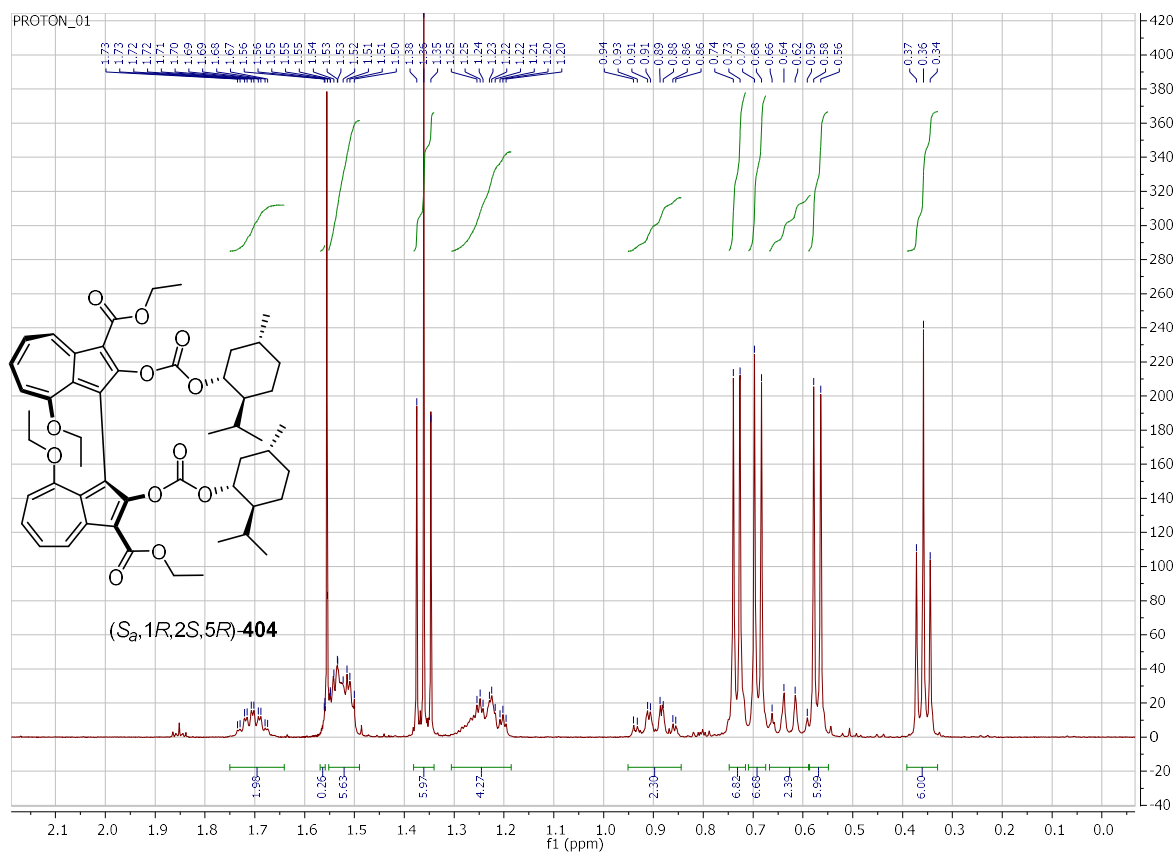


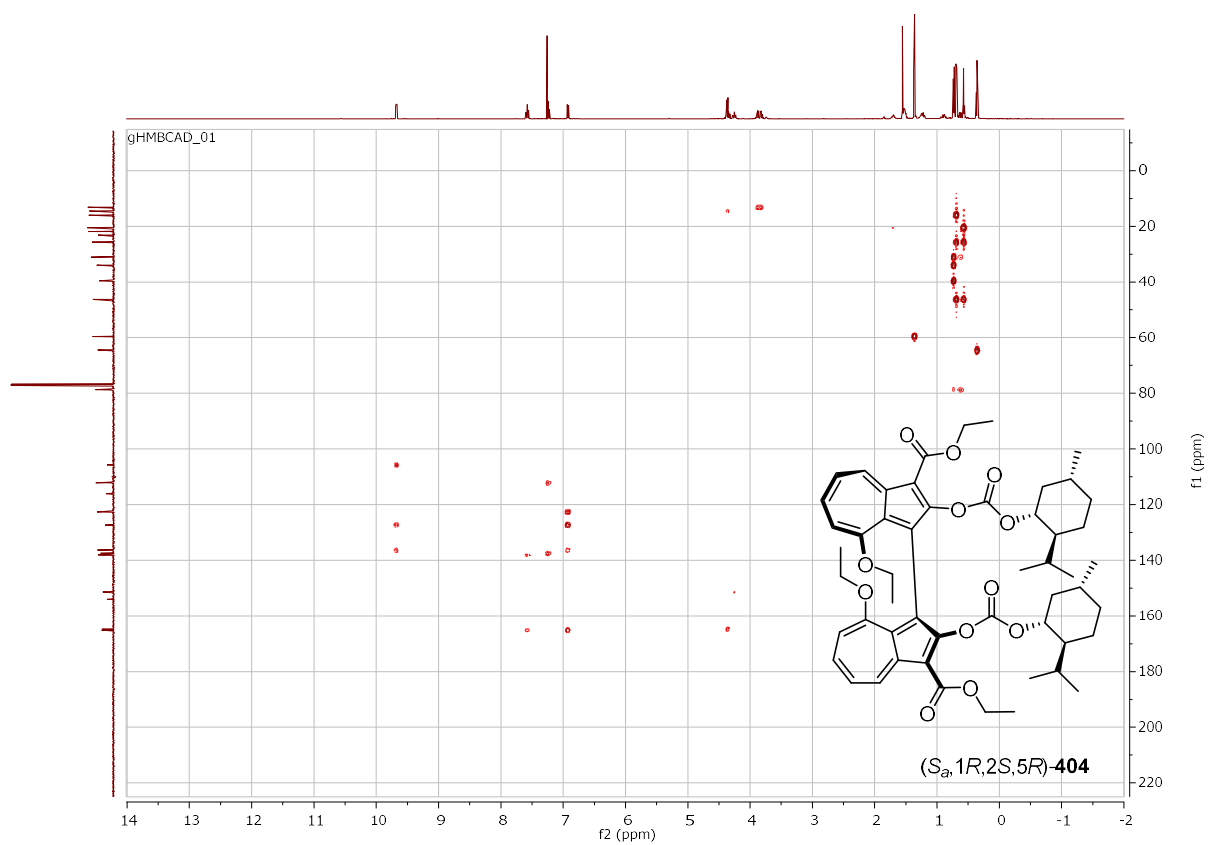
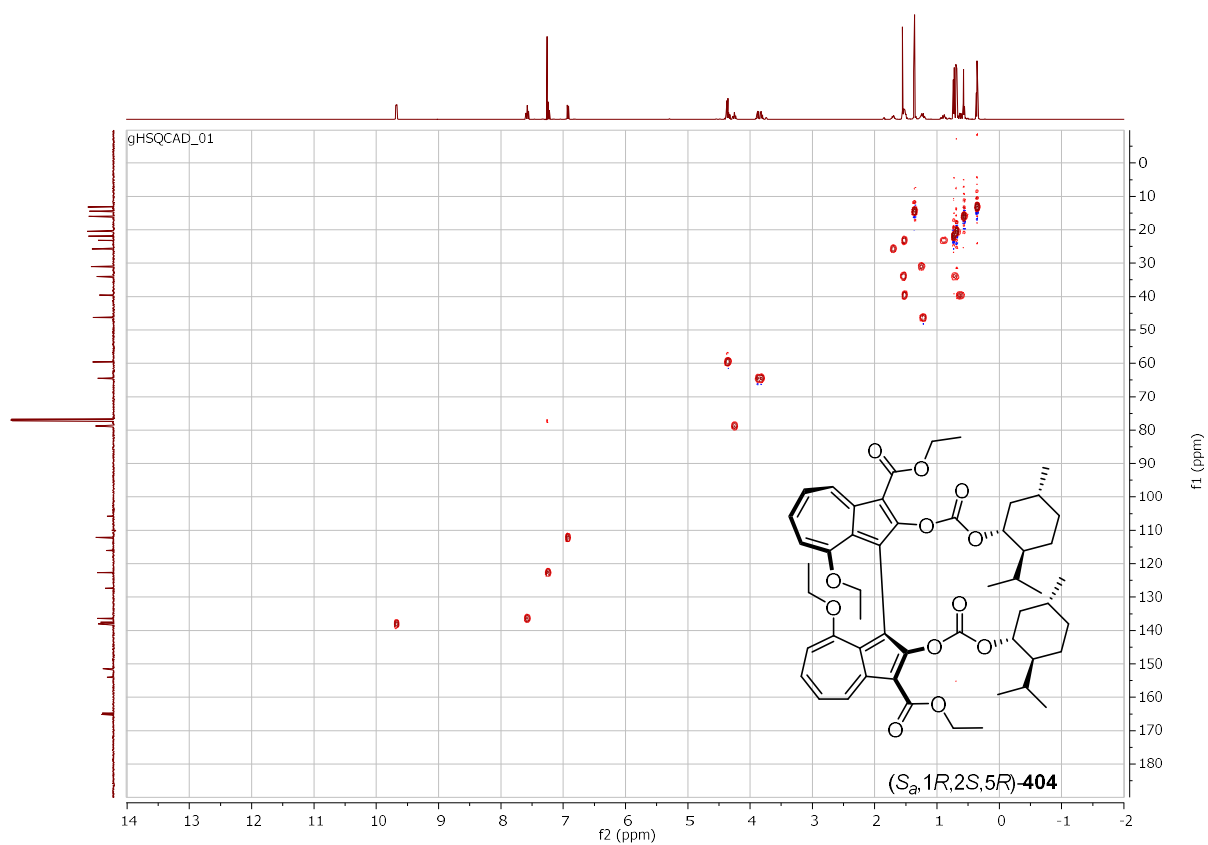


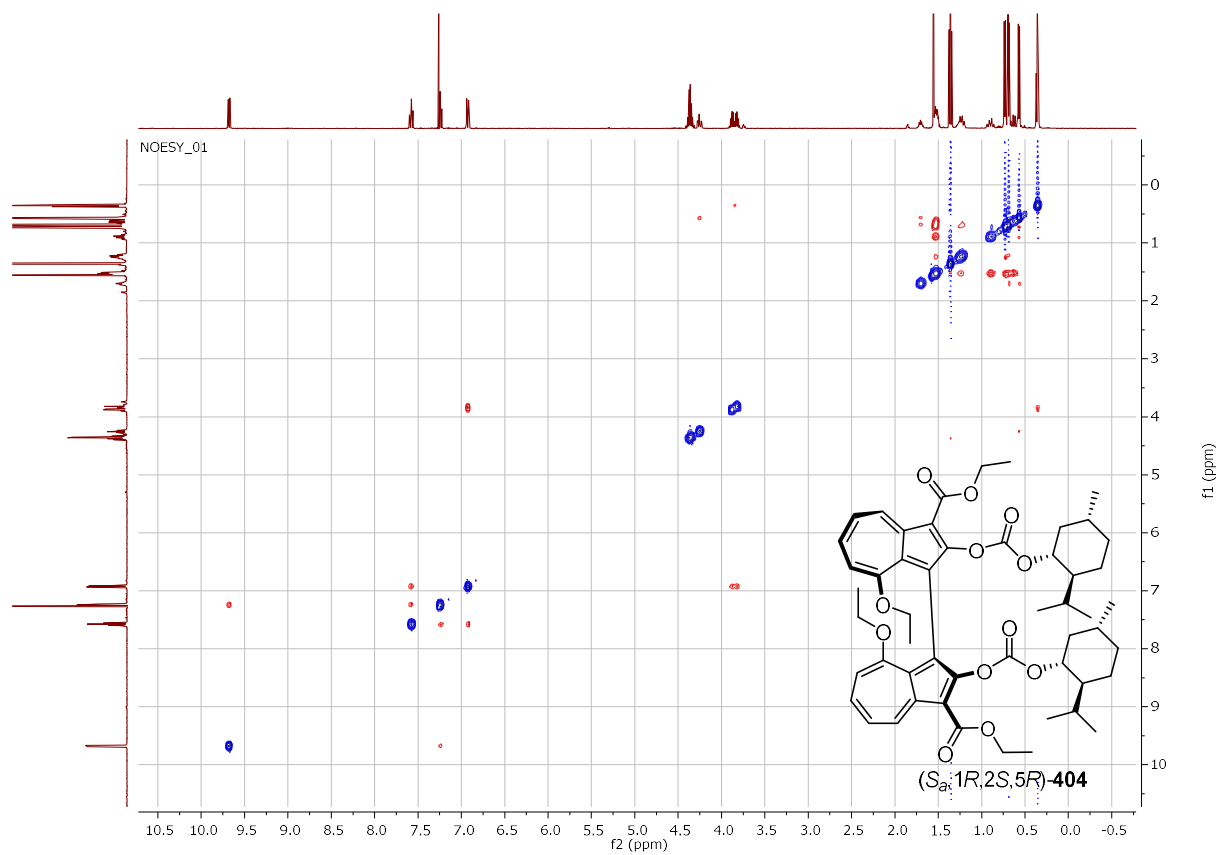
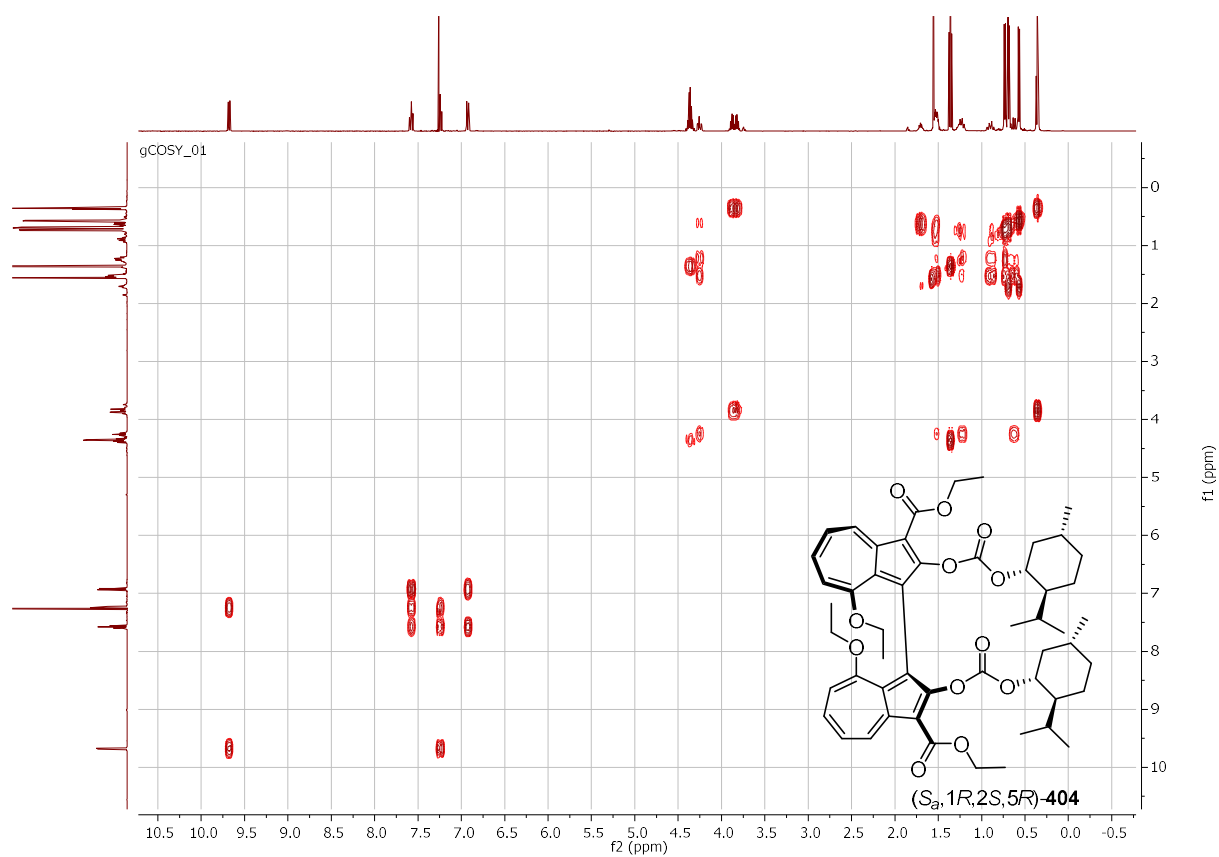


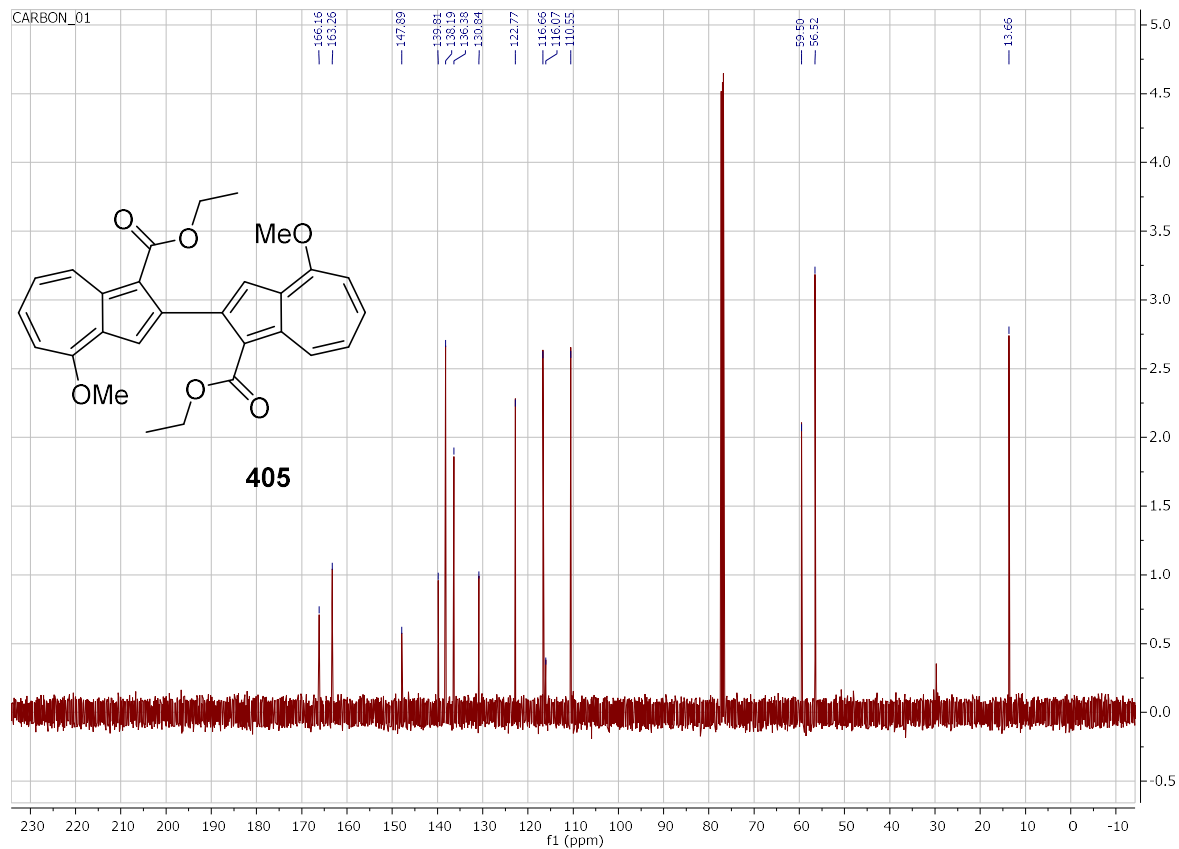
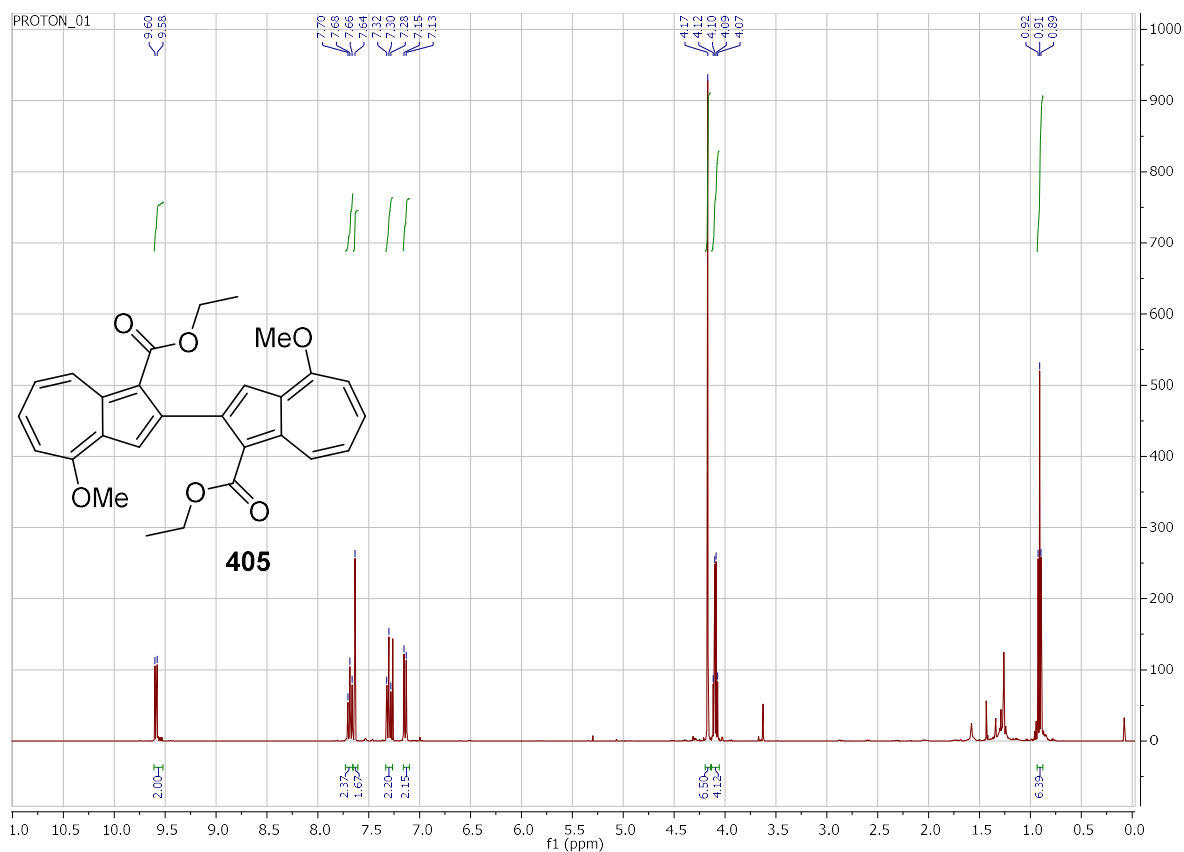


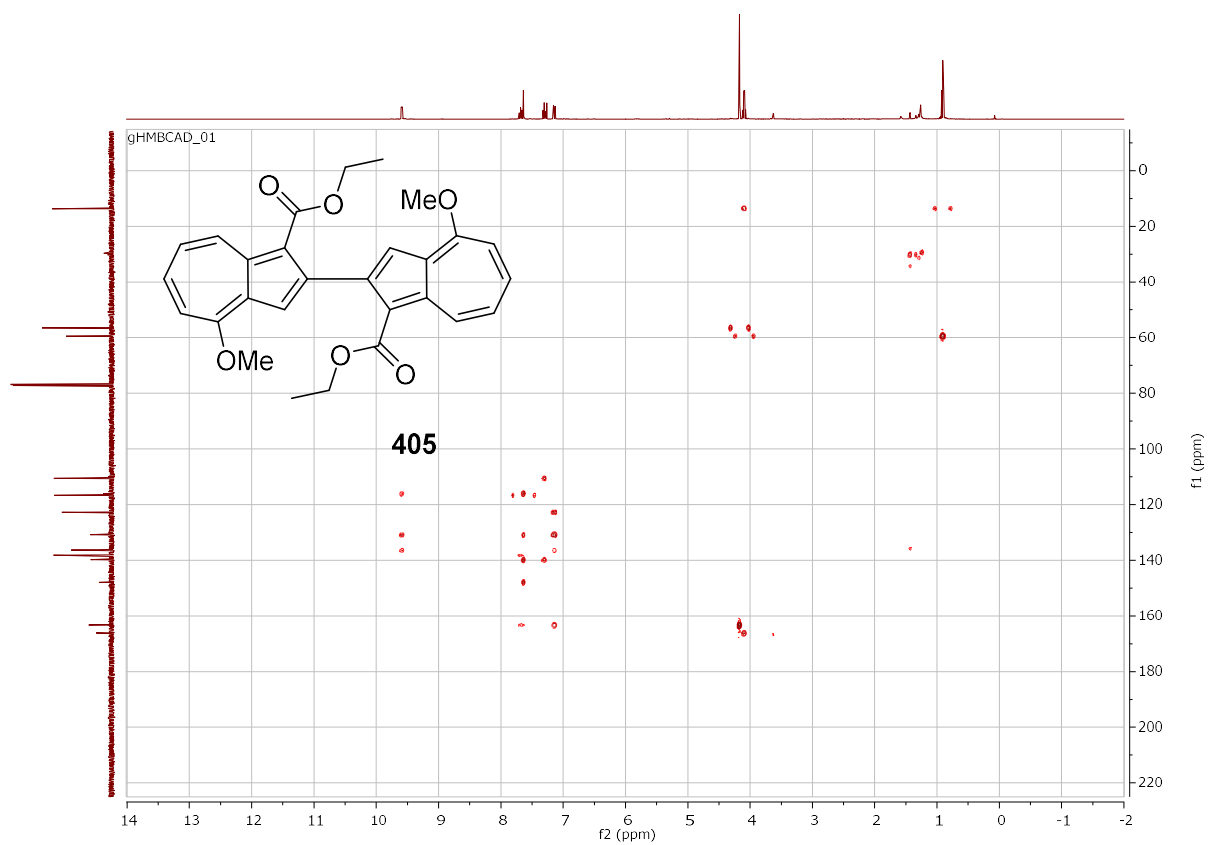
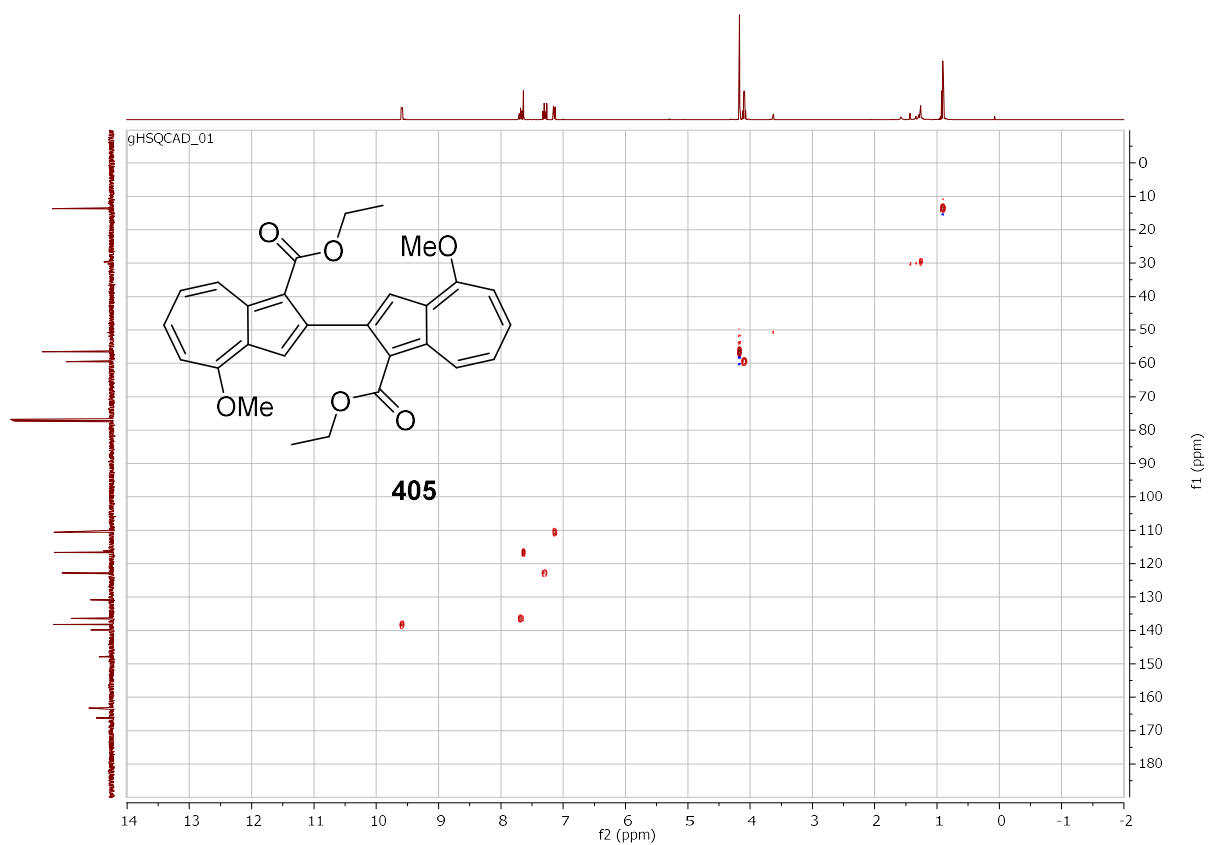


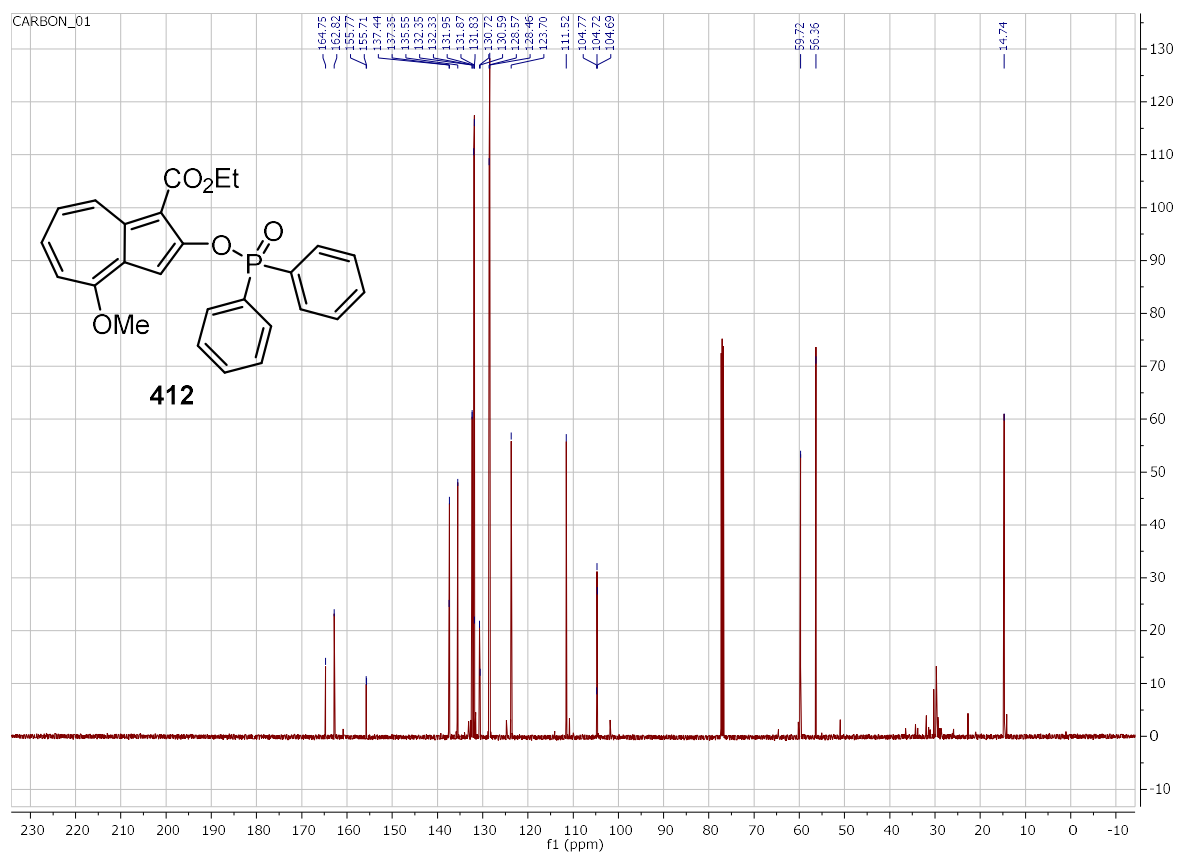
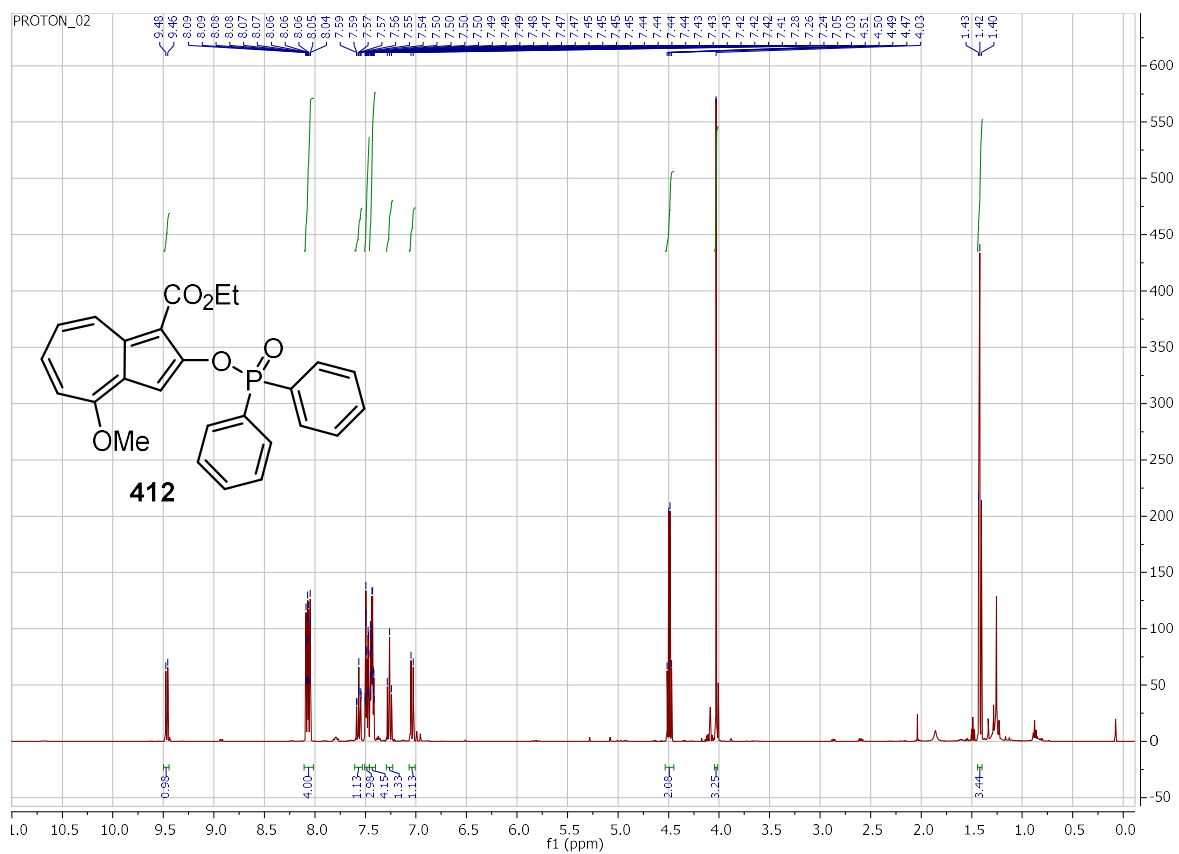


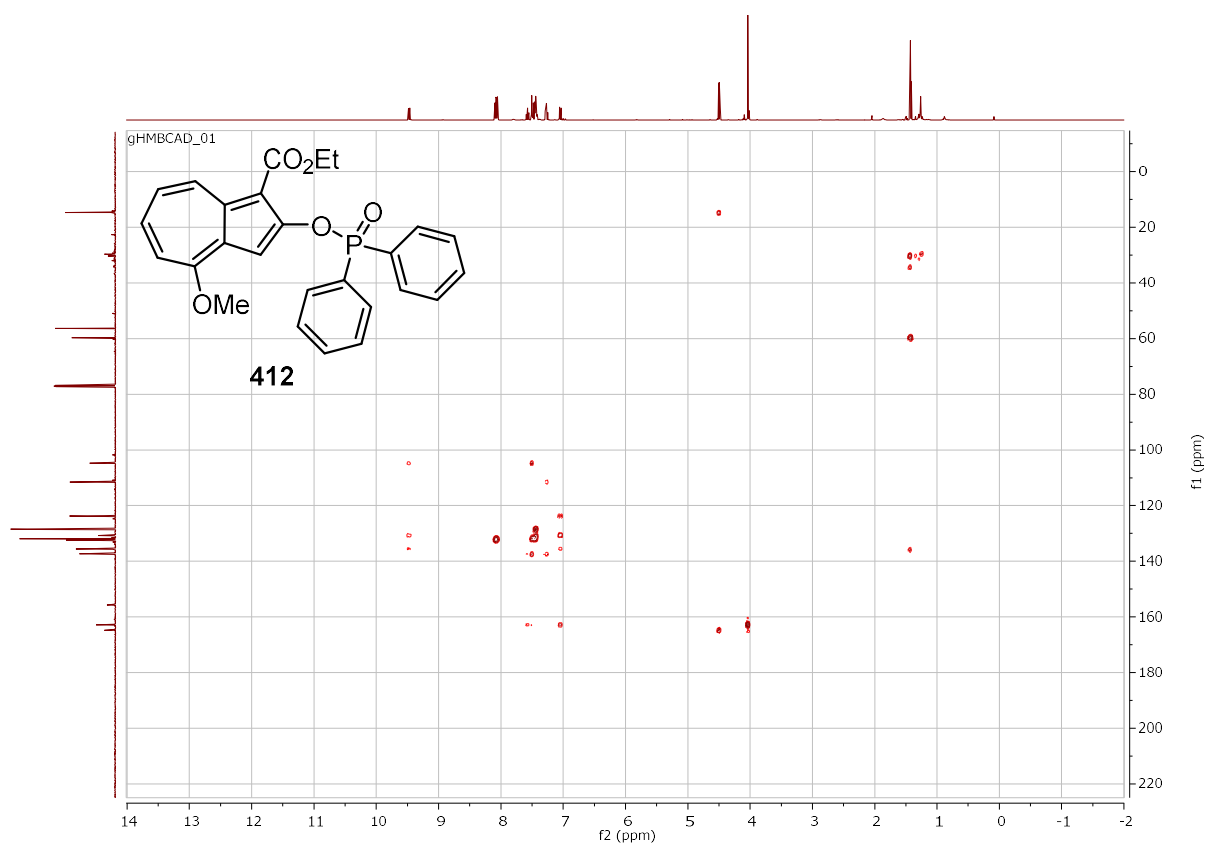
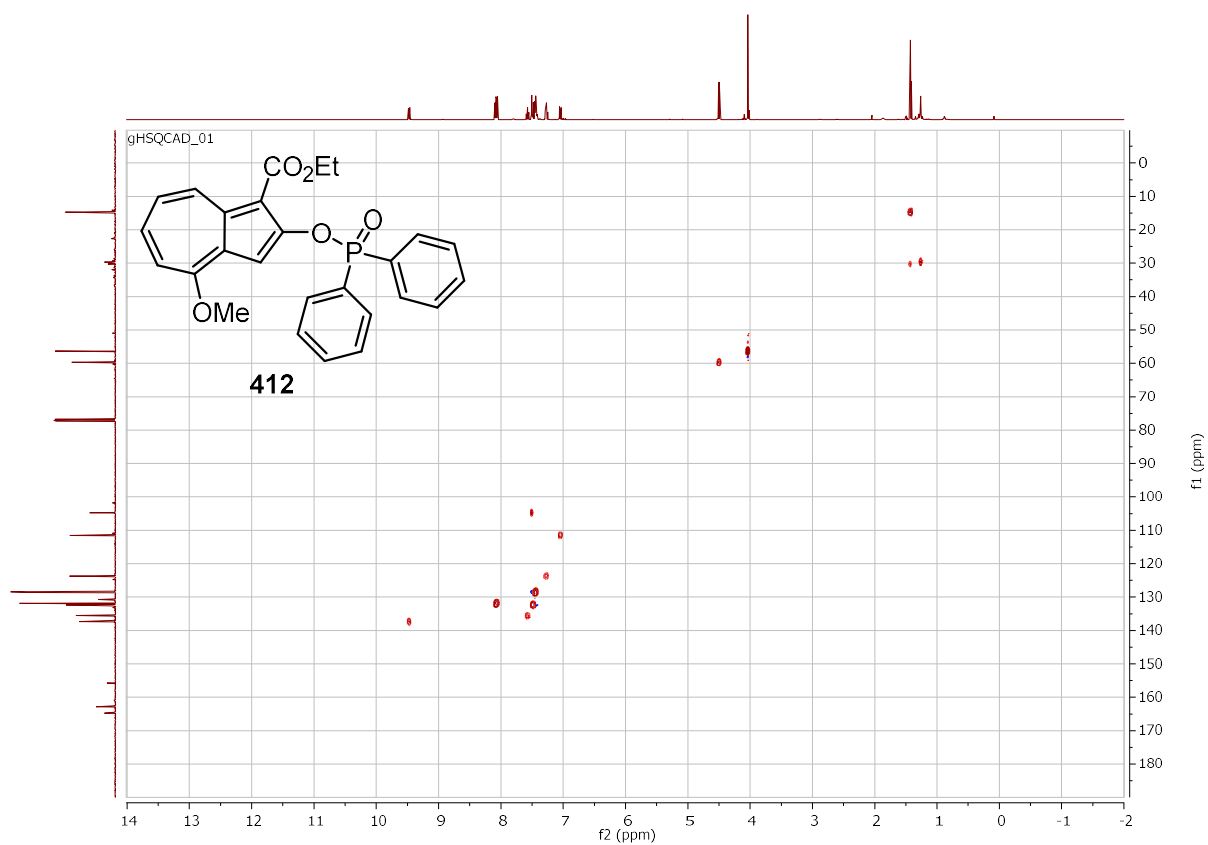


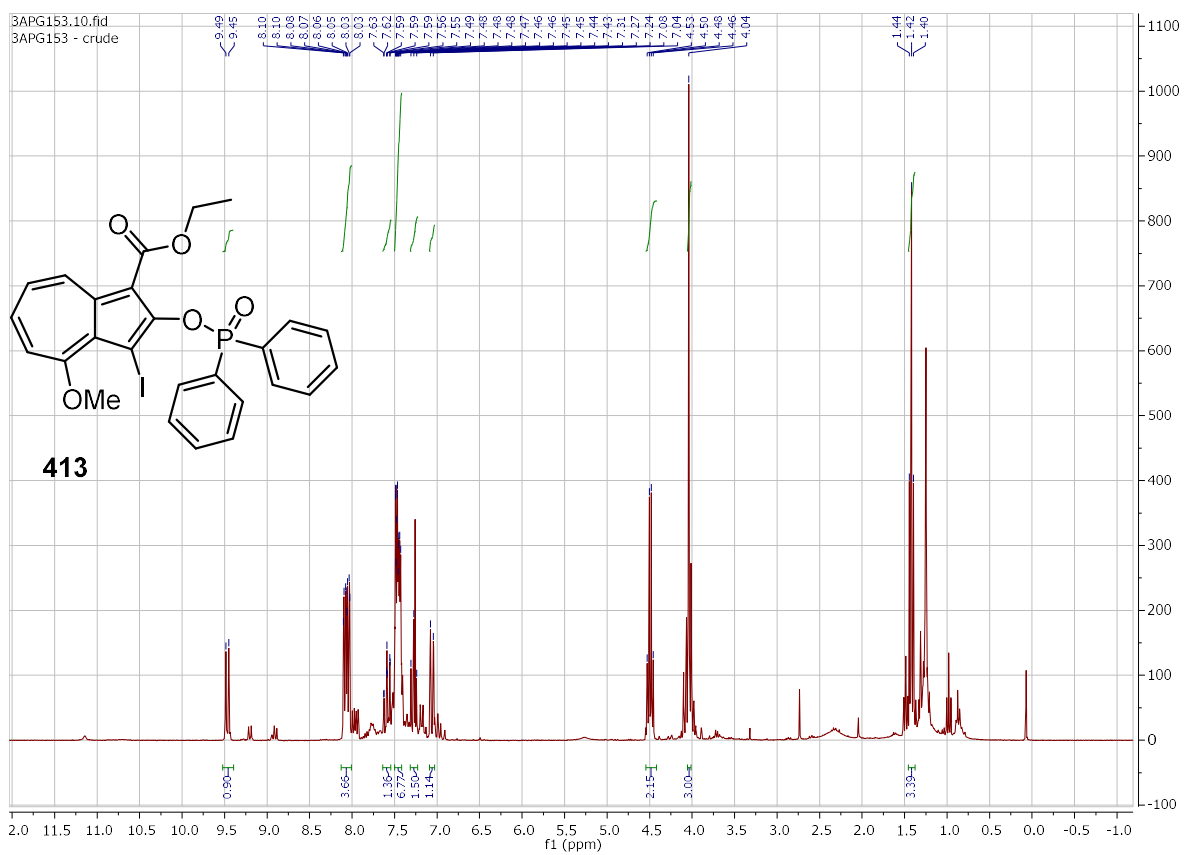
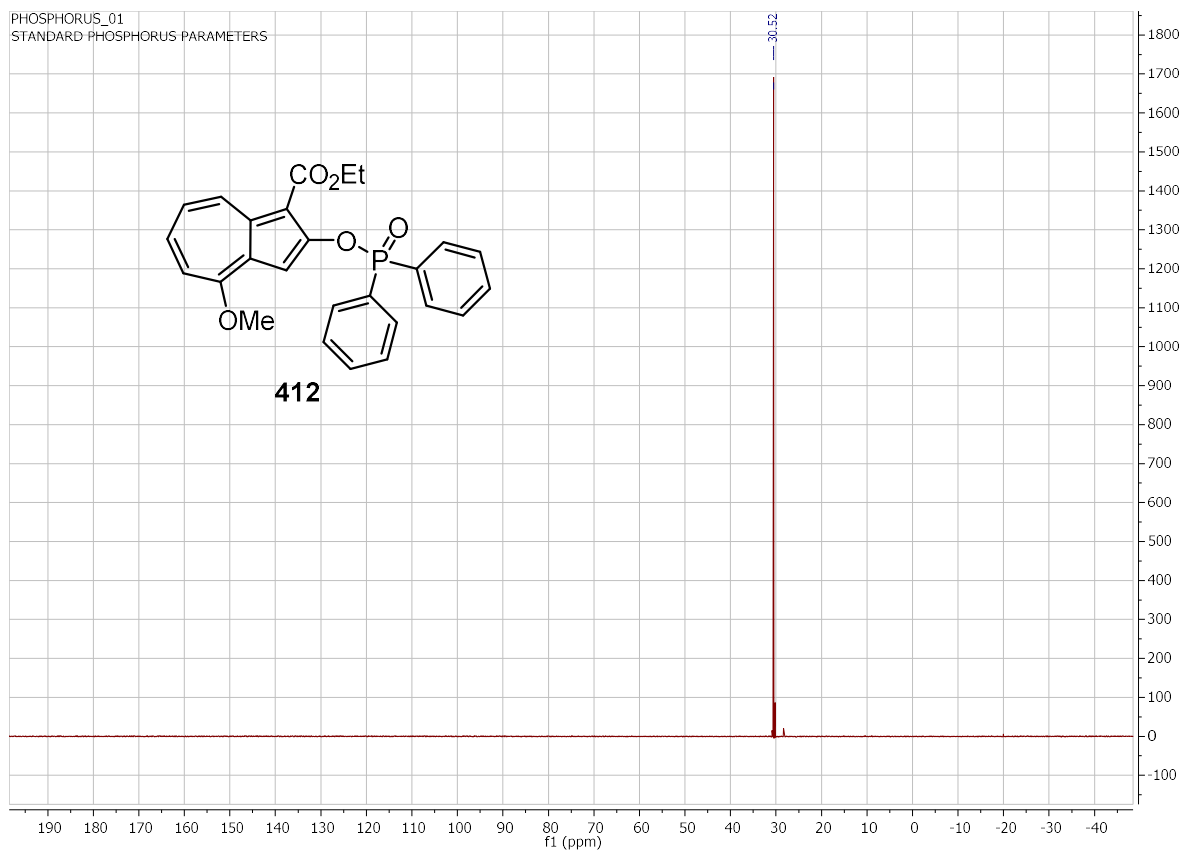


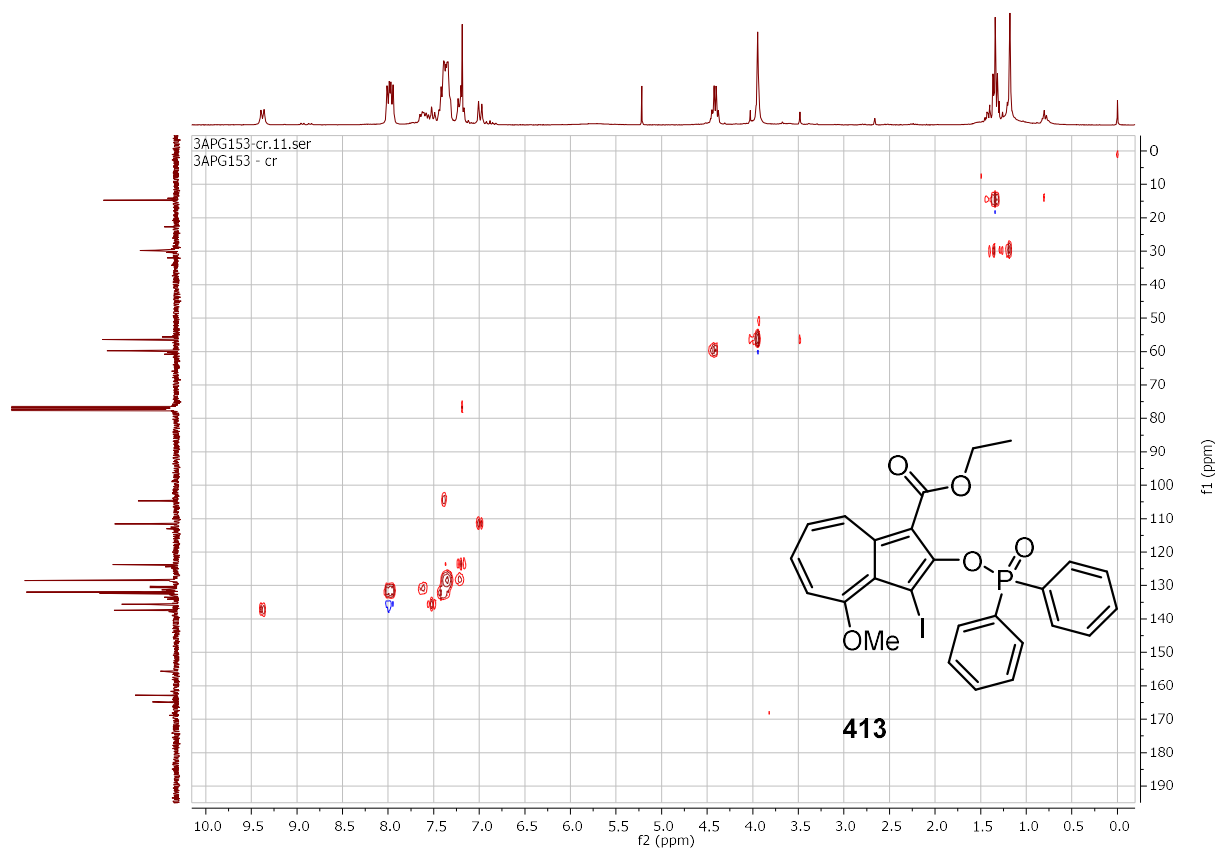
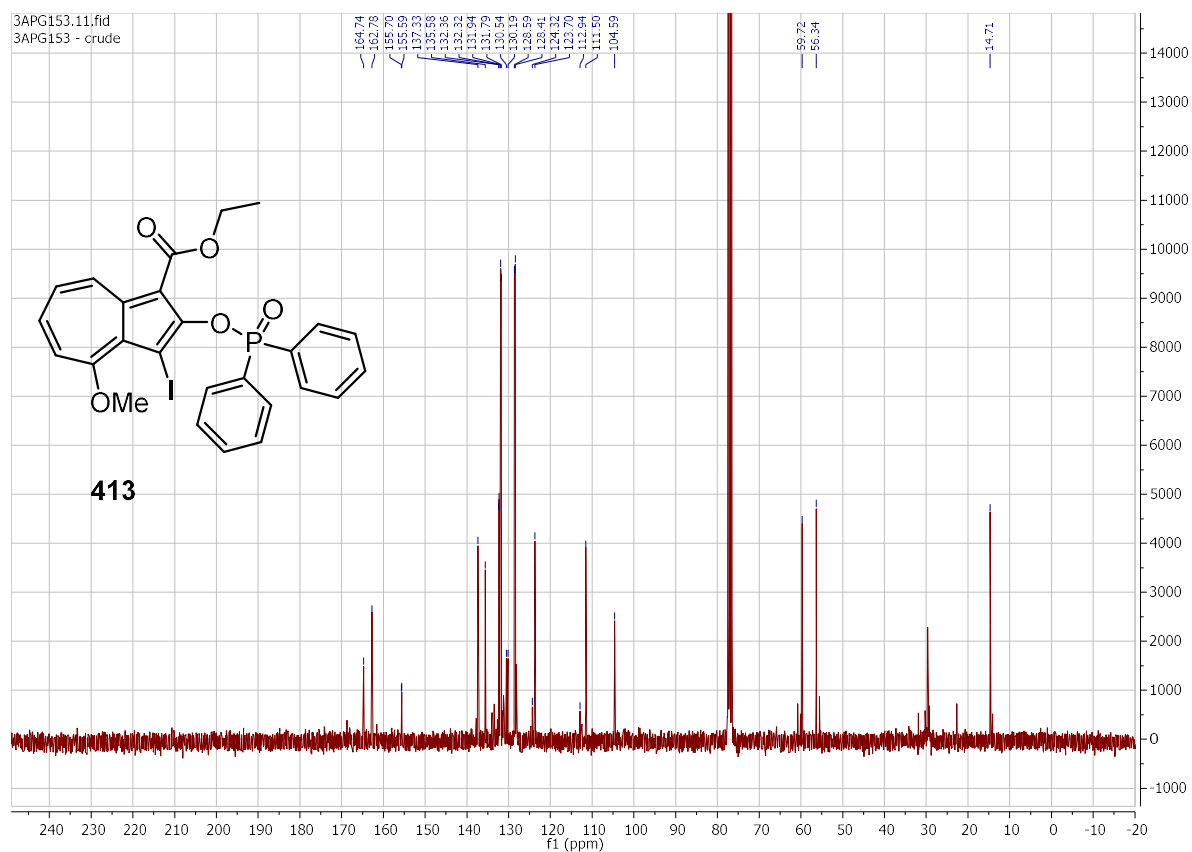


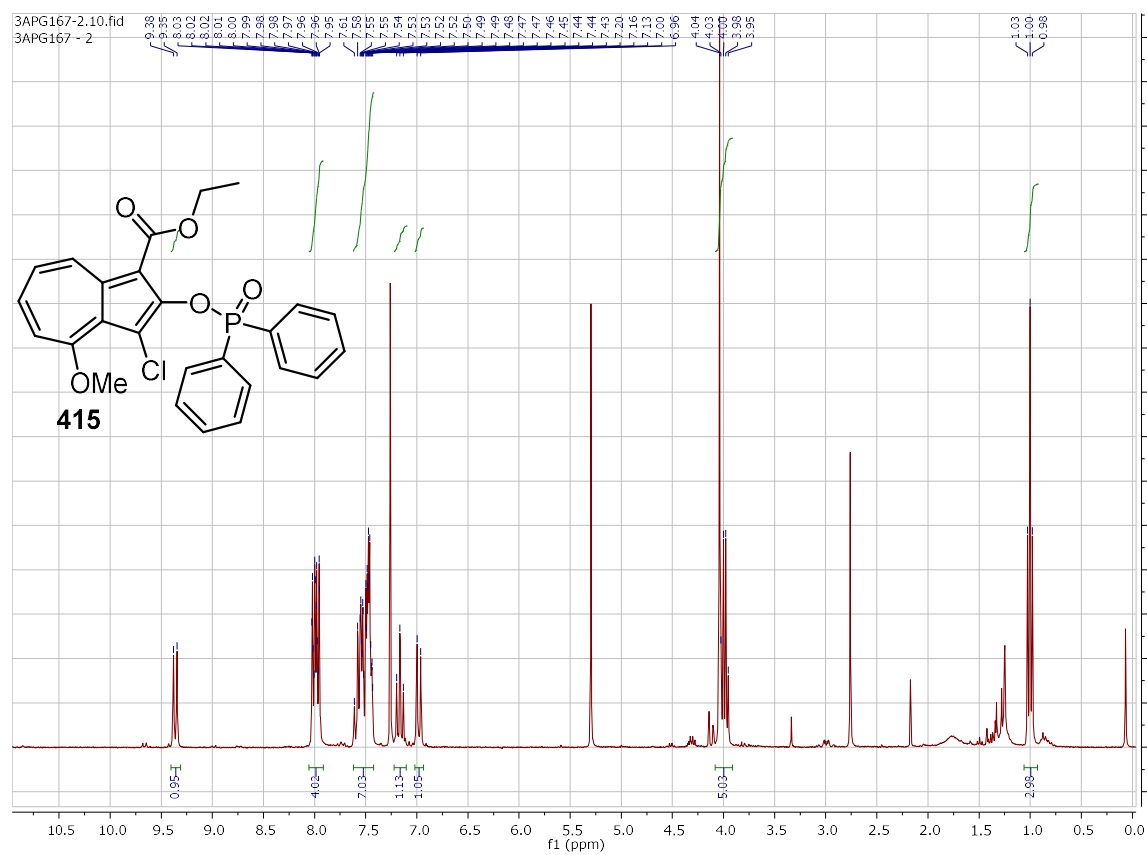
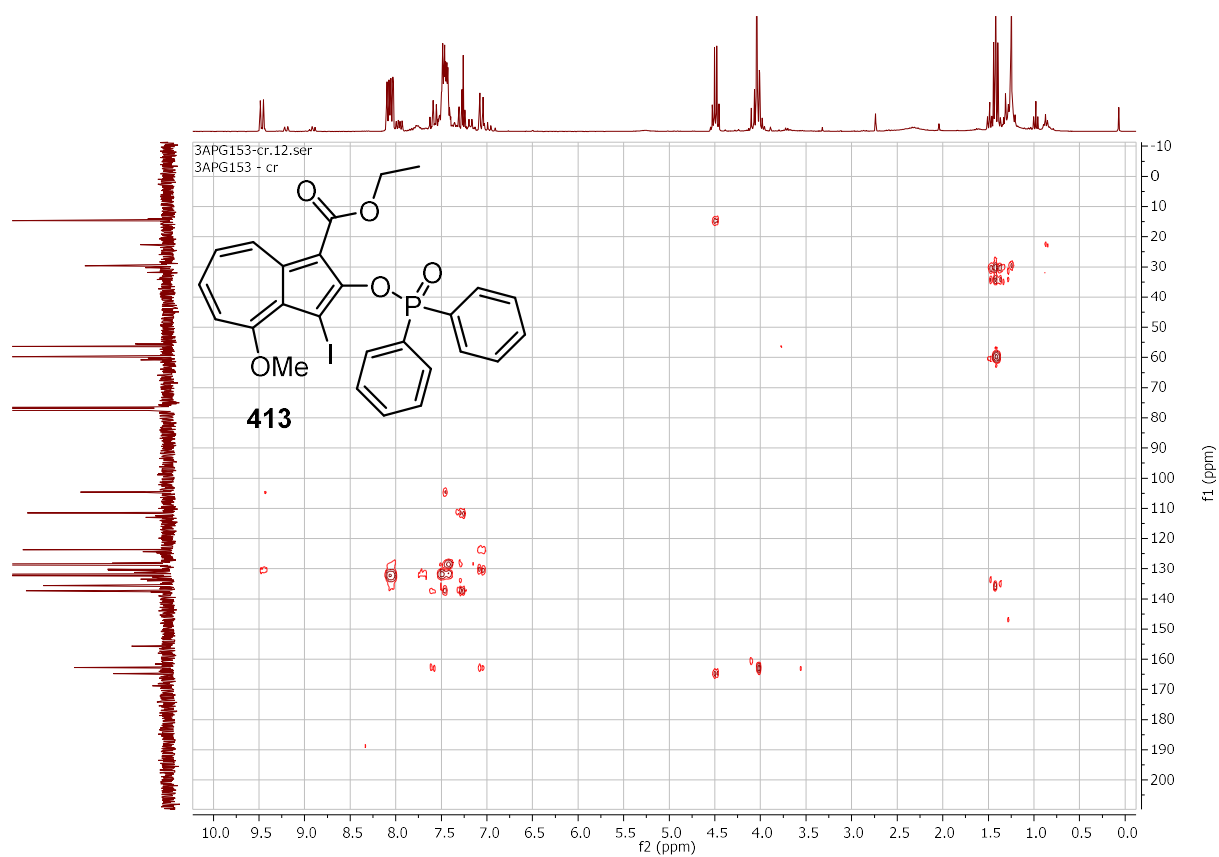


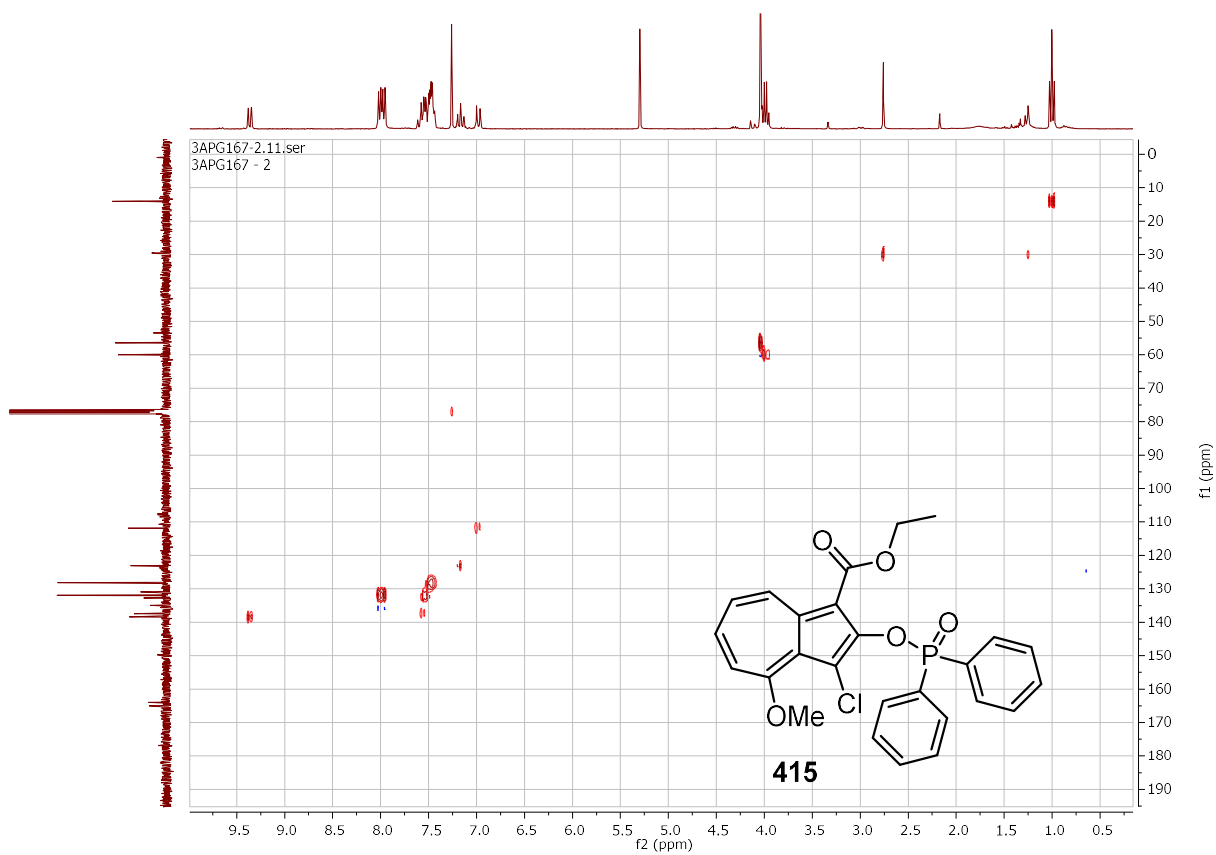
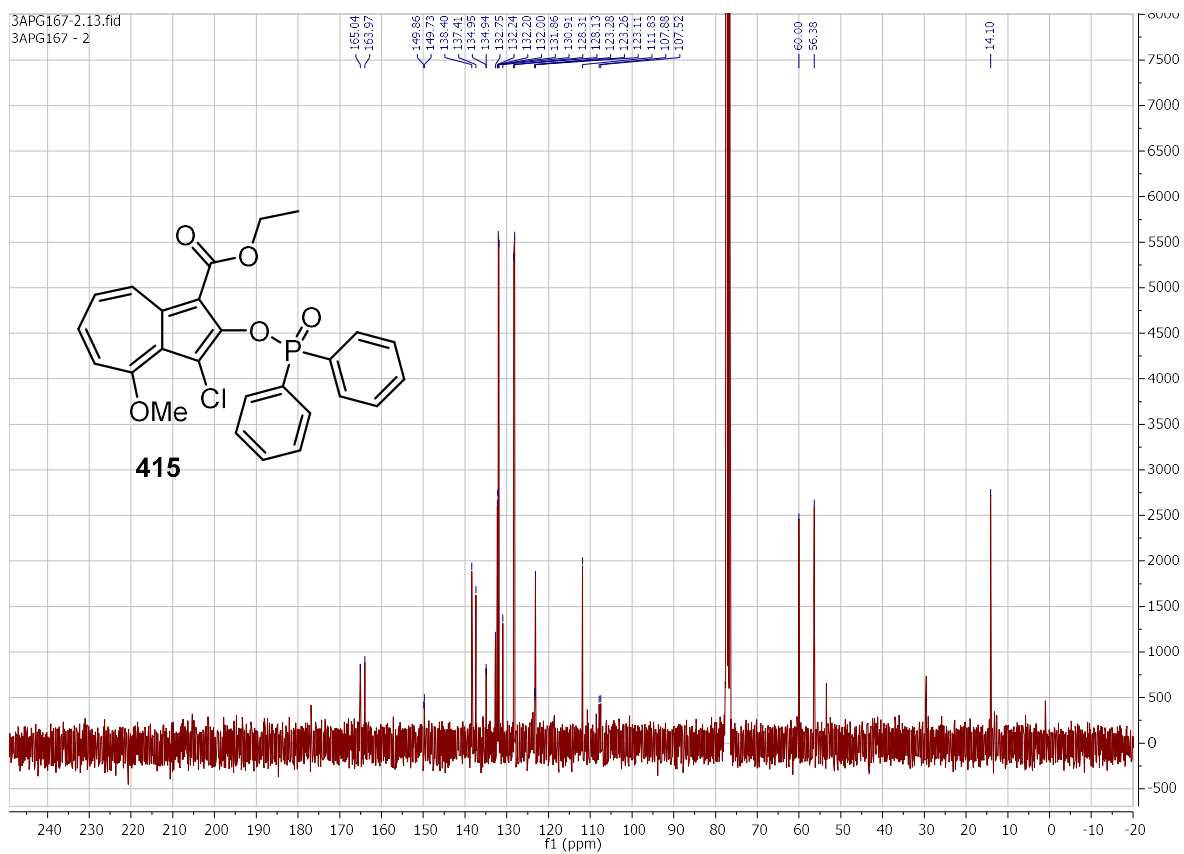


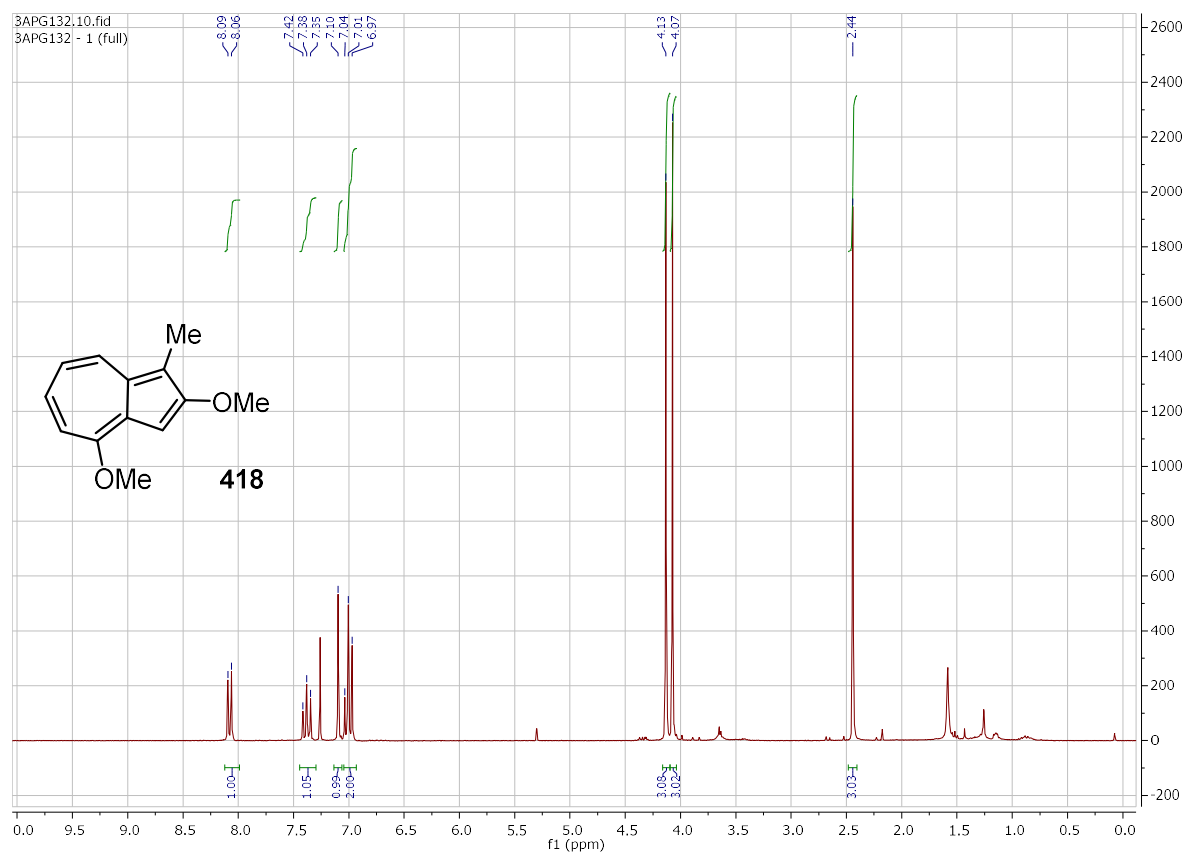
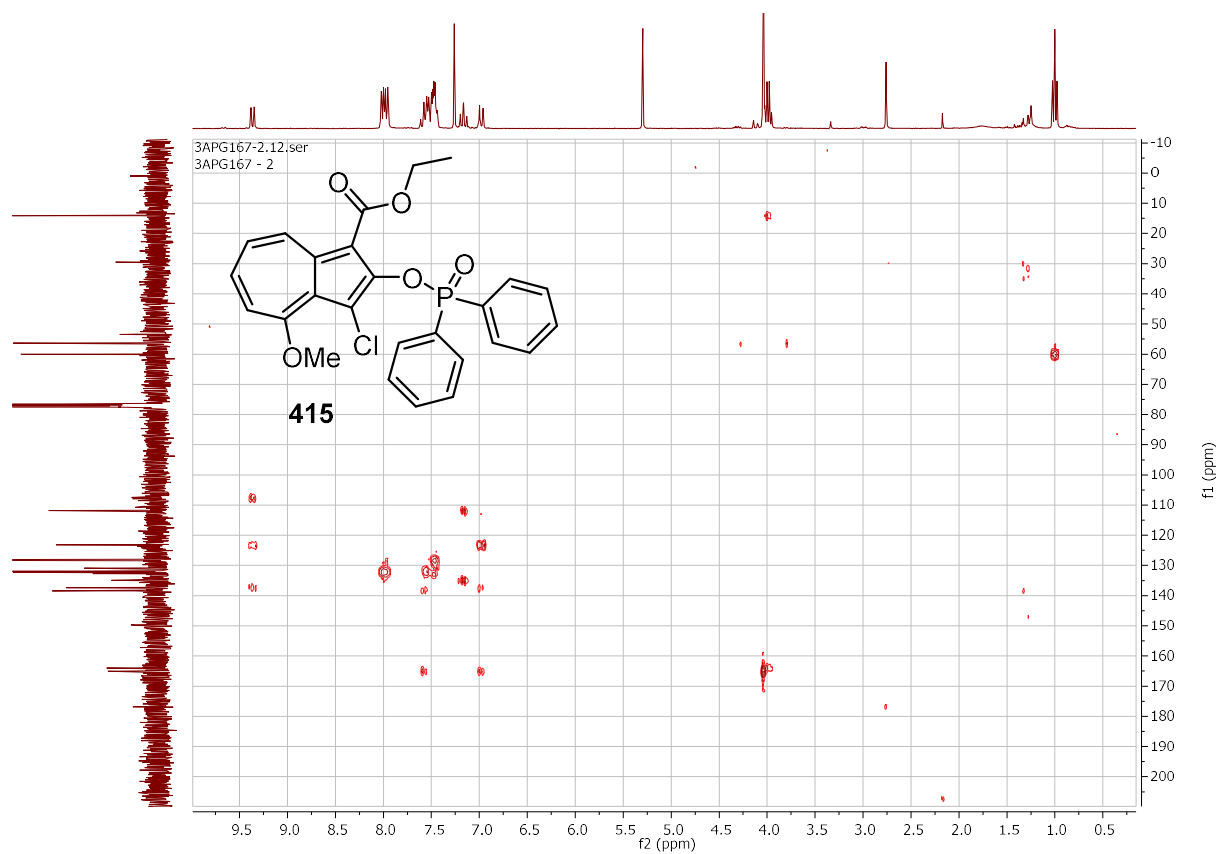


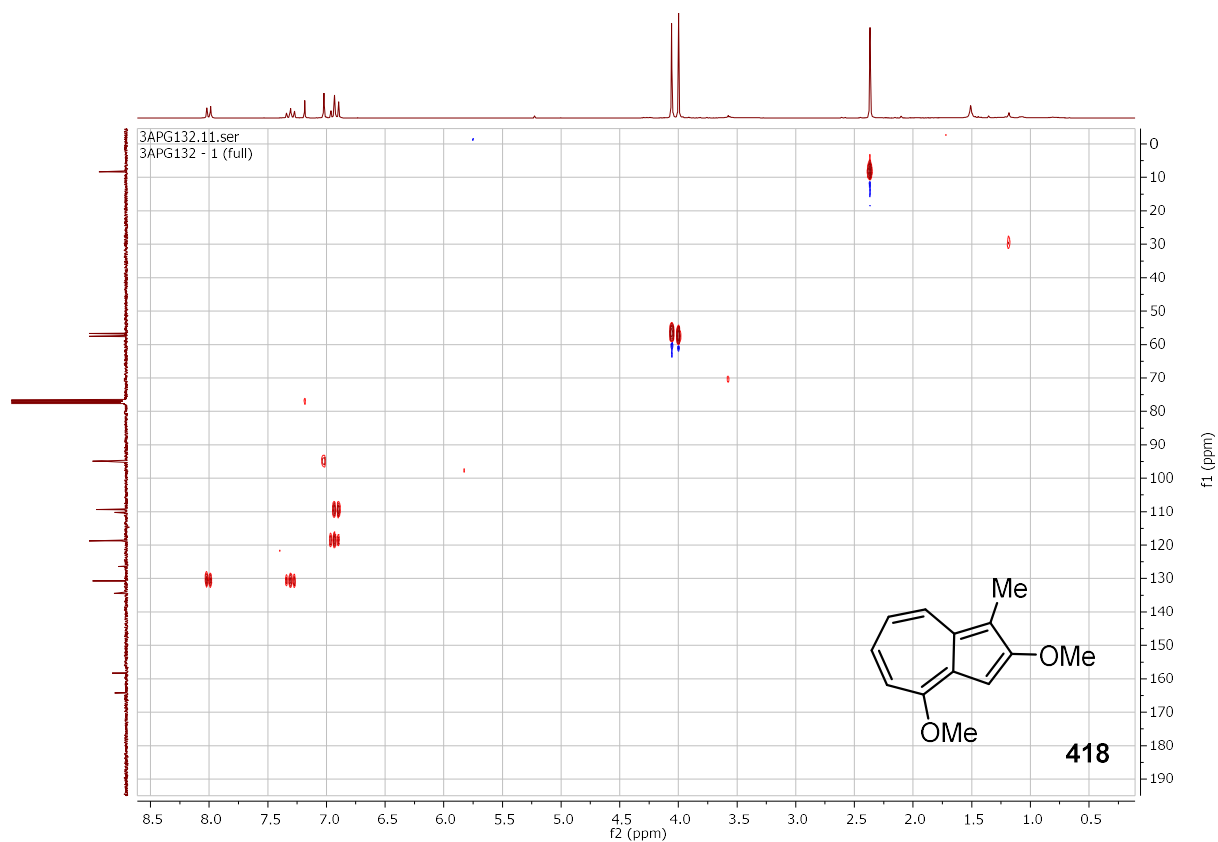
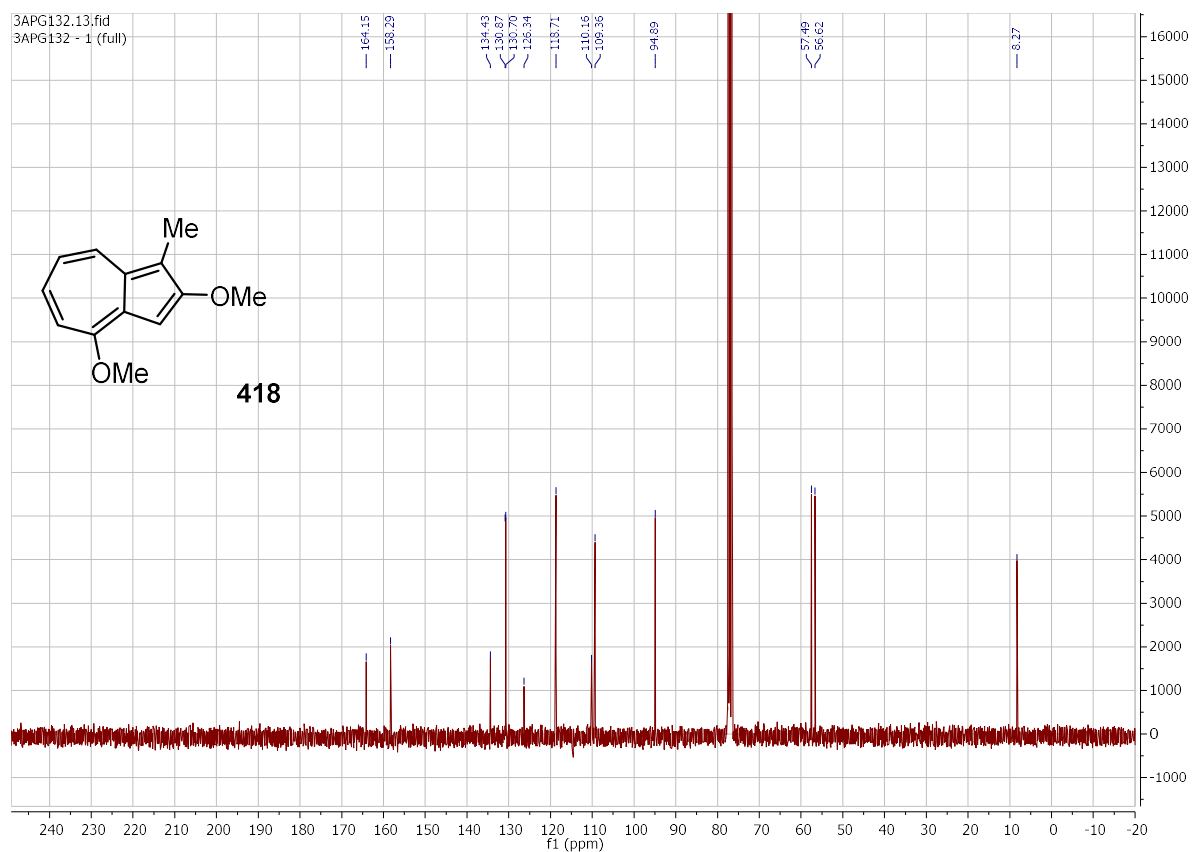


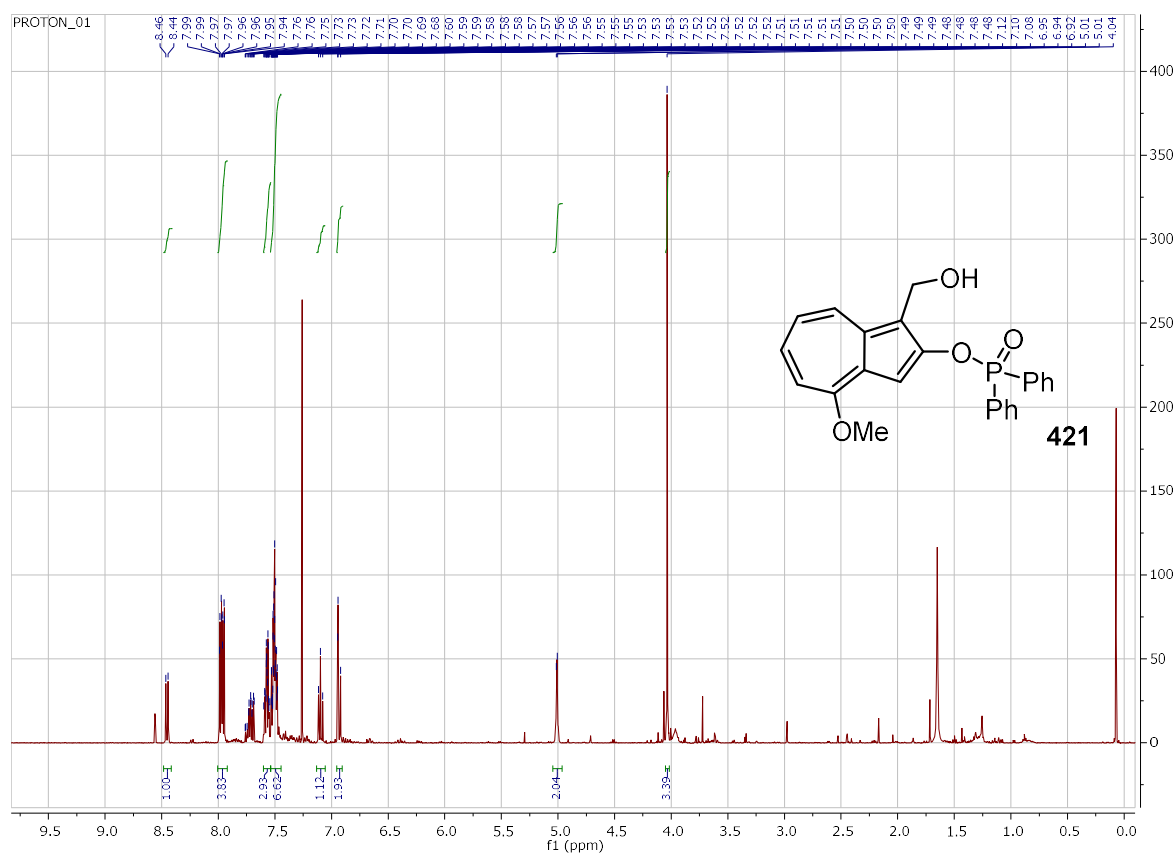
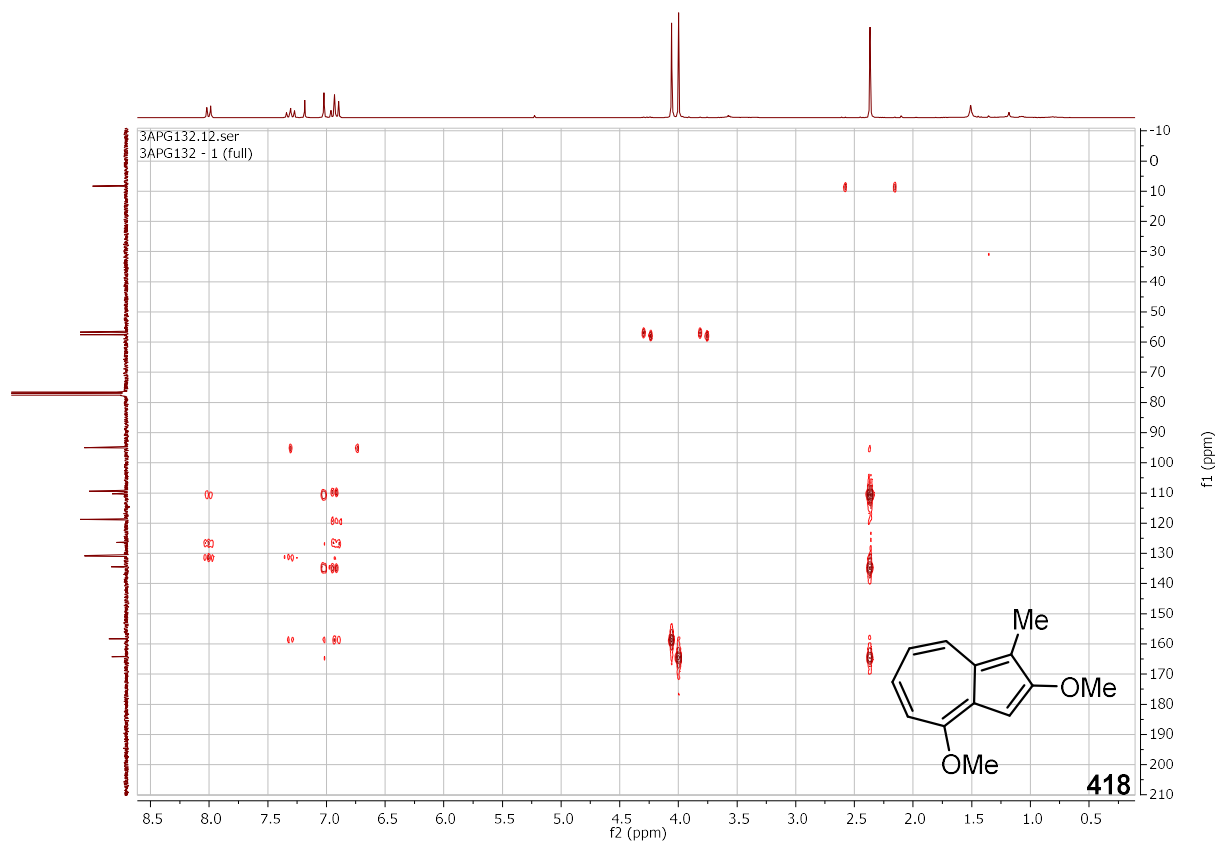


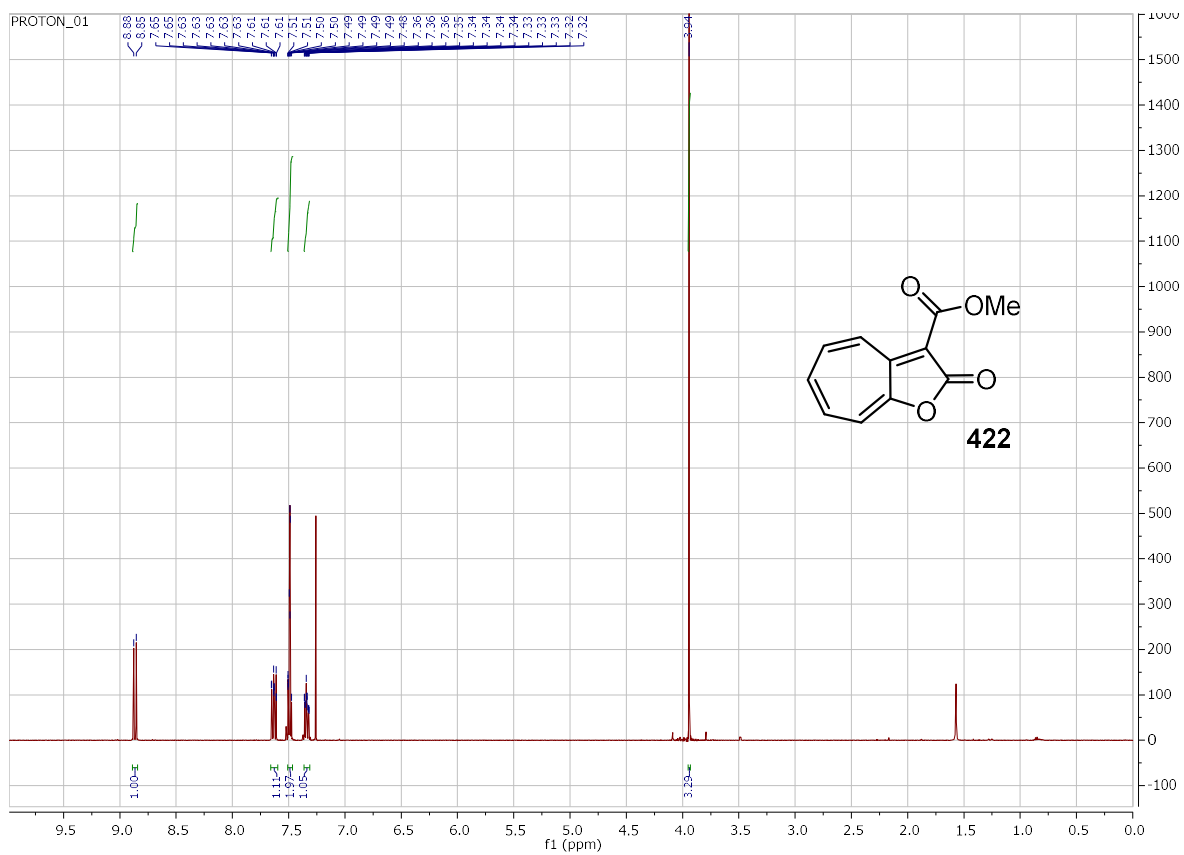
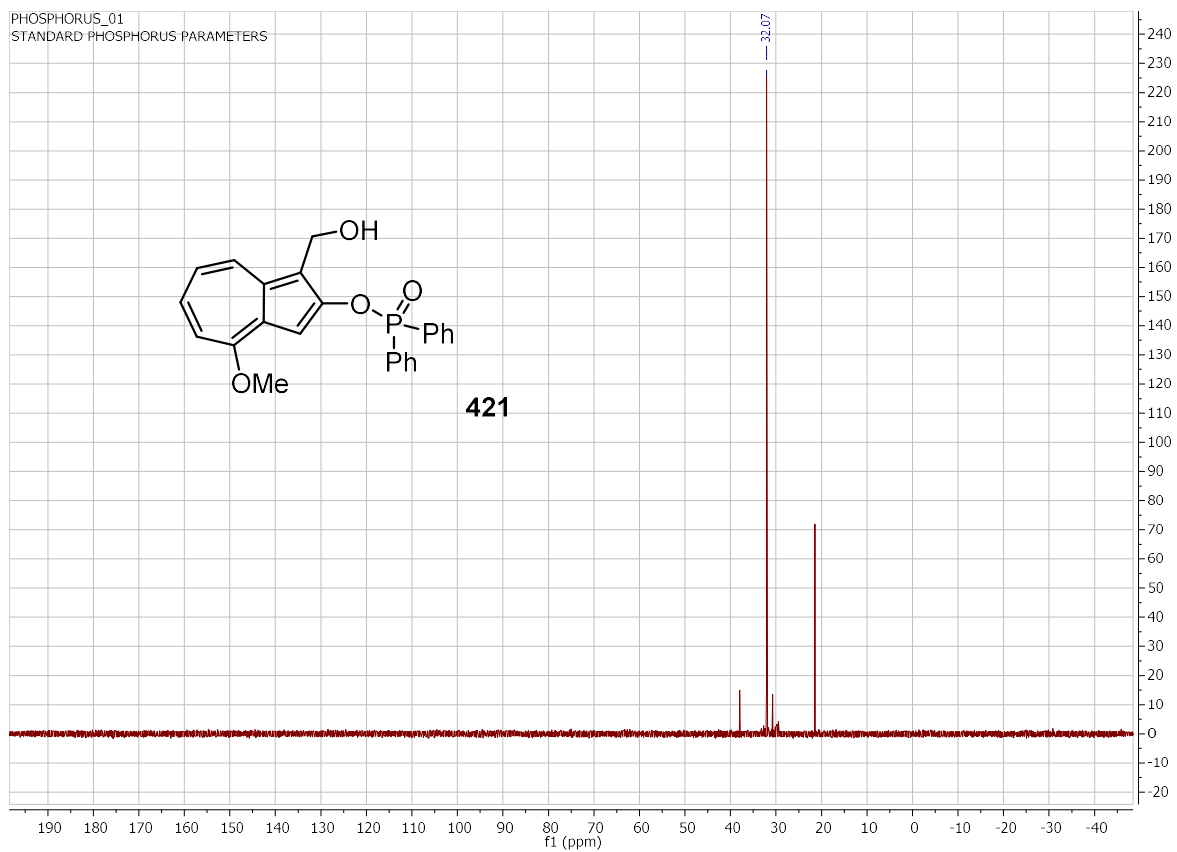


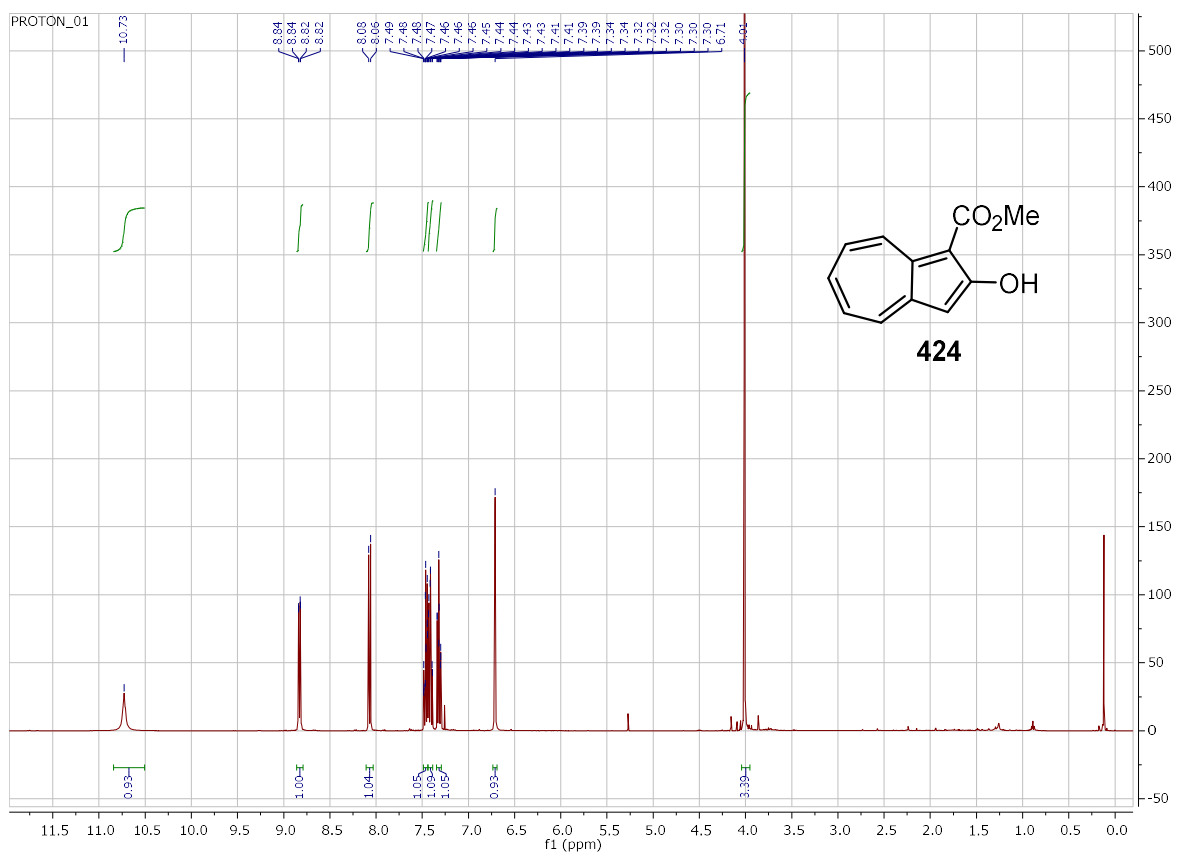
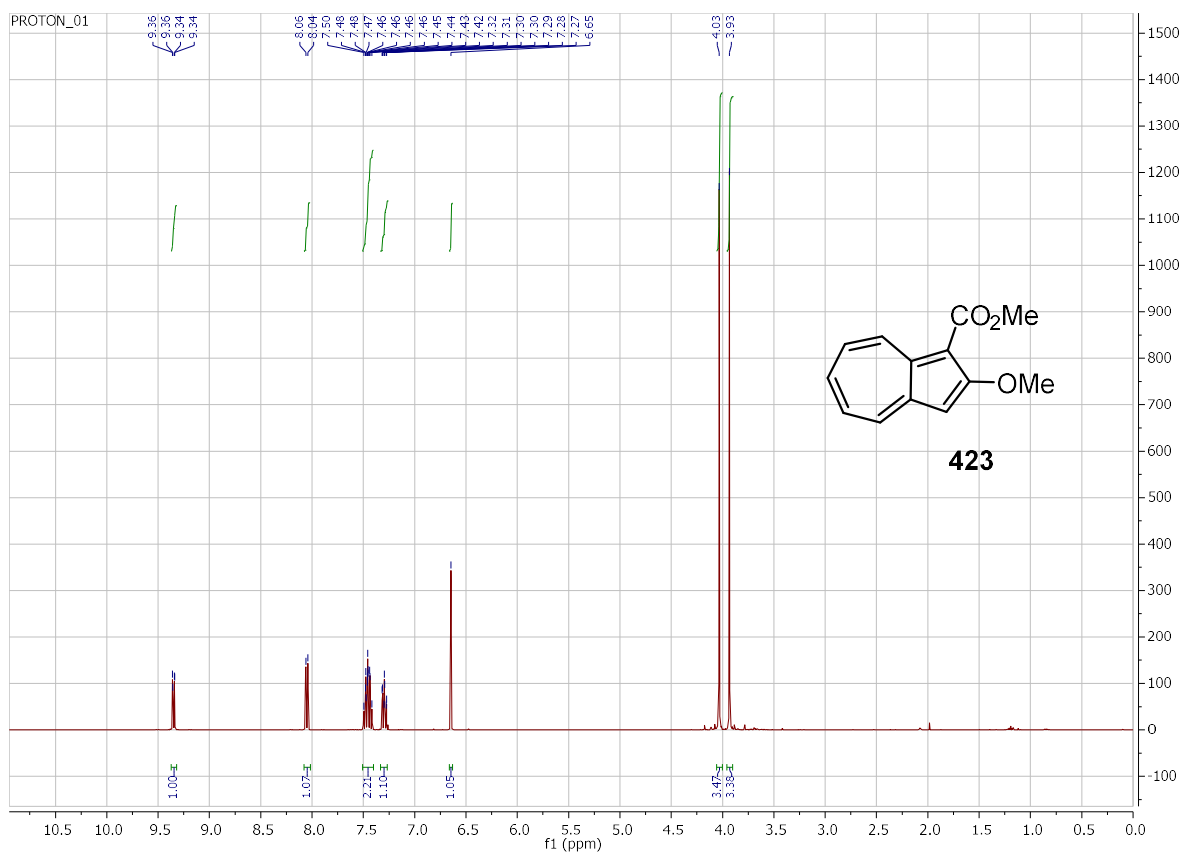


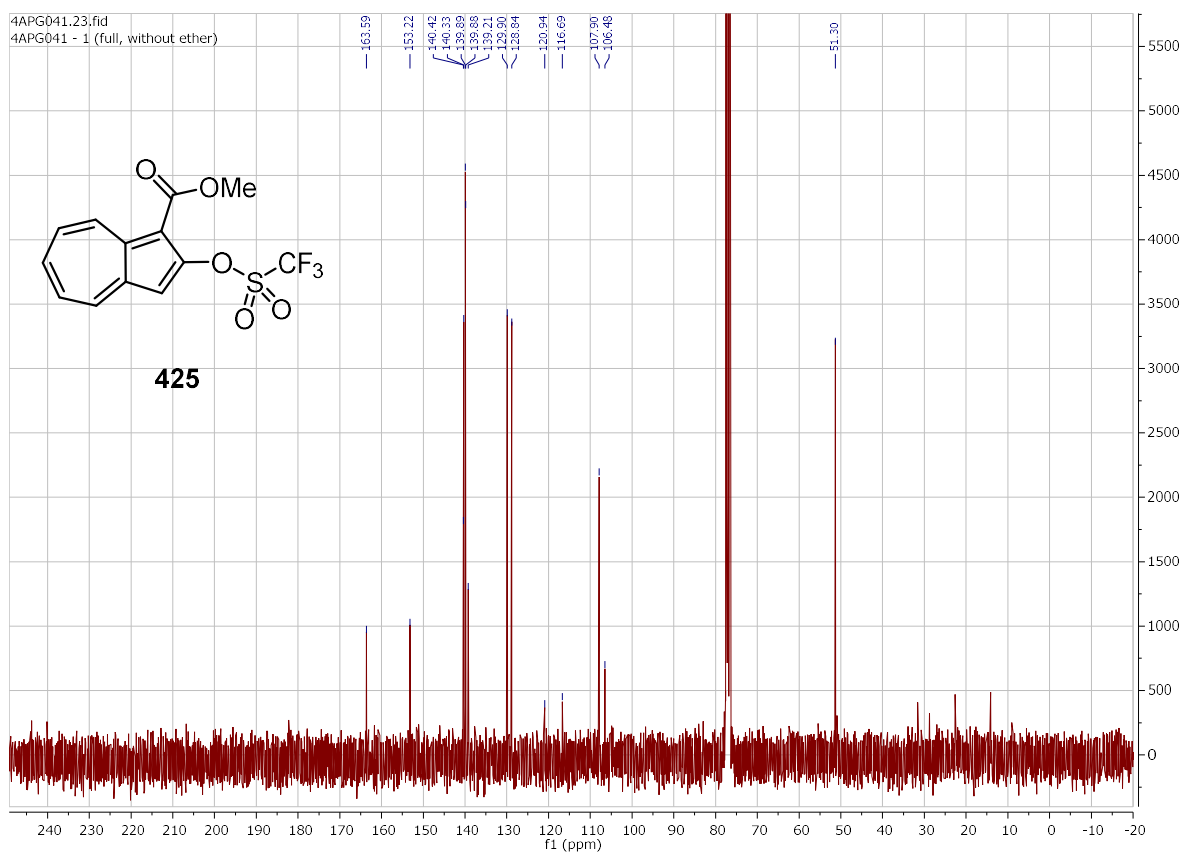
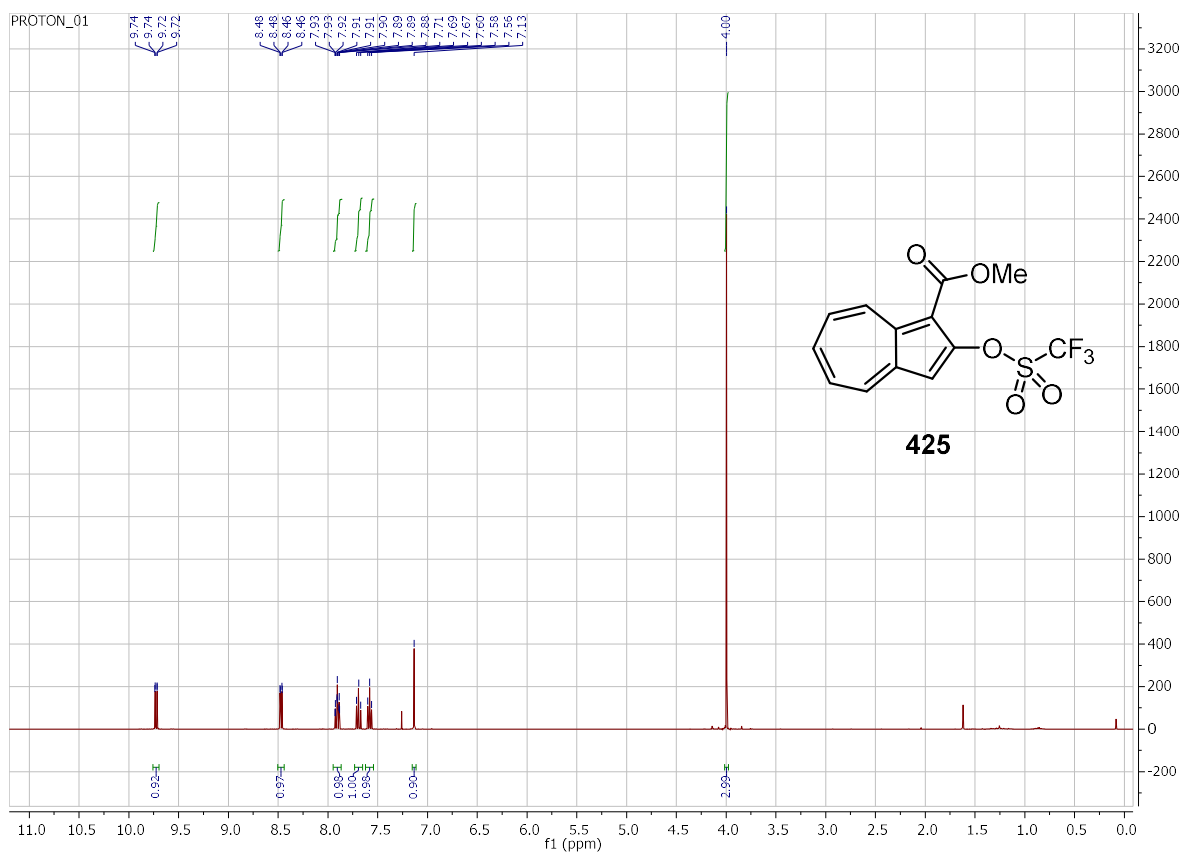


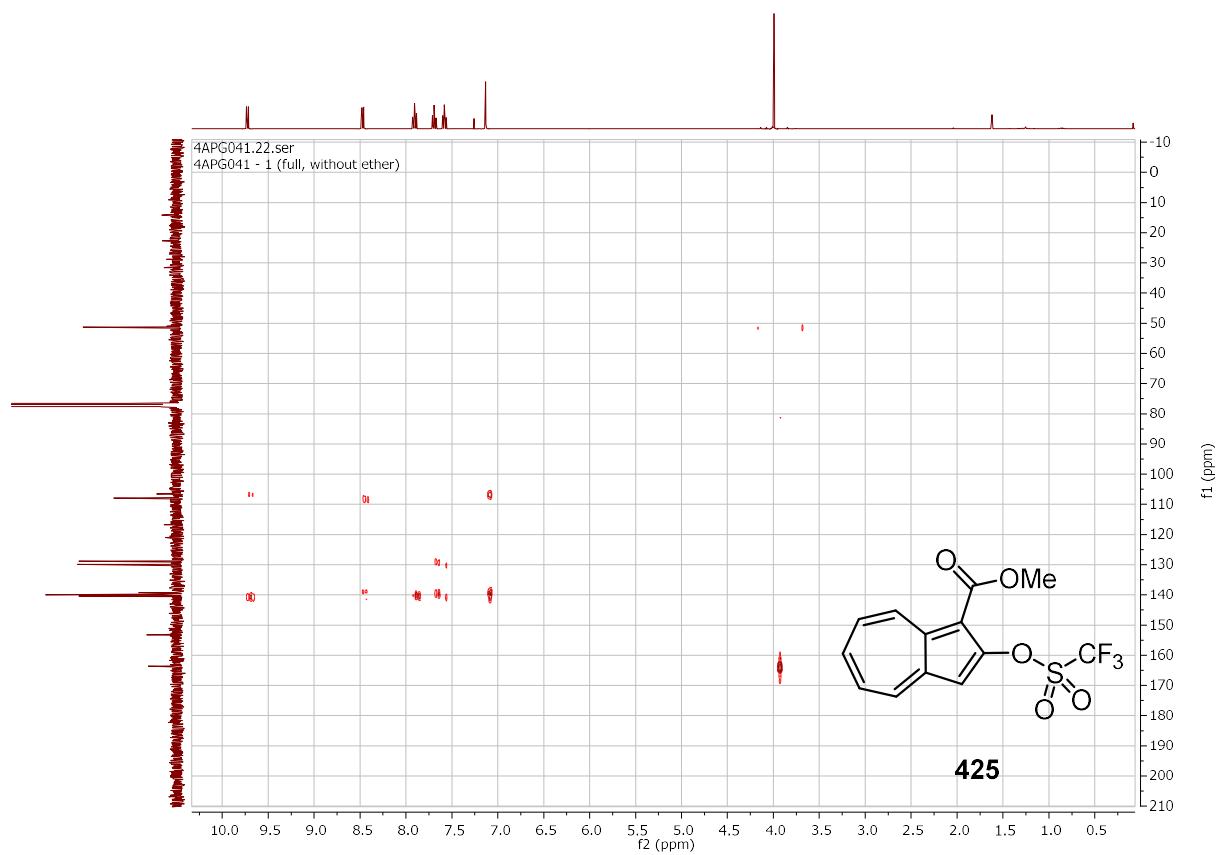
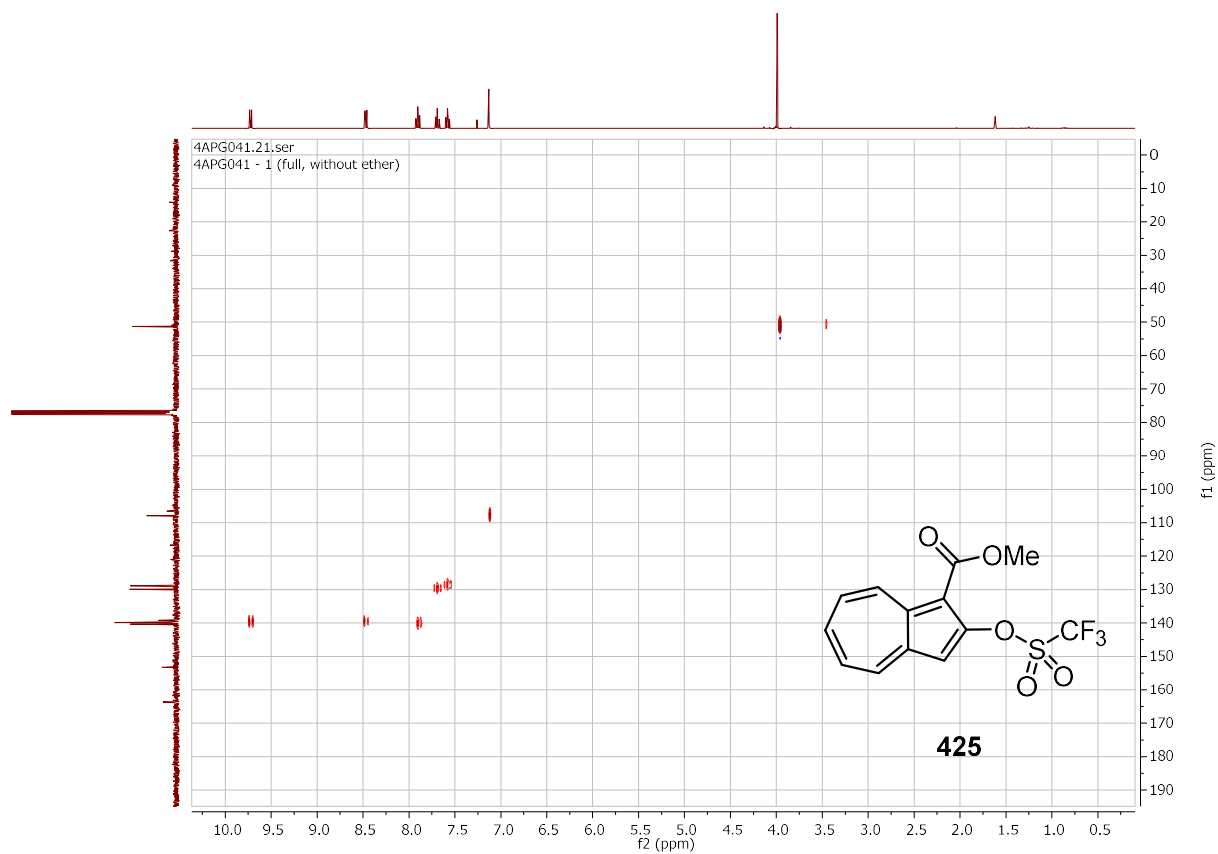


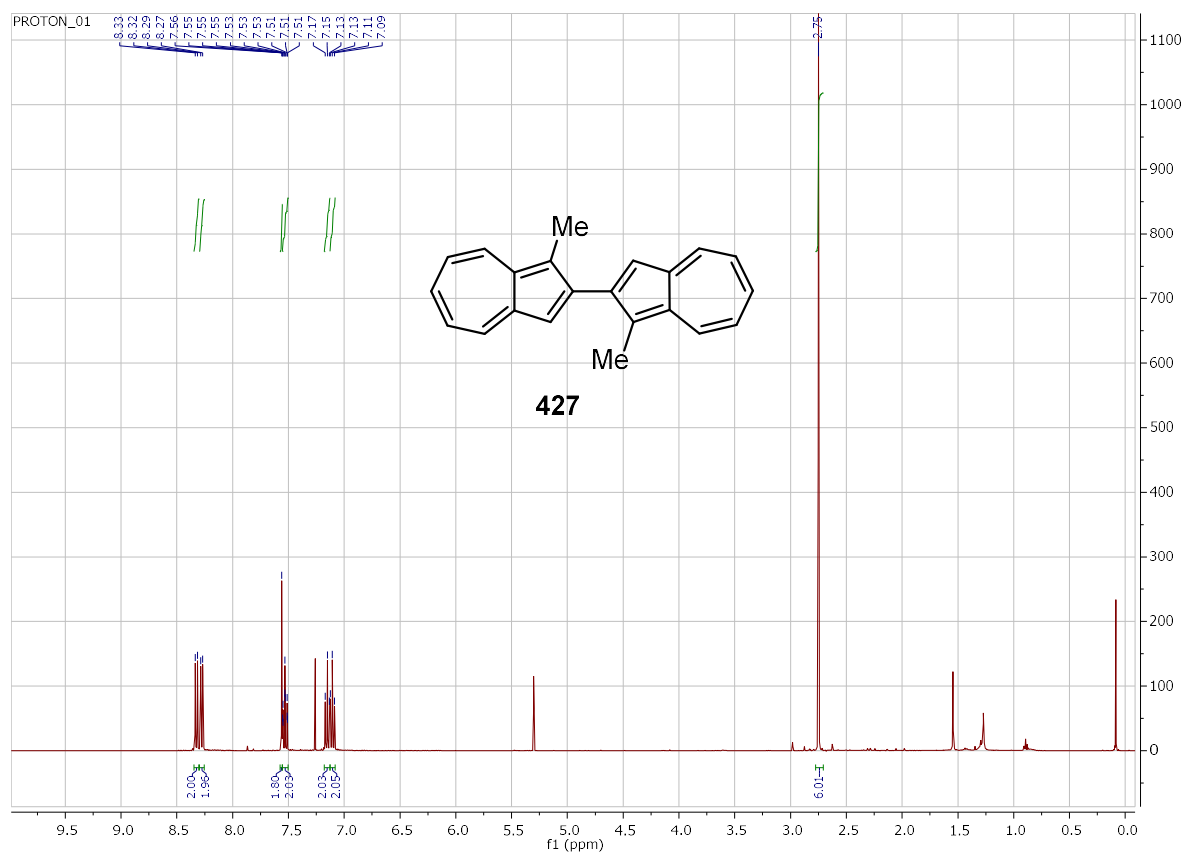
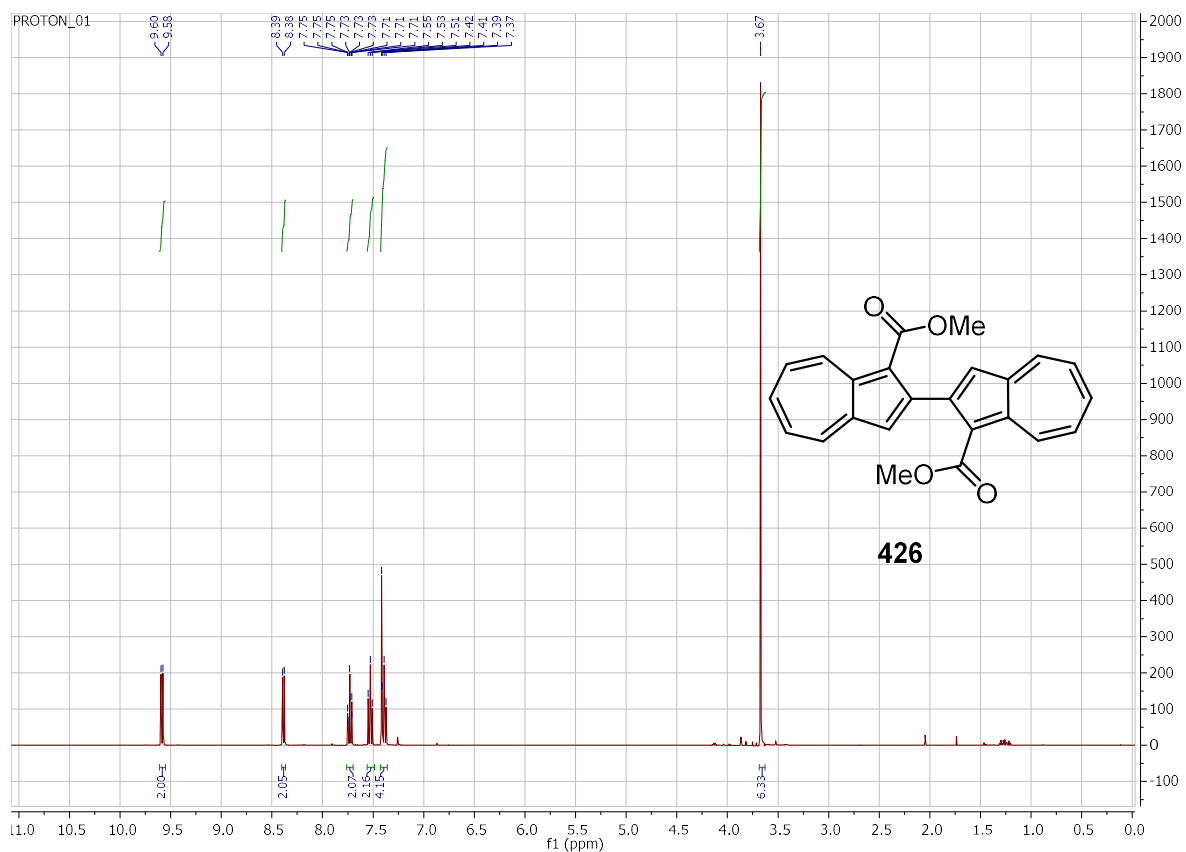


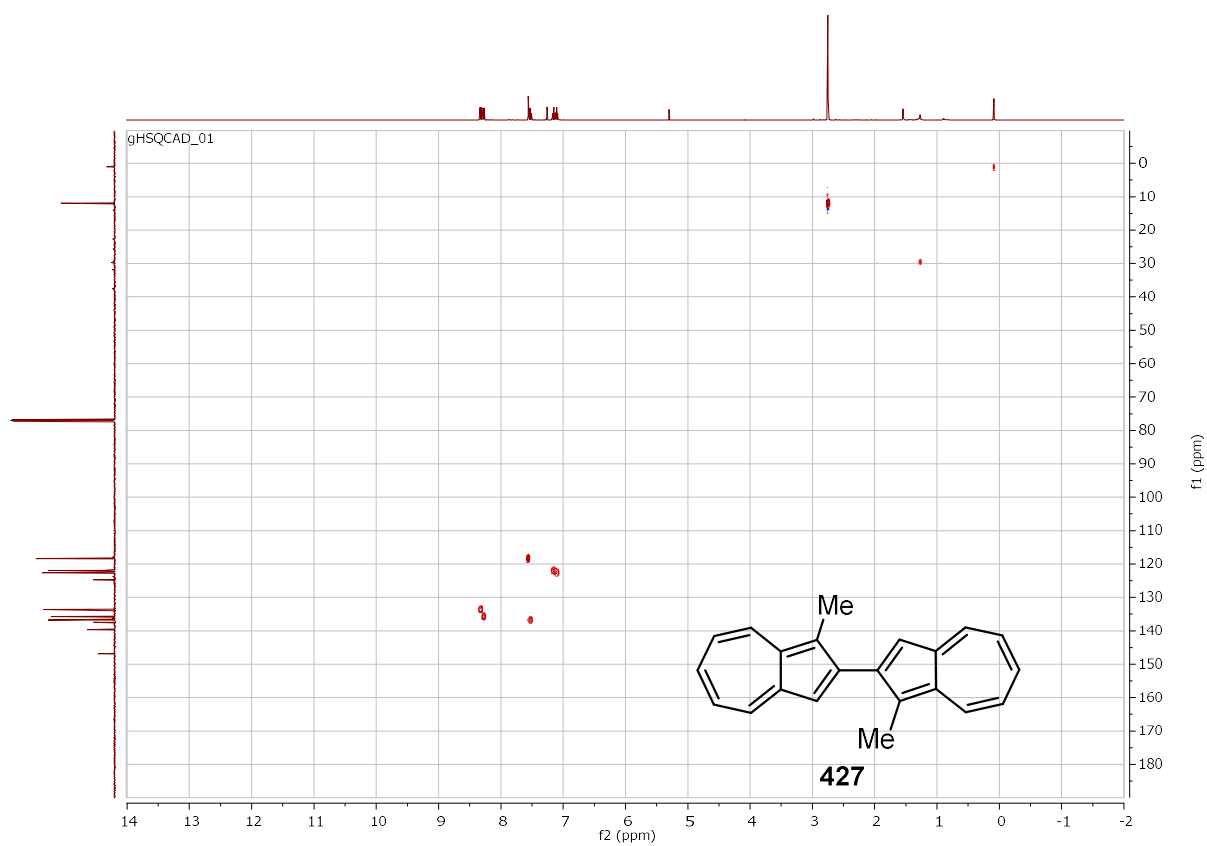
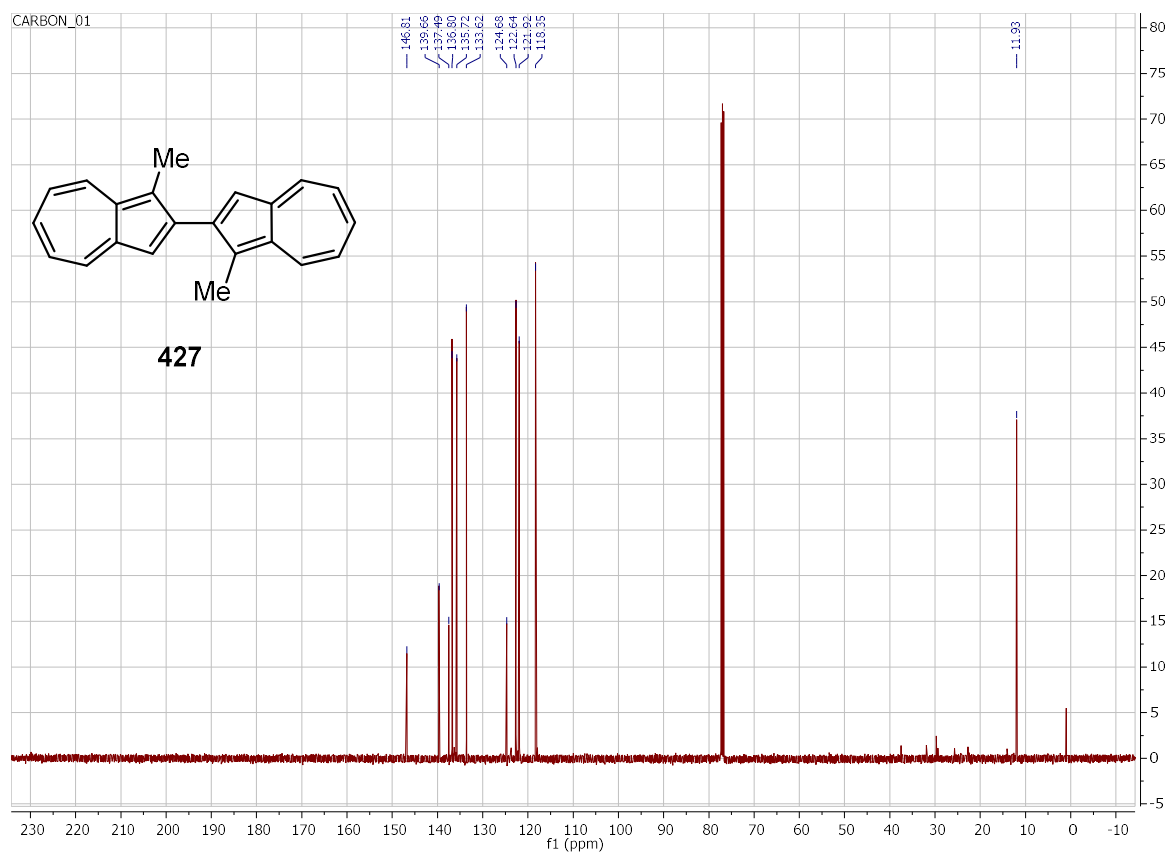


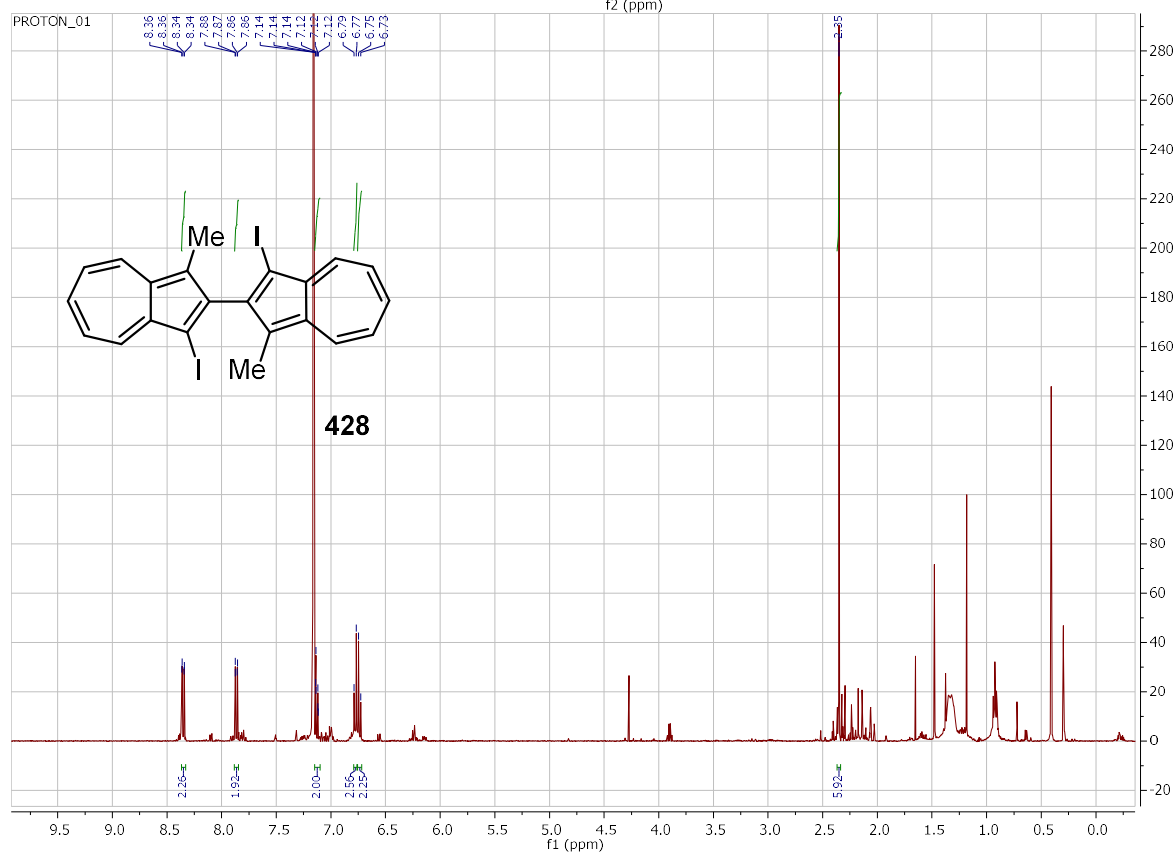
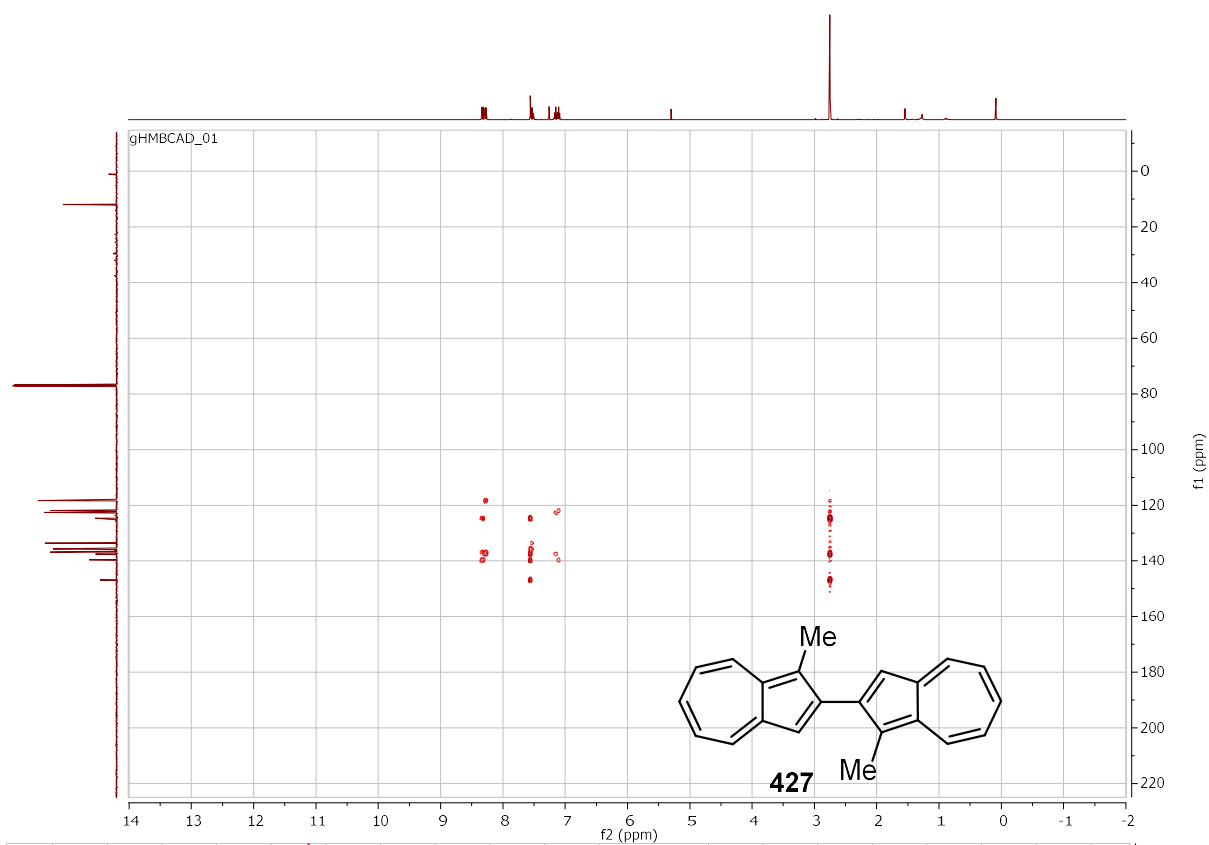


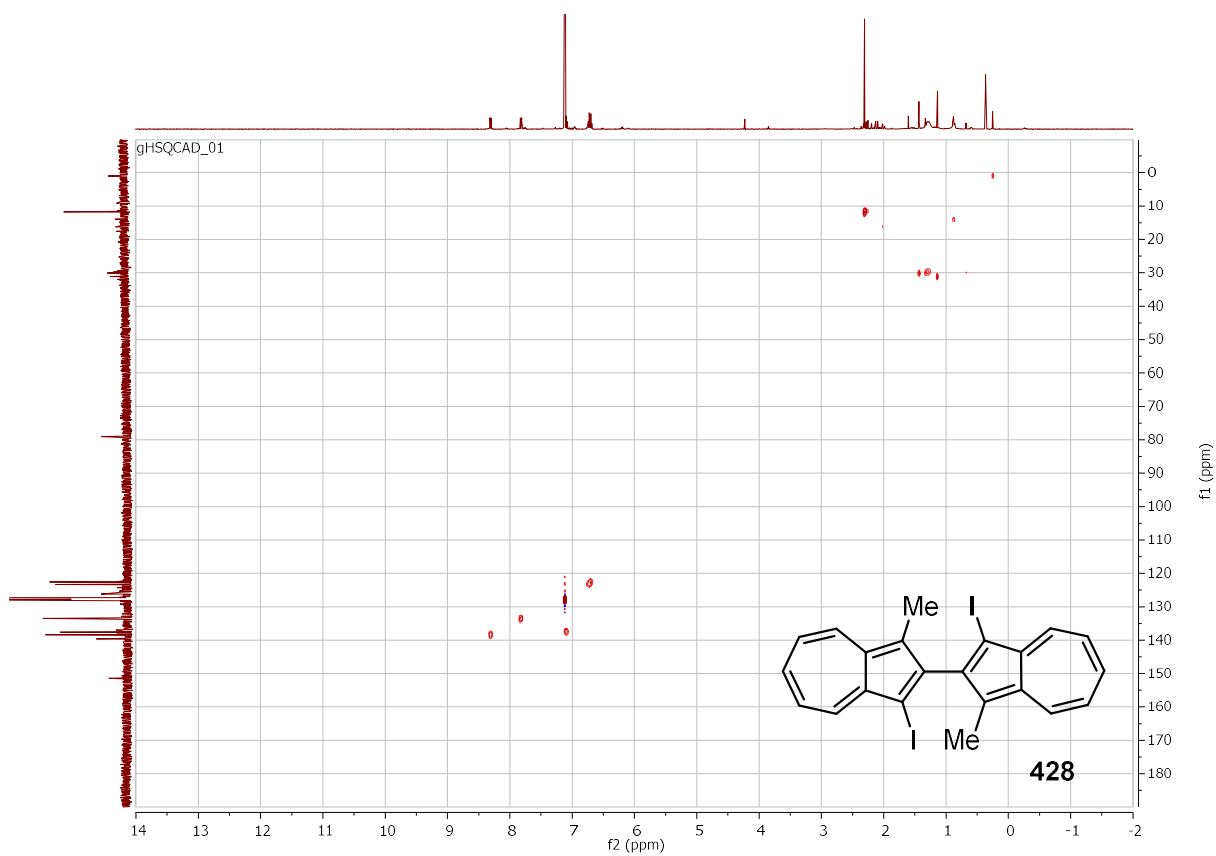
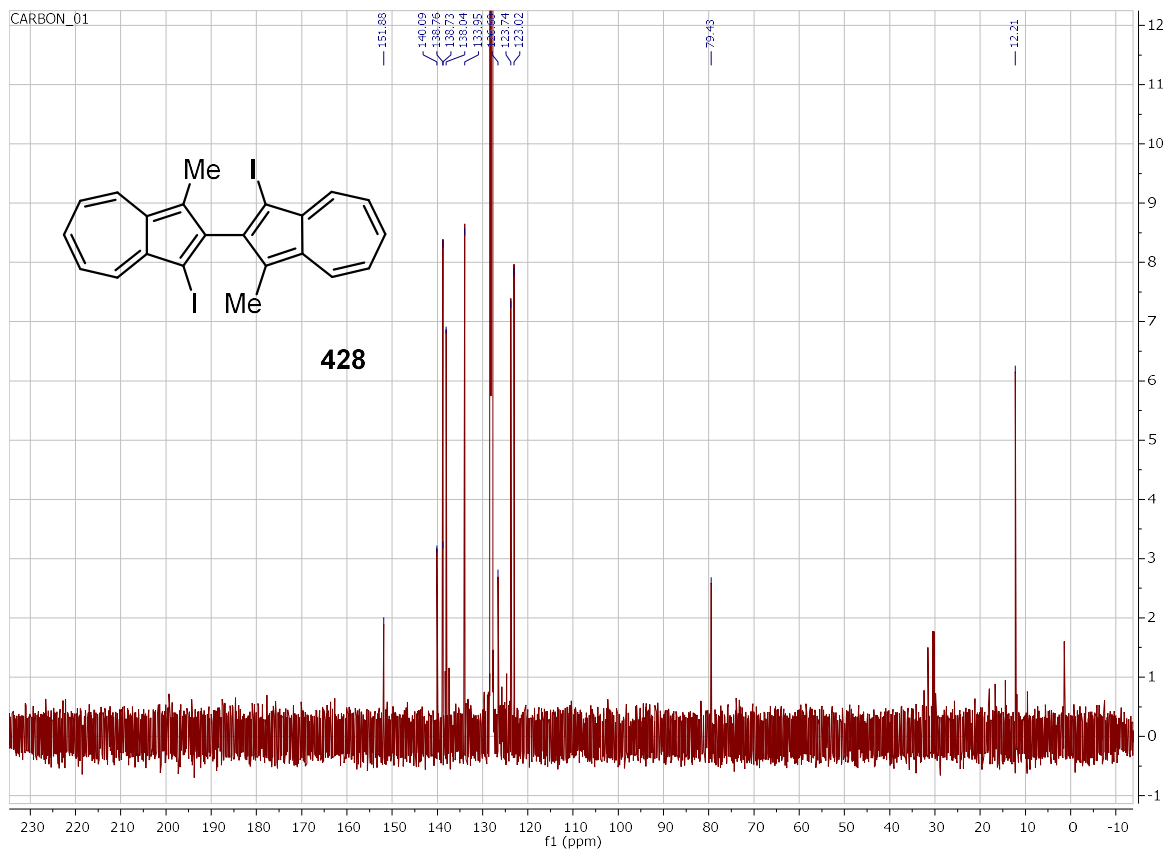


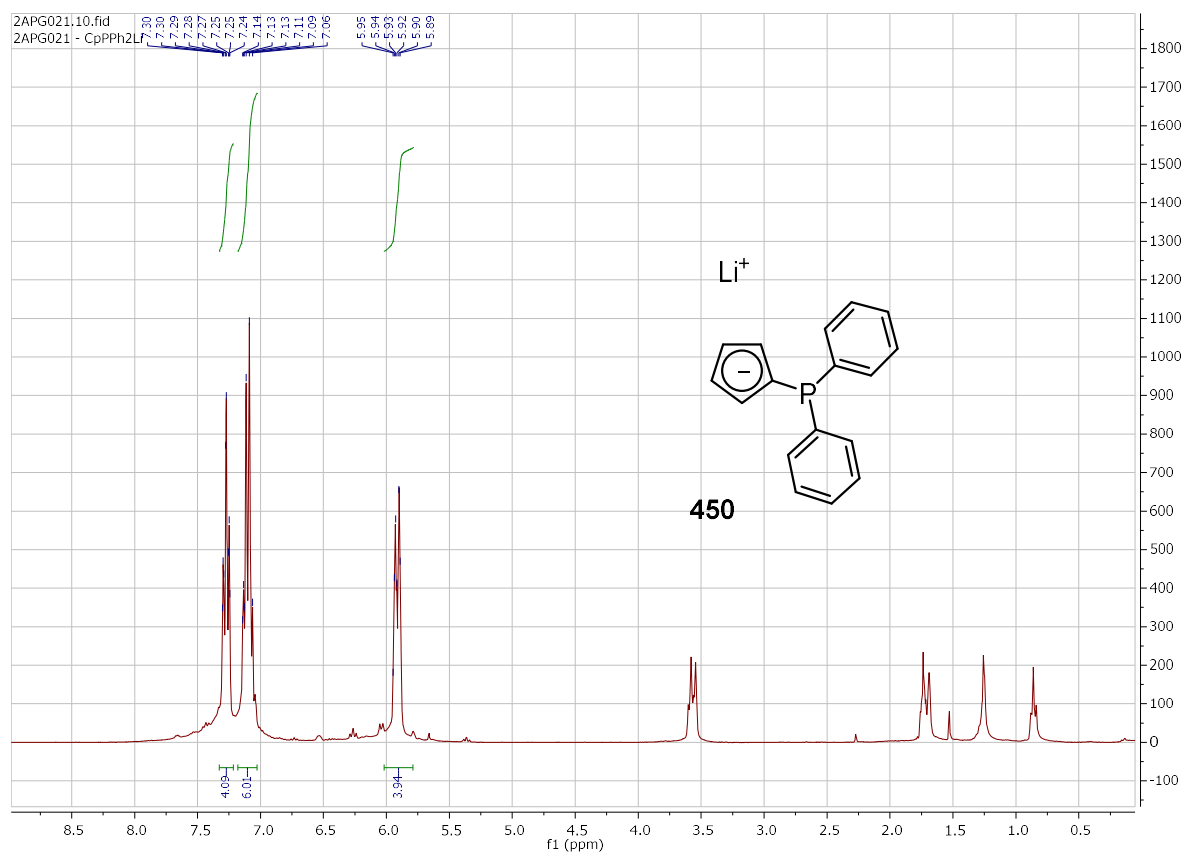
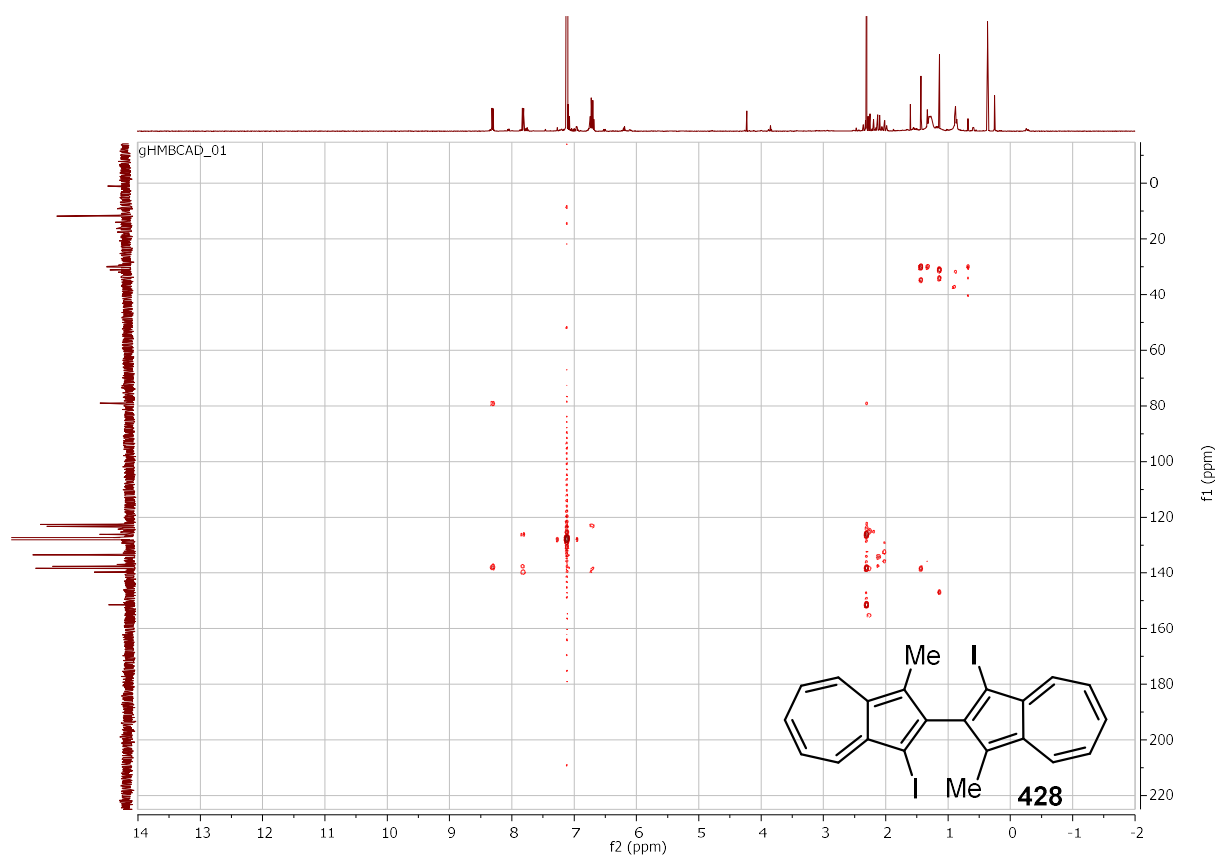


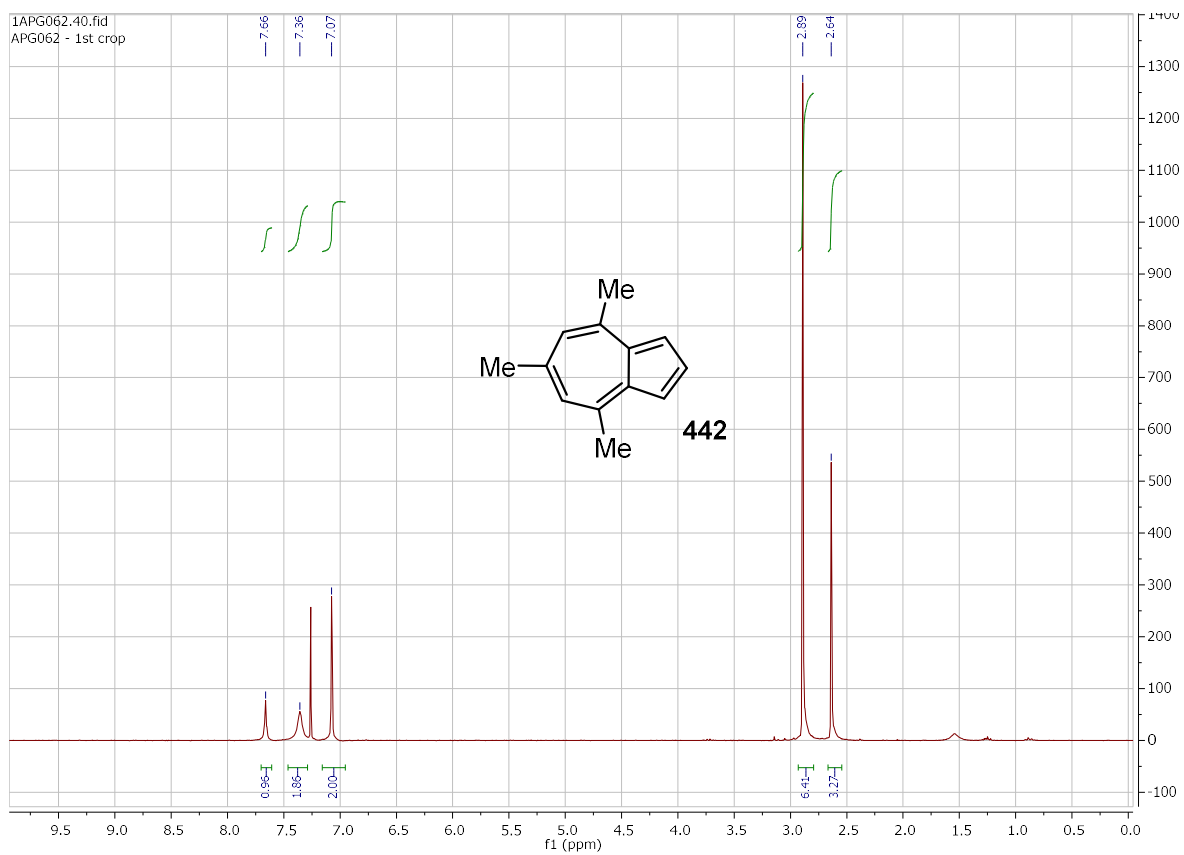
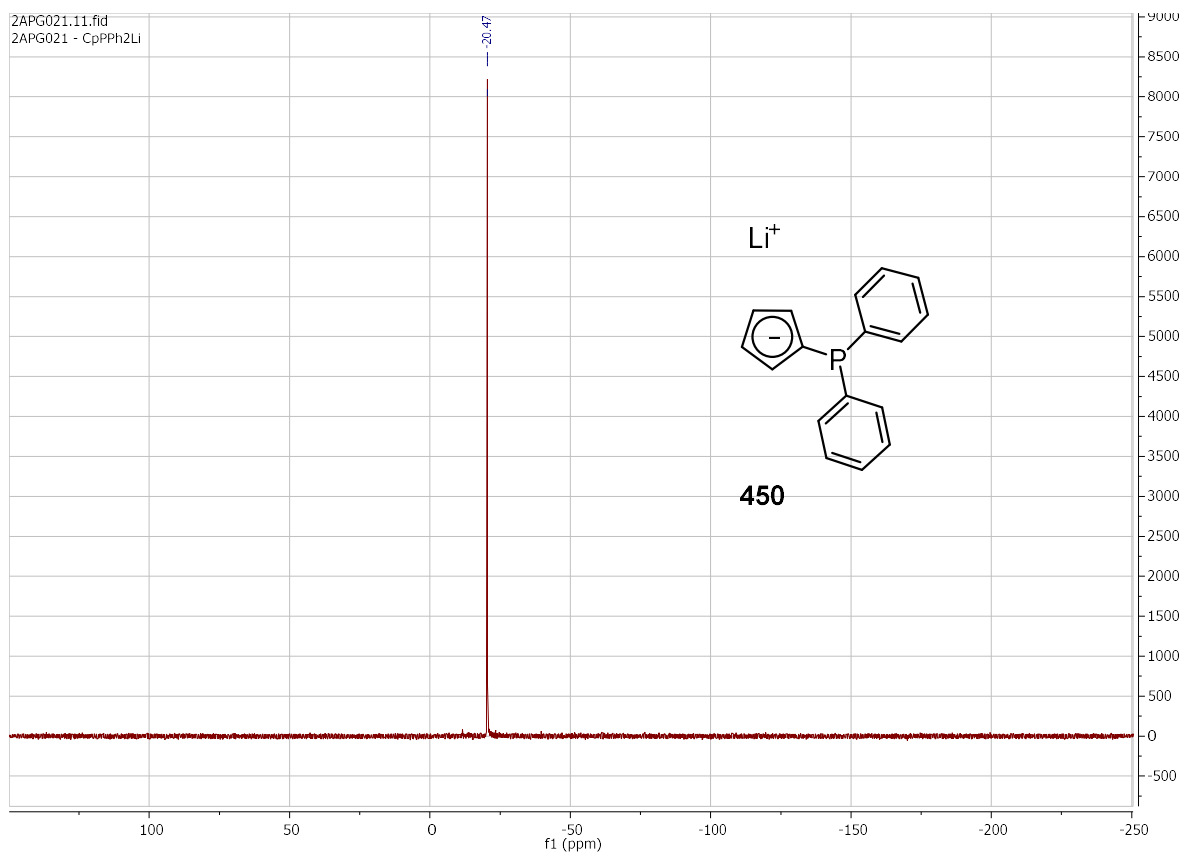


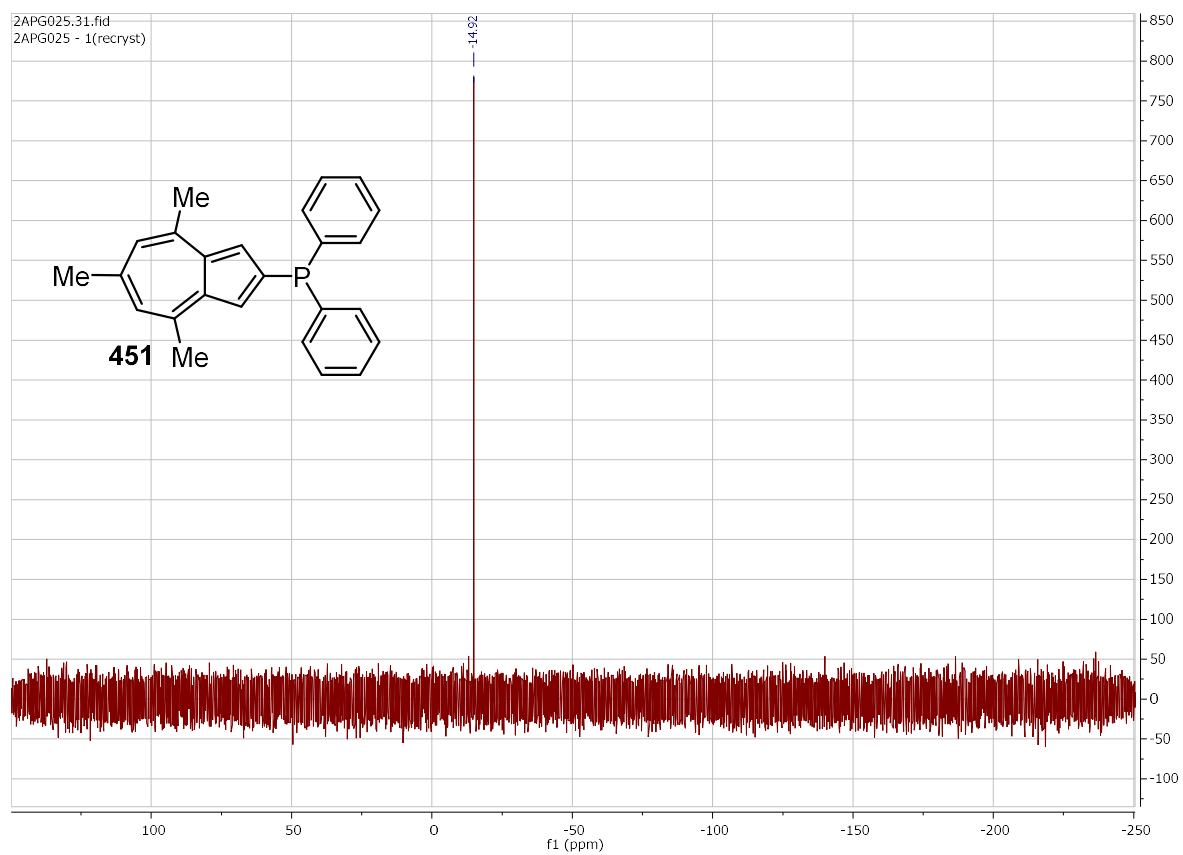
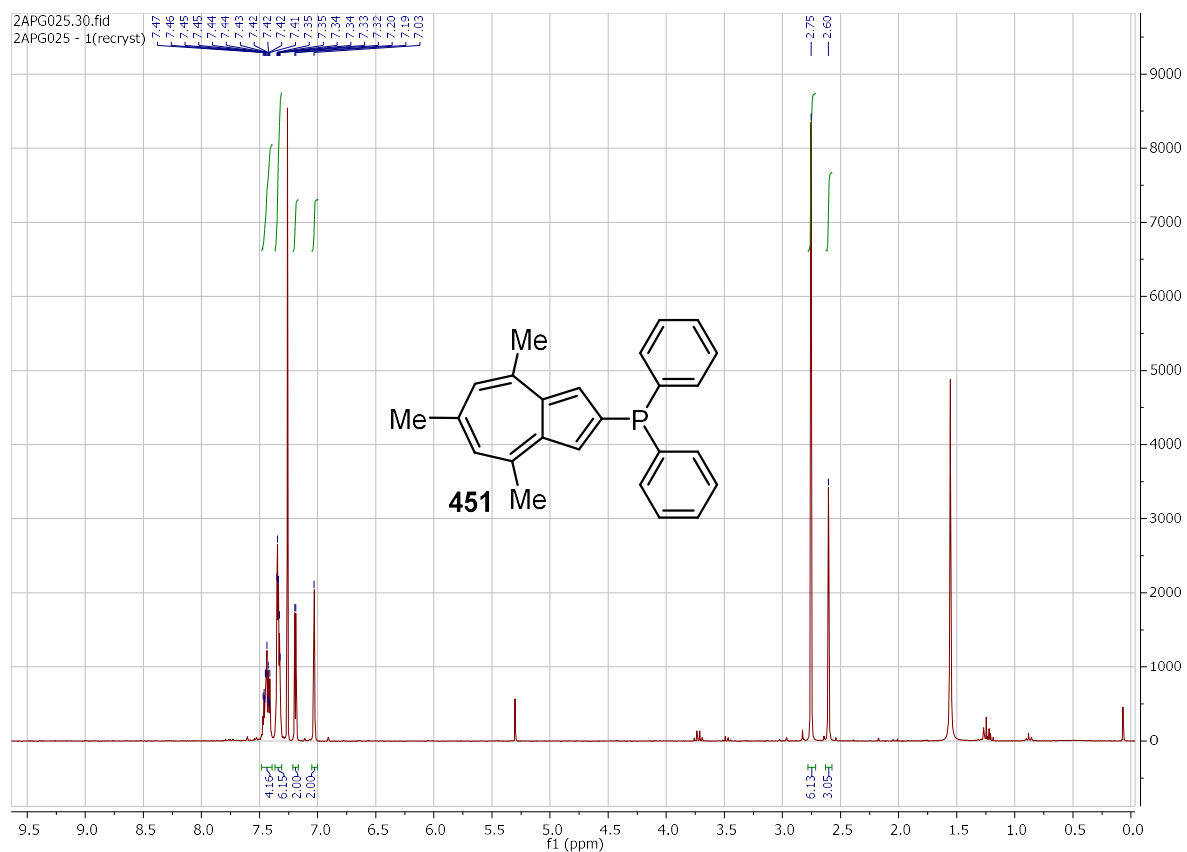


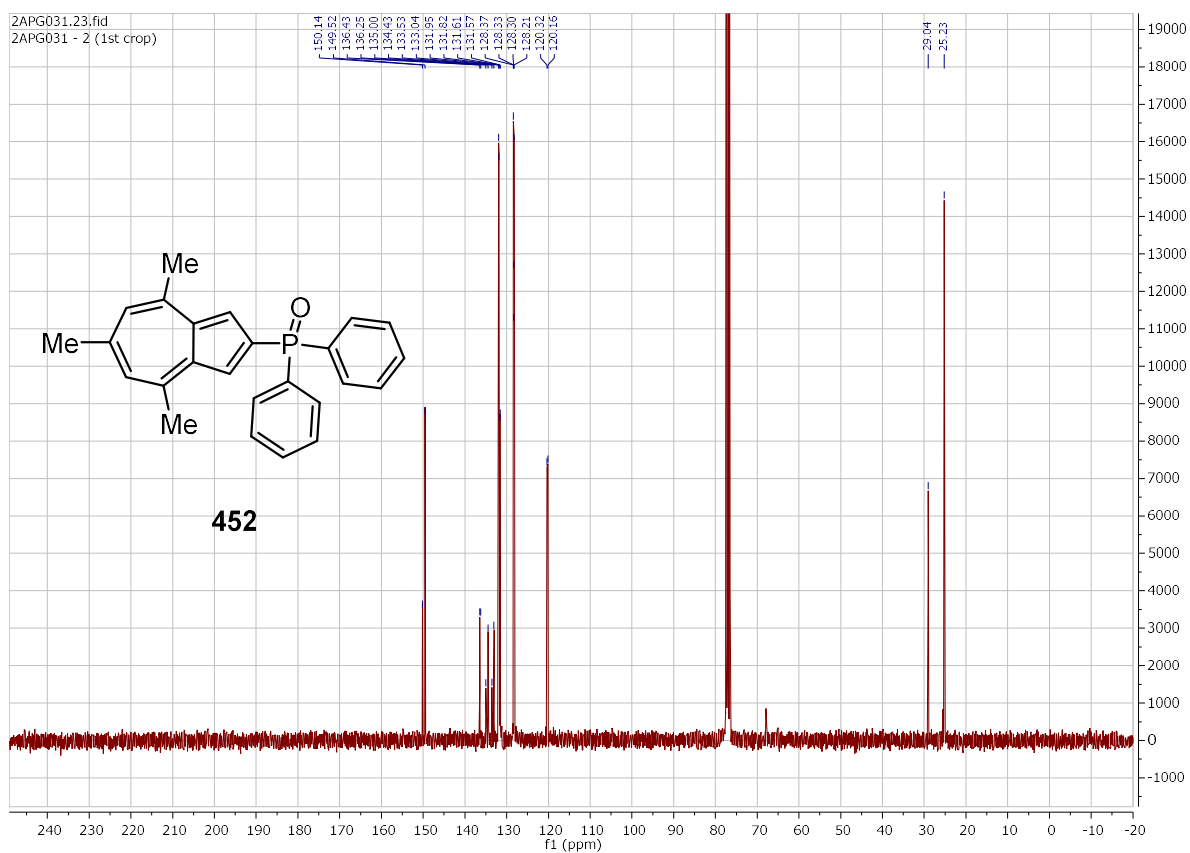
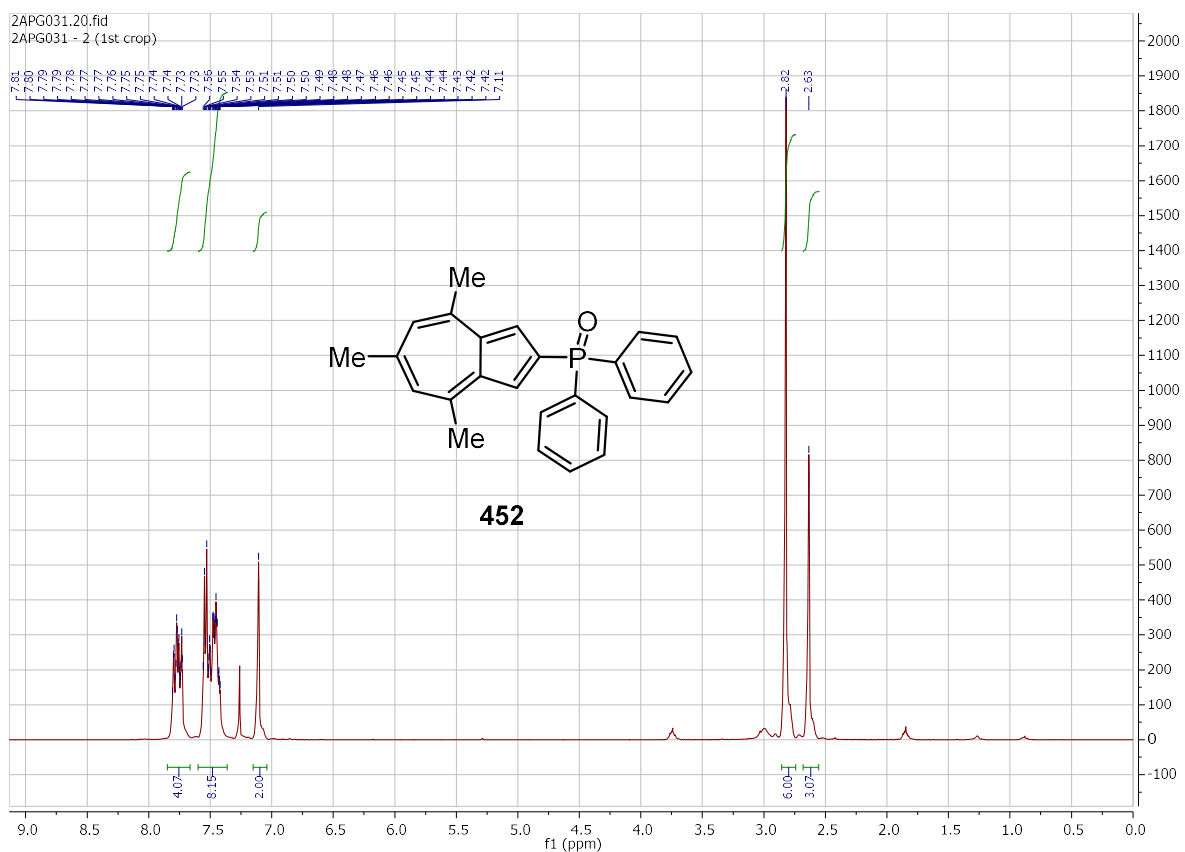


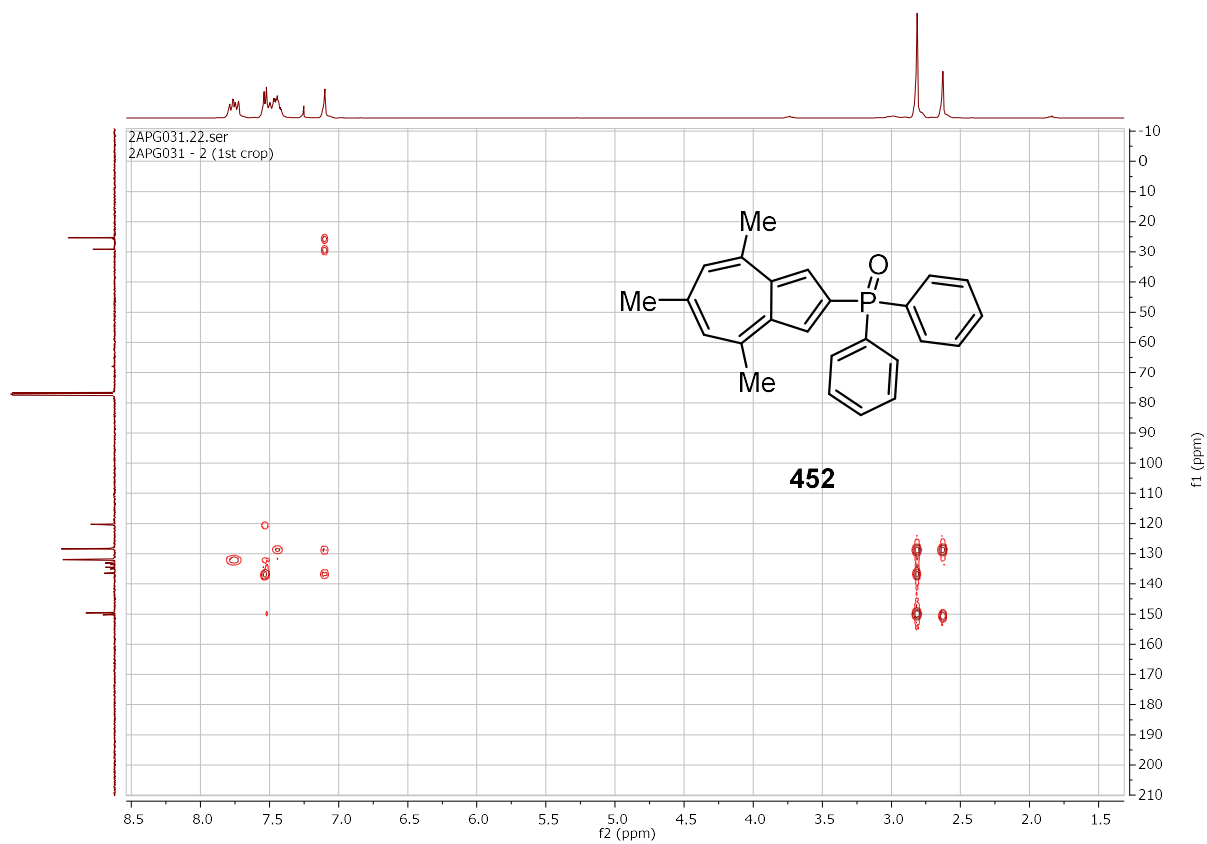
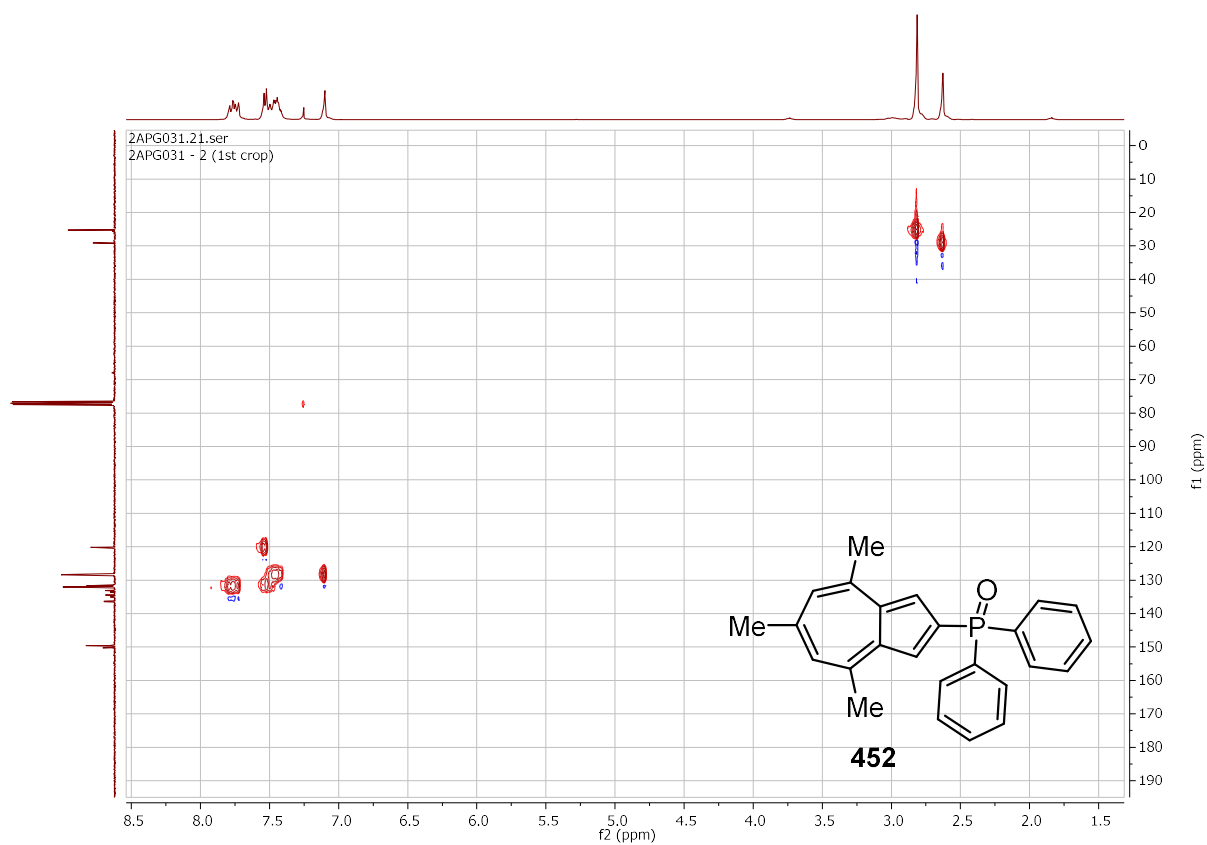


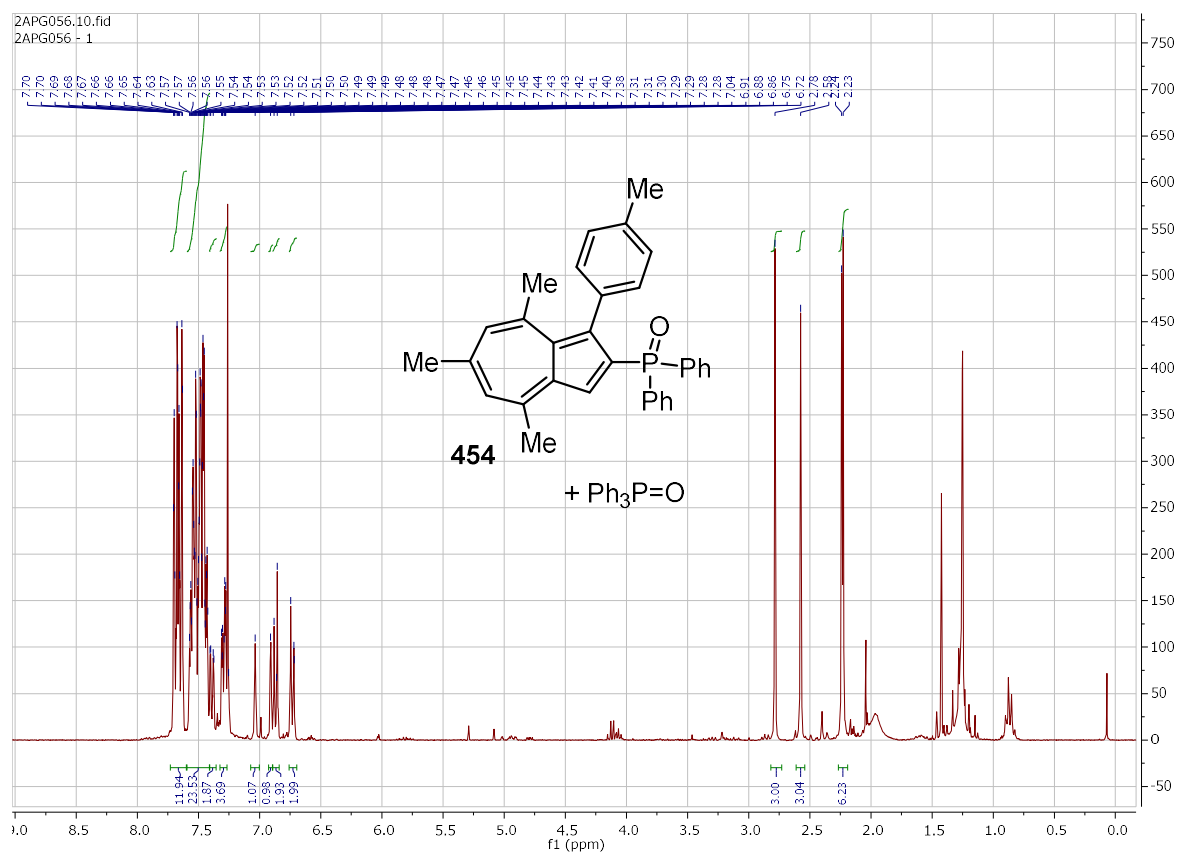
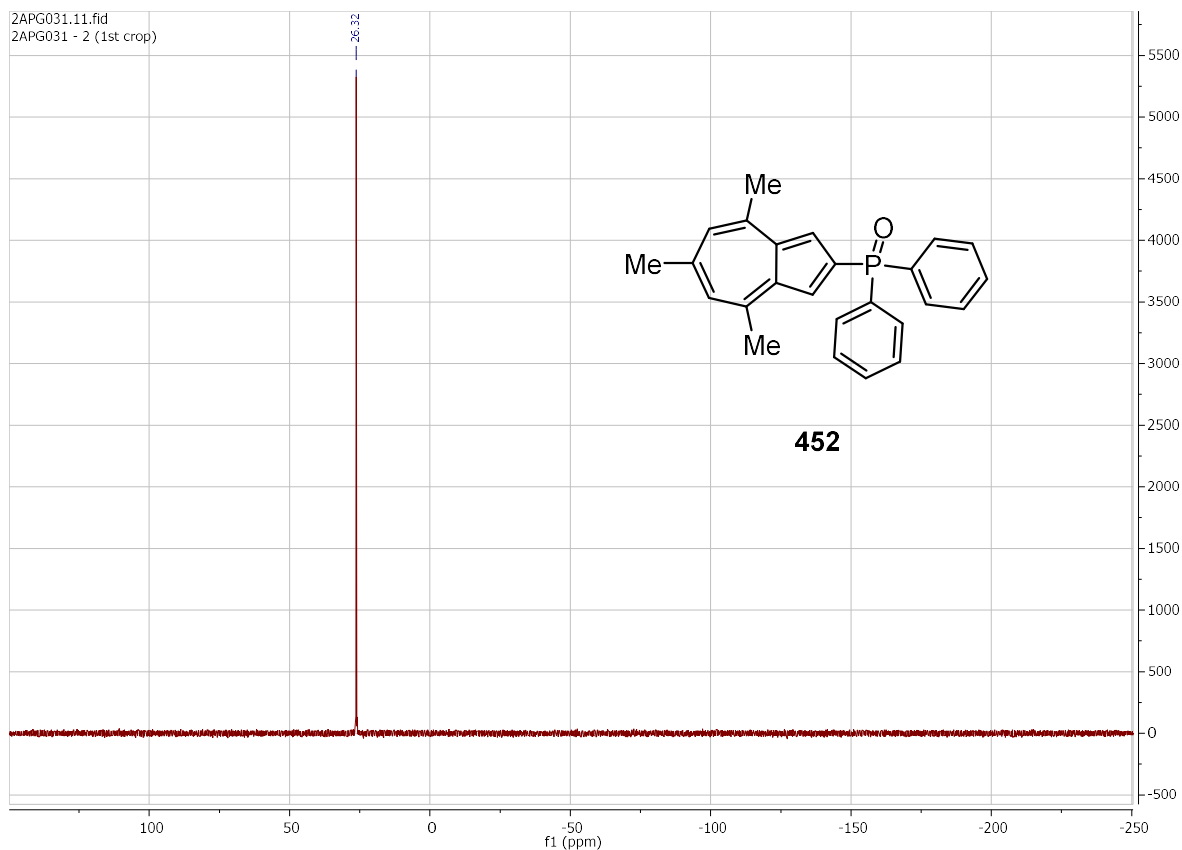


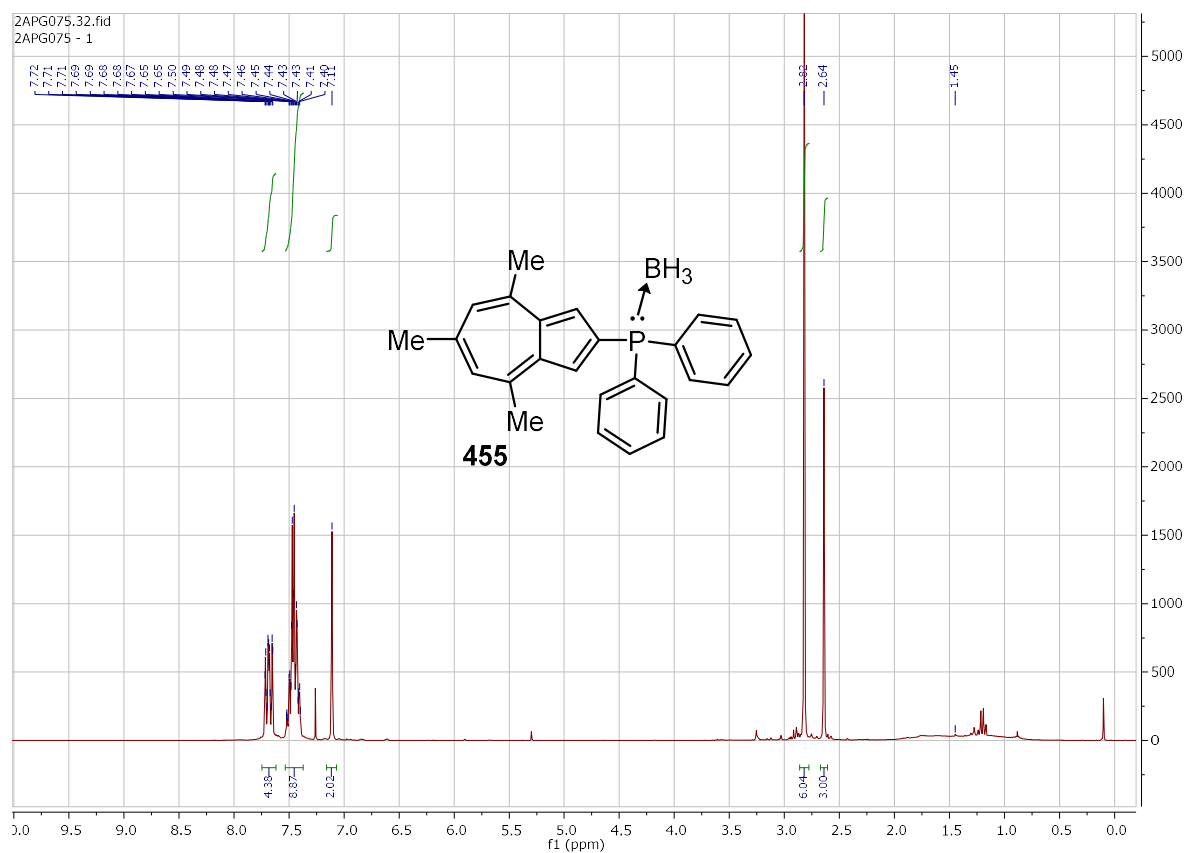
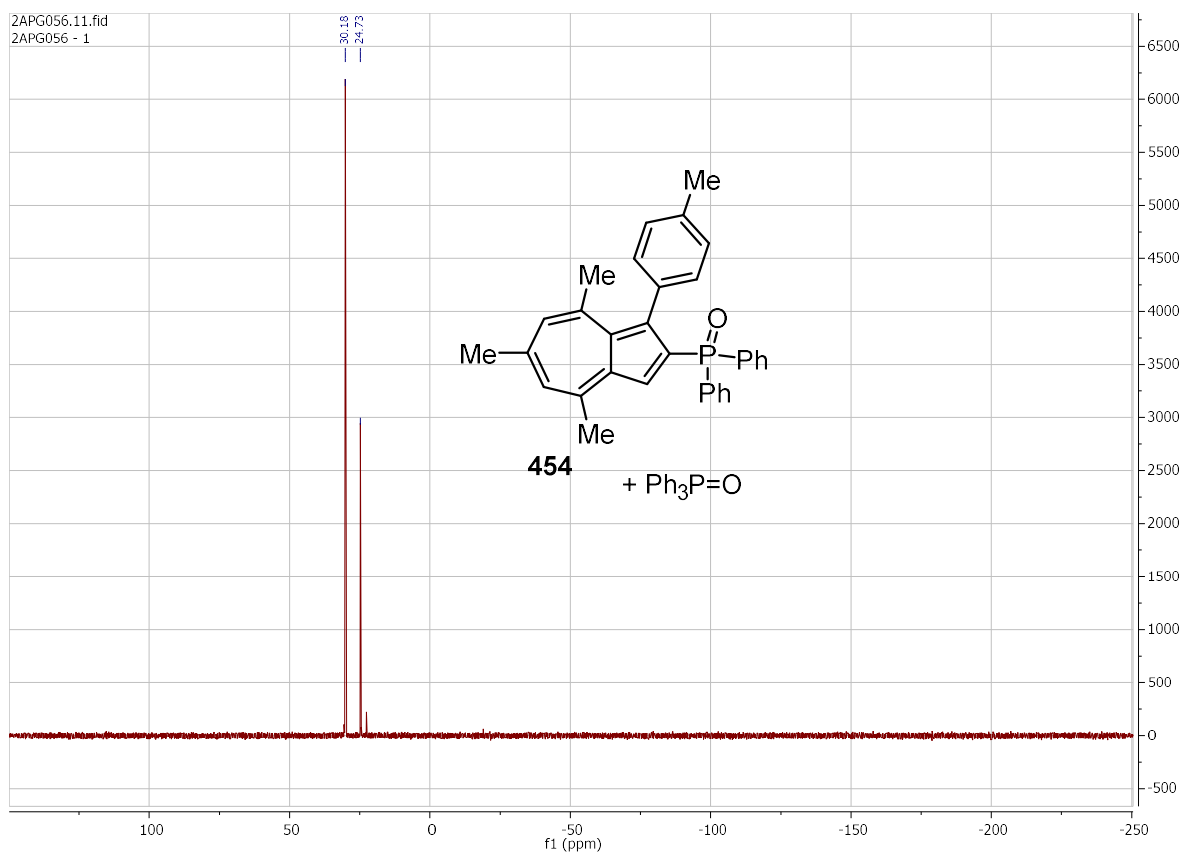


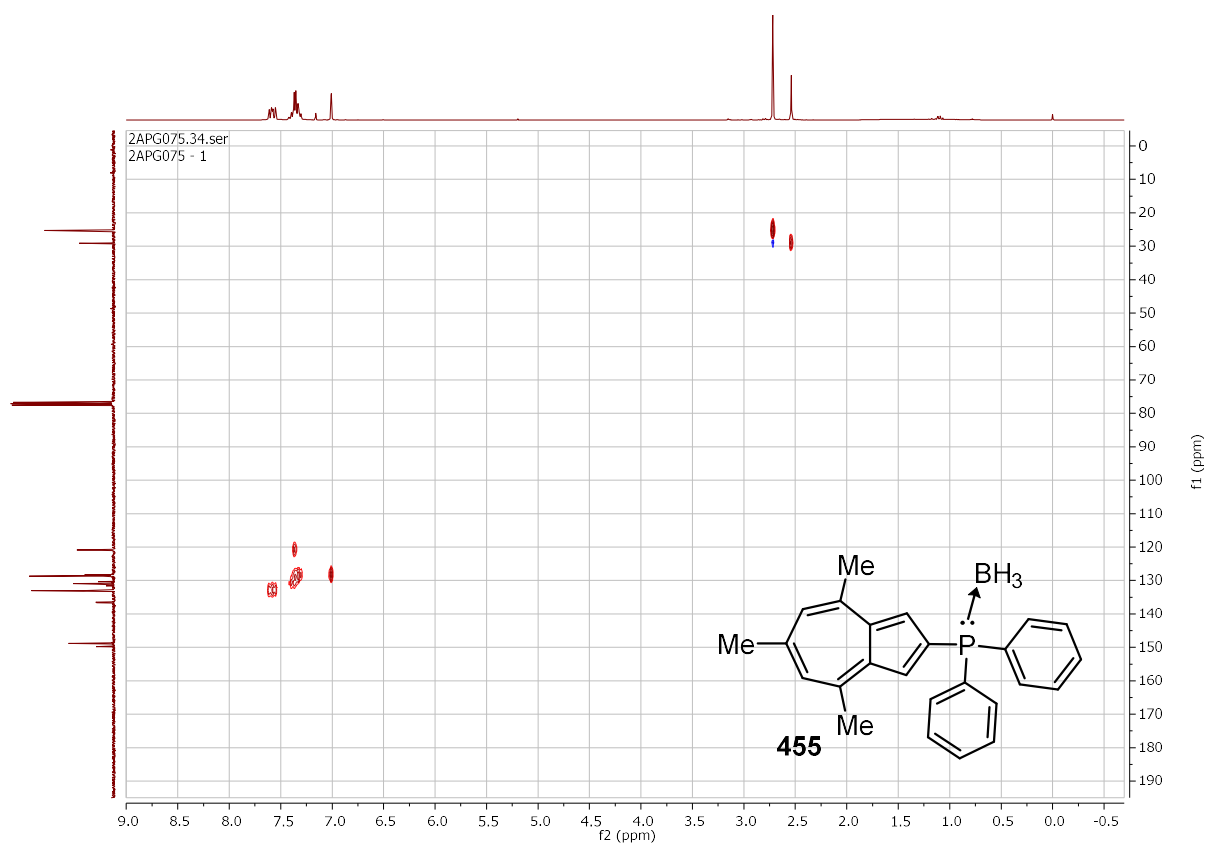
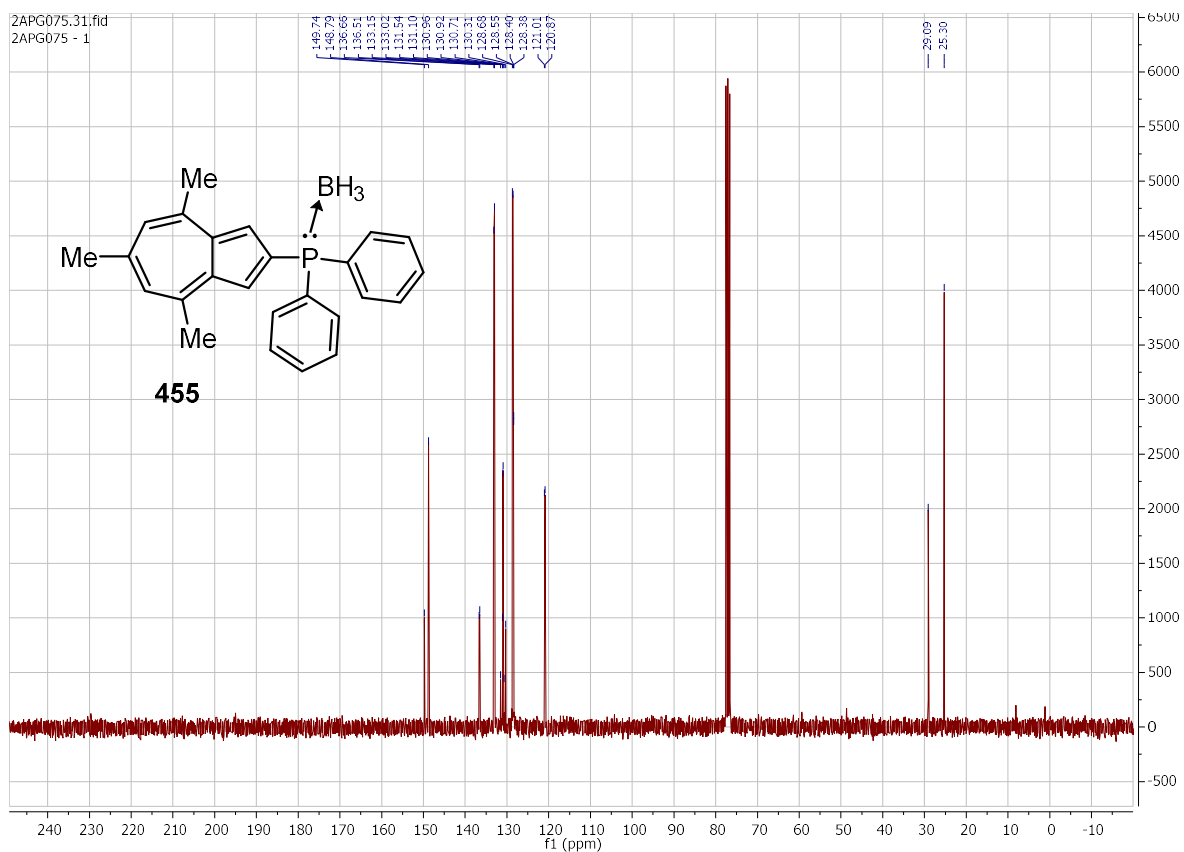


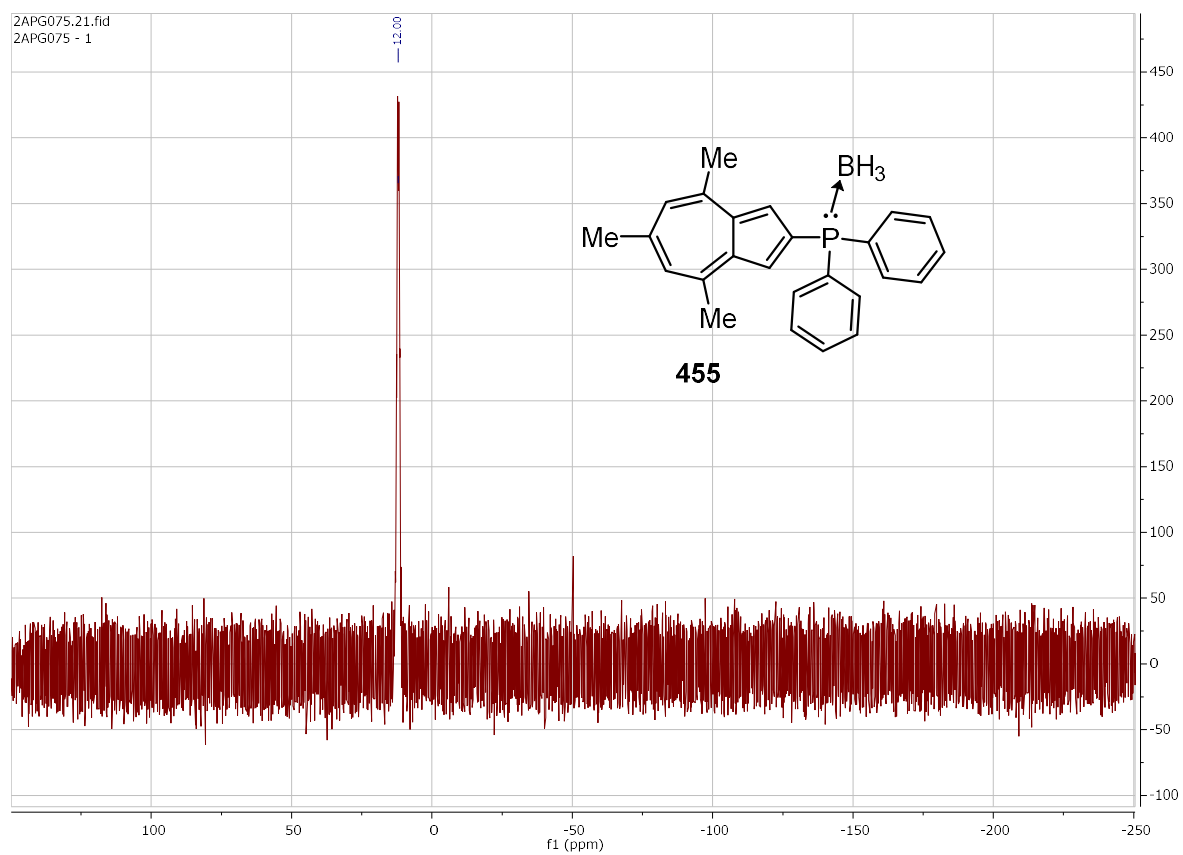
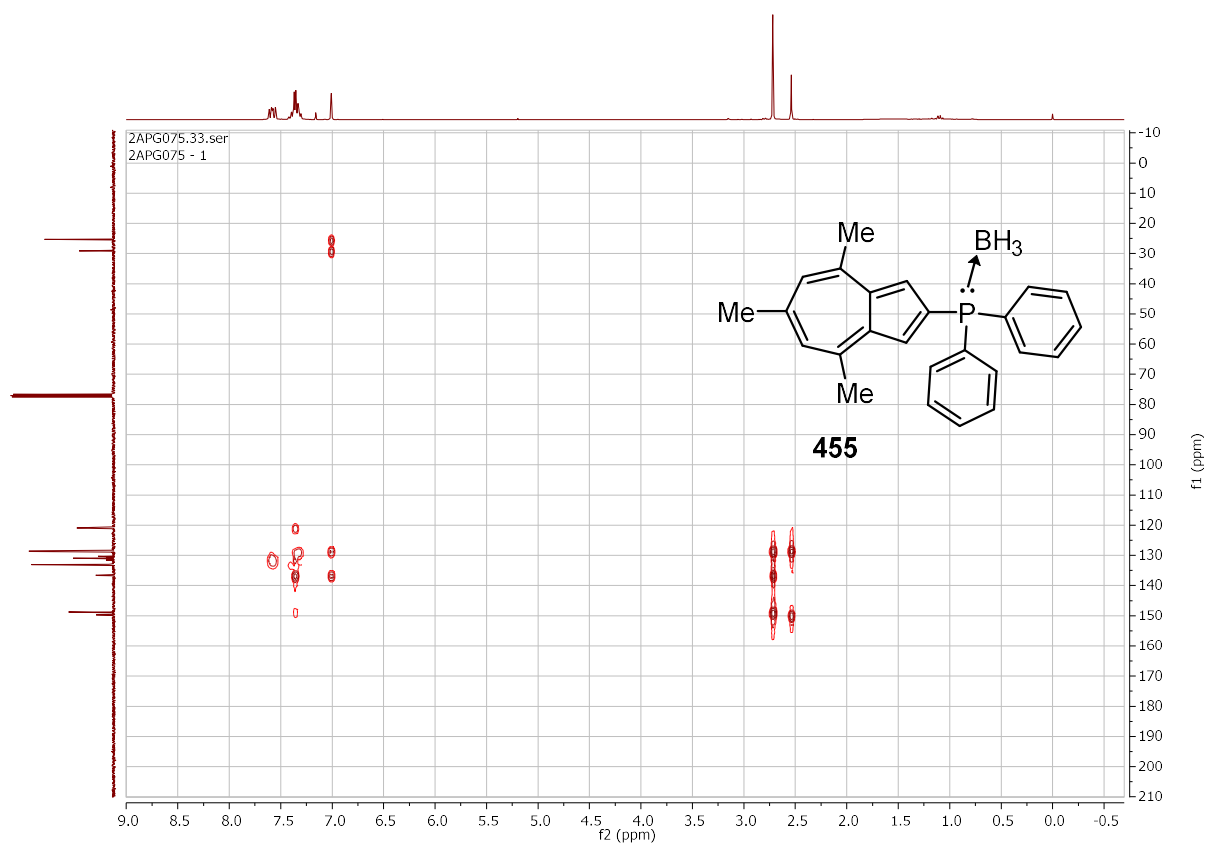


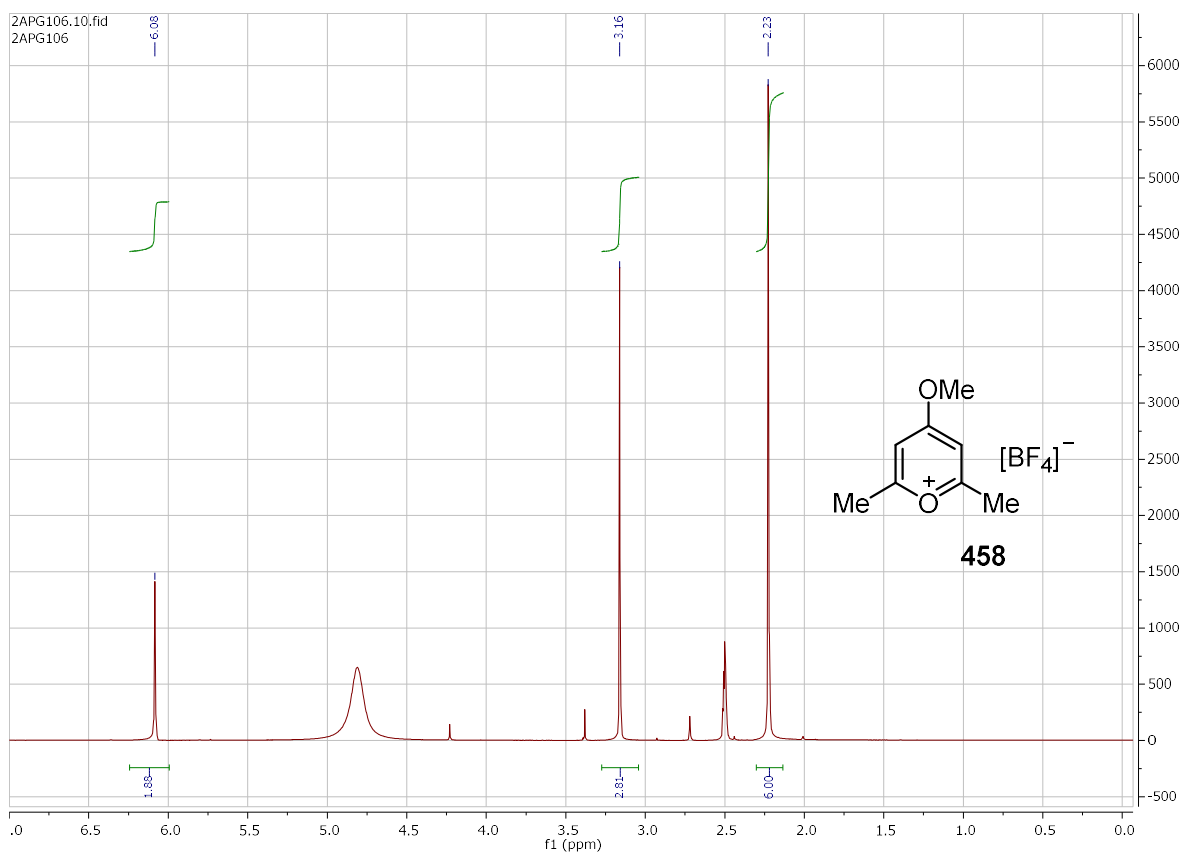
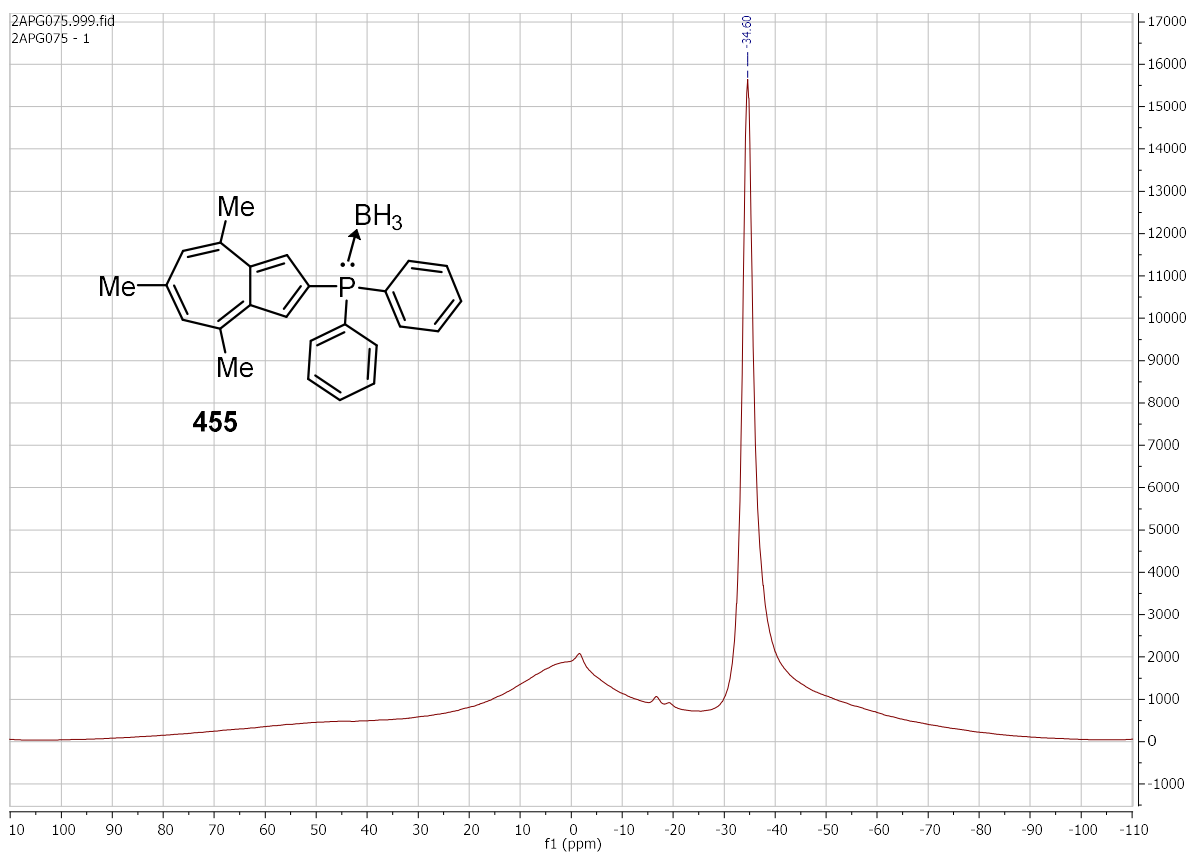


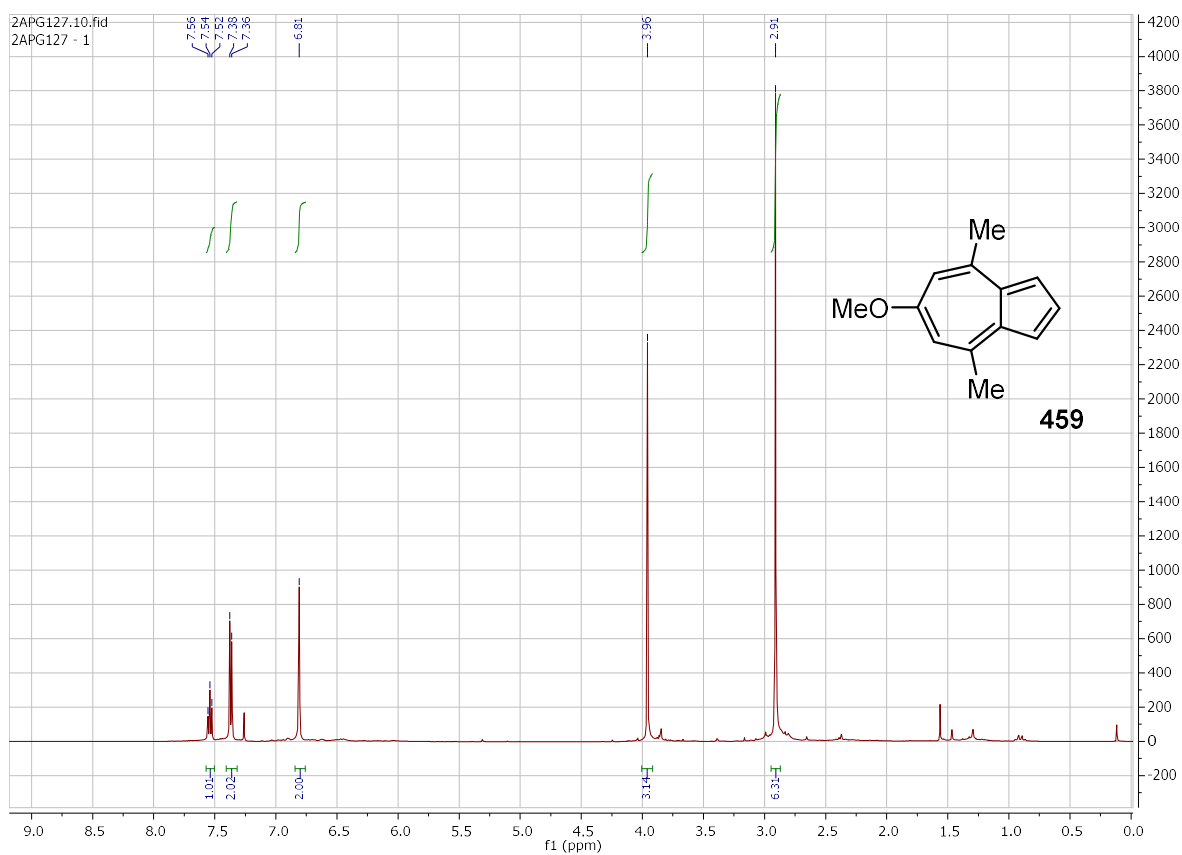
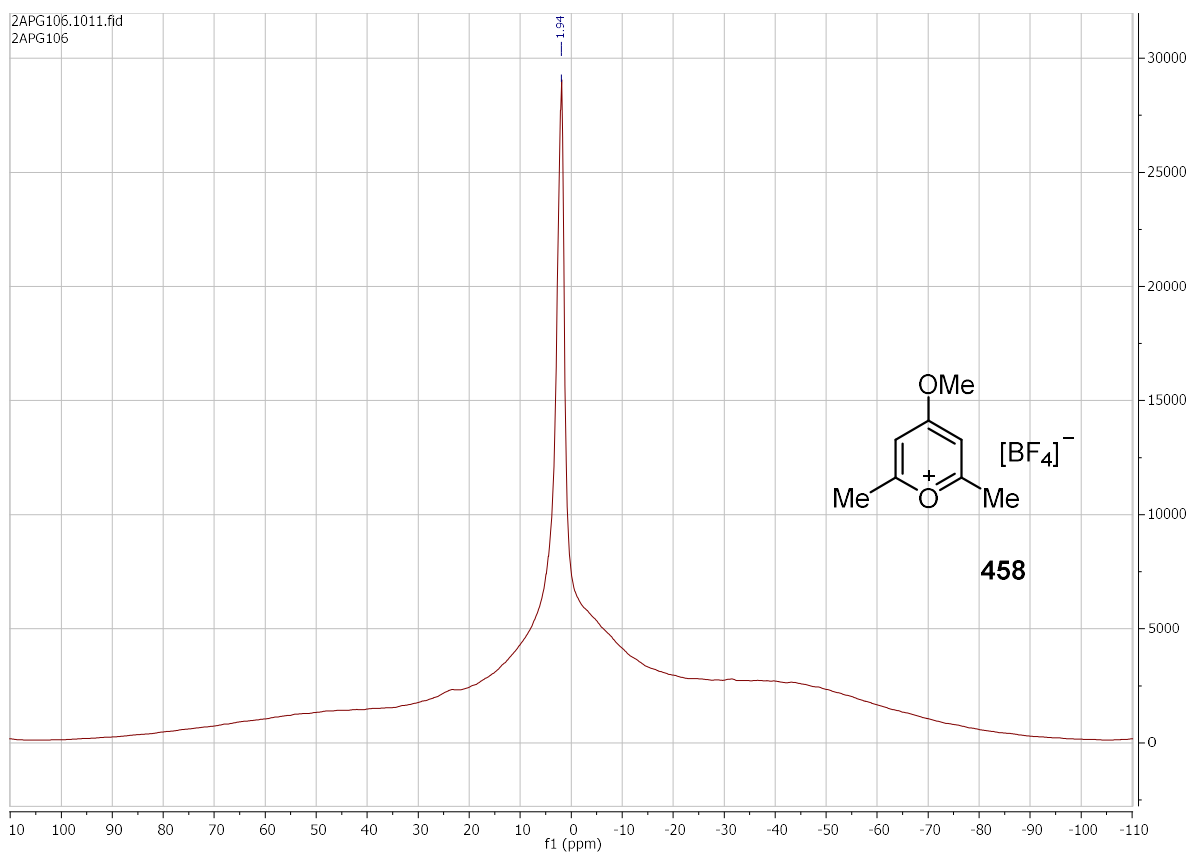


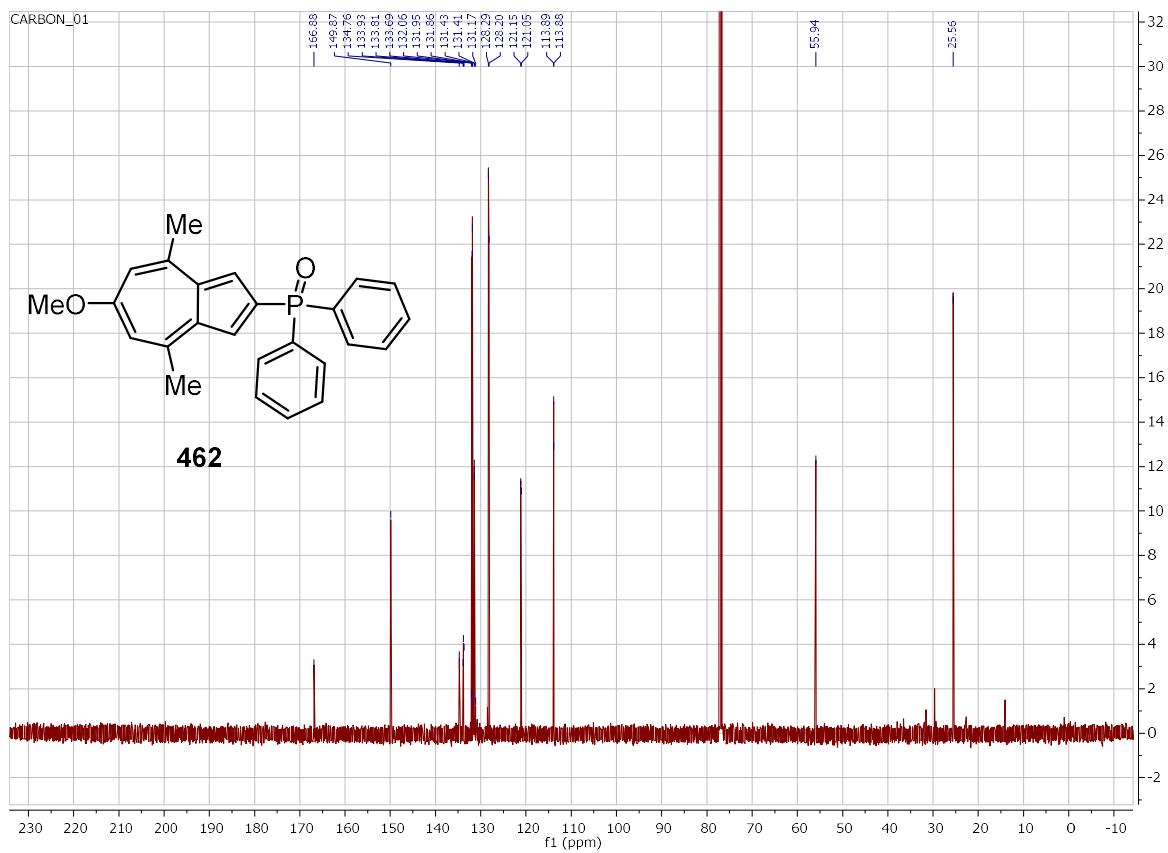
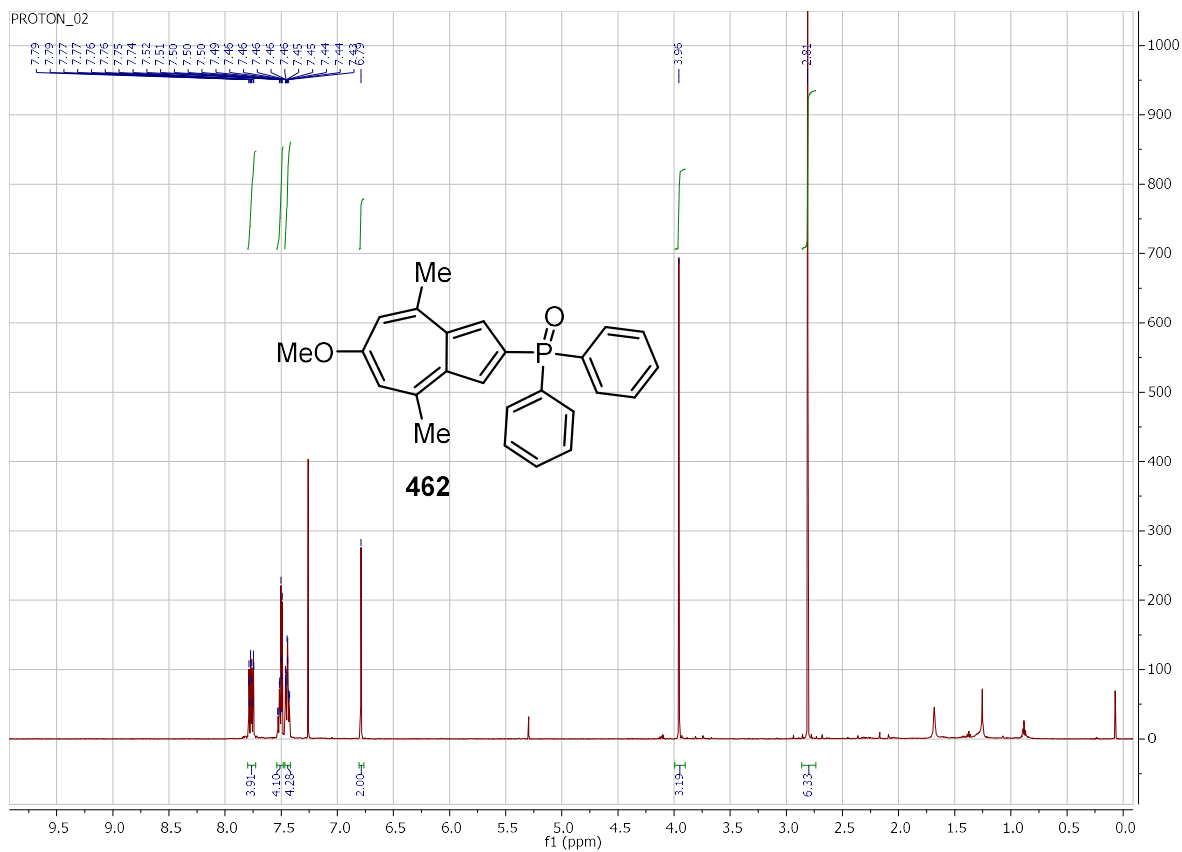


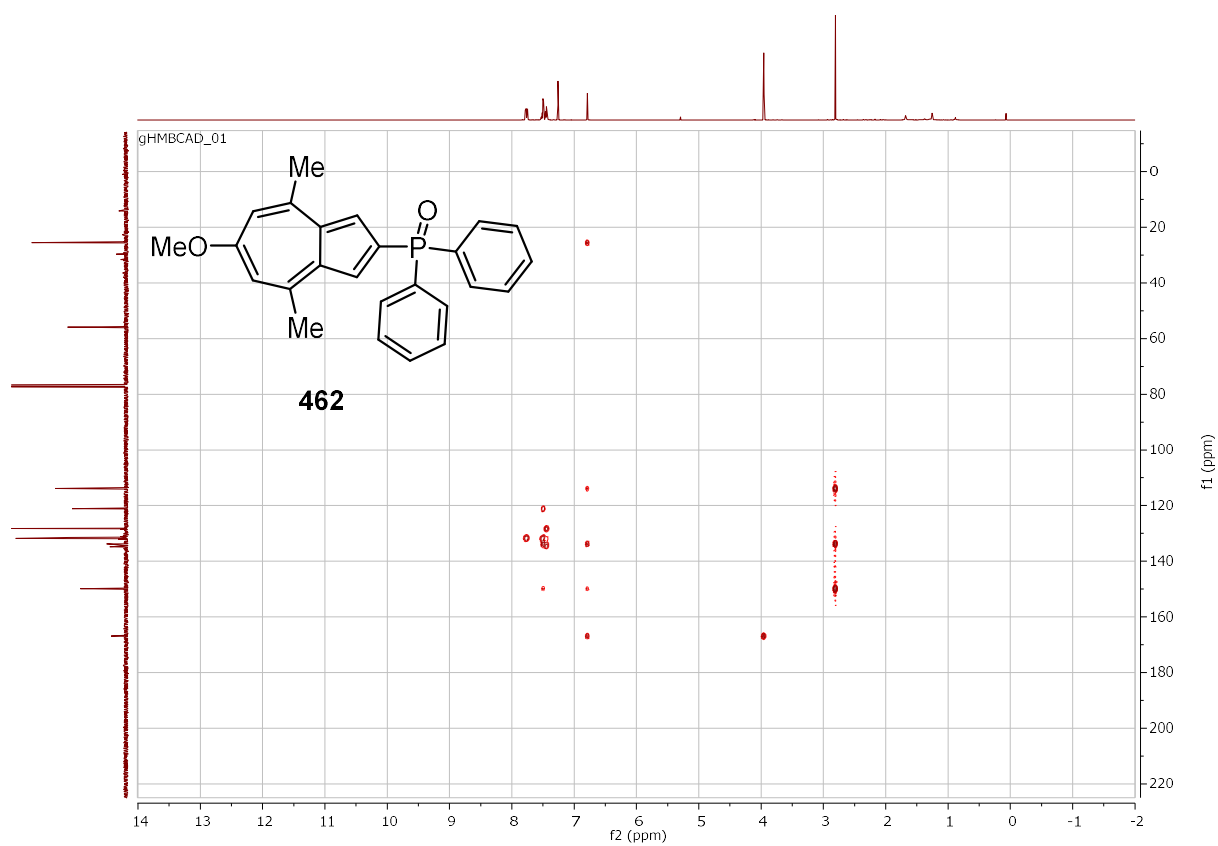
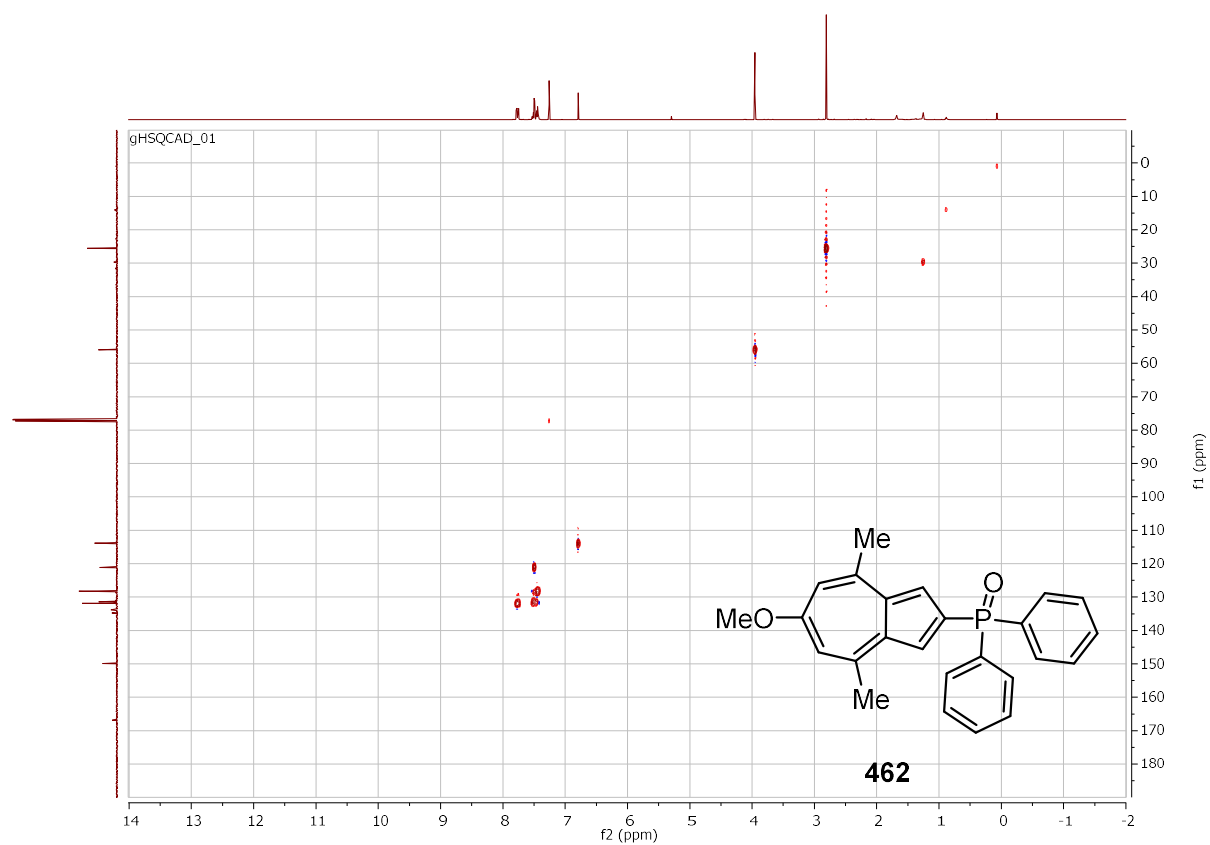


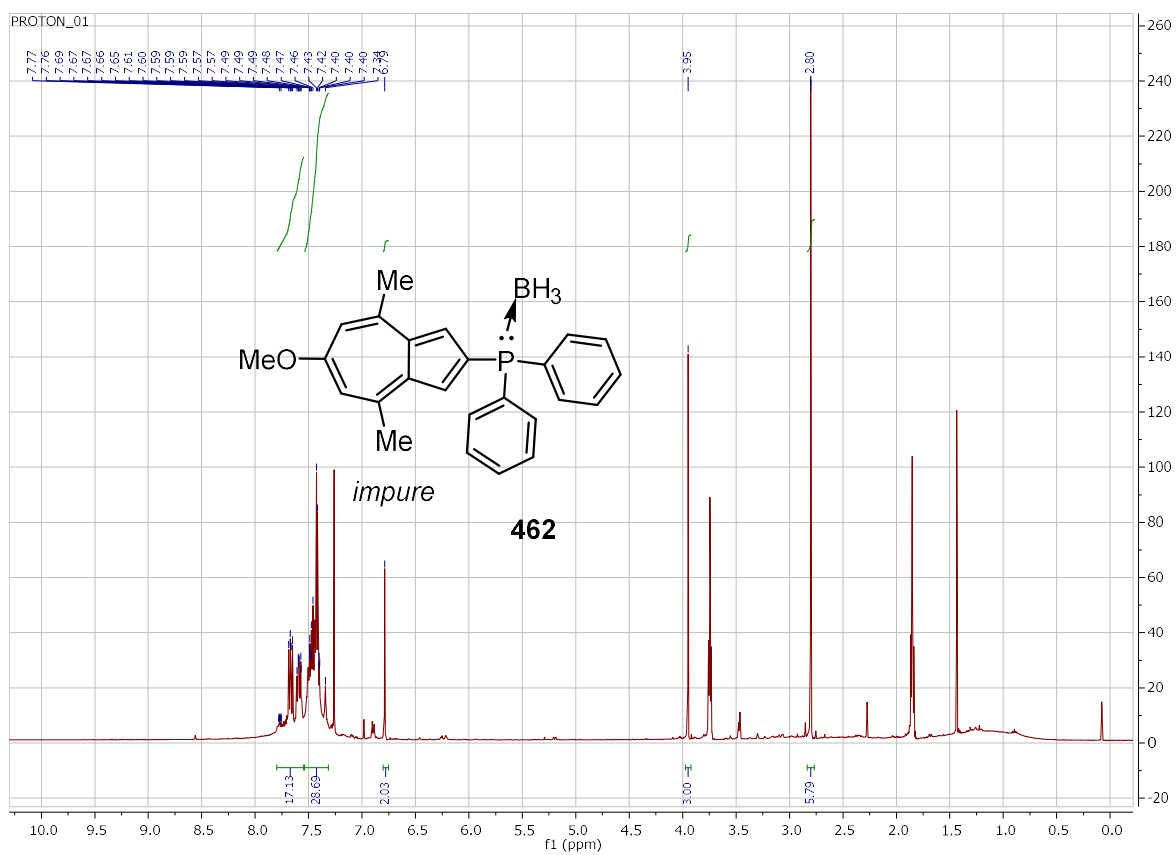
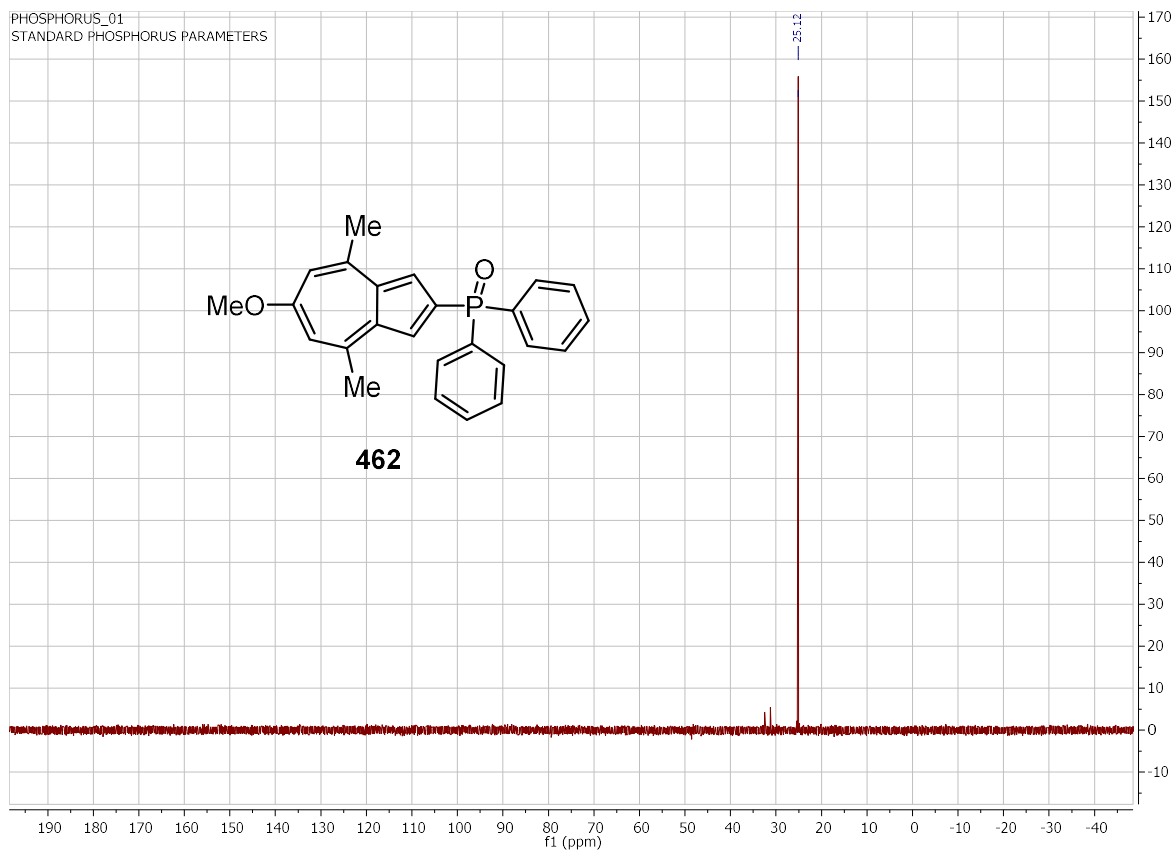


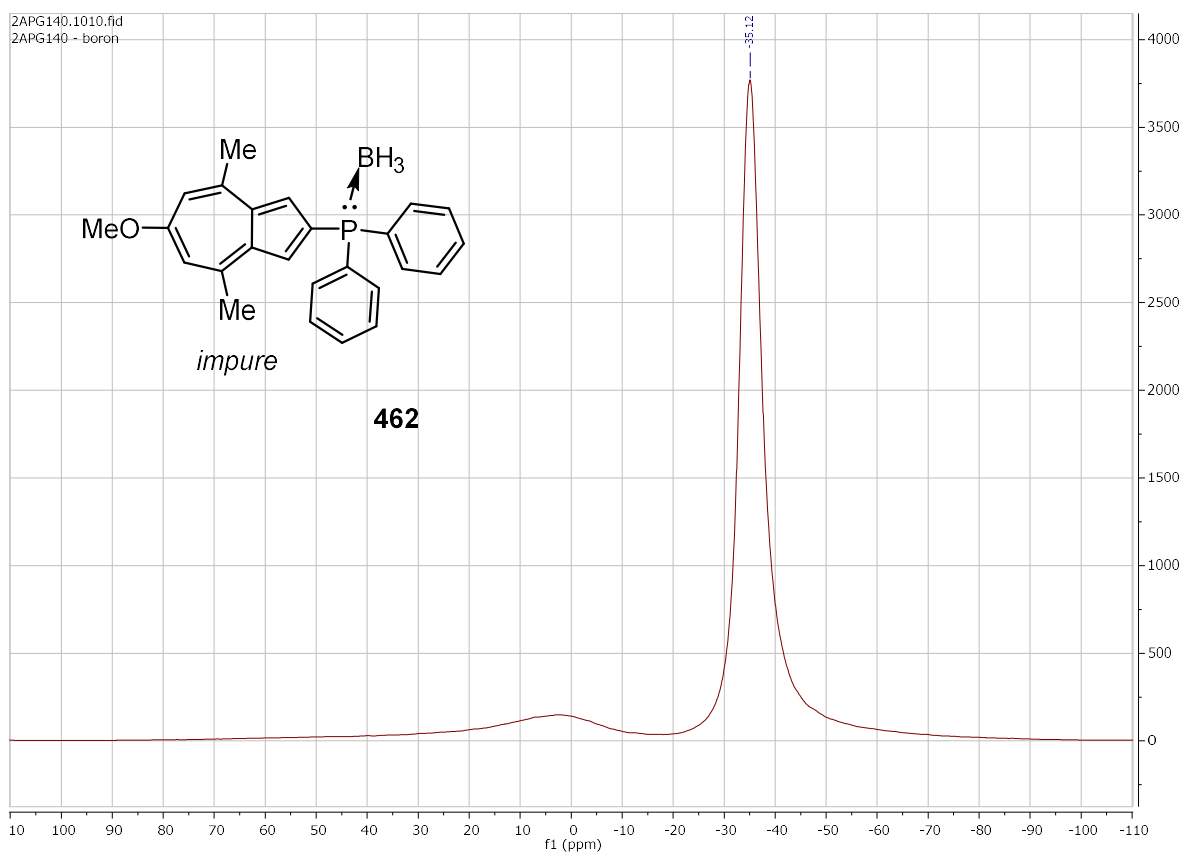
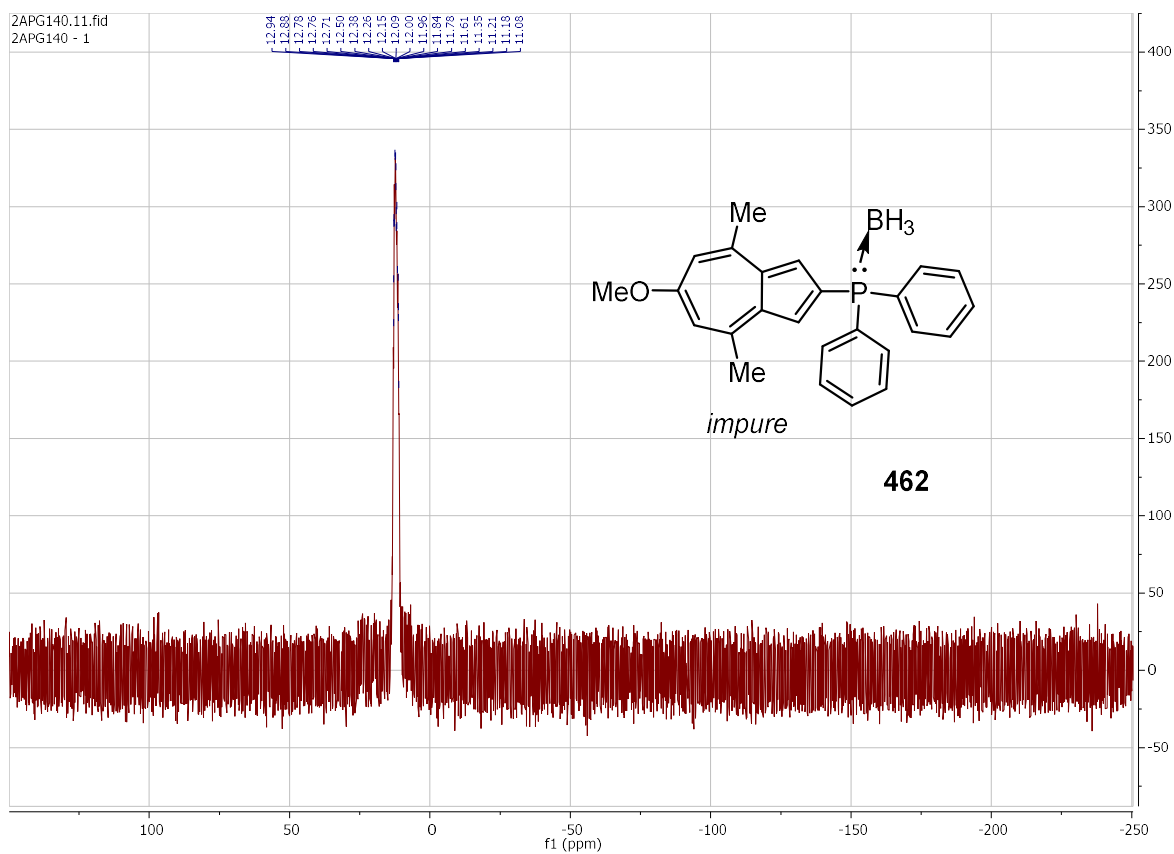


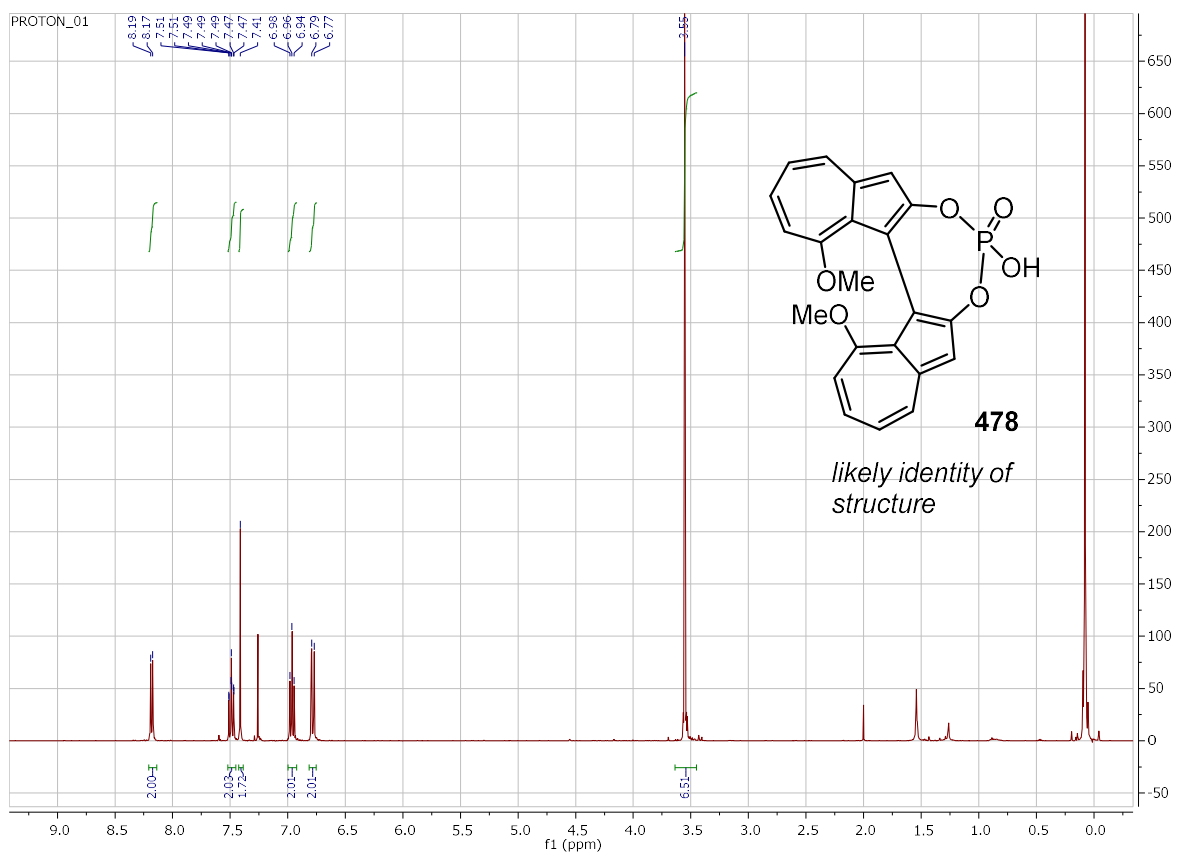
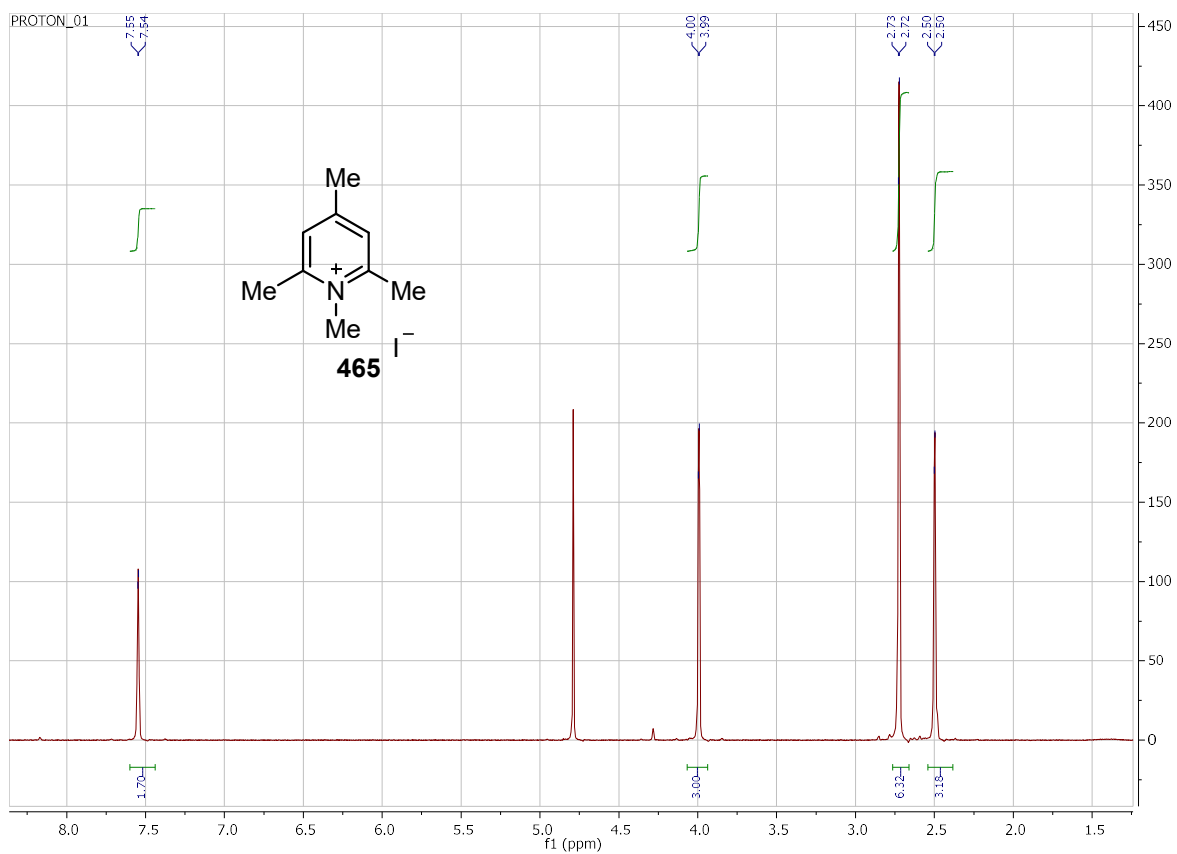


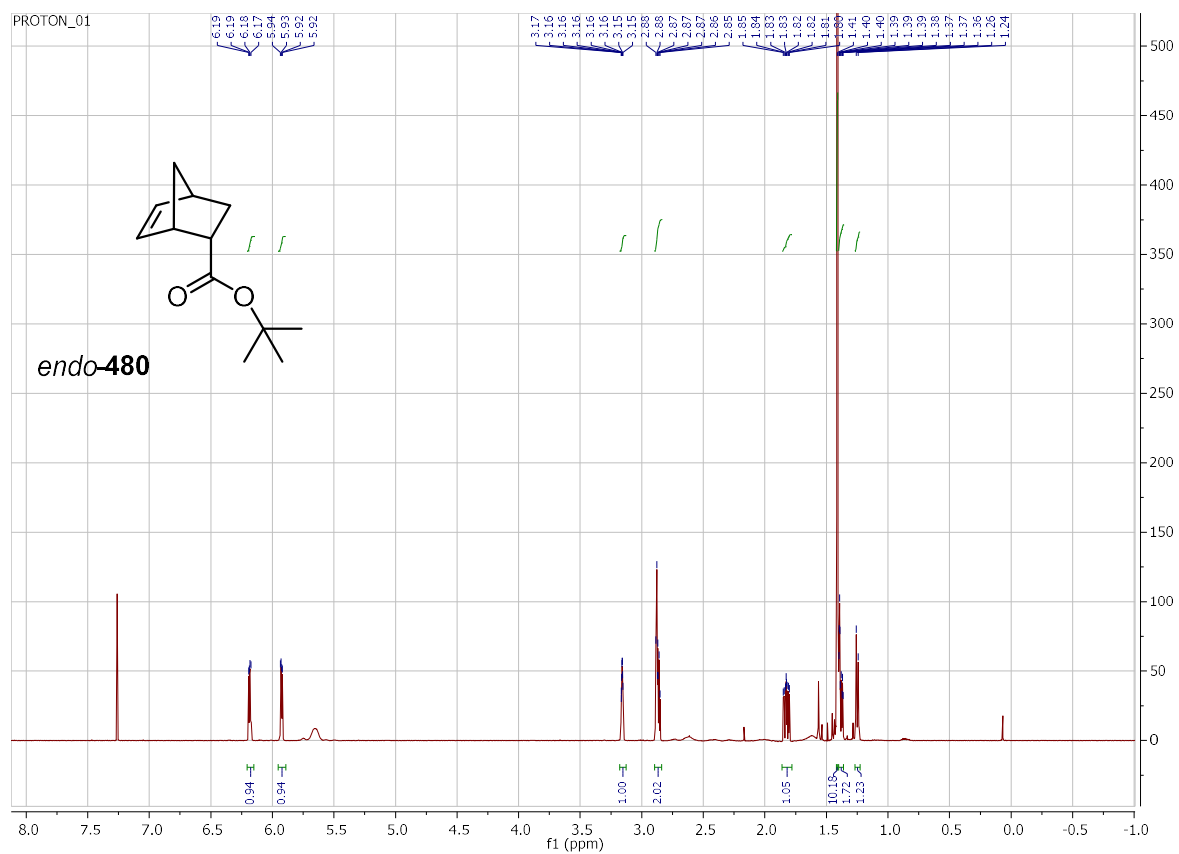












5.2. X-ray crystallography appendix

X-ray crystallography data for (±)-328.

Crystal data and structure refinement.

Identification code	k13sel4
Empirical formula	C ₂₈ H ₂₆ O ₈
Formula weight	490.49
Temperature	150(2) K
Wavelength	0.71073 Å
Crystal system	Triclinic
Space group	P-1
Unit cell dimensions	a = 8.6910(2) Å α = 97.318(1)° b = 9.2470(2) Å β = 102.998(1)° c = 15.8990(4) Å γ = 106.770(1)°
Volume	1166.46(5) Å ³
Z	2
Density (calculated)	1.396 Mg/m ³
Absorption coefficient	0.103 mm ⁻¹
F(000)	516
Crystal size	0.30 x 0.20 x 0.20 mm
Theta range for data collection	3.76 to 27.39°
Index ranges	-11 ≤ h ≤ 11; -11 ≤ k ≤ 11; -20 ≤ l ≤ 20
Reflections collected	22324
Independent reflections	5275 [R(int) = 0.0515]
Reflections observed (>2σ)	3613
Data Completeness	0.994
Absorption correction	Semi-empirical from equivalents
Max. and min. transmission	0.974 and 0.933
Refinement method	Full-matrix least-squares on F ²
Data / restraints / parameters	5275 / 0 / 331
Goodness-of-fit on F ²	1.007
Final R indices [I>2σ(I)]	R1 = 0.0459 wR2 = 0.1040
R indices (all data)	R1 = 0.0798 wR2 = 0.1195
Largest diff. peak and hole	0.189 and -0.241 eÅ ⁻³

Atomic coordinates ($\times 10^4$) and equivalent isotropic displacement parameters ($\text{\AA}^2 \times 10^3$). U(eq) is defined as one third of the trace of the orthogonalized Uij tensor.

Atom	x	y	z	U(eq)
O(1)	10502(2)	9063(1)	8953(1)	38(1)
O(2)	11196(1)	7340(1)	8128(1)	35(1)
O(3)	7279(2)	2119(1)	8318(1)	34(1)
O(4)	8776(1)	4874(1)	7109(1)	32(1)
O(5)	1678(2)	2003(1)	4511(1)	32(1)
O(6)	3133(1)	3438(1)	7940(1)	34(1)
O(7)	3582(1)	4143(1)	6101(1)	32(1)
O(8)	1331(2)	-505(1)	4449(1)	39(1)
C(1)	6219(2)	4369(2)	7628(1)	23(1)
C(2)	7868(2)	5212(2)	7653(1)	24(1)
C(3)	8525(2)	6540(2)	8336(1)	23(1)
C(4)	7252(2)	6557(2)	8763(1)	23(1)
C(5)	7423(2)	7677(2)	9481(1)	27(1)
C(6)	6272(2)	7808(2)	9941(1)	32(1)
C(7)	4654(2)	6839(2)	9791(1)	36(1)
C(8)	3742(2)	5513(2)	9152(1)	34(1)
C(9)	4223(2)	4759(2)	8492(1)	27(1)
C(10)	5785(2)	5182(2)	8299(1)	23(1)
C(11)	5200(2)	2909(2)	6990(1)	23(1)
C(12)	3938(2)	2835(2)	6240(1)	25(1)
C(13)	3277(2)	1357(2)	5705(1)	25(1)
C(14)	4142(2)	430(2)	6127(1)	24(1)
C(15)	3899(2)	-1098(2)	5778(1)	30(1)
C(16)	4678(2)	-2094(2)	6120(1)	34(1)
C(17)	5852(2)	-1815(2)	6918(1)	33(1)
C(18)	6599(2)	-484(2)	7574(1)	29(1)
C(19)	6400(2)	956(2)	7599(1)	26(1)
C(20)	5350(2)	1434(2)	6953(1)	23(1)
C(21)	10127(2)	7770(2)	8516(1)	26(1)
C(22)	12731(2)	8536(2)	8182(1)	40(1)
C(23)	1433(2)	2862(2)	7978(1)	41(1)
C(24)	7930(2)	4147(2)	6205(1)	41(1)
C(25)	1905(2)	4134(2)	6040(1)	36(1)
C(26)	2018(2)	826(2)	4844(1)	27(1)
C(27)	368(2)	1561(2)	3696(1)	36(1)
C(28)	8214(2)	1799(2)	9091(1)	35(1)

Bond lengths [Å] and angles [°].

O(1)-C(21)	1.2167(19)	O(2)-C(21)	1.346(2)
O(2)-C(22)	1.443(2)	O(3)-C(19)	1.3662(19)
O(3)-C(28)	1.4286(2)	O(4)-C(2)	1.360(2)
O(4)-C(24)	1.432(2)	O(5)-C(26)	1.3472(19)
O(5)-C(27)	1.4404(19)	O(6)-C(9)	1.3583(19)
O(6)-C(23)	1.438(2)	O(7)-C(12)	1.3633(18)
O(7)-C(25)	1.437(2)	O(8)-C(26)	1.2145(19)
C(1)-C(10)	1.409(2)	C(1)-C(2)	1.409(2)
C(1)-C(11)	1.481(2)	C(2)-C(3)	1.410(2)
C(3)-C(4)	1.425(2)	C(3)-C(21)	1.462(2)
C(4)-C(5)	1.390(2)	C(4)-C(10)	1.480(2)
C(5)-C(6)	1.388(3)	C(6)-C(7)	1.380(3)
C(7)-C(8)	1.387(2)	C(8)-C(9)	1.393(2)
C(9)-C(10)	1.415(2)	C(11)-C(20)	1.401(2)
C(11)-C(12)	1.407(2)	C(12)-C(13)	1.398(2)
C(13)-C(14)	1.429(2)	C(13)-C(26)	1.468(2)
C(14)-C(15)	1.387(2)	C(14)-C(20)	1.481(2)
C(15)-C(16)	1.387(2)	C(16)-C(17)	1.379(2)
C(17)-C(18)	1.390(2)	C(18)-C(19)	1.389(2)
C(19)-C(20)	1.419(2)		
C(21)-O(2)-C(22)	116.34(14)	C(19)-O(3)-C(28)	119.98(12)
C(2)-O(4)-C(24)	118.86(13)	C(26)-O(5)-C(27)	115.33(13)
C(9)-O(6)-C(23)	120.84(14)	C(12)-O(7)-C(25)	117.53(13)
C(10)-C(1)-C(2)	107.25(13)	C(10)-C(1)-C(11)	128.88(14)
C(2)-C(1)-C(11)	123.87(14)	O(4)-C(2)-C(1)	127.40(14)
O(4)-C(2)-C(3)	121.55(14)	C(1)-C(2)-C(3)	111.05(14)
C(2)-C(3)-C(4)	107.05(14)	C(2)-C(3)-C(21)	127.10(15)
C(4)-C(3)-C(21)	125.50(14)	C(5)-C(4)-C(3)	124.72(15)
C(5)-C(4)-C(10)	128.42(16)	C(3)-C(4)-C(10)	106.86(13)
C(6)-C(5)-C(4)	129.42(17)	C(7)-C(6)-C(5)	127.94(17)
C(6)-C(7)-C(8)	130.25(17)	C(7)-C(8)-C(9)	129.63(17)
O(6)-C(9)-C(8)	120.21(15)	O(6)-C(9)-C(10)	111.66(14)
C(8)-C(9)-C(10)	128.14(15)	C(1)-C(10)-C(9)	126.06(14)
C(1)-C(10)-C(4)	107.78(14)	C(9)-C(10)-C(4)	126.16(14)
C(20)-C(11)-C(12)	107.56(13)	C(20)-C(11)-C(1)	129.54(14)
C(12)-C(11)-C(1)	122.69(13)	O(7)-C(12)-C(13)	129.19(14)
O(7)-C(12)-C(11)	119.40(13)	C(13)-C(12)-C(11)	111.32(13)
C(12)-C(13)-C(14)	106.81(13)	C(12)-C(13)-C(26)	128.35(14)
C(14)-C(13)-C(26)	124.73(14)	C(15)-C(14)-C(13)	124.38(15)
C(15)-C(14)-C(20)	128.66(15)	C(13)-C(14)-C(20)	106.90(13)
C(14)-C(15)-C(16)	129.34(16)	C(17)-C(16)-C(15)	127.96(16)
C(16)-C(17)-C(18)	130.13(15)	C(19)-C(18)-C(17)	129.69(16)
O(3)-C(19)-C(18)	119.84(14)	O(3)-C(19)-C(20)	111.93(13)
C(18)-C(19)-C(20)	128.23(15)	C(11)-C(20)-C(19)	126.86(14)
C(11)-C(20)-C(14)	107.39(13)	C(19)-C(20)-C(14)	125.69(14)
O(1)-C(21)-O(2)	121.51(15)	O(1)-C(21)-C(3)	125.90(16)
O(2)-C(21)-C(3)	112.58(14)	O(8)-C(26)-O(5)	121.58(14)
O(8)-C(26)-C(13)	126.14(15)	O(5)-C(26)-C(13)	112.28(13)

Anisotropic displacement parameters ($\text{\AA}^2 \times 10^3$). The anisotropic displacement factor exponent takes the form: $-2 \pi^2 [h^2 a^{*2} U_{11} + \dots + 2 h k a^* b^* U_{12}]$

Atom	U11	U22	U33	U23	U13	U12
O(1)	34(1)	26(1)	42(1)	-6(1)	9(1)	0(1)
O(2)	24(1)	30(1)	44(1)	-1(1)	9(1)	3(1)
O(3)	38(1)	25(1)	30(1)	3(1)	-5(1)	11(1)
O(4)	27(1)	32(1)	31(1)	-4(1)	5(1)	9(1)
O(5)	33(1)	26(1)	29(1)	6(1)	-2(1)	6(1)
O(6)	25(1)	32(1)	37(1)	1(1)	8(1)	1(1)
O(7)	27(1)	20(1)	44(1)	6(1)	-2(1)	9(1)
O(8)	39(1)	24(1)	37(1)	-2(1)	-7(1)	4(1)
C(1)	24(1)	18(1)	24(1)	3(1)	2(1)	7(1)
C(2)	25(1)	21(1)	24(1)	4(1)	4(1)	10(1)
C(3)	23(1)	20(1)	23(1)	3(1)	1(1)	6(1)
C(4)	26(1)	19(1)	22(1)	5(1)	2(1)	8(1)
C(5)	32(1)	21(1)	25(1)	4(1)	3(1)	8(1)
C(6)	41(1)	27(1)	28(1)	1(1)	9(1)	12(1)
C(7)	42(1)	38(1)	34(1)	4(1)	16(1)	18(1)
C(8)	30(1)	37(1)	36(1)	9(1)	12(1)	11(1)
C(9)	27(1)	24(1)	27(1)	6(1)	4(1)	6(1)
C(10)	26(1)	19(1)	24(1)	6(1)	3(1)	8(1)
C(11)	23(1)	18(1)	26(1)	3(1)	4(1)	5(1)
C(12)	25(1)	18(1)	30(1)	6(1)	6(1)	6(1)
C(13)	25(1)	20(1)	28(1)	3(1)	3(1)	5(1)
C(14)	25(1)	20(1)	27(1)	4(1)	7(1)	4(1)
C(15)	34(1)	22(1)	29(1)	1(1)	5(1)	6(1)
C(16)	42(1)	20(1)	37(1)	3(1)	9(1)	11(1)
C(17)	40(1)	22(1)	40(1)	10(1)	12(1)	15(1)
C(18)	31(1)	26(1)	32(1)	10(1)	6(1)	12(1)
C(19)	24(1)	22(1)	29(1)	4(1)	7(1)	5(1)
C(20)	23(1)	20(1)	26(1)	4(1)	6(1)	6(1)
C(21)	28(1)	24(1)	22(1)	4(1)	1(1)	8(1)
C(22)	26(1)	39(1)	46(1)	0(1)	9(1)	-1(1)
C(23)	25(1)	46(1)	45(1)	10(1)	8(1)	1(1)
C(24)	38(1)	45(1)	30(1)	-8(1)	13(1)	1(1)
C(25)	34(1)	36(1)	41(1)	9(1)	6(1)	18(1)
C(26)	26(1)	22(1)	29(1)	3(1)	5(1)	4(1)
C(27)	33(1)	38(1)	29(1)	8(1)	-4(1)	8(1)
C(28)	36(1)	38(1)	28(1)	8(1)	1(1)	15(1)

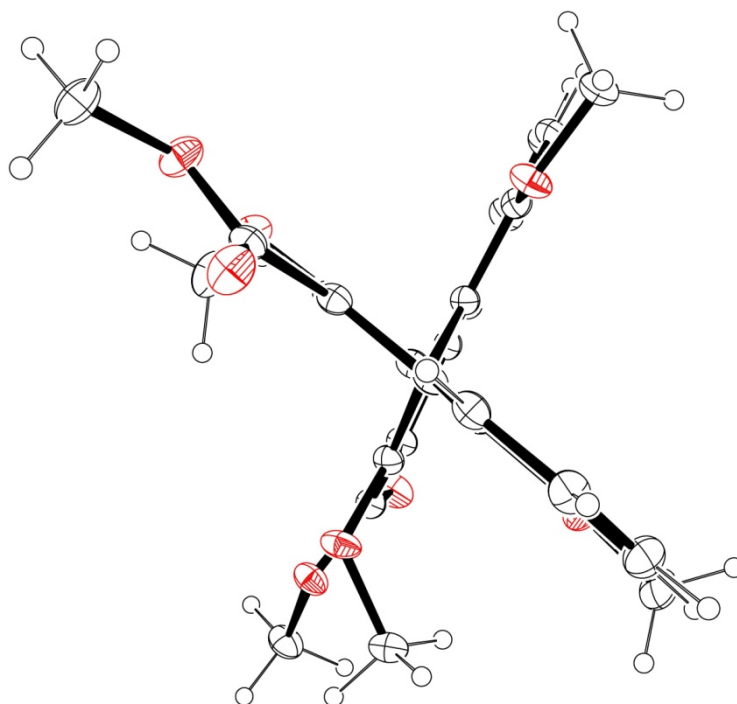
Hydrogen coordinates ($\times 10^4$) and isotropic displacement parameters ($\text{\AA}^2 \times 10^3$).

Atom	x	y	z	U(eq)
H(5)	8481	8466	9688	32
H(6)	6644	8672	10418	39
H(7)	4074	7125	10189	44
H(8)	2622	5051	9166	41
H(15)	3082	-1523	5225	36
H(16)	4364	-3091	5759	41
H(17)	6206	-2667	7039	39
H(18)	7361	-573	8081	35
H(22A)	12473	9400	7956	61
H(22B)	13359	8124	7829	61
H(22C)	13405	8895	8799	61
H(23A)	1415	2564	8547	62
H(23B)	808	1962	7499	62
H(23C)	916	3669	7916	62
H(24A)	7450	3032	6157	62
H(24B)	8727	4346	5850	62
H(24C)	7035	4566	5990	62
H(25A)	1188	3083	6011	53
H(25B)	1483	4490	5508	53
H(25C)	1900	4823	6561	53
H(27A)	697	1009	3236	55
H(27B)	179	2487	3519	55
H(27C)	-663	887	3779	55
H(28A)	7457	1049	9323	52
H(28B)	8774	2755	9539	52
H(28C)	9052	1373	8943	52

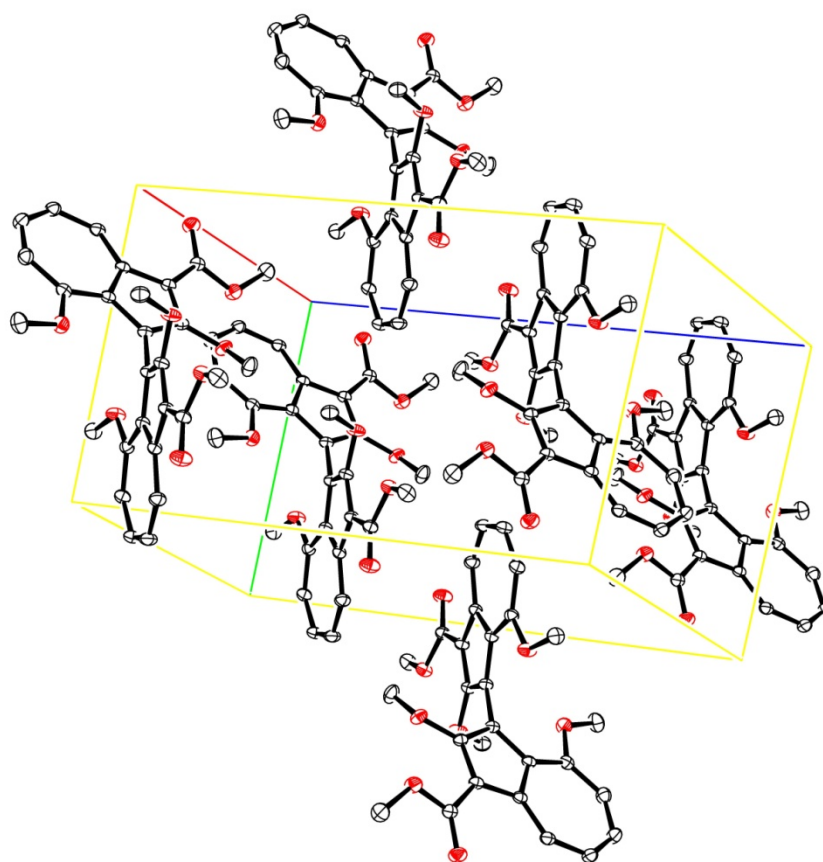
Dihedral angles [°].

Atom1 - Atom2 - Atom3 - Atom4	Dihedral
C(24) - O(4) - C(2) - C(1)	33.7(2)
C(24) - O(4) - C(2) - C(3)	-145.45(16)
C(10) - C(1) - C(2) - O(4)	-178.23(14)
C(11) - C(1) - C(2) - O(4)	1.5(2)
C(10) - C(1) - C(2) - C(3)	1.04(17)
C(11) - C(1) - C(2) - C(3)	-179.25(13)
O(4) - C(2) - C(3) - C(4)	179.04(13)
C(1) - C(2) - C(3) - C(4)	-0.28(17)
O(4) - C(2) - C(3) - C(21)	5.5(2)
C(1) - C(2) - C(3) - C(21)	-173.77(14)
C(2) - C(3) - C(4) - C(5)	179.05(14)
C(21) - C(3) - C(4) - C(5)	-7.3(2)
C(2) - C(3) - C(4) - C(10)	-0.55(16)
C(21) - C(3) - C(4) - C(10)	173.07(13)
C(3) - C(4) - C(5) - C(6)	179.67(16)
C(10) - C(4) - C(5) - C(6)	-0.8(3)
C(4) - C(5) - C(6) - C(7)	0.1(3)
C(5) - C(6) - C(7) - C(8)	-1.0(3)
C(6) - C(7) - C(8) - C(9)	2.1(3)
C(23) - O(6) - C(9) - C(8)	4.9(2)
C(23) - O(6) - C(9) - C(10)	-175.41(14)
C(7) - C(8) - C(9) - O(6)	178.43(17)
C(7) - C(8) - C(9) - C(10)	-1.2(3)
C(2) - C(1) - C(10) - C(9)	178.51(14)
C(11) - C(1) - C(10) - C(9)	-1.2(2)
C(2) - C(1) - C(10) - C(4)	-1.34(16)
C(11) - C(1) - C(10) - C(4)	178.96(14)
O(6) - C(9) - C(10) - C(1)	-0.3(2)
C(8) - C(9) - C(10) - C(1)	179.29(16)
O(6) - C(9) - C(10) - C(4)	179.48(13)
C(8) - C(9) - C(10) - C(4)	-0.9(3)
C(5) - C(4) - C(10) - C(1)	-178.39(15)
C(3) - C(4) - C(10) - C(1)	1.19(16)
C(5) - C(4) - C(10) - C(9)	1.8(2)
C(3) - C(4) - C(10) - C(9)	-178.66(14)
C(10) - C(1) - C(11) - C(20)	-108.2(2)
C(2) - C(1) - C(11) - C(20)	72.1(2)
C(10) - C(1) - C(11) - C(12)	77.7(2)
C(2) - C(1) - C(11) - C(12)	-102.00(19)
C(25) - O(7) - C(12) - C(13)	62.8(2)
C(25) - O(7) - C(12) - C(11)	-121.14(17)
C(20) - C(11) - C(12) - O(7)	-177.71(14)
C(1) - C(11) - C(12) - O(7)	-2.4(2)
C(20) - C(11) - C(12) - C(13)	-0.95(19)
C(1) - C(11) - C(12) - C(13)	174.31(15)
O(7) - C(12) - C(13) - C(14)	176.54(16)
C(11) - C(12) - C(13) - C(14)	0.18(19)
O(7) - C(12) - C(13) - C(26)	0.2(3)
C(11) - C(12) - C(13) - C(26)	-176.15(16)
C(12) - C(13) - C(14) - C(15)	-176.69(16)
C(26) - C(13) - C(14) - C(15)	-0.2(3)

C(12) - C(13) - C(14) - C(20)	0.61(18)
C(26) - C(13) - C(14) - C(20)	177.11(15)
C(13) - C(14) - C(15) - C(16)	178.98(18)
C(20) - C(14) - C(15) - C(16)	2.3(3)
C(14) - C(15) - C(16) - C(17)	2.9(3)
C(15) - C(16) - C(17) - C(18)	-2.1(3)
C(16) - C(17) - C(18) - C(19)	-1.7(3)
C(28) - O(3) - C(19) - C(18)	-8.9(2)
C(28) - O(3) - C(19) - C(20)	170.82(15)
C(17) - C(18) - C(19) - O(3)	-179.61(17)
C(17) - C(18) - C(19) - C(20)	0.7(3)
C(12) - C(11) - C(20) - C(19)	-175.99(16)
C(1) - C(11) - C(20) - C(19)	9.2(3)
C(12) - C(11) - C(20) - C(14)	1.29(18)
C(1) - C(11) - C(20) - C(14)	-173.53(16)
O(3) - C(19) - C(20) - C(11)	1.6(2)
C(18) - C(19) - C(20) - C(11)	-178.67(17)
O(3) - C(19) - C(20) - C(14)	-175.19(15)
C(18) - C(19) - C(20) - C(14)	4.5(3)
C(15) - C(14) - C(20) - C(11)	175.96(17)
C(13) - C(14) - C(20) - C(11)	-1.19(18)
C(15) - C(14) - C(20) - C(19)	-6.7(3)
C(13) - C(14) - C(20) - C(19)	176.14(15)
C(22) - O(2) - C(21) - O(1)	-6.2(2)
C(22) - O(2) - C(21) - C(3)	172.83(14)
C(2) - C(3) - C(21) - O(1)	160.71(16)
C(4) - C(3) - C(21) - O(1)	-11.6(3)
C(2) - C(3) - C(21) - O(2)	-18.2(2)
C(4) - C(3) - C(21) - O(2)	169.42(14)
C(27) - O(5) - C(26) - O(8)	4.4(2)
C(27) - O(5) - C(26) - C(13)	-175.86(15)
C(12) - C(13) - C(26) - O(8)	-170.57(18)
C(14) - C(13) - C(26) - O(8)	13.7(3)
C(12) - C(13) - C(26) - O(5)	9.7(3)
C(14) - C(13) - C(26) - O(5)	-166.05(15)



Axial view of biazulene (\pm)-**328**.



Unit cell of biazulene (\pm)-**328**.

X-ray crystallographic data for (*R*_a,1*R*,2*S*,5*R*)-**404**.

Table 1. Crystal data and structure refinement for s16sel1		
Identification code	s16sel1	
Empirical formula	C _{52.25} H _{66.72} O _{12.12}	
Formula weight	888.70	
Temperature	150.01(10) K	
Wavelength	1.54184 Å	
Crystal system	Orthorhombic	
Space group	P2 ₁ 2 ₁ 2 ₁	
Unit cell dimensions	a = 12.61370(10) Å	α = 90°.
	b = 16.68850(10) Å	β = 90°.
	c = 23.7719(2) Å	γ = 90°.
Volume	5004.07(7) Å ³	
Z	4	
Density (calculated)	1.178 Mg/m ³	
Absorption coefficient	0.673 mm ⁻¹	
F(000)	1906	
Crystal size	0.300 x 0.250 x 0.080 mm ³	
Theta range for data collection	3.236 to 73.128°.	
Index ranges	-15 ≤ h ≤ 15, -19 ≤ k ≤ 20, -22 ≤ l ≤ 29	
Reflections collected	57208	
Independent reflections	9956 [R(int) = 0.0304]	
Completeness to theta = 67.684°	100.0 %	
Absorption correction	Semi-empirical from equivalents	
Max. and min. transmission	1.00000 and 0.71916	
Refinement method	Full-matrix least-squares on F ²	
Data / restraints / parameters	9956 / 0 / 614	
Goodness-of-fit on F ²	1.019	
Final R indices [I > 2σ(I)]	R1 = 0.0347, wR2 = 0.0907	
R indices (all data)	R1 = 0.0373, wR2 = 0.0926	
Absolute structure parameter	0.06(4)	
Extinction coefficient	n/a	
Largest diff. peak and hole	0.402 and -0.184 e.Å ⁻³	

Table 2. Atomic coordinates ($\times 10^4$) and equivalent isotropic displacement parameters ($\text{\AA}^2 \times 10^3$) for s16sel1. $U(\text{eq})$ is defined as one third of the trace of the orthogonalized U_{ij} tensor.

	x	y	z	$U(\text{eq})$
O(1)	2491(1)	5654(1)	3208(1)	42(1)
O(2)	-2287(2)	4345(2)	4036(1)	83(1)
O(3)	-2405(1)	4014(1)	3131(1)	54(1)
O(4)	-639(1)	4012(1)	2472(1)	33(1)
O(5)	-1331(2)	5043(1)	1976(1)	49(1)
O(6)	-1184(1)	3777(1)	1642(1)	45(1)
O(7)	652(1)	6382(1)	2490(1)	41(1)
O(8)	3709(2)	3838(1)	1032(1)	51(1)
O(9)	3064(2)	2970(1)	1664(1)	49(1)
O(10)	1767(1)	3454(1)	2503(1)	29(1)
O(11)	3328(1)	3645(1)	2951(1)	51(1)
O(12)	2278(1)	2573(1)	3092(1)	42(1)
C(1)	4138(2)	5761(3)	2764(1)	77(1)
C(2)	3559(2)	5889(2)	3313(1)	60(1)
C(3)	1773(2)	5585(1)	3623(1)	32(1)
C(4)	1986(2)	5897(1)	4157(1)	38(1)
C(5)	1367(2)	5889(1)	4637(1)	40(1)
C(6)	366(2)	5579(1)	4723(1)	42(1)
C(7)	-293(2)	5196(1)	4345(1)	40(1)
C(8)	-100(2)	5005(1)	3783(1)	32(1)
C(9)	-814(2)	4575(1)	3428(1)	35(1)
C(10)	-1888(2)	4309(2)	3576(1)	47(1)
C(11)	-3505(2)	3784(2)	3217(2)	68(1)
C(12)	-3887(3)	3445(3)	2673(2)	104(2)
C(13)	-298(2)	4494(1)	2910(1)	30(1)
C(14)	-1086(2)	4360(1)	2018(1)	35(1)
C(15)	-1668(2)	3958(1)	1100(1)	40(1)
C(16)	-2572(2)	3369(1)	1032(1)	43(1)
C(17)	-3096(2)	3437(1)	455(1)	42(1)
C(18)	-4009(2)	2842(2)	398(1)	51(1)
C(19)	-2270(2)	3341(2)	-2(1)	51(1)
C(20)	-1372(2)	3947(2)	67(1)	53(1)
C(21)	-824(2)	3877(2)	645(1)	47(1)
C(22)	121(2)	4455(2)	722(1)	52(1)
C(23)	1033(2)	4225(3)	334(2)	80(1)
C(24)	-165(2)	5338(2)	650(2)	64(1)
C(25)	686(2)	4867(1)	2902(1)	27(1)
C(26)	848(2)	5183(1)	3445(1)	29(1)
C(27)	1373(2)	4858(1)	2400(1)	28(1)
C(28)	1640(2)	5466(1)	2013(1)	31(1)
C(29)	1278(2)	6264(1)	2046(1)	37(1)
C(30)	226(3)	7159(2)	2620(1)	53(1)
C(31)	-333(3)	7074(2)	3172(1)	62(1)
C(32)	1514(2)	6896(1)	1676(1)	50(1)
C(33)	2171(3)	6892(2)	1204(1)	57(1)
C(34)	2775(2)	6292(2)	974(1)	53(1)
C(35)	2854(2)	5500(2)	1139(1)	43(1)
C(36)	2362(2)	5121(1)	1593(1)	34(1)
C(37)	2501(2)	4295(1)	1733(1)	33(1)

C(38)	3154(2)	3705(1)	1439(1)	38(1)
C(39)	3709(2)	2338(2)	1423(1)	53(1)
C(40)	3238(3)	1550(2)	1589(1)	62(1)
C(41)	1893(2)	4171(1)	2220(1)	28(1)
C(42)	2555(2)	3257(1)	2864(1)	32(1)
C(43)	2924(2)	2276(1)	3559(1)	41(1)
C(44)	3385(2)	1486(1)	3371(1)	40(1)
C(45)	4010(2)	1074(2)	3841(1)	49(1)
C(46)	4382(2)	251(2)	3644(1)	63(1)
C(47)	3331(3)	1016(2)	4369(1)	54(1)
C(48)	2860(3)	1820(2)	4542(1)	64(1)
C(49)	2194(2)	2189(2)	4065(1)	51(1)
C(50)	1596(4)	2979(2)	4209(2)	77(1)
C(51)	705(4)	2840(3)	4606(2)	96(1)
C(52)	2344(4)	3644(2)	4405(1)	83(1)
O(13)	-4459(14)	4806(11)	4237(8)	67(5)
C(61)	-5190(20)	4161(18)	4229(12)	69(7)
C(62)	-4800(30)	3436(17)	4502(14)	78(8)

Table 3. Bond lengths [Å] for s16sel1.

O(1)-C(3)	1.344(3)	C(16)-H(16B)	0.9900
O(1)-C(2)	1.424(3)	C(17)-C(19)	1.514(4)
O(2)-C(10)	1.204(3)	C(17)-C(18)	1.526(3)
O(3)-C(10)	1.336(3)	C(17)-H(17)	1.0000
O(3)-C(11)	1.454(3)	C(18)-H(18A)	0.9800
O(4)-C(14)	1.349(3)	C(18)-H(18B)	0.9800
O(4)-C(13)	1.384(2)	C(18)-H(18C)	0.9800
O(5)-C(14)	1.184(3)	C(19)-C(20)	1.527(4)
O(6)-C(14)	1.328(3)	C(19)-H(19A)	0.9900
O(6)-C(15)	1.458(3)	C(19)-H(19B)	0.9900
O(7)-C(29)	1.334(3)	C(20)-C(21)	1.542(3)
O(7)-C(30)	1.438(3)	C(20)-H(20A)	0.9900
O(8)-C(38)	1.215(3)	C(20)-H(20B)	0.9900
O(9)-C(38)	1.343(3)	C(21)-C(22)	1.544(4)
O(9)-C(39)	1.450(3)	C(21)-H(21)	1.0000
O(10)-C(42)	1.353(2)	C(22)-C(23)	1.524(4)
O(10)-C(41)	1.383(2)	C(22)-C(24)	1.526(4)
O(11)-C(42)	1.189(3)	C(22)-H(22)	1.0000
O(12)-C(42)	1.310(3)	C(23)-H(23A)	0.9800
O(12)-C(43)	1.464(2)	C(23)-H(23B)	0.9800
C(1)-C(2)	1.510(4)	C(23)-H(23C)	0.9800
C(1)-H(1A)	0.9800	C(24)-H(24A)	0.9800
C(1)-H(1B)	0.9800	C(24)-H(24B)	0.9800
C(1)-H(1C)	0.9800	C(24)-H(24C)	0.9800
C(2)-H(2A)	0.9900	C(25)-C(26)	1.408(3)
C(2)-H(2B)	0.9900	C(25)-C(27)	1.476(3)
C(3)-C(4)	1.398(3)	C(27)-C(41)	1.388(3)
C(3)-C(26)	1.412(3)	C(27)-C(28)	1.411(3)
C(4)-C(5)	1.384(3)	C(28)-C(29)	1.410(3)
C(4)-H(4)	0.9500	C(28)-C(36)	1.468(3)
C(5)-C(6)	1.380(4)	C(29)-C(32)	1.405(3)
C(5)-H(5)	0.9500	C(30)-C(31)	1.494(4)
C(6)-C(7)	1.381(3)	C(30)-H(30A)	0.9900
C(6)-H(6)	0.9500	C(30)-H(30B)	0.9900
C(7)-C(8)	1.395(3)	C(31)-H(31A)	0.9800
C(7)-H(7)	0.9500	C(31)-H(31B)	0.9800
C(8)-C(9)	1.427(3)	C(31)-H(31C)	0.9800
C(8)-C(26)	1.471(3)	C(32)-C(33)	1.395(4)
C(9)-C(13)	1.400(3)	C(32)-H(32)	0.9500
C(9)-C(10)	1.469(3)	C(33)-C(34)	1.373(4)
C(11)-C(12)	1.494(5)	C(33)-H(33)	0.9500
C(11)-H(11A)	0.9900	C(34)-C(35)	1.382(4)
C(11)-H(11B)	0.9900	C(34)-H(34)	0.9500
C(12)-H(12A)	0.9800	C(35)-C(36)	1.397(3)
C(12)-H(12B)	0.9800	C(35)-H(35)	0.9500
C(12)-H(12C)	0.9800	C(36)-C(37)	1.429(3)
C(13)-C(25)	1.389(3)	C(37)-C(41)	1.402(3)
C(15)-C(16)	1.514(3)	C(37)-C(38)	1.463(3)
C(15)-C(21)	1.524(3)	C(39)-C(40)	1.496(4)
C(15)-H(15)	1.0000	C(39)-H(39A)	0.9900
C(16)-C(17)	1.526(3)	C(39)-H(39B)	0.9900
C(16)-H(16A)	0.9900	C(40)-H(40A)	0.9800
		C(40)-H(40B)	0.9800
		C(40)-H(40C)	0.9800
		C(43)-C(44)	1.508(3)

C(43)-C(49)	1.521(4)	C(50)-C(52)	1.529(5)
C(43)-H(43)	1.0000	C(50)-H(50)	1.0000
C(44)-C(45)	1.530(3)	C(51)-H(51A)	0.9800
C(44)-H(44A)	0.9900	C(51)-H(51B)	0.9800
C(44)-H(44B)	0.9900	C(51)-H(51C)	0.9800
C(45)-C(47)	1.523(4)	C(52)-H(52A)	0.9800
C(45)-C(46)	1.525(4)	C(52)-H(52B)	0.9800
C(45)-H(45)	1.0000	C(52)-H(52C)	0.9800
C(46)-H(46A)	0.9800	O(13)-C(61)	1.42(3)
C(46)-H(46B)	0.9800	O(13)-H(13)	0.8400
C(46)-H(46C)	0.9800	C(61)-C(62)	1.46(4)
C(47)-C(48)	1.525(4)	C(61)-H(61A)	0.9900
C(47)-H(47A)	0.9900	C(61)-H(61B)	0.9900
C(47)-H(47B)	0.9900	C(62)-H(62A)	0.9800
C(48)-C(49)	1.540(4)	C(62)-H(62B)	0.9800
C(48)-H(48A)	0.9900	C(62)-H(62C)	0.9800
C(48)-H(48B)	0.9900		
C(49)-C(50)	1.558(4)		
C(49)-H(49)	1.0000		
C(50)-C(51)	1.486(6)		

Table 4. Bond angles [°] for s16sel1.

C(3)-O(1)-C(2)	122.19(17)	C(11)-C(12)-H(12B)	109.5
C(10)-O(3)-C(11)	116.8(2)	H(12A)-C(12)-H(12B)	109.5
C(14)-O(4)-C(13)	118.69(15)	C(11)-C(12)-H(12C)	109.5
C(14)-O(6)-C(15)	118.87(16)	H(12A)-C(12)-H(12C)	109.5
C(29)-O(7)-C(30)	121.65(18)	H(12B)-C(12)-H(12C)	109.5
C(38)-O(9)-C(39)	117.35(19)	O(4)-C(13)-C(25)	121.90(17)
C(42)-O(10)-C(41)	115.79(15)	O(4)-C(13)-C(9)	125.02(18)
C(42)-O(12)-C(43)	117.36(16)	C(25)-C(13)-C(9)	112.54(17)
C(2)-C(1)-H(1A)	109.5	O(5)-C(14)-O(6)	128.6(2)
C(2)-C(1)-H(1B)	109.5	O(5)-C(14)-O(4)	126.24(19)
H(1A)-C(1)-H(1B)	109.5	O(6)-C(14)-O(4)	105.17(16)
C(2)-C(1)-H(1C)	109.5	O(6)-C(15)-C(16)	106.03(19)
H(1A)-C(1)-H(1C)	109.5	O(6)-C(15)-C(21)	108.43(18)
H(1B)-C(1)-H(1C)	109.5	C(16)-C(15)-C(21)	113.09(18)
O(1)-C(2)-C(1)	105.5(2)	O(6)-C(15)-H(15)	109.7
O(1)-C(2)-H(2A)	110.6	C(16)-C(15)-H(15)	109.7
C(1)-C(2)-H(2A)	110.6	C(21)-C(15)-H(15)	109.7
O(1)-C(2)-H(2B)	110.6	C(15)-C(16)-C(17)	112.0(2)
C(1)-C(2)-H(2B)	110.6	C(15)-C(16)-H(16A)	109.2
H(2A)-C(2)-H(2B)	108.8	C(17)-C(16)-H(16A)	109.2
O(1)-C(3)-C(4)	120.30(19)	C(15)-C(16)-H(16B)	109.2
O(1)-C(3)-C(26)	112.16(17)	C(17)-C(16)-H(16B)	109.2
C(4)-C(3)-C(26)	127.5(2)	H(16A)-C(16)-H(16B)	107.9
C(5)-C(4)-C(3)	129.6(2)	C(19)-C(17)-C(16)	109.7(2)
C(5)-C(4)-H(4)	115.2	C(19)-C(17)-C(18)	112.7(2)
C(3)-C(4)-H(4)	115.2	C(16)-C(17)-C(18)	111.0(2)
C(6)-C(5)-C(4)	129.9(2)	C(19)-C(17)-H(17)	107.7
C(6)-C(5)-H(5)	115.0	C(16)-C(17)-H(17)	107.7
C(4)-C(5)-H(5)	115.0	C(18)-C(17)-H(17)	107.7
C(5)-C(6)-C(7)	128.9(2)	C(17)-C(18)-H(18A)	109.5
C(5)-C(6)-H(6)	115.5	C(17)-C(18)-H(18B)	109.5
C(7)-C(6)-H(6)	115.5	H(18A)-C(18)-H(18B)	109.5
C(6)-C(7)-C(8)	128.6(2)	C(17)-C(18)-H(18C)	109.5
C(6)-C(7)-H(7)	115.7	H(18A)-C(18)-H(18C)	109.5
C(8)-C(7)-H(7)	115.7	H(18B)-C(18)-H(18C)	109.5
C(7)-C(8)-C(9)	124.8(2)	C(17)-C(19)-C(20)	111.3(2)
C(7)-C(8)-C(26)	128.3(2)	C(17)-C(19)-H(19A)	109.4
C(9)-C(8)-C(26)	106.93(17)	C(20)-C(19)-H(19A)	109.4
C(13)-C(9)-C(8)	106.00(18)	C(17)-C(19)-H(19B)	109.4
C(13)-C(9)-C(10)	127.6(2)	C(20)-C(19)-H(19B)	109.4
C(8)-C(9)-C(10)	126.4(2)	H(19A)-C(19)-H(19B)	108.0
O(2)-C(10)-O(3)	122.2(2)	C(19)-C(20)-C(21)	112.2(2)
O(2)-C(10)-C(9)	125.9(2)	C(19)-C(20)-H(20A)	109.2
O(3)-C(10)-C(9)	111.9(2)	C(21)-C(20)-H(20A)	109.2
O(3)-C(11)-C(12)	106.6(3)	C(19)-C(20)-H(20B)	109.2
O(3)-C(11)-H(11A)	110.4	C(21)-C(20)-H(20B)	109.2
C(12)-C(11)-H(11A)	110.4	H(20A)-C(20)-H(20B)	107.9
O(3)-C(11)-H(11B)	110.4	C(15)-C(21)-C(20)	108.22(19)
C(12)-C(11)-H(11B)	110.4	C(15)-C(21)-C(22)	113.52(19)
H(11A)-C(11)-H(11B)	108.6	C(20)-C(21)-C(22)	113.9(2)
C(11)-C(12)-H(12A)	109.5	C(15)-C(21)-H(21)	106.9
		C(20)-C(21)-H(21)	106.9
		C(22)-C(21)-H(21)	106.9
		C(23)-C(22)-C(24)	110.7(3)

C(23)-C(22)-C(21)	110.7(2)	C(36)-C(35)-H(35)	115.8
C(24)-C(22)-C(21)	114.0(2)	C(35)-C(36)-C(37)	124.3(2)
C(23)-C(22)-H(22)	107.0	C(35)-C(36)-C(28)	128.5(2)
C(24)-C(22)-H(22)	107.0	C(37)-C(36)-C(28)	107.22(17)
C(21)-C(22)-H(22)	107.0	C(41)-C(37)-C(36)	105.48(17)
C(22)-C(23)-H(23A)	109.5	C(41)-C(37)-C(38)	127.14(19)
C(22)-C(23)-H(23B)	109.5	C(36)-C(37)-C(38)	127.37(18)
H(23A)-C(23)-H(23B)	109.5	O(8)-C(38)-O(9)	122.2(2)
C(22)-C(23)-H(23C)	109.5	O(8)-C(38)-C(37)	125.7(2)
H(23A)-C(23)-H(23C)	109.5	O(9)-C(38)-C(37)	112.11(18)
H(23B)-C(23)-H(23C)	109.5	O(9)-C(39)-C(40)	108.2(2)
C(22)-C(24)-H(24A)	109.5	O(9)-C(39)-H(39A)	110.1
C(22)-C(24)-H(24B)	109.5	C(40)-C(39)-H(39A)	110.1
H(24A)-C(24)-H(24B)	109.5	O(9)-C(39)-H(39B)	110.1
C(22)-C(24)-H(24C)	109.5	C(40)-C(39)-H(39B)	110.1
H(24A)-C(24)-H(24C)	109.5	H(39A)-C(39)-H(39B)	108.4
H(24B)-C(24)-H(24C)	109.5	C(39)-C(40)-H(40A)	109.5
C(13)-C(25)-C(26)	106.60(17)	C(39)-C(40)-H(40B)	109.5
C(13)-C(25)-C(27)	122.10(17)	H(40A)-C(40)-H(40B)	109.5
C(26)-C(25)-C(27)	131.25(17)	C(39)-C(40)-H(40C)	109.5
C(25)-C(26)-C(3)	125.00(18)	H(40A)-C(40)-H(40C)	109.5
C(25)-C(26)-C(8)	107.89(17)	H(40B)-C(40)-H(40C)	109.5
C(3)-C(26)-C(8)	127.10(17)	O(10)-C(41)-C(27)	120.62(16)
C(41)-C(27)-C(28)	106.22(17)	O(10)-C(41)-C(37)	126.28(18)
C(41)-C(27)-C(25)	122.43(16)	C(27)-C(41)-C(37)	113.08(17)
C(28)-C(27)-C(25)	131.34(18)	O(11)-C(42)-O(12)	128.41(19)
C(29)-C(28)-C(27)	124.50(19)	O(11)-C(42)-O(10)	125.48(19)
C(29)-C(28)-C(36)	127.49(18)	O(12)-C(42)-O(10)	106.10(16)
C(27)-C(28)-C(36)	107.99(17)	O(12)-C(43)-C(44)	106.61(18)
O(7)-C(29)-C(32)	120.7(2)	O(12)-C(43)-C(49)	107.2(2)
O(7)-C(29)-C(28)	111.98(17)	C(44)-C(43)-C(49)	112.58(19)
C(32)-C(29)-C(28)	127.3(2)	O(12)-C(43)-H(43)	110.1
O(7)-C(30)-C(31)	106.2(2)	C(44)-C(43)-H(43)	110.1
O(7)-C(30)-H(30A)	110.5	C(49)-C(43)-H(43)	110.1
C(31)-C(30)-H(30A)	110.5	C(43)-C(44)-C(45)	112.0(2)
O(7)-C(30)-H(30B)	110.5	C(43)-C(44)-H(44A)	109.2
C(31)-C(30)-H(30B)	110.5	C(45)-C(44)-H(44A)	109.2
H(30A)-C(30)-H(30B)	108.7	C(43)-C(44)-H(44B)	109.2
C(30)-C(31)-H(31A)	109.5	C(45)-C(44)-H(44B)	109.2
C(30)-C(31)-H(31B)	109.5	H(44A)-C(44)-H(44B)	107.9
H(31A)-C(31)-H(31B)	109.5	C(47)-C(45)-C(46)	111.6(2)
C(30)-C(31)-H(31C)	109.5	C(47)-C(45)-C(44)	109.9(2)
H(31A)-C(31)-H(31C)	109.5	C(46)-C(45)-C(44)	109.8(2)
H(31B)-C(31)-H(31C)	109.5	C(47)-C(45)-H(45)	108.5
C(33)-C(32)-C(29)	128.8(2)	C(46)-C(45)-H(45)	108.5
C(33)-C(32)-H(32)	115.6	C(44)-C(45)-H(45)	108.5
C(29)-C(32)-H(32)	115.6	C(45)-C(46)-H(46A)	109.5
C(34)-C(33)-C(32)	130.8(2)	C(45)-C(46)-H(46B)	109.5
C(34)-C(33)-H(33)	114.6	H(46A)-C(46)-H(46B)	109.5
C(32)-C(33)-H(33)	114.6	C(45)-C(46)-H(46C)	109.5
C(33)-C(34)-C(35)	128.6(2)	H(46A)-C(46)-H(46C)	109.5
C(33)-C(34)-H(34)	115.7	H(46B)-C(46)-H(46C)	109.5
C(35)-C(34)-H(34)	115.7	C(45)-C(47)-C(48)	112.6(2)
C(34)-C(35)-C(36)	128.5(2)	C(45)-C(47)-H(47A)	109.1
C(34)-C(35)-H(35)	115.8	C(48)-C(47)-H(47A)	109.1

C(45)-C(47)-H(47B)	109.1
C(48)-C(47)-H(47B)	109.1
H(47A)-C(47)-H(47B)	107.8
C(47)-C(48)-C(49)	111.5(2)
C(47)-C(48)-H(48A)	109.3
C(49)-C(48)-H(48A)	109.3
C(47)-C(48)-H(48B)	109.3
C(49)-C(48)-H(48B)	109.3
H(48A)-C(48)-H(48B)	108.0
C(43)-C(49)-C(48)	106.8(2)
C(43)-C(49)-C(50)	112.7(2)
C(48)-C(49)-C(50)	116.1(2)
C(43)-C(49)-H(49)	106.9
C(48)-C(49)-H(49)	106.9
C(50)-C(49)-H(49)	106.9
C(51)-C(50)-C(52)	112.8(3)
C(51)-C(50)-C(49)	111.9(3)
C(52)-C(50)-C(49)	112.5(3)
C(51)-C(50)-H(50)	106.4
C(52)-C(50)-H(50)	106.4
C(49)-C(50)-H(50)	106.4
C(50)-C(51)-H(51A)	109.5
C(50)-C(51)-H(51B)	109.5
H(51A)-C(51)-H(51B)	109.5

C(50)-C(51)-H(51C)	109.5
H(51A)-C(51)-H(51C)	109.5
H(51B)-C(51)-H(51C)	109.5
C(50)-C(52)-H(52A)	109.5
C(50)-C(52)-H(52B)	109.5
H(52A)-C(52)-H(52B)	109.5
C(50)-C(52)-H(52C)	109.5
H(52A)-C(52)-H(52C)	109.5
H(52B)-C(52)-H(52C)	109.5
C(61)-O(13)-H(13)	109.5
O(13)-C(61)-C(62)	113(2)
O(13)-C(61)-H(61A)	108.9
C(62)-C(61)-H(61A)	108.9
O(13)-C(61)-H(61B)	108.9
C(62)-C(61)-H(61B)	108.9
H(61A)-C(61)-H(61B)	107.7
C(61)-C(62)-H(62A)	109.5
C(61)-C(62)-H(62B)	109.5
H(62A)-C(62)-H(62B)	109.5
C(61)-C(62)-H(62C)	109.5
H(62A)-C(62)-H(62C)	109.5
H(62B)-C(62)-H(62C)	109.5

Table 5. Anisotropic displacement parameters ($\text{\AA}^2 \times 10^3$) for s16sel1. The anisotropic displacement factor exponent takes the form: $-2p^2[h^2 a^{*2}U^{11} + \dots + 2 h k a^* b^* U^{12}]$

	U ¹¹	U ²²	U ³³	U ²³	U ¹³	U ¹²
O(1)	36(1)	58(1)	32(1)	-9(1)	3(1)	-14(1)
O(2)	54(1)	137(2)	59(1)	-13(1)	24(1)	-35(1)
O(3)	34(1)	68(1)	60(1)	-1(1)	4(1)	-14(1)
O(4)	40(1)	26(1)	33(1)	-3(1)	-6(1)	-4(1)
O(5)	66(1)	35(1)	46(1)	-8(1)	-18(1)	14(1)
O(6)	56(1)	35(1)	42(1)	-10(1)	-19(1)	9(1)
O(7)	49(1)	24(1)	51(1)	2(1)	3(1)	4(1)
O(8)	50(1)	63(1)	41(1)	-7(1)	18(1)	-1(1)
O(9)	58(1)	50(1)	40(1)	-3(1)	14(1)	16(1)
O(10)	32(1)	27(1)	28(1)	0(1)	-3(1)	1(1)
O(11)	41(1)	60(1)	50(1)	21(1)	-14(1)	-17(1)
O(12)	47(1)	30(1)	49(1)	9(1)	-17(1)	-4(1)
C(1)	44(2)	132(3)	56(2)	-25(2)	12(1)	-32(2)
C(2)	39(1)	95(2)	45(1)	-19(1)	3(1)	-24(1)
C(3)	37(1)	31(1)	30(1)	-2(1)	1(1)	-1(1)
C(4)	44(1)	37(1)	34(1)	-7(1)	-2(1)	-5(1)
C(5)	53(1)	39(1)	28(1)	-8(1)	-2(1)	2(1)
C(6)	54(1)	45(1)	28(1)	-7(1)	7(1)	6(1)
C(7)	44(1)	41(1)	34(1)	0(1)	11(1)	4(1)
C(8)	36(1)	29(1)	32(1)	-1(1)	4(1)	1(1)
C(9)	34(1)	33(1)	38(1)	2(1)	3(1)	-1(1)
C(10)	39(1)	50(1)	52(1)	2(1)	6(1)	-8(1)
C(11)	36(1)	82(2)	85(2)	6(2)	4(1)	-17(1)
C(12)	48(2)	156(4)	109(3)	-14(3)	-9(2)	-37(2)
C(13)	35(1)	24(1)	31(1)	1(1)	-2(1)	-1(1)
C(14)	34(1)	33(1)	37(1)	-4(1)	-5(1)	2(1)
C(15)	43(1)	38(1)	38(1)	-9(1)	-11(1)	7(1)
C(16)	47(1)	39(1)	42(1)	-6(1)	-9(1)	4(1)
C(17)	40(1)	40(1)	45(1)	-8(1)	-11(1)	5(1)
C(18)	50(1)	43(1)	61(2)	-5(1)	-12(1)	0(1)
C(19)	47(1)	64(2)	43(1)	-19(1)	-10(1)	3(1)
C(20)	43(1)	75(2)	41(1)	-14(1)	-3(1)	-4(1)
C(21)	39(1)	53(1)	48(1)	-20(1)	-8(1)	7(1)
C(22)	38(1)	65(2)	54(1)	-24(1)	-5(1)	3(1)
C(23)	44(2)	113(3)	83(2)	-52(2)	6(2)	-6(2)
C(24)	49(2)	64(2)	78(2)	-10(2)	-5(1)	-9(1)
C(25)	33(1)	22(1)	26(1)	0(1)	0(1)	1(1)
C(26)	34(1)	25(1)	27(1)	-1(1)	2(1)	1(1)
C(27)	32(1)	30(1)	23(1)	0(1)	-2(1)	-3(1)
C(28)	33(1)	33(1)	27(1)	4(1)	-3(1)	-4(1)
C(29)	42(1)	34(1)	36(1)	4(1)	-5(1)	-4(1)
C(30)	69(2)	33(1)	57(2)	3(1)	-4(1)	18(1)
C(31)	68(2)	45(1)	74(2)	-3(1)	9(2)	24(1)
C(32)	66(2)	35(1)	51(1)	12(1)	-4(1)	-2(1)
C(33)	74(2)	50(1)	48(1)	24(1)	-5(1)	-14(1)
C(34)	59(2)	64(2)	37(1)	18(1)	2(1)	-16(1)
C(35)	41(1)	58(1)	31(1)	7(1)	1(1)	-7(1)
C(36)	32(1)	44(1)	26(1)	3(1)	-2(1)	-6(1)
C(37)	32(1)	42(1)	24(1)	-1(1)	0(1)	-1(1)

C(38)	33(1)	52(1)	29(1)	-7(1)	-1(1)	0(1)
C(39)	48(1)	60(2)	52(1)	-17(1)	6(1)	15(1)
C(40)	74(2)	54(2)	58(2)	-6(1)	7(1)	20(1)
C(41)	32(1)	30(1)	24(1)	0(1)	-2(1)	-1(1)
C(42)	31(1)	35(1)	28(1)	-1(1)	-1(1)	0(1)
C(43)	48(1)	35(1)	40(1)	8(1)	-14(1)	-5(1)
C(44)	38(1)	41(1)	42(1)	11(1)	-2(1)	1(1)
C(45)	40(1)	47(1)	61(1)	21(1)	-11(1)	-4(1)
C(46)	48(1)	57(2)	85(2)	30(2)	11(1)	14(1)
C(47)	71(2)	47(1)	46(1)	15(1)	-11(1)	-3(1)
C(48)	102(3)	51(2)	39(1)	4(1)	-10(1)	-4(2)
C(49)	67(2)	40(1)	46(1)	-1(1)	-1(1)	1(1)
C(50)	114(3)	56(2)	60(2)	-8(1)	8(2)	11(2)
C(51)	118(3)	90(3)	78(2)	-22(2)	10(2)	20(3)
C(52)	161(4)	40(1)	49(2)	-3(1)	15(2)	3(2)
O(13)	53(9)	72(11)	78(11)	-21(9)	15(8)	-19(8)
C(61)	60(14)	78(17)	69(15)	-15(13)	5(12)	-24(14)
C(62)	83(19)	62(16)	90(20)	-16(14)	-5(16)	-18(15)

Table 6. Hydrogen coordinates ($\times 10^4$) and isotropic displacement parameters ($\text{\AA}^2 \times 10^3$) for s16sel1.

	x	y	z	U(eq)
H(1A)	4893	5879	2816	116
H(1B)	3843	6117	2476	116
H(1C)	4054	5202	2645	116
H(2A)	3874	5557	3615	72
H(2B)	3592	6459	3427	72
H(4)	2655	6153	4196	46
H(5)	1679	6135	4958	48
H(6)	93	5635	5093	51
H(7)	-968	5044	4486	48
H(11A)	-3934	4257	3325	81
H(11B)	-3559	3379	3520	81
H(12A)	-4636	3296	2708	157
H(12B)	-3469	2968	2578	157
H(12C)	-3807	3846	2375	157
H(15)	-1952	4517	1103	47
H(16A)	-3108	3469	1327	51
H(16B)	-2299	2817	1082	51
H(17)	-3399	3989	422	50
H(18A)	-4304	2874	18	77
H(18B)	-4561	2972	673	77
H(18C)	-3746	2298	467	77
H(19A)	-2607	3415	-374	62
H(19B)	-1975	2791	13	62
H(20A)	-1660	4495	23	64
H(20B)	-841	3861	-234	64
H(21)	-535	3320	672	56
H(22)	379	4387	1117	63
H(23A)	1639	4578	405	120
H(23B)	808	4280	-58	120
H(23C)	1239	3668	407	120
H(24A)	461	5669	724	96
H(24B)	-730	5480	915	96
H(24C)	-411	5431	264	96
H(30A)	-276	7332	2324	64
H(30B)	802	7560	2649	64
H(31A)	-686	7579	3266	93
H(31B)	183	6941	3465	93
H(31C)	-862	6645	3145	93
H(32)	1180	7393	1758	60
H(33)	2207	7389	1009	68
H(34)	3196	6440	659	64
H(35)	3300	5172	915	52
H(39A)	4445	2378	1565	64
H(39B)	3724	2388	1009	64
H(40A)	3693	1114	1454	93
H(40B)	2532	1497	1421	93
H(40C)	3180	1522	1999	93
H(43)	3505	2664	3645	49
H(44A)	3859	1578	3046	49

H(44B)	2804	1129	3247	49
H(45)	4648	1407	3928	59
H(46A)	4740	-24	3955	95
H(46B)	4876	315	3329	95
H(46C)	3769	-65	3522	95
H(47A)	3769	806	4682	65
H(47B)	2748	630	4302	65
H(48A)	3441	2193	4642	76
H(48B)	2409	1746	4878	76
H(49)	1643	1784	3961	61
H(50)	1270	3171	3850	92
H(51A)	310	3340	4659	143
H(51B)	987	2659	4969	143
H(51C)	232	2429	4452	143
H(52A)	1928	4111	4521	125
H(52B)	2817	3795	4095	125
H(52C)	2766	3452	4723	125
H(13)	-3902	4669	4068	101
H(61A)	-5374	4034	3834	83
H(61B)	-5853	4332	4420	83
H(62A)	-5339	3015	4483	117
H(62B)	-4154	3253	4310	117
H(62C)	-4634	3552	4897	117

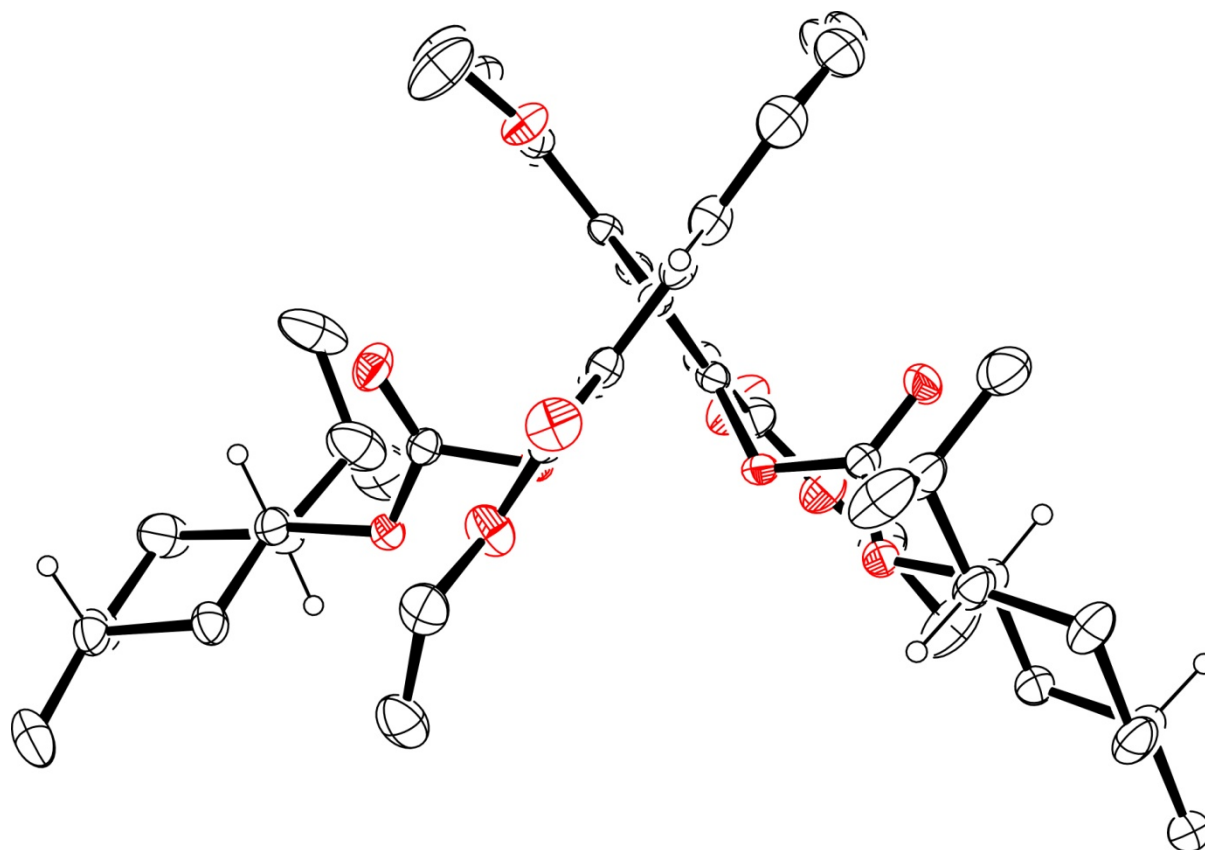
Table 7. Torsion angles [°] for s16sel1.

C(3)-O(1)-C(2)-C(1)	170.8(3)	O(4)-C(13)-C(25)-C(27)	7.9(3)
C(2)-O(1)-C(3)-C(4)	13.1(3)	C(9)-C(13)-C(25)-C(27)	179.84(17)
C(2)-O(1)-C(3)-C(26)	-167.1(2)	C(13)-C(25)-C(26)-C(3)	177.56(18)
O(1)-C(3)-C(4)-C(5)	-179.7(2)	C(27)-C(25)-C(26)-C(3)	0.2(3)
C(26)-C(3)-C(4)-C(5)	0.4(4)	C(13)-C(25)-C(26)-C(8)	-1.5(2)
C(3)-C(4)-C(5)-C(6)	-0.6(4)	C(27)-C(25)-C(26)-C(8)	-178.85(18)
C(4)-C(5)-C(6)-C(7)	-0.8(4)	O(1)-C(3)-C(26)-C(25)	1.5(3)
C(5)-C(6)-C(7)-C(8)	2.2(4)	C(4)-C(3)-C(26)-C(25)	-178.7(2)
C(6)-C(7)-C(8)-C(9)	177.0(2)	O(1)-C(3)-C(26)-C(8)	-179.61(18)
C(6)-C(7)-C(8)-C(26)	-1.9(4)	C(4)-C(3)-C(26)-C(8)	0.2(3)
C(7)-C(8)-C(9)-C(13)	-178.2(2)	C(7)-C(8)-C(26)-C(25)	179.5(2)
C(26)-C(8)-C(9)-C(13)	0.9(2)	C(9)-C(8)-C(26)-C(25)	0.4(2)
C(7)-C(8)-C(9)-C(10)	4.3(4)	C(7)-C(8)-C(26)-C(3)	0.4(3)
C(26)-C(8)-C(9)-C(10)	-176.5(2)	C(9)-C(8)-C(26)-C(3)	-178.69(19)
C(11)-O(3)-C(10)-O(2)	4.0(4)	C(13)-C(25)-C(27)-C(41)	-71.4(2)
C(11)-O(3)-C(10)-C(9)	-175.7(2)	C(26)-C(25)-C(27)-C(41)	105.6(2)
C(13)-C(9)-C(10)-O(2)	175.3(3)	C(13)-C(25)-C(27)-C(28)	107.7(2)
C(8)-C(9)-C(10)-O(2)	-7.8(4)	C(26)-C(25)-C(27)-C(28)	-75.4(3)
C(13)-C(9)-C(10)-O(3)	-5.0(3)	C(41)-C(27)-C(28)-C(29)	-179.70(19)
C(8)-C(9)-C(10)-O(3)	171.9(2)	C(25)-C(27)-C(28)-C(29)	1.1(3)
C(10)-O(3)-C(11)-C(12)	-177.6(3)	C(41)-C(27)-C(28)-C(36)	-0.9(2)
C(14)-O(4)-C(13)-C(25)	-83.5(2)	C(25)-C(27)-C(28)-C(36)	179.92(19)
C(14)-O(4)-C(13)-C(9)	105.6(2)	C(30)-O(7)-C(29)-C(32)	-2.3(3)
C(8)-C(9)-C(13)-O(4)	169.65(18)	C(30)-O(7)-C(29)-C(28)	177.4(2)
C(10)-C(9)-C(13)-O(4)	-12.9(3)	C(27)-C(28)-C(29)-O(7)	0.3(3)
C(8)-C(9)-C(13)-C(25)	-2.0(2)	C(36)-C(28)-C(29)-O(7)	-178.25(19)
C(10)-C(9)-C(13)-C(25)	175.4(2)	C(27)-C(28)-C(29)-C(32)	180.0(2)
C(15)-O(6)-C(14)-O(5)	-1.2(4)	C(36)-C(28)-C(29)-C(32)	1.5(4)
C(15)-O(6)-C(14)-O(4)	178.70(18)	C(29)-O(7)-C(30)-C(31)	-174.2(2)
C(13)-O(4)-C(14)-O(5)	-9.1(3)	O(7)-C(29)-C(32)-C(33)	177.9(3)
C(13)-O(4)-C(14)-O(6)	170.96(17)	C(28)-C(29)-C(32)-C(33)	-1.8(4)
C(14)-O(6)-C(15)-C(16)	-125.2(2)	C(29)-C(32)-C(33)-C(34)	-1.1(5)
C(14)-O(6)-C(15)-C(21)	113.1(2)	C(32)-C(33)-C(34)-C(35)	3.5(5)
O(6)-C(15)-C(16)-C(17)	-174.86(18)	C(33)-C(34)-C(35)-C(36)	-2.2(5)
C(21)-C(15)-C(16)-C(17)	-56.2(3)	C(34)-C(35)-C(36)-C(37)	-179.4(2)
C(15)-C(16)-C(17)-C(19)	55.1(3)	C(34)-C(35)-C(36)-C(28)	-0.4(4)
C(15)-C(16)-C(17)-C(18)	-179.6(2)	C(29)-C(28)-C(36)-C(35)	0.6(4)
C(16)-C(17)-C(19)-C(20)	-56.0(3)	C(27)-C(28)-C(36)-C(35)	-178.2(2)
C(18)-C(17)-C(19)-C(20)	179.8(2)	C(29)-C(28)-C(36)-C(37)	179.7(2)
C(17)-C(19)-C(20)-C(21)	57.8(3)	C(27)-C(28)-C(36)-C(37)	1.0(2)
O(6)-C(15)-C(21)-C(20)	171.9(2)	C(35)-C(36)-C(37)-C(41)	178.5(2)
C(16)-C(15)-C(21)-C(20)	54.6(3)	C(28)-C(36)-C(37)-C(41)	-0.6(2)
O(6)-C(15)-C(21)-C(22)	-60.7(3)	C(35)-C(36)-C(37)-C(38)	-0.5(3)
C(16)-C(15)-C(21)-C(22)	-178.0(2)	C(28)-C(36)-C(37)-C(38)	-179.68(19)
C(19)-C(20)-C(21)-C(15)	-55.2(3)	C(39)-O(9)-C(38)-O(8)	3.6(3)
C(19)-C(20)-C(21)-C(22)	177.5(2)	C(39)-O(9)-C(38)-C(37)	-177.45(19)
C(15)-C(21)-C(22)-C(23)	167.8(3)	C(41)-C(37)-C(38)-O(8)	-176.7(2)
C(20)-C(21)-C(22)-C(23)	-67.7(3)	C(36)-C(37)-C(38)-O(8)	2.2(4)
C(15)-C(21)-C(22)-C(24)	-66.6(3)	C(41)-C(37)-C(38)-O(9)	4.4(3)
C(20)-C(21)-C(22)-C(24)	57.9(3)	C(36)-C(37)-C(38)-O(9)	-176.7(2)
O(4)-C(13)-C(25)-C(26)	-169.70(17)	C(38)-O(9)-C(39)-C(40)	-160.9(2)
C(9)-C(13)-C(25)-C(26)	2.2(2)	C(42)-O(10)-C(41)-C(27)	-99.6(2)
		C(42)-O(10)-C(41)-C(37)	82.0(2)
		C(28)-C(27)-C(41)-O(10)	-178.04(16)
		C(25)-C(27)-C(41)-O(10)	1.2(3)

C(28)-C(27)-C(41)-C(37)	0.5(2)	C(46)-C(45)-C(47)-C(48)	-174.4(3)
C(25)-C(27)-C(41)-C(37)	179.79(17)	C(44)-C(45)-C(47)-C(48)	-52.3(3)
C(36)-C(37)-C(41)-O(10)	178.57(17)	C(45)-C(47)-C(48)-C(49)	57.1(4)
C(38)-C(37)-C(41)-O(10)	-2.4(3)	O(12)-C(43)-C(49)-C(48)	176.09(19)
C(36)-C(37)-C(41)-C(27)	0.1(2)	C(44)-C(43)-C(49)-C(48)	59.2(3)
C(38)-C(37)-C(41)-C(27)	179.12(19)	O(12)-C(43)-C(49)-C(50)	-55.2(3)
C(43)-O(12)-C(42)-O(11)	7.6(3)	C(44)-C(43)-C(49)-C(50)	-172.1(2)
C(43)-O(12)-C(42)-O(10)	-171.70(17)	C(47)-C(48)-C(49)-C(43)	-58.1(3)
C(41)-O(10)-C(42)-O(11)	-0.2(3)	C(47)-C(48)-C(49)-C(50)	175.2(3)
C(41)-O(10)-C(42)-O(12)	179.10(16)	C(43)-C(49)-C(50)-C(51)	166.1(3)
C(42)-O(12)-C(43)-C(44)	-118.4(2)	C(48)-C(49)-C(50)-C(51)	-70.2(4)
C(42)-O(12)-C(43)-C(49)	120.8(2)	C(43)-C(49)-C(50)-C(52)	-65.8(3)
O(12)-C(43)-C(44)-C(45)	-175.36(18)	C(48)-C(49)-C(50)-C(52)	57.9(4)
C(49)-C(43)-C(44)-C(45)	-58.1(3)		
C(43)-C(44)-C(45)-C(47)	52.3(3)		
C(43)-C(44)-C(45)-C(46)	175.5(2)		

Table 8. Hydrogen bonds for s16sel1 [\AA and $^\circ$].

D-H...A	d(D-H)	d(H...A)	d(D...A)	$\angle(\text{DHA})$
O(13)-H(13)...O(2)	0.84	2.11	2.886(19)	153.5



Axial view of ($R_a,1R,2S,5R$)-**404**.

X-ray crystallographic data for (S_a,1*R*,2*S*,5*R*)-**404**.

Table 1. Crystal data and structure refinement for s16sel11.

Identification code	s16sel11	
Empirical formula	C ₅₂ H ₆₆ O ₁₂	
Formula weight	883.04	
Temperature	150.01(10) K	
Wavelength	1.54184 Å	
Crystal system	Orthorhombic	
Space group	P2 ₁ 2 ₁ 2 ₁	
Unit cell dimensions	a = 12.4749(17) Å	α = 90°.
	b = 17.3916(10) Å	β = 90°.
	c = 22.547(3) Å	γ = 90°.
Volume	4891.8(9) Å ³	
Z	4	
Density (calculated)	1.199 Mg/m ³	
Absorption coefficient	0.684 mm ⁻¹	
F(000)	1896	
Crystal size	0.300 x 0.050 x 0.020 mm ³	
Theta range for data collection	3.209 to 66.711°.	
Index ranges	-14 ≤ h ≤ 14, -13 ≤ k ≤ 20, -25 ≤ l ≤ 26	
Reflections collected	34755	
Independent reflections	8646 [R(int) = 0.0993]	
Completeness to theta = 66.711°	99.9 %	
Absorption correction	Semi-empirical from equivalents	
Max. and min. transmission	1.00000 and 0.65916	
Refinement method	Full-matrix least-squares on F ²	
Data / restraints / parameters	8646 / 56 / 634	
Goodness-of-fit on F ²	0.909	
Final R indices [I > 2σ(I)]	R1 = 0.0660, wR2 = 0.1350	
R indices (all data)	R1 = 0.1431, wR2 = 0.1710	
Absolute structure parameter	-0.1(3)	
Extinction coefficient	0.00032(8)	
Largest diff. peak and hole	0.201 and -0.180 e.Å ⁻³	

Table 2. Atomic coordinates ($\times 10^4$) and equivalent isotropic displacement parameters ($\text{\AA}^2 \times 10^3$) for s16sel11. $U(\text{eq})$ is defined as one third of the trace of the orthogonalized U_{ij} tensor.

	x	y	z	$U(\text{eq})$
C(1)	-3550(8)	7000(5)	266(4)	90(3)
C(2)	-2435(8)	6665(5)	355(4)	70(2)
C(3)	-1979(8)	6328(5)	-206(4)	76(3)
C(4)	-897(8)	5966(5)	-110(4)	81(3)
C(5)	-912(7)	5345(5)	375(4)	71(2)
C(6)	162(8)	4925(6)	462(5)	86(3)
C(7)	524(9)	4477(6)	-87(5)	109(4)
C(8)	1065(9)	5464(7)	658(4)	103(4)
C(9)	-1337(7)	5707(5)	928(3)	61(2)
C(10)	-2456(7)	6047(5)	843(4)	68(2)
C(11)	-1156(7)	5326(5)	1930(4)	65(2)
C(12)	-891(7)	4821(4)	2866(3)	55(2)
C(13)	-1461(7)	5038(4)	3377(4)	69(3)
C(14)	-2546(9)	5321(7)	3440(5)	99(4)
O(5)	-2960(13)	5476(9)	2862(6)	115(7)
C(15)	-4057(16)	5753(17)	2917(14)	158(13)
C(16)	-4790(20)	5049(18)	2960(20)	270(30)
O(5A)	-3057(18)	5140(9)	2891(8)	77(7)
C(15A)	-4180(20)	5310(20)	3000(30)	260(40)
C(16A)	-4450(30)	5980(30)	2570(20)	230(30)
C(17)	-737(7)	5009(4)	3865(3)	62(2)
C(18)	-943(10)	5261(5)	4443(4)	86(3)
C(19)	-224(11)	5240(5)	4917(4)	92(4)
C(20)	796(12)	4985(7)	4955(5)	106(4)
C(21)	1405(10)	4633(6)	4534(3)	92(3)
C(22)	1170(9)	4479(5)	3950(3)	73(3)
C(23)	2920(9)	3882(7)	3839(5)	107(4)
C(24)	3455(9)	3466(8)	3322(5)	134(5)
C(25)	275(7)	4723(4)	3615(3)	57(2)
C(26)	176(6)	4635(4)	3002(3)	46(2)
C(27)	972(6)	4457(3)	2557(3)	44(2)
C(28)	1166(6)	3764(4)	2251(3)	45(2)
C(29)	623(6)	3072(4)	2349(3)	51(2)
C(30)	-540(10)	2474(5)	3079(4)	99(4)
C(31)	-927(11)	2752(6)	3665(5)	132(6)
C(32)	743(8)	2372(4)	2063(3)	66(2)
C(33)	1447(8)	2194(5)	1601(3)	72(3)
C(34)	2230(8)	2626(5)	1337(4)	73(3)
C(35)	2533(7)	3366(4)	1454(3)	62(2)
C(36)	2080(6)	3884(4)	1857(3)	50(2)
C(37)	2427(6)	4657(4)	1942(3)	54(2)
C(38)	3332(7)	5033(5)	1647(4)	69(2)
C(39)	4222(11)	6222(7)	1461(7)	141(6)
C(40)	3654(17)	6732(13)	1020(10)	124(8)
C(40A)	4100(30)	7037(13)	1541(15)	129(11)
C(41)	1727(6)	4981(4)	2352(3)	49(2)
C(42)	2228(7)	5971(4)	3004(3)	57(2)
C(43)	2374(8)	7069(4)	3644(4)	69(2)
C(44)	2596(8)	7895(5)	3505(4)	77(3)

C(45)	3508(9)	7995(7)	3035(5)	103(4)
C(46)	3110(19)	8200(20)	2417(10)	209(18)
C(46A)	3700(20)	8732(13)	2855(17)	121(14)
C(47)	4590(10)	7698(9)	3225(7)	166(7)
C(48)	2832(8)	8311(5)	4086(5)	87(3)
C(49)	1909(8)	8238(5)	4523(4)	83(3)
C(50)	1656(8)	7403(5)	4666(4)	76(3)
C(51)	702(9)	7317(6)	5078(4)	93(3)
C(52)	1470(8)	6963(5)	4089(4)	70(2)
O(1)	-1420(5)	5108(3)	1392(2)	68(2)
O(2)	-871(6)	5940(3)	2083(3)	89(2)
O(3)	-1286(4)	4722(3)	2291(2)	61(1)
O(4)	-3033(7)	5487(6)	3877(4)	146(4)
O(6)	1841(5)	4061(3)	3620(2)	72(2)
O(7)	-112(5)	3137(3)	2793(2)	61(2)
O(8)	3958(5)	4719(4)	1314(2)	83(2)
O(9)	3362(6)	5789(4)	1767(3)	105(3)
O(10)	1679(4)	5751(3)	2518(2)	54(1)
O(11)	2790(5)	5565(3)	3299(3)	78(2)
O(12)	2001(5)	6707(3)	3086(2)	66(2)

Table 3. Bond lengths [Å] for s16sel11.

C(1)-C(2)	1.521(12)	C(16A)-H(16D)	0.9800
C(1)-H(1A)	0.9800	C(16A)-H(16E)	0.9800
C(1)-H(1B)	0.9800	C(16A)-H(16F)	0.9800
C(1)-H(1C)	0.9800	C(17)-C(18)	1.399(11)
C(2)-C(3)	1.504(12)	C(17)-C(25)	1.470(11)
C(2)-C(10)	1.539(10)	C(18)-C(19)	1.396(15)
C(2)-H(2)	1.0000	C(18)-H(18)	0.9500
C(3)-C(4)	1.506(12)	C(19)-C(20)	1.350(15)
C(3)-H(3A)	0.9900	C(19)-H(19)	0.9500
C(3)-H(3B)	0.9900	C(20)-C(21)	1.361(14)
C(4)-C(5)	1.537(10)	C(20)-H(20)	0.9500
C(4)-H(4A)	0.9900	C(21)-C(22)	1.376(10)
C(4)-H(4B)	0.9900	C(21)-H(21)	0.9500
C(5)-C(9)	1.495(11)	C(22)-O(6)	1.335(10)
C(5)-C(6)	1.539(12)	C(22)-C(25)	1.413(12)
C(5)-H(5)	1.0000	C(23)-O(6)	1.466(11)
C(6)-C(7)	1.529(13)	C(23)-C(24)	1.525(14)
C(6)-C(8)	1.531(14)	C(23)-H(23A)	0.9900
C(6)-H(6)	1.0000	C(23)-H(23B)	0.9900
C(7)-H(7A)	0.9800	C(24)-H(24A)	0.9800
C(7)-H(7B)	0.9800	C(24)-H(24B)	0.9800
C(7)-H(7C)	0.9800	C(24)-H(24C)	0.9800
C(8)-H(8A)	0.9800	C(25)-C(26)	1.396(9)
C(8)-H(8B)	0.9800	C(26)-C(27)	1.445(9)
C(8)-H(8C)	0.9800	C(27)-C(41)	1.388(9)
C(9)-O(1)	1.480(8)	C(27)-C(28)	1.411(8)
C(9)-C(10)	1.528(11)	C(28)-C(29)	1.397(9)
C(9)-H(9)	1.0000	C(28)-C(36)	1.462(10)
C(10)-H(10A)	0.9900	C(29)-O(7)	1.362(9)
C(10)-H(10B)	0.9900	C(29)-C(32)	1.386(9)
C(11)-O(2)	1.177(10)	C(30)-O(7)	1.426(9)
C(11)-O(1)	1.314(10)	C(30)-C(31)	1.487(11)
C(11)-O(3)	1.339(8)	C(30)-H(30A)	0.9900
C(12)-O(3)	1.398(9)	C(30)-H(30B)	0.9900
C(12)-C(26)	1.403(10)	C(31)-H(31A)	0.9800
C(12)-C(13)	1.405(10)	C(31)-H(31B)	0.9800
C(13)-C(17)	1.424(12)	C(31)-H(31C)	0.9800
C(13)-C(14)	1.446(12)	C(32)-C(33)	1.397(11)
C(14)-O(4)	1.192(12)	C(32)-H(32)	0.9500
C(14)-O(5A)	1.428(13)	C(33)-C(34)	1.368(11)
C(14)-O(5)	1.429(12)	C(33)-H(33)	0.9500
O(5)-C(15)	1.455(13)	C(34)-C(35)	1.367(11)
C(15)-C(16)	1.534(14)	C(34)-H(34)	0.9500
C(15)-H(15A)	0.9900	C(35)-C(36)	1.398(9)
C(15)-H(15B)	0.9900	C(35)-H(35)	0.9500
C(16)-H(16A)	0.9800	C(36)-C(37)	1.426(10)
C(16)-H(16B)	0.9800	C(37)-C(41)	1.392(10)
C(16)-H(16C)	0.9800	C(37)-C(38)	1.464(10)
O(5A)-C(15A)	1.456(14)	C(38)-O(8)	1.214(10)
C(15A)-C(16A)	1.544(14)	C(38)-O(9)	1.343(10)
C(15A)-H(15C)	0.9900	C(39)-C(40A)	1.44(2)
C(15A)-H(15D)	0.9900	C(39)-O(9)	1.482(11)
		C(39)-C(40)	1.509(17)
		C(39)-H(39A)	0.9900

C(39)-H(39B)	0.9900	C(46)-H(46B)	0.9800
C(39)-H(39C)	0.9900	C(46)-H(46C)	0.9800
C(39)-H(39D)	0.9900	C(46A)-H(46D)	0.9800
C(40)-H(40A)	0.9800	C(46A)-H(46E)	0.9800
C(40)-H(40B)	0.9800	C(46A)-H(46F)	0.9800
C(40)-H(40C)	0.9800	C(47)-H(47A)	0.9800
C(40A)-H(40D)	0.9800	C(47)-H(47B)	0.9800
C(40A)-H(40E)	0.9800	C(47)-H(47C)	0.9800
C(40A)-H(40F)	0.9800	C(48)-C(49)	1.521(13)
C(41)-O(10)	1.392(8)	C(48)-H(48A)	0.9900
C(42)-O(11)	1.197(9)	C(48)-H(48B)	0.9900
C(42)-O(12)	1.323(9)	C(49)-C(50)	1.520(12)
C(42)-O(10)	1.348(9)	C(49)-H(49A)	0.9900
C(43)-O(12)	1.481(8)	C(49)-H(49B)	0.9900
C(43)-C(44)	1.496(12)	C(50)-C(51)	1.519(12)
C(43)-C(52)	1.520(12)	C(50)-C(52)	1.527(10)
C(43)-H(43)	1.0000	C(50)-H(50)	1.0000
C(44)-C(48)	1.526(11)	C(51)-H(51A)	0.9800
C(44)-C(45)	1.565(13)	C(51)-H(51B)	0.9800
C(44)-H(44)	1.0000	C(51)-H(51C)	0.9800
C(45)-C(46A)	1.37(2)	C(52)-H(52A)	0.9900
C(45)-C(47)	1.508(16)	C(52)-H(52B)	0.9900
C(45)-C(46)	1.52(2)		
C(45)-H(45)	1.0000		
C(45)-H(45A)	1.0000		
C(46)-H(46A)	0.9800		

Table 4. Bond angles [°] for s16sel11.

C(2)-C(1)-H(1A)	109.5	C(5)-C(9)-H(9)	109.5
C(2)-C(1)-H(1B)	109.5	C(10)-C(9)-H(9)	109.5
H(1A)-C(1)-H(1B)	109.5	C(9)-C(10)-C(2)	110.2(7)
C(2)-C(1)-H(1C)	109.5	C(9)-C(10)-H(10A)	109.6
H(1A)-C(1)-H(1C)	109.5	C(2)-C(10)-H(10A)	109.6
H(1B)-C(1)-H(1C)	109.5	C(9)-C(10)-H(10B)	109.6
C(3)-C(2)-C(1)	112.6(8)	C(2)-C(10)-H(10B)	109.6
C(3)-C(2)-C(10)	109.5(7)	H(10A)-C(10)-H(10B)	108.1
C(1)-C(2)-C(10)	110.3(8)	O(2)-C(11)-O(1)	127.4(7)
C(3)-C(2)-H(2)	108.1	O(2)-C(11)-O(3)	124.9(8)
C(1)-C(2)-H(2)	108.1	O(1)-C(11)-O(3)	107.7(7)
C(10)-C(2)-H(2)	108.1	O(3)-C(12)-C(26)	120.5(6)
C(2)-C(3)-C(4)	112.5(7)	O(3)-C(12)-C(13)	128.0(8)
C(2)-C(3)-H(3A)	109.1	C(26)-C(12)-C(13)	111.3(7)
C(4)-C(3)-H(3A)	109.1	C(12)-C(13)-C(17)	107.6(7)
C(2)-C(3)-H(3B)	109.1	C(12)-C(13)-C(14)	130.2(10)
C(4)-C(3)-H(3B)	109.1	C(17)-C(13)-C(14)	122.0(8)
H(3A)-C(3)-H(3B)	107.8	O(4)-C(14)-O(5A)	122.8(14)
C(3)-C(4)-C(5)	112.6(8)	O(4)-C(14)-O(5)	121.6(12)
C(3)-C(4)-H(4A)	109.1	O(4)-C(14)-C(13)	129.8(11)
C(5)-C(4)-H(4A)	109.1	O(5A)-C(14)-C(13)	105.0(13)
C(3)-C(4)-H(4B)	109.1	O(5)-C(14)-C(13)	108.3(10)
C(5)-C(4)-H(4B)	109.1	C(14)-O(5)-C(15)	108.9(17)
H(4A)-C(4)-H(4B)	107.8	O(5)-C(15)-C(16)	108(2)
C(9)-C(5)-C(6)	107.6(8)	O(5)-C(15)-H(15A)	110.2
C(9)-C(5)-C(6)	113.7(8)	C(16)-C(15)-H(15A)	110.2
C(4)-C(5)-C(6)	114.4(8)	O(5)-C(15)-H(15B)	110.2
C(9)-C(5)-H(5)	106.9	C(16)-C(15)-H(15B)	110.2
C(4)-C(5)-H(5)	106.9	H(15A)-C(15)-H(15B)	108.5
C(6)-C(5)-H(5)	106.9	C(15)-C(16)-H(16A)	109.5
C(7)-C(6)-C(8)	109.2(9)	C(15)-C(16)-H(16B)	109.5
C(7)-C(6)-C(5)	113.3(9)	H(16A)-C(16)-H(16B)	109.5
C(8)-C(6)-C(5)	112.8(8)	C(15)-C(16)-H(16C)	109.5
C(7)-C(6)-H(6)	107.1	H(16A)-C(16)-H(16C)	109.5
C(8)-C(6)-H(6)	107.1	H(16B)-C(16)-H(16C)	109.5
C(5)-C(6)-H(6)	107.1	C(14)-O(5A)-C(15A)	104(3)
C(6)-C(7)-H(7A)	109.5	O(5A)-C(15A)-C(16A)	105(2)
C(6)-C(7)-H(7B)	109.5	O(5A)-C(15A)-H(15C)	110.8
H(7A)-C(7)-H(7B)	109.5	C(16A)-C(15A)-H(15C)	110.8
C(6)-C(7)-H(7C)	109.5	O(5A)-C(15A)-H(15D)	110.8
H(7A)-C(7)-H(7C)	109.5	C(16A)-C(15A)-H(15D)	110.8
H(7B)-C(7)-H(7C)	109.5	H(15C)-C(15A)-H(15D)	108.9
C(6)-C(8)-H(8A)	109.5	C(15A)-C(16A)-H(16D)	109.5
C(6)-C(8)-H(8B)	109.5	C(15A)-C(16A)-H(16E)	109.5
H(8A)-C(8)-H(8B)	109.5	H(16D)-C(16A)-H(16E)	109.5
C(6)-C(8)-H(8C)	109.5	C(15A)-C(16A)-H(16F)	109.5
H(8A)-C(8)-H(8C)	109.5	H(16D)-C(16A)-H(16F)	109.5
H(8B)-C(8)-H(8C)	109.5	H(16E)-C(16A)-H(16F)	109.5
O(1)-C(9)-C(5)	108.5(7)	C(18)-C(17)-C(13)	126.3(9)
O(1)-C(9)-C(10)	107.3(7)	C(18)-C(17)-C(25)	128.4(10)
C(5)-C(9)-C(10)	112.4(7)	C(13)-C(17)-C(25)	105.1(6)
O(1)-C(9)-H(9)	109.5	C(19)-C(18)-C(17)	126.0(10)
		C(19)-C(18)-H(18)	117.0
		C(17)-C(18)-H(18)	117.0

C(20)-C(19)-C(18)	131.5(10)	C(34)-C(33)-H(33)	114.7
C(20)-C(19)-H(19)	114.3	C(32)-C(33)-H(33)	114.7
C(18)-C(19)-H(19)	114.3	C(35)-C(34)-C(33)	129.1(8)
C(19)-C(20)-C(21)	129.1(11)	C(35)-C(34)-H(34)	115.5
C(19)-C(20)-H(20)	115.5	C(33)-C(34)-H(34)	115.5
C(21)-C(20)-H(20)	115.5	C(34)-C(35)-C(36)	128.3(8)
C(20)-C(21)-C(22)	129.5(12)	C(34)-C(35)-H(35)	115.8
C(20)-C(21)-H(21)	115.2	C(36)-C(35)-H(35)	115.8
C(22)-C(21)-H(21)	115.2	C(35)-C(36)-C(37)	124.9(7)
O(6)-C(22)-C(21)	120.4(9)	C(35)-C(36)-C(28)	128.2(7)
O(6)-C(22)-C(25)	111.2(6)	C(37)-C(36)-C(28)	106.8(6)
C(21)-C(22)-C(25)	128.4(9)	C(41)-C(37)-C(36)	106.3(7)
O(6)-C(23)-C(24)	104.2(8)	C(41)-C(37)-C(38)	127.3(7)
O(6)-C(23)-H(23A)	110.9	C(36)-C(37)-C(38)	126.4(7)
C(24)-C(23)-H(23A)	110.9	O(8)-C(38)-O(9)	123.2(8)
O(6)-C(23)-H(23B)	110.9	O(8)-C(38)-C(37)	125.2(8)
C(24)-C(23)-H(23B)	110.9	O(9)-C(38)-C(37)	111.6(7)
H(23A)-C(23)-H(23B)	108.9	C(40A)-C(39)-O(9)	111.4(14)
C(23)-C(24)-H(24A)	109.5	O(9)-C(39)-C(40)	105.4(13)
C(23)-C(24)-H(24B)	109.5	O(9)-C(39)-H(39A)	110.7
H(24A)-C(24)-H(24B)	109.5	C(40)-C(39)-H(39A)	110.7
C(23)-C(24)-H(24C)	109.5	O(9)-C(39)-H(39B)	110.7
H(24A)-C(24)-H(24C)	109.5	C(40)-C(39)-H(39B)	110.7
H(24B)-C(24)-H(24C)	109.5	H(39A)-C(39)-H(39B)	108.8
C(26)-C(25)-C(22)	124.5(7)	C(40A)-C(39)-H(39C)	109.3
C(26)-C(25)-C(17)	109.9(8)	O(9)-C(39)-H(39C)	109.3
C(22)-C(25)-C(17)	125.1(7)	C(40A)-C(39)-H(39D)	109.3
C(25)-C(26)-C(12)	105.9(6)	O(9)-C(39)-H(39D)	109.3
C(25)-C(26)-C(27)	130.5(7)	H(39C)-C(39)-H(39D)	108.0
C(12)-C(26)-C(27)	123.4(6)	C(39)-C(40)-H(40A)	109.5
C(41)-C(27)-C(28)	106.4(6)	C(39)-C(40)-H(40B)	109.5
C(41)-C(27)-C(26)	123.8(6)	H(40A)-C(40)-H(40B)	109.5
C(28)-C(27)-C(26)	129.8(6)	C(39)-C(40)-H(40C)	109.5
C(29)-C(28)-C(27)	125.2(6)	H(40A)-C(40)-H(40C)	109.5
C(29)-C(28)-C(36)	126.7(6)	H(40B)-C(40)-H(40C)	109.5
C(27)-C(28)-C(36)	108.0(6)	C(39)-C(40A)-H(40D)	109.5
O(7)-C(29)-C(32)	119.2(7)	C(39)-C(40A)-H(40E)	109.5
O(7)-C(29)-C(28)	111.8(6)	H(40D)-C(40A)-H(40E)	109.5
C(32)-C(29)-C(28)	129.0(7)	C(39)-C(40A)-H(40F)	109.5
O(7)-C(30)-C(31)	105.1(7)	H(40D)-C(40A)-H(40F)	109.5
O(7)-C(30)-H(30A)	110.7	H(40E)-C(40A)-H(40F)	109.5
C(31)-C(30)-H(30A)	110.7	C(27)-C(41)-C(37)	112.4(6)
O(7)-C(30)-H(30B)	110.7	C(27)-C(41)-O(10)	120.8(6)
C(31)-C(30)-H(30B)	110.7	C(37)-C(41)-O(10)	126.5(7)
H(30A)-C(30)-H(30B)	108.8	O(11)-C(42)-O(12)	128.2(7)
C(30)-C(31)-H(31A)	109.5	O(11)-C(42)-O(10)	125.5(7)
C(30)-C(31)-H(31B)	109.5	O(12)-C(42)-O(10)	106.3(7)
H(31A)-C(31)-H(31B)	109.5	O(12)-C(43)-C(44)	106.8(7)
C(30)-C(31)-H(31C)	109.5	O(12)-C(43)-C(52)	106.0(7)
H(31A)-C(31)-H(31C)	109.5	C(44)-C(43)-C(52)	113.1(7)
H(31B)-C(31)-H(31C)	109.5	O(12)-C(43)-H(43)	110.3
C(29)-C(32)-C(33)	127.6(8)	C(44)-C(43)-H(43)	110.3
C(29)-C(32)-H(32)	116.2	C(52)-C(43)-H(43)	110.3
C(33)-C(32)-H(32)	116.2	C(43)-C(44)-C(48)	108.1(8)
C(34)-C(33)-C(32)	130.7(7)	C(43)-C(44)-C(45)	112.6(8)

C(48)-C(44)-C(45)	112.9(8)	C(44)-C(48)-H(48B)	109.3
C(43)-C(44)-H(44)	107.7	H(48A)-C(48)-H(48B)	107.9
C(48)-C(44)-H(44)	107.7	C(50)-C(49)-C(48)	111.9(8)
C(45)-C(44)-H(44)	107.7	C(50)-C(49)-H(49A)	109.2
C(46A)-C(45)-C(47)	104.4(18)	C(48)-C(49)-H(49A)	109.2
C(47)-C(45)-C(46)	129.3(14)	C(50)-C(49)-H(49B)	109.2
C(46A)-C(45)-C(44)	115.7(15)	C(48)-C(49)-H(49B)	109.2
C(47)-C(45)-C(44)	114.8(11)	H(49A)-C(49)-H(49B)	107.9
C(46)-C(45)-C(44)	114.1(13)	C(51)-C(50)-C(49)	112.8(8)
C(47)-C(45)-H(45)	94.4	C(51)-C(50)-C(52)	110.7(8)
C(46)-C(45)-H(45)	94.4	C(49)-C(50)-C(52)	109.2(8)
C(44)-C(45)-H(45)	94.4	C(51)-C(50)-H(50)	108.0
C(46A)-C(45)-H(45A)	107.2	C(49)-C(50)-H(50)	108.0
C(47)-C(45)-H(45A)	107.2	C(52)-C(50)-H(50)	108.0
C(44)-C(45)-H(45A)	107.2	C(50)-C(51)-H(51A)	109.5
C(45)-C(46)-H(46A)	109.5	C(50)-C(51)-H(51B)	109.5
C(45)-C(46)-H(46B)	109.5	H(51A)-C(51)-H(51B)	109.5
H(46A)-C(46)-H(46B)	109.5	C(50)-C(51)-H(51C)	109.5
C(45)-C(46)-H(46C)	109.5	H(51A)-C(51)-H(51C)	109.5
H(46A)-C(46)-H(46C)	109.5	H(51B)-C(51)-H(51C)	109.5
H(46B)-C(46)-H(46C)	109.5	C(43)-C(52)-C(50)	112.9(7)
C(45)-C(46A)-H(46D)	109.5	C(43)-C(52)-H(52A)	109.0
C(45)-C(46A)-H(46E)	109.5	C(50)-C(52)-H(52A)	109.0
H(46D)-C(46A)-H(46E)	109.5	C(43)-C(52)-H(52B)	109.0
C(45)-C(46A)-H(46F)	109.5	C(50)-C(52)-H(52B)	109.0
H(46D)-C(46A)-H(46F)	109.5	H(52A)-C(52)-H(52B)	107.8
H(46E)-C(46A)-H(46F)	109.5	C(11)-O(1)-C(9)	115.6(6)
C(45)-C(47)-H(47A)	109.5	C(11)-O(3)-C(12)	115.1(6)
C(45)-C(47)-H(47B)	109.5	C(22)-O(6)-C(23)	120.2(7)
H(47A)-C(47)-H(47B)	109.5	C(29)-O(7)-C(30)	121.2(6)
C(45)-C(47)-H(47C)	109.5	C(38)-O(9)-C(39)	115.1(8)
H(47A)-C(47)-H(47C)	109.5	C(42)-O(10)-C(41)	118.0(6)
H(47B)-C(47)-H(47C)	109.5	C(42)-O(12)-C(43)	117.6(6)
C(49)-C(48)-C(44)	111.8(8)		
C(49)-C(48)-H(48A)	109.3		
C(44)-C(48)-H(48A)	109.3		
C(49)-C(48)-H(48B)	109.3		

Table 5. Anisotropic displacement parameters ($\text{\AA}^2 \times 10^3$) for s16sel11. The anisotropic displacement factor exponent takes the form: $-2\pi^2 [h^2 a^{*2} U^{11} + \dots + 2 h k a^* b^* U^{12}]$

	U ¹¹	U ²²	U ³³	U ²³	U ¹³	U ¹²
C(1)	88(8)	83(7)	100(7)	26(6)	-16(6)	9(6)
C(2)	77(6)	67(5)	66(5)	12(4)	-13(4)	-8(5)
C(3)	91(7)	79(6)	59(5)	23(4)	-17(5)	0(5)
C(4)	104(8)	77(6)	63(5)	17(4)	7(5)	-16(6)
C(5)	71(6)	68(5)	73(5)	16(4)	1(4)	-8(5)
C(6)	67(6)	85(7)	105(7)	32(6)	9(5)	-4(5)
C(7)	95(9)	85(8)	147(11)	2(7)	49(8)	1(6)
C(8)	80(8)	128(10)	101(8)	16(7)	-5(6)	9(7)
C(9)	70(6)	62(5)	52(4)	22(4)	-9(4)	-9(4)
C(10)	77(6)	63(5)	63(5)	10(4)	-11(4)	0(5)
C(11)	75(6)	51(5)	69(5)	21(4)	8(4)	1(4)
C(12)	72(5)	43(4)	50(4)	12(3)	10(4)	2(4)
C(13)	75(6)	44(4)	87(6)	16(4)	41(5)	24(4)
C(14)	94(8)	94(8)	108(9)	38(7)	29(7)	41(7)
O(5)	100(12)	74(11)	171(16)	45(10)	47(10)	59(10)
C(15)	106(19)	220(30)	140(20)	40(20)	18(17)	120(20)
C(16)	90(20)	390(70)	320(50)	-40(50)	-70(30)	100(30)
O(5A)	68(12)	31(10)	131(16)	32(9)	17(10)	31(9)
C(15A)	310(70)	90(30)	370(70)	-30(40)	0(60)	-90(40)
C(16A)	70(20)	300(60)	310(60)	200(50)	20(30)	80(30)
C(17)	88(6)	31(3)	66(5)	1(3)	30(5)	7(4)
C(18)	136(9)	40(4)	84(6)	-5(4)	55(7)	-2(5)
C(19)	174(12)	65(6)	37(4)	-10(4)	26(6)	-32(7)
C(20)	150(12)	98(8)	71(7)	-13(6)	1(8)	3(9)
C(21)	143(10)	92(7)	43(4)	-12(4)	-8(5)	-1(7)
C(22)	118(8)	61(5)	39(4)	-4(4)	-6(5)	-4(5)
C(23)	104(9)	125(9)	92(7)	6(7)	-52(7)	25(8)
C(24)	105(10)	194(14)	104(9)	-1(9)	-30(8)	67(10)
C(25)	87(6)	32(4)	52(4)	-4(3)	13(4)	1(4)
C(26)	66(5)	31(3)	41(4)	1(3)	6(3)	5(3)
C(27)	61(5)	37(3)	32(3)	-4(3)	0(3)	-4(3)
C(28)	62(5)	35(4)	39(3)	-6(3)	1(3)	1(3)
C(29)	74(5)	34(4)	44(4)	-6(3)	-4(4)	0(3)
C(30)	169(11)	43(5)	84(6)	-9(4)	55(7)	-35(6)
C(31)	224(15)	72(7)	99(8)	-13(6)	101(10)	-37(8)
C(32)	97(7)	45(4)	55(5)	-12(4)	11(5)	-11(4)
C(33)	103(7)	47(5)	66(5)	-19(4)	14(5)	-10(5)
C(34)	94(7)	60(5)	66(5)	-18(4)	18(5)	10(5)
C(35)	65(5)	67(5)	55(4)	-15(4)	12(4)	10(4)
C(36)	56(4)	46(4)	47(4)	-7(3)	3(3)	7(3)
C(37)	56(5)	60(4)	47(4)	-5(3)	5(3)	-3(4)
C(38)	69(6)	72(6)	68(5)	3(4)	14(5)	-17(5)
C(39)	126(12)	112(10)	185(15)	-13(10)	84(11)	-47(9)
C(40)	102(15)	111(14)	159(17)	40(14)	35(13)	4(12)
C(40A)	130(20)	98(18)	160(20)	-40(16)	76(18)	-46(16)
C(41)	58(5)	50(4)	40(3)	-10(3)	-2(3)	-3(3)
C(42)	64(5)	52(5)	56(4)	-10(4)	0(4)	-8(4)
C(43)	94(7)	49(4)	65(5)	-18(4)	-23(5)	0(4)
C(44)	75(6)	64(6)	92(7)	-16(5)	-7(5)	-6(5)

C(45)	82(8)	112(9)	116(9)	-32(7)	10(7)	-15(7)
C(46)	94(19)	420(50)	111(19)	90(30)	39(15)	80(30)
C(46A)	90(20)	44(13)	230(40)	-9(18)	70(20)	-30(13)
C(47)	96(11)	211(17)	191(17)	-48(14)	42(11)	9(11)
C(48)	82(7)	65(6)	114(8)	-40(5)	-8(6)	-10(5)
C(49)	90(7)	64(6)	96(7)	-32(5)	0(6)	1(5)
C(50)	87(7)	63(6)	79(6)	-23(4)	-21(5)	11(5)
C(51)	110(9)	91(8)	79(7)	-16(5)	7(6)	7(7)
C(52)	90(7)	53(5)	66(5)	-17(4)	-6(5)	-8(4)
O(1)	74(4)	66(4)	63(3)	22(3)	-15(3)	-15(3)
O(2)	151(7)	52(4)	64(4)	12(3)	1(4)	0(4)
O(3)	57(3)	50(3)	77(4)	19(3)	-4(3)	-2(2)
O(4)	126(7)	167(8)	146(7)	36(6)	84(6)	66(7)
O(6)	84(4)	81(4)	50(3)	-4(3)	-21(3)	9(3)
O(7)	95(4)	35(3)	53(3)	-8(2)	21(3)	-13(3)
O(8)	77(4)	104(5)	68(4)	-15(3)	29(3)	-15(4)
O(9)	91(5)	77(5)	145(7)	-20(4)	55(5)	-37(4)
O(10)	75(4)	42(3)	44(2)	-2(2)	0(2)	-11(2)
O(11)	87(4)	57(4)	91(4)	-23(3)	-34(4)	8(3)
O(12)	81(4)	46(3)	72(3)	-15(3)	-13(3)	-1(3)

Table 6. Hydrogen coordinates ($\times 10^4$) and isotropic displacement parameters ($\text{\AA}^2 \times 10^3$) for s16sel11.

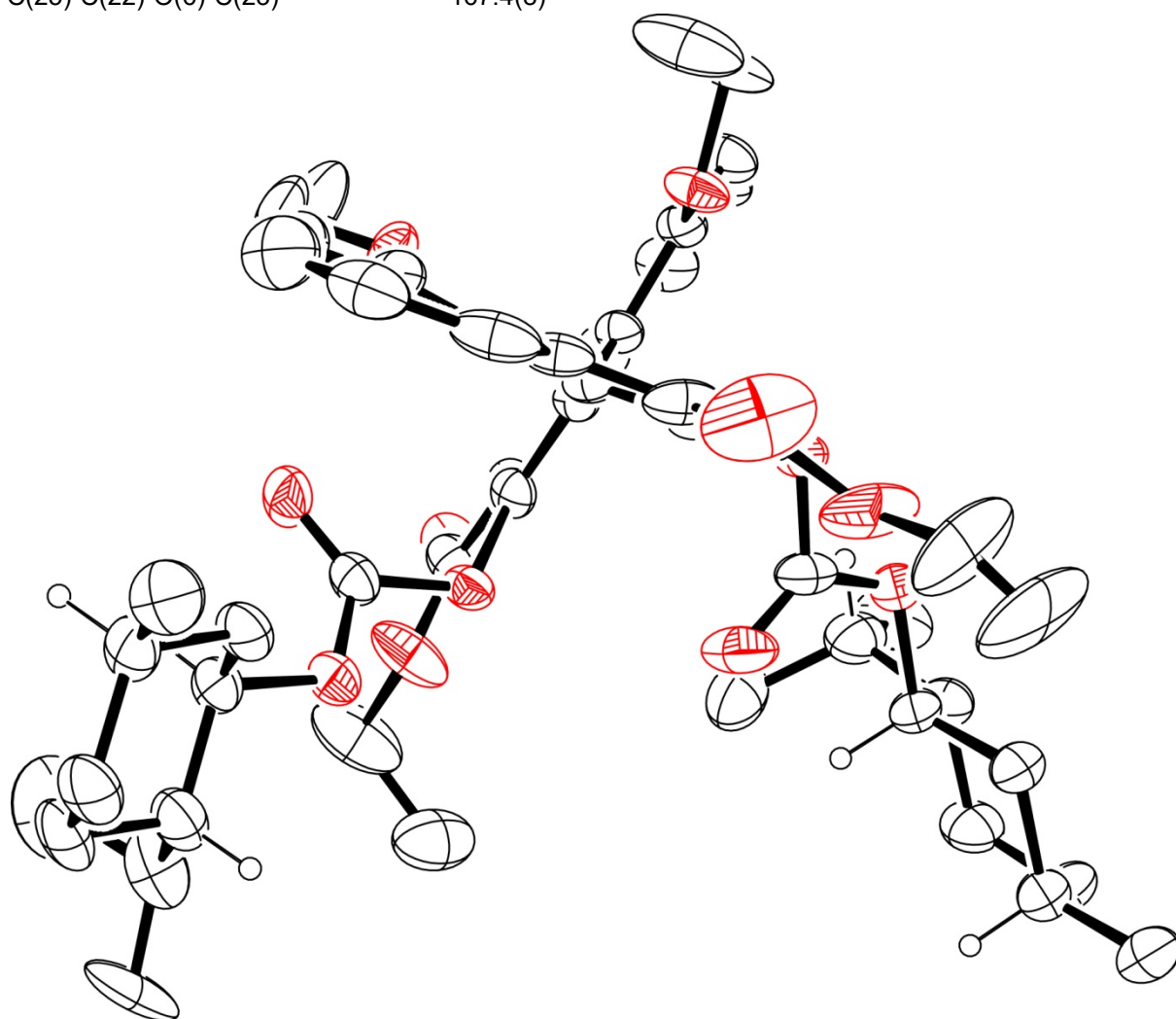
	x	y	z	U(eq)
H(1A)	-3533	7373	-60	135
H(1B)	-3782	7257	631	135
H(1C)	-4053	6586	169	135
H(2)	-1950	7089	488	84
H(3A)	-1914	6739	-508	92
H(3B)	-2480	5935	-361	92
H(4A)	-376	6370	1	98
H(4B)	-651	5732	-487	98
H(5)	-1447	4949	249	85
H(6)	55	4542	787	103
H(7A)	1154	4167	12	164
H(7B)	706	4839	-405	164
H(7C)	-58	4140	-219	164
H(8A)	1714	5163	736	154
H(8B)	850	5735	1020	154
H(8C)	1210	5839	343	154
H(9)	-834	6119	1063	73
H(10A)	-2705	6277	1220	81
H(10B)	-2963	5634	731	81
H(15A)	-4251	6068	2567	189
H(15B)	-4130	6076	3277	189
H(16A)	-5539	5219	2998	399
H(16B)	-4716	4735	2602	399
H(16C)	-4596	4743	3309	399
H(15C)	-4298	5472	3416	311
H(15D)	-4637	4859	2914	311
H(16D)	-5199	6128	2618	339
H(16E)	-3984	6420	2659	339
H(16F)	-4322	5811	2161	339
H(18)	-1636	5464	4521	104
H(19)	-501	5442	5277	110
H(20)	1136	5061	5327	128
H(21)	2094	4471	4662	111
H(23A)	2886	3548	4194	128
H(23B)	3314	4359	3940	128
H(24A)	4208	3368	3419	201
H(24B)	3411	3786	2965	201
H(24C)	3088	2976	3252	201
H(30A)	19	2075	3130	118
H(30B)	-1138	2254	2845	118
H(31A)	-1236	2321	3887	197
H(31B)	-1476	3148	3605	197
H(31C)	-326	2969	3888	197
H(32)	295	1966	2196	79
H(33)	1368	1691	1444	86
H(34)	2617	2376	1030	88
H(35)	3128	3552	1234	75
H(39A)	4718	5867	1255	169
H(39B)	4637	6535	1747	169

H(39C)	4928	6059	1618	169
H(39D)	4205	6101	1032	169
H(40A)	3250	6413	740	186
H(40B)	4183	7040	803	186
H(40C)	3161	7075	1231	186
H(40D)	3348	7155	1627	194
H(40E)	4320	7305	1179	194
H(40F)	4549	7207	1873	194
H(43)	3040	6811	3789	83
H(44)	1926	8122	3335	93
H(45)	3666	8540	3147	124
H(45A)	3292	7697	2675	124
H(46A)	2515	7856	2311	313
H(46B)	3694	8132	2131	313
H(46C)	2863	8731	2412	313
H(46D)	4158	8990	3148	181
H(46E)	3021	9009	2820	181
H(46F)	4065	8726	2470	181
H(47A)	5121	7810	2916	249
H(47B)	4550	7141	3287	249
H(47C)	4804	7949	3596	249
H(48A)	3489	8092	4266	104
H(48B)	2966	8861	4004	104
H(49A)	2095	8512	4894	100
H(49B)	1264	8486	4353	100
H(50)	2296	7175	4867	92
H(51A)	654	6783	5215	140
H(51B)	44	7454	4866	140
H(51C)	791	7658	5421	140
H(52A)	1395	6409	4180	84
H(52B)	790	7139	3908	84

Table 7. Torsion angles [°] for s16sel11.

C(1)-C(2)-C(3)-C(4)	-177.5(7)	C(22)-C(25)-C(26)-C(12)	169.5(7)
C(10)-C(2)-C(3)-C(4)	-54.3(10)	C(17)-C(25)-C(26)-C(12)	-3.0(8)
C(2)-C(3)-C(4)-C(5)	56.1(11)	C(22)-C(25)-C(26)-C(27)	-15.3(12)
C(3)-C(4)-C(5)-C(9)	-56.1(10)	C(17)-C(25)-C(26)-C(27)	172.1(6)
C(3)-C(4)-C(5)-C(6)	176.6(8)	O(3)-C(12)-C(26)-C(25)	-173.9(6)
C(9)-C(5)-C(6)-C(7)	173.2(8)	C(13)-C(12)-C(26)-C(25)	1.1(8)
C(4)-C(5)-C(6)-C(7)	-62.6(11)	O(3)-C(12)-C(26)-C(27)	10.5(10)
C(9)-C(5)-C(6)-C(8)	-62.1(10)	C(13)-C(12)-C(26)-C(27)	-174.4(6)
C(4)-C(5)-C(6)-C(8)	62.0(11)	C(25)-C(26)-C(27)-C(41)	-75.0(10)
C(4)-C(5)-C(9)-O(1)	176.7(7)	C(12)-C(26)-C(27)-C(41)	99.4(9)
C(6)-C(5)-C(9)-O(1)	-55.6(9)	C(25)-C(26)-C(27)-C(28)	104.5(10)
C(4)-C(5)-C(9)-C(10)	58.2(9)	C(12)-C(26)-C(27)-C(28)	-81.1(10)
C(6)-C(5)-C(9)-C(10)	-174.1(7)	C(41)-C(27)-C(28)-C(29)	176.1(7)
O(1)-C(9)-C(10)-C(2)	-178.8(7)	C(26)-C(27)-C(28)-C(29)	-3.4(12)
C(5)-C(9)-C(10)-C(2)	-59.6(9)	C(41)-C(27)-C(28)-C(36)	0.7(8)
C(3)-C(2)-C(10)-C(9)	55.1(10)	C(26)-C(27)-C(28)-C(36)	-178.9(7)
C(1)-C(2)-C(10)-C(9)	179.6(8)	C(27)-C(28)-C(29)-O(7)	-1.6(11)
O(3)-C(12)-C(13)-C(17)	175.8(6)	C(36)-C(28)-C(29)-O(7)	173.0(7)
C(26)-C(12)-C(13)-C(17)	1.2(9)	C(27)-C(28)-C(29)-C(32)	178.4(8)
O(3)-C(12)-C(13)-C(14)	-10.0(15)	C(36)-C(28)-C(29)-C(32)	-7.0(13)
C(26)-C(12)-C(13)-C(14)	175.4(9)	O(7)-C(29)-C(32)-C(33)	179.9(9)
C(12)-C(13)-C(14)-O(4)	178.1(12)	C(28)-C(29)-C(32)-C(33)	-0.1(16)
C(17)-C(13)-C(14)-O(4)	-8.6(19)	C(29)-C(32)-C(33)-C(34)	4.6(18)
C(12)-C(13)-C(14)-O(5A)	16.0(16)	C(32)-C(33)-C(34)-C(35)	-0.7(18)
C(17)-C(13)-C(14)-O(5A)	-170.7(10)	C(33)-C(34)-C(35)-C(36)	-3.5(16)
C(12)-C(13)-C(14)-O(5)	-9.2(17)	C(34)-C(35)-C(36)-C(37)	-178.2(8)
C(17)-C(13)-C(14)-O(5)	164.2(11)	C(34)-C(35)-C(36)-C(28)	-0.2(14)
O(4)-C(14)-O(5)-C(15)	-7(2)	C(29)-C(28)-C(36)-C(35)	7.1(13)
C(13)-C(14)-O(5)-C(15)	179.3(16)	C(27)-C(28)-C(36)-C(35)	-177.6(7)
C(14)-O(5)-C(15)-C(16)	-84(3)	C(29)-C(28)-C(36)-C(37)	-174.7(7)
O(4)-C(14)-O(5A)-C(15A)	7(2)	C(27)-C(28)-C(36)-C(37)	0.7(8)
C(13)-C(14)-O(5A)-C(15A)	171.0(17)	C(35)-C(36)-C(37)-C(41)	176.6(7)
C(14)-O(5A)-C(15A)-C(16A)	116(4)	C(28)-C(36)-C(37)-C(41)	-1.8(8)
C(12)-C(13)-C(17)-C(18)	172.5(7)	C(35)-C(36)-C(37)-C(38)	-2.7(13)
C(14)-C(13)-C(17)-C(18)	-2.2(14)	C(28)-C(36)-C(37)-C(38)	179.0(7)
C(12)-C(13)-C(17)-C(25)	-2.9(8)	C(41)-C(37)-C(38)-O(8)	175.9(8)
C(14)-C(13)-C(17)-C(25)	-177.6(8)	C(36)-C(37)-C(38)-O(8)	-5.0(14)
C(13)-C(17)-C(18)-C(19)	-179.1(8)	C(41)-C(37)-C(38)-O(9)	-7.0(12)
C(25)-C(17)-C(18)-C(19)	-4.6(14)	C(36)-C(37)-C(38)-O(9)	172.1(8)
C(17)-C(18)-C(19)-C(20)	-0.7(18)	C(28)-C(27)-C(41)-C(37)	-1.9(8)
C(18)-C(19)-C(20)-C(21)	-3(2)	C(26)-C(27)-C(41)-C(37)	177.7(7)
C(19)-C(20)-C(21)-C(22)	4(2)	C(28)-C(27)-C(41)-O(10)	172.7(6)
C(20)-C(21)-C(22)-O(6)	-173.6(11)	C(26)-C(27)-C(41)-O(10)	-7.7(11)
C(20)-C(21)-C(22)-C(25)	7.9(19)	C(36)-C(37)-C(41)-C(27)	2.3(9)
O(6)-C(22)-C(25)-C(26)	-8.5(12)	C(38)-C(37)-C(41)-C(27)	-178.4(7)
C(21)-C(22)-C(25)-C(26)	170.1(9)	C(36)-C(37)-C(41)-O(10)	-171.9(7)
O(6)-C(22)-C(25)-C(17)	162.9(7)	C(38)-C(37)-C(41)-O(10)	7.3(13)
C(21)-C(22)-C(25)-C(17)	-18.5(14)	O(12)-C(43)-C(44)-C(48)	172.3(7)
C(18)-C(17)-C(25)-C(26)	-171.6(7)	C(52)-C(43)-C(44)-C(48)	56.1(10)
C(13)-C(17)-C(25)-C(26)	3.7(8)	O(12)-C(43)-C(44)-C(45)	-62.4(11)
C(18)-C(17)-C(25)-C(22)	15.9(13)	C(52)-C(43)-C(44)-C(45)	-178.6(8)
C(13)-C(17)-C(25)-C(22)	-168.7(8)	C(43)-C(44)-C(45)-C(46A)	176(2)
		C(48)-C(44)-C(45)-C(46A)	-62(2)
		C(43)-C(44)-C(45)-C(47)	-62.7(13)

C(48)-C(44)-C(45)-C(47)	60.0(13)	C(24)-C(23)-O(6)-C(22)	-175.3(9)
C(43)-C(44)-C(45)-C(46)	103.5(19)	C(32)-C(29)-O(7)-C(30)	17.5(12)
C(48)-C(44)-C(45)-C(46)	-133.9(19)	C(28)-C(29)-O(7)-C(30)	-162.4(8)
C(43)-C(44)-C(48)-C(49)	-57.7(11)	C(31)-C(30)-O(7)-C(29)	157.5(9)
C(45)-C(44)-C(48)-C(49)	177.1(9)	O(8)-C(38)-O(9)-C(39)	0.1(16)
C(44)-C(48)-C(49)-C(50)	58.6(12)	C(37)-C(38)-O(9)-C(39)	-177.0(10)
C(48)-C(49)-C(50)-C(51)	-177.3(8)	C(40A)-C(39)-O(9)-C(38)	171(2)
C(48)-C(49)-C(50)-C(52)	-53.7(11)	C(40)-C(39)-O(9)-C(38)	111.3(14)
O(12)-C(43)-C(52)-C(50)	-171.9(7)	O(11)-C(42)-O(10)-C(41)	2.8(12)
C(44)-C(43)-C(52)-C(50)	-55.2(11)	O(12)-C(42)-O(10)-C(41)	-176.3(6)
C(51)-C(50)-C(52)-C(43)	176.6(8)	C(27)-C(41)-O(10)-C(42)	91.5(9)
C(49)-C(50)-C(52)-C(43)	51.8(11)	C(37)-C(41)-O(10)-C(42)	-94.7(8)
O(2)-C(11)-O(1)-C(9)	0.6(14)	O(11)-C(42)-O(12)-C(43)	-7.8(13)
O(3)-C(11)-O(1)-C(9)	179.4(6)	O(10)-C(42)-O(12)-C(43)	171.2(6)
C(5)-C(9)-O(1)-C(11)	141.3(7)	C(44)-C(43)-O(12)-C(42)	148.8(8)
C(10)-C(9)-O(1)-C(11)	-97.0(8)	C(52)-C(43)-O(12)-C(42)	-90.3(9)
O(2)-C(11)-O(3)-C(12)	-10.1(13)		
O(1)-C(11)-O(3)-C(12)	171.0(6)		
C(26)-C(12)-O(3)-C(11)	-88.7(8)		
C(13)-C(12)-O(3)-C(11)	97.1(9)		
C(21)-C(22)-O(6)-C(23)	-11.3(13)		
C(25)-C(22)-O(6)-C(23)	167.4(8)		



Axial view of (*S_a*,1*R*,2*S*,5*R*)-**404**.

X-ray crystallographic data for (*R*_a)-**394**.

Table 1. Crystal data and structure refinement for s16sel7.

Identification code	s16sel7	
Empirical formula	C ₃₀ H ₃₀ O ₈	
Formula weight	518.54	
Temperature	150.00(10) K	
Wavelength	1.54184 Å	
Crystal system	Orthorhombic	
Space group	P2 ₁ 2 ₁ 2 ₁	
Unit cell dimensions	a = 7.0912(3) Å	α = 90°.
	b = 9.4533(4) Å	β = 90°.
	c = 37.611(2) Å	γ = 90°.
Volume	2521.3(2) Å ³	
Z	4	
Density (calculated)	1.366 Mg/m ³	
Absorption coefficient	0.817 mm ⁻¹	
F(000)	1096	
Crystal size	0.180 x 0.050 x 0.020 mm ³	
Theta range for data collection	4.824 to 68.414°.	
Index ranges	-8 ≤ h ≤ 8, -6 ≤ k ≤ 11, -45 ≤ l ≤ 45	
Reflections collected	13591	
Independent reflections	4633 [R(int) = 0.0483]	
Completeness to theta = 67.684°	99.8 %	
Absorption correction	Semi-empirical from equivalents	
Max. and min. transmission	1.00000 and 0.71798	
Refinement method	Full-matrix least-squares on F ²	
Data / restraints / parameters	4633 / 0 / 355	
Goodness-of-fit on F ²	1.124	
Final R indices [I > 2σ(I)]	R1 = 0.0643, wR2 = 0.1503	
R indices (all data)	R1 = 0.0725, wR2 = 0.1545	
Absolute structure parameter	-0.11(17)	
Extinction coefficient	n/a	
Largest diff. peak and hole	0.309 and -0.305 e.Å ⁻³	

Table 2. Atomic coordinates ($\times 10^4$) and equivalent isotropic displacement parameters ($\text{\AA}^2 \times 10^3$) for s16sel7. $U(\text{eq})$ is defined as one third of the trace of the orthogonalized U_{ij} tensor.

	x	y	z	$U(\text{eq})$
O(1)	130(6)	4794(4)	3549(1)	29(1)
O(2)	-965(5)	5929(4)	2947(1)	31(1)
O(3)	727(5)	7670(4)	2693(1)	28(1)
O(4)	6558(6)	6337(4)	4056(1)	29(1)
O(5)	3021(6)	6723(4)	4486(1)	32(1)
O(6)	2968(8)	5819(4)	5140(1)	43(1)
O(7)	3121(6)	3515(4)	5266(1)	28(1)
O(8)	3551(5)	2922(4)	3469(1)	24(1)
C(1)	1599(8)	5649(5)	3503(1)	22(1)
C(2)	1852(7)	6621(5)	3222(1)	22(1)
C(3)	414(7)	6698(5)	2949(1)	24(1)
C(4)	-688(8)	7728(6)	2410(1)	29(1)
C(5)	-285(9)	6637(6)	2128(2)	36(1)
C(6)	3611(7)	7328(5)	3278(1)	22(1)
C(7)	4334(8)	8358(5)	3056(1)	25(1)
C(8)	6022(8)	9107(6)	3083(1)	29(1)
C(9)	7407(8)	8966(6)	3339(1)	30(1)
C(10)	7481(7)	8073(5)	3635(1)	26(1)
C(11)	6196(7)	7089(5)	3758(1)	23(1)
C(12)	8209(8)	6670(6)	4272(1)	30(1)
C(13)	7961(9)	5901(6)	4621(2)	37(1)
C(14)	4415(7)	6729(5)	3608(1)	22(1)
C(15)	3171(8)	5699(5)	3743(1)	22(1)
C(16)	3240(7)	4814(5)	4061(1)	22(1)
C(17)	3129(8)	5350(5)	4409(1)	24(1)
C(18)	3119(8)	4249(5)	4664(1)	23(1)
C(19)	3064(8)	4582(6)	5035(1)	27(1)
C(20)	3138(9)	3895(6)	5638(1)	31(1)
C(21)	3345(9)	2572(7)	5854(2)	39(1)
C(22)	3186(7)	2957(5)	4473(1)	22(1)
C(23)	3109(8)	1615(5)	4626(1)	26(1)
C(24)	3064(9)	281(5)	4459(2)	30(1)
C(25)	3125(8)	-19(5)	4105(1)	29(1)
C(26)	3305(8)	901(5)	3816(1)	27(1)
C(27)	3401(7)	2350(6)	3806(1)	22(1)
C(28)	5457(8)	3158(6)	3353(1)	30(1)
C(29)	5392(9)	3641(7)	2974(1)	35(1)
C(30)	3270(7)	3326(5)	4089(1)	20(1)

Table 3. Bond lengths [Å] for s16sel7.

O(1)-C(1)	1.330(6)	C(12)-H(12B)	0.9900
O(1)-H(1)	1.00(7)	C(13)-H(13A)	0.9800
O(2)-C(3)	1.219(7)	C(13)-H(13B)	0.9800
O(3)-C(3)	1.350(6)	C(13)-H(13C)	0.9800
O(3)-C(4)	1.462(6)	C(14)-C(15)	1.409(7)
O(4)-C(11)	1.353(6)	C(15)-C(16)	1.460(7)
O(4)-C(12)	1.459(6)	C(16)-C(17)	1.407(7)
O(5)-C(17)	1.331(6)	C(16)-C(30)	1.411(7)
O(5)-H(5)	0.99(5)	C(17)-C(18)	1.415(7)
O(6)-C(19)	1.237(7)	C(18)-C(22)	1.418(7)
O(7)-C(19)	1.332(6)	C(18)-C(19)	1.431(7)
O(7)-C(20)	1.446(6)	C(20)-C(21)	1.497(8)
O(8)-C(27)	1.382(6)	C(20)-H(20A)	0.9900
O(8)-C(28)	1.438(6)	C(20)-H(20B)	0.9900
C(1)-C(2)	1.412(7)	C(21)-H(21A)	0.9800
C(1)-C(15)	1.434(7)	C(21)-H(21B)	0.9800
C(2)-C(6)	1.431(7)	C(21)-H(21C)	0.9800
C(2)-C(3)	1.450(7)	C(22)-C(23)	1.395(7)
C(4)-C(5)	1.508(7)	C(22)-C(30)	1.485(7)
C(4)-H(4A)	0.9900	C(23)-C(24)	1.409(7)
C(4)-H(4B)	0.9900	C(23)-H(23)	0.9500
C(5)-H(5A)	0.9800	C(24)-C(25)	1.362(8)
C(5)-H(5B)	0.9800	C(24)-H(24)	0.9500
C(5)-H(5C)	0.9800	C(25)-C(26)	1.397(7)
C(6)-C(7)	1.383(7)	C(25)-H(25)	0.9500
C(6)-C(14)	1.477(7)	C(26)-C(27)	1.372(7)
C(7)-C(8)	1.394(8)	C(26)-H(26)	0.9500
C(7)-H(7)	0.9500	C(27)-C(30)	1.412(7)
C(8)-C(9)	1.382(8)	C(28)-C(29)	1.499(7)
C(8)-H(8)	0.9500	C(28)-H(28A)	0.9900
C(9)-C(10)	1.397(7)	C(28)-H(28B)	0.9900
C(9)-H(9)	0.9500	C(29)-H(29A)	0.9800
C(10)-C(11)	1.382(7)	C(29)-H(29B)	0.9800
C(10)-H(10)	0.9500	C(29)-H(29C)	0.9800
C(11)-C(14)	1.425(7)		
C(12)-C(13)	1.509(8)		
C(12)-H(12A)	0.9900		

Table 4. Bond angles [°] for s16sel7.

C(1)-O(1)-H(1)	104(4)	H(13A)-C(13)-H(13B)	109.5
C(3)-O(3)-C(4)	115.5(4)	C(12)-C(13)-H(13C)	109.5
C(11)-O(4)-C(12)	120.0(4)	H(13A)-C(13)-H(13C)	109.5
C(17)-O(5)-H(5)	105(3)	H(13B)-C(13)-H(13C)	109.5
C(19)-O(7)-C(20)	116.4(4)	C(15)-C(14)-C(11)	125.2(5)
C(27)-O(8)-C(28)	114.3(4)	C(15)-C(14)-C(6)	109.0(4)
O(1)-C(1)-C(2)	126.4(5)	C(11)-C(14)-C(6)	125.7(5)
O(1)-C(1)-C(15)	123.2(4)	C(14)-C(15)-C(1)	106.4(4)
C(2)-C(1)-C(15)	110.5(5)	C(14)-C(15)-C(16)	132.1(5)
C(1)-C(2)-C(6)	107.8(4)	C(1)-C(15)-C(16)	121.5(5)
C(1)-C(2)-C(3)	118.3(5)	C(17)-C(16)-C(30)	106.8(4)
C(6)-C(2)-C(3)	133.9(4)	C(17)-C(16)-C(15)	123.7(5)
O(2)-C(3)-O(3)	122.3(5)	C(30)-C(16)-C(15)	129.4(5)
O(2)-C(3)-C(2)	122.6(5)	O(5)-C(17)-C(16)	123.9(5)
O(3)-C(3)-C(2)	115.1(4)	O(5)-C(17)-C(18)	124.7(5)
O(3)-C(4)-C(5)	110.8(4)	C(16)-C(17)-C(18)	111.5(4)
O(3)-C(4)-H(4A)	109.5	C(17)-C(18)-C(22)	106.9(4)
C(5)-C(4)-H(4A)	109.5	C(17)-C(18)-C(19)	119.9(4)
O(3)-C(4)-H(4B)	109.5	C(22)-C(18)-C(19)	133.2(4)
C(5)-C(4)-H(4B)	109.5	O(6)-C(19)-O(7)	120.6(5)
H(4A)-C(4)-H(4B)	108.1	O(6)-C(19)-C(18)	121.4(5)
C(4)-C(5)-H(5A)	109.5	O(7)-C(19)-C(18)	118.0(5)
C(4)-C(5)-H(5B)	109.5	O(7)-C(20)-C(21)	108.5(5)
H(5A)-C(5)-H(5B)	109.5	O(7)-C(20)-H(20A)	110.0
C(4)-C(5)-H(5C)	109.5	C(21)-C(20)-H(20A)	110.0
H(5A)-C(5)-H(5C)	109.5	O(7)-C(20)-H(20B)	110.0
H(5B)-C(5)-H(5C)	109.5	C(21)-C(20)-H(20B)	110.0
C(7)-C(6)-C(2)	124.3(5)	H(20A)-C(20)-H(20B)	108.4
C(7)-C(6)-C(14)	129.4(5)	C(20)-C(21)-H(21A)	109.5
C(2)-C(6)-C(14)	106.3(4)	C(20)-C(21)-H(21B)	109.5
C(6)-C(7)-C(8)	129.1(5)	H(21A)-C(21)-H(21B)	109.5
C(6)-C(7)-H(7)	115.5	C(20)-C(21)-H(21C)	109.5
C(8)-C(7)-H(7)	115.5	H(21A)-C(21)-H(21C)	109.5
C(9)-C(8)-C(7)	127.9(5)	H(21B)-C(21)-H(21C)	109.5
C(9)-C(8)-H(8)	116.1	C(23)-C(22)-C(18)	124.9(4)
C(7)-C(8)-H(8)	116.1	C(23)-C(22)-C(30)	128.1(4)
C(8)-C(9)-C(10)	129.7(5)	C(18)-C(22)-C(30)	107.0(4)
C(8)-C(9)-H(9)	115.1	C(22)-C(23)-C(24)	129.0(5)
C(10)-C(9)-H(9)	115.1	C(22)-C(23)-H(23)	115.5
C(11)-C(10)-C(9)	130.4(5)	C(24)-C(23)-H(23)	115.5
C(11)-C(10)-H(10)	114.8	C(25)-C(24)-C(23)	128.5(5)
C(9)-C(10)-H(10)	114.8	C(25)-C(24)-H(24)	115.8
O(4)-C(11)-C(10)	120.4(5)	C(23)-C(24)-H(24)	115.8
O(4)-C(11)-C(14)	111.8(4)	C(24)-C(25)-C(26)	129.3(5)
C(10)-C(11)-C(14)	127.7(5)	C(24)-C(25)-H(25)	115.4
O(4)-C(12)-C(13)	106.6(5)	C(26)-C(25)-H(25)	115.4
O(4)-C(12)-H(12A)	110.4	C(27)-C(26)-C(25)	130.3(5)
C(13)-C(12)-H(12A)	110.4	C(27)-C(26)-H(26)	114.8
O(4)-C(12)-H(12B)	110.4	C(25)-C(26)-H(26)	114.8
C(13)-C(12)-H(12B)	110.4	C(26)-C(27)-O(8)	114.8(4)
H(12A)-C(12)-H(12B)	108.6	C(26)-C(27)-C(30)	128.9(5)
C(12)-C(13)-H(13A)	109.5	O(8)-C(27)-C(30)	116.2(4)
C(12)-C(13)-H(13B)	109.5	O(8)-C(28)-C(29)	107.9(4)

O(8)-C(28)-H(28A)	110.1	H(29A)-C(29)-H(29B)	109.5
C(29)-C(28)-H(28A)	110.1	C(28)-C(29)-H(29C)	109.5
O(8)-C(28)-H(28B)	110.1	H(29A)-C(29)-H(29C)	109.5
C(29)-C(28)-H(28B)	110.1	H(29B)-C(29)-H(29C)	109.5
H(28A)-C(28)-H(28B)	108.4	C(16)-C(30)-C(27)	126.5(5)
C(28)-C(29)-H(29A)	109.5	C(16)-C(30)-C(22)	107.9(4)
C(28)-C(29)-H(29B)	109.5	C(27)-C(30)-C(22)	125.6(4)

Table 5. Anisotropic displacement parameters ($\text{\AA}^2 \times 10^3$) for s16sel7. The anisotropic displacement factor exponent takes the form: $-2\pi^2 [h^2 a^{*2} U^{11} + \dots + 2 h k a^* b^* U^{12}]$

	U ¹¹	U ²²	U ³³	U ²³	U ¹³	U ¹²
O(1)	28(2)	27(2)	32(2)	4(2)	-1(2)	-6(2)
O(2)	26(2)	32(2)	34(2)	4(2)	-5(2)	-2(2)
O(3)	30(2)	26(2)	27(2)	4(2)	-5(2)	0(2)
O(4)	30(2)	29(2)	28(2)	5(1)	-8(2)	-7(2)
O(5)	52(3)	15(2)	28(2)	-1(1)	2(2)	0(2)
O(6)	76(3)	28(2)	24(2)	-2(2)	1(2)	1(2)
O(7)	30(2)	31(2)	22(2)	4(1)	0(2)	1(2)
O(8)	18(2)	29(2)	25(2)	2(1)	2(1)	0(1)
C(1)	23(3)	18(2)	24(2)	0(2)	1(2)	0(2)
C(2)	25(2)	21(2)	20(2)	0(2)	1(2)	3(2)
C(3)	26(3)	19(2)	26(2)	1(2)	1(2)	2(2)
C(4)	27(3)	29(3)	31(3)	2(2)	-7(2)	6(2)
C(5)	38(3)	35(3)	35(3)	-2(3)	-6(2)	7(3)
C(6)	26(3)	18(2)	21(2)	0(2)	4(2)	0(2)
C(7)	29(3)	21(3)	25(2)	2(2)	4(2)	1(2)
C(8)	34(3)	23(3)	30(3)	3(2)	6(2)	0(2)
C(9)	27(3)	27(3)	35(3)	2(2)	5(2)	-6(2)
C(10)	22(2)	23(3)	31(3)	-1(2)	1(2)	-6(2)
C(11)	25(3)	21(2)	24(2)	0(2)	1(2)	4(2)
C(12)	28(3)	36(3)	27(3)	-2(2)	-8(2)	-3(3)
C(13)	43(4)	31(3)	37(3)	3(2)	-14(3)	0(3)
C(14)	24(2)	21(3)	21(2)	-2(2)	2(2)	1(2)
C(15)	24(2)	20(2)	22(2)	-2(2)	0(2)	1(2)
C(16)	19(2)	26(3)	22(2)	2(2)	0(2)	-8(2)
C(17)	29(3)	15(2)	30(3)	2(2)	2(2)	-1(2)
C(18)	29(3)	12(2)	27(2)	3(2)	0(2)	-1(2)
C(19)	25(3)	26(3)	30(3)	4(2)	1(2)	1(2)
C(20)	27(3)	42(3)	25(3)	2(2)	0(2)	2(3)
C(21)	33(3)	56(4)	30(3)	11(3)	1(2)	2(3)
C(22)	18(2)	19(2)	28(2)	1(2)	1(2)	2(2)
C(23)	32(3)	19(2)	28(3)	4(2)	3(2)	3(2)
C(24)	35(3)	11(2)	42(3)	6(2)	5(3)	1(2)
C(25)	35(3)	11(2)	40(3)	1(2)	7(3)	-5(2)
C(26)	30(3)	23(2)	29(3)	-2(2)	4(2)	0(2)
C(27)	11(2)	32(3)	23(2)	-2(2)	0(2)	1(2)
C(28)	22(3)	32(3)	34(3)	0(2)	6(2)	-1(2)
C(29)	28(3)	47(4)	31(3)	3(2)	4(2)	-3(3)
C(30)	13(2)	20(2)	27(2)	0(2)	1(2)	-1(2)

Table 6. Hydrogen coordinates ($\times 10^4$) and isotropic displacement parameters ($\text{\AA}^2 \times 10^3$) for s16sel7.

	x	y	z	U(eq)
H(1)	-630(110)	4910(80)	3327(19)	50(20)
H(5)	3020(90)	6760(60)	4750(15)	24(14)
H(4A)	-689	8682	2302	35
H(4B)	-1954	7556	2513	35
H(5A)	-1146	6775	1927	54
H(5B)	-467	5688	2227	54
H(5C)	1020	6738	2046	54
H(7)	3575	8588	2856	30
H(8)	6246	9797	2905	35
H(9)	8469	9568	3310	35
H(10)	8596	8155	3773	31
H(12A)	8297	7702	4313	36
H(12B)	9374	6350	4152	36
H(13A)	9016	6129	4779	56
H(13B)	7932	4879	4578	56
H(13C)	6775	6196	4732	56
H(20A)	1950	4383	5702	38
H(20B)	4202	4545	5688	38
H(21A)	3575	2821	6103	59
H(21B)	4410	2019	5763	59
H(21C)	2187	2012	5836	59
H(23)	3083	1597	4879	32
H(24)	2981	-512	4613	35
H(25)	3030	-994	4046	35
H(26)	3373	451	3591	33
H(28A)	6197	2273	3373	35
H(28B)	6065	3888	3503	35
H(29A)	6659	3920	2897	53
H(29B)	4536	4451	2953	53
H(29C)	4937	2867	2823	53

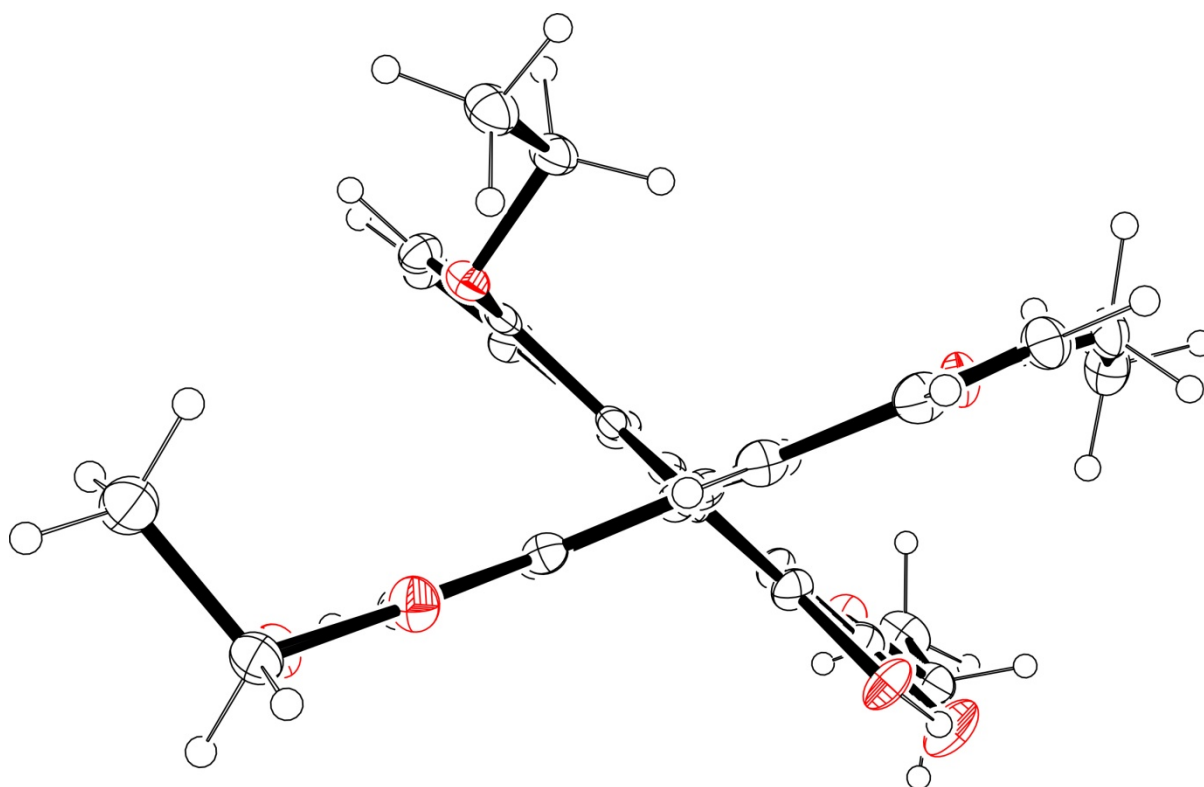
Table 7. Torsion angles [$^\circ$] for s16sel7.

O(1)-C(1)-C(2)-C(6)	179.5(5)	C(14)-C(6)-C(7)-C(8)	0.0(9)
C(15)-C(1)-C(2)-C(6)	-0.3(6)	C(6)-C(7)-C(8)-C(9)	1.8(10)
O(1)-C(1)-C(2)-C(3)	-1.4(8)	C(7)-C(8)-C(9)-C(10)	-0.9(10)
C(15)-C(1)-C(2)-C(3)	178.8(4)	C(8)-C(9)-C(10)-C(11)	-0.7(11)
C(4)-O(3)-C(3)-O(2)	-0.6(7)	C(12)-O(4)-C(11)-C(10)	6.8(7)
C(4)-O(3)-C(3)-C(2)	178.4(4)	C(12)-O(4)-C(11)-C(14)	-172.8(4)
C(1)-C(2)-C(3)-O(2)	-2.3(7)	C(9)-C(10)-C(11)-O(4)	-179.4(5)
C(6)-C(2)-C(3)-O(2)	176.4(5)	C(9)-C(10)-C(11)-C(14)	0.2(10)
C(1)-C(2)-C(3)-O(3)	178.7(4)	C(11)-O(4)-C(12)-C(13)	167.0(5)
C(6)-C(2)-C(3)-O(3)	-2.5(8)	O(4)-C(11)-C(14)-C(15)	-1.3(7)
C(3)-O(3)-C(4)-C(5)	-84.3(6)	C(10)-C(11)-C(14)-C(15)	179.0(5)
C(1)-C(2)-C(6)-C(7)	180.0(5)	O(4)-C(11)-C(14)-C(6)	-178.6(5)
C(3)-C(2)-C(6)-C(7)	1.1(9)	C(10)-C(11)-C(14)-C(6)	1.8(8)
C(1)-C(2)-C(6)-C(14)	0.2(5)	C(7)-C(6)-C(14)-C(15)	-179.8(5)
C(3)-C(2)-C(6)-C(14)	-178.7(5)	C(2)-C(6)-C(14)-C(15)	0.0(5)
C(2)-C(6)-C(7)-C(8)	-179.8(5)	C(7)-C(6)-C(14)-C(11)	-2.2(8)

C(2)-C(6)-C(14)-C(11)	177.6(5)
C(11)-C(14)-C(15)-C(1)	-177.8(5)
C(6)-C(14)-C(15)-C(1)	-0.2(5)
C(11)-C(14)-C(15)-C(16)	4.0(9)
C(6)-C(14)-C(15)-C(16)	-178.4(5)
O(1)-C(1)-C(15)-C(14)	-179.5(5)
C(2)-C(1)-C(15)-C(14)	0.3(6)
O(1)-C(1)-C(15)-C(16)	-1.1(8)
C(2)-C(1)-C(15)-C(16)	178.8(4)
C(14)-C(15)-C(16)-C(17)	66.2(8)
C(1)-C(15)-C(16)-C(17)	-111.8(6)
C(14)-C(15)-C(16)-C(30)	-119.5(7)
C(1)-C(15)-C(16)-C(30)	62.5(8)
C(30)-C(16)-C(17)-O(5)	-178.1(5)
C(15)-C(16)-C(17)-O(5)	-2.7(9)
C(30)-C(16)-C(17)-C(18)	1.1(7)
C(15)-C(16)-C(17)-C(18)	176.5(5)
O(5)-C(17)-C(18)-C(22)	177.9(5)
C(16)-C(17)-C(18)-C(22)	-1.3(7)
O(5)-C(17)-C(18)-C(19)	-2.5(9)
C(16)-C(17)-C(18)-C(19)	178.3(5)
C(20)-O(7)-C(19)-O(6)	-2.3(8)
C(20)-O(7)-C(19)-C(18)	177.6(5)
C(17)-C(18)-C(19)-O(6)	2.2(9)
C(22)-C(18)-C(19)-O(6)	-178.4(6)
C(17)-C(18)-C(19)-O(7)	-177.8(5)
C(22)-C(18)-C(19)-O(7)	1.6(10)
C(19)-O(7)-C(20)-C(21)	-175.9(5)
C(17)-C(18)-C(22)-C(23)	-176.8(5)
C(19)-C(18)-C(22)-C(23)	3.7(10)
C(17)-C(18)-C(22)-C(30)	0.9(6)
C(19)-C(18)-C(22)-C(30)	-178.5(6)
C(18)-C(22)-C(23)-C(24)	176.3(6)
C(30)-C(22)-C(23)-C(24)	-1.0(10)
C(22)-C(23)-C(24)-C(25)	1.5(11)
C(23)-C(24)-C(25)-C(26)	2.2(11)
C(24)-C(25)-C(26)-C(27)	-2.7(12)
C(25)-C(26)-C(27)-O(8)	-179.1(6)
C(25)-C(26)-C(27)-C(30)	-2.7(11)
C(28)-O(8)-C(27)-C(26)	-92.6(6)
C(28)-O(8)-C(27)-C(30)	90.6(5)
C(27)-O(8)-C(28)-C(29)	174.5(4)
C(17)-C(16)-C(30)-C(27)	-179.0(5)
C(15)-C(16)-C(30)-C(27)	5.9(9)
C(17)-C(16)-C(30)-C(22)	-0.4(6)
C(15)-C(16)-C(30)-C(22)	-175.5(5)
C(26)-C(27)-C(30)-C(16)	-175.0(6)
O(8)-C(27)-C(30)-C(16)	1.3(8)
C(26)-C(27)-C(30)-C(22)	6.6(9)
O(8)-C(27)-C(30)-C(22)	-177.0(4)
C(23)-C(22)-C(30)-C(16)	177.3(5)
C(18)-C(22)-C(30)-C(16)	-0.3(6)
C(23)-C(22)-C(30)-C(27)	-4.1(8)
C(18)-C(22)-C(30)-C(27)	178.3(5)

Table 8. Hydrogen bonds for s16sel7 [Å and °].

D-H...A	d(D-H)	d(H...A)	d(D...A)	<(DHA)
O(1)-H(1)...O(2)	1.00(7)	1.74(7)	2.623(5)	145(7)
O(5)-H(5)...O(6)	0.99(5)	1.71(5)	2.603(5)	147(5)



Axial view of (*R_a*)-394.